Die approbierte gedruckte Originalversion dieser Dissertation ist an der TU Wien Bibliothek verfügbar.
The approved original version of this doctoral thesis is available in print at TU Wien Bibliothek.

TECHNISCHE UNIVERSITÄT WIEN
Vienna University of Technology

Dissertation

Novel Organocatalysts for Highly Enantioselective Transformations: Development and Evaluation

Ausgeführt zum Zwecke der Erlangung des akademischen Grades eines Doktors der technischen Wissenschaften
am Institut für Angewandte Synthesechemie unter der Leitung von

Univ. Prof. Dipl.-Ing. Dr.techn. Katharina Schröder
Assoc. Prof. Dipl.-Ing. Dr.techn. Michael Schnürch

eingereicht an der Technischen Universität Wien

von

Dipl.-Ing. Fabian Scharinger
01125653

Wien, 16.11.2023

Table of Contents

Acknowledgement ..... **I**

Abstract ..... **II**

Kurzfassung ..... **III**

List of Abbreviations ..... **IV**

1 The phenomenon of chirality **1**

2 Asymmetric Synthesis **3**

3 Asymmetric Catalysis **5**

3.1 Transition metal catalysis 5

3.1.1 Asymmetric hydrogenations 5

3.1.2 Asymmetric transfer hydrogenations 6

3.1.3 Asymmetric epoxidations 7

3.2 Organocatalysis 9

3.2.1 Covalent activation 10

3.2.1.1 Enamine catalysis 10

3.2.1.2 Iminium catalysis 13

3.2.1.3 Singly Occupied Molecular Orbital catalysis 15

3.2.1.4 Photoredox catalysis 16

3.2.2 Non-covalent activation modes 18

3.2.2.1 Hydrogen-bond activation 18

3.2.2.2 Halogen bonding 20

3.2.2.3 Brønsted acid catalysis 21

3.2.2.4 Brønsted base catalysis 24

3.2.2.5 Phase transfer catalysis 24

3.2.2.6 Asymmetric Counteranion-Directed Catalysis 26

4 Domino reactions **28**

4.1 Asymmetric epoxidation with hydroperoxides 30

4.1.1 Jørgensen catalyst 31

Die approbierte gedruckte Originalversion dieser Dissertation ist an der TU Wien Bibliothek verfügbar.
The approved original version of this doctoral thesis is available in print at TU Wien Bibliothek.

4.1.2 Asymmetric Counteranion Directed Catalysis approach 32

4.2 Azridination of enones 34

5 Bibliography 35

6 Aim of the Thesis 42

7 Chiral Phosphoric Acids as Versatile Tools for Organocatalytic Asymmetric Transfer Hydrogenations 43

8 Counterion Enhanced Organocatalysis: A Novel Approach for the Asymmetric Transfer Hydrogenation of Enones 59

9 Sterically Demanding Flexible Phosphoric Acids for Constructing Efficient and Multi-Purpose Asymmetric Organocatalysts 68

10 Synthesis of Chiral Diazabicycloalkanes *via* Organocatalytic aza-Michael/Aldol Reaction... 80

11 Conclusion 88

Appendix A 91

Appendix B 174

Appendix C 341

Die approbierte gedruckte Originalversion dieser Dissertation ist an der TU Wien Bibliothek verfügbar.
The approved original version of this doctoral thesis is available in print at TU Wien Bibliothek.

Acknowledgement

First and foremost, I would like to express my heartfelt gratitude to my admired supervisor, Prof. Dr. Katharina Schröder. Her unwavering support and the invaluable opportunity she granted me to pursue my PhD thesis are truly appreciated. I am deeply grateful for the trust she placed in me to contribute my ideas to the group's research endeavors.

I would also like to extend my immense appreciation to Prof. Dr. Michael Schnürch, whose guidance and expertise in organic chemistry were instrumental throughout my PhD journey. His assistance with my projects and the wealth of knowledge he provided were crucial to my academic growth.

Furthermore, I wish to acknowledge and appreciate the contributions of all my former and current laboratory colleagues. Ádám Márk Palvölgyi deserves special recognition for his significant role during my journey, as he not only actively participated in nearly all my projects but also served as the go-to expert in organic synthesis, always available for valuable advice. He has also been a dear friend, and I am grateful for his support.

I would like to express my gratitude to my colleagues Kristóf Stágel and Philipp Miksovsky for their unwavering support and for fostering a relaxed and productive laboratory environment. Their fellowship and willingness to collaborate have been truly valuable.

Additionally, I extend my acknowledgments to Alina Lanaridi, Aitor Sainz Martinez, Lisa Eisele, Michael Weise and Blete Hulaj for their professionalism and for contributing to a welcoming and pleasant atmosphere in the lab on a daily basis.

Finally, I would like to share my immense appreciation to my entire family and friends for their unwavering support throughout all the challenges and triumphs of my PhD journey.

Your collective support and encouragement have played an indispensable role in shaping my academic journey, and for that, I am sincerely thankful.

Die approbierte gedruckte Originalversion dieser Dissertation ist an der TU Wien Bibliothek verfügbar.
The approved original version of this doctoral thesis is available in print at TU Wien Bibliothek.

Abstract

Over the past two decades, asymmetric catalysis has emerged as a valuable tool for constructing enantioenriched complex molecules. Within this field, organocatalysis occupies a distinctive role. Unlike traditional metal-complex catalysts, organocatalysis offers several advantages, expanding the realm of possibilities to include various substrates and introducing entirely different activation modes. This thesis is dedicated to a comprehensive exploration of endeavors in the domain of asymmetric organocatalysis and comprises the following parts:

- To introduce the application of phosphoric acids in organocatalysis, a detailed study of an essential reaction in this domain was conducted: The asymmetric transfer hydrogenation. Within this context, recent advancements in organocatalytic techniques employing chiral phosphoric acids for inducing chirality, as well as different hydrogen sources available for transfer hydrogenation were highlighted. This review showcases the diversity and evolution of phosphoric acid catalysts, along with various approaches to harness the potential of the counteranion-directed concept.
- The primary focus of the first experimental part of the thesis centers on the asymmetric transfer hydrogenation of cyclic enones by utilizing bulky counteranions. A comprehensive examination of all catalyst components led to the identification of a potent catalyst that yields astonishing results in terms of both yield and enantioselectivity across diverse cyclohexenone substrates.
- The concept of asymmetric counteranion enhanced catalysis previously introduced was further expanded to a diverse pool of domino reactions with broad applicability. This platform concept involves the creation of an even more potent catalyst comprising a chiral amine and an achiral phosphoric acid. It was demonstrated that bulky, achiral phosphoric acids are excellent candidates to increase stereoinduction in an ion-paired catalyst system, resulting in high yields and enantioselectivities across diverse reactions.
- The final part centers on the aza-Michael/aldol reaction which builds upon a concept related to a reaction previously described. It showcases the first direct organocatalytic synthesis of chiral diazabicycloalkanes via an iminium/enamine domino reaction with excessive screening of all reaction parameters.

Die approbierte gedruckte Originalversion dieser Dissertation ist an der TU Wien Bibliothek verfügbar.
The approved original version of this doctoral thesis is available in print at TU Wien Bibliothek.

Kurzfassung

In den letzten zwanzig Jahren hat sich die asymmetrische Katalyse als ein wertvolles Werkzeug für die Herstellung Enantiomer-angereicherter komplexer Moleküle etabliert. In diesem Bereich nimmt die Organokatalyse eine besondere Rolle ein. Im Gegensatz zu herkömmlichen Metallkomplexkatalysatoren bietet die Organokatalyse erhebliche Vorteile, erweitert die Möglichkeiten auf verschiedene Substrate und führt völlig neue Aktivierungsmechanismen ein. Diese Dissertation widmet sich einer umfassenden Untersuchung der Bestrebungen auf dem Gebiet der asymmetrischen Organokatalyse und besteht aus den folgenden Teilen:

- Um die Anwendung von Phosphorsäuren in der Organokatalyse einzuführen, wurde eine kurze Zusammenfassung über eine wichtige Reaktion in diesem Bereich durchgeführt: die asymmetrische Transferhydrierung. Im Rahmen dieser Analyse wurden die aktuellen Entwicklungen in der Organokatalyse hervorgehoben, die chiralen Phosphorsäuren zur Erzeugung von Chiralität sowie verschiedene verfügbare Wasserstoffquellen für die Transferhydrierung einsetzen. Diese Übersicht zeigt die Vielfalt und Evolution der Phosphorsäurekatalysatoren sowie verschiedene Ansätze zur Nutzung des Konzepts der Gegenionen-gesteuerten Katalyse.
- Der Schwerpunkt des ersten experimentellen Teils der Dissertation liegt auf der asymmetrischen Transferhydrierung von cyclischen Enonen unter Verwendung sperriger Gegenanionen. Eine umfassende Untersuchung aller Katalysatorkomponenten führte zur Identifizierung eines wirksamen Katalysators, der erstaunliche Ergebnisse hinsichtlich Ausbeute und Enantioselektivität bei verschiedenen Cyclohexenon-Substraten liefert.
- Das zuvor eingeführte Konzept der asymmetrischen Gegenanion-verstärkten Katalyse wurde weiter ausgebaut und auf eine breite Palette von Domino-Reaktionen mit weitreichender Anwendbarkeit erweitert. Bei diesem Plattformkonzept erfolgt die Schaffung eines noch leistungsfähigeren Katalysators, bestehend aus einem chiralen Amin- und einer achiralen Phosphorsäure. Es wurde nachgewiesen, dass sperrige, achirale Phosphorsäuren hervorragende Kandidaten sind, um die Stereoinduktion in einem ionengepaarten Katalysatorsystem zu erhöhen, was zu hohen Ausbeuten und Enantioselektivitäten in vielen Reaktionen führt.
- Der letzte Teil konzentriert sich auf die Aza-Michael/Aldol-Reaktion, die auf einem Konzept im Zusammenhang mit einer im vorherigen Teil eingeführten Reaktion beruht. Hier wird die erste direkte organokatalytische Synthese chiraler Diazabicycloalkane mittels einer Iminium/Enamin-Domino-Reaktion durch umfassendes Screening aller Reaktionsparameter vorgestellt.

Die approbierte gedruckte Originalversion dieser Dissertation ist an der TU Wien Bibliothek verfügbar.
The approved original version of this doctoral thesis is available in print at TU Wien Bibliothek.

List of Abbreviations

ACDC	Asymmetric Counteranion-Directed Catalysis
AcCl	Acetylchloride
AcOH	Acetic acid
ATH	Asymmetric transfer hydrogenation
BINAL-H	Binaphthol aluminium hydride
BINAP	2,2'-Bis(diphenylphosphino)-1,1'-binaphthyl
BINOL	1,1-Bi-2-naphthol
BPA	BINOL-derived chiral phosphoric acids
Bu_2O	Dibutylether
CPA	Chiral phosphoric acid
DACH	1,2-Diaminocyclohexane
DEAD	Diethyl azodicarboxylate
DFT	Density functional theory
DIOP	*O*-Isopropylidene-2,3-dihydroxy-1,4-bis(diphenylphosphino)butane
DKR	Dynamic kinetic resolution
DPEN	1,2-Diphenylethylendiamine
EE	Ethyl acetate
ee	Enantiomeric excess
EWG	Electron withdrawing group
HOMO	Highest occupied molecule orbital
IDPi	Chiral imidodiphosphorimidate catalysts
LDA	Lithium diisopropylamide
LUMO	Lowest unoccupied molecule orbital
NADH	Nicotinamide adenine dinucleotide
NFSI	N-Fluorobenzenesulfonimide
NTf	Triflic amide
NTPA	BINOL-derived chiral *N*-triflyl phosphoramides
PE	Petrolether
SET	Single electron transfer
SKA	Silyl ketene acetal
TADDOL	α,α,α',α'-Tetraaryl-2,2-disubstituted 1,3-dioxolane-4,5-dimethanol
TBHP	*Tert*-Butyl hydroperoxide
TMSCl	Trimethylsilyl chloride
TRIP	3,3'-Bis(2,4,6-triisopropylphenyl)-1,1'binaphthyl-2,2'-diyl hydrogenphosphate
TrocCl	2,2,2-Trichloroethyl carbonochloridate

Die approbierte gedruckte Originalversion dieser Dissertation ist an der TU Wien Bibliothek verfügbar.
The approved original version of this doctoral thesis is available in print at TU Wien Bibliothek.
TU Bibliothek Your knowledge hub WIEN

1 The phenomenon of chirality

Chiral molecules, which possess asymmetry in their spatial arrangement, play an important role in various aspects of human life. Prior to the development of asymmetric synthesis, nature had already demonstrated its ability to generate complex chiral molecules through enzymatic reactions. This inherent chirality is vital because chiral molecules that behave like mirror images, referred to as enantiomers, can interact differently with chiral receptors in the body (Figure 1).[1,2]

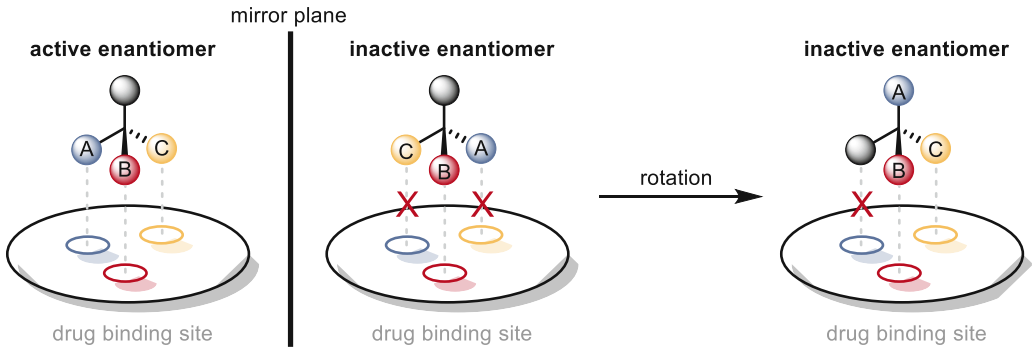


Figure 1. Easson-Stedman hypothetical interaction between the two enantiomers of a racemic drug with a receptor at the drug binding sites.[2]

These variations in interaction can lead to drastically different biological effects. For instance, one enantiomer might be therapeutically beneficial, while its mirror-image counterpart could be inert or even harmful.[3] Consequently, the isolation of specific enantiomers, or the resolution of racemic mixtures (where equal amounts of both enantiomers coexist), is of great importance in fields such as pharmaceuticals and agrochemicals. One traditional method for isolating enantiomers from racemic mixtures is splitting racemates. In kinetic resolution, one enantiomer undergoes a chemical transformation more rapidly than the other. This relies on a notable difference in the speed at which the diastereomeric transition state forms for each enantiomer. Ideally, the reaction is halted before reaching equilibrium, allowing the slower-reacting enantiomer to remain unreacted. Enzymes can perform this task exceptionally well due to their chiral recognition site.

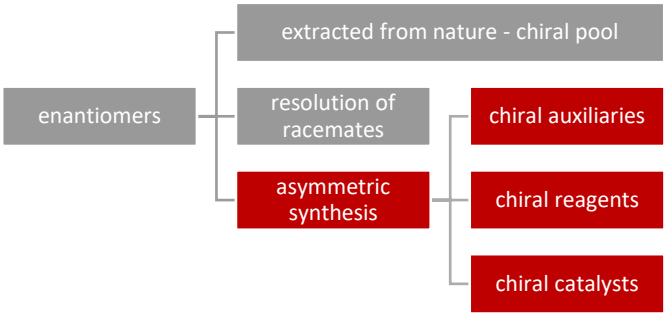


Figure 2. Essential methods to generate enantiomers.

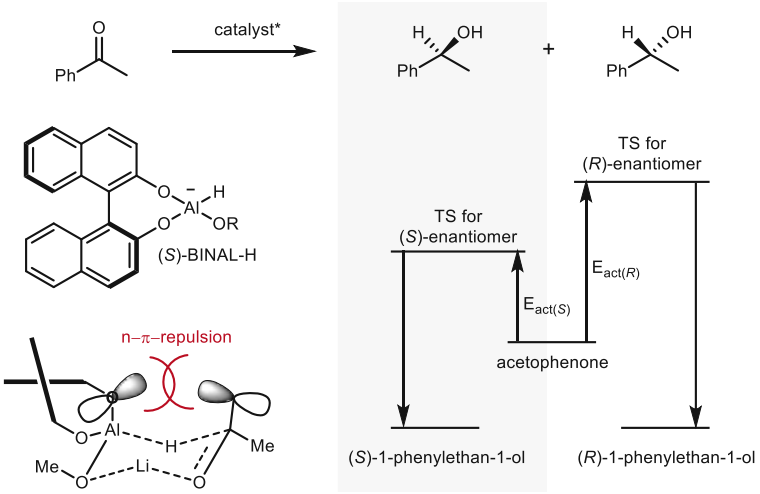
Die approbierte gedruckte Originalversion dieser Dissertation ist an der TU Wien Bibliothek verfügbar.
The approved original version of this doctoral thesis is available in print at TU Wien Bibliothek.
TU Bibliothek Your knowledge hub WIEN

However, this process typically results in yields of less than 50% of the theoretical maximum, making it inefficient.[4] A potential solution to this challenge lies in dynamic kinetic resolution (DKR). In DKR, the enantiomers within the crude mixture must possess the capacity to racemize, which can occur through processes like epimerization on their own or with the assistance of external reagents or catalysts. However, it is important to note that this process is rarely feasible, and in such cases, asymmetric synthesis is considered a valuable option.[1]

Die approbierte gedruckte Originalversion dieser Dissertation ist an der TU Wien Bibliothek verfügbar.
The approved original version of this doctoral thesis is available in print at TU Wien Bibliothek.

2 Asymmetric Synthesis

Asymmetric synthesis aims to create a chiral environment that selectively converts a prochiral starting material into a single enantiomer. This is achieved by introducing a chiral reagent, auxiliary, or catalyst into the reaction.[5] In order to generate an enantioenriched compound through this concept, the chiral compound interacts with the prochiral reactants, forming a diastereomeric transition state which involves lower energy of activation of one enantiomer over the other.[1] As an illustrative example, the asymmetric reduction of acetophenone in **Scheme 1** is demonstrated. In this scenario, a stoichiometric quantity of (*S*)-binaphthol aluminum hydride ((*S*)-BINAL-H) leads to the formation of a diastereomeric six-membered intermediate, where n-π-repulsion provides a certain conformation needed for enantiodiscrimination. Notably, the intermediate state of one enantiomer must possess lower activation energy ($E_{act(S)}$) compared to the transition state associated with the opposite enantiomer ($E_{act(R)}$) of the product. Consequently, this leads to the enrichment of the (*S*)-enantiomer in this particular case.[1,6]

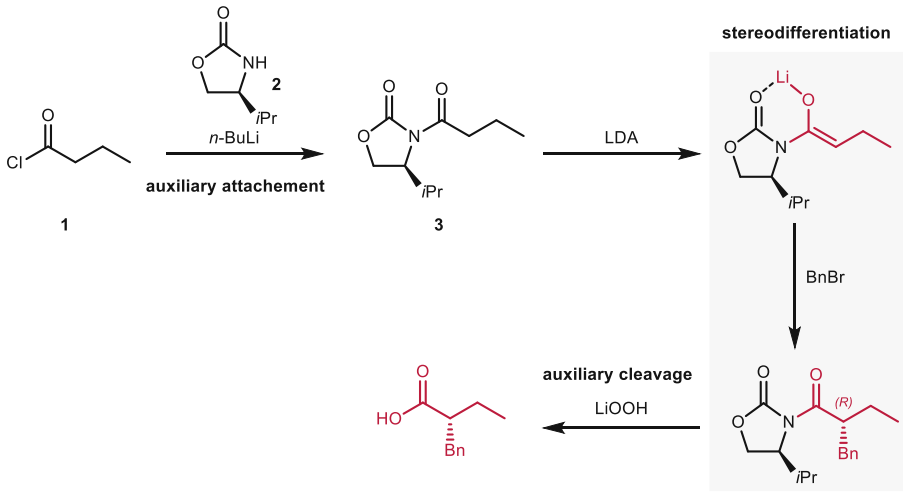


Scheme 1. Asymmetric reduction of acetophenone with (*S*)-BINAL-H.[1,6]

Although the method of employing chiral reagents can achieve a high level of enantiodiscrimination, it requires stoichiometric amounts of these reagents. A similar strategy is employed with chiral auxiliaries which are initially covalently attached to the substrate and enable the subsequent reaction in an enantioselective manner. In the context of the renowned Evans alkylation, the protocol is initiated with the synthesis of activated acid **1** (**Scheme 2**). Subsequently, chiral oxazolidinone **2** is introduced, leading to the formation of compound **3**. Asymmetric induction is achieved through the coordination of a lithium base (Lithium diisopropylamide, LDA) between the (*Z*)-enolate of the substrate and the oxazolidinone moiety. This coordination directs the alkylation to proceed selectively on the less sterically hindered face, concluding in the desired (*R*)-configuration of the product. In the final stage, the chiral auxiliary is cleaved via hydrolysis.[7] In summary, chiral reagents and auxiliaries are

Die approbierte gedruckte Originalversion dieser Dissertation ist an der TU Wien Bibliothek verfügbar.
The approved original version of this doctoral thesis is available in print at TU Wien Bibliothek.

potent tools in asymmetric synthesis, enabling high enantioselectivities of the target compound. Nonetheless, the requirement for stoichiometric quantities of chiral precursors renders this method costly and inefficient in terms of atom efficiency.



Scheme 2. Asymmetric alkylation enabled by Evans oxazolidinone.[7]

Die approbierte gedruckte Originalversion dieser Dissertation ist an der TU Wien Bibliothek verfügbar.
The approved original version of this doctoral thesis is available in print at TU Wien Bibliothek.

3 Asymmetric Catalysis

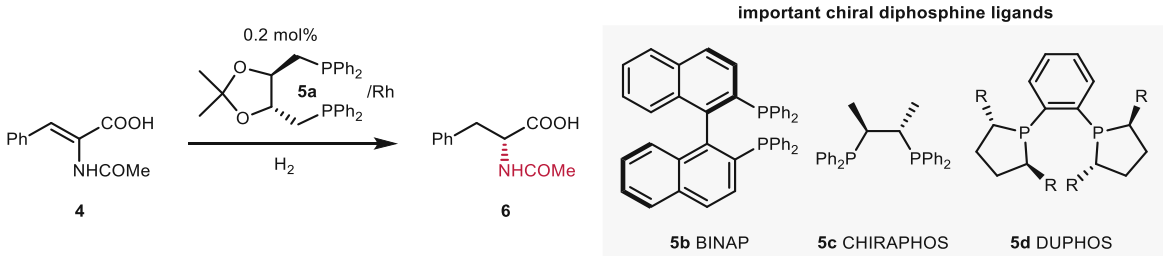
Asymmetric catalysis is a particularly attractive approach to asymmetric synthesis because it allows precise control of stereochemistry using only small amounts of a chiral catalyst. This approach simplifies product isolation and reduces the cost of the expensive chiral compound needed for stereoinduction.[8]

3.1 Transition metal catalysis

Within the realm of asymmetric catalysis, the well-established transition metal catalysis assumes an important role owing to its broad utility in diverse asymmetric transformations. Achieving both high reactivity and selectivity the outcome depends significantly on the choice of transition metal and the intricacies of ligand design, as briefly highlighted on the example of hydrogenation and epoxidation reactions.

3.1.1 Asymmetric hydrogenations

The process of asymmetric hydrogenations utilizing transition metal catalysts holds great importance in both academic research and industrial applications. Its attractiveness stems from its high efficiency, excellent atom economy and its ability to accommodate a broad range of substrates.[9] In this context, Horner[10] and Knowles[11] independently made a noteworthy discovery. They found that by employing the Wilkinson[12] catalyst $RhCl(PPh_3)_3$ and substituting the monodentate phosphine ligands with chiral counterparts, chirality could be induced in the diastereomeric transition state, resulting in a modest enrichment of one enantiomer over the other. In the 1970s, Kagan[13] et al. advanced this approach by utilizing a C_2-symmetric DIOP (*O*-Isopropylidene-2,3-dihydroxy-1,4-bis(diphenylphosphino)butane) ligand, achieving significantly higher ee values of up to 72%. Building upon this strategy, subsequent research unveiled a multitude of new chiral ligands, enabling exceptional enantioselectivity across diverse substrates (**Scheme 3**). In addition to rhodium, ruthenium can also serve as a viable option for such transformations expanding the scope to a variety of alkenes with high enantiodiscrimination.

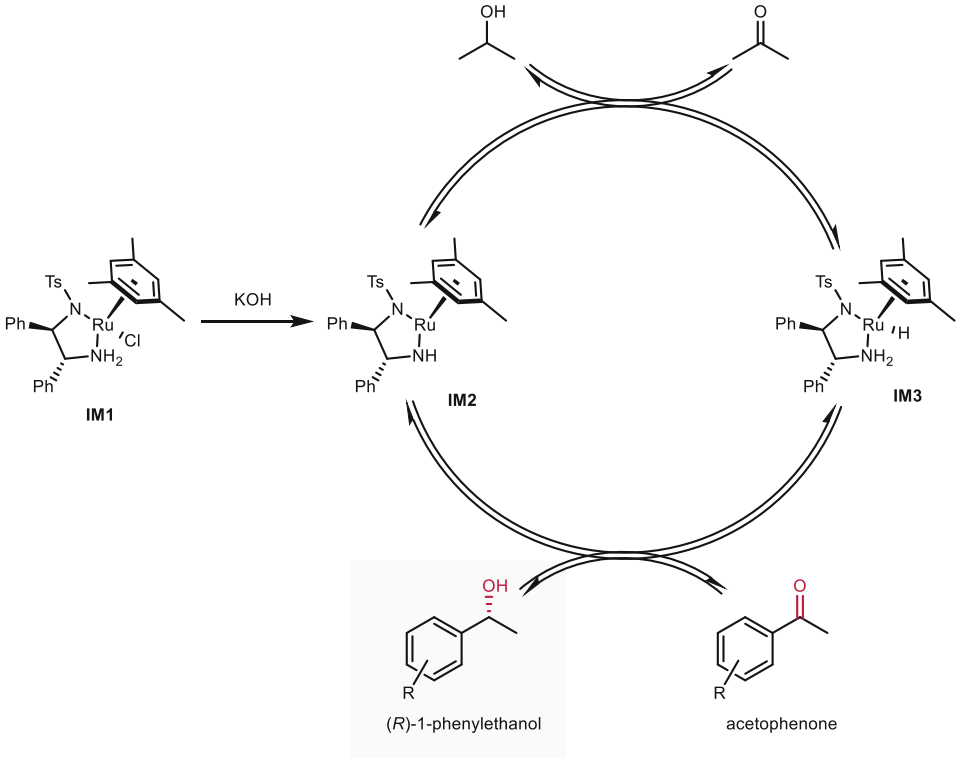


Scheme 3. Asymmetric hydrogenation with chiral diphosphine ligands.[8]

Die approbierte gedruckte Originalversion dieser Dissertation ist an der TU Wien Bibliothek verfügbar.
The approved original version of this doctoral thesis is available in print at TU Wien Bibliothek.

3.1.2 Asymmetric transfer hydrogenations

The asymmetric transfer hydrogenation (ATH) offers an alternative approach to the traditional use of hydrogen gas. The lack of gaseous hydrogen in the case of ATH eliminates the need for high-pressure reactors, resulting in reduced overall process costs and minimizing the risk of explosions. Typically, a donor alcohol, such as 2-propanol, serves as the hydride source. In the context of asymmetric transfer hydrogenation of ketones, it is crucial to recognize that utilizing alcohols as hydrogen donors can lead to diminished yields and enantioselectivity.[14] This is primarily attributed to the reversible character of the process and the unfavourable equilibrium between the ketone and the alcohol.



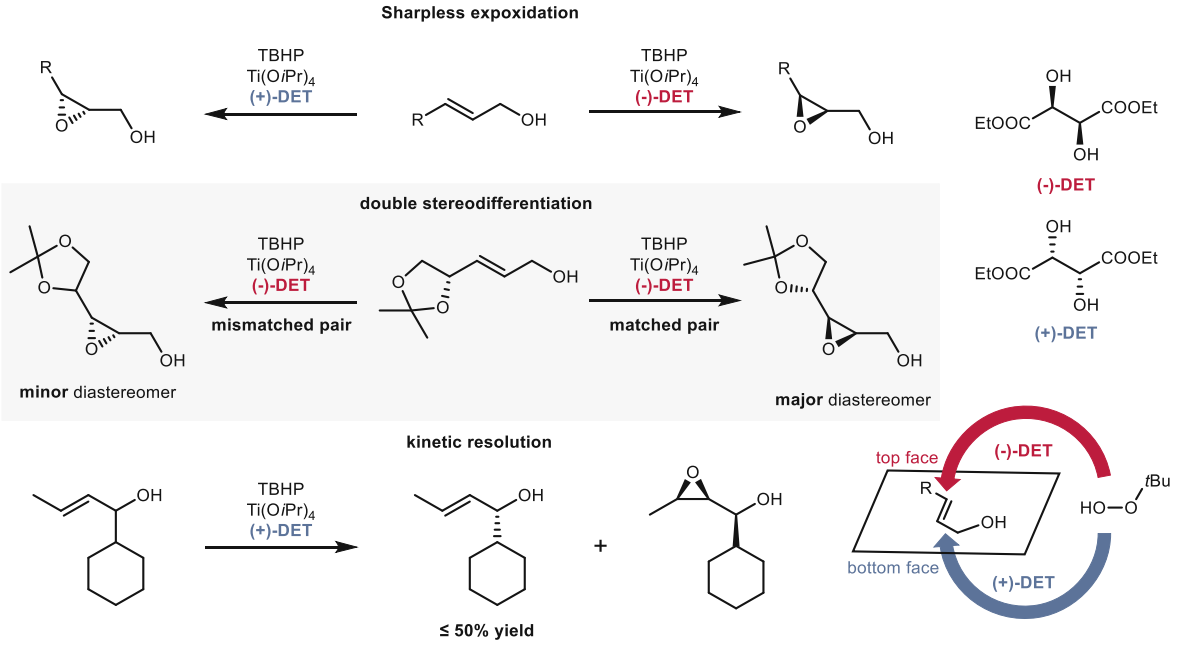
Scheme 4. Mechanism of the asymmetric transfer hydrogenation of enones.[15]

In the case of transfer hydrogenation with 2-propanol, it generally requires the presence of a relatively strong base and a significant excess of donor alcohol to proceed smoothly. When combined with triethylamine, formate can serve as an alternative hydrogen source, offering the potential for improved selectivity and yield. This improvement stems from the irreversible nature of the reaction.[8] Regarding the catalyst, Noyori et al. documented that a monotosylated ruthenium(II) complex exhibits exceptional enantioselectivity across a wide range of aryl/alkyl ketones in combination with a chiral diphenylethylendiamine (DPEN) ligand (**Scheme 4**).[16] The mechanism includes several steps, starting with the base-induced transformation into intermediate **IM2**. Transfer hydrogenation of acetone charges the complex, leading to the formation of the active species **IM3** and acetone as by-product. Subsequently, the diastereomeric transition state facilitates the conversion of the prochiral acetophenone into the desired enantiomer (**Scheme 4**).[15]

Die approbierte gedruckte Originalversion dieser Dissertation ist an der TU Wien Bibliothek verfügbar.
The approved original version of this doctoral thesis is available in print at TU Wien Bibliothek.
TU Bibliothek Your knowledge hub WIEN

3.1.3 Asymmetric epoxidations

An early example in this area can be found in the pioneering efforts of Sharpless et al., who developed a ground-breaking protocol for the asymmetric epoxidation.[17] Here, an allylic alcohol undergoes epoxidation using *tert*-butyl hydroperoxide as oxidant and a titanium complex featuring either (-) or (+)-diethyl tartrate as the chiral ligand. This approach is versatile, allowing for the synthesis of highly substituted epoxides featuring tertiary and quaternary stereocenters. Furthermore, it is applicable to a wide range of functional groups, including alcohols, ethers, amines and various alkenyl and alkynyl moieties. It is important to highlight that only the double bond within the allylic alcohol moiety undergoes epoxidation due to the necessity of substrate-metal coordination.[8]



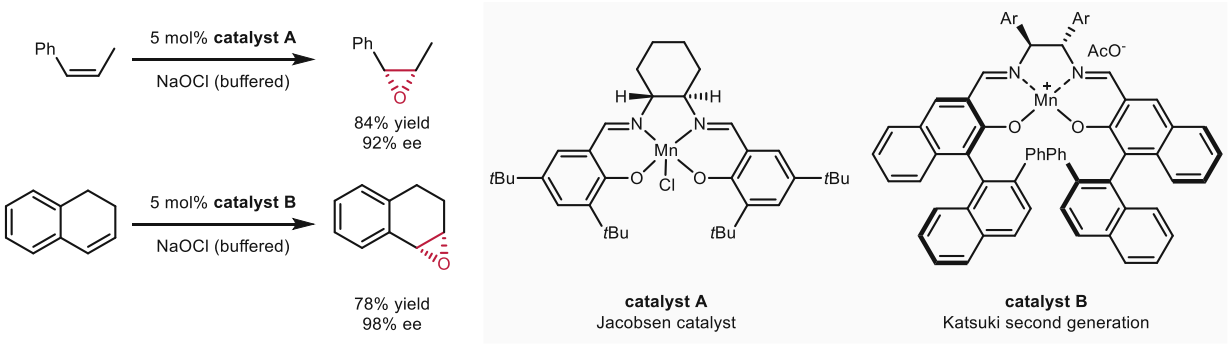
Scheme 5. Sharpless epoxidation.[1,8]

Depending on the ligand enantiomer, the peroxide can either attack from the top or bottom face, resulting in an enantioenriched product. In addition to its utility in ligand-controlled epoxidation of prochiral allylic alcohols, the Sharpless epoxidation also serves as a valuable method for accomplishing dual stereo discrimination. For instance, when a chiral allylic alcohol is placed within a chiral environment created by (-)-DET, it leads to a matched pair scenario. Here, through substrate and catalyst control, the desired diastereomer is generated in a significantly higher amount compared to the mismatched stereoisomer (**Scheme 5**, middle). This strategy can also be applied in the kinetic resolution of chiral allylic alcohols. In this process, double stereodifferentiation occurs through the formation of a diastereomeric complex, leading to the transformation of the matched chiral pair.[18]

Another pioneering method involves the asymmetric epoxidation of alkenes using manganese-salen complexes. In 1990, Jacobsen[19] and Katsuki[20] independently reported the utilization of C_2-symmetric ligands with an ethylenediamine structure and Mn(III) cores. In this approach, a manganese-salen

Die approbierte gedruckte Originalversion dieser Dissertation ist an der TU Wien Bibliothek verfügbar.
The approved original version of this doctoral thesis is available in print at TU Wien Bibliothek.
TU Bibliothek Your knowledge hub WIEN

complex is employed as chiral catalyst, which is converted into its active oxo-Mn(V) form through the use of a stoichiometric amount of oxidant. This concept delivers outstanding performance for unfunctionalized alkenes. Numerous ligands with diverse aromatic substituents and ethylenediamine moieties have been synthesized and evaluated, yet only a handful have demonstrated superior performance compared to Jacobsen's catalyst (**Scheme 6**).[8] It is important to note that these catalysts are not applicable to all types of alkenes, and the most favourable outcomes have been observed when employing alkenes in (*Z*)-configuration.



Scheme 6. Manganese-salen complex.[19,21]

Die approbierte gedruckte Originalversion dieser Dissertation ist an der TU Wien Bibliothek verfügbar.
The approved original version of this doctoral thesis is available in print at TU Wien Bibliothek.

3.2 Organocatalysis

Over the past decades, organocatalysis has emerged as the third pillar of asymmetric catalysis, alongside transition metal and biocatalysis. Organocatalysis employs small organic molecules rather than enzymes or transition metals as catalysts to enable various types of asymmetric transformations. In concept they are designed to mimic or harness the catalytic abilities of enzymes found in biological systems but are significantly smaller and less structural complex. This nature-inspired approach has been influential in the development of organocatalysis and has led to the design of novel catalysts for various chemical reactions.[22]

Organocatalysts offer numerous advantages: They are typically robust, cost-effective, readily accessible and non-toxic. Their resistance to moisture and oxygen makes them suitable for a wide range of reactions, often eliminating the need for inert atmosphere and water exclusion. Additionally, because they do not contain metals, organocatalytic methods are particularly appealing in the pharmaceutical industry where slight metal impurities can be fatal.[22] There are a multitude of activation modes to choose from, encompassing a wide range of interactions. These include non-covalent interactions like hydrogen bonding, electrostatic ion pairs, and halogen bonding, as well as covalent interactions and possible combinations of multiple activation modes within one reaction. Each of these modes has its own subcategories with distinct reaction and catalyst types. To catalytically activate a molecule, specific functional groups on both substrate and catalyst are required. The necessity of these functional groups varies depending on the activation mode of the catalyst.[23]

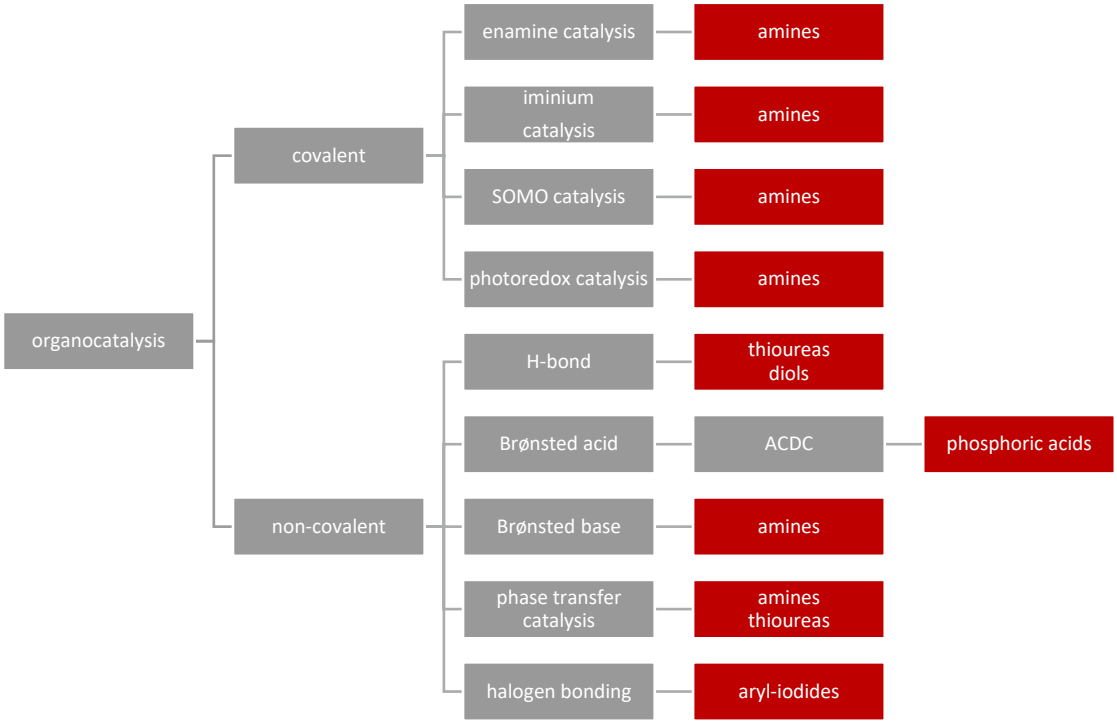


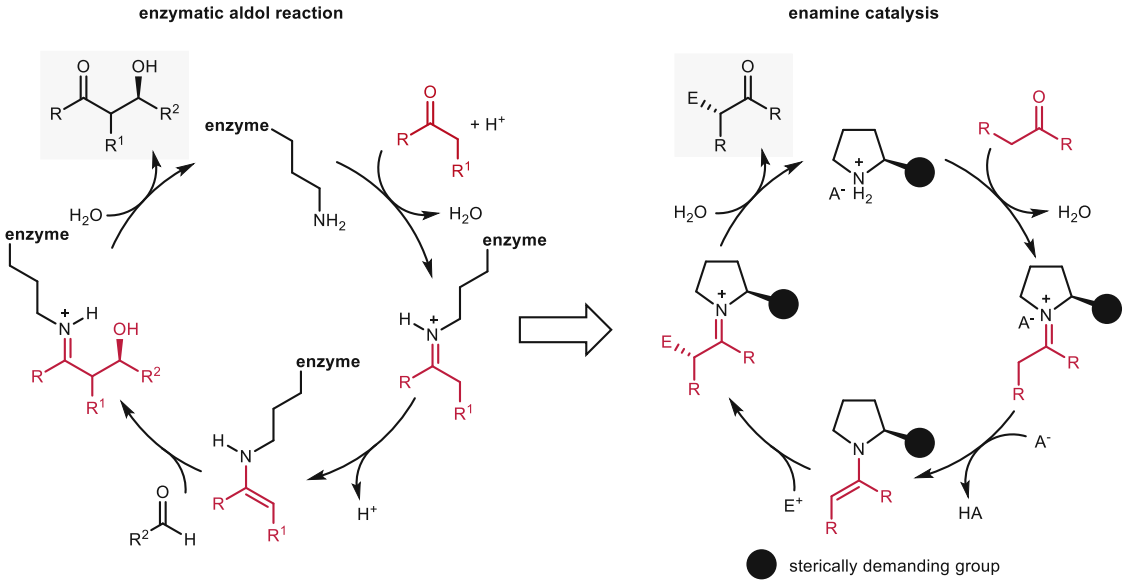
Figure 3. Organocatalytic activation modes. Red = organic compound used as catalysts.

Die approbierte gedruckte Originalversion dieser Dissertation ist an der TU Wien Bibliothek verfügbar.
The approved original version of this doctoral thesis is available in print at TU Wien Bibliothek.

3.2.1 Covalent activation

3.2.1.1 Enamine catalysis

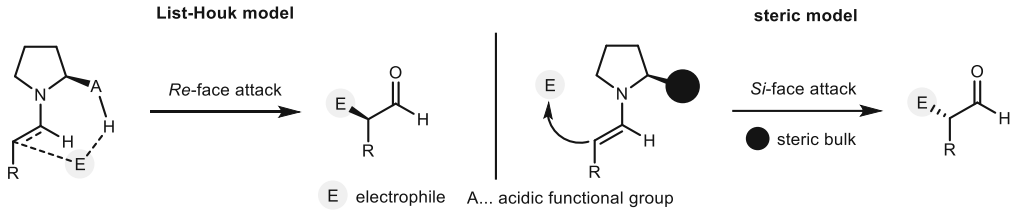
Enamine catalysis has established itself as one of the prominent and widely applied modes of activation in the field of organocatalysis.[24] In this process, a chiral amine is employed as an organocatalyst to convert an aldehyde or ketone into an enamine. This transformation significantly elevates the Highest Occupied Molecular Orbital (HOMO), thereby enhancing its nucleophilic properties. As mentioned in Chapter 3.2, the fundamental idea is drawn from nature, where specific amino acids within the peptide moiety in enzymes or antibodies covalently attach to carbonyl-bearing compounds to create an enamine transition state (**Scheme 7**, left side). In the case of an enzymatic aldol reaction, this process involves the electrophilic carbonyl group of the substrate being targeted by the amine moiety of the enzyme, resulting in enamine formation and subsequent nucleophilic attack on the electrophilic aldehyde to form the corresponding aldol product. Within the detailed mechanism of the organocatalytic pathway, the initial step entails an acid-catalyzed condensation between the carbonyl compound and the amine, yielding an iminium ion (**Scheme 7**, right side). Subsequently, one of the α-acidic protons in the iminium ion is abstracted by the conjugate base of the acid, leading to the nucleophilic enamine intermediate. This intermediate then reacts with an electrophile, providing the desired enantioenriched compound due to catalyst-substrate-reagent interactions. Hydrolysis of the iminium results in the liberation of the final product, along with the regeneration of the catalyst. The co-catalyst, which is a Brønsted acid, can be a protic solvent, an external acid, or a functional group present on the catalyst.[24]



Scheme 7. Biomimetic concept of enamine catalysis.[23,24]

Die approbierte gedruckte Originalversion dieser Dissertation ist an der TU Wien Bibliothek verfügbar.
The approved original version of this doctoral thesis is available in print at TU Wien Bibliothek.

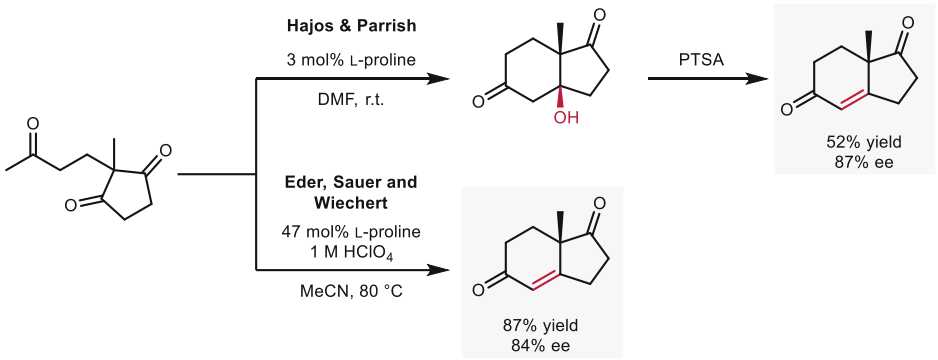
Various transition state models have been devised to anticipate the resulting stereochemistry. In the List-Houk model, for instance, proline, featuring a hydrogen-bond directing group, can create a 6-membered chair-like transition state known as the Zimmermann-Traxler model (**Scheme 8**).[25] This transition state both activates and guides the electrophile resulting in a *Re*-face attack. When a hydrogen-bond directing group is absent and a sterically bulky substituent is present, the outcome is reversed, as the attack occurs from the less hindered *Si*-face.[23]



Scheme 8. Transition state models for electrophilic attack.[23]

Seebach and colleagues explored an alternate mechanism involving proline. Given proline's restricted solubility in various organic solvents, there appears to be a strong driving force to form a soluble oxazolidinone from proline and the substrate which can inverse the enantiomeric outcome compared to List-Houk´s model.[26]

The aldol reaction is a vital tool for carbon-carbon bond formation in enamine catalysis, enabling the synthesis of bioactive compounds and natural products.[27] A pioneering contribution was conducted by Hajos and Parrish, in conjunction with Eder, Sauer, and Wiechert, employing L-proline as an organocatalyst for an intramolecular aldol cyclization. This innovative method facilitated the synthesis of the desired carbocycles with good yields and moderate enantioselectivity (**Scheme 9**).[28,29]



Scheme 9. The Hajos-Parrish-Eder-Sauer-Wiechert Reaction.[28,29]

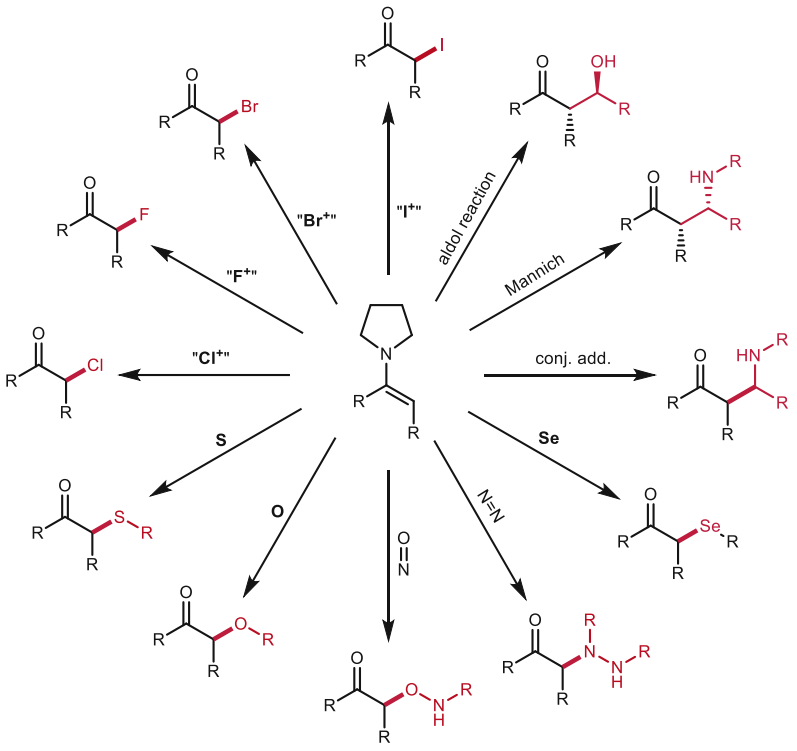
In 2000, List revived the concept of organocatalytic aldol reactions by performing an intermolecular aldol reaction between aromatic or aliphatic aldehydes and acetone, using L-proline as the catalyst (**Scheme 10**). Their efforts yielded remarkable results, with high yields and enantioselectivities achieved, particularly in scenarios involving sterically demanding aliphatic groups on the aldehyde moiety.[30]

Die approbierte gedruckte Originalversion dieser Dissertation ist an der TU Wien Bibliothek verfügbar.
The approved original version of this doctoral thesis is available in print at TU Wien Bibliothek.
TU Bibliothek Your knowledge hub WIEN



Scheme 10. Intermolecular aldol reaction.[30]

List emphasized once more the significance of proline in the field of organocatalysis due to its qualities of being non-toxic, cost-effective, and abundantly available in both enantiomeric forms. Furthermore, this reaction can be effortlessly conducted at room temperature, without the requirement for inert conditions or moisture exclusion. Additionally, any remaining traces of the catalyst can be easily removed through a straightforward extraction process.[30] As of the present day, newly developed organocatalysts continue to draw inspiration from the proline molecule, often showcasing analogous structural elements or being derived from proline itself. Over the years, chemists have developed many different approaches to enamine catalysis using a variety of chiral amines as catalysts for a wide range of reactions involving various electrophilic reagents (**Scheme 11**).[31,32]

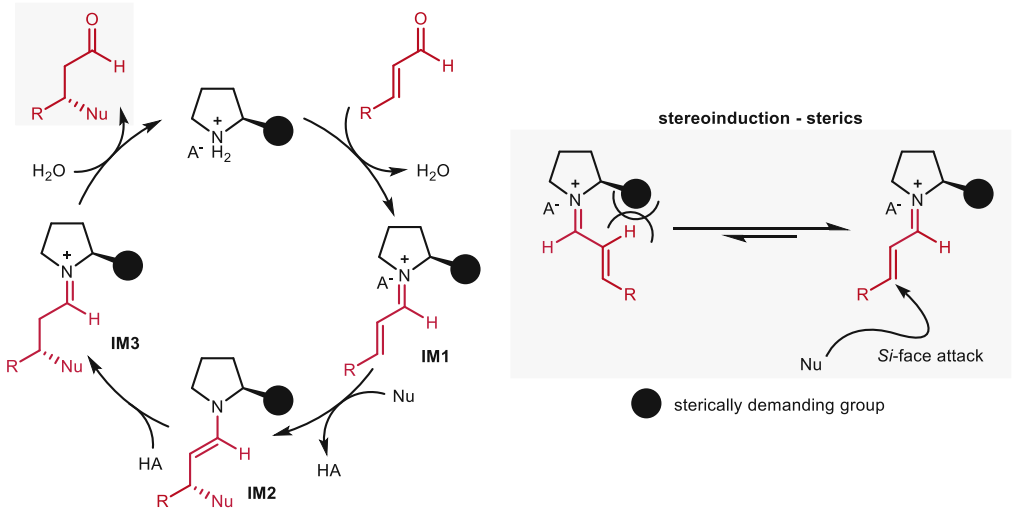


Scheme 11. Possible transformations in enamine catalysis.[32]

Die approbierte gedruckte Originalversion dieser Dissertation ist an der TU Wien Bibliothek verfügbar.
The approved original version of this doctoral thesis is available in print at TU Wien Bibliothek.

3.2.1.2 Iminium catalysis

Iminium catalysis represents another dominant activation mode within the field of organocatalysis. It exhibits parallels with enamine catalysis, even allowing for the use of similar catalysts. The primary distinction lies in the intermediate formed, which, in the case of iminium catalysis, involves a LUMO-lowered species, as opposed to the HOMO-raising intermediate characteristic of enamine catalysis. From a mechanistic standpoint it starts with the covalent formation of the charged iminium species (**Scheme 12**, **IM1**).



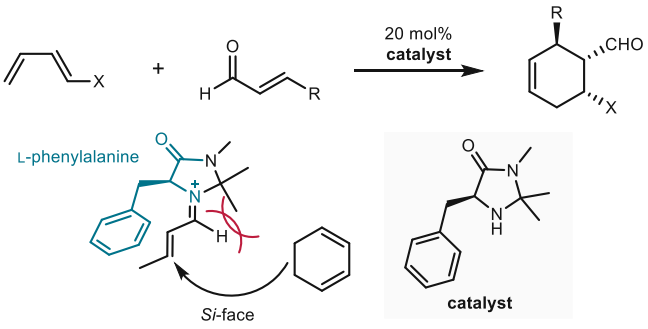
Scheme 12. Concept of iminium activation and stereoinduction.[23]

Subsequently, due to steric effects and potential hydrogen bonding interactions, the more stable (*E*)-imine species is formed. This (*E*)-imine then becomes the target for nucleophilic attack from the sterically accessible face, resulting in the formation of **IM2**. Following the shift in equilibrium from the enamine back to the iminium state, hydrolysis yields the enantioenriched product.

Although iminium catalysis with organic molecules as catalysts has a history dating back to the early 1900s,[33] the first instance of its asymmetric application was unveiled by MacMillan and his colleagues in 2000. They developed a new protocol for Diels-Alder reactions using a sterically bulky, chiral secondary amine as a catalyst.[34] While proline is regarded as a privileged catalyst, it's important to note that not every stereoinduction relies on H-bonding and a chair-like transition state, as illustrated in Chapter 3.2.1.1. Secondary amines with sterically demanding substituents next to the amino-functionality are not naturally occurring and require synthesis and structural optimization. However, MacMillan and his colleagues introduced an innovative concept by synthesizing and employing chiral imidazolidinones as catalysts.[34] The imidazolidinone can be readily prepared using natural derived L-phenylalanine, requiring only a few reaction steps. The stereoinduction through steric repulsion described in Chapter 3.2.1.2. is also applicable in this case, yielding the corresponding (*E*)-imine intermediate (**Scheme 13**). Furthermore, the L-phenylalanine motif can serve as a steric barrier to

Die approbierte gedruckte Originalversion dieser Dissertation ist an der TU Wien Bibliothek verfügbar.
The approved original version of this doctoral thesis is available in print at TU Wien Bibliothek.

hinder the approach of the incoming nucleophile from the *Re*-face. In cases where the substrate includes aromatic groups, it can also engage in π-stacking interactions to exert additional influence on the transition state's structure.[34]



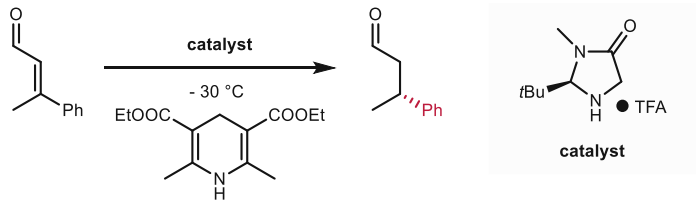
Scheme 13. MacMillan´s imidazolidinone catalyst and demonstration of Diels-Alder reaction.[34]

When considering the acid cocatalyst, it is essential to recognize its potential to impact reactivity and conformation of the transition state, thus affecting the enantiomeric outcome. As detailed in Chapter 3.2.1.1, the Brønsted acid cocatalyst can be present either within the catalyst moiety or an external acid. The acidity of this cocatalyst is closely linked to the basicity of the chiral amine. For instance, imidazolidinone (**catalyst A**, **Scheme 13**) exhibits weak basicity (pK_a= 11.83) in comparison to pyrrolidine (pK_a = 19.89) and, therefore, requires a stronger acid cocatalyst such as trifluoroacetic acid or perchloric acid to function effectively.[35] This relationship is important for catalyst development because one must consider that some acids may not be usable in combination with the desired chiral amine.

3.2.1.2.1 Asymmetric transfer hydrogenation

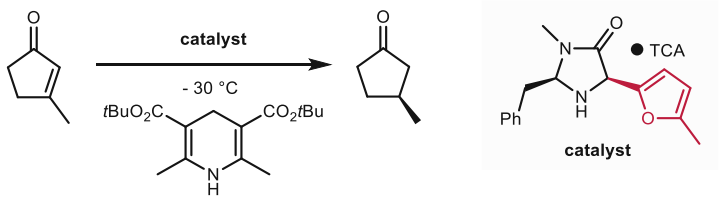
In this biomimetic approach, the hydrogen source for the reduction is a simple Hantzsch ester, resembling biological NADH, instead of hydrogen gas.[36] There are several advantages to this approach: Gaseous hydrogen is challenging to manage and poses safety risks. In contrast, a Hantzsch ester is commercially available, cheap, readily accessible and bench stable.[37] The driving force revolves around delivering a hydride and a proton to the unsaturated, activated functional group of the enal, oxidizing the Hantzsch dihydropyridine into the fully saturated more stable pyridine. Fine-tuning of the substituents on the Hantzsch dihydropyridine can further alter the stereoinduction or reactivity of the catalytic process. In this realm MacMillan and coworkers employed a chiral imidazolidinone catalyst that featured a sterically demanding group positioned directly next to the amine binding site, as detailed in Chapter 3.2.1.2, **Scheme 13**. By lowering the reaction temperature even further, they were able to attain outstanding enantioselectivities along with excellent yields when working with various enals.[38]

Die approbierte gedruckte Originalversion dieser Dissertation ist an der TU Wien Bibliothek verfügbar.
The approved original version of this doctoral thesis is available in print at TU Wien Bibliothek.



Scheme 14. Asymmetric transfer hydrogenation of enals with chiral imidazolidinones.[38]

In order to conduct the same reaction with less reactive enones, modifications to the catalyst structures were necessary to ensure high performance. MacMillan discovered that introducing a furyl substituent was advantageous for improving enantioselectivity without compromising yield in the organocatalytic reaction, two years prior to the development of transfer hydrogenation (**Scheme 15**).[39] In this context, the catalyst also demonstrated exceptional performance, outperforming all other chiral imidazolidinones lacking the furyl moiety.[40]

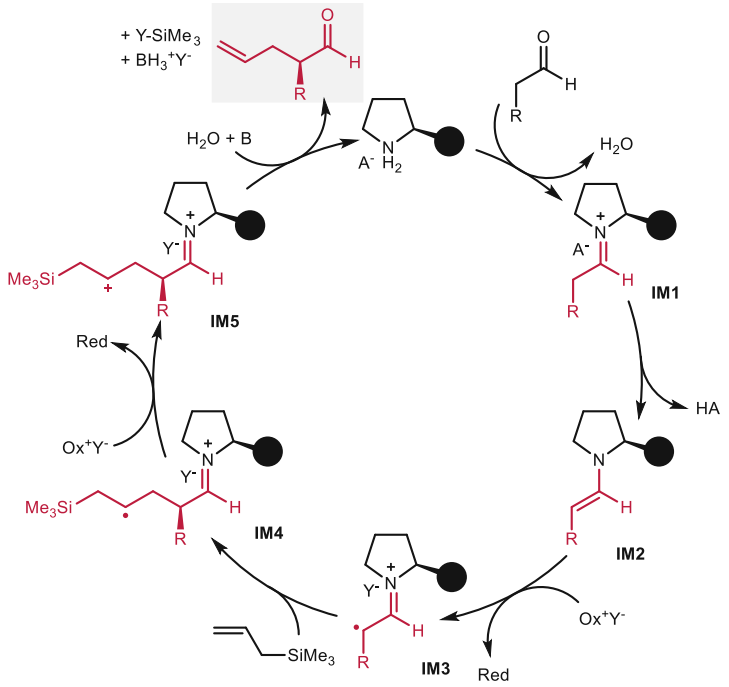


Scheme 15. Asymmetric transfer hydrogenation of enones with modified imidazolidinone catalyst.[40]

3.2.1.3 Singly Occupied Molecular Orbital catalysis

Organo-SOMO catalysis represents another significant cornerstone within organocatalysis, providing an alternative pathway for the α-functionalization of carbonyl compounds through a radical mechanism. The concept relies on generating a radical cation from an enamine species through the utilization of an appropriate oxidant, which facilitates a single electron transfer. In 2007, MacMillan and his colleagues introduced a novel strategy for the α-vinylation of aldehydes.[41] Once again, they employed their imidazolidinone catalyst to convert an aldehyde into the corresponding enamine. Utilizing a mild oxidant such as cerium(IV) (**Scheme 16**, $Ox^{+}Y^{-}$), the enamine can be transformed into an iminium radical cation **IM3**. This transformation is highly selective since the ionization potential of the enamine is lower compared to the initial aldehyde or catalyst. The resulting cationic radical can then engage with a suitable radicophile, such as allyl silane, forming a new cationic radical intermediate **IM4**. A second equivalent of oxidant is required to further oxidize this intermediate, which, following subsequent hydrolysis, yields the desired target molecule.[23]

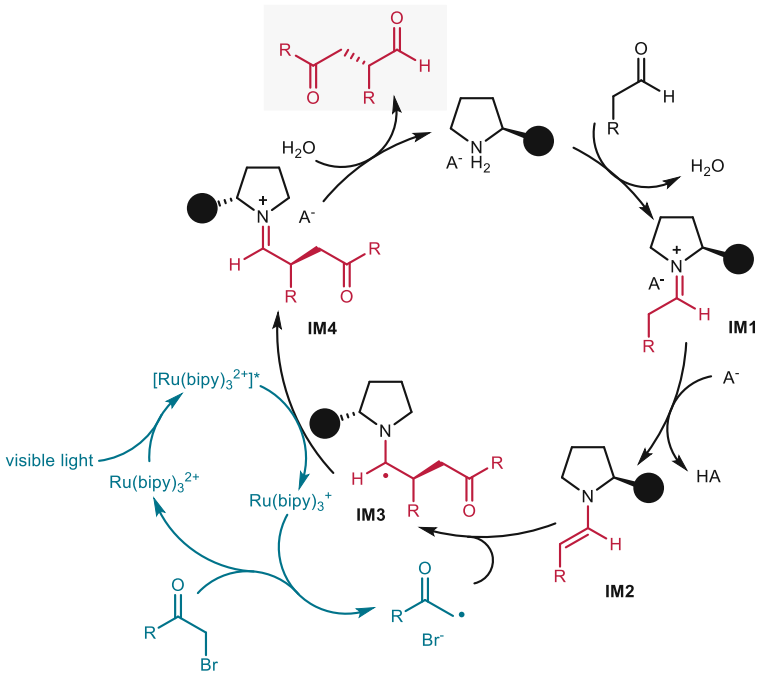
Die approbierte gedruckte Originalversion dieser Dissertation ist an der TU Wien Bibliothek verfügbar.
The approved original version of this doctoral thesis is available in print at TU Wien Bibliothek.



Scheme 16. Mechanism of SOMO catalysis.[23]

3.2.1.4 Photoredox catalysis

In recent years, the combination of photo- with organocatalysis has emerged as a potent technique for synthesizing molecules that are otherwise unattainable. Furthermore, photocatalysis offers additional advantages such as gentle reaction conditions and the flexibility to vary the light source in regards to the energy input, thus offering multiple possibilities in this domain.[42]



Scheme 17. General mechanism of photoredox organocatalysis.[23,43]

Die approbierte gedruckte Originalversion dieser Dissertation ist an der TU Wien Bibliothek verfügbar.
The approved original version of this doctoral thesis is available in print at TU Wien Bibliothek.

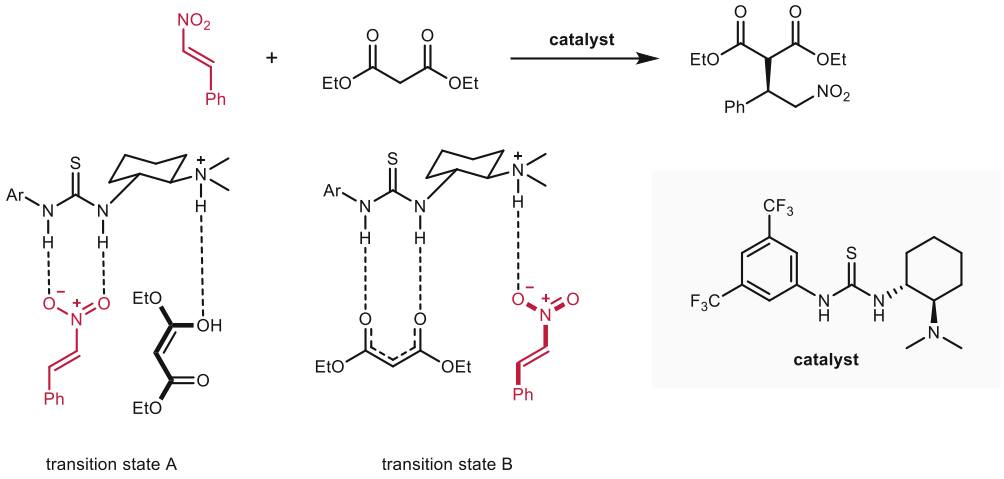
The fundamental concept revolves around the capability of a photoredox catalyst to absorb light, leading to its transformation into an excited state. This kinetically stable species can then engage in redox reactions. A prominent illustration of this concept is the stereoselective α-alkylation of aldehydes (**Scheme 17**). In this process, the initial cycle commences with the formation of the enamine **IM2**, which has been previously described in Chapter 3.2.1.1. However, the crucial step revolves around the photochemical generation of the $Ru(bipy)_3^+$ species, a potent reductant. This species partakes in a single electron transfer (SET) with an α-bromocarbonyl compound, resulting in the formation of a bromide anion and an α-acyl radical. Subsequently, the acyl radical reacts with the enamine, yielding the α-nitrogenated radical **IM3**. This radical undergoes another SET reaction, this time with the photoexcited $Ru(bipy)_3^{2+}$ and an oxidant, leading to the generation of an iminium cation **IM4** while regenerating the $Ru(bipy)_3^+$ species in the process.[23,43]

Die approbierte gedruckte Originalversion dieser Dissertation ist an der TU Wien Bibliothek verfügbar.
The approved original version of this doctoral thesis is available in print at TU Wien Bibliothek.

3.2.2 Non-covalent activation modes

3.2.2.1 Hydrogen-bond activation

In addition to covalent activation of ketones and aldehydes, non-covalent interactions can significantly broaden the range of substrate classes within organocatalysis. The primary interaction in this context is based on hydrogen bond activation, facilitated by a hydrogen bond donor catalyst. Thioureas stand out as the most prevalent H-donor in this regard, offering a high level of reactivity and selectivity, in combination with a straightforward synthesis which often involves commercially available isocyanates as starting materials.[44] An early example involved the Michael addition of 1,3-dicarbonyl compounds to electrophilic nitrostyrene.[45]

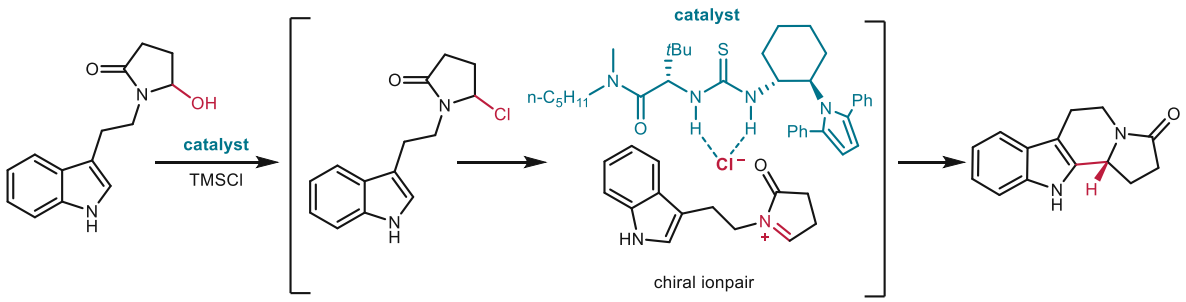


Scheme 18. Activation mode of thiourea-catalyzed Michael addition.[45]

In this regard, the main reaction steps involve reducing the LUMO of the α,β-unsaturated nitro styrene and facilitating enolization of the dicarbonyl reagent through hydrogen bonding. There are two possible transition states for activating both of these function groups. In theory, the urea group on the catalyst has the potential to activate either the electrophile or the nucleophile via hydrogen bonding, as illustrated in **Scheme 18**. In the context of the reaction mentioned above, the group of Pápai conducted DFT calculations and determined that transition state B prevails as the primary pathway due to its lower activation energy barrier.[45]

Apart from the conventional activation methods in organocatalysis, thiourea catalysts possess the ability to extract α-halogens through hydrogen bonding, thereby converting the initially unreactive substrate into an activated iminium state where ion-pairing with the chiral catalyst provides stereioinduction.[40]

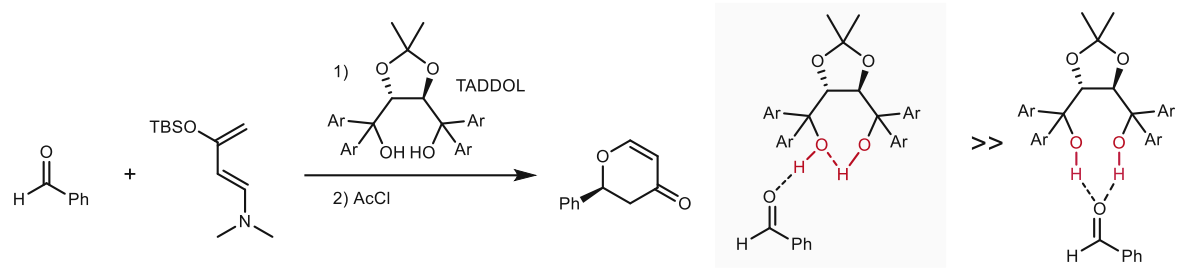
Die approbierte gedruckte Originalversion dieser Dissertation ist an der TU Wien Bibliothek verfügbar.
The approved original version of this doctoral thesis is available in print at TU Wien Bibliothek.



Scheme 19. Pictet-Spengler reaction mechanism.[44,46]

An important early example of this concept was demonstrated within the research group of Jacobsen, focusing on the development of an asymmetric Pictet-Spengler-type cyclization. The mechanism initiates with the conversion of a hydroxy group into a chloride utilizing TMSCl. Subsequently, the urea catalyst facilitates the abstraction of the chloride ion, forming a chiral iminium ion pair. The electron-rich indole then attacks the electrophilic iminium from the sterically unhindered face to give the cyclized product in high enantiodiscrimination (**Scheme 19**).[46]

Diols can also serve as catalysts for hydrogen bonding activation, with the chiral diol TADDOL being a prominent example. TADDOL can be synthesized from tartaric acid, which is available in both enantiomeric forms and is considered a cheap chiral precursor.[47] An early instance of the application of TADDOL in organocatalysis was conducted by Rawal's research group, involving an enantioselective hetero Diels-Alder reaction between benzaldehyde and a diene (**Scheme 20**). It's important to note that, unlike thioureas, which engage in double hydrogen bonding, TADDOL forms a single hydrogen bond for electrophilic activation. This is due to the presence of an intramolecular hydrogen bond in TADDOL, which increases the acidity of the second hydroxyl group and therefore, increasing the H-bond capability.[48]

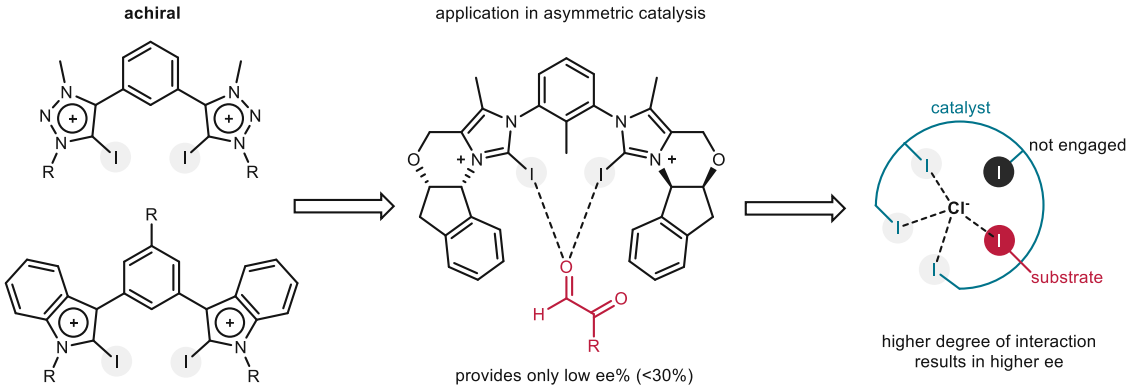


Scheme 20. Hetero Diels-Alder reaction with TADDOL.[48]

Die approbierte gedruckte Originalversion dieser Dissertation ist an der TU Wien Bibliothek verfügbar.
The approved original version of this doctoral thesis is available in print at TU Wien Bibliothek.

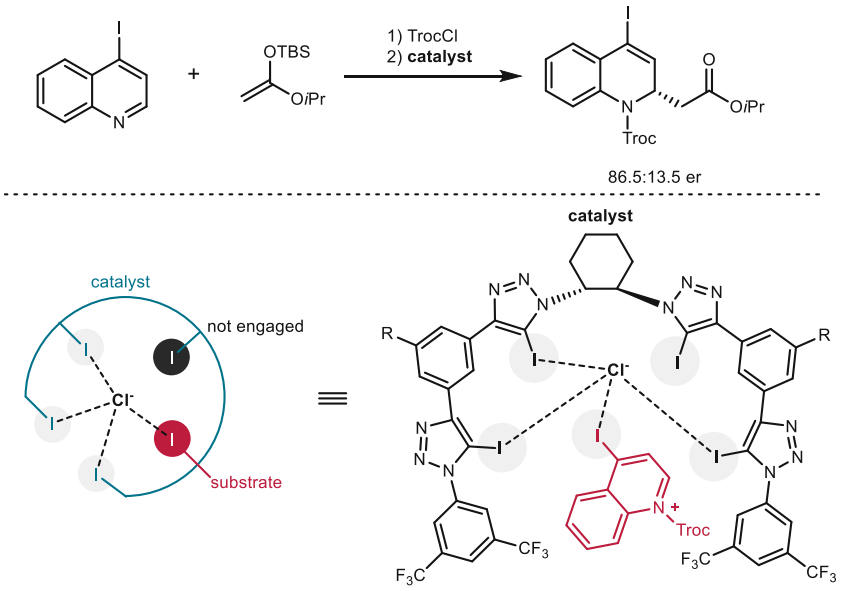
3.2.2.2 Halogen bonding

In the realm of organocatalysis, another emerging non-covalent interaction that gained a lot of attention in recent years is halogen bonding.[49] The foundation of this concept lies in the recognition that, adjacent to a ring with heightened electron density orthogonal to an R-X bond, there exists a region of electron depletion known as the σ-hole. Halogens exhibit a σ-hole interaction wherein the Lewis acidity of these sites increases in correspondence with the size of the interacting halogen (I > Br > Cl > F). Given the relative novelty of this concept, the development of highly enantioselective catalysts remains an ongoing endeavor.[50]



Scheme 21. Example of catalysts exhibiting σ-hole interactions.[50,51]

Initially, achiral halogen bond catalysts were devised with the inclusion of two iodine substituents to facilitate σ-hole interactions. However, when applying this concept in a chiral context, the enantiomeric outcome was less than satisfactory.



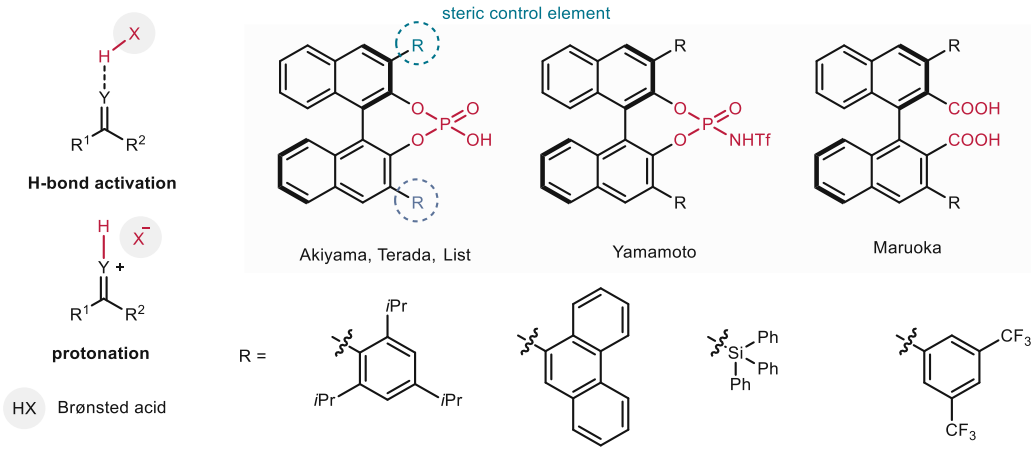
Scheme 22. Example of asymmetric reaction catalyzed by chiral tetraiodo catalyst.[51]

Die approbierte gedruckte Originalversion dieser Dissertation ist an der TU Wien Bibliothek verfügbar.
The approved original version of this doctoral thesis is available in print at TU Wien Bibliothek.

Subsequently, it was discovered by the group of Mancheño in 2023 that increasing the number of σ-hole interactions led to a significant enhancement in enantioselectivity. This can be achieved by increasing the number of halogens within substrate and catalyst (**Scheme 22**).[51]

3.2.2.3 Brønsted acid catalysis

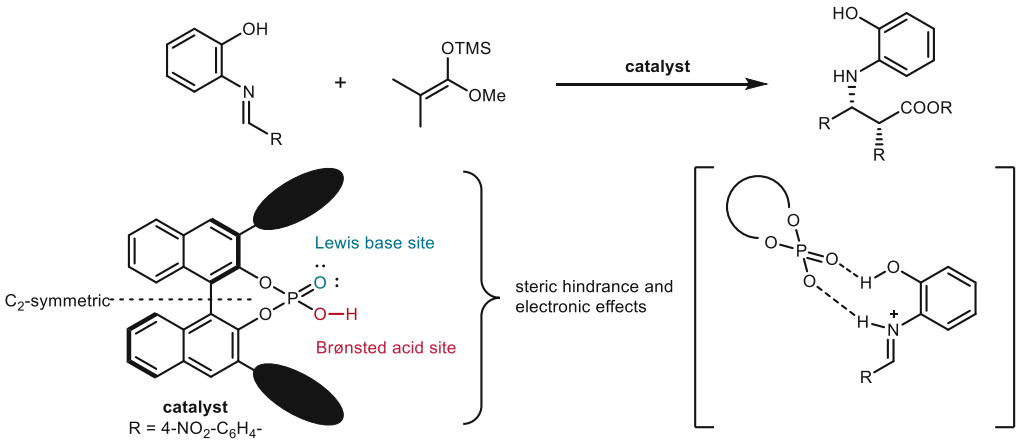
The fundamental concept of Brønsted acid catalysis either depends on the formation of hydrogen bonds due to acidic hydrogens, similar to thioureas discussed in chapter 3.2.2.1, or the protonation of the electrophilic substrate followed by ion-pairing. In this context, the most prevalent catalysts are phosphoric acids obtained from enantiopure BINOL through phosphorylation and subsequent hydrolysis. The stereoinduction primarily arises from the presence of a bulky substituent within the C_2-symmetric phosphoric acid moiety (**Scheme 23**, R-group).



Scheme 23. Concept of Brønsted acid catalysis and examples.[52]

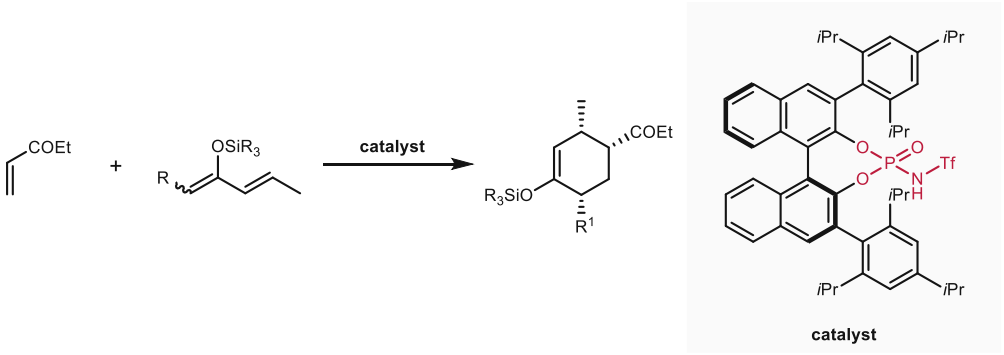
One of the initial approaches for employing this catalyst type involved the enantioselective Mannich-type reaction performed in the research group of Akiyama (**Scheme 24**).[53] In this context, as depicted in **Scheme 23**, the phosphoric acid exhibits sufficient strength to protonate and subsequently lower the LUMO energy of the basic imine. The resulting iminium ion forms an ion pair with the chiral phosphoric acid followed by nucleophilic attack of the TMS-enolate from the less sterically hindered face, yielding the enantioenriched product. Akiyama also demonstrated that the bulky substituent R can significantly impact both the catalyst's reactivity and stereoinduction.[53] Through a steric binding pocket where the substrate and/or reagent can engage with both the Brønsted acid and Lewis base sites of the catalyst, high enantioselectivities can be achieved for a variety of different reactions. For the Akiyama Mannich-type reaction, introducing an extra hydroxy group on the substrate can significantly boost enantioselectivity by promoting interaction between both the Brønsted acid and Lewis base sites on the phosphoric acid and the substrate (**Scheme 24**).[41]

Die approbierte gedruckte Originalversion dieser Dissertation ist an der TU Wien Bibliothek verfügbar.
The approved original version of this doctoral thesis is available in print at TU Wien Bibliothek.



Scheme 24. Brønsted acid catalyzed Mannich-type reaction.[53,54]

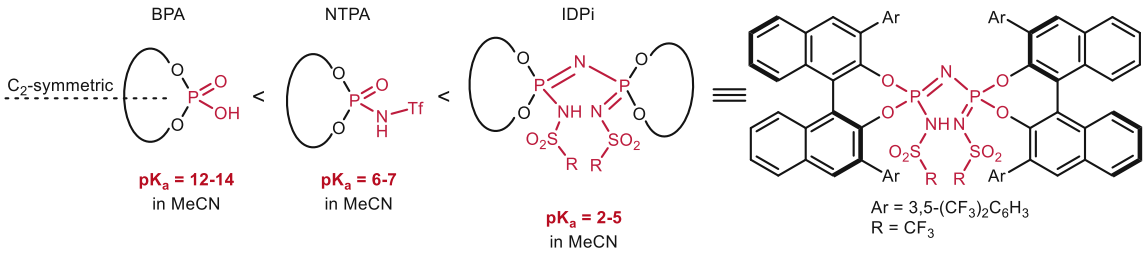
While phosphoric acids are effective at protonating imines, they do not provide sufficient activation for the less basic carbonyl groups present in aldehydes and ketones. To address this challenge, the group of Yamamoto proposed a solution by modifying the structure of phosphoric acids to create phosphoramides (**Scheme 25**). By incorporating an NTf moiety that enhances the stability of the counteranion, a notable increase in the pK_a-value was observed.



Scheme 25. Strong *N*-triflyl phosphoramides for organocatalytic Diels-Alder reaction.[55]

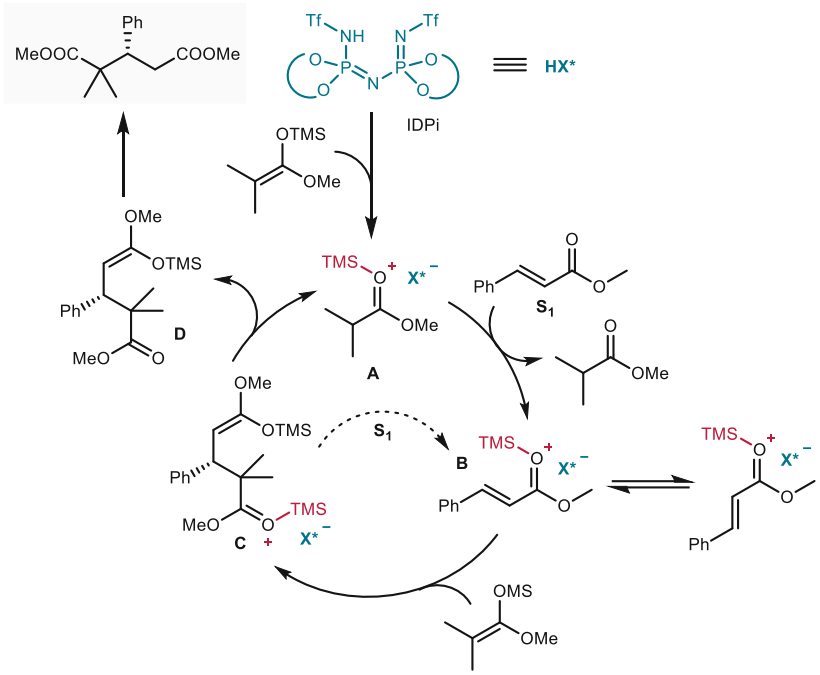
To illustrate the effectiveness of this approach, they applied the newly designed acid in an asymmetric Diels-Alder reaction, achieving significantly higher catalytic efficiency than phosphoric acids (**Scheme 25**).[55] In general, a higher acidity of the catalyst leads to greater reactivity towards less basic substrates, thereby expanding the range of possibilities in catalysis and reaction design. Increasing acidity is just one aspect of Brønsted acid catalysis, while achieving enantioselectivity is a greater challenge. List et al. discovered that a dimer of the chiral substituted TRIP acid created a more rigid and sterically demanding binding site, resulting in enhanced enantioselectivities even with flexible substrates like aldehydes. Furthermore, they found that the acidity can be increased significantly by incorporating an imidodiphosphorimidate moiety (**Scheme 26**).[56–58]

Die approbierte gedruckte Originalversion dieser Dissertation ist an der TU Wien Bibliothek verfügbar.
The approved original version of this doctoral thesis is available in print at TU Wien Bibliothek.



Scheme 26. pK_a values of chiral BINOL-based acids.[56,58]

List also discovered that the ACDC concept could be extended to include reactions involving silylium substrates (silylium-ACDC) in addition to Brønsted acid catalysis. One example is the Mukayama aldol procedure, where the IDPi catalyst can be utilized (**Scheme 27**). In this process, the strong acid initially protonates the silyl ketene acetal (SKA), leading to the formation of the silylated ester **A**.



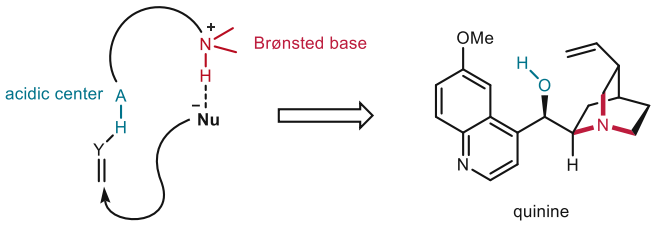
Scheme 27. IDPi-catalyzed Mukayama aldol reaction.[59]

The silicon transfer from **A** to the substrate generates the activated chiral ion pair **B**, which then reacts with the nucleophile to form the doubly silylated intermediate **C**. Subsequently, silylation of the next substrate molecule can occur either directly or through other ester or generic type **A**. Finally, the intermediate **D** undergoes transformation in the acidic environment to yield the desired product.[59]

Die approbierte gedruckte Originalversion dieser Dissertation ist an der TU Wien Bibliothek verfügbar.
The approved original version of this doctoral thesis is available in print at TU Wien Bibliothek.

3.2.2.4 Brønsted base catalysis

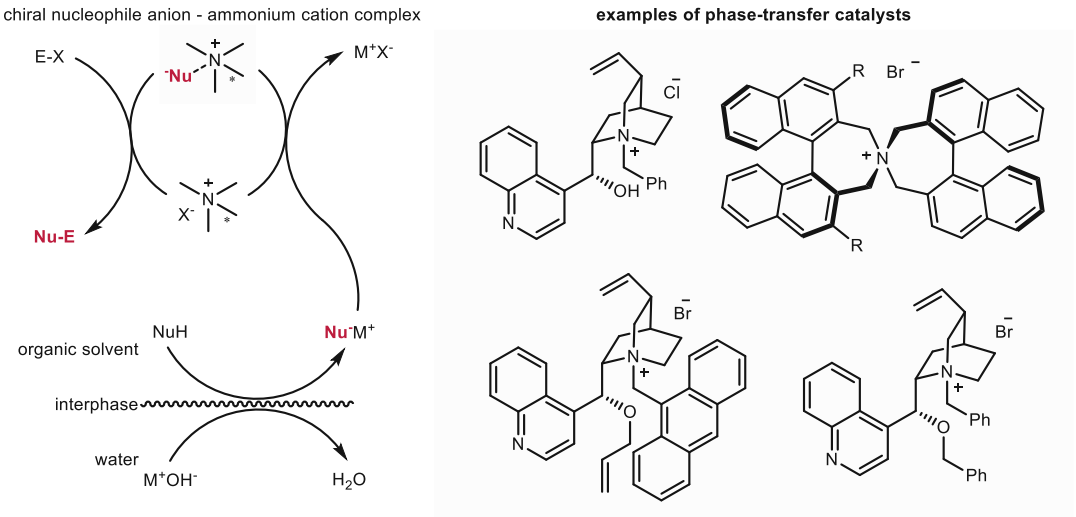
In the realm of organocatalysis, Brønsted base catalysis is another method facilitating a wide array of chemical transformations. A prevalent structural motif involves chinchona alkaloids, thanks to their well-defined rigid structure and cheap cost due to their natural abundance. The utilization of chinchona alkaloids introduces a bifunctional aspect as well, wherein the hydroxy group can engage in hydrogen bonding interactions, thereby further influencing the enantiomeric outcome.[23]



Scheme 28. Brønsted base bifunctional catalyst.[23]

3.2.2.5 Phase transfer catalysis

The fundamental concept of phase transfer catalysis is the generation of a nucleophilic anion by deprotonation of a neutral nucleophile at the interface between a highly basic aqueous layer and an organic solvent. This anion displaces the loosely bound halogen anion within the quaternary ammonium catalyst. Subsequently, the newly created chiral ionic complex transfers the ion-bound nucleophile to the electrophilic substrate, yielding the desired product. Common examples of phase transfer catalysts include quaternary ammonium compounds derived from cinchona alkaloids that have been alkylated and BINOL (1,1'-bi-2-naphthol) based C_2-symmetric structures.[23]

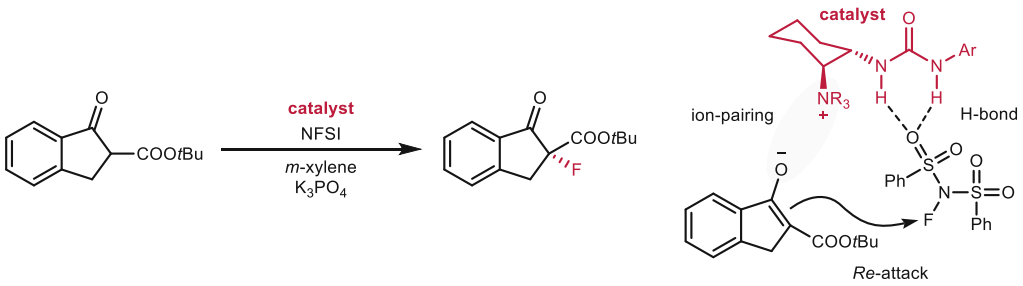


Scheme 29. Mechanism of phase transfer catalysis and prominent examples.[23,60]

To provide an illustrative example, the α-fluorination of β-ketones is presented (**Scheme 30**). In this reaction the ketoester undergoes deprotonation, resulting in the formation of the corresponding potassium enolate. The anion then exchanges with the halogen of the chiral phase transfer catalyst to

Die approbierte gedruckte Originalversion dieser Dissertation ist an der TU Wien Bibliothek verfügbar.
The approved original version of this doctoral thesis is available in print at TU Wien Bibliothek.
TU Bibliothek Your knowledge hub WIEN

form the ionic complex. Subsequently, the nucleophile is poised to undergo substitution with the electrophilic fluorinating agent NFSI, ultimately yielding the desired product with high enantiodiscrimination.[61]



Scheme 30. α-Fluorination via phase transfer catalysis.[61]

Die approbierte gedruckte Originalversion dieser Dissertation ist an der TU Wien Bibliothek verfügbar.
The approved original version of this doctoral thesis is available in print at TU Wien Bibliothek.

3.2.2.6 Asymmetric Counteranion-Directed Catalysis

Asymmetric Counteranion-Directed Catalysis involves the chiral induction in a reaction that proceeds through a cationic intermediate. This is achieved by forming an ion pair with a chiral, enantiomerically pure anion.[62] This concept heavily depends on ion aggregation, which is closely associated with the choice of solvent used in the reaction. To maximize the interaction between both the cation and anion, the formation of contact ion pairs is important. These contact pairs predominantly form in solvents with low dielectric constants that are mostly apolar in nature. Consequently, ether-type solvents such as dioxane, THF, or dibutyl ether are often preferred for this purpose, to ensure a highly enantioselective outcome.[63]

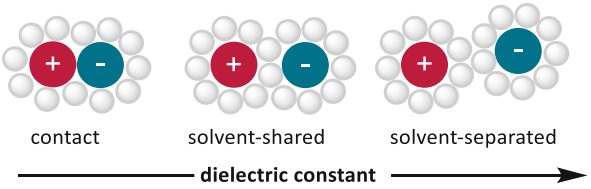
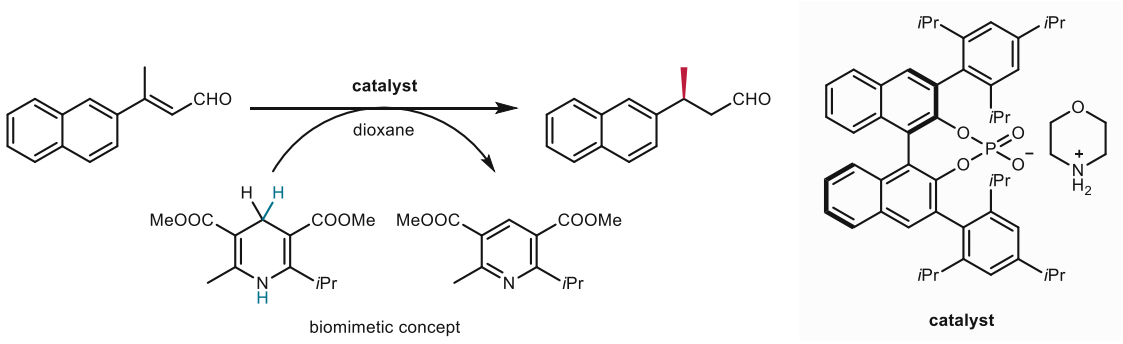


Figure 4. Types of ion pairs.[63]

An early demonstration of the ACDC concept was carried out by List et al., where they employed a modified Akiyama phosphoric acid for the asymmetric transfer hydrogenation of enals. The catalyst, a chiral ion pair comprising a basic morpholine and a chiral phosphoric acid, is highly effective at activating the enal substrate by reducing its LUMO energy to form an iminium intermediate.

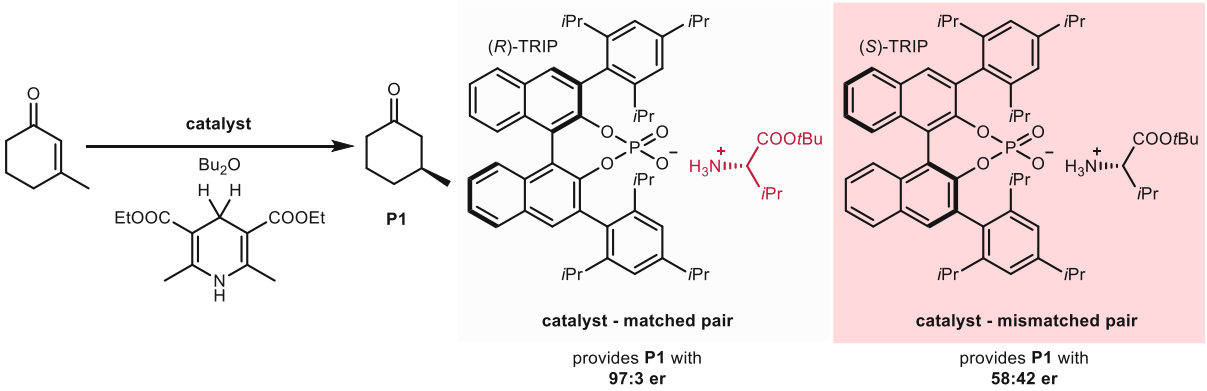


Scheme 31. Asymmetric transfer hydrogenation of enals via ACDC.[36]

The chiral induction through ion pairing, as already depicted in **Scheme 24**, results in remarkably high level of enantiodiscrimination. For the lesser reactive ketones, List observed that switching from a secondary to a primary amine proved advantageous in achieving significantly better results due to the higher nucleophilicity (**Scheme 32**). Furthermore, it was observed that the bulkiness of the ester group on the amine as well as the type of amino acid used as precursor exerted a significant influence on stereoinduction. It is crucial to emphasize that the enantiomers of both the amine and phosphoric acid must “match” in order to provide desired double stereo induction and highly enantioselective

Die approbierte gedruckte Originalversion dieser Dissertation ist an der TU Wien Bibliothek verfügbar.
The approved original version of this doctoral thesis is available in print at TU Wien Bibliothek.
TU Bibliothek Your knowledge hub WIEN

outcome. When an unmatched pair is used, it will provide similar yields but with a substantially lower level of enantioselectivity of the target compound.[62,64]

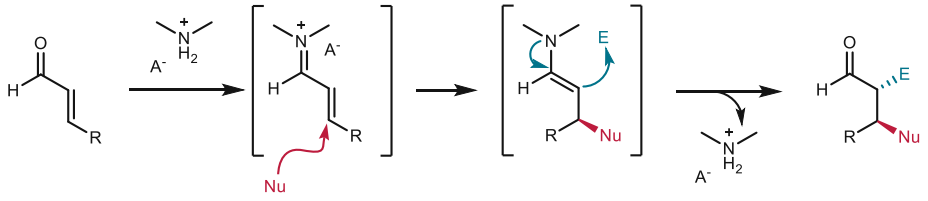


Scheme 32. Double stereoinduction in the asymmetric transfer hydrogenation of enones via ACDC.[64]

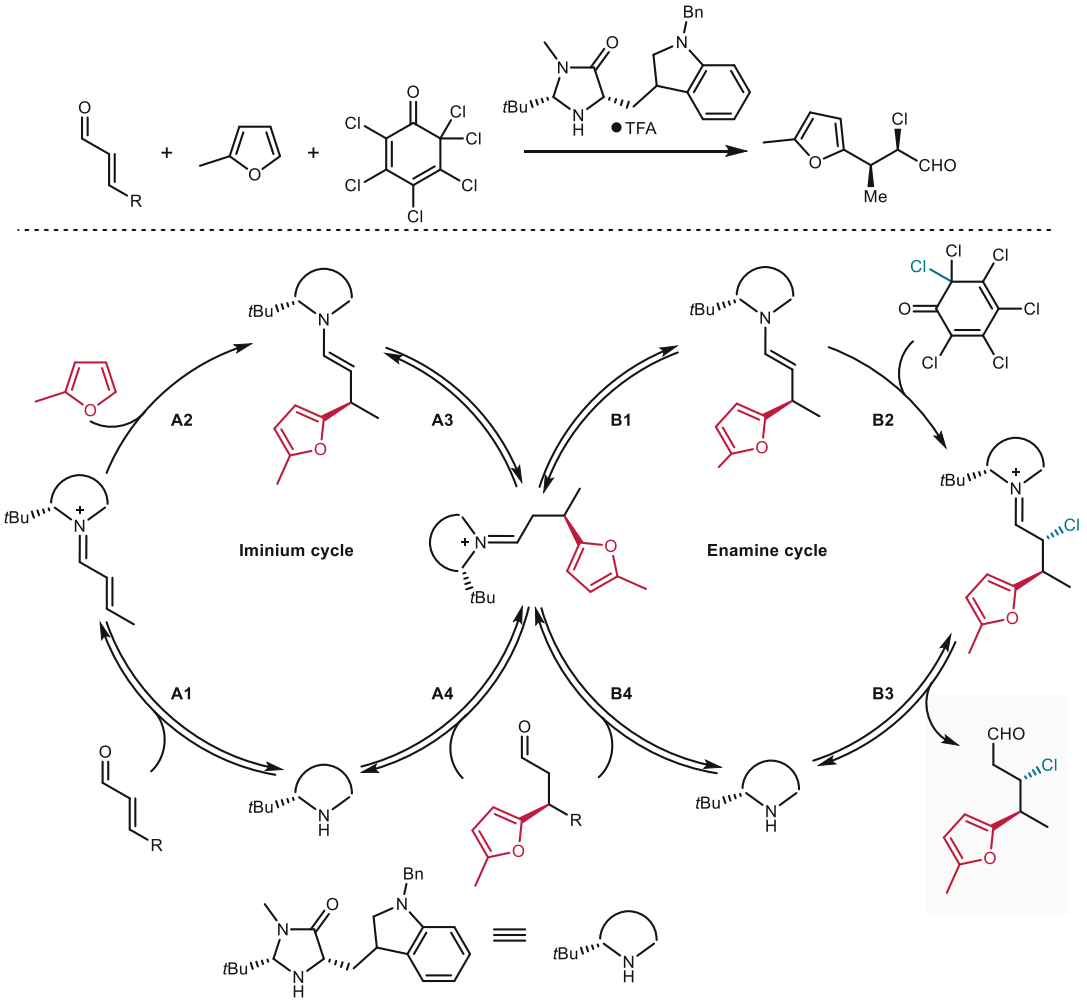
Die approbierte gedruckte Originalversion dieser Dissertation ist an der TU Wien Bibliothek verfügbar.
The approved original version of this doctoral thesis is available in print at TU Wien Bibliothek.

4 Domino reactions

Employing individual reaction steps to construct complex molecules not only proves costly and time-consuming but also necessitates the introduction and subsequent removal of additional functional groups or protective groups. To address this challenge, multicomponent domino reactions have gained prominence. In these reactions, a single catalyst can trigger multiple reaction steps without the need for intermediate isolation. This concept can also be seen as biomimetic, as nature efficiently assembles complex molecules from simple precursors.[65]



Scheme 33. The concept of iminium-enamine domino reactions.[65]



Scheme 34. Example of organo-cascade reaction.[66]

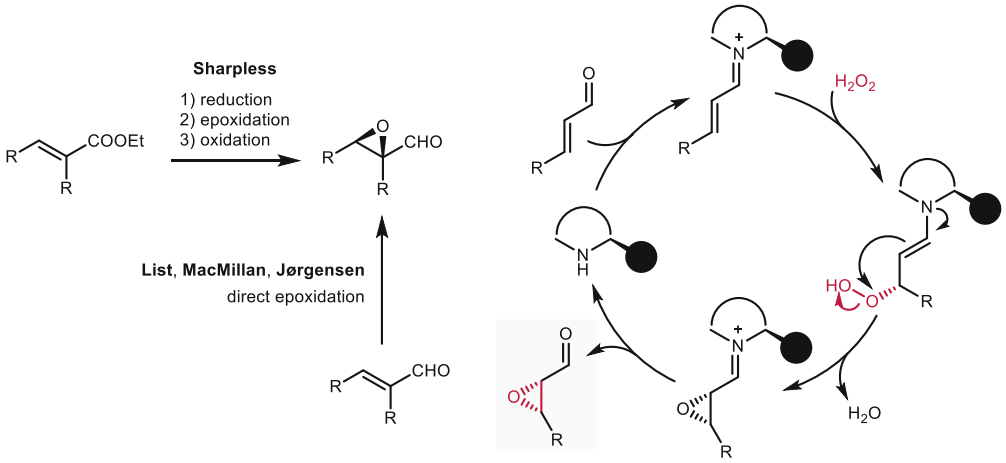
Die approbierte gedruckte Originalversion dieser Dissertation ist an der TU Wien Bibliothek verfügbar.
The approved original version of this doctoral thesis is available in print at TU Wien Bibliothek.

A significant investigation conducted by MacMillan and colleagues focused on the use of various imidazolidinone catalysts in an enantioselective iminium-enamine cascade reaction to introduce furan and chloride as substituents into an activated enal (**Scheme 34**). They emphasized that the stereocontrol exerted by the catalyst overrides the weaker substrate control established during the initial furane addition in the iminium cycle.[66] The initial phase of the mechanism starts with iminium activation **A1**, followed by the addition of furane to the β-position of the enal **A2**. The enamine may potentially revert to the iminium state following catalyst cleavage **A3**, **A4**. Due to the equilibrium between iminium and enamine **B1**, when a suitable electrophile is present, the subsequent enamine pathway can incorporate an electrophile into the α-position of the enal **B2**. This, in turn, is followed by catalyst cleavage, resulting in the formation of a double-substituted aldehyde **B3**.

Die approbierte gedruckte Originalversion dieser Dissertation ist an der TU Wien Bibliothek verfügbar.
The approved original version of this doctoral thesis is available in print at TU Wien Bibliothek.

4.1 Asymmetric epoxidation with hydroperoxides

Chiral epoxides are important building blocks in organic chemistry. The inherent strain within the three-membered ring system renders epoxides susceptible to various nucleophilic ring-opening reactions.[67] Following the ground-breaking discovery of Sharpless (Chapter 3.1.3, **Scheme 5**) in utilizing allylic alcohols for asymmetric epoxidation, organocatalytic methods garnered significant attention. One limitation of the Sharpless approach was the requirement for an allylic-OH group in order to achieve catalyst interaction and a subsequent enantioselective outcome. This hydroxy group is not always essential in the final molecule and necessitates further modification. In contrast, an aldehyde or ketone can be readily targeted by an organocatalyst, broadening the scope of possibilities for various α,β-unsaturated carbonyl-bearing compounds to undergo highly enantioselective epoxidation.[68] Electrophilic oxidants fall short when it comes to epoxidizing electron-poor double bonds in the case of α,β-unsaturated aldehydes or ketones in the Weitz-Scheffer reaction which employs nucleophilic oxidants like peroxides as the only viable option. This choice is driven by the ability of the catalyst to modify the electrophilicity of the substrate's double bond even further through LUMO-lowering interactions and possible hydrogen bond activation of the peroxide species. Hydrogen peroxide is considered an ideal oxidant for this task due to its commercial availability as an aqueous solution and exceptional reactivity with electron-deficient olefins. It provides high atom efficiency, and its only by-product is water.

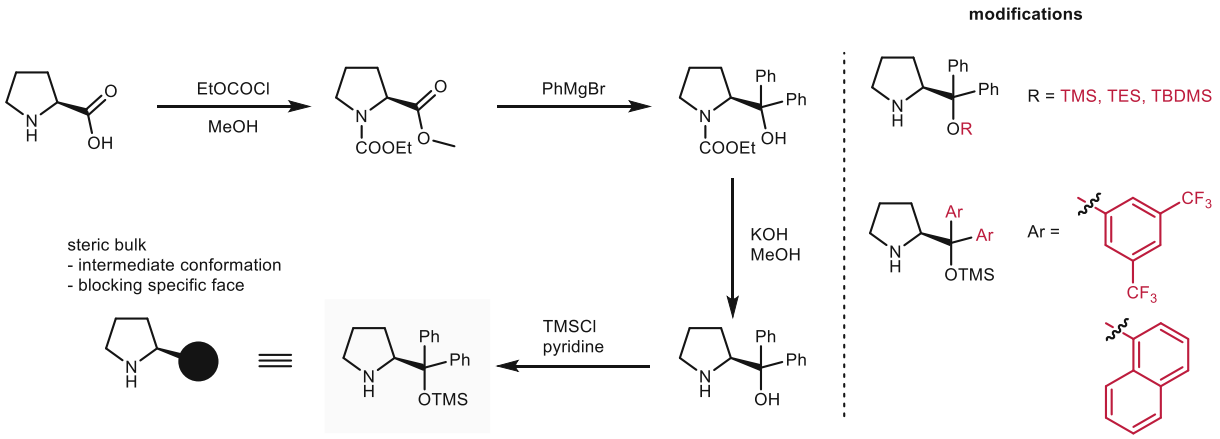


Scheme 35. Representative example for the asymmetric epoxidation of enals.[69]

Die approbierte gedruckte Originalversion dieser Dissertation ist an der TU Wien Bibliothek verfügbar.
The approved original version of this doctoral thesis is available in print at TU Wien Bibliothek.

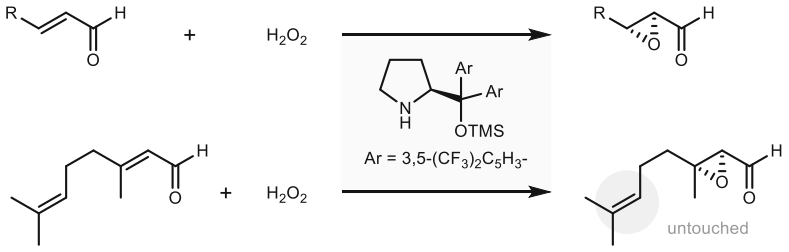
4.1.1 Jørgensen catalyst

While the first generation MacMillan catalyst has demonstrated remarkable efficacy in asymmetric Diels-Alder- and transfer hydrogenation, as discussed in Chapter 3.2.1.2, it provides only low yields and enantioselectivities in asymmetric epoxidations when utilizing hydroperoxides.[70] In the early 2000s, the Jørgensen catalyst emerged as another potent chiral secondary amine, offering an alternative catalyst structure for various transformations. In contrast to MacMillan's imidazolidinone catalyst, the design is quite similar, incorporating sterically demanding groups to effectively block a certain face for electrophilic or nucleophilic attack.[71] The major distinction lies in the precursor and synthesis. By starting with the desired enantiomer of proline and introducing sterically demanding groups through a Grignard reaction, followed by further enhancement of steric hindrance through the introduction of bulky silyl-protecting groups, a versatile steric catalyst is created (**Scheme 36**). Structural modifications can be easily applied to affect steric hindrance or catalyst activity.[69,72] The Jørgensen catalyst proves exceptionally effective in a wide range of asymmetric reactions involving enal substrates.



Scheme 36. Synthesis of Jørgensen catalyst and modifications.[69,72]

During catalyst screening involving various aromatic substituents within the catalyst's structure, Jørgensen discovered that the 3,5-CF_3-substituted pyrrolidine was the most suitable choice. Moreover, Jørgensen showcased that exclusively the double bond experiencing LUMO activation undergoes epoxidation, while other double bonds remain unaffected, ultimately leading to a high level of regio- and enantioselectivity.[69]

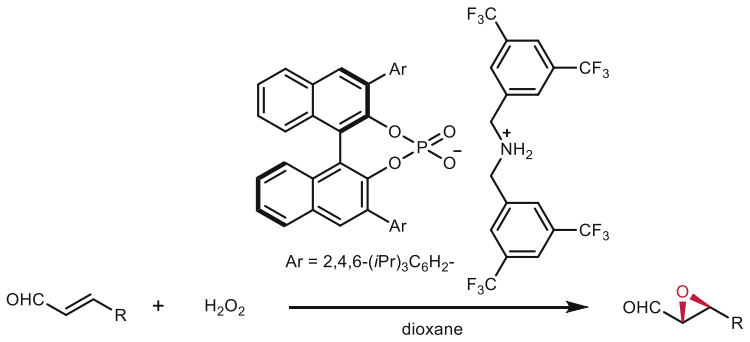


Scheme 37. Jørgensen approach for chemoselective asymmetric epoxidations .[69]

Die approbierte gedruckte Originalversion dieser Dissertation ist an der TU Wien Bibliothek verfügbar.
The approved original version of this doctoral thesis is available in print at TU Wien Bibliothek.

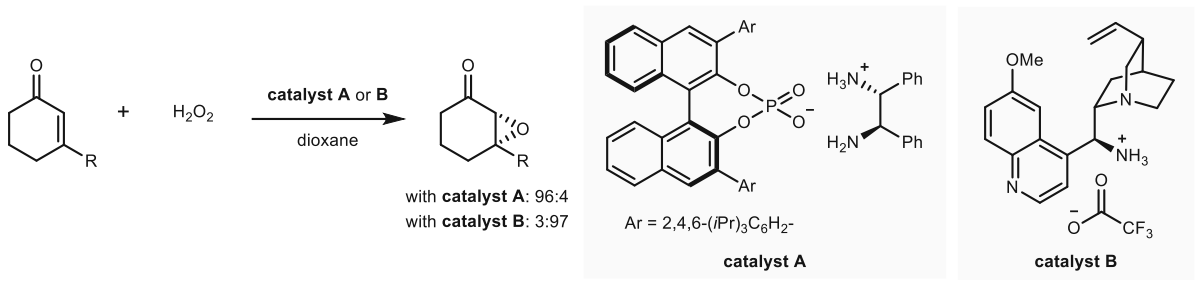
4.1.2 Asymmetric Counteranion Directed Catalysis approach

By employing the asymmetric transfer hydrogenation of enals and enones, List and his colleagues demonstrated that the ACDC concept could yield outstanding results in terms of both yield and enantioselectivity. Notably, the primary driver of stereoselectivity in this context was exclusively the chiral phosphoric acid counteranion, distinguishing it from the approaches of Jørgensen and MacMillan (Chapter 3.2.1.2). Upon closer examination within asymmetric epoxidation, it was however observed that when applying his ATH catalyst, only moderate results could be obtained. Extensive screening of both catalyst components (amine and acid) revealed that only the amine needed to be changed, leading to the identification of a CF_3-substituted dibenzylamine in conjunction with the TRIP phosphoric acid as the best catalyst for this challenging transformation (**Scheme 38**).[73]



Scheme 38. Lists ACDC concept for asymmetric epoxidations.[73]

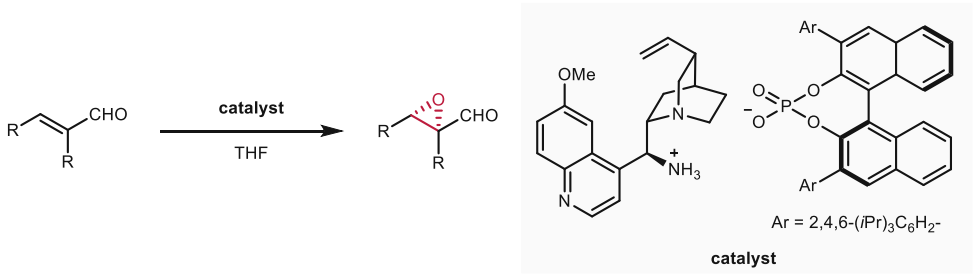
As discussed in Chapter 3.2.2.6, when utilizing enones instead of enals, the reactivity of the secondary amine towards the substrate´s carbonyl group decreases significantly due to the higher steric hindrance and lower electrophilicity. While chiral primary amines can address this issue, in general they should contain sterically demanding groups and/or be structurally rigid.[74] One solution was identified by List et al., who utilized chinchona-based primary amines as catalysts (**Scheme 39**, catalyst B). Through a straightforward one-step synthesis, simple naturally derived chinchona alkaloids could be transformed into the corresponding primary amine via the Mitsunobu-Staudinger reaction.[75] Another potential catalyst involves revisiting the employment of the ACDC concept, this time utilizing a chiral ion pair consisting of matched enantiomers of diphenylethylenediamine and TRIP phosphoric acid (**Scheme 39**, catalyst A).[76]



Scheme 39. Asymmetric epoxidation of enones.[76]

Die approbierte gedruckte Originalversion dieser Dissertation ist an der TU Wien Bibliothek verfügbar.
The approved original version of this doctoral thesis is available in print at TU Wien Bibliothek.

While primary amines exhibit a high reactivity towards enals, the resulting enantioselectivity tends to be unsatisfactory due to the flexibility of the formed iminium or enamine, when compared to the more rigid secondary amines. However, α-branched enals are an exception due to their higher rigidity and can undergo highly enantioselective epoxidation when using an ACDC-salt comprised of primary amino-quinine and the corresponding enantiomer of TRIP (**Scheme 40**).[77–79]

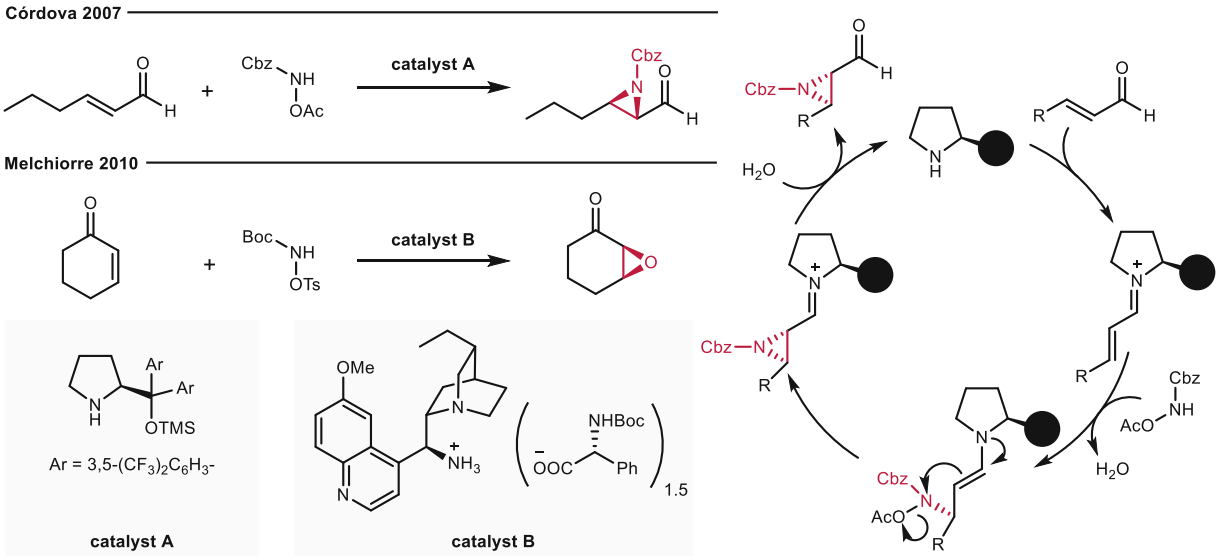


Scheme 40. Asymmetric epoxidation of α-branched enals.[77]

Die approbierte gedruckte Originalversion dieser Dissertation ist an der TU Wien Bibliothek verfügbar.
The approved original version of this doctoral thesis is available in print at TU Wien Bibliothek.

4.2 Azridination of enones

Aziridines belong to a category of saturated heterocycles consisting of a three-membered ring that includes an amine functionality. Similar to other three-membered rings such as cyclopropanes and epoxides, aziridines are subject to high strain. They can be considered nitrogen analogues of epoxides and present some of the most intriguing and demanding heterocyclic structures in the realm of organic chemistry. They hold significance as both essential components in the synthesis of various natural products and important building blocks for complex molecules.[80] In 2007, Córdoba et al. introduced a protocol for synthesizing chiral aziridines using an organocatalytic method similar to asymmetric epoxidation discussed in Chapter 4.1. Their approach involved employing a modified hydroxylamine equipped with a leaving group in conjunction with the Jørgensen catalyst for stereoinduction.[81,82]



Scheme 41. Asymmetric aziridination of enals and enones.[81,83]

Likewise, in the case of ketones, the Melchiorre group devised a comparable protocol through a minor adjustment of the leaving group on the hydroxylamine reagent. They employed the primary amino functionalized quinine in combination with D-Boc-phenylglycine as organocatalyst.[83]

Die approbierte gedruckte Originalversion dieser Dissertation ist an der TU Wien Bibliothek verfügbar.
The approved original version of this doctoral thesis is available in print at TU Wien Bibliothek.

5 Bibliography

(1) Karnik, A. V.; Hasan, M. Diastereomeric Transition States and Stereoselectivity. In *Stereochemistry*; Elsevier, 2021; pp 407–463. https://doi.org/10.1016/B978-0-12-821062-8.00012-0.

(2) McConathy, J.; Owens, M. J. Stereochemistry in Drug Action. *Prim. Care Companion CNS Disord.* **2003**, *5* (2). https://doi.org/10.4088/PCC.v05n0202.

(3) Vargesson, N. Thalidomide-induced Teratogenesis: History and Mechanisms. *Birth Defects Res. Part C Embryo Today Rev.* **2015**, *105* (2), 140–156. https://doi.org/10.1002/bdrc.21096.

(4) Karnik, A. V.; Hasan, M. Racemates: Properties and Methods of Resolution. In *Stereochemistry*; Elsevier, 2021; pp 187–223. https://doi.org/10.1016/B978-0-12-821062-8.00003-X.

(5) Gawley, R. E.; Aubé, J. Introduction, General Principles, and Glossary of Stereochemical Terms. In *Principles of Asymmetric Synthesis*; Elsevier, 2012; pp 1–62. https://doi.org/10.1016/B978-0-08-044860-2.00001-5.

(6) Noyori, R.; Tomino, I.; Tanimoto, Y.; Nishizawa, M. Asymmetric Synthesis via Axially Dissymmetric Molecules. 6. Rational Designing of Efficient Chiral Reducing Agents. Highly Enantioselective Reduction of Aromatic Ketones by Binaphthol-Modified Lithium Aluminum Hydride Reagents. *J. Am. Chem. Soc.* **1984**, *106* (22), 6709–6716. https://doi.org/10.1021/ja00334a041.

(7) Evans, D. A.; Ennis, M. D.; Mathre, D. J. Asymmetric Alkylation Reactions of Chiral Imide Enolates. A Practical Approach to the Enantioselective Synthesis of .Alpha.-Substituted Carboxylic Acid Derivatives. *J. Am. Chem. Soc.* **1982**, *104* (6), 1737–1739. https://doi.org/10.1021/ja00370a050.

(8) Vittorio Caprio, J. M. J. W. *Catalysis in Asymmetric Synthesis, 2nd Edition*; Wiley-VCH, 2009.

(9) Biosca, M.; Diéguez, M.; Zanotti-Gerosa, A. Asymmetric Hydrogenation in Industry; 2021; pp 341–383. https://doi.org/10.1016/bs.acat.2021.08.005.

(10) Horner, L.; Siegel, H.; Büthe, H. Asymmetric Catalytic Hydrogenation with an Optically Active Phosphinerhodium Complex in Homogeneous Solution. *Angew. Chem. Int. Ed.* **1968**, *7* (12), 942–942. https://doi.org/10.1002/anie.196809422.

(11) Knowles, W. S.; Sabacky, M. J. Catalytic Asymmetric Hydrogenation Employing a Soluble, Optically Active, Rhodium Complex. *Chem. Commun.* **1968**, No. 22, 1445. https://doi.org/10.1039/c19680001445.

(12) Osborn, J. A.; Wilkinson, G.; Mrowca, J. J. Tris(Triphenylphosphine)Halorhodium(I); 1967; pp 67–71. https://doi.org/10.1002/9780470132418.ch12.

(13) Dang, T. P.; Kagan, H. B. The Asymmetric Synthesis of Hydratropic Acid and Amino-Acids by Homogeneous Catalytic Hydrogenation. *J. Chem. Soc. D Chem. Commun.* **1971**, No. 10, 481. https://doi.org/10.1039/c29710000481.

(14) Wang, D.; Astruc, D. The Golden Age of Transfer Hydrogenation. *Chem. Rev.* **2015**, *115* (13), 6621–6686. https://doi.org/10.1021/acs.chemrev.5b00203.

(15) Hall, A. M. R.; Dong, P.; Codina, A.; Lowe, J. P.; Hintermair, U. Kinetics of Asymmetric Transfer Hydrogenation, Catalyst Deactivation, and Inhibition with Noyori Complexes As Revealed by Real-Time High-Resolution FlowNMR Spectroscopy. *ACS Catal.* **2019**, *9* (3), 2079–2090. https://doi.org/10.1021/acscatal.8b03530.

Die approbierte gedruckte Originalversion dieser Dissertation ist an der TU Wien Bibliothek verfügbar.
The approved original version of this doctoral thesis is available in print at TU Wien Bibliothek.
TU Bibliothek Your knowledge hub WIEN

(16) Fujii, A.; Hashiguchi, S.; Uematsu, N.; Ikariya, T.; Noyori, R. Ruthenium(II)-Catalyzed Asymmetric Transfer Hydrogenation of Ketones Using a Formic Acid−Triethylamine Mixture. *J. Am. Chem. Soc.* **1996**, *118* (10), 2521–2522. https://doi.org/10.1021/ja954126l.

(17) Katsuki, T.; Sharpless, K. B. The First Practical Method for Asymmetric Epoxidation. *J. Am. Chem. Soc.* **1980**, *102* (18), 5974–5976. https://doi.org/10.1021/ja00538a077.

(18) Martin, V. S.; Woodard, S. S.; Katsuki, T.; Yamada, Y.; Ikeda, M.; Sharpless, K. B. Kinetic Resolution of Racemic Allylic Alcohols by Enantioselective Epoxidation. A Route to Substances of Absolute Enantiomeric Purity? *J. Am. Chem. Soc.* **1981**, *103* (20), 6237–6240. https://doi.org/10.1021/ja00410a053.

(19) Zhang, W.; Loebach, J. L.; Wilson, S. R.; Jacobsen, E. N. Enantioselective Epoxidation of Unfunctionalized Olefins Catalyzed by Salen Manganese Complexes. *J. Am. Chem. Soc.* **1990**, *112* (7), 2801–2803. https://doi.org/10.1021/ja00163a052.

(20) Irie, R.; Noda, K.; Ito, Y.; Matsumoto, N.; Katsuki, T. Catalytic Asymmetric Epoxidation of Unfunctionalized Olefins. *Tetrahedron Lett.* **1990**, *31* (50), 7345–7348. https://doi.org/10.1016/S0040-4039(00)88562-7.

(21) Sasaki, H.; Irie, R.; Hamada, T.; Suzuki, K.; Katsuki, T. Rational Design of Mn-Salen Catalyst (2): Highly Enantioselective Epoxidation of Conjugated Cis Olefins. *Tetrahedron* **1994**, *50* (41), 11827–11838. https://doi.org/10.1016/S0040-4020(01)89298-X.

(22) Berkessel, A.; Gröger, H. *Asymmetric Organocatalysis : From Biomimetic Concepts to Applications in Asymmetric Synthesis*; Wiley-VCH, 2005.

(23) Moyano, A. Activation Modes In Asymmetric Organocatalysis. In *Stereoselective Organocatalysis*; Wiley, 2013; pp 11–80. https://doi.org/10.1002/9781118604755.ch02.

(24) Mukherjee, S.; Yang, J. W.; Hoffmann, S.; List, B. Asymmetric Enamine Catalysis. *Chem. Rev.* **2007**, *107* (12), 5471–5569. https://doi.org/10.1021/cr0684016.

(25) Hoang, L.; Bahmanyar, S.; Houk, K. N.; List, B. Kinetic and Stereochemical Evidence for the Involvement of Only One Proline Molecule in the Transition States of Proline-Catalyzed Intra- and Intermolecular Aldol Reactions. *J. Am. Chem. Soc.* **2003**, *125* (1), 16–17. https://doi.org/10.1021/ja028634o.

(26) Seebach, D.; Beck, A. K.; Badine, D. M.; Limbach, M.; Eschenmoser, A.; Treasurywala, A. M.; Hobi, R.; Prikoszovich, W.; Linder, B. Are Oxazolidinones Really Unproductive, Parasitic Species in Proline Catalysis? – Thoughts and Experiments Pointing to an Alternative View. *Helv. Chim. Acta* **2007**, *90* (3), 425–471. https://doi.org/10.1002/hlca.200790050.

(27) Hosokawa, S. Asymmetric Aldol Reactions in the Total Syntheses of Natural Products. In *Stereoselective Synthesis of Drugs and Natural Products*; Wiley, 2013; pp 1–34. https://doi.org/10.1002/9781118596784.ssd008.

(28) Hajos, Z. G.; Parrish, D. R. Asymmetric Synthesis of Bicyclic Intermediates of Natural Product Chemistry. *J. Org. Chem.* **1974**, *39* (12), 1615–1621. https://doi.org/10.1021/jo00925a003.

(29) Eder, U.; Sauer, G.; Wiechert, R. New Type of Asymmetric Cyclization to Optically Active Steroid CD Partial Structures. *Angew. Chem. Int. Ed.* **1971**, *10* (7), 496–497. https://doi.org/10.1002/anie.197104961.

(30) List, B.; Lerner, R. A.; Barbas, C. F. Proline-Catalyzed Direct Asymmetric Aldol Reactions. *J. Am. Chem. Soc.* **2000**, *122* (10), 2395–2396. https://doi.org/10.1021/ja994280y.

Die approbierte gedruckte Originalversion dieser Dissertation ist an der TU Wien Bibliothek verfügbar.
The approved original version of this doctoral thesis is available in print at TU Wien Bibliothek.
TU Bibliothek Your knowledge hub WIEN

(31) Oliveira, V.; Cardoso, M.; Forezi, L. Organocatalysis: A Brief Overview on Its Evolution and Applications. *Catalysts* **2018**, *8* (12), 605. https://doi.org/10.3390/catal8120605.

(32) *Asymmetric Organocatalysis*; List, B., Ed.; Topics in Current Chemistry; Springer Berlin Heidelberg: Berlin, Heidelberg, 2009; Vol. 291. https://doi.org/10.1007/978-3-642-02815-1.

(33) Knoevenagel, E. Condensation von Malonsäure Mit Aromatischen Aldehyden Durch Ammoniak Und Amine. *Berichte der Dtsch. Chem. Gesellschaft* **1898**, *31* (3), 2596–2619. https://doi.org/10.1002/cber.18980310308.

(34) Ahrendt, K. A.; Borths, C. J.; MacMillan, D. W. C. New Strategies for Organic Catalysis: The First Highly Enantioselective Organocatalytic Diels−Alder Reaction. *J. Am. Chem. Soc.* **2000**, *122* (17), 4243–4244. https://doi.org/10.1021/ja000092s.

(35) An, F.; Maji, B.; Min, E.; Ofial, A. R.; Mayr, H. Basicities and Nucleophilicities of Pyrrolidines and Imidazolidinones Used as Organocatalysts. *J. Am. Chem. Soc.* **2020**, *142* (3), 1526–1547. https://doi.org/10.1021/jacs.9b11877.

(36) Mayer, S.; List, B. Asymmetric Counteranion-Directed Catalysis. *Angew. Chem. Int. Ed.* **2006**, *45* (25), 4193–4195. https://doi.org/10.1002/anie.200600512.

(37) Hantzsch, A. Condensationsprodukte Aus Aldehydammoniak Und Ketonartigen Verbindungen. *Berichte der Dtsch. Chem. Gesellschaft* **1881**, *14* (2), 1637–1638. https://doi.org/10.1002/cber.18810140214.

(38) Ouellet, S. G.; Tuttle, J. B.; MacMillan, D. W. C. Enantioselective Organocatalytic Hydride Reduction. *J. Am. Chem. Soc.* **2005**, *127* (1), 32–33. https://doi.org/10.1021/ja043834g.

(39) Northrup, A. B.; MacMillan, D. W. C. The First General Enantioselective Catalytic Diels-Alder Reaction with Simple (α,β-Unsaturated Ketones. *J. Am. Chem. Soc.* **2002**, *124* (11), 2458–2460. https://doi.org/10.1021/ja017641u.

(40) Tuttle, J. B.; Ouellet, S. G.; MacMillan, D. W. C. Organocatalytic Transfer Hydrogenation of Cyclic Enones. *J. Am. Chem. Soc.* **2006**, *128* (39), 12662–12663. https://doi.org/10.1021/ja0653066.

(41) Kim, H.; MacMillan, D. W. C. Enantioselective Organo-SOMO Catalysis: The α-Vinylation of Aldehydes. *J. Am. Chem. Soc.* **2008**, *130* (2), 398–399. https://doi.org/10.1021/ja077212h.

(42) Romero, N. A.; Nicewicz, D. A. Organic Photoredox Catalysis. *Chem. Rev.* **2016**, *116* (17), 10075–10166. https://doi.org/10.1021/acs.chemrev.6b00057.

(43) Bahamonde, A.; Melchiorre, P. Mechanism of the Stereoselective α-Alkylation of Aldehydes Driven by the Photochemical Activity of Enamines. *J. Am. Chem. Soc.* **2016**, *138* (25), 8019–8030. https://doi.org/10.1021/jacs.6b04871.

(44) Miyabe, H. Hydrogen-Bonding Activation in Chiral Organocatalysts. In *Recent Advances in Organocatalysis*; InTech, 2016. https://doi.org/10.5772/62459.

(45) Hamza, A.; Schubert, G.; Soós, T.; Pápai, I. Theoretical Studies on the Bifunctionality of Chiral Thiourea-Based Organocatalysts: Competing Routes to C−C Bond Formation. *J. Am. Chem. Soc.* **2006**, *128* (40), 13151–13160. https://doi.org/10.1021/ja063201x.

(46) Reisman, S. E.; Doyle, A. G.; Jacobsen, E. N. Enantioselective Thiourea-Catalyzed Additions to Oxocarbenium Ions. *J. Am. Chem. Soc.* **2008**, *130* (23), 7198–7199. https://doi.org/10.1021/ja801514m.

(47) Gratzer, K.; Gururaja, G. N.; Waser, M. Towards Tartaric-Acid-Derived Asymmetric Organocatalysts.

Die approbierte gedruckte Originalversion dieser Dissertation ist an der TU Wien Bibliothek verfügbar.
The approved original version of this doctoral thesis is available in print at TU Wien Bibliothek.
TU Bibliothek Your knowledge hub WIEN

European J. Org. Chem. **2013**, *2013* (21), 4471–4482. https://doi.org/10.1002/ejoc.201201675.

(48) Thadani, A. N.; Stankovic, A. R.; Rawal, V. H. Enantioselective Diels-Alder Reactions Catalyzed by Hydrogen Bonding. *Proc. Natl. Acad. Sci. U. S. A.* **2004**, *101* (16), 5846–5850. https://doi.org/10.1073/pnas.0308545101.

(49) Cavallo, G.; Metrangolo, P.; Milani, R.; Pilati, T.; Priimagi, A.; Resnati, G.; Terraneo, G. The Halogen Bond. *Chem. Rev.* **2016**, *116* (4), 2478–2601. https://doi.org/10.1021/acs.chemrev.5b00484.

(50) Sutar, R. L.; Huber, S. M. Catalysis of Organic Reactions through Halogen Bonding. *ACS Catal.* **2019**, *9* (10), 9622–9639. https://doi.org/10.1021/acscatal.9b02894.

(51) Keuper, A. C.; Fengler, K.; Ostler, F.; Danelzik, T.; Piekarski, D. G.; García Mancheño, O. Fine-tuning Substrate--Catalyst Halogen--Halogen Interactions for Boosting Enantioselectivity in Halogen-Bonding Catalysis. *Angew. Chem. Int. Ed.* **2023**, *202304781*. https://doi.org/10.1002/anie.202304781.

(52) Fages, F. *Asymmetric Organocatalysis*; Springer Berlin Heidelberg, 2005; Vol. 256.

(53) Akiyama, T.; Itoh, J.; Yokota, K.; Fuchibe, K. Enantioselective Mannich-Type Reaction Catalyzed by a Chiral Brønsted Acid. *Angew. Chem. Int. Ed.* **2004**, *43* (12), 1566–1568. https://doi.org/10.1002/anie.200353240.

(54) Simón, L.; Goodman, J. M. A Model for the Enantioselectivity of Imine Reactions Catalyzed by BINOL−Phosphoric Acid Catalysts. *J. Org. Chem.* **2011**, *76* (6), 1775–1788. https://doi.org/10.1021/jo102410r.

(55) Nakashima, D.; Yamamoto, H. Design of Chiral N -Triflyl Phosphoramide as a Strong Chiral Brønsted Acid and Its Application to Asymmetric Diels−Alder Reaction. *J. Am. Chem. Soc.* **2006**, *128* (30), 9626–9627. https://doi.org/10.1021/ja062508t.

(56) Peng, B.; Ma, J.; Guo, J.; Gong, Y.; Wang, R.; Zhang, Y.; Zeng, J.; Chen, W.-W.; Ding, K.; Zhao, B. A Powerful Chiral Super Brønsted C–H Acid for Asymmetric Catalysis. *J. Am. Chem. Soc.* **2022**, *144* (7), 2853–2860. https://doi.org/10.1021/jacs.1c12723.

(57) Čorić, I.; List, B. Asymmetric Spiroacetalization Catalysed by Confined Brønsted Acids. *Nature* **2012**, *483* (7389), 315–319. https://doi.org/10.1038/nature10932.

(58) Schreyer, L.; Properzi, R.; List, B. IDPi Catalysis. *Angew. Chem. Int. Ed.* **2019**, *58* (37), 12761–12777. https://doi.org/10.1002/anie.201900932.

(59) Gatzenmeier, T.; Kaib, P. S. J.; Lingnau, J. B.; Goddard, R.; List, B. The Catalytic Asymmetric Mukaiyama–Michael Reaction of Silyl Ketene Acetals with α,β-Unsaturated Methyl Esters. *Angew. Chem. Int. Ed.* **2018**, *57* (9), 2464–2468. https://doi.org/10.1002/anie.201712088.

(60) Albanese, D. C. M.; Penso, M. New Trends in Asymmetric Phase Transfer Catalysis. *European J. Org. Chem.* **2023**, *26* (19). https://doi.org/10.1002/ejoc.202300224.

(61) Novacek, J.; Waser, M. Syntheses and Applications of (Thio)Urea-Containing Chiral Quaternary Ammonium Salt Catalysts. *European J. Org. Chem.* **2014**, *2014* (4), 802–809. https://doi.org/10.1002/ejoc.201301594.

(62) Mahlau, M.; List, B. Asymmetric Counteranion-Directed Catalysis: Concept, Definition, and Applications. *Angew. Chem. Int. Ed.* **2013**, *52* (2), 518–533. https://doi.org/10.1002/anie.201205343.

(63) Brak, K.; Jacobsen, E. N. Asymmetric Ion-Pairing Catalysis. *Angew. Chem. Int. Ed.* **2013**, *52* (2), 534–561.

Die approbierte gedruckte Originalversion dieser Dissertation ist an der TU Wien Bibliothek verfügbar.
The approved original version of this doctoral thesis is available in print at TU Wien Bibliothek.
TU Bibliothek Your knowledge hub WIEN

https://doi.org/10.1002/anie.201205449.

(64) Martin, N. J. A.; List, B. Highly Enantioselective Transfer Hydrogenation of α,β- Unsaturated Ketones. *J. Am. Chem. Soc.* **2006**, *128* (41), 13368–13369. https://doi.org/10.1021/ja065708d.

(65) Enders, D.; Grondal, C.; Hüttl, M. R. M. Asymmetric Organocatalytic Domino Reactions. *Angew. Chem. Int. Ed.* **2007**, *46* (10), 1570–1581. https://doi.org/10.1002/anie.200603129.

(66) Huang, Y.; Walji, A. M.; Larsen, C. H.; MacMillan, D. W. C. Enantioselective Organo-Cascade Catalysis. *J. Am. Chem. Soc.* **2005**, *127* (43), 15051–15053. https://doi.org/10.1021/ja055545d.

(67) Lauret, C. Epoxy Ketones as Versatile Building Blocks in Organic Synthesis. *Tetrahedron: Asymmetry* **2001**, *12* (17), 2359–2383. https://doi.org/10.1016/S0957-4166(01)00412-8.

(68) Davis, R. L.; Stiller, J.; Naicker, T.; Jiang, H.; Jørgensen, K. A. Asymmetric Organocatalytic Epoxidations: Reactions, Scope, Mechanisms, and Applications. *Angew. Chem. Int. Ed.* **2014**, *53* (29), 7406–7426. https://doi.org/10.1002/anie.201400241.

(69) Marigo, M.; Franzén, J.; Poulsen, T. B.; Zhuang, W.; Jørgensen, K. A. Asymmetric Organocatalytic Epoxidation of α,β-Unsaturated Aldehydes with Hydrogen Peroxide. *J. Am. Chem. Soc.* **2005**, *127* (19), 6964–6965. https://doi.org/10.1021/ja051808s.

(70) Lee, S.; MacMillan, D. W. C. Enantioselective Organocatalytic Epoxidation Using Hypervalent Iodine Reagents. *Tetrahedron* **2006**, *62* (49), 11413–11424. https://doi.org/10.1016/j.tet.2006.07.055.

(71) Palomo, C.; Mielgo, A. Diarylprolinol Ethers: Expanding the Potential of Enamine/Iminium-Ion Catalysis. *Angew. Chem. Int. Ed.* **2006**, *45* (47), 7876–7880. https://doi.org/10.1002/anie.200602943.

(72) Bhaskar Kanth, J. V.; Periasamy, M. Convenient Method for the Synthesis of Chiral α,α-Diphenyl-2-Pyrrolidinemethanol. *Tetrahedron* **1993**, *49* (23), 5127–5132. https://doi.org/10.1016/S0040-4020(01)81877-9.

(73) Wang, X.; List, B. Asymmetric Counteranion-Directed Catalysis for the Epoxidation of Enals. *Angew. Chem. Int. Ed.* **2008**, *47* (6), 1119–1122. https://doi.org/10.1002/anie.200704185.

(74) Dalko, P. I.; Moisan, L. Enantioselective Organocatalysis. *Angew. Chem. Int. Ed.* **2001**, *40* (20), 3726–3748. https://doi.org/10.1002/1521-3773(20011015)40:20<3726::AID-ANIE3726>3.0.CO;2-D.

(75) Vakulya, B.; Varga, S.; Csámpai, A.; Soós, T. Highly Enantioselective Conjugate Addition of Nitromethane to Chalcones Using Bifunctional Cinchona Organocatalysts. *Org. Lett.* **2005**, *7* (10), 1967–1969. https://doi.org/10.1021/ol050431s.

(76) Wang, X.; Reisinger, C. M.; List, B. Catalytic Asymmetric Epoxidation of Cyclic Enones. *J. Am. Chem. Soc.* **2008**, *130* (19), 6070–6071. https://doi.org/10.1021/ja801181u.

(77) Lifchits, O.; Reisinger, C. M.; List, B. Catalytic Asymmetric Epoxidation of α-Branched Enals. *J. Am. Chem. Soc.* **2010**, *132* (30), 10227–10229. https://doi.org/10.1021/ja1037935.

(78) Arimitsu, S.; Yonamine, T.; Higashi, M. Cinchona-Based Primary Amine Catalyzed a Proximal Functionalization of Dienamines: Asymmetric α-Fluorination of α-Branched Enals. *ACS Catal.* **2017**, *7* (7), 4736–4740. https://doi.org/10.1021/acscatal.7b01178.

(79) Lifchits, O.; Mahlau, M.; Reisinger, C. M.; Lee, A.; Farès, C.; Polyak, I.; Gopakumar, G.; Thiel, W.; List, B. The Cinchona Primary Amine-Catalyzed Asymmetric Epoxidation and Hydroperoxidation of α,β-Unsaturated Carbonyl Compounds with Hydrogen Peroxide. *J. Am. Chem. Soc.* **2013**, *135* (17), 6677–

Die approbierte gedruckte Originalversion dieser Dissertation ist an der TU Wien Bibliothek verfügbar.
The approved original version of this doctoral thesis is available in print at TU Wien Bibliothek.
TU Bibliothek Your knowledge hub WIEN

6693. https://doi.org/10.1021/ja402058v.

(80) Tanner, D. Chiral Aziridines—Their Synthesis and Use in Stereoselective Transformations. *Angew. Chem. Int. Ed.* **1994**, *33* (6), 599–619. https://doi.org/10.1002/anie.199405991.

(81) Vesely, J.; Ibrahem, I.; Zhao, G.-L.; Rios, R.; Córdova, A. Organocatalytic Enantioselective Aziridination of α,B-Unsaturated Aldehydes. *Angew. Chem. Int. Ed.* **2007**, *46* (5), 778–781. https://doi.org/10.1002/anie.200603810.

(82) Roma, E.; Tosi, E.; Miceli, M.; Gasperi, T. Asymmetric Organocatalytic Aziridination: Recent Advances. *Asian J. Org. Chem.* **2018**, *7* (12), 2357–2367. https://doi.org/10.1002/ajoc.201800431.

(83) De Vincentiis, F.; Bencivenni, G.; Pesciaioli, F.; Mazzanti, A.; Bartoli, G.; Galzerano, P.; Melchiorre, P. Asymmetric Catalytic Aziridination of Cyclic Enones. *Chem. Asian J.* **2010**, *5* (7), 1652–1656. https://doi.org/10.1002/asia.201000040.

(84) Blaser, H. U. H.-J. F. *Asymmetric Catalysis on Industrial Scale: Challenges, Approaches and Solutions, 2nd Edition*; Wiley-VCH, 2011.

(85) Yang, J. W.; Hechavarria Fonseca, M. T.; List, B. Catalytic Asymmetric Reductive Michael Cyclization. *J. Am. Chem. Soc.* **2005**, *127* (43), 15036–15037. https://doi.org/10.1021/ja055735o.

(86) Uraguchi, D.; Terada, M. Chiral Brønsted Acid-Catalyzed Direct Mannich Reactions via Electrophilic Activation. *J. Am. Chem. Soc.* **2004**, *126* (17), 5356–5357. https://doi.org/10.1021/ja0491533.

(87) Parmar, D.; Sugiono, E.; Raja, S.; Rueping, M. Complete Field Guide to Asymmetric BINOL-Phosphate Derived Brønsted Acid and Metal Catalysis: History and Classification by Mode of Activation; Brønsted Acidity, Hydrogen Bonding, Ion Pairing, and Metal Phosphates. *Chem. Rev.* **2014**, *114* (18), 9047–9153. https://doi.org/10.1021/cr5001496.

(88) Parmar, D.; Sugiono, E.; Raja, S.; Rueping, M. Addition and Correction to Complete Field Guide to Asymmetric BINOL-Phosphate Derived Brønsted Acid and Metal Catalysis: History and Classification by Mode of Activation; Brønsted Acidity, Hydrogen Bonding, Ion Pairing, and Metal Phosphates. *Chem. Rev.* **2017**, *117* (15), 10608–10620. https://doi.org/10.1021/acs.chemrev.7b00197.

(89) Mahoney, W. S.; Stryker, J. M. Hydride-Mediated Homogeneous Catalysis. Catalytic Reduction of α, β-Unsaturated Ketones Using [(Ph3P)CuH]6 and H2. *J. Am. Chem. Soc.* **1989**, *111* (24), 8818–8823. https://doi.org/10.1021/ja00206a008.

(90) Ouellet, S. G.; Tuttle, J. B.; MacMillan, D. W. C. Enantioselective Organocatalytic Hydride Reduction. *J. Am. Chem. Soc.* **2005**, *127* (1), 32–33. https://doi.org/10.1021/ja043834g.

(91) Erkkilä, A.; Majander, I.; Pihko, P. M. Iminium Catalysis. *Chem. Rev.* **2007**, *107* (12), 5416–5470. https://doi.org/10.1021/cr068388p.

(92) Herrera, R. P. Organocatalytic Transfer Hydrogenation and Hydrosilylation Reactions. *Top. Curr. Chem.* **2016**, *374* (3), 29. https://doi.org/10.1007/s41061-016-0032-4.

(93) Martin, N. J. A.; List, B. Highly Enantioselective Transfer Hydrogenation of α,β-Unsaturated Ketones. *J. Am. Chem. Soc.* **2006**, *128* (41), 13368–13369. https://doi.org/10.1021/ja065708d.

(94) Lee, A.; Michrowska, A.; Sulzer-Mosse, S.; List, B. The Catalytic Asymmetric Knoevenagel Condensation. *Angew. Chem. Int. Ed.* **2011**, *50* (7), 1707–1710. https://doi.org/10.1002/anie.201006319.

(95) Singh, G.; Yeboah, E. Recent Applications of Cinchona Alkaloid-Based Catalysts in Asymmetric Addition

Die approbierte gedruckte Originalversion dieser Dissertation ist an der TU Wien Bibliothek verfügbar.
The approved original version of this doctoral thesis is available in print at TU Wien Bibliothek.
TU Bibliothek Your knowledge hub WIEN

Reactions. *Reports Org. Chem.* **2016**, *Volume 6*, 47–75. https://doi.org/10.2147/ROC.S73908.

(96) He, Z. X.; Gong, Y. P.; Zhang, X.; Ma, L. Y.; Zhao, W. Pyridazine as a Privileged Structure: An Updated Review on Anticancer Activity of Pyridazine Containing Bioactive Molecules. *Eur. J. Med. Chem.* **2021**, *209*, 112946. https://doi.org/10.1016/j.ejmech.2020.112946.

(97) Chalem, F.; Farias, P.; Lizarazo, H.; Peña, P. Diftalone: A New Non-Steroidal Anti-Inflammatory Agent: Comparative Study with Phenylbutazone in the Treatment of Rheumatoid Arthritis. *J. Int. Med. Res.* **1977**, *5* (1), 18–25. https://doi.org/10.1177/030006057700500103.

(98) Morita, O.; Kushida, H.; Kunihara, M. Effects of U-97018 on Pressor Responses to Intracerebroventricularly Administered Angiotensin II in Conscious Normotensive Rats. *J. Cardiovasc. Pharmacol.* **1995**, *25* (6), 880–887. https://doi.org/10.1097/00005344-199506000-00005.

(99) Kiledal, S. A.; Jourdain, R.; Vellalath, S.; Romo, D. Multicomponent Enantioselective Synthesis of Tetrahydropyridazinones Employing Chiral α,β-Unsaturated Acylammonium Salts. *Org. Lett.* **2021**, *23* (17), 6622–6627. https://doi.org/10.1021/acs.orglett.1c02044.

(100) Dey, R.; Kumar, P.; Banerjee, P. Lewis Acid Catalyzed Annulation of Cyclopropane Carbaldehydes and Aryl Hydrazines: Construction of Tetrahydropyridazines and Application Toward a One-Pot Synthesis of Hexahydropyrrolo[1,2- b]Pyridazines. *J. Org. Chem.* **2018**, *83* (10), 5438–5449. https://doi.org/10.1021/acs.joc.8b00332.

(101) Momiyama, N.; Tabuse, H.; Noda, H.; Yamanaka, M.; Fujinami, T.; Yamanishi, K.; Izumiseki, A.; Funayama, K.; Egawa, F.; Okada, S.; Adachi, H.; Terada, M. Molecular Design of a Chiral Brønsted Acid with Two Different Acidic Sites: Regio-, Diastereo-, and Enantioselective Hetero-Diels-Alder Reaction of Azopyridinecarboxylate with Amidodienes Catalyzed by Chiral Carboxylic Acid-Monophosphoric Acid. *J. Am. Chem. Soc.* **2016**, *138* (35), 11353–11359. https://doi.org/10.1021/jacs.6b07150.

(102) Attwood, M. R.; Hassall, C. H.; Kröhn, A.; Lawton, G.; Redshaw, S. The Design and Synthesis of the Angiotensin Converting Enzyme Inhibitor Cilazapril and Related Bicyclic Compounds. *J. Chem. Soc., Perkin Trans. 1* **1986**, 1011–1019. https://doi.org/10.1039/P19860001011.

Die approbierte gedruckte Originalversion dieser Dissertation ist an der TU Wien Bibliothek verfügbar.
The approved original version of this doctoral thesis is available in print at TU Wien Bibliothek.

6 Aim of the Thesis

This thesis aims at developing and evaluating novel organocatalysts for various asymmetric reactions. To introduce the topic of organocatalysis, recent advancements in organocatalytic transfer hydrogenation were investigated. The initial research focused on devising a novel catalyst concept for the asymmetric transfer hydrogenation of cyclic enones. Several bulky racemic phosphoric acids were assessed as counteranions in combination with slightly modified, chiral amino acids. The objective was to validate the catalyst concept and demonstrate its efficacy by screening various cyclic enones to achieve high yields and enantioselectivities across the entire scope.

To expand the concept further, the catalyst framework was adapted to incorporate achiral phosphoric acids as counteranions fora broader range of reactions, including the well-documented asymmetric epoxidation and aziridination of enones. Additionally, the aza-Michael/aldol reaction of cyclic enones and Michael-induced ring closure/aldol were developed and evaluated with the new catalyst system. The goal here was to demonstrate the generality and high performance of the newly developed catalyst in various reactions.

Building upon the aza-Michael/aldol cyclization, a new methodology was established to synthesize chiral diazabicycloalkanes using a diamine-type catalyst. The objective was to successfully synthesize this novel moiety with a broad substrate and reagent scope, with a primary focus on achieving high enantioselectivities of the target molecule.

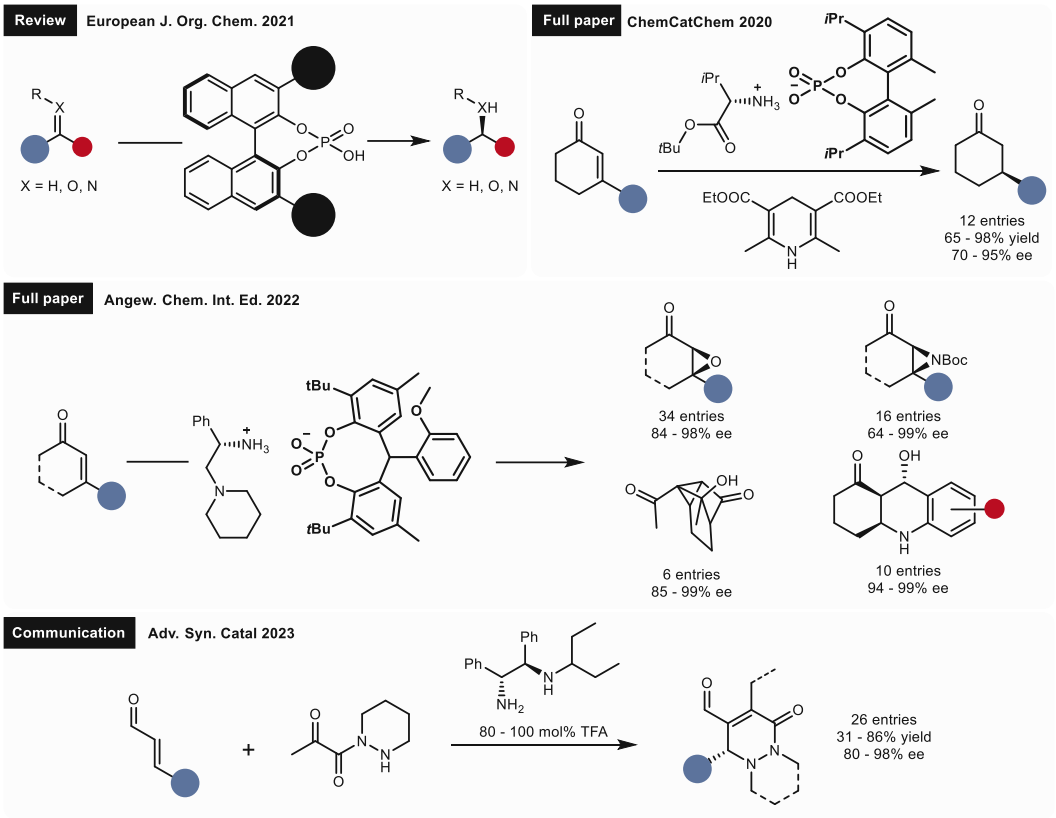


Figure 5. Overview of all projects.

Die approbierte gedruckte Originalversion dieser Dissertation ist an der TU Wien Bibliothek verfügbar.
The approved original version of this doctoral thesis is available in print at TU Wien Bibliothek.
TU Bibliothek Your knowledge hub WIEN

7 Chiral Phosphoric Acids as Versatile Tools for Organocatalytic Asymmetric Transfer Hydrogenations

Asymmetric catalysis is pivotal in modern chemistry, with the asymmetric hydrogenation of unsaturated compounds being particularly noteworthy due to its extensive industrial applications.[84] Inspired by natural oxidoreductases, the introduction of 1,4-dihydropyridines (Hantzsch esters or HEs) as biomimetic hydrogen sources marked the advent of organocatalytic asymmetric transfer hydrogenations (ATH).[85] Notably, these transformations require neither gaseous H_2 nor costly, toxic metal sources, rendering them highly tolerant to air and moisture, simplifying operations, and enhancing safety. Regarding the catalyst, chiral phosphoric acids (CPAs) have gained prominence as potent organocatalysts, thanks to pioneering work by Terada[86], Akiyama[53] and List[36]. These catalysts have found a wide array of applications in both organo- and transition metal catalysis. In the past decade, numerous chiral Brønsted phosphoric acids with similar structural features have been developed. Major structural similarities are the chiral BINOL backbone and large substituents adjacent to the phosphoric acid moiety as essential features for achieving high enantioselectivities in the process.[87,88] From the substrate perspective, this catalyst class is effective in reducing various sp^2-carbon functionalities, including C=C, C=O, and C=N bonds of even complex molecules with high functional group tolerance. In this review, an in-depth examination of recent advancements in the domain of organocatalytic asymmetric transfer hydrogenations has been conducted, encompassing a wide range of substrates and hydrogen sources, all catalyzed by chiral Brønsted phosphoric acids.

The following manuscript is presented in this chapter:

Scharinger, F; Pálvölgyi, Á. M.; Schnürch, M.; Bica-Schröder, K. Chiral Phosphoric Acids as Versatile Tools for Organocatalytic Asymmetric Transfer Hydrogenations. *European J. Org. Chem.* **2021**, *2021* (38), 5367–5381. https://doi.org/10.1002/ejoc.202100894.

As a main author with equal contributions, I authored several chapters and created the corresponding graphical elements for the manuscript.

Die approbierte gedruckte Originalversion dieser Dissertation ist an der TU Wien Bibliothek verfügbar.
The approved original version of this doctoral thesis is available in print at TU Wien Bibliothek.

EurJOC
European Journal of Organic Chemistry

Minireviews
doi.org/10.1002/ejoc.202100894

Chemistry Europe
European Chemical Societies Publishing

Check for updates

Special Collection

Chiral Phosphoric Acids as Versatile Tools for Organocatalytic Asymmetric Transfer Hydrogenations

Ádám Márk Pálvölgyi[+],[a] Fabian Scharinger[+],[a] Michael Schnürch,*[a] and Katharina Bica-Schröder*[a]

Herein, recent developments in the field of organocatalytic asymmetric transfer hydrogenation (ATH) of C=N, C=O and C=C double bonds using chiral phosphoric acid catalysis are reviewed. This still rapidly growing area of asymmetric catalysis relies on metal-free catalysts in combination with biomimetic hydrogen sources. Chiral phosphoric acids have proven to be extremely versatile tools in this area, providing highly active and enantioselective alternatives for the asymmetric reduction of α,β-unsaturated carbonyl compounds, imines and various heterocycles. Eventually, such transformations are more and more often used in multicomponent/cascade reactions, which undoubtedly shows their great synthetic potential and the bright future of organocatalytic asymmetric transfer hydrogenations.

1. Introduction

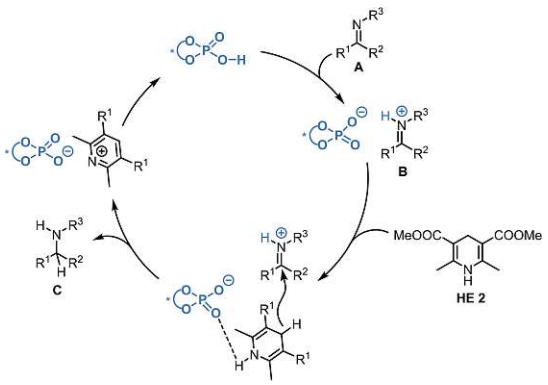
The synthesis of optically active products by asymmetric catalysis plays a crucial role in modern chemistry.[1] In this field, the asymmetric hydrogenation of unsaturated compounds is of special interest, featuring an extreme broad range of industrial applications.[2] Inspired by natural oxidoreductases, the introduction of 1,4-dihydropyridines (Hantzsch esters, **HE**s) as biomimetic hydrogen sources opened the era of organocatalytic asymmetric transfer hydrogenations (ATH).[3–4] As neither gaseous H_2, nor expensive and/or toxic metal sources are required, such asymmetric transformations show great air and moisture tolerance which results in operational simplicity and additionally safer processes. In light of the growing awareness for metal-free, safe and sustainable chemical reactions, the field of organocatalytic ATH received rapidly increasing attention in the last 15 years.

Since the pioneering discoveries by the group of Terada[5] and Akiyama,[6] chiral phosphoric acids (**CPA**s) are amongst the most powerful organocatalysts, and they found a tremendously broad range of applications in organo- and transition-metal-catalysis.[7–9]

While Hantzsch dihydropyridines (**HE**s) are indeed to date the most frequently used hydrogen sources for organocatalytic ATH reactions,[10–12] a few alternative reductants have been developed as well. Bearing a substituent geminal to the transferable hydrogen, benzothiazolines (**BZT**s) and indolines (**IND**s) are highly tunable hydrogen sources as their catalytic activity and selectivity highly depends on the fine tuning of their electronic and steric properties.[13,14] Moreover; ATH reactions using other NADH-analogues like phenanthridines (**PD**s) as well as borane-mediated ATH reactions in combination with CPAs have been also reported. An overview of the most frequently used chiral phosphoric acids and hydrogen sources is depicted in Figure 1.

The typical reaction mechanism of such asymmetric transfer hydrogenations is illustrated with the ATH of ketimine **A** and **HE 2** (Scheme 1). The phosphoric acid acts both as a Brønsted-acid and as a Lewis-base therefore it plays a dual role in the reaction: it activates the substrates *via* protonation generating the iminium species **B**; meanwhile, as a H-bond acceptor it can also direct the hydrogen source, facilitating the subsequent hydride transfer. After the formation of the iminium species **B**, the hydride transfer yields the enantioenriched amine product **C** and the pyridinium salt, which can undergo proton transfer to regenerate the phosphoric acid (Scheme 1).

This Minireview aims to give an overview on the field of chiral phosphoric acid catalyzed asymmetric organocatalytic



Scheme 1. Typical reaction mechanism of CPA-catalyzed asymmetric transfer hydrogenations, illustrated with the ATH of ketimine **A**.

[a] Á. M. Pálvölgyi,[+] F. Scharinger,[+] Prof. M. Schnürch, Prof. K. Bica-Schröder
Institute of Applied Synthetic Chemistry
TU Wien
Getreidemarkt Vienna, 9/163 1060 Wien Austria
E-mail: michael.schnuerch@tuwien.ac.at
katharina.schoeder@tuwien.ac.at

[+] These authors contributed equally to this manuscript.

Special Collection Part of the "Organocatalysis" Special Collection.

© 2021 The Authors. European Journal of Organic Chemistry published by Wiley-VCH GmbH. This is an open access article under the terms of the Creative Commons Attribution License, which permits use, distribution and reproduction in any medium, provided the original work is properly cited.

Die approbierte gedruckte Originalversion dieser Dissertation ist an der TU Wien Bibliothek verfügbar.
The approved original version of this doctoral thesis is available in print at TU Wien Bibliothek.
TU Bibliothek Your knowledge hub

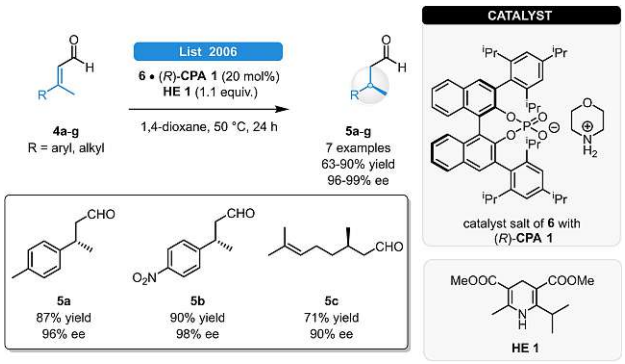
© 2021 The Authors. European Journal of Organic Chemistry published by Wiley-VCH GmbH

ATH reactions with emphasis on recent developments since 2014.

2. Reduction of C=C and C=O Double Bonds

Independently and parallel with the developments of iminium catalysis, in 2005, Mayer and List reported an alternative approach for the ATH of enals (Scheme 2).[15] The combination of morpholine (**6**) with (*R*)-**CPA 1** (also known as (*R*)-TRIP) resulted in high catalytic activities and enantioselectivity for the ATH of 3-alkylcinnamaldehyde derivatives (**5a–g**). Moreover, sterically non-hindered aliphatic substrates could be also efficiently reduced. The reaction was found to be stereoconvergent as the pure (*E*)- and (*Z*)-isomer, as well as the diastereomeric mixture of the enal substrates all resulted in the same product antipode.

The same catalytic concept could be later extended to the ATH of enones (Scheme 3, top).[16] The catalyst salt of L-valine *tert*-butyl ester ((*S*)-**9**), together with the chiral phosphoric acid



Scheme 2. ATH of enals *via* asymmetric counteranion directed catalysis.

(*R*)-**CPA 1** provided >90% yields and excellent enantioselectivity for the ATH of various 3-substituted cyclic enones (**7a–j**). The (*S*)-**CPA 1** gave significantly inferior results, indicating a sharp difference between the matched and mismatched ion-



Ádám Márk Pálvölgyi received his master's degree in organic chemistry in 2017 from the Budapest University of Technology and Economincs. In 2021, he obtained his PhD degree from the Technical University of Vienna (TU Wien) under the supervision of Prof. Katharina Schröder. He is currently a post-doctoral researcher in the same group. His current research focuses on asymmetric organocatalysis and photocatalysis.



Fabian Scharinger carried out his Master's degree in the group of Katharina Schröder in 2019 at the Technical University of Vienna under the co-supervision of Ádám Márk Pálvölgyi. He then continued with his PhD in the same group under the supervision of Prof. Katharina Schröder, focusing on the development of novel organocatalysts and their application in asymmetric synthesis.



Michael Schnürch has carried out his PhD thesis in the group of Prof. Peter Stanetty and received his PhD in 2005 from TU Wien. He was then Post-Doc with Prof. Dalibor Sames at the Columbia University in New York City (as Erwin Schrödinger fellow) and conducted research in the field of decarbonylative coupling reactions and sp^3 C–H activation. After his return, he became Assistant Professor at TU Wien and completed his habilitation in 2013. He was promoted to privatdozent and in 2016 to Associate Professor for Organometallic Chemistry. Additionally, he was the chair of the COST Action CHAOS (C–H Activation in Organic Synthesis) and the European Symposium on Organic Chemistry (ESOC 2019) in Vienna. His research interests are located in the field of synthesis of heterocyclic compounds for the manipulation of cell differentiation and GABAA receptors, C–H activation of sp^3 centers, the substitution of gaseous reagents for solid alternatives, green chemistry, and flow chemistry.



Katharina Schröder (born K. Bica) received her PhD in Technical Chemistry from TU Wien in 2006. After post-doctoral stays in Belfast, UK and Copenhagen, DK, she returned to TU Wien to establish her independent research career focused on green and sustainable chemistry. In 2021, she was appointed Full Professor for Sustainable Chemistry. Katharina Schröder's research interests are based on sustainable organic chemistry, with a special focus on (i) novel catalytic processes for asymmetric synthesis, (ii) on carbon capture and valorization techniques (CCU), particularly on photocatalytic CO_2 activation and (iii) on the recovery of valuable ingredients from industrial waste streams using advanced fluid technologies.

Die approbierte gedruckte Originalversion dieser Dissertation ist an der TU Wien Bibliothek verfügbar.
The approved original version of this doctoral thesis is available in print at TU Wien Bibliothek.
TU Bibliothek Your knowledge hub WIEN

© 2021 The Authors. European Journal of Organic Chemistry published by Wiley-VCH GmbH

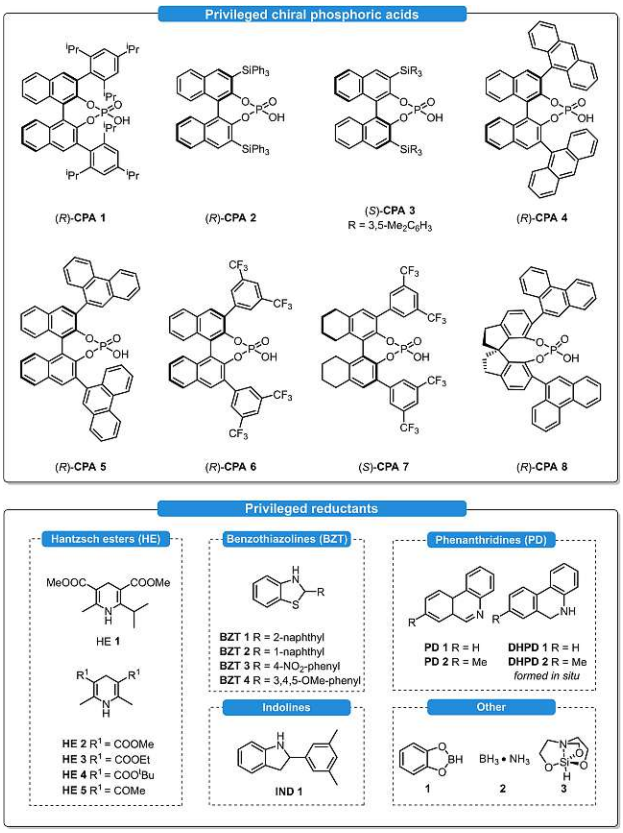
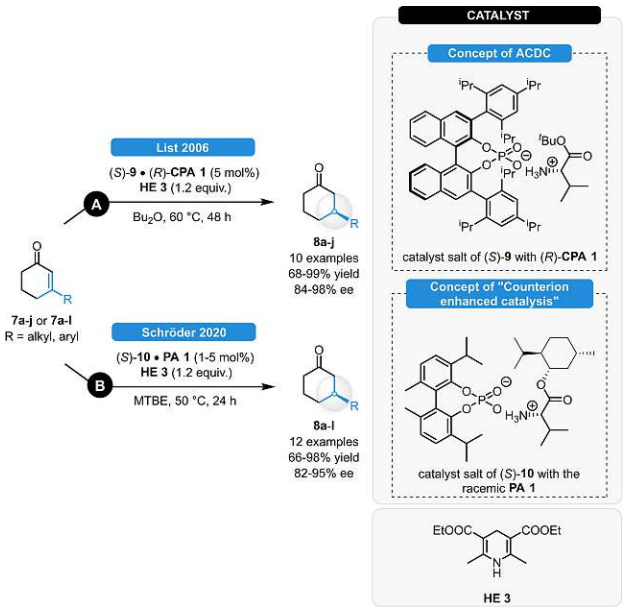


Figure 1. The most typically used chiral phosphoric acids (top) and hydrogen sources (bottom) for asymmetric transfer hydrogenations.

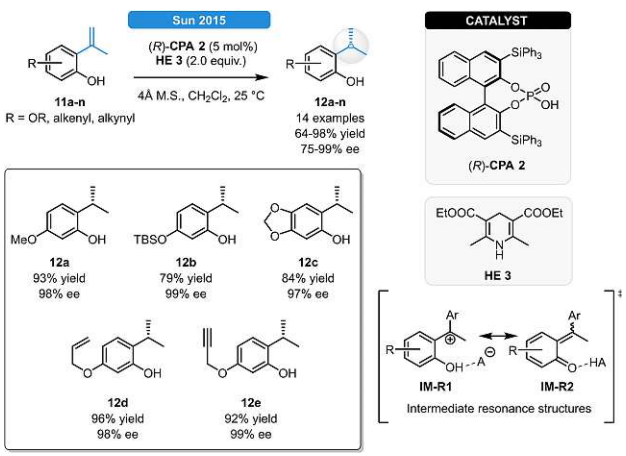


Scheme 3. ATH of cyclic enones *via* asymmetric counteranion directed catalysis (**A**) and *via* "counterion enhanced catalysis" (**B**).

pairing. Based on these discoveries, the general concept of asymmetric counteranion directed catalysis (ACDC) emerged; referring to any asymmetric catalytic reaction in which the enantiodiscrimination is induced through the tight ion-pairing of a cationic intermediate with an enantiomerically pure anion.[17]

We recently showed that the novel concept of "Counterion Enhanced Catalysis" can be also very effective for asymmetric transfer hydrogenations (Scheme 3, bottom).[18] As a conceptual spin-off of the ACDC approach, we relied on rather simple and cheap chiral frameworks composing of amino-acid esters, in combination with achiral or racemic phosphoric acids. After optimization, using the catalyst salt of (*S*)-**10** with the isopropyl-substituted, racemic **PA 1**, similarly high yields and enantioselectivities (82–95 % ee) as compared to ACDC for the ATH of various cyclic enones were observed. Given the significantly cheaper, easier and faster catalyst synthesis, as well as the natural origin of both catalyst components; this methodology could provide a valuable alternative to the current state-of-the-art and it might be also a useful tool for a significantly broader range of future applications.

In 2015 Sun *et al.* reported an elegant strategy for the ATH of electron rich terminal double bonds (Scheme 4). The phosphoric acid (*R*)-**CPA 2**, together with Hantzsch ester **HE 3** provided a convenient access to 1,1-diarylethanes (**12a–n**) in excellent yield and up to >99 % ee.[19] Full chemoselectivity towards the reduction of the terminal alkene bond was observed as various functional groups including silyl ethers, alkenes, alkynes and thioethers were all well tolerated (Scheme 4). As significantly worse results were obtained for styrene substrates without the *ortho*-hydroxyl functionality, the phenolic OH-group is believed to act as a directing group: initial protonation of the substrate **11a–n** results in the formation of an intermediate – described with its extreme resonance **IM-R1** and **IM-R2** forms – in which the (*R*)-**CPA 2** remains in close proximity to the substrate by means of H-bonding with the OH-group as a key factor for the high stereocontrol. DFT calculations showed that even though the (*Z*)-isomer is less stable, it forms preferentially, which was in accordance with the experimentally observed absolute stereochemistry.



Scheme 4. ATH of electron rich stryrenes (left) and the plausible intermediates (right bottom).

Die approbierte gedruckte Originalversion dieser Dissertation ist an der TU Wien Bibliothek verfügbar.
The approved original version of this doctoral thesis is available in print at TU Wien Bibliothek.
TU Bibliothek Your knowledge hub WIEN

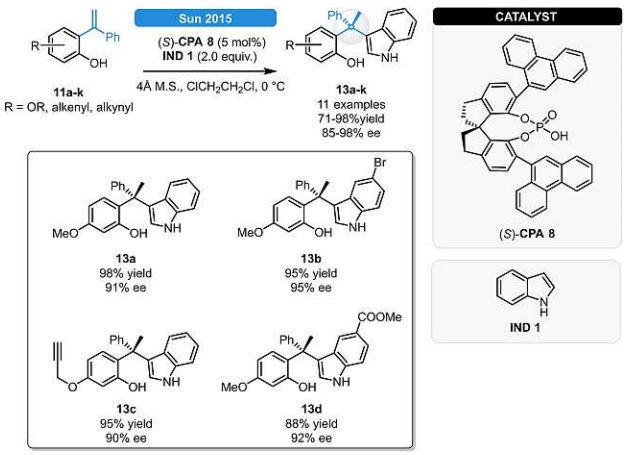
© 2021 The Authors. European Journal of Organic Chemistry published by Wiley-VCH GmbH

When replacing Hantzsch esters with indole nucleophiles, asymmetric hydroarylations could be carried out with high level of stereocontrol (Scheme 5).[19] The best results were obtained with the SPINOL-derived phosphoric acid (*S*)-**CPA 8** resulting in **13a–k** in >90% yields and ee. Eventually, the potential biological activity for either of the product classes was evaluated based on their cytotoxicity on human lung cancer cells, providing IC_{50} values in the low micromolar region.

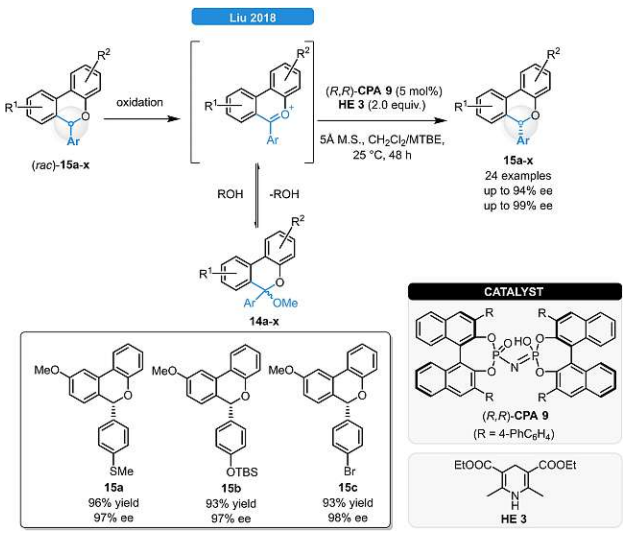
The group of Liu reported a highly enantioselective method for the synthesis of 6*H*-benzo[c]chromenes *via* the ATH of ketals by a redox-deracemization strategy (Scheme 6):[20] The oxidation of racemic **15a–x** and the subsequent enantioselective oxocarbenium-reduction led to the formation of various chromenes. While traditional CPA-catalysis failed to achieve high enantioselectivity and resulted only in 10–55% ee, the C_2-symmetric imidodiphosphoric acid (*R*,*R*)-**CPA 9** in the solvent mixture of CH_2Cl_2 and MTBE provided excellent stereoselectivity for the ATH of *rac*-**15a**. Under the optimized reaction conditions, various α-substituted 6*H*-benzo[c]chromenes bearing different substituents on either of the aromatic rings (*rac*-**15a–x**) could be readily reduced in 86–97% ee.

The asymmetric reduction of C=O double bonds is predominantly achieved *via* transition-metal-catalysis;[21–25] however, a few organocatalytic variants were also reported in the last decade. Antilla and co-workers developed the first CPA-catalyzed ATH reaction of prochiral ketones.[26] The phosphoric acid (*R*)-**CPA 4**, in combination with catecholborane and DMAP resulted in excellent enantioselectivity for the reduction of acetophenone derivatives bearing electron donating and withdrawing groups; meanwhile, moderate selectivity was observed for aliphatic analogues (e.g.: **17e**). Based on ^{11}B NMR studies, it is believed that a chiral boron species is formed. As this features both a Lewis acidic and a Lewis basic moiety, it can simultaneously coordinate to the DMAP and increase the nucleophilicity of an unreacted catecholborane, resulting in the transition state depicted in Scheme 7. Very recently, the authors reported a similar strategy for the C=C reduction of *trans*-chalcones, resulting in 78–96% ee.[27]

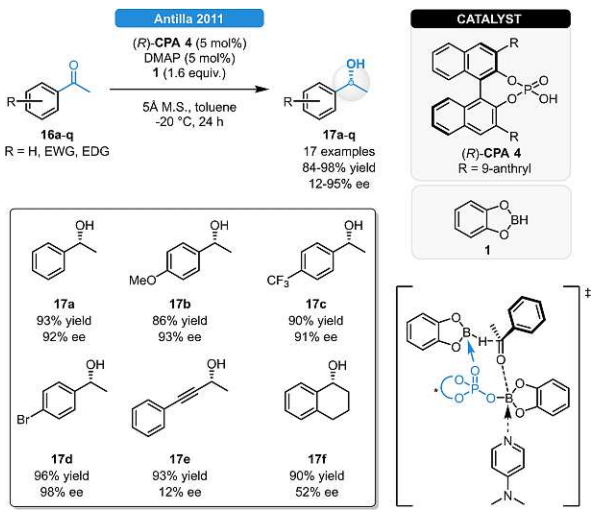
Recently, Yang *et al.* successfully applied CPAs for the asymmetric reduction of bulky aryl ketones using ammonia borane as hydrogen source (Scheme 8). The corresponding secondary alcohols (**19a–r**) were obtained in high yields and in moderate enantioselectivities of 43–77% ee. The CPA could be *in situ* continuously regenerated with the assistance of water and excess of ammonia borane allowing to use only 0.5 mol% of (*S*)-**CPA 3**. According to DFT studies, the phosphoric acid promotes the double hydrogen transfer between the ammonia borane and the ketone, as the transfer of the hydridic and protic hydrogens take place simultaneously through a pericyclic six-membered transition state as a source of asymmetric induction.[28]



Scheme 5. Asymmetric hydroarylation of electron rich stryrenes.



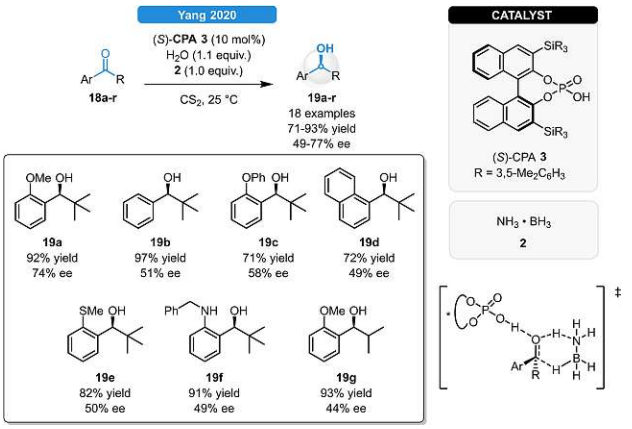
Scheme 6. C_2-symmetric imidodiphosphoric acid-catalyzed ATH of aromatic ketals.



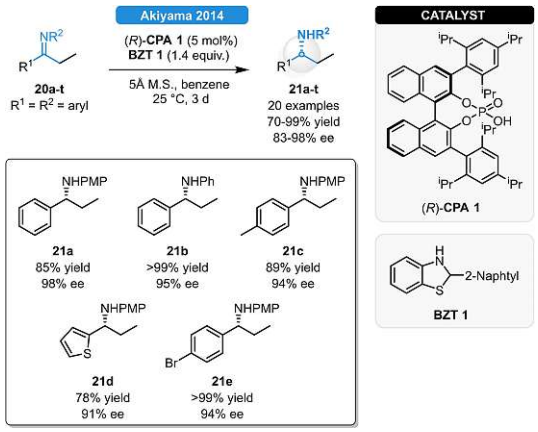
Scheme 7. CPA-catalyzed asymmetric transfer hydrogenation of prochiral ketones.

Die approbierte gedruckte Originalversion dieser Dissertation ist an der TU Wien Bibliothek verfügbar.
The approved original version of this doctoral thesis is available in print at TU Wien Bibliothek.
TU Bibliothek Your knowledge hub WIEN

© 2021 The Authors. European Journal of Organic Chemistry published by Wiley-VCH GmbH



Scheme 8. A CPA-catalyzed asymmetric transfer hydrogenation of bulky aryl ketones.



Scheme 9. Asymmetric transfer hydrogenation of ethyl ketimines.

3. Reduction of C=N Double Bonds

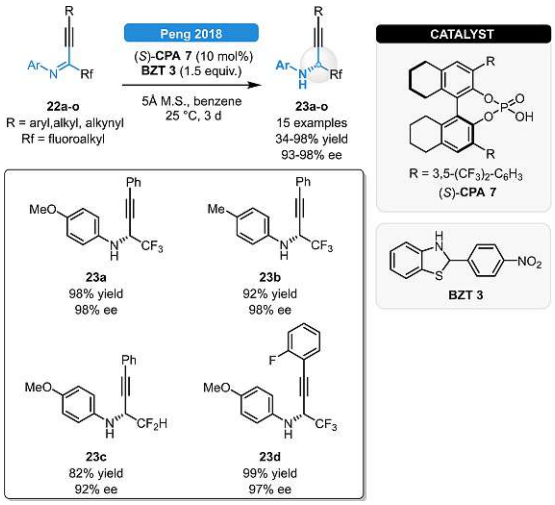
Since the independent pioneering works of Rueping,[29] List,[30] and MacMillan;[31] the synthesis of optically active amines and *N*-heterocycles with the aid of CPAs represents the most extensively studied field of organocatalytic ATH reactions. Herein, recent advancements starting from 2014 will be discussed.

3.1. The ATH of imine derivatives

Based on their previous reports with benzothiazoline-type hydrogen donors, the group of Akiyama reported the ATH of ethyl ketimines as an extension of their previous studies.[32] While traditional Hantzsch esters failed to achieve high yields and enantioselectivity as only up to 53% ee was observed, benzothiazolines provided much better results. After fine tuning the reductant's steric properties, a series of ethyl ketimines (**20a–t**) could be reduced in 70–99% yield and in 90–98% ee (Scheme 9). The different catalytic efficiency of the reductants was examined *via* DFT calculations. This revealed that unlike Hantzsch esters, benzothiazolines exert a significant substituent effect which results in an increased energy difference between the diastereomeric transition states, resulting in significantly higher ee. Eventually, the reaction scope was extended to the reductive amination of aliphatic ethyl ketones, resulting in 70–86% yields and 72–97% ee. Using the same concept, indolines bearing sterically demanding 2-substituents were also found to be suitable hydrogen donors and their catalytic efficiency was demonstrated in the ATH of ketimines as well as for the reductive amination of aliphatic ketones, providing excellent stereocontrol for both substrate classes; meanwhile, the sacrificial hydrogen source could be regenerated *via* treatment with tin powder and HCl in EtOH in 92% yield.[33]

Benzothiazolines were also found to be suitable hydrogen sources for the ATH of alkynyl imines. Peng *et al.* reported a CPA-catalyzed strategy for the synthesis of fluorinated propargylamines (Scheme 10). The best results were obtained using the combination of (*S*)-**CPA 7** and **BZT 3** bearing a *para*-nitrophenyl substituent, as substrates with different electronic properties (**22a–o**) could be reduced with 82–98% yield and >90% ee. Moreover, the propargylamine **23a** was found to be a valuable intermediate for the synthesis of dihydroquinolines.[34] A similar approach was reported by the group of Akiyama for the ATH of aryl-alkynyl-substituted imines, as a small pool of α-trifluoromethyl propargylamines was prepared in excellent, 93–98% enantioselectivity.[35] Both procedures were chemoselective as not even partial reduction of the C≡C bond was observed; moreover, the nature of the hydrogen donor was found to be crucial as no product formation was observed with Hantzsch esters in neither cases.

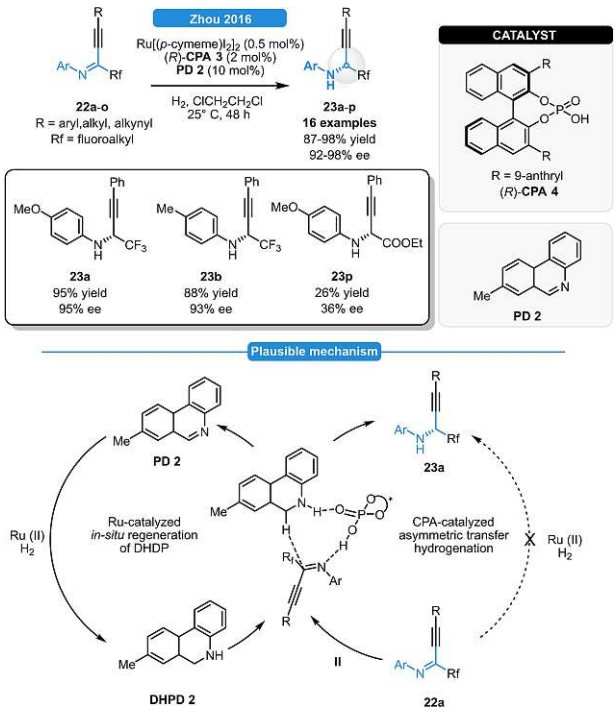
The chemoselective ATH of aryl-alkynyl-imines could be also performed *via* biomimetic reduction relying on Ru/chiral phosphoric acid catalysis in the presence of H_2 as terminal hydrogen source (Scheme 11).[36] In 2016, Zhou *et al.* reported a



Scheme 10. Asymmetric transfer hydrogenation of fluorinated alkynyl ketimines.

© 2021 The Authors. European Journal of Organic Chemistry published by Wiley-VCH GmbH

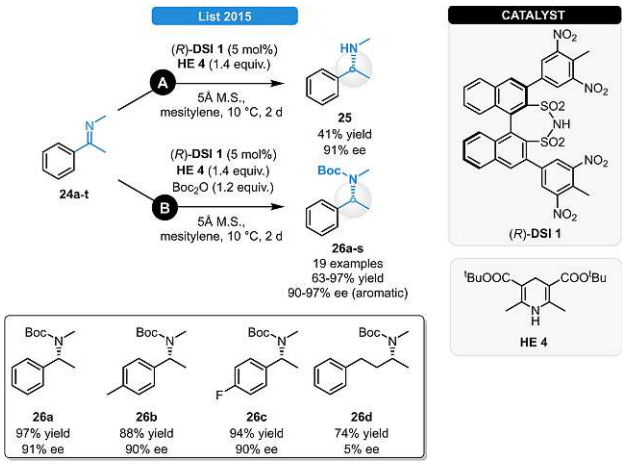
Die approbierte gedruckte Originalversion dieser Dissertation ist an der TU Wien Bibliothek verfügbar.
The approved original version of this doctoral thesis is available in print at TU Wien Bibliothek.
TU Bibliothek Your knowledge hub WIEN



Scheme 11. Asymmetric transfer hydrogenation of fluorinated alkynyl ketimines *via* Ru/CPA combined catalysis.

highly efficient procedure for the synthesis of fluorinated propalgylamines by such elegant method, which also allowed to use only a catalytic amount of biomimetic reductant. After parameter optimization, various aromatic propalgylimines (e.g.: **22a–b**) could be successfully reduced in high yields and in 92–98% ee by using catalytic amount of Ru[(*p*-cymeme)I_2]$_2$, (*R*)-CPA **4** and phenanthridine PD **2** in the presence H_2 as terminal hydrogen source. The reaction was found to be completely chemoselective to C=N reduction; meanwhile, the importance of the Rf-group became also evident as the **23p** was obtained only in moderate yield and ee. The plausible reaction mechanism comprises of two cycles. At first, **PD 2** undergoes reduction *via* Ru/H_2, affording **DHDP 2**. Then, the ATH of the substrate (e.g.: **22a**) with **DHDP 2** in the presence of the organocatalyst (*R*)-**CPA 4** provides the propalgylamine products (e.g.: **23a**). The high level of asymmetric induction could be attributed to the extreme slow direct substrate reduction *via* Ru/H_2.

While the aforementioned strategies all required an *N*-aryl imine for high levels of asymmetric induction, several advances have been reported later for the ATH of *N*-alkyl analogues (Scheme 12). Addressing this issue, List and co-workers initially investigated the ATH of *N*-methyl imine **24a**.[37] Only moderate catalytic activities and poor enantioselectivity (<30% ee) was observed when using CPA catalysis; however, this was significantly improved when a chiral disulfonimide (DSI) was applied instead. The Brønsted acid (*R*)-**DSI 1** afforded the desired product in excellent stereocontrol, albeit only in a moderate yield of 41% as the salt formation with the product **25** resulted in continuous catalyst deactivation. (Scheme 12, pathway **A**). In



Scheme 12. Chiral DSI-catalyzed asymmetric transfer hydrogenation of *N*-alkyl imines.

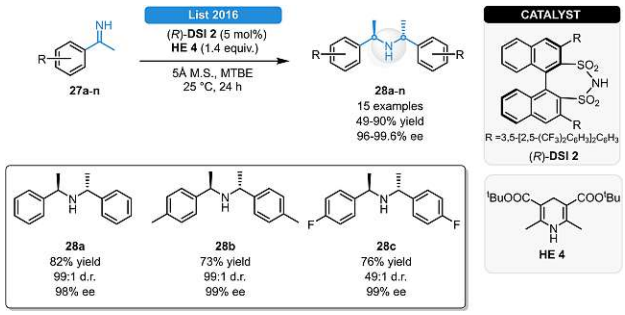
order to solve this problem, the amine product **25** was *in situ* derivatized with Boc_2O (Scheme 12, pathway **B**), yielding **26a** in excellent yield and ee. With this latter method, various aromatic *N*-alkyl imines could be successfully reduced in high yields and enantioselectivities (**26a–s**); however, *ortho* and *meta* substitutions and aliphatic groups were not well tolerated, resulting in close-to-racemic products (e.g.: **26d**). Providing synthetic utility for the optically active products, APIs like the antianginal (*R*)-Fendiline as well as (*S*)-Rivastigmine, a drug for Parkinson treatment were also synthesized. Based on the same methodology, the reduction of *N*-alkyl aryl imino esters was realized by Marsden *et al.* After the subsequent removal of the Boc-group, various *N*-alkylated arylglycines were synthetized in 67–95% yield and 50–90% ee. Offering a great synthetic potential, diverse peptide building blocks and *N*-heterocycles were also prepared after further derivatizations.[38] Detailed NMR studies revealed that in case of the ATH of *N*-alkylimines, several different complexation modes occur when using CPAs, meanwhile only the (*E*) and (*Z*) binary complexes are formed in those reactions relying of DSI-catalysis, which explains the superiority of the latter catalyst class for these transformations.[39]

Relying on chiral DSI-catalysis, the List group reported the synthesis of C_2-symmetric secondary amines *via* reductive condensation of N–H imines (Scheme 13). Using the acid (*R*)-**DSI 2** and Hantzsch ester **HE 4**, a series of optically active aromatic C_2-symmetric secondary amines (**28a–n**) were prepared in moderate to good yields and in excellent stereocontrol. Without desiccant, partial hydrolysis of the products was observed resulting in inferior reactivity, indicating the important role of the molecular sieve in trapping the ammonia byproduct.[40]

Reductive amination provides another strategy for the synthesis of secondary or tertiary amines. It was already demonstrated by MacMillan and List in 2006, that the reduction of *in situ* formed imines can be achieved in a highly enantioselective fashion both for aldehyde and ketone substrates.[31,41]

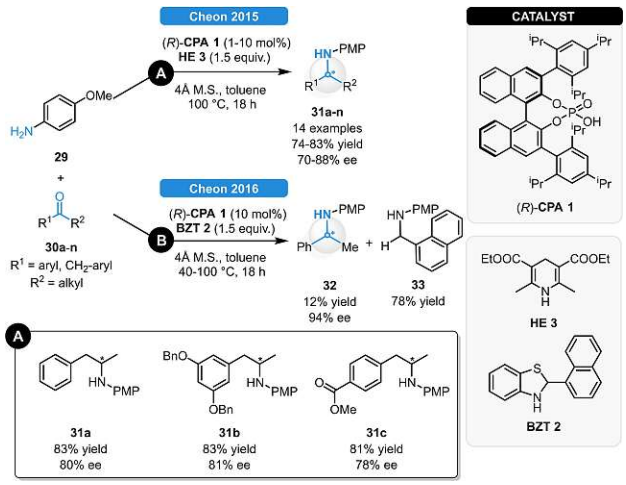
Die approbierte gedruckte Originalversion dieser Dissertation ist an der TU Wien Bibliothek verfügbar.
The approved original version of this doctoral thesis is available in print at TU Wien Bibliothek.
TU Bibliothek Your knowledge hub WIEN

© 2021 The Authors. European Journal of Organic Chemistry published by Wiley-VCH GmbH

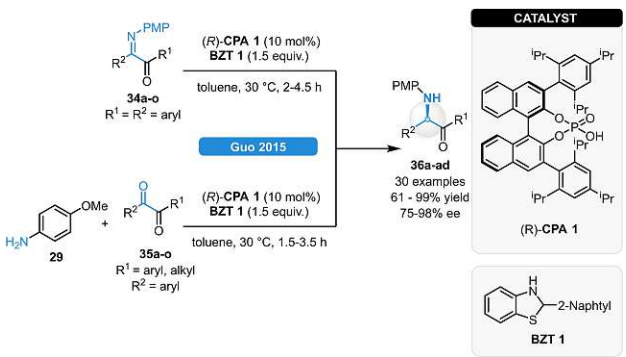


Scheme 13. Chiral DSI-catalyzed asymmetric reductive condensation of *N*–H imines.

In 2015, Cheon *et al.* presented a new method for the synthesis of β-aryl amines (Scheme 14, **A**). The reductive amination of various benzyl methyl ketones bearing substituents with different steric- and electronic properties (**30a**–**n**) could be converted to the desired *N*-PMP β-aryl amines (**31a**–**n**) in good yields and 70–88% ee.[42] Furthermore, gram-scale experiments could be carried out as well using only 1 mol% (*R*)-**CPA 1** without any decrease of the catalytic performance. Later on, the same group investigated the same reaction relying on benzothiazoline reductants (Scheme 14, **B**).[43] While Hantzsch esters provided the corresponding chiral amines **31a**–**n** exclusively; variable ratios of chiral and achiral product (e.g.: **32a** and **33**) were obtained when using benzothiazolines as hydrogen donors. This unexpected phenomenon could be explained with the vulnerability of the reductant to *p*-anisidine. As a competing pathway to the desired ketimine generation, this results in the formation of an aldimine species, which is then reduced with the remaining **BZT 2** to the achiral amine **33** (Scheme 14, **B**).



Scheme 14. Synthesis of β-aryl amines *via* reductive amination, relying on Hantzsch ester (**A**) or benzothiazoline reductants (**B**).

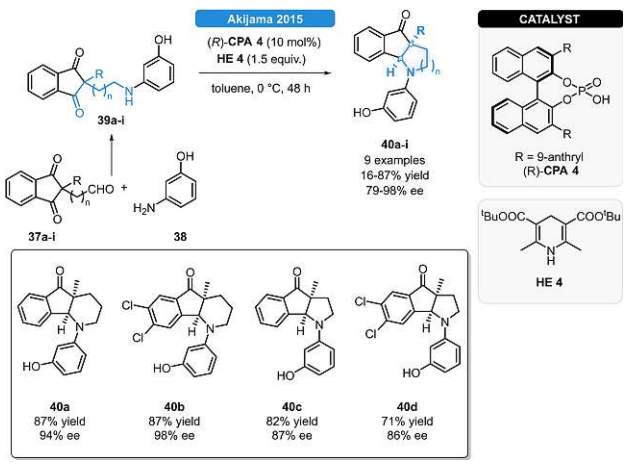


Scheme 15. Strategies for the synthesis of α-amino ketones *via* ATH and reductive amination.

The group of Guo reported the synthesis of optically active α-amino ketones *via* direct ATH of imines and reductive amination of diketones, respectively (Scheme 15).[44] Using (*R*)-**CPA 1** together with the sterically demanding benzothiazoline **BZT 1**, a wide range of substrates could be used for both reaction types, providing a straightforward access to α-amino ketones (**36a**–**ad**) in 61–99% yield and in 75–98% ee. Gram-scale experiments could be carried out with decreased phosphoric acid and Hantzsch ester loadings of 2 mol% and 1.2 equivalent; respectively, without any loss of the catalytic performance.

In 2015, the Akiyama group reported the synthesis of fused piperidine and pyrrolidine-based polyheterocycles *via* desymmetrization-type reductive amination (Scheme 16): The indandione-derived aldehyde **37a**–**i** was reacted with *m*-hydroxyaniline (**38**), followed by CPA-catalyzed reduction. The 9-anthracenyl-substituted (*R*)-**CPA 4**, together with the Hantzsch ester **HE 4** provided excellent enantioselectivities for adducts featuring 5–6 and 5–5 fused skeleton. Significantly worse results were obtained using *m*-anisidine, suggesting that the reaction proceed through a cyclic transition state in which the (*R*)-**CPA 4** activates both the aldehyde and the amine sources *via* hydrogen bonding.[45]

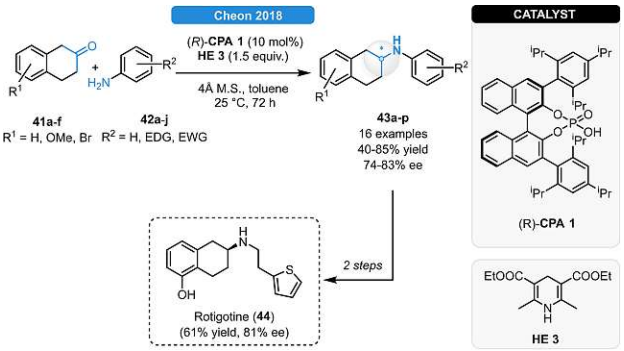
As the first example on the reductive amination of cyclic ketones, Cheon *et al.* disclosed the CPA-catalyzed synthesis of β-aminotetralins (Scheme 17).[46] Various β-tetralones (**41a**–**f**) and anilines (**42a**–**j**) bearing EWG or EDG groups could be



Scheme 16. Synthesis of polyheterocycles *via* reductive amination.

Die approbierte gedruckte Originalversion dieser Dissertation ist an der TU Wien Bibliothek verfügbar.
The approved original version of this doctoral thesis is available in print at TU Wien Bibliothek.
TU Bibliothek Your knowledge hub WIEN

© 2021 The Authors. European Journal of Organic Chemistry published by Wiley-VCH GmbH

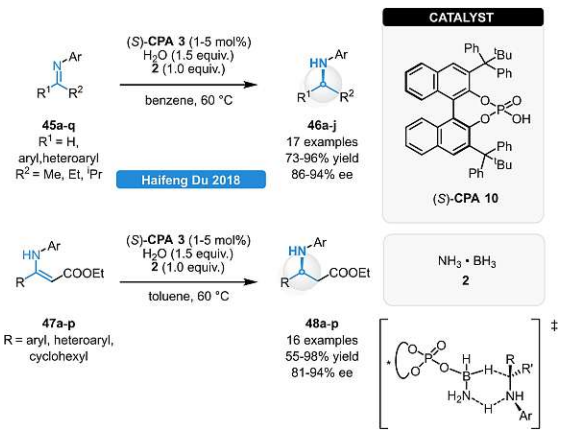


Scheme 17. Reductive amination of β-tetralones.

readily reacted and the corresponding β-aminotetralins (**43 a**–**p**) were obtained in moderate to good yields and in enantioselectivities up to 83 % ee; moreover, the synthetic utility was demonstrated by the enantioselective synthesis of the dopamine agonist drug Rotigotine (**44**).

Using 1-hydrosilatrane (**3**), a novel hydrogen source was introduced for the reductive amination of ketones by Adler *et al.* Even though high yields and up to 84 % ee could be achieved, a rather high phosphoric acid loading of 30 mol% was required.[47]

The chiral ammonia borane composing of the (*S*)-**CPA 10** and ammonia borane (**2**) was also successfully applied for the ATH of β-enamino esters (**45 a**–**q**) and ketimines (**47 a**–**q**) with good yields and good to excellent stereocontrol (Scheme 18). It was proven, that the phosphoric acid acts as a simple Brønsted acid to generate the reactive chiral ammonia borane. Importantly, this species is continuously regenerated with the assistance of water and ammonia borane which also allows to lower the CPA loading below 1 mol%. The hydrogen transfer between the active species and the substrate is realized through a six-membered transition state, as the transfer of the hydridic and protic hydrogens takes place in a simultaneous manner.[48]



Scheme 18. CPA-catalyzed, ammonia borane-mediated ATH of ketimines and β-enamino esters.

4. Asymmetric Transfer Hydrogenation of N-Heterocycles

Enantioenriched (partially) saturated *N*-heterocycles are undoubtedly crucial intermediates both for the agrochemical and pharmaceutical industries (Figure 2).[49,50]

Since the pioneering works of Rueping on the field of chiral phosphoric acid catalyzed ATH of benzoxazines, benzoxazinones and benzothiazines,[51] as well as on the dearomatization of quinolines,[52] quinolones,[53] quinoxalines,[53] and pyridines,[54] various methodologies were published for the asymmetric reduction of *N*-heterocycles. This chapter aims to give an overview on recent advancements starting from 2014.

Serving as a benchmark reactions, various procedures were reported for the asymmetric reduction of 2-phenylquinoline (**49**), relying on classical CPA catalysis in alternative reaction media,[55] bitetralone-modified CPAs,[56] cyclophane- and cathenane-based CPAs,[57–59] bisphosphoric acids,[60,61] as well as using BIFOL-[62] and SPINOL-derivatives (Scheme 19).[63]

Tang *et al.* explored a novel, AOX-mediated (AOX: aza-*o*-xylene) methodology to access dihydroquinolines (Scheme 20).[64] In the presence of a Brønsted acid, the 1,2-dihydroquinoline substrate (**52**) undergoes dearomatization forming a reactive and highly electrophilic aza-*o*-xylene (AOX) intermediate which then readily reacts with the **HE 3** reductant. After optimization, a series of 2,2,4-trimethyltetrahydroquinolines (**53 a**–**k**) were obtained in high yields and in high to excellent enantioselectivities. This method provides not just a mild and metal-free AOX-formation, but it is also beneficial because of the rather simple substrate synthesis.

In 2014, Zhou an co-workers reported the ATH of 2-arylquinoline-3-amines (Scheme 21, top).[65] Even though no reaction was observed when using unprotected or phthaloyl-protected amines, tosyl (Ts) or *tert*-butoxycarbonyl (Boc) protected substrates could be smoothly converted to the

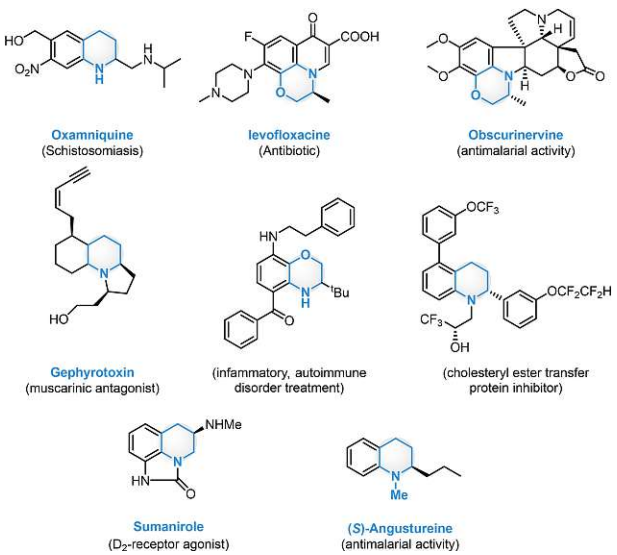
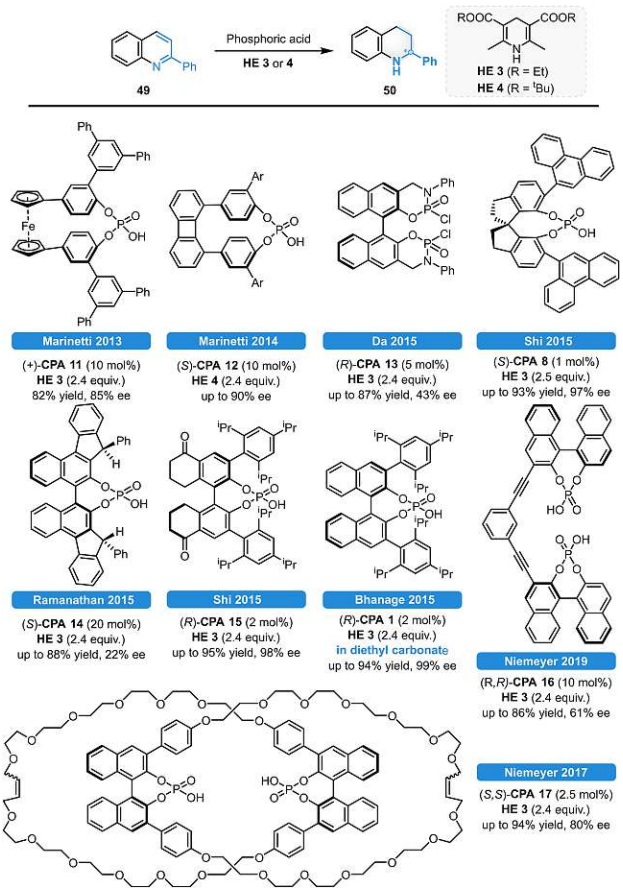


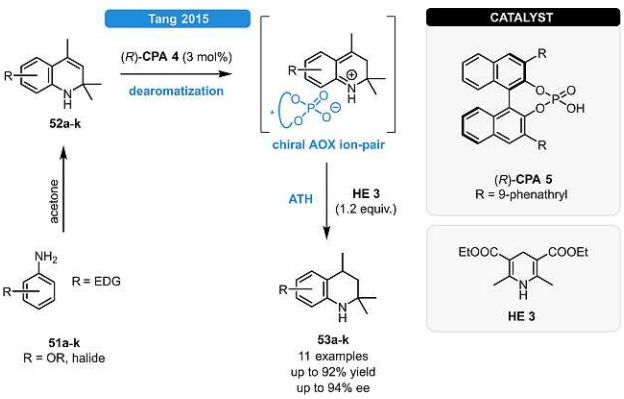
Figure 2. Various biological activity of saturated *N*-heterocycles.

Die approbierte gedruckte Originalversion dieser Dissertation ist an der TU Wien Bibliothek verfügbar.
The approved original version of this doctoral thesis is available in print at TU Wien Bibliothek.
TU Bibliothek Your knowledge hub WIEN

© 2021 The Authors. European Journal of Organic Chemistry published by Wiley-VCH GmbH

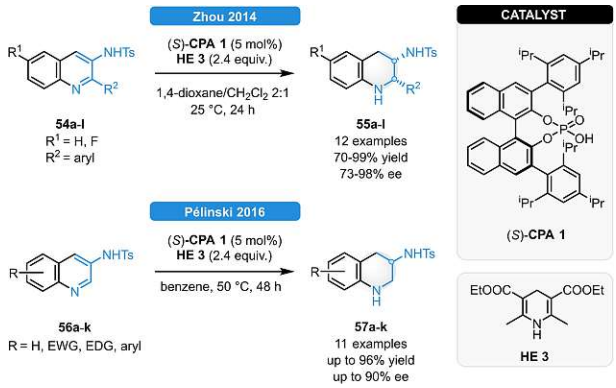


Scheme 19. Recent advances for the ATH of **49**.



Scheme 20. Formation of tetrahydroquinolines *via* AOX-formation.

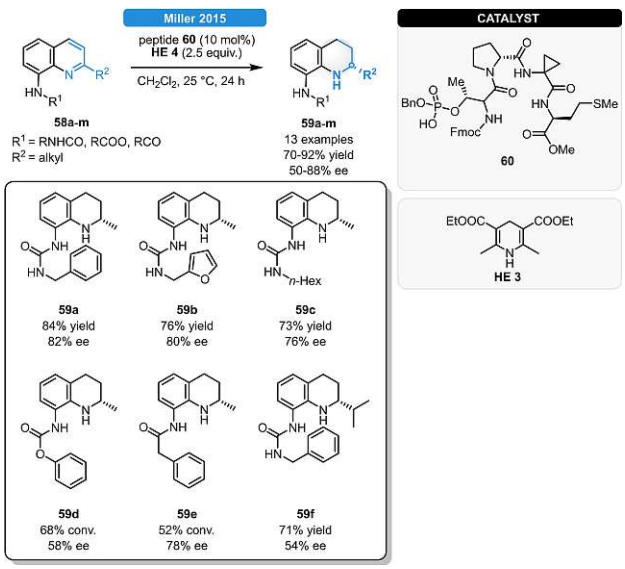
corresponding tetrahydroquinolines. When using (*S*)-**CPA 1**, a series of 2-aryl substituted quinolines (**54a–l**) could be reduced in good yields, excellent *cis* -diastereoselectivity and in 73–98% ee. Importantly, the Ts-group could be easily removed without loss of optical purity. As a result of isotopic labelling, no deuterium could be found at position C2, indicating that the reaction proceeds *via* an endocyclic imine intermediate and dynamic kinetic resolution is also involved for achieving high stereocontol. In analogy to this, the group of Pélinski showed



Scheme 21. ATH of quinoline-3-amines.

that quinoline-3-amines featuring no C2-substituents (**56a–k**) can be successfully reduced in good yields and moderate to excellent ee as well; however, the protection of the amine functionality was found to be crucial for achieving high reactivity and enantioselectivity (Scheme 21, bottom).[66]

Miller *et al.* constructed phosphothreonine (pThr)-containing peptides which could be successfully used as novel CPA scaffolds. In total, 11 different tetrapeptides were screened for the ATH of 8-aminoquinolines and after structural optimization, comparable results to those with (*R*)-**CPA 1** were observed when using the peptide **60**. Various *N*-protected substrates including aromatic and aliphatic ureas, carbamates and amides (**58a–m**) were well tolerated, resulting in 70–92% yield and in 50–88% ee (Scheme 22). Even though such frameworks lack the C_2-symmetry and they also feature numerous rotatable bonds, the still rather high level of asymmetric induction could be rationalized through strong hydrogen bonding interactions between the substrate and the β-turn of the peptide catalyst.[67]



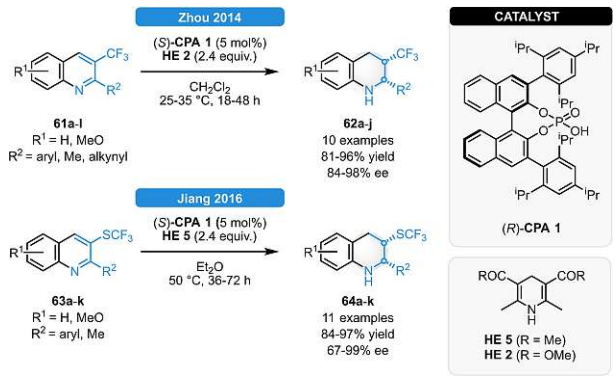
Scheme 22. pThr-containing peptides with CPA scaffold for the ATH of 8-aminoquinolines.

Die approbierte gedruckte Originalversion dieser Dissertation ist an der TU Wien Bibliothek verfügbar.
The approved original version of this doctoral thesis is available in print at TU Wien Bibliothek.
TU Bibliothek Your knowledge hub WIEN

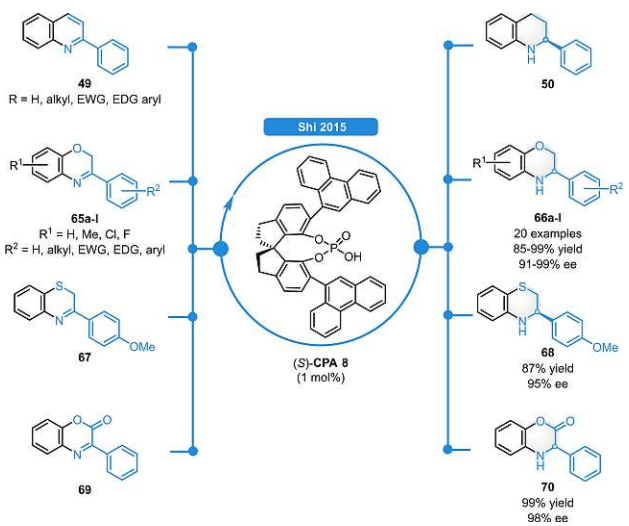
© 2021 The Authors. European Journal of Organic Chemistry published by Wiley-VCH GmbH

Zhou and co-workers investigated the asymmetric reduction of 3-(trifluoromethyl)quinolines.[68] A series of 2-arylsubstituted substrates (**61 a–l**) could be reduced in excellent yield and in 84–98% ee. The presence of an aryl group in the C2-position was found to be crucial for high diastereoselectivity: when using 2-methyl or 2-alkynyl substituents, the corresponding products were obtained in high enantioselectivity; albeit with poor diastereocontrol (Scheme 23, top). Under similar conditions, the ATH of 3-(trifluoromethyl-thio)quinolines (**63 a–l**) was achieved by the Jiang group (Scheme 23, bottom).[69] Tetrahydroquinolines with C2-aryl substituents (**64 a–l**) were formed in high yield and excellent diastereo- and enantioselectivity; meanwhile, the C2-methyl analogue was obtained with inferior d.r. and ee values.

In 2015, Shi *et al.* successfully applied SPINOL-derived phosphoric acids for the ATH of 1,4-benzoxazines.[63] Using (*S*)-**CPA 8**, a broad range of 2-aryl substituted substrates (**65 a–l**) could be reduced in 85–99% yield and in excellent enantioselectivities (91–>99% ee) with very low catalyst loading (Scheme 24). Notably, this method was also suitable for the ATH



Scheme 23. ATH of 3-(trifluoromethyl)quinolines (top) and 3-(trifluoromethyl-thio)quinolines (bottom).



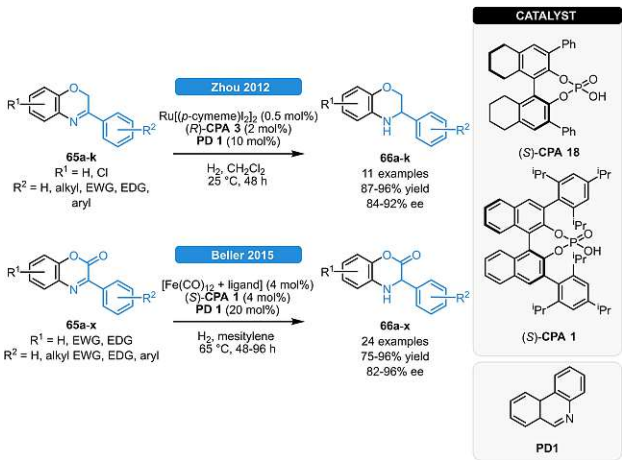
Scheme 24. ATH of various *N*-heterocycles catalyzed by SPINOL-derived acid (*S*)-**CPA 8**.

of diverse *N*-heterocycles including quinolines (**49**), 1,4-benzothiazolines (**67**), and benzoxazinanones (**69**) resulting in similarly high catalytic efficiency for all substrate classes.

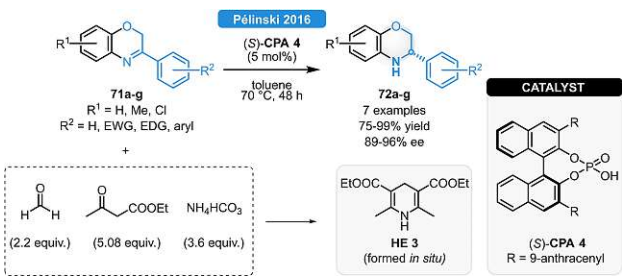
In analogy to their Ru/CPA-catalyzed asymmetric transfer hydrogenation of imines (Scheme 11), the group of Zhou applied the same strategy for the ATH of 1,4-benzoxazines, benzoxazinanones and related *N*-heterocycles (Scheme 25, top),[70,71] while Beller and co-workers reported a relay Fe/CPA-catalyzed asymmetric transfer hydrogenation of 1,4-benzoxazinanones (Scheme 25, bottom).[72] Both approaches relied on the use of sub-stochiometric amount of phenanthridine biomimetic reductant in the presence of H_2 as terminal reductant.

Following the pioneering work of Zhou relying on the elegant combination of transition-metal- and organocatalysis,[73] Pélinski *et al.* reported a new, purely organocatalytic strategy for the ATH of 1,4-benzoxazines relying on *in situ* formed dihydropyridine hydrogen sources (Scheme 26).[74] The multicomponent reaction of NH_4HCO_3, formaldehyde and ethyl acetoacetate led to the *in situ* generation of **HE 3** and the substrates **71 a–g** could be reduced in 91–99% yield and in 89–96% ee. Even though such a nonpolar reaction medium is generally not suitable for the synthesis of Hantzsch esters, its immediate consumption in the subsequent ATH reaction could readily shift the equilibrium, ensuring high reactivity.

In addition to the asymmetric reductions in homogenous phase, various catalyst immobilization strategies were also



Scheme 25. ATH of *N*-heterocycles *via* Ru/CPA catalysis.



Scheme 26. ATH of 1,4-benzoxazines with *in situ* formed Hantzsch esters.[74]

© 2021 The Authors. European Journal of Organic Chemistry published by Wiley-VCH GmbH

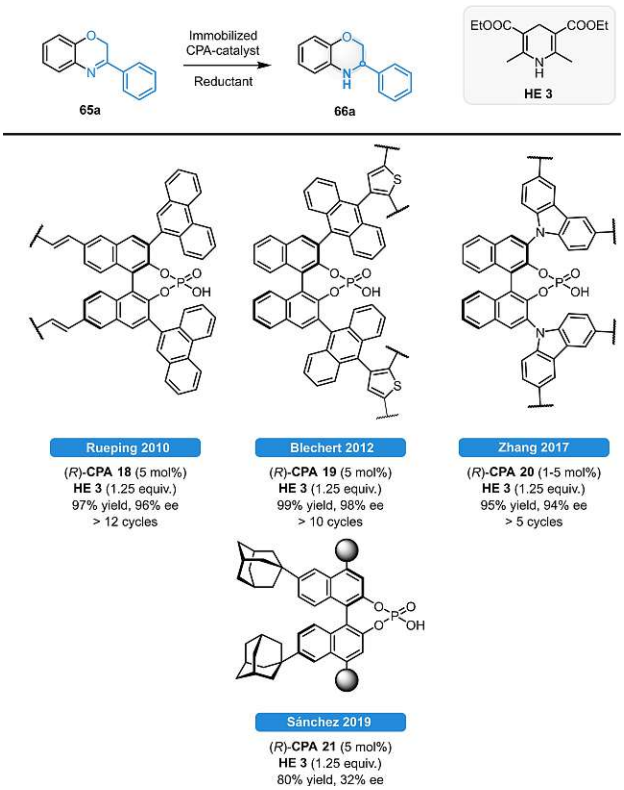
Die approbierte gedruckte Originalversion dieser Dissertation ist an der TU Wien Bibliothek verfügbar.
The approved original version of this doctoral thesis is available in print at TU Wien Bibliothek.
TU Bibliothek Your knowledge hub WIEN

developed for the ATH of 1,4-benzoxazine derivatives (Scheme 27).[75] In 2010, Rueping *et al.* reported the first immobilized chiral CPAs, as they successfully developed a series of polymer-supported catalysts *via* radical polymerization of 7,7′-styrene- or divinylbenzene-linked CPA monomers. As the supported catalyst was made in form of small sticks, they could be used in an unusual „tea-bag setup": After completion of the reaction, the catalyst could be separated by simply pulling out the polymer stick from the reaction mixture. The catalyst (*R*)-**CPA 18** provided excellent yield and enantioselectivity for the ATH of 1,4-benzoxazine **65 a** and it could be used for at least 12 consecutive cycles. Blechert *et al.* prepared CPA-derived microporous polymer networks *via* $FeCl_3$-mediated oxidative coupling of CPA monomers with 3-(anthracen-9-yl)thiophene units (Scheme 27).[76] The immobilized catalyst (*R*)-**CPA 19** provided full conversion and 98% ee for the ATH reaction of **65 a**; meanwhile, the catalyst could be reused for 10 cycles without any loss of reactivity and selectivity. Notably, the same catalyst was suitable for the ATH of 2-aryl quinolines, but also for Friedel-Crafts and Aza-ene reactions. A similar approach was later presented by Zhang and co-workers. Using carbazole-substitution on the 3,3′-position of the CPA they made a catalyst framework analogue to (*R*)-**CPA 19**, resulting in high yields and enantioselectivities even when using only 1 mol% catalyst.[77] Recently, the same reaction was investigated using adamantyl-BINOL as platform for chiral porous polymer frameworks ((*R*)-**CPA 21**). The product **66 a** could be isolated in good yield; however, only moderate enantioselectivity was observed.[78] Even though they cannot be considered as pure organocatalysts, metal-organic frameworks (MOFs) can also provide a nice alternative for the heterogenization of chiral Brønsted acids resulting in a highly porous catalyst framework and offering a high density of catalytic sites. Jiang *et al.* first described the synthesis of three different CPA-based 3D In-MOFs. They observed, that despite to their different structures, the CPAs are periodically aligned within the channels which makes the MOF framework catalytically active towards transfer hydrogenations of imines and benzoxazines.[79] Very recently they extended their concept to non-noble metal-based structures. With the CPA-based 3D Ca-MOF they could achieve similarly high catalytic activity and enantioselectivities to those obtained with 3D Ir-MOFs.[80]

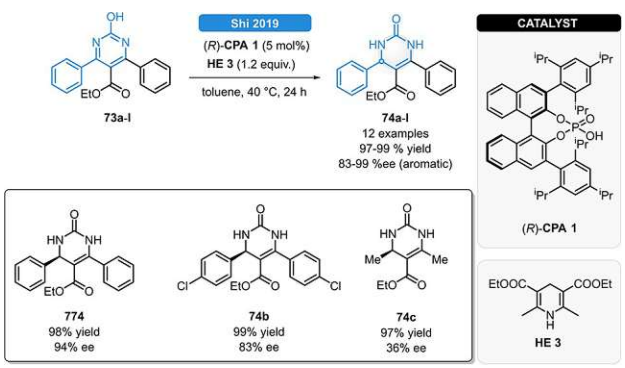
As an alternative to the Biginelli reaction, Shi *et al.* described the synthesis of 3,4-dihydropyrimidin-2(1*H*)-ones (DHPDs, **77 a–l**) *via* asymmetric reduction of pyridines (Scheme 28).[81] Using the phosphoric acid (*R*)-**CPA 1**, a small set of 3,4-diarylpyridines (**73 a–l**) could be reduced in excellent yield and enantioselectivities. The high reactivity could be maintained for aliphatic substrates; however, lower ee values were observed.

Very recently, the group of Akiyama reported the asymmetric dehydroxy-hydrogenation of 3-indolylmethanols (Scheme 29).[82] Relying on (*R*)-**CPA 22** and **BZT 1**, variously substituted indolyl- (**75 a–l**) and indolyl propalgyl methanols (**78 a–n**) could be reduced in high yields and in >90% ee; meanwhile substituents on the alkyne and on the arene moieties were both well tolerated. In order to demonstrate synthetic applicability, the product **76 a** was transformed to the leukotriene production inhibitor **77** *via* Suzuki-Miyaura cross-coupling without any loss of optical purity. The high enantioselectivity is originated from the tight ion-pairing of the **CPA 22** with the dehydrated alkylideneindoleninium ion.

In the same year, Song *et al.* applied *in situ* formed CPA-boron complexes for the direct ATH of C2-aryl-substituted, *N*-unprotected indoles.[83] The $[H]_8$-derived (*R*)-**CPA 7** provided excellent enantioselectivities for a wide range of indole substrates. For achieving high enantioselectivities, low temperature and 3.0 equivalent of H_2O were both necessary.



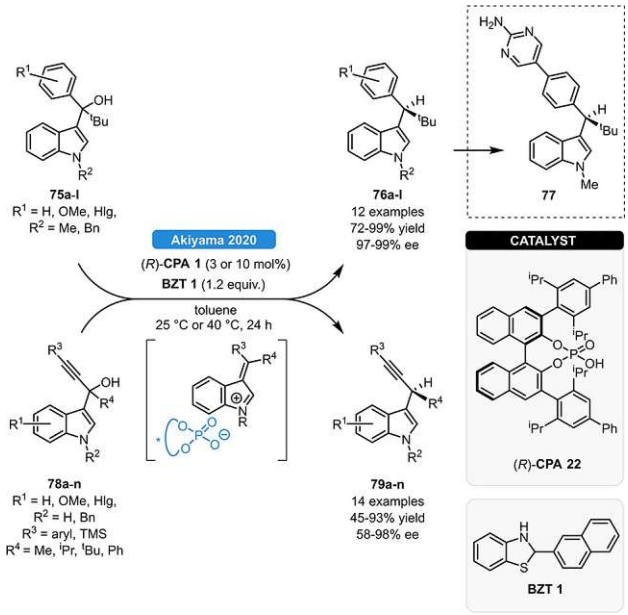
Scheme 27. Catalyst immobilization strategies for the ATH of 1,4-benzoxazines.



Scheme 28. Synthesis of DHPDs.

Die approbierte gedruckte Originalversion dieser Dissertation ist an der TU Wien Bibliothek verfügbar.
The approved original version of this doctoral thesis is available in print at TU Wien Bibliothek.
TU Bibliothek Your knowledge hub WIEN

© 2021 The Authors. European Journal of Organic Chemistry published by Wiley-VCH GmbH

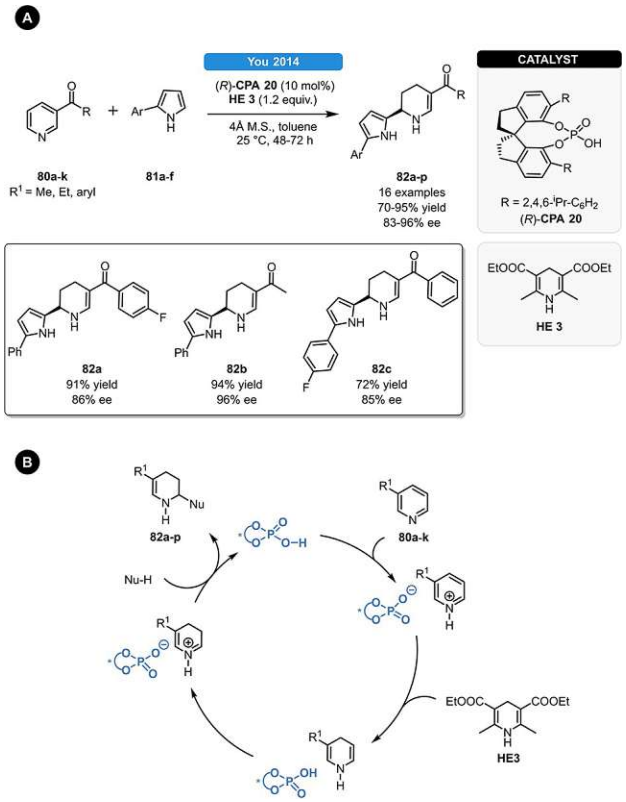


Scheme 29. Dehydroxy-hydrogenation of 3-indolylmethanol derivatives.

5. Organocatalytic Cascade and One-Pot Reactions

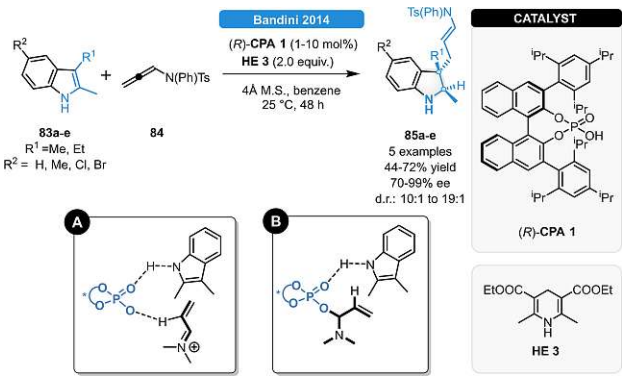
Cascade and one-pot reactions are extreme versatile tools for the rapid construction of high molecular complexity. The overall reaction can be considered as a sequence of several reaction steps that either take place simultaneously or one after the other. As these reaction steps proceed in a single operation under identical/very similar reaction conditions without the necessity of isolating the reaction intermediates, such transformations provide a highly step- and atom economic alternative to classical multi-step synthetic strategies. Allowing selective and well distinct modes of substrate activations, organocatalysts are particularly suitable for such kind of transformations. One of the first CPA- catalyzed organocatalytic cascade reaction was performed in the group of Rueping in 2008. The three-component reaction of an enamine, a vinyl ketone and a Hantzsch ester proceeded *via* a six-step cascade, all being catalyzed by the same phosphoric acid (*R*)-**CPA 4**, providing an easy access to tetrahydropyridines and azadecalinones in a highly enantioselective fashion.[84]

In 2014, You *et al.* reported an asymmetric dearomatization/aza-Friedel-Crafts alkylation cascade for the synthesis of substituted piperidines (Scheme 30, **A**).[85] When using the SPINOL-derived (*R*)-**CPA 20**, various 3-substituted pyridines (**80 a**–**k**) and 2-arylpyrroles (**81 a**–**f**) could be readily reacted under mild reaction conditions, furnishing the highly functionalized piperidine **82 a**–**p** in high yields and in good to excellent enantioselectivity. The authors proposed that after the initial ATH reaction, the generated enamine isomerizes to the corresponding iminium form, which can react with the 2-arylpyrrole nucleophiles (Scheme 30, **B**).



Scheme 30. Synthesis of piperidines *via* asymmetric dearomatization/aza-Friedel-Crafts alkylation cascade reaction.

In the same year, Bandini *et al.* reported a metal-free strategy for the synthesis of 3,3-disubstituted indolines (Scheme 31). The (*R*)-**CPA 1** as single catalyst could successfully promote a highly enantioselective dearomatization/transfer hydrogenation cascade *via* the electrophilic activation of allenamides. The condensation of 2,3-disubstituted or 2,3,5-trisubstituted indoles (**83 a**–**e**) with *N*-aryl allenamide **84** resulted in the formation of indolenine intermediates, which were subsequently reduced *in-situ* to the indoline products (**85 a**–**e**) in excellent diastereo- and enantioselectivity. It is



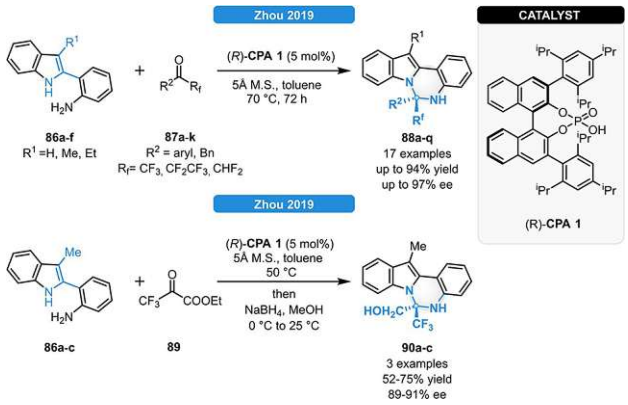
Scheme 31. Dearomatization/ATH cascade for the synthesis of highly functionalized indole moieties (top) and the possible activation modes (bottom, **A** and **B**).

Die approbierte gedruckte Originalversion dieser Dissertation ist an der TU Wien Bibliothek verfügbar.
The approved original version of this doctoral thesis is available in print at TU Wien Bibliothek.
TU Bibliothek Your knowledge hub WIEN

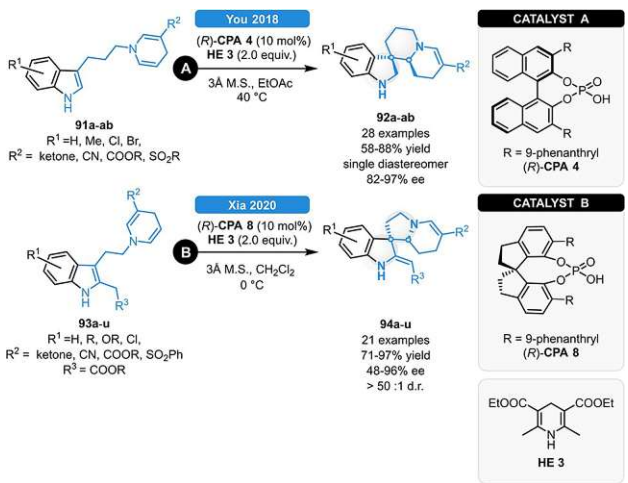
© 2021 The Authors. European Journal of Organic Chemistry published by Wiley-VCH GmbH

believed that the selective protonation of the allenamide at the β-position provides an α,β-unsaturated iminium intermediate, and subsequent Michael-addition and transfer hydrogenation affords the products. The (*R*)-**CPA 1** acts as a bifunctional catalyst activating the allenamide **84** either *via* non-covalent or covalent interactions (Scheme 31, **A** and **B**).[86]

In 2019, Zhou and co-workers reported a CPA-catalyzed condensation/amine addition cascade for the synthesis of 5,6-dihydroindolo[1,2-*c*]quinazolines (Scheme 32, top)[87]. Various 2-(1*H*-indolyl)anilines (**86a–g**) and fluorinated ketones (**87a–k**) could be readily reacted in the presence of 5 mol% (*R*)-**CPA 1**. The CF_3-group was found to play a crucial role in the reaction: as a potent hydrogen-bond acceptor, interactions either with the indole N–H or with the chiral phosphoric acid could result in higher enantiocontrol. When using the α-ketoester **89** as reagent, the cascade reaction followed by subsequent reduction with $NaBH_4$ provided an easy access to the highly enantioenriched α-diamino acid derivatives **90a–c** (Scheme 32, bottom).[87]



Scheme 32. CPA-mediated synthesis of 5,6-dihydroindolo[1,2-c]quinazolines (top) and its application for the preparation of α-diamino acid derivatives (bottom).

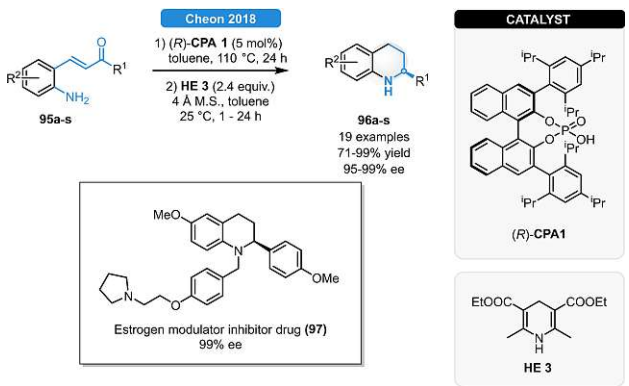


Scheme 33. Different concepts for the synthesis of spiroindolines *via* CPA-catalyzed cascade reactions.

In 2018, You and co-workers realized the synthesis of spiroindolines *via* cascade isomerization/spirocyclization/transfer hydrogenation reaction (Scheme 33, **A**). Under optimized reaction conditions, a wide range of indolyl dihydropyridine substrates (**91a–ab**) featuring various ketone moieties, esters, cyano or sulfonyl groups on the 1,4-dihydropyridine sub-unit were well tolerated, providing the corresponding spiroindoline **92a–ab** in 58–88% yields and in 82–97% ee; moreover, EDG groups and halogen atoms in the R^1 position were also compatible with the reaction. The reaction was found to be extremely diastereoselective, providing a single diastereomeric product in most of the cases.[88] Recently, Xia and co-workers reported a similar method for the synthesis of 2,7-diazaspiro[4.4]nonane indolines (**94a–u**, Scheme 33, **B**). Using the SPINOL-derived (*R*)-**CPA 8**, a comparably broad range of substrates could be applied resulting in excellent diastereoselectivity and 60–96% ee. The nature of the R^2 and R^3-groups was found to be crucial: electron-poor and sterically demanding R^2-groups resulted in high enantioselectivity; meanwhile, the electron withdrawing R^3-ester unit facilitated the formation of the spiro-products and inhibited the alternative Pictet-Spengler pathway.[89]

In 2018, the group of Cheol-Hong Cheon managed to synthesize 2-substituted tetrahydroquinolines in a highly enantioselective fashion by a dehydrative cyclization/ATH reaction sequence (Scheme 34).[90] Unlike previous works, the two-step, one-pot transformation could be carried out by using a chiral phosphoric acid as sole catalyst. After identifying the (*R*)-**CPA 1** as most suitable catalyst, a broad range of 2-aminochalcones (**95a–u**) could be converted to the corresponding 2-substituted tetrahydroquinolines in uniformly high 94–99% ee. Moreover, the strategy was applicable for the synthesis of the estrogen modulator inhibitor **97** in significantly higher yield and identical enantioselectivity than previous literature reports.

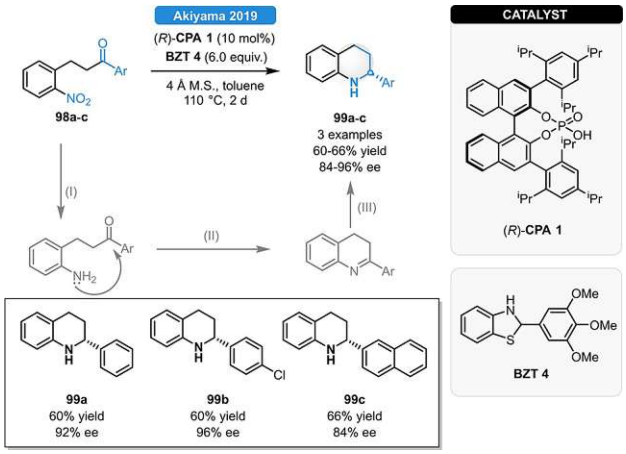
Recently, the Akiyama group established a highly enantioselective methodology for the synthesis of 2-aryltetrahydroquinolines (**99a–c**).[91] After optimizing the reduction of various achiral nitroarenes, a three-step reaction cascade was developed: the initial reduction of the nitroarene (I) was followed by intra-



Scheme 34. Synthesis of tetrahydroquinolines *via* dehydrative cyclization/ATH cascade reaction.

© 2021 The Authors. European Journal of Organic Chemistry published by Wiley-VCH GmbH

Die approbierte gedruckte Originalversion dieser Dissertation ist an der TU Wien Bibliothek verfügbar.
The approved original version of this doctoral thesis is available in print at TU Wien Bibliothek.
TU Bibliothek Your knowledge hub WIEN



Scheme 35. One-pot synthesis of chiral quinolines *via* reduction of nitroarenes in a reduction/cyclization/reduction cascade.

molecular cyclization (II) and asymmetric transfer hydrogenation (III). Relying on (*R*)-**CPA 1** and **BZT 4** as a H-donor, the corresponding products were obtained in 60–66 % yield and in 84–96 % ee (Scheme 35).

6. Conclusions

Organocatalytic asymmetric transfer hydrogenations relying on biomimetic hydrogen sources have proven to be very attractive and popular alternatives to classical transition-metal-based ATH reactions. The introduction of BINOL-derived chiral phosphoric acids could basically revolutionize this field, providing straightforward protocols for the reduction of an extremely diverse pool of substrates featuring C=C, C=N and C=O double bonds. Apart from providing a safe, simple and metal-free alternative for asymmetric hydrogenations, several advances could also successfully tackle the challenge of high catalyst loadings, relying on catalyst amounts similar to those used in transition-metal catalysis. Apart from all these advantages, chiral phosphoric acid-catalyzed ATH reactions are more and more often applied for cascade transformations as well as in total synthesis, indicating its high potential for various industrial applications. Given the juvenileness of this particular field of organocatalysis, a broad range of novel future applications is still expected.

Acknowledgements

Financial support by the Austrian Science Fund (project P29146-N34) is gratefully acknowledged.

Conflict of Interest

The authors declare no conflict of interest.

Keywords: Asymmetric Transfer Hydrogenation · Catalysis · Chiral Phosphoric Acids · Metal-Free Hydrogenation · Organocatalysis

[1] I. Ojima, *Catalytic Asymmetric Synthesis, 3rd Edition*, Wiley-VCH, Weinheim, **2010**.
[2] H. U. Blaser, H.-J. Federsel, *Asymmetric Catalysis on Industrial Scale: Challenges, Approaches and Solutions, 2nd Edition*, Wiley-VCH, Weinheim, **2010**.
[3] J. W. Yang, M. T. Hechavarria Fonseca, B. List, *J. Am. Chem. Soc.* **2005**, *127*, 15036–15037.
[4] Y. Huang, A. M. Walji, C. H. Larsen, D. W. C. MacMillan, *J. Am. Chem. Soc.* **2005**, *127*, 15051–15053.
[5] D. Uraguchi, M. Terada, *J. Am. Chem. Soc.* **2004**, *126*, 5356–5357.
[6] T. Akiyama, J. Itoh, K. Yokota, K. Fuchibe, *Angew. Chem. Int. Ed.* **2004**, *43*, 1566–1568; *Angew. Chem.* **2004**, *116*, 1592–1594.
[7] D. Parmar, E. Sugiono, S. Raja, M. Rueping, *Chem. Rev.* **2014**, *114*, 9047–9153.
[8] D. Parmar, E. Sugiono, S. Raja, M. Rueping, *Chem. Rev.* **2017**, *117*, 10608–10620.
[9] J. Merad, C. Lalli, G. Bernadat, J. Maury, G. Masson, *Chem. A Eur. J.* **2018**, *24*, 3925–3943.
[10] C. Zheng, S. L. You, *Chem. Soc. Rev.* **2012**, *41*, 2498–2518.
[11] S. L. You, *Chem. Asian J.* **2007**, *2*, 820–827.
[12] C. Zheng, S.-L. You, *Chem. Soc. Rev.* **2012**, *41*, 2498.
[13] C. Zhu, K. Saito, M. Yamanaka, T. Akiyama, *Acc. Chem. Res.* **2015**, *48*, 388–398.
[14] C. Zhu, T. Akiyama, *Org. Lett.* **2009**, *11*, 4180–4183.
[15] S. Mayer, B. List, *Angew. Chem. Int. Ed.* **2006**, *45*, 4193–4195; *Angew. Chem.* **2006**, *118*, 4299–4301.
[16] N. J. A. Martin, B. List, *J. Am. Chem. Soc.* **2006**, *128*, 13368–13369.
[17] M. Mahlau, B. List, *Angew. Chem. Int. Ed.* **2013**, *52*, 518–533; *Angew. Chem.* **2013**, *125*, 540–556.
[18] F. Scharinger, Á. Márk Pálvölgyi, V. Zeindlhofer, M. Schnürch, C. Schröder, K. Bica-Schröder, *ChemCatChem* **2020**, *12*, 3776–3782.
[19] Z. Wang, F. Ai, Z. Wang, W. Zhao, G. Zhu, Z. Lin, J. Sun, *J. Am. Chem. Soc.* **2015**, *137*, 383–389.
[20] Y. Li, M. Wan, S. Sun, Z. Fu, H. Huang, L. Liu, *Org. Chem. Front.* **2018**, *5*, 1280–1283.
[21] D. Wang, D. Astruc, *Chem. Rev.* **2015**, *115*, 6621–6686.
[22] M. Kitamura, T. Ohkuma, S. Inoue, N. Sayo, H. Kumobayashi, S. Akutagawa, T. Ohta, H. Takaya, R. Noyori, *J. Am. Chem. Soc.* **1988**, *110*, 629–631.
[23] A. Fujii, S. Hashiguchi, N. Uematsu, T. Ikariya, R. Noyori, *J. Am. Chem. Soc.* **1996**, *118*, 2521–2522.
[24] R. Noyori, T. Ohkuma, *Angew. Chem. Int. Ed.* **2001**, *40*, 40–73; *Angew. Chem.* **2001**, *113*, 40–75.
[25] T. Ikariya, A. J. Blacker, *Acc. Chem. Res.* **2007**, *40*, 1300–1308.
[26] Z. Zhang, P. Jain, J. C. Antilla, *Angew. Chem. Int. Ed.* **2011**, *50*, 10961–10964; *Angew. Chem.* **2011**, *123*, 11153–11156.
[27] F. Na, S. S. Lopez, A. Beauseigneur, L. W. Hernandez, Z. Sun, J. C. Antilla, *Org. Lett.* **2020**, *22*, 5953–5957.
[28] Q. Zhou, W. Meng, X. Feng, H. Du, J. Yang, *Tetrahedron Lett.* **2020**, *61*, 151394.
[29] M. Rueping, E. Sugiono, C. Azap, T. Theissmann, M. Bolte, *Org. Lett.* **2005**, *7*, 3781–3783.
[30] S. Hoffmann, A. M. Seayad, B. List, *Angew. Chem. Int. Ed.* **2005**, *44*, 7424–7427; *Angew. Chem.* **2005**, *117*, 7590–7593.
[31] R. I. Storer, D. E. Carrera, Y. Ni, D. W. C. MacMillan, *J. Am. Chem. Soc.* **2006**, *128*, 84–86.
[32] K. Saito, K. Horiguchi, Y. Shibata, M. Yamanaka, T. Akiyama, *Chem. A Eur. J.* **2014**, *20*, 7616–7620.
[33] K. Saito, H. Miyashita, T. Akiyama, *Org. Lett.* **2014**, *16*, 5312–5315.
[34] M. W. Chen, Q. Yang, Z. Deng, Y. Zhou, Q. Ding, Y. Peng, *J. Org. Chem.* **2018**, *83*, 8688–8694.
[35] M. Miyagawa, K. Takashima, T. Akiyama, *Synlett* **2018**, *29*, 1607–1610.
[36] M. W. Chen, B. Wu, Z. P. Chen, L. Shi, Y. G. Zhou, *Org. Lett.* **2016**, *18*, 4650–4653.
[37] V. N. Wakchaure, P. S. J. Kaib, M. Leutzsch, B. List, *Angew. Chem. Int. Ed.* **2015**, *54*, 11852–11856; *Angew. Chem.* **2015**, *127*, 12019–12023.
[38] J. Mazuela, T. Antonsson, M. J. Johansson, L. Knerr, S. P. Marsden, *Org. Lett.* **2017**, *19*, 5541–5544.

Die approbierte gedruckte Originalversion dieser Dissertation ist an der TU Wien Bibliothek verfügbar.
The approved original version of this doctoral thesis is available in print at TU Wien Bibliothek.
TU Bibliothek Your knowledge hub WIEN

© 2021 The Authors. European Journal of Organic Chemistry published by Wiley-VCH GmbH

[39] K. Rothermel, M. Žabka, J. Hioe, R. M. Gschwind, *J. Org. Chem.* **2019**, *84*, 13221–13231.
[40] V. N. Wakchaure, B. List, *Angew. Chem. Int. Ed.* **2016**, *55*, 15775–15778; *Angew. Chem.* **2016**, *128*, 16007–16010.
[41] S. Hoffmann, M. Nicoletti, B. List, *J. Am. Chem. Soc.* **2006**, *128*, 13074–13075.
[42] K.-H. Kim, C.-Y. Lee, C.-H. Cheon, *J. Org. Chem.* **2015**, *80*, 6367–6374.
[43] K. H. Kim, T. Akiyama, C. H. Cheon, *Chem. Asian J.* **2016**, *11*, 274–279.
[44] W. Wen, Y. Zeng, L. Y. Peng, L. N. Fu, Q. X. Guo, *Org. Lett.* **2015**, *17*, 3922–3925.
[45] K. Mori, A. Miyake, T. Akiyama, *Chem. Commun.* **2015**, *51*, 16107–16110.
[46] D. Y. Park, K. H. Kim, C. H. Cheon, *Adv. Synth. Catal.* **2018**, *360*, 462–467.
[47] V. Skrypai, S. E. Varjosaari, F. Azam, T. M. Gilbert, M. J. Adler, *J. Org. Chem.* **2019**, *84*, 5021–5026.
[48] Q. Zhou, W. Meng, J. Yang, H. Du, *Angew. Chem. Int. Ed.* **2018**, *57*, 12111–12115; *Angew. Chem.* **2018**, *130*, 12287–12291.
[49] Y. G. Zhou, *Acc. Chem. Res.* **2007**, *40*, 1357–1366.
[50] E. Vitaku, D. T. Smith, J. T. Njardarson, *J. Med. Chem.* **2014**, *57*, 10257–10274.
[51] M. Rueping, A. P. Antonchick, T. Theissmann, *Angew. Chem. Int. Ed.* **2006**, *45*, 6751–6755; *Angew. Chem.* **2006**, *118*, 6903–6907.
[52] M. Rueping, A. P. Antonchick, T. Theissmann, *Angew. Chem. Int. Ed.* **2006**, *45*, 3683–3686; *Angew. Chem.* **2006**, *118*, 3765–3768.
[53] M. Rueping, F. Tato, F. R. Schoepke, *Chem. A Eur. J.* **2010**, *16*, 2688–2691.
[54] M. Rueping, A. P. Antonchick, *Angew. Chem. Int. Ed.* **2007**, *46*, 4562–4565; *Angew. Chem.* **2007**, *119*, 4646–4649.
[55] G. V. More, B. M. Bhanage, *Tetrahedron: Asymmetry* **2015**, *26*, 1174–1179.
[56] Y. Wang, W. Liu, W. Ren, Y. Shi, *Org. Lett.* **2015**, *17*, 4976–4979.
[57] K. Isaac, J. Stemper, V. Servajean, P. Retailleau, J. Pastor, G. Frison, K. Kaupmees, I. Leito, J. F. Betzer, A. Marinetti, *J. Org. Chem.* **2014**, *79*, 9639–9646.
[58] J. Stemper, K. Isaac, V. Duret, P. Retailleau, A. Voituriez, J. F. Betzer, A. Marinetti, *Chem. Commun.* **2013**, *49*, 6084–6086.
[59] R. Mitra, H. Zhu, S. Grimme, J. Niemeyer, *Angew. Chem. Int. Ed.* **2017**, *56*, 11456–11459; *Angew. Chem.* **2017**, *129*, 11614–11617.
[60] P. Wang, Y. E. Jia, J. Z. Zhao, D. Zhao, R. Yuan, C. S. Da, *Asian J. Org. Chem.* **2015**, *4*, 430–433.
[61] S. Thölke, H. Zhu, D. Jansen, F. Octa-Smolin, M. Thiele, K. Kaupmees, I. Leito, S. Grimme, J. Niemeyer, *Eur. J. Org. Chem.* **2019**, *2019*, 5190–5195.
[62] N. Someshwar, M. Karthick, C. R. Ramanathan, *Synlett* **2017**, *28*, 2253–2261.
[63] Y. Zhang, R. Zhao, R. L. Y. Bao, L. Shi, *Eur. J. Org. Chem.* **2015**, *2015*, 3344–3351.
[64] G. Li, H. Liu, G. Lv, Y. Wang, Q. Fu, Z. Tang, *Org. Lett.* **2015**, *17*, 4125–4127.
[65] X. F. Cai, R. N. Guo, G. S. Feng, B. Wu, Y. G. Zhou, *Org. Lett.* **2014**, *16*, 2680–2683.
[66] A. Aillerie, V. Lemau De Talencé, C. Dumont, S. Pellegrini, F. Capet, T. Bousquet, L. Pélinski, *New J. Chem.* **2016**, *40*, 9034–9037.
[67] C. R. Shugrue, S. J. Miller, *Angew. Chem. Int. Ed.* **2015**, *54*, 11173–11176; *Angew. Chem.* **2015**, *127*, 11325–11328.
[68] R. N. Guo, Z. P. Chen, X. F. Cai, Y. G. Zhou, *Synthesis* **2014**, *46*, 2751–2756.
[69] J. Zhou, Q. F. Zhang, W. H. Zhao, G. F. Jiang, *Org. Biomol. Chem.* **2016**, *14*, 6937–6941.
[70] Q. Chen, K. Gao, Y. Duan, Z. Ye, L. Shi, Y. Yang, Y. Zhou, *J. Am. Chem. Soc.* **2012**, *134*, 2442–2448.
[71] Z. P. Chen, M. W. Chen, R. N. Guo, Y. G. Zhou, *Org. Lett.* **2014**, *16*, 1406–1409.
[72] L. Q. Lu, Y. Li, K. Junge, M. Beller, *J. Am. Chem. Soc.* **2015**, *137*, 2763–2768.
[73] Q. A. Chen, M. W. Chen, C. Bin Yu, L. Shi, D. S. Wang, Y. Yang, Y. G. Zhou, *J. Am. Chem. Soc.* **2011**, *133*, 16432–16435.
[74] A. Aillerie, C. Gosset, C. Dumont, V. Skrzypczak, P. Champetter, S. Pellegrini, T. Bousquet, L. Pélinski, *RSC Adv.* **2016**, *6*, 54185–54188.
[75] M. Rueping, E. Sugiono, A. Steck, T. Theissmann, *Adv. Synth. Catal.* **2010**, *352*, 281–287.
[76] D. S. Kundu, J. Schmidt, C. Bleschke, A. Thomas, S. Blechert, *Angew. Chem. Int. Ed.* **2012**, *51*, 5456–5459; *Angew. Chem.* **2012**, *124*, 5552–5555.
[77] X. Zhang, A. Kormos, J. Zhang, *Org. Lett.* **2017**, *19*, 6072–6075.
[78] C. Monterde, R. Navarro, M. Iglesias, F. Sánchez, *J. Catal.* **2019**, *377*, 609–618.
[79] X. Chen, H. Jiang, X. Li, B. Hou, W. Gong, X. Wu, X. Han, F. Zheng, Y. Liu, J. Jiang, Y. Cui, *Angew. Chem. Int. Ed.* **2019**, *58*, 14748–14757; *Angew. Chem.* **2019**, *131*, 14890–14899.
[80] X. Chen, Z. Qiao, B. Hou, H. Jiang, W. Gong, J. Dong, H. Y. Li, Y. Cui, Y. Liu, *Nano Res.* **2021**, *14*, 466–472.
[81] F.-J. J. Meng, L. Shi, G.-S. S. Feng, L. Sun, Y.-G. G. Zhou, *J. Org. Chem.* **2019**, *84*, 4435–4442.
[82] H. Osakabe, S. Saito, M. Miyagawa, T. Suga, T. Uchikura, T. Akiyama, *Org. Lett.* **2020**, *22*, 2225–2229.
[83] K. Yang, Y. Lou, C. Wang, L. Qi, T. Fang, F. Zhang, H. Xu, L. Zhou, W. Li, G. Zhang, P. Yu, Q. Song, *Angew. Chem. Int. Ed.* **2020**, *59*, 3294–3299; *Angew. Chem.* **2020**, *132*, 3320–3325.
[84] M. Rueping, A. P. Antonchick, *Angew. Chem. Int. Ed.* **2008**, *47*, 5836–5838; *Angew. Chem.* **2008**, *120*, 5920–5922.
[85] S. G. Wang, S. L. You, *Angew. Chem. Int. Ed.* **2014**, *53*, 2194–2197; *Angew. Chem.* **2014**, *126*, 2226–2229.
[86] C. Romano, M. Jia, M. Monari, E. Manoni, M. Bandini, *Angew. Chem. Int. Ed.* **2014**, *53*, 13854–13857; *Angew. Chem.* **2014**, *126*, 14074–14077.
[87] X. W. Wang, M. W. Chen, B. Wu, B. Wang, Y. G. Zhou, *J. Org. Chem.* **2019**, *84*, 8300–8308.
[88] Z.-L. Xia, C. Zheng, S.-G. Wang, S.-L. You, *Angew. Chem. Int. Ed.* **2018**, *57*, 2653–2656; *Angew. Chem.* **2018**, *130*, 2683–2686.
[89] Z. Pan, Y. Liu, F. Hu, Q. Liu, W. Shang, X. Ji, C. Xia, *Org. Lett.* **2020**, *22*, 1589–1593.
[90] D. Y. Park, S. Y. Lee, J. Jeon, C.-H. Cheon, *J. Org. Chem.* **2018**, *83*, 12486–12495.
[91] M. Miyagawa, R. Yamamoto, N. Kobayashi, T. Akiyama, *Synlett* **2019**, *30*, 499–502.

Manuscript received: July 27, 2021
Revised manuscript received: September 16, 2021

Die approbierte gedruckte Originalversion dieser Dissertation ist an der TU Wien Bibliothek verfügbar.
The approved original version of this doctoral thesis is available in print at TU Wien Bibliothek.
TU Bibliothek Your knowledge hub WIEN

© 2021 The Authors. European Journal of Organic Chemistry published by Wiley-VCH GmbH

8 Counterion Enhanced Organocatalysis: A Novel Approach for the Asymmetric Transfer Hydrogenation of Enones

The task of achieving selective reduction of enones presents a formidable challenge, given the intricate issues of regio- and stereoselectivity.[89] In the domain of catalytic approaches tackling this challenge, organocatalysis has emerged as a highly successful strategy.[14] To improve both handling and stereocontrol of the hydrogen source, typically hydrogen gas, a transition was made from typical donors employed in transition metal catalysis such as isopropanol to the Hantzsch ester dihydropyridine. This biomimetic approach where the Hantzsch ester resembles coenzyme NADPH, can donate both a hydride and a proton to the respective double bond and its driving force is the formation of the more stable pyridine structure.[90] Within organocatalysis, iminium-based asymmetric transfer hydrogenations have arisen as a particularly efficient and metal-free alternative for achieving selective reductions of enones through 1,4-addition reactions.[90–92] In this context, List developed an ACDC catalyst, comprising a chiral amine and phosphoric acid, as a chiral ion-paired catalyst that exhibited impressive performance and selectivity when performing the ATH on various prochiral enones. While this innovative method proves to be highly efficient, it does come with a limitation – specifically, the requirement of employing a chiral phosphoric acid that matches the enantiomer of the amine. In general, chiral mismatched pairs typically result in significantly lower stereoinduction.[93] Moreover, if the opposite enantiomer of the product is desired, both catalyst components must be replaced. In our approach, we closely examined the fundamental concept of ion pairing but took a different route by employing racemic bulky phosphoric acids as counteranions to further enhance the already-established enantioselectivity provided by the chiral amine. The bulky counteranion can serve two purposes: it can act as a steric shield, blocking a specific face from nucleophilic attack or it can alter the conformation of the LUMO-activated intermediate to achieve a high degree of stereoinduction. To achieve this goal, a wide range of chiral amines were examined, which had been synthesized from readily accessible amino acids. Once the desired amine was identified, it was paired with several achiral phosphoric acids, easily synthesized in two steps via oxidative microwave coupling. This catalyst combination produced results similar to those achieved by List's cutting-edge catalyst in terms of yield and enantiomeric excess, all while circumventing the necessity for double stereoinduction. This offers a more straightforward and cost-effective approach to the same objective. The experimental studies were complemented by theoretical investigation to study the impact of both chiral and achiral cations on the enantiomerization of various biphenyl anions. The potential chirality transfer between the ions was studies through polarizable MD simulations in cooperation with partners from the University of Vienna.

Die approbierte gedruckte Originalversion dieser Dissertation ist an der TU Wien Bibliothek verfügbar.
The approved original version of this doctoral thesis is available in print at TU Wien Bibliothek.
TU Bibliothek Your knowledge hub WIEN

The following manuscript is presented in this chapter:

Scharinger, F.; Márk Pálvölgyi, Á.; Zeindlhofer, V.; Schnürch, M.; Schröder, C.; Bica-Schröder, K. Counterion Enhanced Organocatalysis: A Novel Approach for the Asymmetric Transfer Hydrogenation of Enones. *ChemCatChem* **2020**, *12* (14), 3776–3782. https://doi.org/10.1002/cctc.202000414.

In my role as a primary author with equal contribution, I carried out all major experiments and made substantial contributions to the draft of the manuscript.

Die approbierte gedruckte Originalversion dieser Dissertation ist an der TU Wien Bibliothek verfügbar.
The approved original version of this doctoral thesis is available in print at TU Wien Bibliothek.

Counterion Enhanced Organocatalysis: A Novel Approach for the Asymmetric Transfer Hydrogenation of Enones

Fabian Scharinger[+],[a] Ádám Márk Pálvölgyi[+],[a] Veronika Zeindlhofer,[b] Michael Schnürch,[a] Christian Schröder,[b] and Katharina Bica-Schröder*[a]

Dedicated to Prof. Johannes Fröhlich on the occasion of his 60th birthday

We present a novel strategy for organocatalytic transfer hydrogenations relying on an ion-paired catalyst of natural L-amino acids as main source of chirality in combination with racemic, atropisomeric phosphoric acids as counteranion. The combination of a chiral cation with a structurally flexible anion resulted in a novel chiral framework for asymmetric transfer hydrogenations with enhanced selectivity through synergistic effects. The optimized catalytic system, in combination with a Hantzsch ester as hydrogen source for biomimetic transfer hydrogenation, enabled high enantioselectivity and excellent yields for a series of α,β-unsaturated cyclohexenones under mild conditions. Moreover, owing to the use of readily available and chiral pool-derived building blocks, it could be prepared in a straightforward and significantly cheaper way compared to the current state of the art.

Introduction

Asymmetric transfer hydrogenation has emerged as a powerful and convenient tool for the reduction of prochiral carbonyl compounds.[1] The selective reduction of enones is a particularly challenging task due to the inherent question of regio- and stereoselectivity.[2] Among many catalytic protocols that have been described for this particular reaction, the flourishing area of organocatalysis offers attractive solutions, and iminium-based asymmetric transfer hydrogenations provide an efficient and metal-free alternative for the selective reduction of enones via 1,4-addition.[3–5]

Over the past years, two types of catalysts have emerged as particularly well suited for organocatalytic transfer hydrogenations of enals and enones. In 2004, the group of MacMillan reported a series of imidazolidinone derivatives as powerful benchmark catalysts for highly asymmetric conjugate hydrogenations of α,β-unsaturated aldehydes and ketones (Figure 1, left).[5,6] In parallel, List and co-workers described a novel method for the non-asymmetric transfer hydrogenation of cinnamaldehyde derivatives using secondary ammonium salts as catalysts.[7] Two years later, a new methodology in asymmetric transfer hydrogenation was reported by Mayer and List as they observed high catalytic activity and enantioselectivity in the reaction of enals and enones catalyzed by ammonium salts composed of an achiral or chiral cation and an enantiopure sterically demanding phosphate anion, TRIP (Figure 1, right).[8,9] Based on the early success of List's catalytic system, a new general concept emerged in the field of organocatalysis, known as Asymmetric Counteranion-Directed Catalysis (ACDC), which refers to any catalytic reaction, in which the enantiodiscrimination is induced through the tight ion-pairing of a cationic intermediate with an enantiomerically pure anion.[10] The ion-bound nature of this attractive approach for chiral induction offers considerable flexibility for fine-tuning of the electronic and steric properties compared to conventional covalent ligand systems.[11] Since the discovery of ACDC, or in general, of asymmetric ion-pairing catalysis, several other highly enantioselective reactions proceeding through cationic intermediates have been reported.[12–15] While different asymmetric induction modes can be realized in asymmetric ion-pairing catalysis, the formation of ion pairs between ammonium cations and bulky chiral phosphate anions is particularly prominent.[16–21]

While these elegant strategies are certainly among the most important discoveries in the field of organocatalysis for the last decades, they still do have some limitations. MacMillan's imidazolidinones are excellent catalysts for the asymmetric transfer hydrogenation of enals; however, the reactivity for enones is inferior thus requiring higher catalyst loadings.[6] In contrast, List et al. could successfully reach high reactivity and selectivity for the asymmetric transfer hydrogenation of enals and enones even with low catalyst loading based on the chiral TRIP counteranion. However, this approach requires a rather expensive catalyst, prepared in a five-step synthesis with rather

[a] F. Scharinger,[+] Á. Márk Pálvölgyi,[+] Prof. M. Schnürch, Prof. K. Bica-Schröder
Institute of Applied Synthetic Chemistry
TU Wien
Getreidemarkt 9/163
1060 Wien (Austria)
E-mail: katharina.schroeder@tuwien.ac.at
[b] V. Zeindlhofer, Prof. C. Schröder
Department of Computational Biological Chemistry
University of Vienna
Währinger Str. 17
1090 Wien (Austria)
[+] These authors contributed equally to this manuscript.

Supporting information for this article is available on the WWW under https://doi.org/10.1002/cctc.202000414

© 2020 The Authors. Published by Wiley-VCH Verlag GmbH & Co. KGaA. This is an open access article under the terms of the Creative Commons Attribution License, which permits use, distribution and reproduction in any medium, provided the original work is properly cited.

Die approbierte gedruckte Originalversion dieser Dissertation ist an der TU Wien Bibliothek verfügbar.
The approved original version of this doctoral thesis is available in print at TU Wien Bibliothek.

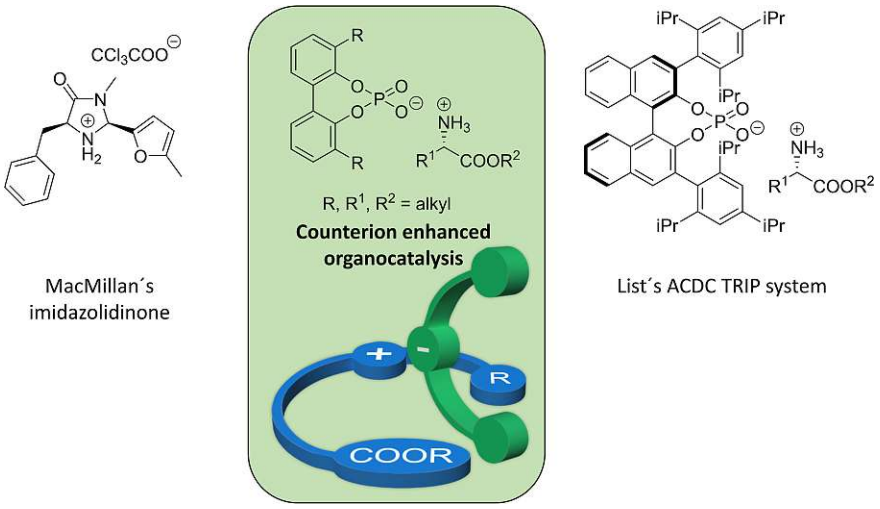


Figure 1. Iminium-based organocatalytic reduction of enones and different catalytic systems, including MacMillan's imidazolidinone catalyst (left), List's TRIP phosphate (right) as well as the novel counterion enhanced approach reported in here (middle).

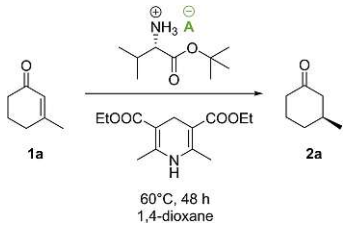
low overall yields. Moreover, a careful structural optimization is required for the bulky phosphate anion of the catalyst: while the TRIP counteranion provides indeed high selectivity in the ATH of ketones and aldehydes, a significant decrease in the enantiodiscrimination could be observed just with a slight modification of the phosphate unit, resulting in moderate selectivity or even close-to-racemic products. Given these limitations; a straightforward, cheaper and chiral-pool derived catalytic system that combines high catalytic activity with excellent enantioselectivity would be highly desirable.

In here, we propose a novel concept of asymmetric ion-paired organocatalysis with a fixed element of chirality based on ion aggregation between a chiral amino acid cation and C_2-symmetric atropisomeric phosphate anion. This concept of an ion-paired catalyst framework offers novel opportunities for ligand design with unprecedented flexibility compared to conventional ligand design relying on covalently constructed ligands. Eventually, this unique approach results in an easily accessible, cheap and chiral pool-derived a catalytic system that is yet able to reduce a set of α,β-unsaturated ketones with high yields and selectivity.

Results and Discussion

To prove the concept of counterion enhanced asymmetric transfer hydrogenations, we initially focused on the reduction of 3-methyl-2-cyclohexenone. The reaction was performed with the common Hantzsch ethyl ester as mild reductant using standard conditions that have been previously established by List et al (Scheme 1).[5]

For a first evaluation of the concept, different salts of (L)-valine *t*-butyl ester, including the non-chiral trifluoroacetate salt, but also salts with tropoisomeric biphenyl phosphate as well as enantiopure or racemic binaphthyl phosphate anions were used as catalysts (Table 1). While no reaction was



Scheme 1. Proof of concept: asymmetric transfer hydrogenation of 3-methyl-2-cyclohexenone (**1 a**) by using different salts of L-valine *t*-butyl ester.

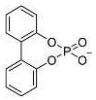
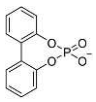
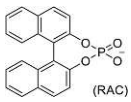
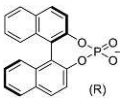
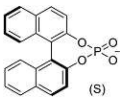
observed with the biphenolate anion **3** due to the lower acidity of 2,2′-biphenol (Table 1, entry 1), the reaction proceeded with moderate yield in the presence of biphenyl phosphate **4** (Table 1, entries 4 and 5). Most importantly, an increase of enantioselectivity to 64%ee – an increase by 10%ee compared to the trifluoroacetate salt - could be observed, indicating that the tropoisomeric and C2-symmetric biphenyl phosphate anion plays a role in enantiodiscrimination (Table 1, entries 2 vs. 4). It is worthwhile noticing that this is not the case with different binaphthyl phosphate anions, as the observed enantioselectivity with racemic or enantiopure binaphthyl phosphate was identical to the values obtained for trifluoroacetate (Table 1, entries 2 vs. 6–8). This clearly shows that matched/mismatched effects between the chiral amino acid and the counteranion do not influence the enantioselectivity of the product.

Further studies showed that this effect is even more pronounced in MTBE as a solvent, where an enantioselectivity of 74%ee compared to 51%ee obtained with the trifluoroacetate anion was found (Table 1, entries 3 vs. 5). In fact, when studying the impact of different solvents in this reaction, we found that the best selectivity is observed in solvents with low dielectric constants such as MTBE ($\varepsilon = 4.5$) or toluene ($\varepsilon = 2.4$), whereas lower enantioselectivity was found in more polar solvents such as water ($\varepsilon = 80.1$), see ESI Table S2, page S24 for details.

Die approbierte gedruckte Originalversion dieser Dissertation ist an der TU Wien Bibliothek verfügbar.
The approved original version of this doctoral thesis is available in print at TU Wien Bibliothek.
TU Bibliothek Your knowledge hub WIEN

© 2020 The Authors. Published by Wiley-VCH Verlag GmbH & Co. KGaA

Table 1. Proof of concept in the counterion enhanced asymmetric transfer hydrogenation of 3-methyl-2-cyclohexenone (**1a**) using L-valine *t*-butyl ester as cation source.

Entry[a]	Anion		Conv.[c][%]	Yield[c] [%]	ee[c] [%]	Δee[d]
1		**3**	< 1	< 1	n.d.	n.d.
2			78	49	54	-
3[b]			92	88	51	-
4		**4**	40	27	64	10
5[b]		**4**	**75**	**72**	**74**	**23**
6	 (RAC)	**8**	13	13	54	0
7	 (R)	**8**	22	13	54	0
8	 (S)	**8**	20	15	54	0

[a] Performed with 0.18 mmol 3-methyl-2-cyclohexenone (**1a**), 20 mol% catalyst and 0.22 mmol Hantzsch ethyl ester in 0.55 mL 1,4-dioxane for 48 hours at 60 °C, [b] MTBE used as solvent, [c] Determined by GC analysis on BGB5 column using *n*-dodecane as internal standard and chiral GC analysis using a BGB175 chiral capillary column, [d] Δee defined as the difference between the reaction with phosphate anion **4** and trifluoracetate anion in 1,4-dioxane and MTBE, respectively.

This increase in the enantioselectivity can be attributed to the solvent's polarity, resulting in the formation of contact ion pairs in apolar solvents and hence a stronger interaction between cation and anion in the catalyst. In contrast to conventional salts that are defined by a strictly charge-ordered structure of atomic ions without dipole moment, organic salts, e.g. ionic liquids, possess a complex network with remarkable structural heterogeneity of the composing molecular ions.[22] On a supramolecular length scale, ion pairs, or more precisely ion aggregates exist for a lifetime of a few picoseconds; however, ion pair destabilization occurs as pairs readily dissociate into individual ions in pure salt melts. This situation changes drastically when organic salts are dissolved in molecular solvents: A number of experimental techniques, including NMR measurements or cyclic voltammetry proved the existence of long-lived ion pairs, suggesting that the ion pair formation is insignificant in neat salts but dominant in electrolyte solutions. Although a key feature of organic salts in solution, ion aggregation has been scarcely exploited for interionic chirality transfer. An outstanding example in this regard was published by Leitner and co-workers in their work on asymmetric hydrogenations featuring a proline-based chiral ionic liquid as solvent or additive in combination with atropisomeric phosphine ligands.[23] Impressive enantioselectivity was obtained through a complex of [{(*R*)-binap}Rh{(*S*)-MeProl}]$^+$, accompanied by *N*-bis-(trifluoromethane)sulfonimide anion.

We reasoned that the catalytic system could be improved by tuning the steric demand and rotation barrier of the atropisomeric phosphate anion. For this purpose, a set of biphenyl phosphoric acids were prepared via microwave-assisted oxidative coupling of phenols with *t*-butyl peroxide. This straightforward coupling step, followed by reaction with $POCl_3$ and successive hydrolysis gave access to the phosphoric acids (**4**–**7**) with variable substituent pattern in acceptable overall yield, starting from cheap and readily available phenols (see ESI S10–S13 for details). With this set of phosphoric acids in hand, the selectivity in asymmetric transfer hydrogenation could be considerably improved and varied between 74 and 80 %ee. Best results were obtained with the isopropyl substituted phosphoric acid **6** as anion source, providing up to 80 %ee with nearly quantitative yield (Figure 2, also see ESI Table S3, page S25 for details). Furthermore, other acids traditionally used in organocatalysis have been investigated. The ee values were below 60 % for all cases under the same reaction conditions, further highlighting the benefits of the atropisomeric phosphoric acids **4**–**7** (see ESI Table S4, page S26 for details).

Successively, we performed an extensive screening of the amino acid as cation source for further optimization of the catalytic system. Little difference in enantioselectivity (between 72–80 %ee) were found between L-valine, L-leucine, L-isoleucine and L-*t*-leucine *t*-butyl esters, whereas aromatic species such as L-phenylalanine *t*-butyl ester where less efficient. L-Proline *t*-butyl ester with a secondary ammonium cation gave also significantly lower selectivity (see ESI Table S5, page S27 for details). Finally, modifications on the ester moiety

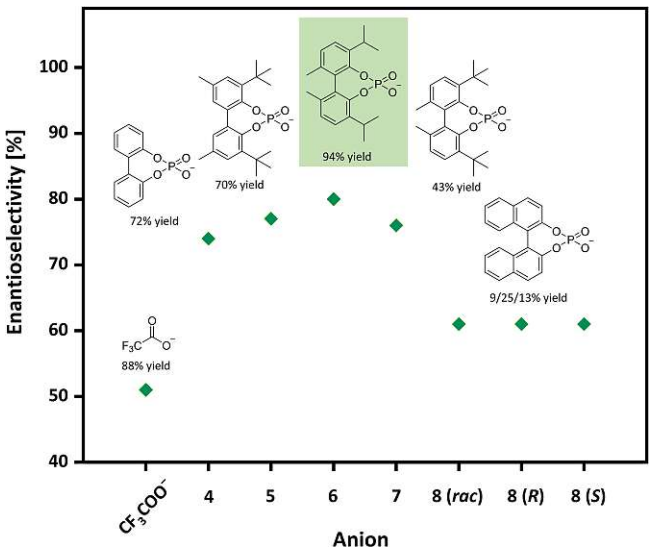


Figure 2. Impact of different phosphate anions vs. TFA anion on the enantioselectivity. All reactions were carried out in MTBE at 60 °C using L-valine *t*-butyl ester as cation source.

Die approbierte gedruckte Originalversion dieser Dissertation ist an der TU Wien Bibliothek verfügbar.
The approved original version of this doctoral thesis is available in print at TU Wien Bibliothek.
TU Bibliothek Your knowledge hub WIEN

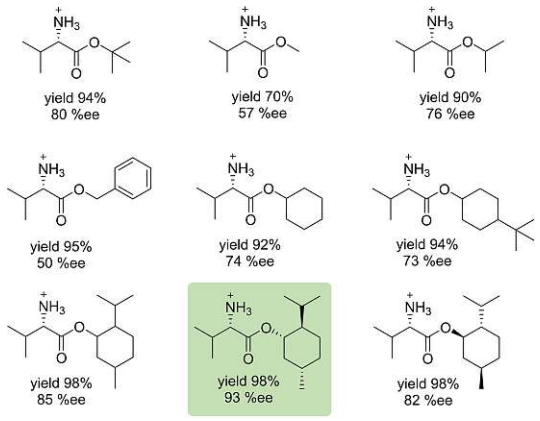
© 2020 The Authors. Published by Wiley-VCH Verlag GmbH & Co. KGaA

of (L)-valine revealed that sterically demanding aliphatic groups such as *t*-butyl, 4-*t*-butyl cyclohexyl or menthyl are indeed required for reaching high selectivity, as can be easily seen when comparing the results with those obtained for methyl or benzyl esters. Eventually, the best results were obtained when matching (L)-valine with the (+)-(1*S*,2*R*,5*S*) menthol, as the resulting ester in combination with phosphoric acid **6** resulted in an excellent yield of 98% and an enantioselectivity of 93% ee. This is in contrast to the mismatched ester-system obtained with (−)-(1*R*,2*S*,5*R*) menthol, which gave only 82%ee (Scheme 2).

With the ideal cationic and anionic moiety identified, it was also possible to reduce the catalyst loading to lower amounts: When studying different catalyst loadings at 25 °C, the high selectivity was maintained even at 5 mol% catalyst, although losses in yield had to be taken into account. Eventually, a reaction temperature of 50 °C provided an ideal compromise between yield and selectivity, providing the desired product **2a** in 98% yield and 95%ee (Table 2, entry 9).

For further studies on scope and limitation of the newly established catalytic system, the substrate pool was widened to investigate the asymmetric transfer hydrogenation of different 3-substituted cyclohexenones under the previously optimized reaction conditions (Table 3). Enantioselectivity exceeded 90% frequently, thereby demonstrating the versatility and broad application range of the newly established system.

In general, atropisomerism is a type of axial chirality that may arise in systems where free rotation about a single covalent



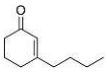
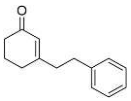
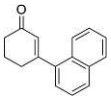
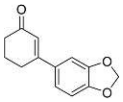
Scheme 2. Optimization of the (L)-valine ester moiety as cations source for. All reactions were carried out in MTBE at 60 °C using phosphate anion **6**.

Table 2. Optimization of conditions and parameters for the asymmetric transfer hydrogenation of 3-methyl-2-cyclohexenone (**1a**) using (*L*)-valine (+)-(1*R*,3*R*,4*S*) menthyl ester and the isopropyl substituted phosphoric acid **6** as anion source.

Entry[a]	T [°C]	Catalyst [mol%]	Hantzsch ester	Yield[b]/%	ee[c] [%]
1	60	20	ethyl	98	93
2	50	20	ethyl	98	95
3	40	20	ethyl	96	95
4	25	20	ethyl	59	96
5	25	10	ethyl	43	96
6	25	5	ethyl	29	96
7	25	1	ethyl	11	96
8	50	10	ethyl	99	94
9	**50**	**5**	**ethyl**	**98**	**95**
10	50	1	ethyl	68	93
11[d]	25	20	methyl	14	83
12[d]	25	20	ethyl	17	88
13[d]	25	20	*i*-propyl	58	69
14[d]	25	20	*t*-butyl	58	67

[a] Performed with 0.18 mmol 3-methyl-2-cyclohexenone, 0.009-0.036 mmol catalyst and 0.22 mmol Hantzsch ester in 0.55 mL MTBE at the given temperature for 48 hours, [b] Determined by GC analysis on a BGB5 column using *n*-dodecane as internal standard, [c] Determined by chiral GC analysis using a BGB175 chiral capillary column, [d] Performed with (L)-valine *t*-butyl ester instead of (L)-valine (+)-(1*R*,3*R*,4*S*) menthyl ester.

Table 3. Substrate scope for the counterion enhanced transfer hydrogenation of enones.

Entry[a]	Substrate		Yield [d] [%]	ee[e] [%]
1		**1a**	98 (72)[f]	95 (*S*)
2		**1b**	85 (76)[f]	92 (*S*)
3		**1c**	70 (55)[f]	91 (*S*)
4		**1d**	91 (87)	93 (*S*)
5		**1e**	85 (60)[f]	86 (*S*)
6		**1f**	75 (68)[f]	88 (*S*)
7[b]		**1g**	66 (60)	92 (*S*)
8[c]		**1h**	94 (80)[f]	89 (*S*)
9		**1i**	86 (84)	82 (*S*)
10		**1j**	94 (91)	90 (*S*)
11		**1k**	65 (62)	94 (*S*)
12		**1l**	89 (86)	70 (*S*)

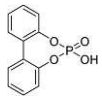
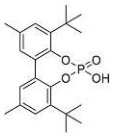
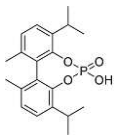
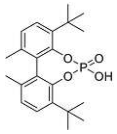
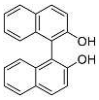
[a] Performed with 1.8 mmol ketone, 5 mol% catalyst and 2.2 mmol Hantzsch ethyl ester in 5.5 mL MTBE at 50 °C for 48 hours, [b] 20 mol% catalyst, [c] 10 mol% catalyst, [d] Determined by GC or GC–MS analysis. Isolated yields after flash column chromatography are given in parenthesis, [e] Determined by chiral GC analysis using a BGB175 or BGB173 chiral capillary column, or by chiral HPLC analysis using a Diacel Chiralcel AS–H column. Absolute configurations have been determined by measuring the optical rotation and comparing with literature data, [f] Lower isolated yield because of high volatility of the product.

Die approbierte gedruckte Originalversion dieser Dissertation ist an der TU Wien Bibliothek verfügbar.
The approved original version of this doctoral thesis is available in print at TU Wien Bibliothek.
TU Bibliothek Your knowledge hub WIEN

© 2020 The Authors. Published by Wiley-VCH Verlag GmbH & Co. KGaA

bond is hindered.[24] The isomerization pathways of biphenyls with bulky ortho-substituents were studied in detail by Masson, showing that conformers with isomerization barriers >23 kcal/mol can be separated at room temperature.[25] Less information is available for biphenols or biphenyl phosphoric acids. For more insight on the behavior of the atropisomeric phosphoric acids, we calculated isomerization barriers for compounds **4**–**8** (Table 4). The pure electrostatic barriers were corrected by frequency contributions to result in the Gibbs free energy barrier (ΔG) at a temperature of 333.15 K. Optimizations, energy evaluations and frequency calculations were performed on the B3LYP-D3/def2TZVP[26–28] level of theory with the program package ORCA.[29] Correlation in the uniform electron gas was modeled according to the Vosko-Wilk-Nusair VWN5 formalism.[30] A detailed description of the computational methodology can be found in the ESI (S32–S33).

Table 4. Barrier energies for the phosphoric acids on the B3LYP-D3/def2TZVP level of theory.

Entry	Biphenol/ Phosphoric acid		Isomerization barrier ΔG [kcal/mol]	Dihedral angle around the aryl-aryl bound	
				Ground state	Transition state
1			11.5[31]	110°	0°
2		**4**	10.0	43°	0°
3		**5**	12.0	49°	0°
4		**6**	41.2	56°	21°
5		**7**	48.2	61°	29°
6			42.7[25]	75°	26°

In general, comparison of the isomerization barriers between biphenols and biphenyl phosphoric acids is not straightforward. In case of biphenol, at least five ground state isomers can be identified, resulting in multiple isomerization pathways.[31] Sahnoun et al. estimate a value of 11.5 kcal/mol for the lowest possible pathway.[31]

Due to the additional O–P–O bridge, the phosphoric acids are restricted in the rotation of the aryl-aryl bond, hence allowing only one pathway. The phosphoric acids **4** and **5** have similar rotational barriers of 10 and 12 kcal/mol, indicating that substituents in 3,3′-position have only a minor impact on the rotation barrier. As visible from Figure 3 (top), their transition states for the isomerization are both planar. However, barriers for the acids **6** and **7** increase to 41.2 and 48.2 kcal/mol, respectively, which can be attributed to the methyl groups in 6,6′-position. Apart from the steric hindrance of the rotation, this substitution pattern also forces an out-of-plane transition state (Figure 3, bottom).

Moreover, the optimal dihedral angle of 2,2′-biphenol and biphenyl phosphoric acid differs significantly due to the constraints of the phosphate bridge on the rotation of the two phenyl rings (Table 4). In case of 2,2′-biphenol two hydroxyl hydrogens are able to form hydrogen bonds to the opposite oxygen.

The rotational barrier itself cannot explain the different enantioselectivity observed in the ATH reaction. For example,

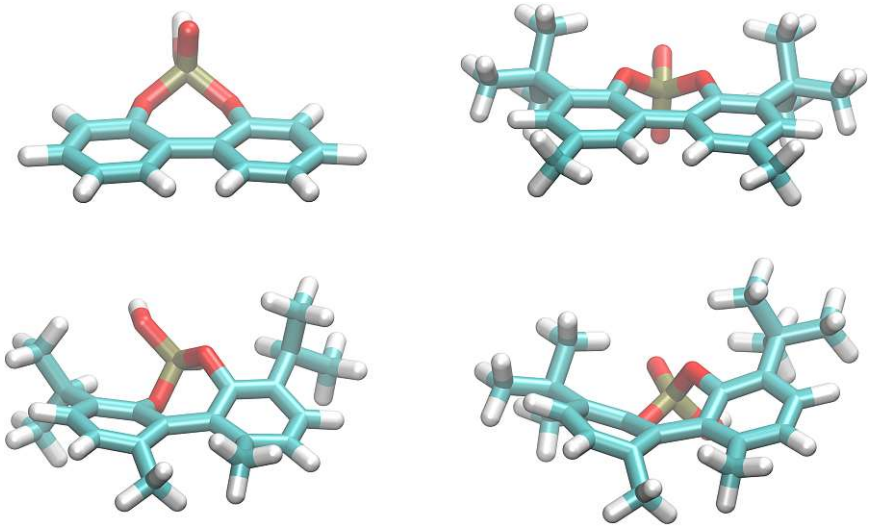


Figure 3. Optimized geometry of the transition states of compounds **4**–**7**.

Die approbierte gedruckte Originalversion dieser Dissertation ist an der TU Wien Bibliothek verfügbar.
The approved original version of this doctoral thesis is available in print at TU Wien Bibliothek.
TU Bibliothek Your knowledge hub WIEN

© 2020 The Authors. Published by Wiley-VCH Verlag GmbH & Co. KGaA

anions arising from phosphoric acid **5** and **7** gave similar enantioselectivity, despite a considerable difference in their rotational barriers (Figure 2,). Additionally, the rotational barrier of the binaphthyl phosphate **8** is considerably higher compared to biphenyl phosphate **4**. However, the latter resulted in considerably higher yield and enantioselectivity (see Table 1, entries 4 vs. 6–8), indicating that a complex interplay of the steric demand, anion geometry and rotation barrier is responsible for the different performance in the ATH reaction.

The most promising catalyst system was investigated further via non-polarizable molecular dynamics simulations. To model the ion pair prior to the enantioselective reaction step, we further investigated the iminium cation formed (+)-(1*S*,2*R*,5*S*) menthyl-L-valinate and 3-methyl-2-cyclohexenone, in combination with phosphate anion **6**. Simulations were performed for one intermediate ion pair at 60 °C in methyl butyl ether, a solvent with a comparable dielectric constant to MTBE (see ESI S34-S37 for details). To explore any structural difference in the ion pairs, the (*E*) and (*Z*) form of the cation and both enantiomers of the anion were considered in four different simulations. The ion pairs incorporating the (*R*)-enantiomer of the anion are shown in Figure 4.

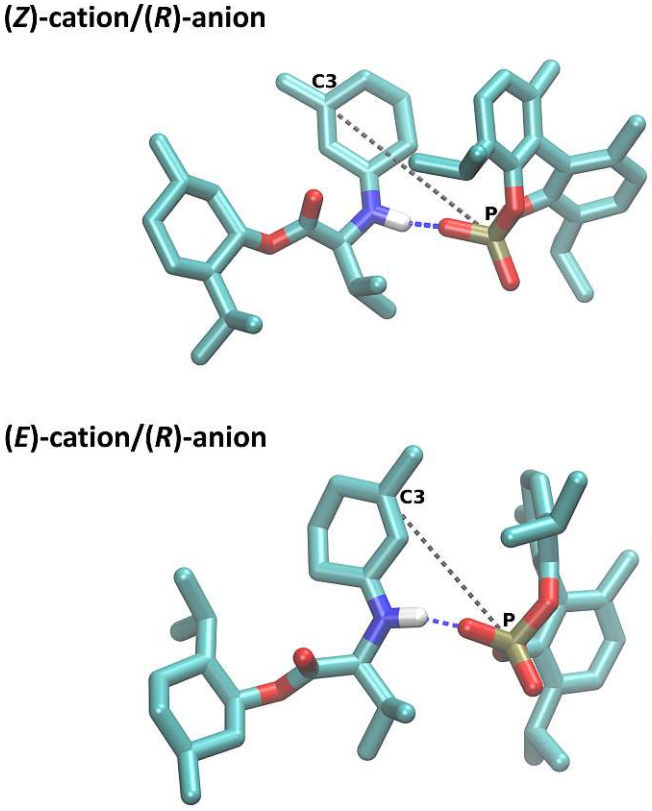


Figure 4. Snapshots of the (*Z*)-cation/(*R*)-anion (top) and (*E*)-cation/(*R*)-anion (bottom) pairs from the simulations. All solvent molecules as well as all hydrogens except the nitrogen-bound hydrogen were omitted for clarity.

Table 5. Average number of hydrogen bonds and interionic distances obtained from molecular dynamics simulations.

Ion pair	Average number of hydrogen bonds	Average interionic distance (center of mass) [Å]	Average distance C3-P [Å]
Z-cat/R-an	0.90 ± 0.04	7.2 ± 0.8	6.7 ± 0.5
Z-cat/S-an	0.85 ± 0.07	6.9 ± 0.9	6.6 ± 0.6
E-cat/R-an	0.90 ± 0.05	7.1 ± 0.9	5.5 ± 0.4
E-cat/S-an	0.87 ± 0.03	6.8 ± 0.9	5.2 ± 0.4

From the average interionic distance calculated respective to center of mass, it can be seen that the ions form stable pairs throughout the simulation. In all systems, the hydrogen bond between cation and anion (see Figure 4 and Table 5) is present for more than 85 % of the simulation time. This hydrogen bond promotes a certain orientation of the ion pair, with the phosphate group of the anion oriented towards the nitrogen of the cation. This also affects the average distance between the prochiral C3-atom of the cation and the P-atom of the anion. In the unfavored (*Z*)-form, the methyl group bound to the prochiral C3 points on the opposite side of the nitrogen-bound hydrogen, resulting in an interionic distance of approx. 6.5 Å away. In contrast, the C3-P distance is shorter by about 1 Å in the favored (*E*)-form, providing a closer ion pair and thus might be ideal for chiral induction.

Conclusion

In here, we reported a novel concept of counterion catalysis for organocatalytic asymmetric transfer hydrogenations. The ion-paired catalysts, based on cheap amino acid-derived cations and flexible phosphate anions could be readily synthetized from natural compounds, providing a significantly cheaper alternative to the current start-of-art ACDC methodology. After careful parameter optimization, a series of different enones could be reduced with high yields and enantioselectivity under mild conditions even with low catalyst loadings.

From the simulation data, we can conclude that interionic interactions are strong enough to form a stable ion pair in apolar solvents such as MTBE, and that the hydrogen bond both favors a certain arrangement of the ion pair, with the C3 atom relatively close to the anion. The exact interplay between the ions, and the mechanism of a possible chirality transfer remains unclear, and it will be further evaluated in future studies addressing the influence of aggregate formation rather than a single ion pair.

Current investigations focus on the exploration of the reaction scope for counterion enhanced organocatalysis with chiral amino acid derived cations and atropisomeric phosphate anions. Overall, we expect that the concept of counterion enhanced catalysis relying on chiral cations and atropisomeric anions will find broad utility in organocatalysis, but also in transition metal catalyzed process.

Die approbierte gedruckte Originalversion dieser Dissertation ist an der TU Wien Bibliothek verfügbar.
The approved original version of this doctoral thesis is available in print at TU Wien Bibliothek.
TU Bibliothek Your knowledge hub WIEN

© 2020 The Authors. Published by Wiley-VCH Verlag GmbH & Co. KGaA

Experimental Section

Representative procedure for the asymmetric transfer hydrogenation

A glass vial equipped with a magnetic stir bar was charged with ketone (1.8 mmol, 1.0 equiv.) in MTBE (5.5 mL, 0.33 M), followed by the addition of the catalyst (55.4 mg, 0.09 mmol, 5 mol%) and Hantzsch ester (552 mg, 2.2 mmol, 1.2 equiv.). The reaction mixture was stirred at 50 °C for 48 h. After cooling to room temperature, diethyl ether (5 mL) and 4 M HCl (10 mL) was added and the mixture was stirred until the phases were transparent (30 min). The phases were separated and the organic phase was washed with 4 M HCl (3×20 mL). The organic phase was dried over Na_2SO_4 and concentrated under reduced pressure. Purification by column chromatography (15% Et_2O: PE, vanillin staining agent or UV visualization) gave the 3-substituted cyclohexanones.

Acknowledgements

Financial support by the Austrian Science Fund (project P29146-N34) is gratefully acknowledged.

Conflict of Interest

The authors declare no conflict of interest.

Keywords: organocatalysis · asymmetric synthesis · transfer hydrogenation · ion aggregation · phosphoric acid · counterion catalysis

[1] D. Wang, D. Astruc, *Chem. Rev.* **2015**, *115*, 6621–6686.
[2] W. S. Mahoney, J. M. Stryker, *J. Am. Chem. Soc.* **1989**, *111*, 8818–8823.
[3] A. Erkkilä, I. Majander, P. M. Pihko, *Chem. Rev.* **2007**, *107*, 5416–5470.
[4] R. P. Herrera, *Top. Curr. Chem.* **2016**, *374*, 29.
[5] S. G. Ouellet, J. B. Tuttle, D. W. C. MacMillan, *J. Am. Chem. Soc.* **2005**, *127*, 32–33.
[6] J. B. Tuttle, S. G. Ouellet, D. W. C. MacMillan, *J. Am. Chem. Soc.* **2006**, *128*, 12662–12663.
[7] J. W. Yang, M. T. Hechavarria Fonseca, B. List, *Angew. Chem. Int. Ed.* **2004**, *43*, 6660–6662; *Angew. Chem.* **2004**, *116*, 6829–6832.
[8] S. Mayer, B. List, *Angew. Chem. Int. Ed.* **2006**, *45*, 4193–4195; *Angew. Chem.* **2006**, *118*, 4299–4301.
[9] N. J. A. Martin, B. List, *J. Am. Chem. Soc.* **2006**, *128*, 13368–13369.
[10] M. Mahlau, B. List, *Angew. Chem. Int. Ed.* **2013**, *52*, 518–533; *Angew. Chem.* **2013**, *125*, 540–556.
[11] K. Brak, E. N. Jacobsen, *Angew. Chem. Int. Ed.* **2013**, *52*, 534–561; *Angew. Chem.* **2013**, *125*, 558–588.
[12] G. L. Hamilton, E. J. Kang, M. Mba, F. D. Toste, *Science* **2007**, *317*, 496–499.
[13] S. Liao, B. List, *Angew. Chem. Int. Ed.* **2010**, *49*, 628–631; *Angew. Chem.* **2010**, *122*, 638–641.
[14] P. García-García, F. Lay, C. Rabalakos, B. List, *Angew. Chem. Int. Ed.* **2009**, *48*, 4363–4366; *Angew. Chem.* **2009**, *121*, 4427–4430.
[15] V. Rauniyar, Z. J. Wang, H. E. Burks, F. D. Toste, *J. Am. Chem. Soc.* **2011**, *133*, 8486–8489.
[16] D. Qian, J. Sun, *Chem. Eur. J.* **2019**, *25*, 3740–3751.
[17] G. B. Rowland, E. B. Rowland, Y. Liang, J. A. Perman, J. C. Antilla, *Org. Lett.* **2007**, *9*, 2609–2611.
[18] L. Ren, T. Lei, L.-Z. Gong, *Chem. Commun.* **2011**, *47*, 11683.
[19] X. Cheng, S. Vellalath, R. Goddard, B. List, *J. Am. Chem. Soc.* **2008**, *130*, 15786–15787.
[20] M. Rueping, E. Sugiono, C. Azap, T. Theissmann, M. Bolte, *Org. Lett.* **2005**, *7*, 3781–3783.
[21] R. I. Storer, D. E. Carrera, Y. Ni, D. W. C. MacMillan, *J. Am. Chem. Soc.* **2006**, *128*, 84–86.
[22] R. Hayes, G. G. Warr, R. Atkin, *Chem. Rev.* **2015**, *115*, 6357–6426.
[23] D. Chen, M. Schmitkamp, G. Franciò, J. Klankermayer, W. Leitner, *Angew. Chem. Int. Ed.* **2008**, *47*, 7339–7341; *Angew. Chem.* **2008**, *120*, 7449–7451.
[24] J. Chandrasekhar, R. Dick, J. Van Veldhuizen, D. Koditek, E.-I. Lepist, M. E. McGrath, L. Patel, G. Phillips, K. Sedillo, J. R. Somoza, et al., *J. Med. Chem.* **2018**, *61*, 6858–6868.
[25] E. Masson, *Org. Biomol. Chem.* **2013**, *11*, 2859.
[26] A. D. Becke, *J. Chem. Phys.* **1993**, *98*, 5648–5652.
[27] S. Grimme, J. Antony, S. Ehrlich, H. Krieg, *J. Chem. Phys.* **2010**, *132*, 154104.
[28] F. Weigend, R. Ahlrichs, *Phys. Chem. Chem. Phys.* **2005**, *7*, 3297.
[29] F. Neese, *Wiley Interdiscip. Rev.: Comput. Mol. Sci.* **2012**, *2*, 73–78.
[30] S. H. Vosko, L. Wilk, M. Nusair, *Can. J. Phys.* **1980**, *58*, 1200–1211.
[31] R. Sahnoun, S. Koseki, Y. Fujimura, *J. Phys. Chem. A* **2006**, *110*, 2440–2447.

Manuscript received: March 9, 2020
Revised manuscript received: April 22, 2020
Accepted manuscript online: April 28, 2020
Version of record online: June 15, 2020

Die approbierte gedruckte Originalversion dieser Dissertation ist an der TU Wien Bibliothek verfügbar.
The approved original version of this doctoral thesis is available in print at TU Wien Bibliothek.
TU Bibliothek Your knowledge hub WIEN

© 2020 The Authors. Published by Wiley-VCH Verlag GmbH & Co. KGaA

9 Sterically Demanding Flexible Phosphoric Acids for Constructing Efficient and Multi-Purpose Asymmetric Organocatalysts

In the initial studies of the ACDC concept, List et al. demonstrated exceptional performance using a chiral, highly sterically demanding phosphoric acid. Combining the renowned TRIP phosphoric acid with various chiral or achiral amines yielded a privileged catalyst, flourishing in multiple applications.[62,73,77,93] Another privileged catalyst in the domain of iminium-catalysis is primary amino functionalized quinine, a slightly modified naturally derived compound known for its substantial rigidity. This quality makes it an ideal catalyst for enamine or iminium catalysis, showcasing remarkable performance in various tasks.[94,95] In our approach, we aimed to create a versatile catalyst suitable for transformations such as epoxidation, aziridination, and more complex domino reactions involving an iminium/enamine strategy. We started by screening several diamines, preferably derived from commercially available amino acids. Subsequently, we optimized the chiral diamine structure via screening of the secondary amine moiety. From the perspective of the phosphoric acid, we employed achiral, sterically demanding, and rigid phosphoric acids as counterions to reduce the flexibility of the catalytic complex and potential beneficial conformational changes. As an initial model reaction, we selected the asymmetric epoxidation of enones, given its significant role as a chiral building block. Subsequently, we transitioned to the asymmetric aziridination of enones to further illustrate the catalyst's performance. In the final section, we introduced a novel procedure for the synthesis of intricate chiral compounds, utilizing our concept of counteranion-enhanced catalysis.

The following manuscript is presented in this chapter:

Scharinger, F.; Pálvölgyi, Á. M.; Weisz, M.; Weil, M.; Stanetty, C.; Schnürch, M.; Bica-Schröder, K. Sterically Demanding Flexible Phosphoric Acids for Constructing Efficient and Multi-Purpose Asymmetric Organocatalysts. *Angew. Chem. Int. Ed.* **2022**, *61* (26). https://doi.org/10.1002/anie.202202189.

In my role as a main author, I carried out all major experiments and was responsible for manuscript preparation.

Die approbierte gedruckte Originalversion dieser Dissertation ist an der TU Wien Bibliothek verfügbar.
The approved original version of this doctoral thesis is available in print at TU Wien Bibliothek.

Check for updates

Organocatalysis

How to cite:
International Edition: doi.org/10.1002/anie.202202189
German Edition: doi.org/10.1002/ange.202202189

Sterically Demanding Flexible Phosphoric Acids for Constructing Efficient and Multi-Purpose Asymmetric Organocatalysts

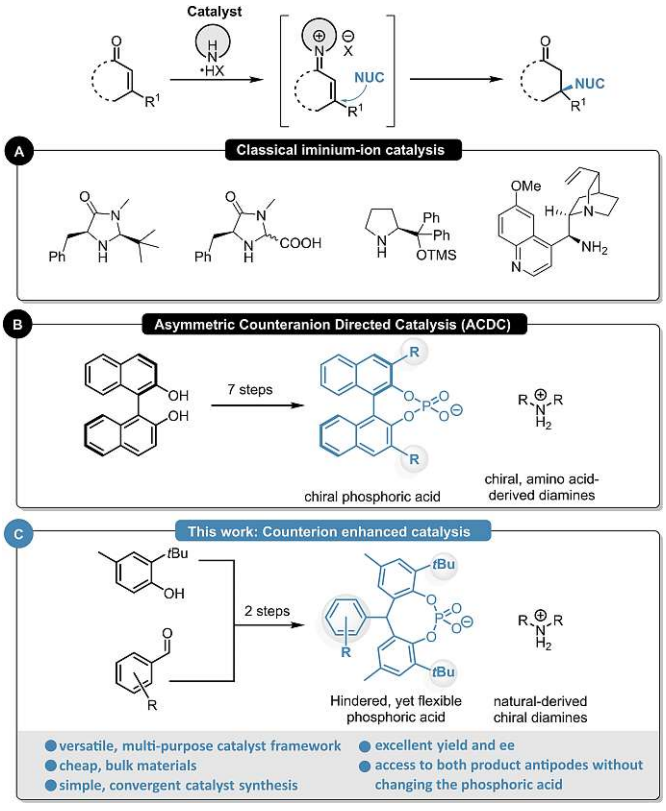
*Fabian Scharinger, Ádám Márk Pálvölgyi, Melanie Weisz, Matthias Weil, Christian Stanetty, Michael Schnürch, and Katharina Bica-Schröder**

Abstract: Herein, we present a novel approach for various asymmetric transformations of cyclic enones. The combination of readily accessible chiral diamines and sterically demanding flexible phosphoric acids resulted in a simple and highly tunable catalyst framework. The careful optimization of the catalyst components led to the identification of a particularly powerful and multi-purpose organocatalyst, which was successfully applied for asymmetric epoxidations, aziridinations, aza-Michael-initiated cyclizations, as well as for a novel Robinson-like Michael-initiated ring closure/aldol cyclization. High catalytic activities and excellent stereocontrol was observed for all four reaction types, indicating the excellent versatility of our catalytic system. Furthermore, a simple change in the diamine's configuration provided easy access to both product antipodes in all cases.

Introduction

The synthesis of optically active products is one of the major challenges in modern chemistry and in this field, asymmetric organocatalysis is of special interest.[1] As no toxic and/or expensive transition metals are required, such transformations generally feature great air- and moisture tolerance,[2–5] therefore providing a simple and robust access to enantioenriched products. Iminium-ion catalysis represents one of the most important organocatalytic activation modes and it has become a powerful and widely applied tool for the enantioselective β-functionalization of α,β-unsaturated aldehydes and ketones.[6] Landmark discoveries from the group of MacMillan,[7–9] Jørgensen,[10–12] and List[13–15] resulted in powerful methods for various iminium-ion-catalyzed asymmetric transformations (Scheme 1A). Parallel to traditional iminium-ion catalysis, the field of BINOL-derived chiral phosphoric acids also emerged to be indispensable, providing elegant examples for the β-functionalization of enals and enones using enantiomerically pure, chiral phosphoric acids (CPAs) via Asymmetric Counteranion Directed Catalysis (ACDC, Scheme 1B).[16–18] Despite these remarkable advances, most of the existing methods suffer either from their difficult tunability for obtaining the opposite product antipode and/or from multi-step catalyst synthesis with tedious separations resulting in rather expensive catalyst systems.[19,20]

Incited by these limitations and based on our previous experiences,[21,22] we envisioned to apply our concept of



Scheme 1. Different catalytic concepts for the asymmetric functionalization of enones: classical iminium-ion catalysis (A), Asymmetric Counteranion-Directed Catalysis (B) and the concept of counterion enhanced catalysis (C).

[*] F. Scharinger, Á. M. Pálvölgyi, M. Weisz, C. Stanetty, Prof. M. Schnürch, Prof. K. Bica-Schröder
Institute of Applied Synthetic Chemistry, TU Wien
Getreidemarkt 9/163, 1060 Wien (Austria)
E-mail: katharina.schroeder@tuwien.ac.at
Prof. M. Weil
Institute of Chemical Technologies and Analytics, TU Wien
Getreidemarkt 9/163, 1060 Wien (Austria)

© 2022 The Authors. Angewandte Chemie International Edition published by Wiley-VCH GmbH. This is an open access article under the terms of the Creative Commons Attribution License, which permits use, distribution and reproduction in any medium, provided the original work is properly cited.

Die approbierte gedruckte Originalversion dieser Dissertation ist an der TU Wien Bibliothek verfügbar. The approved original version of this doctoral thesis is available in print at TU Wien Bibliothek.
TU Wien Bibliothek Your knowledge hub

counterion enhanced catalysis for various asymmetric β-functionalization reactions of cyclic enones (Scheme 1C). By combining easily accessible chiral diamines with sterically demanding yet flexible phosphoric acids, simple and highly tunable multi-purpose catalyst frameworks were obtained. Within this contribution we will report a set of different transformations which could be carried out with such catalyst system, resulting in excellent enantioselectivities for both product antipodes.

Results and Discussion

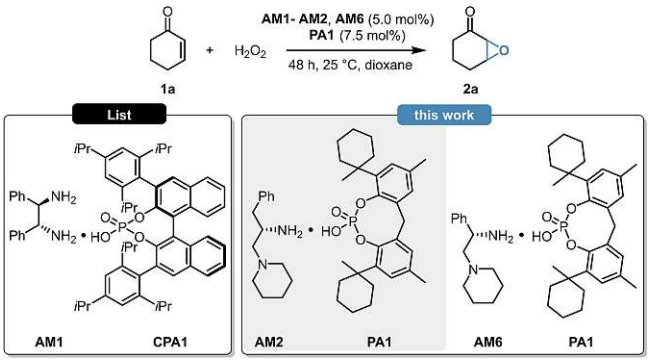
Asymmetric Epoxidation of Enones

Enantioenriched epoxides play a crucial role for the pharmaceutical and agricultural industries, both as intermediates and actual APIs. Based on the landmark discovery of K. B. Sharpless et al., the asymmetric epoxidation of unsaturated compounds is of special interest in this field. Seminal examples relying on (transition)metal catalysis,[23–25] phase transfer catalysis,[26–28] bifunctional base catalysis,[29,30] and iminium-ion/enamine catalysis[31–33] have been all successfully applied, resulting in various tools for asymmetric epoxidations. Despite these remarkable advances, the asymmetric epoxidation of α,β-unsaturated ketones still remained a challenge. The current state of the art catalyst for this purpose was reported by the group of B. List. Their elegant strategy applied double stereoinduction by combining the chiral amine **AM1** with the chiral phosphoric acid **CPA1**, also known as (*S*)-TRIP (Table 1, left).[34] Instead of relying on such a double stereoinduction approach, we envisioned to use our concept of counterion enhanced catalysis, using simple and flexible phosphoric acids in combination with amino-acid-derived diamines as cheap and readily available chiral frameworks (Table 1, right). To test our concept, the asymmetric epoxidation of 2-cyclohexen-1-one (**1a**) was chosen as benchmark reaction. Initially, we aimed to investigate if the use of a flexible phosphoric acid instead of other, commonly used acids can lead to an increased catalytic activity and/or enantioselectivity. For this purpose, the epoxidation of **1a** was performed by using the chiral diamine **AM2** or **AM6** in combination with the phosphoric acid **PA1**, and the results were compared to control experiments performed with TFA. When using **PA1** instead of TFA, a significant increase both in catalytic activity and enantioselectivity was observed (Table 1, entries 3 vs. 4 and 5 vs. 6), indicating a strong counterion effect. To our delight, the simple and cheap, unoptimized catalyst framework of **AM6** and **PA1** could already provide excellent results with only marginal differences to the current state-of-art (Table 1, entries 2 vs. 6).

Encouraged by these initial findings, we then aimed for optimizing our catalyst framework. In order to find the ideal amine source, various diamines (**AM2**–**AM12**) were synthesized from simple and cheap amino-acid precursors and their catalytic efficiency was evaluated in the epoxidation of **1a** (Scheme 2). At first, we sought to optimize the tertiary amine patterns of the diamines by using different, L-phenylalanine-derived amines (**AM2**–**AM5**).

Compared to the initially used piperidine unit, both the ring expansion and the ring shrinkage resulted in a significant decrease of catalytic activity and it also led to inferior enantioselectivity (Scheme 2, top). This was particularly pronounced when using the morpholine-modified amine **AM5**, which provided only 20 % conversion. With the

Table 1: Proof of concept studies.

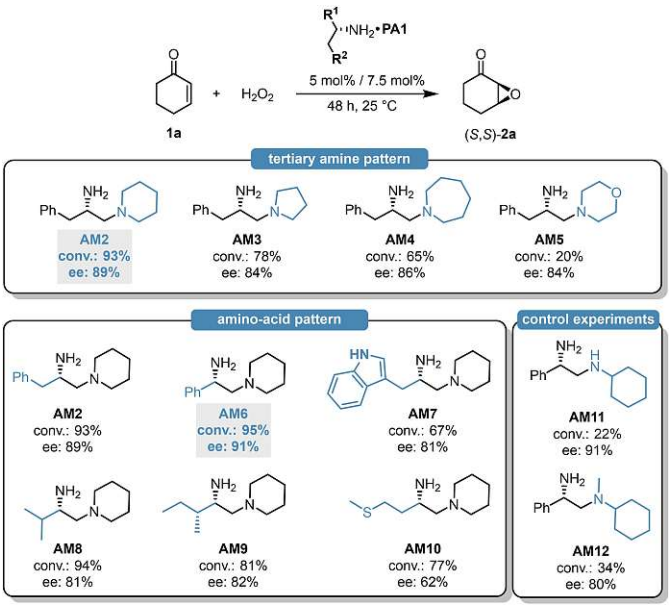


Entry[a]	Amine	Acid	Conv. [%][b]	ee [%][c]		Δee
1[d]	**AM1**	TFA	95	90 (*R*,*R*)	⊢	**2**
2[d]	**AM1**	**CPA1**	98	92 (*R*,*R*)		
3	**AM2**	TFA	54	67 (*S*,*S*)	⊢	**22**
4	**AM2**	**PA1**	93	89 (*S*,*S*)		
5	**AM6**	TFA	91	79 (*S*,*S*)	⊢	**12**
6	**AM6**	**PA1**	95	91 (*S*,*S*)		

[a] Reactions were performed with 0.30 mmol 2-cyclohexen-1-one (**1a**), 5.0 mol% amine, 7.5 mol% acid and 1.5 equiv H_2O_2 (50% aq.) in 1.25 mL dioxane at 25 °C for 48 h. [b] Determined by GC analysis on a BGB5 column using *n*-dodecane as internal standard. [c] Determined by chiral GC analysis on a BGB175 column. [d] Literature values performed at 50 °C for 24 h.

© 2022 The Authors. Angewandte Chemie International Edition published by Wiley-VCH GmbH

Die approbierte gedruckte Originalversion dieser Dissertation ist an der TU Wien Bibliothek verfügbar. The approved original version of this doctoral thesis is available in print at TU Wien Bibliothek. TU Bibliothek Your knowledge hub WIEN



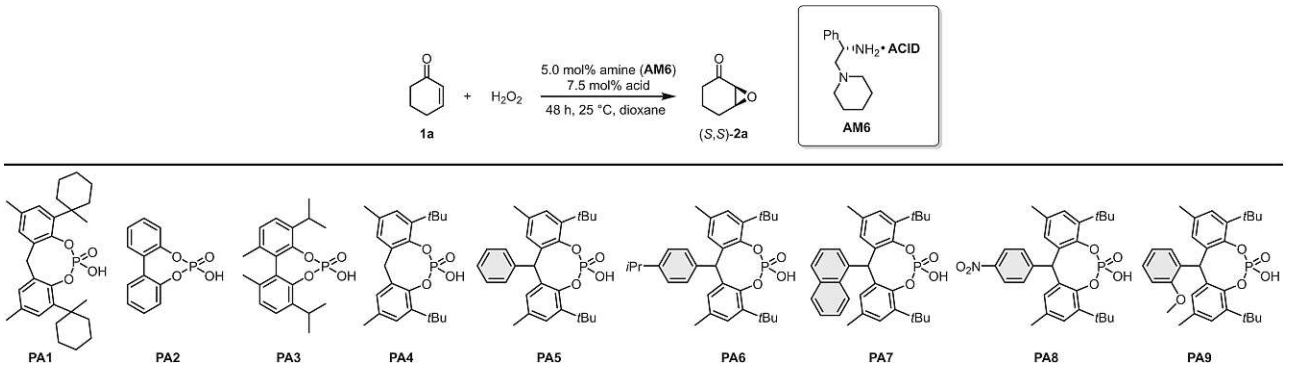
Scheme 2. Screening of different amino-acid-derived diamines using **PA1** as counterion. The reaction conditions were identical to those in Table 1.

suitable tertiary amine modification in hand, we also aimed for screening different amino acids (**AM6**–**AM10**). This revealed, that the diamine **AM2** and **AM6**, derived from aromatic amino-acids like L-phenylalanine and L-phenylglycine result in excellent yield and stereocontrol; meanwhile, the introduction of either heteroaromatic- or aliphatic amino-acids led to inferior catalytic activity and/or enantioselectivity (Scheme 2, bottom). Based on these findings, **AM6** was chosen as ideal diamine, resulting in 95 % conversion and 91 % ee. Even though L- and D-phenylglycine are non-proteinogenic amino acids, they are eventually crucial building blocks for lactam antibiotics what makes them cheap and commercially available bulk materials.[35] The cyclic tertiary amine pattern was still found to be crucial, as both the phenylglycine-derived **AM11**–**AM12** resulted in significantly inferior catalytic activities.

We then continued our optimization by screening different solvents. While the reaction proceeded quite smoothly indeed in ether-type reaction media, significantly worse results were obtained when using other solvents such as toluene or chloroform. We suspect that dioxane is an ideal solvent because it can fulfill two key requirements: (I) its low dielectric constant facilitates the formation of tight ion-pairs, resulting in an effective steric shielding around the iminium-ion and providing higher ee values; and (II) it forms a homogeneous system with the 50 % aqueous H_2O_2, which can improve not just the catalytic performance but it also leads to better reproducibility (for details, see Supporting Information page S24).

With the suitable diamine and solvent in hand, we continued the optimization by investigating the effect of different counterions (Table 2). For this purpose, a set of sterically demanding phosphoric acids (**PA1**–**PA9**) were prepared either via direct phosphorylation of the corresponding diols (**PA1**–**PA2, PA4**) or in a convenient two step

Table 2: Acid screening.



Entry[a]	Acid	Conv. [%][b]	ee [%][c]	Entry[a]	Acid	Conv. [%][b]	ee [%][c]
1	no acid	0	n.d.	9	**PA4**	85	92 (96.0 : 4.0)
2	p-toluenesulfonic acid	90	83 (91.5 : 8.5)	10	**PA5**	98	93 (96.5 : 3.5)
3	2,5-dinitrobenzoic acid	94	67 (83.5 : 16.5)	11	**PA6**	96	94 (97.0 : 3.0)
4	TFA	95	72 (86.0 : 14.0)	12	**PA7**	95	94 (97.0 : 3.0)
5	camphorsulfonic acid	87	82 (91.0 : 9.0)	13	**PA8**	95	93 (96.5 : 3.5)
6	**PA1**	95	91 (95.5 : 4.5)	14	**PA9**	95	95 (97.5 : 2.5)
7	**PA2**	12	69 (84.5 : 15.5)	**15**[d]	**PA9**	**96**	**95** (97.5 : 2.5)
8	**PA3**	97	90 (95.0 : 5.0)	16[e]	**PA9**	48	86 (93.0 : 7.0)

[a] Reactions were performed with 0.30 mmol 2-cyclohexen-1-one (**1a**), 5 mol% amine **AM6**, 7.5 mol% acid and 1.5 equiv H_2O_2 (50% aq.) in 1.25 mL dioxane at 25 °C for 48 h. [b] Determined by GC analysis on a BGB5 column using *n*-dodecane as internal standard. [c] Determined by chiral GC analysis on a BGB175 column. Enantiomeric ratios in parenthesis. [d] Reaction was performed with 1.0 equiv acid. [e] Reaction was performed with 2.0 equiv acid.

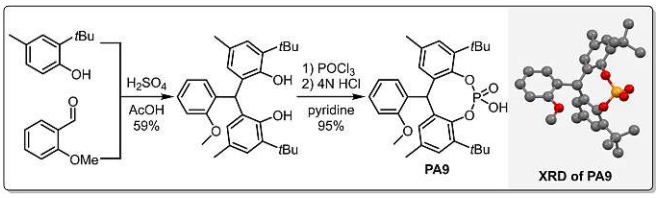
© 2022 The Authors. Angewandte Chemie International Edition published by Wiley-VCH GmbH

Die approbierte gedruckte Originalversion dieser Dissertation ist an der TU Wien Bibliothek verfügbar.
The approved original version of this doctoral thesis is available in print at TU Wien Bibliothek.
TU Bibliothek Your knowledge hub WIEN

procedure starting from simple phenols via Friedel–Crafts alkylation and subsequent phosphorylation (**PA5**–**PA9**, Scheme 3). The detailed synthesis of **PA1**–**PA9** can be found in the Supporting Information (Supporting Information page S11–S17).

While the simple biphenyl-derived **PA2** provided poor solubility and therefore low conversion and moderate stereocontrol (Table 2, entry 7), both the yield and enantioselectivity could be improved with **PA3**, indicating that an increased steric bulk might be indeed beneficial (Table 2, entry 8). To our delight, compounds **PA5**–**PA9** all gave excellent results, providing the asymmetric epoxide (*S*,*S*)-**2a** in 95–98 % yield and in 93–98 % ee (Table 2, entries 9–14). Taking into account the slightly higher yield of the phosphoric acid synthesis, but also the higher enantioselectivity, **PA9** has been chosen as optimal acid additive. Furthermore, the amine-to-acid ratio could be decreased to 1/1 without any loss of catalytic performance (Table 2, entries 14 vs. 15). The phosphoric acids **PA5**–**PA9** are sterically very demanding, yet feature no hindered rotation; therefore, the resulting ion-pair might behave as a single stereoisomeric catalyst. This could be an important aspect not just to avoid the generation of matched/mismatched diastereomers between the amine and the phosphoric acid, but it also results in a simple catalyst system which provides a convenient access to both product antipodes. Indeed, after simply changing from L-**AM6** to the diamine D-**AM6**, (*R*,*R*)-**2a** was obtained with the same excellent 95 % ee. To further test our concept, other classical Brønsted acids were also applied under the optimized reaction conditions (Table 2, entries 2–5). These provided the product (*S*,*S*)-**2a** in good yields; albeit, significantly decreased enantioselectivity of 67–83 % ee were observed (Table 2, entries 2–5). This clearly indicates the superiority of our phosphoric acids, which might be a consequence of the more efficient steric shielding upon iminium-ion formation.

In order to probe our hypothesis whether these phosphoric acids can eventually form stable enantiomers under the reaction conditions, ^{31}P NMR spectra of the [**AM6**][**PA3**] and [**AM6**][**PA9**] catalyst salts were recorded at different temperatures between −30 °C and +27 °C. The formation of the catalyst salt [**AM6**][**PA3**] resulted in complete peak splitting already at room temperature, indicating the formation of diastereomers and therefore suggesting that—as a consequence of its hindered rotation—compound **PA3** is chiral and it can form distinguishable enantiomers in a chiral environment at room temperature.



Scheme 3. General synthesis of **PA5**–**PA9** with the example of **PA9** (left) and the XRD crystallographic data for **PA9** (right). The deposition number for the XRD of **PA9**-MeOH adduct is CCDC 2112844.[36]

In contrast, no peak splitting in the NMR spectra of [**AM6**][**PA9**] could be observed, suggesting that such ion-paired catalysts based on flexible phosphoric acids might indeed act as a single stereoisomer under the reaction conditions. The detailed NMR study can be found in the Supporting Information (Supporting Information page S153–S159).

Having all crucial reaction parameters optimized, we aimed for exploring the scope and limitations of our catalyst system. Cyclohexenones with various β-substituents including alkyl, cycloalkyl and aryl groups were all well tolerated, resulting in a rather broad substrate scope as the corresponding epoxide products (**2a**–**2n**) were obtained in 95–98 % enantioselectivity for both product antipodes (Scheme 4). To our delight, the reaction scope could be expanded not just to other cyclic enones (**2o**), but eventually also to the epoxidation of acyclic substrates, still providing excellent enantioselectivities (**2p**–**q**). In accordance to literature—and for the sake of higher yield and enantioselectivity—a catalyst loading of 10 mol % was used for all reaction except when using the sterically unhindered substrate **1a**.[34]

Asymmetric Aziridination of Enones

To investigate the robustness of our catalytic system, we envisioned to expand the reaction scope to asymmetric aziridinations. As structural analogues to oxirans, aziridines are important building blocks for the synthesis of numerous APIs as well, as depicted in Figure 1.[37–40]

During the 1990s, numerous advances have been published for the asymmetric aziridination of olefins via Lewis-acid catalysis in the presence of chiral ligands,[41,42] as well as for the synthesis of aziridines via the addition of ylides or carbenes to imines.[43,44] With the rise of organocatalysis, several metal-free strategies emerged providing not just a less toxic and/or expensive alternative, but also expanding the reaction scope towards enals.[45,46] As for the current state of the art for the asymmetric aziridination of enones, the group of Melchiorre reported an elegant strategy via simple iminium-ion catalysis. The combination of a cinchona-derived chiral diamine and a chiral acid resulted in moderate to high catalytic activities and high stereocontrol for various enones via double stereoinduction; however, rather high catalyst loadings of 20 mol % was required.[47,48]

We started our optimization with the aziridination of 2-cyclohexen-1-one (**1a**). To our surprise, dioxane, which was the most suitable solvent for asymmetric epoxidation, resulted in nearly no product formation; whereas the

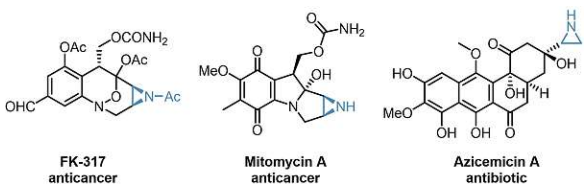
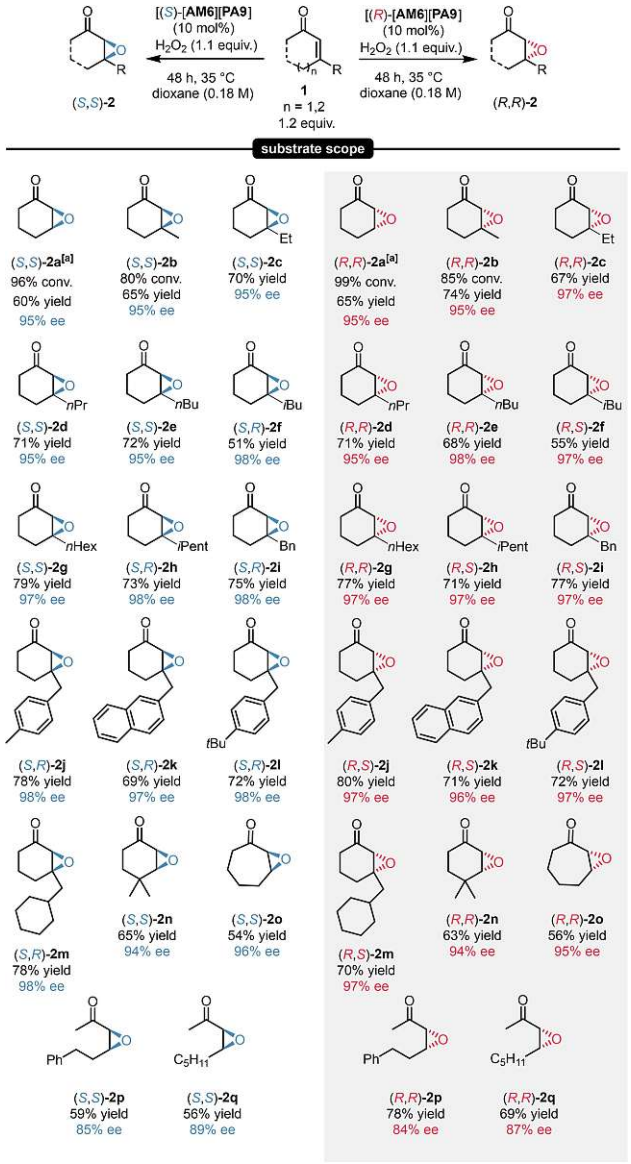


Figure 1. Examples of biologically active aziridines.

© 2022 The Authors. Angewandte Chemie International Edition published by Wiley-VCH GmbH

Die approbierte gedruckte Originalversion dieser Dissertation ist an der TU Wien Bibliothek verfügbar. The approved original version of this doctoral thesis is available in print at TU Wien Bibliothek. TU Bibliothek Your knowledge hub WIEN



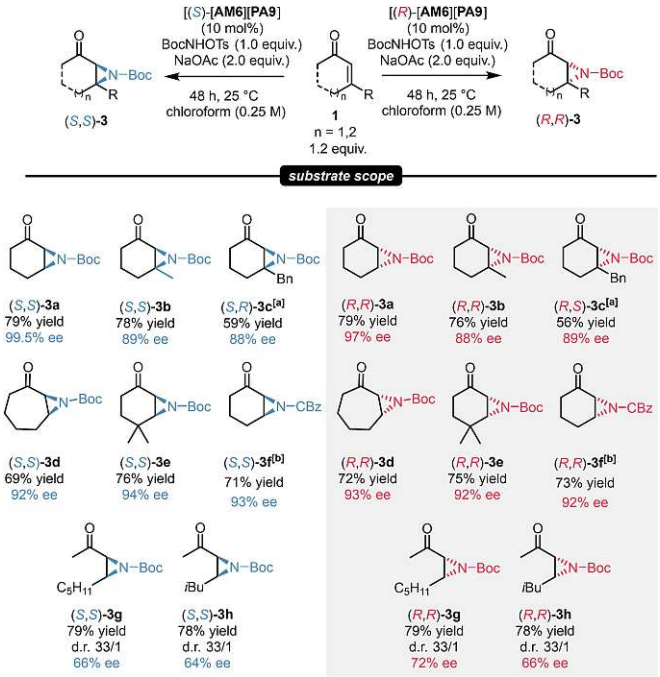
Scheme 4. Substrate scope for asymmetric epoxidations. Reactions were performed with 1.0–3.0 mmol enone (1.0 equiv **1a–q**), 10 mol% [**AM6**][**PA9**] and 1.1 equiv H_2O_2 (50% aq.) in dioxane (0.18 M) at 35 °C for 48 h. Yields refer to pure products after isolation by column chromatography. The enantiomeric excess was determined by chiral GC (BGB 175) or chiral HPLC (Chiralpak® IB or AS-H columns) analysis. Products **2a–f** and **2o** were isolated with lower yields because of their high volatility. [a] Reactions performed with 5.0 mol% [**AM6**][**PA9**] at 25 °C for 48 h. For **2o--q**, an additional work-up step with 1 N NaOH was required. For details, see Supporting Information page S26.

reaction in chloroform in the presence of $NaHCO_3$ as acid scavenger proceeded smoothly at room temperature, providing the product (*S*,*S*)-**3a** in high yield and in an excellent 97% ee. Further attempts by screening different solvents and acid scavengers gave almost all inferior results. Nevertheless, changing from $NaHCO_3$ to NaOAc provided even higher yields and an ee of 99.5% when using the catalyst salt of [**AM6**][**PA9**], which was already found to be very efficient for our asymmetric epoxidations. The detailed optimization can be found in the Supporting Information (Supporting Information pages S35–S36).

Gratifyingly, under these optimized conditions, the catalyst salt [**AM6**][**PA9**] was applicable for a set of enones. The reaction showed good tolerance for 3-alkyl- and 3-arylcycloalkenes; moreover, CBz-protecting aziridines could be also prepared. The aziridines **3a–f** were obtained in good to high yields and in excellent enantioselectivity values of 88–99.5% ee by using only 10 mol% catalyst loading. Furthermore, our catalytic system was found to be suitable for the aziridination of acyclic enones, as the product **3g–h** were obtained in good yields, high diastereoselectivity and moderate ee. To the best of our knowledge, this is the first example for the asymmetric aziridination of enones without the necessity of an ion-paired catalyst featuring both chiral cation and anion. Similarly to our findings described in the previous chapter, our strategy provided an access to both product antipodes with essentially the same enantioselectivities (Scheme 5).

Asymmetric Michael-Addition-Initiated Cascade Reactions

To further examine the versatility of our catalytic system, we also envisioned to expand our reaction scope to the



Scheme 5. Substrate scope for asymmetric aziridinations. Reactions were performed with 1.2 mmol substrate, 10 mol% catalyst [**AM6**][**PA9**], 1.0 mmol *tert*-butyl (tosyloxy)carbamate (1.0 equiv), 2.0 mmol (2.0 equiv) NaOAc in 4 mL chloroform (0.25 M). Yields refer to pure products after isolation by column chromatography. The enantiomeric excess values were determined by chiral HPLC analysis on a Chiralpak® AS-H or on a Chiralpak® IA-3 column. [a] Reaction was performed with 2.0 mmol (2.0 equiv) $NaHCO_3$ instead of NaOAc. [b] Reaction was performed with 1.0 mmol (1.0 equiv) CBzNHOTs instead of BocNHOTs.

Die approbierte gedruckte Originalversion dieser Dissertation ist an der TU Wien Bibliothek verfügbar. The approved original version of this doctoral thesis is available in print at TU Wien Bibliothek.
TU Bibliothek Your knowledge hub WIEN

© 2022 The Authors. Angewandte Chemie International Edition published by Wiley-VCH GmbH

direction of cascade-cyclizations. We initially turned our attention towards the synthesis of octahydroacridines via a direct aza-Michael/aldol sequence. While *N*-heterocycles such as quinolines and acridines (Figure 2) are known to exert anti-inflammatory, antiviral and anticancer activities,[49–52] the application and activity of chiral octahydroacridins are not yet fully explored.[53]

So far, the only procedure for the synthesis of such stable octahydroacridines was reported by the group of Yang in 2018. Even though they could use modified proline-derivatives as elegant and reasonably affordable organocatalysts, the use of *N*-tosyl-protected reagents was found to be crucial for achieving high enantioselectivities (Scheme 6, **A**).[53] Therefore, such method requires not just only additional pre-functionalization, but it also leads to a less atom economic process. Consequently; to solve these aforementioned issues, we aimed for the development of a direct aza-Michael/aldol sequence for the synthesis of octahydroacridines relying on protecting-group-free reagents (Scheme 6, **B**).

Initially, the reaction of **1a** and 2-aminobenzaldehyde (**4a**) was investigated in the presence of our state-of-art organocatalyst [**AM6**][**PA9**] (Table 3). A short optimization showed that the amount of solvent was crucial and higher concentrations (>0.4 M) led to significantly lower ee values. The unprotected octahydroacridine **5a** product was found to be sensitive to acidic and basic environment, therefore they could not be isolated by conventional column chromatography. Nevertheless, when the reaction was performed in chloroform, the isolation of the partially precipitated product could be carried out by simple filtration, which provided the pure **5a** in 64 % yield and basically as a single enantiomer (>99 % ee, Table 3, entry 2). When the reaction was carried out in dioxane or toluene—resulting in homogeneous reaction conditions—**5a** could be still isolated in 96 % ee by a fast short-path Pasteur-column, indicating that the precipitation had eventually no effect on the enantioselectivity of the product (Table 3, entries 2 vs. 3, 4). Through additional control experiments we found that our catalyst [**AM6**][**PA9**] has indeed better performance for such transformations compared to state-of-art organocatalysts: the cinchona-derivative (*S*,*S*)-**AM13** and (*R*,*R*)-**AM1** (DPEN) both gave high conversions; albeit, resulting in degradation products and in limited yields of 2–11 % for **5a** both with TFA and with **6** as counterion (Table 3, entries 5–11).

With these promising results in hand, a small scope of five different compounds was explored. By using the catalyst [**AM6**][**PA9**], the octahydroacridine products **5a–e** could be isolated in 55–64 % yield and in excellent enantioselectivities of 93–>99 % ee. Similarly to our previous results, **5a–e** could be accessed in both enantiomeric forms (Scheme 7).

Herein, we propose the plausible reaction mechanism (Scheme 8). As a first step, the enone **1a** reacts with the aminocatalyst, resulting in the formation of the iminium

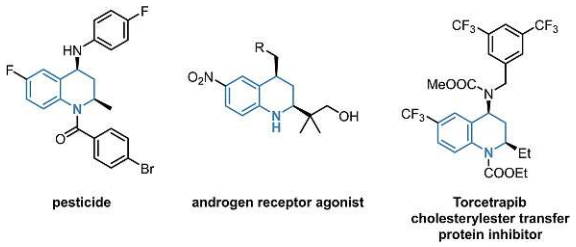
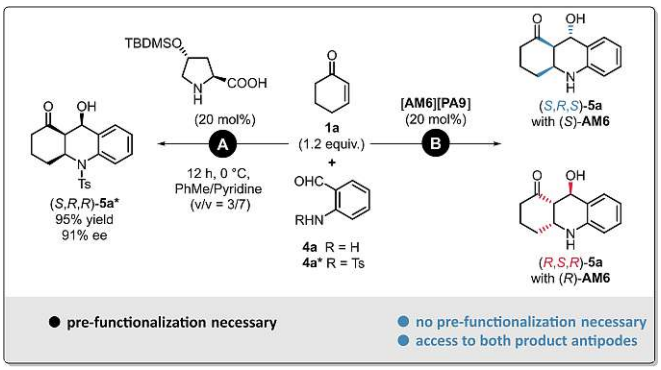
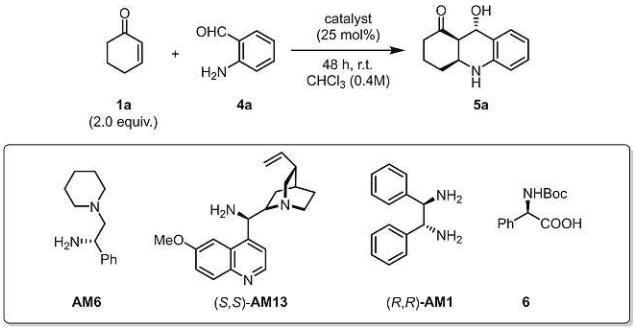


Figure 2. Examples of biologically active tetrahydroquinolines and acridins.



Scheme 6. Different concepts for the synthesis of asymmetric octahydroacridins: Aza-Michael/Aldol sequence by using pre-functionalized reagents (**A**),[39] and by our concept relying on a protecting-group-free reagent (**B**).

Table 3: Screening of different solvents and catalysts for the synthesis of octahydroacridine **5a**.

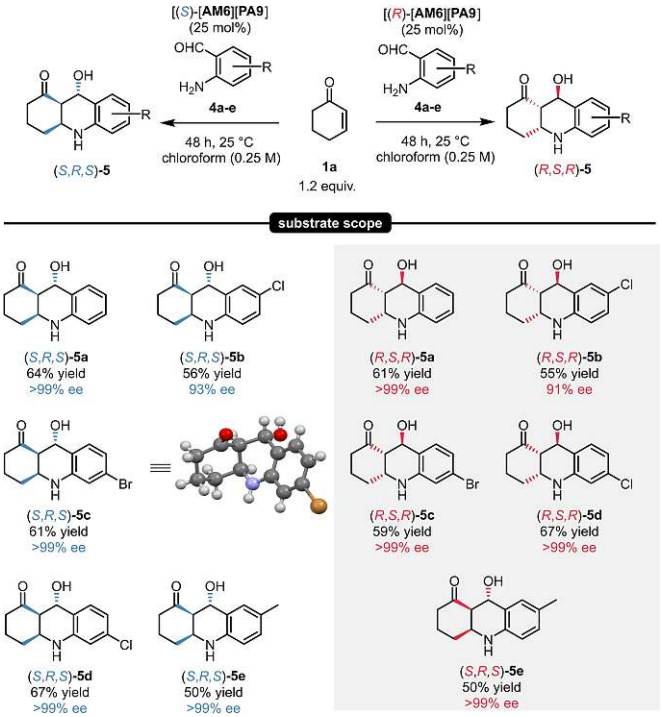


Entry[a]	Amine	Acid	Conv. [%][b]	Yield of **5a**[c]	ee [%][d]
1	**AM6**	none	trace	n.d.	n.d.
2	**AM6**	**PA9** (**1.0** equiv)	**>99**	**48** (**64**)	**>99**
3[e]	**AM6**	**PA9** (1.0 equiv)	79		96
4[f]	**AM6**	**PA9** (1.0 equiv)	90		96
5	**AM13**	**PA9** (1.0 equiv)	85	11	>99
6	**AM1**	**PA9** (1.0 equiv)	99	11	>99
7	**AM13**	TFA (1.0 equiv)	98	2	70
8	**AM13**	TFA (2.0 equiv)	88	n.d.	n.d.
9	**AM1**	TFA (1.0 equiv)	99	n.d.	n.d.
10	**AM13**	**6** (1.0 equiv)	>99	7	>99
11	**AM13**	**6** (2.0 equiv)	>99	18	>99

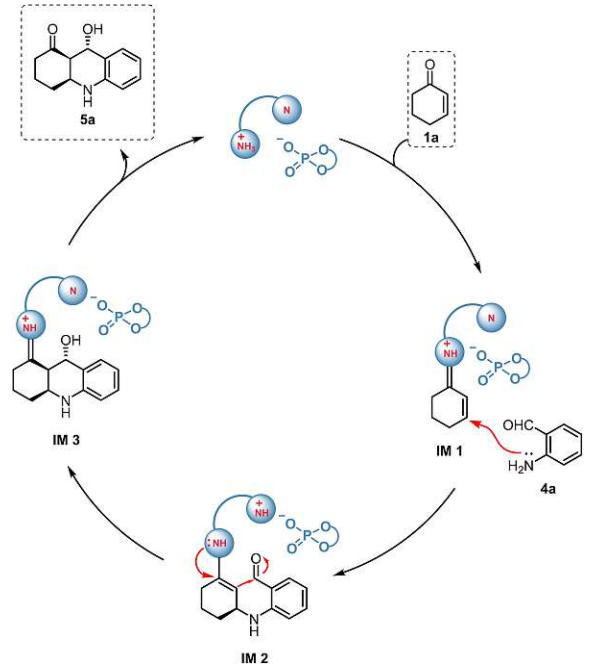
[a] Reactions were performed on a 0.2 mmol scale in 1 mL chloroform (0.2 M) at 25 °C for 48 hours. [b] Determined by GC-MS analysis on a BGB 5 column. [c] Isolated yields after precipitation from the reaction mixture with *n*-hexane/*i*-PrOH. The yield in parenthesis corresponds to 1.0 mmol scale. [d] Determined by chiral HPLC on a Chiralpak® AS-H column.

Die approbierte gedruckte Originalversion dieser Dissertation ist an der TU Wien Bibliothek verfügbar.
The approved original version of this doctoral thesis is available in print at TU Wien Bibliothek.
TU Bibliothek Your knowledge hub WIEN

© 2022 The Authors. Angewandte Chemie International Edition published by Wiley-VCH GmbH



Scheme 7. Substrate scope for the synthesis of octahydroacridines via direct aza-michael-aldol sequence. Reactions were performed with 1.0 mmol 2-aminobenzaldeyhde (**4a–e**, 1.0 equiv), 1.2 equiv 2-cyclohexen-1-one (**1a**) and 25 mol% catalyst [**AM6**][**PA9**] at 25 °C for 48 h. Yields refer to pure products after precipiation. Enantiomeric excess values were determined by chiral HPLC analysis on a Chiralpak® AS-H column. The deposition number for the XRD of (*S*,*R*,*S*)-**5c** is CCDC 2112845.[36]

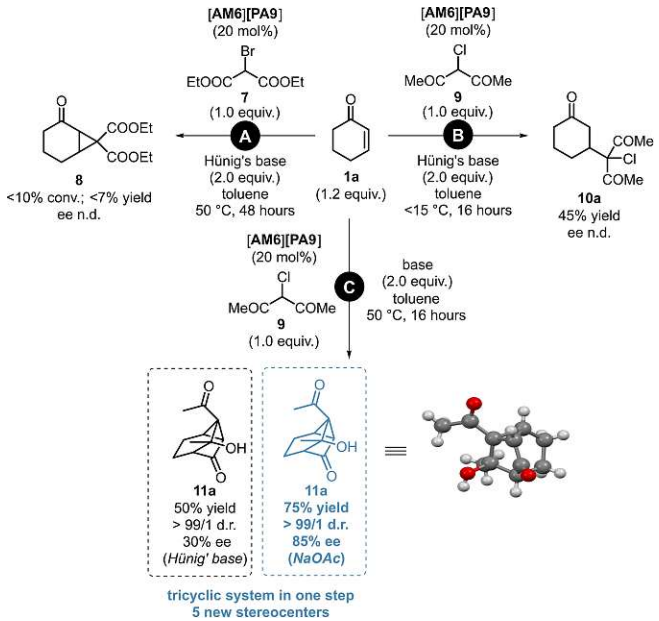


Scheme 8. Plausible reaction mechanism for the aza-Michael/aldol sequence, using **4a** as a representative reagent.

intermediate **IM1**, which then undergoes a Michael-addition with **4a**. The generated conjugated enamine (**IM2**) then initiates an intramolecular aldol reaction and the cyclization. Finally, hydrolysis of **IM3** leads to the desired product **5a**.

Being motivated to find yet another application for our powerful and multi-purpose catalyst [**AM6**][**PA9**], we envisioned to apply it in Michael-Initiated Ring Closure (MIRC) reactions of **1a**, by initially aiming for the synthesis of the cyclopropane derivative **8**. Despite several attempts using diethyl-2-bromomalonate (**7**) as reagent, the reaction was found to be extremely sluggish even at 50 °C and only traces of product **8** could be observed (Scheme 9, **A**). When a similar reagent, 3-cloroacetylacetone (**9**) was applied, the Michael-product **10a** was formed in moderate yields under kinetic contol; meanwhile, no cyclopropane-formation was observed (Scheme 9, **B**). However; we discovered an unprecedented Robinson-like annulation sequence when using 3-chloroacetylacetone (**9**) as reagent in the presence of *N*,*N*-diisopropylethylamine at 50 °C under thermodynamic control. The reaction afforded the tricyclic product **11a** with five new stereocenters in a promising 50 % isolated yield and in a moderate 30 % ee (Scheme 9, **C**, black). Moreover, this result could be significantly improved when using NaOAc as acid-scavenger, as **11a** was obtained in 75 % yield, as a single diastreomer and in 85 % ee (Scheme 9, **C**).

Even though these results were already quite promising, we aimed for further improving this process. Gratifyingly,



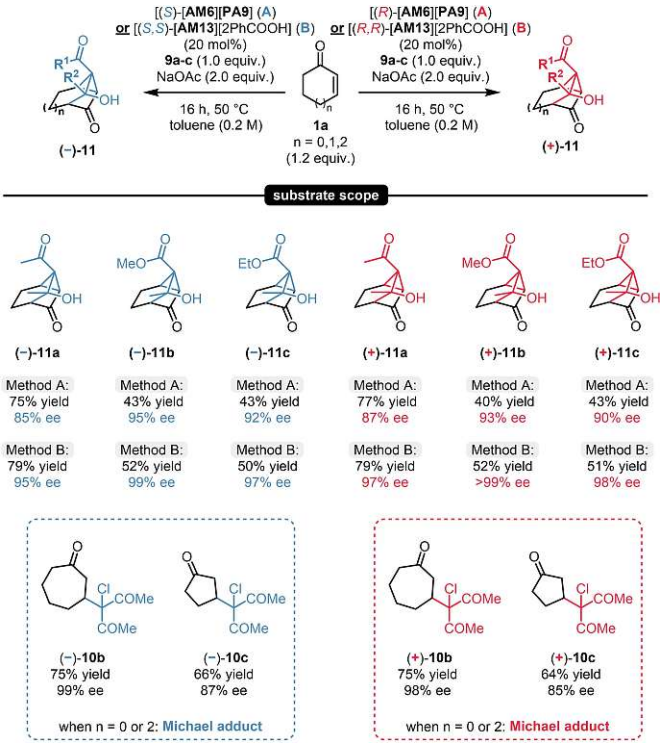
Scheme 9. Towards the discovery of a novel Robinson-like MIRC-reaction/intramolecular aldol sequence: Initial trial for MIRC reaction (**A**), simple Michael addition under kinetic control (**B**) and the novel cyclization under thermodynamic control (**C**). Reactions were performed on a 1.0 mmol scale by using 1.2 equiv **1a**, 1.0 equiv reagent (**7** or **9**) and 2.0 equiv base in 5 mL toluene (0.2 M) at 15 °C or 50 °C for 16 hours. Yields refer to pure products after flash column chromatography. Enantiomeric excess values for **11a** were determined by chiral HPLC analysis on a Chiralpak® OJ column. The deposition number for the XRD of **11a** is CCDC 2112843.[36]

Die approbierte gedruckte Originalversion dieser Dissertation ist an der TU Wien Bibliothek verfügbar.
The approved original version of this doctoral thesis is available in print at TU Wien Bibliothek.
TU Bibliothek Your knowledge hub WIEN

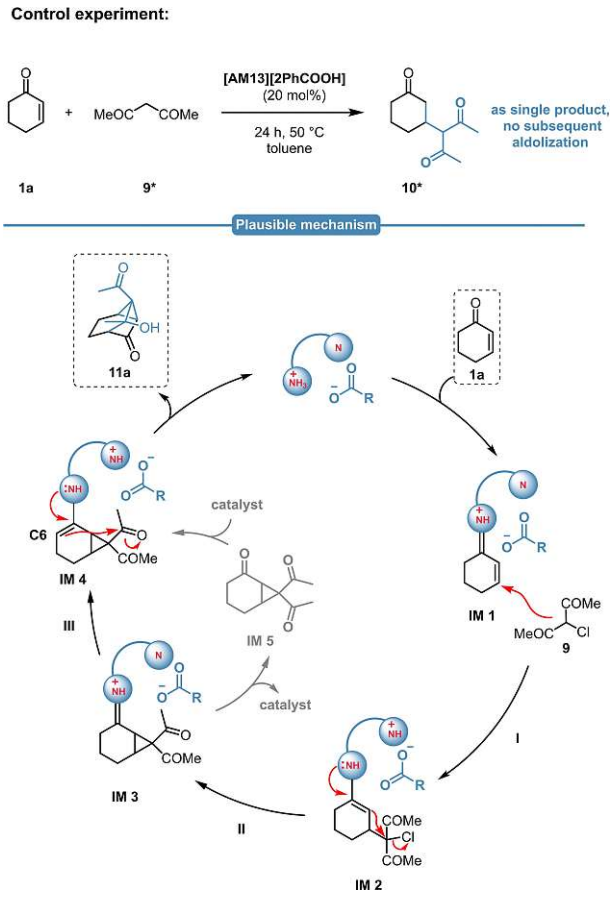
© 2022 The Authors. Angewandte Chemie International Edition published by Wiley-VCH GmbH

when changing to the classical quinine and quinidine-derived organocatalysts [**AM13**][**2PhCOOH**], even better results were obtained: The product **11a** could be obtained in 79 % yield, as a single diastereomer, and in an excellent 95 % ee and 97 % ee for the (−) and (+)-antipodes; respectively (see entries for **11a** in Scheme 10). We then aimed to explore the possible limitations and reaction scope of such MIRC/aldol annulation sequence. We found that the reaction was limited to the six-membered substrate **1a**, as the reaction with other cyclic enones resulted in the formation of the corresponding Michael adducts **10b–c**. Nevertheless, the reaction scope could be easily expanded by using readily available chlorinated β-ketoester reagents, resulting in **11b–c** in excellent enantioselectivities for both product antipodes by using both organocatalytic strategies with [**AM6**][**PA9**] and [**AM13**]-[**2PhCOOH**] (Scheme 10).

The control reaction with acetylacetone (**9***) resulted in the formation of the Michael adduct (**10***) as single product and no sign for the subsequent intramolecular aldolization was detected (Scheme 11, top). This might suggest, that the cyclopropane intermediate is indeed required for an ideal geometry for the subsequent second ring closing step, which makes a concurrent aldolization/cyclopropanation pathway unlikely. Based on these experimental findings, herein we propose a plausible mechanism for the MIRC/aldol sequence (Scheme 11, bottom). At first, the catalyst reacts



Scheme 10. Scope of the MIRC/aldol sequence. Reactions were performed with 1.0 mmol chlorinated reagent (**9a–c**, 1.0 equiv), 1.2 equiv 2-cyclohexen-1-one (**1a**) and 25 mol % catalyst [**AM6**][**PA9**] or [**AM13**][**2PhCOOH**] at 50 °C for 16 h. Yields refer to pure products after isolation by column chromatography. Enantiomeric excess values were determined by chiral HPLC analysis on a Chiralpak® OJ column.



Scheme 11. Control experiment with **9*** (top) and the plausible reaction mechanism of the MIRC/aldol sequence (bottom).

with the enone **1a**, resulting in the formation of the imunium intermediate **IM1**, which then undergoes a Michael-addition with **9** (**I**). Through the conjugated enamine **IM2** this is followed by the subsequent cyclopropane ring closure (**II**), resulting in **IM3**. This step might be followed by a direct intramolecular proton shuttle (**III**) and the generated enamine **IM4** subsequently initiates the intramolecular aldol reaction, yielding the tricyclic product **11a**. This is in accordance with our experimental observations, as the corresponding cyclopropane (**IM5**) could be never isolated; however, its formation cannot be completely outruled.

Conclusion

Herein we reported a novel concept of counterion enhanced catalysis for various asymmetric functionalization of enones. By combining sterically demanding flexible phosphoric acids with amino-acid-derived chiral diamines, simple and highly tunable organocatalytic frameworks were obtained. After a careful parameter optimization, a particularly powerful and multi-purpose organocatalyst was found, which could be successfully applied in asymmetric epoxidations, aziridinations, aza-Michael/aldol cascade cyclization, as well as in a Robinson-like asymmetric MIRC/aldol cyclization. For all

Die approbierte gedruckte Originalversion dieser Dissertation ist an der TU Wien Bibliothek verfügbar.
The approved original version of this doctoral thesis is available in print at TU Wien Bibliothek.
TU Bibliothek Your knowledge hub WIEN

© 2022 The Authors. Angewandte Chemie International Edition published by Wiley-VCH GmbH

four reaction types, excellent enantioselectivities were obtained, providing an easy access to both product enantiomers in all cases. Further investigations focusing on broadening the scope of our catalytic concept, especially for complex cyclizations are currently ongoing in our research group.

Acknowledgements

Financial support by the Austrian Science Fund (project P29146-N34) is gratefully acknowledged. This project has also received generous funding from the European Research Council (ERC) under the European Union's Horizon 2020 research and innovation programme (Grant agreement No. 864991).

Conflict of Interest

The authors declare no conflict of interest.

Data Availability Statement

The data that support the findings of this study are available from the corresponding author upon reasonable request.

Keywords: Asymmetric Catalysis · Aziridination · Cyclization · Epoxidation · Phosphoric Acids

[1] J. Seayad, B. List, *Org. Biomol. Chem.* **2005**, *3*, 719.
[2] B. Vakulya, S. Varga, T. Soós, *J. Org. Chem.* **2008**, *73*, 3475–3480.
[3] S. V. Kochetkov, A. S. Kucherenko, S. G. Zlotin, *Org. Biomol. Chem.* **2018**, *16*, 6423–6429.
[4] Y. Zhou, Q. Liu, Y. Gong, *Org. Biomol. Chem.* **2012**, *10*, 7618.
[5] A. Carlone, G. Bartoli, M. Bosco, F. Pesciaioli, P. Ricci, L. Sambri, P. Melchiorre, *Eur. J. Org. Chem.* **2007**, 5492–5495.
[6] A. Erkkilä, I. Majander, P. M. Pihko, *Chem. Rev.* **2007**, *107*, 5416–5470.
[7] N. A. Paras, D. W. C. MacMillan, *J. Am. Chem. Soc.* **2001**, *123*, 4370–4371.
[8] S. P. Brown, N. C. Goodwin, D. W. C. MacMillan, *J. Am. Chem. Soc.* **2003**, *125*, 1192–1194.
[9] D. W. C. MacMillan, *Nature* **2008**, *455*, 304–308.
[10] P. Melchiorre, K. A. Jørgensen, *J. Org. Chem.* **2003**, *68*, 4151–4157.
[11] M. Marigo, S. Bachmann, N. Halland, A. Braunton, K. A. Jørgensen, *Angew. Chem. Int. Ed.* **2004**, *43*, 5507–5510; *Angew. Chem.* **2004**, *116*, 5623–5626.
[12] M. Marigo, T. C. Wabnitz, D. Fielenbach, K. A. Jørgensen, *Angew. Chem. Int. Ed.* **2005**, *44*, 794–797; *Angew. Chem.* **2005**, *117*, 804–807.
[13] M. T. Hechavarria Fonseca, B. List, *Angew. Chem. Int. Ed.* **2004**, *43*, 3958–3960; *Angew. Chem.* **2004**, *116*, 4048–4050.
[14] J. W. Yang, M. T. Hechavarria Fonseca, B. List, *Angew. Chem. Int. Ed.* **2004**, *43*, 6660–6662; *Angew. Chem.* **2004**, *116*, 6829–6832.
[15] J. Zhou, V. Wakchaure, P. Kraft, B. List, *Angew. Chem. Int. Ed.* **2008**, *47*, 7656–7658; *Angew. Chem.* **2008**, *120*, 7768–7771.
[16] M. Mahlau, B. List, *Angew. Chem. Int. Ed.* **2013**, *52*, 518–533; *Angew. Chem.* **2013**, *125*, 540–556.
[17] N. J. A. Martin, B. List, *J. Am. Chem. Soc.* **2006**, *128*, 13368–13369.
[18] S. Mayer, B. List, *Angew. Chem. Int. Ed.* **2006**, *45*, 4193–4195; *Angew. Chem.* **2006**, *118*, 4299–4301.
[19] M. Klussmann, L. Ratjen, S. Hoffmann, V. Wakchaure, R. Goddard, B. List, *Synlett* **2010**, 2189–2192.
[20] S. Saha, C. Schneider, *Chem. Eur. J.* **2015**, *21*, 2348–2352.
[21] F. Scharinger, Á. Márk Pálvölgyi, V. Zeindlhofer, M. Schnürch, C. Schröder, K. Bica-Schröder, *ChemCatChem* **2020**, *12*, 3776–3782.
[22] Á. M. Pálvölgyi, J. Smith, M. Schnürch, K. Bica-Schröder, *J. Org. Chem.* **2021**, *86*, 850–860.
[23] T. Katsuki, K. B. Sharpless, *J. Am. Chem. Soc.* **1980**, *102*, 5974–5976.
[24] R. Irie, K. Noda, Y. Ito, N. Matsumoto, T. Katsuki, *Tetrahedron Lett.* **1990**, *31*, 7345–7348.
[25] D. Enders, J. Zhu, G. Raabe, *Angew. Chem. Int. Ed. Engl.* **1996**, *35*, 1725–1728; *Angew. Chem.* **1996**, *108*, 1827–1829.
[26] R. Helder, J. C. Hummelen, R. W. P. M. Laane, J. S. Wiering, H. Wynberg, *Tetrahedron Lett.* **1976**, *17*, 1831–1834.
[27] H. Sasai, E. Emori, T. Arai, M. Shibasaki, *Tetrahedron Lett.* **1996**, *37*, 5561–5564.
[28] E. J. Corey, F.-Y. Zhang, *Org. Lett.* **1999**, *1*, 1287–1290.
[29] T. Genski, G. Macdonald, X. Wei, N. Lewis, R. J. K. Taylor, *Synlett* **1999**, 795–797.
[30] M. Terada, M. Nakano, *Heterocycles* **2008**, *76*, 1049.
[31] S. Lee, D. W. C. MacMillan, *Tetrahedron* **2006**, *62*, 11413–11424.
[32] J. Li, N. Fu, L. Zhang, P. Zhou, S. Luo, J.-P. Cheng, *Eur. J. Org. Chem.* **2010**, 6840–6849.
[33] X. Wang, B. List, *Angew. Chem. Int. Ed.* **2008**, *47*, 1119–1122; *Angew. Chem.* **2008**, *120*, 1135–1138.
[34] X. Wang, C. M. Reisinger, B. List, *J. Am. Chem. Soc.* **2008**, *130*, 6070–6071.
[35] U. Müller, F. van Assema, M. Gunsior, S. Orf, S. Kremer, D. Schipper, A. Wagemans, C. A. Townsend, T. Sonke, R. Bovenberg, M. Wubbolts, *Metab. Eng.* **2006**, *8*, 196–208.
[36] Deposition Numbers 2112844 (for **PA9**), 2112845 (for (*S*,*R*,*S*)-**5a**) and 211843 (for **11a**) contains the supplementary crystallographic data for this paper. These data are provided free of charge by the joint Cambridge Crystallographic Data Centre and Fachinformationszentrum Karlsruhe Access Structures service.
[37] Y. Ogasawara, H. Liu, *J. Am. Chem. Soc.* **2009**, *131*, 18066–18068.
[38] D. M. Vyas, D. Benigni, R. A. Partyka, T. W. Doyle, *J. Org. Chem.* **1986**, *51*, 4307–4309.
[39] J.-C. Andrez, *Beilstein J. Org. Chem.* **2009**, *5*, 33.
[40] M. Kim, E. Vedejs, *J. Org. Chem.* **2004**, *69*, 7262–7265.
[41] Z. Li, K. R. Conser, E. N. Jacobsen, *J. Am. Chem. Soc.* **1993**, *115*, 5326–5327.
[42] D. A. Evans, M. T. Bilodeau, M. M. Faul, *J. Am. Chem. Soc.* **1994**, *116*, 2742–2753.
[43] K. B. Hansen, N. S. Finney, E. N. Jacobsen, *Angew. Chem. Int. Ed. Engl.* **1995**, *34*, 676–678; *Angew. Chem.* **1995**, *107*, 750–752.
[44] V. K. Aggarwal, A. Thompson, R. V. H. Jones, M. C. H. Standen, *J. Org. Chem.* **1996**, *61*, 8368–8369.
[45] J. Vesely, I. Ibrahem, G.-L. Zhao, R. Rios, A. Córdova, *Angew. Chem. Int. Ed.* **2007**, *46*, 778–781; *Angew. Chem.* **2007**, *119*, 792–795.
[46] H. Arai, N. Sugaya, N. Sasaki, K. Makino, S. Lectard, Y. Hamada, *Tetrahedron Lett.* **2009**, *50*, 3329–3332.
[47] F. De Vincentiis, G. Bencivenni, F. Pesciaioli, A. Mazzanti, G. Bartoli, P. Galzerano, P. Melchiorre, *Chem. Asian J.* **2010**, *5*, 1652–1656.

© 2022 The Authors. Angewandte Chemie International Edition published by Wiley-VCH GmbH

Die approbierte gedruckte Originalversion dieser Dissertation ist an der TU Wien Bibliothek verfügbar.
The approved original version of this doctoral thesis is available in print at TU Wien Bibliothek.
TU Bibliothek Your knowledge hub WIEN

[48] F. Pesciaioli, F. De Vincentiis, P. Galzerano, G. Bencivenni, G. Bartoli, A. Mazzanti, P. Melchiorre, *Angew. Chem. Int. Ed.* **2008**, *47*, 8703–8706; *Angew. Chem.* **2008**, *120*, 8831–8834.
[49] M. Kaya, Y. Yıldırır, G. Y. Çelik, *Pharm. Chem. J.* **2015**, *48*, 722–726.
[50] D. B. Damon, R. W. Dugger, G. Magnus-Aryitey, R. B. Ruggeri, R. T. Wester, M. Tu, Y. Abramov, *Org. Process Res. Dev.* **2006**, *10*, 464–471.
[51] S. Kitamura, T. Harada, H. Hiramatsu, R. Shimizu, H. Miyagawa, Y. Nakagawa, *Bioorg. Med. Chem. Lett.* **2014**, *24*, 1715–1718.
[52] N. Nagata, M. Miyakawa, S. Amano, K. Furuya, N. Yamamoto, H. Nejishima, K. Inoguchi, *Bioorg. Med. Chem. Lett.* **2011**, *21*, 6310–6313.
[53] S. Li, J. Wang, P.-J. Xia, Q.-L. Zhao, C.-M. Wang, J.-A. Xiao, X.-Q. Chen, H.-Y. Xiang, H. Yang, *J. Org. Chem.* **2018**, *83*, 12284–12290.

Manuscript received: February 10, 2022
Accepted manuscript online: April 12, 2022
Version of record online: ■■, ■■

Die approbierte gedruckte Originalversion dieser Dissertation ist an der TU Wien Bibliothek verfügbar.
The approved original version of this doctoral thesis is available in print at TU Wien Bibliothek.
TU Wien Bibliothek Your knowledge hub

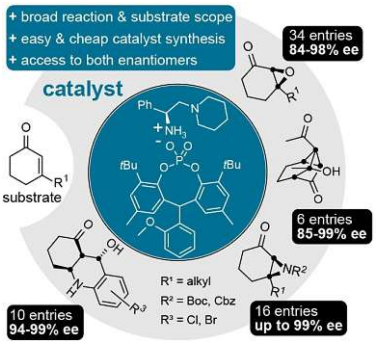
© 2022 The Authors. Angewandte Chemie International Edition published by Wiley-VCH GmbH

Research Articles

Organocatalysis

F. Scharinger, Á. M. Pálvölgyi, M. Weisz, M. Weil, C. Stanetty, M. Schnürch, K. Bica-Schröder* _____ **e202202189**

Sterically Demanding Flexible Phosphoric Acids for Constructing Efficient and Multi-Purpose Asymmetric Organocatalysts



The ability of counterion enhanced catalysis to promote the asymmetric functionalization of enones was demonstrated. Combining the use of sterically demanding phosphoric acids with simple chiral diamines allowed for the preparation of simple ion-paired and highly tunable organocatalysts. The latter could be applied in four different asymmetric transformations, providing a highly enantioselective access to both product antipodes in all cases.

Die approbierte gedruckte Originalversion dieser Dissertation ist an der TU Wien Bibliothek verfügbar.
The approved original version of this doctoral thesis is available in print at TU Wien Bibliothek.
TU Bibliothek Your knowledge hub WIEN

© 2022 The Authors. Angewandte Chemie International Edition published by Wiley-VCH GmbH

10 Synthesis of Chiral Diazabicycloalkanes *via* Organocatalytic aza-Michael/Aldol Reaction

Diazabicycloalkanes and pyridazines constitute an essential and diverse group of nitrogen-containing heterocycles, well-known for their biological activity.[96–98] Symmetric diazabicycloalkanes feature a unique structure defined by a compact bicyclic ring system interconnected by two nitrogen atoms. While various established methods exist for producing chiral pyridazines[99–101], the one-step synthesis of the more intricate chiral diazabicycloalkane moiety continues to pose an ongoing challenge. The conventional indirect approach to synthesize the bicyclic moiety begins with the creation of the chiral precursor, followed by annulation to yield the bicyclic product. One of the initial methods for producing the cyclic intermediate relied on enamine catalysis, which necessitated multiple reaction steps.[102] We devised a direct approach to synthesize the annulated product, utilizing an organocatalytic aza-Michael/aldol reaction with enals. In this strategy, a cascade reaction is initiated by the aza-Michael addition, followed by an intramolecular cyclization. This method offers a practical and straightforward means to produce a range of nitrogen-containing heterocycles, particularly those that are traditionally challenging to synthesize. The primary objective was to synthesize the diazabicycloalkane moiety in a highly enantioselective manner. Initially, we applied an iminium/enamine domino reaction, employing a reagent featuring both nucleophilic and electrophilic functional groups. These compounds can lead to self-condensation, and therefore, the search for a catalyst that ensures high selectivity was necessary. We conducted extensive catalyst screening to identify the optimal catalyst structure, followed by fine-tuning of the reaction conditions and the final evaluation of various enal substrates.

The following manuscript is presented in this chapter:

Submitted Manuscript – Under Revision

Scharinger, F.; Weil, M.; Stanetty, C.; Schnürch, M.; Bica-Schröder, K. Synthesis of Chiral Diazabicycloalkanes via Organocatalytic aza-Michael/Aldol Reaction. *Adv. Synth. Catal.* **2023.**

In my role as a main author, I carried out all experiments and was responsible for manuscript preparation.

Die approbierte gedruckte Originalversion dieser Dissertation ist an der TU Wien Bibliothek verfügbar.
The approved original version of this doctoral thesis is available in print at TU Wien Bibliothek.

Synthesis of Chiral Diazabicycloalkanes *via* Organocatalytic aza-Michael/Aldol Reaction

Fabian Scharinger,[a] Matthias Weil,[b] Michael Schnürch[a] and Katharina Bica-Schröder[a]*

[a] F. Scharinger, Prof. M. Schnürch, Prof. K. Bica-Schröder
Institute of Applied Synthetic Chemistry, TU Wien
Getreidemarkt 9/163, 1060 Vienna (Austria)
E-mail: katharina.schroeder@tuwien.ac.at
[b] Prof. M. Weil
Institute of Chemical Technologies and Analytics, TU Wien
Getreidemarkt 9/163, 1060 Vienna (Austria)

Die approbierte gedruckte Originalversion dieser Dissertation ist an der TU Wien Bibliothek verfügbar.
The approved original version of this doctoral thesis is available in print at TU Wien Bibliothek.

Abstract: We introduce a strategy for the one-step synthesis of chiral diazabicycloalkanes that delivers the annulated ring system in a single reaction step. The method entails a direct aza-Michael/aldol reaction of enals in conjunction with modified oxopropanamides and establishes the chiral center via iminium-enamine tandem catalysis. For this purpose, we developed simple diphenylethylendiamine frameworks as dual activation organocatalyst, effectively engaging both the substrate and reagent, thus leading to yields of 31-86% and enantioselectivities in the range of 80-98%. The final product features not only the diazabicycloalkane moiety but includes also additional functionalities, such as aldehyde motives that can be modified *in situ* without loss of enantioselectivity, and an sp^2-bearing methyl group. Our approach accommodates a wide array of enals with high functional group tolerance. Additionally, we demonstrated the adjustability of enantioselectivity and yield by modulating the acid cocatalyst's quantity, thus offering multiple optimization possibilities.

Diazabicycloalkanes and pyridazines represent a vital and diverse class of nitrogen-containing heterocycles, renowned for their wide-ranging biological activity.[1] These compounds exhibit a versatile profile, finding application not only in approved and experimental drugs but as well as agrochemicals (Figure 1).[1–7]

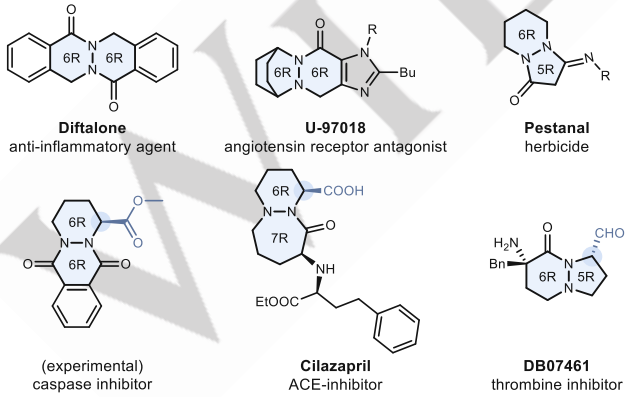
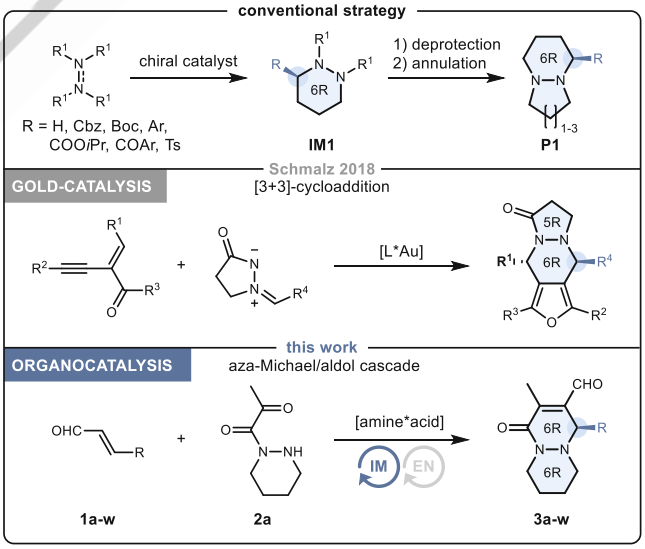


Figure 1. Examples of bioactive diazabicycloalkanes.[2–7]

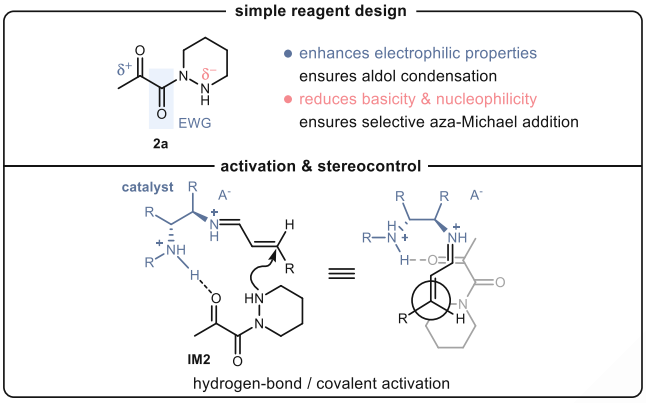
Symmetric diazabicycloalkanes boast a distinctive structure characterized by a condensed bicyclic ring system bridged by two nitrogen atoms. While there are several well-established methods for synthesizing chiral pyridazines,[8–14] the one-step synthesis of the more complex chiral diazabicycloalkane moiety remains an ongoing challenge. The typical indirect strategy for synthesizing the bicyclic moiety involves the preparation of the chiral precursor **IM1**, followed by annulation to form the final product, **P1** (Scheme 1, top). One of the initial approaches for synthesizing **IM1** relied on enamine catalysis, which requires multiple reaction steps.[15] Other methods utilized for this purpose include hetero-Diels-Alder reactions,[10] [3+3] cycloadditions,[16–19] Michael-induced multi-component,[8] as well as organo-cascade[11,14,20] and transition-metal cascade reactions.[21] To synthesize the annulated product **P1**, a multi-step synthesis starting from **IM1** is often required, involving protecting-group cleavage and subsequent modifications to enable cyclization.[15,22] Schmalz and coworkers demonstrated the direct synthesis of chiral pyrazolopyridazines through [3+3]-cycloaddition utilizing a chiral gold catalyst (Scheme 1, center).[17] However, to our knowledge, direct synthesis approaches for generating bicyclic ring structures such as chiral pyridazinopyridazines (Scheme 1, **3a-w**) have not been reported yet.



Scheme 1. Strategies for the synthesis of diazabicycloalkanes.

We developed a direct methodology for the synthesis of the annulated product **P1**, involving the use of an organocatalytic aza-Michael/aldol reaction of enals (Scheme 1, bottom). In this strategy, a cascade reaction is employed, initiated by the aza-Michael addition, followed by an intramolecular cyclization.[23] This methodology provides a viable and simple approach to access various nitrogen-containing heterocycles, especially those that are challenging to synthesize.[23] For the aza-Michael cascade

reaction, common *N*-nucleophiles, including aniline derivatives,[24–26] aromatic amines,[27–29] tosyl-protected amines,[30–32] and carbamate-protected hydroxylamines,[33–35] are known to provide the optimal reactivity and stereocontrol. In our approach, we encounter the challenge that none of the well-established nucleophiles above can be used for the direct transfer of the pyridazine structure **2a**. To address this synthetic hurdle, we envision incorporating a pyruvic acid moiety into the reagent design (Scheme 2, top). This choice ensures reduced nucleophilic and basic properties of the attacking amino group, which is crucial to minimize side reactions such as self-condensation and provides optimal reaction conditions to provide high enantiodiscrimination.

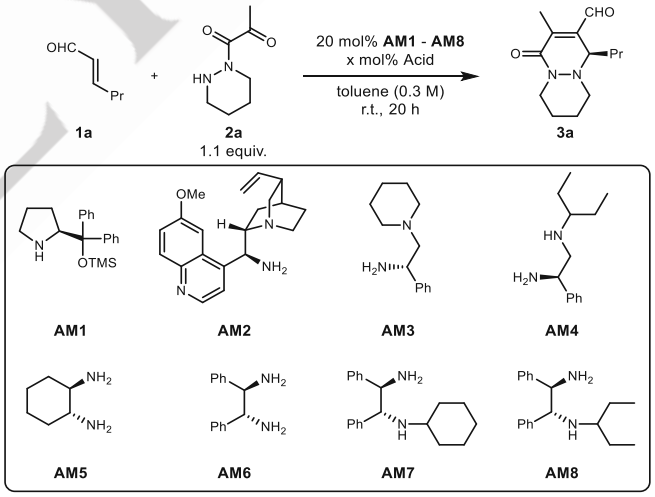


Scheme 2. Reagent design and activation concept.

Moreover, the attached activated ketone functionality in **2a** not only enables aldol condensation but also facilitates high stereocontrol through interactions with the organocatalyst (Scheme 2, bottom). Furthermore, this choice introduces an sp^2-bearing methyl group in the final product **3a-z**, which is a structural feature known to have a significant impact on biological activity.[36,37] As substrate class enals were chosen for their high reactivity upon activation to an iminium species, which also introduces an essential functional group in the final product, thereby expanding possibilities in subsequent post-modifications (Scheme 5).[38]

In our pursuit of optimizing the yield and enantioselectivity of product **3a**, we conducted a screening of various catalysts in the domain of iminium catalysis, focusing on enals **1a-w** as the substrate class. As the first choice, we selected the widely recognized Hayashi-Jørgensen catalyst **AM1** due to its well-established reputation for exhibiting high generality and applicability, particularly in organocatalytic C-N bond formation of enals.[29,39–43] Contrary to expectations, the catalyst performance was unsatisfactory, regardless of the presence of benzoic acid as a cocatalyst (Table 1, entry 1-2). This outcome strongly indicated that the activation of the ketone functionality on reagent **2a** was a fundamental requirement for achieving at least moderate yield. Furthermore, the product obtained from the reaction was racemic, indicating a lack of the desired catalyst-substrate-reagent interaction with this specific secondary amino-catalyst. On the contrary, the privileged primary amine catalyst **AM2** derived from quinine[44,45] exhibited the capability to achieve considerably higher yields, owing to its efficient substrate and reagent activation. However, this catalyst still resulted in undesirably low enantioselectivities of **3a** (Table 1, entry 3). The catalyst **AM3** shares similar features with the quinine-amine, possessing both primary and tertiary amino groups, thereby providing a comparable activation mode. However, in contrast to the quinine-based catalyst, **AM3** exhibits lower steric hindrance, rendering it more flexible and is generally a less desirable organocatalyst.[46] To our surprise, experimental data showed that the low enantioselectivity did not arise from lacking steric hindrance but rather from the presence of a tertiary amino group in both **AM2** and **AM3**, since the enantiodiscrimination in **AM3** surpassed the more rigid **AM2** (Table 1, entry 4). This can be further demonstrated by employing **AM4**, which contains a secondary amine, achieving a similar yield, but more importantly, a significantly higher ee. To further enhance the enantiodiscrimination, the chiral backbone was replaced from the amino acid derived **AM4** to the C2-symmetric diphenylethylenediamine **AM6** since the ee was significantly lower for diaminocyclohexane **AM5**. The secondary amino modification from **AM4** and the chiral backbone from **AM6** accordingly lead to good yields and 85% ee at room temperature and 91% ee at 0 °C with **AM8**. **AM7** can be considered as an alternative catalyst, but since the yield is slightly lower, further optimizations and the final substrate scope was performed with **AM8**.

Table 1. Catalyst screening

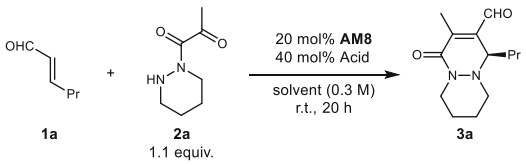


Entry[a]	Amine	Acid	Yield [%][b]	ee [%][c]
1	**AM1**	-	6	rac
2	**AM1**	BA (20 mol%)	17	rac
3	**AM2**	TFA (40 mol%)	87	26 (S)
4	**AM3**	TFA (40 mol%)	70	48 (S)
5	**AM4**	TFA (40 mol%)	89	74 (R)
6	**AM5**	TFA (40 mol%)	96	21 (R)
7	**AM6**	TFA (40 mol%)	62	76 (R)
8	**AM7**	TFA (40 mol%)	60	85 (R)
9	**AM8**	TFA (40 mol%)	79	85 (R)
10[d]	**AM8**	TFA (40 mol%)	61	91 (R)

[a] Reactions were performed with 0.05 mmol **1a**, 1.1 equiv. **2a** and 20 mol% catalyst at 25 °C for 20 h. [b] Determined by GC analysis on a BGB5 column using *n*-dodecane as internal standard. [c] Determined by chiral HPLC on Chiralpak ASH-column. [d] Reaction performed at 0 °C.

Die approbierte gedruckte Originalversion dieser Dissertation ist an der TU Wien Bibliothek verfügbar.
The approved original version of this doctoral thesis is available in print at TU Wien Bibliothek.
TU Bibliothek Your knowledge hub WIEN

Table 2. Solvent and acid screening



Entry[a]	Solvent	Acid	Yield [%][b]	ee [%][c]
1	MeOH	TFA	16	n.d.
2	THF	TFA	51	53
3	dioxane	TFA	25	80
4	$CHCl_3$	TFA	62	78
5	DCM	TFA	56	79
6	Et_2O	TFA	32	68
7	toluene	TFA	79	85
8	toluene	TCA	67	75
9	toluene	PTSA	69	80
10	toluene	AcOH	18	n.d.
11	toluene	BA	19	n.d.
12	toluene	PFBA	60	35

[a] Reactions were performed with 0.05 mmol **1a**, 1.1 equiv. **2a** and 20 mol% diamine, 40 mol% acid, at 25 °C for 20 h. [b] Determined by GC analysis on a BGB5 column using *n*-dodecane as internal standard. [c] Determined by chiral HPLC on Chiralpak ASH-column.

Solvent screening indicated that solvents more polar than toluene, such as diethyl ether, chloroform, dioxane, THF and methanol, are not optimal for this reaction, as they resulted in either low yields or significantly lower enantiodiscrimination (Table 2, entry 1-6). In terms of the acid cocatalyst, weaker acidic compounds, such as acetic acid (AcOH) or benzoic acid (BA), produced unsatisfactory results. However, increasing the acidity by using pentafluorobenzoic acid (PFBA) led to significantly higher yields, although the overall ee remained low. The use of stronger acids, such as trifluoroacetic acid (TFA) along with compounds such as trichloroacetic acid (TCA) or p-toluenesulfonic acid (PTSA), resulted in substantially improved yields and ee values (Table 2, entry 7-12). In our pursuit to improve the enantioselectivity, we found that increasing the amount of trifluoroacetic acid (TFA) significantly enhances this property (Figure 2). For the synthesis of **3a**, adding more TFA leads to an exponential increase in enantioselectivity, but it also reduces the yield in a linear manner. Similarly, the more sterically demanding and less reactive **1o** follows the same pattern. Based on these findings, the final conditions for the scope and limitations were established as follows: For less hindered and highly reactive enals **1a-n**, a TFA:**AM8** ratio of 5:1 was selected, while for hindered cinnamic aldehydes **1o-w**, the ratio was adjusted to 4:1 to enhance their reactivity.

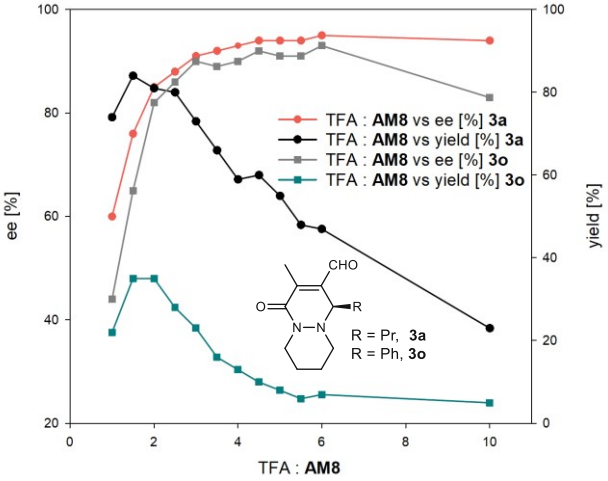
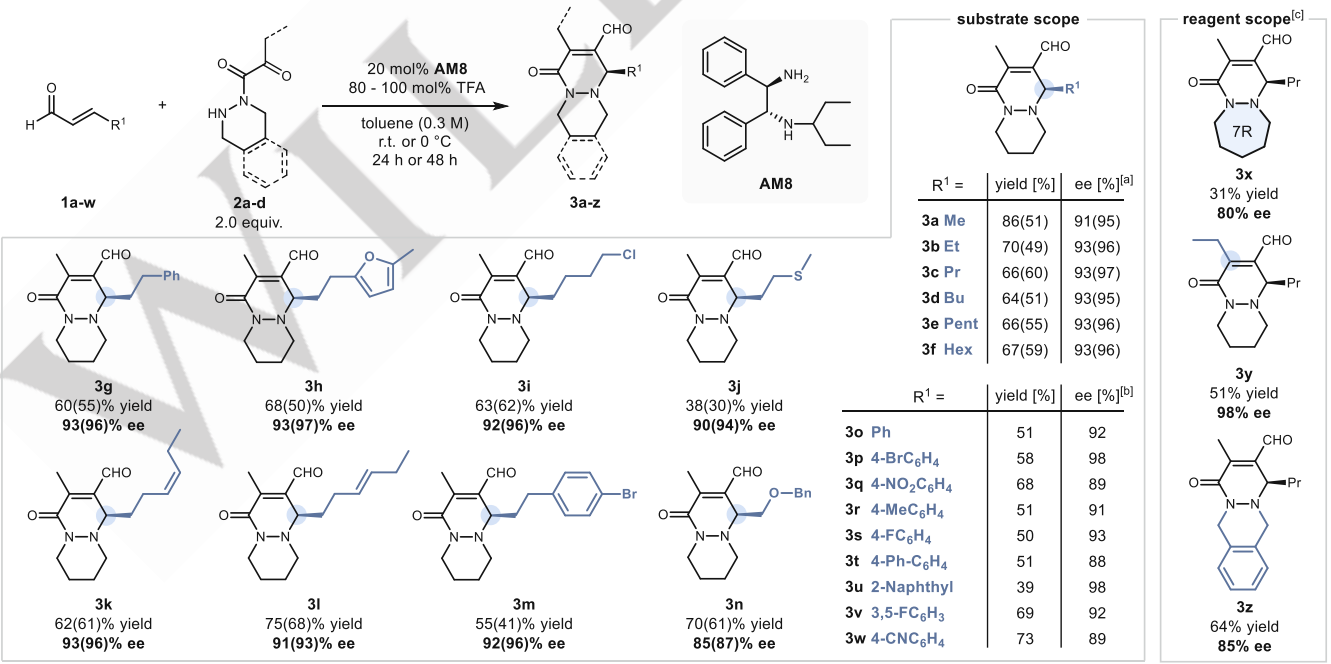


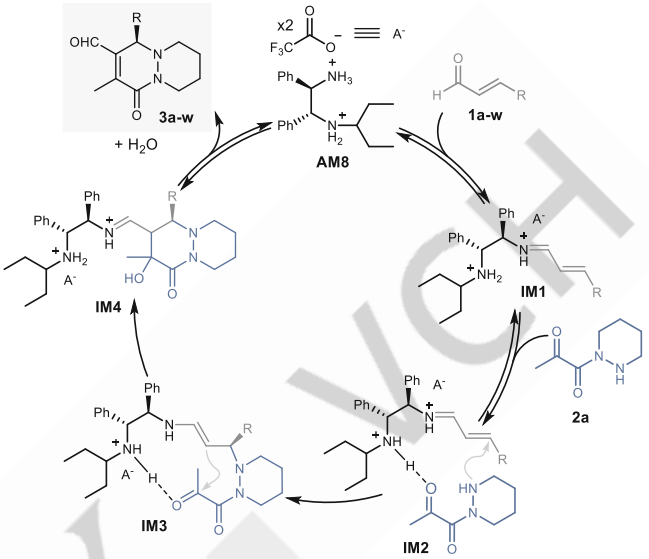
Figure 2. TFA quantity screening. Reactions were performed with 0.05 mmol **1a** or **1o**, 1.1 equiv. **2a** and 20 mol% **AM8** at 25 °C for 20 h. Yield determined by GC analysis on a BGB5 column using *n*-dodecane as internal standard. Enantiomeric excess determined by chiral HPLC on Chiralpak ASH-column.



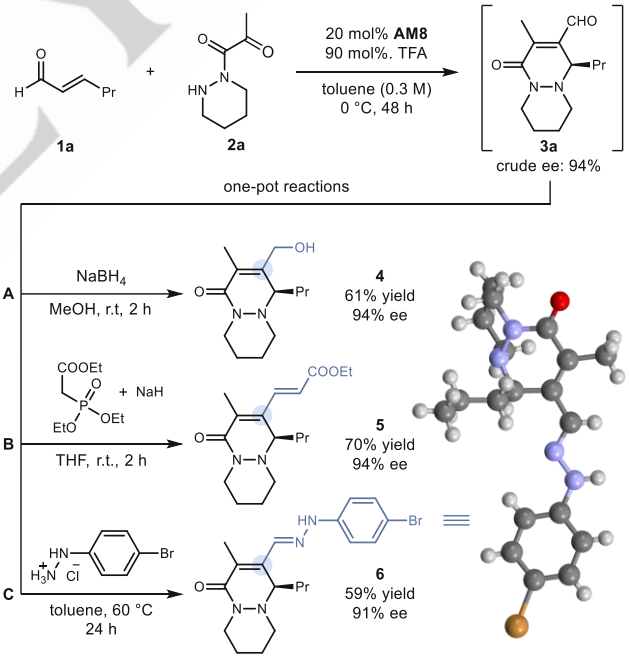
Scheme 3. Scope and limitation. Reactions were performed with 0.25 mmol enal (**1a–w**, 1.0 equiv.), 2.0 equiv. **2a-d**, 20 mol% **AM8** at 25 °C. [a] Reaction conditions: 20 h at r.t. and 0 °C (indicated in parenthesis) with 100 mol% TFA. [b] Reaction conditions: 48 h at r.t with 80 mol% TFA. [c] Reaction conditions: 48 h at 0 °C with 100 mol% TFA. Reaction conditions for **3g-n**: 20 h at r.t. and 48 h at 0 °C (indicated in parenthesis) with 100 mol% TFA. Yields refer to pure products after isolation by column chromatography. Enantiomeric excess determined by chiral HPLC on Chiralpak ASH & IB-column.

Die approbierte gedruckte Originalversion dieser Dissertation ist an der TU Wien Bibliothek verfügbar.
The approved original version of this doctoral thesis is available in print at TU Wien Bibliothek.
TU Bibliothek Your knowledge hub WIEN

Having established the optimal reaction conditions, we proceeded to test a wide range of enal substrates. Initially, we started with enals that differed only in the number of carbon atoms (Scheme 3, **1a-f**). For the less hindered and highly reactive aldehydes, we employed a TFA:**AM8** ratio of 5:1 to optimize enantioselectivity. This approach provided us with a reliable means to attain high ee values across diverse substrates. For comparison, we also conducted these reactions at both room temperature and 0 °C (Scheme 3, parenthesis), employing the same reaction time. The results showed that the sterically least hindered enal **1a** achieved the highest yield. However, due to the high reaction rate, we anticipated a decrease in enantioselectivity, which was indeed observed. As we increased the chain length of the aldehyde, the yield reached a plateau at around 67% with an average enantioselectivity of 93% at room temperature. At 0 °C, with the same reaction time, we noted a lower yield compared to room temperature, due to the lower reaction rate. However, on the positive side, an increase in ee was observed, resulting in ee values of up to 97%. For the more functionalized substrates **1g-n**, we opted for longer reaction times at 0 °C to maximize yield. In fact, **3g**, **3i**, **3k**, **3l**, and **3n** were obtained in similar yields compared to room temperature, while reaching excellent enantioselectivity of up to 97%. In the case of the more sterically demanding cinnamic aldehyde **1o**, already shown in Figure 2, the yield was notably lower, requiring a reduction in the amount of TFA used for the reaction to enhance the reaction rate and increase the yield. Despite this, it was still possible to achieve high enantioselectivities up to 98%. Comparatively, the average yield was lower when compared to the less sterically hindered substrates, except cinnamic aldehydes with additional electron withdrawing groups **1q**, **1v**, **1w** which provided yields of 68 - 73%. Furthermore, we implemented modifications to the reagent structure to investigate the possibility of introducing a larger ringsize or alternative aliphatic moieties on the reagent side. The utilization of a 7-membered ring framework (Scheme 3, **3x**) led to the successful generation of the target compound; however, this alteration resulted in a notable reduction in both yield and enantioselectivity. Similar results were achieved with **3z** which structure resembles the pattern of the anti-flammatory agent Diftalone (Figure 1). These findings underscore the role of conformational changes on the reagent side, not only in influencing the reactivity, but also in impacting its enantiodiscrimination. The introduction of an ethyl group to replace the methyl group yielded even higher enantioselectivity of up to 98%, with only marginal yield decrease (Scheme 3, **3y**). This phenomenon points towards increased steric repulsion within the catalyst's intermediate state (Scheme 4, **IM2**). Eventually, we successfully demonstrated the suitability and applicability of a broad range of enal substrates for this reaction, affording moderate to high product yields, along with exceptional enantioselectivities and the possibility of reagent modification. Based on the observed trends, we present a plausible reaction mechanism in Scheme 4. The reaction starts with the iminium activation of the enal **1a-w**, forming intermediate **IM1** (see references for evidence of this intermediate utilizing similar diamine catalysts in combination with enals/enones)[47–49]. The reagent **2a** is then directed via hydrogen bonding, forming the aza-Michael adduct **IM2** (see references for literature data on aza-Michael additions to iminium-activated enals and hydrogen bond direction/activation of reagents)[39,42,50][49,51–53]. In **IM3**, the enamine reattacks the activated carbonyl group on the reagent side, forming intermediate **IM4**. Hydrolysis of **IM4** provides the corresponding product **3a-n**.



Scheme 4. Proposed reaction mechanism for the synthesis of pyridazinopyridazines.



Scheme 5. One-pot modifications. Reactions were performed with 0.25 mmol 2-hexenal (1.0 equiv.), 2.0 equiv. **2a** and 20 mol% catalyst **AM8,** 90 mol% TFA at 0 °C for 48 h. Experimental details in supporting information (page 21). Yields refer to pure products after isolation by column chromatography. Enantiomeric excess determined by chiral HPLC on Chiralpak ASH & IA3 -column. The deposition number for the XRD of **6** is CCDC 2286183[55]

To demonstrate the robustness and practicality of the diazabicycloalkane product, we carried out one-pot reactions without isolating **3a**. For the straightforward aldehyde reduction, we simply added methanol and $NaBH_4$ directly to the crude

Die approbierte gedruckte Originalversion dieser Dissertation ist an der TU Wien Bibliothek verfügbar.
The approved original version of this doctoral thesis is available in print at TU Wien Bibliothek.
TU Bibliothek Your knowledge hub WIEN

mixture of **3a** at room temperature. Remarkably, no racemization occurred, and the enantioselectivity of the final product **4** remained identical to that of the intermediate **3a**. Similarly, in the Horner-Wadsworth-Emmons reaction,[54] the activated Wittig reagent was introduced into the crude mixture at 0 °C. Once again, no racemization was detected, and complete conversion of **3a** to product **5** was achieved in a short reaction time. Under more rigorous conditions involving hydrazone formation at 60 °C towards product **6**, a slight decrease in enantioselectivity was observed. It is worth noting that while racemization could account for this phenomenon, the residual enal-substrate **1a** might undergo rapid reactions with **2a** at elevated temperatures, leading to a decrease in the enantioselectivity of **3a** before the hydrazone formation in the subsequent step. Nevertheless, these results highlight the robustness of the diazabicycloalkane moiety and its potential for efficient one-pot reactions without compromising enantioselectivity.

In this study, we present the direct organocatalytic synthesis of chiral, condensed diazabicycloalkanes via tandem enamine-iminium catalysis in a single step. Through an organocatalytic aza-Michael/aldol reaction of enals, we achieved yields of 31-86% and enantioselectivities of 80-98% on a wide range of enal-substrates tolerating both sterically unhindered **1a-n** and hindered enals **1o-w**. Interestingly, we observed that the ee could be significantly influenced by increasing the amount of acid cocatalyst, offering alternative avenues for reaction optimization, focusing on either yield or enantioselectivity, if necessary. The ideal catalyst was identified as modified diphenylethylenediamine **AM8** with both primary and secondary amino groups. We found that these functionalities were essential for attaining high yields and ee, proposing a necessary dual activation of both the substrate and reagent. The resulting compound incorporates a methyl group, possessing notable biological significance, as well as an aldehyde group that we demonstrated to undergo stable post-modifications.

Acknowledgements

This project has received funding from the European Research Council (ERC) under the European Union's Horizon 2020 research and innovation program (Grant agreement No. 864991)

Keywords: aza-Michael/aldol • diazabicycloalkane • nitrogen heterocycles • organocatalysis • pyridazine

[1] Z. X. He, Y. P. Gong, X. Zhang, L. Y. Ma, W. Zhao, *Eur. J. Med. Chem.* **2021**, *209*, 112946.

[2] F. Chalem, P. Farias, H. Lizarazo, P. Peña, *J. Int. Med. Res.* **1977**, *5*, 18–25.

[3] O. Morita, H. Kushida, M. Kunihara, *J. Cardiovasc. Pharmacol.* **1995**, *25*, 880–887.

[4] S. García-Ortega, P. J. Holliman, D. L. Jones, *Sci. Total Environ.* **2006**, *366*, 826–836.

[5] G. Charrier, Jean-Damien;Brenchley, *Caspase Inhibitors and Uses Thereof*, **2011**, US7968716B2.

[6] T. Szucs, *Drugs* **1991**, *41*, 18–24.

[7] R. St. Charles, J. H. Matthews, E. Zhang, A. Tulinsky, *J. Med. Chem.* **1999**, *42*, 1376–1383.

[8] S. A. Kiledal, R. Jourdain, S. Vellalath, D. Romo, *Org. Lett.* **2021**, *23*, 6622–6627.

[9] R. Dey, P. Kumar, P. Banerjee, *J. Org. Chem.* **2018**, *83*, 5438–5449.

[10] N. Momiyama, H. Tabuse, H. Noda, M. Yamanaka, T. Fujinami, K. Yamanishi, A. Izumiseki, K. Funayama, F. Egawa, S. Okada, H. Adachi, M. Terada, *J. Am. Chem. Soc.* **2016**, *138*, 11353–11359.

[11] H. J. Leng, F. Peng, S. Zingales, W. Huang, B. Wang, Q. Zhao, R. Zhou, G. He, C. Peng, B. Han, *Chem. Eur. J.* **2015**, *21*, 18100–18108.

[12] S. Gao, J. R. Chen, X. Q. Hu, H. G. Cheng, L. Q. Lu, W. J. Xiao, *Adv. Synth. Catal.* **2013**, *355*, 3539–3544.

[13] M. Fernández, J. L. Vicario, E. Reyes, L. Carrillo, D. Badía, *Chem. Commun.* **2012**, *48*, 2092.

[14] S. Kumarn, A. J. Oelke, D. M. Shaw, D. A. Longbottom, S. V. Ley, *Org. Biomol. Chem.* **2007**, *5*, 2678–2689.

[15] M. R. Attwood, C. H. Hassall, A. Kröhn, G. Lawton, S. Redshaw, *J. Chem. Soc., Perkin Trans. 1* **1986**, 1011–1019.

[16] L. Liang, Y. Huang, *Org. Lett.* **2016**, *18*, 2604–2607.

[17] Q. Du, J. M. Neudörfl, H. G. Schmalz, *Chem. Eur. J.* **2018**, *24*, 2379–2383.

[18] X. Xu, M. P. Doyle, *Acc. Chem. Res.* **2014**, *47*, 1396–1405.

[19] Y. Qian, P. J. Zavalij, W. Hu, M. P. Doyle, *Org. Lett.* **2013**, *15*, 1564–1567.

[20] A. J. Oelke, S. Kumarn, D. A. Longbottom, S. V. Ley, *Synlett* **2006**, *209*, 2548–2552.

[21] X. Xu, P. Y. Zavalij, M. P. Doyle, *Angew. Chem. Int. Ed.* **2012**, *51*, 9829–9833.

[22] S. Radl, in *Compr. Heterocycl. Chem. III*, Elsevier, **2008**, pp. 365–479.

[23] Y. Song, D. Du, *Adv. Synth. Catal.* **2021**, *363*, 4667–4694.

[24] Z.-X. Jia, Y.-C. Luo, Y. Wang, L. Chen, P.-F. Xu, B. Wang, *Chem. Eur. J.* **2012**, *18*, 12958–12961.

[25] X.-F. Wang, J. An, X.-X. Zhang, F. Tan, J.-R. Chen, W.-J. Xiao, *Org. Lett.* **2011**, *13*, 808–811.

[26] H. Sundén, R. Rios, I. Ibrahem, G.-L. Zhao, L. Eriksson, A. Córdova, *Adv. Synth. Catal.* **2007**, *349*, 827–832.

[27] S. Mukherjee, S. Shee, T. Poisson, T. Besset, A. T. Biju, *Org. Lett.* **2018**, *20*, 6998–7002.

[28] D. Enders, C. Wang, G. Raabe, *Synthesis (Stuttg).* **2009**, *24*, 4119–4124.

[29] M. Giardinetti, J. Marrot, X. Moreau, V. Coeffard, C. Greck, *J. Org. Chem.* **2016**, *81*, 6855–6861.

[30] X.-J. Zhou, J.-Q. Zhao, X.-M. Chen, J.-R. Zhuo, Y.-P. Zhang, Y.-Z. Chen, X.-M. Zhang, X.-Y. Xu, W.-C. Yuan, *J. Org. Chem.* **2019**, *84*, 4381–4391.

[31] Y. Huang, C. Zheng, G. Zhao, *RSC Adv.* **2013**, *3*, 16999.

[32] B.-L. Zhao, D.-M. Du, *Asian J. Org. Chem.* **2015**, *4*, 1120–1126.

[33] S. Izumi, Y. Kobayashi, Y. Takemoto, *Org. Lett.* **2016**, *18*, 696–699.

[34] M. Moczulski, P. Drelich, Ł. Albrecht, *Org. Biomol. Chem.* **2018**, *16*, 376–379.

[35] I. Ibrahem, R. Rios, J. Vesely, G.-L. Zhao, A. Córdova, *Chem. Commun.* **2007**, 849–851.

[36] D. Aynetdinova, M. C. Callens, H. B. Hicks, C. Y. X. Poh, B. D. A. Shennan, A. M. Boyd, Z. H. Lim, J. A. Leitch, D. J. Dixon, *Chem. Soc. Rev.* **2021**, *50*, 5517–5563.

Die approbierte gedruckte Originalversion dieser Dissertation ist an der TU Wien Bibliothek verfügbar.
The approved original version of this doctoral thesis is available in print at TU Wien Bibliothek.
TU Bibliothek Your knowledge hub WIEN

[37] H. Schönherr, T. Cernak, *Angew. Chem. Int. Ed.* **2013**, *52*, 12256–12267.

[38] A. Erkkilä, I. Majander, P. M. Pihko, *Chem. Rev.* **2007**, *107*, 5416–5470.

[39] S.-J. Lee, J.-G. Ahn, J. Seo, H.-J. Ha, C.-W. Cho, *Org. Biomol. Chem.* **2018**, *16*, 9477–9486.

[40] A. Córdova, S. Lin, A. Tseggai, *Adv. Synth. Catal.* **2012**, *354*, 1363–1372.

[41] H.-M. Guo, T.-F. Yuan, H.-Y. Niu, J.-Y. Liu, R.-Z. Mao, D.-Y. Li, G.-R. Qu, *Chem. Eur. J.* **2011**, *17*, 4095–4098.

[42] I. Arenas, A. Ferrali, C. Rodríguez-Escrich, F. Bravo, M. A. Pericàs, *Adv. Synth. Catal.* **2017**, *359*, 2414–2424.

[43] D. Enders, C. Joie, K. Deckers, *Chem. Eur. J.* **2013**, *19*, 10818–10821.

[44] P. Melchiorre, *Angew. Chem. Int. Ed.* **2012**, *51*, 9748–9770.

[45] G. Singh, E. Yeboah, *Reports Org. Chem.* **2016**, *Volume 6*, 47–75.

[46] P. I. Dalko, L. Moisan, *Angew. Chem. Int. Ed.* **2001**, *40*, 3726–3748.

[47] K. H. Kim, S. Lee, D. W. Lee, D. H. Ko, D. C. Ha, *Tetrahedron Lett.* **2005**, *46*, 5991–5994.

[48] M. Wang, L. Lin, J. Shi, X. Liu, Y. Kuang, X. Feng, *Chem. Eur. J.* **2011**, *17*, 2365–2368.

[49] J. Wang, X. Liu, S. Dong, L. Lin, X. Feng, *J. Org. Chem.* **2013**, *78*, 6322–6327.

[50] A. R. Ranade, G. I. Georg, *J. Org. Chem.* **2014**, *79*, 984–992.

[51] J. H. Shim, M. J. Kim, J. Y. Lee, K. H. Kim, D. C. Ha, *Tetrahedron Lett.* **2020**, *61*, 152295.

[52] S. Li, J. Wang, P.-J. Xia, Q.-L. Zhao, C.-M. Wang, J.-A. Xiao, X.-Q. Chen, H.-Y. Xiang, H. Yang, *J. Org. Chem.* **2018**, *83*, 12284–12290.

[53] H. Zong, H. Huang, G. Bian, L. Song, *J. Org. Chem.* **2014**, *79*, 11768–11773.

[54] W. S. Wadsworth, W. D. Emmons, *J. Am. Chem. Soc.* **1961**, *83*, 1733–1738.

[55] Deposition numbers 2286183 contain the supplementary crystallographic data for this paper. These data are provided free of charge by the joint Cambridge Crystallographic Data Centre and Fachinformationszentrum Karlsruhe Access Structures service.

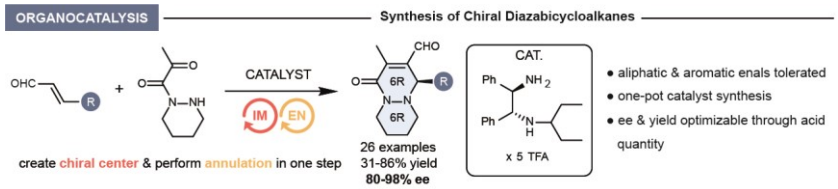
Die approbierte gedruckte Originalversion dieser Dissertation ist an der TU Wien Bibliothek verfügbar.
The approved original version of this doctoral thesis is available in print at TU Wien Bibliothek.

TU Bibliothek Your knowledge hub WIEN

Synthesis of Chiral Diazabicycloalkanes via Organocatalytic aza-Michael/Aldol Reaction

Adv. Synth. Catal. **Year**, *Volume*, Page – Page

Fabian Scharinger,[a] Matthias Weil,[b] Michael Schnürch[a] and Katharina Bica-Schröder[a]*



Die approbierte gedruckte Originalversion dieser Dissertation ist an der TU Wien Bibliothek verfügbar.
The approved original version of this doctoral thesis is available in print at TU Wien Bibliothek.

WILEY VCH

11 Conclusion

To introduce the topic and utility of organocatalysis we summarized recent advancements within the realm of organocatalytic asymmetric transfer hydrogenation (ATH) of sp^2-hybridized C=N, C=O, and C=C bonds using chiral phosphoric acids as catalysis (**Figure 6**). We then demonstrated that chiral phosphoric acids have emerged as remarkably versatile tools in this domain, offering highly efficient and enantioselective pathways for the reduction of α,β-unsaturated carbonyl compounds including imines and diverse heterocycles. To conclude the review, we have summarized and emphasized the utilization of chiral phosphoric acids in multicomponent and cascade reactions, underscoring their suitability and practicality in these domains.

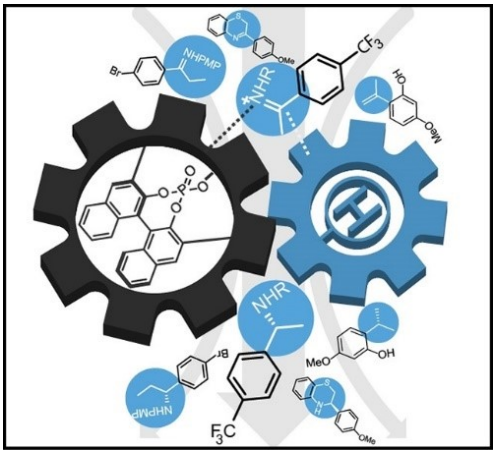


Figure 6. Asymmetric transfer hydrogenation via phosphoric acid catalysts.

The second part of the thesis introduces a novel approach that we have coined counterion enhanced organocatalysis for organocatalytic asymmetric transfer hydrogenations. This innovative method utilizes ion-paired catalysts, comprising cost-effective cations derived from amino acids and flexible, racemic phosphate anions. These catalysts can be easily synthesized from natural compounds, offering a significantly more economical alternative compared to the current state-of-the-art ACDC methodology. We discovered that the chiral amine, a D-menthyl ester derived from L-valine, could already yield modest enantioselectivities when combined with commercially available acids like TFA. However, by increasing the steric hindrance of the counteranion using a phosphoric acid derived from thymol, we were able to achieve outstanding enantioselectivities for a broad range of enone substrates. Simulation data suggests that interionic interactions are robust enough to form stable ion pairs in apolar solvents such as MTBE concluding a possible interconversion of the phosphoric acid atropisomer. Furthermore, hydrogen bonding between the catalyst components facilitates a particular ion pair configuration, resulting in a reduced distance between the sterically hindering ester group and the phosphoric acid which corresponds to a high stereocontrol. Our ongoing investigations are centered on expanding the scope of counterion-enhanced organocatalysis using chiral amino

Die approbierte gedruckte Originalversion dieser Dissertation ist an der TU Wien Bibliothek verfügbar.
The approved original version of this doctoral thesis is available in print at TU Wien Bibliothek.
TU Bibliothek Your knowledge hub WIEN

acid-derived cations and possible atropisomeric, or racemic phosphate anions. In conclusion, we anticipate that the concept of counterion-enhanced catalysis, relying on chiral cations and bulky anions, will have broad applications not only in organocatalysis but also in transition metal catalysis.

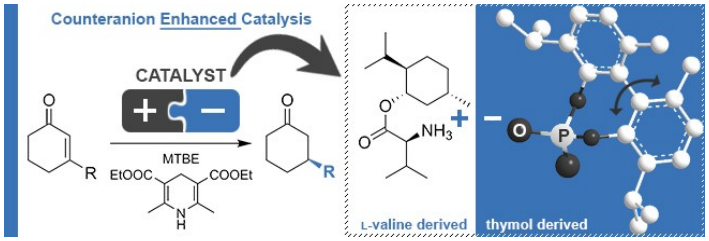


Figure 7. Concept of counteranion enhanced organocatalysis within asymmetric transfer hydrogenation of enones.

In the second project, we have further expanded the innovative concept of counterion-enhanced organocatalysis for diverse asymmetric functionalizations of enones. We achieved this by combining sterically demanding, flexible phosphoric acids with chiral diamines derived from amino acids, resulting in the creation of straightforward and highly adaptable organocatalytic frameworks. After meticulous parameter optimization, we identified a remarkably robust and versatile organocatalyst. This catalyst proved effective in various asymmetric reactions, including epoxidations, aziridinations, aza-Michael/aldol cascade cyclizations, and a Robinson-like asymmetric Michael induced ring closure/aldol cyclization. We achieved outstanding enantioselectivities in all four reaction types, enabling the straightforward synthesis of both product enantiomers. Our ongoing research endeavors are currently focused on expanding the applicability of this catalytic concept, especially in complex cyclization reactions.

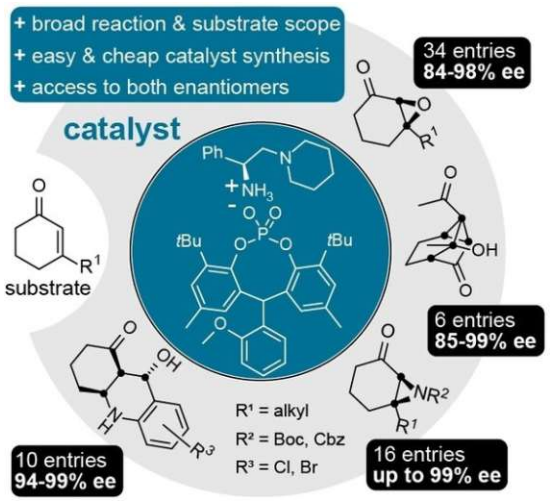


Figure 8. Iminium/enamine catalysis with achiral phosphoric acids.

Die approbierte gedruckte Originalversion dieser Dissertation ist an der TU Wien Bibliothek verfügbar.
The approved original version of this doctoral thesis is available in print at TU Wien Bibliothek.

In the third project, we introduced a pioneering method for the direct organocatalytic synthesis of chiral, condensed diazabicycloalkanes using domino iminium/enamine catalysis. By conducting a straightforward organocatalytic aza-Michael/aldol reaction with enals, we achieved favorable to high yields and exceptional enantioselectivities of up to 98% across a broad spectrum of enal substrates. This method proved effective for both sterically unhindered enals and their more hindered counterparts with equally good results. Interestingly, we observed that the enantiomeric excess could be significantly influenced by increasing the amount of acid cocatalyst. This finding opens up alternative avenues for reaction optimization, allowing us to prioritize either yield or enantioselectivity as needed. The most effective catalyst we identified was a modified diphenylethylenediamine, possessing both primary and secondary amino groups. We found that these functionalities were essential for achieving high yields and enantiomeric excess, suggesting a dual activation of both the substrate and reagent. The resulting compound includes a methyl group, which holds significant biological relevance, as well as an aldehyde group that we demonstrated to be amenable to stable post-modifications.

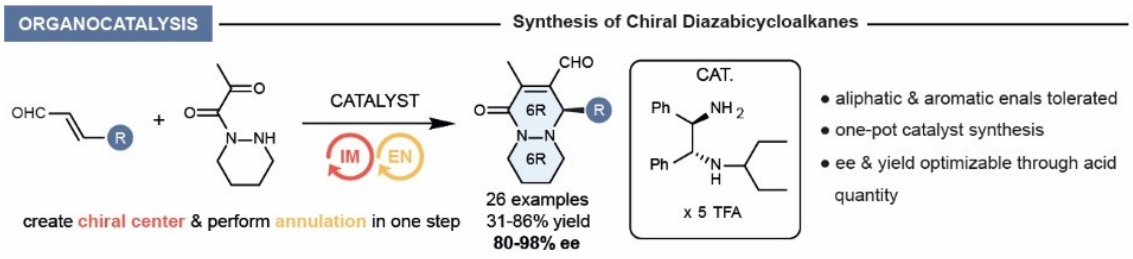


Figure 9. Organocatalytic synthesis of diazabicycloalkanes.

Die approbierte gedruckte Originalversion dieser Dissertation ist an der TU Wien Bibliothek verfügbar.
The approved original version of this doctoral thesis is available in print at TU Wien Bibliothek.

Appendix A

Supporting information:

Counterion Enhanced Organocatalysis: A Novel Approach for the Asymmetric Transfer Hydrogenation of Enones

Die approbierte gedruckte Originalversion dieser Dissertation ist an der TU Wien Bibliothek verfügbar.
The approved original version of this doctoral thesis is available in print at TU Wien Bibliothek.

ChemCatChem

Supporting Information

Counterion Enhanced Organocatalysis: A Novel Approach for the Asymmetric Transfer Hydrogenation of Enones

Fabian Scharinger[+], Ádám Márk Pálvölgyi[+], Veronika Zeindlhofer, Michael Schnürch, Christian Schröder, and Katharina Bica-Schröder*

Die approbierte gedruckte Originalversion dieser Dissertation ist an der TU Wien Bibliothek verfügbar.
The approved original version of this doctoral thesis is available in print at TU Wien Bibliothek.

1. General remarks 3
2. Synthesis of L-amino acid derivatives 4
3. General synthesis of the phosphoric acids 10
4. Synthesis of the Hantzsch ester 14
5. Synthesis of ATH substrates 15
6. General procedure and optimization of the ATH reactions 18
7. Computational studies 32
8. NMR specta of L-amino acid derivatives 38
9. NMR specta of phosphoric acids and its intermediates 45
10. NMR specta of ATH substrates 54
11. NMR specta of ATH products 59
12. Chiral GC and HPLC traces 65
13. References 81

Die approbierte gedruckte Originalversion dieser Dissertation ist an der TU Wien Bibliothek verfügbar.
The approved original version of this doctoral thesis is available in print at TU Wien Bibliothek.

1. General remarks

All purchased chemicals from commercial suppliers were used without further purification. Dry solvents were pre-distilled and desiccated on aluminium oxide columns (PURESOLV, Innovative Technology).

Column chromatography was performed on standard manual glass columns using Merck (40-60 µm) silica gel with pre-distilled solvents (PE : petrolether, EtOAc : ethyl acetate, Et_2O : diethyl ether). For TLC analysis, precoated aluminium-backed plates were purchased from Merck (silica gel 60 F_{254}). UV active compounds were detected at 254 nm. Non-UV active compounds have been detected using vanillin staining solution (5% vanillin in EtOH + H_2SO_4).

^{1}H, ^{13}C, and ^{31}P NMR spectra were recorded on a Bruker Advance UltraShield 200 MHz or 400 MHz spectrometer and chemical shifts are reported in ppm using TMS (tetramethylsilane) as internal standard. Coupling constants (*J*) are given in Hz. For NMR purpose, the following abbreviations are used: s (singlet), d (doublet), t (triplet), q (quartet), m (multiplet), brs (broad singlet), dd (doublet of doublets), ddd (doublets of doublet of doublets), td (triplet of doublets), dt (doublet of triplets).

GC analysis have been performed on a Thermo Scientific Focus on BGB5 column by using FID detector. Chiral GC measurements were performed on chiral BGB columns (BGB173 or BGB175) by using FID detector.

Chiral HPLC measurements were carried out on a DIONEX UPLC equipped with a photodiode array (PDA) plus detector (190–360 nm), using a Diacel Chiralcel AS-H column (250×4.60 mm, 5 µm).

Optical rotation was measured on an Anton Paar MCP500 polarimeter at the specific conditions and the results have been compared to literature values. Concentrations are given in g / 100 ml.

HR-MS analysis was performed using HTC PAL system auto sampler, an Agilent 1100/1200 HPLC and Agilent 6230 AJS ESI-TOF mass spectrometer.

Microwave reactions were performed on a Biotage Initiator Classic in 20 ml pressure tight glass vials.

Melting points above room temperature were measured on an automated melting point system OPTI MELT of Stanford Research Systems and are uncorrected.

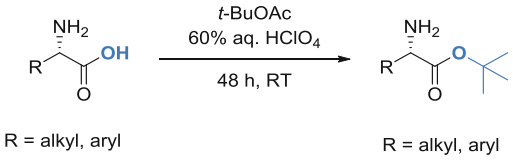
Infrared spectra were recorded on a Perkin-Elmer Spectrum 65 FT IR spectrometer equipped with a specac MK II Golden Gate Single Reflection ATR unit.

Die approbierte gedruckte Originalversion dieser Dissertation ist an der TU Wien Bibliothek verfügbar.
The approved original version of this doctoral thesis is available in print at TU Wien Bibliothek.
TU Bibliothek Your knowledge hub WIEN

2. Synthesis of L-amino acid derivatives

2.1 General procedure for the synthesis of L-amino acid *tert*-butyl esters

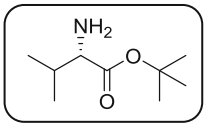
Compound have been prepared by the following literature procedure: [1]



R = alkyl, aryl R = alkyl, aryl

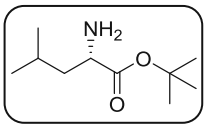
To a solution of the corresponding L-amino acid (1.0 equiv.) in *tert*-butyl acetate (18.0 equiv.), $HClO_4$ (60 % aqueous solution, 1.5 equiv.) was added dropwise at 0°C. The reaction mixture was stirred 18 h at room temperature. Distilled H_2O was added, and the reaction mixture was extracted with distilled H_2O (2×) and 1 N HCl (3×). The combined aqueous phases were then adjusted to pH 10 with a saturated Na_2CO_3 solution. The resulting solution was then extracted with CH_2Cl_2. The combined organic phases were dried over anhydrous Na_2SO_4 and concentrated under reduced pressure to give the L-amino acid *tert*-butyl esters, which were find to be pure without further purifications.

tert-Butyl L-valinate [1]



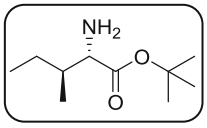
Light yellow oil (67% yield). **^{1}H NMR (400 MHz, $CDCl_3$) δ** 3.17 (d, *J* = 4.8 Hz, 1H, C*H*-NH_2), 2.03 – 1.97 (m, 1H, C*H*-$(CH_3)_2$), 1.57 (s, 2H, NH_2), 1.46 (s, 9H, 3 × CH_3-C), 0.97 (d, *J* = 6.9 Hz, 3H, CH_3-CH), 0.89 (d, *J* = 6.9 Hz, 3H, CH_3-CH).

tert-Butyl L-leucinate [1]



Light yellow oil (69% yield). **^{1}H NMR (400 MHz, $CDCl_3$) δ** 3.26 (t, *J* = 8.0 Hz, 1H, C*H*-NH_2), 1.74 – 1.67 (m, 1H, C*H*-$(CH_3)_2$), 1.48 – 1.37 (m, 12H, CH_{2a}-CH-NH_2, NH_2, 3 × CH_3-C), 1.33 – 1.27 (m, 1H, CH_{2b}-CH-NH_2), 0.86 (t, *J* = 9.0 Hz, 6H, 2 × CH_3-CH).

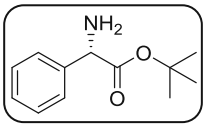
tert-Butyl L-isoleucinate [2]



Light yellow oil (36% yield). **^{1}H NMR (400 MHz, $CDCl_3$) δ** 3.22 (d, *J* = 4.8 Hz, 1H, C*H*-NH_2), 1.73 – 1.67 (m, 1H, C*H*-CH_3), 1.48 (s, 2H, NH_2), 1.46 (s, 9H, 3 × CH_3-C), 1.12 – 1.23 (m, 2H, CH_2-CH_3), 1.12 – 0.70 (m, 6H, 2 x CH_3).

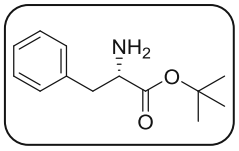
Die approbierte gedruckte Originalversion dieser Dissertation ist an der TU Wien Bibliothek verfügbar.
The approved original version of this doctoral thesis is available in print at TU Wien Bibliothek.
TU Bibliothek Your knowledge hub WIEN

tert-Butyl-(*S*)-2-amino-2-phenylacetate [2]



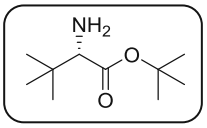
Light yellow solid (61% yield). **^{1}H NMR (400 MHz, $CDCl_3$) δ** 7.30 – 7.16 (m, 5H, *H*-arom), 4.39 (s, 1H, C*H*-NH_2), 1.99 (s, 2H, NH_2), 1.30 (s, 9H, 3 × CH_3-C).

tert-Butyl L-phenylalaninate [2]



Light yellow oil (65% yield). **^{1}H NMR (400 MHz, $CDCl_3$) δ** 7.23 – 7.14 (m, 5H, *H*-arom), 3.54 (t, *J* = 7.8 Hz, 1H, C*H*-NH_2), 2.97 (dd, *J* = 16.0 Hz, 8.0 Hz, 1H, CH_{2a}-CH-NH_2), 2.77 (dd, *J* = 16.0 Hz, 8.0 Hz, 1H, CH_{2b}-CH-NH_2), 1.40 (s, 2H, NH_2), 1.35 (s, 9H, 3 × CH_3-C).

tert-Butyl (S)-2-amino-3,3-dimethylbutanoate [1]

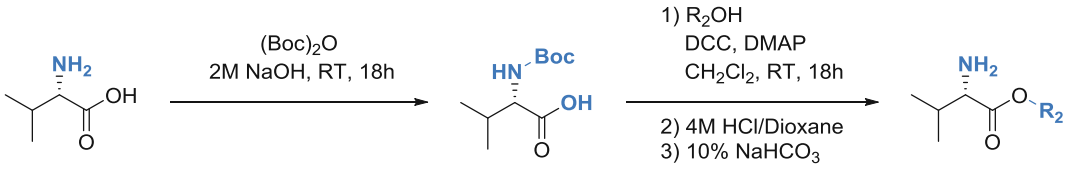


Light yellow oil (72% yield). **^{1}H NMR (400 MHz, $CDCl_3$) δ** 2.95 (s, 1H, C*H*-NH_2), 1.41 (s, 11H, NH_2, 3 × CH_3-C), 0.90 (s, 9H, 3 × CH_3-C).

Die approbierte gedruckte Originalversion dieser Dissertation ist an der TU Wien Bibliothek verfügbar.
The approved original version of this doctoral thesis is available in print at TU Wien Bibliothek.

2.2 General procedure for the synthesis of L-amino acid esters via DCC/DMAP coupling

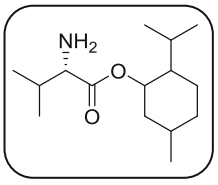
L-Valine mentyl esters (all three diastereomers), L-valine cyclohexyl ester and L-valine 4-(*tert*-butyl)cyclohexyl ester have been prepared by the following two step general procedure: [3]



A solution of L-valine (5.0 g, 43 mmol, 1.0 equiv.) in 2 N NaOH (43 mL) was cooled to 0°C and Boc_2O (11.3 g, 51.6 mmol, 1.2 equiv.) was added slowly *via* syringe. The ice bath was removed and the reaction mixture stirred for 18 h at room temperature. The mixture was acidified (pH = 2) by using a 4 N HCl and extracted with EtOAc (3 × 50 mL). The combined organic phases were dried over anhydrous Na_2SO_4 and concentrated to give (*tert*-butoxycarbonyl)-L-valine as a colorless oil (8.3 g, 90%).

To a solution of (*tert*-butoxycarbonyl)- L-valine (1.0 equiv.) in dry CH_2Cl_2, DCC (1.1 equiv.) was added at room temperature. The suspension was cooled to 0°C followed by the addition of the corresponding alcohol (1.0 equiv.) and DMAP (0.1 equiv.). The reaction mixture was stirred for 18 h at room temperature followed by the addition of EtOAc. After 10 min of stirring, the dicyclohexyl urea was filtered off, rinsed with EtOAc and the filtrate was successively washed with 1 N HCl solution, saturated $NaHCO_3$ solution, dried over anhydrous Na_2SO_4 and concentrated under reduced pressure. 4 N HCl in dioxane was added and the resulting mixture was stirred for 3 h at room temperature. The solvent was removed, Et_2O was added and stirred for 10 min. The amino acid HCl salt was filtered off, washed with Et_2O (3×) and dried in vacuo. The salt was suspended in CH_2Cl_2, saturated $NaHCO_3$ was added and stirred for 2 h at room temperature. The organic phase was separated, washed with saturated $NaHCO_3$ (3×) and concentrated under reduced pressure to yield the corresponding esters.

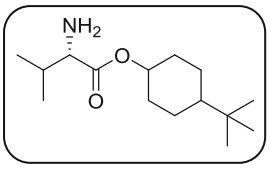
Menthyl valinates (all diastereomers)



Colorless oil (DL: 58% yield, D: 55% yield, L: 58% yield). **^{1}H NMR (400 MHz, $CDCl_3$) δ** 4.73 (td, *J* = 10.9, 4.4 Hz, 1H, C*H*-O), 3.29 (d, *J* = 4.8 Hz, 1H, C*H*-NH_2), 2.15 – 2.01 (m, 1H, C*H*-$(CH_3)_2$), 2.00 – 1.01 (m, 10H, NH_2, *H*-menthol), 0.99 (d, *J* = 6.9 Hz, 3H, CH_3-CH), 0.90 (m, 9H, 2 × CH_3-CH, CH_3-CH-menthol), 0.76 (d, *J* = 7.0 Hz, 3H, CH_3-menthol); **^{13}C NMR (100 MHz, $CDCl_3$) δ** 175.30, 74.88, 60.40, 47.08, 41.01, 34.37, 31.90, 31.53, 26.11, 23.09, 22.15, 21.01, 19.79, 16.65, 15.89.

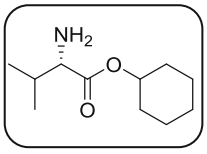
Die approbierte gedruckte Originalversion dieser Dissertation ist an der TU Wien Bibliothek verfügbar.
The approved original version of this doctoral thesis is available in print at TU Wien Bibliothek.
TU Bibliothek Your knowledge hub WIEN

4-(tert-Butyl)cyclohexyl-L-valinate



Colorless oil (18% yield). **^{1}H NMR (400 MHz, $CDCl_3$) δ** 4.73 – 4.66 (m, 1H, C*H*-O), 3.30 (d, *J* = 4.8 Hz, 1H, C*H*-NH_2), 2.25 (s, 2H, N*H*$_2$), 2.12 – 1.94 (m, 3H, C*H*-$(CH_3)_2$, C*H*$_2$-CH-O), 1.85 – 1.75 (m, 2H, C*H*$_2$-CH-O), 1.41 – 1.22 (m, 2H, C*H*$_2$-CH-C-tbu), 1.18 – 1.00 (m, 2H, C*H*$_2$-CH-C-tbu), 0.99 (d, *J* = 6.9 Hz, 3H, C*H*$_3$-CH), 0.92 (d, *J* = 6.9 Hz, 3H, C*H*$_3$-CH), 0.85 (s, 9H, 3 × C*H*$_3$-C).

Cyclohexyl L-valinate [4]

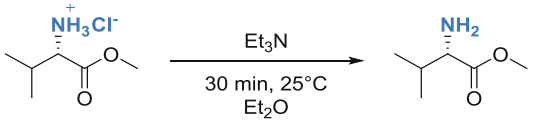


Colorless oil (49% yield). **^{1}H NMR (400 MHz, $CDCl_3$) δ** 4.93 – 4.64 (m, 1H, C*H*-O), 3.24 (d, *J* = 4.9 Hz, 1H, C*H*-NH_2), 2.05 – 1.97 (m, 1H, C*H*-$(CH_3)_2$), 1.81 (bs, 2H, N*H*$_2$), 1.74 – 1.00 (m, 10H, C*H*-cyclohexyl), 0.96 (d, *J* = 6.9 Hz, 3H, C*H*$_3$-CH), 0.88 (d, *J* = 6.9 Hz, 3H, C*H*$_3$-CH).

Die approbierte gedruckte Originalversion dieser Dissertation ist an der TU Wien Bibliothek verfügbar.
The approved original version of this doctoral thesis is available in print at TU Wien Bibliothek.

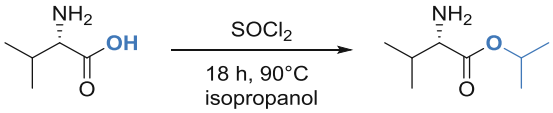
2.3 Synthesis of other L-amino acid esters

Methyl L-valinate [5]



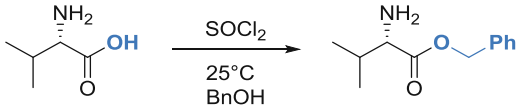
To a slurry of L-valine methyl-ester hydrochloride (1.27 g, 7.6 mmol, 1.0 equiv.) in dry MeOH (1 mL), Et_3N (1.6 mL, 12 mmol, 1.6 equiv.) was added. After 10 min of stirring, dry Et_2O (30 mL) was added, the solution was cooled to 0°C and it was stirred for another 30 min. The triethylamine hydrochloride salt was filtered off and the filtrate was concentrated to yield the product as a colorless oil (800 mg, 81%). **^{1}H NMR (400 MHz, $CDCl_3$) δ** 3.70 (s, 3H, C*H*$_3$-O), 3.28 (d, *J* = 5.1 Hz, 1H, C*H*-NH_2), 2.11 – 1.93 (m, 1H, C*H*-$(CH_3)_2$), 1.45 (s, 2H, N*H*$_2$), 0.95 (d, *J* = 6.9 Hz, 3H, C*H*$_3$-CH), 0.88 (d, *J* = 6.9 Hz, 3H, C*H*$_3$-CH).

Isopropyl L-valinate [6]



To a solution of L-valine (1.0 g, 8.5 mmol, 1.0 equiv.) in isopropanol (26 mL, 341 mmol, 40 equiv.) was added thionyl chloride (3.1 mL, 43 mmol, 5.0 equiv.) at 0°C. The reaction mixture was then refluxed for 18 h. After cooling to room temperature, the solvent was evaporated, Et_2O (50 mL) was added and the amino acid hydrochloride salt was filtered off. CH_2Cl_2 (50 mL) was added, followed by the addition of sat. $NaHCO_3$ (50 mL) and the two phases were stirred for 30 min. The organic phase was washed several times with sat. $NaHCO_3$ (3 × 25 mL), dried over anhydrous Na_2SO_4 and concentrated to give the product as a colorless liquid (380 mg, 23%). **^{1}H NMR (400 MHz, $CDCl_3$) δ** 5.09 – 5.02 (m, 1H, C*H*-O), 3.26 (d, *J* = 4.9 Hz, 1H, C*H*-NH_2), 2.07 – 1.99 (m, 1H, C*H*-$(CH_3)_2$), 1.82 (s, 2H, N*H*$_2$), 1.42 – 1.16 (m, 6H, 2 x C*H*$_3$-CH-O), 0.98 (d, *J* = 6.9 Hz, 3H, C*H*$_3$-CH), 0.91 (d, *J* = 6.9 Hz, 3H, C*H*$_3$-CH).

Benzyl L-valinate [7]



To a solution of L-valine (1.0 g, 8.5 mmol, 1.0 equiv.) in benzyl alcohol (26 mL, 341 mmol, 40 equiv.) was added thionyl chloride (3.1 mL, 43 mmol, 5.0 equiv.) at 0°C. The reaction mixture was then stirred for 18 hours at room temperature. Et_2O (50 mL) was added and the amino acid hydrochloride salt was

Die approbierte gedruckte Originalversion dieser Dissertation ist an der TU Wien Bibliothek verfügbar.
The approved original version of this doctoral thesis is available in print at TU Wien Bibliothek.
TU Bibliothek Your knowledge hub WIEN

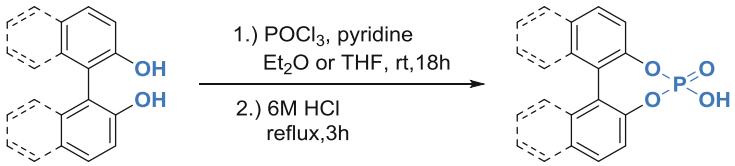
filtered off. CH_2Cl_2 (50 mL) was added, followed by the addition of sat. $NaHCO_3$ (50 mL) and the two phases were stirred for 30 min. The organic phase was washed several times with sat. $NaHCO_3$ (3 × 25 mL), dried over anhydrous Na_2SO_4 and concentrated under reduced pressure to give the product as a colorless liquid (1.12 g, 62%). **^{1}H NMR (400 MHz, $CDCl_3$) δ** 7.37 – 7.32 (m, 5H, *H*-arom), 5.15 (dd, *J* = 12.0 Hz, 16.0 Hz, 1H, C*H*$_2$-arom), 3.34 (d, *J* = 4.0 Hz, 1H, C*H*-NH_2), 2.08 – 2.01 (m, 1H, C*H*-$(CH_3)_2$), 1.68 (s, 2H, N*H*$_2$), 0.96 (d, *J* = 6.9 Hz, 3H, C*H*$_3$-CH), 0.88 (d, *J* = 6.9 Hz, 3H, C*H*$_3$-CH).

Die approbierte gedruckte Originalversion dieser Dissertation ist an der TU Wien Bibliothek verfügbar.
The approved original version of this doctoral thesis is available in print at TU Wien Bibliothek.

3. General synthesis of the phosphoric acids

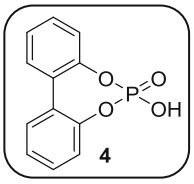
The phosphoric acids have been prepared following either a one or a two-step reaction pathway:

1.) One step procedure: [8]



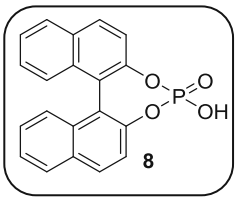
To a solution of the corresponding diol (1.0 equiv.) in dry Et_2O or THF pyridine (2.0 equiv.) was added. The reaction mixture was cooled to 0°C and $POCl_3$ (1.4 equiv.) was added slowly *via* syringe. The resulting reaction mixture was stirred for 18 h at room temperature. The pyridinium hydrochloride was filtered off and it was rinsed several times with Et_2O. The filtrate was concentrated and recrystallized from *n*-heptane. The white solid was filtered off, washed with *n*-heptane (3×) and hydrolyzed with 6 N HCl for 3 h at reflux temperature. Filtration gave the products as a white solid.

6-Hydroxydibenzo[d,f][1,3,2]dioxaphosphepine 6-oxide [8]



White solid (81% yield). **^{1}H NMR (400 MHz, DMSO-d_6) δ** 7.63 (dd, *J* = 7.6, 1.7 Hz, 2H, *H*-arom), 7.50 (td, *J* = 7.8, 1.7 Hz, 2H, *H*-arom), 7.39 (tt, *J* = 7.5, 1.3 Hz, 2H, *H*-arom), 7.32 – 7.21 (m, 2H, *H*-arom); **^{31}P NMR (162 MHz, DMSO-d_6)** 1.72. *Analytical data were in accordance with the literature.*[8]

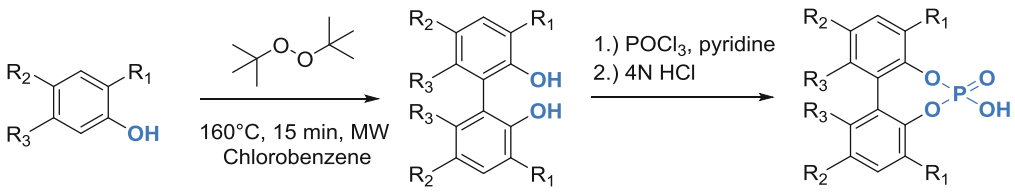
4-Hydroxydinaphtho[2,1-d:1',2'-f][1,3,2]dioxaphosphepine 4-oxide



White solid ((*S*,*R*): 89% yield, (*R*): 93% yield, (*S*): 94% yield). **^{1}H NMR (400 MHz, DMSO-d_6) δ** 8.18 (d, *J* = 8.9 Hz, 2H, *H*-arom), 8.08 (d, *J* = 1.3 Hz, 2H, *H*-arom), 7.57 (dd, *J* = 8.8, 0.9 Hz, 2H, *H*-arom), 7.52 (ddd, *J* = 8.1, 6.7, 1.2 Hz, 2H, *H*-arom), 7.37 (ddd, *J* = 8.3, 6.8, 1.4 Hz, 2H, *H*-arom), 7.23 (dd, *J* = 8.5, 1.1 Hz, 2H, *H*-arom); **^{31}P NMR (162 MHz, DMSO-d_6)** 2.66. *Analytical data were in accordance with the literature.*[8]

Die approbierte gedruckte Originalversion dieser Dissertation ist an der TU Wien Bibliothek verfügbar.
The approved original version of this doctoral thesis is available in print at TU Wien Bibliothek.

2.) Two step procedure: [9, 10]



R_1 = *i*-Pr, R_2 = H, R_3 = CH_3
R_1 = *t*-Bu, R_2 = H, R_3 = CH_3
R_1 = *t*-Bu, R_2 = CH_3, R_3 = H

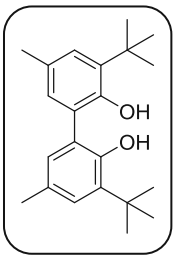
R_1 = *i*-Pr, R_2 = H, R_3 = CH_3
R_1 = *t*-Bu, R_2 = H, R_3 = CH_3
R_1 = *t*-Bu, R_2 = CH_3, R_3 = H

R_1 = *i*-Pr, R_2 = H, R_3 = CH_3
R_1 = *t*-Bu, R_2 = H, R_3 = CH_3
R_1 = *t*-Bu, R_2 = CH_3, R_3 = H

In a 20 mL microwave vial equipped with a stir bar, the corresponding phenol (1.0 equiv.) was dissolved in chlorobenzene (1.66 M). Di-*tert*-butyl peroxide (1.05 equiv.) was then added *via* syringe. The vial was capped and the reaction mixture was stirred for 15 min at room temperature. The vial was then placed in the microwave reactor and heated to 160°C (high absorption setting) and stirred for 15 min. The reaction mixture was allowed to cool down and volatiles have been removed under reduced pressure. The resulting crude mixture was purified by column chromatography (EtOAc: PE, UV visualization) to afford the desired 2,2'-diols (**Step A**).

To a solution of the corresponding 2,2'-diol (1.0 equiv.) in pyridine, $POCl_3$ (2.0 equiv.) was added slowly *via* syringe at 0°C. After stirring the reaction mixture for 24 h at 95°C, it was cooled to room temperature and distilled H_2O was added slowly. The resulting clear solution was stirred for another 18 h at 95 °C. After cooling down to room temperature, 4 N HCl was added slowly. The precipitate of the product was filtered off and washed with 4 N HCl. The solid product was further hydrolyzed by re-dissolving it in CH_2Cl_2 and washing several times with 4 N HCl (3-4×) After being dried over anhydrous Na_2SO_4, removal of the solvent gave the phosphoric acids (**Step B**).

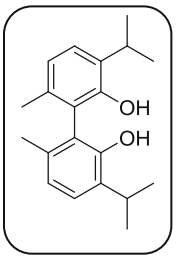
*3,3'-Di-tert-butyl-5,5'-dimethyl-[1,1'-biphenyl]-2,2'-diol (**STEP A**)* [11]



Column chromatography (1.5% EtOAc in light petrol) afforded the product as pale yellow solid (53% yield). **^{1}H NMR (400 MHz, $CDCl_3$) δ** 7.20 (d, *J* = 2.1 Hz, 2H, *H*-arom), 6.94 (d, *J* = 2.1 Hz, 2H, *H*-arom), 5.24 (s, 2H, 2 × O*H*), 2,36 (s, 6H, 2 × CH_3), 1.48 (s, 18H, 6 × CH_3-C).

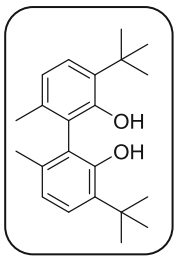
Die approbierte gedruckte Originalversion dieser Dissertation ist an der TU Wien Bibliothek verfügbar.
The approved original version of this doctoral thesis is available in print at TU Wien Bibliothek.

*3,3'-Diisopropyl-6,6'-dimethyl-[1,1'-biphenyl]-2,2'-diol (**STEP A**)* [12]



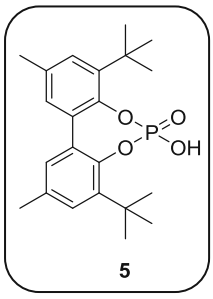
Column chromatography (2% EtOAc in light petrol) afforded the product as light yellow oil (58% yield). **^{1}H NMR (400 MHz, $CDCl_3$) δ** 7.19 (d, *J* = 7.7 Hz, 2H, *H*-arom), 6.89 (d, *J* = 7.8 Hz, 2H, *H*-arom), 4.76 (s, 2H, 2 × O*H*), 3.32 – 3.25 (m, 2H, 2 × C*H*-$(CH_3)_2$), 1.96 (s, 6H, 2 × CH_3), 1.26 (dd, *J* = 6.9, 2.7 Hz, 12H, 4 × CH_3-CH); **^{13}C NMR (100 MHz, $CDCl_3$) δ** 150.99, 135.67, 132.57, 126.75, 122.22, 119.38, 27.17, 22.64, 22.50, 19.26.

*3,3'-Di-tert-butyl-6,6'-dimethyl-[1,1'-biphenyl]-2,2'-diol (**STEP A**)* [13]



Column chromatography (1.5% EtOAc in light petrol) afforded the product as white solid (45% yield). **^{1}H NMR (400 MHz, $CDCl_3$) δ** 7.27 (d, *J* = 8.0 Hz, 2H, *H*-arom), 6.87 (d, *J* = 8.0 Hz, 2H, *H*-arom), 5.01 (s, 2H, 2 × O*H*), 1.94 (s, 6H, 2 × CH_3), 1.42 (s, 18H, 6 × CH_3-C); **^{13}C NMR (100 MHz, $CDCl_3$) δ** 152.35, 134.08, 127.50, 121.97, 120.26, 34.79, 29.64, 19.28.

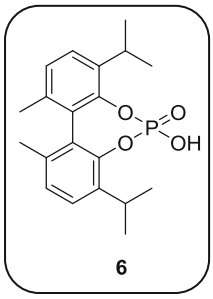
*4,8-Di-tert-butyl-6-hydroxy-2,10-dimethyldibenzo[d,f][1,3,2]dioxaphosphepine 6-oxide (**STEP B**)* [14]



5

Grey solid (63% yield). **^{1}H NMR (400 MHz, $CDCl_3$) δ** 7.26 (s, 2H, *H*-arom), 7.02 (s, 2H, *H*-arom), 2.36 (s, 6H, 2 × CH_3), 1.50 (s, 18H, 6 × CH_3-C); **^{31}P NMR (162 MHz, $CDCl_3$) δ** 0.48. *Analytical data were in accordance with the literature.*[15]

*6-Hydroxy-4,8-diisopropyl-1,11-dimethyldibenzo[d,f][1,3,2]dioxaphosphepine-6-oxide (**STEP B**)*

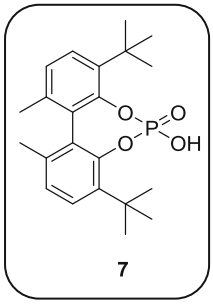


6

Brown solid (85% yield). **^{1}H NMR (400 MHz, $CDCl_3$) δ** 7.27 (d, *J* = 8.0 Hz, 2H, *H*-arom), 7.15 (d, *J* = 8.0 Hz, 2H, *H*-arom), 3.49 – 3.45 (m, 2H, 2 × C*H*-$(CH_3)_2$), 2.14 (s, 6H, 2 × CH_3), 1.27 (dd, *J* = 25.5, 6.9 Hz, 12H, 4 × CH_3-CH); **^{31}P NMR (162 MHz, $CDCl_3$) δ** 2.40; **^{13}C NMR (100 MHz, $CDCl_3$) δ** 145.40, 137.74, 136.08, 128.02, 127.11, 126.31, 26.60, 24.10, 22.75, 19.67; **IR ATR (ν_{max}/cm^{-1})** 2963 (O-H), 2872 (C-H), 1610 (C=C), 1204 (C-O), 967 (C-H), 818 (C-H arom); **HRMS (ESI-TOF)** $[M + Na]^+$ calc. 383.1388, found 383.1389.

Die approbierte gedruckte Originalversion dieser Dissertation ist an der TU Wien Bibliothek verfügbar.
The approved original version of this doctoral thesis is available in print at TU Wien Bibliothek.
TU Bibliothek Your knowledge hub WIEN

*4,8-Di-tert-butyl-6-hydroxy-1,11-dimethyldibenzo[d,f][1,3,2]dioxaphosphepine 6-oxide (**STEP B**)*



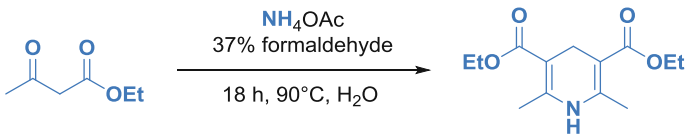
7

White solid (66% yield). **^{1}H NMR (400 MHz, $CDCl_3$) δ** 7.38 (dd, *J* = 8.0, 1.5 Hz, 2H, *H*-arom), 7.11 (dd, *J* = 11.8, 8.2 Hz, 2H, *H*-arom), 2.01 (d, *J* = 27.3 Hz, 6H, 2 × CH_3), 1.48 (d, *J* = 12.4 Hz, 18H, 6 × CH_3-C); **^{31}P NMR (162 MHz, $CDCl_3$) δ** 3.99; **^{13}C NMR (100 MHz, $CDCl_3$) δ** 144.48, 144.31, 140.81, 140.72, 134.81, 130.10, 129.91, 128.89, 35.18, 31.26, 21.10; **IR ATR (ν_{max}/cm^{-1})** 2961 (O-H), 2872 (C-H), 1610 (C=C), 1308 (C-O), 1023 (C-H), 901 (C-H arom); **HRMS (ESI-TOF)** $[M + Na]^+$ calc. 411.1701, found 411.1732.

Die approbierte gedruckte Originalversion dieser Dissertation ist an der TU Wien Bibliothek verfügbar.
The approved original version of this doctoral thesis is available in print at TU Wien Bibliothek.

4. Synthesis of the Hantzsch ester

Diethyl 2,6-dimethyl-1,4-dihydropyridine-3,5-dicarboxylate [16]



Compound was prepared by the following modified literature procedure.

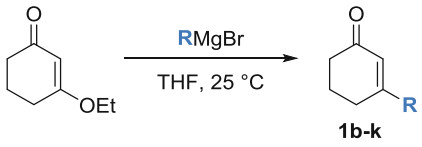
A mixture of formaldehyde (37% aqueous solution, 4.0 g, 49 mmol, 1.0 equiv.), NH_4OAc (7.6 g, 99 mmol, 2.0 equiv.), ethyl acetoacetate (26 g, 0.2 mol, 4.0 equiv.) and distilled H_2O (100 mL) was refluxed at 90°C for 18 h. After cooling the reaction mixture to room temperature, cold distilled H_2O (100 mL) was added, the crude product was filtered off, washed with cold distilled H_2O (100 mL) and dried in vacuo. Recrystallization from MeOH gave the product as a yellow solid (7.5 g, 60%). **^{1}H NMR (400 MHz, $CDCl_3$) δ** 5.19 (s, 1H, N*H*), 4.16 (q, *J* = 7.1 Hz, 4H, 2 × C*H*$_2$-O), 3.26 (s, 2H, C*H*$_2$), 2.19 (s, 6H, 2 × C*H*$_3$), 1.28 (t, *J* = 7.1 Hz, 6H, 2 × C*H*$_3$-CH$_2$-O).

Die approbierte gedruckte Originalversion dieser Dissertation ist an der TU Wien Bibliothek verfügbar.
The approved original version of this doctoral thesis is available in print at TU Wien Bibliothek.

5. Synthesis of ATH substrates

3-Methyl-2-cyclohexenone, 3-methyl-cyclopentenone and isophorone have been purchased from commercial supplier (*Sigma Aldrich*).

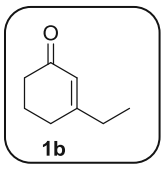
The remaining 3-alkylcyclohexenones and 3-arylcyclohexanones have been prepared by the following procedure, starting from 3-ethoxycyclohexenone (*Acros Organics*): [17]



1b-k

A 3 M solution of the Grignard reagent was prepared freshly from freshly ground Mg (1.0 equiv.), alkyl/aryl bromide (1.0 equiv.) in dry THF, and it was refluxed for 1 h. After being cooled to 0°C, 3-ethoxycyclohexenone (1.0 equiv.) was added slowly and the reaction mixture was stirred for 18 h at room temperature. The reaction was quenched with 1 N HCl solution (50 mL) at 0°C. Et_2O was added and the organic phase was washed with 1 N HCl solution (3 × 25 mL), sat. $NaHCO_3$ (3 × 25 mL), dried over anhydrous Na_2SO_4 and concentrated under reduced pressure. The crude products were purified by column chromatography (Et_2O: PE, UV TLC visualization) to provide the pure products.

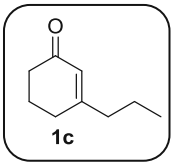
3-Ethyl-2-cyclohexenone [18]



1b

Column chromatography (25% Et_2O in PE) afforded the product as a yellow oil (67% yield). **^{1}H NMR (400 MHz, $CDCl_3$) δ** 5.87 (s, 1H, C*H*), 2.45 – 2.11 (m, 6H, CH_2-CO, CH_2-CH_2-CO, CH_2-C-ethyl), 2.07 – 1.81 (m, 2H, CH_2-CH_3), 1.09 (t, *J* = 7.4 Hz, 3H, CH_3).

3-Propyl-2-cyclohexenone [19]

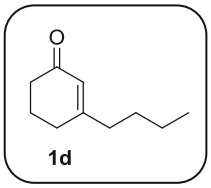


1c

Column chromatography (25% Et_2O in PE) afforded the product as a yellow oil (60% yield). **^{1}H NMR (400 MHz, $CDCl_3$) δ** 5.87 (s, 1H, C*H*), 2.53 – 2.07 (m, 6H, CH_2-CO, CH_2-CH_2-CO, CH_2-C-propyl), 2.07 – 1.73 (m, 2H, CH_2-CH_2-CH_3), 1.68 – 1.36 (m, 2H, CH_2-CH_3), 0.93 (t, *J* = 7.4 Hz, 3H, CH_3).

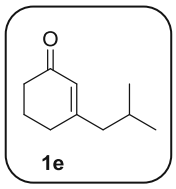
Die approbierte gedruckte Originalversion dieser Dissertation ist an der TU Wien Bibliothek verfügbar.
The approved original version of this doctoral thesis is available in print at TU Wien Bibliothek.

3-Butyl-2-cyclohexenone [20]



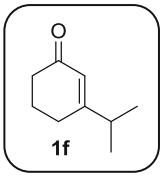
Column chromatography (30% Et_2O in PE) afforded the product as a yellow oil (74% yield). **^{1}H NMR (400 MHz, $CDCl_3$) δ** 5.86 (s, 1H, C*H*), 2.48 – 2.09 (m, 6H, CH_2-CO, CH_2-CH_2-CO, CH_2-C-butyl), 2.06 – 1.79 (m, 2H, CH_2-CH_2-CH_2-CH_3), 1.61 – 1.15 (m, 4H, CH_2-CH_2-CH_3), 0.91 (t, *J* = 7.0 Hz, 3H, CH_3).

3-Isobutyl-2-cyclohexenone [21]



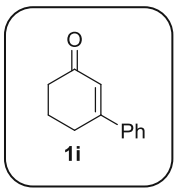
Column chromatography (25% Et_2O in PE) afforded the product as a yellow oil (69% yield). **^{1}H NMR (400 MHz, $CDCl_3$) δ** 5.84 (s, 1H, C*H*), 2.54 – 2.17 (m, 4H, CH_2-CO, CH_2-CH_2-CO), 2.18 – 1.56 (m, 5H, CH_2-C-isobutyl, CH_2-CH$(CH_3)_2$, CH_2-C*H*$(CH_3)_2$), 0.90 (d, *J* = 6.5 Hz, 6H, 2 × CH_3-CH).

3-Isopropyl-2-cyclohexenone [22]



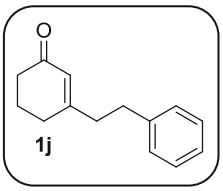
Column chromatography (25% Et_2O in PE) afforded the product as a yellow oil (10% yield). **^{1}H NMR (400 MHz, $CDCl_3$) δ** 5.88 (s, 1H, C*H*), 2.61 – 2.17 (m, 5H, CH_2-CO, CH_2-CH_2-CO, C*H*-$(CH_3)_2$), 2.13 – 1.81 (m, 2H, CH_2-C-isopropyl), 1.10 (d, *J* = 6.9 Hz, 6H, 2 × CH_3-CH).

3-Phenyl-2-cyclohexenone [23]



Column chromatography (30% Et_2O in PE) afforded the product as a white solid (88% yield). **^{1}H NMR (400 MHz, $CDCl_3$) δ** 7.53 – 7.41 (m, 5H, *H*-arom), 6.42 (s, 1H, C*H*), 2.85 – 2.78 (m, 2H, CH_2-CO), 2.62 – 2.49 (m, 2H, CH_2-CH_2-CO), 2.18 – 2.14 (m, 2H, CH_2-C-phenyl).

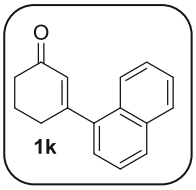
3-Phenethyl-2-cyclohexenone [24]



The formation of the grignard-reagent and the reaction have been carried out at 40°C. Column chromatography (30% Et_2O in PE) afforded the product as a light yellow oil (91% yield). **^{1}H NMR (200 MHz, $CDCl_3$) δ** 7.34 – 7.15 (m, 5H, *H*-arom), 5.90 (s, 1H, C*H*), 2.89 – 2.76 (m, 2H, CH_2-CO), 2.58 – 2.47 (m, 2H, CH_2-CH_2-CO), 2.40 – 2.26 (m, 4H, phenyl-CH_2-CH_2) 2.05 – 1.92 (m, 2H, CH_2-C-phenyl).

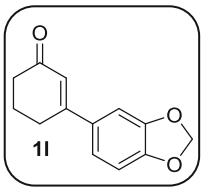
Die approbierte gedruckte Originalversion dieser Dissertation ist an der TU Wien Bibliothek verfügbar.
The approved original version of this doctoral thesis is available in print at TU Wien Bibliothek.

3-(Naphtalen-1-yl)-2-cyclohexenone [25]



Column chromatography (30% - 50% Et_2O in PE) afforded the product as a yellow oil (94% yield). **^{1}H NMR (200 MHz, $CDCl_3$) δ** 7.92 – 7.82 (m, 3H, *H*-arom), 7.54 – 7.45 (m, 3H, *H*-arom), 7.35 – 7.28 (m, 1H, *H*-arom), 6.21 (s, 1H, C*H*), 2.82 – 2.74 (m, 2H, CH_2-CO), 2.64 – 2.56 (m, 2H, CH_2-CH_2-CO), 2.33 – 2.19 (m, 2H, CH_2-C-arom).

3-Piperonyl-2-cyclohexenone [26]



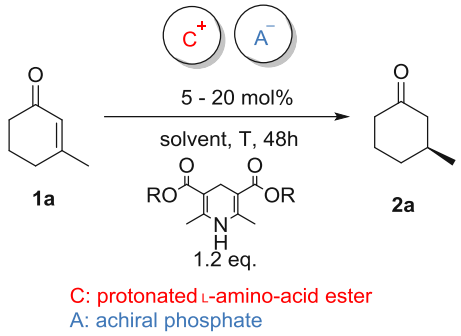
Column chromatography (30% Et_2O in PE) afforded the product as a yellow foam (90% yield). **^{1}H NMR (200 MHz, $CDCl_3$) δ** 7.06 (ddd, *J* = 8.0 Hz, 4.0 Hz, 2.0 Hz, 2H, *H*-arom), 6.83 (d, *J* = 8.0 Hz, 1H, *H*-arom), 6.33 (s, 1H, C*H*), 6.01 (s, 2H, OCH_2), 2.76 – 2.67 (t, *J* = 6.0 Hz, 2H, CH_2-CO), 2.50 – 2.41 (t, *J* = 6.0 Hz, 2H, CH_2-CH_2-CO), 2.19 – 2.06 (m, 2H, CH_2-C-arom).

Die approbierte gedruckte Originalversion dieser Dissertation ist an der TU Wien Bibliothek verfügbar.
The approved original version of this doctoral thesis is available in print at TU Wien Bibliothek.

6. General procedure and optimization of the ATH reactions

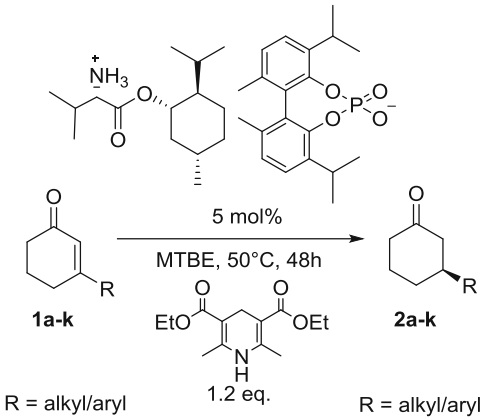
6.1 General procedures

General procedure for parameter optimization



An 8 mL screw cap vial equipped with a magnetic stir bar was charged with 3-methylcyclohexenone (0.18 mmol, 1.0 equiv.) in the appropriate solvent (0.55 mL, 0.33 M), followed by the addition of the catalyst (0.009 – 0.036 mmol, 5 mol% – 20 mol%) and the appropriate Hantzsch ester (0.22 mmol, 1.2 equiv.). The reaction mixture was stirred at the given temperature for 48 h. The conversion and yield have been determined by GC measurement by using *n*-dodecane as internal standard, while chiral GC have been used to determine the enantiomeric excess.

General procedure for scope and limitations



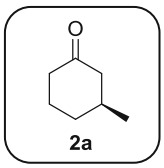
A 20 mL microwave vial equipped with a magnetic stir bar was charged with ketone (1.8 mmol, 1.0 equiv.) in MTBE (5.5 mL, 0.33 M), followed by the addition of the catalyst (55.4 mg, 0.09 mmol, 5 mol%) and Hantzsch ester (552 mg, 2.2 mmol, 1.2 equiv.). The reaction mixture was stirred at 50°C for 48 h. After cooling to room temperature, Et_2O (5 mL) and 4 M HCl (10 mL) was added and the mixture was stirred until the phases were transparent (30 min). The phases were separated and the organic phase

Die approbierte gedruckte Originalversion dieser Dissertation ist an der TU Wien Bibliothek verfügbar.
The approved original version of this doctoral thesis is available in print at TU Wien Bibliothek.
TU Bibliothek Your knowledge hub WIEN

was washed with 4 M HCl (3 × 20 mL). The organic phase was dried over Na_2SO_4 and concentrated under reduced pressure. Purification by column chromatography (Et_2O: PE, vanillin staining agent or UV visualization) gave the 3-substituted cyclohexanones.

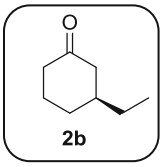
6.2 Analytical data of ATH products

(S)-3-Methylcyclohexanone



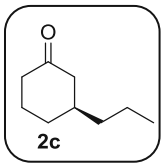
Column chromatography (25% Et_2O in PE) afforded the product as a colorless oil. GC yield: 98%, isolated yield: 72% due to high volatility, 95% ee. $[\alpha]_D^{20}$: −11.1 (c = 1.0, $CHCl_3$); **^{1}H NMR (400 MHz, $CDCl_3$) δ** 2.41 – 2.21 (m, 3H), 2.09 – 1.82 (m, 4H), 1.76 – 1.57 (m, 1H), 1.42 – 1.24 (m, 1H), 1.02 (d, *J* = 6.4 Hz, 3H). **Determination of the enantiomeric excess** BGB175 column (85°C isotherm 20 min, 30°C/min to 220°C): t_R (*S*) = 9.0 min, t_R (*R*) = 9.6 min.

(S)-3-Ethylcyclohexanone



Column chromatography (25% Et_2O in light petrol) afforded the product as a colorless oil. GC yield: 85%, isolated yield: 76% due to high volatility, 92% ee. $[\alpha]_D^{20}$: −15.6 (c = 1.0, $CHCl_3$); **^{1}H NMR (400 MHz, $CDCl_3$) δ** 2.45 – 2.23 (m, 3H), 2.09 – 1.87 (m, 3H), 1.76 – 1.63 (m, 2H), 1.41 – 1.28 (m, 3H), 0.91 (t, *J* = 7.5 Hz, 3H). **Determination of the enantiomeric excess** BGB173 column (52°C isotherm 110 min, 30°C/min to 220°C): t_R (*R*) = 51.0 min, t_R (*S*) = 54.9 min.

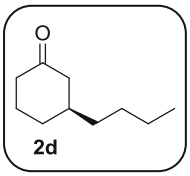
(S)-3-Propylcyclohexanone



Column chromatography (25% Et_2O in PE) afforded the product as a colorless oil. GC yield: 70%, isolated yield: 55% due to high volatility, 91% ee. $[\alpha]_D^{20}$: −14.7 (c = 1.0, $CHCl_3$); **^{1}H NMR (400 MHz, $CDCl_3$) δ** 2.42 – 2.22 (m, 3H), 2.06 – 1.86 (m, 3H), 1.80 – 1.74 (m, 1H), 1.67 – 1.59 (m, 1H), 1.35 – 1.26 (m, 5H), 0.92 – 0.86 (m, 3H). **Determination of the enantiomeric excess** BGB175 column (70°C isotherm 60 min, 1°C/min to 150 °C, 5 min at 150°C, 30°C /min to 220°C): t_R (*S*) = 50.6 min, t_R (*R*) = 53.1 min.

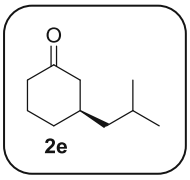
Die approbierte gedruckte Originalversion dieser Dissertation ist an der TU Wien Bibliothek verfügbar.
The approved original version of this doctoral thesis is available in print at TU Wien Bibliothek.

(S)-3-Butylcyclohexanone



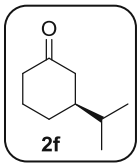
Column chromatography (25% Et_2O in PE) afforded the product as a colorless oil. GC yield: 91%, isolated yield: 87%, 93% ee. $[\alpha]_D^{20}$: −15.0 (c = 1.0, $CHCl_3$); **^{1}H NMR (400 MHz, $CDCl_3$) δ** 2.44 – 1.56 (m, 7H), 1.40 – 1.09 (m, 7H), 0.91 – 0.82 (m, 4H). **Determination of the enantiomeric excess** BGB175 column (70 °C isotherm 60 min, 1°C/min to 150°C, 5 min at 150°C, 30 °C /min to 220°C): t_R (*S*) = 76.9 min, t_R (*R*) = 78.1 min.

(S)-3-Isobutylcyclohexanone



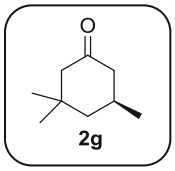
Column chromatography (25% Et_2O in PE) afforded the product as a colorless oil. GC yield: 85%, isolated yield: 60% due to high volatility, 86% ee. $[\alpha]_D^{20}$: −11.3 (c = 1.0, $CHCl_3$); **^{1}H NMR (400 MHz, $CDCl_3$) δ** 2.42 – 2.21 (m, 2H), 2.03 – 1.61 (m, 4H), 1.66 – 1.41 (m, 2H), 1.33 – 1.10 (m, 3H), 0.89 – 0.84 (m, 6H). **Determination of the enantiomeric excess** BGB175 column (70 °C isotherm 5 min, 0.5 °C/min to 110°C, 5 min at 110°C, 30°C /min to 220°C): t_R (*R*) = 39.2 min, t_R (*S*) = 40.7 min.

(S)-3-Isopropylcyclohexanone



Column chromatography (25% Et_2O in PE) afforded the product as a colorless oil. GC yield: 75%, isolated yield: 68% due to high volatility, 88% ee. $[\alpha]_D^{20}$: −12.4 (c = 1.0, $CHCl_3$); **^{1}H NMR (400 MHz, $CDCl_3$) δ** 2.44 – 1.23 (m, 10H), 0.92 (d, *J* = 6.0 Hz, 3H), 0.90 (d, *J* = 6.0 Hz, 3H). **Determination of the enantiomeric excess** BGB175 column (85°C isotherm 20 min, 30°C/min to 220°C): t_R (*R*) = 20.75 min, t_R (*S*) = 20.96 min.

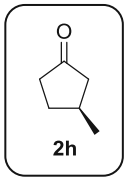
(S)-3,5,5-Trimethylcyclohexanone



Column chromatography (25% Et_2O in PE) afforded the product as a colorless oil. GC yield: 66%, isolated yield: 60% due to high volatility, 92% ee. $[\alpha]_D^{20}$: −11.9 (c = 1.0, $CHCl_3$); **^{1}H NMR (400 MHz, $CDCl_3$) δ** 2.33 – 2.14 (m, 2H), 1.92 – 1.83 (m, 3H), 1.60 – 1.56 (m, 1H), 1.38 – 1.25 (m, 2H), 1.05 – 1.01 (m, 5H), 0.88 (s, 3H). **Determination of the enantiomeric excess** BGB175 column (85°C isotherm 20 min, 30°C/min to 220°C): t_R (*S*) = 13.4 min, t_R (*R*) = 17.9 min.

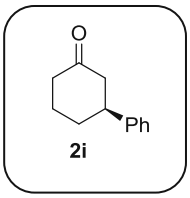
Die approbierte gedruckte Originalversion dieser Dissertation ist an der TU Wien Bibliothek verfügbar.
The approved original version of this doctoral thesis is available in print at TU Wien Bibliothek.

(S)-3-Methylcyclopentanone



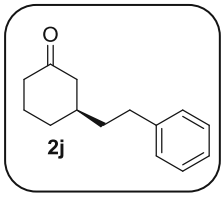
Column chromatography (25% Et_2O in PE) afforded the product as a colorless oil. GC yield: 94%, isolated yield: 80% due to high volatility, 89% ee. $[\alpha]_D^{20}$: −13.2 (c = 1.0, $CHCl_3$); **^{1}H NMR (200 MHz, $CDCl_3$) δ** 3.22 – 2.70 (m, 1H), 2.51 – 1.81 (m, 5H), 1.32 – 1.29 (m, 1H), 1.11 – 1.02 (m, 3H). **Determination of enantiomeric excess** BGB175 column (85°C isotherm 20 min, 30°C/min to 220°C): t_R (*S*) = 8.1 min, t_R (*R*) = 8.5 min.

(S)-3-Phenylcyclohexanone



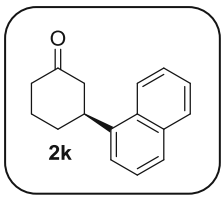
Column chromatography (25% Et_2O in light petrol) afforded the product as a colorless oil. GC yield: 86%, isolated yield: 84%, 82% ee. $[\alpha]_D^{20}$: −17.2 (c = 1.0, $CHCl_3$); **^{1}H NMR (200 MHz, $CDCl_3$) δ** 7.39 – 7.37 (m, 2H), 7.32 – 7.27 (m, 3H), 3.11 – 3.00 (m, 1H), 2.68 – 2.44 (m, 4H), 2.23 – 2.15 (m, 2H), 1.93 – 1.81 (m, 2H). **Determination of the enantiomeric excess** BGB175 column (120°C isotherm 55 min, 30°C /min to 220°C): t_R (*R*) = 48.8 min, t_R (*S*) = 49.5 min.

(S)-3-Phenethylcyclohexanone



Column chromatography (25% Et_2O in light petrol) afforded the product as a colorless oil. GC yield: 94%, isolated yield: 91%, 90% ee. **^{1}H NMR (200 MHz, $CDCl_3$) δ** 7.37 – 7.22 (m, 5H), 2.75 – 2.33 (m, 5H), 2.14 – 1.70 (m, 7H), 1.49 – 1.38 (m, 1H). **Determination of the enantiomeric excess** Chiralcel Diacel AS-H column (*n*-heptane/*i*-PrOH 97/3 V/V%, 1 mL/min, 25˚C, λ = 220 nm): t_R (*R*) = 15.6 min, t_R (*S*) = 16.6 min.

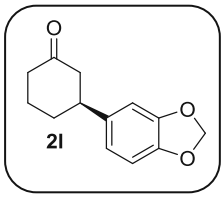
(S)-3-(Naphtalen-1-yl)cyclohexanone



Column chromatography (25% Et_2O in light petrol) afforded the product as a colorless oil. GC yield: 65%, isolated yield: 62%, 94% ee. $[\alpha]_D^{20}$: −49.2 (c = 1.0, $CHCl_3$); **^{1}H NMR (200 MHz, $CDCl_3$) δ** 8.05 – 7.75 (m, 3H), 7.54 – 7.38 (m, 4H), 3.92 – 3.82 (m, 1H), 2.75 – 1.94 (m, 8H). **Determination of the enantiomeric excess** Chiracel Diacel AS-H column (*n*-heptane/*i*-PrOH 95/5 V/V%, 1mL/min, 25˚C, λ = 220 nm): t_R (*R*) = 13.8 min, t_R (*S*) = 22.7 min.

Die approbierte gedruckte Originalversion dieser Dissertation ist an der TU Wien Bibliothek verfügbar.
The approved original version of this doctoral thesis is available in print at TU Wien Bibliothek.
TU Bibliothek Your knowledge hub WIEN

(S)-3-Piperonycyclohexanone

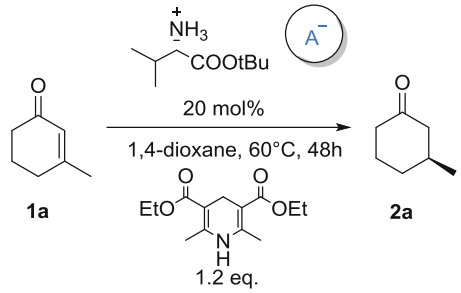


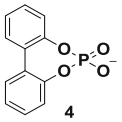
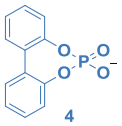
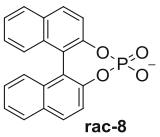
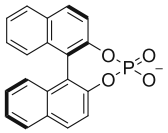
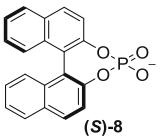
Column chromatography (25% Et_2O in light petrol) afforded the product as a colorless oil. GC yield: 65%, isolated yield: 62%, 94% ee. $[\alpha]_D^{20}$**:** -15.3 (c = 1, $CHCl_3$); **^{1}H NMR (200 MHz, $CDCl_3$) δ** 6.74 – 6.63 (m, 3H), 5.93 (s, 2H), 2.98 – 2.87 (m, 2H), 2.54 – 2.39 (m, 4H), 2.17 – 2.02 (m, 2H), 1.83 – 1.73 (m, 2H). **Determination of enantiomeric excess** Chiralcel Diacel AS-H column (*n*-heptane/*i*-PrOH 85/15 V/V%, 1 mL/min, 25˚C, λ = 220 nm): t_R (*S*) = 23.5 min, t_R (*R*) = 28.0 min.

Die approbierte gedruckte Originalversion dieser Dissertation ist an der TU Wien Bibliothek verfügbar.
The approved original version of this doctoral thesis is available in print at TU Wien Bibliothek.

6.3 Optimization of reaction conditions

Table S1.: Proof of concept in 1,4-dioxane

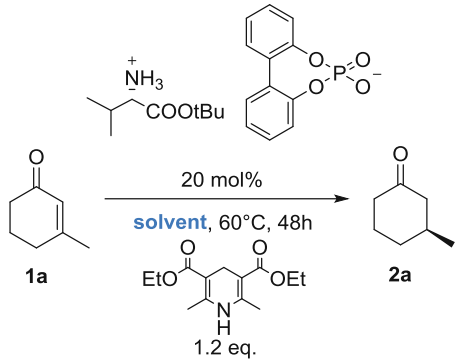


Entry[a]	Counteranion	Yield[b] [%]	ee[c] [%]	Δee[d] [%]
1		49	54 (*S*)	-
2		49	54 (*S*)	-
3	 **4**	**27**	**64 (*S*)**	**+ 10**
4[e]	 **4**	**72**	**74 (*S*)**	**+ 23**
5	 **rac-8**	13	54 (*S*)	0
6	 **(*R*)-8**	13	54 (*S*)	0
7	 **(*S*)-8**	15	54 (*S*)	0

[a] Performed with 0.18 mmol 3-methyl-2-cyclohexenone, 0.036 mmol catalyst, 0.22 mmol Hantzsch ethyl ester in 0.55 mL 1,4-dioxane at 60°C for 48 hours. [b] Determined by GC analysis using *n*-dodecane as internal standard. [c] Determined by chiral GC analysis using a BGB175 chiral capillary column. Absolute configurations have been determined by measuring the optical rotation and comparing with literature data. [d] ee difference compare to the reaction with TFA counteranion. [e] MTBE was used as solvent.

Die approbierte gedruckte Originalversion dieser Dissertation ist an der TU Wien Bibliothek verfügbar.
The approved original version of this doctoral thesis is available in print at TU Wien Bibliothek.
TU Bibliothek Your knowledge hub WIEN

Table S2.: Solvent screening

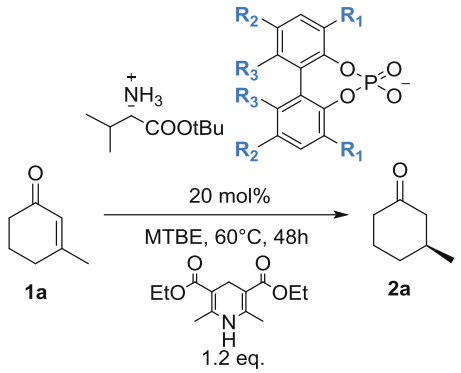


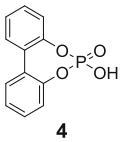
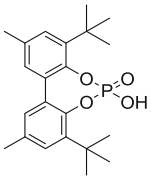
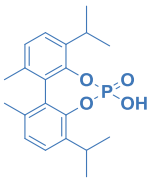
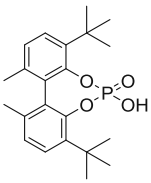
Entry[a]	Solvent	Yield[b] [%]	ee[c] [%]
1	EtOAc	48	67 (*S*)
2	BuOAc	41	62 (*S*)
3	THF	60	68 (*S*)
4	1,4-Dioxane	27	64 (*S*)
5	**MTBE**	**72**	**74 (*S*)**
6	Bu_2O	16	62 (*S*)
7	Toluene	17	75 (*S*)
8	$CHCl_3$	23	53 (*S*)
9	H_2O	9	42 (*S*)
10	MeOH	10	30 (*S*)
11	EtOH	20	50 (*S*)
12	^{i}PrOH	26	57 (*S*)
13	^{t}BuOH	30	60 (*S*)
14	Acetonitrile	17	37 (*S*)

[a] Performed with 0.18 mmol 3-methyl-2-cyclohexenone, 0.036 mmol catalyst, 0.22 mmol Hantzsch ethyl ester in 0.55 mL solvent at 60°C for 48 hours. [b] Determined by GC analysis using *n*-dodecane as internal standard. [c] Determined by chiral GC analysis using a BGB175 chiral capillary column. Absolute configurations have been determined by measuring the optical rotation and comparing with literature data.

Die approbierte gedruckte Originalversion dieser Dissertation ist an der TU Wien Bibliothek verfügbar.
The approved original version of this doctoral thesis is available in print at TU Wien Bibliothek.

Table S3.: Phosphoric acid screening

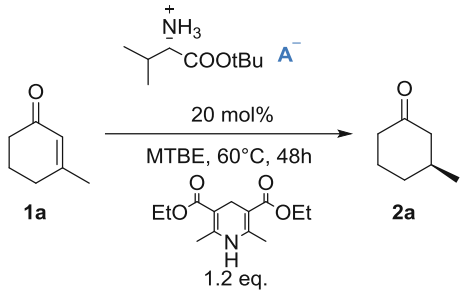


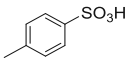
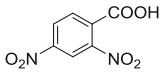
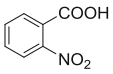
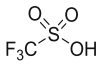
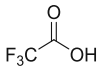
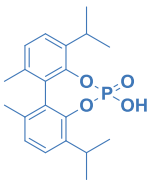
Entry[a]	Phosphoric acid	Yield[b] [%]	ee[c] [%]
1	 **4**	72	74 (*S*)
2	 **5**	70	77 (*S*)
3	 **6**	**94**	**80 (*S*)**
4	 **7**	43	76 (*S*)

[a] Performed with 0.18 mmol 3-methyl-2-cyclohexenone, 0.036 mmol catalyst, 0.22 mmol Hantzsch ethyl ester in 0.55 mL MTBE at 60°C for 48 hours. [b] Determined by GC analysis using *n*-dodecane as internal standard. [c] Determined by chiral GC analysis using a BGB175 chiral capillary column. Absolute configurations have been determined by measuring the optical rotation and comparing with literature data.

Die approbierte gedruckte Originalversion dieser Dissertation ist an der TU Wien Bibliothek verfügbar.
The approved original version of this doctoral thesis is available in print at TU Wien Bibliothek.

Table S4.: Comparison of selectivity by screening other acids

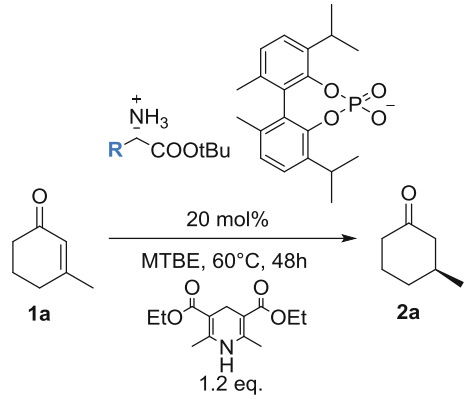


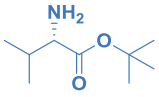
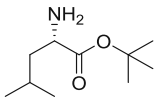
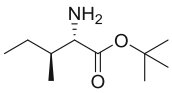
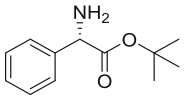
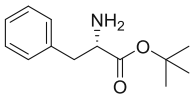
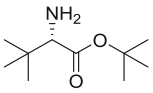
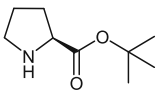
Entry[a]	Acid	Yield[b] [%]	ee[c] [%]
1		34	58 (*S*)
2		91	37 (*S*)
3		93	45 (*S*)
4		45	55 (*S*)
5		40	52 (*S*)
6		88	51 (*S*)
7	 **6**	**94**	**80 (*S*)**

[a] Performed with 0.18 mmol 3-methyl-2-cyclohexenone, 0.036 mmol catalyst, 0.22 mmol Hantzsch ethyl ester in 0.55 mL MTBE at 60°C for 48 hours. [b] Determined by GC analysis using *n*-dodecane as internal standard. [c] Determined by chiral GC analysis using a BGB175 chiral capillary column. Absolute configurations have been determined by measuring the optical rotation and comparing with literature data.

Die approbierte gedruckte Originalversion dieser Dissertation ist an der TU Wien Bibliothek verfügbar.
The approved original version of this doctoral thesis is available in print at TU Wien Bibliothek.

Table S5: L-Amino acid screening

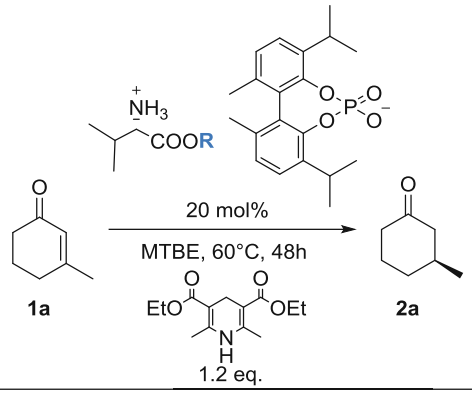


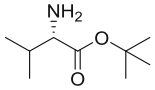
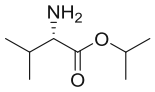
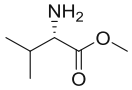
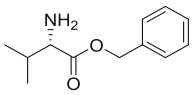
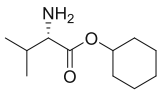
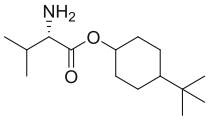
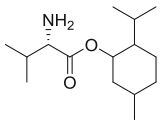
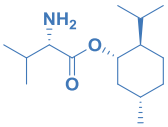
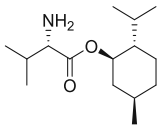
Entry[a]	L-amino acid	Yield[b] [%]	ee[c] [%]
1		**94**	**80 (*S*)**
2		52	77 (*S*)
3		73	72 (*S*)
4		55	9 (*S*)
5		83	60 (*S*)
6		91	76 (*S*)
7		73	33 (S)

[a] Performed with 0.18 mmol 3-methyl-2-cyclohexenone, 0.036 mmol catalyst, 0.22 mmol Hantzsch ethyl ester in 0.55 mL MTBE at 60°C for 48 hours. [b] Determined by GC analysis using *n*-dodecane as internal standard. [c] Determined by chiral GC analysis using a BGB175 chiral capillary column. Absolute configurations have been determined by measuring the optical rotation and comparing with literature data.

Die approbierte gedruckte Originalversion dieser Dissertation ist an der TU Wien Bibliothek verfügbar.
The approved original version of this doctoral thesis is available in print at TU Wien Bibliothek.

Table S6: Ester screening

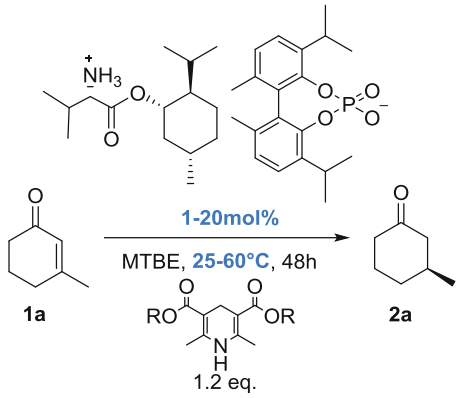


Entry[a]	L-valine ester	Yield[b] [%]	ee[c] [%]
1		94	80 (*S*)
2		90	76 (*S*)
3		70	57 (*S*)
4		95	50 (*S*)
5		92	74 (*S*)
6		94	73 (*S*)
7		98	85 (*S*)
8		**98**	**93 (*S*)**
9		98	82 (*S*)

[a] Performed with 0.18 mmol 3-methyl-2-cyclohexenone, 0.036 mmol catalyst, 0.22 mmol Hantzsch ethyl ester in 0.55 mL MTBE at 60°C for 48 hours. [b] Determined by GC analysis using *n*-dodecane as internal standard. [c] Determined by chiral GC using a BGB175 chiral capillary column. Absolute configurations have been determined by measuring the optical rotation and comparing with literature data.

Die approbierte gedruckte Originalversion dieser Dissertation ist an der TU Wien Bibliothek verfügbar.
The approved original version of this doctoral thesis is available in print at TU Wien Bibliothek.

Table S7: Screening of catalyst loading and temperature

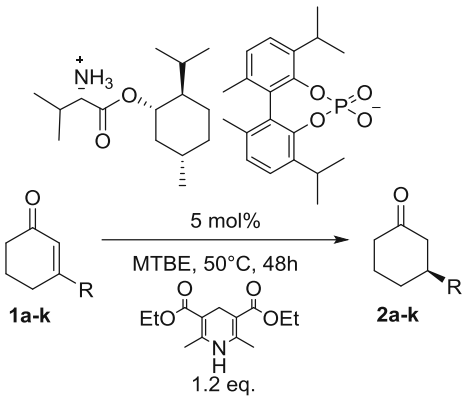


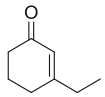
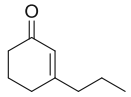
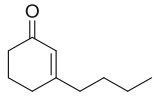
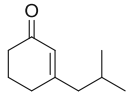
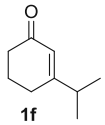
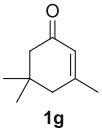
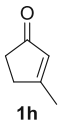
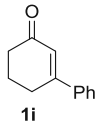
Entry[a]	Temperature	Catalyst loading [mol%]	Hantzsch ester	Yield[b] [%]	ee[c] [%]
1	60	20	ethyl	98	93 (*S*)
2	50	20	ethyl	98	95 (*S*)
3	40	20	ethyl	96	95 (*S*)
4	25	20	ethyl	59	96 (*S*)
5	25	10	ethyl	43	96 (*S*)
6	25	5	ethyl	29	96 (*S*)
7	25	1	ethyl	11	96 (*S*)
8	50	10	ethyl	99	94 (*S*)
9	**50**	**5**	**ethyl**	**98**	**95 (*S*)**
10	50	1	ethyl	68	93 (*S*)
11[d]	25	20	methyl	14	83 (*S*)
12[d]	25	20	ethyl	17	88 (*S*)
13[d]	25	20	*i*-propyl	58	69 (*S*)
14[d]	25	20	*t*-butyl	58	67 (*S*)

[a] Performed with 0.18 mmol 3-methyl-2-cyclohexenone, 0.009-0.036 mmol catalyst, 0.22 mmol Hantzsch ester in 0.55 mL MTBE at the given temperature for 48 hours. [b] Determined by GC analysis using *n*-dodecane as internal standard. [c] Determined by chiral GC analysis using a BGB175 chiral capillary column. Absolute configurations have been determined by measuring the optical rotation and comparing with literature data. [d] Performed with (L)-valine *t*-butyl ester instead of (L)-valine (+)-(1*R*,3*R*,4*S*) menthyl ester.

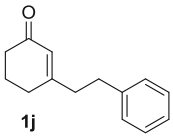
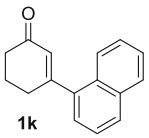
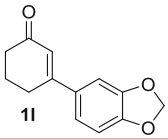
Die approbierte gedruckte Originalversion dieser Dissertation ist an der TU Wien Bibliothek verfügbar.
The approved original version of this doctoral thesis is available in print at TU Wien Bibliothek.

6.4 Reaction scope and limitations



Entry[a]	Substrate	Yield[d] [%]	ee[e] [%]
1	 1a	98 (72)[f]	95 (*S*)
2	 1b	85 (76)[f]	92 (*S*)
3	 1c	70 (55)[f]	91 (*S*)
4	 1d	91 (87)	93 (*S*)
5	 1e	85 (60)[f]	86 (*S*)
6	 1f	75 (68)[f]	88 (*S*)
7[b]	 1g	66 (60)	92 (*S*)
8[c]	 1h	94 (80)[f]	89 (*S*)
9	 1i	86 (84)	82 (*S*)

Die approbierte gedruckte Originalversion dieser Dissertation ist an der TU Wien Bibliothek verfügbar.
The approved original version of this doctoral thesis is available in print at TU Wien Bibliothek.

10	 1j	94 (91)	90 (*S*)
11	 1k	65 (62)	94 (*S*)
12	 1l	89 (86)	70 (*S*)

[a] Performed with 1.8 mmol ketone, 5 mol% catalyst and 2.2 mmol Hantzsch ethyl ester in 5.5 mL MTBE at 50°C for 48 h. [b] 20 mol% catalyst. [c] 10 mol% catalyst. [d] Determined by GC or GC-MS analysis. Isolated yields after flash column chromatography are given in parenthesis. [e] Determined by chiral GC analysis using a BGB175 or BGB173 chiral capillary column, or by chiral HPLC analysis using a Diacel Chiralcel AS-H column. Absolute configurations have been determined by measuring the optical rotation and comparing with literature data. [f] Lower isolated yield because of high volatility of the product.

Die approbierte gedruckte Originalversion dieser Dissertation ist an der TU Wien Bibliothek verfügbar.
The approved original version of this doctoral thesis is available in print at TU Wien Bibliothek.

7. Computational studies

7.1 Quantummechanical calculation of rotational barriers

7.1.1 Choice of method and basis set

Although several studies on the calculation of rotational barriers in substituted biphenyls have been published[27,28,29], the only systematic protocol so far has been established by Masson.[30] A key finding of Masson's study is that for accurate barrier energies, inclusion of vibrational corrections is crucial. Since frequency computations as well as transition state optimizations for molecules as large as the substituted phosphoric acids can become quite expensive, a compromise between accuracy and efficiency is necessary in terms of the method.

The popular as well as efficient B3LYP functional[31] has been shown to perform well for the estimation of rotational barriers for unsubstituted and substituted biphenyls[29,30,32].However, as also noted by Masson, empirical dispersion correction terms such as Grimme's DFT-D or DFT-D3[33,34] are necessary to obtain accurate energies with B3LYP, so we chose B3LYP-D3 as a functional. The correlation of the uniform electron gas in the B3LYP functional was modeled according to the Vosko-Wilk-Nusair VWN5 formalism.[35]

Since Masson achieved good results with DFT/def2-TZVPP[36], we tested both the single-polarized def2-TZVP and double-polarized def2-TZVPP set for compound **4**. Since energies on the B3LYP-D3 level of theory differed only by 0.07 kcal/mol between both basis sets, we chose the computationally cheaper def2-TZVP basis set. Summarizing, all geometry optimizations, energy evaluations and frequency calculations (at 333.15K) were performed on the B3LYP-D3/def2-TZVP level of theory. All computations were performed with ORCA.[37] For further validation of the method, we compared the B3LYP-D3/def2-TZVP electronic barrier energies of phosphoric acid **4** against single point electronic energies on the same geometry computed on the benchmark DLPNO-CCSD(T)/def2-QZVP[36,38] level of theory. Only a small energy difference of 0.28 kcal/mol could be observed.

Masson also addresses the role of solvent when computing rotational barriers. In all studies on the computation of biphenyl racemization barriers published so far, good agreement with experiment is achieved without the consideration of solvent effects. Possible justification can be found in a study by Graybill and Leffler[39], who found a compensation of enthalpy and entropy in different solvents. For a more detailed discussion, see References 30 and 39.

However, Masson emphasizes that solvent effects cannot be confidently neglected for negatively charged biphenyls. Since solvent effects and likely specific interactions with both solvent and cation

Die approbierte gedruckte Originalversion dieser Dissertation ist an der TU Wien Bibliothek verfügbar.
The approved original version of this doctoral thesis is available in print at TU Wien Bibliothek.

need to be considered when computing rotational barriers of the anionic forms of phosphoric acids **4**-**7**, the barrier of the corresponding anions will be the topic of more detailed future work.

7.1.2 Optimization of transition states

The systematic search for rotational transition states is not straightforward. Usually, fixing the torsional dihedral angle around the aryl-aryl bond to 0 degrees and optimizing this constrained structure yields good guesses for rotational transition states of substituted biphenyl.[30] The situation is trickier when the planar transition state is hindered by bulky ortho-substituents such as the isopropyl and tert-butyl groups in phosphoric acids **6** and **7**. For all phosphoric acids, we optimized the structure while fixing one of the dihedral angles to 0° and used the result as guesses for the transition state optimizations. In addition, for phosphoric acid **6** we performed a systematic transition state search with the nudged elastic band (NEB) method implemented in ORCA.[40,41] We also used the result of this NEB calculation to construct another transition state guess for phosphoric acid **7**. The imaginary frequencies of all transition states corresponded to an out-of-plane torsion of the phenyl rings.

For phosphoric acids **4** and **5**, fully planar transition states as depicted in Figure S1 are obtained when using the constrained structures as transition state guesses.

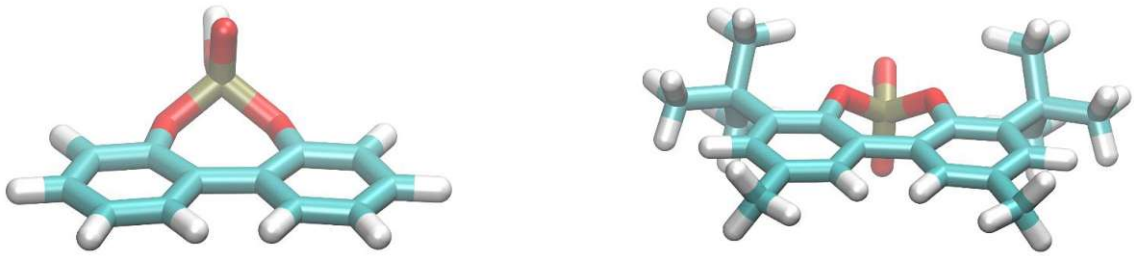


*Figure S1: Rotational transition states for phosphoric acids **4** and **5**.*

As already mentioned, compounds **6** and **7** have methyl groups in the 6,6'-position, which hinder the planar transition state. Instead, they adopt a conformation in which the aryl-aryl-bond is out-of-plane and the two rings roughly coplanar. This peculiar transition state geometry for ortho-substituted biphenyls has been anticipated by Baddeley as early as 1946.[42] Ling and Harris proposed the associated mechanism in 1964.[43] They suggested an asynchronous nature of the racemization, with 6,6'-groups passing over each other subsequently instead of synchronously, minimizing the barrier energy. The out-of-plane transition states as well as the asynchronous nature of the racemization has been confirmed by Masson's calculation.[30] The asynchronous mechanism is also visible in the case of both phosphoric acids **6** and **7**. By constraining different dihedral angles during pre-optimization, two different transition states can be obtained. The first transition state corresponds to passing of the methyl groups prior to

Die approbierte gedruckte Originalversion dieser Dissertation ist an der TU Wien Bibliothek verfügbar.
The approved original version of this doctoral thesis is available in print at TU Wien Bibliothek.

reaching the transition state, in the second transition state the ester oxygens of the phosphate groups have passed instead (Figure S2 and S3, left and right). No pathway is favored over the other, the electronic barriers of the two transition states for both phosphoric acid **6** and **7** only differ by 0.01 kcal/mol.

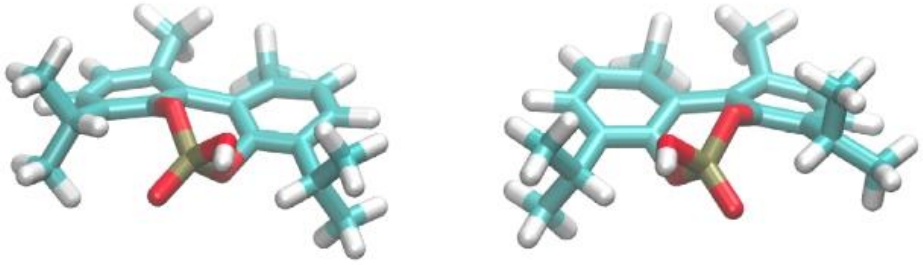


*Figure S2: Asynchronous transition states for phosphoric acid **6**.*

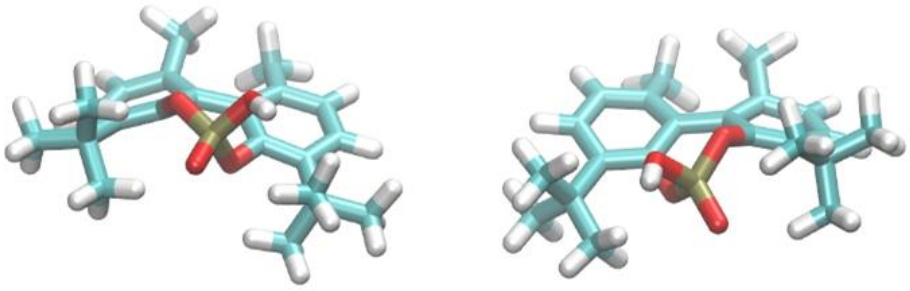


*Figure S3: Asynchronous transition states for phosphoric acid **7**.*

7.2 Molecular Dynamics Simulations

7.2.1 Simulation setup

Force fields for the anionic form of anion **6** and the iminium intermediate evolving from the L-valine (+)-(1*S*,2*R*,5*S*)-menthyl-cation were obtained from PARAMCHEM[44,45] without further modification. Since no force field for MTBE was available, we chose n-methylbutylether as a solvent. The solvent parameters were taken from the CGenFF force field[46]. Simulation boxes contained a single ion pair and 216 molecules of n-methylbutylether. To consider all possible isomers and stereisomers, both the (*E*)- and (*Z*)-form of the cation as well as both anion enantiomers were considered, yielding four different systems (see Table S8.). 10 replica simulations of every system were conducted under the following conditions: All simulations were performed with the program package CHARMM.[47] Initial configurations were created with PACKMOL.[48] All simulations were conducted in the NpT ensemble

Die approbierte gedruckte Originalversion dieser Dissertation ist an der TU Wien Bibliothek verfügbar.
The approved original version of this doctoral thesis is available in print at TU Wien Bibliothek.
TU Bibliothek Your knowledge hub WIEN

and employed the CHARMM CPT algorithm, the leapfrog integrator and the Hoover thermostat. A temperature of 330 K, a pressure of 1 atm and a non-bonded cutoff of 11 Å were used. Electrostatics were treated using the Particle Mesh Ewald method, with a grid size of approximately 1 Å, cubic splines of order 6 and a K of 0.41 $Å^{-1}$. The SHAKE algorithm was employed to fix the length of bonds to hydrogens.

Boxes were first equilibrated for 2 ns using a timestep of 1 fs, followed by production simulations of at least 38 ns (see Table S8 for system details) under the same conditions. Coordinates were written to disk every 250 steps.

Table S8: Overview over all four simulated systems.

System number	Cation-Isomer	Anion-Isomer	Average boxsize [A]	Number of replica	Simulation time per replica [ns]
1	Z	R	36.1	10	38
2	Z	S	36.1	10	58
3	E	R	36.1	10	38
4	E	S	36.1	10	78

For trajectory analysis, the MDAnalysis library[49] as well as self-written python code was used. Plots were created with R (ggplot).[50] Hydrogen bonds were analyzed using CHARMM and a cutoff distance of 2.4 Å and a cutoff angle of 135°. Every 10^{th} step of the trajectory was considered in the analysis.

7.2.2 Statistical considerations

To ensure statistical convergence of the simulations, several measures were taken. For both cation isomers (E and Z) 10 different conformers opimized for RMSD diversity were generated using a genetic algorithm implemented in OpenBabel. [51] Sampling of anion conformations was not done due to the structural rigidity of the anion. For each of the 10 replica/systems, a different cation conformer was used to create an initial configuration. Since we were especially interested in ion-ion-interactions, we monitored the distribution of several atom-atom interionic distances to assess sampling. Every system was simulated until the distributions reached convergence, the respective times for every system are listed in Table S8. These converged distributions are depicted in Figure S4 and show that especially the N23-O48 and N23-O49 distance distributions show full overlap.

To illustrate the distribution prior to convergence, the distributions of the E/S system after 38 ns and the full simulation time of 78 ns are depicted in Figure S5. It can be clearly seen that the N23-O48 and

Die approbierte gedruckte Originalversion dieser Dissertation ist an der TU Wien Bibliothek verfügbar.
The approved original version of this doctoral thesis is available in print at TU Wien Bibliothek.

N23-O49 distance distributions are different at 38 ns, but after a simulation time of 78 ns the distributions have equalized.

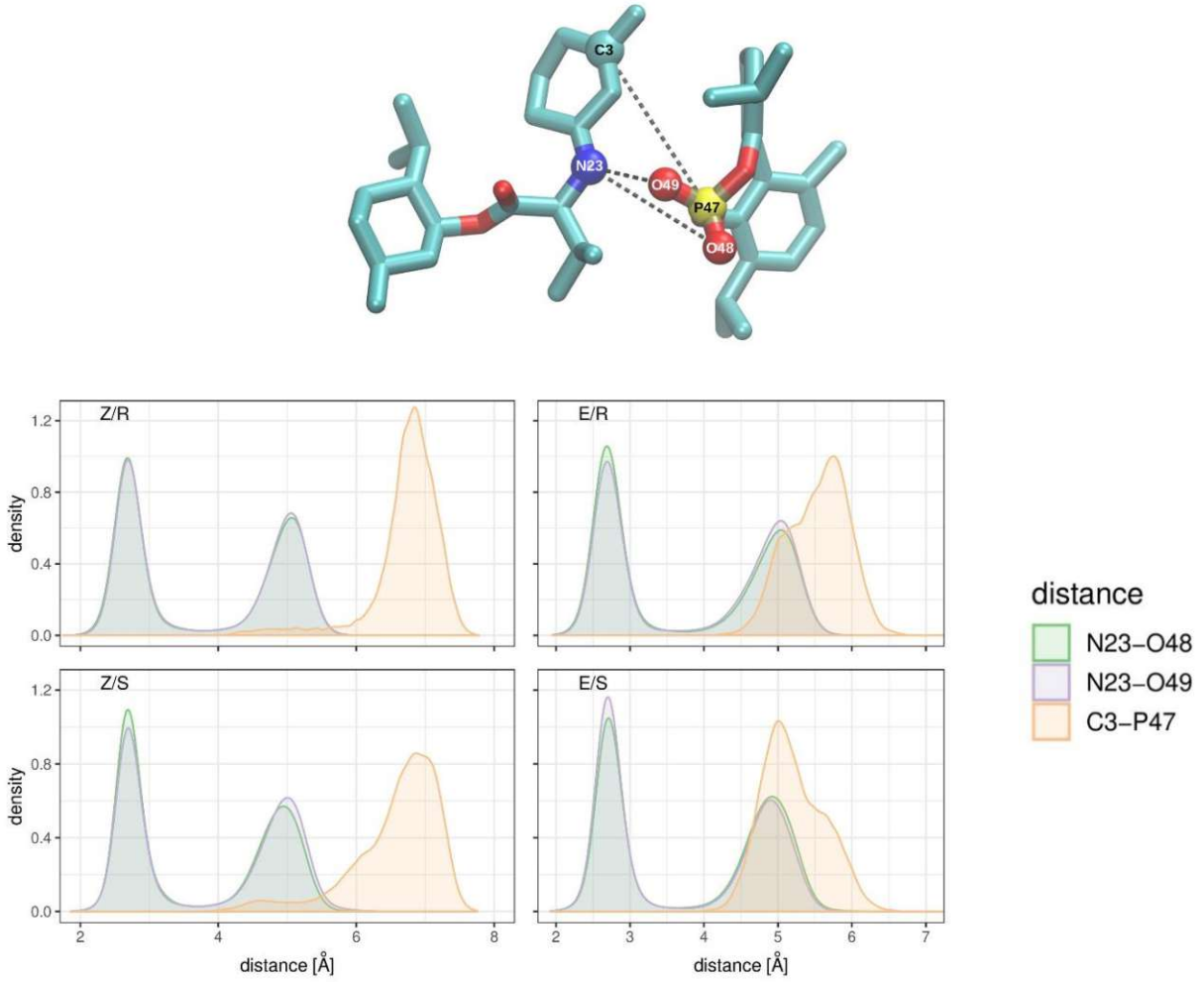


Figure S4. Interionic distances illustrated for the E-cation/S-anion pair (top) and the distributions after the full simulation time (bottom). Simulation times for the different systems are listed in Table S8.

Die approbierte gedruckte Originalversion dieser Dissertation ist an der TU Wien Bibliothek verfügbar.
The approved original version of this doctoral thesis is available in print at TU Wien Bibliothek.

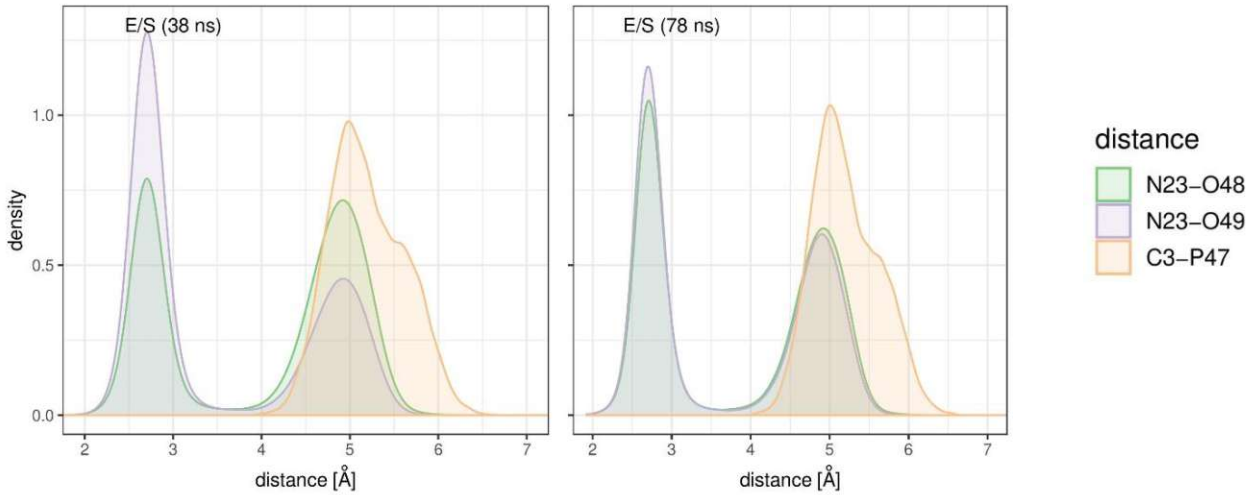
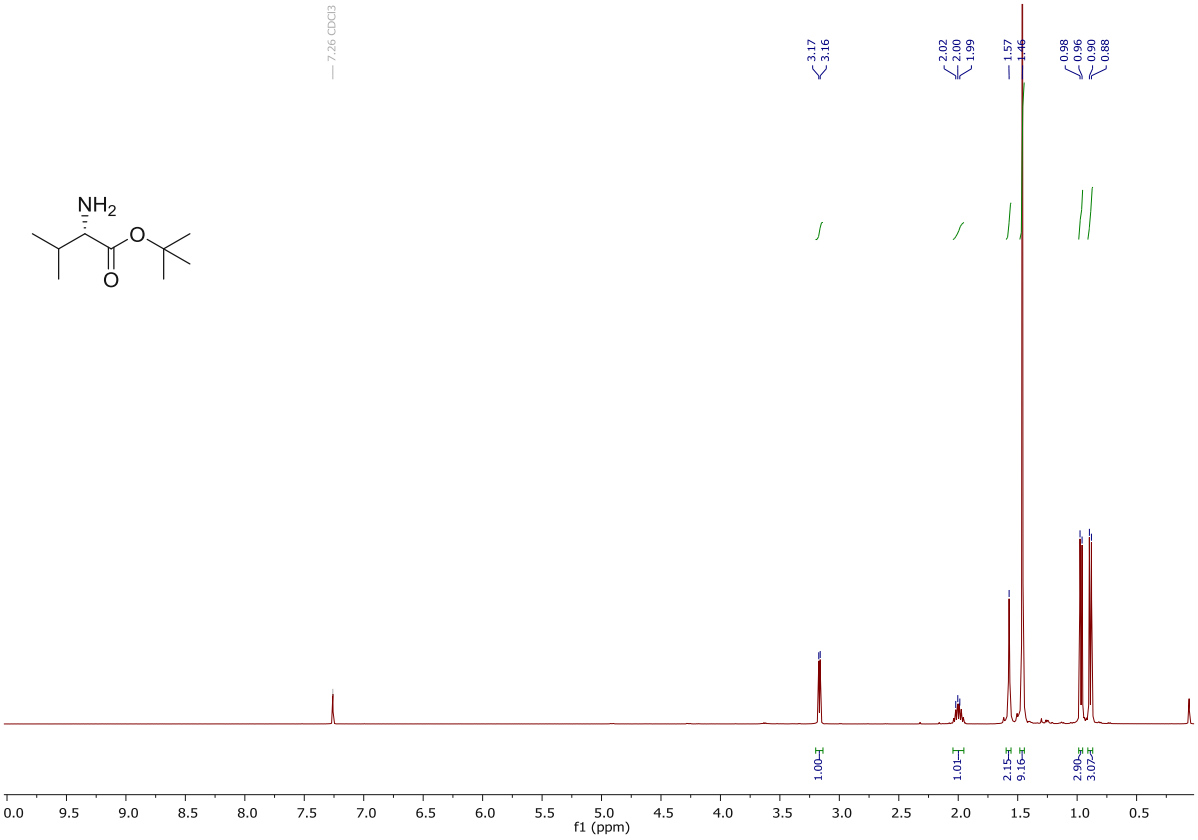
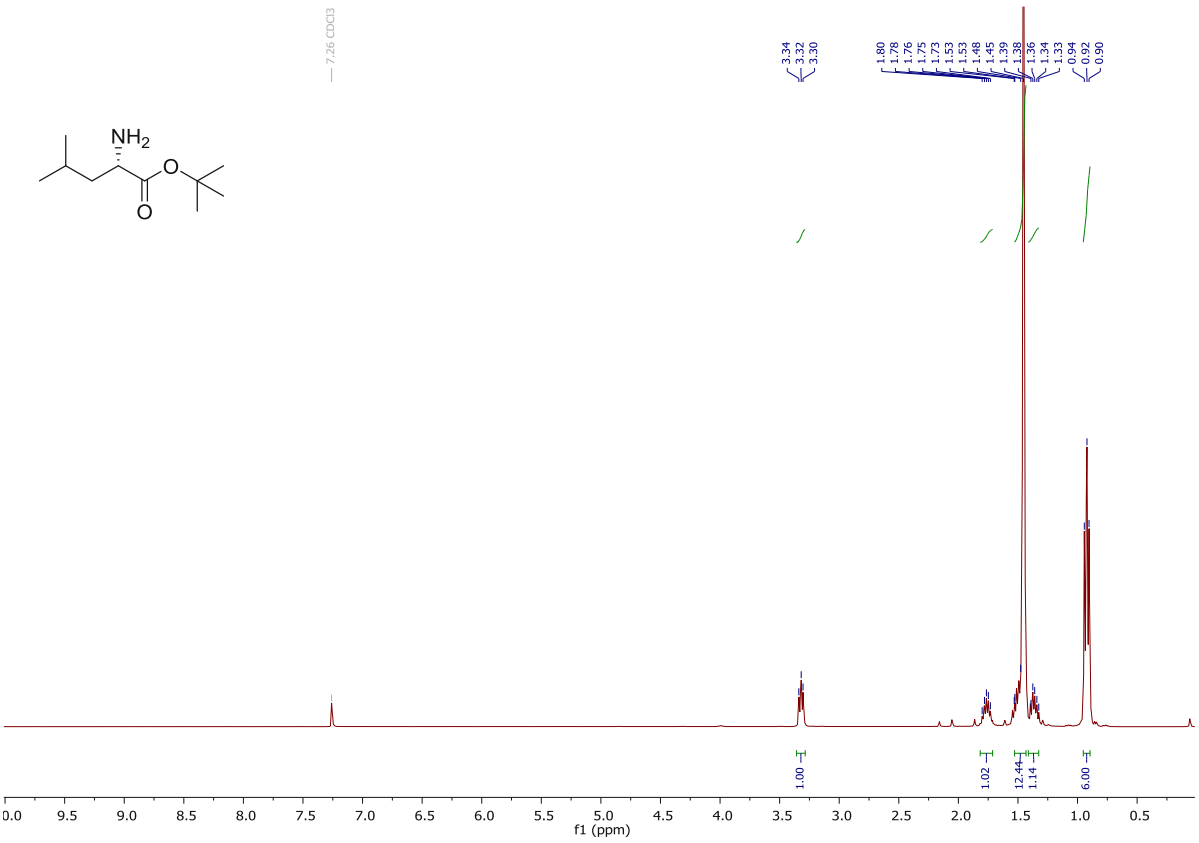


Figure S5. Distribution of interionic distances for the E-cation/S-anion pair after 38 ns (left) and 78 ns (right) simulation time. It is clearly visible that 78 ns are necessary to converge the distributions.

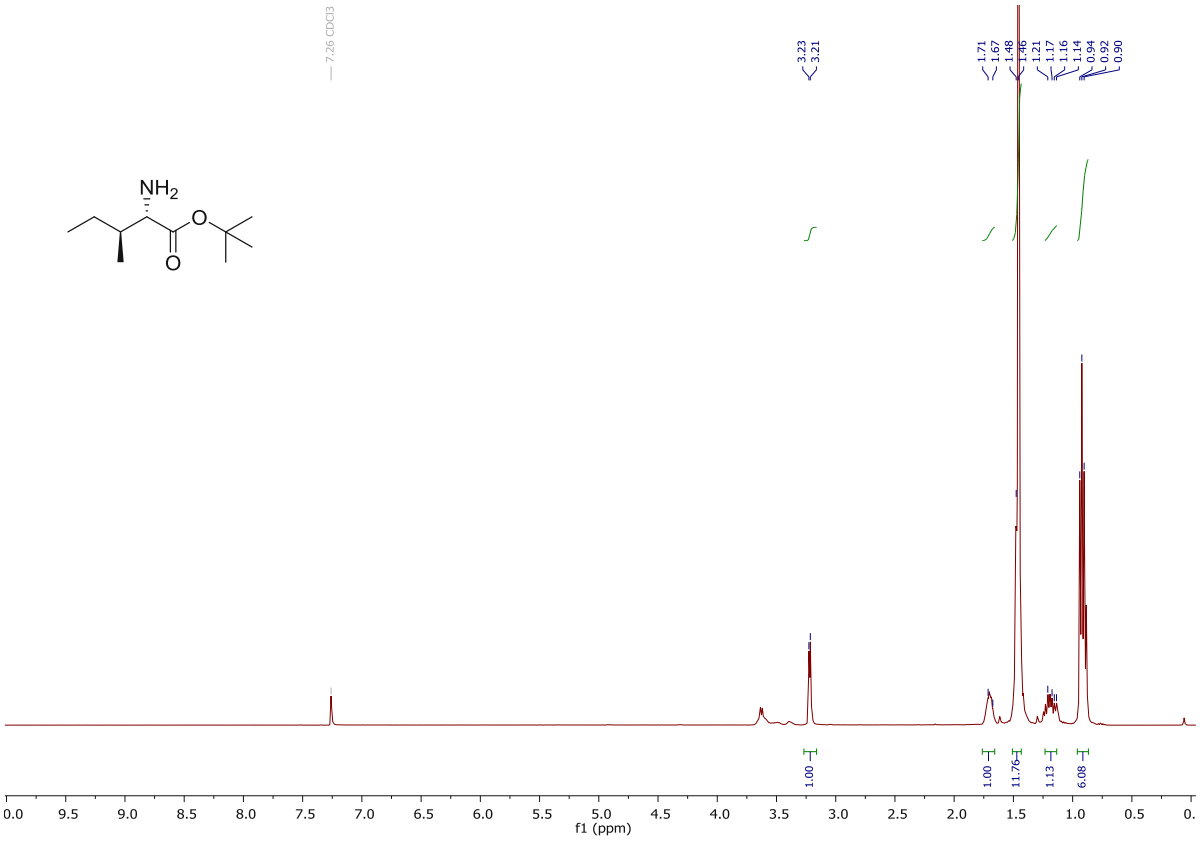
Die approbierte gedruckte Originalversion dieser Dissertation ist an der TU Wien Bibliothek verfügbar.
The approved original version of this doctoral thesis is available in print at TU Wien Bibliothek.

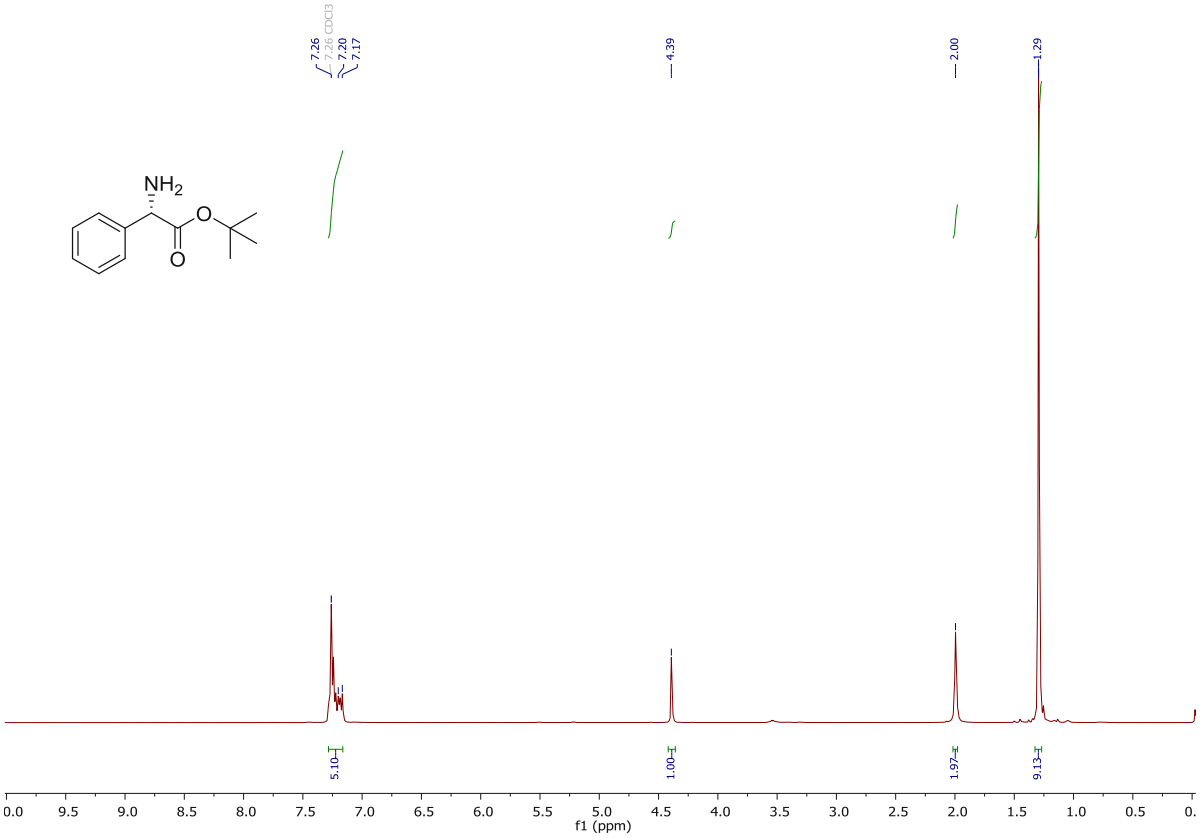
8. NMR specta of L-amino acid derivatives





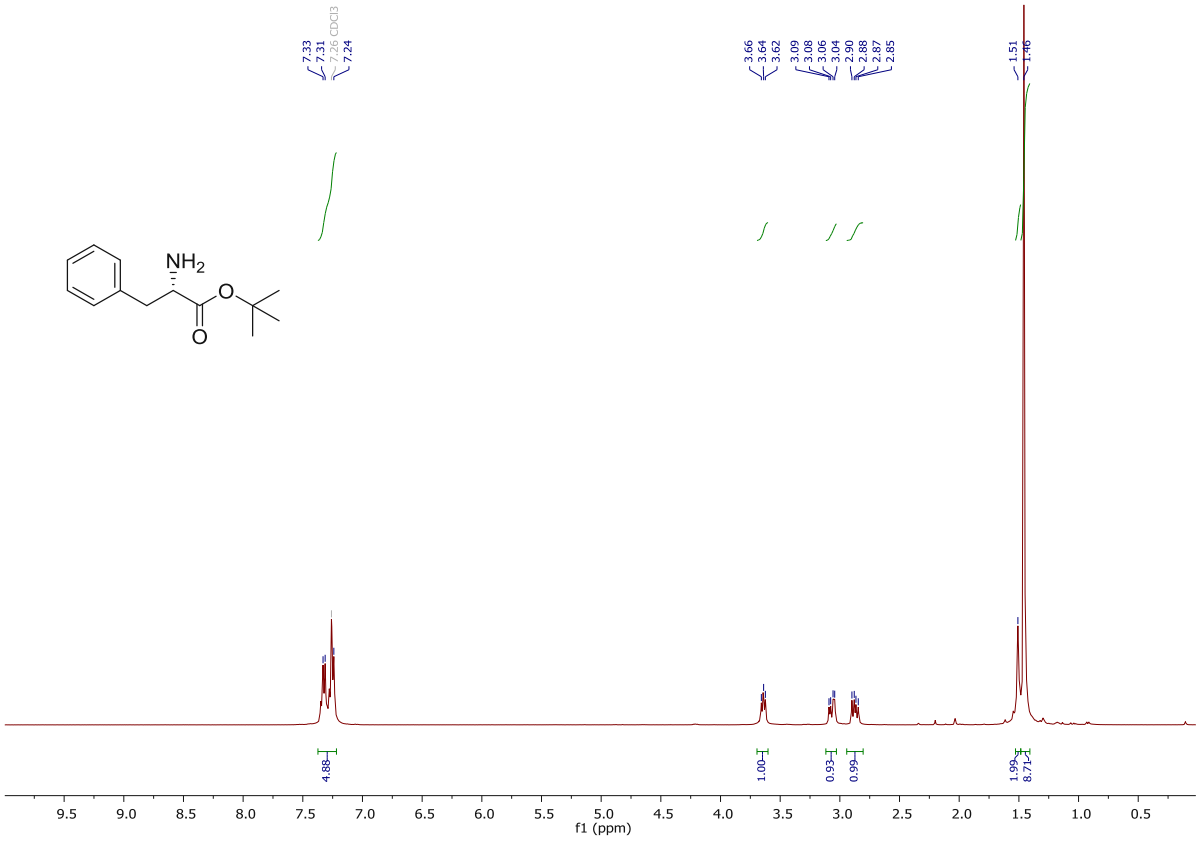
Die approbierte gedruckte Originalversion dieser Dissertation ist an der TU Wien Bibliothek verfügbar.
The approved original version of this doctoral thesis is available in print at TU Wien Bibliothek.

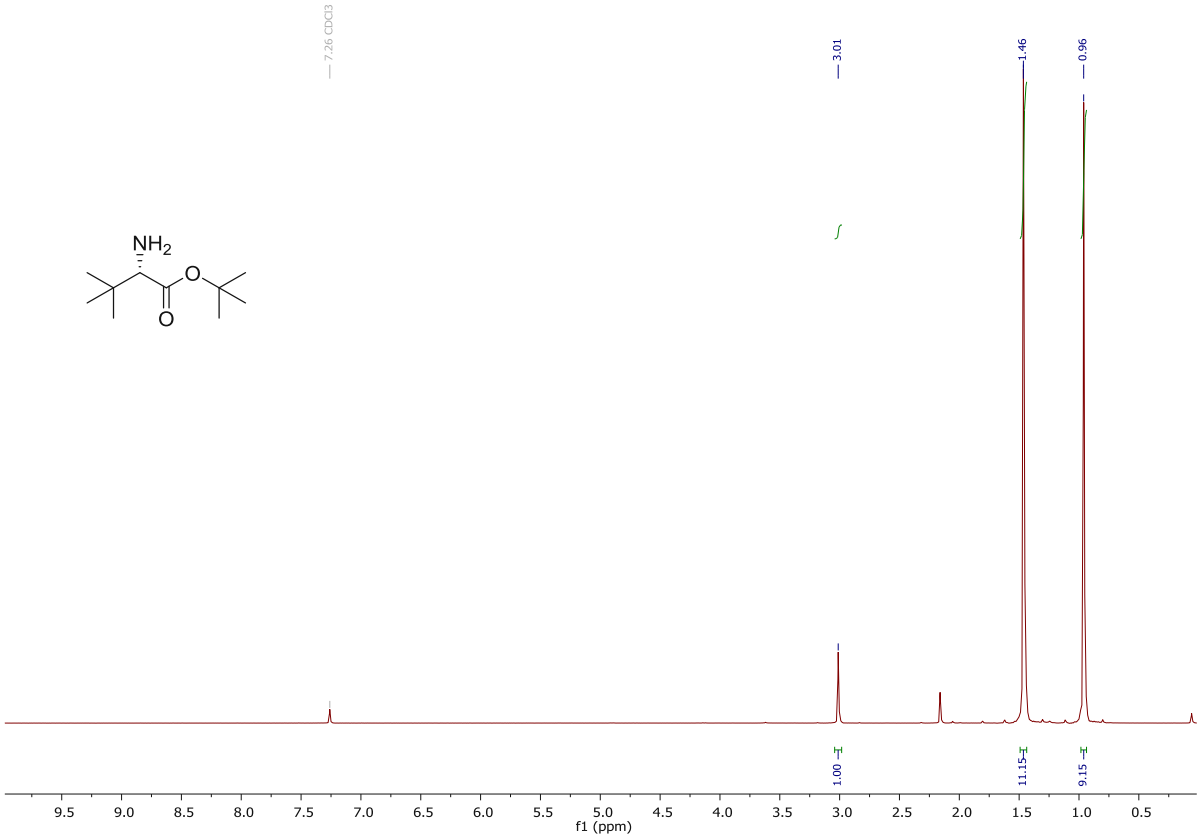




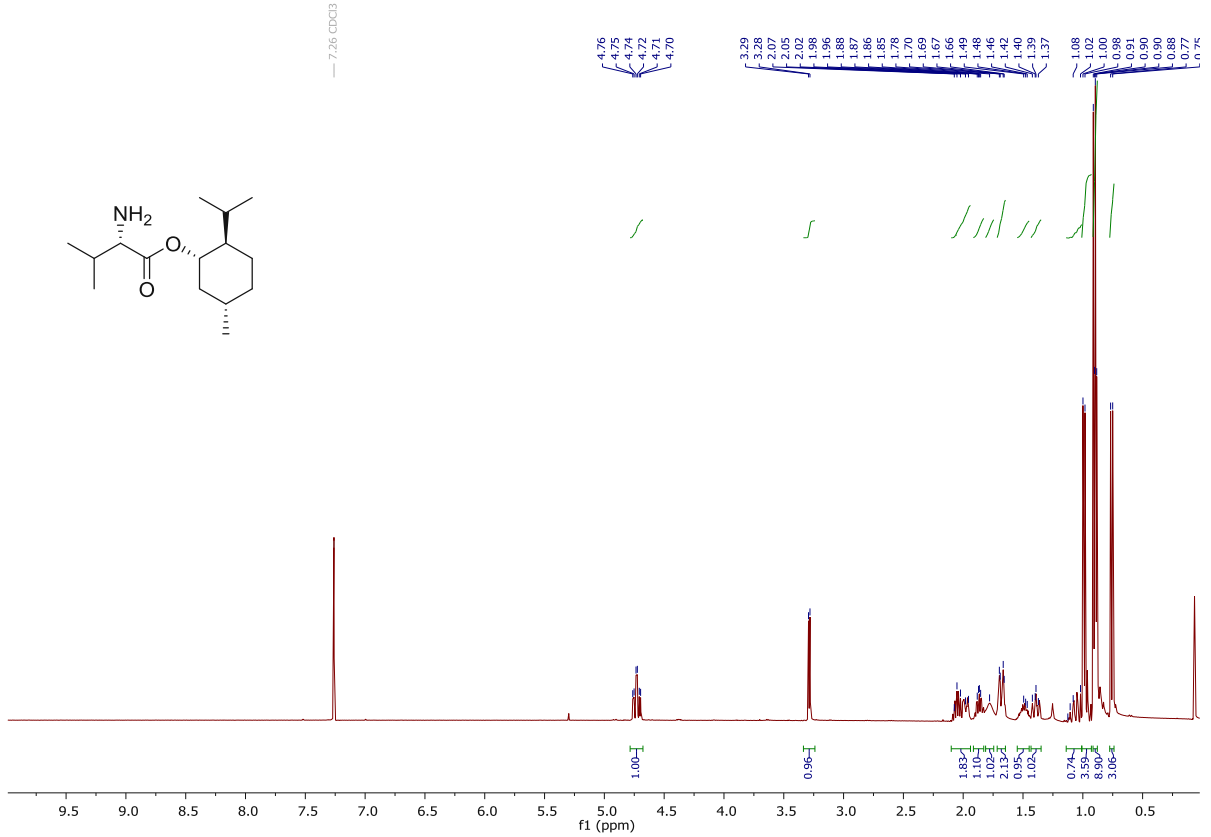
Die approbierte gedruckte Originalversion dieser Dissertation ist an der TU Wien Bibliothek verfügbar.
The approved original version of this doctoral thesis is available in print at TU Wien Bibliothek.

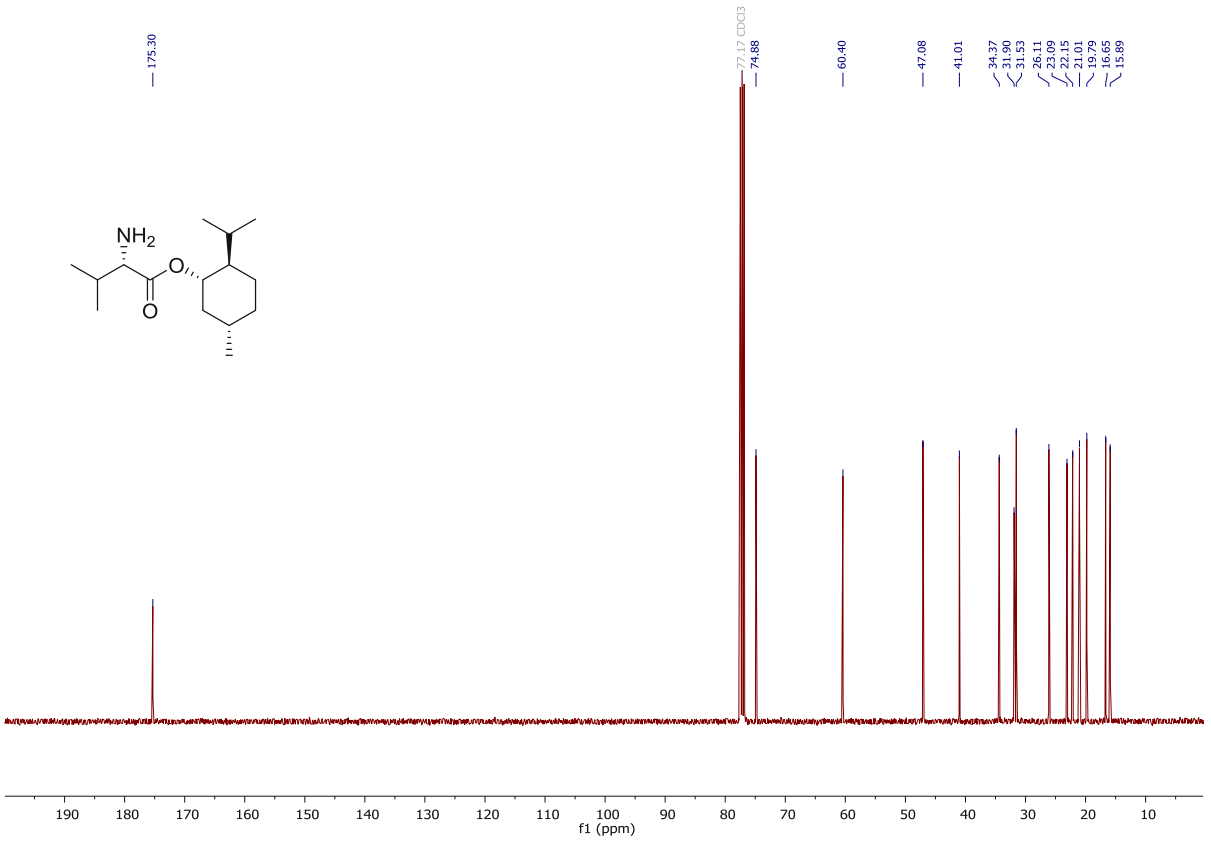
Die approbierte gedruckte Originalversion dieser Dissertation ist an der TU Wien Bibliothek verfügbar.
The approved original version of this doctoral thesis is available in print at TU Wien Bibliothek.



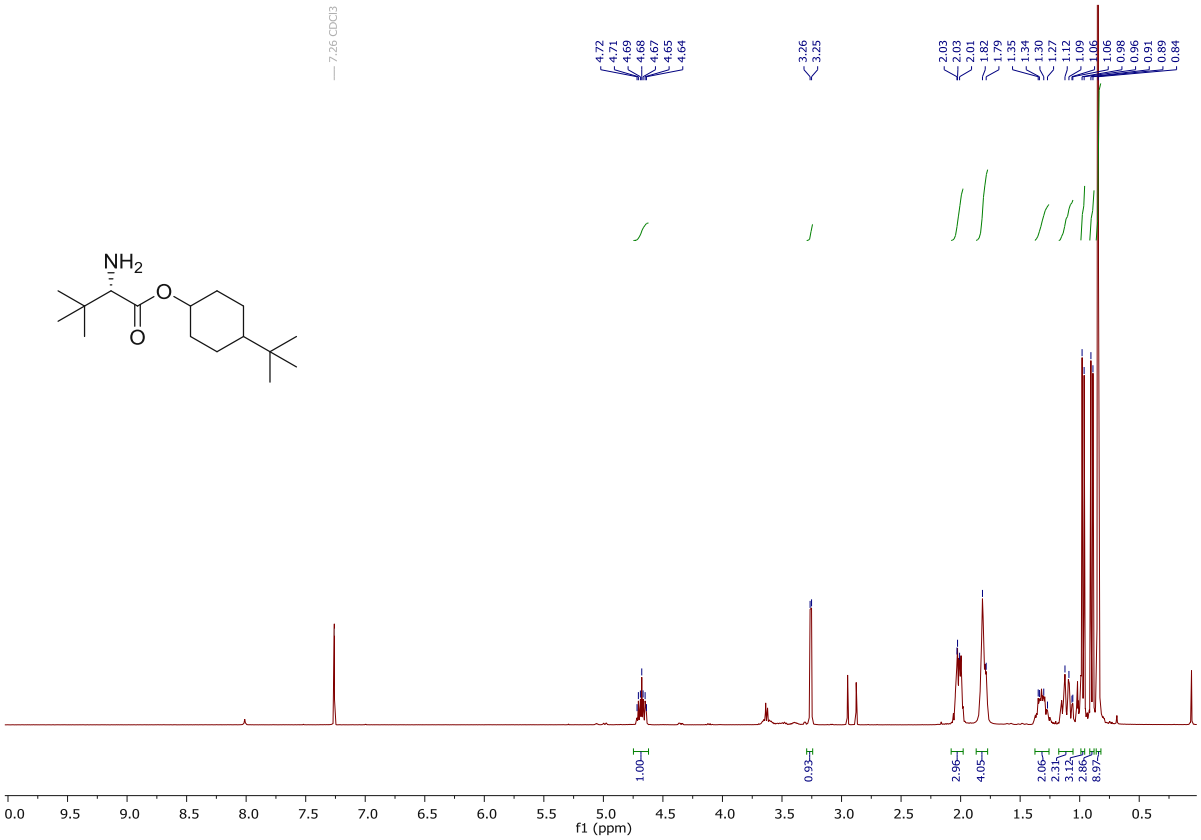


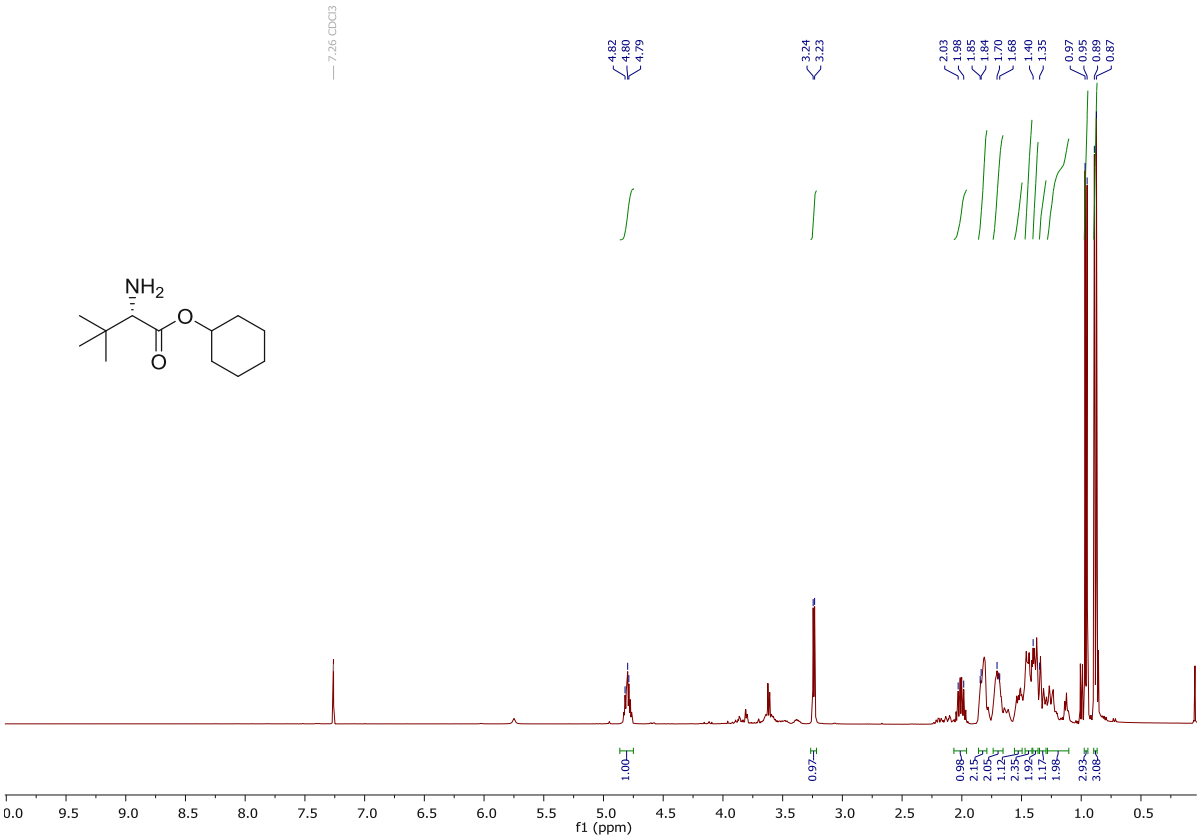
Die approbierte gedruckte Originalversion dieser Dissertation ist an der TU Wien Bibliothek verfügbar.
The approved original version of this doctoral thesis is available in print at TU Wien Bibliothek.



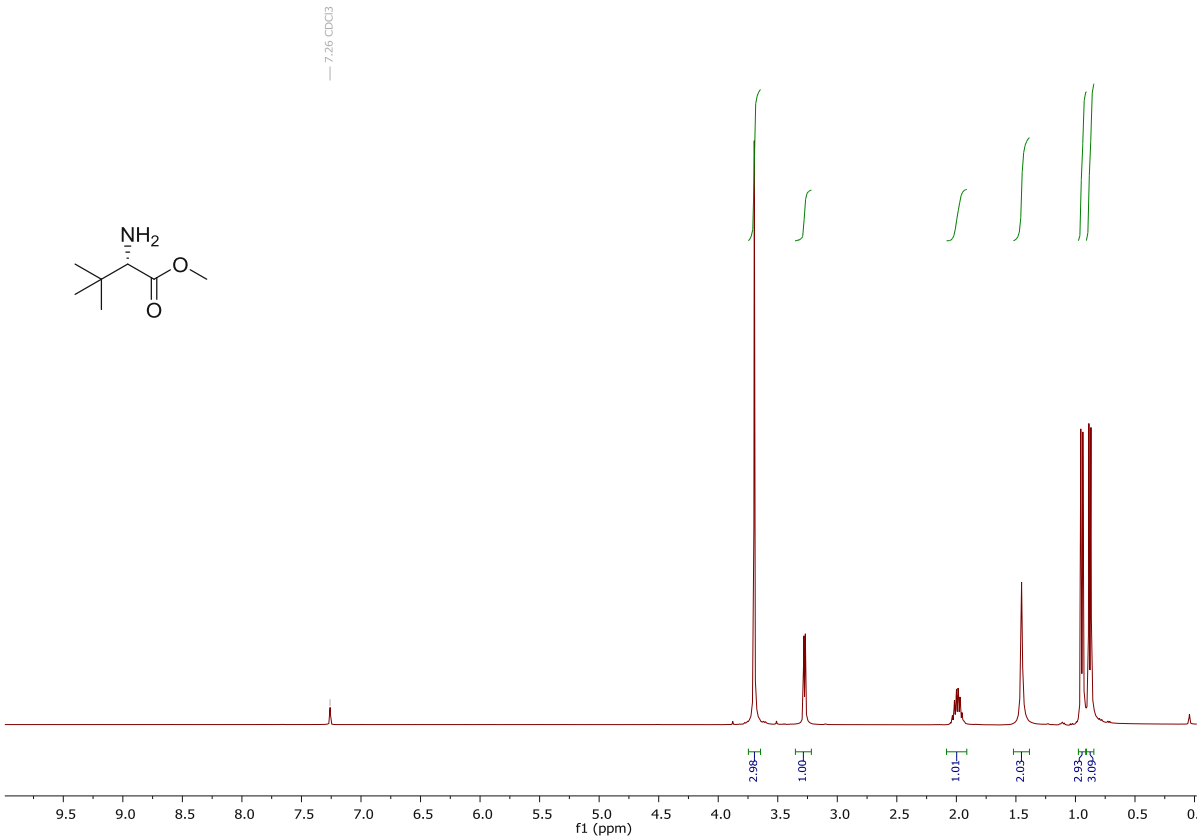


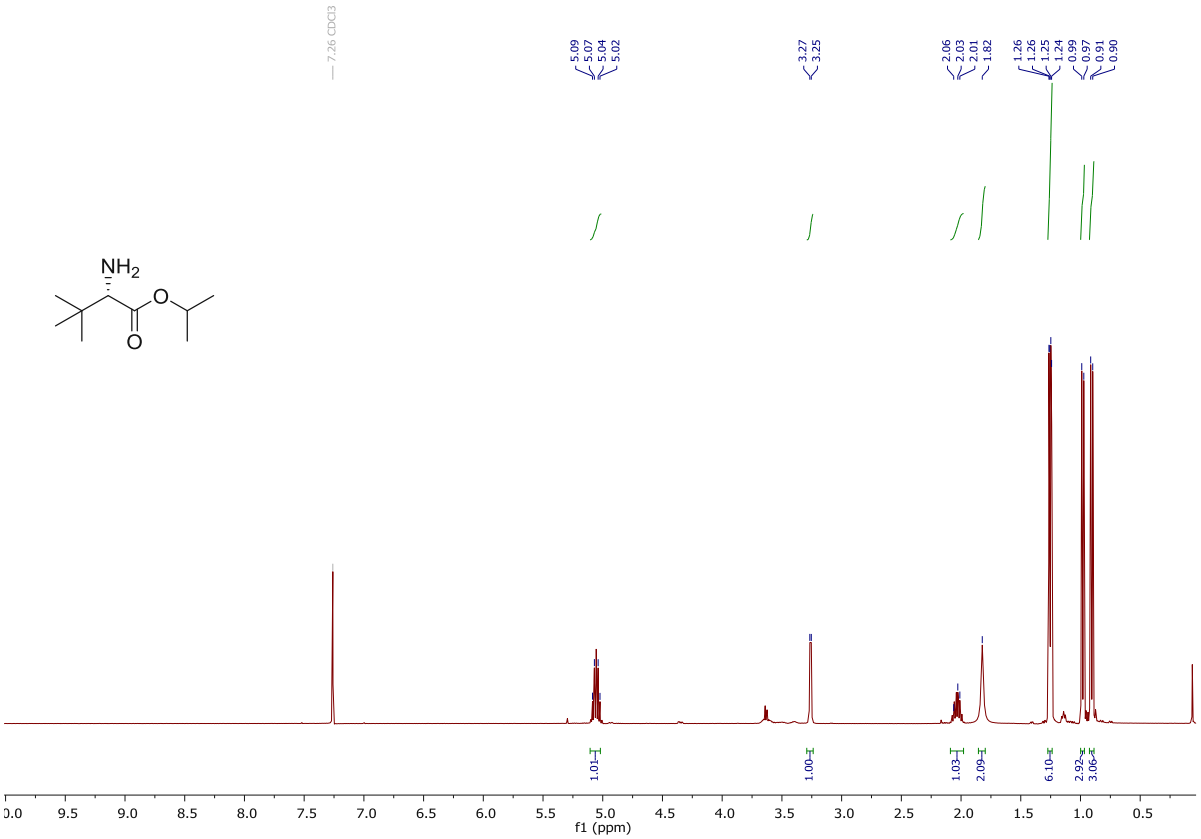
Die approbierte gedruckte Originalversion dieser Dissertation ist an der TU Wien Bibliothek verfügbar.
The approved original version of this doctoral thesis is available in print at TU Wien Bibliothek.

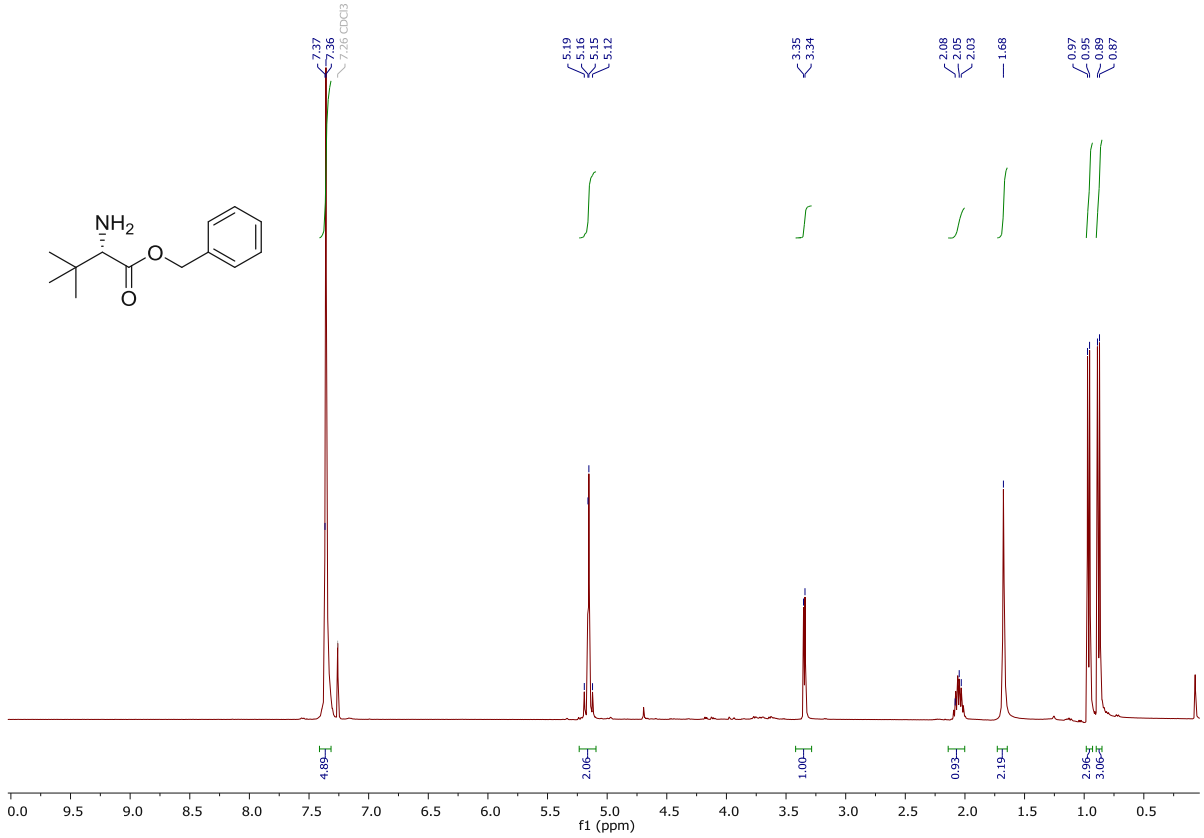




Die approbierte gedruckte Originalversion dieser Dissertation ist an der TU Wien Bibliothek verfügbar.
The approved original version of this doctoral thesis is available in print at TU Wien Bibliothek.

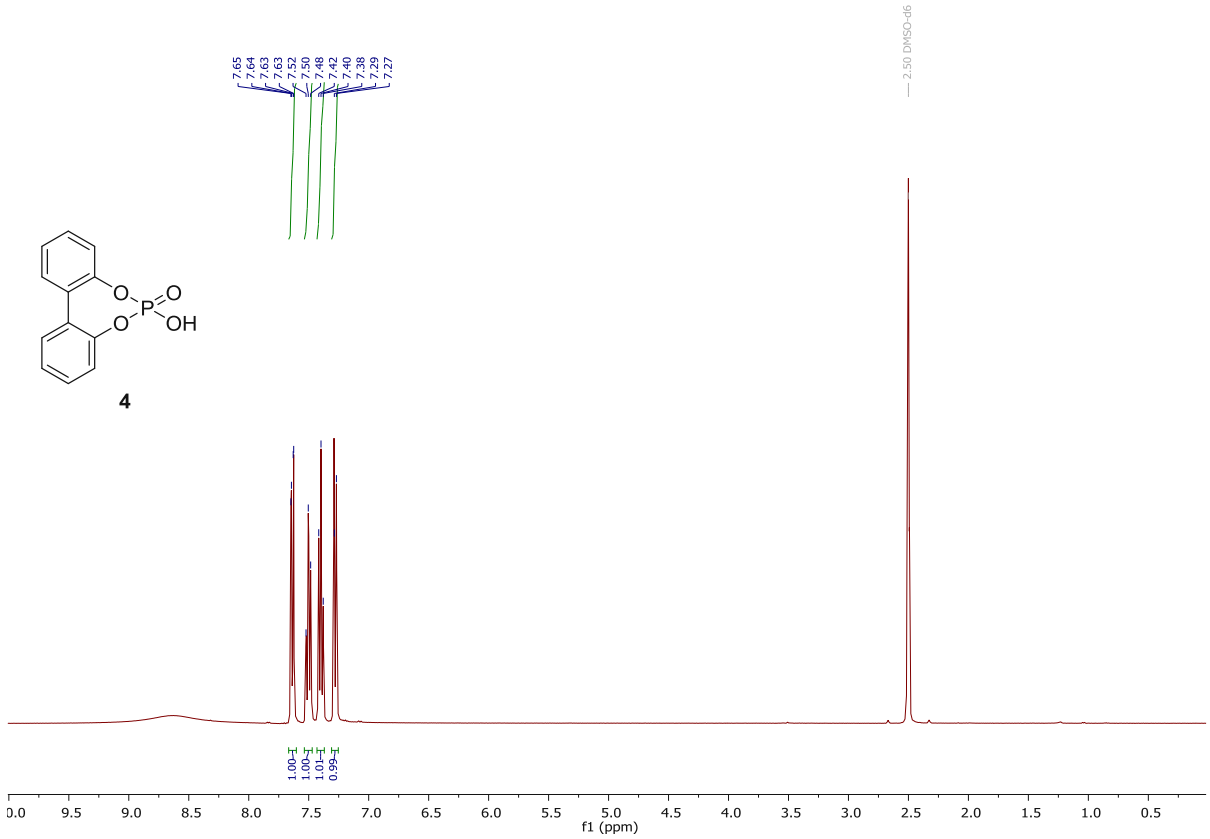




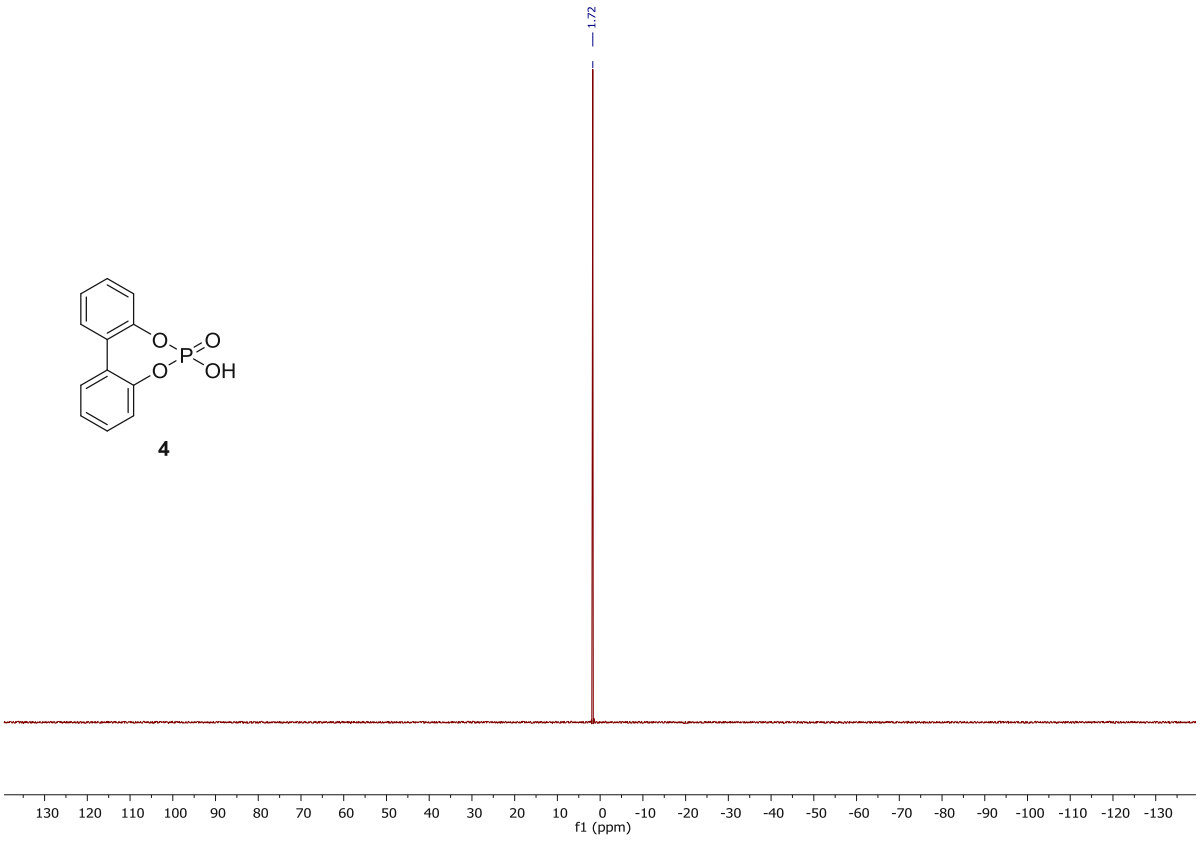


Die approbierte gedruckte Originalversion dieser Dissertation ist an der TU Wien Bibliothek verfügbar.
The approved original version of this doctoral thesis is available in print at TU Wien Bibliothek.

9. NMR specta of phosphoric acids and its intermediates

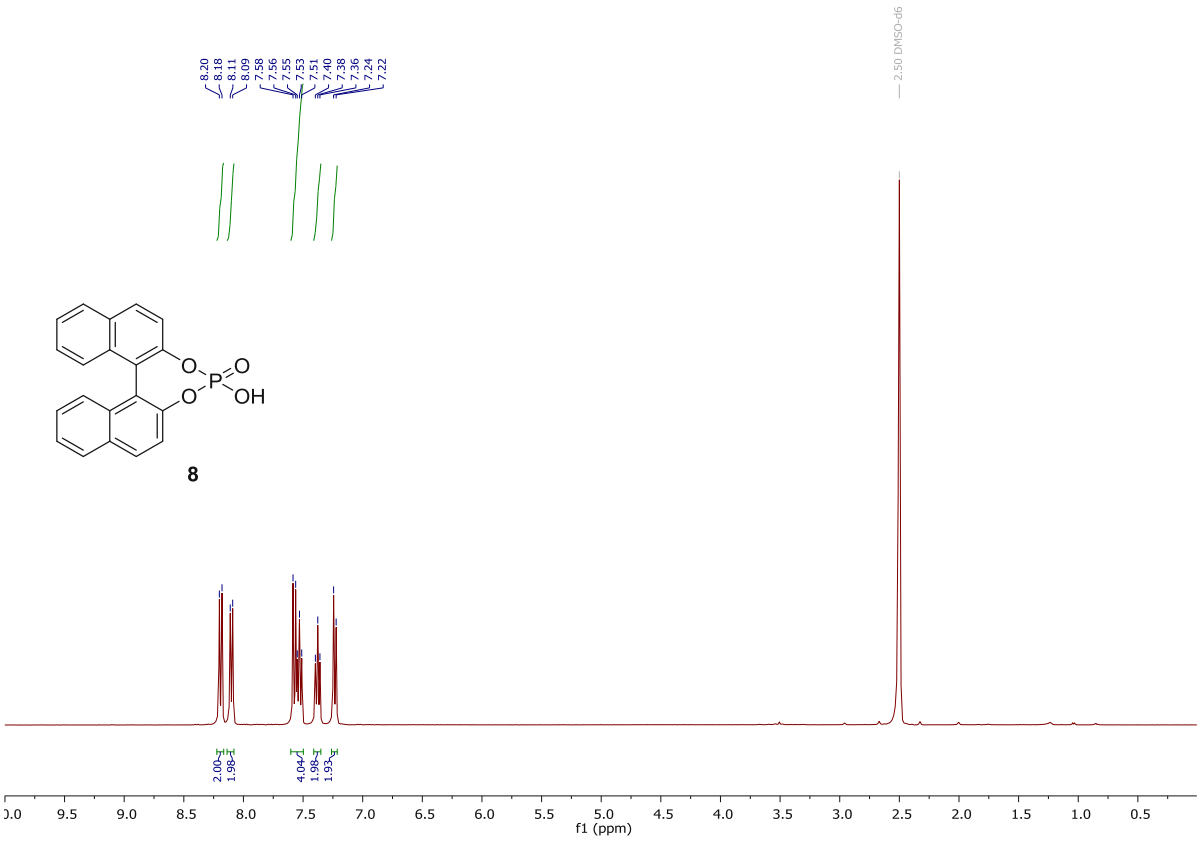


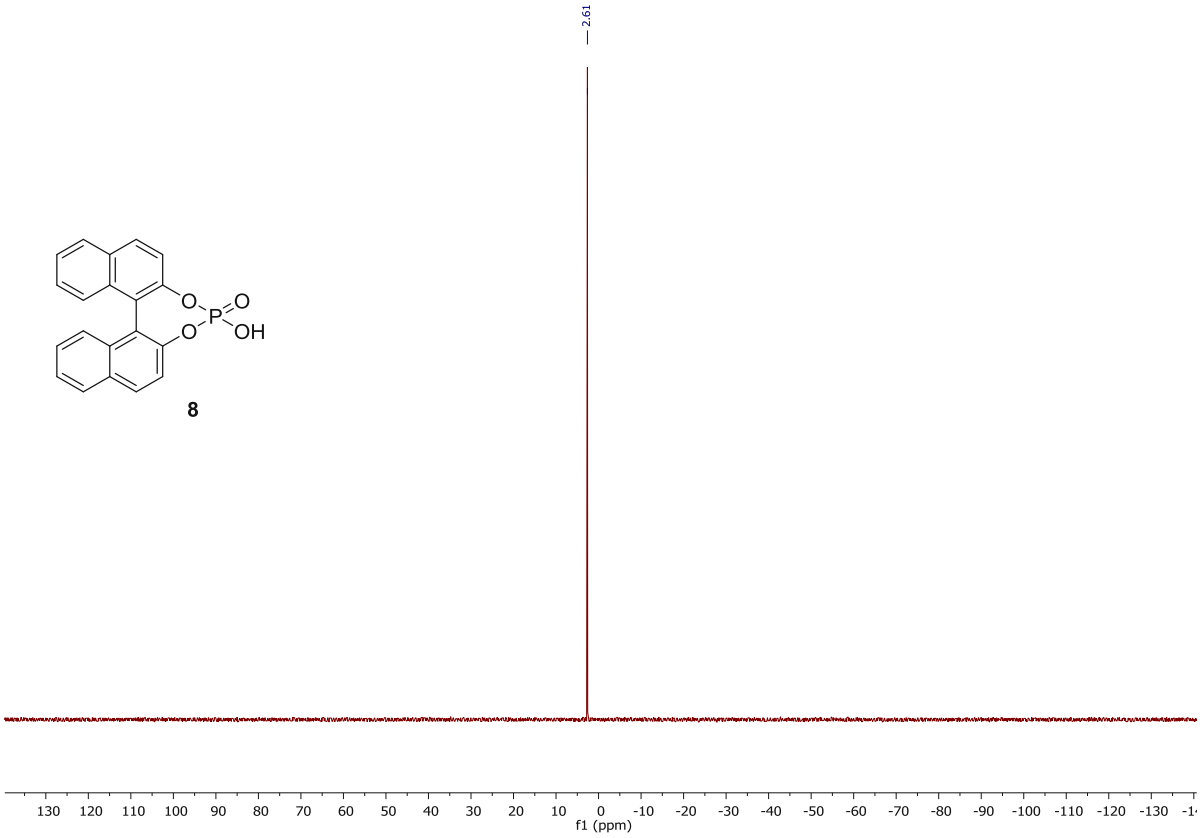
4



4

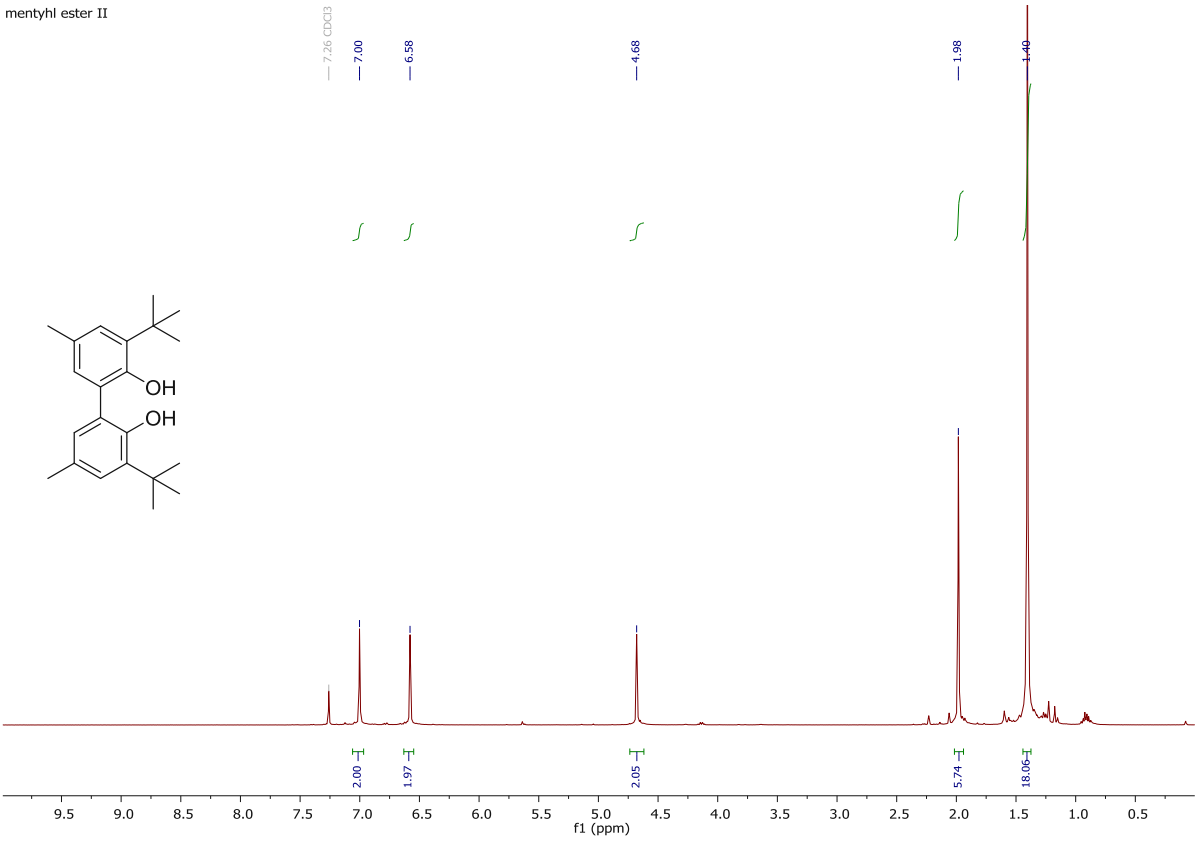
Die approbierte gedruckte Originalversion dieser Dissertation ist an der TU Wien Bibliothek verfügbar.
The approved original version of this doctoral thesis is available in print at TU Wien Bibliothek.

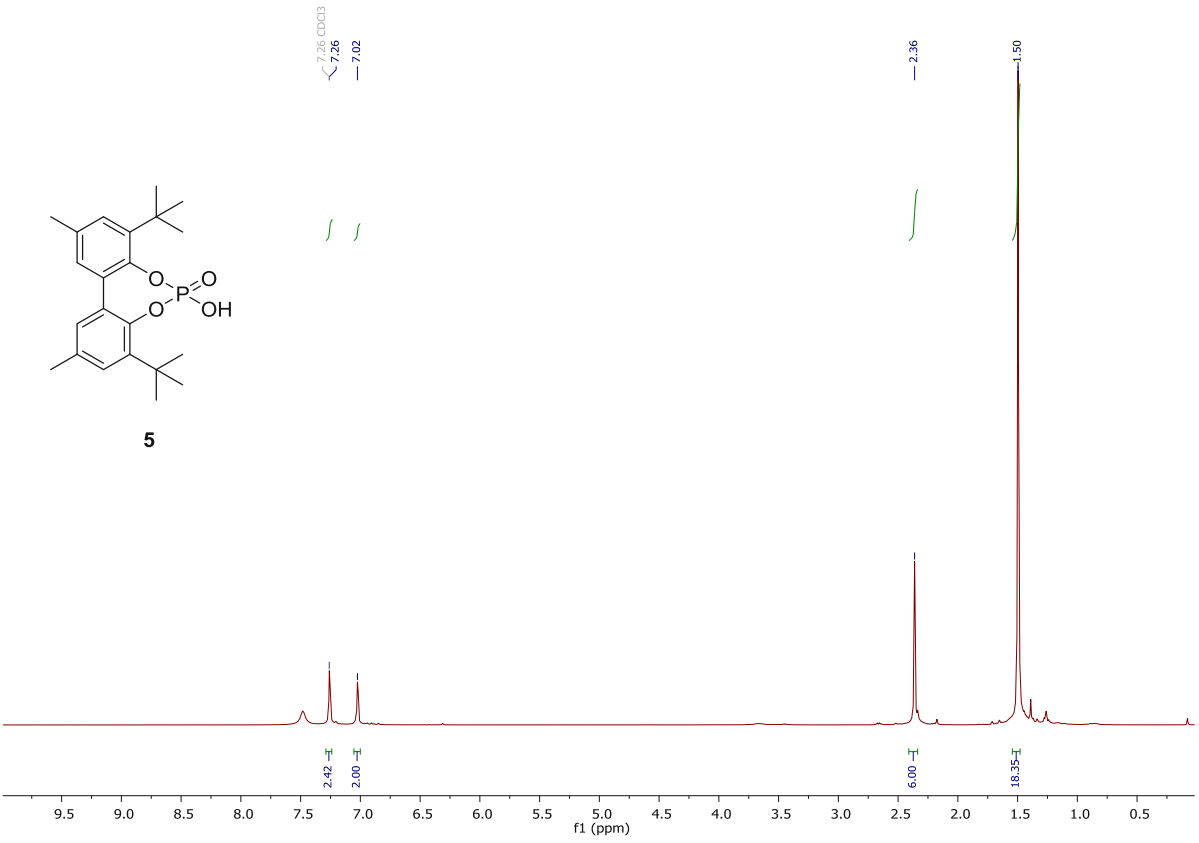




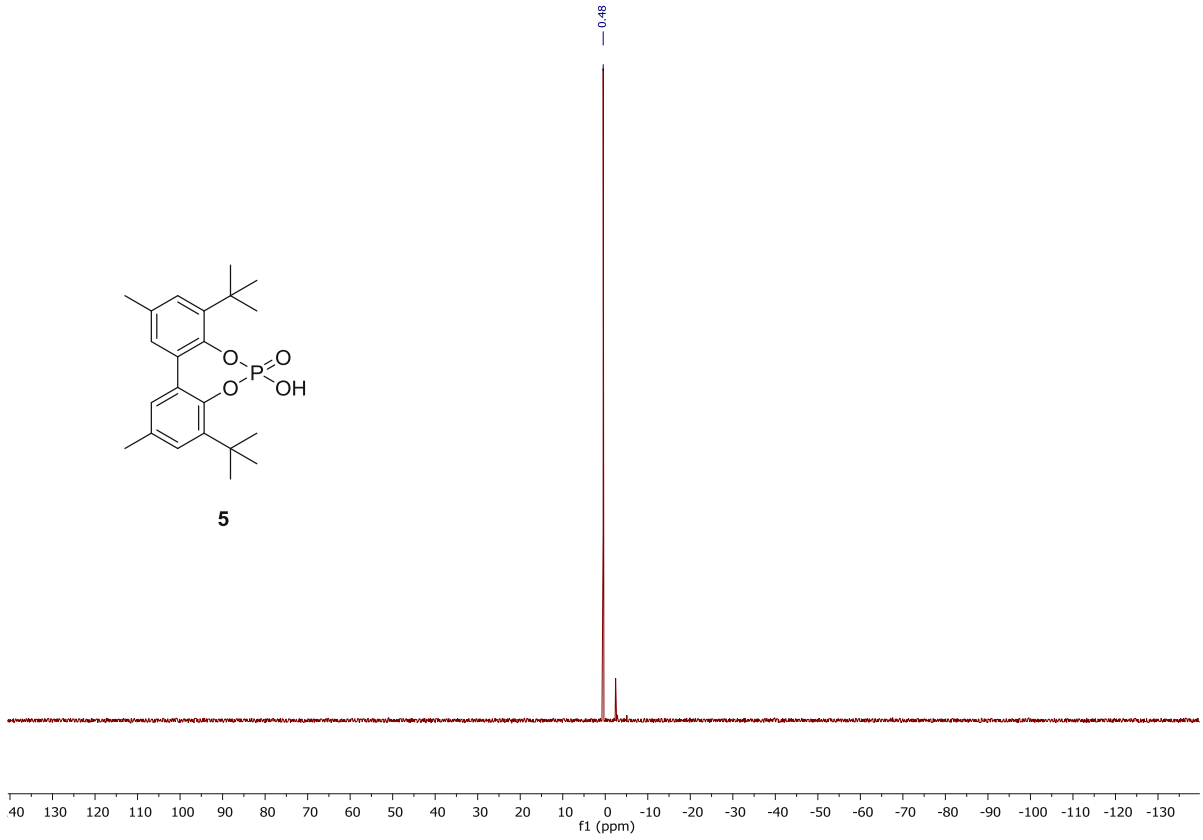
Die approbierte gedruckte Originalversion dieser Dissertation ist an der TU Wien Bibliothek verfügbar.
The approved original version of this doctoral thesis is available in print at TU Wien Bibliothek.

Die approbierte gedruckte Originalversion dieser Dissertation ist an der TU Wien Bibliothek verfügbar.
The approved original version of this doctoral thesis is available in print at TU Wien Bibliothek.

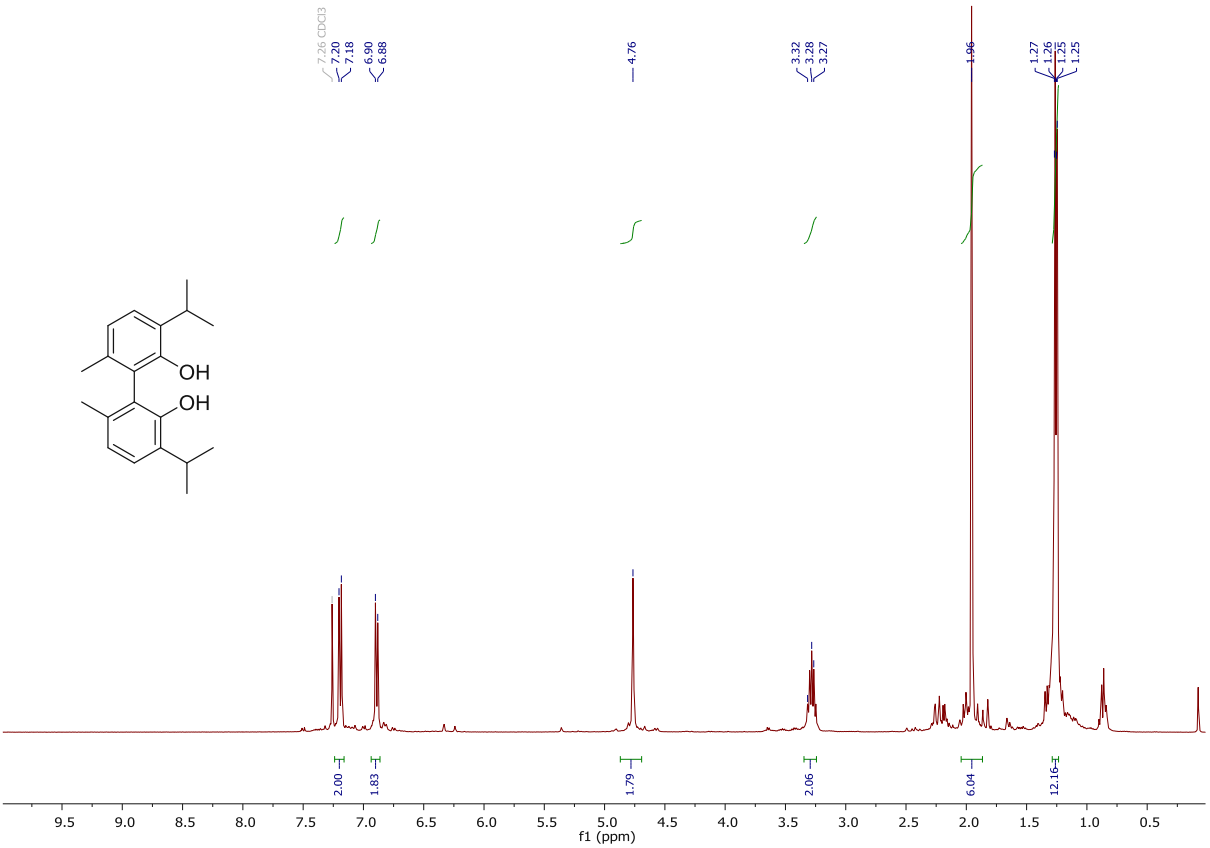




5

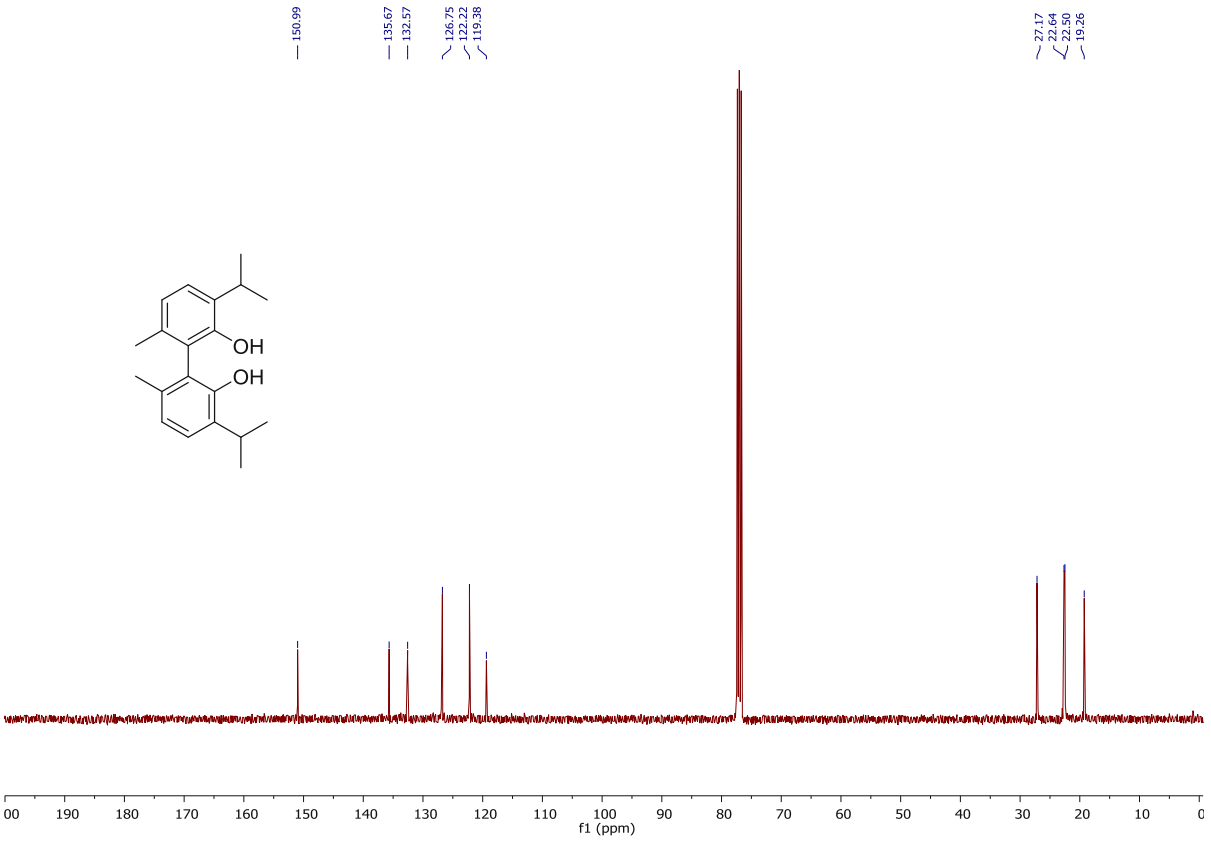


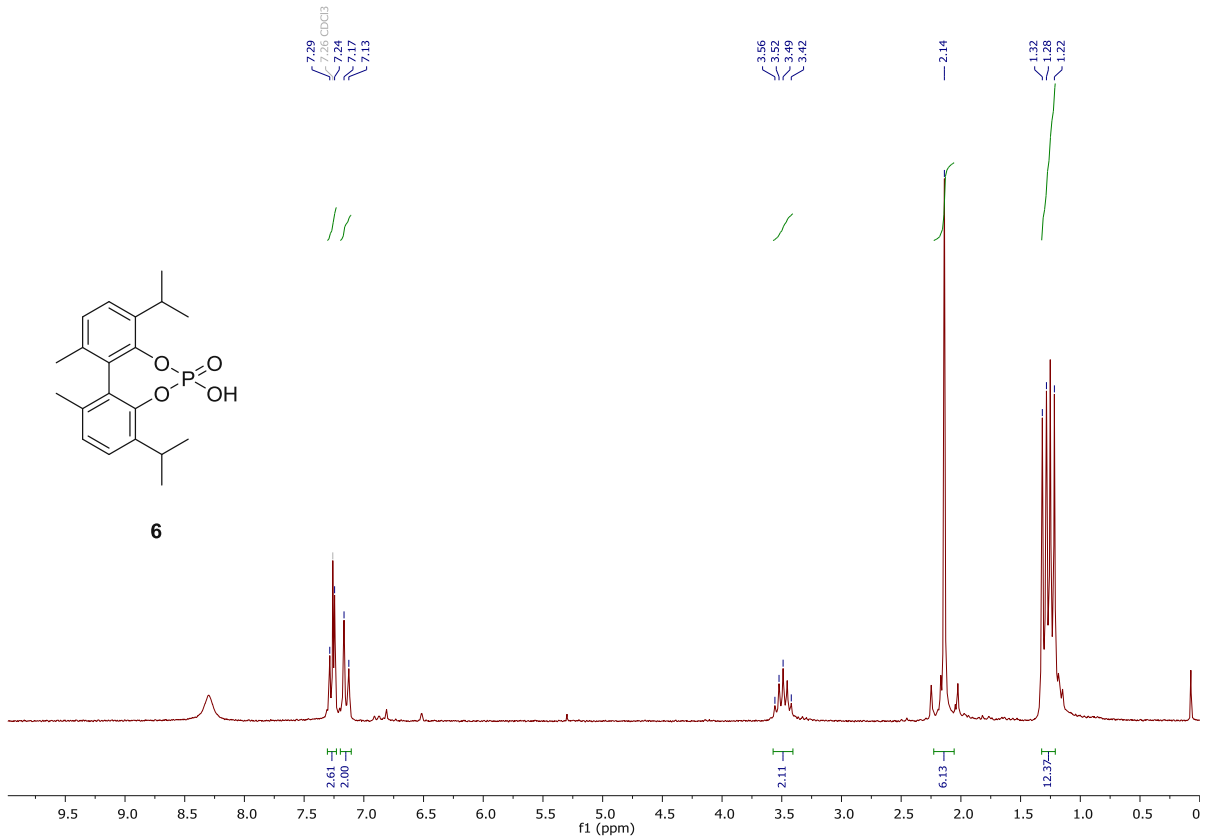
5



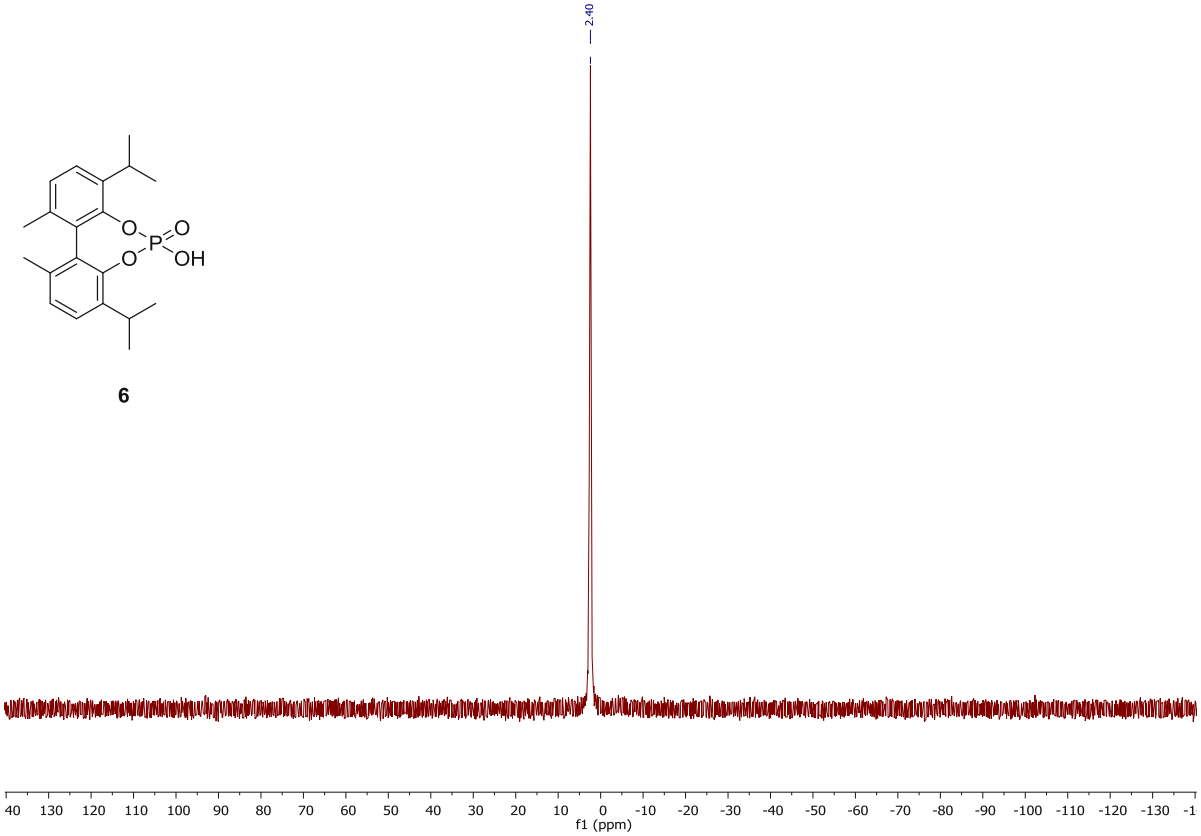
Die approbierte gedruckte Originalversion dieser Dissertation ist an der TU Wien Bibliothek verfügbar.
The approved original version of this doctoral thesis is available in print at TU Wien Bibliothek.
TU Bibliothek Your knowledge hub WIEN

Die approbierte gedruckte Originalversion dieser Dissertation ist an der TU Wien Bibliothek verfügbar.
The approved original version of this doctoral thesis is available in print at TU Wien Bibliothek.

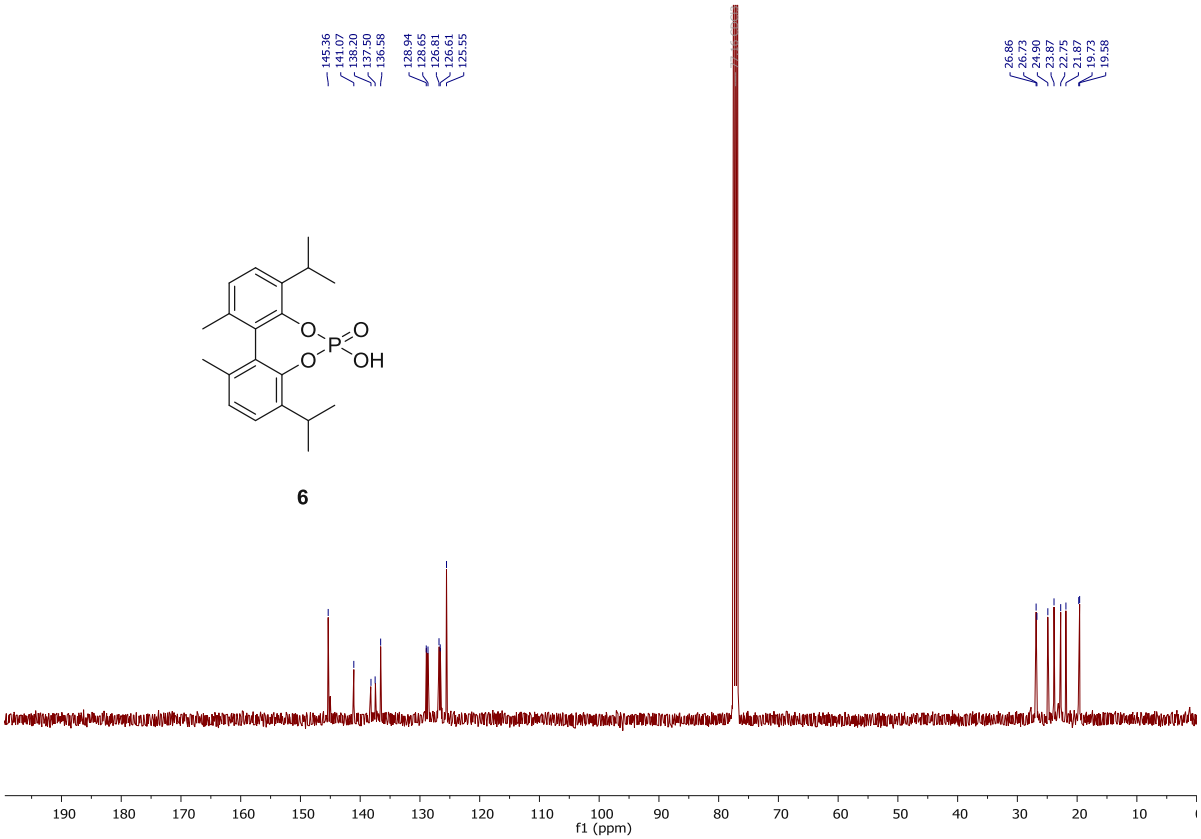




6



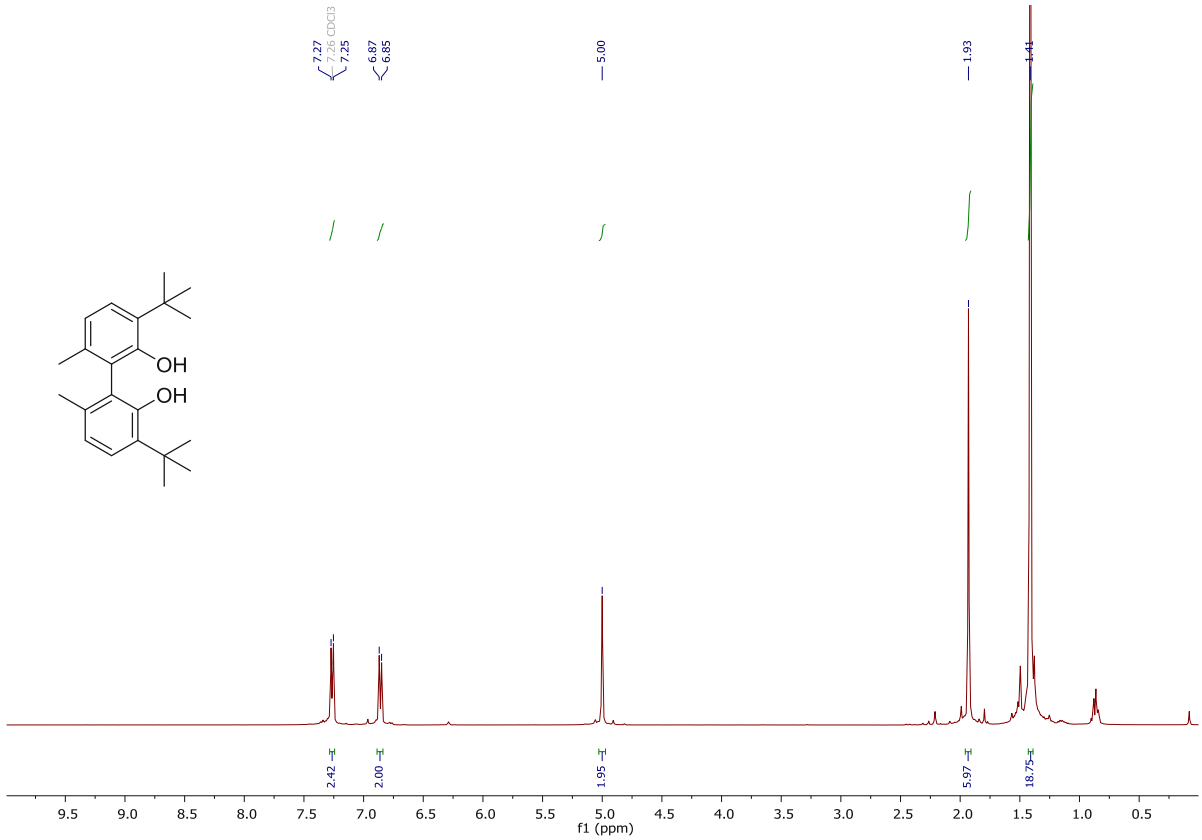
6

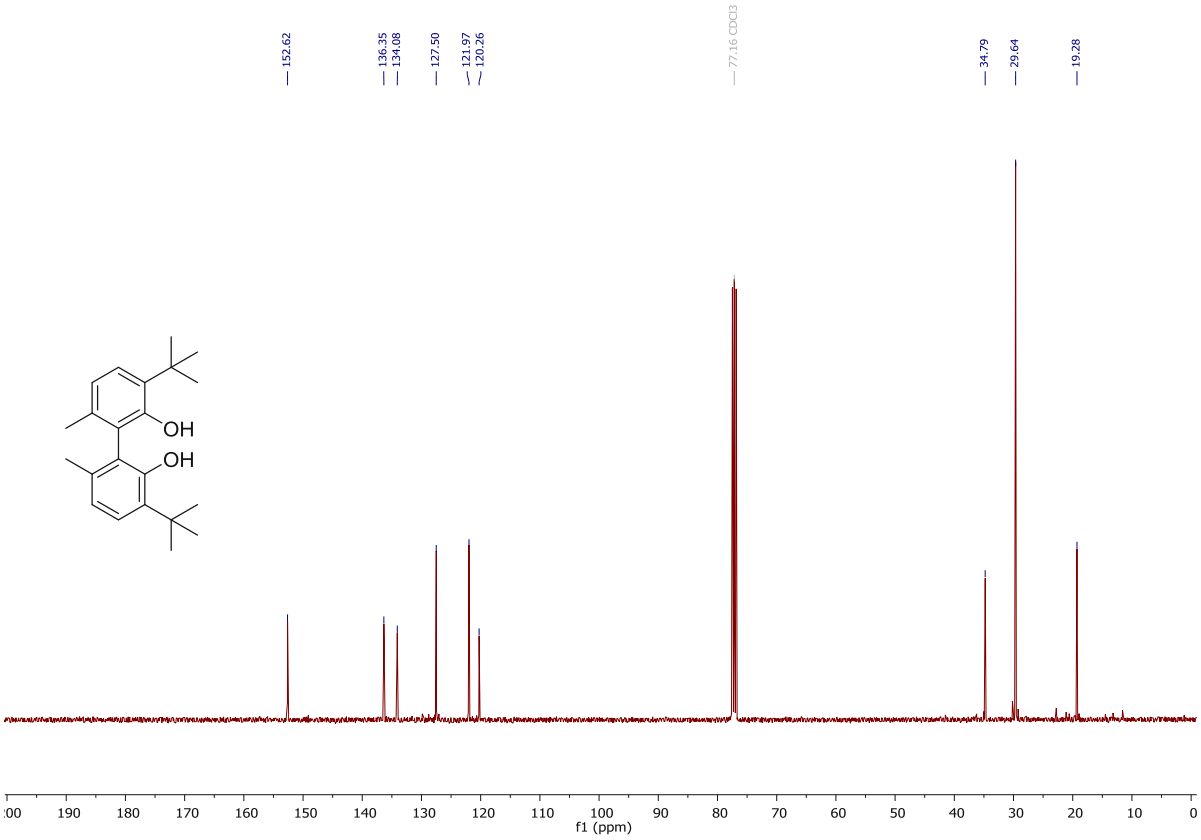


6

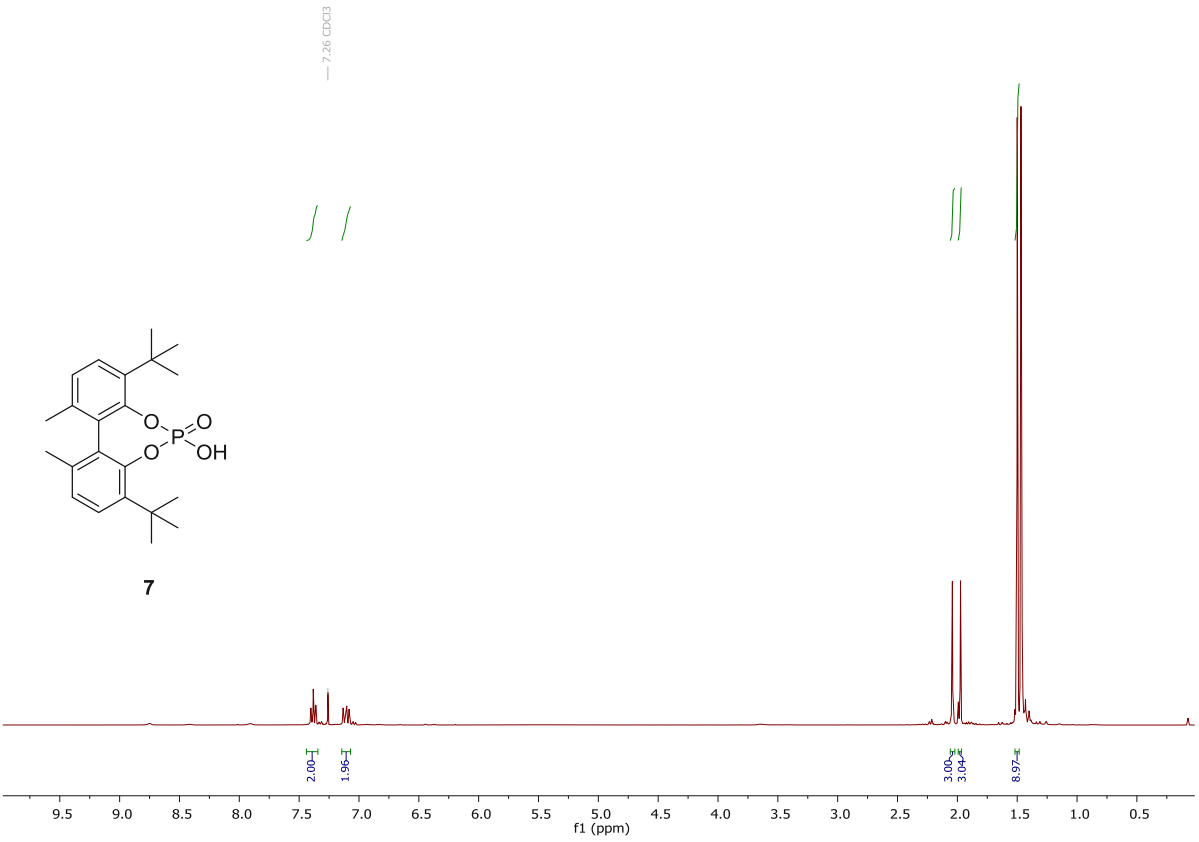
Die approbierte gedruckte Originalversion dieser Dissertation ist an der TU Wien Bibliothek verfügbar.
The approved original version of this doctoral thesis is available in print at TU Wien Bibliothek.

Die approbierte gedruckte Originalversion dieser Dissertation ist an der TU Wien Bibliothek verfügbar.
The approved original version of this doctoral thesis is available in print at TU Wien Bibliothek.

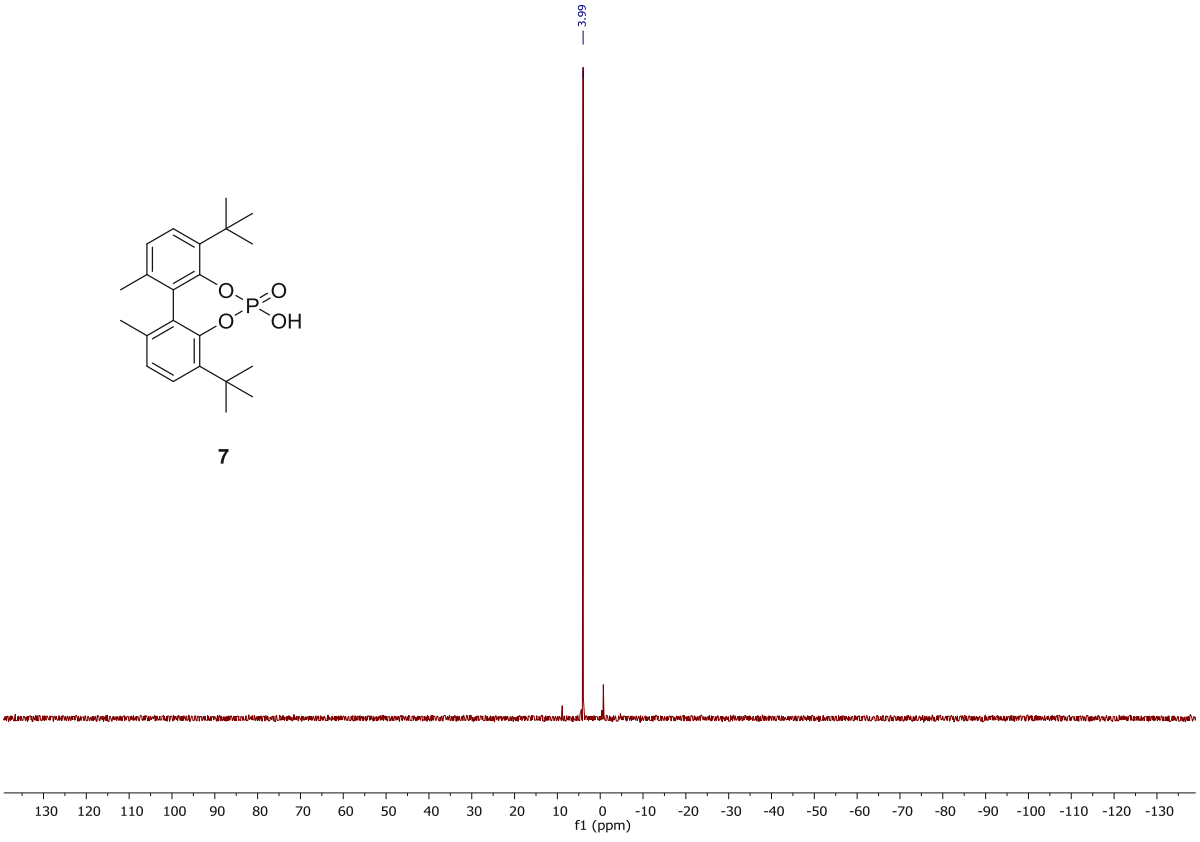




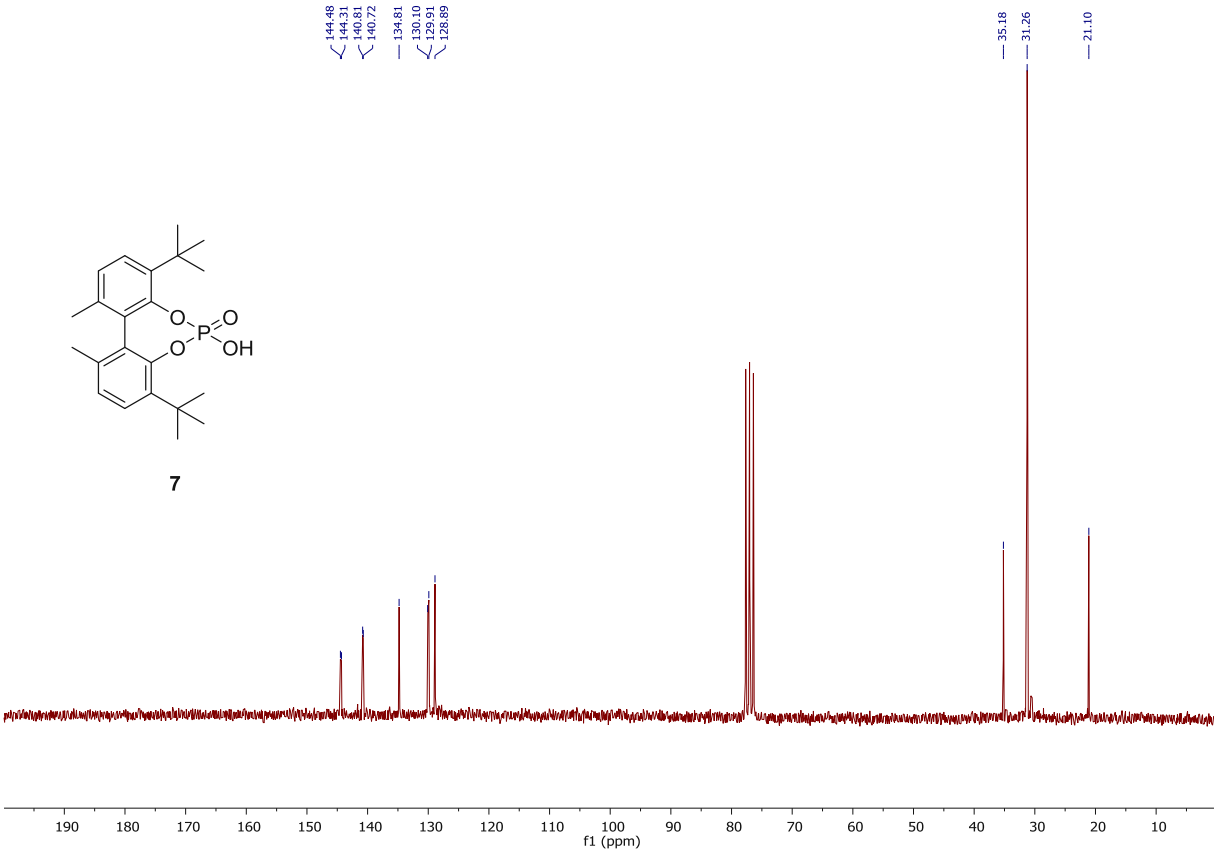
Die approbierte gedruckte Originalversion dieser Dissertation ist an der TU Wien Bibliothek verfügbar.
The approved original version of this doctoral thesis is available in print at TU Wien Bibliothek.



7



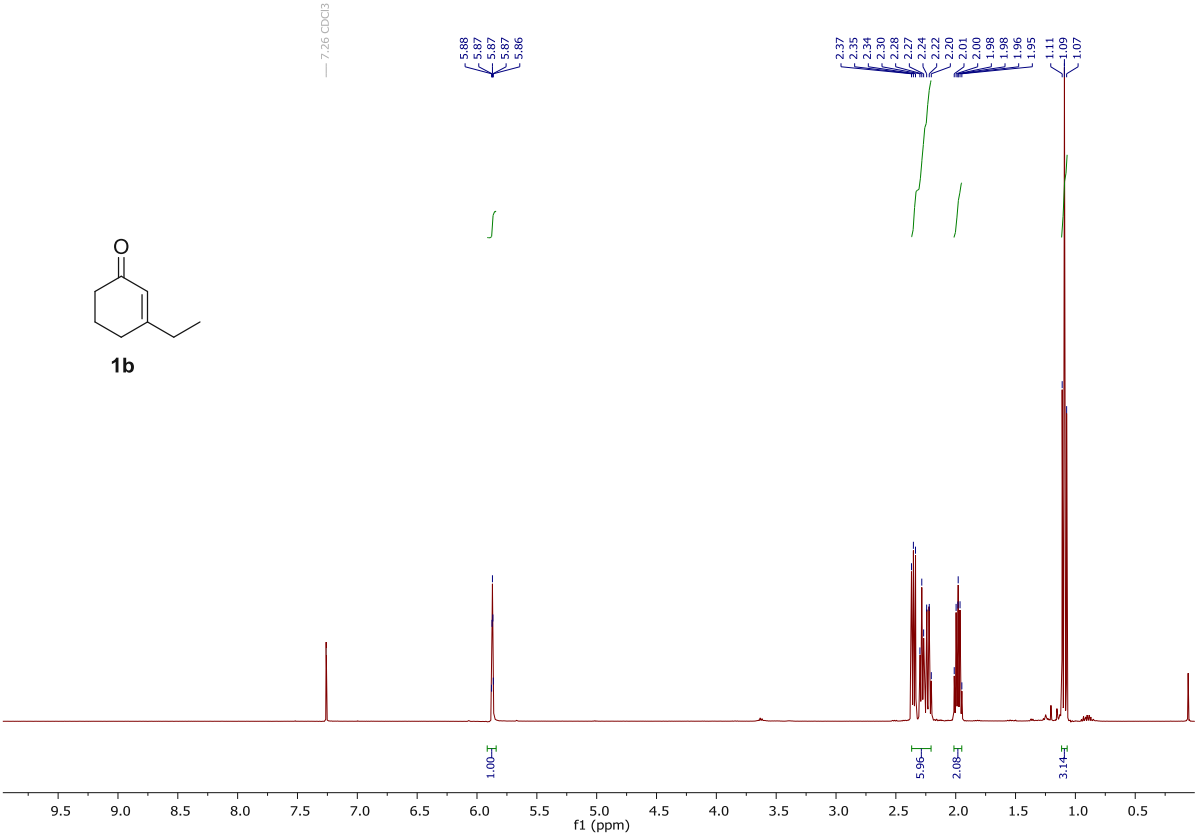
7



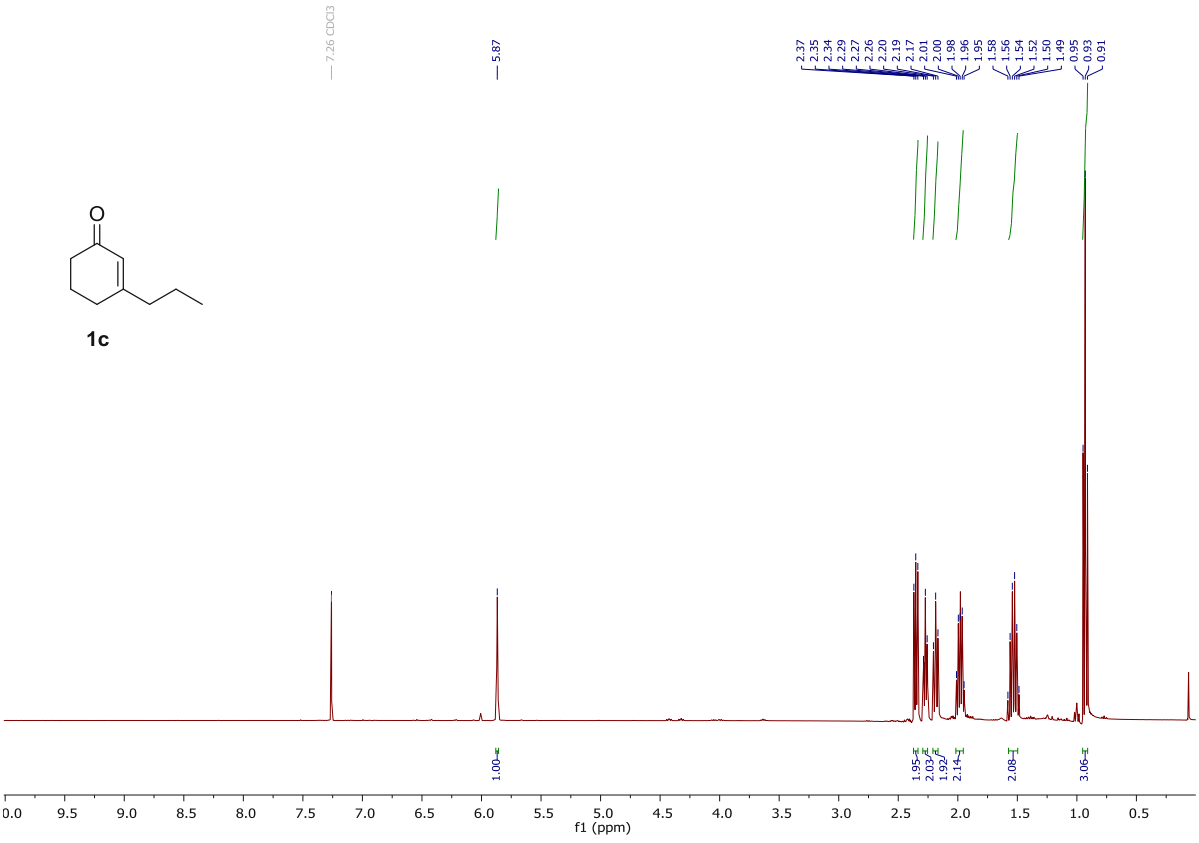
7

Die approbierte gedruckte Originalversion dieser Dissertation ist an der TU Wien Bibliothek verfügbar.
The approved original version of this doctoral thesis is available in print at TU Wien Bibliothek.

10. NMR specta of ATH substrates

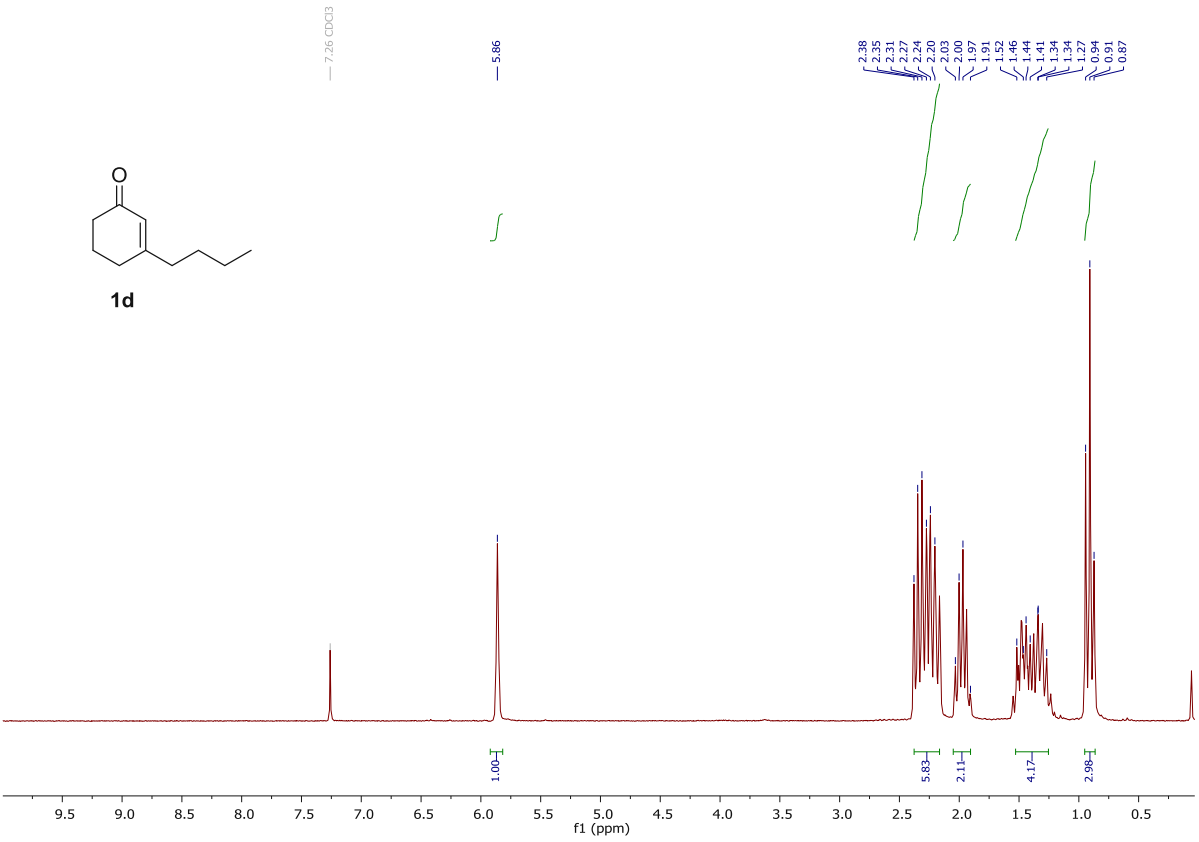


1b

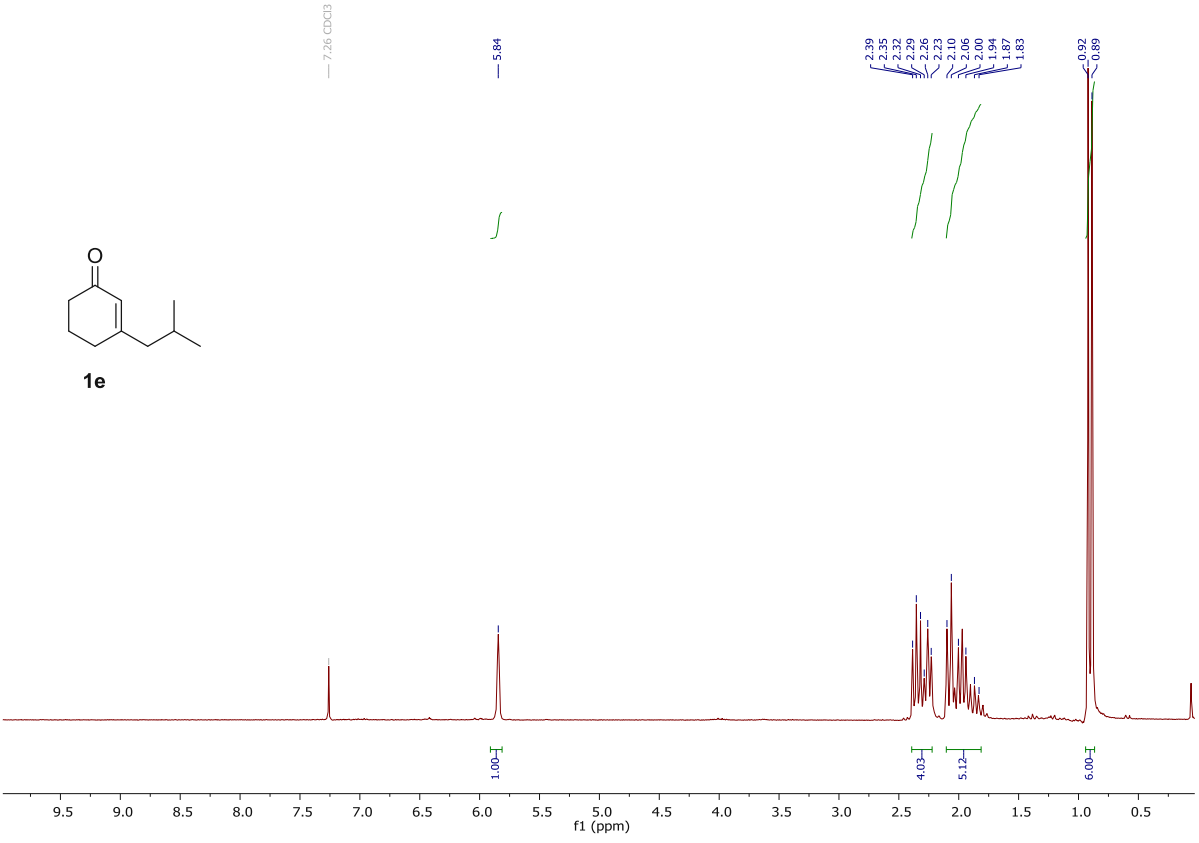


1c

Die approbierte gedruckte Originalversion dieser Dissertation ist an der TU Wien Bibliothek verfügbar.
The approved original version of this doctoral thesis is available in print at TU Wien Bibliothek.

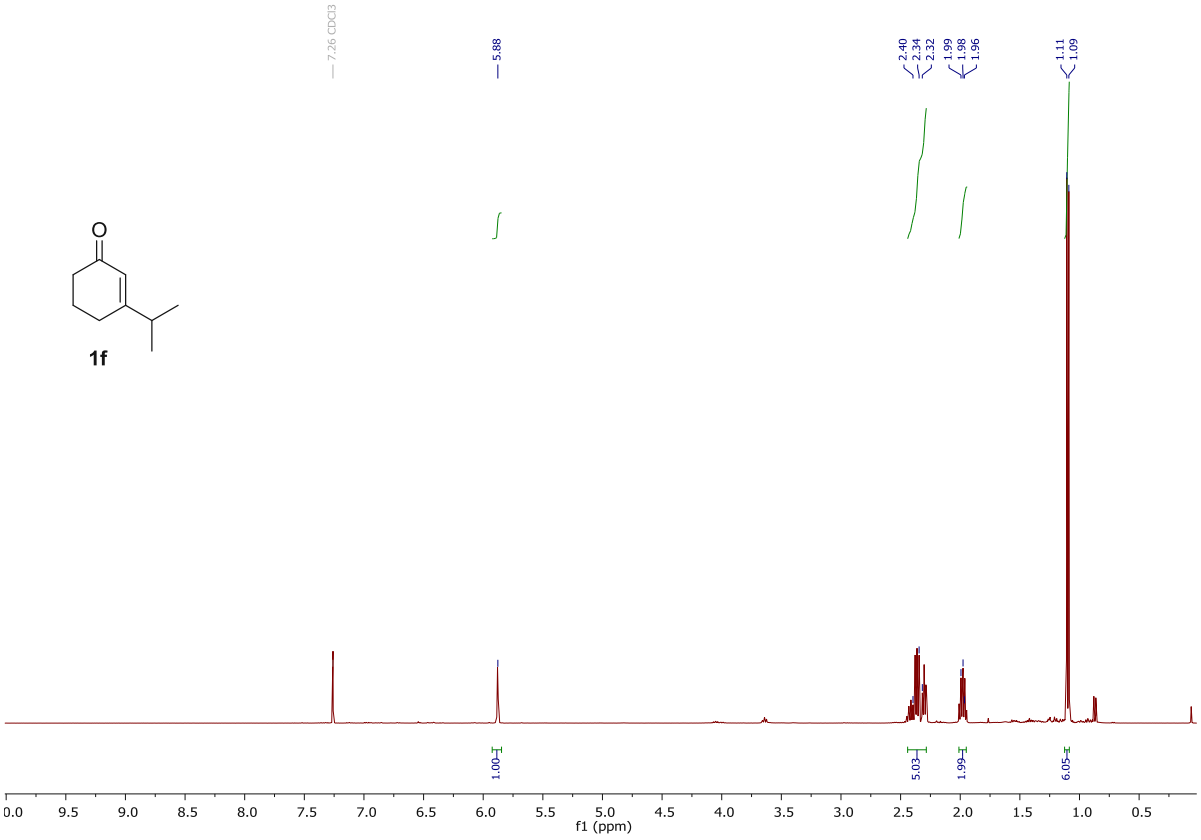


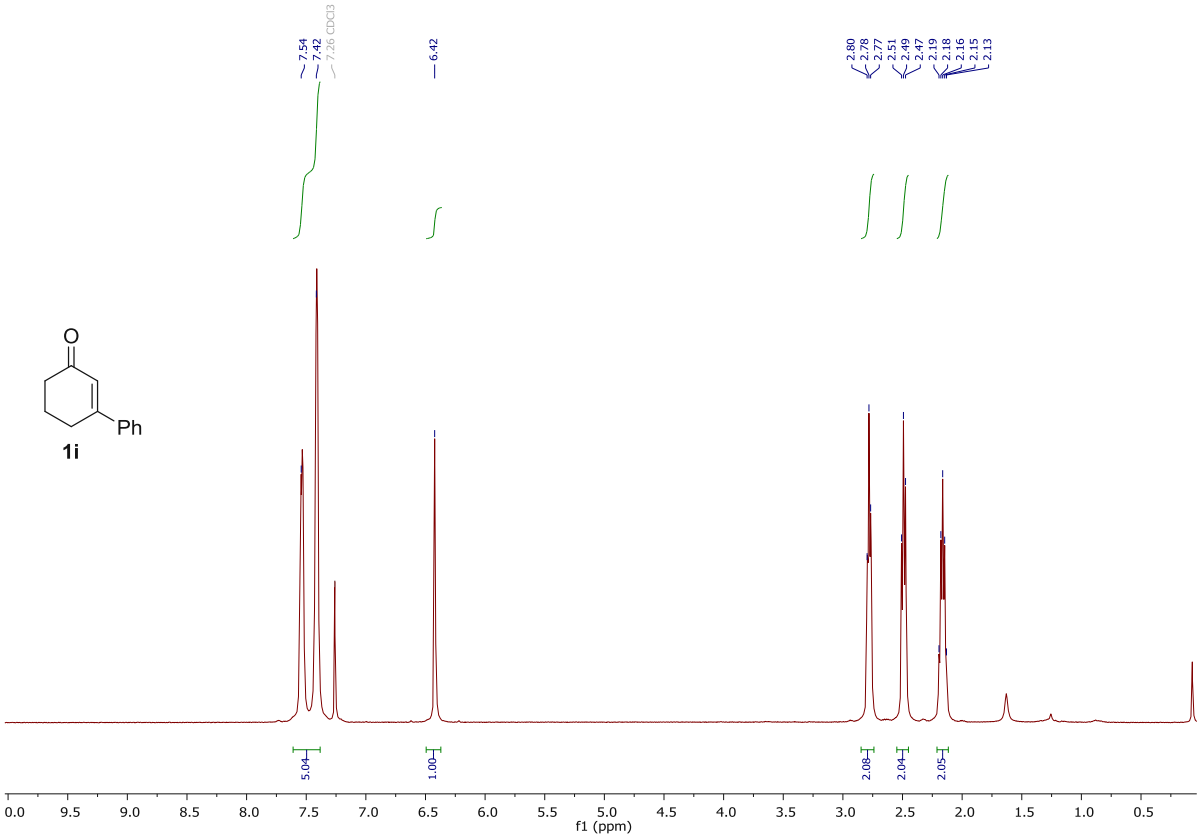
1d



1e

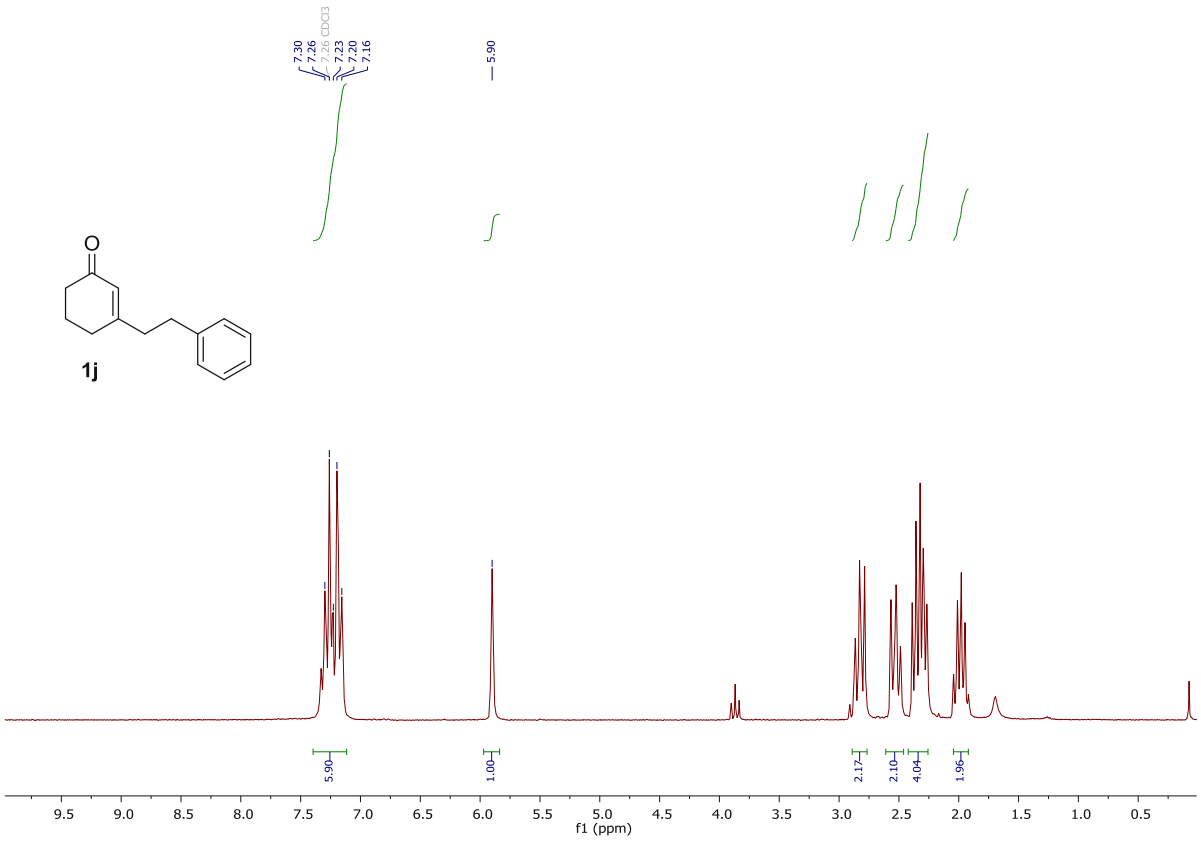
Die approbierte gedruckte Originalversion dieser Dissertation ist an der TU Wien Bibliothek verfügbar.
The approved original version of this doctoral thesis is available in print at TU Wien Bibliothek.

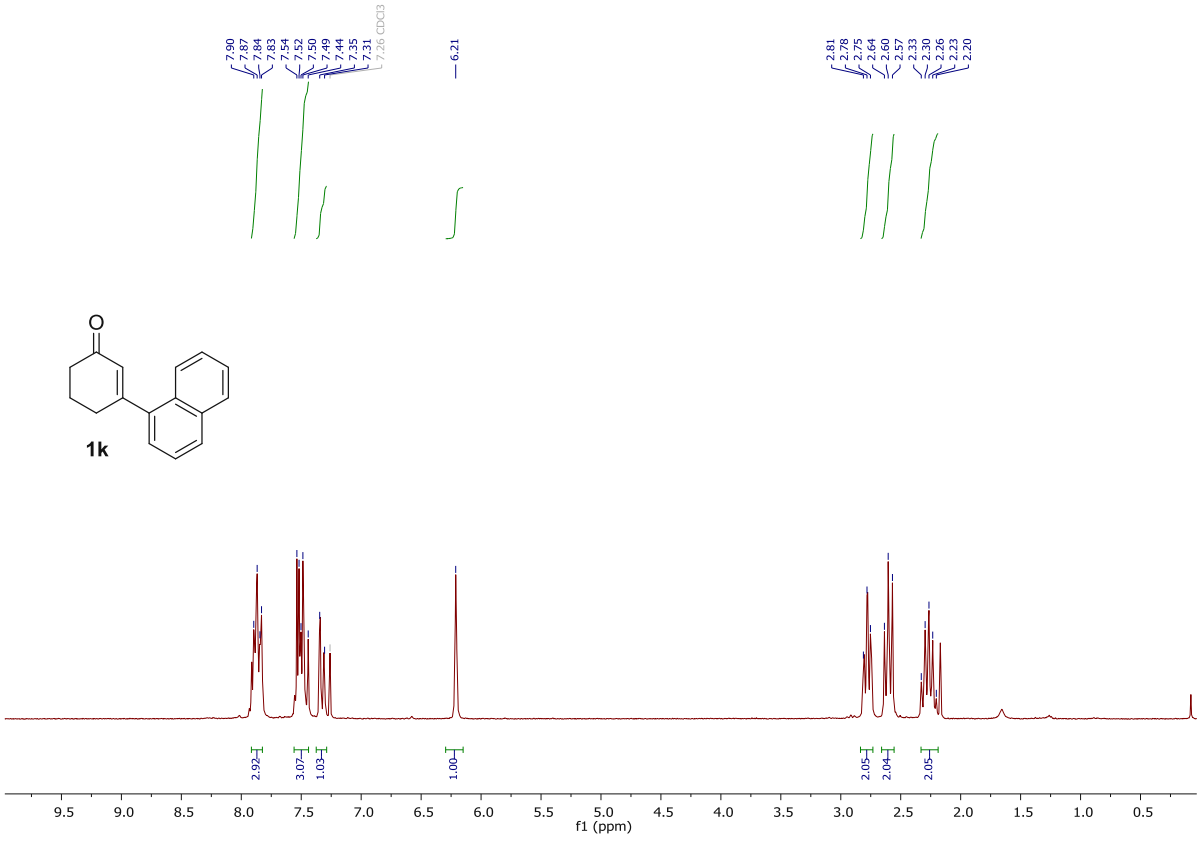


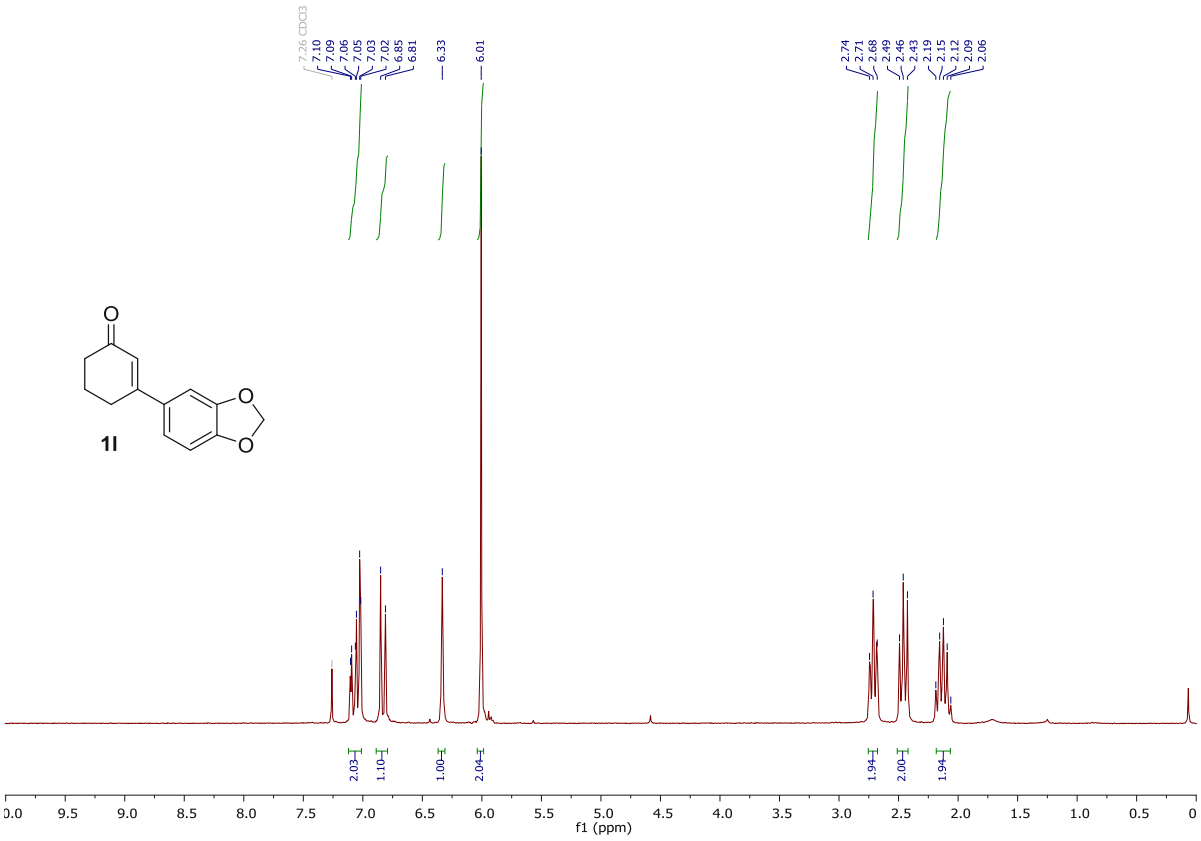


Die approbierte gedruckte Originalversion dieser Dissertation ist an der TU Wien Bibliothek verfügbar.
The approved original version of this doctoral thesis is available in print at TU Wien Bibliothek.

Die approbierte gedruckte Originalversion dieser Dissertation ist an der TU Wien Bibliothek verfügbar.
The approved original version of this doctoral thesis is available in print at TU Wien Bibliothek.

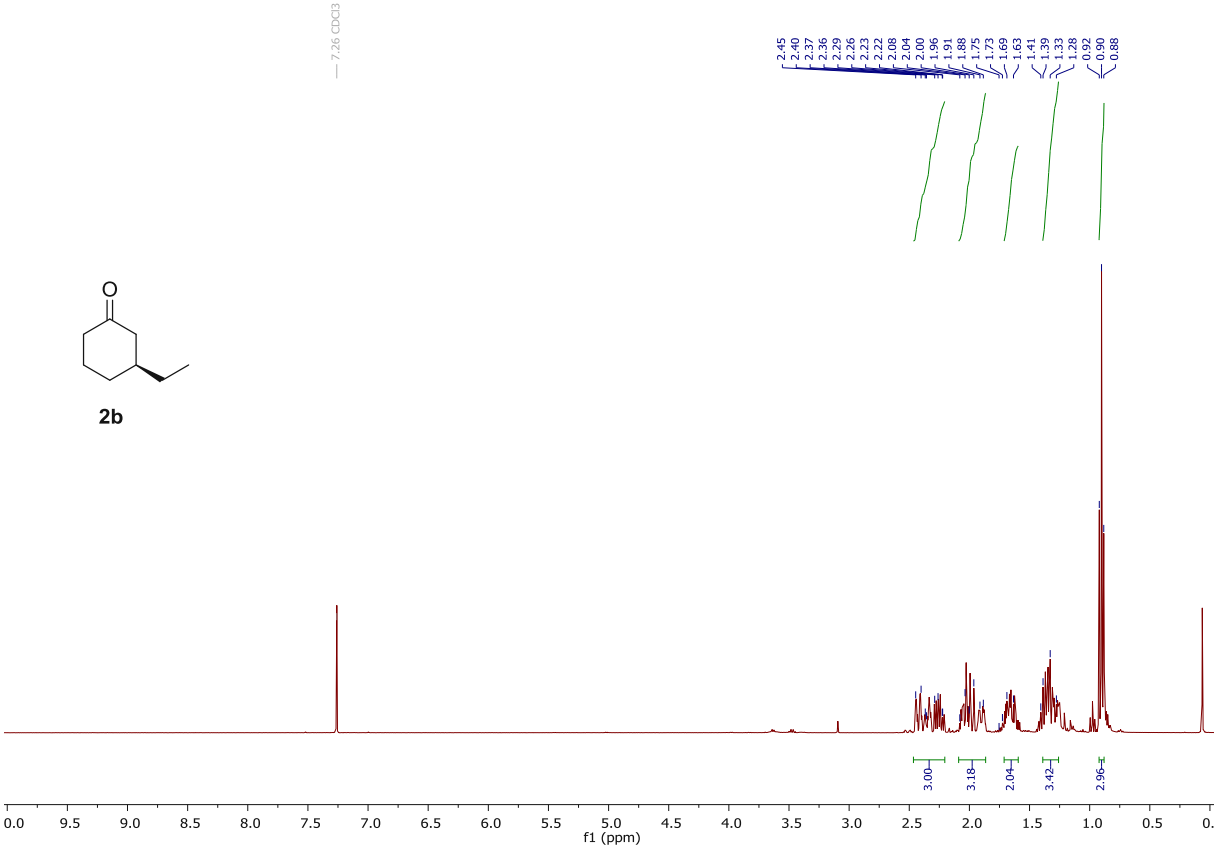




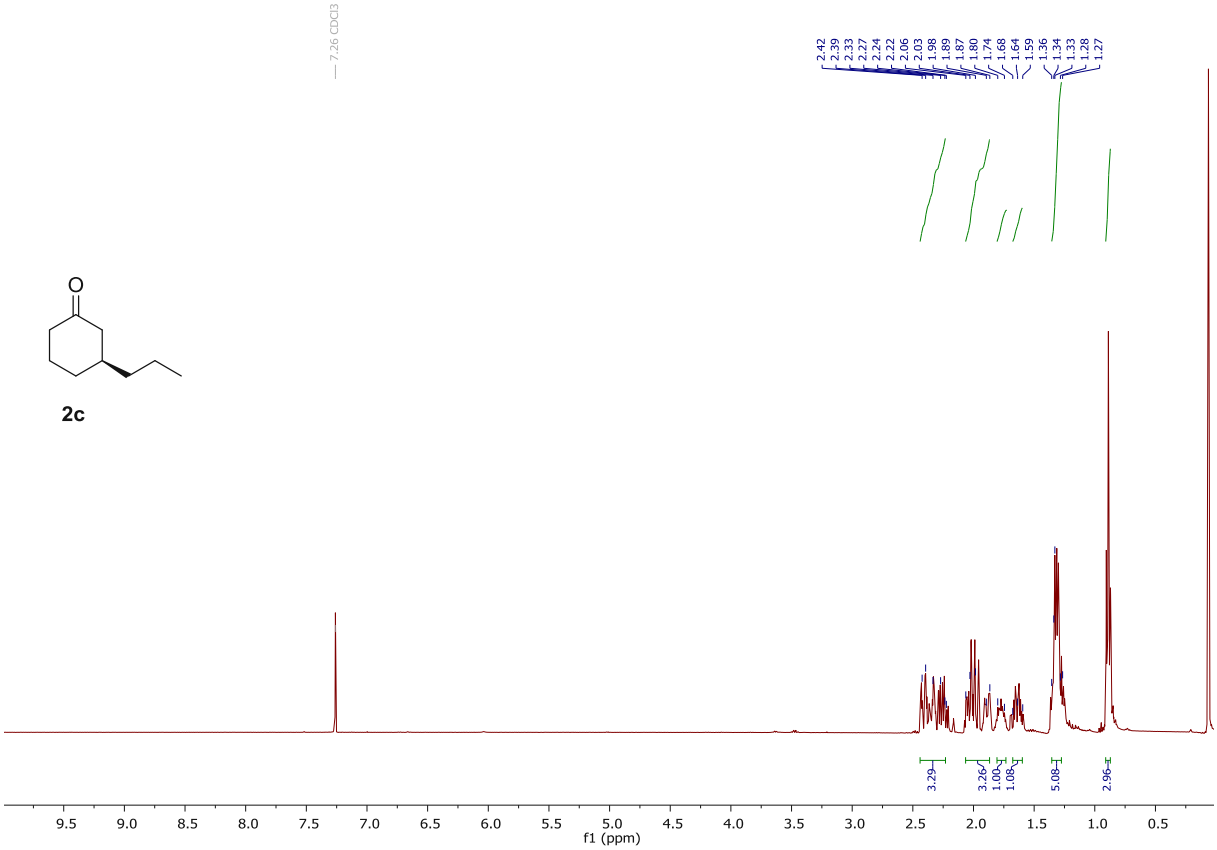


Die approbierte gedruckte Originalversion dieser Dissertation ist an der TU Wien Bibliothek verfügbar.
The approved original version of this doctoral thesis is available in print at TU Wien Bibliothek.

11. NMR specta of ATH products



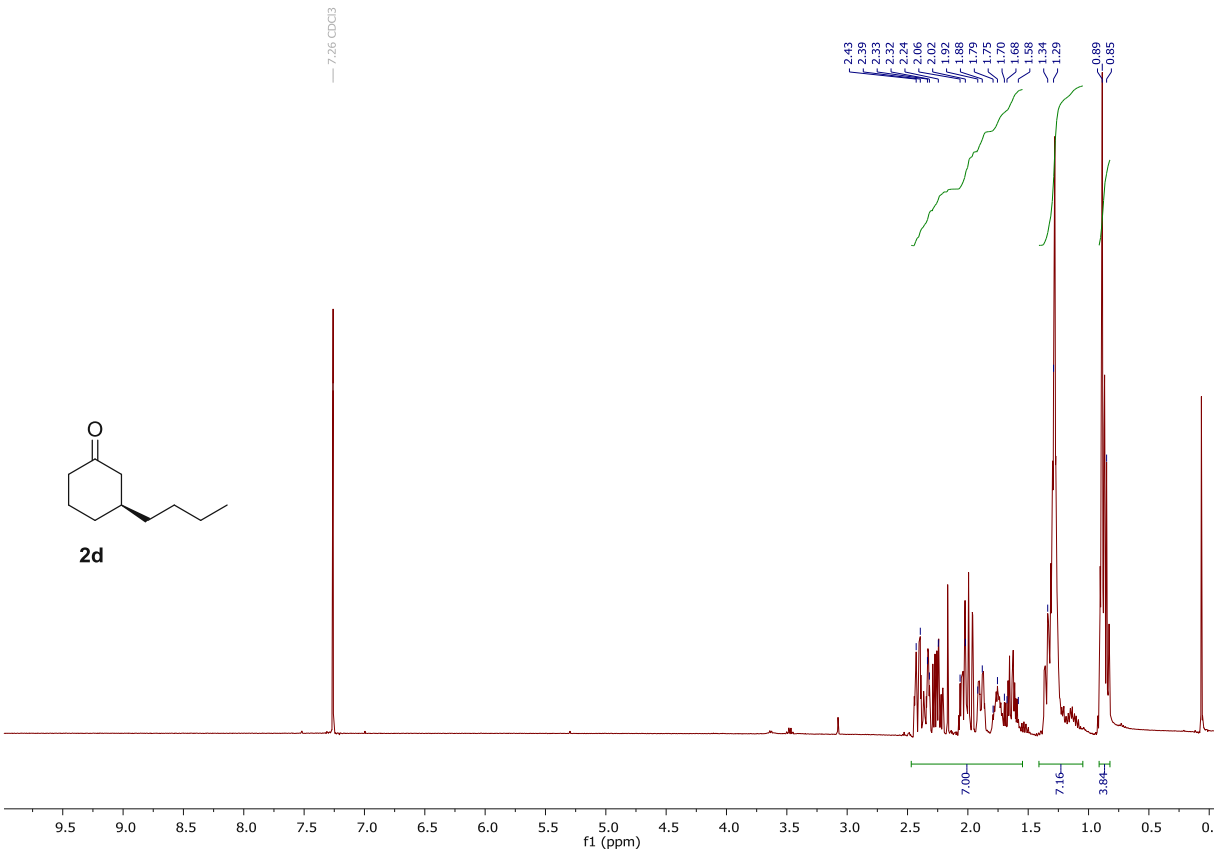
2b



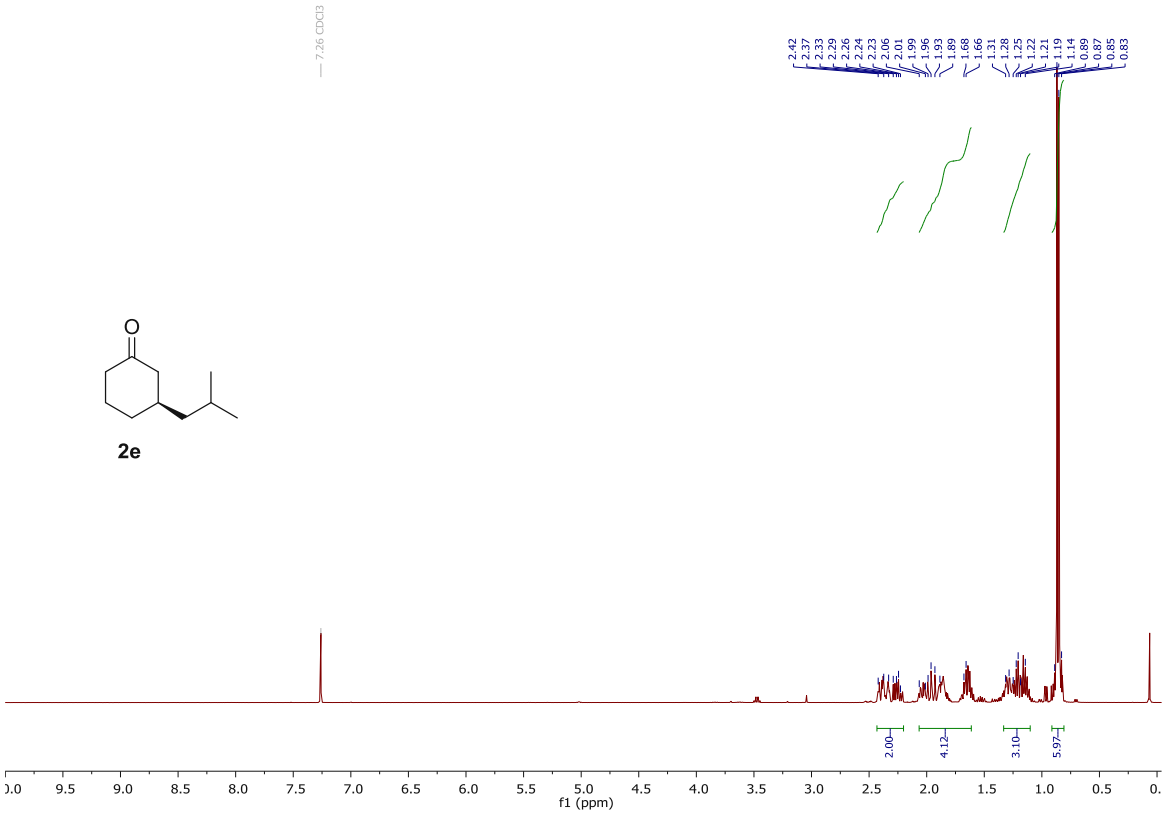
2c

Die approbierte gedruckte Originalversion dieser Dissertation ist an der TU Wien Bibliothek verfügbar.
The approved original version of this doctoral thesis is available in print at TU Wien Bibliothek.

Die approbierte gedruckte Originalversion dieser Dissertation ist an der TU Wien Bibliothek verfügbar.
The approved original version of this doctoral thesis is available in print at TU Wien Bibliothek.

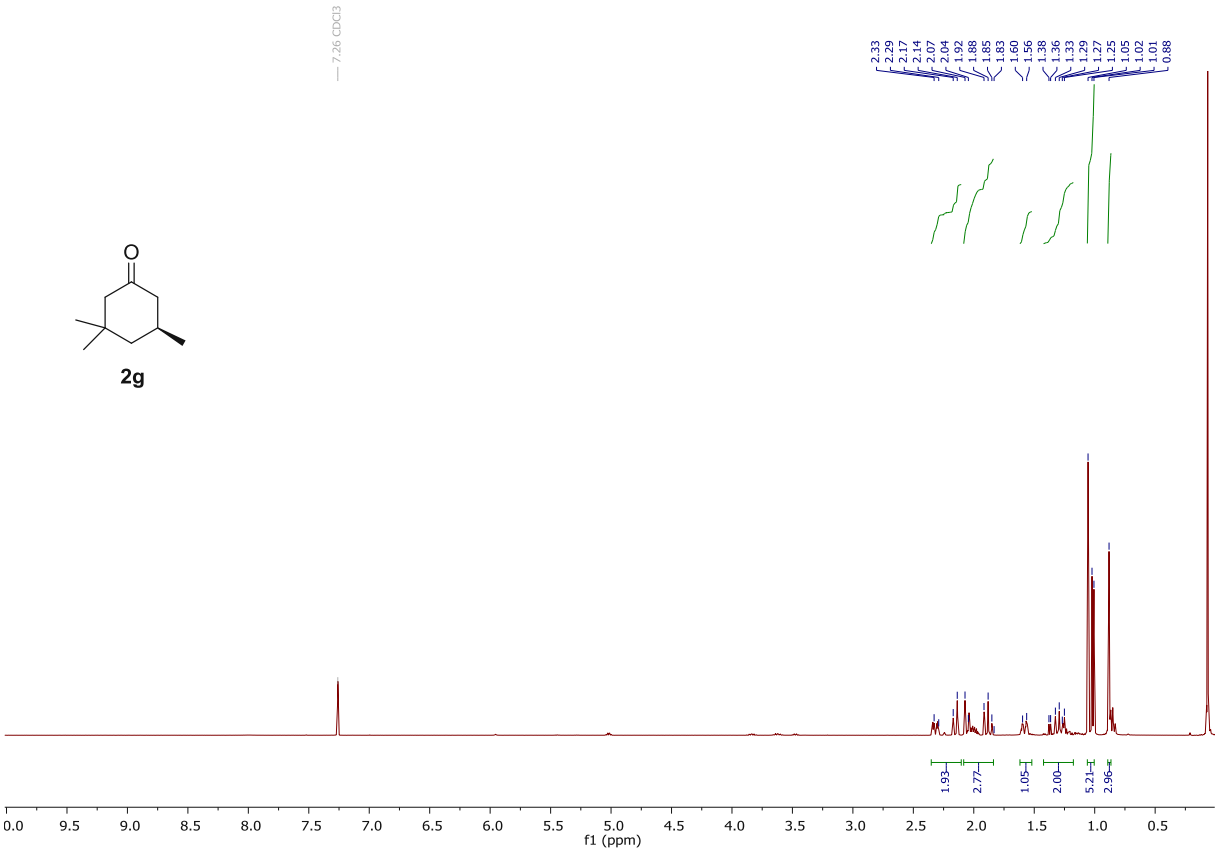


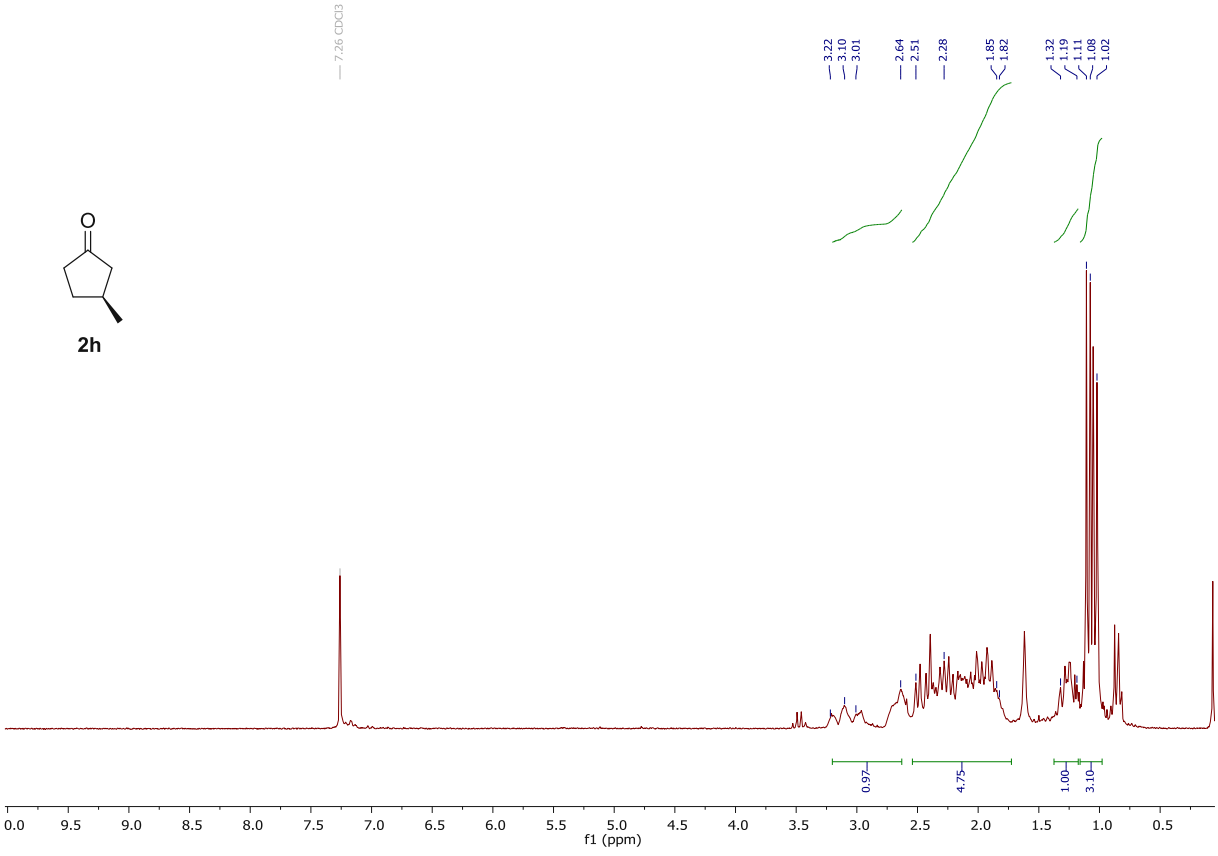
2d



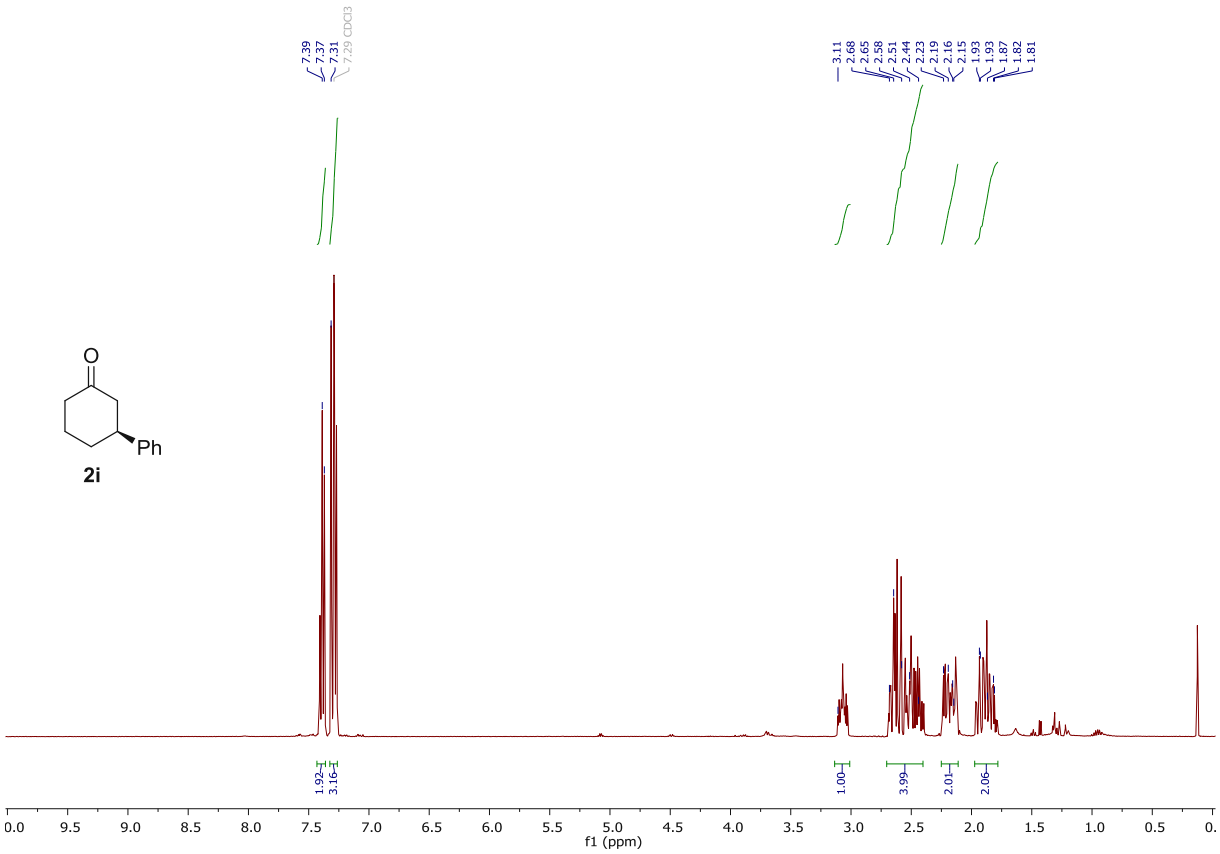
2e

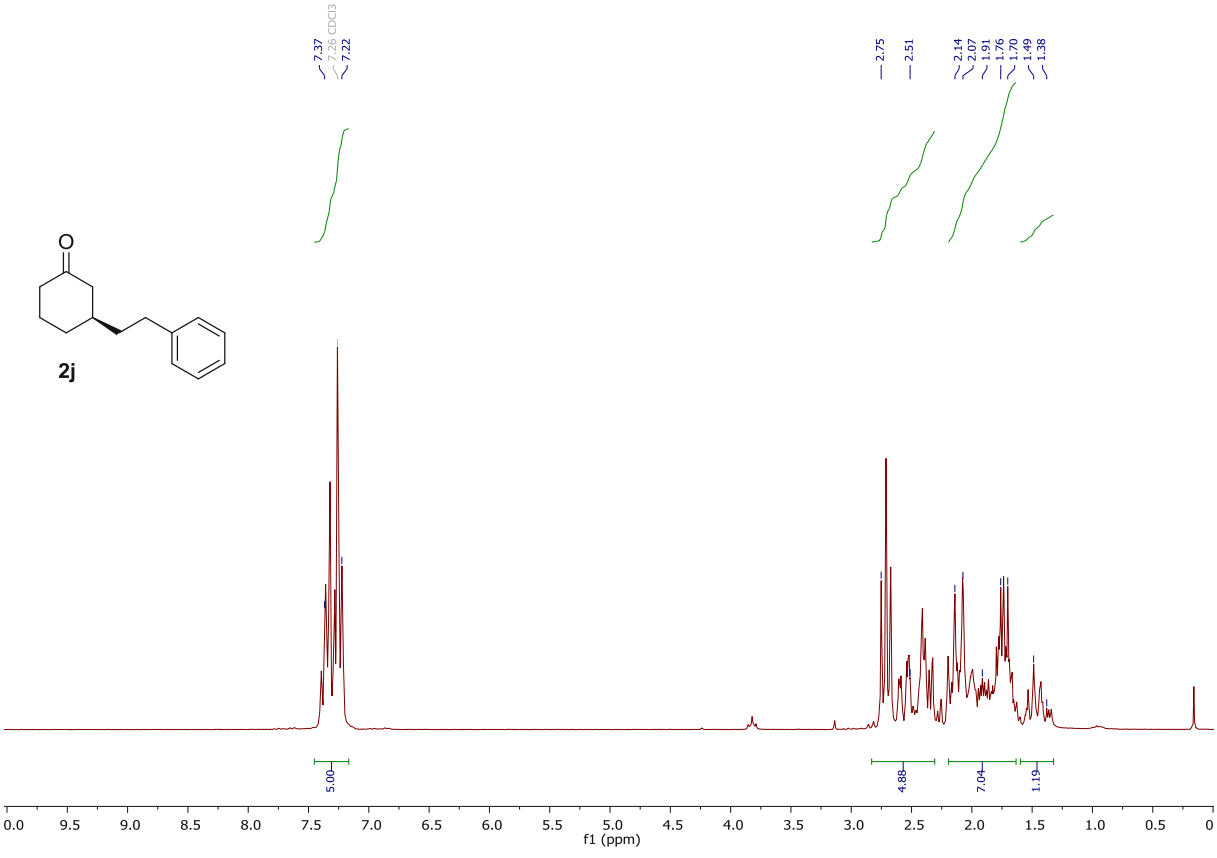
Die approbierte gedruckte Originalversion dieser Dissertation ist an der TU Wien Bibliothek verfügbar.
The approved original version of this doctoral thesis is available in print at TU Wien Bibliothek.

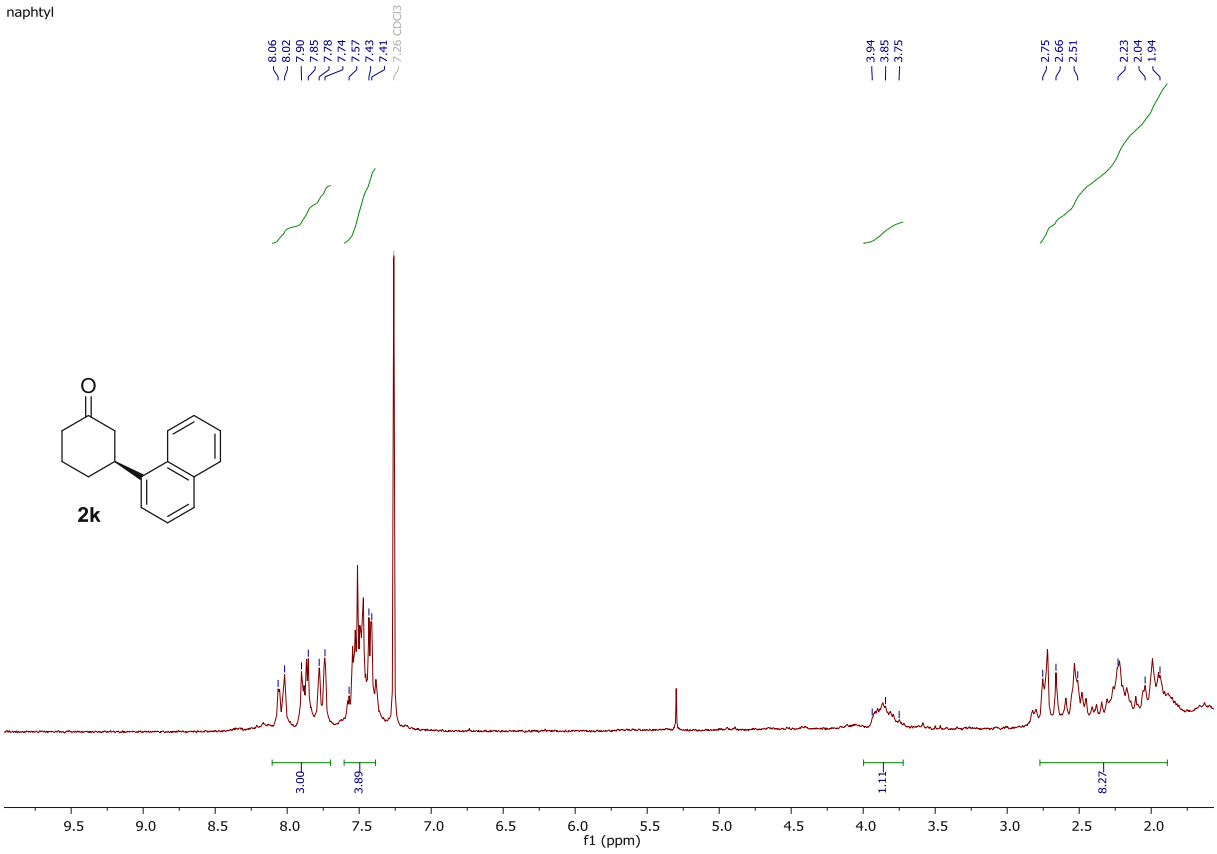


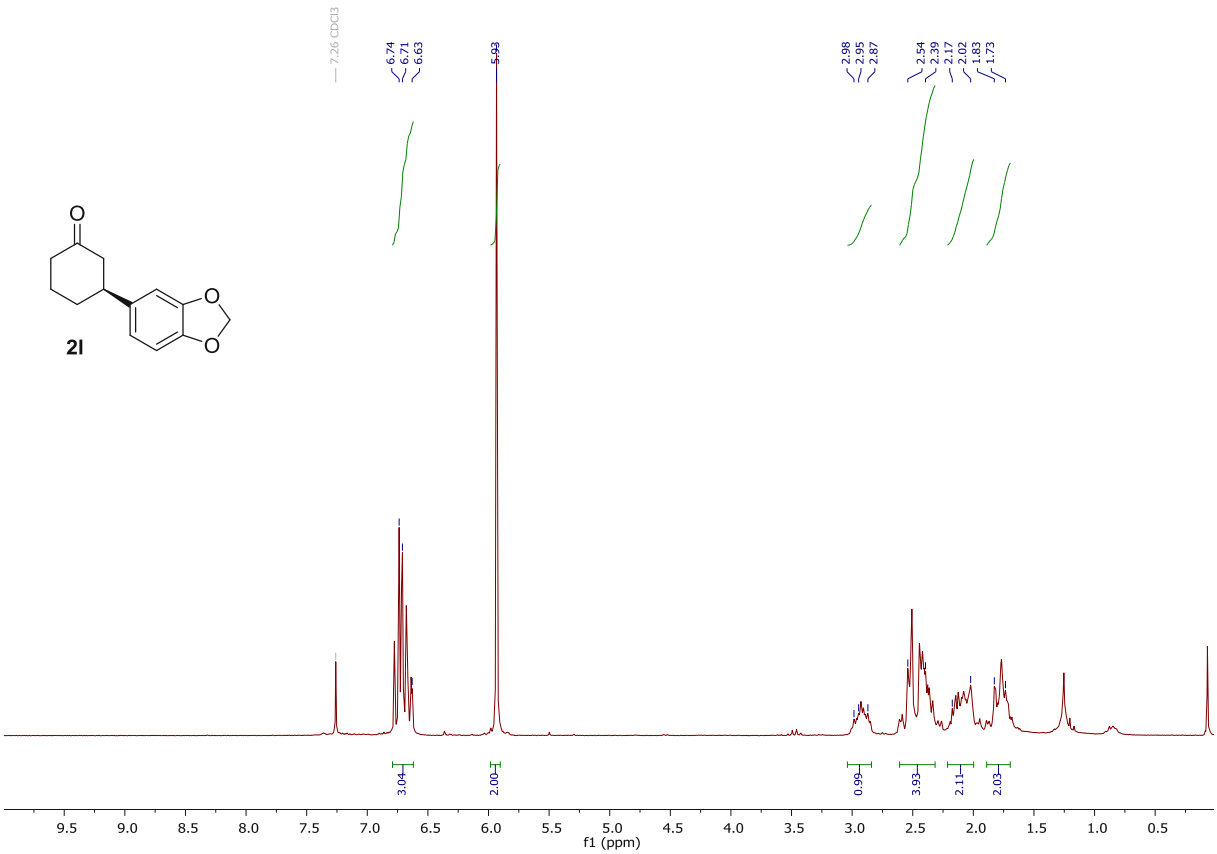


Die approbierte gedruckte Originalversion dieser Dissertation ist an der TU Wien Bibliothek verfügbar.
The approved original version of this doctoral thesis is available in print at TU Wien Bibliothek.

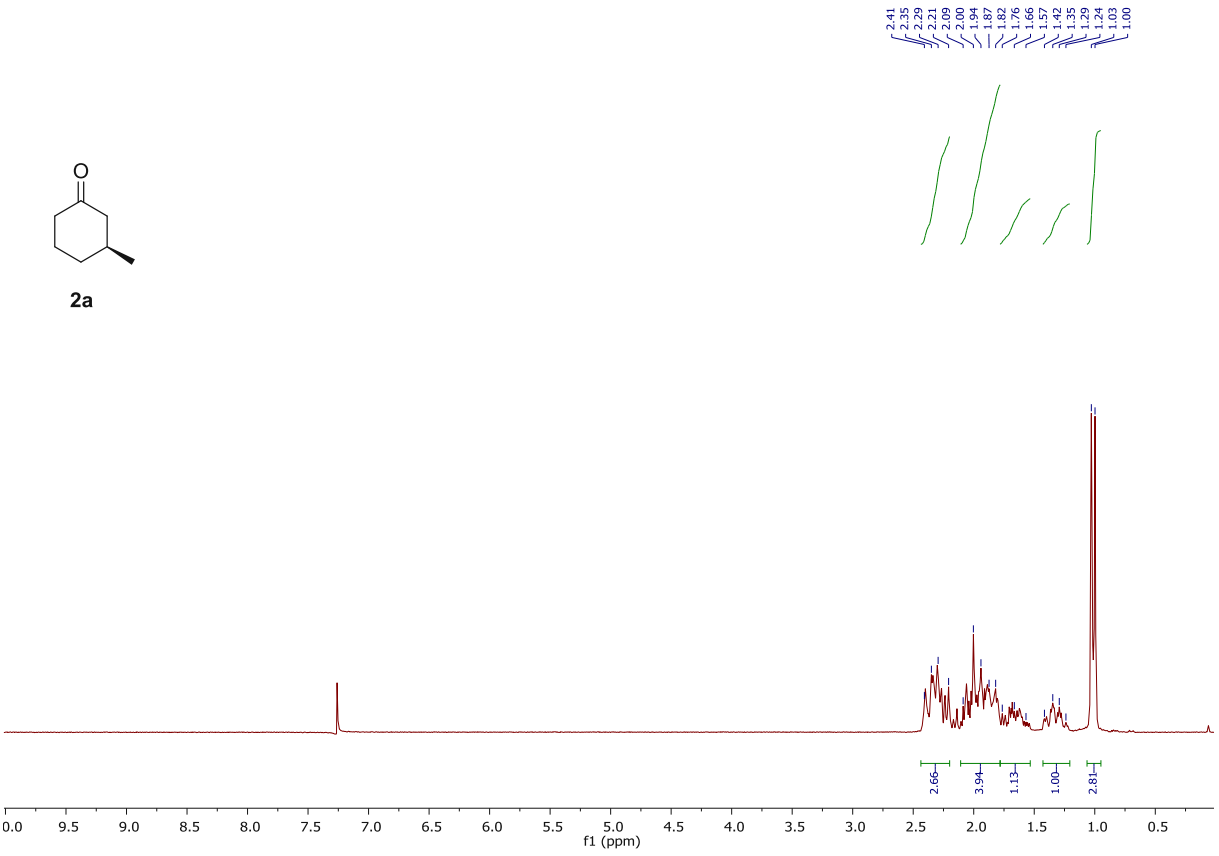






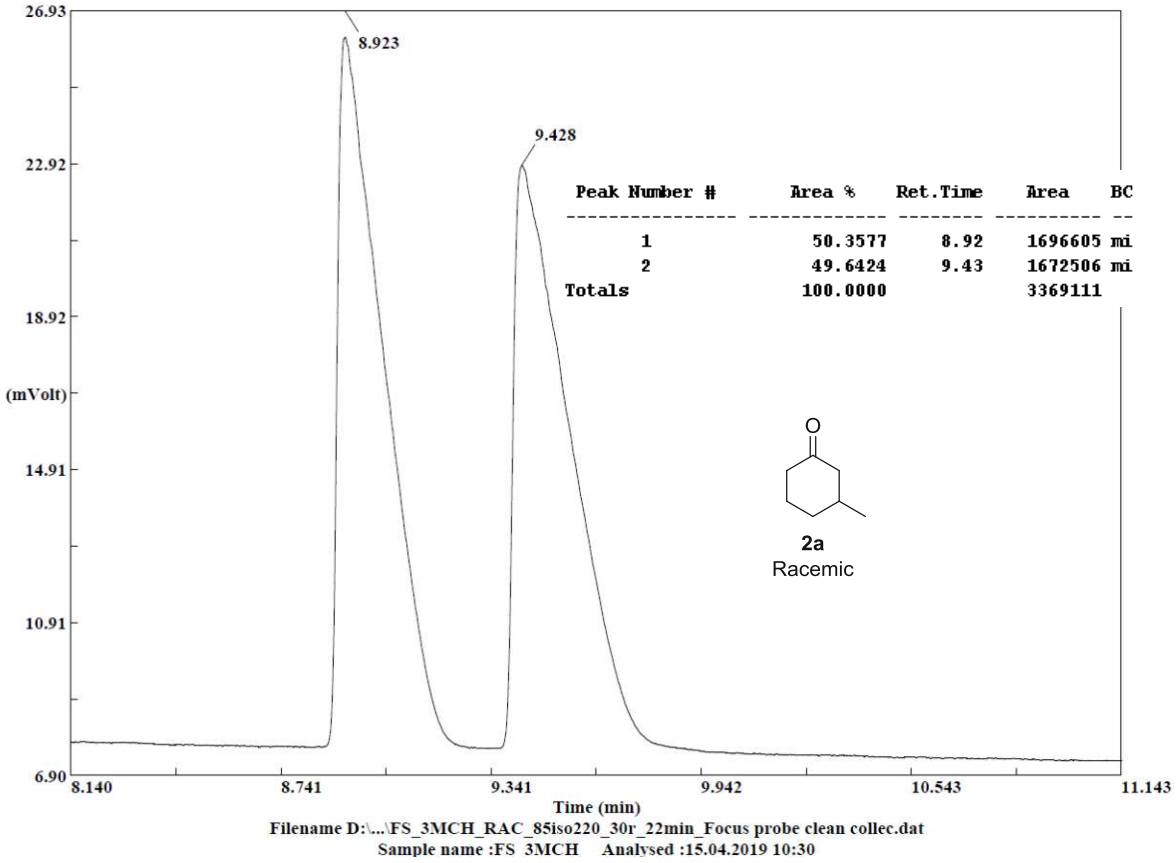


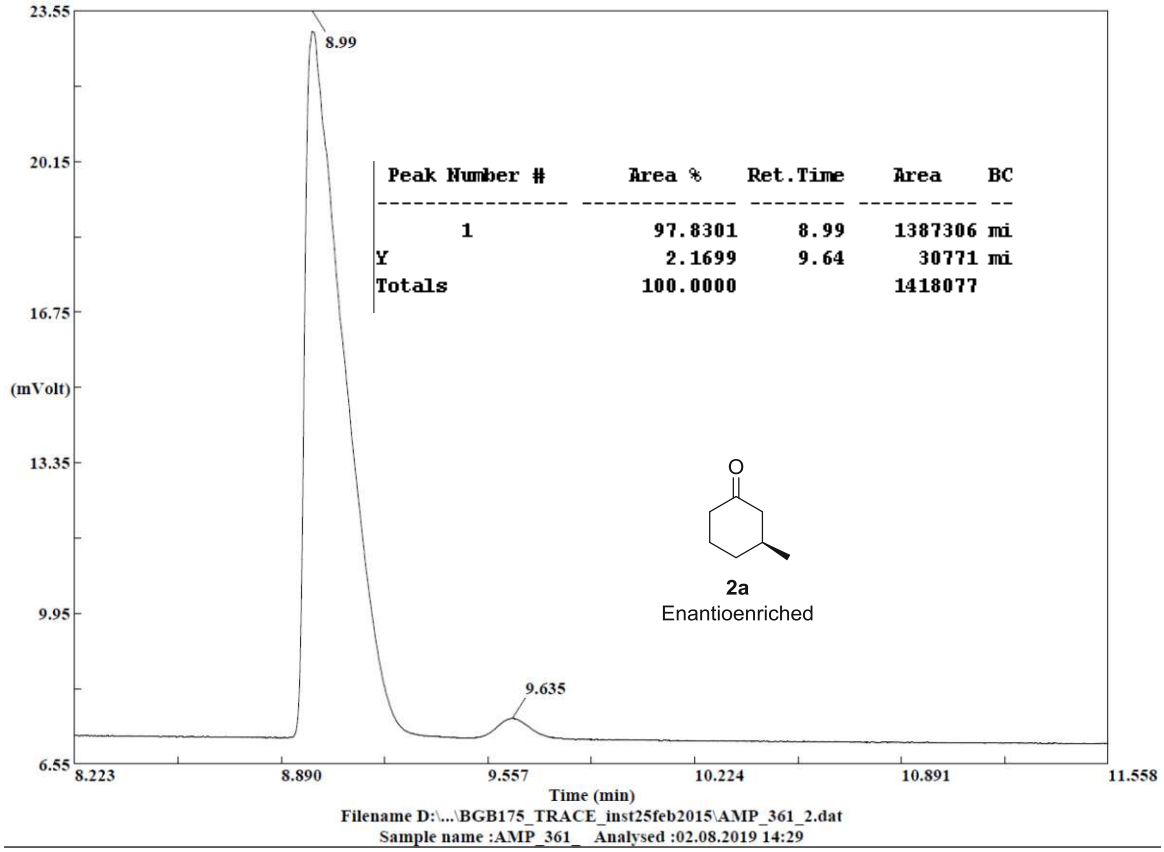
Die approbierte gedruckte Originalversion dieser Dissertation ist an der TU Wien Bibliothek verfügbar.
The approved original version of this doctoral thesis is available in print at TU Wien Bibliothek.



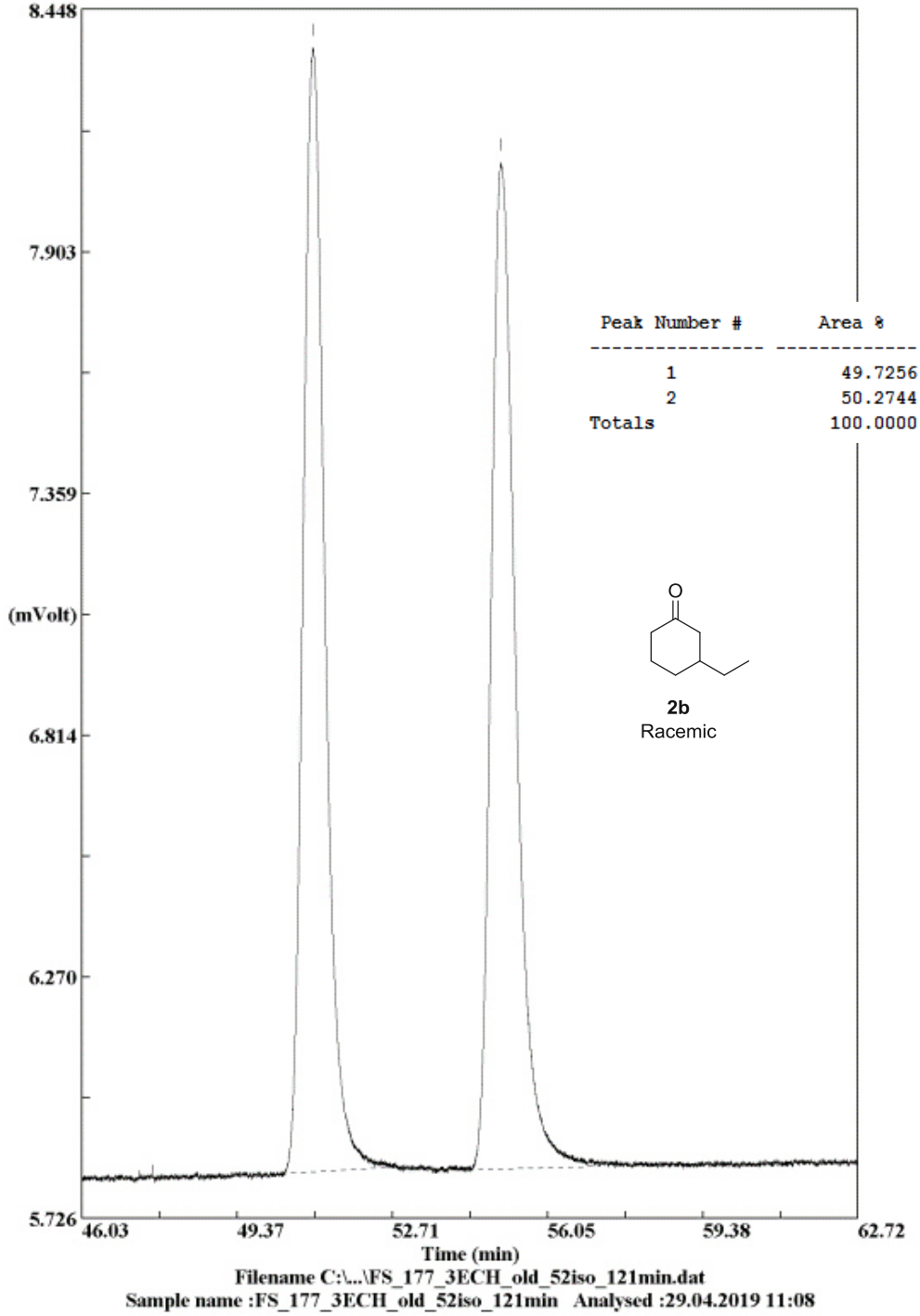
Die approbierte gedruckte Originalversion dieser Dissertation ist an der TU Wien Bibliothek verfügbar.
The approved original version of this doctoral thesis is available in print at TU Wien Bibliothek.

12. Chiral GC and HPLC traces





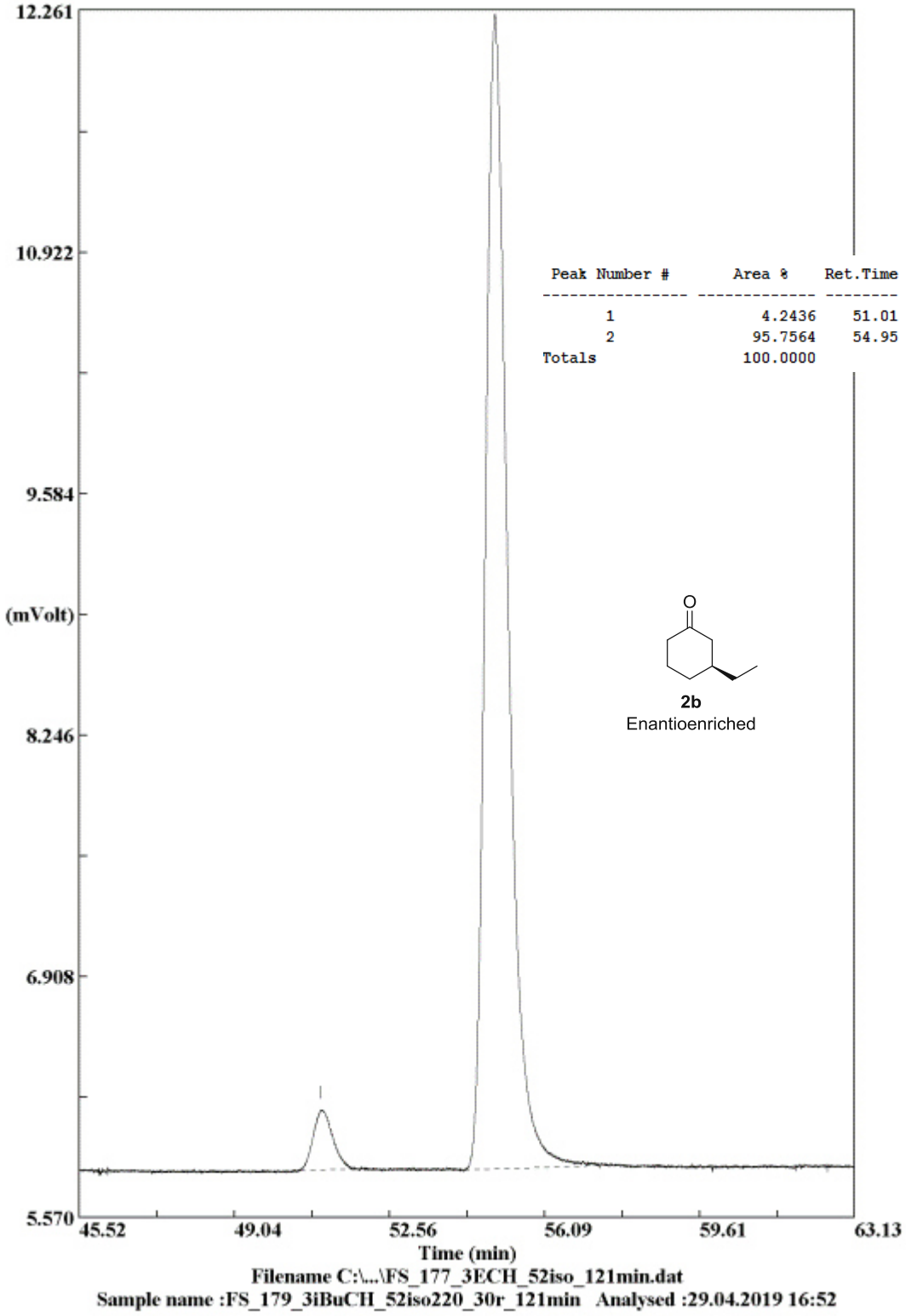
Die approbierte gedruckte Originalversion dieser Dissertation ist an der TU Wien Bibliothek verfügbar.
The approved original version of this doctoral thesis is available in print at TU Wien Bibliothek.



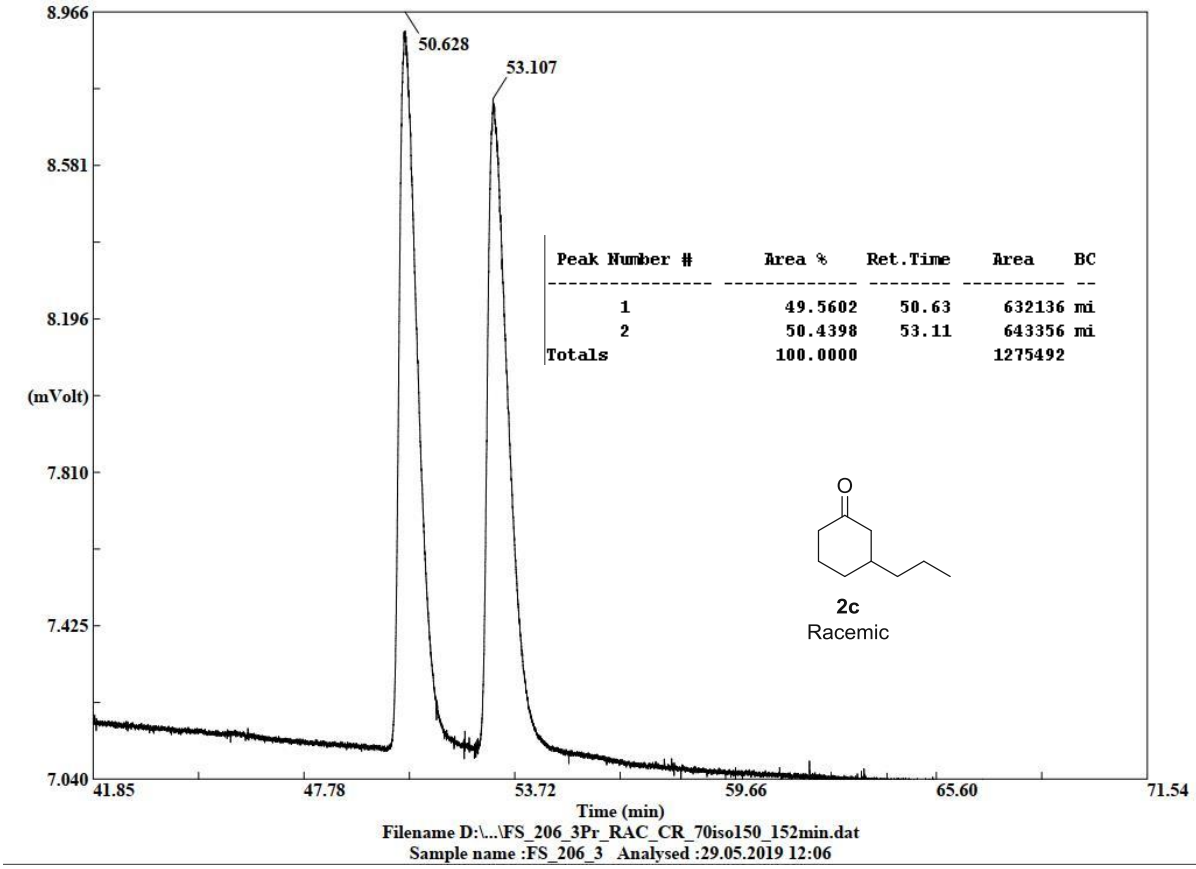
Peak Number #	Area %	Ret.Time	Area	BC
1	49.7256	50.99	828902	mi
2	50.2744	55.04	838049	mi
Totals	100.0000		1666951	

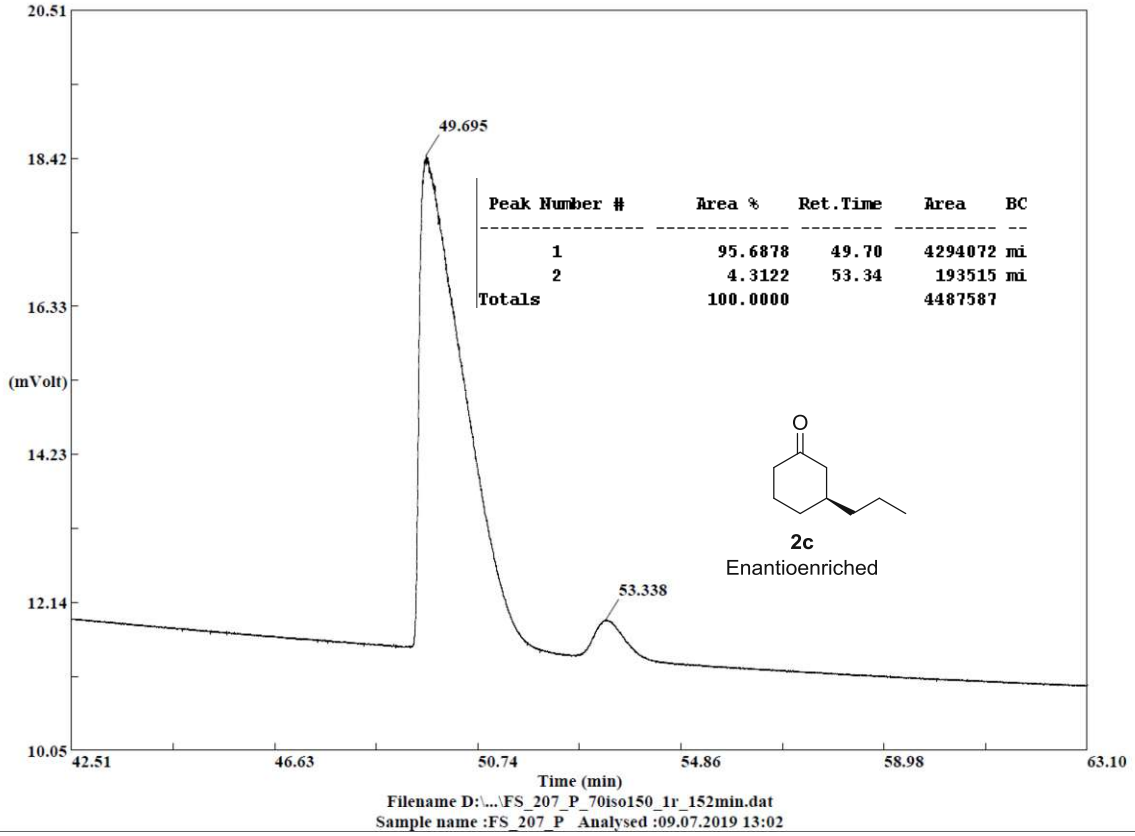
2b
Racemic

Die approbierte gedruckte Originalversion dieser Dissertation ist an der TU Wien Bibliothek verfügbar.
The approved original version of this doctoral thesis is available in print at TU Wien Bibliothek.

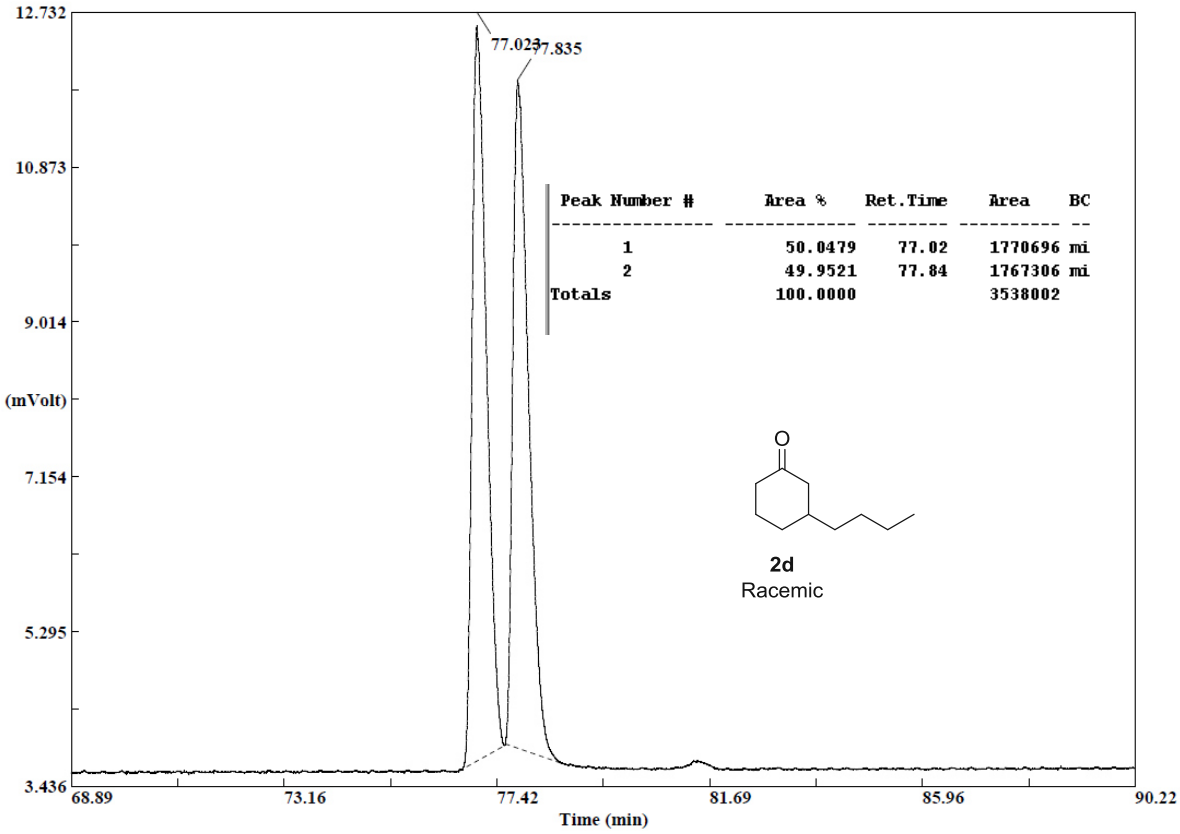


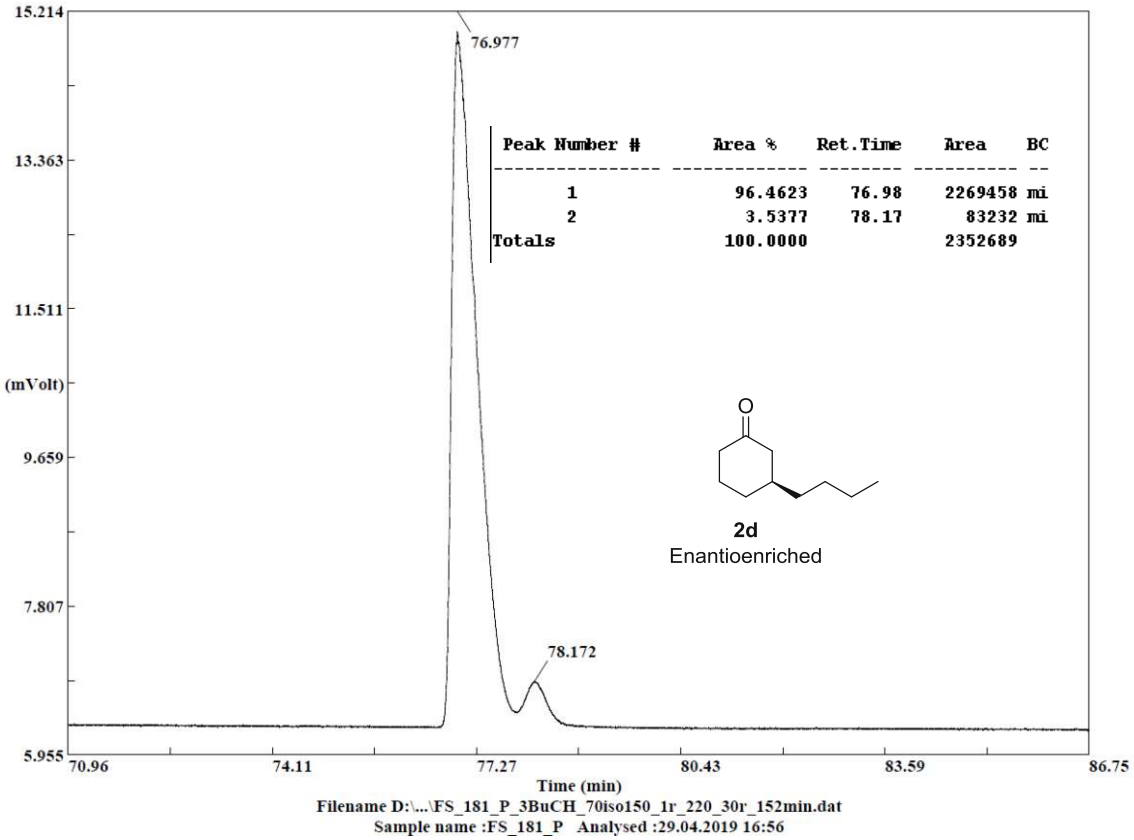
Die approbierte gedruckte Originalversion dieser Dissertation ist an der TU Wien Bibliothek verfügbar.
The approved original version of this doctoral thesis is available in print at TU Wien Bibliothek.



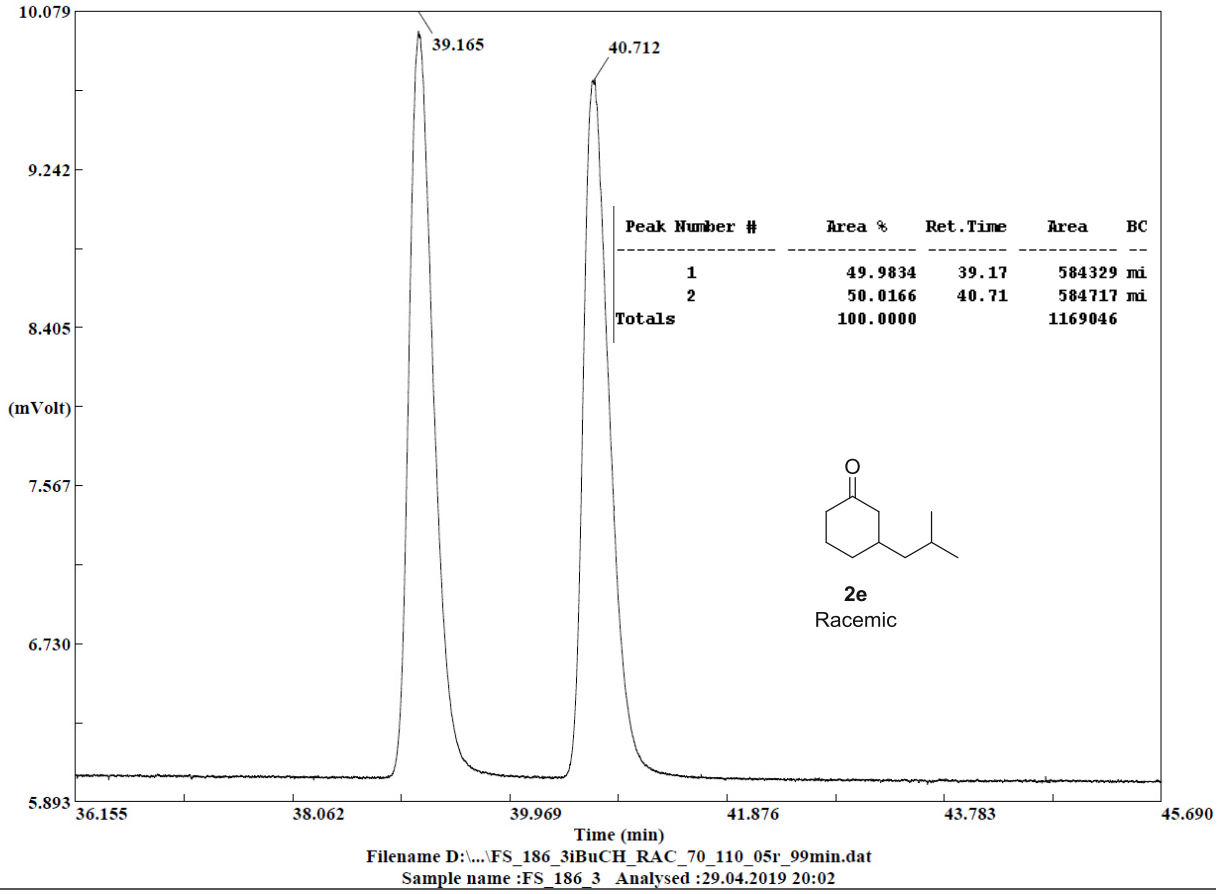


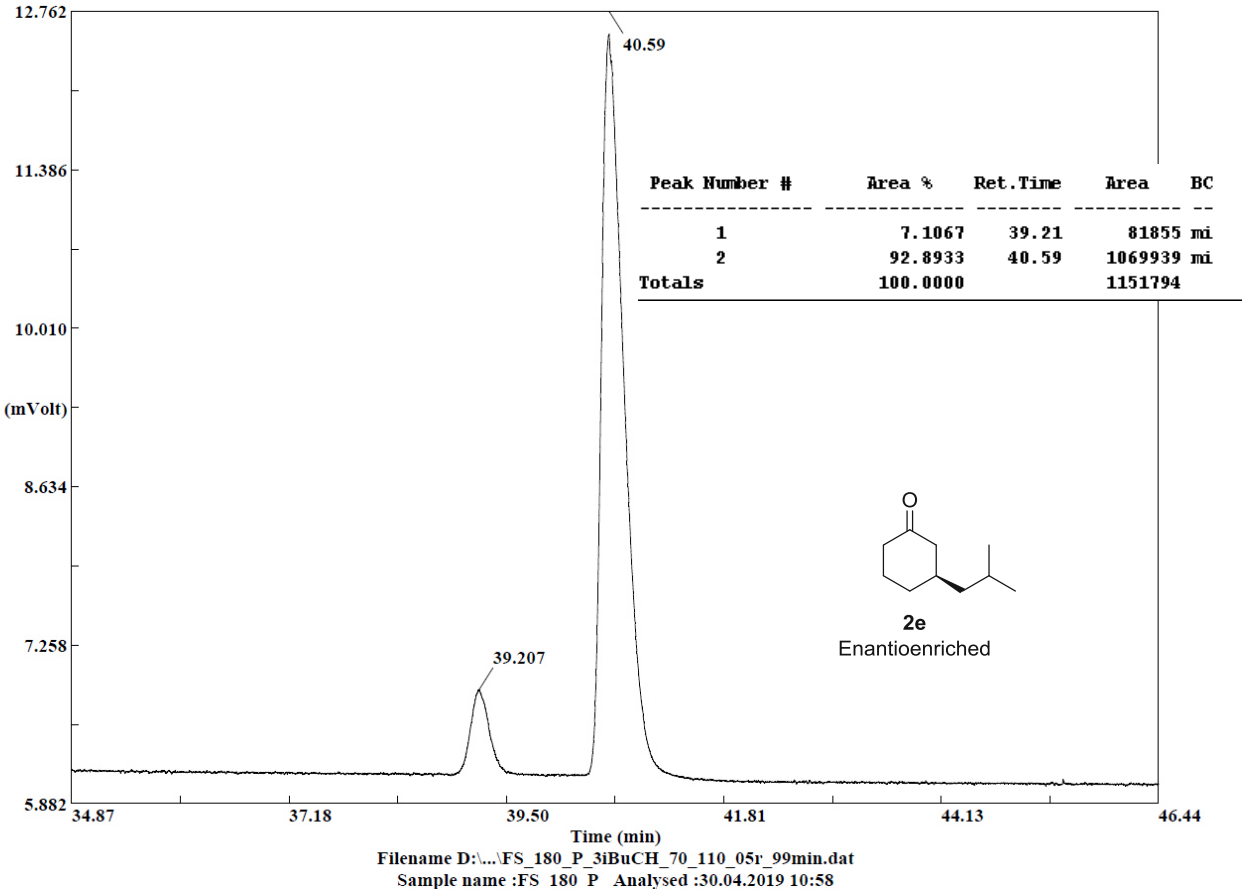
Die approbierte gedruckte Originalversion dieser Dissertation ist an der TU Wien Bibliothek verfügbar.
The approved original version of this doctoral thesis is available in print at TU Wien Bibliothek.



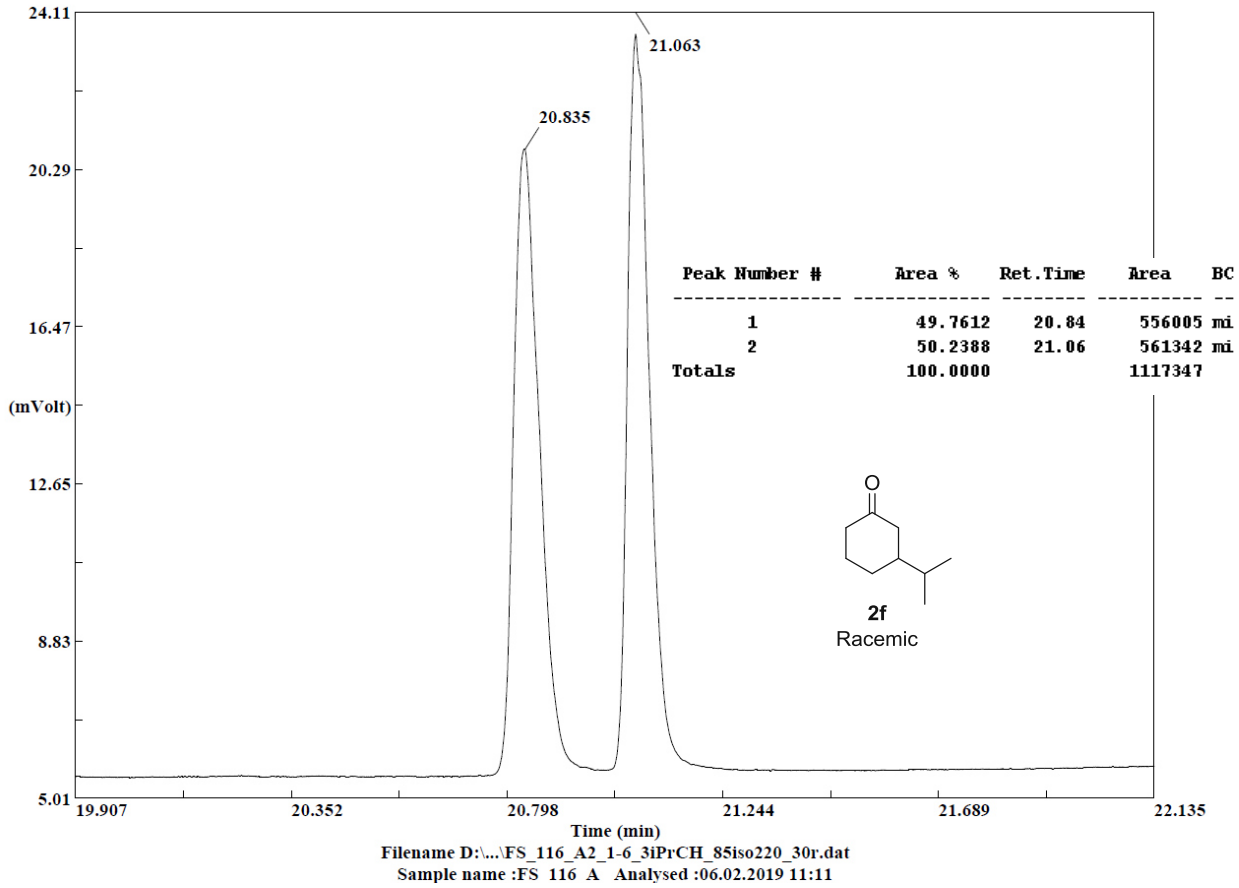


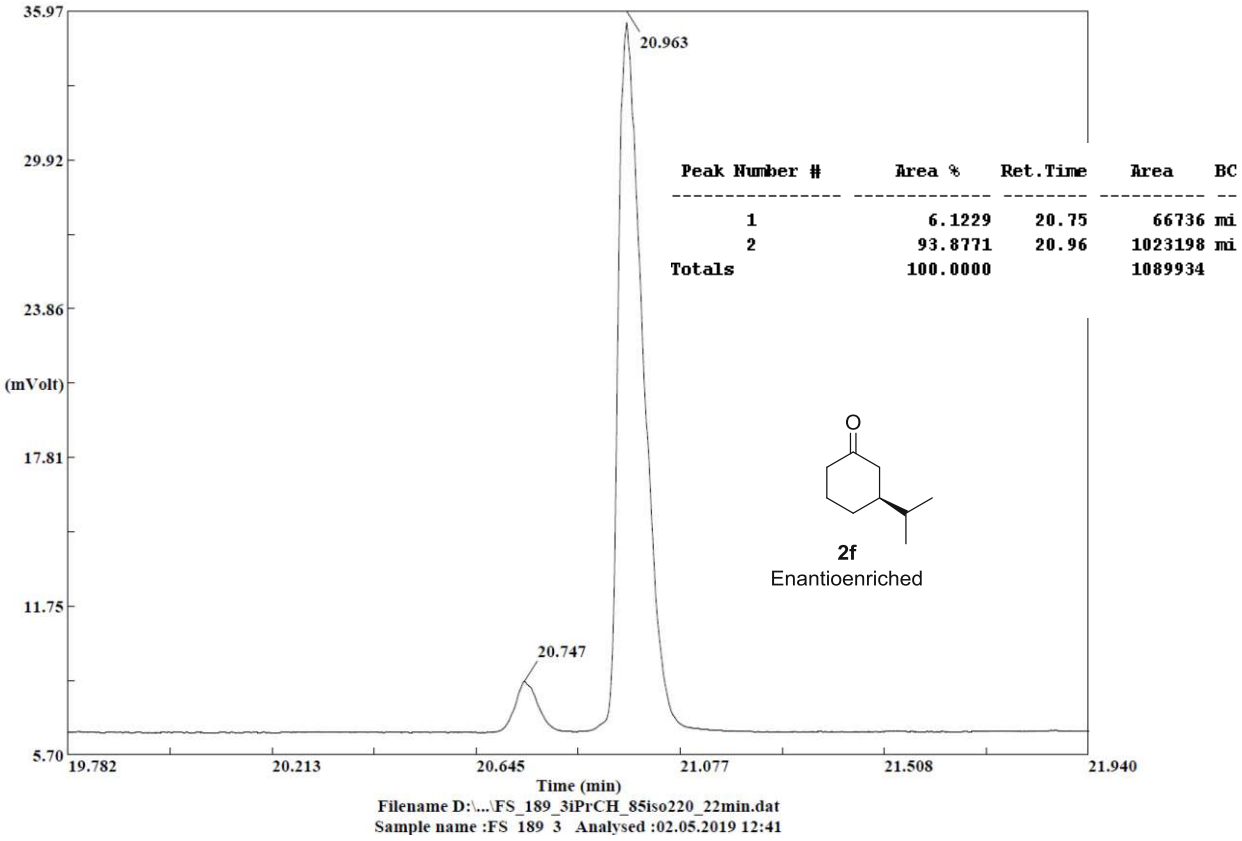
Die approbierte gedruckte Originalversion dieser Dissertation ist an der TU Wien Bibliothek verfügbar.
The approved original version of this doctoral thesis is available in print at TU Wien Bibliothek.



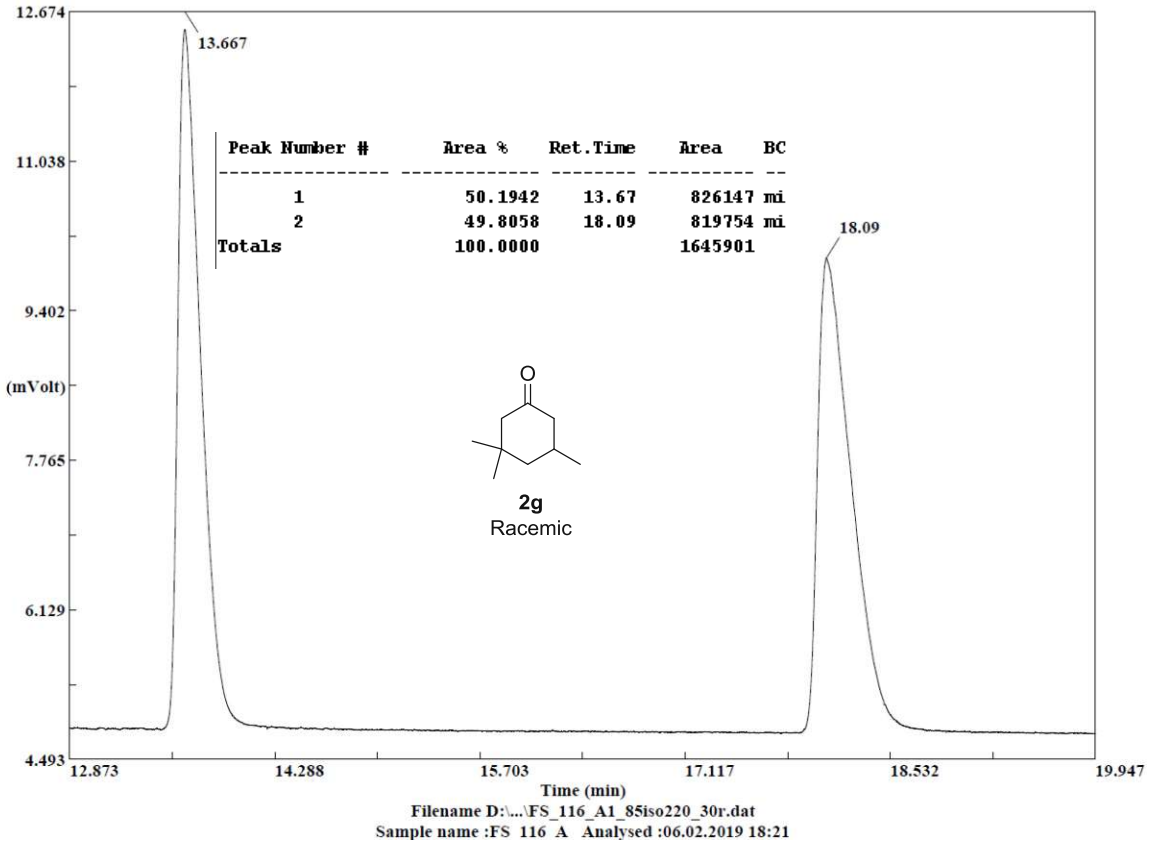


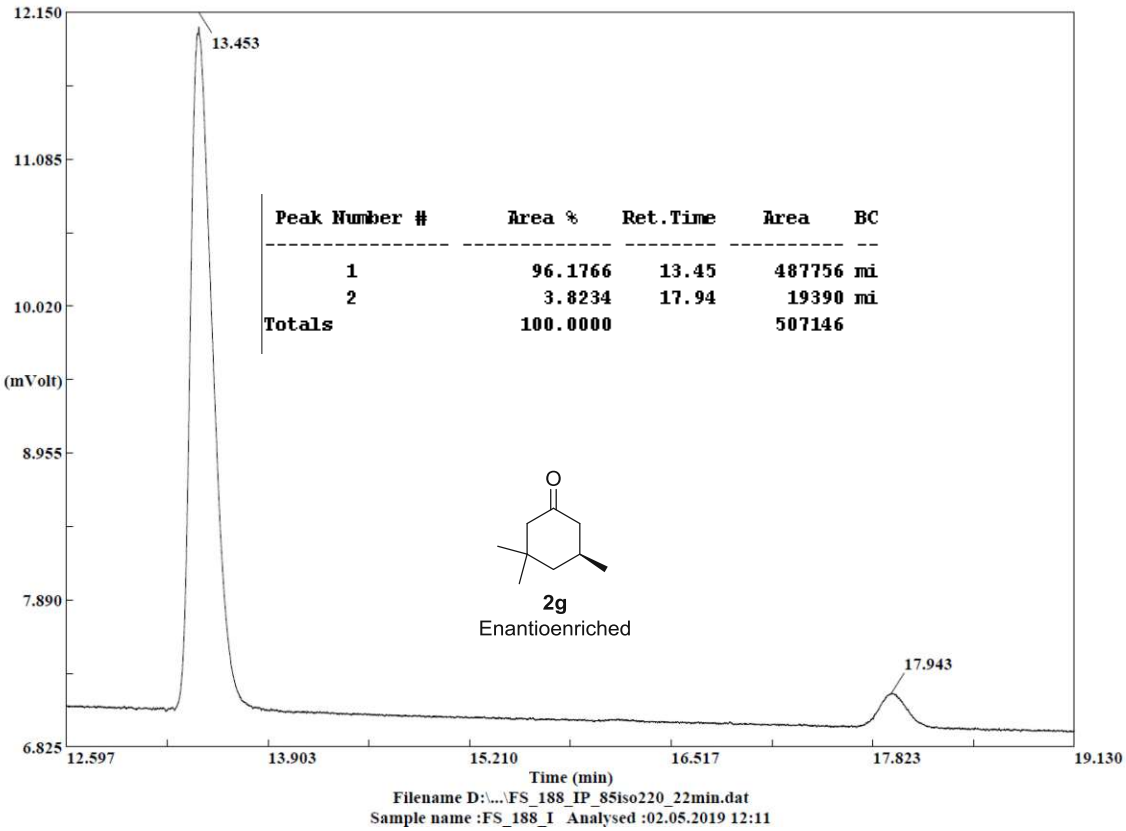
Die approbierte gedruckte Originalversion dieser Dissertation ist an der TU Wien Bibliothek verfügbar.
The approved original version of this doctoral thesis is available in print at TU Wien Bibliothek.



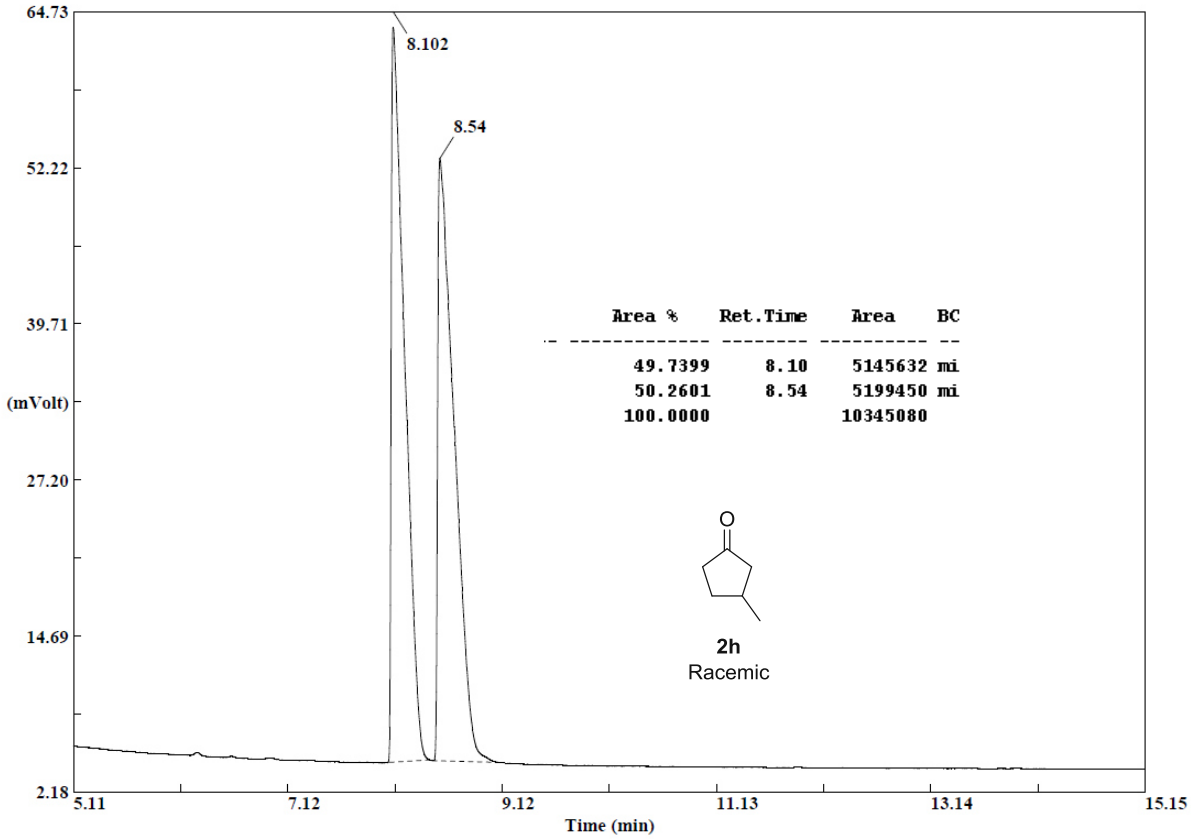


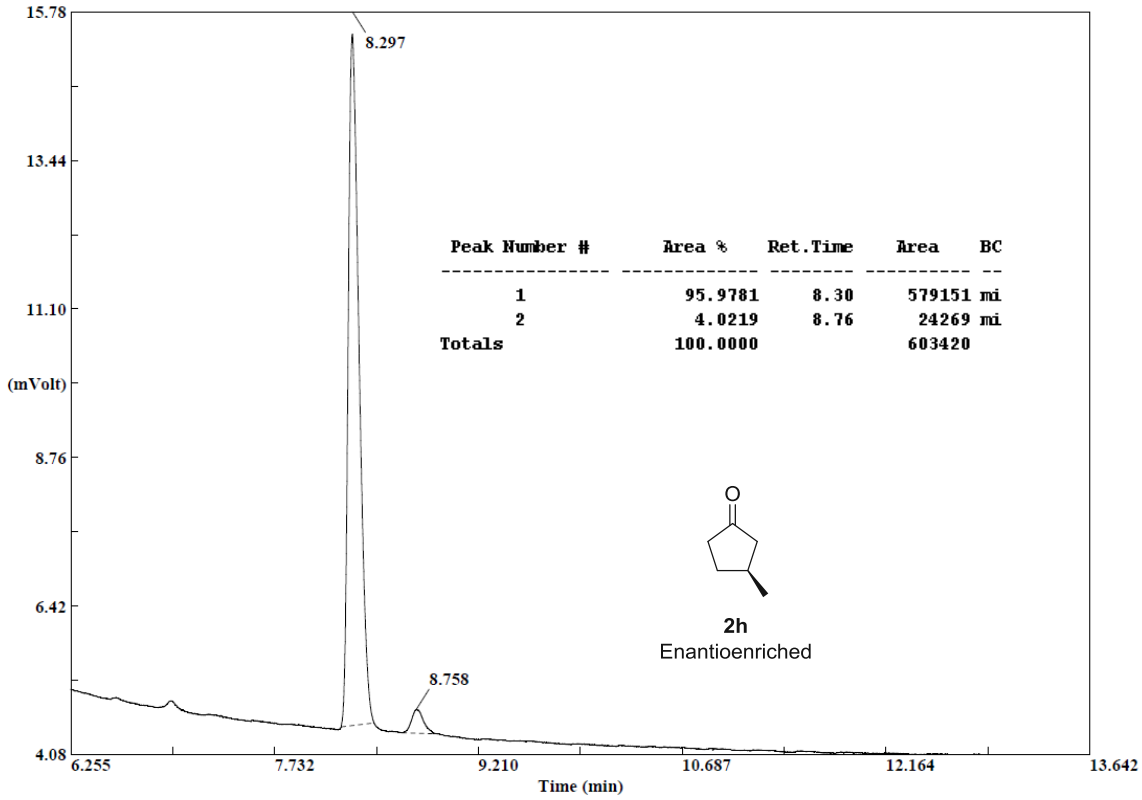
Die approbierte gedruckte Originalversion dieser Dissertation ist an der TU Wien Bibliothek verfügbar.
The approved original version of this doctoral thesis is available in print at TU Wien Bibliothek.



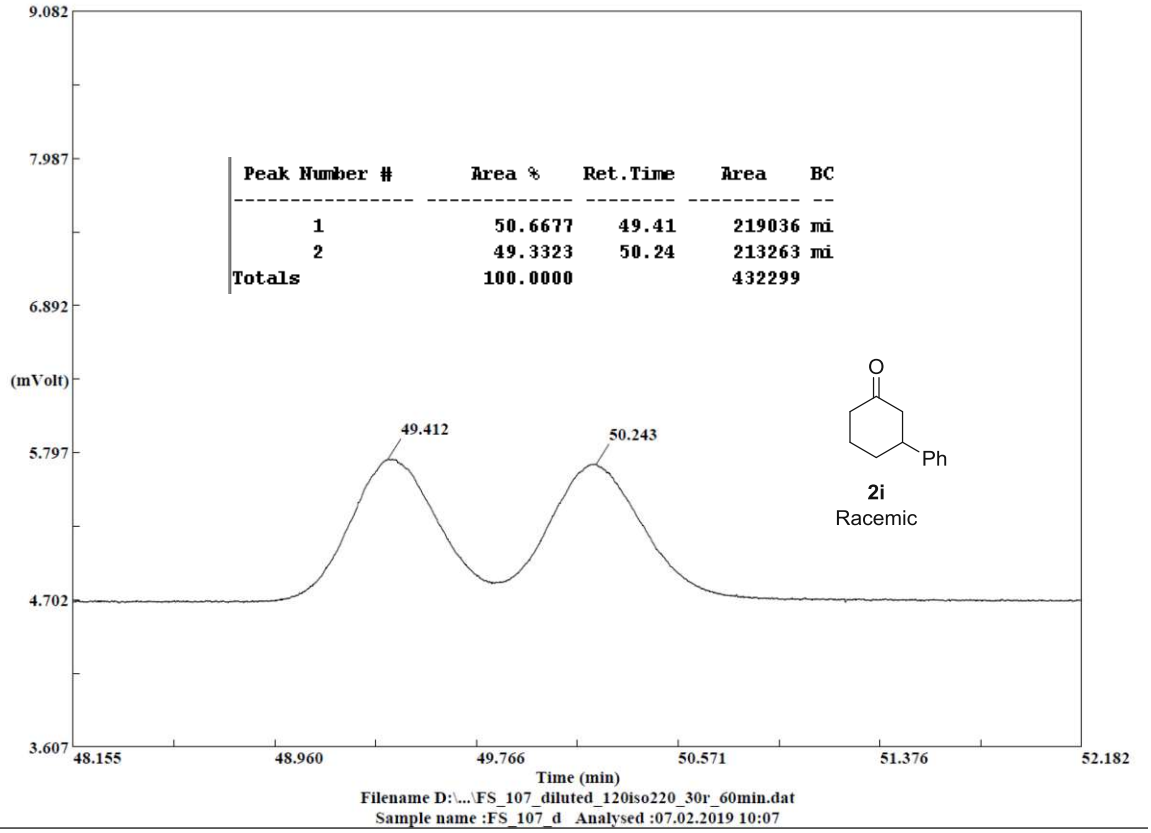


Die approbierte gedruckte Originalversion dieser Dissertation ist an der TU Wien Bibliothek verfügbar.
The approved original version of this doctoral thesis is available in print at TU Wien Bibliothek.

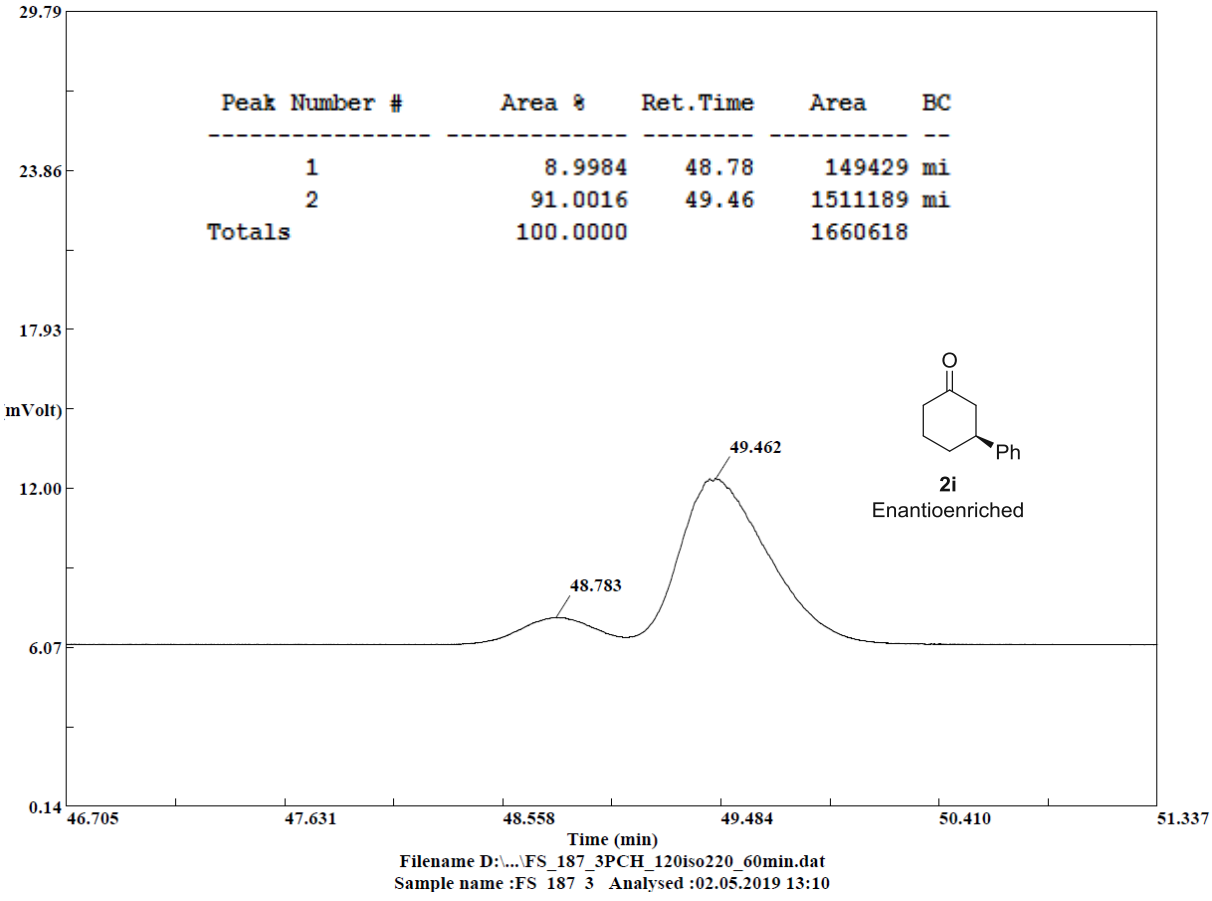




Die approbierte gedruckte Originalversion dieser Dissertation ist an der TU Wien Bibliothek verfügbar.
The approved original version of this doctoral thesis is available in print at TU Wien Bibliothek.

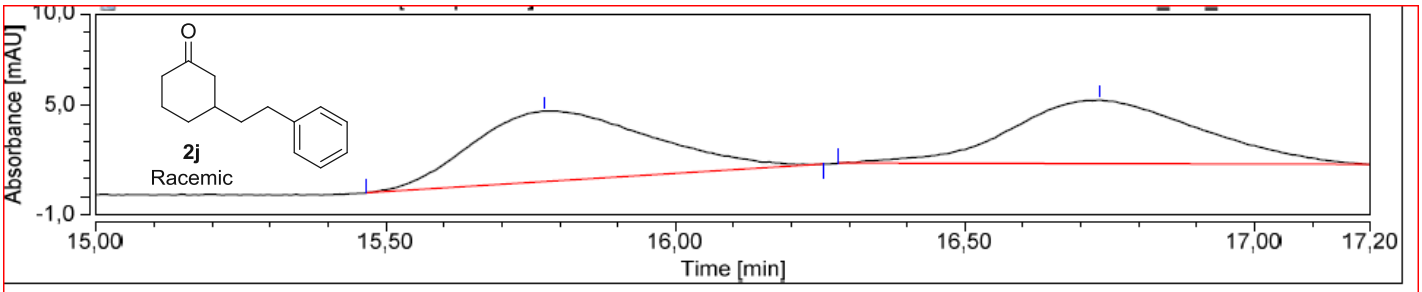


Peak Number #	Area %	Ret.Time	Area	BC
1	50.6677	49.41	219036	mi
2	49.3323	50.24	213263	mi
Totals	100.0000		432299	



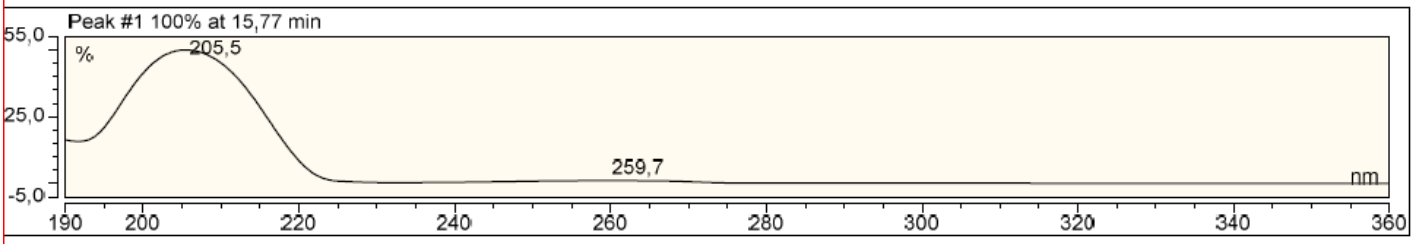
Peak Number #	Area %	Ret.Time	Area	BC
1	8.9984	48.78	149429	mi
2	91.0016	49.46	1511189	mi
Totals	100.0000		1660618	

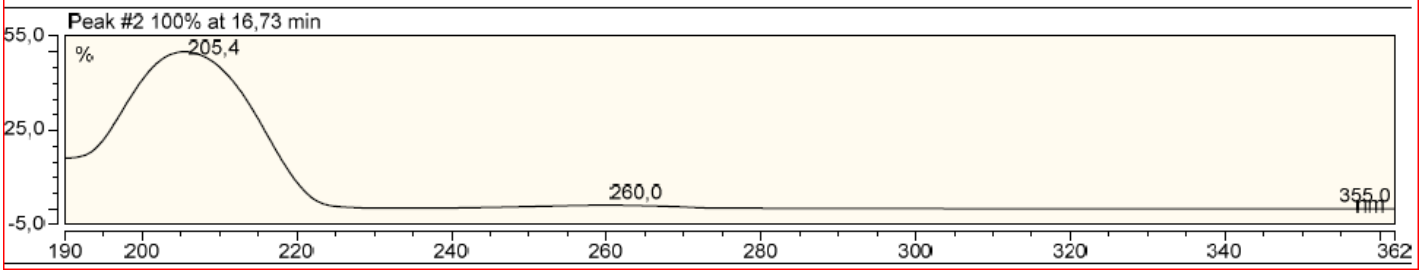
Die approbierte gedruckte Originalversion dieser Dissertation ist an der TU Wien Bibliothek verfügbar.
The approved original version of this doctoral thesis is available in print at TU Wien Bibliothek.



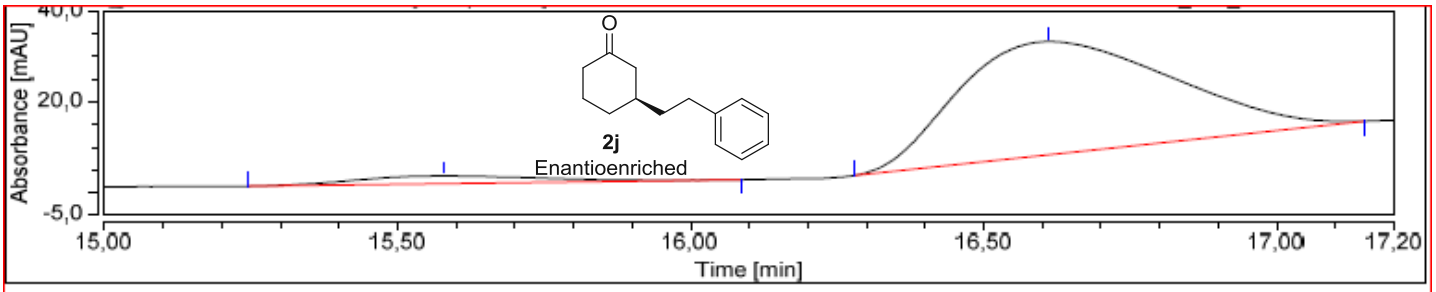
Integration Results

No.	Peak Name	Retention Time min	Area mAU*min	Height mAU	Relative Area %	Relative Height %	Amount n.a.
1		15,773	1,368	3,867	51,01	52,59	n.a.
2		16,732	1,314	3,486	48,99	47,41	n.a.
Total:			**2,682**	**7,353**	**100,00**	**100,00**	



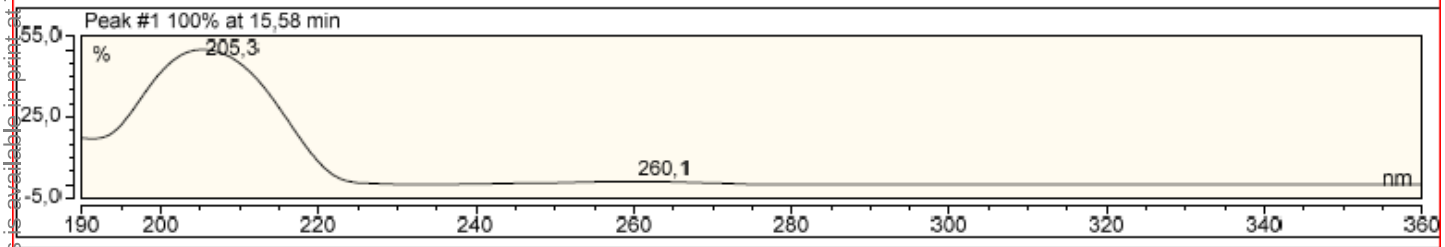


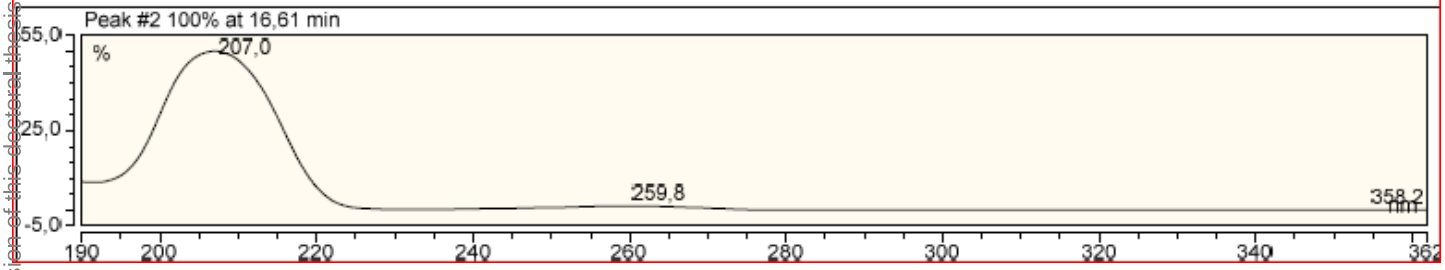
Die approbierte gedruckte Originalversion dieser Dissertation ist an der TU Wien Bibliothek verfügbar.
The approved original version of this doctoral thesis is available in print at TU Wien Bibliothek.



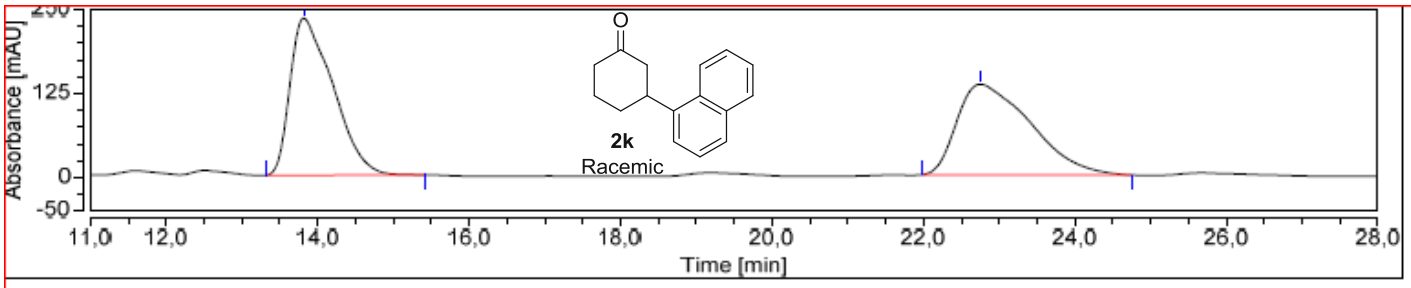
Integration Results

No.	Peak Name	Retention Time min	Area mAU*min	Height mAU	Relative Area %	Relative Height %	Amount n.a.
1		15,578	0,610	1,737	5,46	6,49	n.a.
2		16,610	10,569	25,025	94,54	93,51	n.a.
Total:			**11,179**	**26,762**	**100,00**	**100,00**	



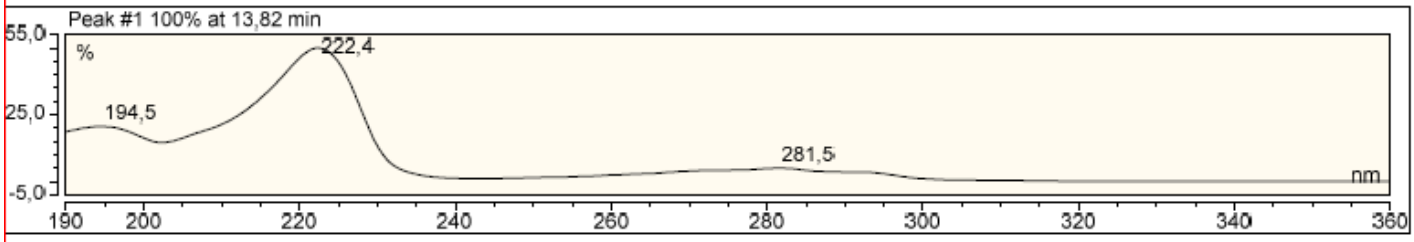


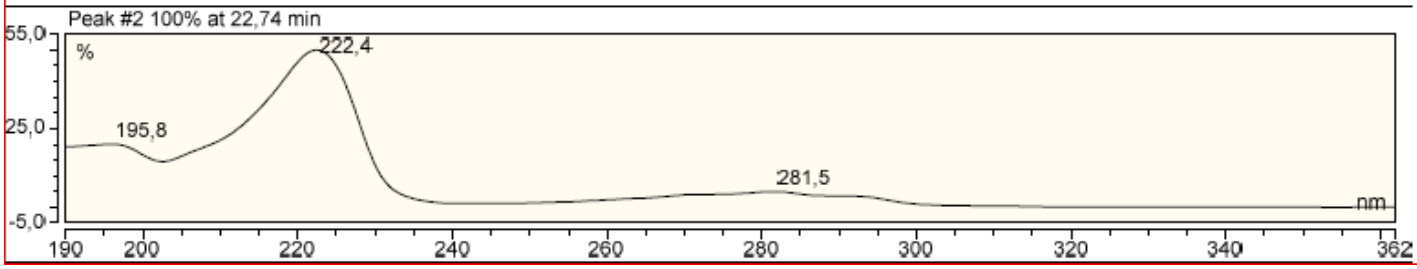
Die approbierte gedruckte Originalversion dieser Dissertation ist an der TU Wien Bibliothek verfügbar.
The approved original version of this doctoral thesis is available in print at TU Wien Bibliothek.



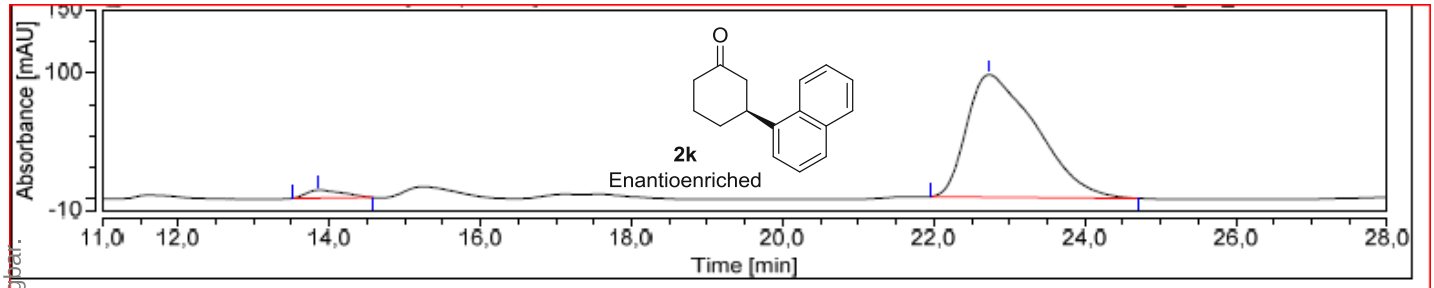
Integration Results

No.	Peak Name	Retention Time min	Area mAU*min	Height mAU	Relative Area %	Relative Height %	Amount n.a.
1		13,815	153,307	233,921	50,31	63,43	n.a.
2		22,743	151,414	134,857	49,69	36,57	n.a.
Total:			**304,720**	**368,778**	**100,00**	**100,00**	



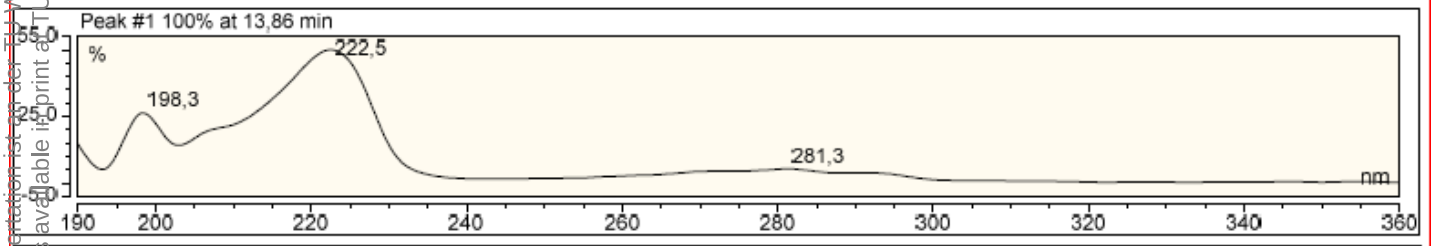


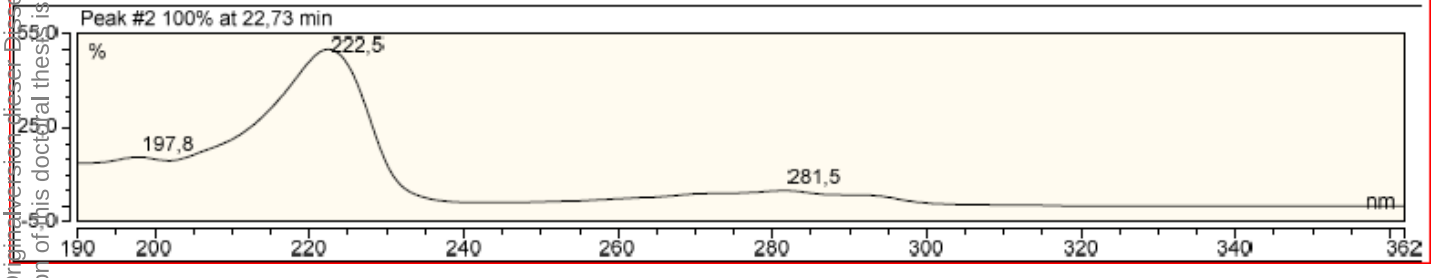
Die approbierte gedruckte Originalversion dieser Dissertation ist an der TU Wien Bibliothek verfügbar.
The approved original version of this doctoral thesis is available in print at TU Wien Bibliothek.



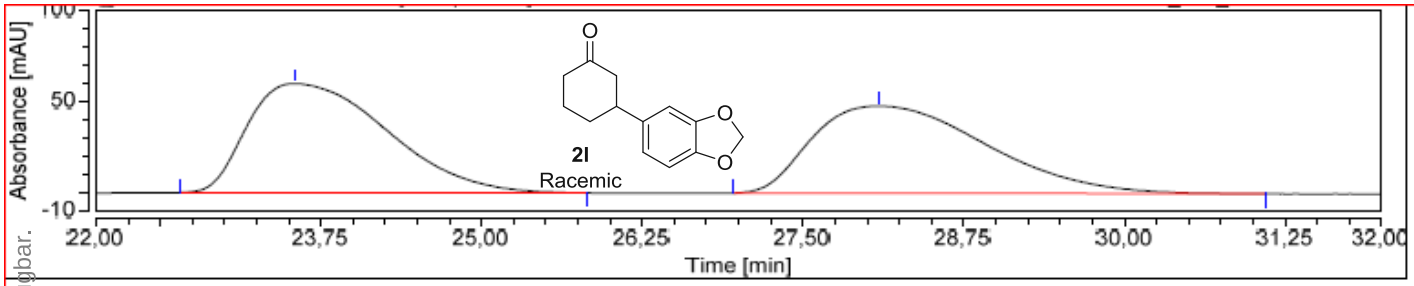
Integration Results

Nr.	Peak Name	Retention Time min	Area mAU*min	Height mAU	Relative Area %	Relative Height %	Amount n.a.
1		13,857	3,534	6,383	3,29	6,14	n.a.
2		22,732	103,836	97,530	96,71	93,86	n.a.
Total:			**107,370**	**103,913**	**100,00**	**100,00**	



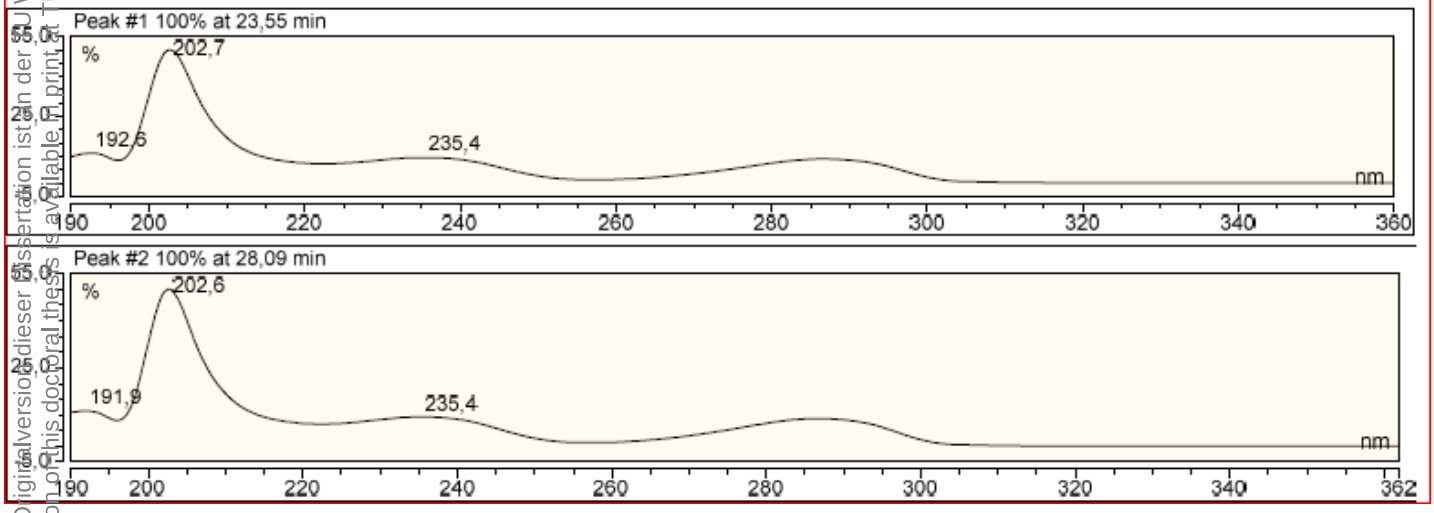


Die approbierte gedruckte Originalversion dieser Dissertation ist an der TU Wien Bibliothek verfügbar.
The approved original version of this doctoral thesis is available in print at TU Wien Bibliothek.

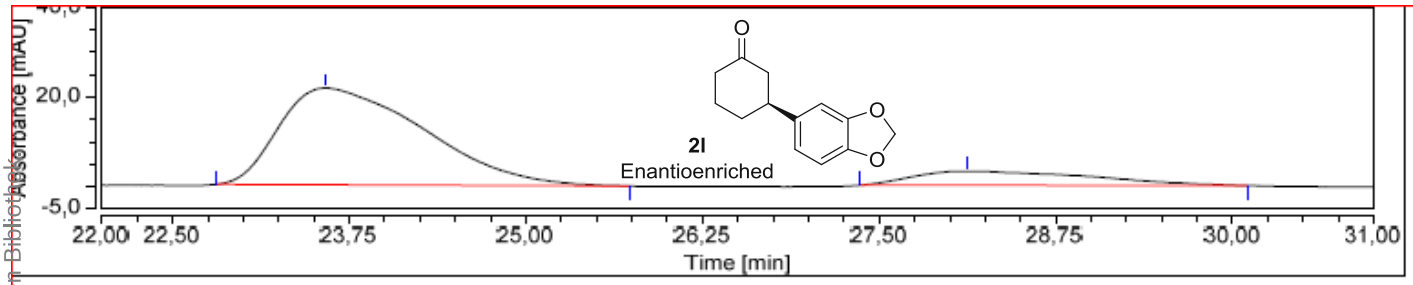


Integration Results

No	Peak Name	Retention Time min	Area mAU*min	Height mAU	Relative Area %	Relative Height %	Amount n.a.
1		23,547	74,644	59,680	49,97	55,57	n.a.
2		28,085	74,741	47,719	50,03	44,43	n.a.
Total:			**149,386**	**107,399**	**100,00**	**100,00**	

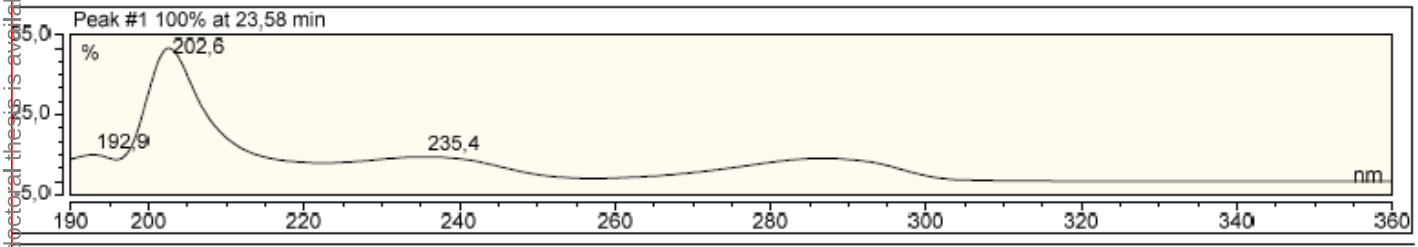


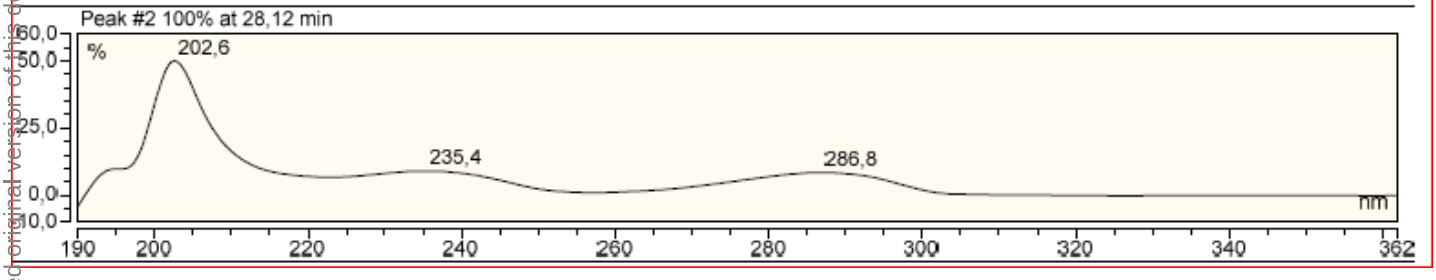
Die approbierte gedruckte Originalversion dieser Dissertation ist an der TU Wien Bibliothek verfügbar.
The approved original version of this doctoral thesis is available in print at TU Wien Bibliothek.



Integration Results

No.	Peak Name	Retention Time min	Area mAU*min	Height mAU	Relative Area %	Relative Height %	Amount n.a.
1		23,583	25,752	21,686	84,92	87,25	n.a.
2		28,123	4,573	3,168	15,08	12,75	n.a.
Total:			**30,325**	**24,854**	**100,00**	**100,00**	





Die approbierte gedruckte Originalversion dieser Dissertation ist an der TU Wien Bibliothek verfügbar.
The approved original version of this doctoral thesis is available in print at TU Wien Bibliothek.

13. References

1 H. Chen, Y. Feng, Z. Xu, T. Ye, *Tetrahedron* **2005**, *61*, 11132–11140.

2 J. Han, J. Lian, X. Tian, S. Zhou, X. Zhen, S. Liu, *Eur. J. Org. Chem*. **2014**, *32*, 7232–7238.

3 T. Akama et al. *Bioorg. Med. Chem. Lett*. **2018**, *28*, 6–10.

4 S. Kandil, J. Balzarini, S. Rat, A. Brancale, A. D. Westwell, C. McGuigan, *Bioorg. Med. Chem. Lett.* **2016**, *26*, 5618–5623.

5 S. Thétiot-Laurent et al. *ChemBioChem*. **2017**, *18*, 300-315.

6 T. J. Trivedi, K. S. Rao, T. Singh, S. K. Mandal, N. Sutradhar, A. B. Panda, A. Kumar, *ChemSusChem.* **2011**, *4*, 604–608.

7 J. You, B. Liu, Y. Wang, *J. Chin. Chem. Soc.-Taip.* **2009**, *56*, 1010-1017.

8 W. Kuchen, H. F. *Phosphorus Sulfur*. **1980**, *8*, 139–145.

9 S. Grant-Overton, J. A. Buss, E. H. Smith, E. G. Gutierrez, E. J. Moorhead, V. S. Lin, A. G. Wenzel, *Synth. Commun*. **2015**, *45*, 331–337.

10 E. G. Gutierrez, E. J. Moorhead, E. H. Smith, V. S. Lin, L. K. G. Ackerman, C. E. Knezevic, V. Sun, S. Grant, A. G. Wenzel, *Eur. J. Org. Chem*. **2010**, *16*, 3027–3031.

11 L. Iu, J. A. Fuentes, M. E. Janka, K. J. Fontenot, M. L. Clarke, *Angew. Chem. Int. Ed.* **2019**, *58*, 2120–2124.

12 D. R. Armstrong, C. Cameron, D. C. Nonhebel, P. G. Perkins, *J. Chem. Soc.* **1983**, *5*, 587–589.

13 R. Singh, C. Czekelius, R. R. Schrock, P. Müller, A. H. Hoveyda, *Organometallics* **2007**, *26*, 2528–2539.

14 T. Wenliang, CAN149:307958, **2008**.

15 Wenliang, T. *Production of Substituted Biphenyl Acid-Form Phosphate Ammonium Salt.* CAN149:307958, **2008**.

16 L. M. Schneider, V. M. Schmiedel, T. Pecchioli, D. Lentz, C. Merten, M. Christmann, *Org. Lett.* **2017**, *19*, 2310–2313.

17 N. J. A. Martin, B. List, *J. Am. Chem. Soc.* **2006**, *128*, 13368–13369.

18 B.-D. Chong, Y.-I. Ji, S.-S. Oh, J.-D. Yang, W. Baik, S. Koo, *J. Org. Chem.* **2002**, *62*, 9323–9325..

19 E. Brenna, M. Crotti, M. De Pieri,F. G. Gatti, G. Manenti, D. Monti, *Adv. Synth. Catal.* **2018**, *360*, 3677–3686.

20 S. T. Cohen-Anisfeld, P. T. Lansbury, *J. Am. Chem. Soc.* **1993**, *115*, 10531–10537.

21 M. D´Augustin, L. Palais, A. Alexakis, *Angew. Chem.* **2005**, *117*, 1400–1402.

22 J.-G. Jun, T. H. Ha, B. P. Mundy, K. E. Bartelt, R. S. Bain, J. H. Cardellina, *J. Chem. Soc. Perkin Trans. 1* **1994**, 18, 2643.

Die approbierte gedruckte Originalversion dieser Dissertation ist an der TU Wien Bibliothek verfügbar.
The approved original version of this doctoral thesis is available in print at TU Wien Bibliothek.
TU Bibliothek Your knowledge hub WIEN

[23] E. D. Scott, N. Amishiro, S. E. Denmark, N. Amishiro, *J. Org. Chem.* **2003**, *68* (18), 6997–7003.

[24] V. Jurkauskas, J. P. Sadighi, S. L. Buchwald, *Org. Lett*. **2003**, *5*, 2417-2420.

[25] Y. Fall, H. Doucet, M. Santelli, *Tetrahedron* **2009**, *2*, 489-495.

[26] M. K. Das, S. De, Shubhashish; A. Bisai, *Org. Biomol. Chem*. **2015**, *13*, 3585-3588.

[27] F. Cecacci, G. Mancini, P. Mencarelli, C. Villani, *Tetrahedron: Asymmetry* **2003**, *14*, 3117–3122.

[28] L. Luzzani, M. Mancinelli, A. Mazzanti, S. Lepri, R. Ruzziconi, M. Schlosser, *Org. Biomol. Chem.* **2012**, *10*, 1847–1855.

[29] R. Sahnoun, S. Koseki, Y. Fujimura, *J. Phys. Chem. A* **2006**, *110*, 2440–2447.

[30] E. Masson, *Org. Biomol. Chem.* **2013**, *11*, 2859.

[31] A. D. Becke, *J. Chem. Phys.* **1993**, *98*, 5648–5652.

[32] M. P. Johansson, J. Olsen, *J. Chem. Theory Comput.* **2008**, *4*, 1460–1471.

[33] S. Grimme, J. Antony, S. Ehrlich, H. Krieg, *J. Chem. Phys.* **2010**, *132*, 154104.

[34] S. Grimme, S. Erlich, L. Georigk, *J. Comput. Chem* **2011**, *32*, 1456–1465.

[35] S. H. Vosko, L. Wilk, M. Nusair, *Can. J. Phys.* **1980**, *58*, 1200–1211.

[36] F. Weigend, R. Ahlrichs, *Phys. Chem. Chem. Phys.* **2005**, *7*, 3297–3305.

[37] F. Neese, *Wiley Interdisciplinary Reviews: Computational Molecular Science* **2012**, *2*, 73–78.

[38] C. Riplinger, F. Neese, *J. Chem. Phys.* **2013**, *138*, 034106.

[39] J. E. Leffler, B. M. Graybill, *J. Phys. Chem.* **1959**, *63*, 1457–1460.

[40] G. Henkelman, B. P. Uberuaga, H. J. Jónsson, *Chem. Phys.* **2000**, *113*, 9901–9904.

[41] D. Sheppard, R. Terrell, G. Henkelman, *J. Chem. Phys.* **2008**, *128*, 134106.

[42] G. Baddeley, *Nature* **1946**, *157*, 694–695.

[43] C. C. K. Ling, M. M. Harris, *J. Chem. Soc.* **1964**, *0*, 1825–1835.

[44] K. Vanommeslaeghe, A. D. MacKerell, *J. Chem. Inf. Model.* **2012**, *52*, 3144–3154.

[45] K. Vanommeslaeghe, E. P. Raman, A. D. MacKerell, *J. Chem. Inf. Model* **2012,** *52*, 3155–3168.

[46] K. Vanommeslaeghe, E. Hatcher, C. Acharya, S. Kundu, S. Zhong, J. Shim, E. Darian, O. Guvench, P. Lopes, I. Vorobyov et al., *J. Comput. Chem* **2010**, *31*, 671–690.

[47] B. R. Brooks, C. L. Brooks, A. D. Mackerell, L. Nilsson, R. J. Petrella, B. Roux, Y. Won, G. Archontis, C. Bartels, S. Boresch et al., *J. Comput. Chem* **2009**, *30*, 1545–1614.

[48] L. Martínez, R. Andrade, G. Birgin, J. M. Martínez, *J. Comput. Chem*. **2009**, *30*, 2157-2164.

[49] N. Michaud-Agrawal, E. J. Denning, T. B. Woolf, O. Beckstein, *J. Comput. Chem* **2011**, *32*, 2319–2327.

[50] H. Wickham. ggplot2: Elegant Graphics for Data Analysis. Springer-Verlag New York, 2016.

[51] The Open Babel Package, version 2.4.1
https://openbabel.readthedocs.io/en/latest/3DStructureGen/multipleconformers.html

Die approbierte gedruckte Originalversion dieser Dissertation ist an der TU Wien Bibliothek verfügbar.
The approved original version of this doctoral thesis is available in print at TU Wien Bibliothek.
TU Bibliothek Your knowledge hub WIEN

Appendix B

Supporting information:

Sterically Demanding Flexible Phosphoric Acids for Constructing Efficient and Multi-Purpose Asymmetric Organocatalysts

Die approbierte gedruckte Originalversion dieser Dissertation ist an der TU Wien Bibliothek verfügbar.
The approved original version of this doctoral thesis is available in print at TU Wien Bibliothek.

Supporting Information

Sterically Demanding Flexible Phosphoric Acids for Constructing Efficient and Multi-Purpose Asymmetric Organocatalysts

Fabian Scharinger[a], Ádám Márk Pálvölgyi[a], Melanie Weisz[a], Matthias Weil[b], Christian Stanetty[a], Michael Schnürch[a] and Katharina Bica-Schröder*[a]

[a] Institute of Applied Synthetic Chemistry, TU Wien, Getreidemarkt 9/163, 1060 Wien, Austria

[b] Institute of Chemical Technologies and Analytics, TU Wien, Getreidemarkt 9/163, 1060 Wien, Austria

Die approbierte gedruckte Originalversion dieser Dissertation ist an der TU Wien Bibliothek verfügbar.
The approved original version of this doctoral thesis is available in print at TU Wien Bibliothek.

TABLE OF CONTENTS

GENERAL REMARKS 3

1. PREPARATION OF ETHYL ACETAMIDOCYANOACETATE (OXYMA, 13) 4

2. PREPARATION OF DIAMINES 5

Step 1: Boc-protection 5
Step 2: DCC/DMAP/Oxyma coupling 6
Step 3: Deprotection 7
Step 4: Reduction 8

3. SYNTHESIS OF THE PHOSPHORIC ACIDS 11

Preparation of 1,1´-biphenols *via* Friedel-Crafts alkylation 12
Preparation of 23 *via* oxidative coupling 14
General procedure to all phosphorylations and hydrolysis 14

4. SUBSTRATE SYNTHESIS 18

5. PARAMETER OPTIMIZATION FOR ASYMMETRIC EPOXIDATIONS 21

5.1. Preliminary phosphoric acid screening 21
5.2 Amino-modification screening 22
5.3 Amino acid screening 23
5.4 Solvent screening 24
5.5 Final phosphoric acid screening, screening of conventional acids 25

6. GENERAL PROCEDURE AND ANALYTICAL DATA FOR THE ASYMMETRIC EPOXIDATIONS 26

7. PARAMETER OPTIMIZATION FOR THE ASYMMETRIC AZIRIDINATIONS 35

7.1 Solvent screening 35
7.2 Base screening 36

8. GENERAL PROCEDURE AND ANALYTICAL DATA FOR THE ASYMMETRIC AZIRIDINATIONS 37

9. GENERAL PROCEDURE AND ANALYTICAL DATA FOR THE ASYMMETRIC AZA-MICHAEL ADDITIONS 42

10. GENERAL PROCEDURE AND ANALYTICAL DATA FOR THE ASYMMETRIC MICHAEL-INITIATED RING-CLOSURE/INTRAMOLECULAR ALDOL SEQUENCE 46

11. CHIRAL HPLC AND CHIRAL GC CHROMATOGRAMS FOR THE ASYMMETRIC EPOXIDATIONS 49

12. CHIRAL HPLC CHROMATOGRAMS FOR THE ASYMMETRIC AZIRIDINATIONS 66

13. CHIRAL HPLC CHROMATOGRAMS FOR THE ASYMMETRIC AZA-MICHAEL/ALDOL REACTIONS 74

14. CHIRAL HPLC CHROMATOGRAMS FOR THE ASYMMETRIC MICHAEL-INITIATED RING CLOSURE/INTRAMOLECULAR ALDOL SEQUENCE 80

15. NMR SPECTRA OF CHIRAL DIAMINES 84

16. NMR SPECTRA OF PHOSPHORIC ACIDS AND INTERMEDIATES 93

17. NMR SPECTRA OF LITERATURE UNKNOWN ENONE SUBSTRATES 109

18. NMR SPECTRA FOR THE ASYMMETRIC EPOXIDATIONS 111

19. NMR SPECTRA FOR THE ASYMMETRIC AZIRIDINATIONS 128

20. NMR SPECTRA OF ASYMMETRIC AZA-MICHAEL/ALDOL REACTIONS 136

21. NMR SPECTRA OF ASYMMETRIC MICHAEL-INDUCED RING-CLOSURE/ALDOL REACTION SEQUENCE 144

22. EXTENDED 1D/2D-NMR EXPERIMENTS SUPPORTING THE STRUCTURE OF COMPOUND 11 148

23. NMR STUDIES FOR PHOSPHORIC ACIDS 153

24. XRD DATA FOR COMPOUNDS 5C, 11A AND PA9 160

Die approbierte gedruckte Originalversion dieser Dissertation ist an der TU Wien Bibliothek verfügbar.
The approved original version of this doctoral thesis is available in print at TU Wien Bibliothek.

General remarks

All purchased chemicals from commercial suppliers were used without further purification, unless noted otherwise. Dry solvents were pre-distilled and desiccated on aluminium oxide columns (PURESOLV, Innovative Technology).

Column chromatography was performed on standard manual glass columns using Merck (40-60 µm) silica gel with pre-distilled solvents (PE: petrolether, EtOAc: ethyl acetate, Et_2O: diethyl ether). For TLC analysis, precoated aluminium-backed plates were purchased from Merck (silica gel 60 F_{254}). UV active compounds were detected at 254 nm. Non-UV active compounds have been detected using vanillin staining solution (5% vanillin in EtOH + H_2SO_4).

^{1}H, ^{13}C, ^{19}F and ^{31}P NMR spectra were recorded on a Bruker Advance UltraShield 200 MHz or 400 MHz spectrometer and chemical shifts are reported in ppm using TMS (tetramethylsilane) as internal standard. Coupling constants (*J*) are given in Hz. For assignation purpose, the following abbreviations are used: s (singlet), d (doublet), t (triplet), q (quartet), m (multiplet), brs (broad singlet), dd (doublet of doublets), ddd (doublets of doublet of doublets), td (triplet of doublets), dt (doublet of triplets).

GC measurement have been performed on a Thermo Scientific Focus on BGB5 column by using FID detector. Chiral GC measurements were performed on chiral BGB columns (BGB 173, BGB 175) by using FID detector.

GC-MS measurements have been performed on a Thermo Scientific DSQ II on BGB5 column (30m), equipped with a quadrupole MS detector DSQ II.

Chiral HPLC measurements were carried out on a DAIONEX UPLC equipped with a photodiode array (PDA) plus detector (190–360 nm), using a Diacel Chiracel AS-H, IB and OJ columns (all 250 × 4.60 mm, 5 µm).

Optical rotation was measured on an Anton Paar MCP500 polarimeter at the specific conditions and the results have been compared to literature values. Concentrations are given in g / 100 mL.

HR-MS analysis was performed using HTC PAL system auto sampler, an Agilent 1100/1200 HPLC and Agilent 6230 AJS ESI-TOF mass spectrometer.

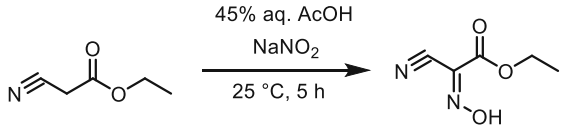
Microwave reactions were performed on a Biotage Initiator Classic in 20 ml pressure tight glass vials.

Melting points above room temperature were measured on an automated melting point system OPTI MELT of Stanford Research Systems and are uncorrected.

Infrared spectra were recorded on a Perkin-Elmer Spectrum 65 FT IR spectrometer equipped with a specac MK II Golden Gate Single Reflection ATR unit.

Die approbierte gedruckte Originalversion dieser Dissertation ist an der TU Wien Bibliothek verfügbar.
The approved original version of this doctoral thesis is available in print at TU Wien Bibliothek.
TU Bibliothek Your knowledge hub WIEN

1. Preparation of ethyl acetamidocyanoacetate (oxyma, 13)



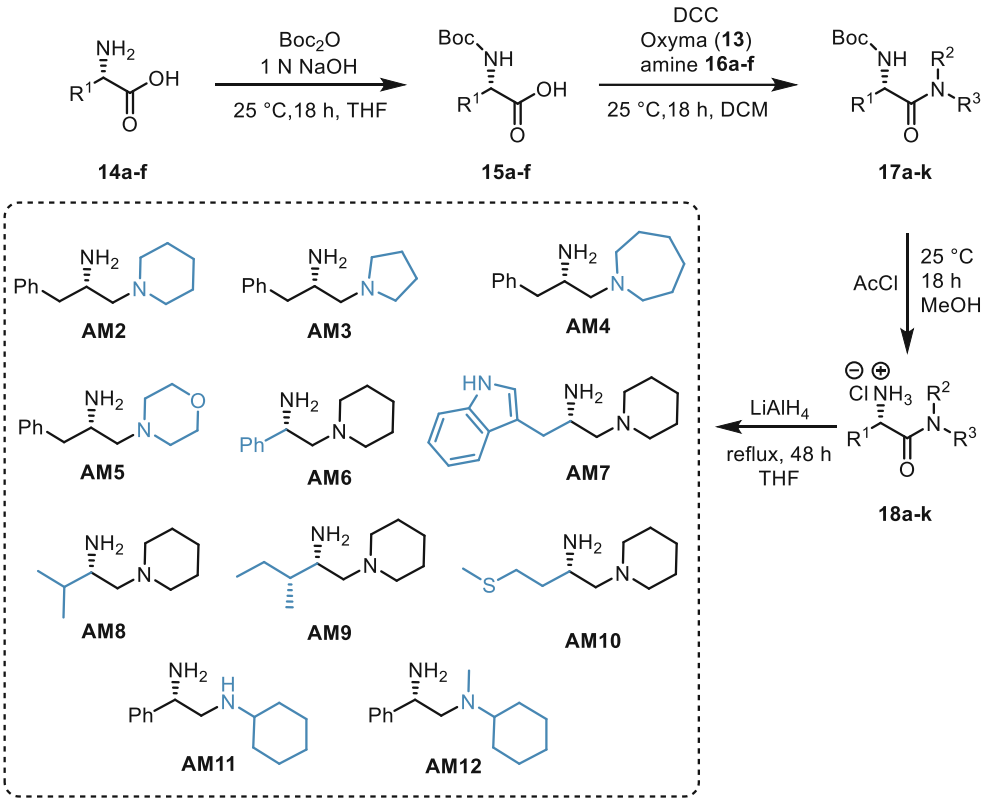
12 **13**

According to literature procedure.[1] A solution of ethyl cyanoacetate (**12**, 10 g, 88.0 mmol, 1.0 equiv.) in aqueous acetic acid (45 w/w %, 40 mL) was stirred at 0 °C for 15 min. Sodium nitrite (18.3 g, 265.0 mmol, 3.0 equiv.) was added portion-wise and the reaction mixture was stirred 18 h at room temperature. Et_2O (50 mL) and water were added until a clear solution was obtained. The aqueous phase was extracted with Et_2O (2×), the combined organic phases were washed with water (2×), brine (1×) and dried over anhydrous Na_2SO_4. Removal of the solvent gave **13** as a slight yellow solid (12.3 g, 98% yield). **^{1}H NMR (400 MHz, $CDCl_3$) δ** 4.45 (q, *J* = 7.1 Hz, 2H), 1.41 (t, *J* = 7.1 Hz, 3H). The O*H* proton was not detected.

Die approbierte gedruckte Originalversion dieser Dissertation ist an der TU Wien Bibliothek verfügbar.
The approved original version of this doctoral thesis is available in print at TU Wien Bibliothek.

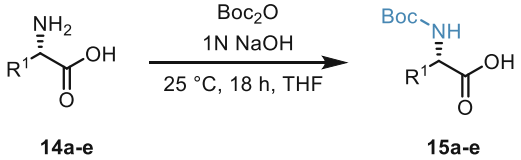
2. Preparation of diamines

Diamines **AM2**-**AM12** were prepared according to a four-step synthetic procedure, as depicted in Scheme S1.



Scheme S1. General procedure for the synthesis of diamines **AM2-AM12.**

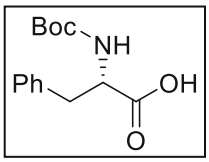
Step 1: Boc-protection



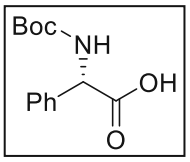
General procedure[2]: To the solution of amino acid **14a-e** (1.0 equiv.) in a mixture of THF / 1 N NaOH (1:1, 0.4 M), di-*tert*-butyl-dicarbonate (1.2 equiv.) was added. The solution was stirred for 18 h at room temperature. The THF was removed *in vacuo*, the resulting aqueous solution was diluted with DCM and it was acidified to pH 2 with a 1 N HCl solution. The aqueous phase was extracted with DCM (3×), the combined organic phases were washed with brine and dried over anhydrous Na_2SO_4. Removal of the solvent afforded the product **15a-e** as a white solid or colorless, viscous liquid.

N-Boc-L-tryptophan (**15f**) was bought from Fluka and it was used without further purifications.

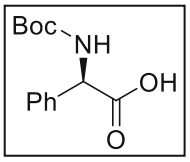
Die approbierte gedruckte Originalversion dieser Dissertation ist an der TU Wien Bibliothek verfügbar.
The approved original version of this doctoral thesis is available in print at TU Wien Bibliothek.



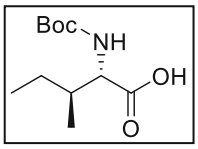
(*tert*-butoxycarbonyl)-L-Phenylalanine, 15a.[3] Performed on a 30.0 mmol scale. Viscous liquid (8.0 g, 99% yield). **^{1}H NMR (200 MHz, $CDCl_3$)** δ 7.18 – 7.31 (m, 5H), 4.94 (d, *J* = 8.3 Hz, 1H), 4.61 (d, *J* = 8.3 Hz, 1H), 3.09 – 3.25 (m, 2H), 1.42 (s, 9H). The COO*H* proton was not detected.



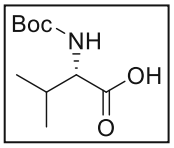
(*tert*-butoxycarbonyl)-L-Phenyglycine, (*S*)-**15b.**[4] Performed on a 17.0 mmol scale. White powder (4.1 g, 99% yield). **^{1}H NMR (200 MHz, $CDCl_3$) δ** 7.51 (brs, 1H), 7.29 – 7.43 (m, 5H), 5.13 (d, *J* = 8.1 Hz, 1H), 1.40 (s, 9H). The COO*H* proton was not detected.



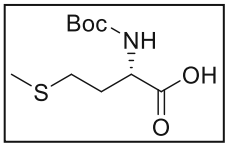
(*tert*-butoxycarbonyl)-D-Phenyglycine, (*R*)-**15b.**[5] Performed on a 19.8 mmol scale. White powder (4.79 g, 96% yield). **^{1}H NMR (200 MHz, $CDCl_3$) δ** 7.50 (brs, 1H), 7.29 – 7.42 (m, 5H), 5.13 (d, *J* = 8.1 Hz, 1H), 1.40 (s, 9H). The COO*H* proton was not detected.



(*tert*-butoxycarbonyl)-L-Isoleucine, 15c.[6] Performed on a 24.0 mmol scale. Viscous liquid (5.5 g, 99% yield). **^{1}H NMR (200 MHz, $CDCl_3$) δ** 3.48 (brs, 1H), 2.40 – 2.73 (m, 1H), 1.83 – 2.05 (m, 1H), 1.48 – 1.60 (m, 2H), 1.43 (s, 9H), 0.90 – 1.20 (m, 6H). The COO*H* proton was not detected.

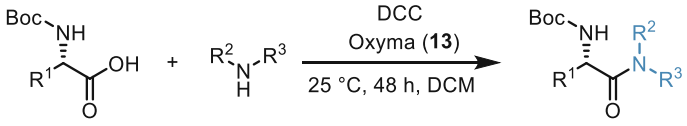


(*tert*-butoxycarbonyl)-L-Valine, 15d.[3] Performed on a 51.0 mmol scale. Viscous liquid (10.5 g, 94% yield). **^{1}H NMR (200 MHz, $CDCl_3$) δ** 5.05 (d, *J* = 9.1 Hz, 1H), 4.25 (dd, *J* = 8.8, 4.3 Hz, 1H), 2.09 – 2.26 (m, 1H), 1.44 (s, 9H), 0.99 (d, *J* = 6.8 Hz, 3H), 0.92 (d, *J* = 6.9 Hz, 3H). The COO*H* proton was not detected.



(*tert*-butoxycarbonyl)-L-Methionine, 15e.[7] Performed on a 14.0 mmol scale. Viscous liquid (3.4 g, >99% yield). **^{1}H NMR (200 MHz, $CDCl_3$) δ** 5.17 (brs, 1H), 4.43 (brs, 1H), 2.58 (dd, 8.4, 6.2 Hz, 2H), 2.11 (s, 3H), 1.97 (m, 2H), 1.44 (s, 9H). The COO*H* proton was not detected.

Step 2: DCC/DMAP/Oxyma coupling

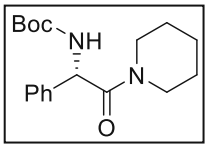


15a-f **16a-f** **17a-k**

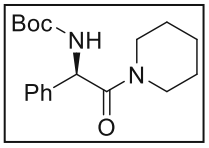
General procedure:[8] To a solution of the Boc-protected amino acid **15a-f** (1.0 equiv.) in dry DCM (0.2 M), DCC (2.0 equiv.), oxyma **13** (1.1 equiv.) and amine **16a-f** (2.5 equiv.) were added at 0 °C. The

Die approbierte gedruckte Originalversion dieser Dissertation ist an der TU Wien Bibliothek verfügbar.
The approved original version of this doctoral thesis is available in print at TU Wien Bibliothek.
TU Bibliothek Your knowledge hub WIEN

resulting turbid solution was stirred for another 15 min at 0 °C, allowed to warm up and it was stirred at room temperature for 48 h. Then cold EtOAc (50 mL) was added, the mixture was stirred for 10 min, the DCU was filtered off and the clear solution was concentrated *in vacuo*. The crude mixture was re-dissolved in EtOAc (25 mL) and it was washed with 1 N HCl (1×). The formed solid was filtered off and the filtrate was repeatedly washed with 1 N HCl (2×), 1 N NaOH (3×) and brine (1×). The combined organic phases were dried over anhydrous Na_2SO_4. Solvent removal afforded the crude products **17a-i** as white solids, which were used without further purification with the exception of (*S*)-**17b** and (*R*)-**17b**.

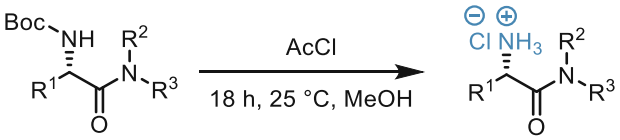


***tert*-butyl (*S*)-(2-Oxo-1-phenyl-2-(piperidin-1-yl)ethyl)carbamate**, (*S*)-**17b.**[9] Performed on a 17.0 mmol scale. Purified by column chromatography (30% EE in PE, R_f = 0.38). White solid (2.0 g, 79% yield). **^{1}H NMR (200 MHz, $CDCl_3$) δ** 7.38 – 7.16 (m, 5H), 6.08 (d, *J* = 7.7 Hz, 1H), 5.51 (d, *J* = 7.7 Hz, 1H), 3.66 (dt, *J* = 11.5, 4.2 Hz, 1H), 3.78 – 3.13 (m, 4H), 1.54 – 1.27 (m, 14H).



***tert*-butyl (*R*)-(2-Oxo-1-phenyl-2-(piperidin-1-yl)ethyl)carbamate**, (*R*)-**17b.**[9] Performed on a 17.0 mmol scale. Purified by column chromatography (30% EE in PE, R_f = 0.38). White solid (2.1 g, 80% yield). **^{1}H NMR (200 MHz, $CDCl_3$) δ** 7.37 – 7.17 (m, 5H), 6.08 (d, *J* = 7.7 Hz, 1H), 5.51 (d, *J* = 7.7 Hz, 1H), 3.66 (dt, *J* = 11.5, 4.2 Hz, 1H), 3.78 – 3.13 (m, 4H), 1.56 – 1.27 (m, 14H).

Step 3: Deprotection

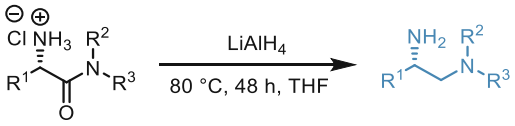


17a-i **18a-i**

General procedure:[8] To a solution of Boc-amide **17a-i** (1.0 equiv.) in dry MeOH (0.41 M), acetyl chloride (8.0 equiv.) was added at 0 °C. After 15 min, the ice bath was removed and the solution was stirred for another 18 h at 25 ˚C. The solvent was removed and the solid was dried under reduced pressure (1 h, 0.7 mbar). Et_2O was added to the solid and the dispersion was stirred for 15 min. The product was filtered off. The crude products **18a-i** were used directly for the next step without further purifications.

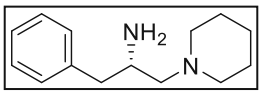
Die approbierte gedruckte Originalversion dieser Dissertation ist an der TU Wien Bibliothek verfügbar.
The approved original version of this doctoral thesis is available in print at TU Wien Bibliothek.
TU Bibliothek Your knowledge hub WIEN

Step 4: Reduction

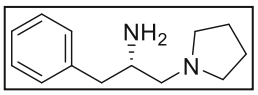


18a-i **AM2-AM10**

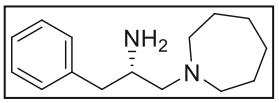
General procedure:[10] To a stirred solution of salt **18a-i** (1.0 equiv.) in THF (0.13-0.15 M) $LiAlH_4$ (5.0 equiv.) was added in small portions at 0 °C. The resulting dispersion was stirred for 15 min and it was subsequently stirred at reflux for 48 h. After cooling to room temperature, distilled H_2O (1 mL per g $LiAlH_4$), and 15 % aqueous NaOH (2 mL per g $LiAlH_4$) were added at 0 °C and the mixture was stirred for 10 min. Anhydrous Na_2SO_4 was added to remove the previously added water, and the product was taken up in EtOAc. The solid was filtered off and it was washed with EtOAc. The filtrate was washed with 1 N NaOH (2×) and brine (1×) and it was dried over anhydrous Na_2SO_4. Removal of the solvent – and if necessary, column chromatography – afforded the pure product **AM2-AM10** as yellow oil or yellow solid.



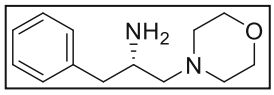
(*S*)-1-Phenyl-3-(piperidin-1-yl)propan-2-amine, AM2.[11] Performed on a 3.0 mmol scale. Yellow oil (0.60 g, 85% yield). **^{1}H NMR (400 MHz, $CDCl_3$) δ** 7.32 – 7.25 (m, 2H), 7.23 – 7.16 (m, 3H), 3.66 – 3.59 (m, 4H), 3.23 – 3.11 (m, 1H), 2.71 (dd, *J* = 13.3, 4.5 Hz, 1H), 2.54 – 2.41 (m, 3H), 2.33 – 2.15 (m, 4H), 1.44 (brs, 2H).



(*S*)-1-Phenyl-3-(pyrrolidin-1-yl)propan-2-amine, AM3.[12] Performed on a 4.0 mmol scale. Purified by column chromatography (15% MeOH in EtOAc + 2% Et_3N, R_f = 0.23). Yellow oil (0.44 g, 59% yield). **^{1}H NMR (200 MHz, $CDCl_3$) δ** 7.39 – 7.16 (m, 5H), 3.27 – 3.09 (m, 1H), 2.79 (dd, *J* = 13.3, 4.5 Hz, 1H), 2.65 – 2.42 (m, 6H), 2.34 (dd, *J* = 11.8, 4.3 Hz, 1H), 1.77 – 1.61 (m, 4H), 1.46 (brs, 2H).

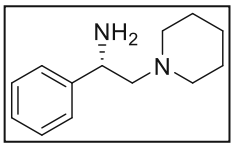


(*S*)-1-(Azepan-1-yl)-3-phenylpropan-2-amine, AM4.[12] Performed on a 3.0 mmol scale. Yellow oil (0.62 g, 99% yield). **^{1}H NMR (400 MHz, $CDCl_3$) δ** 7.34 – 7.15 (m, 5H), 3.13 – 3.03 (m, 1H), 2.76 – 2.42 (m, 7H), 2.32 – 2.24 (m, 1H), 1.71 – 1.49 (m, 10H).

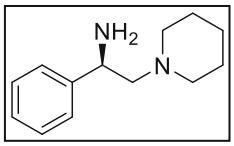


(*S*)-1-Morpholino-3-phenylpropan-2-amine, AM5.[13] Performed on a 4.0 mmol scale. White solid (0.35 g, 45% yield). **^{1}H NMR (400 MHz, $CDCl_3$) δ** 7.34 – 7.14 (m, 5H), 3.78 – 3.59 (m, 4H), 3.26 – 3.13 (m, 1H), 2.73 (dd, *J* = 13.3, 4.5 Hz, 1H), 2.59 – 2.45 (m, 3H), 2.42 – 2.20 (m, 4H), 1.51 (brs, 2H).

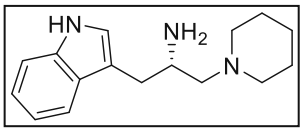
Die approbierte gedruckte Originalversion dieser Dissertation ist an der TU Wien Bibliothek verfügbar.
The approved original version of this doctoral thesis is available in print at TU Wien Bibliothek.



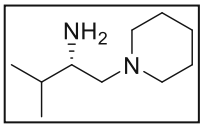
(*S*)-1-Phenyl-2-(piperidin-1-yl)ethan-1-amine, (*S*)-**AM6.**[14] Performed on a 6.1 mmol scale. Purified by column chromatography (10% MeOH in DCM + 0.8% Et_3N, R_f = 0.25). Yellow oil (0.99 g, 77% yield). **^{1}H NMR (200 MHz, $CDCl_3$) δ** 7.42 – 7.16 (m, 5H), 4.10 (dd, *J* = 9.6, 4.4 Hz, 1H), 2.67 – 2.19 (m, 6H), 1.89 (s, 2H), 1.73 – 1.50 (m, 4H), 1.49 – 1.33 (m, 2H).



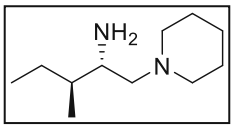
(*R*)-1-Phenyl-2-(piperidin-1-yl)ethan-1-amine, (*R*)-**AM6.**[14] Performed on a 6.1 mmol scale. Purified by column chromatography (10% MeOH in DCM + 0.8% Et_3N, R_f = 0.25). Yellow oil (0.95 g, 76% yield). **^{1}H NMR (200 MHz, $CDCl_3$) δ** 7.42 – 7.16 (m, 5H), 4.10 (dd, *J* = 9.6, 4.4 Hz, 1H), 2.67 – 2.19 (m, 6H), 1.89 (s, 2H), 1.73 – 1.50 (m, 4H), 1.49 – 1.33 (m, 2H).



(*S*)-1-(1*H*-Indol-3-yl)-3-(piperidin-1-yl)propan-2-amine, **AM7.** Performed on a 5.0 mmol scale. Purified by column chromatography (10% MeOH in DCM + 0.8% Et_3N, R_f = 0.21). Yellow solid (0.37 g, 30% yield). $[\alpha]_D^{20}$ = + 11.60 (c 0.96, CH_2Cl_2). **^{1}H NMR (400 MHz, $CDCl_3$) δ** 8.44 (s, 1H), 7.62 (dt, *J* = 7.9, 1.0 Hz, 1H), 7.36 (dt, *J* = 8.1, 1.0 Hz, 1H), 7.18 (ddd, *J* = 8.1, 7.0, 1.3 Hz, 1H), 7.11 (ddd, *J* = 8.0, 7.0, 1.1 Hz, 1H), 7.06 (s, 1H), 3.38 – 3.26 (m, 1H), 2.90 (ddd, *J* = 14.2, 4.5, 0.9 Hz, 1H), 2.83 (d, *J* = 12.0, 2H), 2.66 (dd, *J* = 14.2, 8.4 Hz, 2H), 2.40 – 2.21 (m, 6H), 1.56 (pd, *J* = 6.0, 3.6 Hz, 4H), 1.42 (p, *J* = 6.0 Hz, 2H). **^{13}C NMR (101 MHz, $CDCl_3$) δ** 136.52, 127.85, 122.83, 122.00, 119.32, 119.09, 113.08, 111.31, 65.87, 55.23, 48.34, 31.55, 26.23, 24.59. **IR ATR (vmax/cm^{-1})** 3367, 2917, 2839, 1499, 1355. **HRMS (ESI)** Cald for $C_{16}H_{24}N_3$ $[M+H]^+$ 258.1965, Found 258.1972.

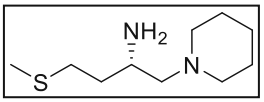


(*S*)-3-Methyl-1-(piperidin-1-yl)butan-2-amine, **AM8.**[14] Performed on a 4.0 mmol scale. Light yellow oil (0.60 g, 80% yield). **^{1}H NMR (400 MHz, $CDCl_3$) δ** 2.66 (ddd, *J* = 10.3, 5.6, 3.4 Hz, 1H), 2.16 – 2.10 (m, 2H), 2.46 (s, 2H), 2.06 – 2.00 (m, 2H), 1.63 – 1.45 (m, 7H), 1.44 – 1.35 (m, 2H), 0.89 (d, *J* = 6.8 Hz, 6H).

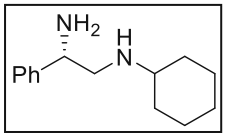


(2*S*,3*S*)-3-Methyl-1-(piperidin-1-yl)pentan-2-amine, **AM9.**[15] Performed on a 3.0 mmol scale. Dark yellow oil (0.48 g, 96% yield). **^{1}H NMR (400 MHz, $CDCl_3$) δ** 2.76 (ddd, *J* = 10.5, 5.6, 3.2 Hz, 1H), 2.53 – 2.35 (m, 2H), 2.23 – 1.85 (m, 5H), 1.57 – 1.35 (m, 7H), 1.32 – 1.07 (m, 3H), 0.95 – 0.80 (m, 6H). **^{13}C NMR (101 MHz, $CDCl_3$) δ** 63.46, 51.80, 39.26, 26.35, 25.42, 24.70, 15.20, 11.72.

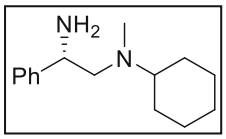
Die approbierte gedruckte Originalversion dieser Dissertation ist an der TU Wien Bibliothek verfügbar.
The approved original version of this doctoral thesis is available in print at TU Wien Bibliothek.
TU Bibliothek Your knowledge hub WIEN



(*S*)-4-(Methylthio)-1-(piperidin-1-yl)butan-2-amine, AM10. Performed on a 5.0 mmol scale. Red oil (0.56 g, 60% yield). $[\alpha]_D^{20}$ = + 7.19 (c 1.0, CH_2Cl_2). **^{1}H NMR (400 MHz, $CDCl_3$) δ** 2.99 (ddt, *J* = 9.6, 8.4, 4.2 Hz, 1H), 2.65 – 2.38 (m, 4H), 2.26 – 2.09 (m, 4H), 2.07 (s, 3H), 1.68 – 1.32 (m, 10H). **^{13}C NMR (101 MHz, $CDCl_3$) δ** 66.29, 55.14, 46.79, 35.28, 31.29, 26.26, 24.59, 15.62. **IR ATR (vmax/cm^{-1})** 2928, 2852, 1439. **HRMS (ESI)** Cald for $C_{10}H_{23}N_2S$ $[M+H]^+$ 203.1576, Found 203.1576.



(*S*)-*N*^{1}-Cyclohexyl-2-phenylethane-1,2-diamine, AM11. Performed on a 5.0 mmol scale. Red oil (0.60 g, 58% yield). $[\alpha]_D^{20}$ = + 44.37 (c 0.93, CH_2Cl_2). ^{1}H NMR (400 MHz, **$CDCl_3$**) δ 7.26 – 7.21 (m, 3H), 7.21 – 7.12 (m, 2H), 3.90 (dd, *J* = 8.5, 4.8 Hz, 1H), 2.78 (dd, *J* = 11.7, 4.8 Hz, 1H), 2.63 (dd, *J* = 11.7, 8.5 Hz, 1H), 2.33 (tt, *J* = 10.4, 3.8 Hz, 1H), 1.77 (dddd, *J* = 10.8, 9.3, 3.5, 1.5 Hz, 2H), 1.68 – 1.58 (m, 3H), 1.56 – 1.47 (m, 2H), 1.19 – 1.03 (m, 4H), 1.01 – 0.91 (m, 3H). **^{13}C NMR (101 MHz, $CDCl_3$) δ** 145.17, 128.61, 127.23, 126.50, 56.89, 56.23, 55.12, 33.99, 33.78, 26.31, 25.17. **HRMS (ESI)** Cald for $C_{14}H_{23}N_2$ $[M+H]^+$ 219.1856, Found 219.1874.

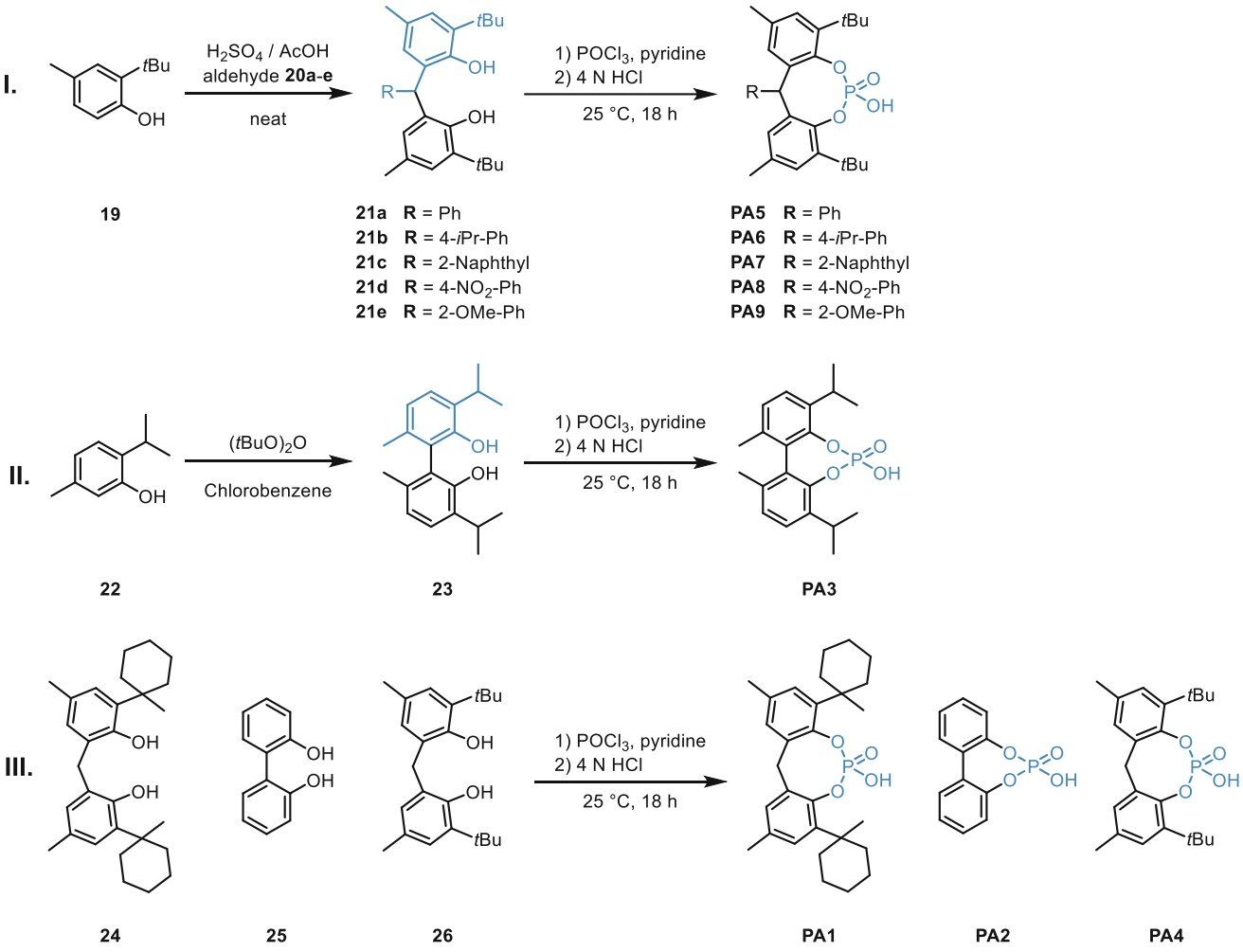


(*S*)-*N*^{1}-Cyclohexyl-N^1-methyl-2-phenylethane-1,2-diamine, AM12. Performed on a 5.0 mmol scale. Red oil (0.46 g, 42% yield). $[\alpha]_D^{20}$ = + 33.17 (c 0.75, CH_2Cl_2). **^{1}H NMR (200 MHz, $CDCl_3$) δ** 7.41 – 7.07 (m, 5H), 3.98 (t, *J* = 6.9 Hz, 1H), 2.48 – 2.32 (m, 2H), 2.26 (s, 3H), 1.89 (s, 2H), 1.80 – 1.46 (m, 5H), 1.33 – 0.92 (m, 5H). **^{13}C NMR (101 MHz, $CDCl_3$) δ** 144.74, 128.32, 126.99, 126.74, 63.77, 62.72, 53.48, 37.84, 29.17, 28.31, 26.39, 26.11, 26.10. **HRMS (ESI)** Cald for $C_{15}H_{25}N_2$ $[M+H]^+$ 233.2012, Found 233.2014.

Die approbierte gedruckte Originalversion dieser Dissertation ist an der TU Wien Bibliothek verfügbar.
The approved original version of this doctoral thesis is available in print at TU Wien Bibliothek.

3. Synthesis of the phosphoric acids

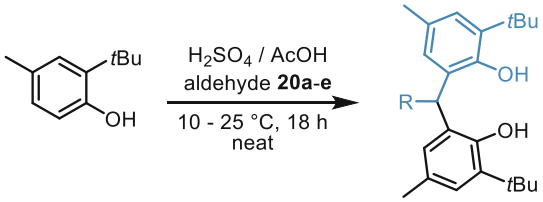
Phosphoric acids **PA5**-**PA9** were prepared according to a two-step procedure *via* Friedel-Crafts alkylation and subsequent phosphorylation (Scheme S2, **I.**). Phosphoric acid **PA3** was prepared according to two-step procedure *via* oxidative coupling and subsequent phosphorylation (Scheme S2, **II.**). Phosphoric acids **PA1**-**PA2** and **PA4** were prepared *via* direct phosphorylation of commercially available diols **24**-**26** (Scheme S2, **III.**).



Scheme S2. General procedure for the synthesis of phosphoric acids.

Die approbierte gedruckte Originalversion dieser Dissertation ist an der TU Wien Bibliothek verfügbar.
The approved original version of this doctoral thesis is available in print at TU Wien Bibliothek.

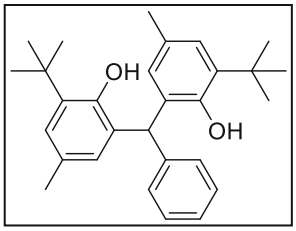
Preparation of 1,1´-biphenols *via* Friedel-Crafts alkylation



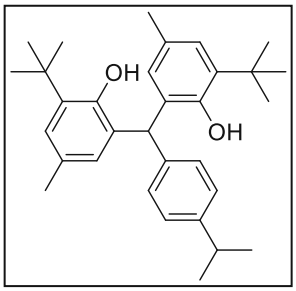
19

21a **R** = Ph
21b **R** = 4-*i*Pr-Ph
21c **R** = 2-Naphthyl
21d **R** = 4-NO_2-Ph
21e **R** = 2-OMe-Ph

General procedure:[16] To a solution of phenol **19** (2.0 equiv.) in acetic acid (0.58 M), aldehyde **20a-e** (1.0 equiv.) was added at room temperature. Then concentrated sulfuric acid (1.3 equiv.) was added dropwise over about 7-10 °C (*excessive cooling below this point might result in the freezing of acetic acid!*) and the mixture was stirred for 15 min. The cooling bath was removed and the solution was stirred for 18 h at room temperature. Distilled H_2O was added, the precipitate was filtered off and it was subsequently washed with distilled H_2O until the filtrate became colourless. Purification of the crude products (noted below) afforded **21a-e** as white or slightly coloured solid.

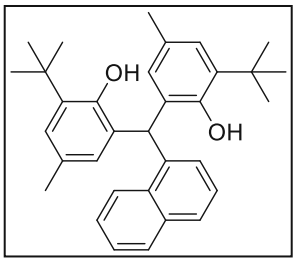


6,6'-(Phenylmethylene)bis(2-(*tert*-butyl)-4-methylphenol), 21a.[16] Performed on a 6.0 mmol scale. Purified by washing the crude precipitate several times with cold *n*-hexane. White solid (1.4 g, 55% yield). **^{1}H NMR (200 MHz, $CDCl_3$) δ** 7.43 – 7.29 (m, 3H), 7.25 – 7.15 (m, 2H), 7.12 – 7.03 (d, *J* = 2.2 Hz, 2H), 6.50 (d, *J* = 2.2 Hz, 2H), 5.61 (s, 1H), 4.83 (bs, 2H), 2.19 (s, 6H), 1.38 (s, 18H).

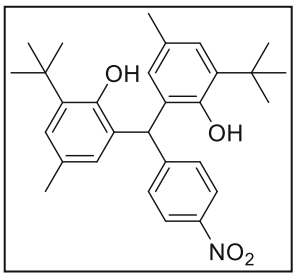


6,6'-((4-Isopropylphenyl)methylene)bis(2-(*tert*-butyl)-4-methylphenol) , 21b. Performed on a 6.0 mmol scale. The crude precipitate was dissolved in DCM, washed with sat. $NaHCO_3$ (2×), brine (1×), and the combined organic phases were dried over anhydrous Na_2SO_4 and concentrated *in vacuo*. The crude product was purified by column chromatography (5% EtOAc in PE, R_f = 0.45). White solid (0.95 g, 34% yield). **M.p.** 177 – 178 °C. **^{1}H NMR (400 MHz, $CDCl_3$) δ** 7.21 (d, *J* = 8.2 Hz, 2H), 7.11 (d, *J* = 8.2 Hz, 2H), 7.05 (d, *J* = 2.2 Hz, 2H), 6.52 (d, *J* = 2.1 Hz, 2H), 5.54 (s, 1H), 4.81 (s, 2H), 2.93 (m, 1H), 2.19 (s, 6H), 1.38 (s, 18H), 1.27 (d, *J* = 6.9 Hz, 6H). **^{13}C NMR (101 MHz, $CDCl_3$) δ** 151.00, 148.07, 137.71, 137.64, 129.66, 129.46, 128.44, 127.95, 127.24, 127.21, 47.14, 34.77, 33.84, 29.92, 24.08, 21.20. **IR ATR (vmax/cm^{-1})** 3535, 3476, 2960, 1441, 1164. **HRMS (ESI)** Cald for $C_{32}H_{41}O_2$ $[M-H]^-$ 457.3112, Found 457.3114.

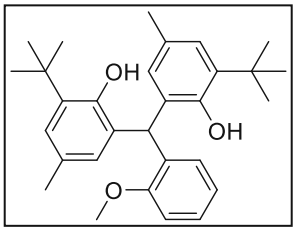
Die approbierte gedruckte Originalversion dieser Dissertation ist an der TU Wien Bibliothek verfügbar.
The approved original version of this doctoral thesis is available in print at TU Wien Bibliothek.
TU Bibliothek Your knowledge hub WIEN



6,6'-(Naphthalen-1-ylmethylene)bis(2-(*tert*-butyl)-4-methylphenol), 21c. Performed on a 6.0 mmol scale. The crude precipitate was dissolved in DCM, extracted with sat. $NaHCO_3$ (2×), brine (1×), the combined organic phase dried over anhydrous Na_2SO_4 and concentrated. Purified by column chromatography (5 % EtOAc in PE, R_f = 0.41). White solid (1.48 g, 52% yield). **M.p.** 107 – 110 °C. **^{1}H NMR (200 MHz, $CDCl_3$) δ** 7.96 – 7.80 (m, 3H), 7.54 – 7.35 (m, 3H), 7.17 – 7.03 (m, 3H), 6.45 (d, *J* = 2.1 Hz, 2H), 6.31 (s, 1H), 4.73 (bs, 2H), 2.14 (s, 6H), 1.40 (s, 18H). **^{13}C NMR (101 MHz, $CDCl_3$) δ** 150.87, 137.77, 136.53, 134.24, 132.08, 129.79, 128.97, 128.52, 128.31, 128.10, 127.32, 127.18, 126.86, 126.02, 125.74, 124.14, 43.27, 34.78, 29.98, 21.19. **HRMS (ESI)** Cald for $C_{33}H_{37}O_2$ $[M-H]^-$ 465.2799, found 465.2796.



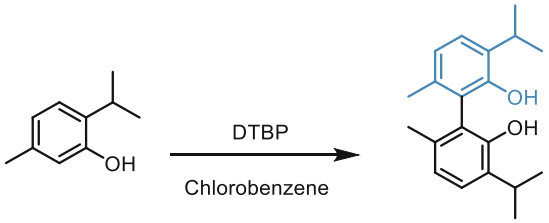
6,6'-((4-Nitrophenyl)methylene)bis(2-(*tert*-butyl)-4-methylphenol), 21d.[17] Performed on a 6.0 mmol scale. The crude precipitate was dissolved in DCM, washed with sat. $NaHCO_3$ (2×), brine (1×), and the combined organic phases were dried over anhydrous Na_2SO_4 and concentrated *in vacuo*. Pink solid (2.5 g, 89% yield). **M.p.** 212 – 214 °C. **^{1}H NMR (400 MHz, $CDCl_3$) δ** 8.24 – 8.11 (m, 2H), 7.34 (dd, *J* = 8.9, 0.7 Hz, 2H), 7.07 (d, *J* = 2.1 Hz, 2H), 6.52 – 6.43 (m, 2H), 5.82 (s, 1H), 4.91 (s, 2H), 2.20 (d, *J* = 0.7 Hz, 6H), 1.38 (s, 18H). **^{13}C NMR (101 MHz, $CDCl_3$) δ** 150.54, 149.79, 146.88, 137.33, 130.33, 130.00, 127.79, 127.65, 127.47, 123.80, 46.22, 34.49, 29.93, 21.05. **IR ATR (vmax/cm^{-1})** 3505, 2954, 1515, 1443, 1346. **HRMS (ESI)** Cald for $C_{29}H_{34}NO_4$ $[M-H]^-$ 460.2493, found 460.2491.



6,6'-((2-Methoxyphenyl)methylene)bis(2-(*tert*-butyl)-4-methylphenol), 21e.[18] Performed on a 6.0 mmol scale. The crude precipitate was dissolved in DCM, washed with sat. $NaHCO_3$ (2×), brine (1×), and the combined organic phases were dried over anhydrous Na_2SO_4 and concentrated *in vacuo*. Purified by column chromatography (3 % EtOAc in PE, R_f = 0.40). White solid (1.6 g, 59% yield). The crude product could be also purified by recrystallization from either acetic acid or *n*-hexane, affording **21e** with the same purity. **M.p.** 172 – 174 °C. **^{1}H NMR (200 MHz, $CDCl_3$) δ** 7.37 – 7.21 (m, 1H), 7.09 – 6.86 (m, 5H), 6.55 (d, *J* = 2.1 Hz, 2H), 5.91 (s, 1H), 4.95 (s, 2H), 3.81 (s, 3H), 2.19 (s, 6H), 1.37 (s, 18H). **^{13}C NMR (101 MHz, $CDCl_3$) δ** 156.83, 151.17, 137.49, 130.77, 129.28, 128.73, 128.64, 127.63, 127.43, 127.10, 121.37, 111.05, 55.90, 39.73, 34.82, 29.88, 21.21. **IR ATR (vmax/cm^{-1})** 3537, 2949, 1486, 1440, 1178, 1106. **HRMS (ESI)** Cald for $C_{30}H_{37}O_3$ $[M-H]^-$ 445.2748, found 445.2765.

Die approbierte gedruckte Originalversion dieser Dissertation ist an der TU Wien Bibliothek verfügbar.
The approved original version of this doctoral thesis is available in print at TU Wien Bibliothek.
TU Bibliothek Your knowledge hub WIEN

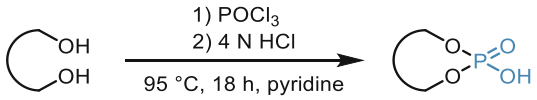
Preparation of 23 *via* oxidative coupling



22 **23**

According to modified literature procedure:[19] In a 20 mL microwave vial equipped with a stir bar, the phenol **22** (0.73 g, 4.85 mmol, 1.0 equiv.) was dissolved in chlorobenzene (1.66 M). Di-*tert*-butyl peroxide (DTBP, 0.93 mL, 5.10 mmol, 1.05 equiv.) was then added *via* syringe. The vial was capped and the reaction mixture was stirred for 15 min at room temperature. The vial was then placed in the microwave reactor and heated to 160 °C (*high absorption setting!*) and stirred for 15 min. The reaction mixture was allowed to cool down and volatiles have been removed under reduced pressure. The resulting crude mixture was purified by column chromatography (2% EtOAc in PE, R_f = 0.30). White solid (1.1 g, 76% yield). **^{1}H NMR (400 MHz, $CDCl_3$) δ** 7.19 (d, *J* = 7.7 Hz, 2H), 6.89 (d, *J* = 7.8 Hz, 2H), 4.76 (s, 2H), 3.32 – 3.25 (m, 2H), 1.96 (s, 6H), 1.26 (dd, *J* = 6.9, 2.7 Hz, 12H).

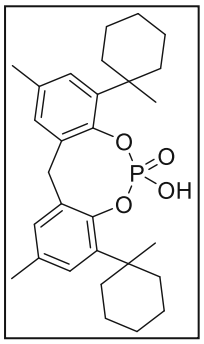
General procedure to all phosphorylations and hydrolysis



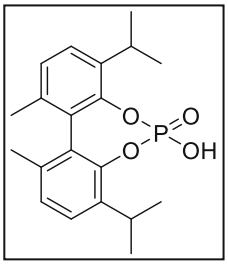
21a-e, 23-26 **PA1-PA9**

According to literature procedure:[20] To a solution of the diol **21a-e**, **23-26** (1.0 equiv.) in pyridine (0.34 M), $POCl_3$ (2.0 equiv.) was added slowly *via* syringe at 0 °C. After stirring the reaction mixture for 24 h at 95 °C, it was cooled to room temperature and H_2O (25 equiv.) was added slowly. The resulting clear solution was stirred for another 18 h at 95 °C. After cooling to room temperature, 4 N HCl was added slowly. The precipitate was filtered off and it was washed with 4 N HCl. The filtrate was extracted with DCM, and the organic phase was washed several times with 4 N HCl (3×), brine (3×), H_2O and it was dried over anhydrous Na_2SO_4. Removal of the solvent afforded **PA1**-**PA9**.

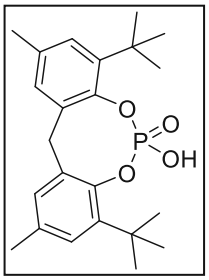
Die approbierte gedruckte Originalversion dieser Dissertation ist an der TU Wien Bibliothek verfügbar.
The approved original version of this doctoral thesis is available in print at TU Wien Bibliothek.



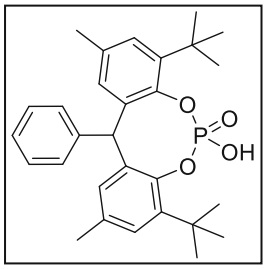
6-Hydroxy-2,10-dimethyl-4,8-bis(1-methylcyclohexyl)-12*H*-dibenzo[d,g] [1,3,2] dioxaphosphocine 6-oxide, PA1. Performed on a 7.1 mmol scale. White powder (3.4 g, 98% yield). **M.p.** 264 – 266 °C. **^{1}H NMR (400 MHz, $CDCl_3$) δ** 7.06 (t, *J* = 1.9 Hz, 2H), 6.96 (d, *J* = 2.1 Hz, 2H), 4.06 (s, 2H), 2.29 (s, 6H), 2.17 (dd, *J* = 13.4, 7.9 Hz, 4H), 1.69 – 1.52 (m, 8H), 1.44 (t, *J* = 9.1 Hz, 8H), 1.30 (s, 6H). The COO*H* proton was not detected. **^{13}C NMR (101 MHz, $CDCl_3$) δ** 147.79, 147.70, 139.60, 139.53, 134.26, 130.79, 130.76, 129.55, 129.53, 128.17, 38.62, 37.64, 35.39, 27.09, 26.62, 22.96, 21.15. **^{31}P NMR (162 MHz, $CDCl_3$) δ** −9.53. **IR ATR (vmax/cm^{-1})** 2922, 2856, 1604, 1440, 1194, 1018, 967. **HRMS (ESI)** Cald for $C_{29}H_{38}O_4P$ $[M-H]^-$ 481.2513, found 481.2514.



6-Hydroxy-4,8-diisopropyl-1,11-dimethyldibenzo[d,f][1,3,2]dioxaphosphepine-6-oxide, PA3. Performed on a 6.7 mmol scale. Brown foam (2.0 g, 83% yield). **^{1}H NMR (400 MHz, $CDCl_3$) δ** 8.35 (brs, 1H), 7.27 (d, *J* = 8.0 Hz, 2H), 7.15 (d, *J* = 8.0 Hz, 2H), 3.49-3.45 (m, 2H), 2.14 (s, 6H), 1.27 (dd, *J* = 25.5, 6.9 Hz, 12H). **^{31}P NMR (162 MHz, $CDCl_3$) δ** 2.14.

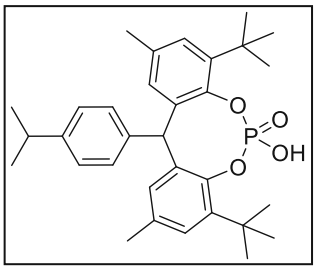


4,8-Di-*tert*-butyl-6-hydroxy-2,10-dimethyl-12*H*-dibenzo[d,g][1,3,2]dioxaphosphocine-6-oxide, PA4.[21] Performed on a 9.0 mmol scale. White powder (3.6 g, >99% yield). **^{1}H NMR (400 MHz, $CDCl_3$) δ** 12.35 (brs, 1H), 7.04 (d, *J* = 1.5 Hz, 2H), 6.96 (dd, *J* = 2.1, 0.8 Hz, 2H), 4.05 (s, 2H), 2.28 (s, 6H), 1.41 (s, 18H). **^{31}P NMR (162 MHz, $CDCl_3$) δ** −9.64.

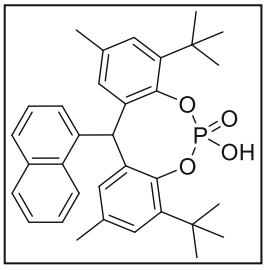


4,8-Di-*tert*-butyl-6-hydroxy-2,10-dimethyl-12-phenyl-12*H*-dibenzo [d,g]-[1,3,2]dioxaphosphocine 6-oxide, PA5. Performed on a 0.7 mmol scale. White powder (0.3 g, 87% yield). **M.p.** 254 – 256 °C. **^{1}H NMR (400 MHz, DMSO-d_6) δ** 7.26 (dd, *J* = 8.3, 6.6 Hz, 2H), 7.22 – 7.16 (m, 1H), 7.13 – 7.05 (m, 4H), 7.03 – 6.97 (m, 2H), 6.03 (s, 1H), 2.23 (s, 6H), 1.39 (s, 18H). The COO*H* proton was not detected. **^{13}C NMR (101 MHz, DMSO-d_6) δ** 146.64 (d, *J* = 7.8 Hz), 141.91, 140.86 (d, *J* = 4.7 Hz), 135.26 (d, *J* = 3.1 Hz), 133.37 (d, *J* = 1.7 Hz), 128.04, 126.98, 34.80, 31.10. **^{31}P NMR (162 MHz, DMSO-d_6) δ** −12.85. **IR ATR (vmax/cm^{-1})** 2959, 1739, 1602, 1439, 1011, 932. **HRMS (ESI)** Cald for $C_{29}H_{34}O_4P$ $[M-H]^-$ 477.2200, found 477.2201.

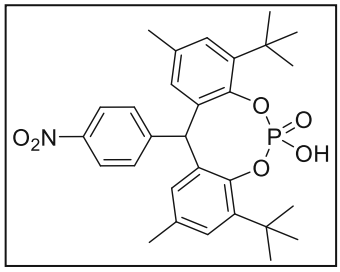
Die approbierte gedruckte Originalversion dieser Dissertation ist an der TU Wien Bibliothek verfügbar.
The approved original version of this doctoral thesis is available in print at TU Wien Bibliothek.
TU Bibliothek Your knowledge hub WIEN



4,8-Di-*tert*-butyl-6-hydroxy-12-(4-isopropylphenyl)-2,10-dimethyl-12*H*-dibenzo[d,g][1,3,2]dioxaphosphocine 6-oxide, PA6. Performed on a 2.0 mmol scale. White powder (0.91 g, 89% yield). **M.p.** 212 – 215 °C. **^{1}H NMR (400 MHz, $CDCl_3$) δ** 7.20 (d, *J* = 8.1 Hz, 2H), 7.14 (d, *J* = 8.2 Hz, 2H), 7.03 (s, 4H), 6.27 (s, 1H), 2.89 (h, *J* = 6.9 Hz, 1H), 2.25 (s, 6H), 1.41 (s, 19H), 1.26 (d, *J* = 6.9 Hz, 6H). The COO*H* proton was not detected. **^{13}C NMR (101 MHz, $CDCl_3$) δ** 147.31, 147.22, 146.87, 140.84, 140.78, 138.09, 134.42, 134.06, 129.53, 128.16, 127.06, 126.13, 35.07, 33.76, 31.11, 24.15, 21.39. **^{31}P NMR (162 MHz, $CDCl_3$) δ** −10.48. **IR ATR (vmax/cm^{-1})** 2960, 1502, 1512, 1442, 1218, 1106, 1018, 939. **HRMS (ESI)** Cald for $C_{32}H_{40}O_4P$ $[M-H]^-$ 519.2670, found 519.2670.

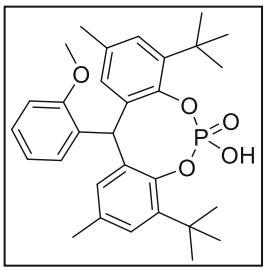


4,8-Di-*tert*-butyl-6-hydroxy-2,10-dimethyl-12-(naphthalen-1-yl)-12*H*-dibenzo [d,g][1,3,2]dioxaphosphocine 6-oxide, PA7. Performed on a 3.2 mmol scale. White powder (1.1 g, 67% yield). **M.p.** 284 – 287 °C (decomp.). **^{1}H NMR (400 MHz, $CDCl_3$) δ** 7.81 – 7.67 (m, 4H), 7.39 – 7.25 (m, 2H), 7.20 – 7.13 (m, 1H), 6.95 (t, *J* = 2.0 Hz, 2H), 6.86 (s, 1H), 6.75 (d, *J* = 2.2 Hz, 2H), 2.10 (s, 6H), 1.35 (s, 18H). The COO*H* proton was not detected. **^{13}C NMR (101 MHz, $CDCl_3$) δ** 147.42, 147.32, 140.81, 140.75, 135.20, 134.41, 133.93, 133.91, 133.58, 133.55, 132.75, 128.66, 128.60, 128.07, 126.93, 126.40, 126.37, 125.72, 125.53, 124.78, 40.43, 35.05, 30.86, 21.40. **^{31}P NMR (162 MHz, $CDCl_3$) δ** −9.10. **IR ATR (vmax/cm^{-1})** 2950, 1601, 1438, 1196, 1123, 1015, 958. **HRMS (ESI)** Cald for $C_{33}H_{36}O_4P$ $[M-H]^-$ 527.2357, found 527.2356.



4,8-Di-*tert*-butyl-6-hydroxy-2,10-dimethyl-12-(4-nitrophenyl)-12*H*-dibenzo[d,g][1,3,2]dioxaphosphocine 6-oxide, PA8. Performed on a 5.4 mmol scale. Red solid (2.1 g, 74% yield). **M.p.** 199 – 202 °C. **^{1}H NMR (200 MHz, $CDCl_3$) δ** 10.83 (brs, 1H), 8.09 – 7.95 (m, 2H), 7.28 – 7.21 (m, 2H), 7.06 (s, 2H), 6.88 (d, *J* = 2.1 Hz, 2H), 6.02 (s, 1H), 2.22 (s, 6H), 1.32 (s, 18H). **^{13}C NMR (101 MHz, $CDCl_3$) δ** 149.27, 146.72, 146.63, 146.47, 141.80, 141.75, 134.91, 134.90, 133.20, 129.65, 128.20, 123.11, 35.16, 31.11, 21.30. **^{31}P NMR (162 MHz, $CDCl_3$) δ** −11.54**IR ATR (vmax/cm^{-1})** 2962, 1596, 1517, 1443, 1346, 898. **HRMS (ESI)** Cald for $C_{29}H_{33}NO_6P$ $[M-H]^-$ 522.2051, found 522.2052.

Die approbierte gedruckte Originalversion dieser Dissertation ist an der TU Wien Bibliothek verfügbar.
The approved original version of this doctoral thesis is available in print at TU Wien Bibliothek.



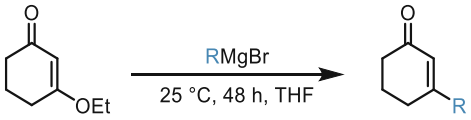
4,8-Di-*tert*-butyl-6-hydroxy-12-(2-methoxyphenyl)-2,10-dimethyl-12*H*-dibenzo[d,g][1,3,2]dioxaphosphocine 6-oxide, **PA9.** Performed on a 3.6 mmol scale. White solid (1.7 g, 95% yield). **M.p.** 174 – 176 °C. **^{1}H NMR (400 MHz, CD_2Cl_2) δ** 10.08 (brs, 1H), 7.64 (ddd, *J* = 7.8, 1.6, 0.8 Hz, 1H), 7.27 (td, *J* = 7.7, 1.6 Hz, 1H), 7.05 (s, 2H), 7.02 – 6.93 (m, 3H), 6.87 (dd, *J* = 8.2, 1.2 Hz, 1H), 6.47 (s, 1H), 3.52 (s, 3H), 2.25 (s, 6H), 1.42 (s, 18H). **^{13}C NMR (101 MHz, CD_2Cl_2) δ** 158.54, 147.36, 147.27, 141.03, 140.97, 134.70, 134.67, 134.30, 134.29, 129.75, 129.34, 128.36, 127.88, 127.86, 126.99, 120.27, 112.13, 56.08, 38.08, 35.25, 31.15, 21.33. **^{31}P NMR (162 MHz, CD_2Cl_2) δ** −10.56. **IR ATR (vmax/cm^{-1})** 2959, 1599, 1459, 1436, 1245, 1199, 1107, 955. **HRMS (ESI)** Cald for $C_{30}H_{36}O_5P$ $[M-H]^-$ 507.2306, found 507.2304.

Die approbierte gedruckte Originalversion dieser Dissertation ist an der TU Wien Bibliothek verfügbar.
The approved original version of this doctoral thesis is available in print at TU Wien Bibliothek.

4. Substrate synthesis

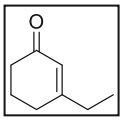
3-Methyl-2-cyclohexenone (**1a**), 3-methyl-2-cyclopentenone (**1b**) and 4,4-dimethyl-2-cyclohexenone (**1n**) have been purchased from commercial supplier (Sigma Aldrich). 3-Ethoxy-2-cyclohexenone (**27**) has been purchased from Acros Organics. All of these were used without further purifications.

1c-**m** were prepared *via* Grignard-reaction, as depicted in Scheme 4.

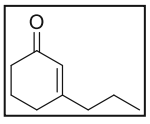


27 **1c-m**

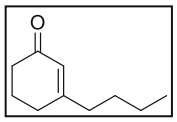
General procedure:[22] A 3 M solution of the Grignard reagent was prepared freshly from freshly ground Mg (1.0 equiv.), alkyl/aryl bromide (1.0 equiv.) in dry Et_2O (2.0 M for alkyl halide, 1.0 M for aryl halide) and it was stirred for 1 h. After being cooled to 0 °C, 3-ethoxy-2-cyclohexenone (**27**, 1.0 equiv.) in dry THF (10 mL) was added slowly, and the reaction mixture was stirred for 18 h at room temperature. The reaction mixture was quenched with 1 N HCl solution (50 mL) at 0 °C. Et_2O was added and the organic phase was washed with 1 N HCl solution (3 × 25 mL), sat. $NaHCO_3$ (3 × 25 mL), dried over anhydrous Na_2SO_4 and concentrated under reduced pressure. The crude products were purified by column chromatography (PE: Et_2O, UV and vaniline TLC visualization) to provide the pure products.



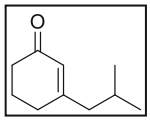
3-Ethyl-2-cyclohexenone, 1c.[22] Performed on a 14.0 mmol scale. Purified by column chromatography (25% Et_2O in PE). Yellow oil (1.20 g, 69% yield). **^{1}H NMR (400 MHz, $CDCl_3$) δ** 5.87 (s, 1H), 2.45 – 2.11 (m, 6H), 2.07 – 1.81 (m, 2H), 1.09 (t, *J* = 7.4 Hz, 3H).



3-Propyl-2-cyclohexenone, 1d.[23] Performed on a 14.0 mmol scale. Purified by column chromatography (20% Et_2O in PE). Yellow oil (1.72 g, 89% yield). **^{1}H NMR (400 MHz, $CDCl_3$) δ** 5.84 (s, 1H), 2.36 – 2.31 (m, 2H), 2.25 (tdd, *J* = 6.2, 1.5, 0.7 Hz, 2H), 2.20 – 2.13 (m, 2H), 2.01 – 1.92 (m, 2H), 1.51 (h, *J* = 7.4 Hz, 2H), 0.91 (t, *J* = 7.4 Hz, 3H).

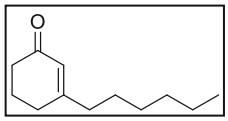


3-Butyl-2-cyclohexenone, 1e.[24] Performed on a 14.0 mmol scale. Purified by column chromatography (30% Et_2O in PE). Yellow oil (1.53 g, 74% yield). **^{1}H NMR (400 MHz, $CDCl_3$) δ** 5.86 (s, 1H), 2.48 – 2.09 (m, 6H), 2.06 – 1.79 (m, 2H), 1.61 – 1.15 (m, 4H), 0.91 (t, *J* = 7.0 Hz, 3H).

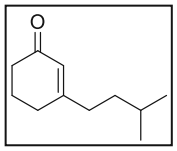


3-Isobutyl-2-cyclohexenone, 1f. [22] Performed on a 14.0 mmol scale. Purified by column chromatography (25% Et_2O in PE). Yellow oil (1.10 g, 69% yield). **^{1}H NMR (400 MHz, $CDCl_3$) δ** 5.84 (s, 1H), 2.54 – 2.17 (m, 4H), 2.18 – 1.56 (m, 5H), 0.90 (d, *J* = 6.5 Hz, 6H).

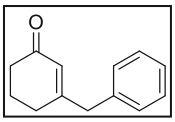
Die approbierte gedruckte Originalversion dieser Dissertation ist an der TU Wien Bibliothek verfügbar.
The approved original version of this doctoral thesis is available in print at TU Wien Bibliothek.
TU Bibliothek Your knowledge hub WIEN



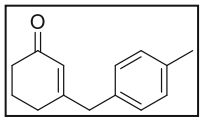
3-Hexyl-2-cyclohexenone, 1g.[25] Performed on a 14.0 mmol scale. Purified by column chromatography (30% Et_2O in PE). Yellow oil (1.96 g, 60% yield**). ^{1}H NMR (400 MHz, $CDCl_3$)** δ 5.85 (p, *J* = 1.4 Hz, 1H), 2.33 (dd, *J* = 7.5, 6.0 Hz, 2H), 2.26 (td, *J* = 6.1, 1.5 Hz, 2H), 2.23 – 2.16 (m, 2H), 2.03 – 1.92 (m, 2H), 1.53 – 1.41 (m, 2H), 1.35 – 1.20 (m, 6H), 0.93 – 0.82 (m, 3H).



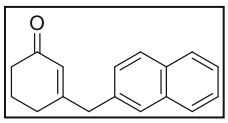
3-(3-Methylbutyl)-2-cyclohexen-1-one, 1h.[26] Performed on a 14.0 mmol scale. Purified by column chromatography (30% Et_2O in PE). Yellow oil (2.1 g, 89% yield). **^{1}H NMR (400 MHz, $CDCl_3$) δ** 5.85 (s, 1H), 2.33 (dd, *J* = 7.4, 6.0 Hz, 2H), 2.27 (ddt, *J* = 7.1, 5.5, 1.1 Hz, 2H), 2.22 – 2.16 (m, 2H), 2.00 – 1.91 (m, 2H), 1.54 (dp, *J* = 13.3, 6.7 Hz, 1H), 1.40 – 1.31 (m, 2H), 0.88 (d, *J* = 6.6 Hz, 6H).



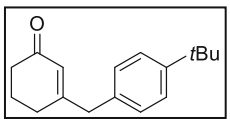
3-Benzylcyclohex-2-en-1-one, 1i.[27] Performed on a 18.0 mmol scale (1 M Grignard solution). Purified by column chromatography (35% Et_2O in PE). Yellow oil (1.8 g, 54% yield). **^{1}H NMR (400 MHz, $CDCl_3$) δ** 7.30 – 7.25 (m, 2H), 7.24 – 7.18 (m, 1H), 7.14 – 7.10 (m, 2H), 5.83 (s, 1H), 3.47 (s, 2H), 2.32 (dd, *J* = 7.5, 6.0 Hz, 2H), 2.25 – 2.17 (m, 2H), 1.98 – 1.86 (m, 2H).



3-(4-Methylbenzyl)cyclohex-2-en-1-one, 1j.[28] Performed on a 14.0 mmol scale (1 M Grignard solution). Purified by column chromatography (30% Et_2O in PE). Yellow oil (0.91 g, 32% yield). **^{1}H NMR (400 MHz, $CDCl_3$) δ** 7.14 – 7.09 (m, 2H), 7.07 – 7.02 (m, 2H), 5.86 (s, 1H), 3.46 (s, 2H), 2.39 – 2.29 (m, 5H), 2.27 – 2.21 (m, 2H), 1.99 – 1.90 (m, 2H).



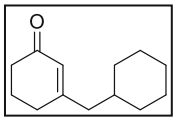
3-(Naphthalen-2-ylmethyl)cyclohex-2-en-1-one, 1k. Performed on a 18.0 mmol scale (1 M Grignard solution). Purified by column chromatography (35% Et_2O in PE). White solid (1.0 g, 24% yield). **M.p.** 75 – 77 °C. **^{1}H NMR (400 MHz, $CDCl_3$) δ** 7.64 – 7.54 (m, 3H), 7.44 – 7.39 (m, 1H), 7.31 – 7.22 (m, 2H), 7.13 – 7.02 (m, 1H), 5.73 (s, 1H), 3.46 (s, 2H), 2.15 (dd, *J* = 7.4, 6.0 Hz, 2H), 2.07 (td, *J* = 6.1, 1.5 Hz, 2H), 1.79 – 1.67 (m, 2H). **^{13}C NMR (101 MHz, $CDCl_3$) δ** 200.04, 164.65, 134.64, 132.54, 128.56, 127.84, 127.82, 127.66, 127.34, 127.24, 126.41, 125.92, 44.82, 37.46, 29.38, 22.80. **IR ATR (vmax/cm^{-1})** 3056, 1664, 811, 745. **HRMS (ESI)** Cald for $C_{17}H_{17}O$ $[M+H]^+$ 237.1274, Found 237.1228.



3-(4-(*Tert*-butyl)benzyl)cyclohex-2-en-1-one, 1l. Performed on a 14.0 mmol scale (1 M Grignard solution). Purified by column chromatography (30% Et_2O in PE). Yellow oil (1.7 g, 39% yield). **^{1}H NMR (400 MHz, $CDCl_3$) δ** 7.35 – 7.29 (m, 2H), 7.11 – 7.06 (m, 2H), 5.85 (s, 1H), 3.47 (s, 2H), 2.36 (dd, *J* = 7.4, 6.0 Hz, 2H), 2.30 – 2.22 (m, 2H), 2.02 – 1.92

Die approbierte gedruckte Originalversion dieser Dissertation ist an der TU Wien Bibliothek verfügbar.
The approved original version of this doctoral thesis is available in print at TU Wien Bibliothek.
TU Bibliothek Your knowledge hub WIEN

(m, 2H), 1.31 (s, 9H). **^{13}C NMR (101 MHz, $CDCl_3$) δ** 200.15, 165.24, 149.92, 133.97, 128.92, 126.92, 125.73, 44.12, 37.46, 34.59, 31.50, 29.49, 22.80. **IR ATR (vmax/cm^{-1})** 2951, 1665, 812, 746. **HRMS (ESI)** Cald for $C_{17}H_{23}O$ $[M+H]^+$ 243.1744, Found 243.1749.

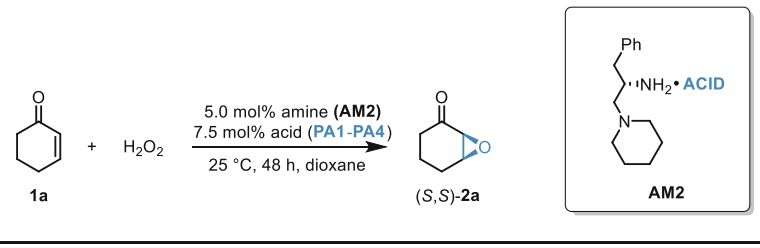


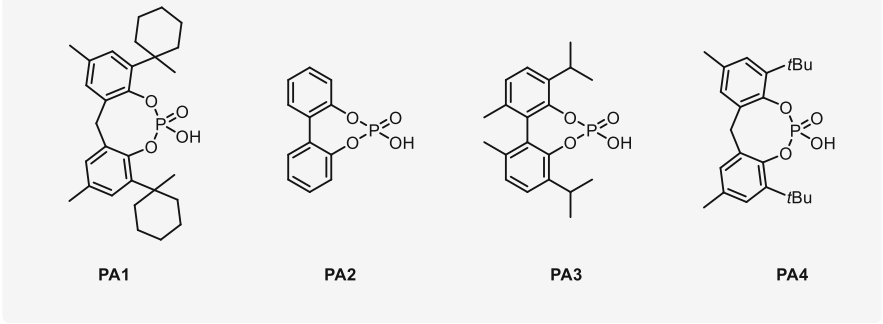
3-(Cyclohexylmethyl)cyclohex-2-en-1-one, **1m.**[29] Performed on a 21.0 mmol scale. Purified by column chromatography (30% Et_2O in PE). Yellow oil (1.5 g, 71% yield). **^{1}H NMR (400 MHz, $CDCl_3$) δ** 5.83 (s, 1H), 2.37 – 2.31 (m, 2H), 2.25 (td, *J* = 6.1, 1.6 Hz, 2H), 2.08 (d, *J* = 7.2 Hz, 2H), 1.97 (dq, *J* = 7.7, 6.3 Hz, 2H), 1.74 – 1.59 (m, 5H), 1.52 (ddq, *J* = 11.0, 7.2, 3.6 Hz, 1H), 1.28 – 1.07 (m, 3H), 0.97 – 0.83 (m, 2H).

Die approbierte gedruckte Originalversion dieser Dissertation ist an der TU Wien Bibliothek verfügbar.
The approved original version of this doctoral thesis is available in print at TU Wien Bibliothek.

5. Parameter optimization for asymmetric epoxidations

5.1. Preliminary phosphoric acid screening



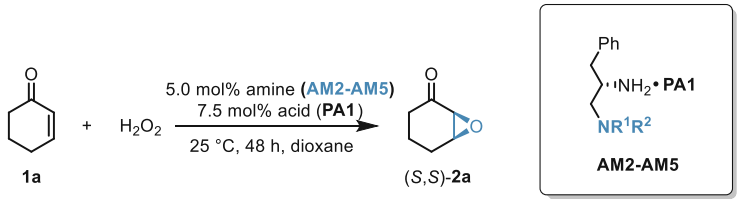


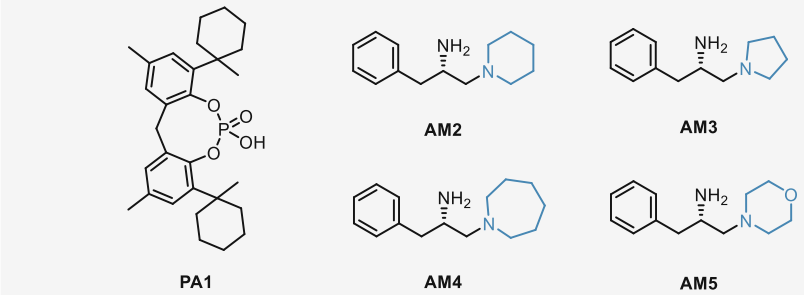
entry[a]	amine	acid	conv. [%][b]	ee [%][c]
1	AM2	PA1	93	88
2	AM2	**PA2**	7	25
3	AM2	**PA3**	93	79
4	AM2	**PA4**	60	88

[a] Performed with 0.30 mmol 2-cyclohexen-1-one (**1a**), 0.015 mmol catalyst (5 mol% **AM2**, 7.5 mol% **PA1**-**PA4**) and 1.5 equiv. H_2O_2 (50% aq.) in 1.25 mL dioxane at 25 °C for 48 hours. [b] Determined by GC analysis using *n*-dodecane as internal standard. [c] Determined by chiral GC analysis using a BGB175 chiral capillary column. Absolute configuration has been determined by measuring the optical rotation and comparing with literature data.

Die approbierte gedruckte Originalversion dieser Dissertation ist an der TU Wien Bibliothek verfügbar.
The approved original version of this doctoral thesis is available in print at TU Wien Bibliothek.

5.2 Amino-modification screening



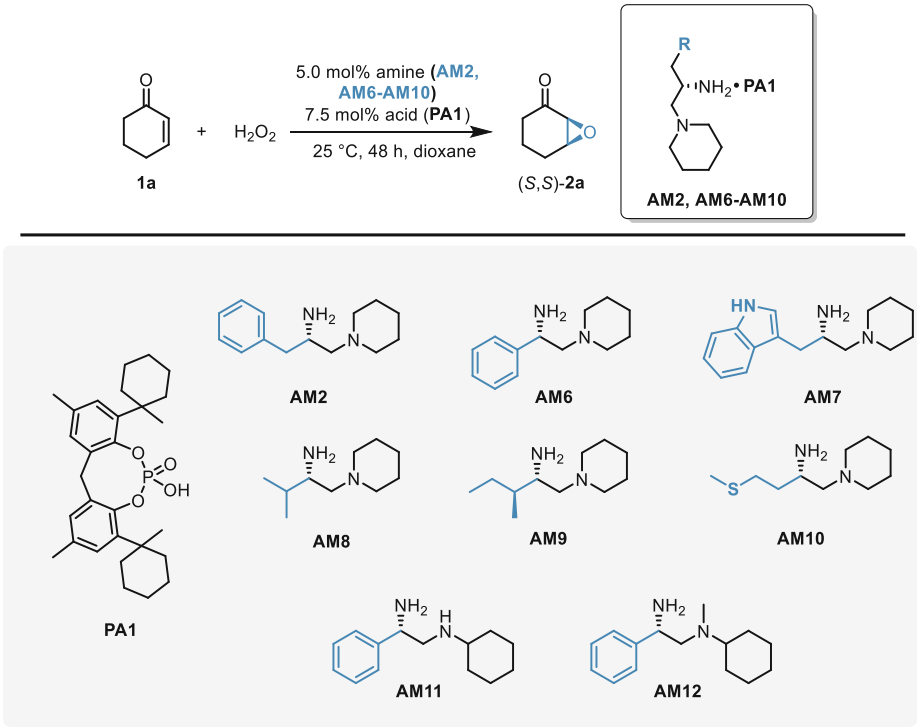


entry[a]	amine	acid	conv. [%][b]	ee [%][c]
1	AM2	PA1	93	89
2	AM3		78	84
3	AM4		65	86
4	AM5		20	84

[a] Performed with 0.30 mmol 2-cyclohexen-1-one (**1a**), 0.015 mmol catalyst (5 mol% **AM2**-**AM6**, 7.5 mol% **PA1**) and 1.5 equiv. H_2O_2 (50% aq.) in 1.25 mL dioxane at 25 °C for 48 hours. [b] Determined by GC analysis using *n*-dodecane as internal standard. [c] Determined by chiral GC analysis using a BGB175 chiral capillary column. Absolute configuration has been determined by measuring the optical rotation and comparing with literature data.

Die approbierte gedruckte Originalversion dieser Dissertation ist an der TU Wien Bibliothek verfügbar.
The approved original version of this doctoral thesis is available in print at TU Wien Bibliothek.

5.3 Amino acid screening

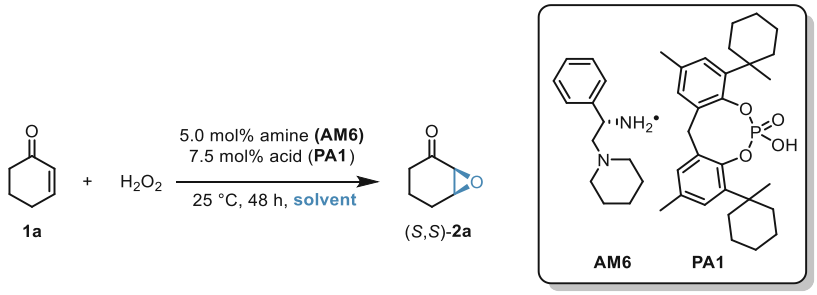


entry[a]	amine	acid	conv. [%][b]	ee [%][c]
1	**AM2**	**PA1**	93	89
2	**AM6**		**95**	**91**
3	**AM7**		67	81
4	**AM8**		94	81
5	**AM9**		81	82
6	**AM10**		77	62
7	**AM11**		22	91
8	**AM12**		34	80

[a] Performed with 0.30 mmol 2-cyclohexen-1-one (**1a**) 0.015 mmol catalyst (5 mol% **AM2**, **AM6**-**AM10**, 7.5 mol% **PA1**) and 1.5 equiv. H_2O_2 (50% aq.) in 1.25 mL dioxane at 25 °C for 48 hours. [b] Determined by GC analysis using *n*-dodecane as internal standard. [c] Determined by chiral GC analysis using a BGB175 chiral capillary column. Absolute configuration has been determined by measuring the optical rotation and comparing with literature data.

Die approbierte gedruckte Originalversion dieser Dissertation ist an der TU Wien Bibliothek verfügbar.
The approved original version of this doctoral thesis is available in print at TU Wien Bibliothek.

5.4 Solvent screening

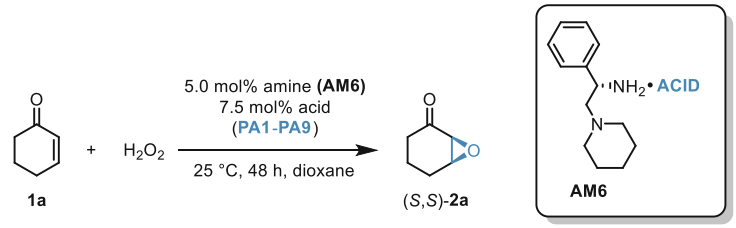


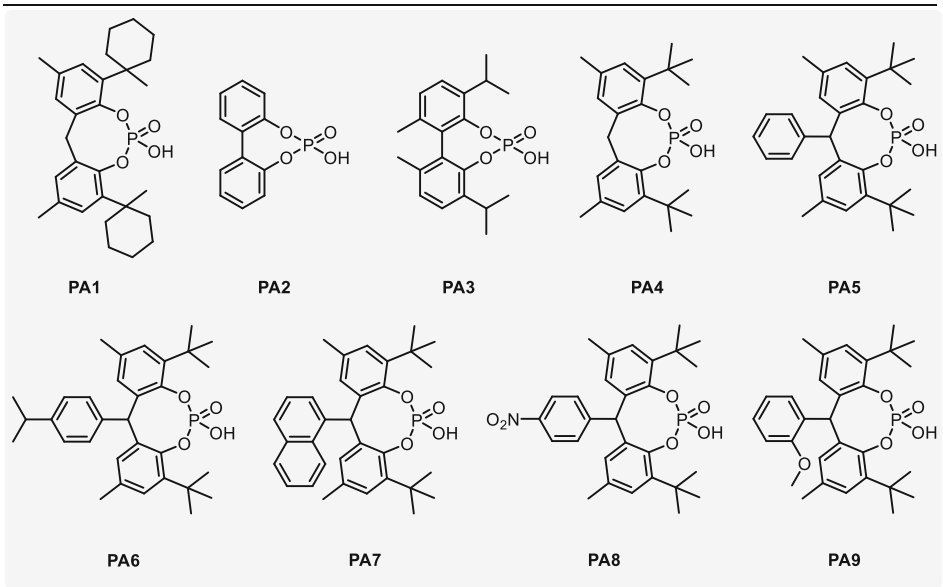
entry[a]	amine	acid	solvent	conv. [%][b]	ee [%][c]
1			**dioxane**	**95**	**91**
2			DME	73	87
3			2MeTHF	81	87
4	**AM6**	**PA1**	THF	18	87
5			MTBE	94	83
6			$CHCl_3$	42	84
7			toluene	42	60

[a] Performed with 0.30 mmol 2-cyclohexen-1-one (**1a**), 0.015 mmol catalyst (5 mol% **AM6**, 7.5 mol% **PA1**) and 1.5 equiv. H_2O_2 (50% aq.) in 1.25 mL solvent at 25 °C for 48 hours. [b] Determined by GC analysis using *n*-dodecane as internal standard. [c] Determined by chiral GC analysis using a BGB175 chiral capillary column. Absolute configuration has been determined by measuring the optical rotation and comparing with literature data.

Die approbierte gedruckte Originalversion dieser Dissertation ist an der TU Wien Bibliothek verfügbar.
The approved original version of this doctoral thesis is available in print at TU Wien Bibliothek.

5.5 Final phosphoric acid screening, screening of conventional acids



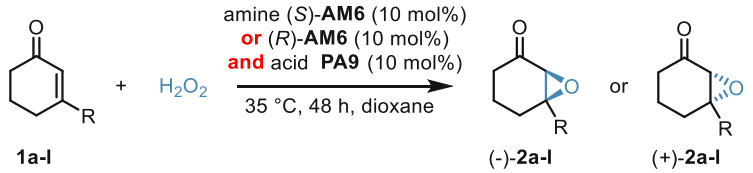


entry[a]	amine	acid	conv. [%][b]	ee [%][c]
1	AM6	no acid	0	n.d.
2		*p*TsOH	90	83 (91.5: 8.5)
3		2,5-dinitrobenzoic acid	94	67 (83.5: 16.5)
4		TFA	95	72 (86.0: 14.0)
5		Camphorsulfonic acid	87	82 (91.0: 9.0)
6		**PA1**	95	91 (95.5: 4.5)
7		**PA2**	12	69 (84.5: 15.5)
8		**PA3**	97	90 (95.0: 5.0)
9		**PA4**	85	92 (96.0: 4.0)
10		**PA5**	98	93 (96.5: 3.5)
11		**PA6**	96	94 (97.0: 3.0)
12		**PA7**	95	94 (97.0: 3.0)
13		**PA8**	95	93 (96.5: 3.5)
14		**PA9**	95	95 (97.5: 2.5)
15[d]		**PA9**	**96**	**95 (97.5: 2.5)**
16[e]		**PA9**	48	86 (93.0: 7.0)

[a] Performed with 0.30 mmol 2-cyclohexen-1-one (**1a**), 0.015 mmol catalyst (5 mol% **AM6**, 5.0-10.0 mol% **PA1-PA9** or other acid) and 1.5 equiv. H_2O_2 (50% aq.) in 1.5 mL dioxane at 25 °C for 48 hours. [b] Determined by GC analysis using *n*-dodecane as internal standard. [c] Determined by chiral GC analysis using a BGB175 chiral capillary column. Enantiomeric ratios in parenthesis. Absolute configuration has been determined by measuring the optical rotation and comparing with literature data. [d] Performed with an amine-to-acid ratio of 1/1 (5 mol% **AM6**, 5 mol% **PA9**). [e] Performed with an amine-to-acid ratio of 1/2 (5 mol% **AM6**, 10 mol% **PA9**).

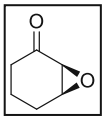
Die approbierte gedruckte Originalversion dieser Dissertation ist an der TU Wien Bibliothek verfügbar.
The approved original version of this doctoral thesis is available in print at TU Wien Bibliothek.

6. General procedure and analytical data for the asymmetric epoxidations

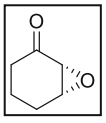


Reactions were performed on a 1.0 – 3.0 mmol scale. In a 20 mL screw cap vial the catalyst was prepared *in situ* by stirring the amine **AM6** (10 mol%) and phosphoric acid **PA9** (10 mol%) in anhydrous dioxane (0.18 M) for 20 min. Then the enone **1a-l** (1.0-3.0 mmol) was added and the reaction mixture was stirred for another 15 min at room temperature. Finally, 50% aqueous hydrogen peroxide (1.1 equiv.) was added and the resulting clear solution was stirred for 48 h at 35 °C. The reaction mixture was allowed to cool down to room temperature. Et_2O, distilled H_2O and brine were added, the aqueous phase was extracted with Et_2O (3×) and the combined organic phases were washed with brine and dried over Na_2SO_4, filtered and concentrated *in vacuo*. The crude products were purified by column chromatography (PE: Et_2O, vanillin staining agent) to provide the pure epoxyketones (−)-**2a-l** and (+)-**2a-l**.

For epoxides **2o-q** additional/modified workup is required: After 48 h at 35 °C, EtOAc was added and the reaction mixture was extracted with brine (2×) and concentrated *in vacuo.* The crude was taken up in small amounts of EtOAc, filtered through a silica filled pasteur pipette and eluted with EtOAc (5 mL). The solution was removed and approx. 3 mL dioxane and 1 mL Et_2O was added, followed by 1 equiv. 1N NaOH. After 30 min stirring the mixture was extracted with Brine (2×), concentrated and purified by column chromatography (PE:EE mixtures, vanillin staining agent) to provide the pure epoxyketones **2o-q**.



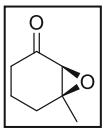
(1*S*,6*S*)-7-Oxabicyclo[4.1.0]heptan-2-one, (*S*,*S*)-2a.[27] Performed on a 3.0 mmol scale. Purified by column chromatography (25% Et_2O in PE, R_f = 0.2). Colourless liquid (201 mg, 60% yield, reduced yield due to high volatility). $[\alpha]_D^{20}$ = − 141.77 (c 1.0, CH_2Cl_2). **^{1}H NMR (400 MHz, $CDCl_3$) δ** 3.59 – 3.54 (m, 1H), 3.19 (d, *J* = 3.9 Hz, 1H), 2.56 – 2.47 (m, 1H), 2.24 (m, 1H), 2.11 – 1.99 (m, 1H), 1.98 – 1.83 (m, 2H), 1.70 – 1.60 (m, 1H). **^{13}C NMR (101 MHz, $CDCl_3$) δ** 206.04, 56.02, 55.20, 36.45, 22.94, 17.10. The **enantiomeric ratio** was determined to be 97.3:2.7 er (95% ee) by chiral GC analysis (BGB 175 column, 110 °C isothermal for 20 min, 30 °C/min to 220 °C, 25 min method), major enantiomer: t_r = 12.15 min, minor enantiomer: t_r = 13.43 min,).



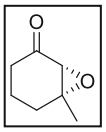
(1*R*,6*R*)-7-Oxabicyclo[4.1.0]heptan-2-one, (*R*,*R*)-2a.[27] Performed on a 2.5 mmol scale. Purified by column chromatography (25% Et_2O in PE, R_f = 0.2). Colourless liquid (185 mg, 65% yield, reduced yield due to high volatility). $[\alpha]_D^{20}$ = + 175.60 (c 1.0, CH_2Cl_2). The

Die approbierte gedruckte Originalversion dieser Dissertation ist an der TU Wien Bibliothek verfügbar.
The approved original version of this doctoral thesis is available in print at TU Wien Bibliothek.
TU Bibliothek Your knowledge hub WIEN

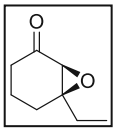
enantiomeric ratio was determined to be 97.3:2.7 er (95% ee) by chiral GC analysis (BGB 175 column, 110 °C isothermal for 20 min, 30 °C/min to 220 °C, 25 min method), minor enantiomer: t_r = 12.49 min, major enantiomer: t_r = 13.29 min.



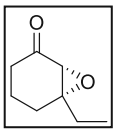
(1*S*,6*S*)-6-Methyl-7-oxabicyclo[4.1.0]heptan-2-one, (*S*,*S*)-2b.[27] Performed on a 3.0 mmol scale. Purified by column chromatography (25% Et_2O in PE, R_f = 0.33). Colourless liquid (246 mg, 65% yield, reduced yield due to high volatility). $[\alpha]_D^{20} = -152.99$ (c 1.0, CH_2Cl_2). **^{1}H NMR (400 MHz, $CDCl_3$) δ** 3.06 (s, 1H), 2.47 (dtd, *J* = 17.6, 4.1, 1.0 Hz, 1H), 2.16 – 1.79 (m, 4H), 1.68 – 1.58 (m, 1H), 1.43 (s, 3H). **^{13}C NMR (101 MHz, $CDCl_3$) δ** 206.83, 62.52, 62.09, 35.79, 28.50, 22.32, 17.28). The **enantiomeric ratio** was determined to be 97.4:2.6 er (95% ee) by chiral GC analysis (BGB 175 column, 110 °C isothermal for 20 min, 30 °C/min to 220 °C, 25 min method), minor enantiomer: t_r = 12.30 min, major enantiomer: t_r = 13.92 min.



(1*R*,6*R*)-6-Methyl-7-oxabicyclo[4.1.0]heptan-2-one, (*R*,*R*)-2b.[27] Performed on a 3.0 mmol scale. Purified by column chromatography (25% Et_2O in PE, R_f = 0.33). Colourless liquid (244 mg, 65% yield, reduced yield due to high volatility). $[\alpha]_D^{20} = +164.20$ (c 1.0, CH_2Cl_2). The **enantiomeric ratio** was determined to be 97.5:2.5 er (95% ee) by chiral GC analysis (BGB 175 column, 110 °C isothermal for 20 min, 30 °C/min to 220 °C, 25 min method), major enantiomer: t_r = 12.15 min, minor enantiomer: t_r = 14.17 min.

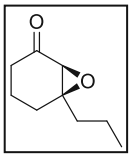


(1*S*,6*S*)-6-Ethyl-7-oxabicyclo[4.1.0]heptan-2-one, (*S*,*S*)-2c.[27] Performed on a 2.15 mmol scale. Purified by column chromatography (25% Et_2O in PE, R_f = 0.30). Colourless liquid (211 mg, 70% yield, reduced yield due to high volatility). $[\alpha]_D^{20} = -141.97$ (c 1.0, CH_2Cl_2). **^{1}H NMR (400 MHz, $CDCl_3$) δ** 3.07 (s, 1H), 2.53 – 2.45 (m, 1H), 2.14 – 1.81 (m, 4H), 1.78 – 1.60 (m, 3H), 0.96 (t, *J* = 7.5 Hz, 3H). **^{13}C NMR (101 MHz, $CDCl_3$) δ** 207.14, 66.24, 60.90, 36.09, 28.93, 26.28, 17.50, 8.79. The **enantiomeric ratio** was determined to be 97.1:2.9 er (94% ee) by chiral GC analysis (BGB 175 column, 110 °C isothermal for 20 min, 30 °C/min to 220 °C, 25 min method), major enantiomer: t_r = 16.3 min, minor enantiomer: t_r = 17.55 min.

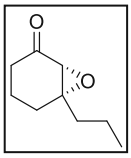


(1*R*,6*R*)-6-Ethyl-7-oxabicyclo[4.1.0]heptan-2-one, (*R*,*R*)-2c.[27] Performed on a 1.75 mmol scale. Purified by column chromatography (25% Et_2O in PE, R_f = 0.30). Colourless liquid (164 mg, 67% yield, reduced yield due to high volatility). $[\alpha]_D^{20} = +139.87$ (c 1.0, CH_2Cl_2). The **enantiomeric ratio** was determined to be 98.3:1.7 er (97% ee) by chiral GC analysis (BGB 175 column, 110 °C isothermal for 20 min, 30 °C/min to 220 °C, 25 min method), minor enantiomer: t_r = 16.44 min, major enantiomer: t_r = 17.09 min.

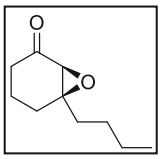
Die approbierte gedruckte Originalversion dieser Dissertation ist an der TU Wien Bibliothek verfügbar.
The approved original version of this doctoral thesis is available in print at TU Wien Bibliothek.
TU Bibliothek Your knowledge hub WIEN



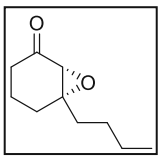
(1*S*,6*S*)-6-Propyl-7-oxabicyclo[4.1.0]heptan-2-one, (*S*,*S*)-2d.[30] Performed on a 2.15 mmol scale. Purified by column chromatography (20% Et_2O in PE, R_f = 0.31). Colourless liquid (237 mg, 71% yield, reduced yield due to high volatility). $[\alpha]_D^{20}$ = − 117.34 (c 1.0, CH_2Cl_2). **^{1}H NMR (400 MHz, $CDCl_3$) δ** 3.06 (s, 1H), 2.49 (dt, *J* = 17.3, 4.6 Hz, 1H), 2.16 – 1.80 (m, 4H), 1.75 – 1.53 (m, 3H), 1.51 – 1.37 (m, 2H), 0.92 (td, *J* = 7.3, 1.4 Hz, 3H). **^{13}C NMR (101 MHz, $CDCl_3$) δ** 207.14, 65.43, 61.28, 38.15, 36.07, 26.46, 18.10, 17.47, 14.11. The **enantiomeric ratio** was determined to be 97.7:2.3 er (95% ee) by chiral HPLC analysis (Chiralpak® AS-H column, *n*-Hexane/*i*-PrOH = 90:10, 1 mL/min, λ = 210 nm, 25 °C), minor enantiomer: t_r = 7.47 min, major enantiomer: t_r = 11.6 min.



(1*R*,6*R*)-6-Propyl-7-oxabicyclo[4.1.0]heptan-2-one, (*R*,*R*)-2d.[30] Performed on a 2.15 mmol scale. Purified by column chromatography (20% Et_2O in PE, R_f = 0.31). Colourless liquid (244 mg, 75% yield, reduced yield due to high volatility). $[\alpha]_D^{20}$ = + 136.06 (c 1.0, CH_2Cl_2). The **enantiomeric ratio** was determined to be 97.8:2.2 er (96% ee) by chiral HPLC analysis (Chiralpak® AS-H column, *n*-Hexane/*i*-PrOH = 90:10, 1 mL/min, λ = 210 nm, 25 °C), major enantiomer: t_r = 7.41 min, minor enantiomer: t_r = 11.85 min. $[\alpha]_D^{20}$ = + 136.06 (c 1.0, CH_2Cl_2).

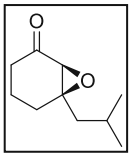


(1*S*,6*S*)-6-Butyl-7-oxabicyclo[4.1.0]heptan-2-one, (*S*,*S*)-2e.[27] Performed on a 2.0 mmol scale. Purified by column chromatography (25% Et_2O in PE, R_f = 0.28). Colourless liquid (242 mg, 72% yield, reduced yield due to high volatility). $[\alpha]_D^{20}$ = − 126.95 (c 1.0, CH_2Cl_2). **^{1}H NMR (400 MHz, $CDCl_3$) δ** 3.05 (s, 1H), 2.53 – 2.44 (m, 1H), 2.14 – 1.80 (m, 4H), 1.76 – 1.51 (m, 3H), 1.43 – 1.26 (m, 4H), 0.89 (t, *J* = 7.1 Hz, 3H). **^{13}C NMR (101 MHz, $CDCl_3$) δ** 207.14, 65.56, 61.30, 36.05, 35.82, 26.88, 26.51, 22.71, 17.48, 14.02. The **enantiomeric ratio** was determined to be 98.6:1.4 er (97% ee) by chiral HPLC analysis (Chiralpak® IB column, *n*-Hexane/*i*-iPrOH = 98:2, 1 mL/min, λ = 210 nm, 25 °C), major enantiomer: t_r = 5.14 min, minor enantiomer: t_r = 5.53 min.

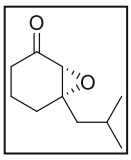


(1*R*,6*R*)-6-Butyl-7-oxabicyclo[4.1.0]heptan-2-one, (*R*,*R*)-2e.[27] Performed on a 1.0 mmol scale. Purified by column chromatography (25% Et_2O in PE, R_f = 0.28). Colourless liquid (114 mg, 68% yield, reduced yield due to high volatility). $[\alpha]_D^{20}$ = + 111.66 (c 1.0, CH_2Cl_2). The **enantiomeric ratio** was determined to be 97.6:2.4 er (95% ee) by chiral HPLC analysis (Chiralpak® IB column, *n*-Hexane/*i*-PrOH = 98:2, 1 mL/min, λ = 210 nm, 25 °C), minor enantiomer: t_r = 5.17 min, major enantiomer: t_r = 5.57 min.

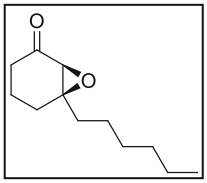
Die approbierte gedruckte Originalversion dieser Dissertation ist an der TU Wien Bibliothek verfügbar.
The approved original version of this doctoral thesis is available in print at TU Wien Bibliothek.
TU Bibliothek Your knowledge hub WIEN



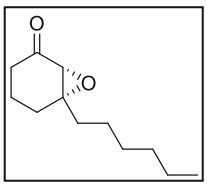
(1*S*,6*R*)-6-Isobutyl-7-oxabicyclo[4.1.0]heptan-2-one, (*S*,*R*)-2f.[27] Performed on a 1.5 mmol scale. Purified by column chromatography (15% Et_2O in PE, R_f = 0.27). Colourless liquid (130 mg, 51% yield, reduced yield due to high volatility). $[\alpha]_D^{20} = -93.41$ (c 1.0, CH_2Cl_2). **^{1}H NMR (400 MHz, $CDCl_3$) δ** 3.03 (s, 1H), 2.54 – 2.46 (m, 1H), 2.13 – 1.79 (m, 5H), 1.70 – 1.60 (m, 2H), 1.39 (dd, *J* = 14.1, 8.2 Hz, 1H), 0.96 (d, *J* = 6.6 Hz, 3H), 0.90 (d, *J* = 6.6 Hz, 3H). **^{13}C NMR (101 MHz, $CDCl_3$) δ** 207.20, 64.79, 61.66, 45.26, 36.07, 26.36, 25.19, 23.26, 22.66, 17.44. The **enantiomeric ratio** was determined to be 98.8:1.2 er (98% ee) by chiral HPLC analysis (Chiralpak® IB column, *n*-Hexane/*i*-PrOH = 98:2, 1 mL/min, λ = 210 nm, 25 °C), major enantiomer: t_r = 5.14 min, minor enantiomer: t_r = 5.54 min).



(1*R*,6*S*)-6-Isobutyl-7-oxabicyclo[4.1.0]heptan-2-one, (*R*,*S*)-2f.[27] Performed on a 2.0 mmol scale. Purified by column chromatography (15% Et_2O in PE, R_f = 0.27). Colourless liquid (181 mg, 55% yield, reduced yield due to high volatility). $[\alpha]_D^{20} = +123.84$ (c 1.0, CH_2Cl_2). The **enantiomeric ratio** was determined to be 98.8:1.2 er (98% ee) by chiral HPLC analysis (Chiralpak® IB column, *n*-Hexane/*i*-PrOH = 98:2, 1 mL/min, λ = 210 nm, 25 °C), minor enantiomer: t_r = 5.14 min, major enantiomer: t_r = 5.52 min.

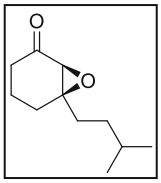


(1*S*,6*S*)-6-Hexyl-7-oxabicyclo[4.1.0]heptan-2-one, (*S*,*S*)-2g.[27] Performed on a 1.8 mmol scale. Purified by column chromatography (25% Et_2O in PE, R_f = 0.45). Colourless liquid (258 mg, 79% yield). $[\alpha]_D^{20} = -96.77$ (c 1.0, CH_2Cl_2). **^{1}H NMR (400 MHz, $CDCl_3$) δ** 3.06 (s, 1H), 2.54 – 2.45 (m, 1H), 2.15 – 1.80 (m, 4H), 1.74 – 1.55 (m, 3H), 1.40 (ttd, *J* = 8.5, 6.2, 1.6 Hz, 2H), 1.34 – 1.21 (m, 6H), 0.91 – 0.84 (m, 3H). **^{13}C NMR (101 MHz, $CDCl_3$) δ** 207.19, 65.62, 61.34, 36.15, 36.09, 31.77, 29.28, 26.54, 24.73, 22.63, 17.52, 14.15. The **enantiomeric ratio** was determined to be 98.6:1.4 er (97% ee) by chiral HPLC analysis (Chiralpak® IB column, *n*-Hexane/*i*-PrOH = 98:2, 1 mL/min, λ = 210 nm, 25 °C), major enantiomer: t_r = 4.83 min, minor enantiomer: t_r = 5.37 min.

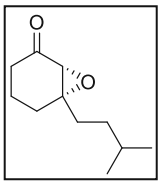


(1*R*,6*R*)-6-Hexyl-7-oxabicyclo[4.1.0]heptan-2-one, (*R*,*R*)-2g.[27] Performed on a 1.8 mmol scale. Purified by column chromatography (25% Et_2O in PE, R_f = 0.45). Colourless liquid (250 mg, 77% yield). $[\alpha]_D^{20} = +83.40$ (c 1.0, CH_2Cl_2). The **enantiomeric ratio** was determined to be 98.3:1.7 er (97% ee) by chiral HPLC analysis (Chiralpak® IB column, *n*-Hexane/*i*-PrOH = 98:2, 1 mL/min, λ = 210 nm, 25 °C), minor enantiomer: t_r = 4.89 min, major enantiomer: t_r = 5.47 min.

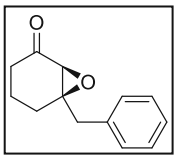
Die approbierte gedruckte Originalversion dieser Dissertation ist an der TU Wien Bibliothek verfügbar.
The approved original version of this doctoral thesis is available in print at TU Wien Bibliothek.
TU Bibliothek Your knowledge hub WIEN



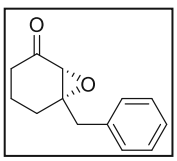
(1*S*,6*R*)-6-Isopentyl-7-oxabicyclo[4.1.0]heptan-2-one, (*S*,*R*)-2h. Performed on a 1.8 mmol scale. Purified by column chromatography (10% Et_2O in PE, R_f = 0.36). Colourless liquid (236 mg, 73% yield). $[\alpha]_D^{20}$ = − 106.04 (c 1.0, CH_2Cl_2). **^{1}H NMR (400 MHz, $CDCl_3$) δ** 3.06 (s, 1H), 2.54 – 2.44 (m, 1H), 2.15 – 1.80 (m, 4H), 1.74 – 1.47 (m, 4H), 1.32 – 1.23 (m, 2H), 0.88 (dd, *J* = 6.6, 1.9 Hz, 6H). **^{13}C NMR (101 MHz, $CDCl_3$) δ** 207.16, 65.78, 61.32, 36.07, 34.03, 33.66, 28.10, 26.61, 22.54, 17.54. The **enantiomeric ratio** was determined to be 99:1 er (98% ee) by chiral HPLC analysis (Chiralpak® IB column, *n*-Hexane/*i*-PrOH = 98:2, 1 mL/min, λ = 210 nm, 25 °C), major enantiomer: t_r = 4.85 min, minor enantiomer: t_r = 5.21 min. **HRMS** (ESI) Cald for $C_{11}H_{19}O_2$ $[M+H]^+$ 183.1380, Found 183.1329.



(1*R*,6*S*)-6-Isopentyl-7-oxabicyclo[4.1.0]heptan-2-one, (*R*,*S*)-2h. Performed on a 1.5 mmol scale. Purified by column chromatography (10% Et_2O in PE, R_f = 0.36). Colourless liquid (194 mg, 71% yield). $[\alpha]_D^{20}$ = + 106.85 (c 1.0, CH_2Cl_2). The **enantiomeric ratio** was determined to be 99:1 er (98% ee) by chiral HPLC analysis (Chiralpak® IB column, *n*-Hexane/*i*-PrOH = 98:2, 1 mL/min, λ = 210 nm, 25 °C), minor enantiomer: t_r = 4.85 min, major enantiomer: t_r = 5.20 min.

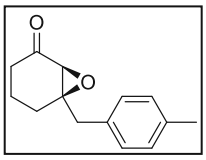


(1*S*,6*R*)-6-Benzyl-7-oxabicyclo[4.1.0]heptan-2-one, (*S*,*R*)-2i.[27] Performed on a 1.6 mmol scale. Purified by column chromatography (35% Et_2O in PE, R_f = 0.25). Colourless liquid (243 mg, 75% yield). $[\alpha]_D^{20}$ = − 103.00 (c 1.0, CH_2Cl_2). **^{1}H NMR (400 MHz, $CDCl_3$) δ** 7.30 – 7.11 (m, 5H), 3.06 (s, 1H), 2.93 (d, *J* = 1.5 Hz, 2H), 2.49 – 2.38 (m, 1H), 2.08 – 1.73 (m, 4H), 1.62 – 1.50 (m, 1H). **^{13}C NMR (101 MHz, $CDCl_3$) δ** 206.69, 135.58, 129.71, 128.70, 127.18, 65.42, 60.65, 42.38, 36.07, 26.45, 17.39. The **enantiomeric ratio** was determined to be 99:1 er (98% ee) by chiral HPLC analysis (Chiralpak® IB column, *n*-Hexane/*i*-PrOH = 98:2, 1 mL/min, λ = 210 nm, 25 °C), major enantiomer: t_r = 8.97 min, minor enantiomer: t_r = 10.1 min.

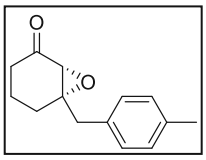


(1*R*,6*S*)-6-Benzyl-7-oxabicyclo[4.1.0]heptan-2-one, (*R*,*S*)-2i.[27] Performed on a 1.6 mmol scale. Purified by column chromatography (35% Et_2O in PE, R_f = 0.25). Colourless liquid (252 mg, 77% yield). $[\alpha]_D^{20}$ = + 107.82 (c 1.0, CH_2Cl_2). The **enantiomeric ratio** was determined to be 98.2:1.8 er (96% ee) by Chiral HPLC analysis (Chiralpak® IB column, *n*-Hexane/*i*-PrOH = 98:2, 1 mL/min, λ = 210 nm, 25 °C), major enantiomer: t_r = 9.10 min, minor enantiomer: t_r = 10.02 min.

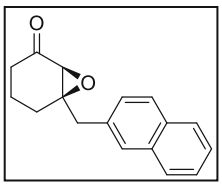
Die approbierte gedruckte Originalversion dieser Dissertation ist an der TU Wien Bibliothek verfügbar.
The approved original version of this doctoral thesis is available in print at TU Wien Bibliothek.
TU Bibliothek Your knowledge hub WIEN



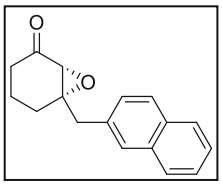
(1*S*,6*R*)-6-(4-Methylbenzyl)-7-oxabicyclo[4.1.0]heptan-2-one, (*S*,*R*)-2j. Performed on a 1.1 mmol scale. Purified by column chromatography (20% Et_2O in PE, R_f = 0.29). White solid (186 mg, 78% yield). **M.p. =** 54 – 56 °C. $[\alpha]_D^{20}$ = – 107.96 (c 1.0, CH_2Cl_2). **^{1}H NMR (400 MHz, $CDCl_3$) δ** 7.15 – 7.07 (m, 4H), 3.11 (s, 1H), 2.99 – 2.89 (m, 2H), 2.54 – 2.44 (m, 1H), 2.33 (s, 3H), 2.13 – 1.76 (m, 4H), 1.67 – 1.56 (m, 1H). **^{13}C NMR (101 MHz, $CDCl_3$) δ** 206.78, 136.78, 132.47, 129.58, 129.38, 65.55, 60.68, 41.97, 36.08, 26.43, 21.18, 17.41. The **enantiomeric ratio** was determined to be 99:1 er (98% ee) by chiral HPLC (Chiralpak® IB column, *n*-Hexane/*i*-PrOH = 98:2, 1 mL/min, λ = 210 nm, 25 °C), major enantiomer: t_r = 8.16 min, minor enantiomer: t_r = 8.98 min. **IR ATR (vmax/cm^{-1})** 2951, 1705, 817, 781. **HRMS (ESI)** Cald for $C_{14}H_{17}O_2$ $[M+H]^+$ 217.1223, Found 217.1208.



(1*R*,6*S*)-6-(4-Methylbenzyl)-7-oxabicyclo[4.1.0]heptan-2-one, (*R*,*S*)-2j. Performed on a 1.18 mmol scale. Purified by column chromatography (20% Et_2O in PE, R_f = 0.29). White solid (204 mg, 80% yield). $[\alpha]_D^{20}$ = + 93.69 (c 1.0, CH_2Cl_2). The **enantiomeric ratio** was determined to be 98.4:1.6 er (97% ee) by chiral HPLC (Chiralpak® IB column, *n*-Hexane/*i*-PrOH = 98:2, 1 mL/min, λ = 210 nm, 25 °C), minor enantiomer: t_r = 8.19 min, major enantiomer: t_r = 8.90 min.

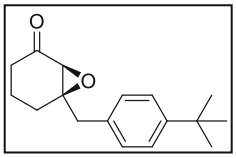


(1*S*,6*R*)-6-(Naphthalen-2-ylmethyl)-7-oxabicyclo[4.1.0]heptan-2-one, (*S*,*R*)-2k. Performed on a 0.9 mmol scale. Purified by column chromatography (15% Et_2O in PE, R_f = 0.14). Colourless liquid (158 mg, 69% yield). $[\alpha]_D^{20}$ = – 87.52 (c 1.0, CH_2Cl_2). **^{1}H NMR (400 MHz, $CDCl_3$) δ** 7.86 – 7.78 (m, 3H), 7.69 – 7.65 (m, 1H), 7.52 – 7.44 (m, 2H), 7.35 (dd, *J* = 8.4, 1.8 Hz, 1H), 3.18 (s, 1H), 3.14 (s, 2H), 2.55 – 2.45 (m, 1H), 2.17 – 1.80 (m, 4H), 1.60 (ddt, *J* = 12.6, 6.0, 4.1 Hz, 1H). **^{13}C NMR (101 MHz, $CDCl_3$) δ** 206.56, 133.50, 133.13, 132.56, 128.34 (d, *J* = 2.9 Hz), 127.76, 127.68, 126.32, 125.90, 65.43, 60.66, 42.49, 36.03, 26.43, 17.33. The **enantiomeric ratio** was determined to be 98.8:1.2 er (97% ee) by chiral HPLC (Chiralpak® OJ column, *n*-Hexane/*i*-PrOH = 85:15, 1 mL/min, λ = 210 nm, 25 °C), major enantiomer: t_r = 28.97 min, minor enantiomer: t_r = 35.43 min. **IR ATR (vmax/cm^{-1})** 3053, 2944, 1707, 811. **HRMS (ESI)** Cald for $C_{17}H_{17}O_2$ $[M+H]^+$ 253.1223, Found 253.1208.

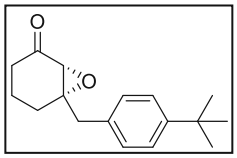


(1*R*,6*S*)-6-(Naphthalen-2-ylmethyl)-7-oxabicyclo[4.1.0]heptan-2-one, (*R*,*S*)-2k. Performed on a 0.9 mmol scale. Purified by column chromatography (15% Et_2O in PE, R_f = 0.14). Colourless liquid (162 mg, 71% yield). $[\alpha]_D^{20}$ = + 87.73 (c 1.0, CH_2Cl_2). The **enantiomeric ratio** was determined to be 98.2:1.8 er (96% ee) by chiral HPLC (Chiralpak® OJ column, *n*-Hexane/*i*-PrOH = 85:15, 1 mL/min, λ = 210 nm, 25 °C), minor enantiomer: t_r = 28.86 min, major enantiomer: t_r = 34.91 min.

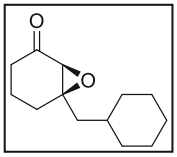
Die approbierte gedruckte Originalversion dieser Dissertation ist an der TU Wien Bibliothek verfügbar.
The approved original version of this doctoral thesis is available in print at TU Wien Bibliothek.
TU Bibliothek Your knowledge hub WIEN



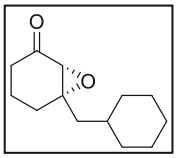
(1*S*,6*R*)-6-(4-(Tert-butyl)benzyl)-7-oxabicyclo[4.1.0]heptan-2-one, (*S*,*R*)-2l. Performed on a 1.22 mmol scale. Purified by column chromatography (20% Et_2O in PE, R_f = 0.28). White solid (227 mg, 72% yield). **M.p. =** 46 – 48 °C. $[\alpha]_D^{20} = -90.48$ (c 1.0, CH_2Cl_2). **^{1}H NMR (400 MHz, $CDCl_3$) δ** 7.32 (d, *J* = 8.3 Hz, 2H), 7.13 (d, *J* = 8.5 Hz, 2H), 3.10 (s, 1H), 3.00 – 2.87 (m, 2H), 2.54 – 2.42 (m, 1H), 2.13 – 1.79 (m, 4H), 1.69 – 1.57 (m, 1H), 1.31 (s, 9H). **^{13}C NMR (101 MHz, $CDCl_3$) δ** 206.89, 150.07, 132.43, 129.39, 125.62, 65.55, 60.66, 41.84, 36.10, 34.60, 31.49, 26.54, 17.42. The **enantiomeric ratio** was determined to be 99:1 er (98% ee) by chiral HPLC (Chiralpak® IB column, *n*-Hexane/*i*-PrOH = 98:2, 1 mL/min, λ = 210 nm, 25 °C), major enantiomer: t_r = 6.15 min, minor enantiomer: t_r = 6.62 min **IR ATR (vmax/cm^{-1})** 2945, 1708, 836. **HRMS (ESI)** Cald for $C_{17}H_{23}O_2$ $[M+H]^+$ 259.1693, Found 259.1682**.**



(1*R*,6*S*)-6-(4-(Tert-butyl)benzyl)-7-oxabicyclo[4.1.0]heptan-2-one, (*R*,*S*)-2l. Performed on a 1.05 mmol scale. Purified by column chromatography (25% Et_2O in PE, R_f = 0.33). White solid (194 mg, 72% yield). $[\alpha]_D^{20} = +80.41$ (c 1.0, CH_2Cl_2). The **enantiomeric ratio** was determined to be 98.5:1.5 er (97% ee) by chiral HPLC (Chiralpak® IB column, *n*-Hexane/*i*-PrOH = 98:2, 1 mL/min, λ = 210 nm, 25 °C), minor enantiomer: t_r = 6.25 min, major enantiomer: t_r = 6.79 min.

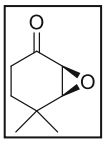


(1*S*,6*R*)-6-(Cyclohexylmethyl)-7-oxabicyclo[4.1.0]heptan-2-one, (*S*,*R*)-2m. Performed on a 1.57 mmol scale. Purified by column chromatography (25% Et_2O in PE, Rf = 0.31). Colourless liquid (219 mg, 67% yield). $[\alpha]_D^{20} = -100.68$ (c 1.0, CH_2Cl_2). **^{1}H NMR (400 MHz, $CDCl_3$) δ** 3.03 (s, 1H), 2.54 – 2.45 (m, 1H), 2.13 – 1.82 (m, 4H), 1.77 – 1.59 (m, 7H), 1.58 – 1.44 (m, 1H), 1.39 (dd, *J* = 13.7, 8.0 Hz, 1H), 1.31 – 1.06 (m, 3H), 1.02 – 0.84 (m, 2H). **^{13}C NMR (101 MHz, $CDCl_3$) δ** 207.19, 64.41, 61.60, 43.86, 35.94, 34.44, 33.82, 33.23, 26.38, 26.26, 26.16, 26.13, 17.31. The **enantiomeric ratio** was determined to be 98.8:1.2 er (98% ee) by chiral HPLC (Chiralpak® IB column, *n*-Hexane/*i*-PrOH = 99:1, 1 mL/min, λ = 220 nm, 25 °C), major enantiomer: t_r = 5.84 min, minor enantiomer: t_r = 6.58 min. **HRMS (ESI)** Cald for $C_{13}H_{21}O_2$ $[M+H]^+$ 209.1536, Found 209.1507.

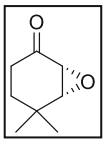


(1*R*,6*S*)-6-(Cyclohexylmethyl)-7-oxabicyclo[4.1.0]heptan-2-one, (*R*,*S*)-2m. Performed on a 1.57 mmol scale. Purified by column chromatography (25% Et_2O in PE, R_f = 0.31). Colourless liquid (230 mg, 70% yield). $[\alpha]_D^{20} = +106.21$ (c 1.0, CH_2Cl_2). The **enantiomeric ratio** was determined to be 98.8:1.2 er (98% ee) by chiral HPLC (Chiralpak® IB column, *n*-Hexane/*i*-PrOH = 99:1, 1 mL/min, λ = 220 nm, 25 °C), minor enantiomer: t_r = 5.76 min, major enantiomer: t_r = 6.43 min.

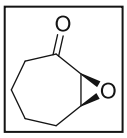
Die approbierte gedruckte Originalversion dieser Dissertation ist an der TU Wien Bibliothek verfügbar.
The approved original version of this doctoral thesis is available in print at TU Wien Bibliothek.
TU Bibliothek Your knowledge hub WIEN



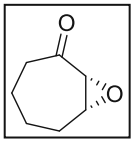
(1*S*,6*S*)-5,5-Dimethyl-7-oxabicyclo[4.1.0]heptan-2-one, (*S*,*S*)-2n.[27] Performed on a 2.83 mmol scale. Purified by column chromatography (20% Et_2O in PE, R_f = 0.29). Colourless liquid (258 mg, 65% yield). $[\alpha]_D^{20} = -148.55$ (c 1.0, CH_2Cl_2). **^{1}H NMR (400 MHz, $CDCl_3$) δ** 3.21 (d, *J* = 4.0 Hz, 1H), 3.16 (dd, *J* = 4.0, 1.3 Hz, 1H), 2.39 (ddd, *J* = 18.9, 6.4, 3.0 Hz, 1H), 2.18 (ddd, *J* = 18.8, 11.7, 7.0 Hz, 1H), 1.95 – 1.84 (m, 1H), 1.33 (dddd, *J* = 13.7, 7.0, 3.0, 1.3 Hz, 1H), 1.21 (s, 3H), 1.05 (s, 3H). **^{13}C NMR (101 MHz, $CDCl_3$) δ** 206.15, 64.28, 56.07, 33.29, 30.90, 29.93, 27.56, 23.02. The **enantiomeric ratio** was determined to be 97.2:2.8 er (94% ee) by chiral GC (BGB 175 column, 110 °C isothermal for 20 min, 30 °C/min to 220 °C, 25 min method), major enantiomer: t_r = 13.42 min, minor enantiomer: t_r = 15.45 min.



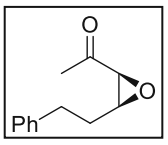
(1*R*,6*R*)-5,5-Dimethyl-7-oxabicyclo[4.1.0]heptan-2-one, (*R*,*R*)-2n.[27] Performed on a 2.41 mmol scale. Purified by column chromatography (20% Et_2O in PE, R_f = 0.29). Colourless liquid (213 mg, 63% yield). $[\alpha]_D^{20} = +156.13$ (c 1.0, CH_2Cl_2). The **enantiomeric ratio** was determined to be 96.7:3.3 er (93% ee) by chiral GC (BGB 175 column, 110 °C isothermal for 20 min, 30 °C/min to 220 °C, 25 min method), major enantiomer: t_r = 13.69 min, minor enantiomer: t_r = 15.00 min.



(1*S*,7*S*)-8-Oxabicyclo[5.1.0]octan-2-one, (*S*,*S*)-2o.[27] Performed on a 0.91 mmol scale. Purified by column chromatography (3% EE in PE, R_f = 0.4). Colourless liquid (62 mg, 54% yield). $[\alpha]_D^{20} = -15.03$ (c 0.66, CH_2Cl_2). **^{1}H NMR (400 MHz, CD_2Cl_2) δ** 3.31 – 3.25 (m, 2H), 2.57 – 2.50 (m, 1H), 2.21 – 2.16 (m, 1H), 1.78 – 1.56 (m, 4H), 0.95 – 0.87 (m, 1H). **^{13}C NMR (101 MHz, CD_2Cl_2) δ** 210.46, 59.40, 55.08, 40.52, 27.41, 23.52, 22.95. The **enantiomeric ratio** was determined to be 98:2 er (96% ee) by chiral GC (BGB 175 column, 110 °C isothermal for 30 min, 30 °C/min to 220 °C, 38 min method), major enantiomer: t_r = 15.80 min, minor enantiomer: t_r = 16.78 min.



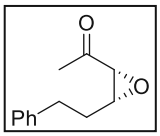
(1*R*,7*R*)-8-Oxabicyclo[5.1.0]octan-2-one, (*R*,*R*)-2o.[27] Performed on a 0.91 mmol scale. Purified by column chromatography (3% EE in PE, R_f = 0.4). Colourless liquid (64 mg, 56% yield). $[\alpha]_D^{20} = +17.07$ (c 0.71, CH_2Cl_2). The **enantiomeric ratio** was determined to be 97.5:2.5 er (95% ee) by chiral GC (BGB 175 column, 110 °C isothermal for 30 min, 30 °C/min to 220 °C, 38 min method), minor enantiomer: t_r = 16.00 min, major enantiomer: t_r = 16.47 min.



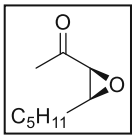
1-((2*S*,3*S*)-3-phenethyloxiran-2-yl)ethan-1-one, (*S*,*S*)-2p.[27] Performed on a 0.57 mmol scale. Purified by column chromatography (5% EE in PE, R_f = 0.45). Colourless liquid (65 mg, 59% yield). $[\alpha]_D^{20} = -13.34$ (c 0.62, CH_2Cl_2). **^{1}H NMR (400 MHz, $CDCl_3$) δ** 7.25 – 7.23 (m, 2H), 7.16 – 7.10 (m, 3H), 3.09 (d, *J* = 4.0 Hz, 1H), 3.03 – 3.01 (m, 1H), 2.74 – 2.67 (m, 2H), 1.93 (s, 3H), 1.90 – 1.85 (m, 2H). **^{13}C NMR (101 MHz, $CDCl_3$) δ** 205.63, 140.42, 128.64, 128.35, 126.35, 59.93,

Die approbierte gedruckte Originalversion dieser Dissertation ist an der TU Wien Bibliothek verfügbar.
The approved original version of this doctoral thesis is available in print at TU Wien Bibliothek.
TU Bibliothek Your knowledge hub WIEN

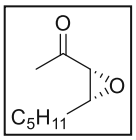
57.51, 33.47, 32.01, 24.55. The **enantiomeric ratio** was determined to be 92.5:7.5 er (85% ee) by chiral GC (BGB 173 column, 150 °C isothermal for 40 min, 30 °C/min to 220 °C, 48 min method), major enantiomer: t_r = 13.92 min, minor enantiomer: t_r = 14.46 min.



1-((2R,3R)-3-phenethyloxiran-2-yl)ethan-1-one, (*R*,*R*)-2p.[27] Performed on a 0.57 mmol scale. Purified by column chromatography (5% EE in PE, R_f = 0.45). Colourless liquid (60 mg, 55% yield). $[\alpha]_D^{20}$ = + 15.32 (c 0.62, CH_2Cl_2). The **enantiomeric ratio** was determined to be 92:8 er (84% ee) by chiral GC (BGB 173 column, 150 °C isothermal for 40 min, 30 °C/min to 220 °C, 48 min method), minor enantiomer: t_r = 13.91 min, major enantiomer: t_r = 14.46 min.



(2*S*,3*S*)-3-Hexyloxiran-2-yl)ethan-1-one, (*S*,*S*)-2q.[27] Performed on a 0.71 mmol scale. Purified by column chromatography (3% EE in PE, R_f = 0.3). Colourless liquid (62 mg, 56% yield). $[\alpha]_D^{20}$ = − 33.78 (c 0.71, CH_2Cl_2). **^{1}H NMR (400 MHz, $CDCl_3$) δ** 3.10 (d, *J* = 4.0 Hz, 1H), 3.02 – 2.99 (m, 1H), 1.99 (s, 3H), 1.57 – 1.56 (m, 2H), 1.43 – 1.37 (m, 2H), 1.27 – 1.25 (m, 4H), 0.83 (t, *J* = 6.0 Hz, 3H). **^{13}C NMR (101 MHz, $CDCl_3$) δ** 206.610, 59.95, 58.09, 31.74, 31.40, 25.45, 24.34, 22.48, 13.92. The **enantiomeric ratio** was determined to be 94.5:5.5 er (89% ee) by chiral GC (BGB 175 column, 110 °C isothermal for 30 min, 30 °C/min to 220 °C, 38 min method), minor enantiomer: t_r = 14.14 min, major enantiomer: t_r = 14.90 min.

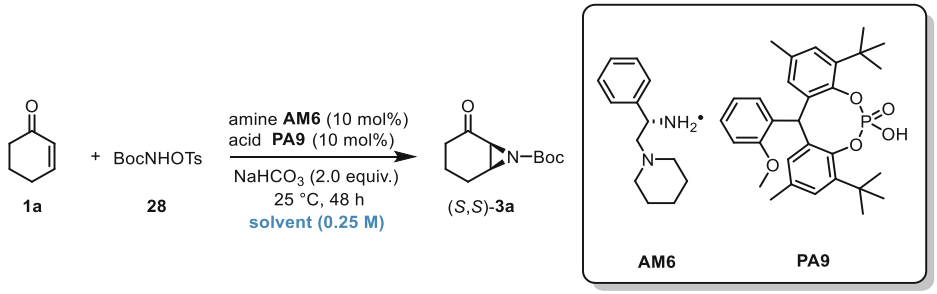


(2*R*,3*R*)-3-Benzyloxiran-2-yl)ethan-1-one, (*R*,*R*)-2q.[27] Performed on a 0.71 mmol scale. Purified by column chromatography (3% EE in PE, R_f = 0.3). Colourless liquid (63 mg, 57% yield). $[\alpha]_D^{20}$ = 42.09 (c 0.66, CH_2Cl_2). The **enantiomeric ratio** was determined to be 93.5:6.5 er (87% ee) by chiral GC (BGB 175 column, 110 °C isothermal for 30 min, 30 °C/min to 220 °C, 38 min method), major enantiomer: t_r = 14.09 min, minor enantiomer: t_r = 15.00 min.

Die approbierte gedruckte Originalversion dieser Dissertation ist an der TU Wien Bibliothek verfügbar.
The approved original version of this doctoral thesis is available in print at TU Wien Bibliothek.

7. Parameter optimization for the asymmetric aziridinations

7.1 Solvent screening

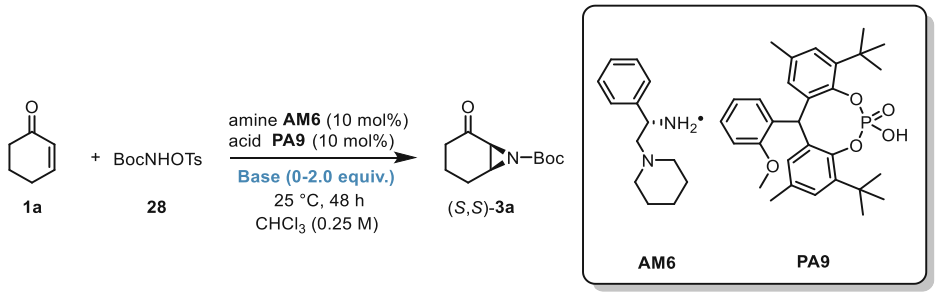


entry[a]	amine	acid	solvent	conv. [%][b]	ee [%][c]
1	**AM6**	**PA9**	dioxane	11	n.d.
2			MTBE	7	n.d.
3			DCM	99	64
4			**$CHCl_3$**	**98**	**98**

[a] Performed with 0.30 mmol 2-cyclohexen-1-one (**1a**, 1.2 equiv.), 0.25 mmol **28** (1.0 equiv.), 0.025 mmol catalyst (10 mol% **AM6**, 10 mol% **PA9**) and 0.60 mmol (2.0 equiv.) $NaHCO_3$ in 1.0 mL solvent at 25 °C for 48 hours. [b] Determined by GC-MS analysis. [c] Determined by chiral HPLC analysis using a Chiralpak® AS-H column. Absolute configuration has been determined by measuring the optical rotation and comparing with literature data.

Die approbierte gedruckte Originalversion dieser Dissertation ist an der TU Wien Bibliothek verfügbar.
The approved original version of this doctoral thesis is available in print at TU Wien Bibliothek.

7.2 Base screening

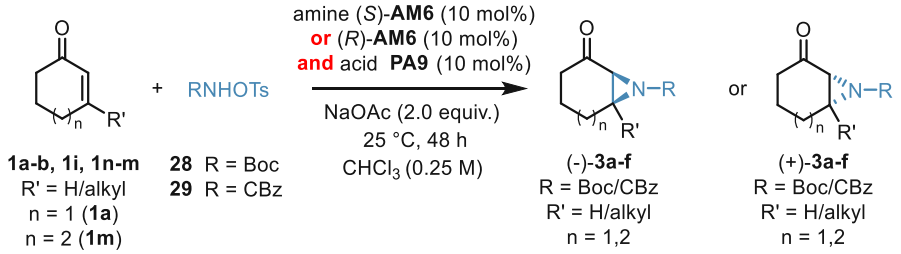


entry[a]	amine	acid	base	conv. [%][b]	ee [%][c]
1			$NaHCO_3$ (0 equiv.)	traces	n.d.
2			$NaHCO_3$ (1.0 equiv.)	36	57
3			$NaHCO_3$ (2.0 equiv.)	98	98
4			Na_2CO_3 (2.0 equiv.)	25	n.d.
5	**AM6**	**PA9**	*i*Pr_2NEt (2.0 equiv.)	traces	n.d.
6			Pyridine (2.0 equiv.)	23	68
7			Lutidine (2.0 equiv.)	traces	n.d
8			Cs_2CO_3 (2.0 equiv.)	5	n.d.
9			**NaOAc (2.0 equiv.)**	**98**	**99.5**

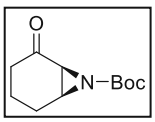
[a] Performed with 0.30 mmol 2-cyclohexen-1-one (**1a**, 1.2 equiv.), 0.25 mmol **28** (1.0 equiv.), 0.025 mmol catalyst (10 mol% **AM6**, 10 mol% **PA9**) and 0-0.60 mmol (0-2.0 equiv.) base in 1.0 mL chloroform at 25 °C for 48 hours. [b] Determined by GC-MS analysis. [c] Determined by chiral HPLC analysis using a Chiralpak® AS-H column. Absolute configuration has been determined by measuring the optical rotation and comparing with literature data.

Die approbierte gedruckte Originalversion dieser Dissertation ist an der TU Wien Bibliothek verfügbar.
The approved original version of this doctoral thesis is available in print at TU Wien Bibliothek.

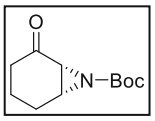
8. General procedure and analytical data for the asymmetric aziridinations



All reactions were performed on a 1.0 mmol scale. In a 20 mL screw cap vial the catalyst was prepared *in situ* by stirring the amine **AM6** (20.4 mg, 10 mol%) and phosphoric acid **PA9** (50.86 mg, 10 mol%) in $CHCl_3$ (4.0 mL, 0.25 M) for 20 min. Then the enone **1a-b**, **1i**, **1n-m** (1.2 mmol, 1.2 equiv.) was added and the reaction mixture was stirred for another 15 min at room temperature. Then, reagent **28**-**29** (1.0 mmol, 1.0 equiv.) and NaOAc (165 mg, 2.0 mmol, 2.0 equiv.) were added. The reaction mixture was stirred at room temperature for 48 h. The crude reaction mixture was washed with brine (1×) and the aqueous phase was extracted with CH_2Cl_2 (3×). The combined organic phases were dried over anhydrous Na_2SO_4 and the solvent was removed under reduced pressure. The crude product was then purified by column chromatography (PE/EE mixtures, vanillin staining agent) to afford the pure aziridines (−)**3a-f** and (+)-**3a-f**.

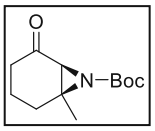


***tert*-Butyl (1*S*,6*S*)-2-oxo-7-azabicyclo[4.1.0]heptane-7-carboxylate, (*S*,*S*)-3a.**[31] Purified by column chromatography (20% EtOAc in PE). White solid (167 mg, 79% yield). $[\alpha]_D^{20} =$ − 143.5 (c 1.0, $CHCl_3$). **^{1}H NMR (400 MHz, $CDCl_3$) δ** 3.08 – 3.05 (m, 1H), 2.88 (d, *J* = 5.8 Hz, 1H), 2.53 – 2.40 (m, 1H), 2.27 – 2.19 (m, 1H), 2.09 – 1.90 (m, 2H), 1.82 – 1.73 (m, 1H), 1.67 – 1.59 (m, 1H), 1.44 (s, 9H). **^{13}C NMR (101 MHz, $CDCl_3$) δ** 204.3, 160.6, 82.2, 43.2, 40.4, 36.9, 27.8, 22.6, 17.3. The **enantiomeric excess** was determined to be 99.5% ee by chiral HPLC (Chiralpak® AS-H column, *n*-Heptane/*i*-PrOH = 95:5, 0.5 mL/min, λ = 220 nm, 25 °C), major enantiomer: t_r = 21.60 min, minor enantiomer: t_r = 23.50 min.

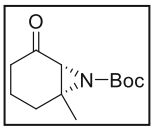


***tert*-Butyl (1*R*,6*R*)-2-oxo-7-azabicyclo[4.1.0]heptane-7-carboxylate, (*R*,*R*)-3a.**[31] Purified by column chromatography (20% EtOAc in PE). $[\alpha]_D^{20} =$ + 106.7 (c 1.0, $CHCl_3$). White solid (166 mg, 79% yield). The **enantiomeric excess** was determined to be 97% ee by chiral HPLC (Chiralpak® AS-H column, *n*-Heptane/*i*-PrOH = 95:5, 0.5 mL/min, λ = 220 nm, 25 °C), minor enantiomer: t_r = 21.69 min, major enantiomer: t_r = 23.12 min.

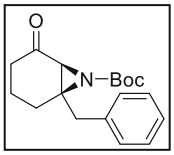
Die approbierte gedruckte Originalversion dieser Dissertation ist an der TU Wien Bibliothek verfügbar.
The approved original version of this doctoral thesis is available in print at TU Wien Bibliothek.
TU Bibliothek Your knowledge hub WIEN



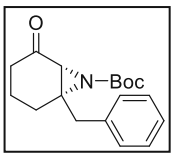
***tert*-Butyl (1*S*,6*S*)-1-methyl-5-oxo-7-azabicyclo[4.1.0]heptane-7-carboxylate, (*S*,*S*)-3b.**[31] Purified by column chromatography (20% EtOAc in PE). Colourless oil (175 mg, 78% yield). $[\alpha]_D^{20} = -80.7$ (c 1.0, $CHCl_3$). **^{1}H NMR (400 MHz, $CDCl_3$) δ** 2.77 (s, 1H), 2.50 – 2.37 (m, 1H), 2.16 – 2.09 (m, 1H), 2.06 – 1.92 (m, 2H), 1.71 – 1.57 (m, 2H), 1.45 (s, 9H), 1.39 (s, 3H). **^{13}C NMR (101 MHz, $CDCl_3$) δ** 205.6, 159.0, 82.0, 49.68, 47.6, 36.2, 29.3, 28.1, 20.4, 17.5. The **enantiomeric excess** was determined to be 89% ee by chiral HPLC (Chiralpak® AS-H column, *n*-Heptane/ Chiralpak® AS-H column, *n*-Heptane/*i*-PrOH = 90:10, 1 mL/min, λ = 220 nm, 25 °C), minor enantiomer: t_r = 7.70 min, major enantiomer: t_r = 8.52 min.



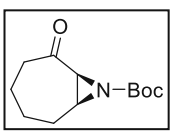
***tert*-Butyl (1*R*,6*R*)-1-methyl-5-oxo-7-azabicyclo[4.1.0]heptane-7-carboxylate, (*R*,*R*)-3b.**[31] Purified by column chromatography (20% EtOAc in PE). Colourless oil (172 mg, 76% yield). $[\alpha]_D^{20} = +81.7$ (c 1.0, $CHCl_3$). The **enantiomeric excess** was determined to be 88% ee by chiral HPLC (Chiralpak® AS-H column, *n*-Heptane/*i*-PrOH = 90:10, 1 mL/min, λ = 220 nm, 25 °C), major enantiomer: t_r = 7.70 min, minor enantiomer: t_r = 8.65 min.



***tert*-Butyl (1*R*,6*S*)-1-Benzyl-5-oxo-7-azabicyclo[4.1.0]heptane-7-carboxylate, (*R*,*S*)-3c.**[31] Reaction was performed with 2.0 equiv. $NaHCO_3$ instead of 2.0 equiv. NaOAc on a 0.8 mmol scale. Purified by column chromatography (20% EtOAc in PE). Colourless oil (141 mg, 59% yield). $[\alpha]_D^{20} = -139.1$ (c 1.0, $CHCl_3$). **^{1}H NMR (400 MHz, $CDCl_3$) δ** 7.33 - 7.20 (m, 5H), 3.24 (d, *J* = 14.3 Hz, 1H), 3.06 (s, 1H), 2.47 – 2.35 (m, 2H), 2.08 – 2.00 (m, 1H), 1.99 – 1.86 (m, 2H), 1.66 – 1.51 (m, 2H), 1.49 (s, 9H). **^{13}C NMR (101 MHz, $CDCl_3$) δ** 205.1, 158.6, 136.4, 129.5, 128.9, 127.3, 82.4, 51.3, 48.8, 41.4, 36.2, 28.1, 26.2, 17.6. The **enantiomeric excess** was determined to be 88% ee by chiral HPLC (Chiralpak® AS-H column, *n*-Heptane/*i*-PrOH = 90:10, 1 mL/min, λ = 220 nm, 25 °C), minor enantiomer: t_r = 6.45 min, major enantiomer: t_r = 15.17 min.



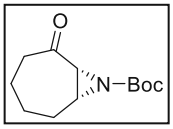
***tert*-Butyl (1*S*,6*R*)-1-Benzyl-5-oxo-7-azabicyclo[4.1.0]heptane-7-carboxylate, (*S*,*R*)-3c.**[31] Reaction was performed with 2.0 equiv. $NaHCO_3$ instead of 2.0 equiv. NaOAc on a 0.8 mmol scale. Purified by column chromatography (20% EtOAc in PE). Colourless oil (135 mg, 56% yield). $[\alpha]_D^{20} = +137.5$ (c 1.0, $CHCl_3$). The **enantiomeric excess** was determined to be 89% ee by chiral HPLC Chiralpak® AS-H column, *n*-Heptane/*i*-PrOH = 90:10, 1 mL/min, λ = 220 nm, 25 °C), major enantiomer: t_r = 6.43 min, minor enantiomer: t_r = 15.20 min.



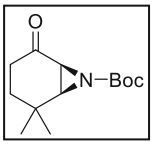
***tert*-butyl (1*S*,7*S*)-2-Oxo-8-azabicyclo[5.1.0]octane-8-carboxylate, (*S*,*S*)-3d.**[31] Purified by column chromatography (10% EtOAc in PE). Colourless oil (155 mg, 69% yield). $[\alpha]_D^{20} = -116.13$ (c 0.98, CH_2Cl_2). **^{1}H NMR (400 MHz, $CDCl_3$) δ** 2.95 (d, *J* = 5.9, 1H), 2.82

Die approbierte gedruckte Originalversion dieser Dissertation ist an der TU Wien Bibliothek verfügbar.
The approved original version of this doctoral thesis is available in print at TU Wien Bibliothek.
TU Bibliothek Your knowledge hub WIEN

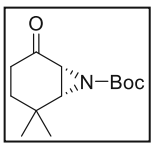
(dd, *J* = 5.9, *J* = 1.6 Hz, 1H), 2.70 – 2.66 (m, 1H), 2.38 – 2.35 (m, 1H), 2.21 - 2.19 (m, 1H), 1.72 – 1.49 (m, 5H), 1.38 (s, 9H). **^{13}C NMR (101 MHz, $CDCl_3$) δ** 209.3, 160.9, 82.0, 47.3, 40.8, 40.4, 27.9, 23.7, 23.5. The **enantiomeric excess** was determined to be 92% ee by chiral HPLC (Chiralpak® AS-H column, *n*-Heptane/*i*-PrOH = 90:10, 1 mL/min, λ = 220 nm, 25 °C), minor enantiomer: t_r = 7.20 min, major enantiomer: t_r = 8.44 min.



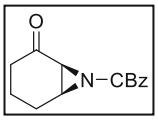
***tert*-butyl (1*R*,7R)-2-Oxo-8-azabicyclo[5.1.0]octane-8-carboxylate, (*R*,*R*)-3d.**[31] Purified by column chromatography (10% EtOAc in PE). Colourless oil (163 mg, 72% yield). The **enantiomeric excess** was determined to be 93% ee by chiral HPLC (Chiralpak® AS-H column, *n*-Heptane/*i*-PrOH = 90:10, 1 mL/min, λ = 220 nm, 25 °C), major enantiomer: t_r = 7.18 min, major enantiomer: t_r = 8.48 min.



***tert*-Butyl (1*S*,6*S*)-2,2-Dimethyl-5-oxo-7-azabicyclo[4.1.0]heptane-7-carboxylate, (*S*,*S*)-3e.**[31] Purified by column chromatography (15% EtOAc in PE). Colourless oil (175 mg, 76% yield). $[\alpha]_D^{20}$ = − 100.1 (c 1.0, $CHCl_3$). **^{1}H NMR (400 MHz, $CDCl_3$) δ** 2.92 (d, *J* = 5.9, 1H), 2.66 (dd, *J* = 5.9, *J* = 1.6 Hz, 1H), 2.35 (ddd, *J* = 19.1, *J* = 6.5, *J* = 2.4 Hz, 1H), 2.21 – 2.11 (m, 1H), 1.96 – 1.84 (m, 1H), 1.44 (s, 9H), 1.32 – 1.24 (m, 1H), 1.21 (s, 3H), 1.03 (s, 3H). **^{13}C NMR (101 MHz, $CDCl_3$) δ** 204.7, 160.5, 82.2, 50.2, 44.2, 33.8, 30.4, 28.0, 27.7, 23.4. The **enantiomeric excess** was determined to be 93% ee by chiral HPLC (Chiralpak® AS-H column, *n*-Heptane/*i*-PrOH = 90:10, 1 mL/min, λ = 220 nm, 25 °C), major enantiomer: t_r = 6.85 min, minor enantiomer: t_r = 8.56 min.



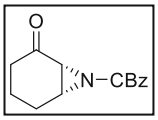
***tert*-Butyl (1*R*,6*R*)-2,2-Dimethyl-5-oxo-7-azabicyclo[4.1.0]heptane-7-carboxylate, (*R*,*R*)-3e.**[31] Purified by column chromatography (15% EtOAc in PE). Colourless oil (182 mg, 75% yield). $[\alpha]_D^{20}$ = + 103.4 (c 1.0, $CHCl_3$). The **enantiomeric excess** was determined to be 92% ee by chiral HPLC (Chiralpak® AS-H column, *n*-Heptane/*i*-PrOH = 90:10, 1 mL/min, λ = 220 nm, 25 °C), minor enantiomer: t_r = 7.35 min, major enantiomer: t_r = 8.94 min.



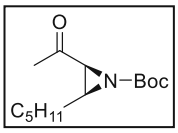
(1*S*,6*S*)-7-(2-Oxo-2-phenyl-1λ^2-ethyl)-7-azabicyclo[4.1.0]heptan-2-one, (*S*,*S*)-3f.[31] Purified by column chromatography (gradient elution, 20% to 33% EtOAc in PE). Colourless oil (174 mg, 71% yield). $[\alpha]_D^{20}$ = − 75.77 (c 1.34, CH_2Cl_2). **^{1}H NMR (400 MHz, $CDCl_3$)** δ 7.28 - 7.22 (m, 5H), 5.04 (dd, *J* = 12.0 Hz, 14.0 Hz, 2H), 3.06 - 3.05 (m, 1H), 2.89 (d, *J* = 8.0 Hz, 1H), 2.40 - 2.35 (m, 1H), 2.17 - 2.13 (m, 1H), 1.99 - 1.78 (m, 2H), 1.72 - 1.66 (m, 1H), 1.57 - 1.51 (m, 1H). **^{13}C NMR (101 MHz, $CDCl_3$)** δ 203.7, 161.5, 133.4, 128.6, 128.5, 128.3, 68.6, 42.9, 40.6, 36.9, 30.4, 22.5, 17.1. The **enantiomeric excess** was determined to be 93% ee by chiral HPLC (Chiralpak® AS-H column,

Die approbierte gedruckte Originalversion dieser Dissertation ist an der TU Wien Bibliothek verfügbar.
The approved original version of this doctoral thesis is available in print at TU Wien Bibliothek.
TU Bibliothek Your knowledge hub WIEN

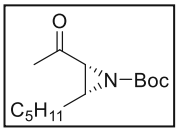
n-Heptane/*i*-PrOH = 95:5, 1 mL/min, λ = 220 nm, 25 °C), major enantiomer: t_r = 31.89 min, minor enantiomer: t_r = 49.23 min.



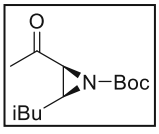
(1*R*,6*R*)-7-(2-Oxo-2-phenyl-1λ²-ethyl)-7-azabicyclo[4.1.0]heptan-2-one, (*R*,*R*)-3f.[31] Purified by column chromatography (gradient elution, 20% to 33% EtOAc in PE). Colourless oil (180 mg, 73% yield). $[\alpha]_D^{20}$ = + 84.71 (c 0.95, CH_2Cl_2).The **enantiomeric excess** was determined to be 92% ee by chiral HPLC (AS-H column, *n*-Heptane/*i*-PrOH = 95:5, 1 mL/min, λ = 220 nm, 25 °C), minor enantiomer: t_r = 32.34 min, major enantiomer: t_r = 48.69 min.



(*tert*-butyl (2*S*,3*S*)-2-Acetyl-3-pentylaziridine-1-carboxylate, (*S*,*S*)-3g.[31] Purified by column chromatography (12% EtOAc in PE). Colourless oil (175 mg, 78% yield). $[\alpha]_D^{20}$ = – 5.3 (c 1.0, CH_2Cl_2). **^{1}H NMR (400 MHz, $CDCl_3$)** δ 2.91 (d, *J* = 2.8 Hz, 1H), 2.60 – 2.56 (m, 1H), 2.20 (s, 3H), 1.54 – 1.51 (m, 1H), 1.43 – 1.34 (m, 12H), 1.27 – 1.22 (m, 4H), 0.82 (t, *J* = 8.0 Hz, 3H). **^{13}C NMR (101 MHz, $CDCl_3$)** δ 202.7, 159.1, 81.7, 46.7, 45.6, 31.3, 29.1, 28.0, 26.5, 22.5, 14.0. The **diastereometic ratio** was 33/1 d.r. based on the ^{1}H NMR spectrum. The **enantiomeric excess** was determined to be 64% ee by chiral HPLC (Chiralpak® IA-3 column, *n*-Hexane/*i*-PrOH = 99:1, 1 mL/min, λ = 235 nm, 25 °C), minor enantiomer: t_r = 7.78 min, major enantiomer: t_r = 11.88 min.

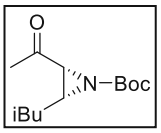


(*tert*-butyl (2*R*,3*R*)-2-Acetyl-3-pentylaziridine-1-carboxylate, (*R*,*R*)-3g.[31] Purified by column chromatography (12% EtOAc in PE). Colourless oil (170 mg, 75% yield). $[\alpha]_D^{20}$ = + 5.5 (c 1.0, CH_2Cl_2). The **diastereometic ratio** was 33/1 d.r. based on the ^{1}H NMR spectrum. The **enantiomeric excess** was determined to be 70% ee by chiral HPLC (Chiralpak® IA-3 column, *n*-Hexane/*i*-PrOH = 99:1, 1 mL/min, λ = 235 nm, 25 °C), major enantiomer: t_r = 7.72 min, minor enantiomer: t_r = 12.14 min.



(*tert*-butyl (2*S*,3*S*)-2-Acetyl-3-isobutylaziridine-1-carboxylate, (*S*,*S*)-3h. Purified by column chromatography (10% EtOAc in PE). Colourless oil (164 mg, 68% yield). $[\alpha]_D^{20}$ = – 8.56 (c 1.0, CH_2Cl_2). **^{1}H NMR (400 MHz, $CDCl_3$)** δ 2.91 (d, *J* = 2.8 Hz, 1H), 2.62 – 2.59 (m, 1H), 2.21 (s, 3H), 1.80 – 1.73 (m, 1H), 1.48 – 1.43 (m, 1H), 1.39 (s, 9H), 1.25 – 1.19 (m, 1H), 0.92 – 0.90 (m, 6H). **^{13}C NMR (101 MHz, $CDCl_3$)** δ 202.6, 159.1, 81.7, 46.9, 44.4, 40.3, 29.3, 27.9, 26.9, 22.7, 22.0. The **diastereometic ratio** was 33/1 d.r. based on the ^{1}H NMR spectrum. The **enantiomeric excess** was determined to be 64% ee by chiral HPLC (Chiralpak® IA-3 column, *n*-Hexane/*i*-PrOH = 99:1, 1 mL/min, λ = 235 nm, 25 °C), minor enantiomer: t_r = 7.66 min, major enantiomer: t_r = 12.30 min. **IR ATR (vmax/cm^{-1})** 2958, 1724, 1423, 1149, 802. **HRMS (ESI)** Cald for $C_8H_{16}NO_2$ $[M+H-BOC]^+$ 142.1226, Found 142.1233.

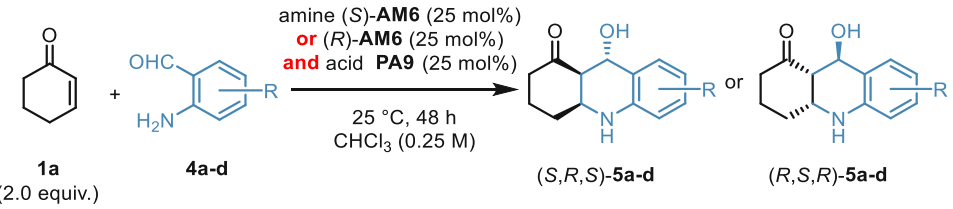
Die approbierte gedruckte Originalversion dieser Dissertation ist an der TU Wien Bibliothek verfügbar.
The approved original version of this doctoral thesis is available in print at TU Wien Bibliothek.
TU Bibliothek Your knowledge hub WIEN



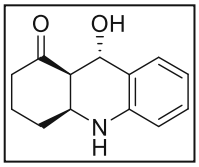
(*tert*-butyl (2*R*,3*R*)-2-Acetyl-3-isobutylaziridine-1-carboxylate, (*R*,*R*)-3h. Purified by column chromatography (10% EtOAc in PE). Colourless oil (170 mg, 70% yield). $[\alpha]_D^{20} =$ + 8.91 (c 1.0, CH_2Cl_2). The **diastereometic ratio** was 33/1 d.r. based on the ^{1}H NMR spectrum. The **enantiomeric excess** was determined to be 66% ee by chiral HPLC (Chiralpak® IA-3 column, *n*-Hexane/*i*-PrOH = 99:1, 1 mL/min, λ = 235 nm, 25 °C), major enantiomer: t_r = 7.66 min, minor enantiomer: t_r = 12.34 min.

Die approbierte gedruckte Originalversion dieser Dissertation ist an der TU Wien Bibliothek verfügbar.
The approved original version of this doctoral thesis is available in print at TU Wien Bibliothek.

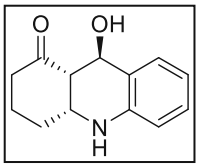
9. General procedure and analytical data for the asymmetric aza-Michael additions



In an 8 mL screw cap vial the catalyst was prepared *in situ* by stirring the amine **AM6** (25 mol%) and phosphoric acid **PA9** (25 mol%) in $CHCl_3$ (0.25 M) for 20 min. Then, 2-cyclohexen-1-one (**1a**, 2.0 equiv.) was added and the reaction mixture was stirred for another 20 min at room temperature. Then aminobenzaldehyde **4a-d** was added in one portion. The reaction mixture was stirred at room temperature for 48 h. After this 15 % *i*-PrOH in *n*-hexane was added and the mixture was placed in an ultrasound bath for 1min. The solid was filtered off, it was successively washed with low amounts of 15% *i*-PrOH in *n*-hexane (3×) (13% *i*-PrOH in *n*-hexane for **5e**) and with pure *n*-hexane (3×) and it was dried *in vacuo* to provide the pure product **5a-d** as white powder.

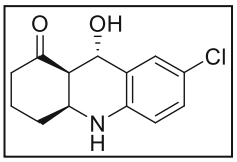


(4a*S*,9*R*,9a*S*)-9-Hydroxy-3,4,4a,9,9a,10-hexahydroacridin-1(2*H*)-one, (*S*,*R*,*S*)-**5a.** Performed with 1.24 mmol 2-aminobenzaldehyde (**4a**). White powder (171 mg, 64% yield). **M.p. =** 197 – 199 °C. $[\alpha]_D^{20} = -178.7$ (c 0.66, CH_2Cl_2). **^{1}H NMR (400 MHz, DMSO-d_6) δ** 7.09 (dd, *J* = 7.6, 1.6 Hz, 1H), 6.91 (ddd, *J* = 8.0, 7.2, 1.6 Hz, 1H), 6.55 – 6.47 (m, 2H), 5.76 (s, 1H), 5.02 (d, *J* = 5.5 Hz, 1H), 4.74 (dd, *J* = 5.5, 2.1 Hz, 1H), 3.84 (q, *J* = 3.2 Hz, 1H), 2.77 (dt, *J* = 2.4, 1.2 Hz, 1H), 2.46 – 2.33 (m, 1H), 2.13 – 1.92 (m, 4H), 1.88 – 1.78 (m, 1H). **^{13}C NMR (101 MHz, DMSO-d_6) δ** 210.06, 144.74, 130.57, 127.62, 121.84, 115.86, 114.04, 63.00, 53.99, 48.42, 40.52, 28.74, 21.85. The **enantiomeric excess** was determined to be >99% ee by chiral HPLC (Chiralpak® IB column, *n*-Hexane/*i*-PrOH = 85:15, 1 mL/min, λ = 220 nm, 25 °C), minor enantiomer: t_r = 18.61 min, major enantiomer: t_r = 22.48 min. **IR ATR (vmax/cm^{-1})** 3370, 3167, 1692, 1496, 750. **HRMS (ESI)** Cald for $C_{13}H_{15}NO_2$ $[M]^+$ 217.1103, Found 217.1058.

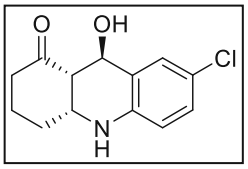


(4a*R*,9*S*,9a*R*)-9-Hydroxy-3,4,4a,9,9a,10-hexahydroacridin-1(2*H*)-one, (*R*,*S*,*R*)-**5a.** Performed with 1.24 mmol 2-aminobenzaldehyde (**4a**). White powder (164 mg, 61% yield). $[\alpha]_D^{20} = +132.9$ (c 0.48, CH_2Cl_2). The **enantiomeric excess** was determined to be >99% ee by chiral HPLC (Chiralpak® IB column, *n*-Hexane/*i*-PrOH = 85:15, 1 mL/min, λ = 220 nm, 25 °C), major enantiomer: t_r = 18.67 min, minor enantiomer: t_r = 22.48 min.

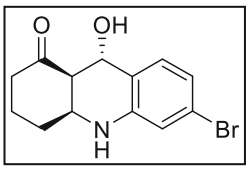
Die approbierte gedruckte Originalversion dieser Dissertation ist an der TU Wien Bibliothek verfügbar.
The approved original version of this doctoral thesis is available in print at TU Wien Bibliothek.
TU Bibliothek Your knowledge hub WIEN



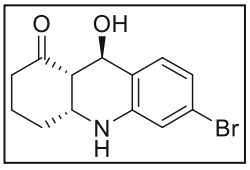
(4a*S*,9*R*,9a*S*)-7-Chloro-9-hydroxy-3,4,4a,9,9a,10-hexahydroacridin-1(2*H*)-one, (*S*,*R*,*S*)-**5b.** Performed with 0.60 mmol 2-amino-5-chlorobenzaldehyde (**4b**). White powder (90 mg, 56% yield). **M.p. =** 184 – 186 °C. $[\alpha]_D^{20} = -130.9$ (c 0.80, CH_2Cl_2). **^{1}H NMR (400 MHz, DMSO-d_6) δ** 7.10 (d, *J* = 2.5 Hz, 1H), 6.94 (dd, *J* = 8.6, 2.6 Hz, 1H), 6.51 (d, *J* = 8.6 Hz, 1H), 6.01 (s, 1H), 5.21 (d, *J* = 5.3 Hz, 1H), 4.71 (dd, *J* = 5.3, 2.3 Hz, 1H), 3.82 (q, *J* = 3.1 Hz, 1H), 2.79 (ddt, *J* = 3.6, 2.3, 1.1 Hz, 1H), 2.46 – 2.35 (m, 1H), 2.08 (ddd, *J* = 14.8, 3.9, 1.8 Hz, 1H), 1.97 (t, *J* = 3.0 Hz, 3H), 1.89 – 1.78 (m, 1H). **^{13}C NMR (101 MHz, DMSO-d_6) δ** 209.94, 143.57, 129.75, 127.42, 123.45, 118.85, 115.50, 62.71, 53.33, 48.49, 40.46, 28.57, 21.89. The **enantiomeric excess** was determined to be 93% ee by chiral HPLC (Chiralpak® AS-H column, *n*-Hexane/*i*-PrOH = 65:35, 1 mL/min, λ = 220 nm, 25 °C), major enantiomer: t_r = 7.93 min, minor enantiomer: t_r =14.53 min. **IR ATR (vmax/cm^{-1})** 3371, 3192, 1692, 1500, 820. **HRMS (ESI)** Cald for $C_{13}H_{14}ClNO_2$ $[M]^+$ 251.0713, Found 251.0689.



(4a*R*,9*S*,9a*R*)-7-Chloro-9-hydroxy-3,4,4a,9,9a,10-hexahydroacridin-1(2*H*)-one, (*R*,*S*,*R*)-**5b.** Performed with 0.6 mmol 2-amino-5-chlorobenzaldehyde (**4c**). White powder (89 mg, 55% yield). $[\alpha]_D^{20} = +137.0$ (c 0.66, CH_2Cl_2). The **enantiomeric excess** was determined to be 91% ee by chiral HPLC (Chiralpak® AS-H column, *n*-Hexane/*i*-PrOH = 65:35, 1 mL/min, λ = 220 nm, 25 °C), minor enantiomer: t_r = 7.82 min, major enantiomer: t_r =13.89 min.



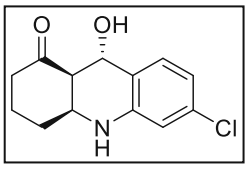
(4a*S*,9*R*,9a*S*)-6-Bromo-9-hydroxy-3,4,4a,9,9a,10-hexahydroacridin-1(2*H*) - (*S*,*R*,*S*)-**5c.** Performed with 0.6 mmol 2-amino-4-bromobenzaldehyde (**4c**). White powder (90 mg, 61% yield). **M.p. =** 183 – 185 °C. $[\alpha]_D^{20} = -118.6$ (c 0.62, CH_2Cl_2). **^{1}H NMR (400 MHz, DMSO-d_6) δ** 7.02 (d, *J* = 8.0 Hz, 1H), 6.70 – 6.61 (m, 2H), 6.12 (s, 1H), 5.13 (d, *J* = 5.4 Hz, 1H), 4.70 (dd, *J* = 5.4, 2.3 Hz, 1H), 3.84 (q, *J* = 2.8, 2.4 Hz, 1H), 2.79 (td, *J* = 2.5, 1.2 Hz, 1H), 2.46 – 2.36 (m, 1H), 2.11 – 2.02 (m, 1H), 1.99 – 1.91 (m, 3H), 1.85 (pt, *J* = 6.9, 4.2, 3.4 Hz, 1H). **^{13}C NMR (101 MHz, DMSO-d_6) δ** 209.87, 146.30, 132.37, 120.96, 120.58, 118.05, 115.72, 62.59, 53.26, 48.16, 40.48, 28.52, 21.81. The **enantiomeric excess** was determined to be >99% ee by chiral HPLC (Chiralpak® AS-H column, *n*-Hexane/*i*-PrOH = 65:35, 1 mL/min, λ = 220 nm, 25 °C), major enantiomer: t_r = 8.74 min, minor enantiomer: t_r = 12.08 min. **IR ATR (vmax/cm^{-1})** 3368, 3225, 1692, 1607, 1491, 989. **HRMS (ESI)** Cald for $C_{13}H_{14}BrNO_2$ $[M]^+$ 295.0208, Found 295.0199.



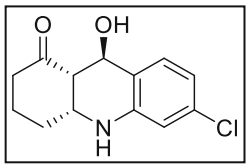
(4a*R*,9*S*,9a*R*)-6-Bromo-9-hydroxy-3,4,4a,9,9a,10-hexahydroacridin-1(2*H*)-one, (*R*,*S*,*R*)-**5c.** Performed with 0.6 mmol 2-amino-4-bromobenzaldehyde (**4c**). White powder (87 mg, 59% yield). $[\alpha]_D^{20} = +125.2$ (c 0.74, CH_2Cl_2). The

Die approbierte gedruckte Originalversion dieser Dissertation ist an der TU Wien Bibliothek verfügbar.
The approved original version of this doctoral thesis is available in print at TU Wien Bibliothek.
TU Bibliothek Your knowledge hub WIEN

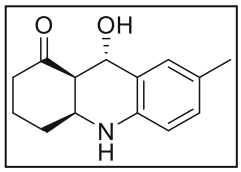
enantiomeric excess was to be >99% ee by chiral HPLC (Chiralpak® AS-H column, *n*-Hexane/*i*-PrOH = 65:35, 1 mL/min, λ = 220 nm, 25 °C), minor enantiomer: t_r = 9.83 min, major enantiomer: t_r = 12.74 min.



(4a*S*,9*R*,9a*S*)-6-Chloro-9-hydroxy-3,4,4a,9,9a,10-hexahydroacridin-1(2*H*) -one, (*S*,*R*,*S*)-**5d**. Performed with 0.6 mmol 2-amino-4-chlorobenzaldehyde (**4d**). White powder (109 mg, 69% yield). **M.p. =** 172 – 174 °C. $[\alpha]_D^{20}$ = − 185.5 (c 0.483, CH_2Cl_2). **^{1}H NMR (400 MHz, DMSO-d$_6$) δ** 7.08 (d, *J* = 7.8 Hz, 1H), 6.51 (d, *J* = 7.4 Hz, 2H), 6.13 (s, 1H), 5.10 (d, *J* = 5.4 Hz, 1H), 4.71 (dd, *J* = 5.4, 2.3 Hz, 1H), 3.85 (q, *J* = 2.8, 2.4 Hz, 1H), 2.79 (td, *J* = 2.6, 1.3 Hz, 1H), 2.43 (td, *J* = 12.1, 6.1 Hz, 1H), 2.12 – 2.02 (m, 1H), 1.97 (q, *J* = 6.4, 3H), 1.86 (dq, *J* = 8.5, 5.8, 4.8 Hz, 1H). **^{13}C NMR (101 MHz, DMSO-d$_6$) δ** 209.71, 145.96, 131.99, 131.90, 120.57, 115.13, 112.73, 62.46, 53.27, 48.09, 40.41, 28.47, 21.73. The **enantiomeric excess** was determined to be >99% ee by chiral HPLC (Chiralpak® AS-H column, *n*-Hexane/*i*-PrOH = 65:35, 1 mL/min, λ = 220 nm, 25 °C), major enantiomer: t_r = 8.22 min, minor enantiomer: t_r = 11.70 min. **IR ATR (νmax/cm^{-1})** 3366, 3169, 1692, 1613, 1476, 992. **HRMS (ESI)** Cald for $C_{13}H_{15}ClNO_2$ $[M+H]^+$ 252.0786, Found 252.0790.

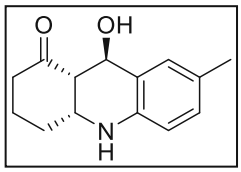


(4a*R*,9*S*,9a*R*)-6-Chloro-9-hydroxy-3,4,4a,9,9a,10-hexahydroacridin-1(2*H*) -one, (*R*,*S*,*R*)-**5d**. Performed with 0.6 mmol 2-amino-4-chlorobenzaldehyde (**4d**). White powder (109 mg, 69% yield). $[\alpha]_D^{20}$ = + 180.0 (c 0.48, CH_2Cl_2). The **enantiomeric excess** was determined to be >99% ee by chiral HPLC (Chiralpak® AS-H column, *n*-Hexane/*i*-PrOH = 65:35, 1 mL/min, λ = 220 nm, 25 °C), minor enantiomer: t_r = 8.27 min, majorenantiomer: t_r = 11.65 min.



(4a*S*,9*R*,9a*S*)-9-Hydroxy-7-methyl-3,4,4a,9,9a,10-hexahydroacridin-1(2H)-one, (*S*,*R*,*S*)-**5e**. Performed with 0.74 mmol 2-amino-5-methylbenzaldehyde (**4e**). White powder (86 mg, 50% yield). **M.p. =** 183 – 185 °C. $[\alpha]_D^{20}$ = − 178,36 (c 0.304, CH_2Cl_2). **^{1}H NMR (400 MHz, DMSO-d$_6$)** δ 6.92 (d, *J* = 2.2 Hz, 1H), 6.74 (dd, *J* = 8.1, 2.1 Hz, 1H), 6.41 (d, *J* = 8.1 Hz, 1H), 5.57 (s, 1H), 4.95 (d, *J* = 5.6 Hz, 1H), 4.70 (dd, *J* = 5.6, 2.1 Hz, 1H), 3.81 (q, *J* = 3.2 Hz, 1H), 2.75 (dt, *J* = 3.7, 1.7 Hz, 1H), 2.41 (td, *J* = 14.1, 13.3, 6.3 Hz, 1H), 2.15 (s, 3H), 2.11 – 1.89 (m, 4H), 1.83 (ddd, *J* = 11.2, 8.2, 4.3 Hz, 1H). **^{13}C NMR (101 MHz, DMSO-d$_6$)** δ 209.96, 142.35, 130.82, 128.20, 124.03, 121.77, 114.07, 62.91, 54.19, 48.53, 40.44, 28.77, 21.81, 20.15. The **enantiomeric excess** was determined to be >99% ee by chiral HPLC (Chiralpak® AS-H column, *n*-Hexane/*i*-PrOH = 70:30, 1 mL/min, λ = 220 nm, 25 °C), major enantiomer: t_r = 8.99 min, minor enantiomer: t_r = 24.2 min. **IR ATR (νmax/cm^{-1})** 3374, 3194, 1695, 1624, 1457, 990. **HRMS (ESI)** Cald for $C_{14}H_{18}NO_2$ $[M+H]^+$ 232.1332, Found 232.1335.

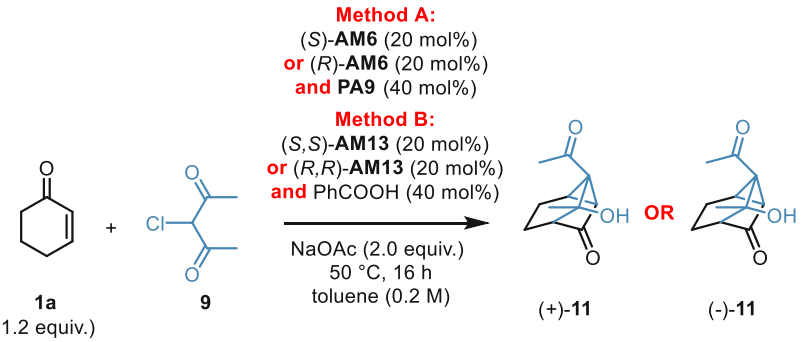
Die approbierte gedruckte Originalversion dieser Dissertation ist an der TU Wien Bibliothek verfügbar.
The approved original version of this doctoral thesis is available in print at TU Wien Bibliothek.
TU Bibliothek Your knowledge hub WIEN



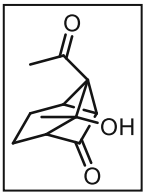
(4a*R*,9*S*,9a*R*)-9-Hydroxy-7-methyl-3,4,4a,9,9a,10-hexahydroacridin-1(2*H*)-one, (*R*,*S*,*R*)-**5e**. Performed with 0.74 mmol 2-amino-5-methylbenzaldehyde (**4e**). White powder (85 mg, 50% yield). $[\alpha]_D^{20} = +177.97$ (c 0.295, CH_2Cl_2). The **enantiomeric excess** was determined to be >99% ee by chiral HPLC (Chiralpak® AS-H column, *n*-Hexane/*i*-PrOH = 70:30, 1 mL/min, λ = 220 nm, 25 °C), minor enantiomer: t_r = 9.14 min, major enantiomer: t_r = 23.3 min.

Die approbierte gedruckte Originalversion dieser Dissertation ist an der TU Wien Bibliothek verfügbar.
The approved original version of this doctoral thesis is available in print at TU Wien Bibliothek.

10. General procedure and analytical data for the asymmetric Michael-Initiated Ring-Closure/Intramolecular Aldol Sequence

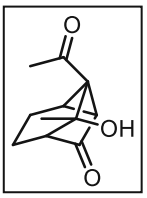


Reactions were performed on a 1.0 mmol scale. In a 20 mL screw cap vial the catalyst was prepared *in situ* by stirring the amine (**AM6** or **AM13**, 20 mol%) and acid (**PA9** or PhCOOH**,** 40 mol%) in anhydrous toluene (0.20 M) for 20 min. Then, 2-cyclohexen-1-one (**1a**, 1.2 equiv.) was added and the reaction mixture was stirred for another 20 min at room temperature. Then 3-chloroacetylacetone (**9,** 1.0 equiv.) and NaOAc (2.0 equiv.) were added and the reaction mixture was stirred at 50 ˚C for 16 hours. After being cooled down to room temperature, the reaction was quenched with H_2O (10 mL) and the aqueous phase was extracted with toluene (2×) and EtOAc (2×). The combined organic phases were washed with saturated $NaHCO_3$ (2×), dried over anhydrous Na_2SO_4 and the solvents were removed *in vacuo*. The crude product was purified by column chromatography (gradient elution, PE/EE mixtures).

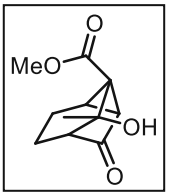


1-Acetyl-8-hydroxy-8-methyltricyclo[3.2.1.0^{2,7}]octan-6-one (−)-**11a.** Purified by column chromatography (33% EtOAc in PE to 100% EtOAc, R_f = 0.35 in PE/EtOAc 1/1). White solid (155 mg, 77% yield). **M.p. =** 85 – 87 °C. $[\alpha]_D^{20} = -114.14$ (c 1.02, CH_2Cl_2). **^{1}H NMR (600 MHz, $CDCl_3$)** δ 3.99 (bs, 1H, O*H*), 2.60 (ddt, *J* = 8.5, 3.0, 1.5 Hz, 1H, *H*2), 2.48 (dd, *J* = 8.6, 1.5 Hz, 1H, *H*7), 2.13 – 1.99 (m, 4H, *H*3a, *H*3b, *H*4a, *H*5), 1.99-1.94 (m, 1H, *H*4b), 1.93 (s, 3H, COC*H*$_3$), 1.62 (s, 3H, C*H*$_3$). **^{13}C NMR (150 MHz, $CDCl_3$)** δ 209.79, 206.08, 74.99, 52.43, 52.26, 38.68, 36.29, 25.41, 25.12, 15.47. The product was obtained as a single diastereomer. The **enantiomeric excess** was determined by chiral HPLC to be 85% ee and 95% ee by using [(*S*)-**AM6**][**PA9**] and [(*S,S*)-**AM13**][2PhCOOH], respectively (Chiralpak® OJ column, *n*-Hexane/*i*-PrOH = 90:10, 1 mL/min, λ = 220 nm, 25 °C), major enantiomer: t_r = 22.09 min, minor enantiomer: t_r = 26.02 min. **IR ATR (νmax/cm^{-1})** 3045, 2976, 1717, 1682, 1353, 1225, 876. **HRMS (ESI)** Cald for $C_{11}H_{15}O_3$ $[M+H]^+$ 195.1021, Found 195.1018**.**

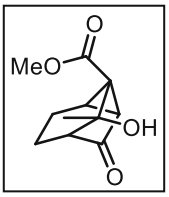
Die approbierte gedruckte Originalversion dieser Dissertation ist an der TU Wien Bibliothek verfügbar.
The approved original version of this doctoral thesis is available in print at TU Wien Bibliothek.



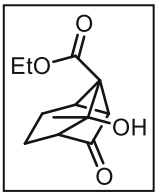
1-Acetyl-8-hydroxy-8-methyltricyclo[3.2.1.0^{2,7}]octan-6-one (+)-**11a.** White solid (152 mg, 79% yield). $[\alpha]_D^{20}$ = + 111.91 (c 1.0, CH_2Cl_2). The product was obtained as a single diastereomer. The **enantiomeric excess** was determined by chiral HPLC to be 87% ee and 97% ee by using [(*R*)-**AM6**][**PA9**] and [(*R*,*R*)-**AM13**][2PhCOOH], respectively (Chiralpak® OJ column, *n*-Hexane/*i*-PrOH = 90 : 10, 1 mL/min, λ = 220 nm, 25 °C), minor enantiomer: t_r = 22.83 min, major enantiomer: t_r = 25.22 min.



Methyl-8-hydroxy-8-methyl-6-oxotricyclo[3.2.1.0^{2,7}]octane-1-carboxylate (−)-**11b.** Purified by column chromatography (25% EtOAc in PE to 33% EtOAc in PE). Light yellow oil (119 mg, 52% yield). $[\alpha]_D^{20}$ = − 21.30 (c 1.0, CH_2Cl_2). **^{1}H NMR (400 MHz, $CDCl_3$)** δ 3.67 (s, 3H), 3.65 (s, 1H), 2.53 – 2.52 (m, 1H), 2.34 (d, *J* = 8.0 Hz, 1H), 1.97 – 1.87 (m, 5H), 1.56 (s, 3H). **^{13}C NMR (100 MHz, $CDCl_3$)** δ 210.2, 171.1, 74.4, 53.2, 52.2, 44.3, 38.9, 36.3, 25.5, 21.9, 15.1. The **enantiomeric excess** was determined by chiral HPLC to be 95% ee and 99% ee by using [(*S*)-**AM6**][**PA9**] and [(*S*,*S*)-**AM13**][2PhCOOH], respectively (Chiralpak® OJ column, *n*-Hexane/*i*-PrOH = 93:7, 0.8 mL/min, λ = 220 nm, 25 °C), major enantiomer: t_r = 29.66 min, minor enantiomer: t_r = 32.41 min. **IR ATR (vmax/cm^{-1})** 3511, 2954, 1721, 1483, 1221, 871. **HRMS (ESI)** Cald for $C_{11}H_{14}O_4Na$ $[M+Na]^+$ 233.0784, Found 233.0790**.**

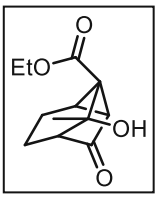


Methyl-8-hydroxy-8-methyl-6-oxotricyclo[3.2.1.0^{2,7}]octane-1-carboxylate (+)-**11b.** Purified by column chromatography (25% EtOAc in PE to 50% EtOAc in PE). Light yellow oil (119 mg, 52% yield). $[\alpha]_D^{20}$ = + 23.1 (c 1.0, CH_2Cl_2). The **enantiomeric excess** was determined by chiral HPLC to be 94% ee and 99% ee by using [(*R*)-**AM6**][**PA9**] and [(*R*,*R*)-**AM13**][2PhCOOH], respectively (Chiralpak® OJ column, *n*-Hexane/*i*-PrOH = 93:7, 0.8 mL/min, λ = 220 nm, 25 °C), minor enantiomer: t_r = 30.45 min, major enantiomer: t_r = 31.73 min.

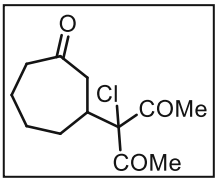


Ethyl-8-hydroxy-8-methyl-6-oxotricyclo[3.2.1.0^{2,7}]octane-1-carboxylate (−)-**11c.** Purified by column chromatography (25% EtOAc in PE to 50% EtOAc in PE). Light yellow oil (112 mg, 50% yield). $[\alpha]_D^{20}$ = − 25.4 (c 1.0, CH_2Cl_2). **^{1}H NMR (400 MHz, $CDCl_3$)** δ 3.67 (s, 3H), 3.65 (s, 1H), 2.53 – 2.52 (m, 1H), 2.34 (d, *J* = 8.0 Hz, 1H), 1.97 – 1.87 (m, 5H), 1.56 (s, 3H). **^{13}C NMR (100 MHz, $CDCl_3$)** δ 210.2, 171.1, 74.4, 53.2, 52.2, 44.3, 38.9, 36.3, 25.5, 21.9, 15.1. The **enantiomeric excess** was determined by chiral HPLC to be 92% ee and 97% ee by using [(*S*)-**AM6**][**PA9**] and [(*S*,*S*)-**AM13**][2PhCOOH], respectively (Chiralpak® OJ column, *n*-Hexane/*i*-PrOH = 93:7, 0.8 mL/min, λ = 220 nm, 25 °C), major enantiomer: t_r = 29.66 min, minor enantiomer: t_r = 32.41 min. **IR ATR (vmax/cm^{-1})** 3511, 2954, 1721, 1483, 1221, 871. **HRMS (ESI)** Cald for $C_{12}H_{17}O_4$ $[M+H]^+$ 225.1122, Found 225.1123**.**

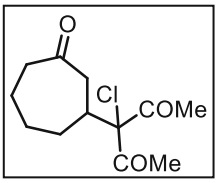
Die approbierte gedruckte Originalversion dieser Dissertation ist an der TU Wien Bibliothek verfügbar.
The approved original version of this doctoral thesis is available in print at TU Wien Bibliothek.
TU Bibliothek Your knowledge hub WIEN



Methyl-8-hydroxy-8-methyl-6-oxotricyclo[3.2.1.0^{2,7}]octane-1-carboxylate (+)-**11c.** Purified by column chromatography (25% EtOAc in PE to 50% EtOAc in PE). Light yellow oil (114 mg, 51% yield). $[\alpha]_D^{20} =$ + 21.5 (c 1.0, CH_2Cl_2). The **enantiomeric excess** was determined by chiral HPLC to be 90% ee and 98% ee by using [(*R*)-**AM6**][**PA9**] and [(*R*,*R*)-**AM13**][2PhCOOH], respectively (Chiralpak® OJ column, *n*-Hexane/*i*-PrOH = 93:7, 0.8 mL/min, λ = 220 nm, 25 °C), minor enantiomer: t_r = 30.45 min, major enantiomer: t_r = 31.73 min.



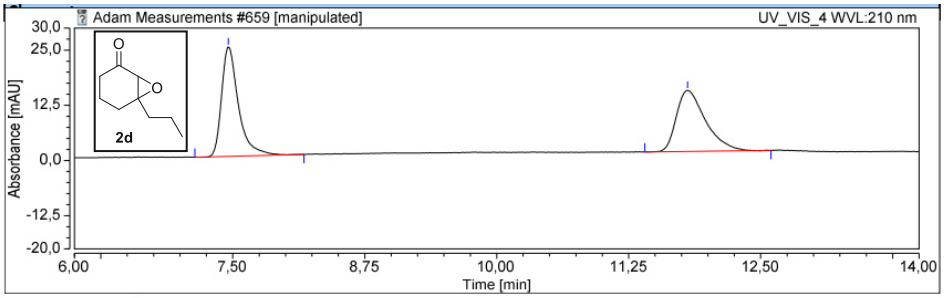
3-Chloro-3-(3-oxocycloheptyl)pentane-2,4-dione (−)-**10b.** Purified by column chromatography (12% EtOAc in PE to 20% EtOAc in PE). Colorless oil (173 mg, 71% yield). $[\alpha]_D^{20} =$ − 8.56 (c 1.0, CH_2Cl_2). **^{1}H NMR (400 MHz, $CDCl_3$)** δ 2.88 – 2.83 (m, 1H), 2.60 – 2.47 (m, 3H), 2.27 – 2.26 (m, 6H), 2.23 – 2.19 (m, 1H), 1.94 – 1.91 (m, 2H), 1.68 – 1.65 (m, 1H), 1.54 – 1.47 (m, 1H), 1.40 – 1.35 (m, 2H). **^{13}C NMR (100 MHz, $CDCl_3$)** δ 211.7, 200.0, 88.7, 45.4, 43.4, 42.0, 32.3, 28.9, 27.4, 24.4. The **enantiomeric excess** was determined by chiral HPLC to be 99% ee by using [(*S*,*S*)-**AM13**][2PhCOOH] (Chiralpak® IA-3 column, *n*-Hexane/*i*-PrOH = 95 : 5, 1 mL/min, λ = 205 nm, 25 °C), major enantiomer: t_r = 13.02 min, minor enantiomer: t_r = 14.78 min. **IR ATR (vmax/cm^{-1})**, 2932, 2861, 1699, 1356, 1154. **HRMS (ESI)** Cald for $C_{12}H_{17}ClO_3Na$ $[M+Na]^+$ 267.0758, Found 267.0762**.**



3-Chloro-3-(3-oxocycloheptyl)pentane-2,4-dione (+)-**10b.** Purified by column chromatography (12% EtOAc in PE to 20% EtOAc in PE). Colorless oil (166 mg, 69% yield). $[\alpha]_D^{20} =$ + 8.66 (c 1.0, CH_2Cl_2). The **enantiomeric excess** was determined by chiral HPLC to be 99% ee by using [(*R*,*R*)-**AM13**][2PhCOOH] (Chiralpak® IA-3 column, *n*-Hexane/*i*-PrOH = 95 : 5, 1 mL/min, λ = 205 nm, 25 °C), minor enantiomer: t_r = 13.20 min, major enantiomer: t_r = 14.60 min.

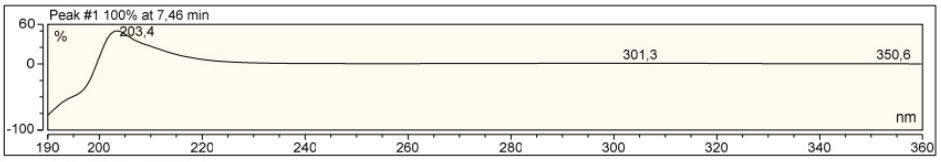
Die approbierte gedruckte Originalversion dieser Dissertation ist an der TU Wien Bibliothek verfügbar.
The approved original version of this doctoral thesis is available in print at TU Wien Bibliothek.

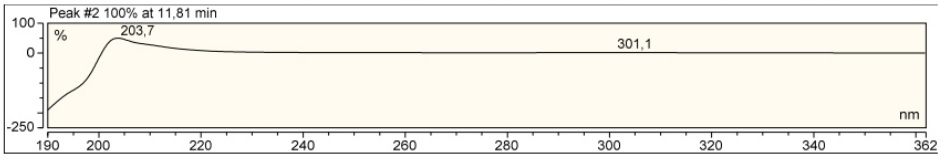
11. Chiral HPLC and chiral GC chromatograms for the asymmetric epoxidations

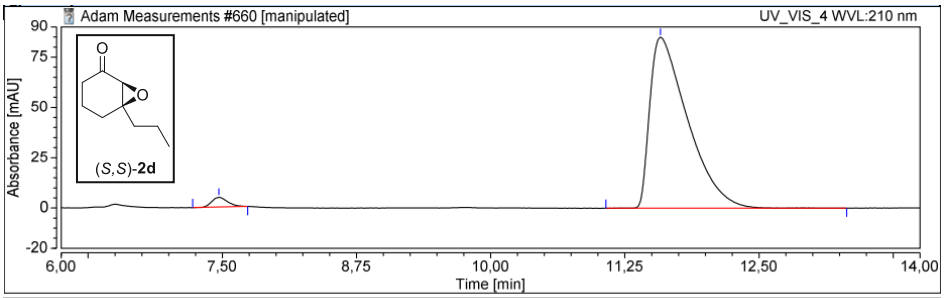


Integration Results

No.	Peak Name	Retention Time min	Area mAU*min	Height mAU	Relative Area %	Relative Height %	Amount n.a.
1		7,458	4,595	24,824	51,04	64,18	n.a.
2		11,807	4,408	13,857	48,96	35,82	n.a.
Total:			**9,003**	**38,681**	**100,00**	**100,00**	

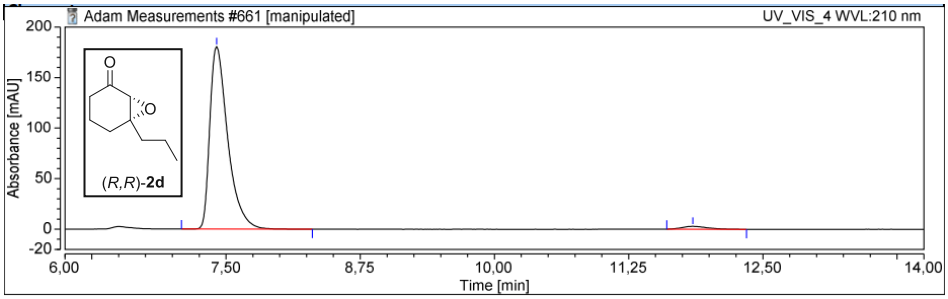






Integration Results

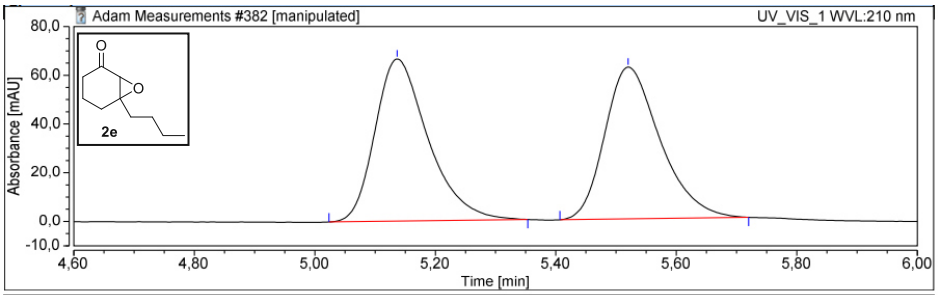
No.	Peak Name	Retention Time min	Area mAU*min	Height mAU	Relative Area %	Relative Height %	Amount n.a.
1		7,468	0,826	4,837	2,34	5,39	n.a.
2		11,582	34,524	84,956	97,66	94,61	n.a.
Total:			**35,350**	**89,793**	**100,00**	**100,00**	



Integration Results

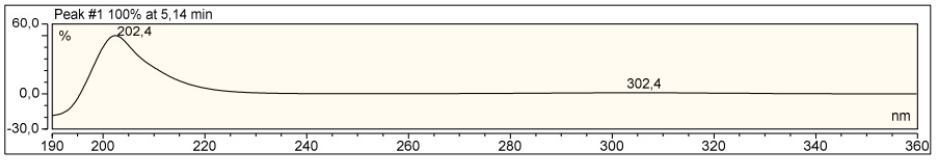
No.	Peak Name	Retention Time min	Area mAU*min	Height mAU	Relative Area %	Relative Height %	Amount n.a.
1		7,412	34,883	180,338	97,84	98,45	n.a.
2		11,848	0,771	2,837	2,16	1,55	n.a.
Total:			**35,654**	**183,174**	**100,00**	**100,00**	

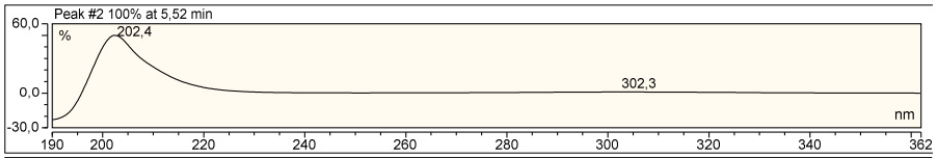
Die approbierte gedruckte Originalversion dieser Dissertation ist an der TU Wien Bibliothek verfügbar.
The approved original version of this doctoral thesis is available in print at TU Wien Bibliothek.
TU Bibliothek Your knowledge hub WIEN

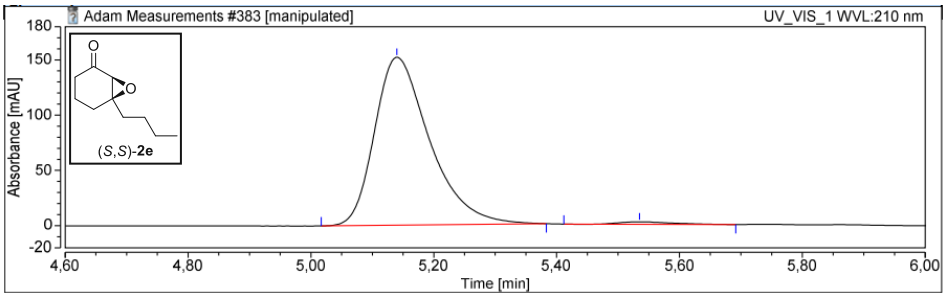


Integration Results

No.	Peak Name	Retention Time min	Area mAU*min	Height mAU	Relative Area %	Relative Height %	Amount n.a.
1		5,137	6,787	66,589	50,55	51,65	n.a.
2		5,520	6,639	62,336	49,45	48,35	n.a.
Total:			**13,426**	**128,925**	**100,00**	**100,00**	

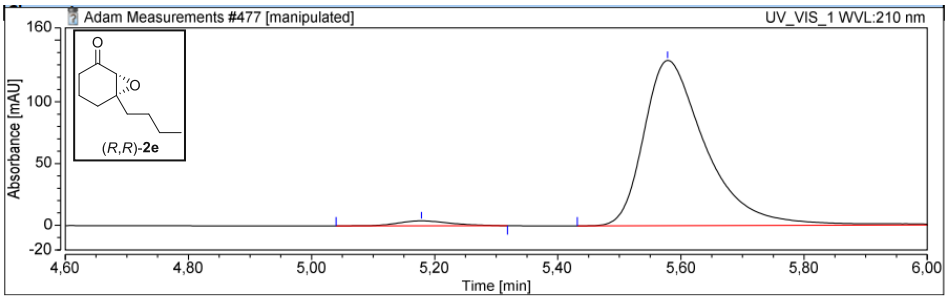






Integration Results

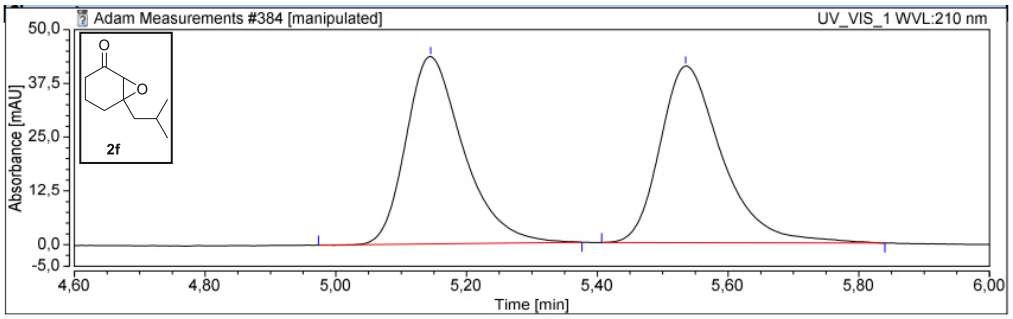
No.	Peak Name	Retention Time min	Area mAU*min	Height mAU	Relative Area %	Relative Height %	Amount n.a.
1		5,140	15,796	151,947	98,64	98,55	n.a.
2		5,535	0,217	2,236	1,36	1,45	n.a.
Total:			**16,013**	**154,182**	**100,00**	**100,00**	



Integration Results

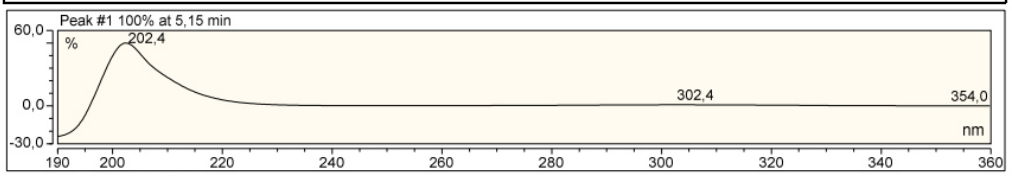
No.	Peak Name	Retention Time min	Area mAU*min	Height mAU	Relative Area %	Relative Height %	Amount n.a.
1		5,178	0,392	4,012	2,44	2,90	n.a.
2		5,578	15,682	134,115	97,56	97,10	n.a.
Total:			**16,075**	**138,128**	**100,00**	**100,00**	

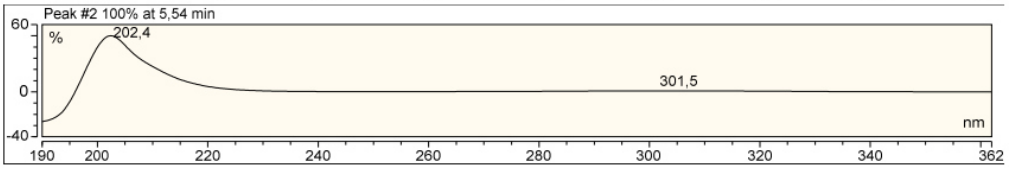
Die approbierte gedruckte Originalversion dieser Dissertation ist an der TU Wien Bibliothek verfügbar.
The approved original version of this doctoral thesis is available in print at TU Wien Bibliothek.

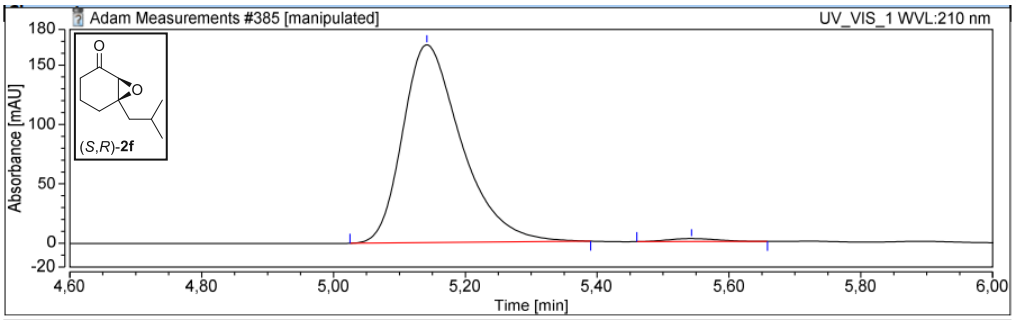


Integration Results

No.	Peak Name	Retention Time min	Area mAU*min	Height mAU	Relative Area %	Relative Height %	Amount n.a.
1		5,145	4,430	43,569	49,54	51,48	n.a.
2		5,535	4,513	41,069	50,46	48,52	n.a.
Total:			**8,943**	**84,638**	**100,00**	**100,00**	

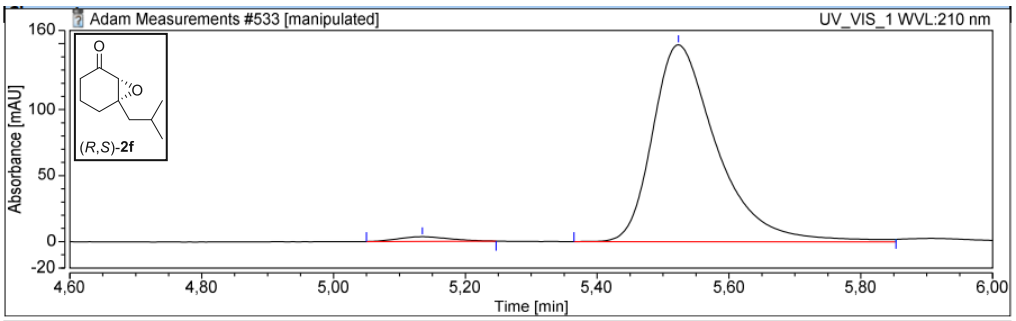






Integration Results

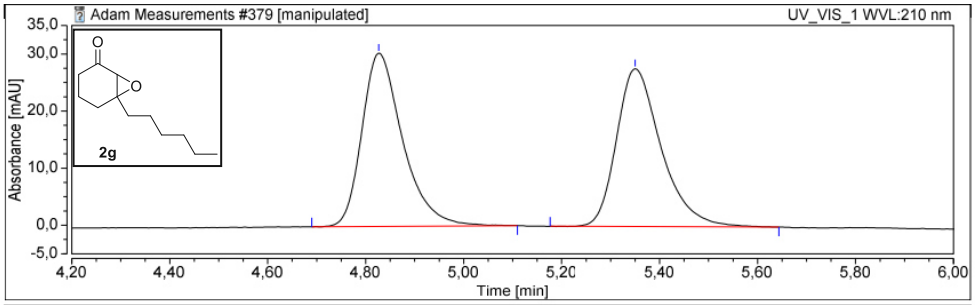
No.	Peak Name	Retention Time min	Area mAU*min	Height mAU	Relative Area %	Relative Height %	Amount n.a.
1		5,142	17,225	166,593	98,78	98,53	n.a.
2		5,543	0,213	2,477	1,22	1,47	n.a.
Total:			**17,438**	**169,070**	**100,00**	**100,00**	



Integration Results

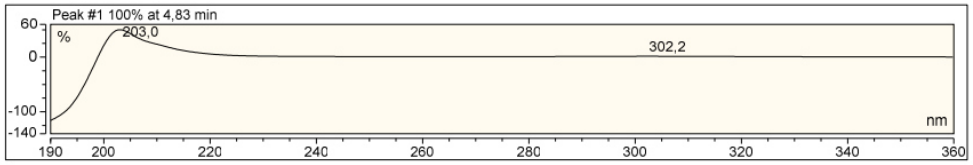
No.	Peak Name	Retention Time min	Area mAU*min	Height mAU	Relative Area %	Relative Height %	Amount n.a.
1		5,135	0,313	3,488	1,82	2,28	n.a.
2		5,523	16,867	149,230	98,18	97,72	n.a.
Total:			**17,180**	**152,718**	**100,00**	**100,00**	

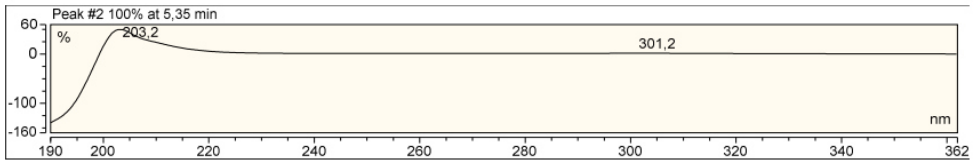
Die approbierte gedruckte Originalversion dieser Dissertation ist an der TU Wien Bibliothek verfügbar.
The approved original version of this doctoral thesis is available in print at TU Wien Bibliothek.

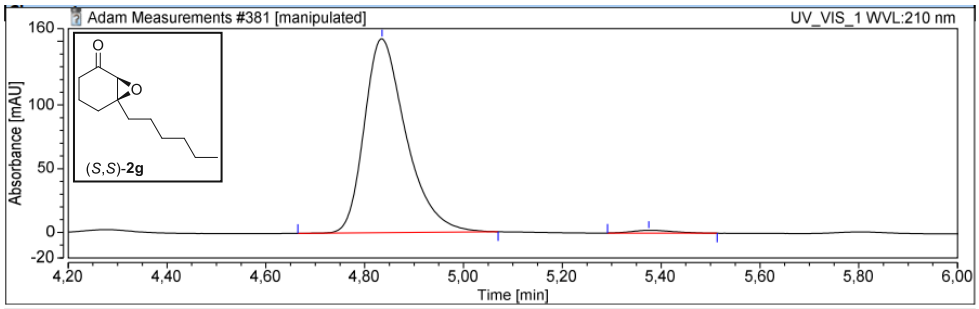


Integration Results

No.	Peak Name	Retention Time min	Area mAU*min	Height mAU	Relative Area %	Relative Height %	Amount n.a.
1		4,827	2,932	30,374	50,12	52,35	n.a.
2		5,350	2,918	27,647	49,88	47,65	n.a.
Total:			**5,851**	**58,022**	**100,00**	**100,00**	

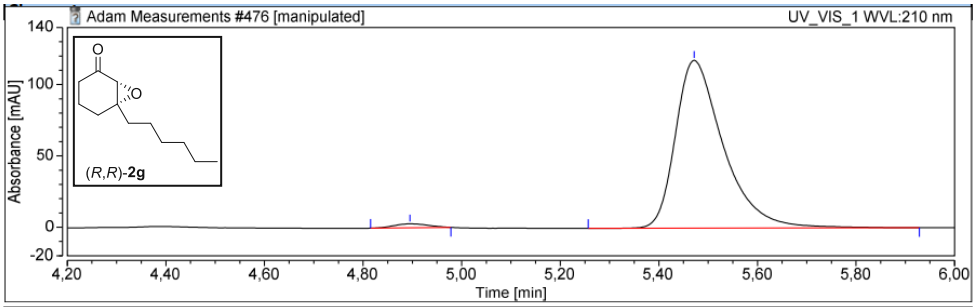






Integration Results

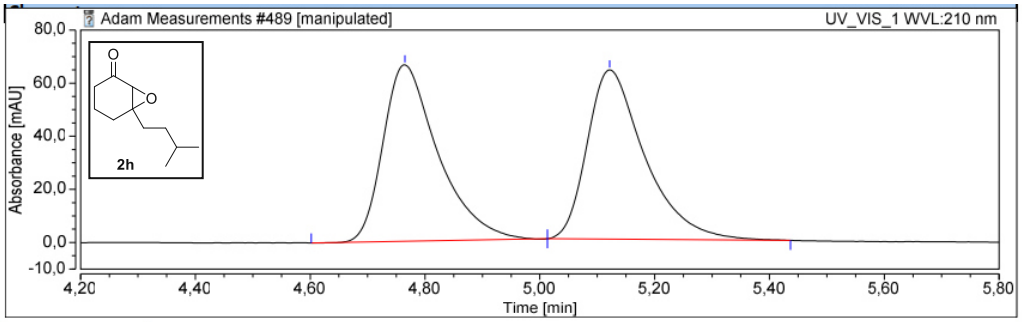
No.	Peak Name	Retention Time min	Area mAU*min	Height mAU	Relative Area %	Relative Height %	Amount n.a.
1		4,835	14,893	152,260	98,61	98,57	n.a.
2		5,375	0,210	2,202	1,39	1,43	n.a.
Total:			**15,103**	**154,462**	**100,00**	**100,00**	



Integration Results

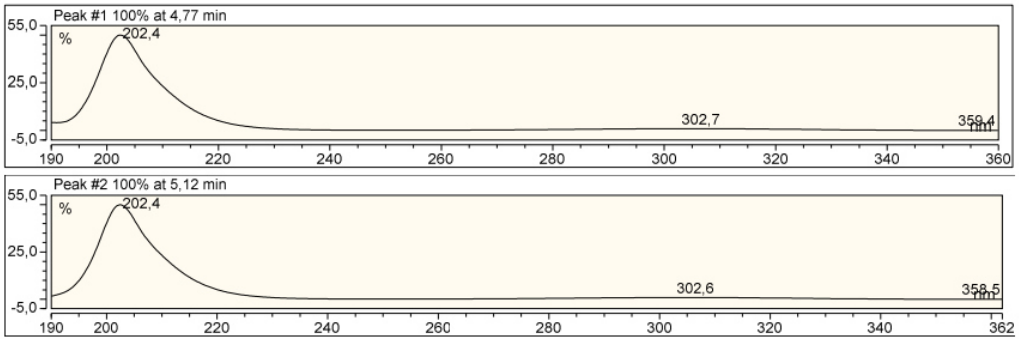
No.	Peak Name	Retention Time min	Area mAU*min	Height mAU	Relative Area %	Relative Height %	Amount n.a.
1		4,895	0,228	2,842	1,69	2,36	n.a.
2		5,472	13,273	117,672	98,31	97,64	n.a.
Total:			**13,501**	**120,514**	**100,00**	**100,00**	

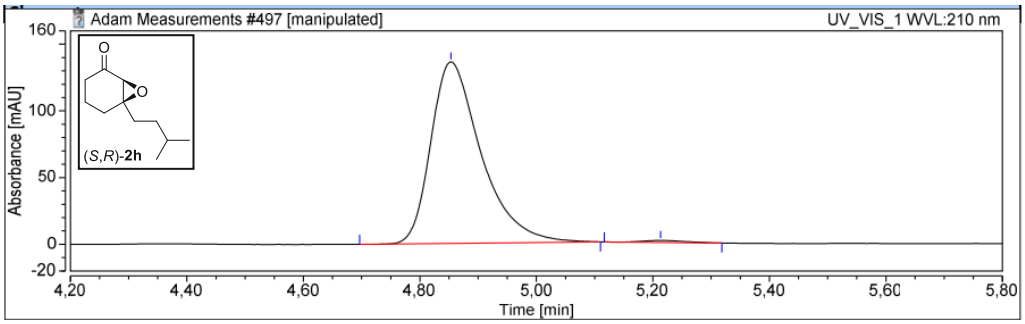
Die approbierte gedruckte Originalversion dieser Dissertation ist an der TU Wien Bibliothek verfügbar.
The approved original version of this doctoral thesis is available in print at TU Wien Bibliothek.
TU Bibliothek Your knowledge hub WIEN



Integration Results

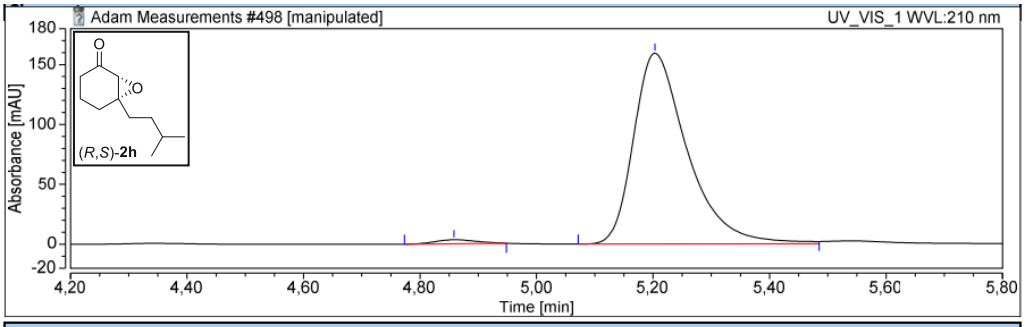
No.	Peak Name	Retention Time min	Area mAU*min	Height mAU	Relative Area %	Relative Height %	Amount n.a.
1		4,765	7,355	66,478	49,81	51,03	n.a.
2		5,122	7,411	63,786	50,19	48,97	n.a.
Total:			**14,766**	**130,264**	**100,00**	**100,00**	





Integration Results

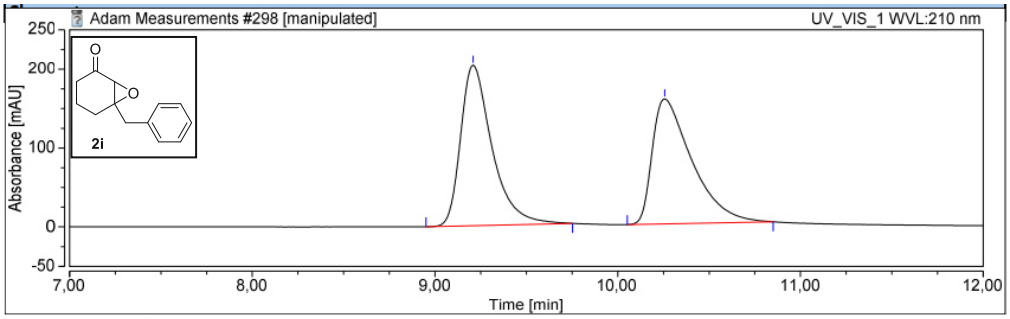
No.	Peak Name	Retention Time min	Area mAU*min	Height mAU	Relative Area %	Relative Height %	Amount n.a.
1		4,853	13,612	136,137	99,07	98,92	n.a.
2		5,213	0,127	1,487	0,93	1,08	n.a.
Total:			**13,739**	**137,623**	**100,00**	**100,00**	



Integration Results

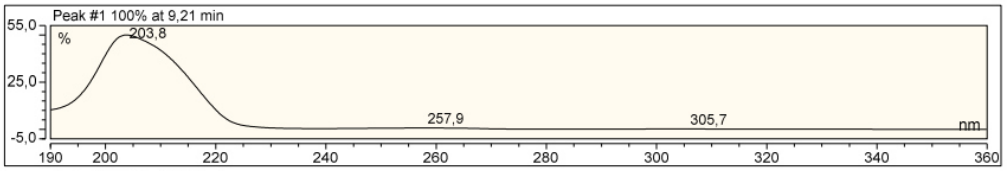
No.	Peak Name	Retention Time min	Area mAU*min	Height mAU	Relative Area %	Relative Height %	Amount n.a.
1		4,858	0,273	3,372	1,57	2,07	n.a.
2		5,203	17,064	159,392	98,43	97,93	n.a.
Total:			**17,336**	**162,764**	**100,00**	**100,00**	

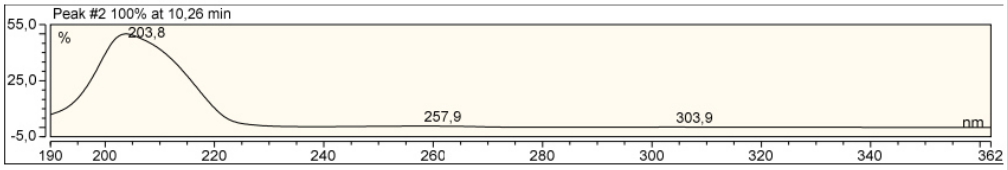
Die approbierte gedruckte Originalversion dieser Dissertation ist an der TU Wien Bibliothek verfügbar.
The approved original version of this doctoral thesis is available in print at TU Wien Bibliothek.
TU Bibliothek Your knowledge hub WIEN

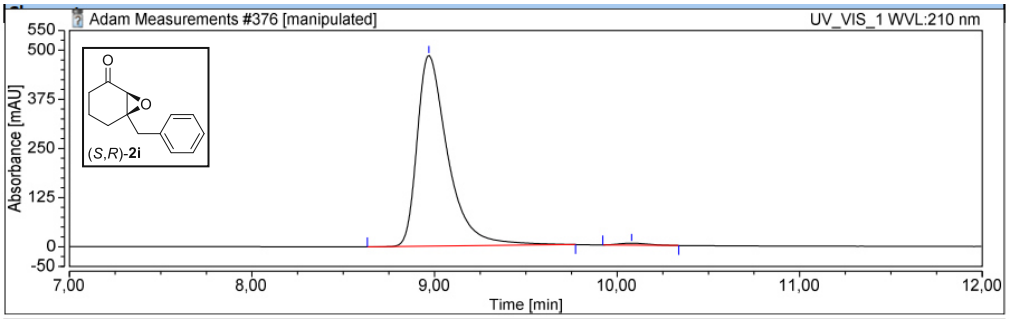


Integration Results

No.	Peak Name	Retention Time min	Area mAU*min	Height mAU	Relative Area %	Relative Height %	Amount n.a.
1		9,208	40,527	203,644	50,41	56,22	n.a.
2		10,257	39,869	158,596	49,59	43,78	n.a.
Total:			**80,396**	**362,240**	**100,00**	**100,00**	

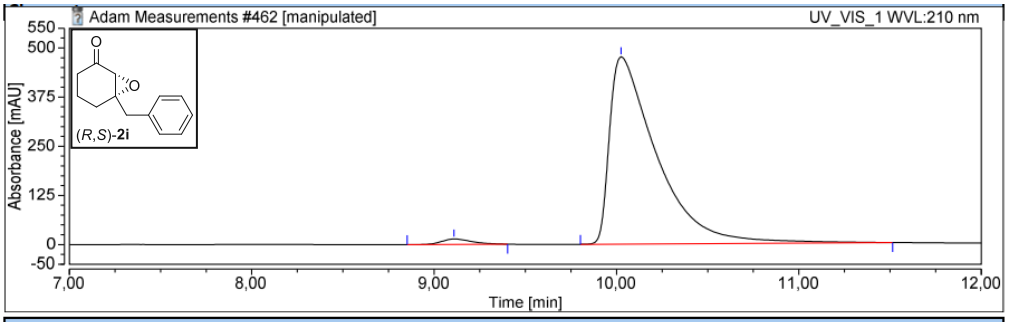






Integration Results

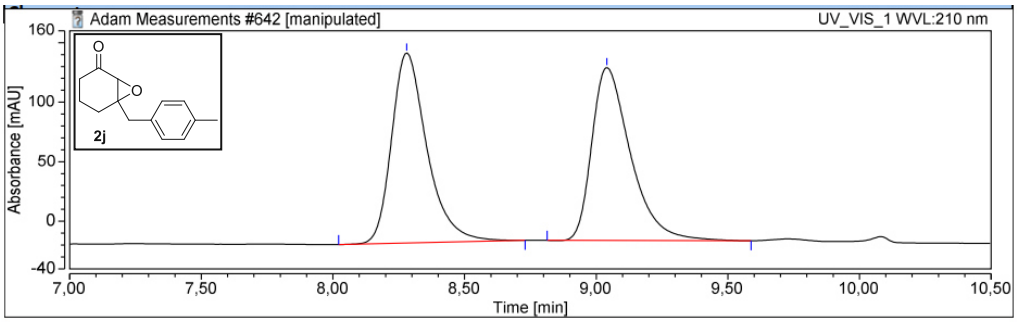
No.	Peak Name	Retention Time min	Area mAU*min	Height mAU	Relative Area %	Relative Height %	Amount n.a.
1		8,968	94,483	484,939	99,03	98,98	n.a.
2		10,080	0,921	4,991	0,97	1,02	n.a.
Total:			**95,404**	**489,930**	**100,00**	**100,00**	



Integration Results

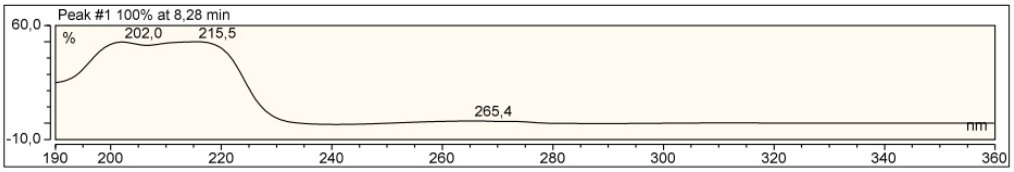
No.	Peak Name	Retention Time min	Area mAU*min	Height mAU	Relative Area %	Relative Height %	Amount n.a.
1		9,108	2,599	13,727	1,79	2,80	n.a.
2		10,025	142,665	476,291	98,21	97,20	n.a.
Total:			**145,264**	**490,017**	**100,00**	**100,00**	

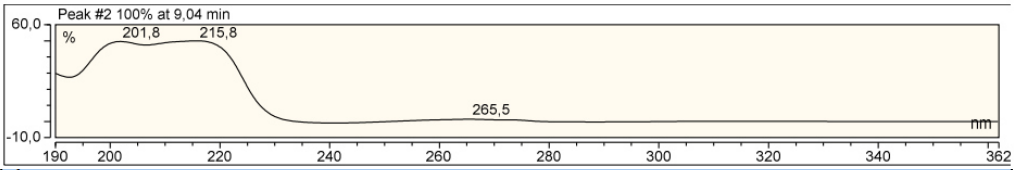
Die approbierte gedruckte Originalversion dieser Dissertation ist an der TU Wien Bibliothek verfügbar.
The approved original version of this doctoral thesis is available in print at TU Wien Bibliothek.

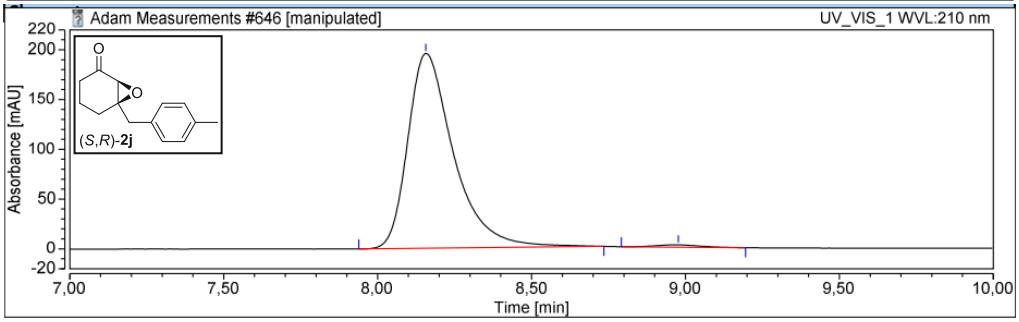


Integration Results

No.	Peak Name	Retention Time min	Area mAU*min	Height mAU	Relative Area %	Relative Height %	Amount n.a.
1		8,280	24,897	159,683	50,16	52,38	n.a.
2		9,040	24,737	145,187	49,84	47,62	n.a.
Total:			**49,634**	**304,870**	**100,00**	**100,00**	

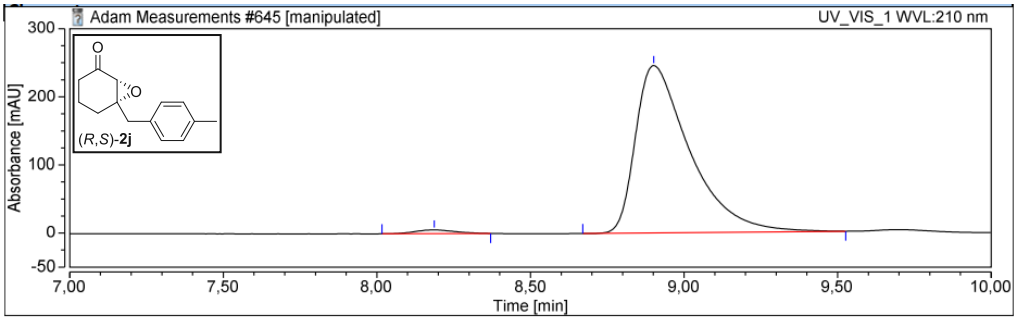






Integration Results

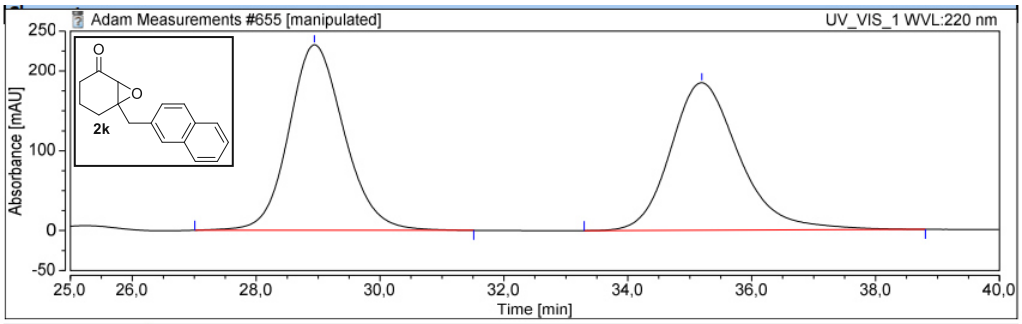
No.	Peak Name	Retention Time min	Area mAU*min	Height mAU	Relative Area %	Relative Height %	Amount n.a.
1		8,157	33,838	195,881	98,91	98,84	n.a.
2		8,977	0,372	2,301	1,09	1,16	n.a.
Total:			**34,210**	**198,181**	**100,00**	**100,00**	



Integration Results

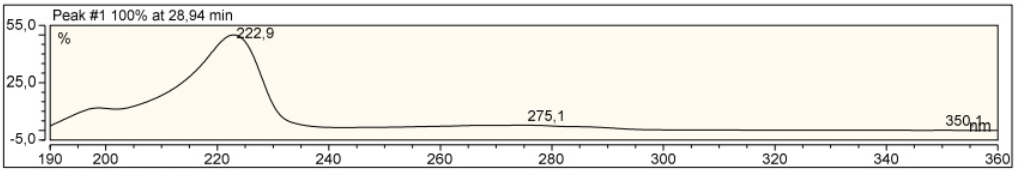
No.	Peak Name	Retention Time min	Area mAU*min	Height mAU	Relative Area %	Relative Height %	Amount n.a.
1		8,187	0,804	5,406	1,57	2,15	n.a.
2		8,902	50,376	245,891	98,43	97,85	n.a.
Total:			**51,179**	**251,297**	**100,00**	**100,00**	

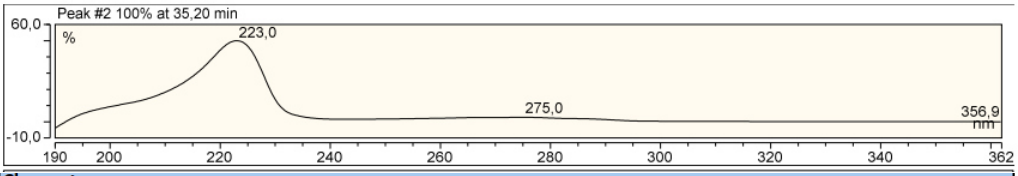
Die approbierte gedruckte Originalversion dieser Dissertation ist an der TU Wien Bibliothek verfügbar.
The approved original version of this doctoral thesis is available in print at TU Wien Bibliothek.

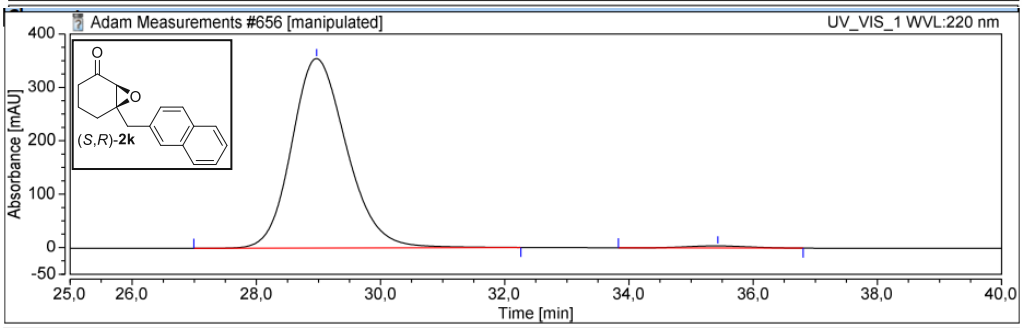


Integration Results

No.	Peak Name	Retention Time min	Area mAU*min	Height mAU	Relative Area %	Relative Height %	Amount n.a.
1		28,938	240,597	232,494	50,36	55,71	n.a.
2		35,195	237,191	184,809	49,64	44,29	n.a.
Total:			**477,788**	**417,303**	**100,00**	**100,00**	

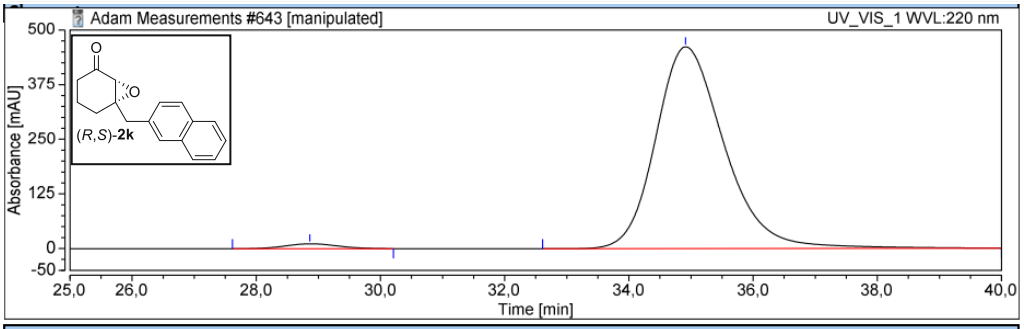






Integration Results

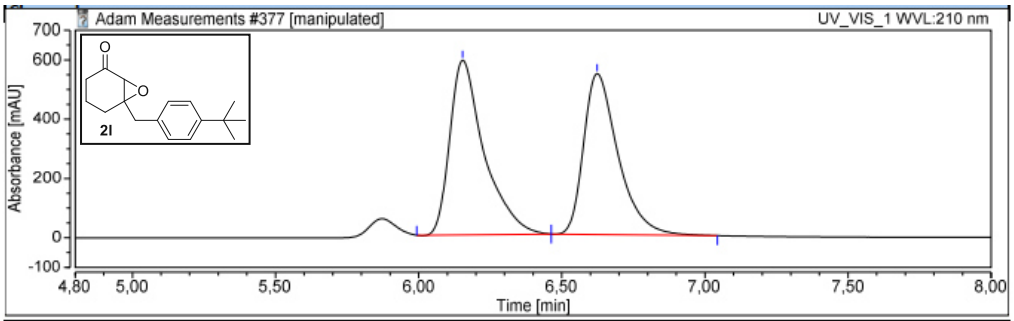
No.	Peak Name	Retention Time min	Area mAU*min	Height mAU	Relative Area %	Relative Height %	Amount n.a.
1		28,968	363,984	355,021	98,76	98,90	n.a.
2		35,430	4,569	3,950	1,24	1,10	n.a.
Total:			**368,553**	**358,971**	**100,00**	**100,00**	



Integration Results

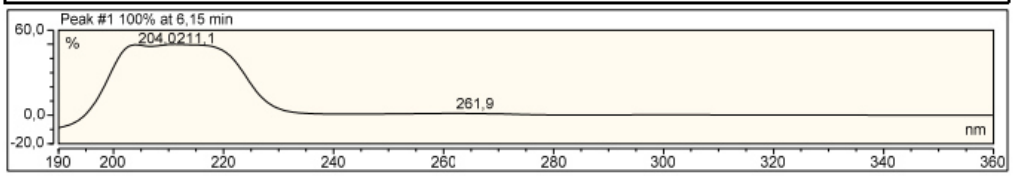
No.	Peak Name	Retention Time min	Area mAU*min	Height mAU	Relative Area %	Relative Height %	Amount n.a.
1		28,863	11,190	11,318	1,85	2,39	n.a.
2		34,912	592,545	461,747	98,15	97,61	n.a.
Total:			**603,735**	**473,065**	**100,00**	**100,00**	

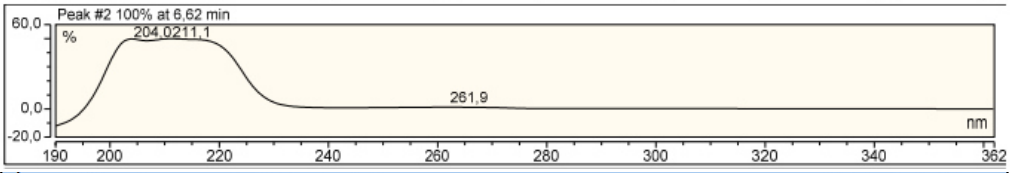
Die approbierte gedruckte Originalversion dieser Dissertation ist an der TU Wien Bibliothek verfügbar.
The approved original version of this doctoral thesis is available in print at TU Wien Bibliothek.

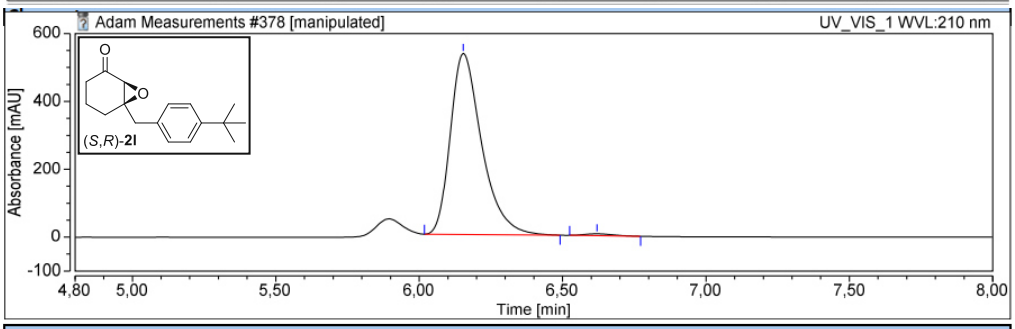


Integration Results

No.	Peak Name	Retention Time min	Area mAU*min	Height mAU	Relative Area %	Relative Height %	Amount n.a.
1		6,153	81,787	589,335	51,87	52,03	n.a.
2		6,623	75,882	543,317	48,13	47,97	n.a.
Total:			**157,669**	**1132,652**	**100,00**	**100,00**	

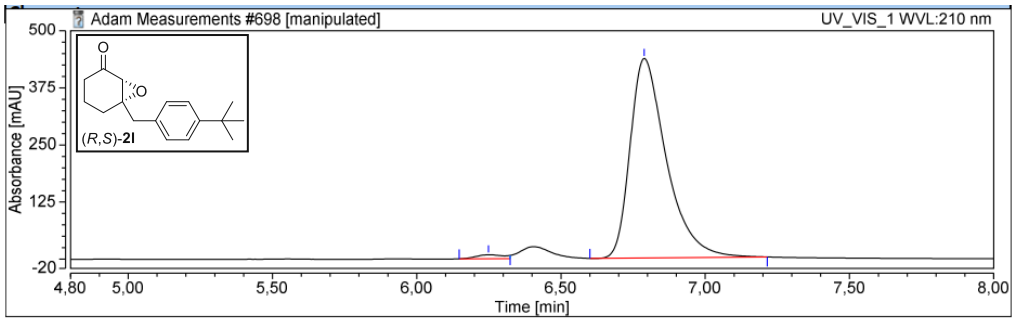






Integration Results

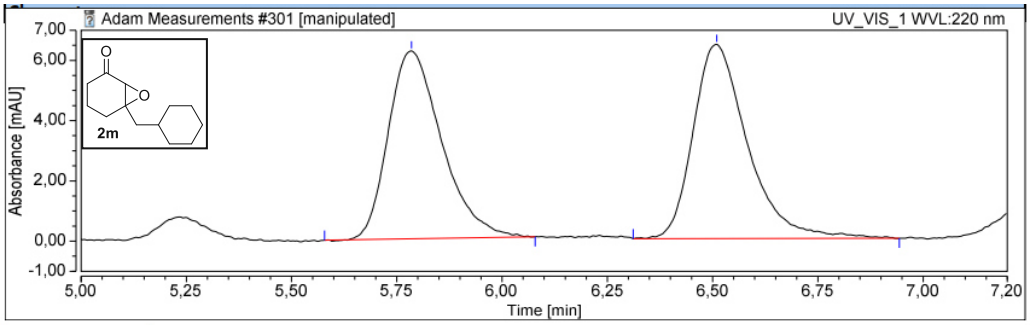
No.	Peak Name	Retention Time min	Area mAU*min	Height mAU	Relative Area %	Relative Height %	Amount n.a.
1		6,153	67,757	533,581	99,09	98,97	n.a.
2		6,620	0,623	5,530	0,91	1,03	n.a.
Total:			**68,380**	**539,111**	**100,00**	**100,00**	



Integration Results

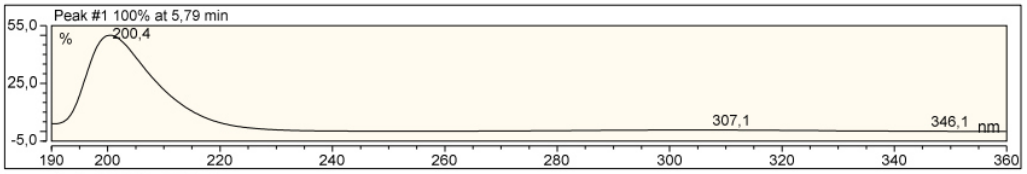
No.	Peak Name	Retention Time min	Area mAU*min	Height mAU	Relative Area %	Relative Height %	Amount n.a.
1		6,248	0,965	8,695	1,49	1,95	n.a.
2		6,788	63,685	436,689	98,51	98,05	n.a.
Total:			**64,651**	**445,384**	**100,00**	**100,00**	

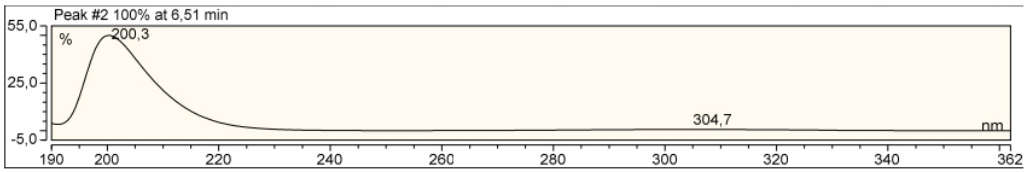
Die approbierte gedruckte Originalversion dieser Dissertation ist an der TU Wien Bibliothek verfügbar.
The approved original version of this doctoral thesis is available in print at TU Wien Bibliothek.

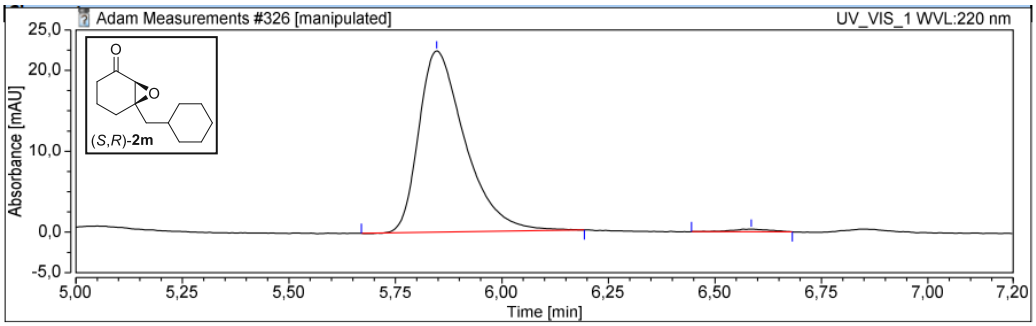


Integration Results

No.	Peak Name	Retention Time min	Area mAU*min	Height mAU	Relative Area %	Relative Height %	Amount n.a.
1		5,785	0,915	6,236	48,69	49,18	n.a.
2		6,510	0,965	6,444	51,31	50,82	n.a.
Total:			**1,880**	**12,680**	**100,00**	**100,00**	

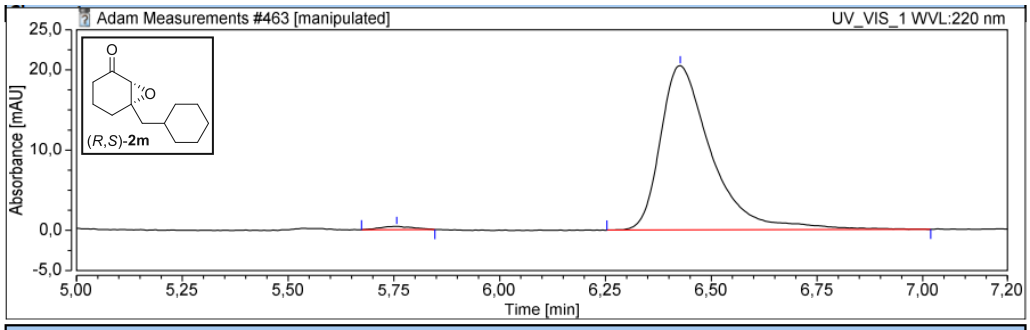






Integration Results

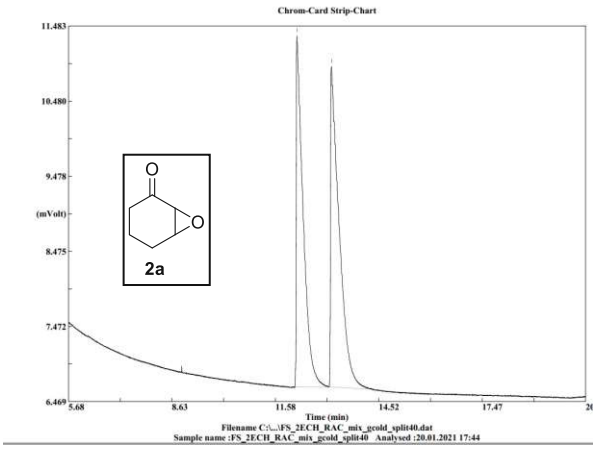
No.	Peak Name	Retention Time min	Area mAU*min	Height mAU	Relative Area %	Relative Height %	Amount n.a.
1		5,847	2,816	22,418	98,83	98,52	n.a.
2		6,585	0,033	0,336	1,17	1,48	n.a.
Total:			**2,850**	**22,754**	**100,00**	**100,00**	



Integration Results

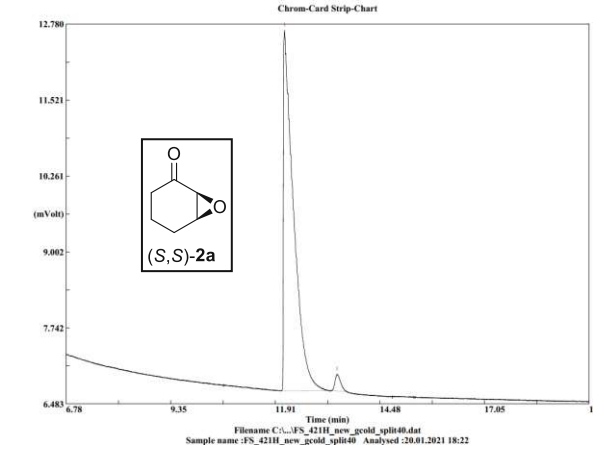
No.	Peak Name	Retention Time min	Area mAU*min	Height mAU	Relative Area %	Relative Height %	Amount n.a.
1		5,757	0,037	0,417	1,29	2,00	n.a.
2		6,427	2,852	20,464	98,71	98,00	n.a.
Total:			**2,890**	**20,881**	**100,00**	**100,00**	

Die approbierte gedruckte Originalversion dieser Dissertation ist an der TU Wien Bibliothek verfügbar.
The approved original version of this doctoral thesis is available in print at TU Wien Bibliothek.



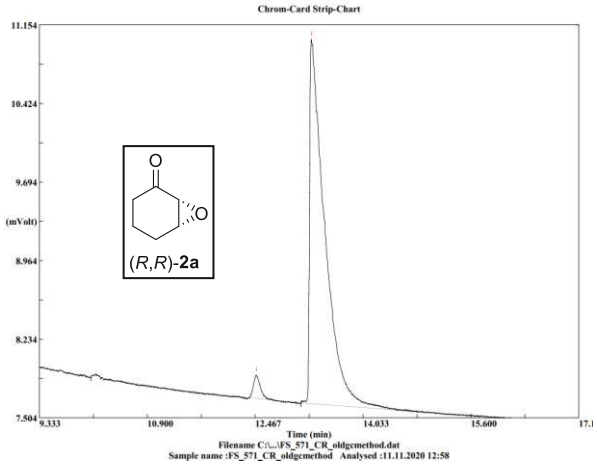
Analysed : 20.01.2021 17:44 Printed : 21.02.2021 14:24
Sample ID : FS_2ECH_RAC_mix_gcold_split40
Channel : Channel A
Analysis Type : UnkNown (Area) Calc. Method : Area %

Peak Number #	Area %	Ret.Time	Area	BC
1	47.3050	12.19	631914	mi
2	52.6950	13.17	703914	mi
Totals	100.0000		1335828	



Operator ID : Company Name :
Analysed : 20.01.2021 18:22 Printed : 21.02.2021 14:05
Sample ID : FS_421H_new_gcold_split40
Channel : Channel A
Analysis Type : UnkNown (Area) Calc. Method : Area %

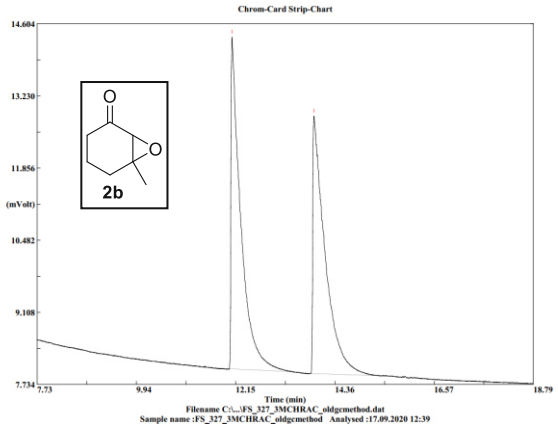
Peak Number #	Area %	Ret.Time	Area	BC
1	97.2837	12.15	1017860	mi
2	2.7163	13.43	28420	mi
Totals	100.0000		1046280	



Analysed : 11.11.2020 12:58 Printed : 02.01.2021 14:0
Sample ID : FS_571_CR_oldgcmethod Channel : Channel A
Analysis Type : UnkNown (Area) Calc. Method : Area %

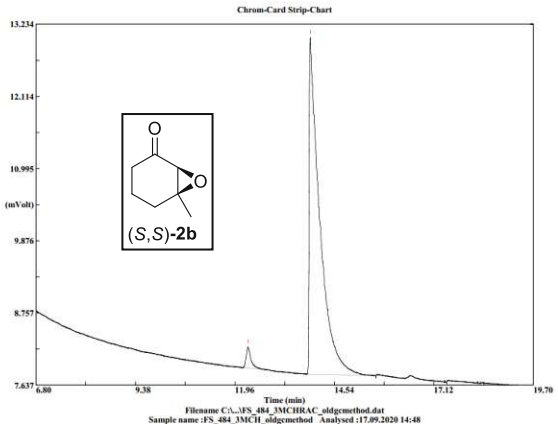
Peak Number #	Area %	Ret.Time	Area	BC
1	2.7457	12.49	14506	mi
2	97.2543	13.29	513798	mi
Totals	100.0000		528304	

Die approbierte gedruckte Originalversion dieser Dissertation ist an der TU Wien Bibliothek verfügbar.
The approved original version of this doctoral thesis is available in print at TU Wien Bibliothek.
TU Bibliothek Your knowledge hub WIEN



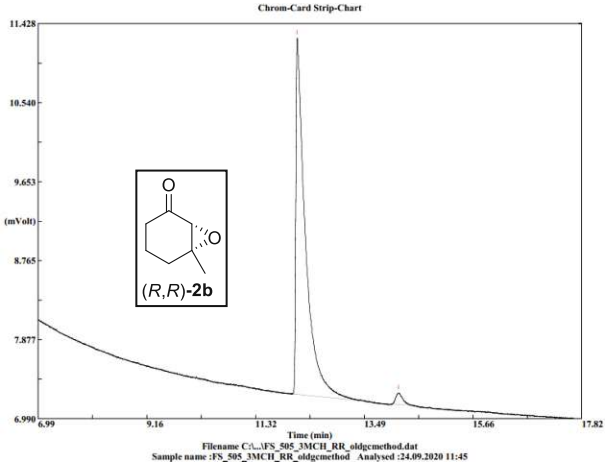
Analysed : 17.09.2020 12:39 Printed : 17.09.2020 13:32
Sample ID : FS_327_3MCHRAC_oldgcmethod
Channel : Channel A
Analysis Type : UnkNown (Area) Calc. Method : Area %

Peak Number #	Area %	Ret.Time	Area	BC
1	50.4849	12.07	944865	mi
2	49.5151	13.90	926713	mi
Totals	100.0000		1871578	



Analysed : 17.09.2020 14:48 Printed : 08.10.2020 16:52
Sample ID : FS_484_3MCH_oldgcmethodChannel : Channel A
Analysis Type : UnkNown (Area) Calc. Method : Area %

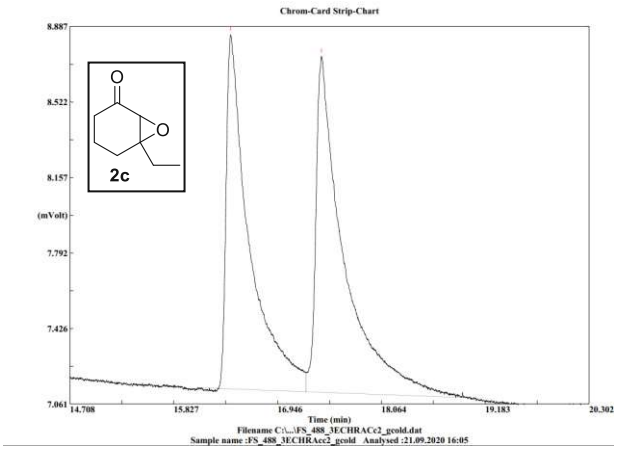
Peak Number #	Area %	Ret.Time	Area	BC
1	2.6285	12.30	26364	mi
2	97.3716	13.92	976642	mi
Totals	100.0000		1003006	



Analysed : 24.09.2020 11:45 Printed : 08.10.2020 16:50
Sample ID : FS_505_3MCH_RR_oldgcmethod
Channel : Channel A
Analysis Type : UnkNown (Area) Calc. Method : Area %

Peak Number #	Area %	Ret.Time	Area	BC
1	97.5301	12.15	527793	mi
2	2.4699	14.17	13366	mi
Totals	100.0000		541159	

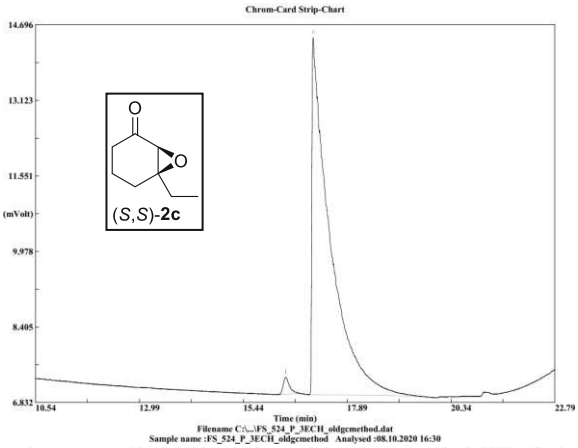
Die approbierte gedruckte Originalversion dieser Dissertation ist an der TU Wien Bibliothek verfügbar.
The approved original version of this doctoral thesis is available in print at TU Wien Bibliothek.
TU Bibliothek Your knowledge hub WIEN



Filename C:\...\FS_488_3ECHRACc2_gcold.dat
Sample name :FS_488_3ECHRAcc2_gcold Analysed :21.09.2020 16:05

Analysed : 21.09.2020 16:05 Printed : 21.09.2020 16:38
Sample ID : FS_488_3ECHRAcc2_gcold Channel : Channel A
Analysis Type : UnkNown (Area) Calc. Method : Area %

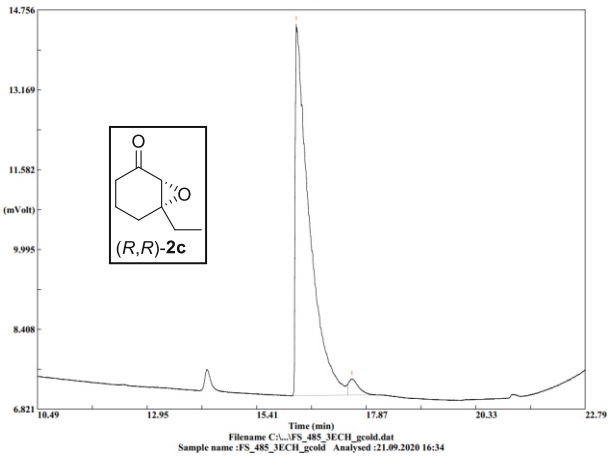
Peak Number #	Area %	Ret.Time	Area	BC
1	47.3646	16.44	297390	mi
2	52.6354	17.42	330484	mi
Totals	100.0000		627874	



Filename C:\...\FS_524_P_3ECH_oldgcmethod.dat
Sample name :FS_524_P_3ECH_oldgcmethod Analysed :08.10.2020 16:30

Analysed : 08.10.2020 16:30 Printed : 08.10.2020 17:40
Sample ID : FS_524_P_3ECH_oldgcmethod
Channel : Channel A
Analysis Type : UnkNown (Area) Calc. Method : Area %

Peak Number #	Area %	Ret.Time	Area	BC
1	1.6644	16.44	36903	mi
2	98.3356	17.09	2180270	mi
Totals	100.0000		2217173	

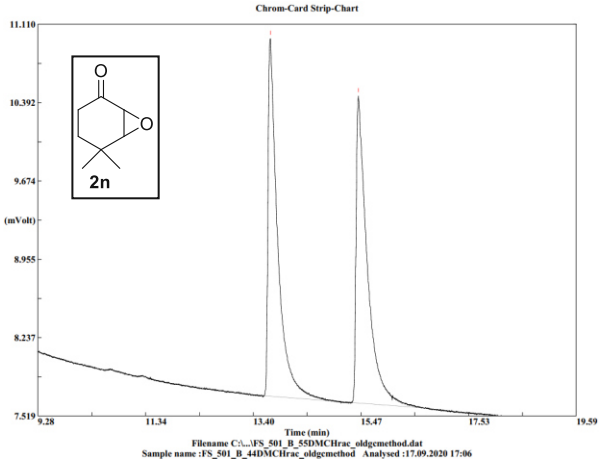


Filename C:\...\FS_485_3ECH_gcold.dat
Sample name :FS_485_3ECH_gcold Analysed :21.09.2020 16:34

Analysed : 21.09.2020 16:34 Printed : 03.01.2021 13:27
Sample ID : FS_485_3ECH_gcold Channel : Channel A
Analysis Type : UnkNown (Area) Calc. Method : Area %

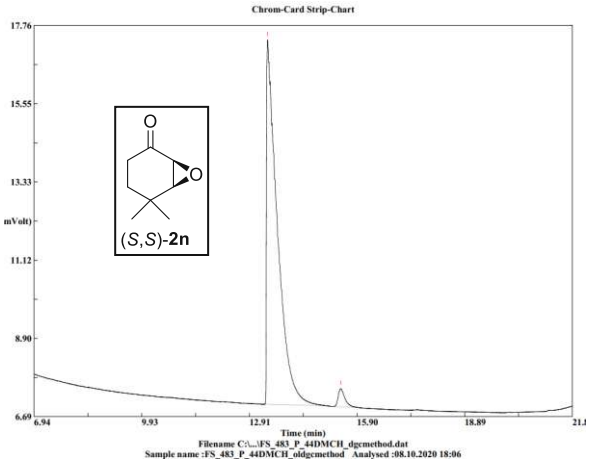
Peak Number #	Area %	Ret.Time	Area	BC
1	97.0875	16.30	1630936	mi
2	2.9125	17.55	48927	mi
Totals	100.0000		1679862	

Die approbierte gedruckte Originalversion dieser Dissertation ist an der TU Wien Bibliothek verfügbar.
The approved original version of this doctoral thesis is available in print at TU Wien Bibliothek.



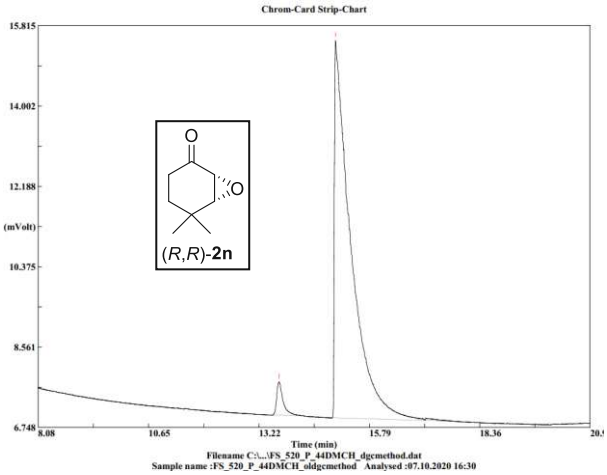
Analysed : 17.09.2020 17:06 Printed : 17.09.2020 20:22
Sample ID : FS_501_B_44DMCHrac_oldgcmethod
Channel : Channel A
Analysis Type : UnkNown (Area) Calc. Method : Area %

Peak Number #	Area %	Ret.Time	Area	BC
1	49.5526	13.73	409531	mi
2	50.4474	15.42	416926	mi
Totals	100.0000		826457	



Analysed : 08.10.2020 18:06 Printed : 08.10.2020 22:37
Sample ID : FS_483_P_44DMCH_oldgcmethod
Channel : Channel A
Analysis Type : UnkNown (Area) Calc. Method : Area %

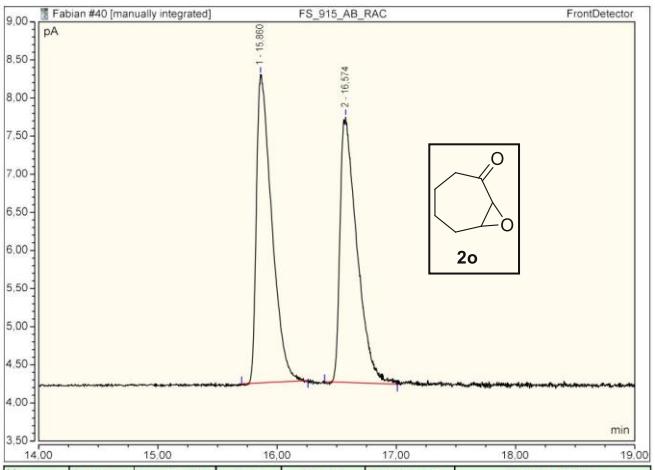
Peak Number #	Area %	Ret.Time	Area	BC
1	97.1759	13.42	2140601	mi
2	2.8241	15.45	62209	mi
Totals	100.0000		2202810	



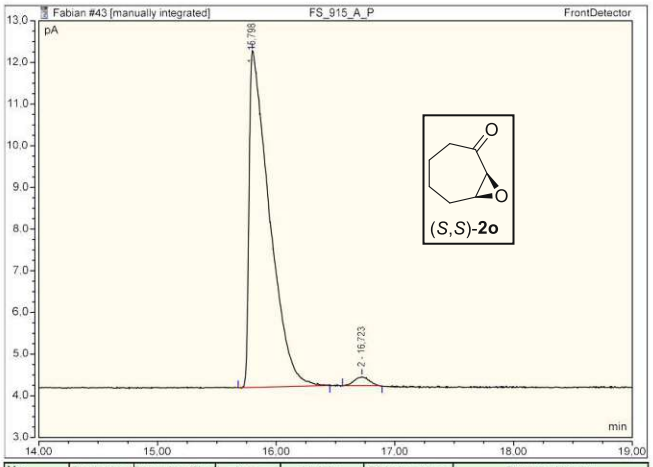
Analysed : 07.10.2020 16:30 Printed : 08.10.2020 16:55
Sample ID : FS_520_P_44DMCH_oldgcmethod
Channel : Channel A
Analysis Type : UnkNown (Area) Calc. Method : Area %

Peak Number #	Area %	Ret.Time	Area	BC
1	3.2889	13.69	75117	mi
2	96.7111	15.00	2208821	mi
Totals	100.0000		2283938	

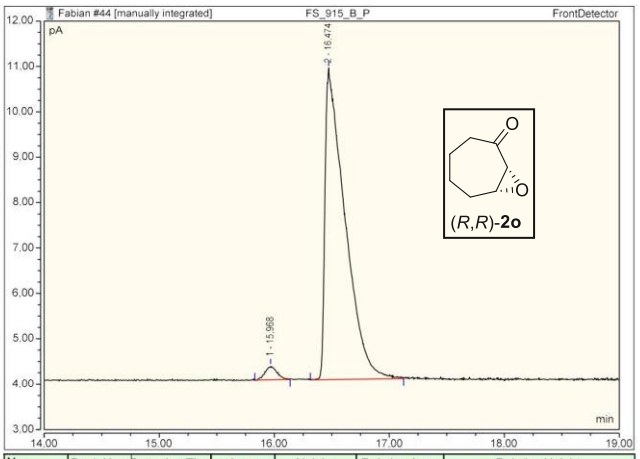
Die approbierte gedruckte Originalversion dieser Dissertation ist an der TU Wien Bibliothek verfügbar.
The approved original version of this doctoral thesis is available in print at TU Wien Bibliothek.



No.	Peak Nam	Retention Time min	Area pA*min	Height pA	Relative Area %	Relative Height %
1		15,860	0,602	4,046	51,29	53,74
2		16,574	0,572	3,483	48,71	46,26
Total:			**1,174**	**7,530**	**100,00**	**100,00**

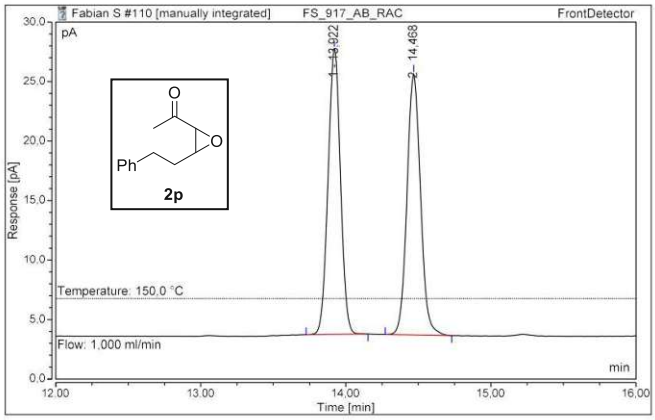


No.	Peak Nam	Retention Time min	Area pA*min	Height pA	Relative Area %	Relative Height %
1		15,798	1,593	8,088	98,16	97,33
2		16,723	0,030	0,222	1,84	2,67
Total:			**1,623**	**8,310**	**100,00**	**100,00**

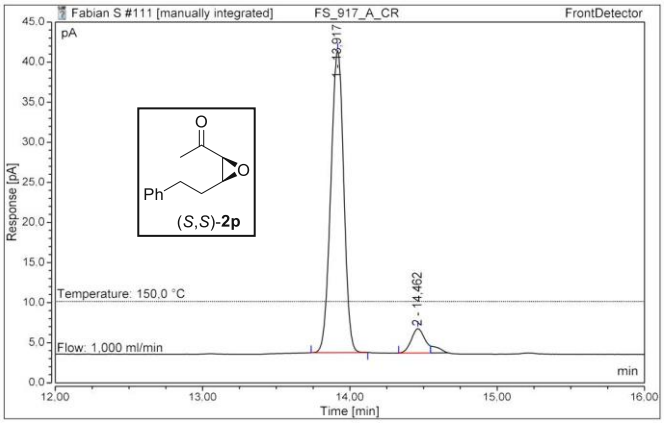


No.	Peak Nam	Retention Time min	Area pA*min	Height pA	Relative Area %	Relative Height %
1		15,968	0,036	0,307	2,54	4,27
2		16,474	1,376	6,866	97,46	95,73
Total:			**1,411**	**7,172**	**100,00**	**100,00**

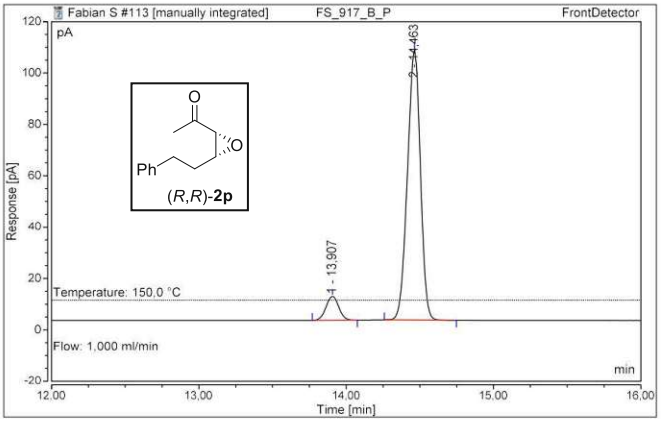
Die approbierte gedruckte Originalversion dieser Dissertation ist an der TU Wien Bibliothek verfügbar.
The approved original version of this doctoral thesis is available in print at TU Wien Bibliothek.



No.	Peak Name	Retention Time min	Area pA*min	Height pA	elative Area %	elative Heig %	Amount n.a.
1		13,922	2,383	24,005	50,19	52,25	n.a.
2		14,468	2,365	21,937	49,81	47,75	n.a.
Total:			**4,749**	**45,942**	**100,00**	**100,00**	

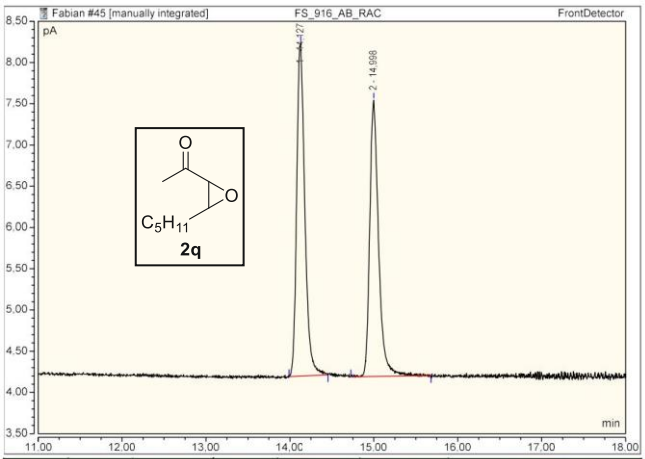


No.	Peak Name	Retention Time min	Area pA*min	Height pA	elative Area %	elative Heig %	Amount n.a.
1		13,917	3,847	37,673	92,30	92,49	n.a.
2		14,462	0,321	3,058	7,70	7,51	n.a.
Total:			**4,168**	**40,732**	**100,00**	**100,00**	

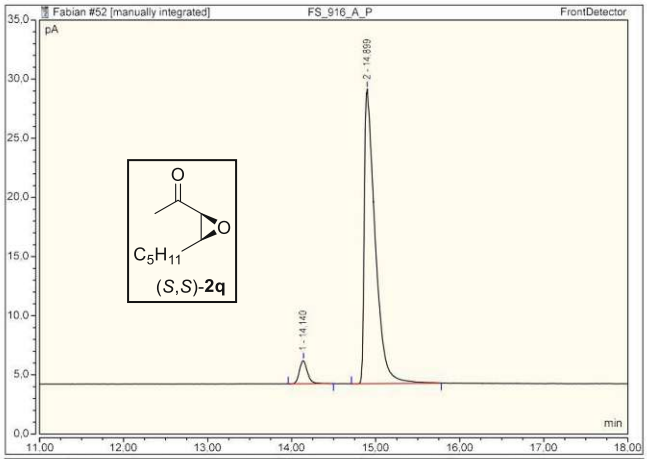


No.	Peak Name	Retention Time min	Area pA*min	Height pA	elative Area %	elative Heig %	Amount n.a.
1		13,907	0,922	9,262	7,94	8,11	n.a.
2		14,463	10,683	104,973	92,06	91,89	n.a.
Total:			**11,605**	**114,235**	**100,00**	**100,00**	

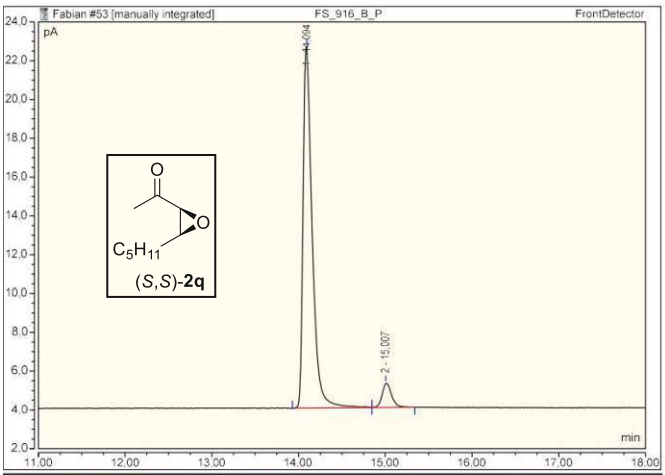
Die approbierte gedruckte Originalversion dieser Dissertation ist an der TU Wien Bibliothek verfügbar.
The approved original version of this doctoral thesis is available in print at TU Wien Bibliothek.



No.	Peak Nam	Retention Time min	Area pA*min	Height pA	Relative Area %	Relative Height %
1		14,127	0,453	4,037	52,54	54,66
2		14,998	0,409	3,349	47,46	45,34
Total:			**0,862**	**7,387**	**100,00**	**100,00**



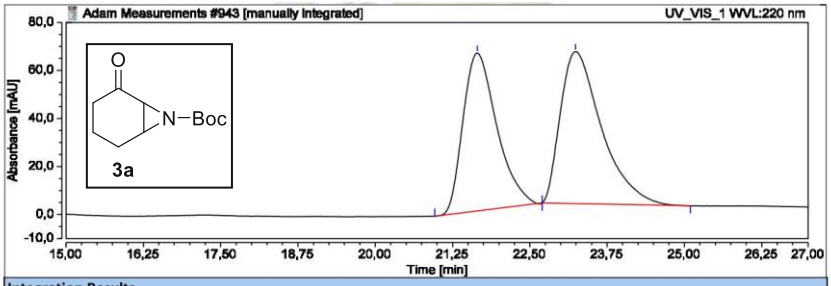
No.	Peak Nam	Retention Time min	Area pA*min	Height pA	Relative Area %	Relative Height %
1		14,140	0,215	1,998	5,48	7,42
2		14,899	3,708	24,919	94,52	92,58
Total:			**3,923**	**26,917**	**100,00**	**100,00**



No.	Peak Nam	Retention Time min	Area pA*min	Height pA	Relative Area %	Relative Height %
1		14,094	2,276	18,662	93,47	93,69
2		15,007	0,159	1,258	6,53	6,31
Total:			**2,435**	**19,920**	**100,00**	**100,00**

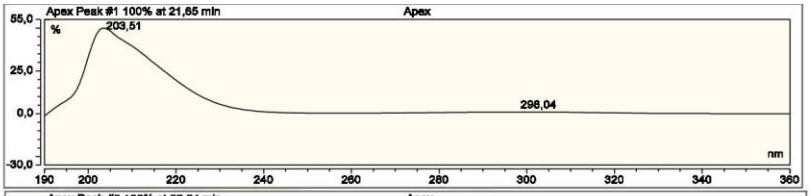
Die approbierte gedruckte Originalversion dieser Dissertation ist an der TU Wien Bibliothek verfügbar.
The approved original version of this doctoral thesis is available in print at TU Wien Bibliothek.

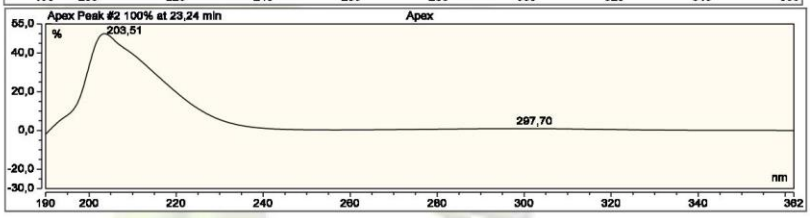
12. Chiral HPLC chromatograms for the asymmetric aziridinations

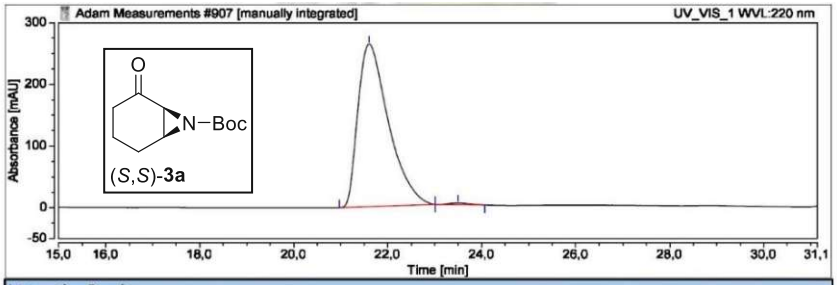


Integration Results

No.	Peak Name	Retention Time min	Area mAU*min	Height mAU	Relative Area %	Relative Height %	Amount n.a.
1		21,652	41,589	65,703	46,00	50,93	n.a.
2		23,238	48,818	63,311	54,00	49,07	n.a.
Total:			90,407	129,013	100,00	100,00	

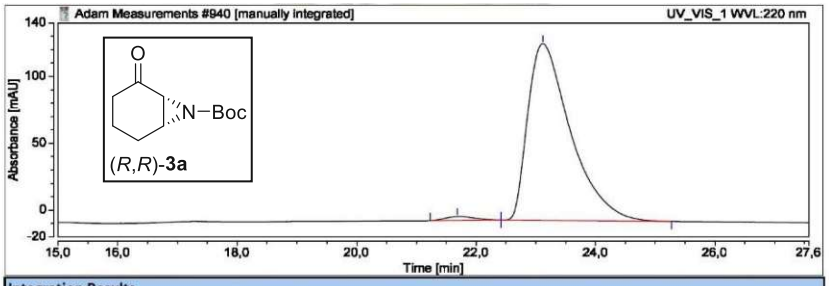






Integration Results

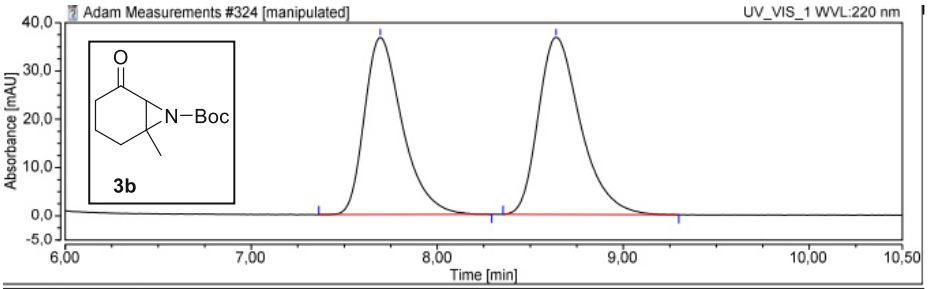
No.	Peak Name	Retention Time min	Area mAU*min	Height mAU	Relative Area %	Relative Height %	Amount n.a.
1		21,602	198,100	263,717	99,35	99,02	n.a.
2		23,495	1,306	2,612	0,65	0,98	n.a.
Total:			199,406	266,329	100,00	100,00	



Integration Results

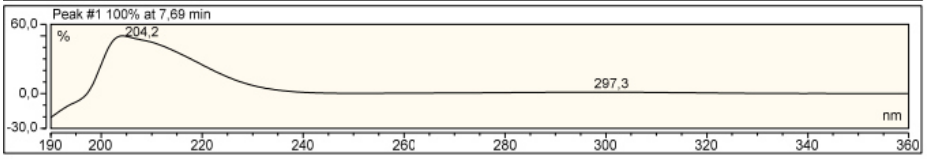
No.	Peak Name	Retention Time min	Area mAU*min	Height mAU	Relative Area %	Relative Height %	Amount n.a.
1		21,688	1,661	2,985	1,49	2,21	n.a.
2		23,115	109,869	132,193	98,51	97,79	n.a.
Total:			111,531	135,179	100,00	100,00	

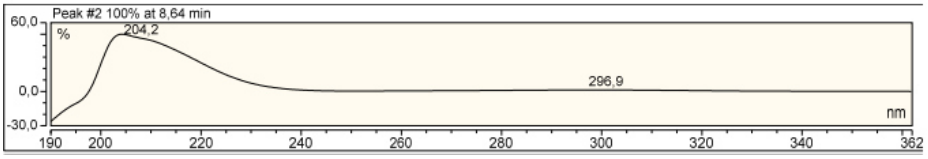
Die approbierte gedruckte Originalversion dieser Dissertation ist an der TU Wien Bibliothek verfügbar.
The approved original version of this doctoral thesis is available in print at TU Wien Bibliothek.

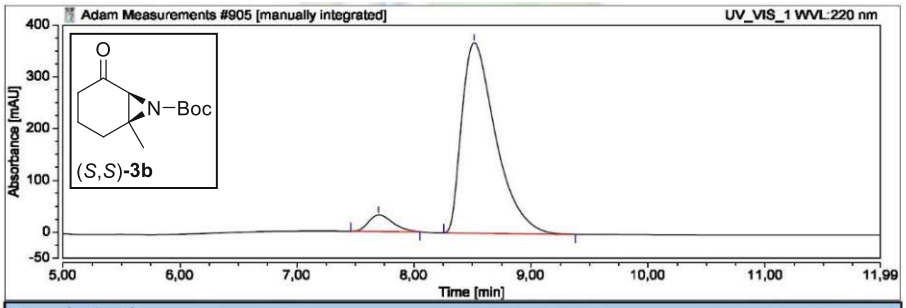


Integration Results

No.	Peak Name	Retention Time min	Area mAU*min	Height mAU	Relative Area %	Relative Height %	Amount n.a.
1		7,693	8,662	36,652	47,23	49,99	n.a.
2		8,638	9,678	36,661	52,77	50,01	n.a.
Total:			**18,340**	**73,313**	**100,00**	**100,00**	

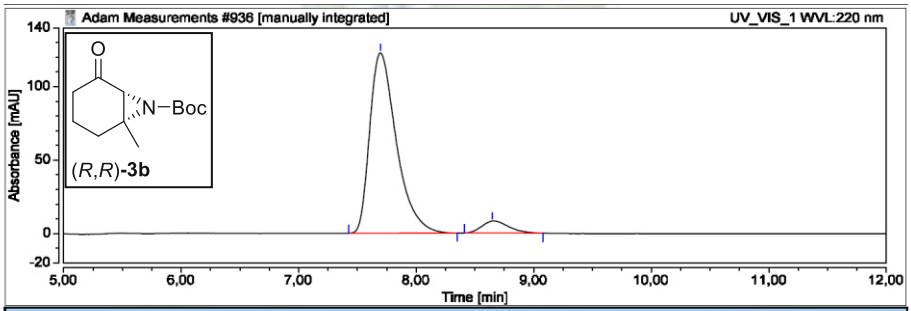






Integration Results

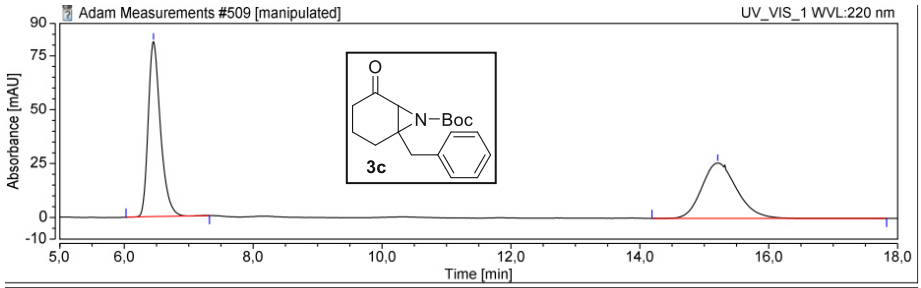
No.	Peak Name	Retention Time min	Area mAU*min	Height mAU	Relative Area %	Relative Height %	Amount n.a.
1		7,700	7,735	32,028	5,89	8,01	n.a.
2		8,515	123,616	367,736	94,11	91,99	n.a.
Total:			**131,351**	**399,764**	**100,00**	**100,00**	



Integration Results

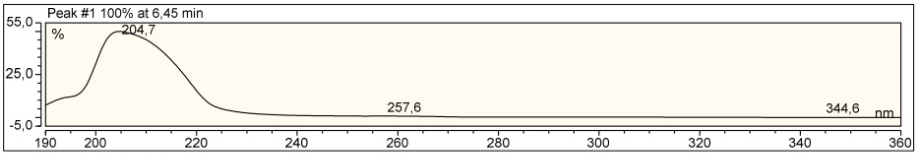
No.	Peak Name	Retention Time min	Area mAU*min	Height mAU	Relative Area %	Relative Height %	Amount n.a.
1		7,695	32,247	122,738	93,76	93,77	n.a.
2		8,650	2,145	8,157	6,24	6,23	n.a.
Total:			**34,392**	**130,894**	**100,00**	**100,00**	

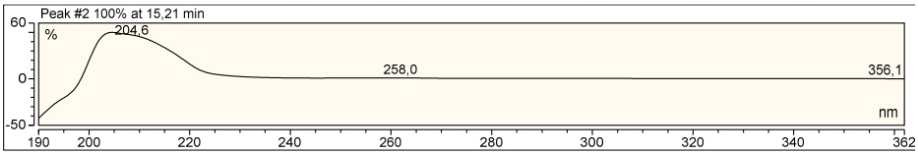
Die approbierte gedruckte Originalversion dieser Dissertation ist an der TU Wien Bibliothek verfügbar.
The approved original version of this doctoral thesis is available in print at TU Wien Bibliothek.

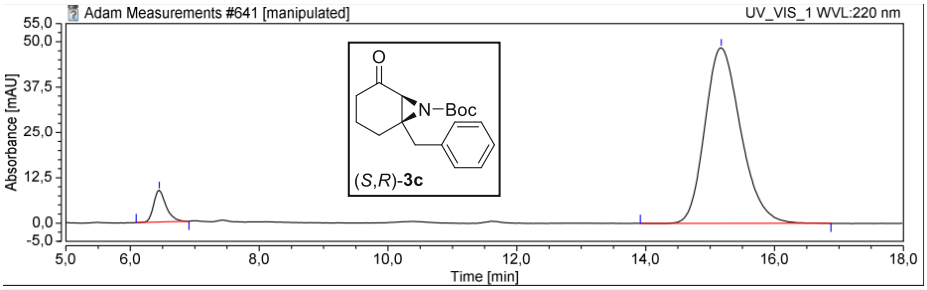


Integration Results

No.	Peak Name	Retention Time min	Area mAU*min	Height mAU	Relative Area %	Relative Height %	Amount n.a.
1		6,452	17,893	81,063	52,73	75,96	n.a.
2		15,207	16,041	25,661	47,27	24,04	n.a.
Total:			**33,934**	**106,724**	**100,00**	**100,00**	

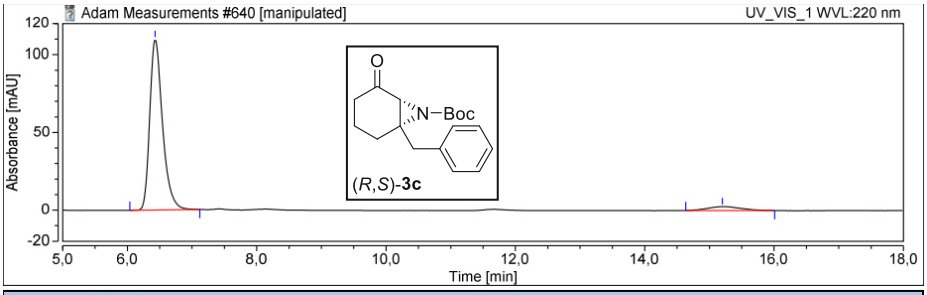






Integration Results

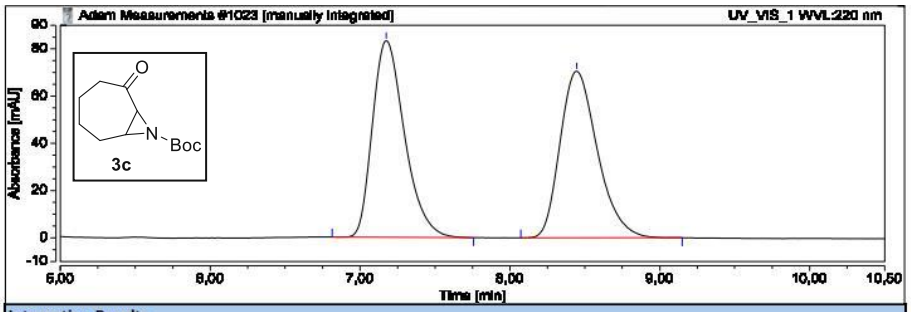
No.	Peak Name	Retention Time min	Area mAU*min	Height mAU	Relative Area %	Relative Height %	Amount n.a.
1		6,448	1,949	8,700	5,89	15,24	n.a.
2		15,172	31,151	48,379	94,11	84,76	n.a.
Total:			**33,099**	**57,079**	**100,00**	**100,00**	



Integration Results

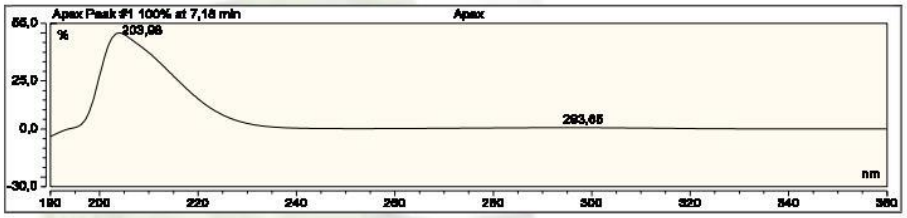
No.	Peak Name	Retention Time min	Area mAU*min	Height mAU	Relative Area %	Relative Height %	Amount n.a.
1		6,430	25,076	109,691	94,45	97,79	n.a.
2		15,200	1,474	2,476	5,55	2,21	n.a.
Total:			**26,550**	**112,167**	**100,00**	**100,00**	

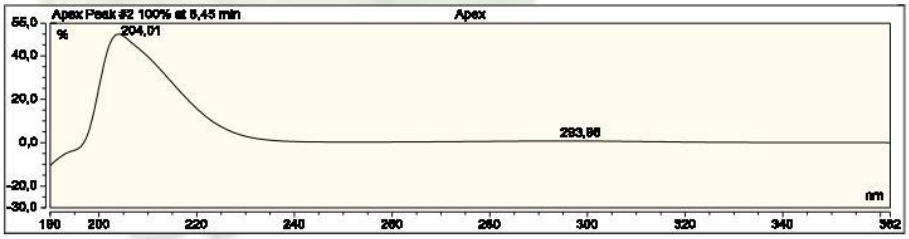
Die approbierte gedruckte Originalversion dieser Dissertation ist an der TU Wien Bibliothek verfügbar.
The approved original version of this doctoral thesis is available in print at TU Wien Bibliothek.
TU Bibliothek Your knowledge hub WIEN

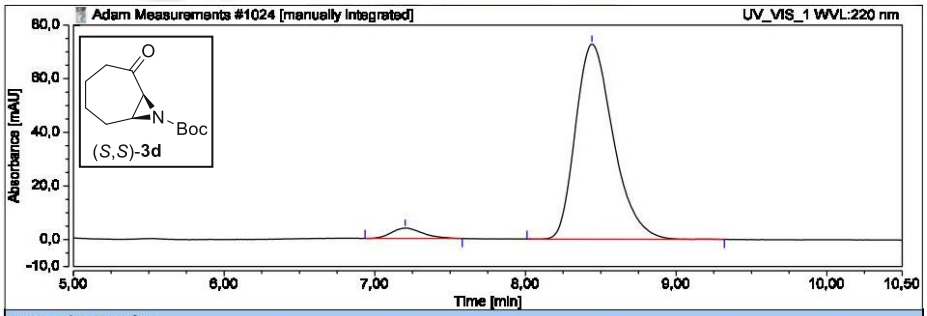


Integration Results

No.	Peak Name	Retention Time min	Area mAU*min	Height mAU	Relative Area %	Relative Height %	Amount n.a.
1		7,175	20,561	83,238	50,24	54,11	n.a.
2		8,445	20,362	70,580	49,76	45,89	n.a.
Total:			40,923	153,818	100,00	100,00	

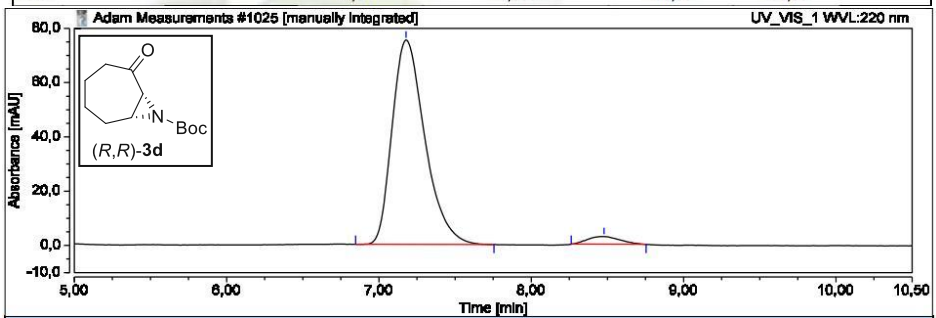






Integration Results

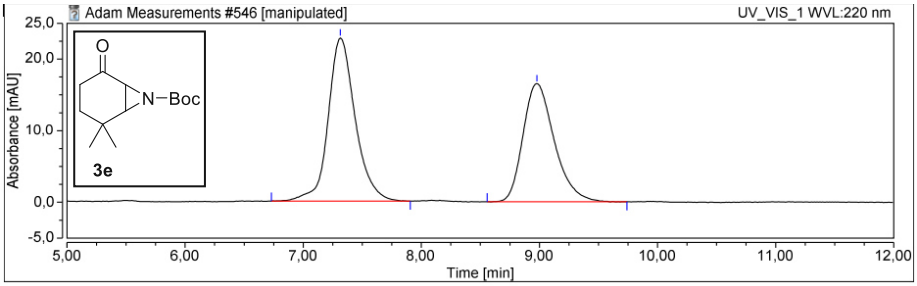
No.	Peak Name	Retention Time min	Area mAU*min	Height mAU	Relative Area %	Relative Height %	Amount n.a.
1		7,202	0,934	3,886	4,23	5,07	n.a.
2		8,442	21,137	72,797	95,77	94,93	n.a.
Total:			22,071	76,683	100,00	100,00	



Integration Results

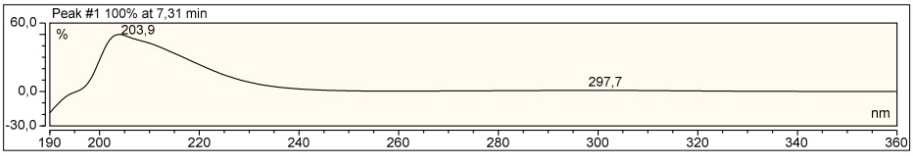
No.	Peak Name	Retention Time min	Area mAU*min	Height mAU	Relative Area %	Relative Height %	Amount n.a.
1		7,178	18,762	75,330	96,36	96,32	n.a.
2		8,478	0,708	2,881	3,64	3,68	n.a.
Total:			19,470	78,211	100,00	100,00	

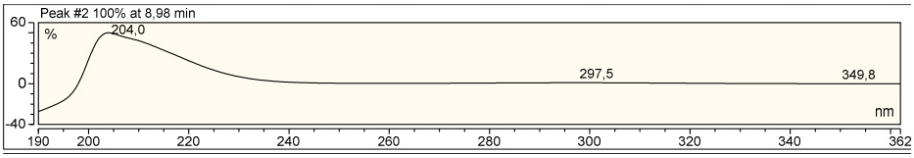
Die approbierte gedruckte Originalversion dieser Dissertation ist an der TU Wien Bibliothek verfügbar.
The approved original version of this doctoral thesis is available in print at TU Wien Bibliothek.
TU Bibliothek Your knowledge hub

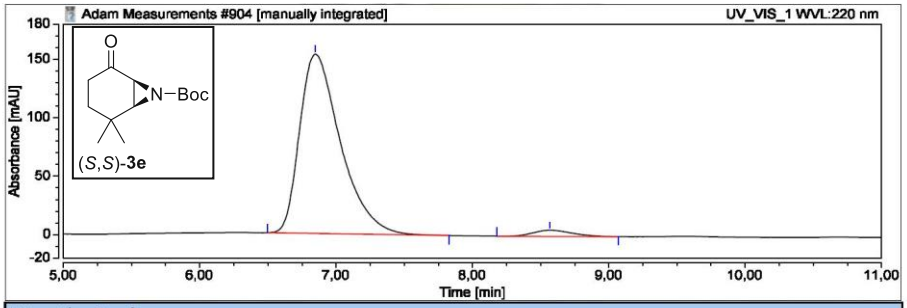


Integration Results

No.	Peak Name	Retention Time min	Area mAU*min	Height mAU	Relative Area %	Relative Height %	Amount n.a.
1		7,313	6,044	22,816	54,42	58,01	n.a.
2		8,978	5,062	16,513	45,58	41,99	n.a.
Total:			**11,107**	**39,329**	**100,00**	**100,00**	

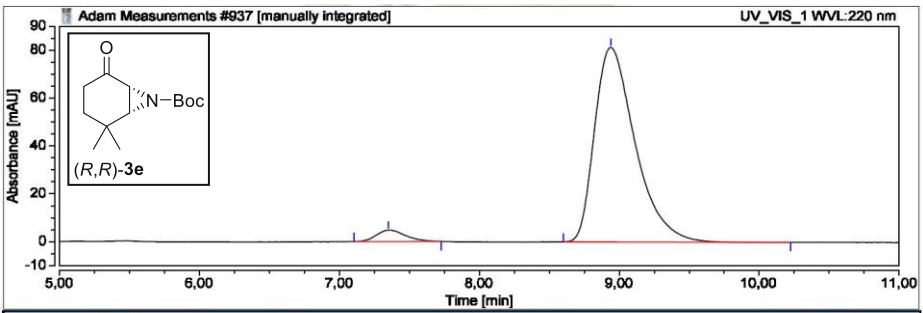






Integration Results

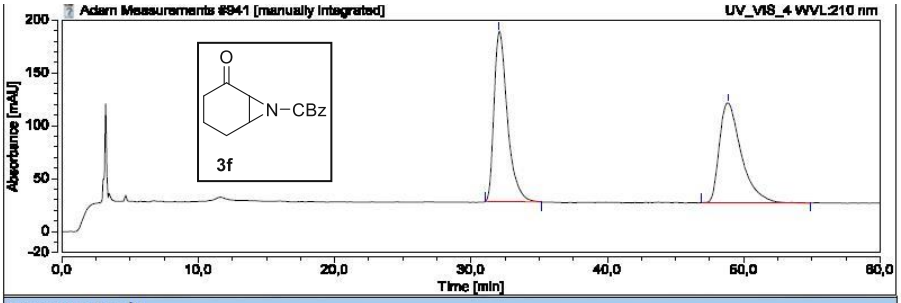
No.	Peak Name	Retention Time min	Area mAU*min	Height mAU	Relative Area %	Relative Height %	Amount n.a.
1		6,848	53,232	153,311	96,81	96,65	n.a.
2		8,567	1,754	5,307	3,19	3,35	n.a.
Total:			**54,987**	**158,618**	**100,00**	**100,00**	



Integration Results

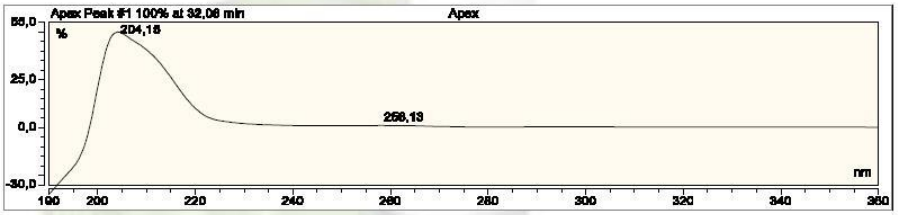
No.	Peak Name	Retention Time min	Area mAU*min	Height mAU	Relative Area %	Relative Height %	Amount n.a.
1		7,352	1,157	4,802	4,07	5,58	n.a.
2		8,938	27,260	81,282	95,93	94,42	n.a.
Total:			**28,417**	**86,083**	**100,00**	**100,00**	

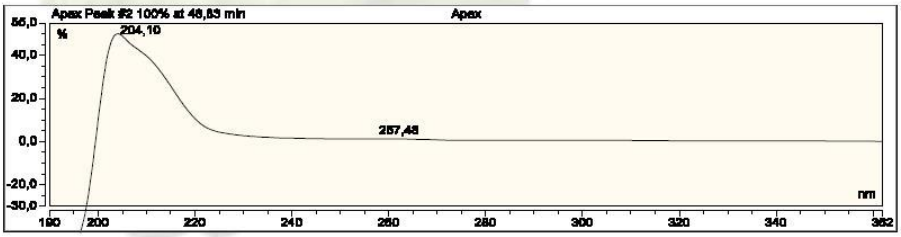
Die approbierte gedruckte Originalversion dieser Dissertation ist an der TU Wien Bibliothek verfügbar.
The approved original version of this doctoral thesis is available in print at TU Wien Bibliothek.

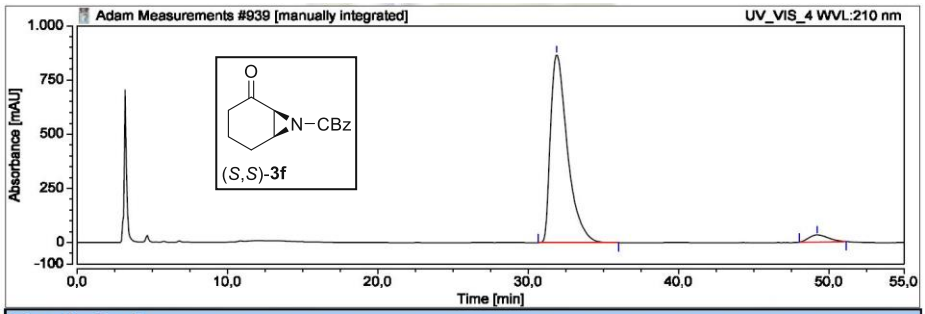


Integration Results

No.	Peak Name	Retention Time min	Area mAU*min	Height mAU	Relative Area %	Relative Height %	Amount n.a.
1		32,075	182,240	161,429	51,08	63,08	n.a.
2		48,833	174,535	94,465	48,92	36,92	n.a.
Total:			356,775	255,894	100,00	100,00	

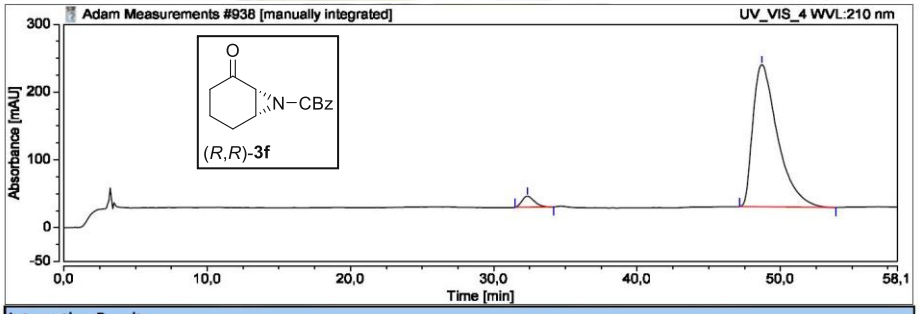






Integration Results

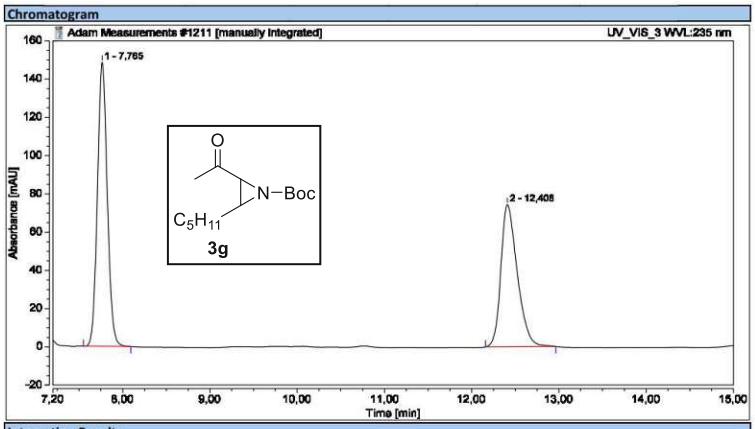
No.	Peak Name	Retention Time min	Area mAU*min	Height mAU	Relative Area %	Relative Height %	Amount n.a.
1		31,887	1131,020	868,181	95,85	96,39	n.a.
2		49,230	48,947	32,518	4,15	3,61	n.a.
Total:			1179,967	900,699	100,00	100,00	



Integration Results

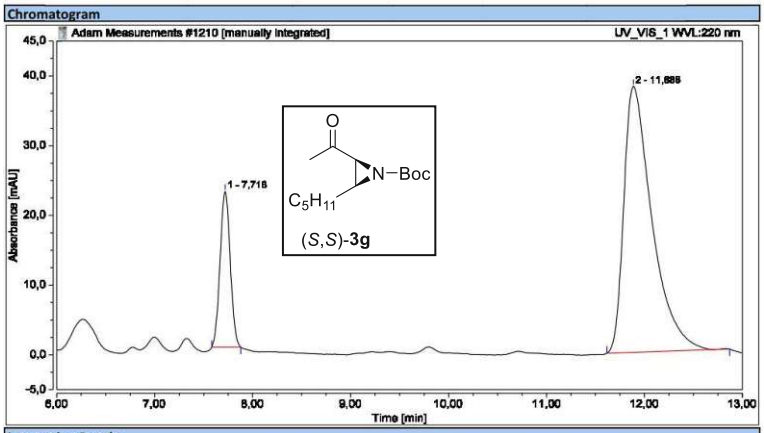
No.	Peak Name	Retention Time min	Area mAU*min	Height mAU	Relative Area %	Relative Height %	Amount n.a.
1		32,345	16,201	16,417	3,72	7,25	n.a.
2		48,693	418,917	209,865	96,28	92,75	n.a.
Total:			435,117	226,282	100,00	100,00	

Die approbierte gedruckte Originalversion dieser Dissertation ist an der TU Wien Bibliothek verfügbar.
The approved original version of this doctoral thesis is available in print at TU Wien Bibliothek.
TU Bibliothek Your knowledge hub WIEN



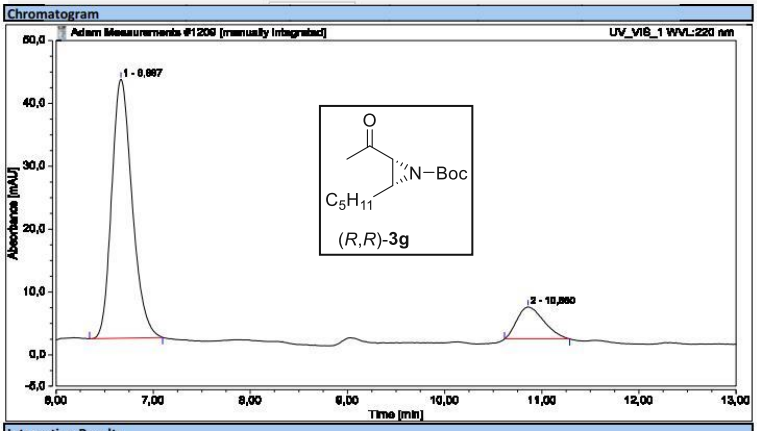
Integration Results

No.	Peak Name	Retention Time min	Area mAU*min	Height mAU	Relative Area %	Relative Height %	Amount
1		7,765	19,483	148,459	54,66	66,63	n.a.
2		12,408	16,164	74,360	45,34	33,37	n.a.
Total:			35,647	222,819	100,00	100,00	



Integration Results

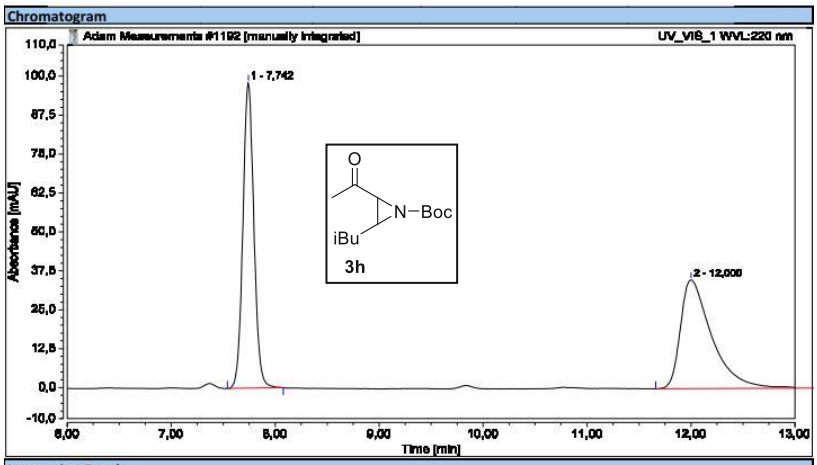
No.	Peak Name	Retention Time min	Area mAU*min	Height mAU	Relative Area %	Relative Height %	Amount
1		7,718	2,678	22,368	17,41	36,97	n.a.
n.a.	1	n.a.	n.a.	n.a.	n.a.	n.a.	n.a.
2		11,888	12,702	38,142	82,59	63,03	n.a.
Total:			15,379	60,509	100,00	100,00	



Integration Results

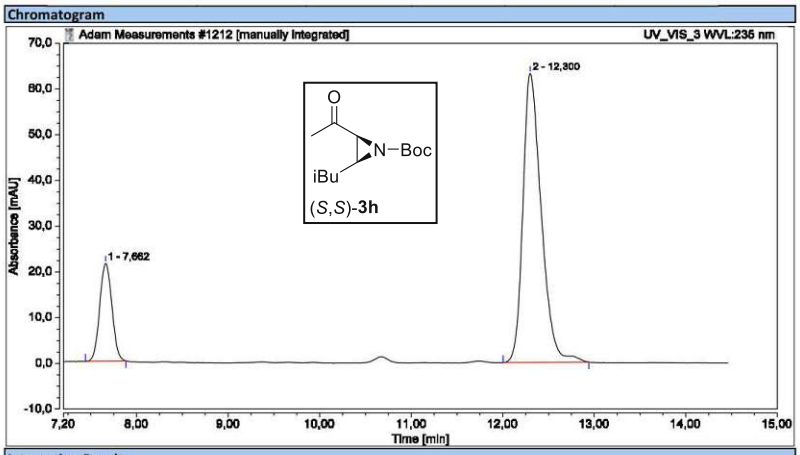
No.	Peak Name	Retention Time min	Area mAU*min	Height mAU	Relative Area %	Relative Height %	Amount
1		6,667	10,050	41,182	86,10	89,04	n.a.
n.a.	1	n.a.	n.a.	n.a.	n.a.	n.a.	n.a.
2		10,860	1,622	5,067	13,90	10,96	n.a.
Total:			11,672	46,250	100,00	100,00	

Die approbierte gedruckte Originalversion dieser Dissertation ist an der TU Wien Bibliothek verfügbar.
The approved original version of this doctoral thesis is available in print at TU Wien Bibliothek.



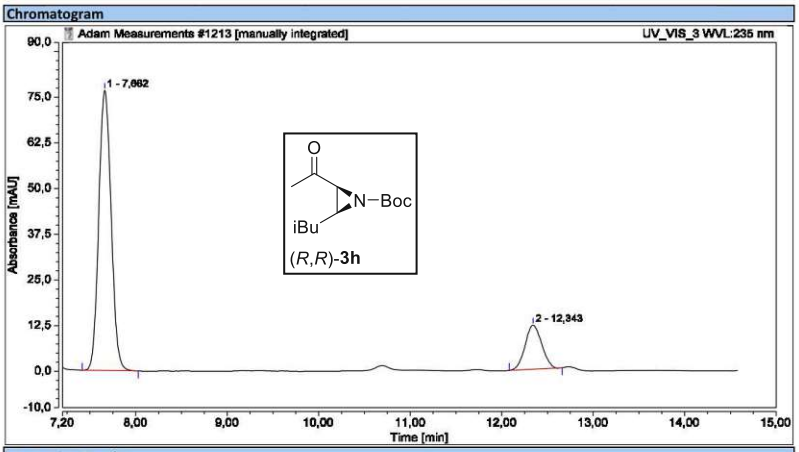
Integration Results

No.	Peak Name	Retention Time min	Area mAU*min	Height mAU	Relative Area %	Relative Height %	Amount
1		7,742	12,006	98,132	49,66	73,76	n.a.
n.a.	1	n.a.	n.a.	n.a.	n.a.	n.a.	n.a.
2		12,000	12,168	34,906	50,34	26,24	n.a.
Total:			**24,174**	**133,038**	**100,00**	**100,00**	



Integration Results

No.	Peak Name	Retention Time min	Area mAU*min	Height mAU	Relative Area %	Relative Height %	Amount
1		7,662	3,293	21,402	18,29	25,29	n.a.
2		12,300	14,712	63,214	81,71	74,71	n.a.
Total:			**18,005**	**84,616**	**100,00**	**100,00**	

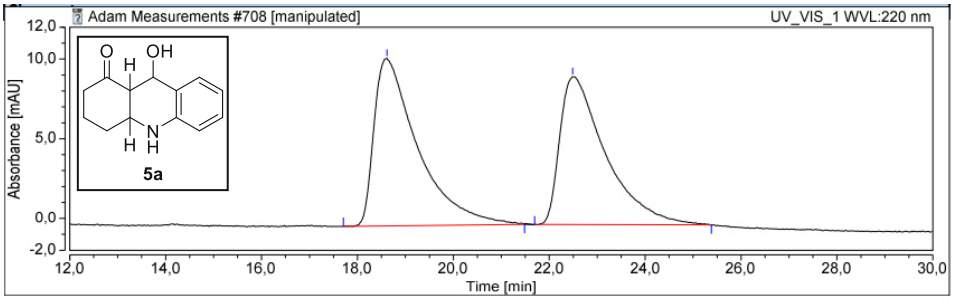


Integration Results

No.	Peak Name	Retention Time min	Area mAU*min	Height mAU	Relative Area %	Relative Height %	Amount
1		7,662	12,010	76,685	82,62	86,41	n.a.
2		12,343	2,526	12,057	17,38	13,59	n.a.
Total:			**14,536**	**88,742**	**100,00**	**100,00**	

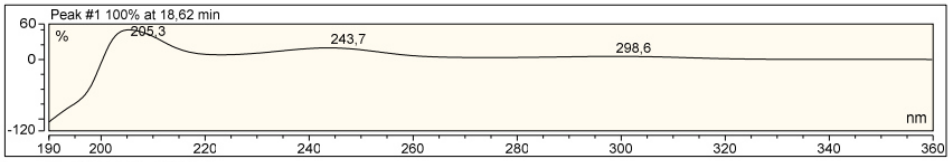
Die approbierte gedruckte Originalversion dieser Dissertation ist an der TU Wien Bibliothek verfügbar.
The approved original version of this doctoral thesis is available in print at TU Wien Bibliothek.
TU Bibliothek Your knowledge hub WIEN

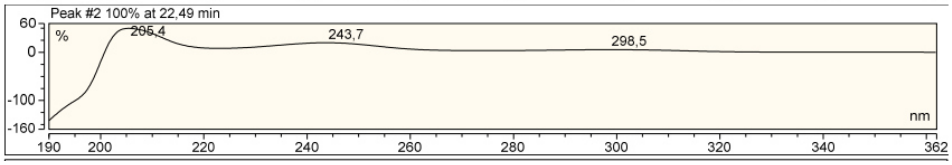
13. Chiral HPLC chromatograms for the asymmetric Aza-Michael/aldol reactions

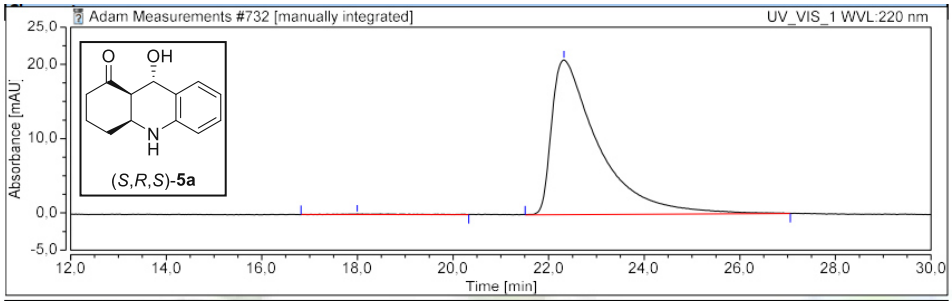


Integration Results

No.	Peak Name	Retention Time min	Area mAU*min	Height mAU	Relative Area %	Relative Height %	Amount n.a.
1		18,615	11,080	10,513	51,95	53,10	n.a.
2		22,487	10,249	9,285	48,05	46,90	n.a.
Total:			**21,329**	**19,798**	**100,00**	**100,00**	

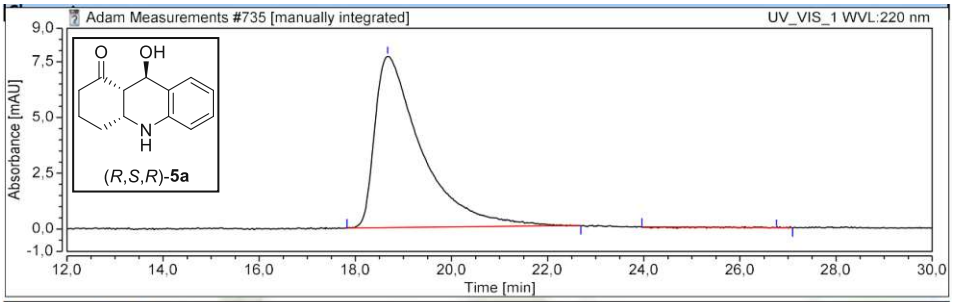






Integration Results

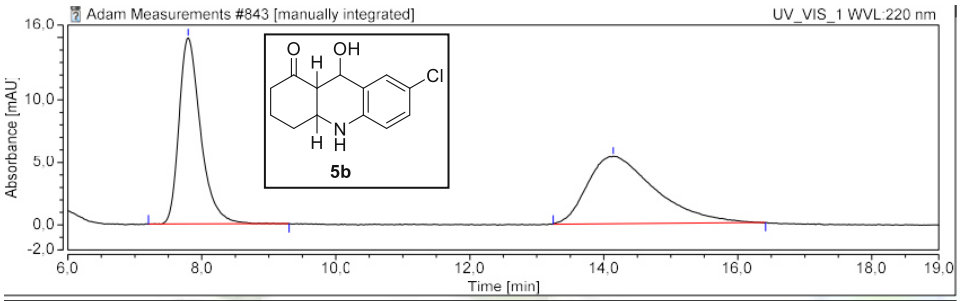
No.	Peak Name	Retention Time min	Area mAU*min	Height mAU	Relative Area %	Relative Height %	Amount n.a.
1		17,995	0,077	0,085	0,33	0,40	n.a.
2		22,322	23,598	20,827	99,67	99,60	n.a.
Total:			**23,676**	**20,912**	**100,00**	**100,00**	



Integration Results

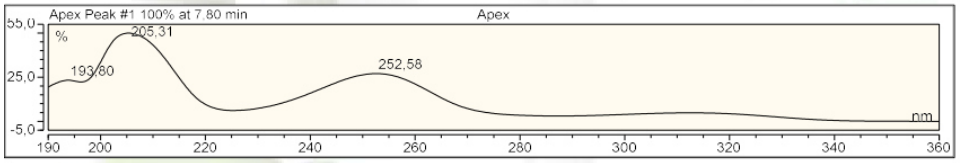
No.	Peak Name	Retention Time min	Area mAU*min	Height mAU	Relative Area %	Relative Height %	Amount n.a.
1		18,672	8,605	7,694	99,87	99,56	n.a.
2		26,758	0,011	0,034	0,13	0,44	n.a.
Total:			**8,616**	**7,728**	**100,00**	**100,00**	

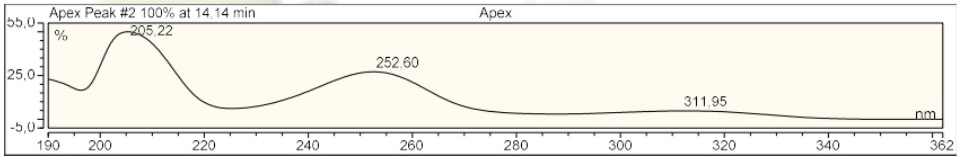
Die approbierte gedruckte Originalversion dieser Dissertation ist an der TU Wien Bibliothek verfügbar.
The approved original version of this doctoral thesis is available in print at TU Wien Bibliothek.
TU Bibliothek Your knowledge hub WIEN

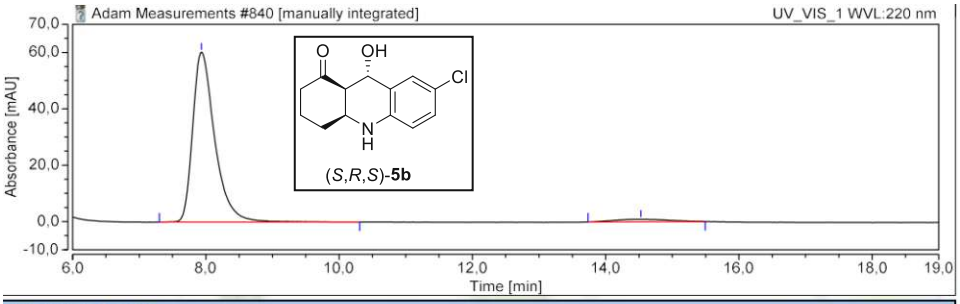


Integration Results

No.	Peak Name	Retention Time min	Area mAU*min	Height mAU	Relative Area %	Relative Height %	Amount n.a.
1		7,795	5,544	14,898	46,85	73,40	n.a.
2		14,140	6,290	5,399	53,15	26,60	n.a.
Total:			**11,834**	**20,298**	**100,00**	**100,00**	

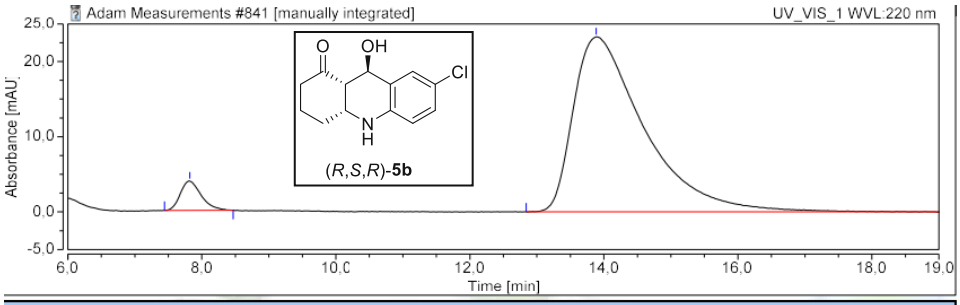






Integration Results

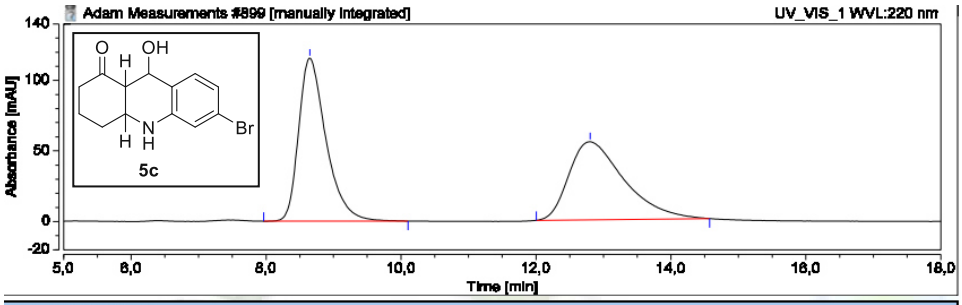
No.	Peak Name	Retention Time min	Area mAU*min	Height mAU	Relative Area %	Relative Height %	Amount n.a.
1		7,933	23,159	60,331	96,45	98,51	n.a.
2		14,530	0,854	0,913	3,55	1,49	n.a.
Total:			**24,012**	**61,244**	**100,00**	**100,00**	



Integration Results

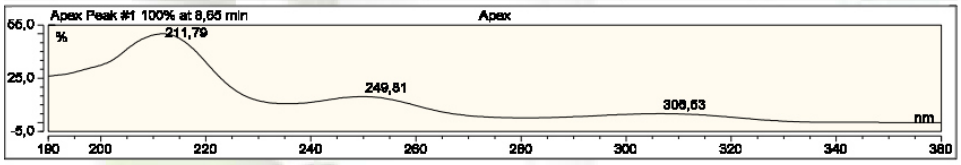
No.	Peak Name	Retention Time min	Area mAU*min	Height mAU	Relative Area %	Relative Height %	Amount n.a.
1		7,818	1,398	3,912	4,68	14,38	n.a.
2		13,885	28,503	23,293	95,32	85,62	n.a.
Total:			**29,902**	**27,204**	**100,00**	**100,00**	

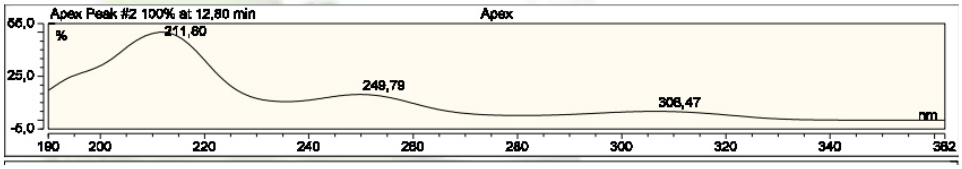
Die approbierte gedruckte Originalversion dieser Dissertation ist an der TU Wien Bibliothek verfügbar.
The approved original version of this doctoral thesis is available in print at TU Wien Bibliothek.

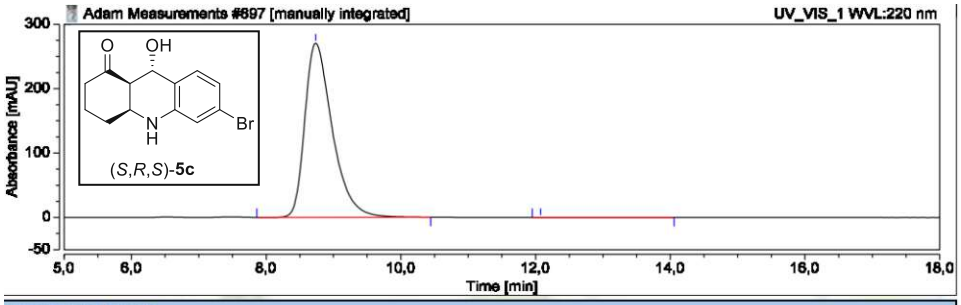


Integration Results

No.	Peak Name	Retention Time min	Area mAU*min	Height mAU	Relative Area %	Relative Height %	Amount n.a.
1		8,648	54,332	115,562	50,92	67,64	n.a.
2		12,802	52,375	55,290	49,08	32,36	n.a.
Total:			**106,706**	**170,852**	**100,00**	**100,00**	

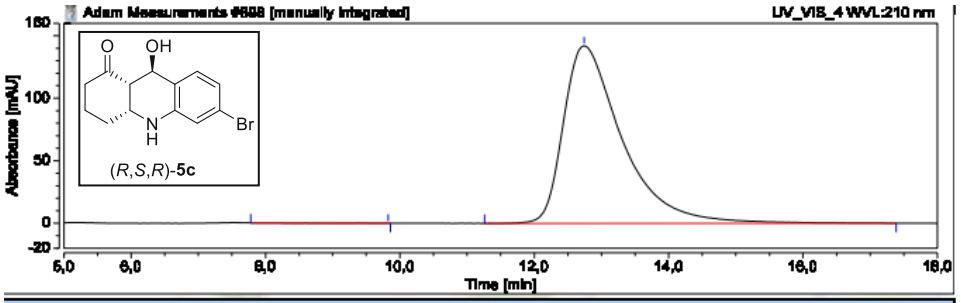






Integration Results

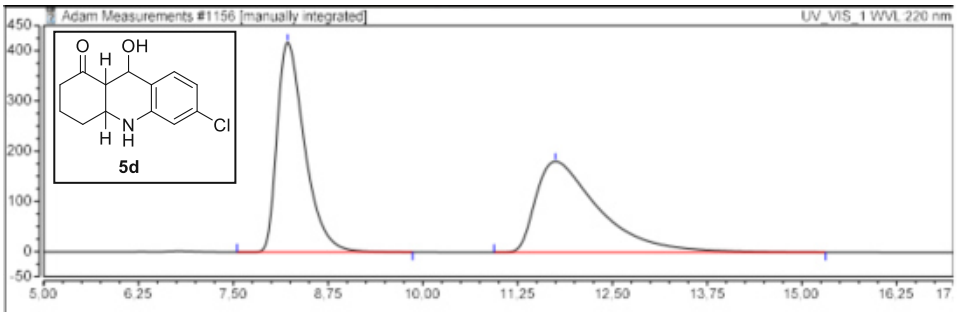
No.	Peak Name	Retention Time min	Area mAU*min	Height mAU	Relative Area %	Relative Height %	Amount n.a.
1		8,737	127,712	270,429	99,99	99,99	n.a.
2		12,077	0,015	0,018	0,01	0,01	n.a.
Total:			**127,727**	**270,447**	**100,00**	**100,00**	



Integration Results

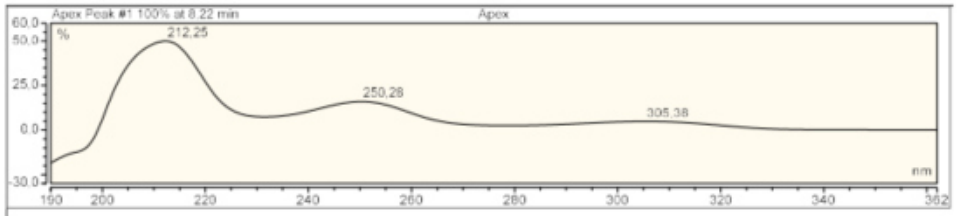
No.	Peak Name	Retention Time min	Area mAU*min	Height mAU	Relative Area %	Relative Height %	Amount n.a.
1		9,825	0,054	0,027	0,04	0,02	n.a.
2		12,742	143,659	142,132	99,96	99,98	n.a.
Total:			**143,714**	**142,159**	**100,00**	**100,00**	

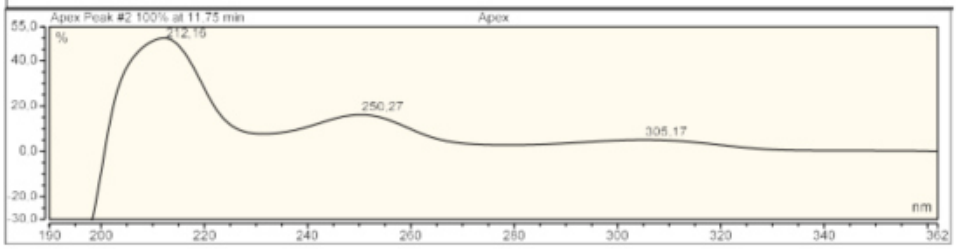
Die approbierte gedruckte Originalversion dieser Dissertation ist an der TU Wien Bibliothek verfügbar.
The approved original version of this doctoral thesis is available in print at TU Wien Bibliothek.
TU Bibliothek Your knowledge hub WIEN

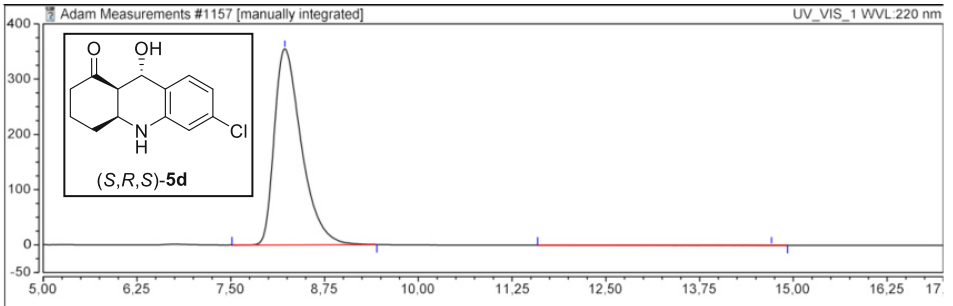


Integration Results

No.	Peak Name	Retention Time min	Area mAU*min	Height mAU	Relative Area %	Relative Height %	Amount n.a.
1		8,217	176,197	417,600	50,19	69,77	n.a.
2		11,748	174,889	180,952	49,81	30,23	n.a.
Total:			**351,087**	**598,552**	**100,00**	**100,00**	



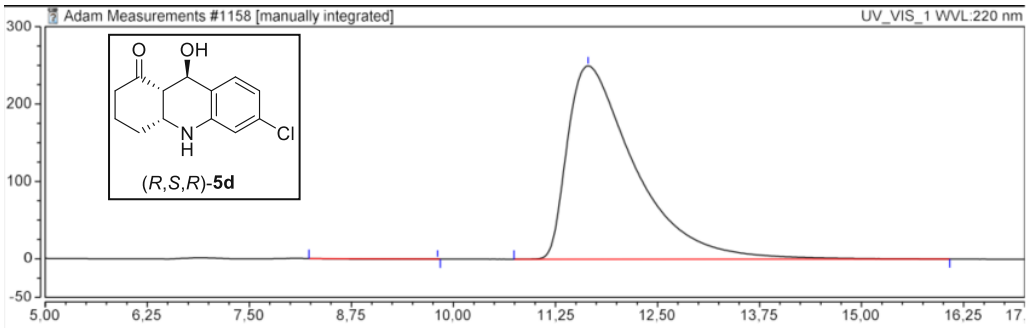




Integration Results

No.	Peak Name	Retention Time min	Area mAU*min	Height mAU	Relative Area %	Relative Height %	Amount n.a.
1		8,220	148,851	354,859	99,95	99,99	n.a.
2		14,708	0,070	0,048	0,05	0,01	n.a.
Total:			**148,922**	**354,907**	**100,00**	**100,00**	

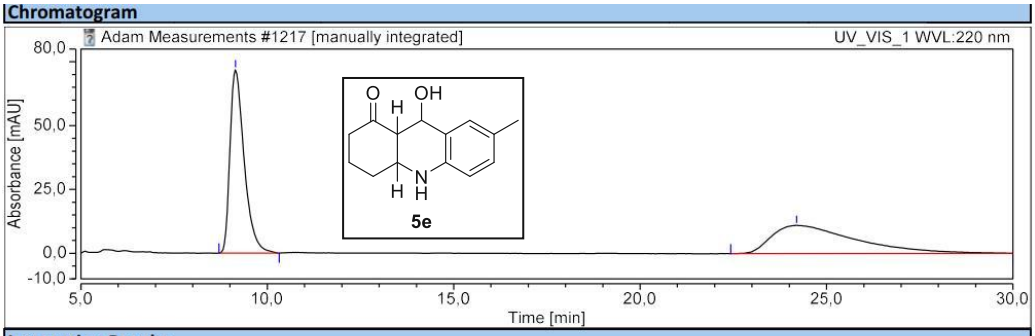
Die approbierte gedruckte Originalversion dieser Dissertation ist an der TU Wien Bibliothek verfügbar.
The approved original version of this doctoral thesis is available in print at TU Wien Bibliothek.



Integration Results

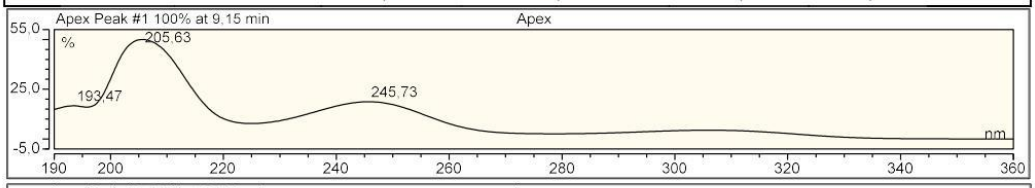
No.	Peak Name	Retention Time min	Area mAU*min	Height mAU	Relative Area %	Relative Height %	Amount n.a.
1		9,807	0,299	0,066	0,12	0,03	n.a.
2		11,648	239,830	249,853	99,88	99,97	n.a.
Total:			**240,130**	**249,918**	**100,00**	**100,00**	

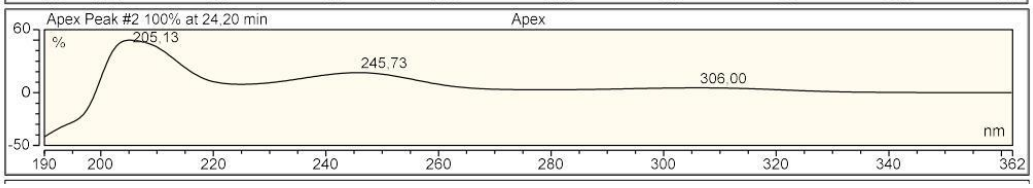
Chromatogram



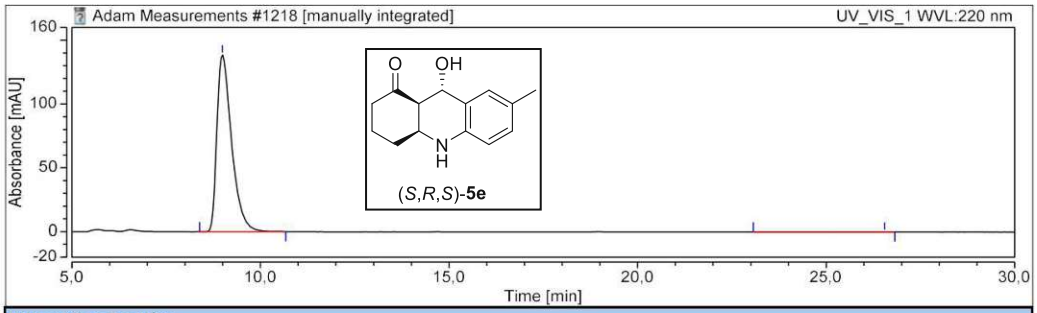
Integration Results

No.	Peak Name	Retention Time min	Area mAU*min	Height mAU	Relative Area %	Relative Height %	Amount n.a.
1		9,145	31,759	71,805	52,60	86,68	n.a.
2		24,197	28,614	11,034	47,40	13,32	n.a.
Total:			**60,373**	**82,839**	**100,00**	**100,00**	



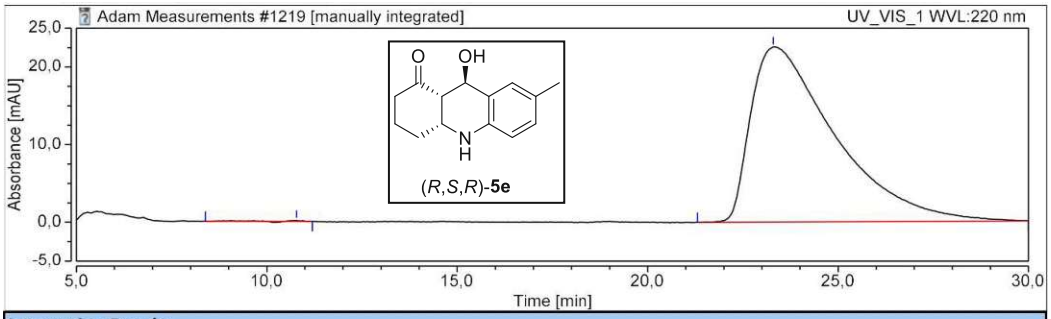


Die approbierte gedruckte Originalversion dieser Dissertation ist an der TU Wien Bibliothek verfügbar.
The approved original version of this doctoral thesis is available in print at TU Wien Bibliothek.



Integration Results

No.	Peak Name	Retention Time min	Area mAU*min	Height mAU	Relative Area %	Relative Height %	Amount n.a.
1		8,990	62,774	138,581	99,93	99,96	n.a.
2		26,548	0,042	0,054	0,07	0,04	n.a.
Total:			**62,815**	**138,635**	**100,00**	**100,00**	

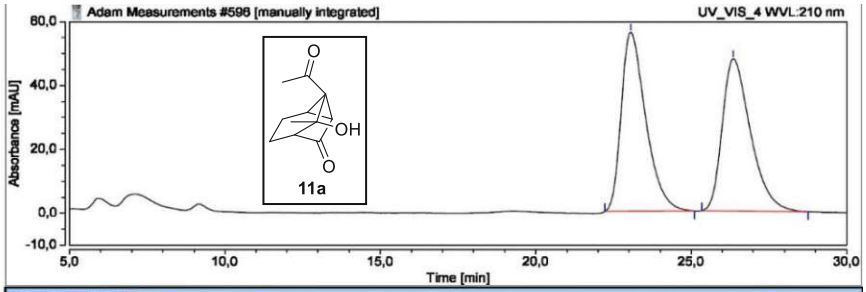


Integration Results

No.	Peak Name	Retention Time min	Area mAU*min	Height mAU	Relative Area %	Relative Height %	Amount n.a.
1		10,780	0,067	0,156	0,12	0,69	n.a.
2		23,300	57,614	22,542	99,88	99,31	n.a.
Total:			**57,681**	**22,698**	**100,00**	**100,00**	

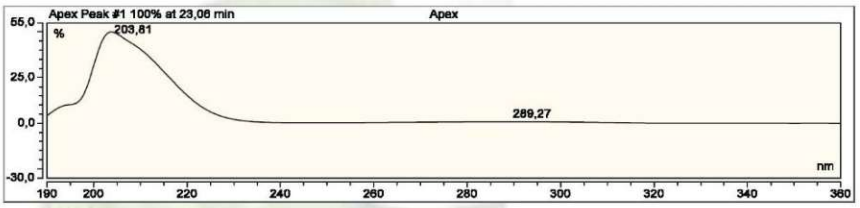
Die approbierte gedruckte Originalversion dieser Dissertation ist an der TU Wien Bibliothek verfügbar.
The approved original version of this doctoral thesis is available in print at TU Wien Bibliothek.

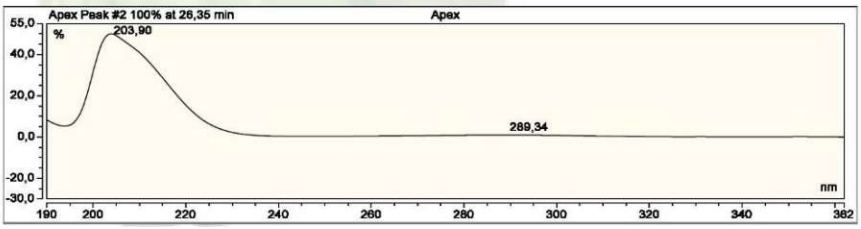
14. Chiral HPLC chromatograms for the asymmetric Michael-Initiated Ring Closure/intramolecular aldol sequence

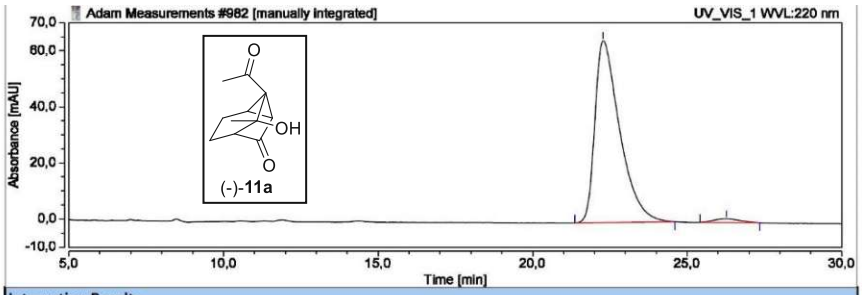


Integration Results

No.	Peak Name	Retention Time min	Area mAU*min	Height mAU	Relative Area %	Relative Height %	Amount n.a.
1		23,055	51,224	56,148	50,46	54,09	n.a.
2		26,350	50,286	47,652	49,54	45,91	n.a.
Total:			101,511	103,800	100,00	100,00	

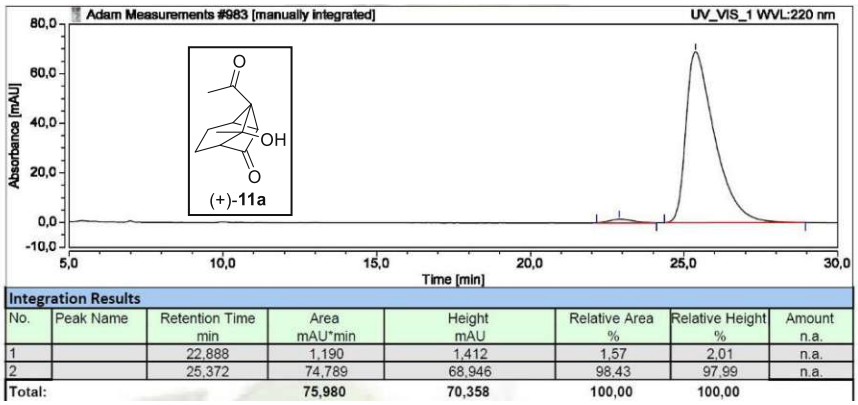






Integration Results

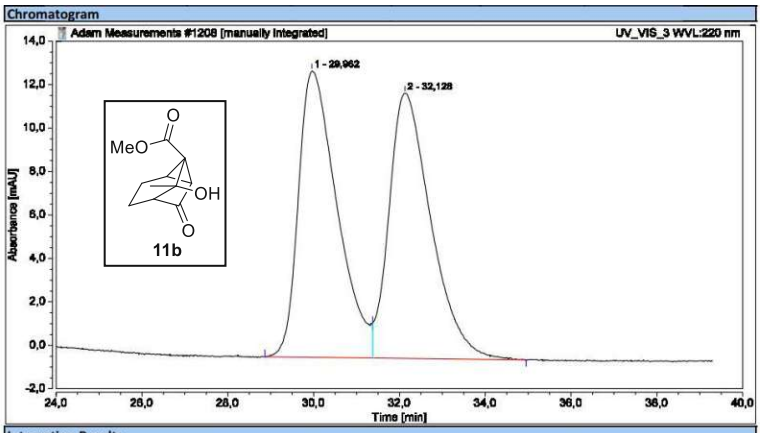
No.	Peak Name	Retention Time min	Area mAU*min	Height mAU	Relative Area %	Relative Height %	Amount n.a.
1		22,285	60,385	64,902	97,92	97,95	n.a.
2		26,267	1,281	1,357	2,08	2,05	n.a.
Total:			61,666	66,258	100,00	100,00	



Integration Results

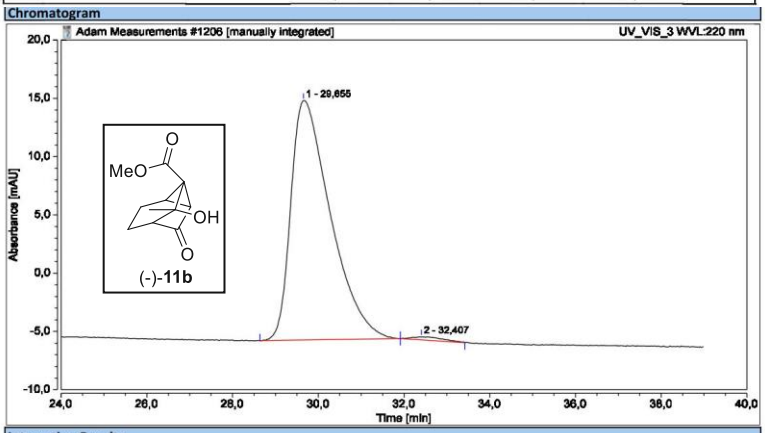
No.	Peak Name	Retention Time min	Area mAU*min	Height mAU	Relative Area %	Relative Height %	Amount n.a.
1		22,888	1,190	1,412	1,57	2,01	n.a.
2		25,372	74,789	68,946	98,43	97,99	n.a.
Total:			75,980	70,358	100,00	100,00	

Die approbierte gedruckte Originalversion dieser Dissertation ist an der TU Wien Bibliothek verfügbar.
The approved original version of this doctoral thesis is available in print at TU Wien Bibliothek.
TU Bibliothek Your knowledge hub WIEN



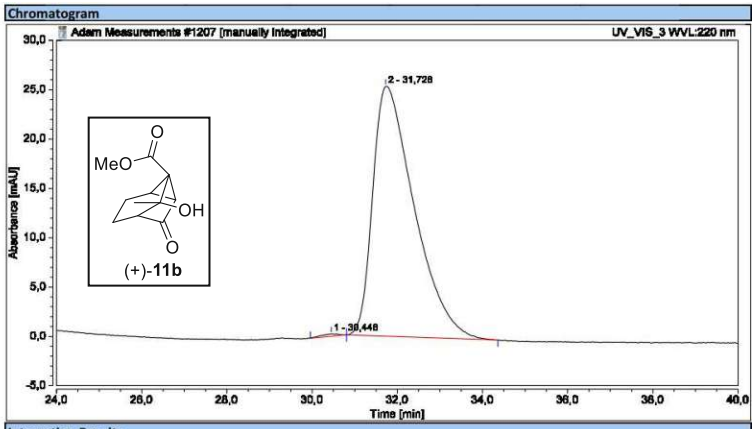
Integration Results

No.	Peak Name	Retention Time min	Area mAU*min	Height mAU	Relative Area %	Relative Height %	Amount
1		29,962	13,735	13,195	49,84	51,92	n.a.
2		32,128	13,821	12,221	50,16	48,08	n.a.
Total:			27,556	25,417	100,00	100,00	



Integration Results

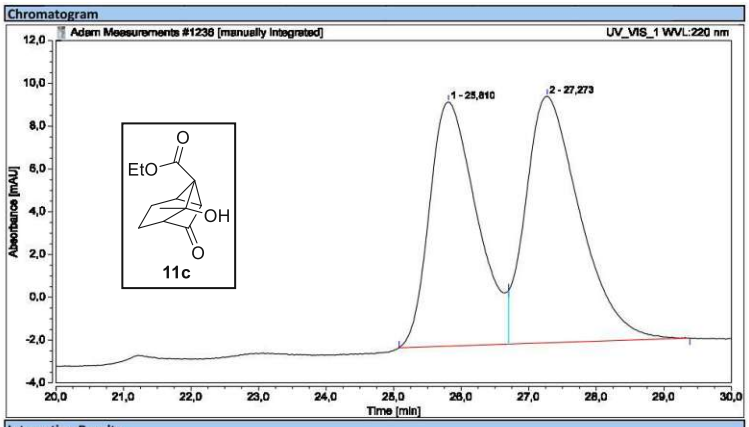
No.	Peak Name	Retention Time min	Area mAU*min	Height mAU	Relative Area %	Relative Height %	Amount
1		29,655	21,989	20,568	98,93	98,63	n.a.
2		32,407	0,237	0,286	1,07	1,37	n.a.
Total:			22,227	20,854	100,00	100,00	



Integration Results

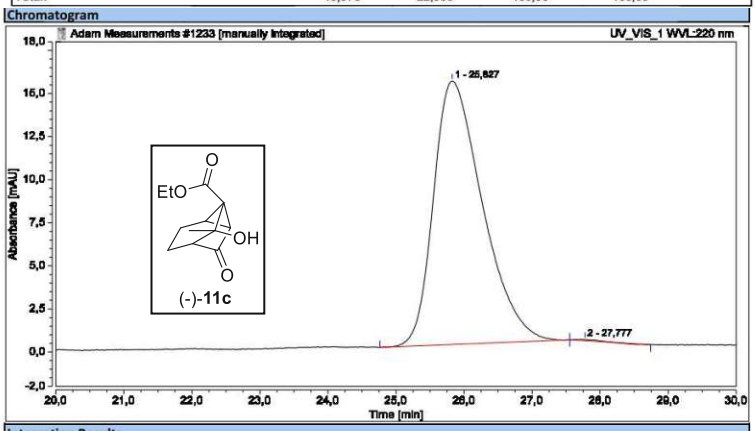
No.	Peak Name	Retention Time min	Area mAU*min	Height mAU	Relative Area %	Relative Height %	Amount
1		30,448	0,116	0,253	0,40	0,99	n.a.
2		31,728	28,566	25,346	99,60	99,01	n.a.
Total:			28,683	25,599	100,00	100,00	

Die approbierte gedruckte Originalversion dieser Dissertation ist an der TU Wien Bibliothek verfügbar.
The approved original version of this doctoral thesis is available in print at TU Wien Bibliothek.
TU Bibliothek Your knowledge hub WIEN



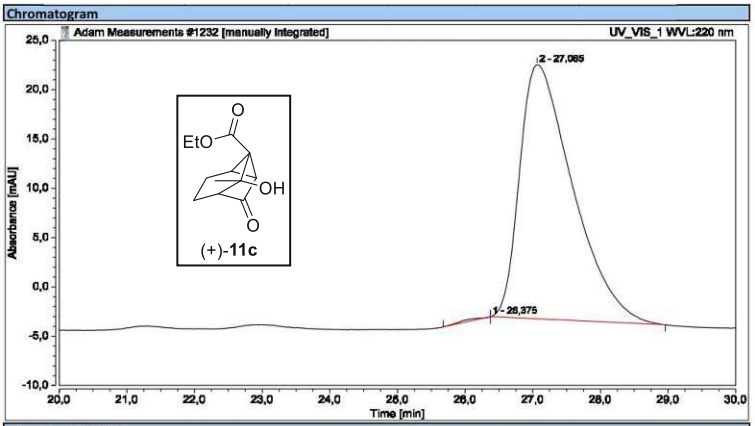
Integration Results

No.	Peak Name	Retention Time min	Area mAU*min	Height mAU	Relative Area %	Relative Height %	Amount
n.a.	1	n.a.	n.a.	n.a.	n.a.	n.a.	n.a.
1		25,810	9,238	11,420	46,24	49,76	n.a.
2		27,273	10,738	11,529	53,76	50,24	n.a.
Total:			19,976	22,950	100,00	100,00	



Integration Results

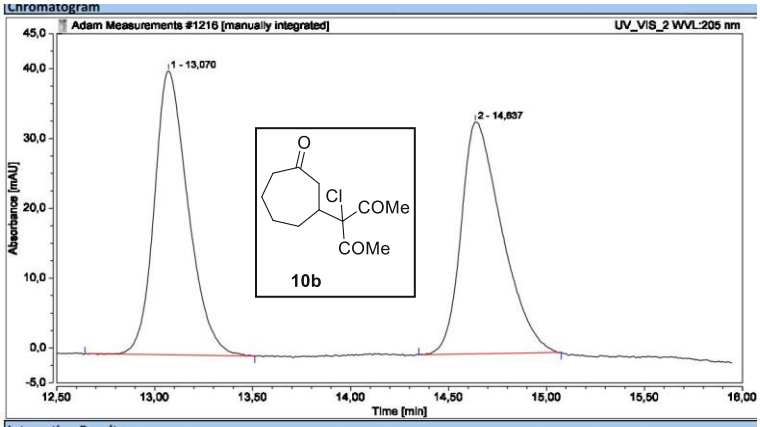
No.	Peak Name	Retention Time min	Area mAU*min	Height mAU	Relative Area %	Relative Height %	Amount
n.a.	1	n.a.	n.a.	n.a.	n.a.	n.a.	n.a.
1		25,827	12,754	15,297	99,85	99,46	n.a.
2		27,777	0,019	0,083	0,15	0,54	n.a.
Total:			12,774	15,381	100,00	100,00	



Integration Results

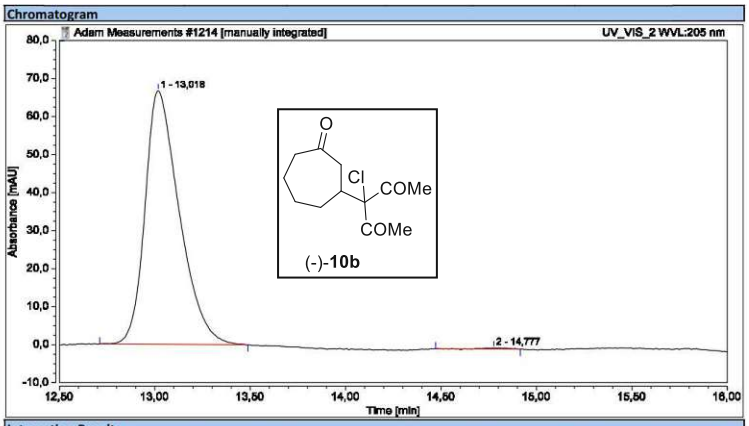
No.	Peak Name	Retention Time min	Area mAU*min	Height mAU	Relative Area %	Relative Height %	Amount
n.a.	1	n.a.	n.a.	n.a.	n.a.	n.a.	n.a.
1		26,375	0,073	0,000	0,31	0,00	n.a.
2		27,065	23,477	25,768	99,69	100,00	n.a.
Total:			23,550	25,768	100,00	100,00	

Die approbierte gedruckte Originalversion dieser Dissertation ist an der TU Wien Bibliothek verfügbar.
The approved original version of this doctoral thesis is available in print at TU Wien Bibliothek.
TU Bibliothek Your knowledge hub WIEN



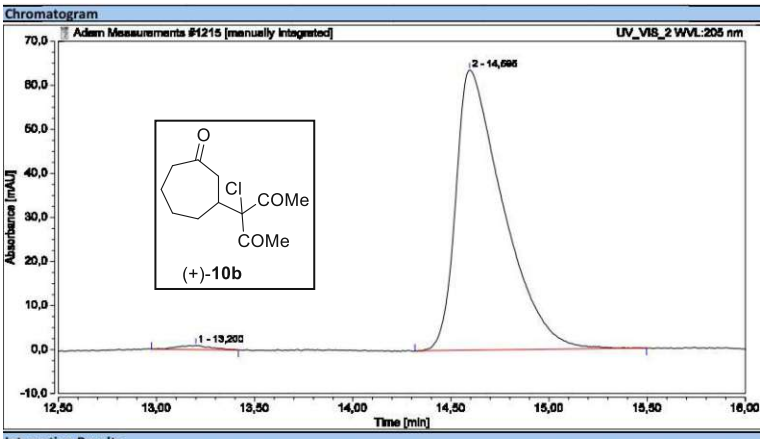
Integration Results

No.	Peak Name	Retention Time min	Area mAU*min	Height mAU	Relative Area %	Relative Height %	Amount
1		13,070	8,141	40,617	50,30	55,04	n.a.
2		14,637	8,045	33,175	49,70	44,96	n.a.
Total:			16.186	73.793	100.00	100.00	



Integration Results

No.	Peak Name	Retention Time min	Area mAU*min	Height mAU	Relative Area %	Relative Height %	Amount
1		13,018	13,877	66,661	99,76	99,50	n.a.
2		14,777	0,034	0,335	0,24	0,50	n.a.
Total:			13,911	66,996	100,00	100,00	

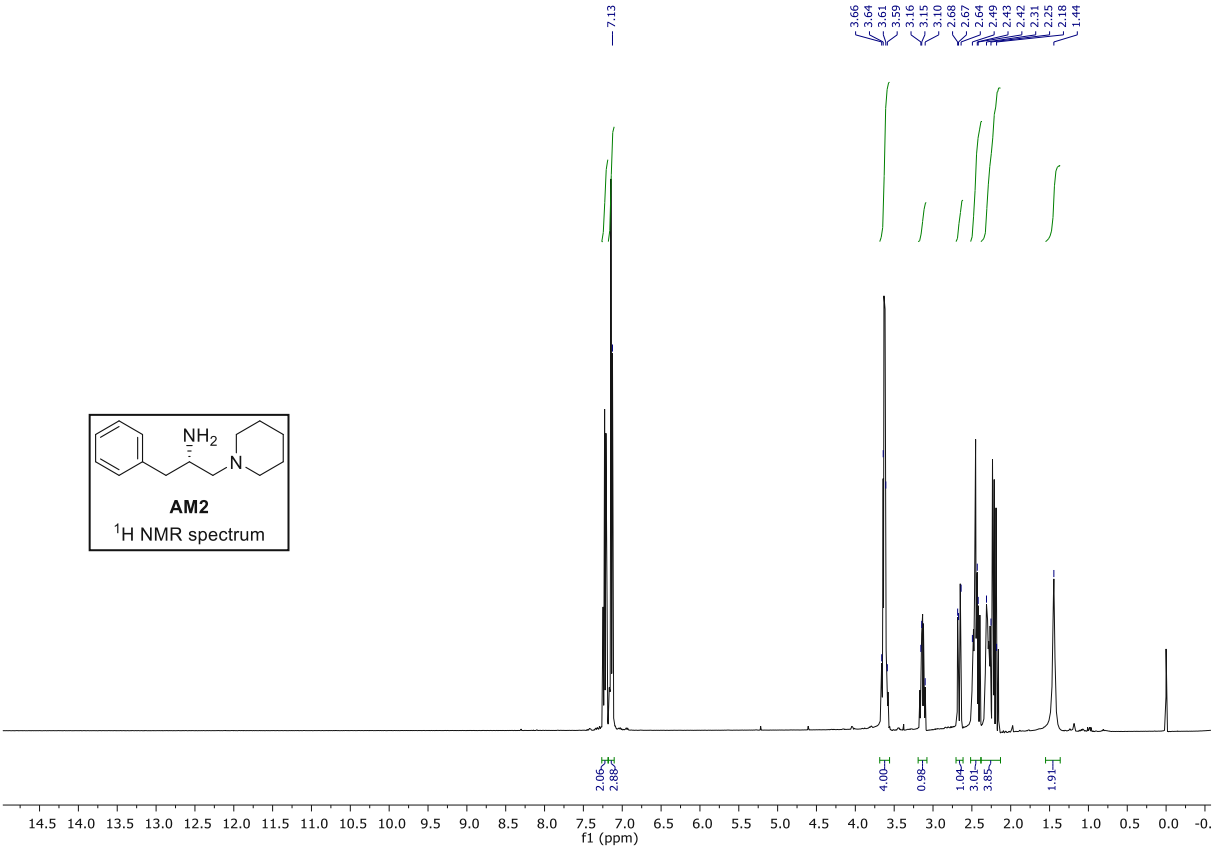


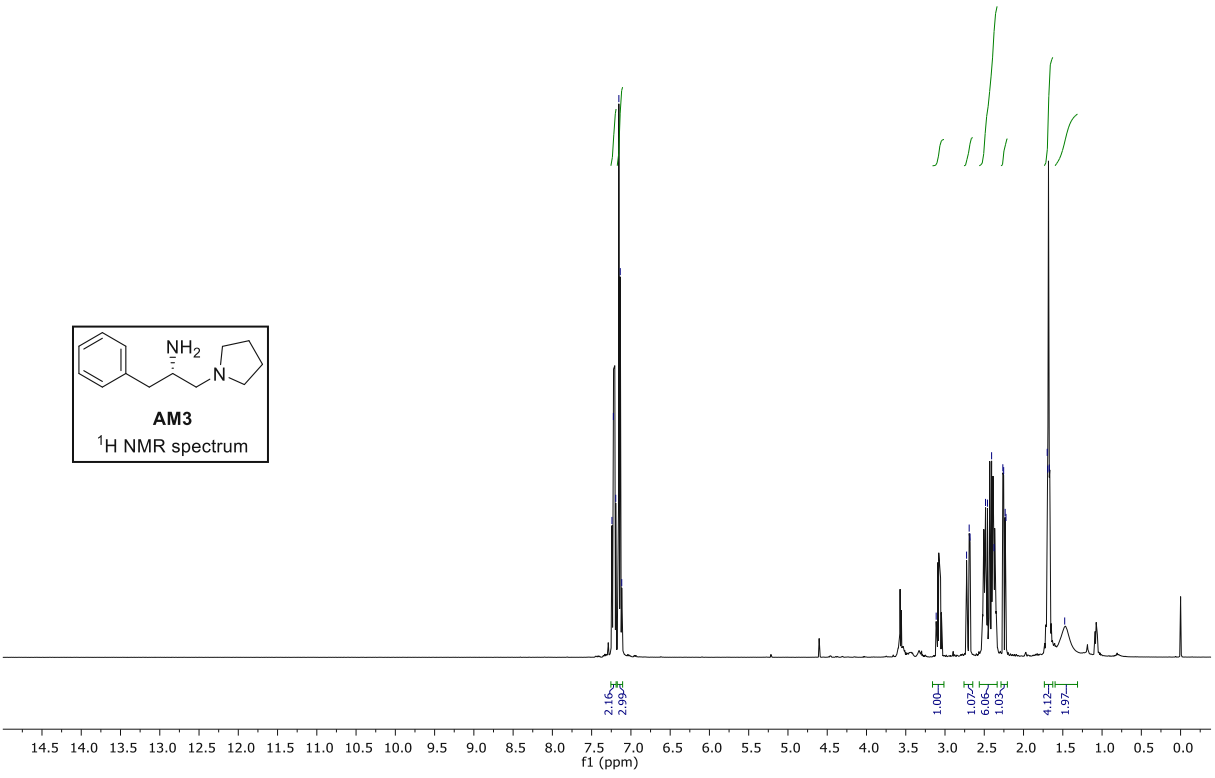
Integration Results

No.	Peak Name	Retention Time min	Area mAU*min	Height mAU	Relative Area %	Relative Height %	Amount
1		13,200	0,185	0,953	1,03	1,48	n.a.
2		14,595	17,860	63,620	98,97	98,52	n.a.
Total:			18,045	64,573	100,00	100,00	

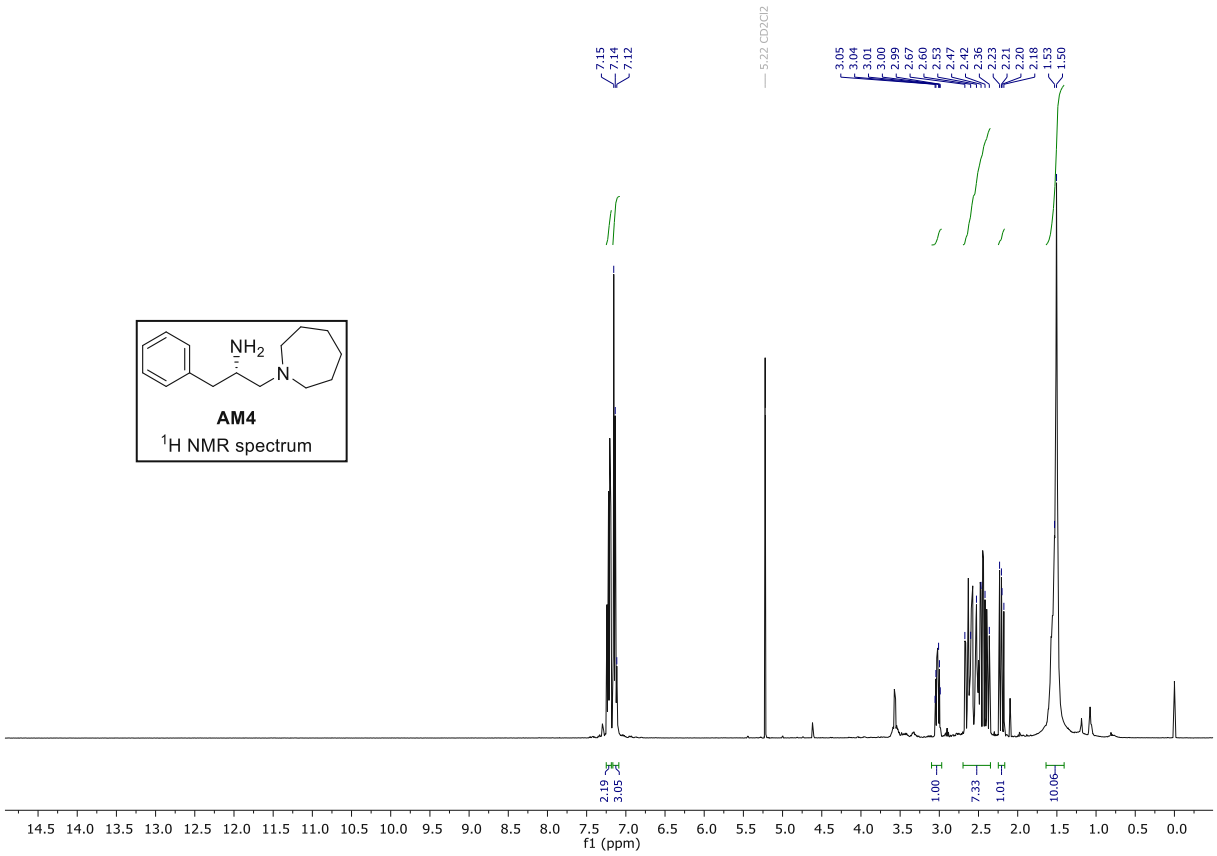
Die approbierte gedruckte Originalversion dieser Dissertation ist an der TU Wien Bibliothek verfügbar.
The approved original version of this doctoral thesis is available in print at TU Wien Bibliothek.

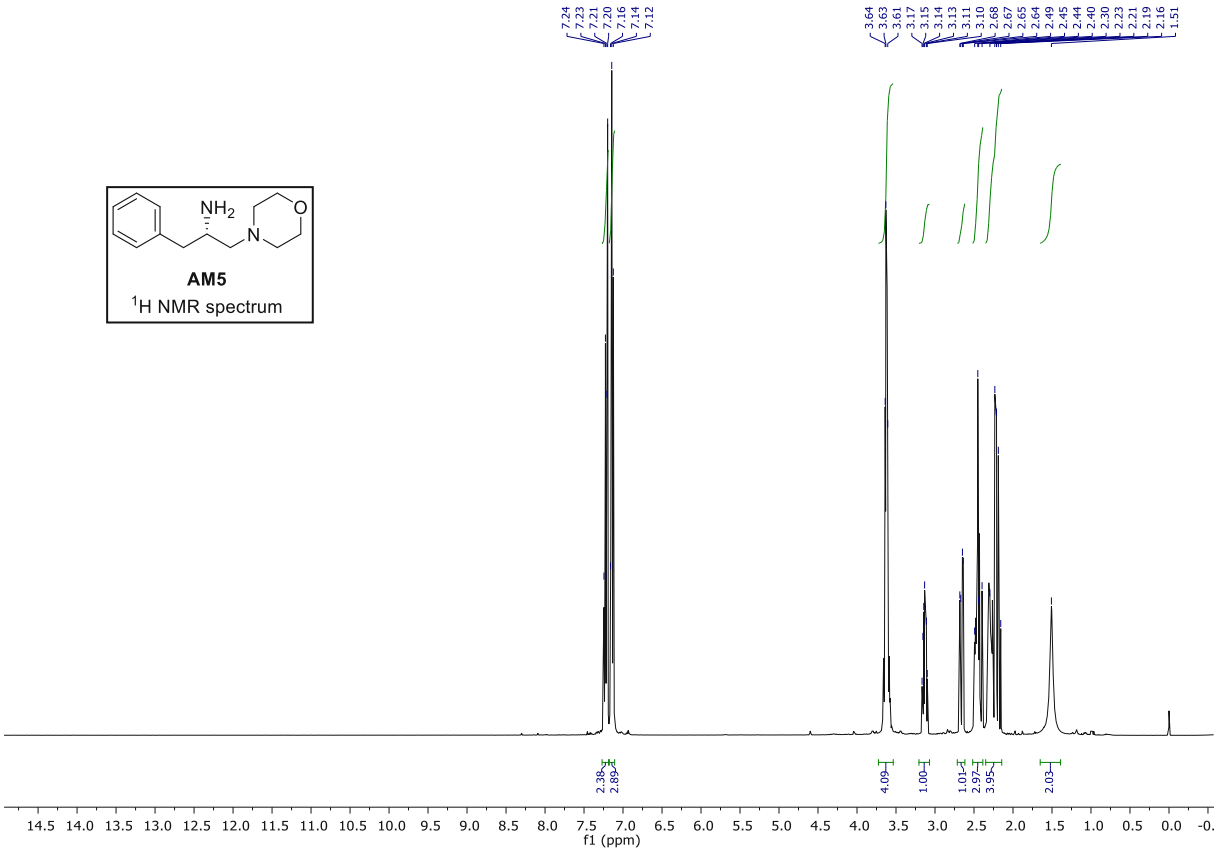
15. NMR spectra of chiral diamines



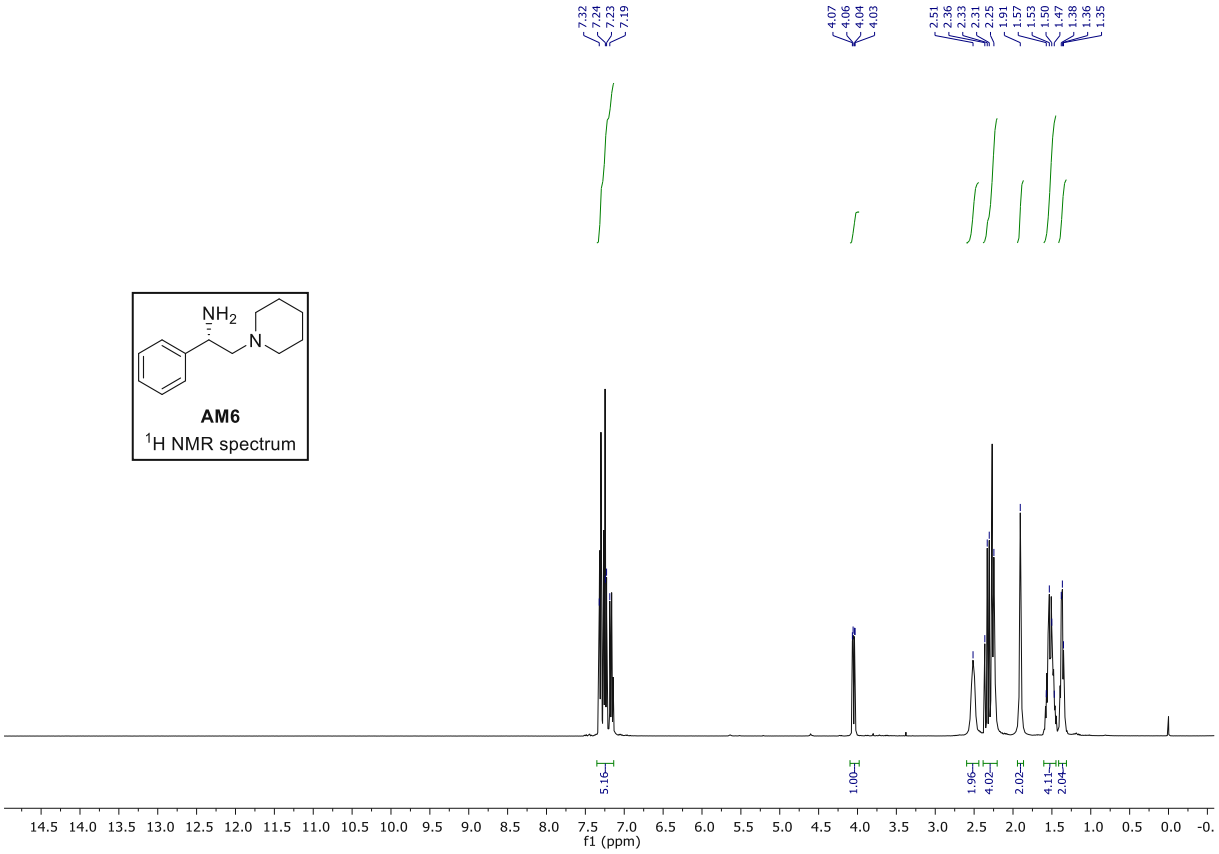


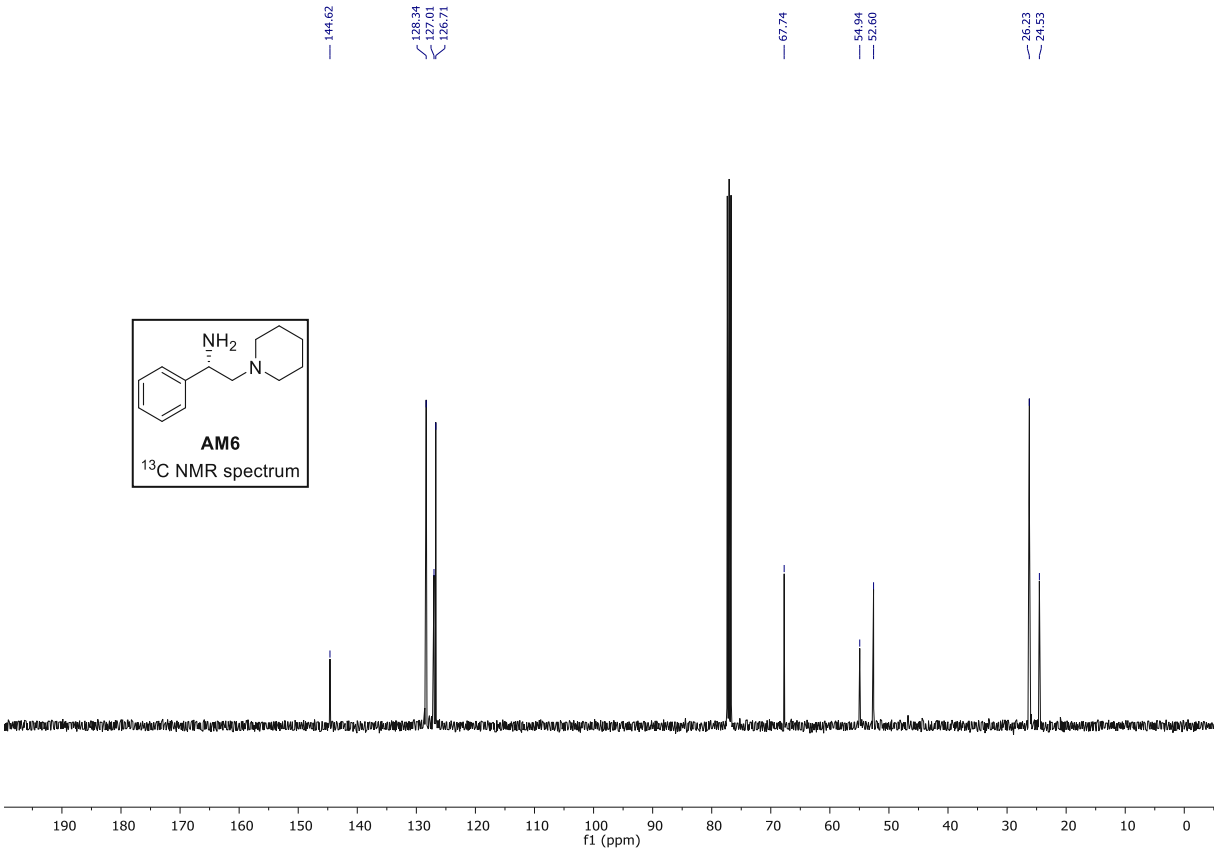
Die approbierte gedruckte Originalversion dieser Dissertation ist an der TU Wien Bibliothek verfügbar.
The approved original version of this doctoral thesis is available in print at TU Wien Bibliothek.



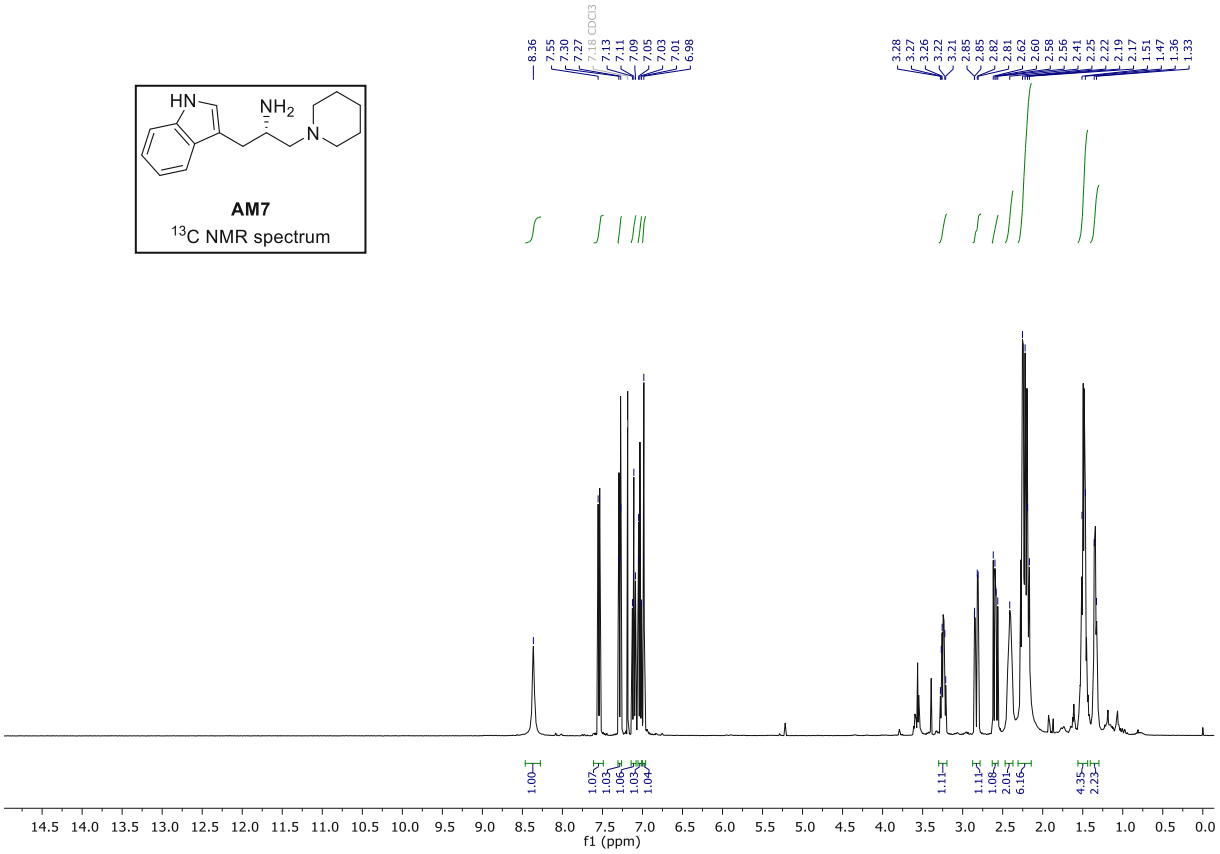


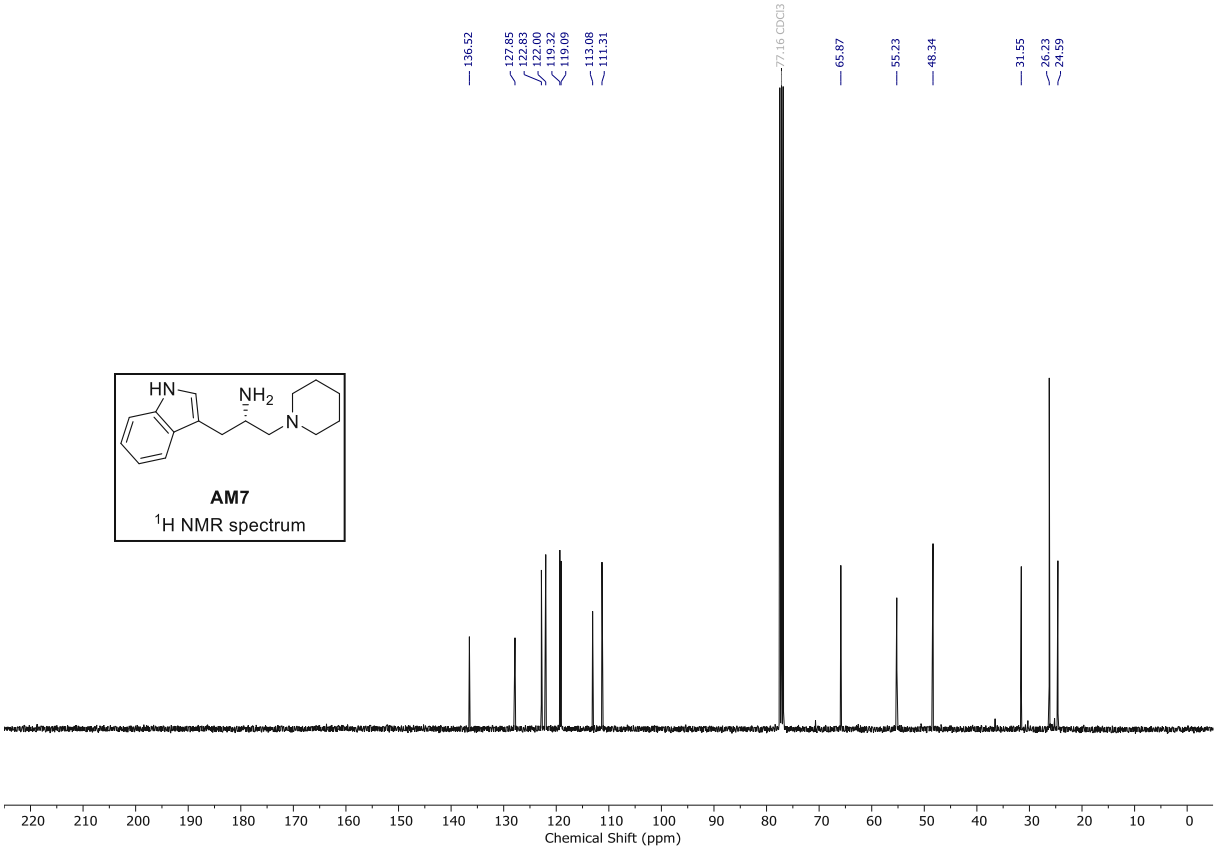
Die approbierte gedruckte Originalversion dieser Dissertation ist an der TU Wien Bibliothek verfügbar.
The approved original version of this doctoral thesis is available in print at TU Wien Bibliothek.



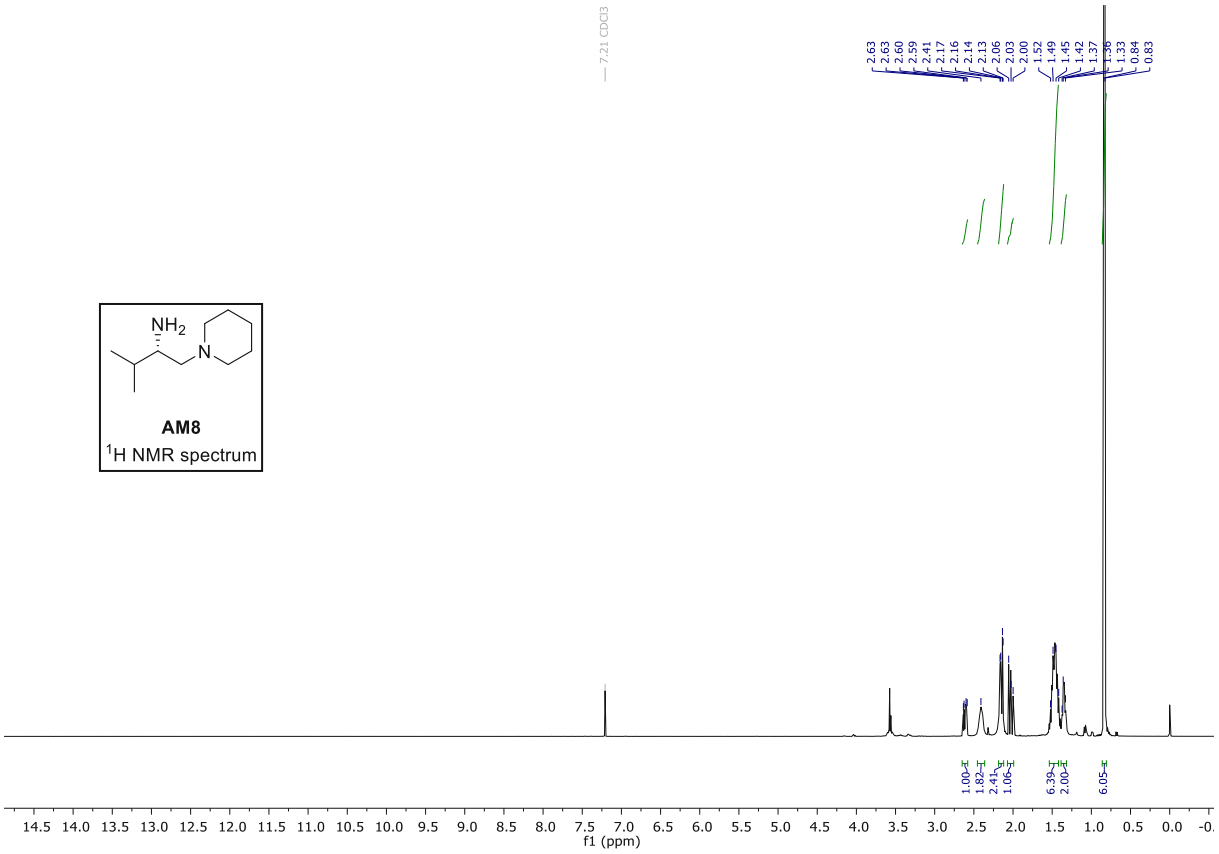


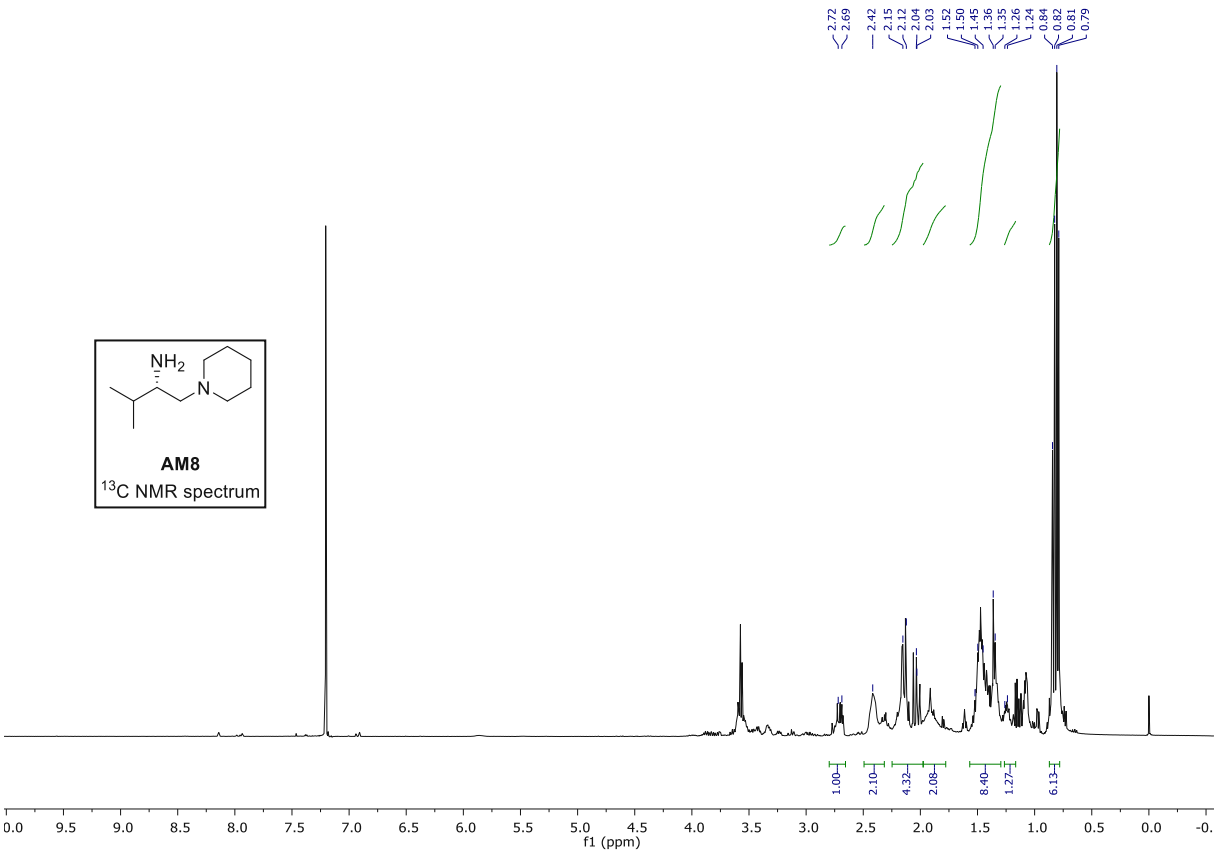
Die approbierte gedruckte Originalversion dieser Dissertation ist an der TU Wien Bibliothek verfügbar.
The approved original version of this doctoral thesis is available in print at TU Wien Bibliothek.
TU Bibliothek Your knowledge hub WIEN



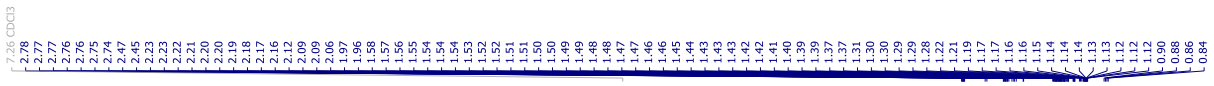


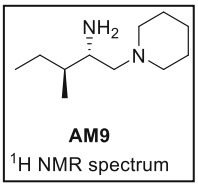
Die approbierte gedruckte Originalversion dieser Dissertation ist an der TU Wien Bibliothek verfügbar.
The approved original version of this doctoral thesis is available in print at TU Wien Bibliothek.





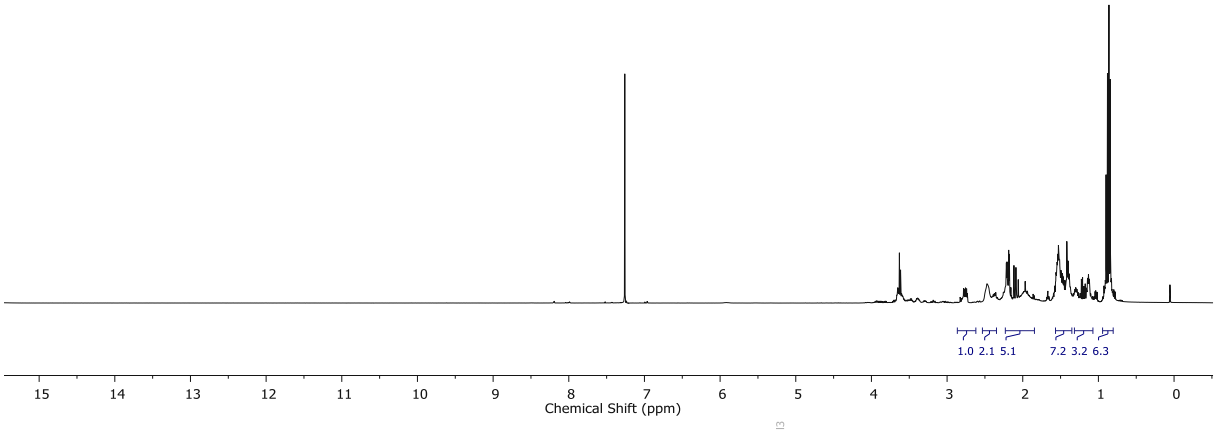
Die approbierte gedruckte Originalversion dieser Dissertation ist an der TU Wien Bibliothek verfügbar.
The approved original version of this doctoral thesis is available in print at TU Wien Bibliothek.

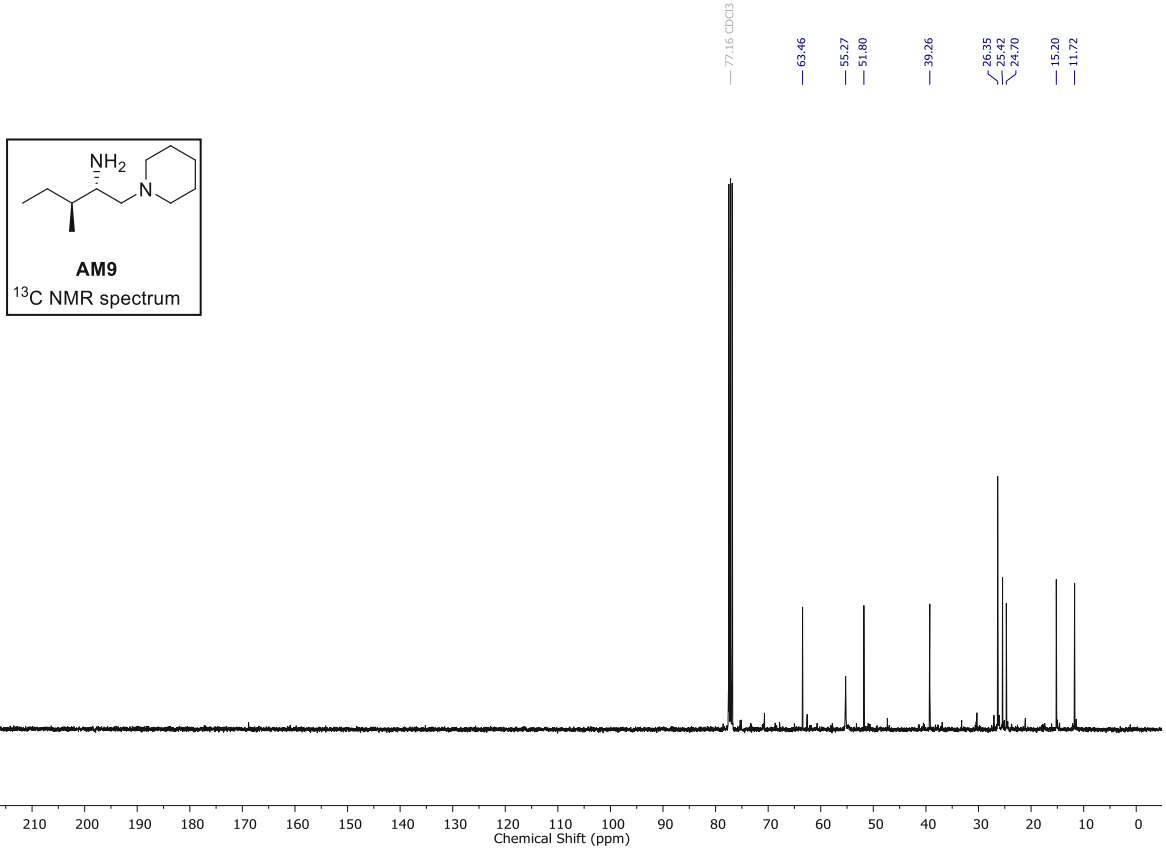




AM9

^{1}H NMR spectrum

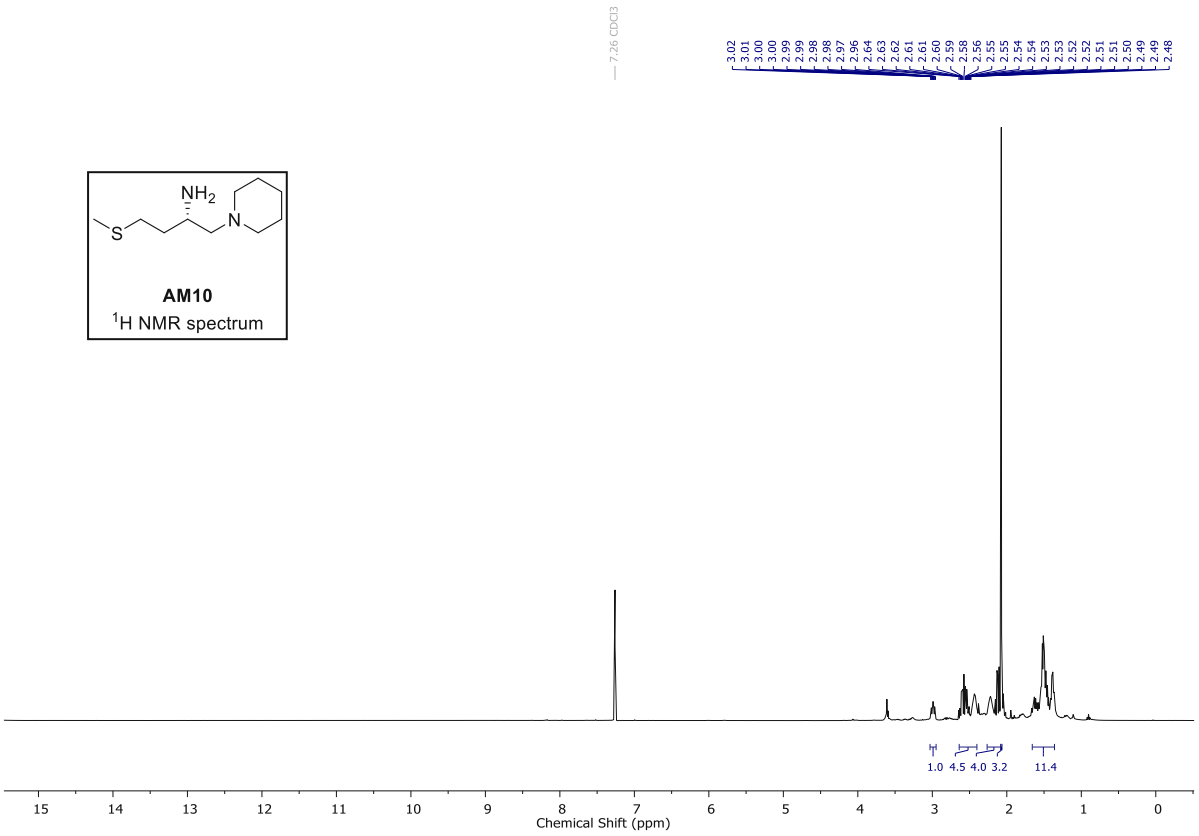


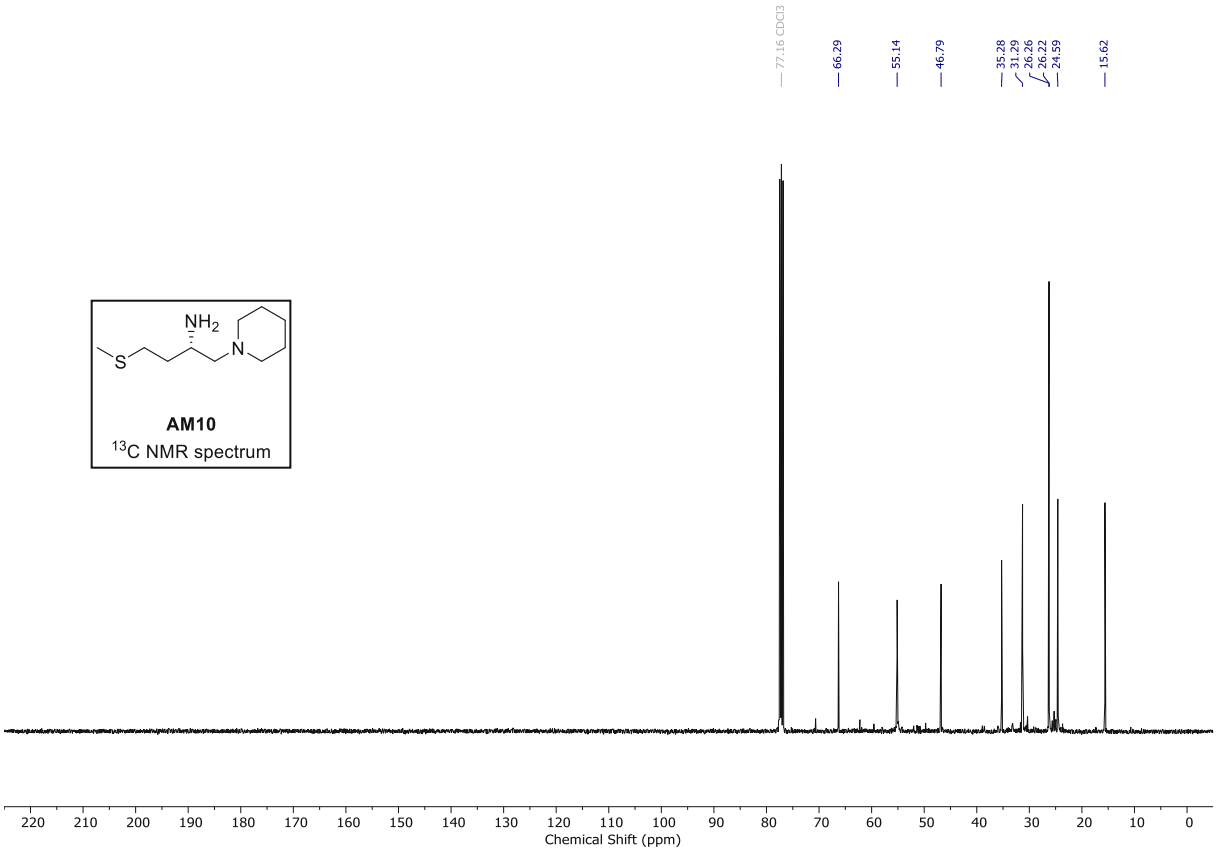


AM9

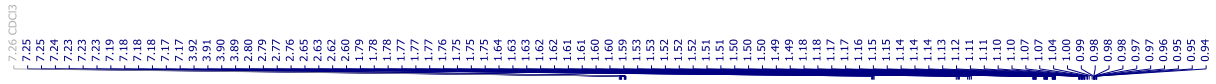
^{13}C NMR spectrum

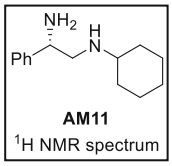
Die approbierte gedruckte Originalversion dieser Dissertation ist an der TU Wien Bibliothek verfügbar.
The approved original version of this doctoral thesis is available in print at TU Wien Bibliothek.

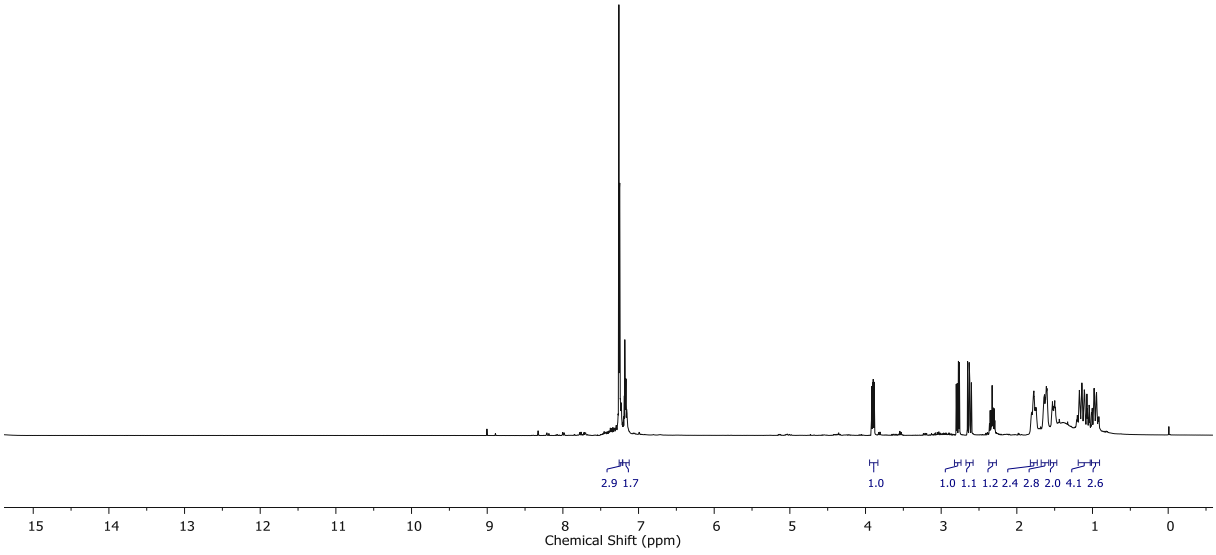


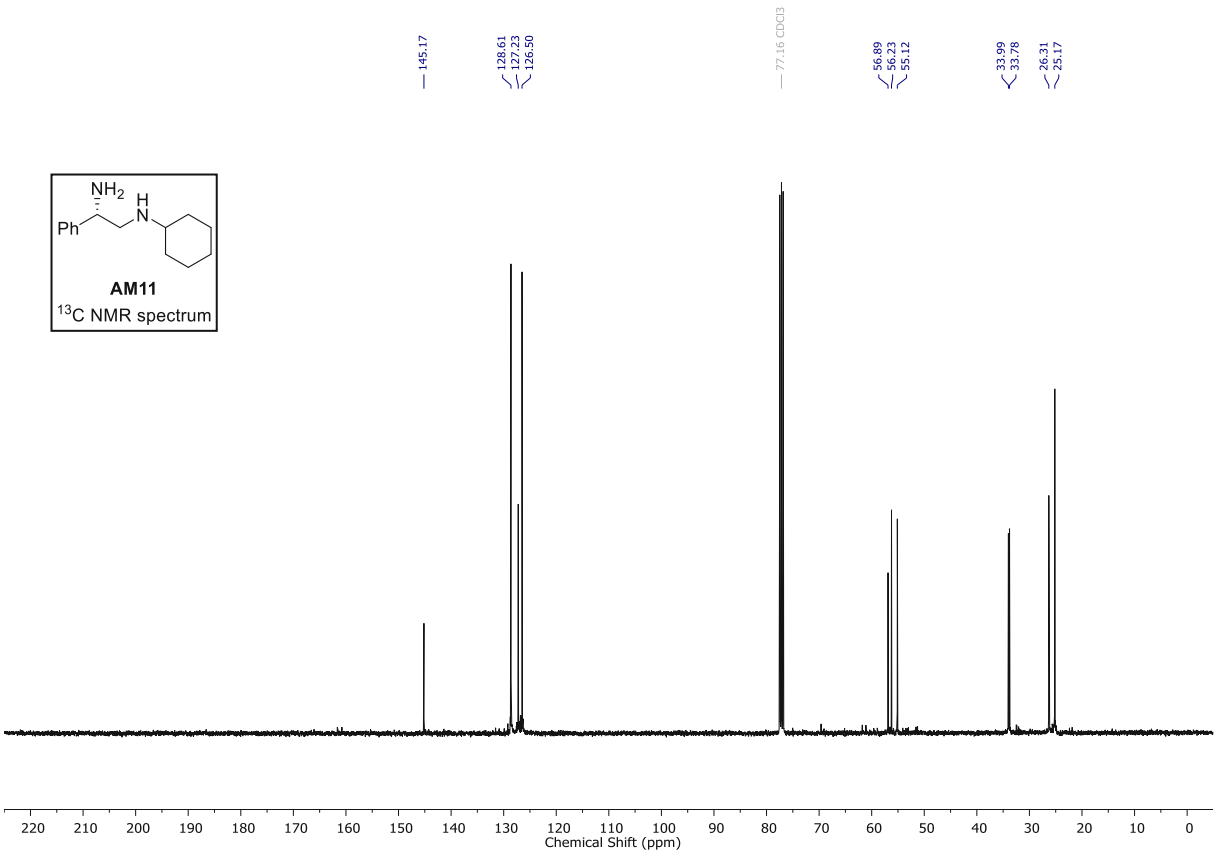


Die approbierte gedruckte Originalversion dieser Dissertation ist an der TU Wien Bibliothek verfügbar.
The approved original version of this doctoral thesis is available in print at TU Wien Bibliothek.



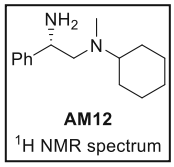




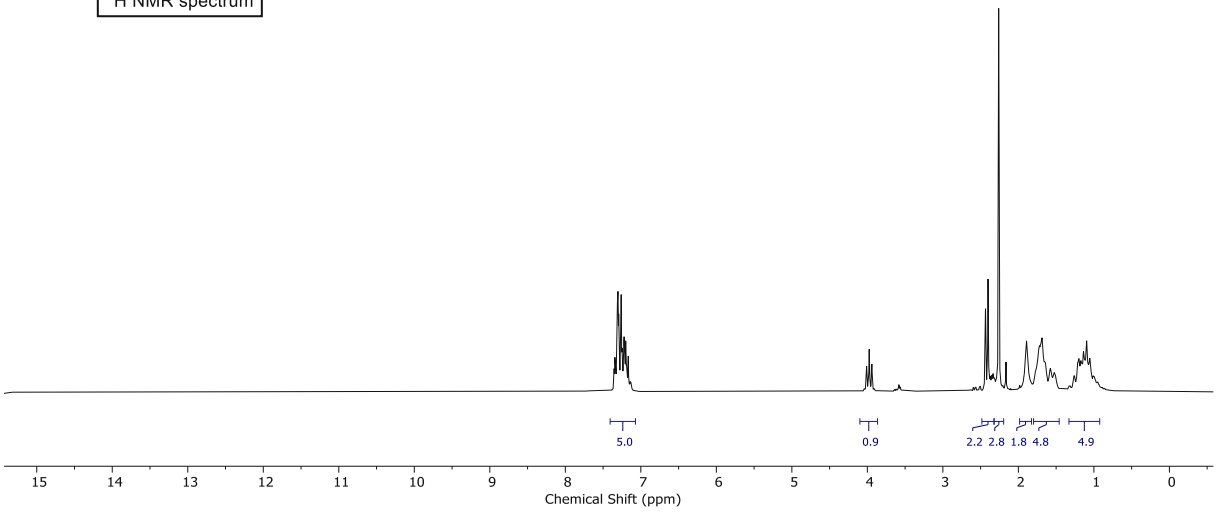


Die approbierte gedruckte Originalversion dieser Dissertation ist an der TU Wien Bibliothek verfügbar.
The approved original version of this doctoral thesis is available in print at TU Wien Bibliothek.

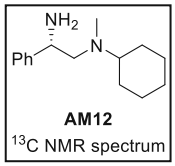




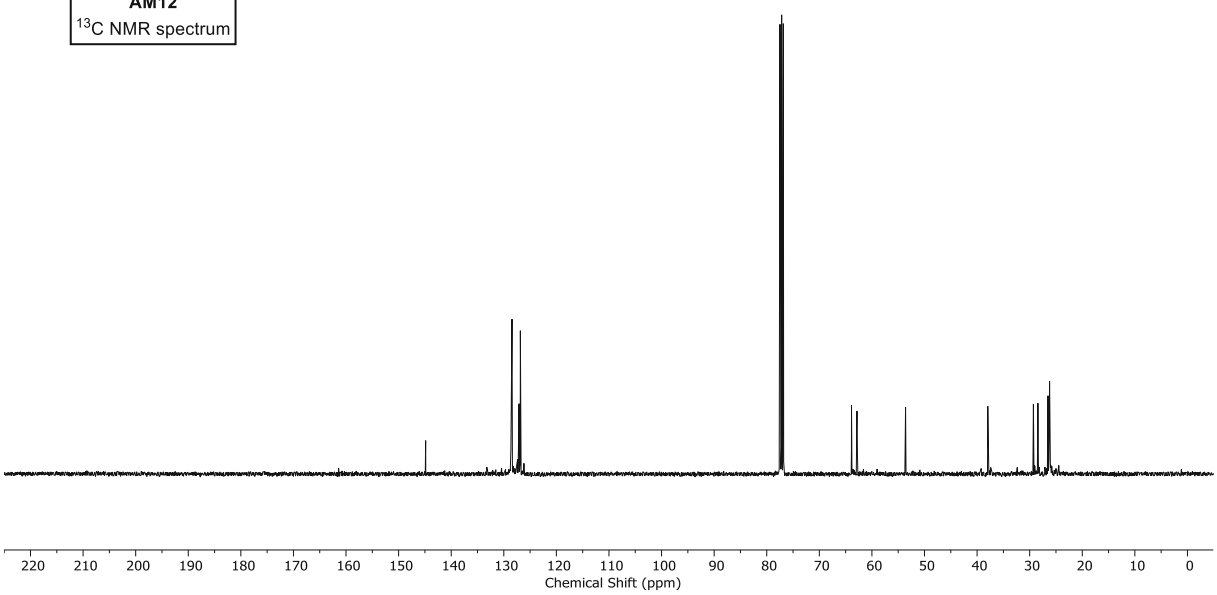
AM12
^{1}H NMR spectrum





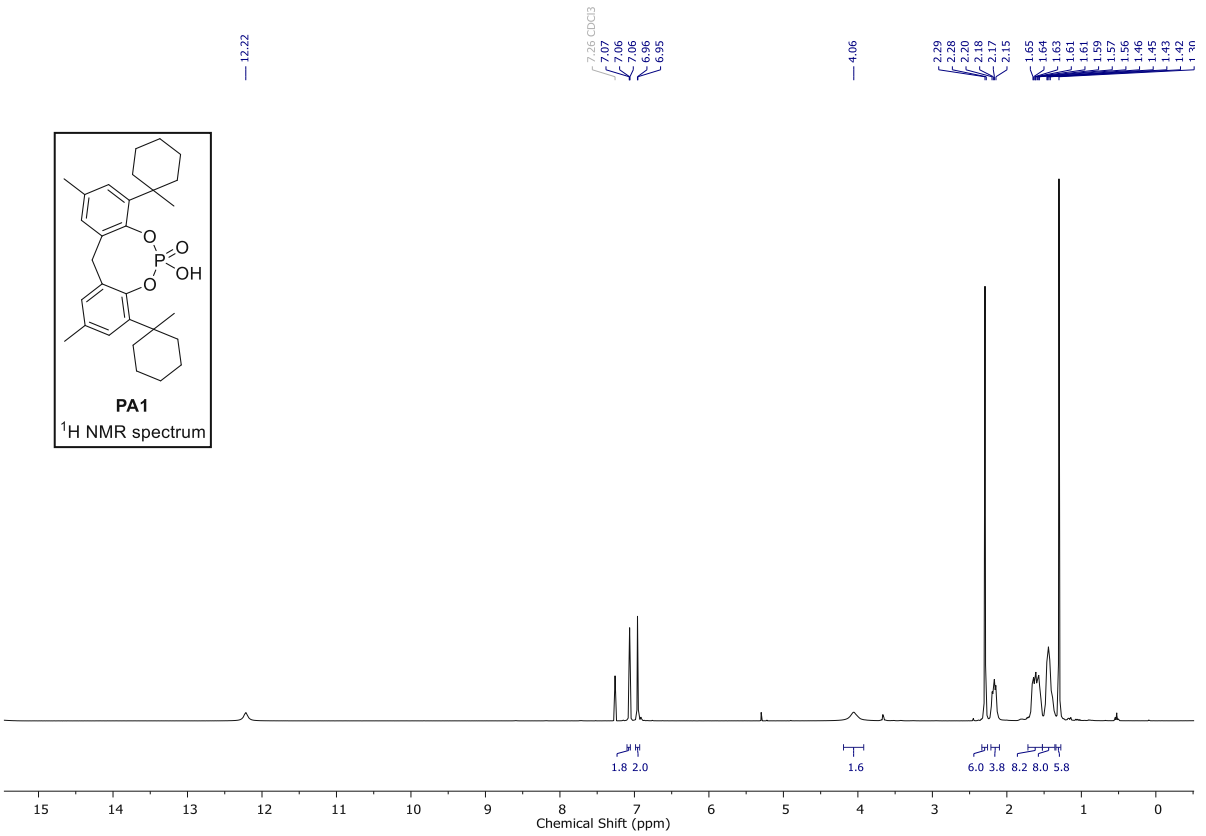


AM12
^{13}C NMR spectrum

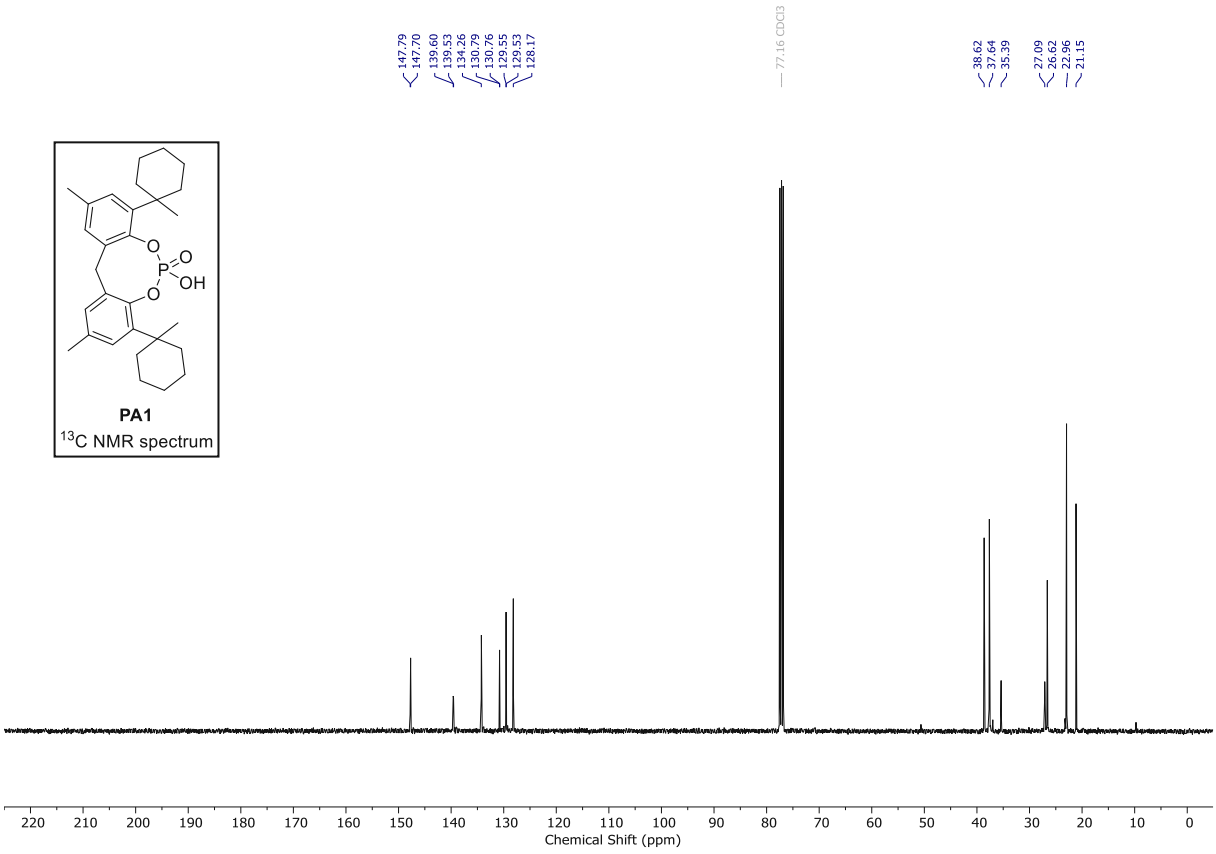


Die approbierte gedruckte Originalversion dieser Dissertation ist an der TU Wien Bibliothek verfügbar.
The approved original version of this doctoral thesis is available in print at TU Wien Bibliothek.

16. NMR spectra of phosphoric acids and intermediates

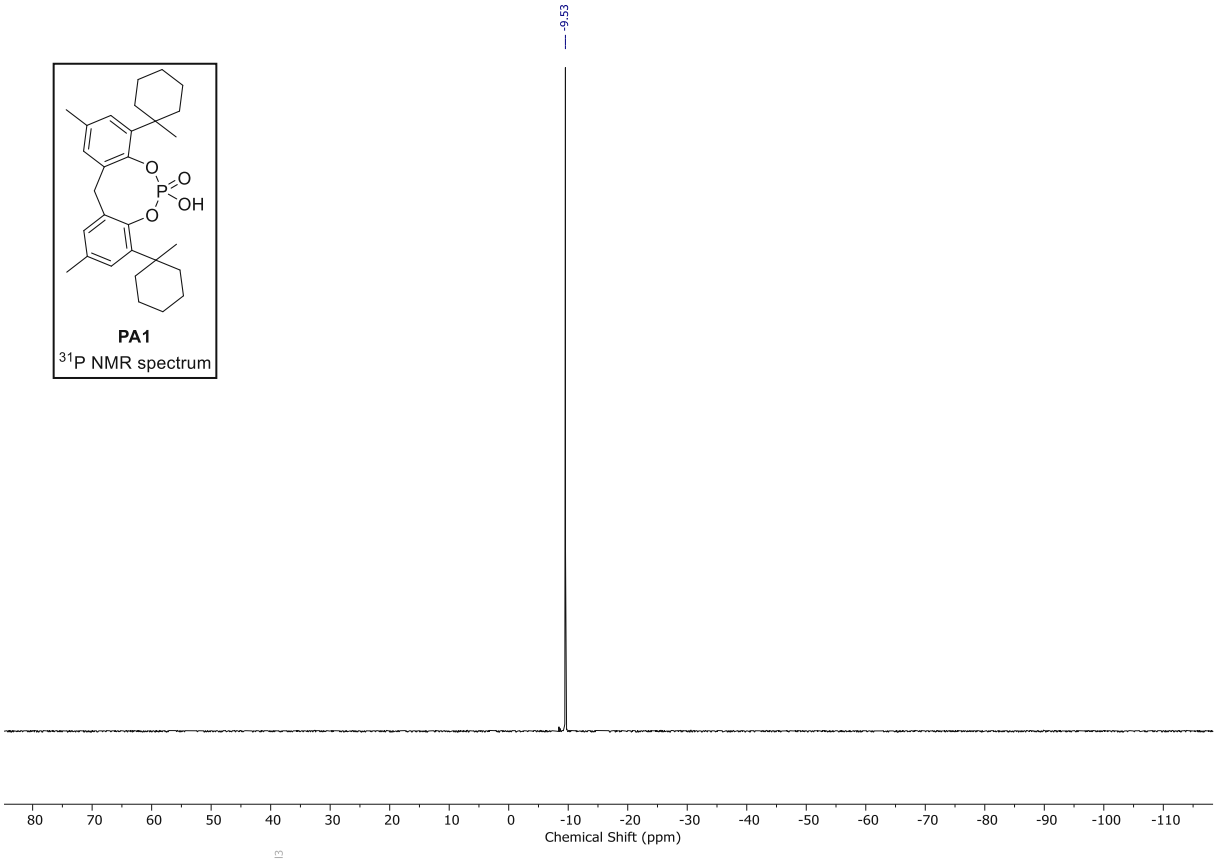


PA1
^{1}H NMR spectrum



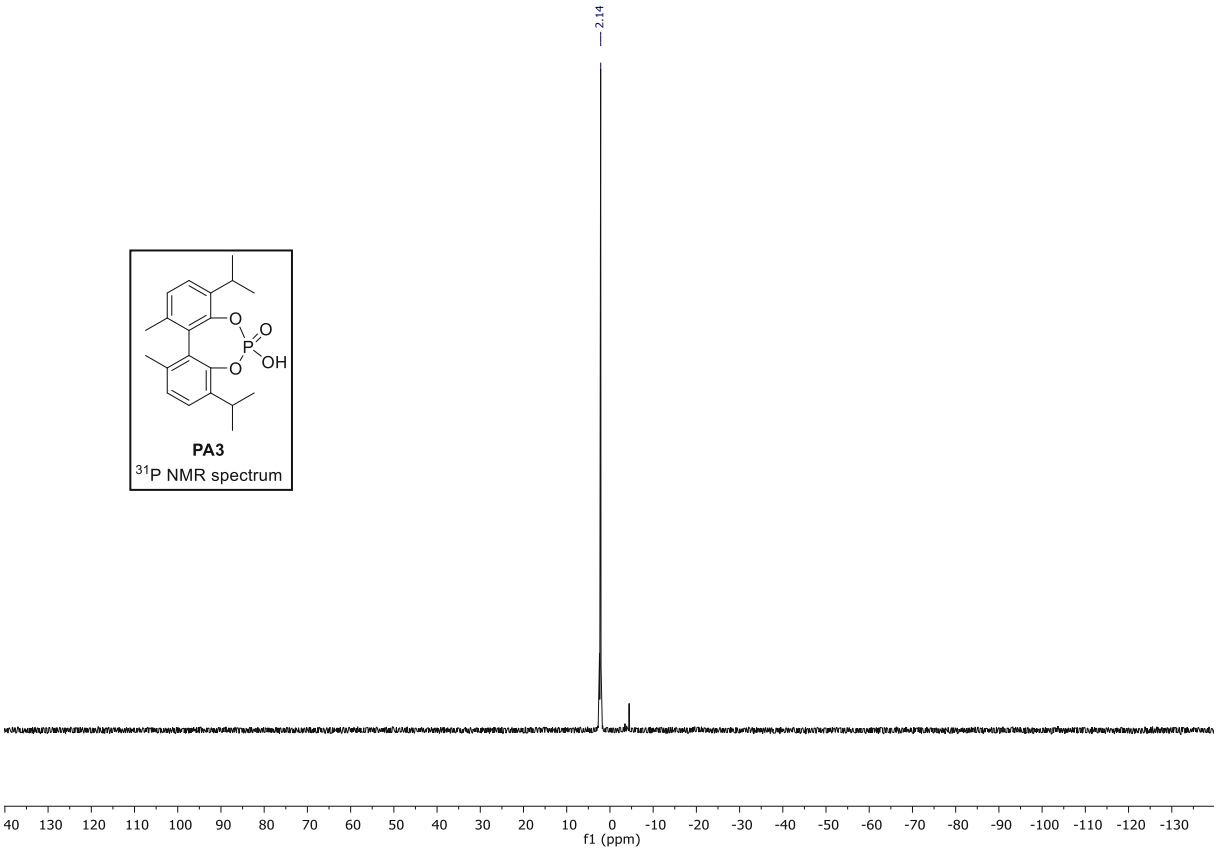
PA1
^{13}C NMR spectrum

Die approbierte gedruckte Originalversion dieser Dissertation ist an der TU Wien Bibliothek verfügbar.
The approved original version of this doctoral thesis is available in print at TU Wien Bibliothek.

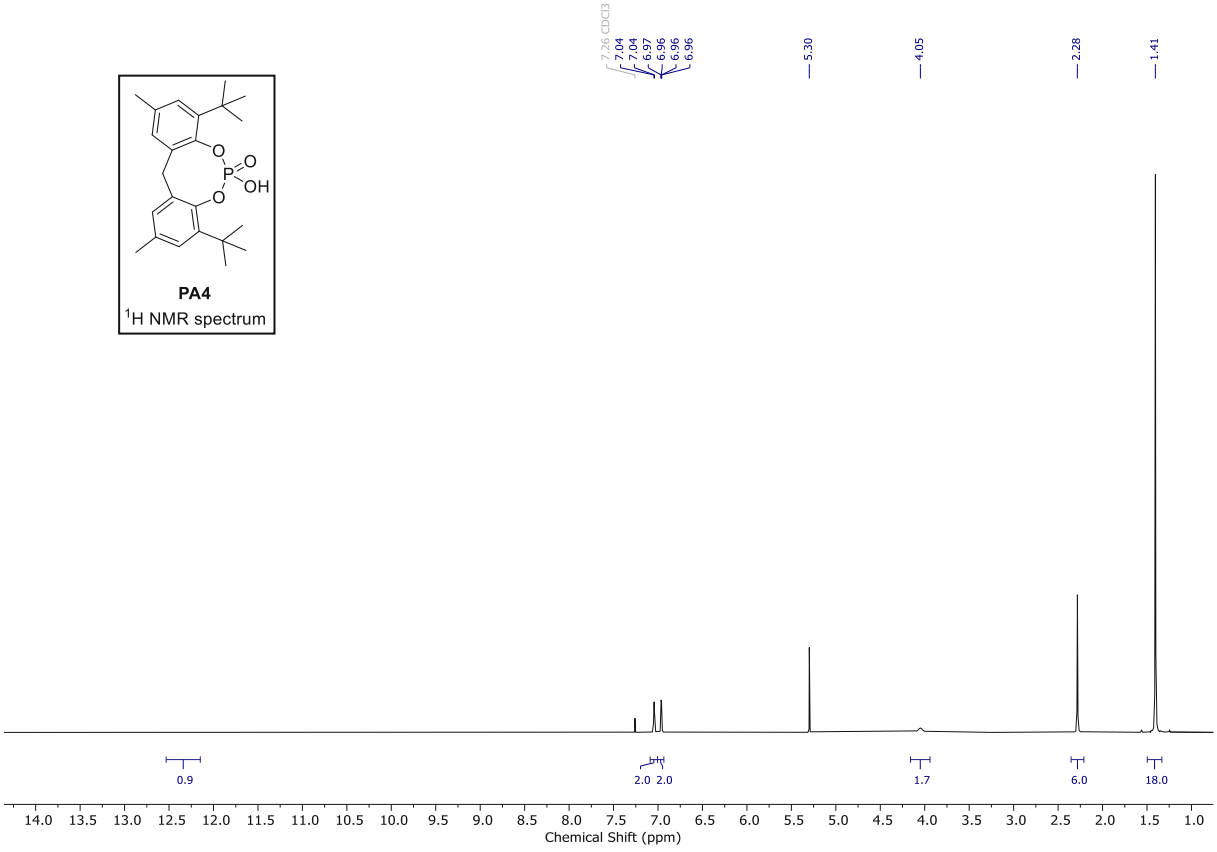


Die approbierte gedruckte Originalversion dieser Dissertation ist an der TU Wien Bibliothek verfügbar.
The approved original version of this doctoral thesis is available in print at TU Wien Bibliothek.

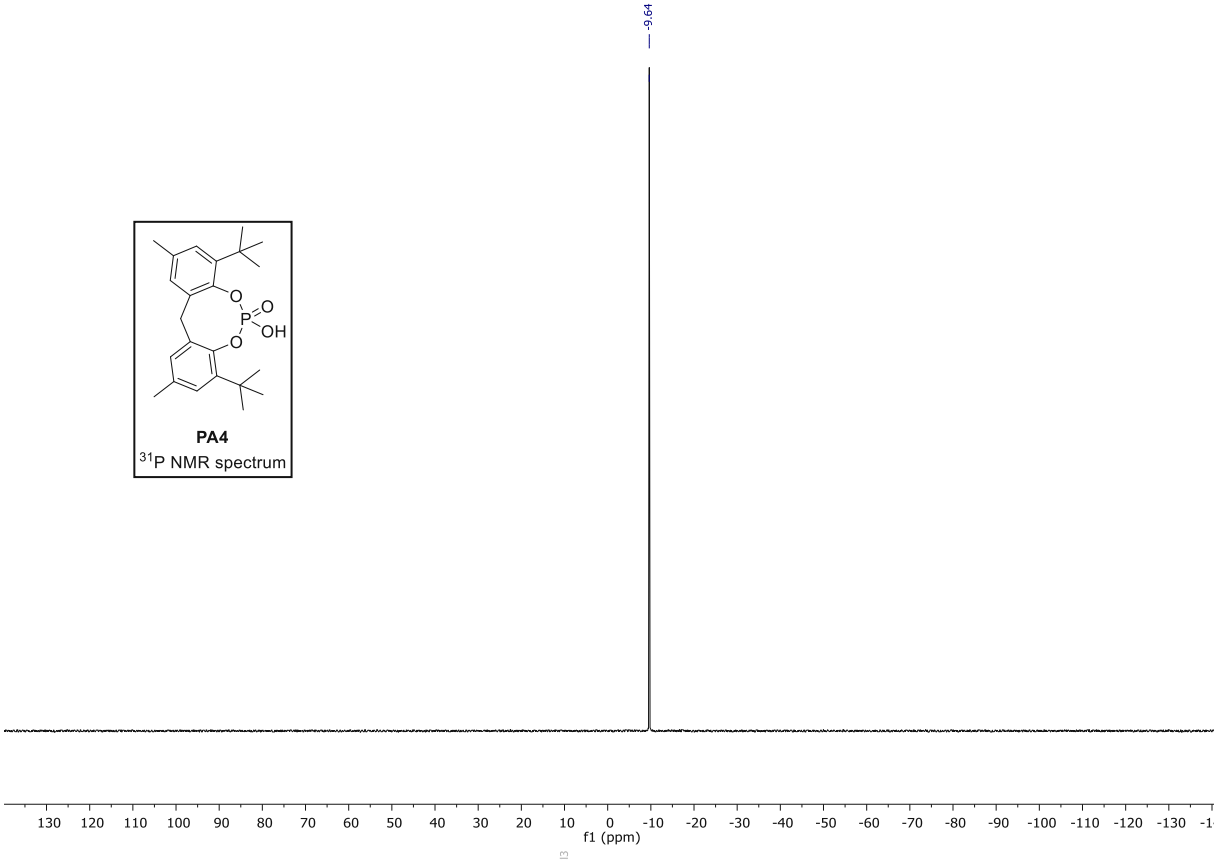
PA3
^{31}P NMR spectrum

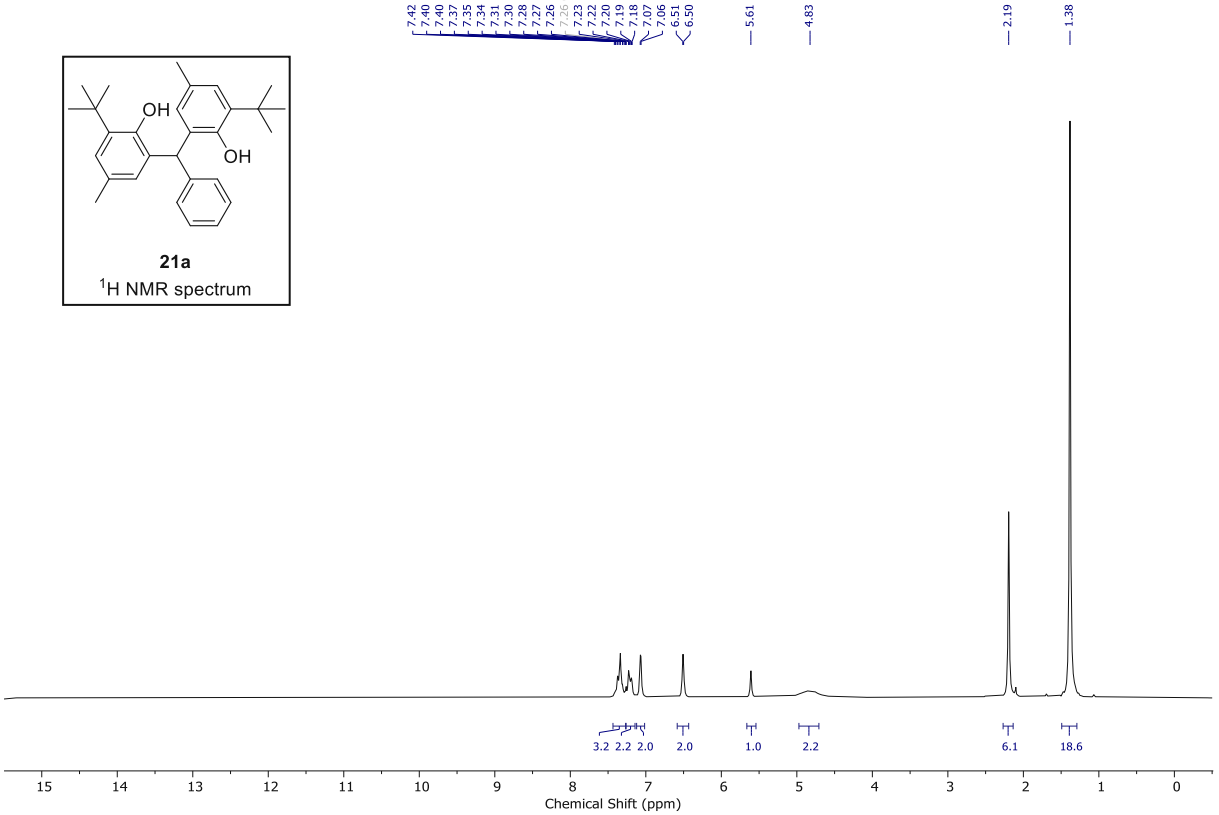


PA4
^{1}H NMR spectrum



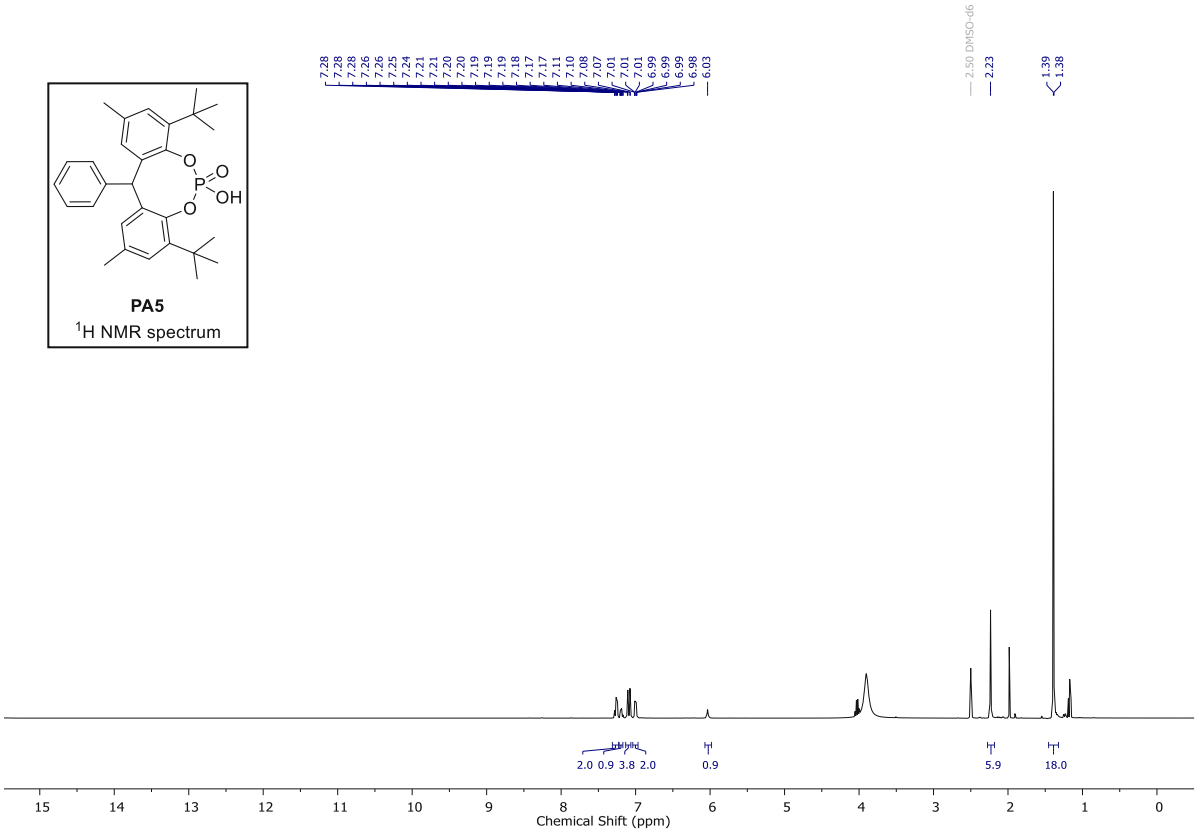
Die approbierte gedruckte Originalversion dieser Dissertation ist an der TU Wien Bibliothek verfügbar.
The approved original version of this doctoral thesis is available in print at TU Wien Bibliothek.



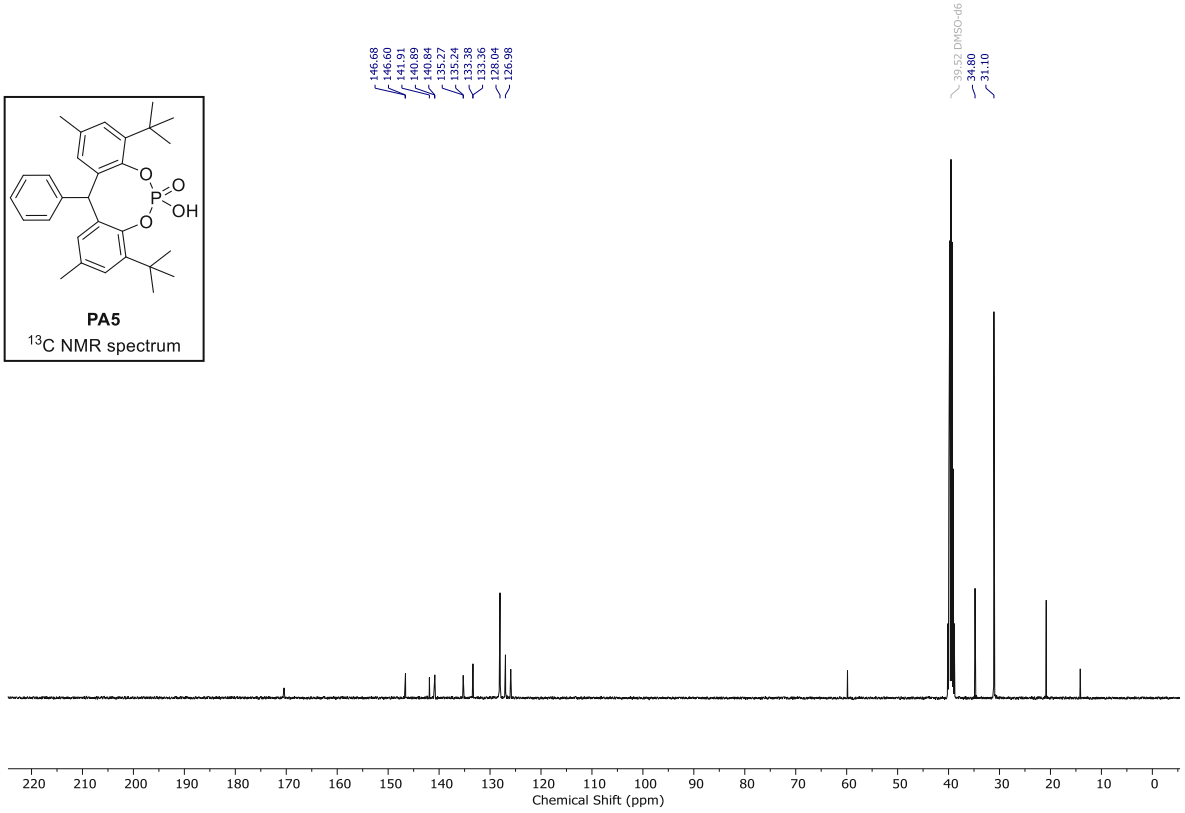


Die approbierte gedruckte Originalversion dieser Dissertation ist an der TU Wien Bibliothek verfügbar.
The approved original version of this doctoral thesis is available in print at TU Wien Bibliothek.

PA5
^{1}H NMR spectrum

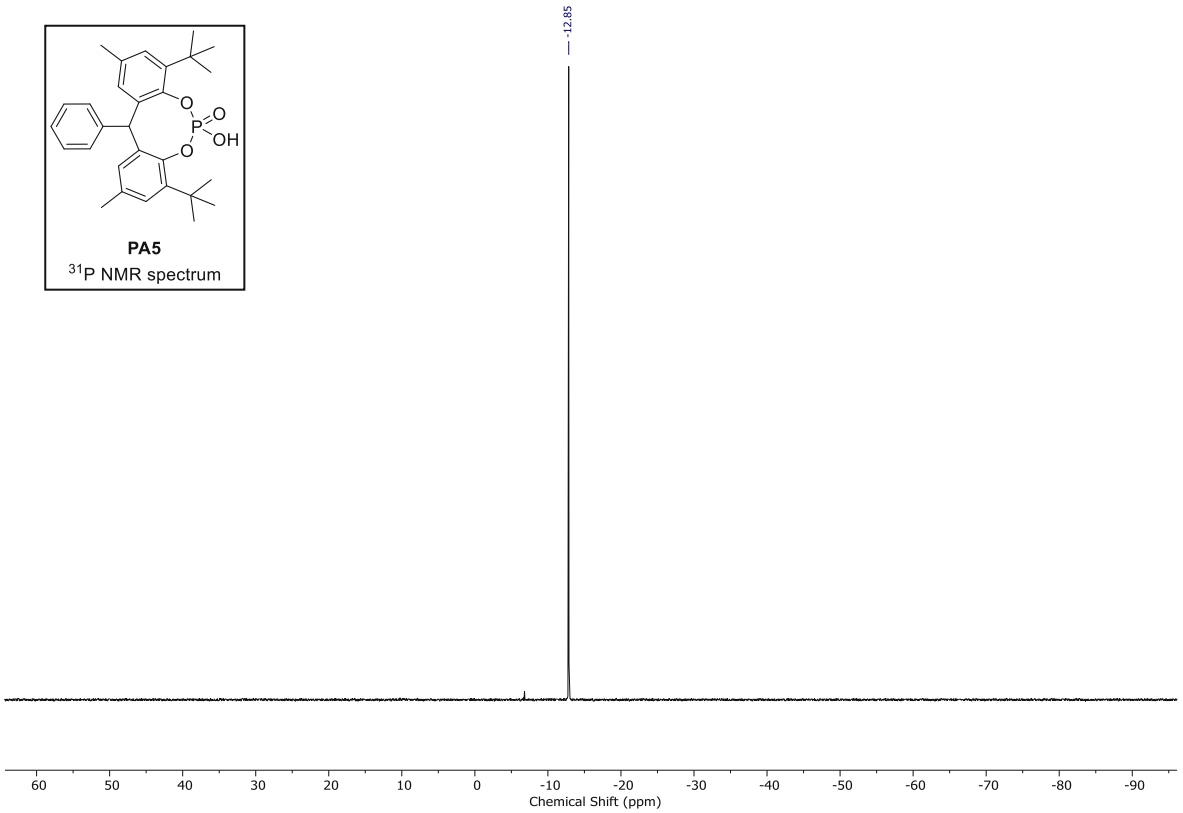


PA5
^{13}C NMR spectrum

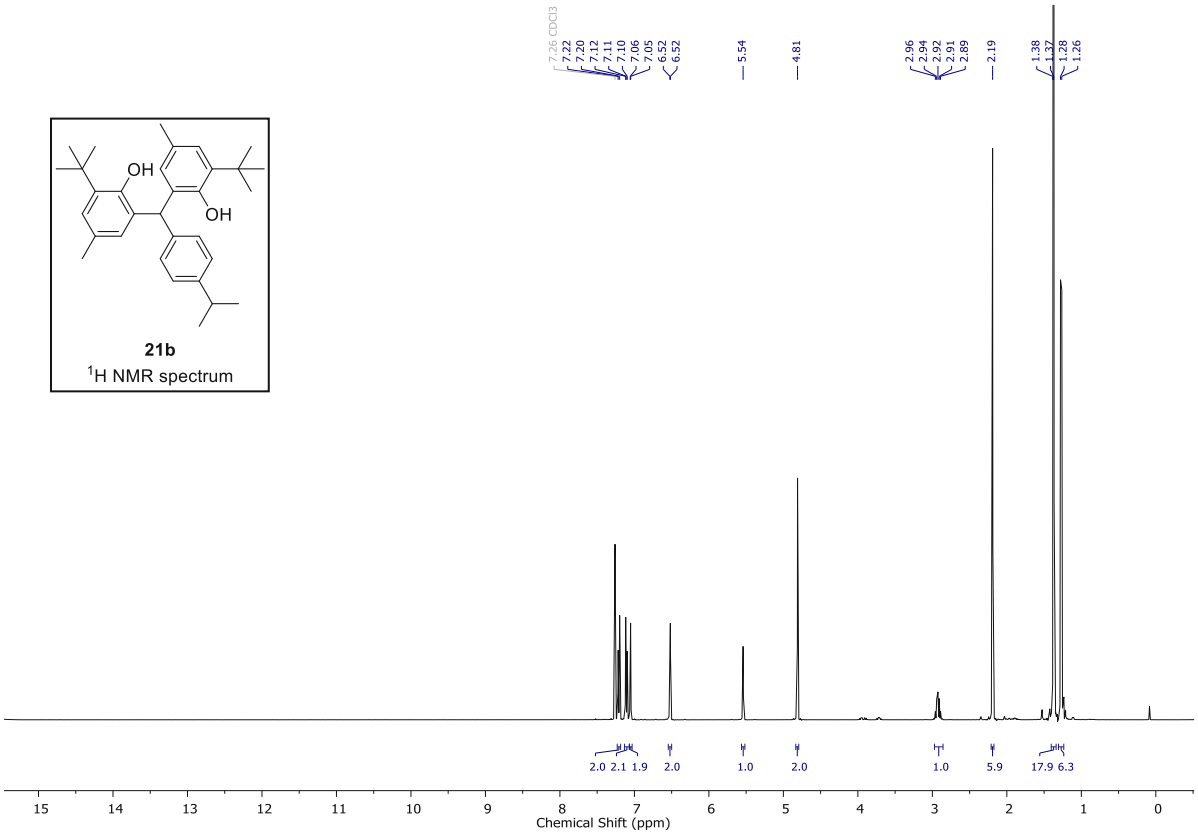


Die approbierte gedruckte Originalversion dieser Dissertation ist an der TU Wien Bibliothek verfügbar.
The approved original version of this doctoral thesis is available in print at TU Wien Bibliothek.

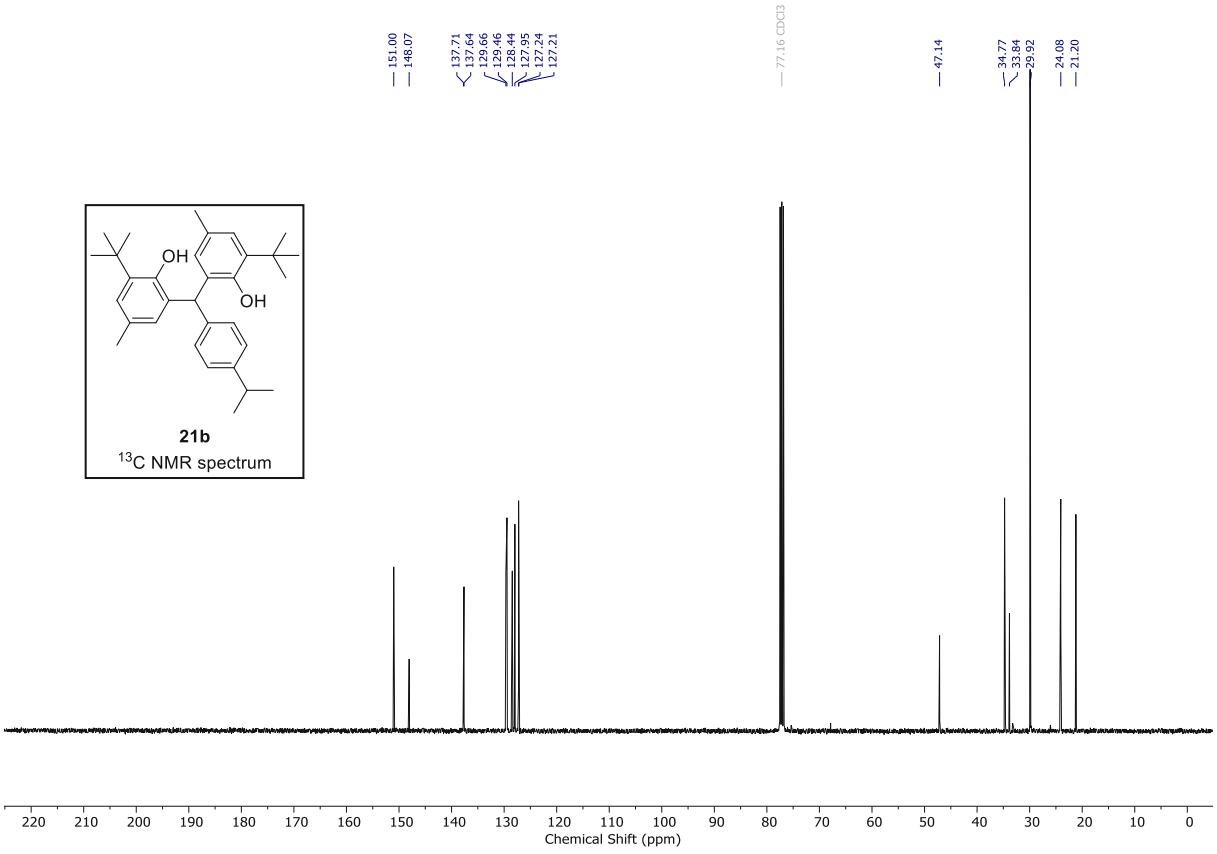
PA5
^{31}P NMR spectrum

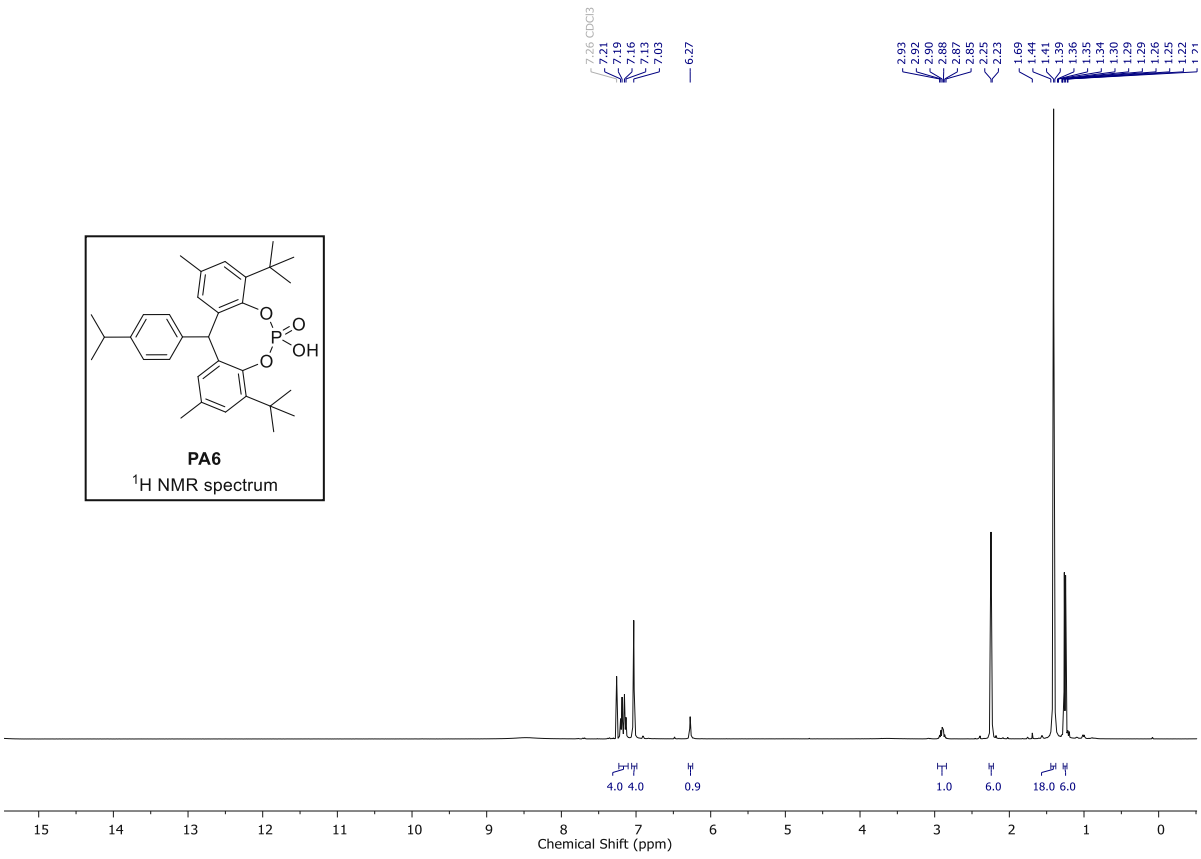


21b
^{1}H NMR spectrum

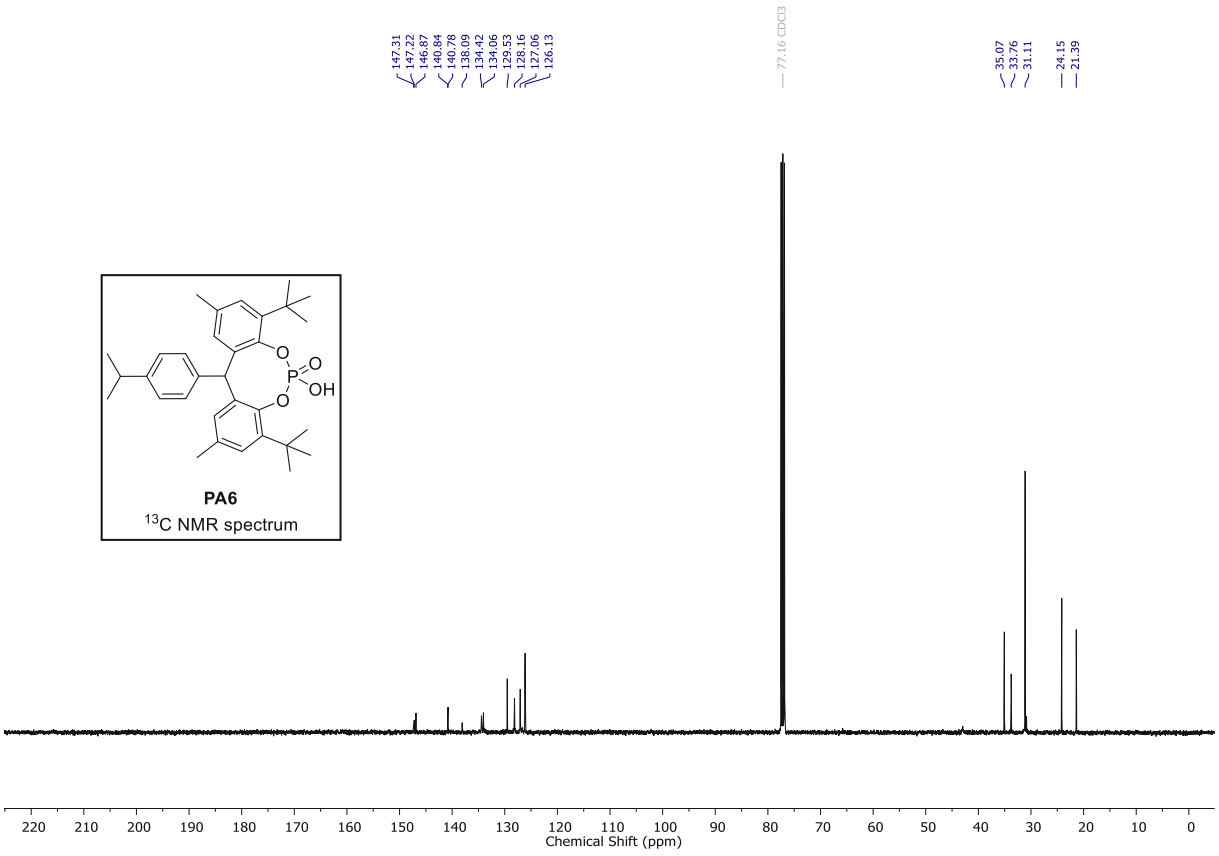


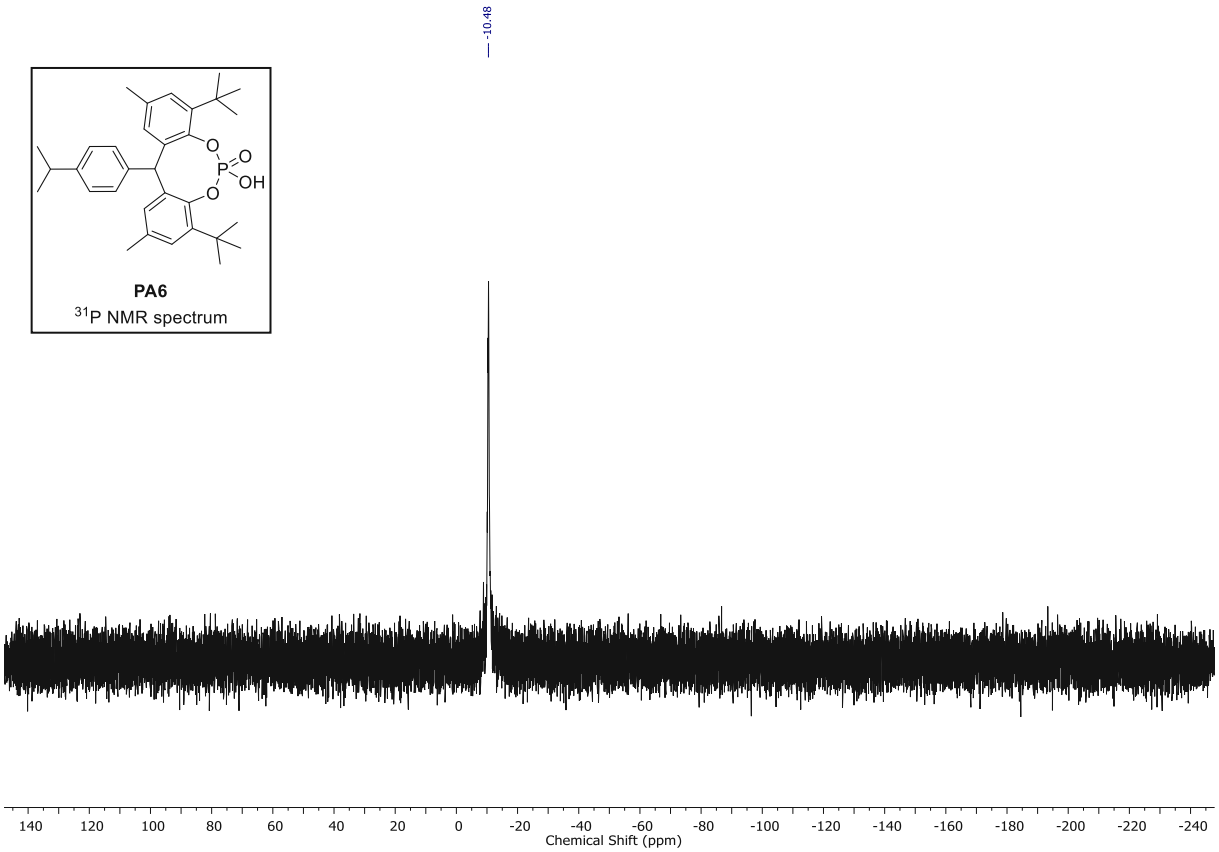
Die approbierte gedruckte Originalversion dieser Dissertation ist an der TU Wien Bibliothek verfügbar.
The approved original version of this doctoral thesis is available in print at TU Wien Bibliothek.
TU Bibliothek Your knowledge hub WIEN



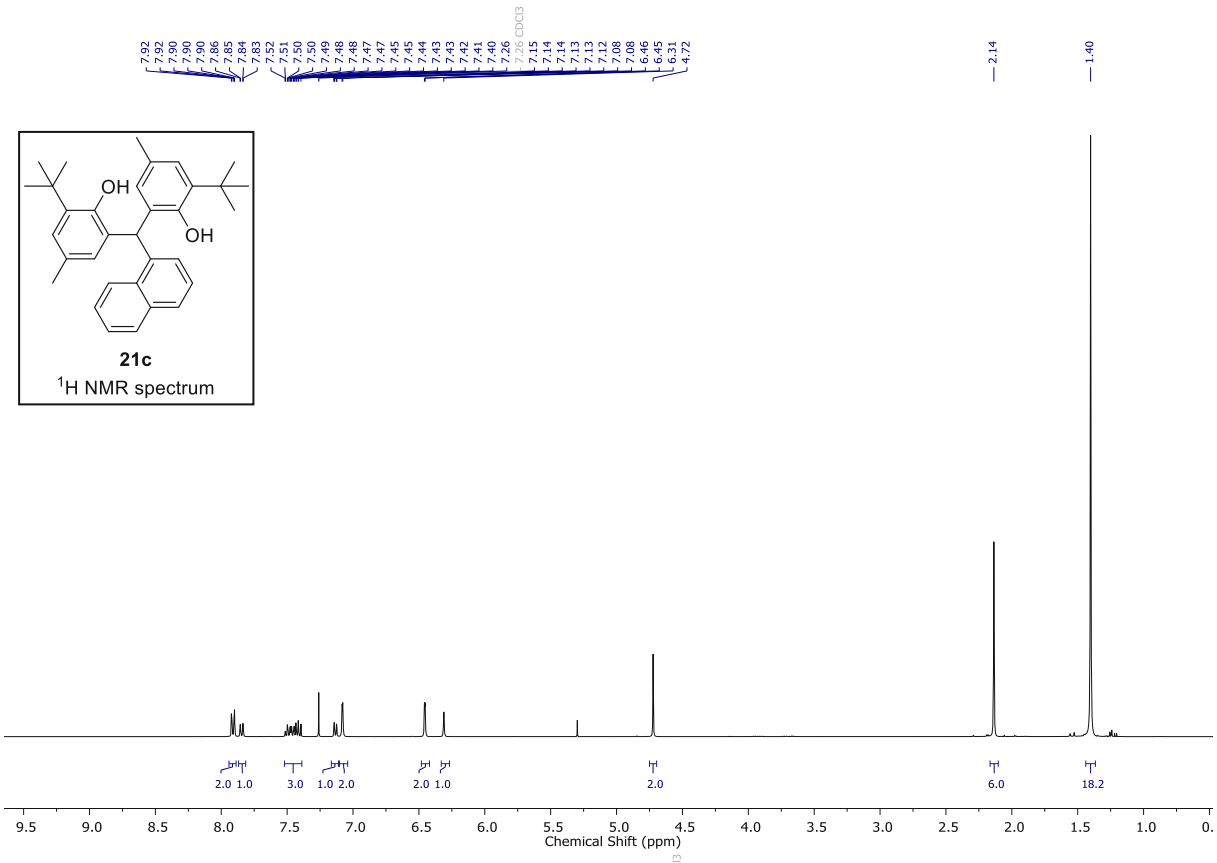


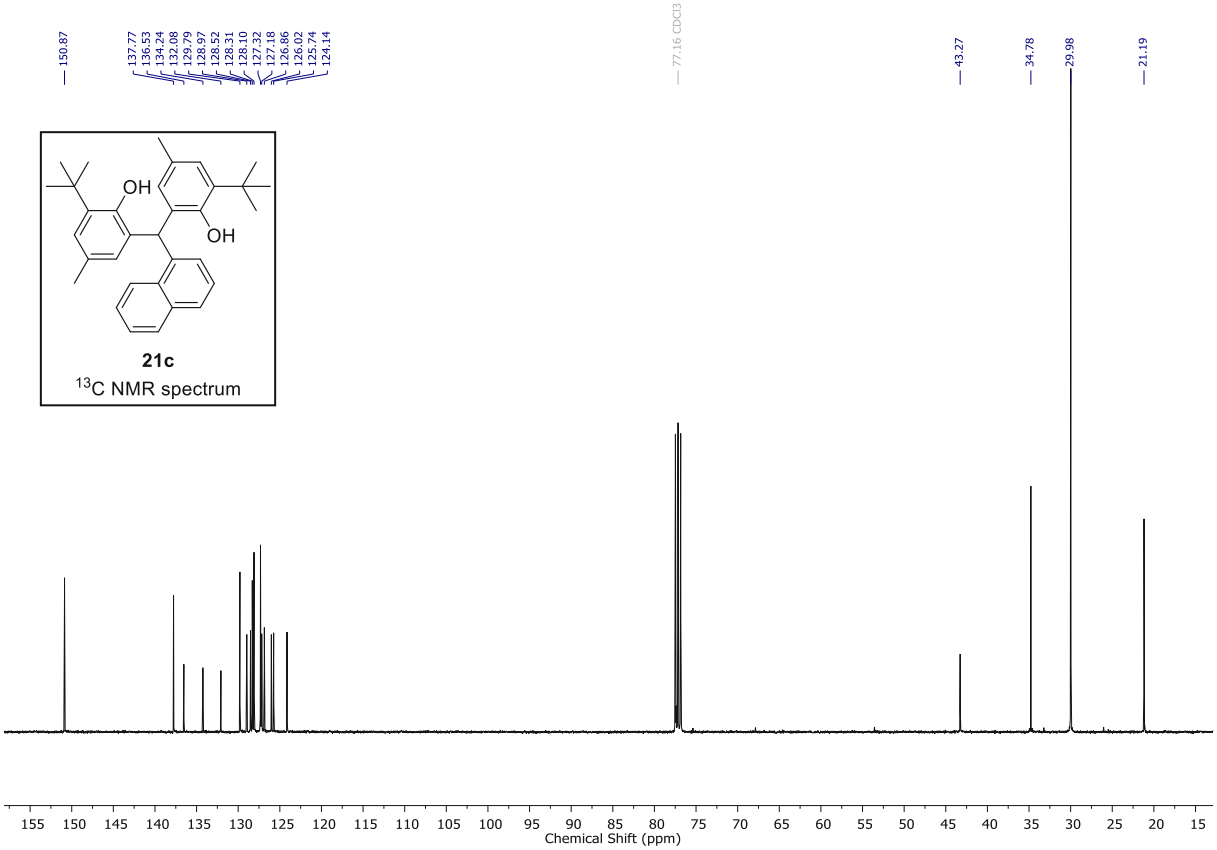
Die approbierte gedruckte Originalversion dieser Dissertation ist an der TU Wien Bibliothek verfügbar.
The approved original version of this doctoral thesis is available in print at TU Wien Bibliothek.



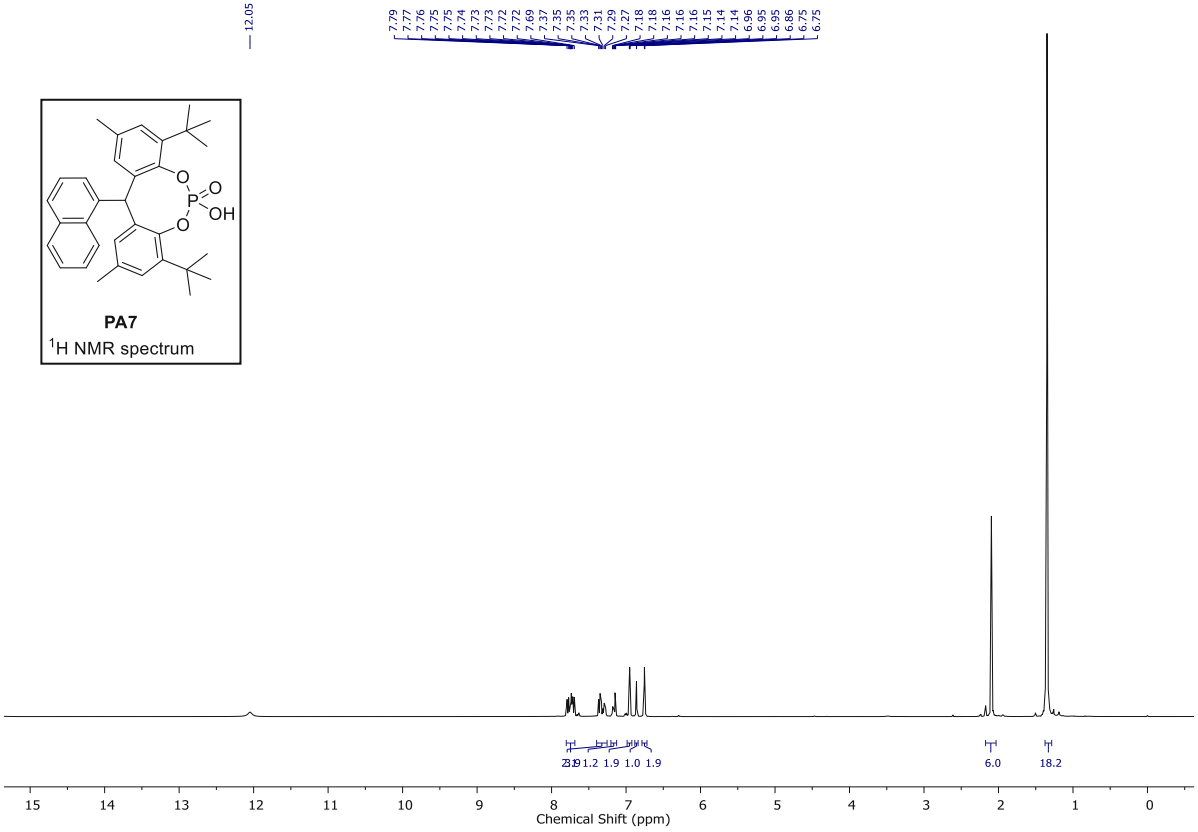


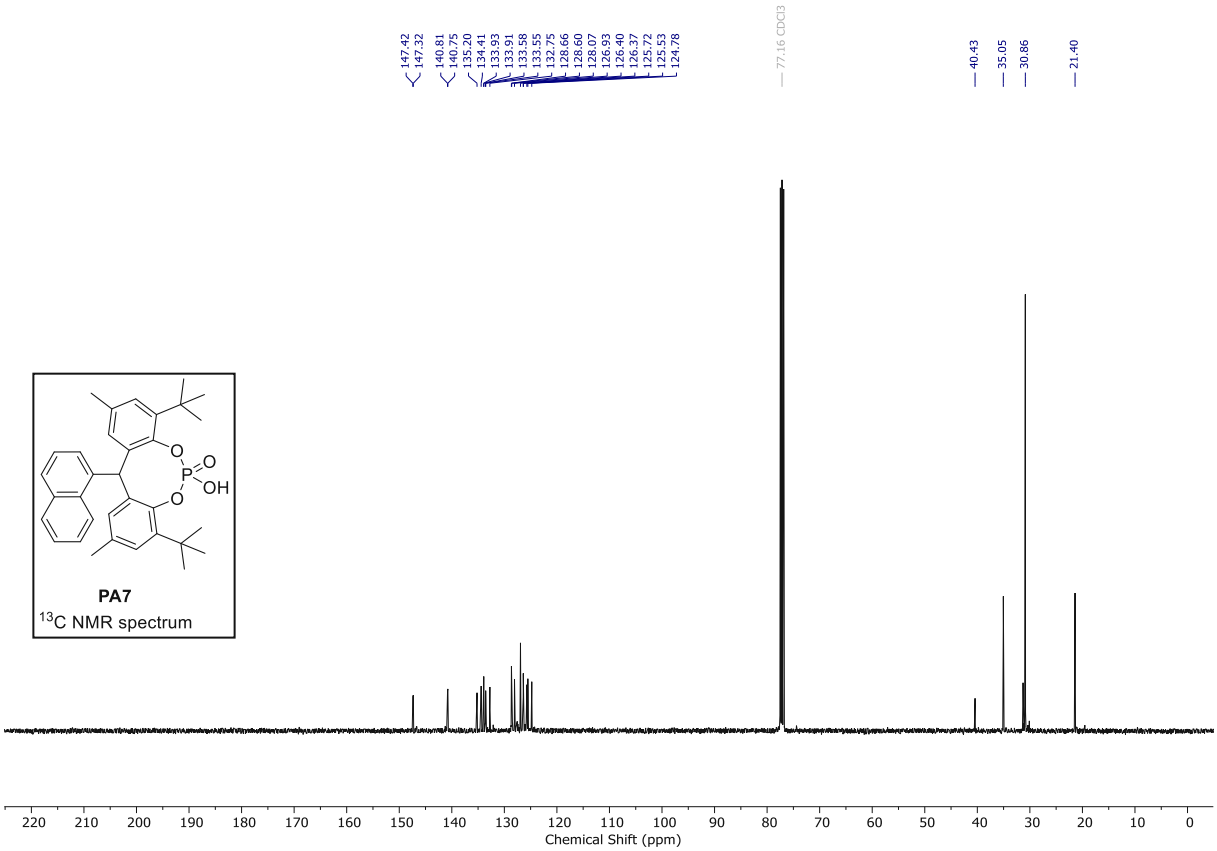
Die approbierte gedruckte Originalversion dieser Dissertation ist an der TU Wien Bibliothek verfügbar.
The approved original version of this doctoral thesis is available in print at TU Wien Bibliothek.



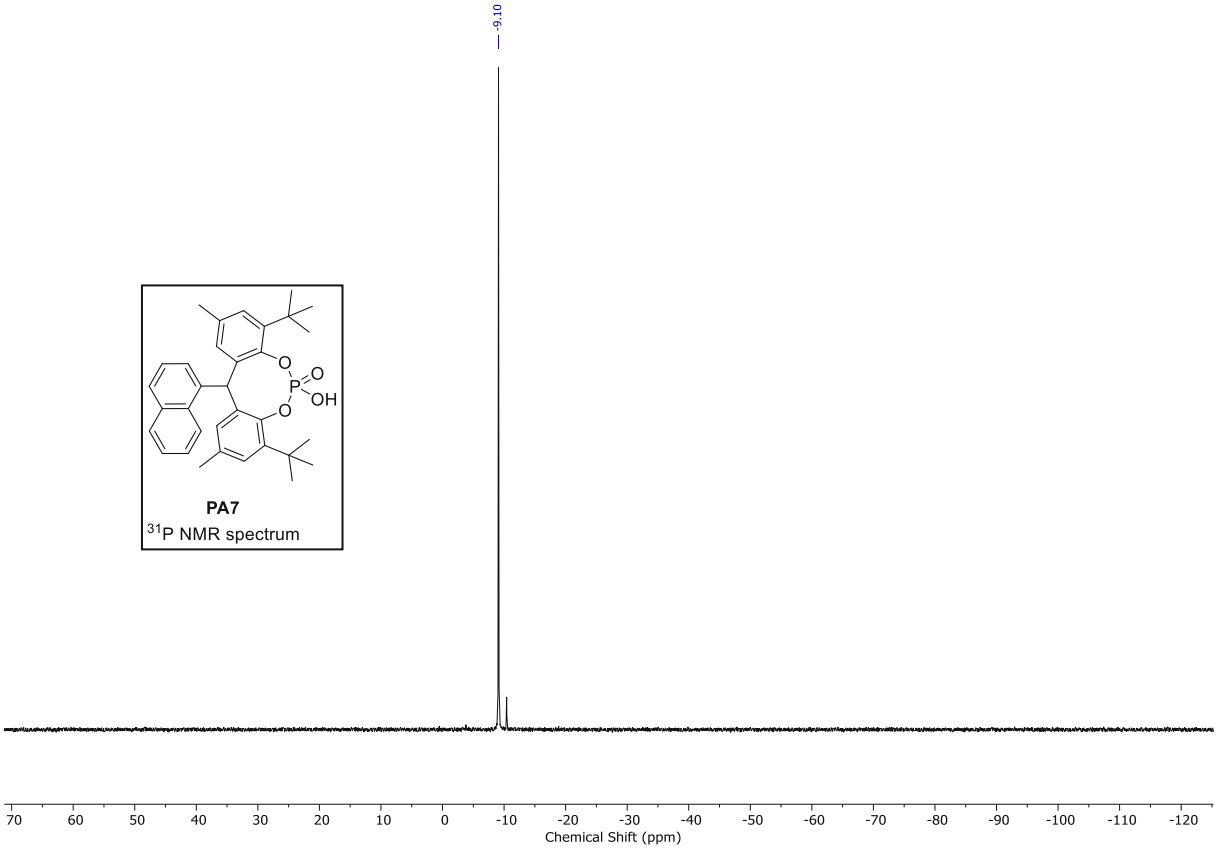


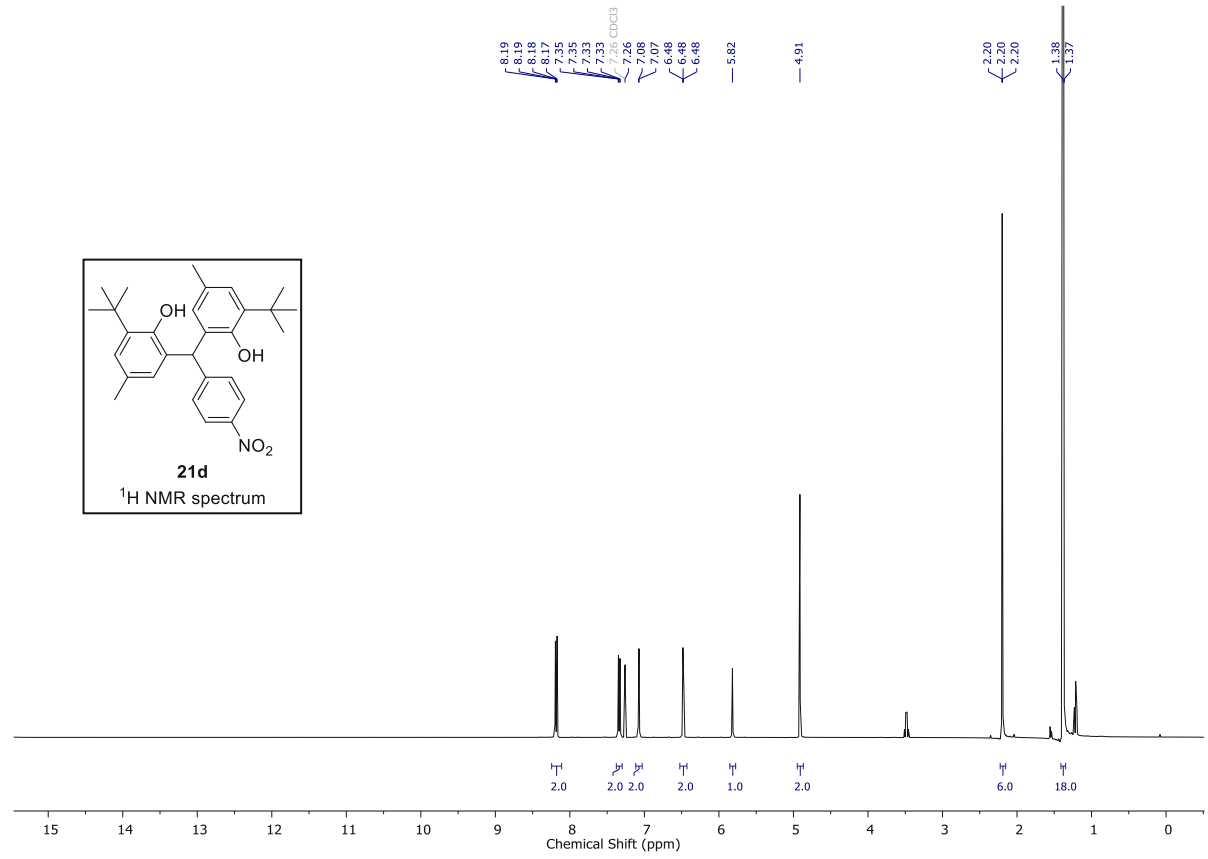
Die approbierte gedruckte Originalversion dieser Dissertation ist an der TU Wien Bibliothek verfügbar.
The approved original version of this doctoral thesis is available in print at TU Wien Bibliothek.



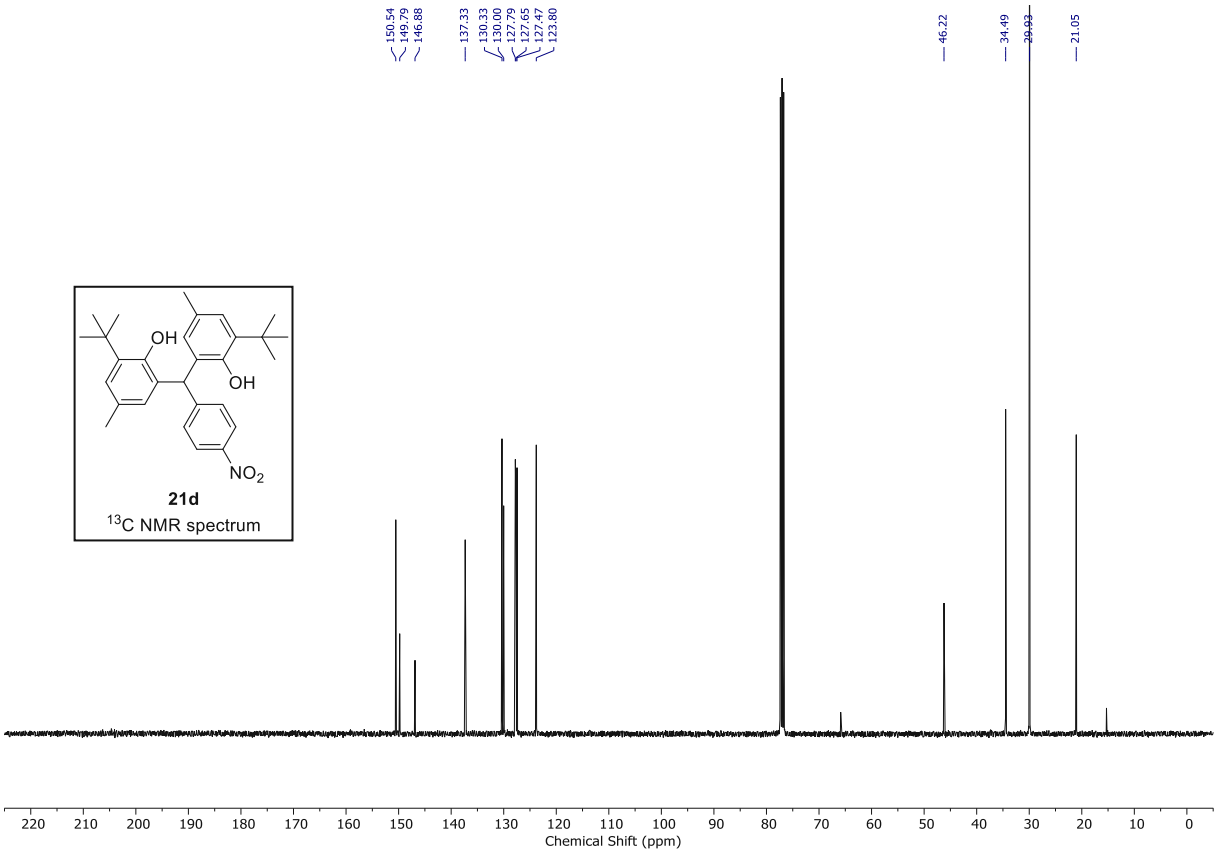


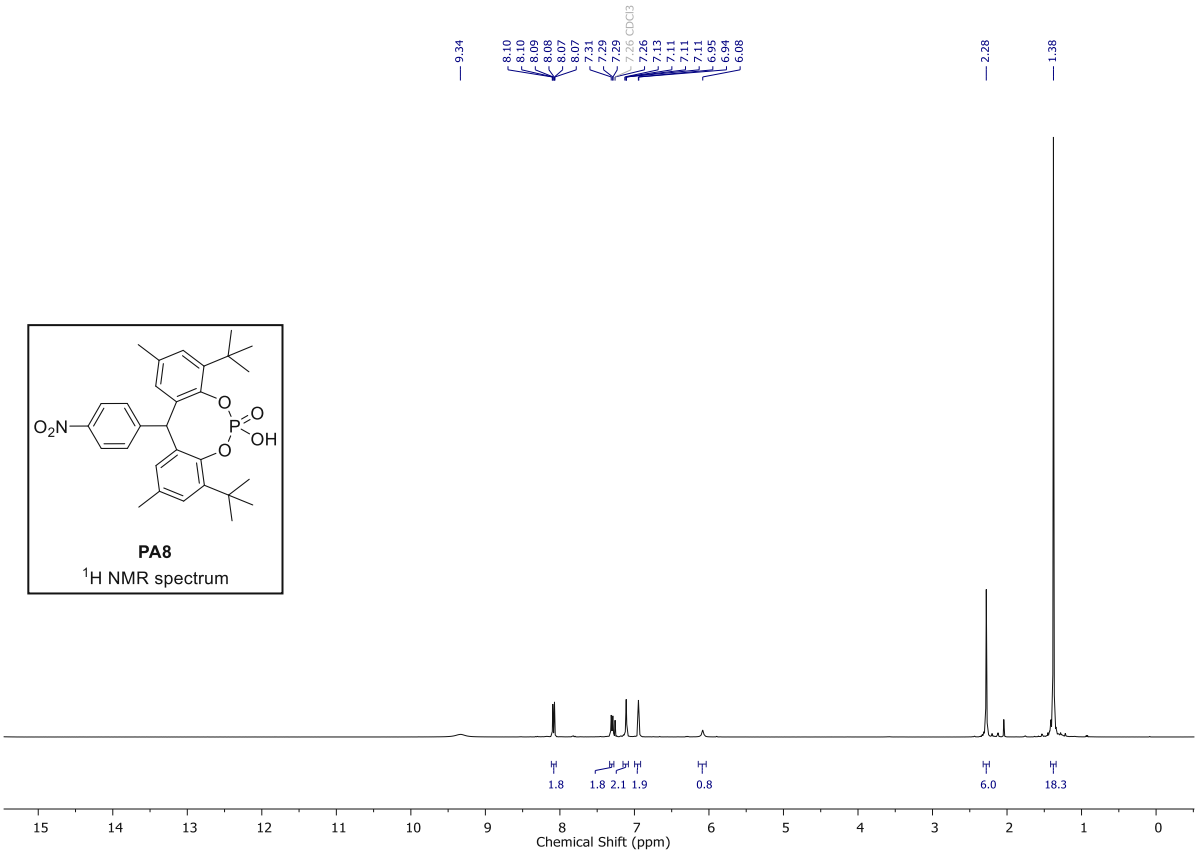
Die approbierte gedruckte Originalversion dieser Dissertation ist an der TU Wien Bibliothek verfügbar.
The approved original version of this doctoral thesis is available in print at TU Wien Bibliothek.



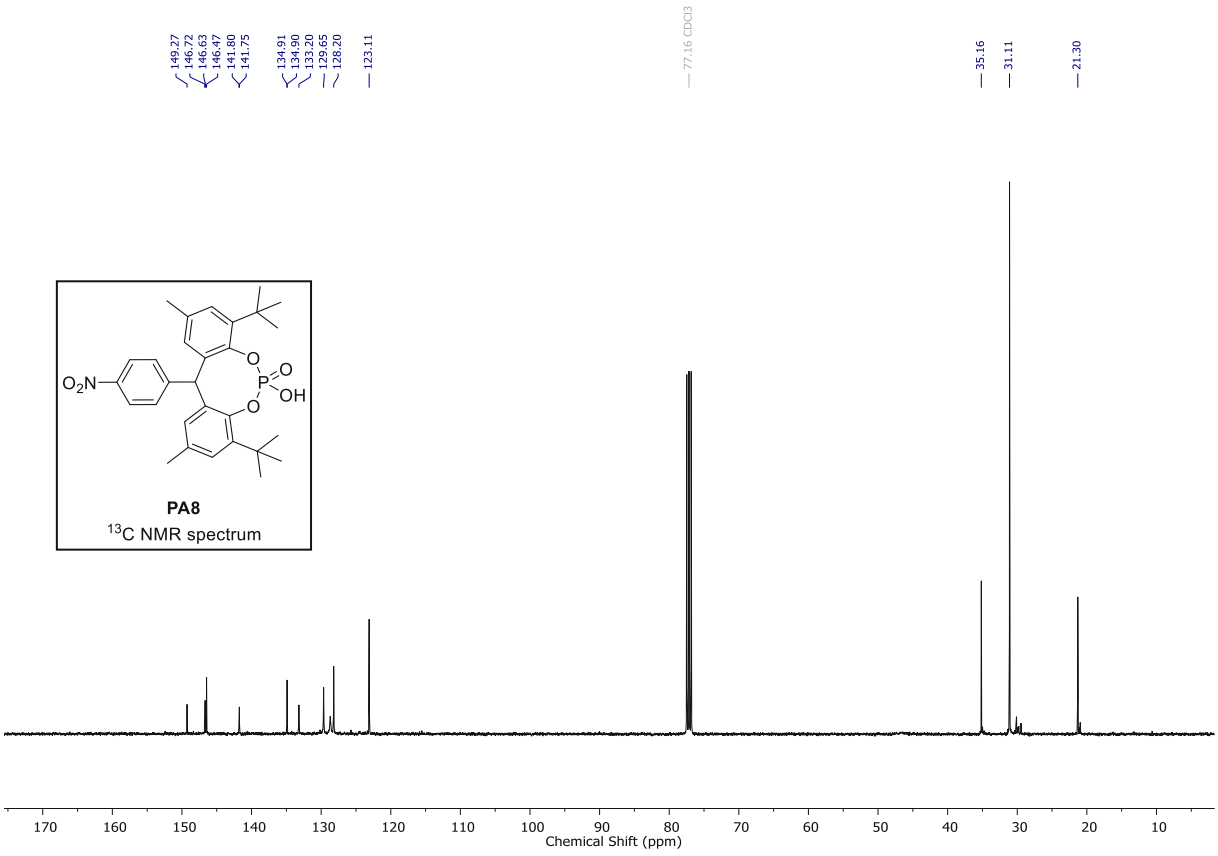


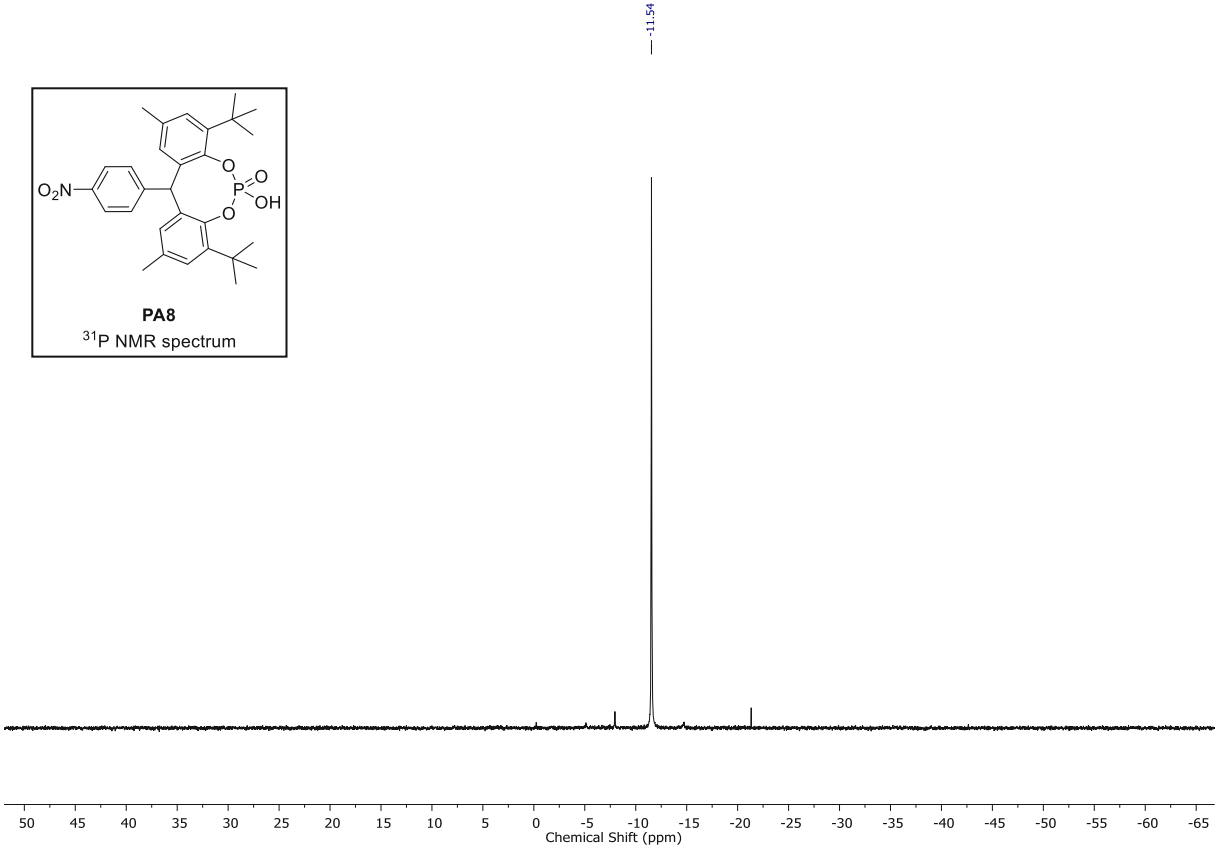
Die approbierte gedruckte Originalversion dieser Dissertation ist an der TU Wien Bibliothek verfügbar.
The approved original version of this doctoral thesis is available in print at TU Wien Bibliothek.



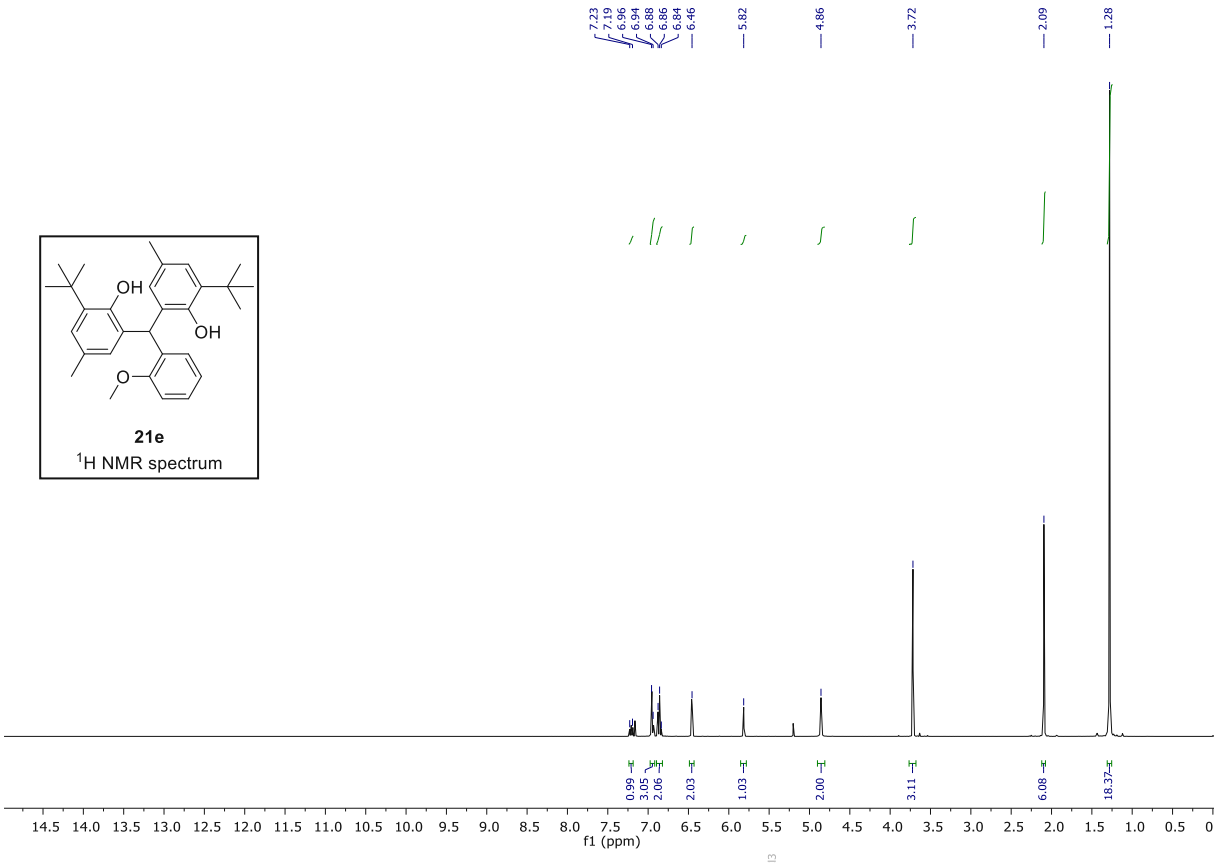


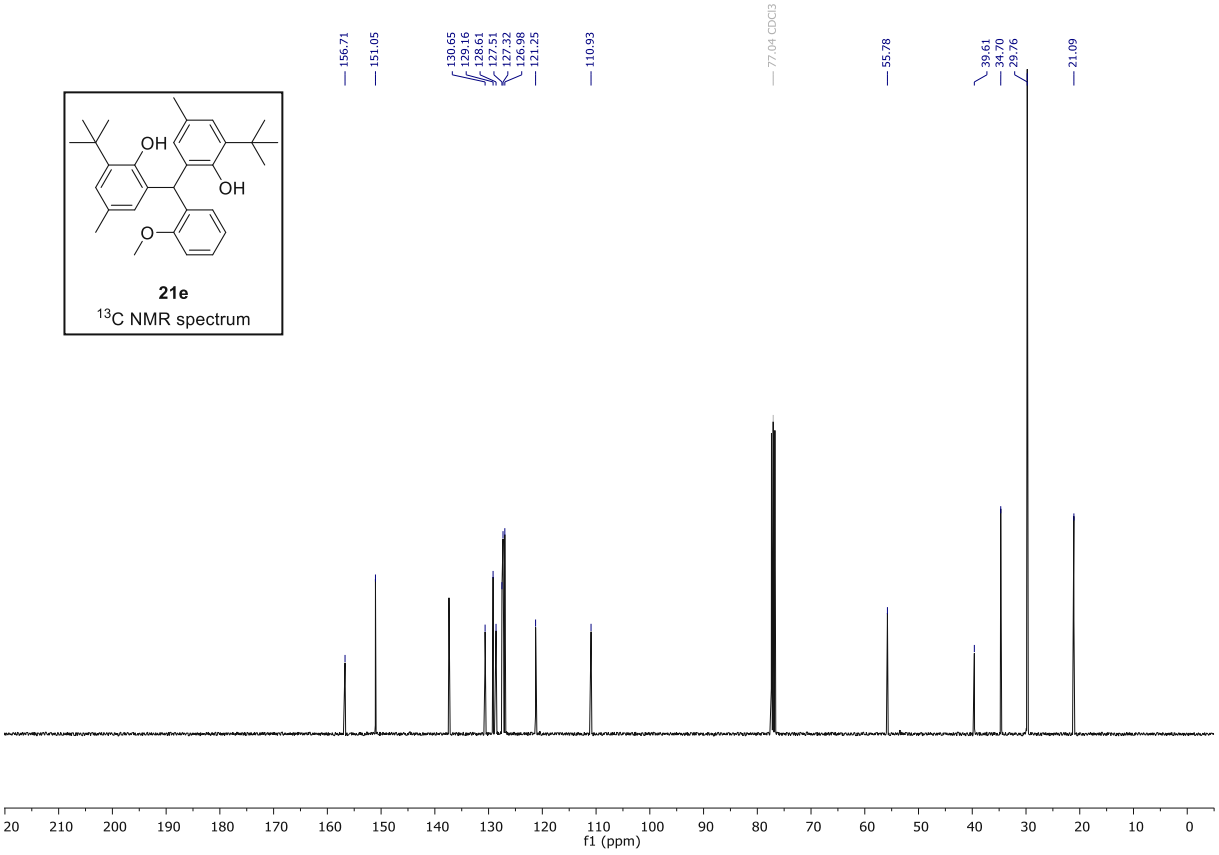
Die approbierte gedruckte Originalversion dieser Dissertation ist an der TU Wien Bibliothek verfügbar.
The approved original version of this doctoral thesis is available in print at TU Wien Bibliothek.



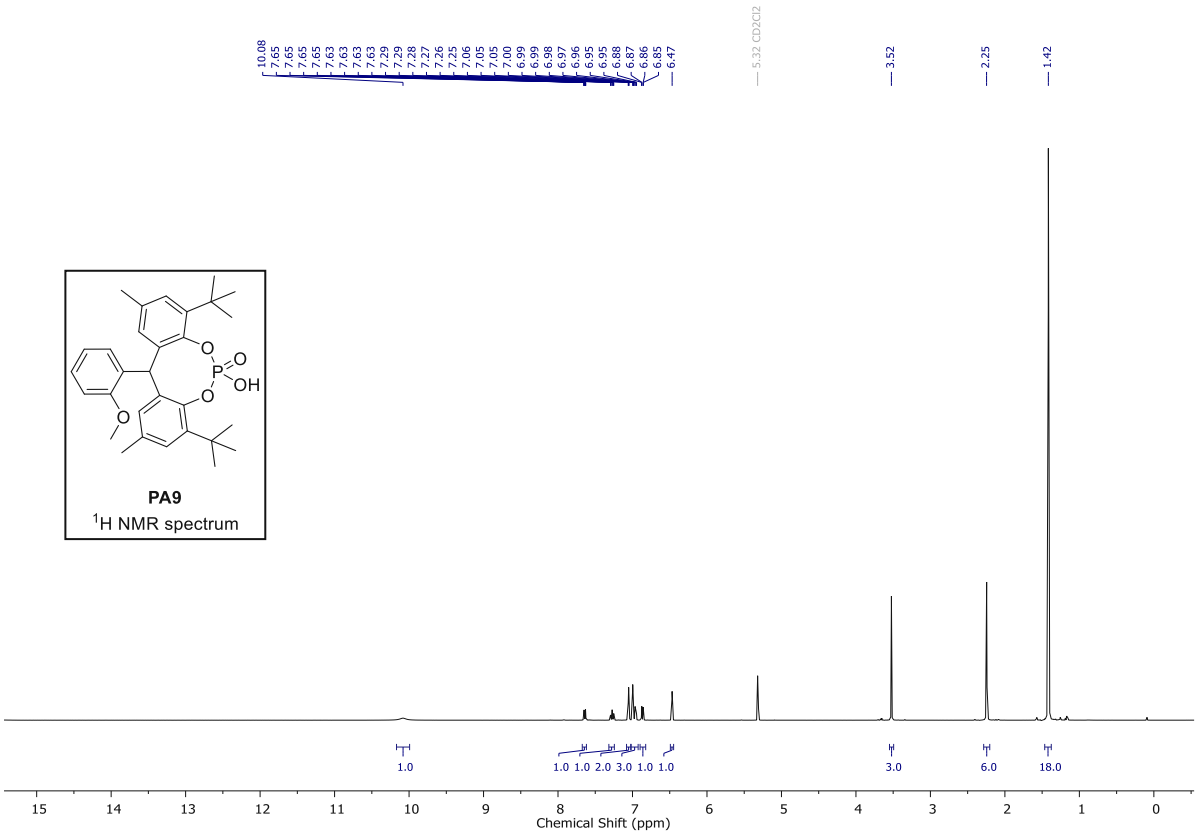


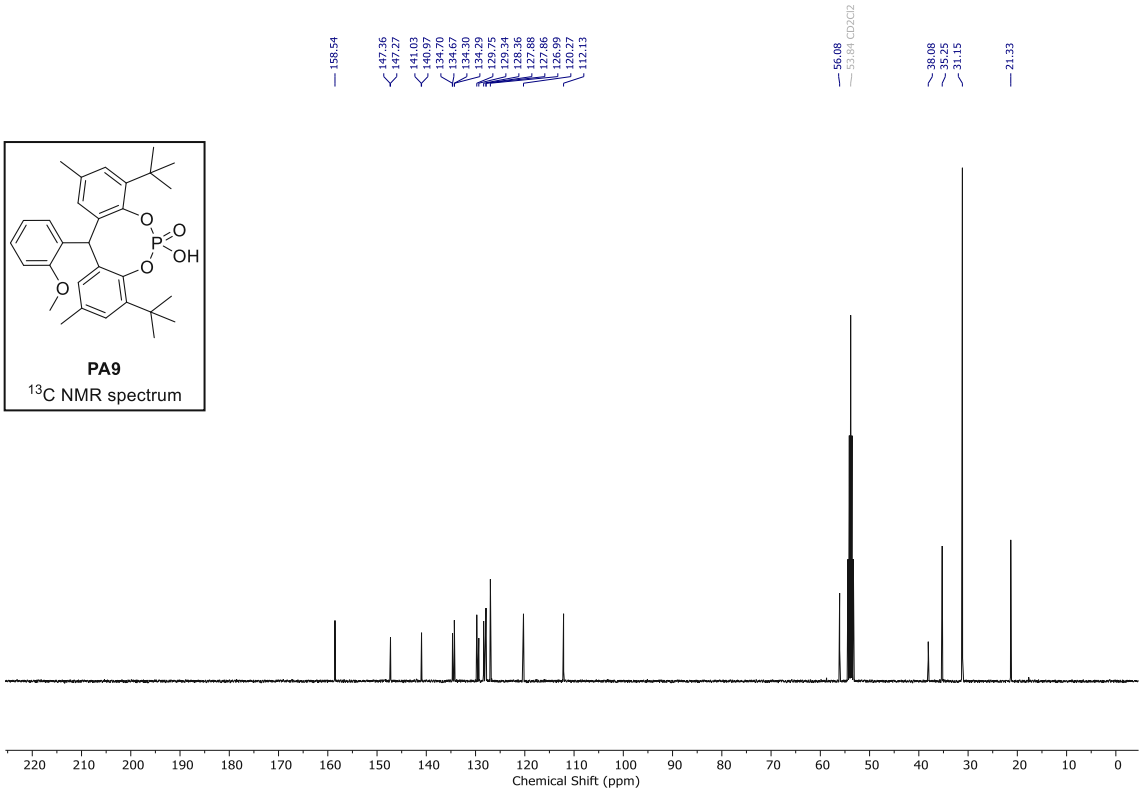
Die approbierte gedruckte Originalversion dieser Dissertation ist an der TU Wien Bibliothek verfügbar.
The approved original version of this doctoral thesis is available in print at TU Wien Bibliothek.



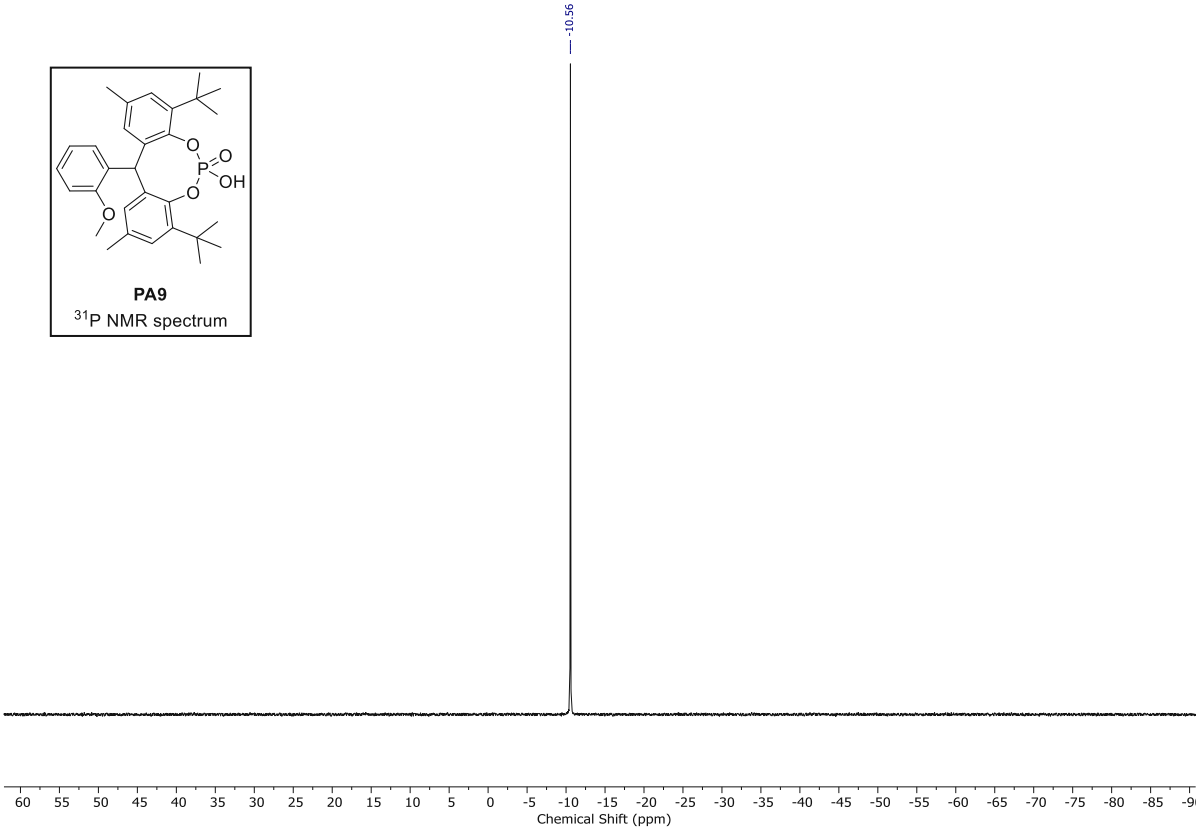


Die approbierte gedruckte Originalversion dieser Dissertation ist an der TU Wien Bibliothek verfügbar.
The approved original version of this doctoral thesis is available in print at TU Wien Bibliothek.



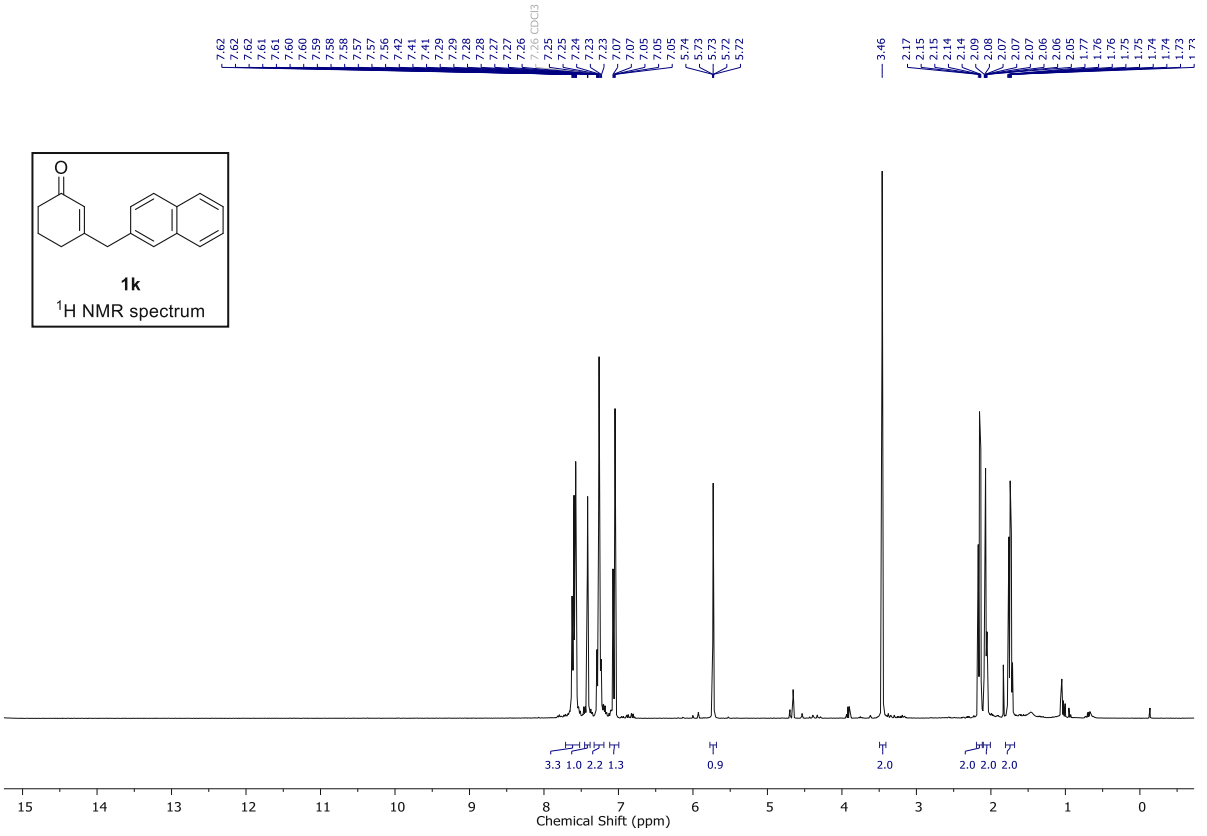


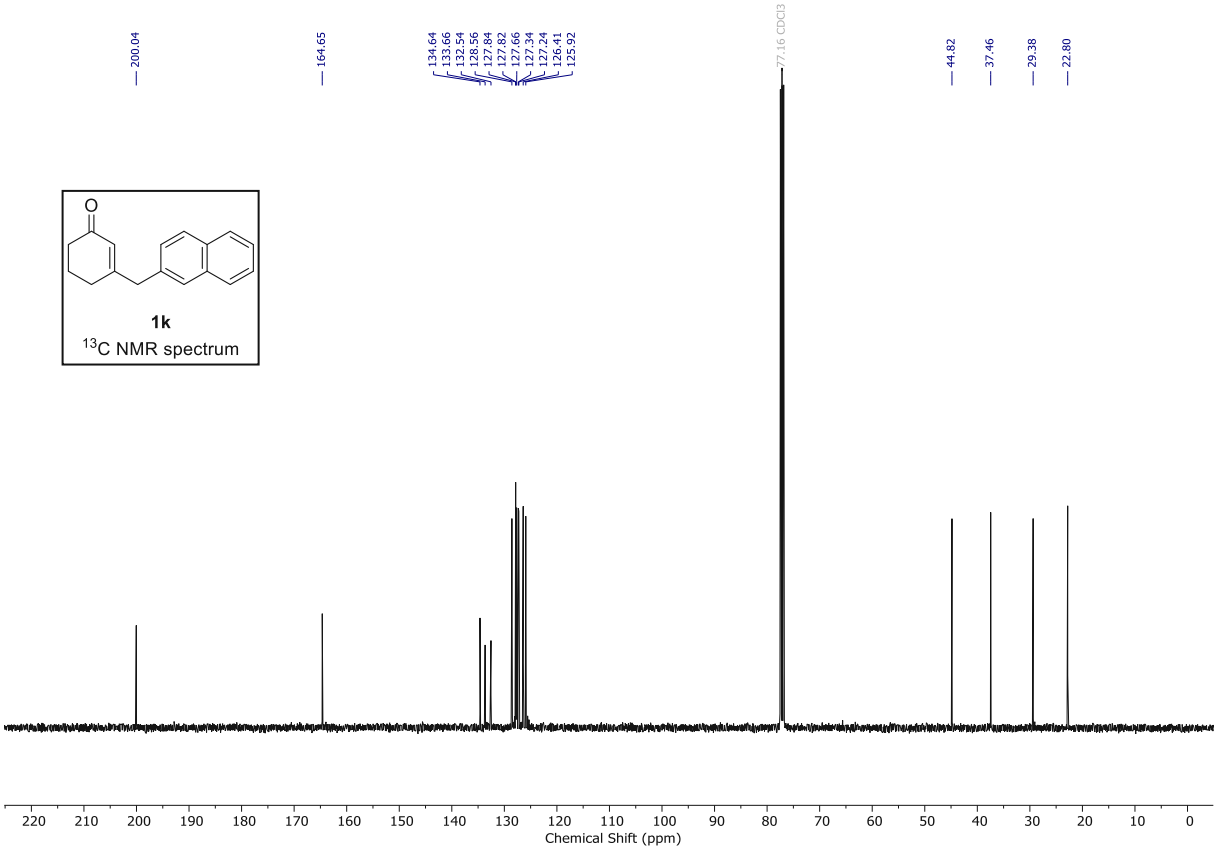
Die approbierte gedruckte Originalversion dieser Dissertation ist an der TU Wien Bibliothek verfügbar.
The approved original version of this doctoral thesis is available in print at TU Wien Bibliothek.



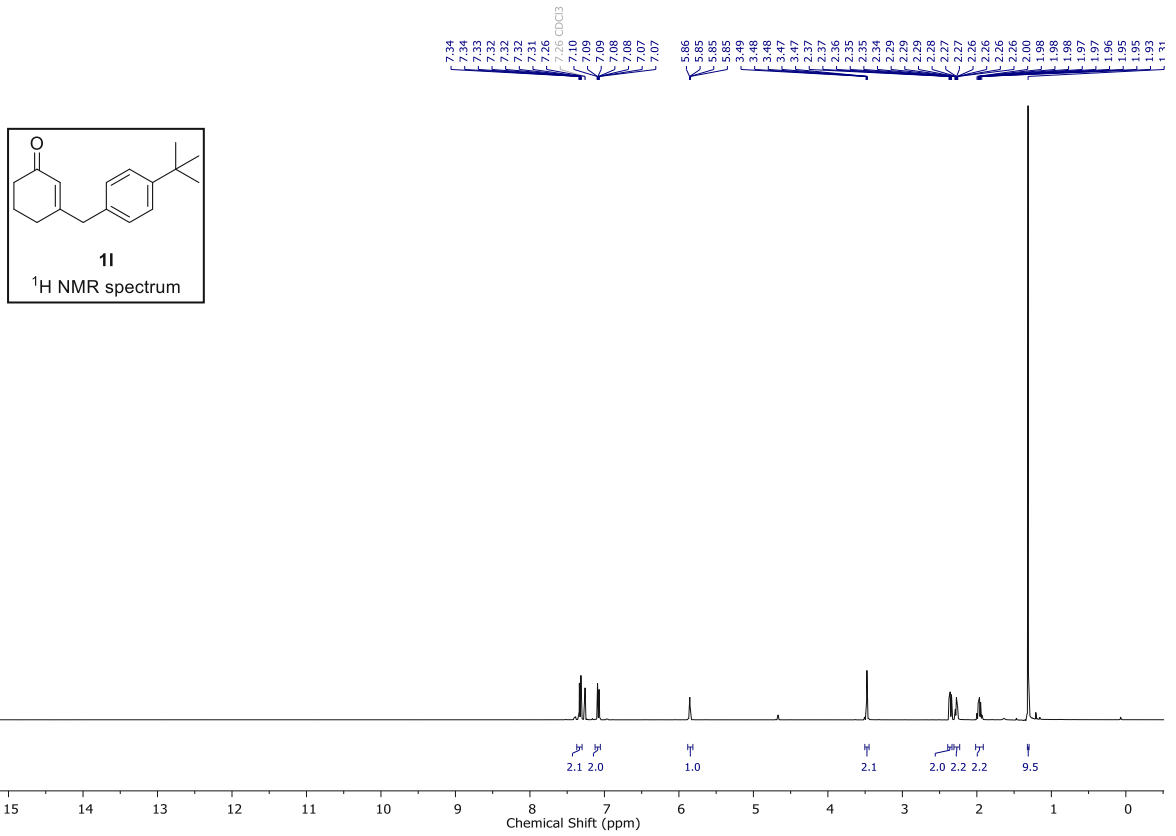
Die approbierte gedruckte Originalversion dieser Dissertation ist an der TU Wien Bibliothek verfügbar.
The approved original version of this doctoral thesis is available in print at TU Wien Bibliothek.

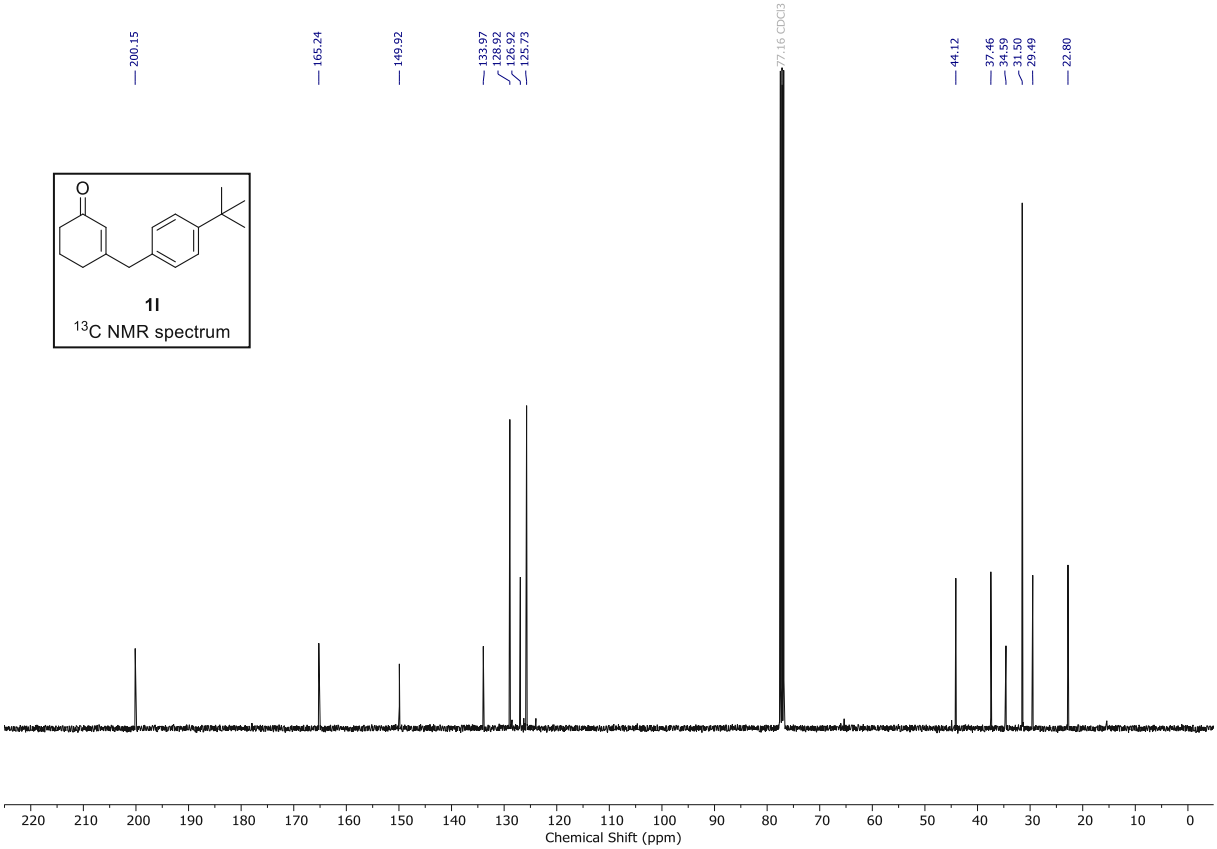
17. NMR spectra of literature unknown enone substrates





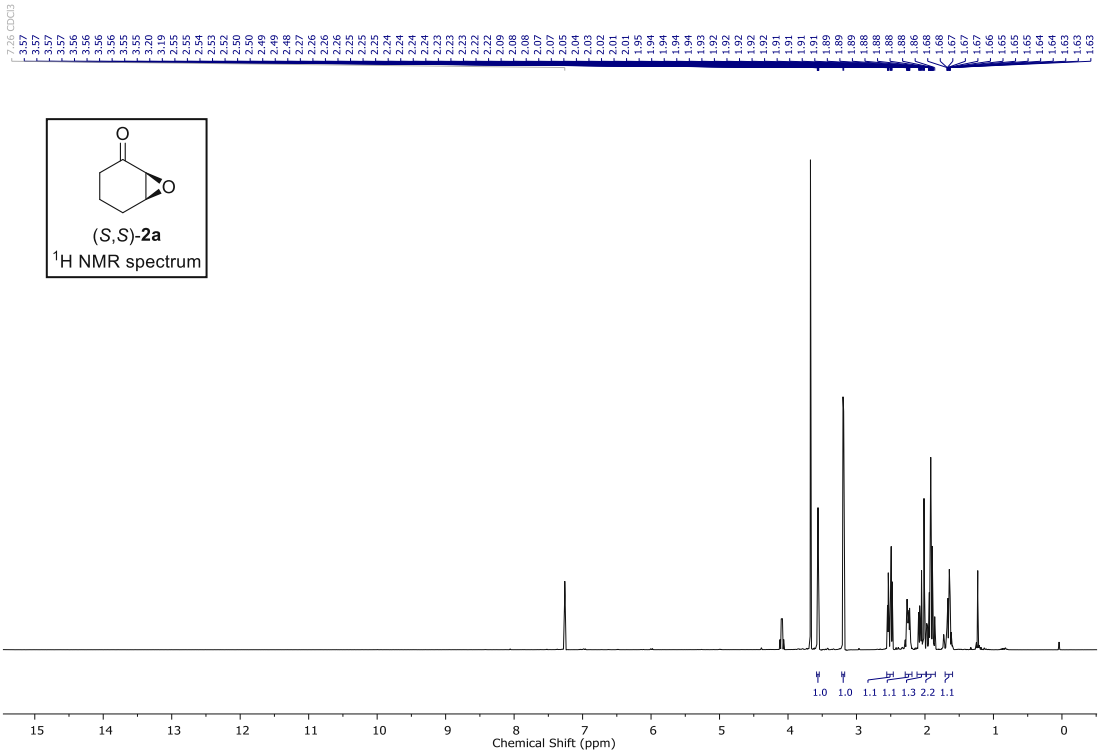
Die approbierte gedruckte Originalversion dieser Dissertation ist an der TU Wien Bibliothek verfügbar.
The approved original version of this doctoral thesis is available in print at TU Wien Bibliothek.

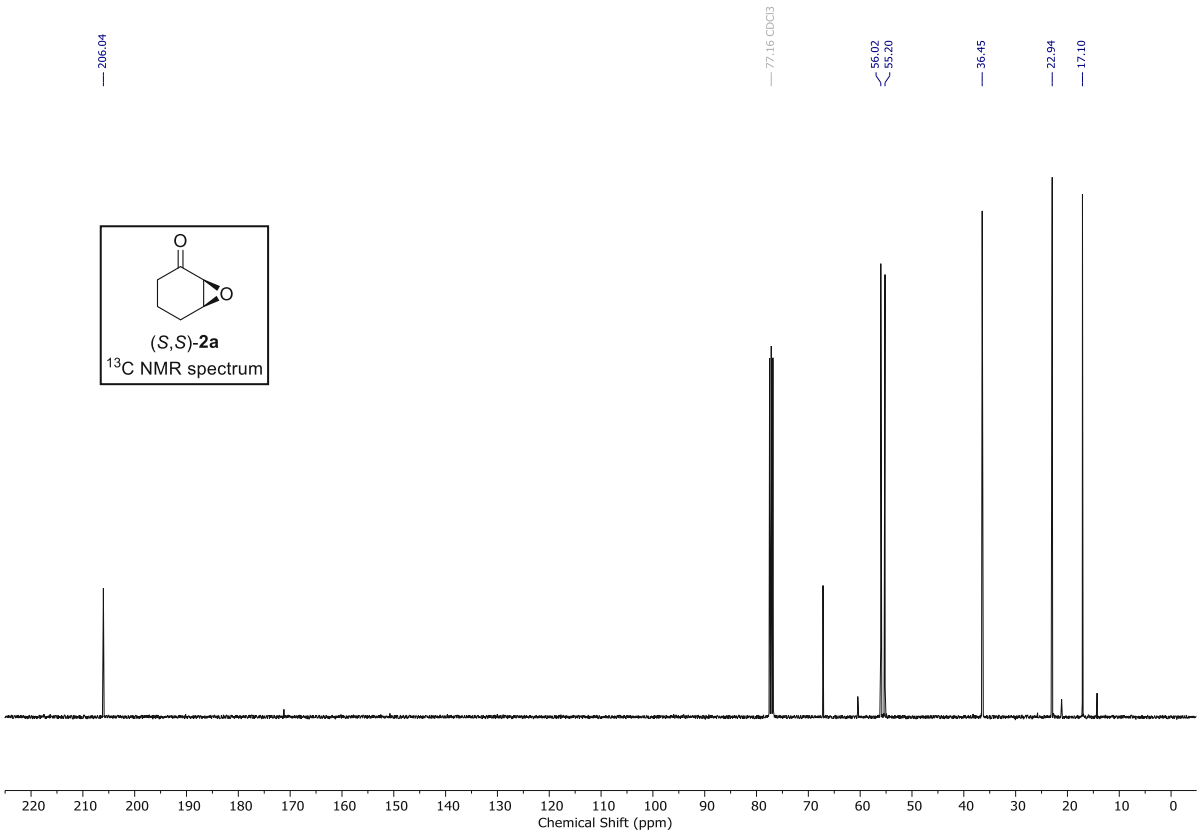




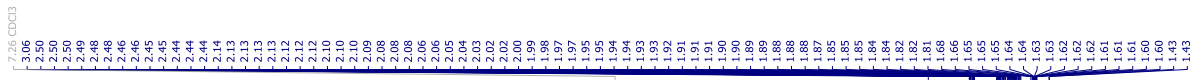
Die approbierte gedruckte Originalversion dieser Dissertation ist an der TU Wien Bibliothek verfügbar.
The approved original version of this doctoral thesis is available in print at TU Wien Bibliothek.

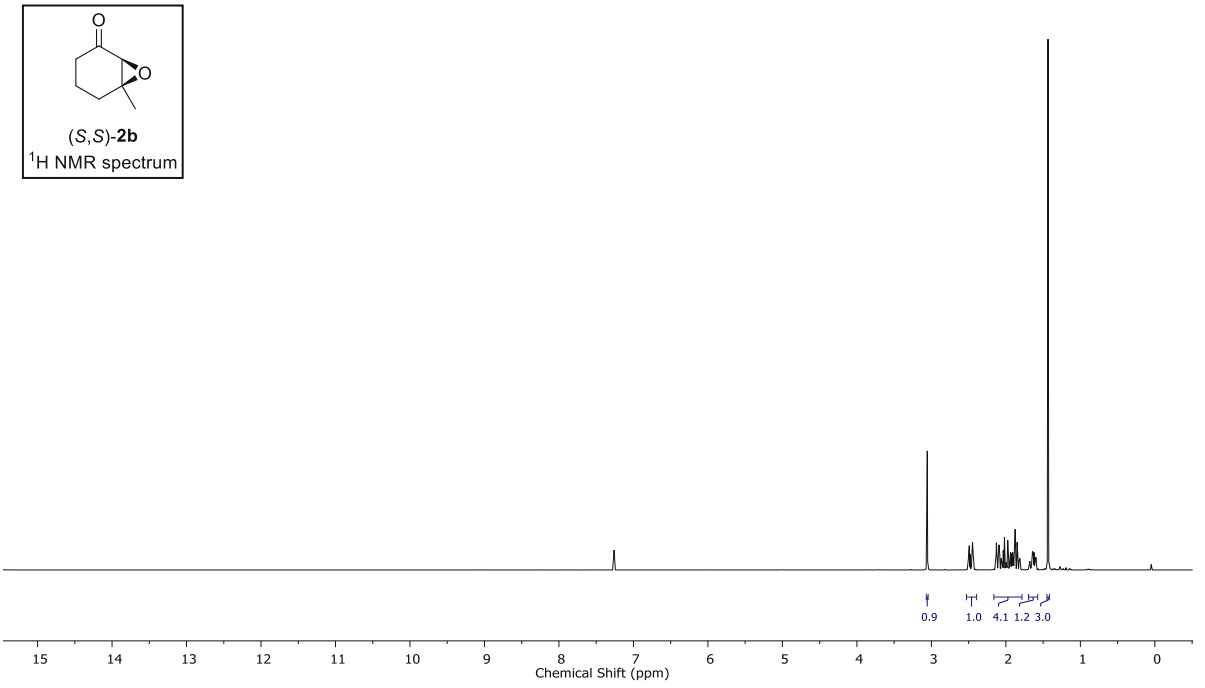
18. NMR spectra for the asymmetric epoxidations

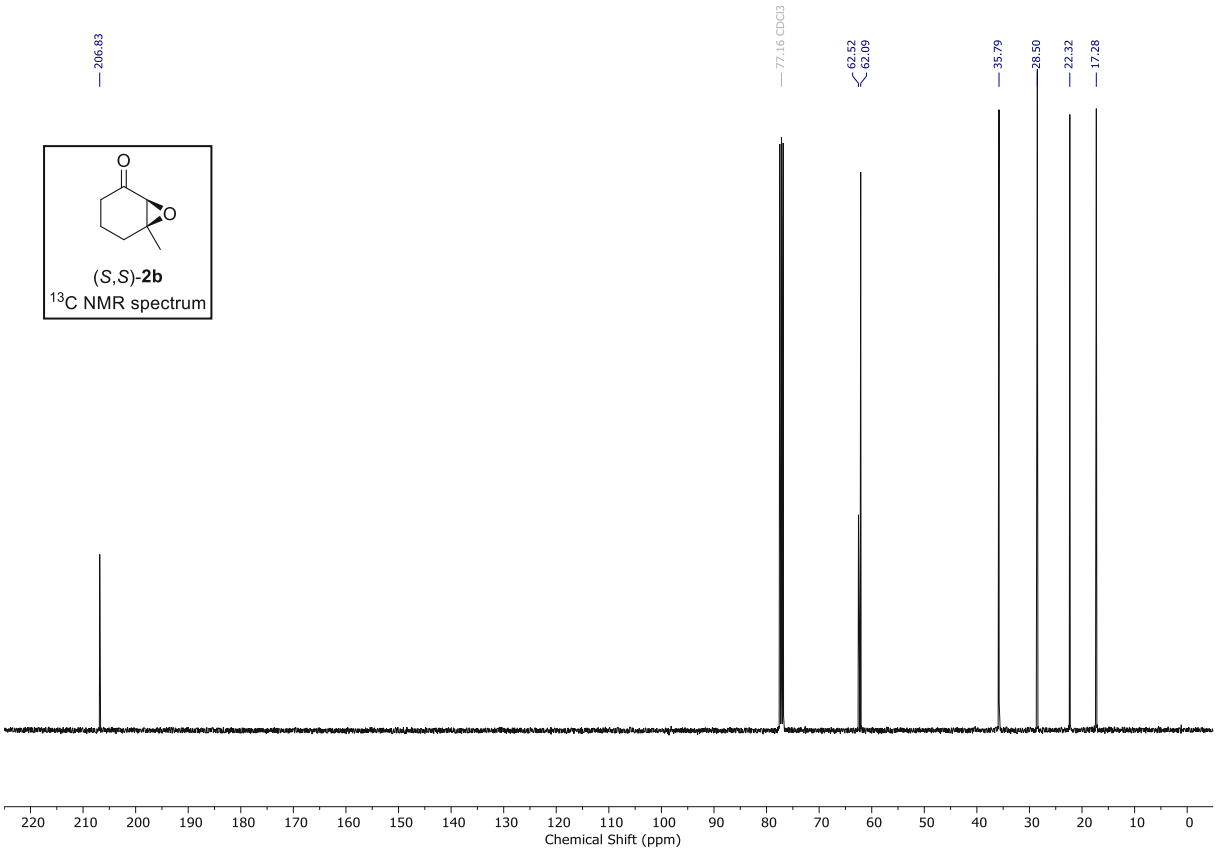




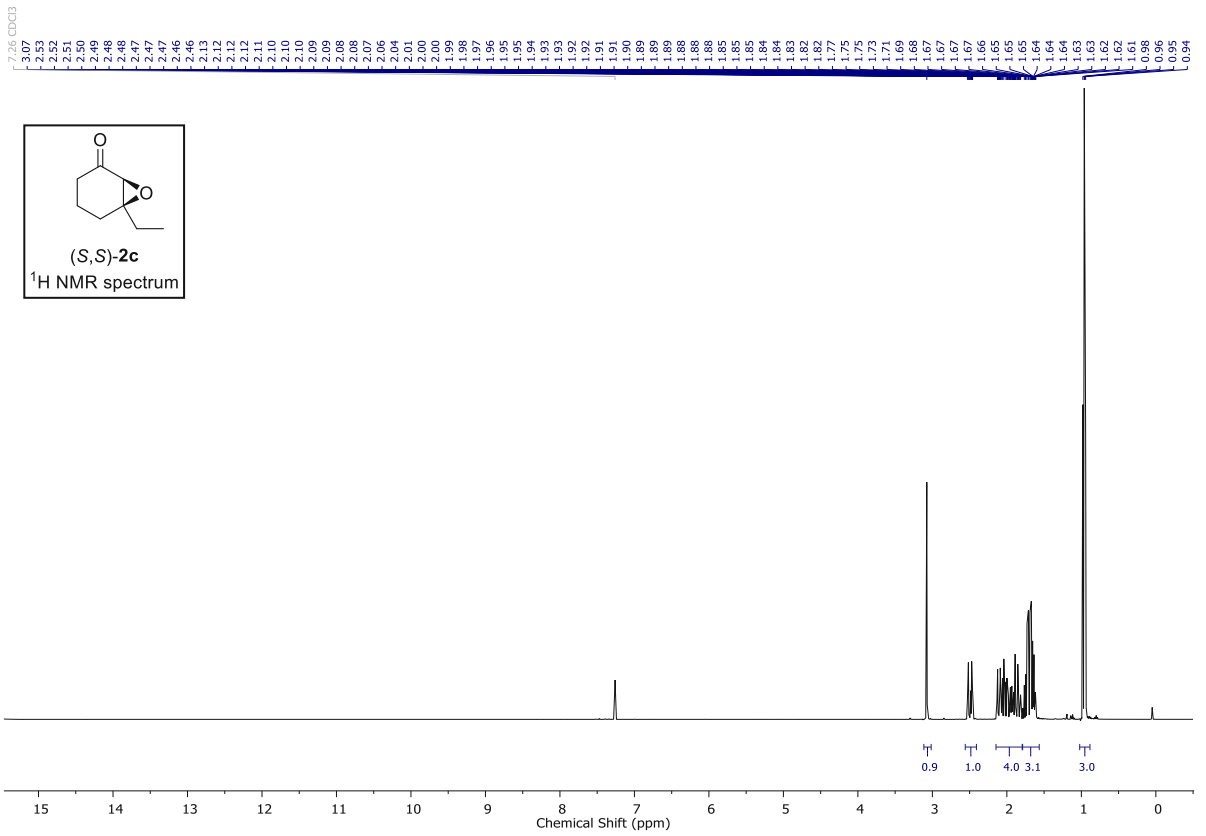
Die approbierte gedruckte Originalversion dieser Dissertation ist an der TU Wien Bibliothek verfügbar.
The approved original version of this doctoral thesis is available in print at TU Wien Bibliothek.

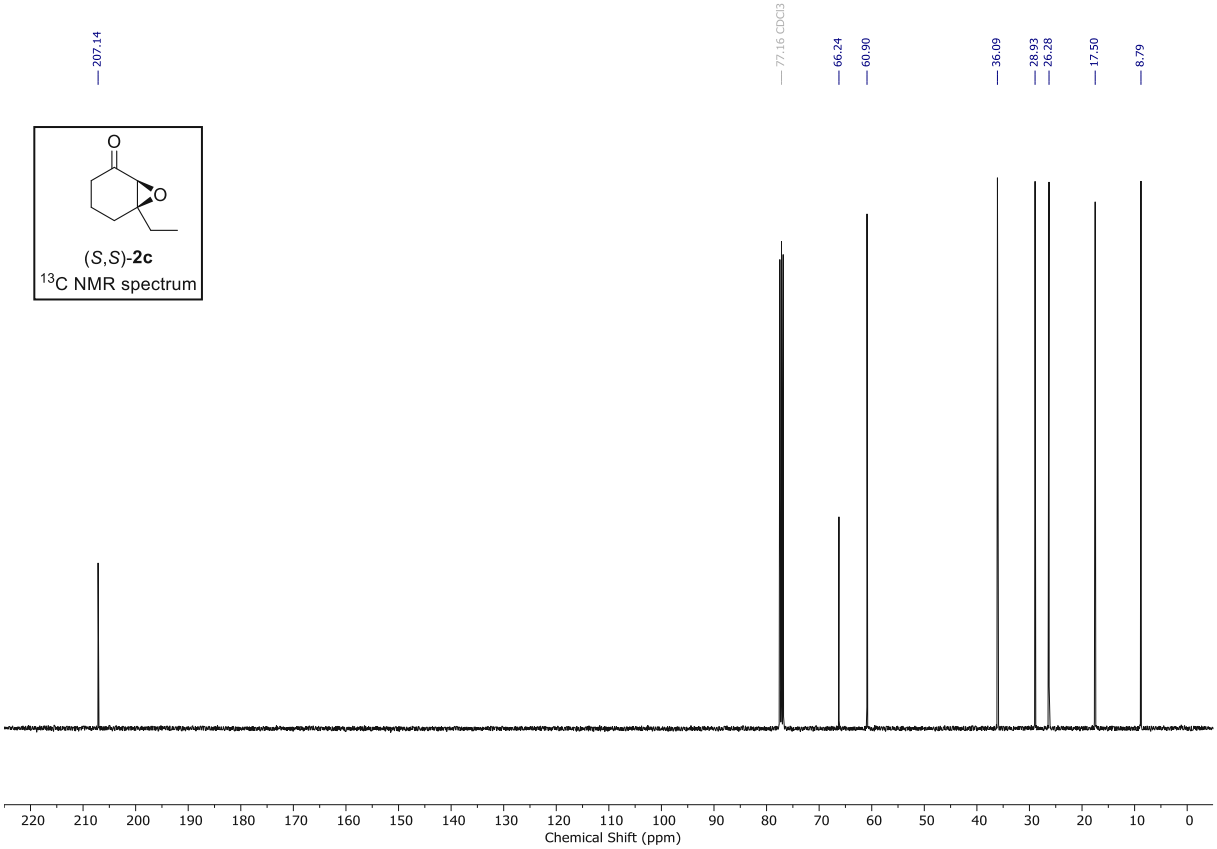






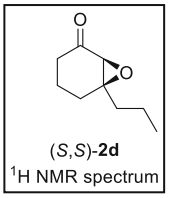
Die approbierte gedruckte Originalversion dieser Dissertation ist an der TU Wien Bibliothek verfügbar.
The approved original version of this doctoral thesis is available in print at TU Wien Bibliothek.

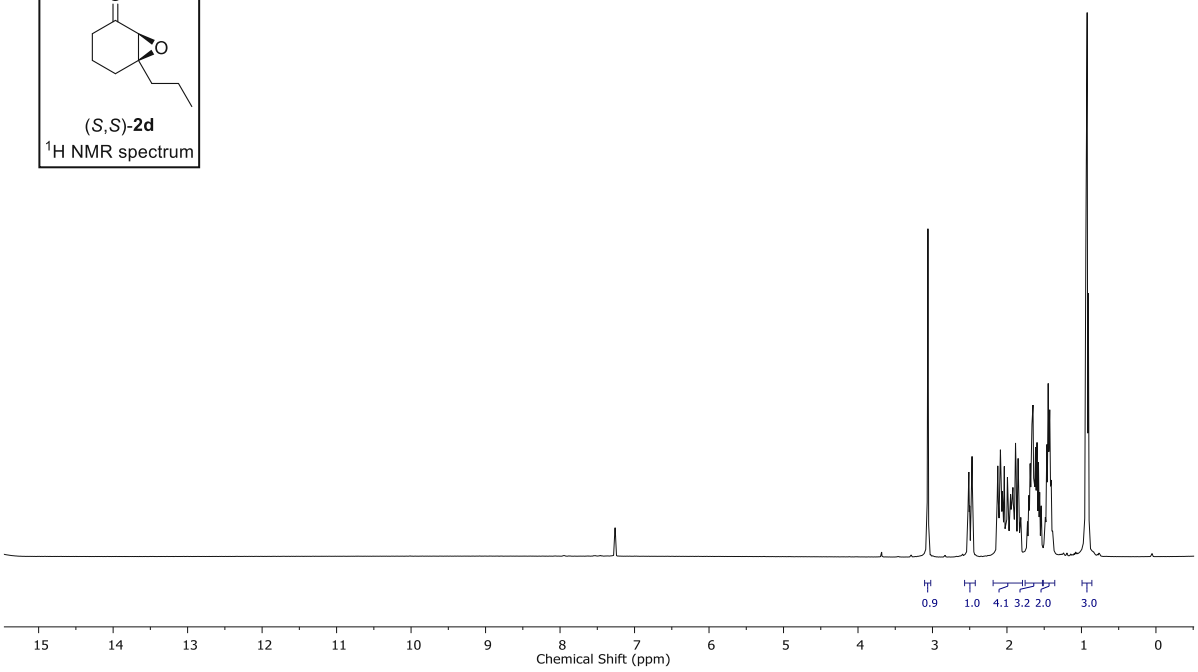


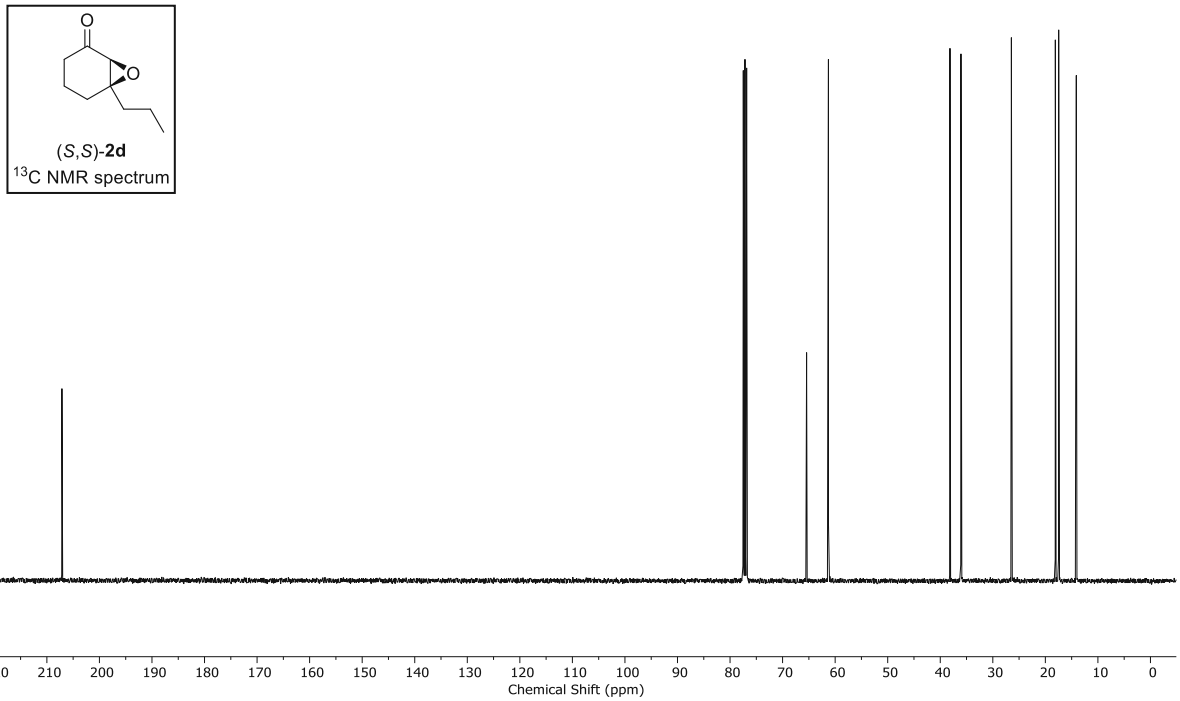


Die approbierte gedruckte Originalversion dieser Dissertation ist an der TU Wien Bibliothek verfügbar.
The approved original version of this doctoral thesis is available in print at TU Wien Bibliothek.

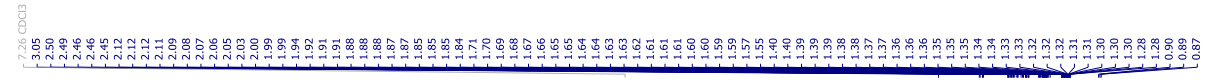


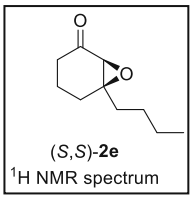


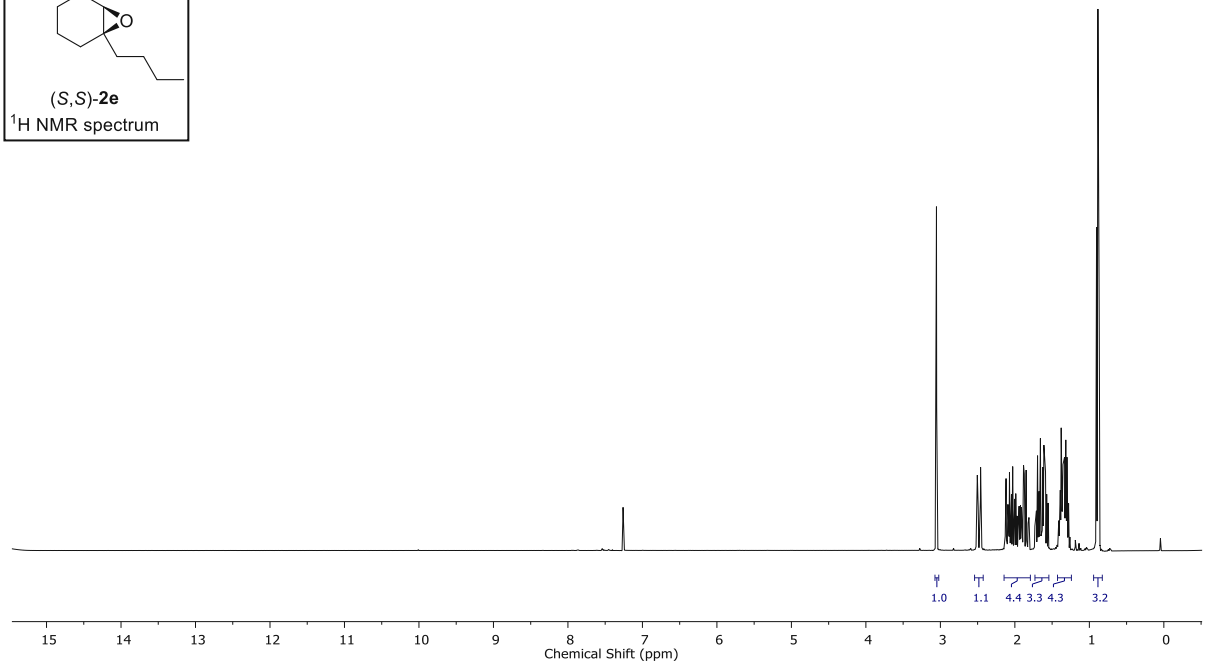


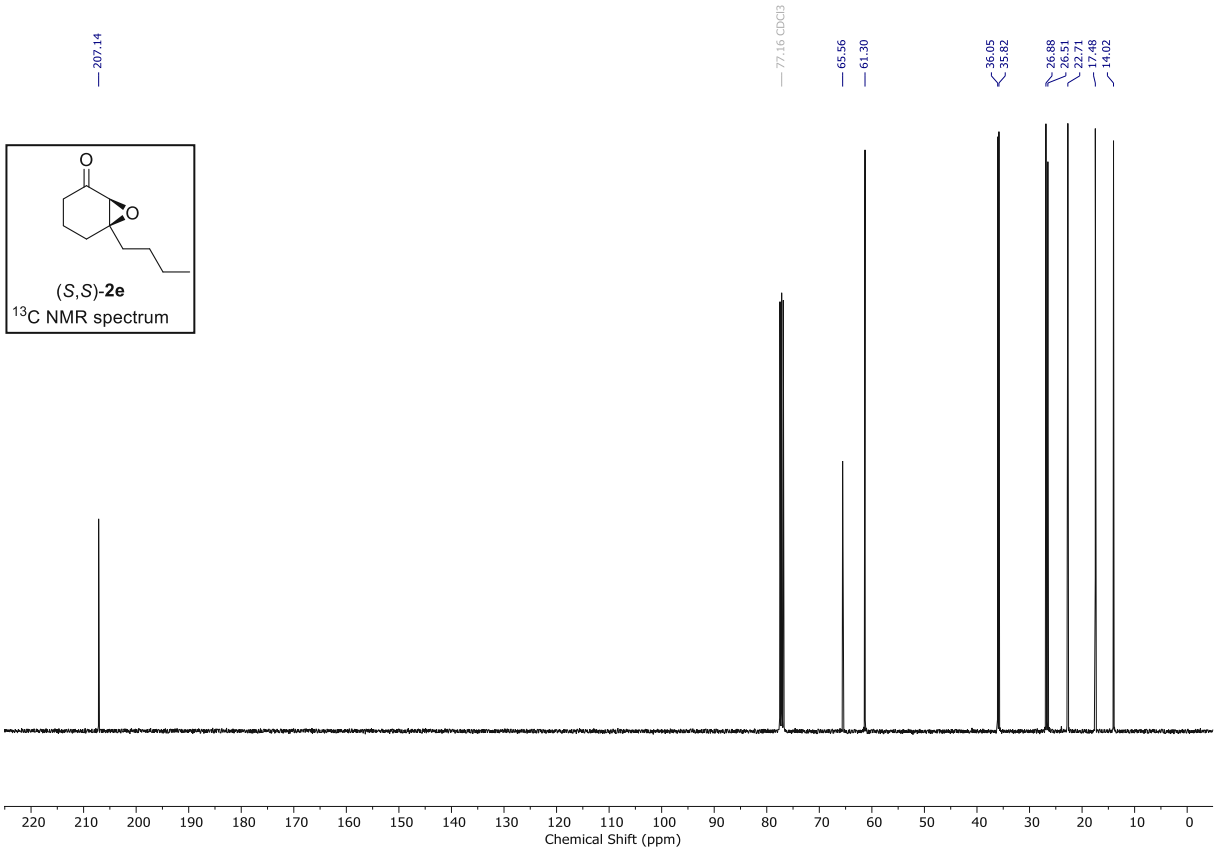


Die approbierte gedruckte Originalversion dieser Dissertation ist an der TU Wien Bibliothek verfügbar.
The approved original version of this doctoral thesis is available in print at TU Wien Bibliothek.

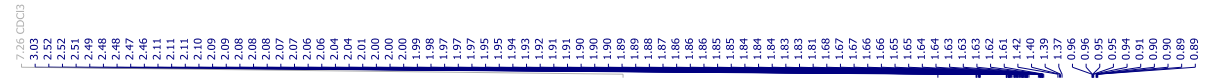


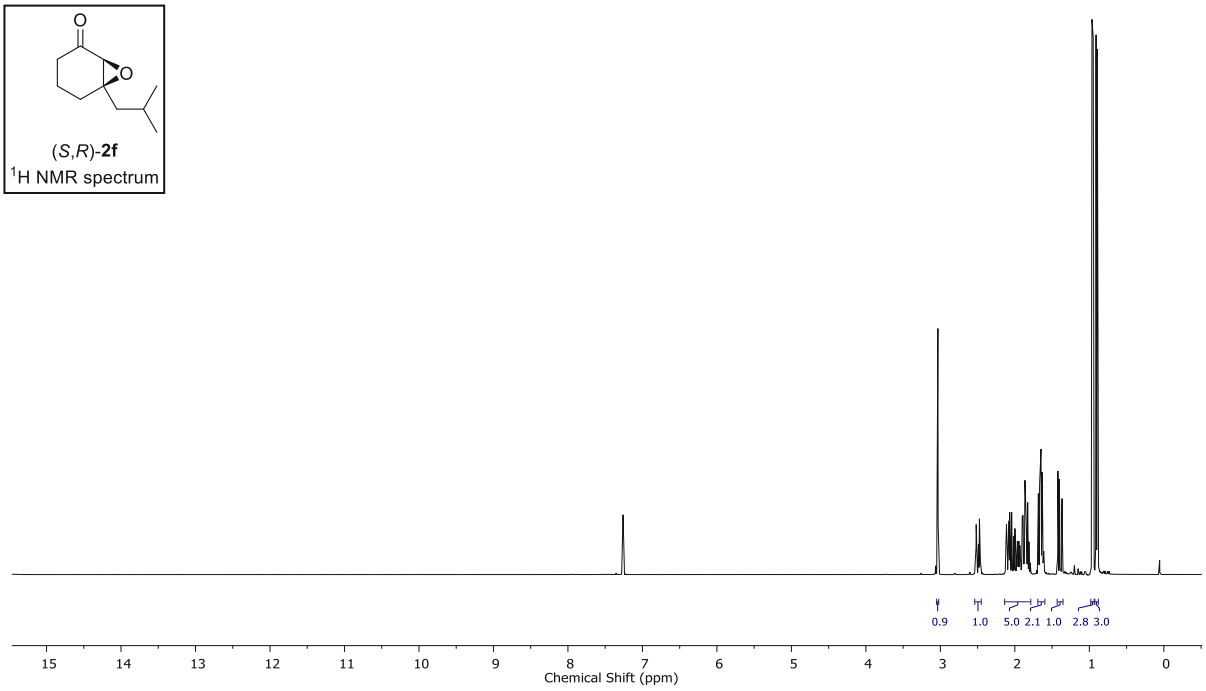




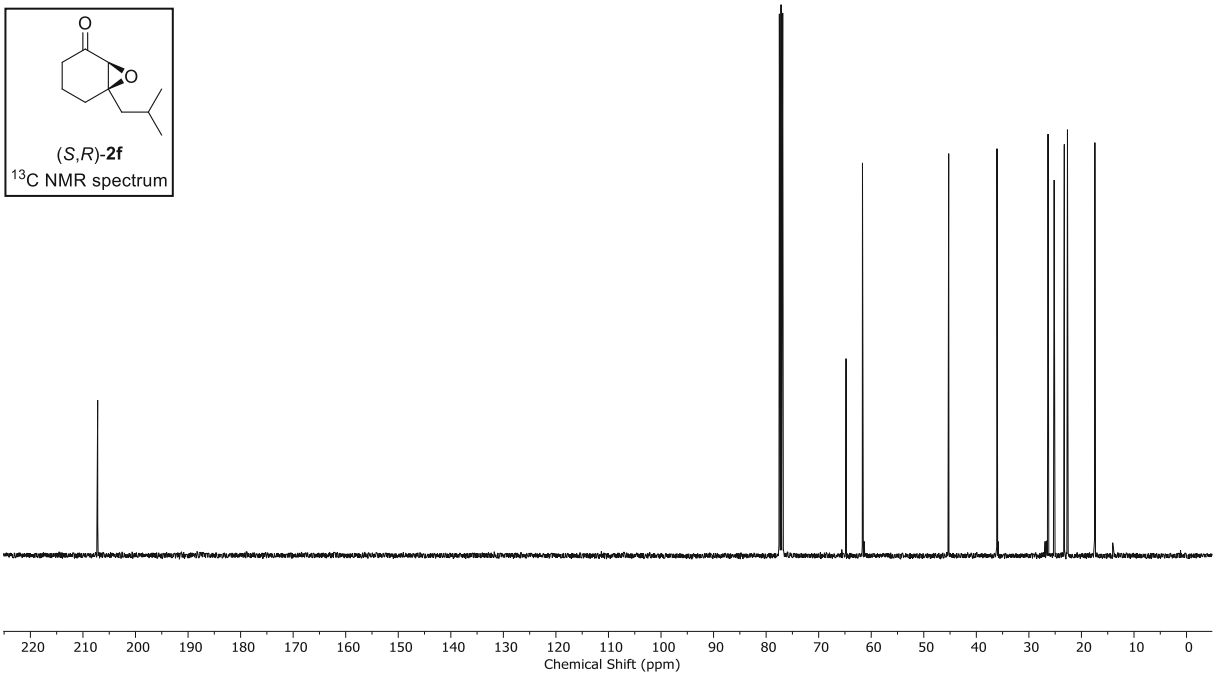


Die approbierte gedruckte Originalversion dieser Dissertation ist an der TU Wien Bibliothek verfügbar.
The approved original version of this doctoral thesis is available in print at TU Wien Bibliothek.

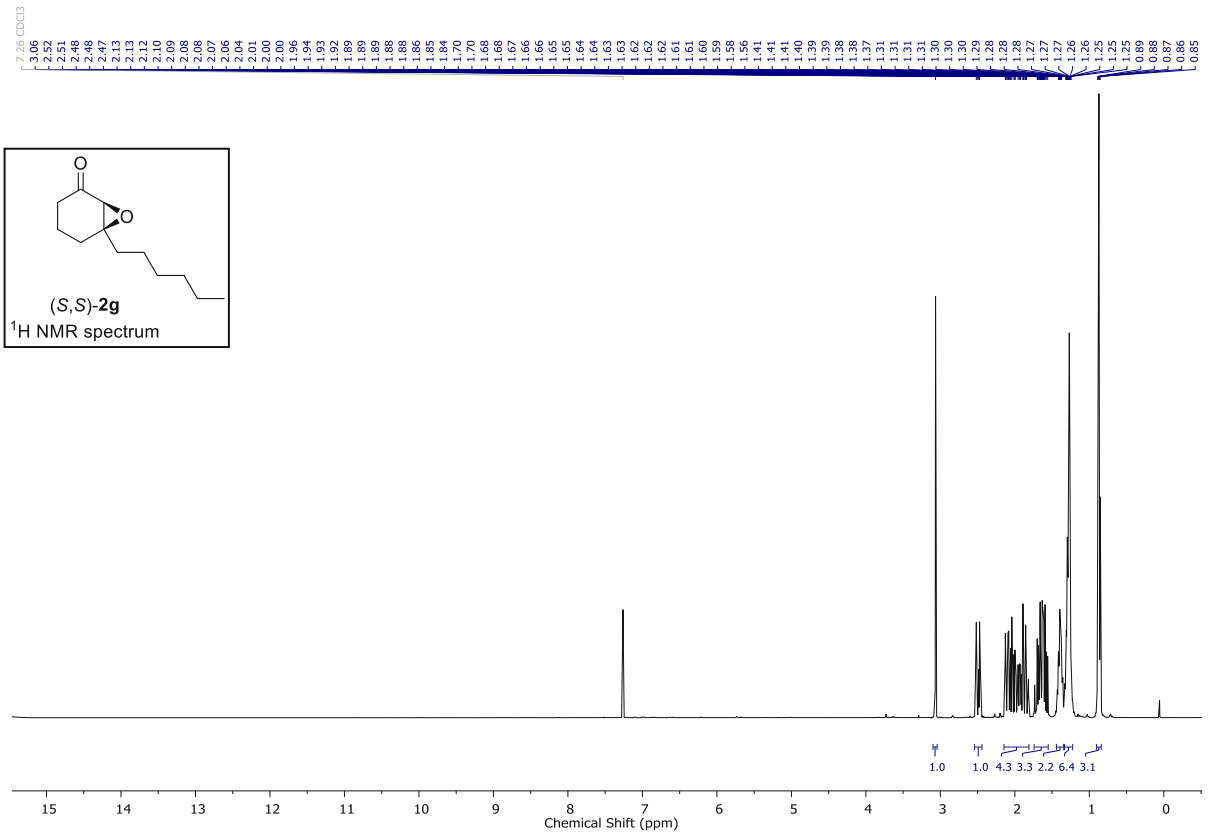


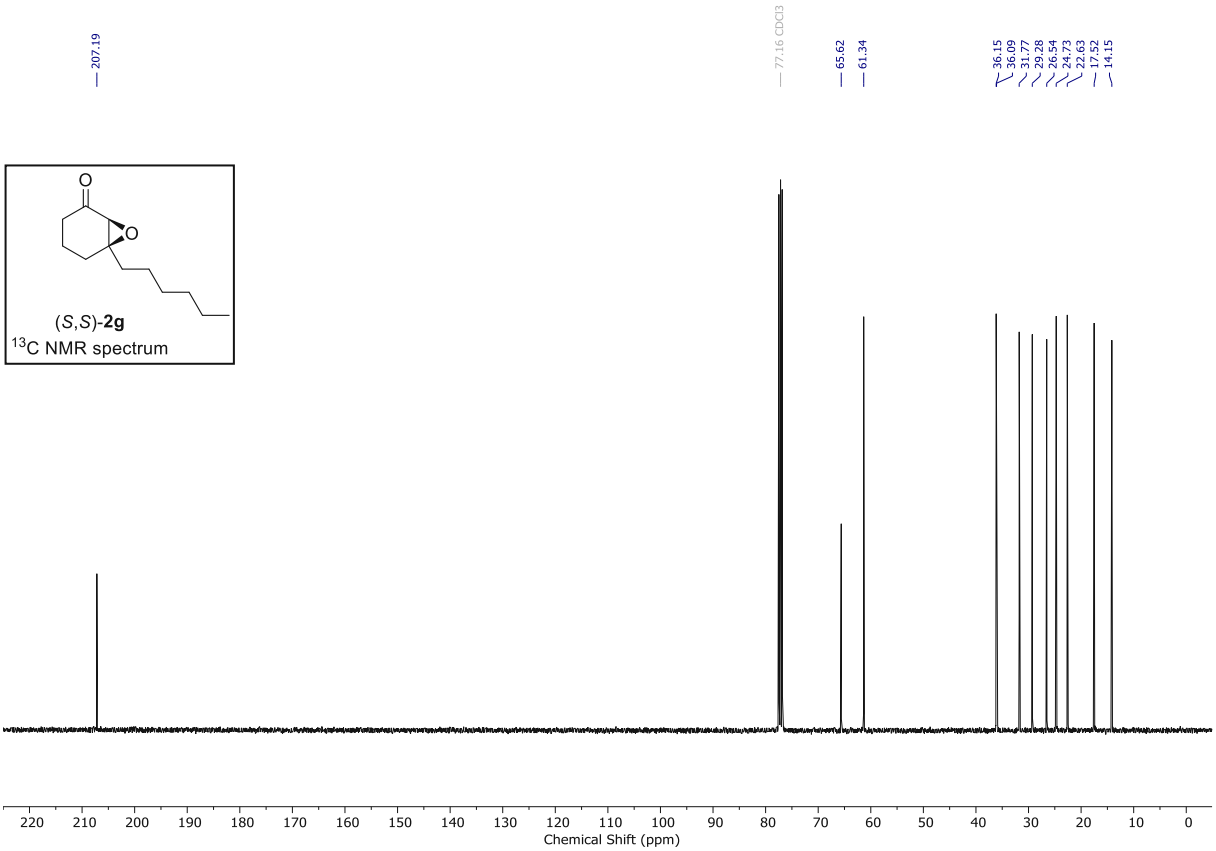






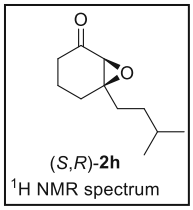
Die approbierte gedruckte Originalversion dieser Dissertation ist an der TU Wien Bibliothek verfügbar.
The approved original version of this doctoral thesis is available in print at TU Wien Bibliothek.



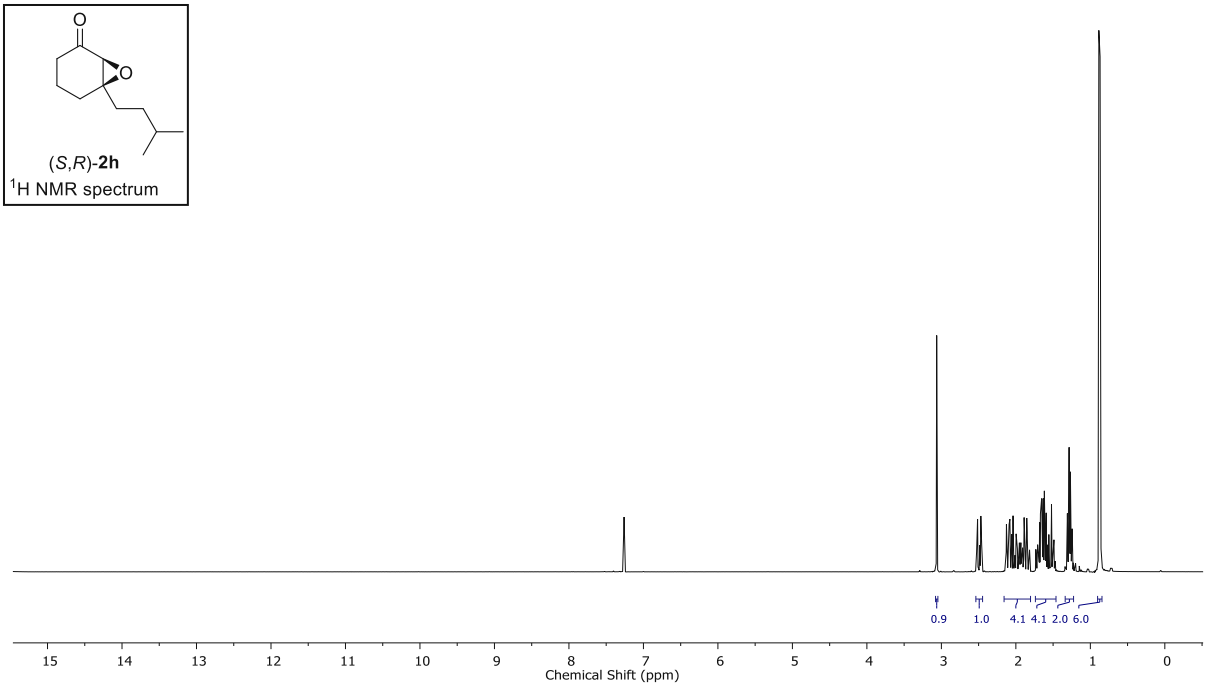


Die approbierte gedruckte Originalversion dieser Dissertation ist an der TU Wien Bibliothek verfügbar.
The approved original version of this doctoral thesis is available in print at TU Wien Bibliothek.

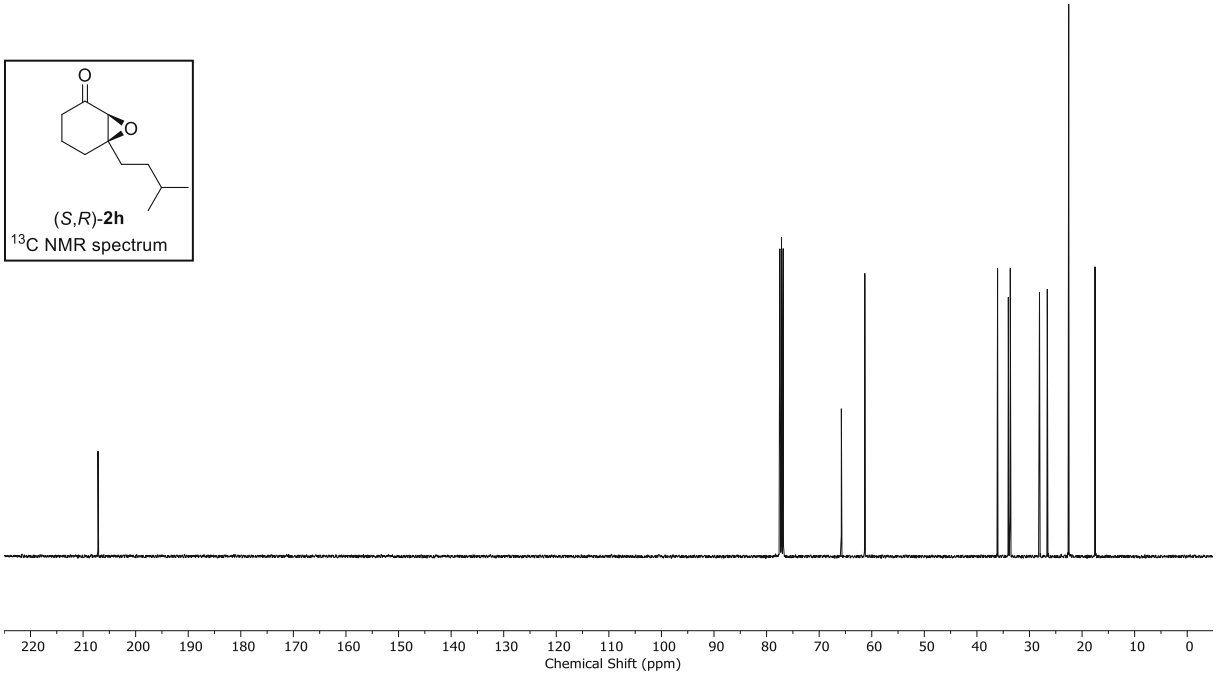




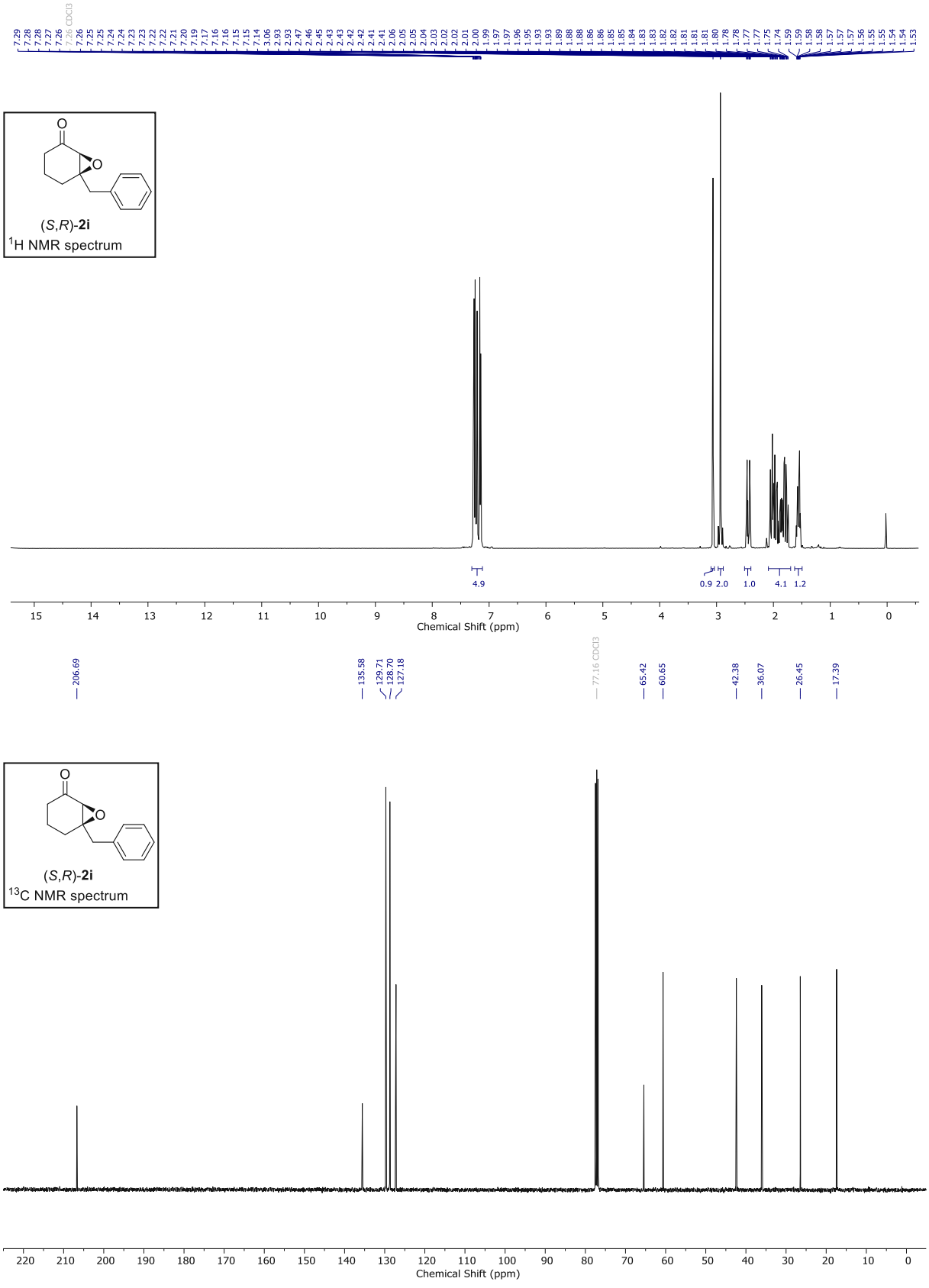
(*S*,*R*)-**2h**
^{1}H NMR spectrum



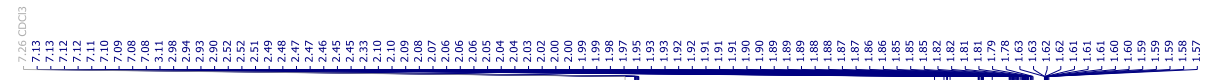
(*S*,*R*)-**2h**
^{13}C NMR spectrum

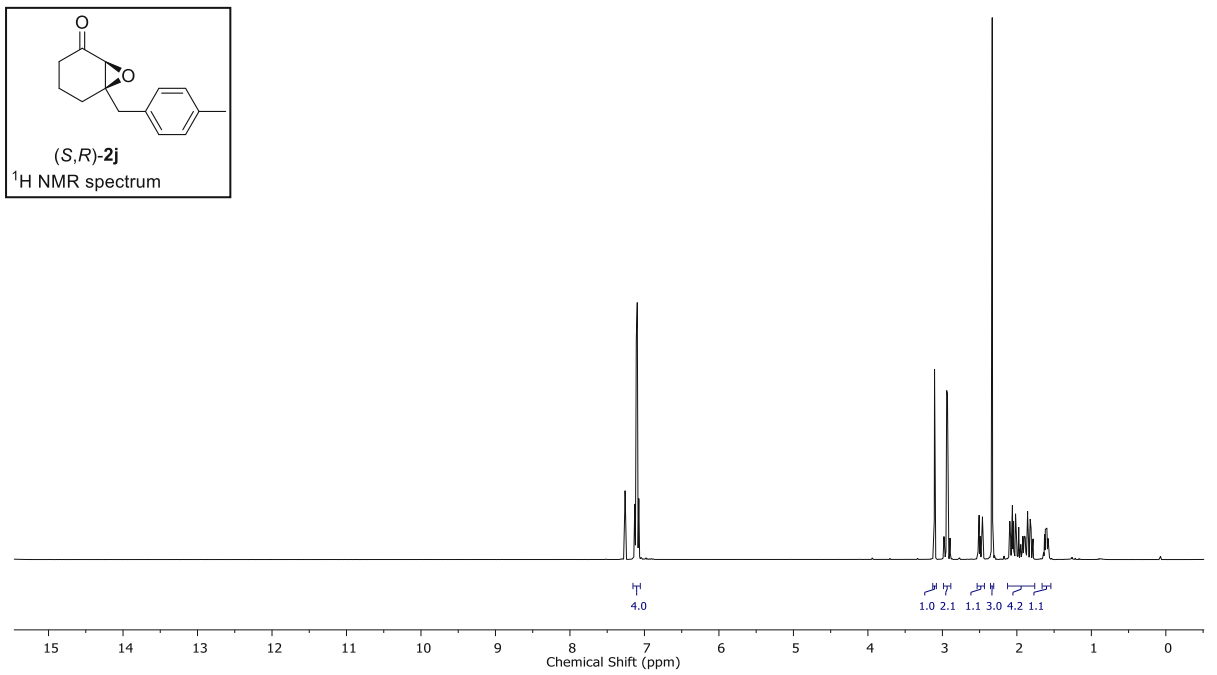


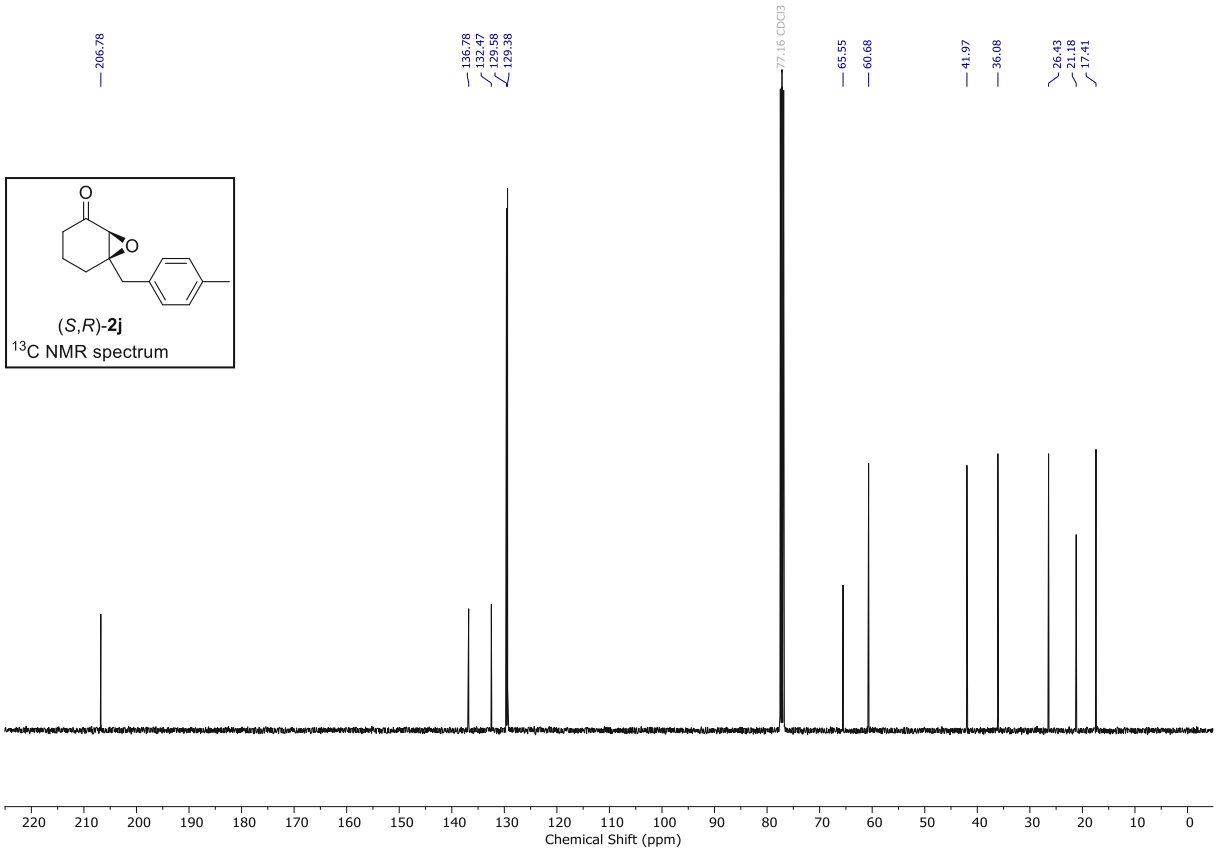
Die approbierte gedruckte Originalversion dieser Dissertation ist an der TU Wien Bibliothek verfügbar.
The approved original version of this doctoral thesis is available in print at TU Wien Bibliothek.



Die approbierte gedruckte Originalversion dieser Dissertation ist an der TU Wien Bibliothek verfügbar.
The approved original version of this doctoral thesis is available in print at TU Wien Bibliothek.

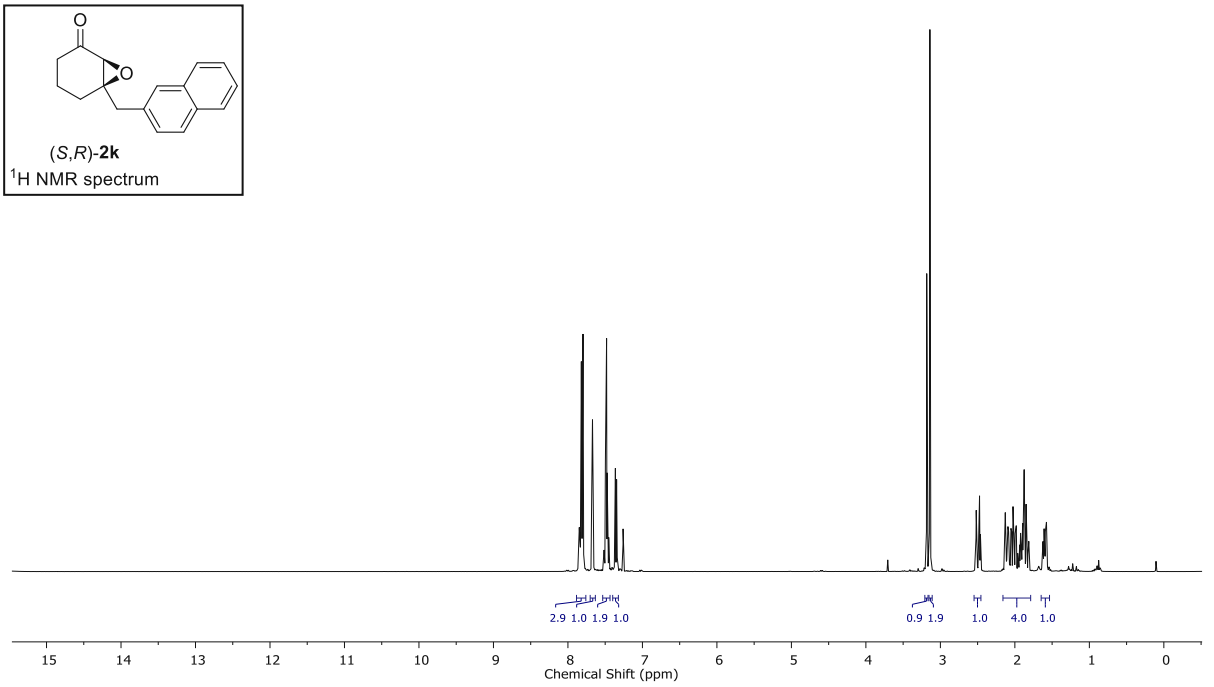


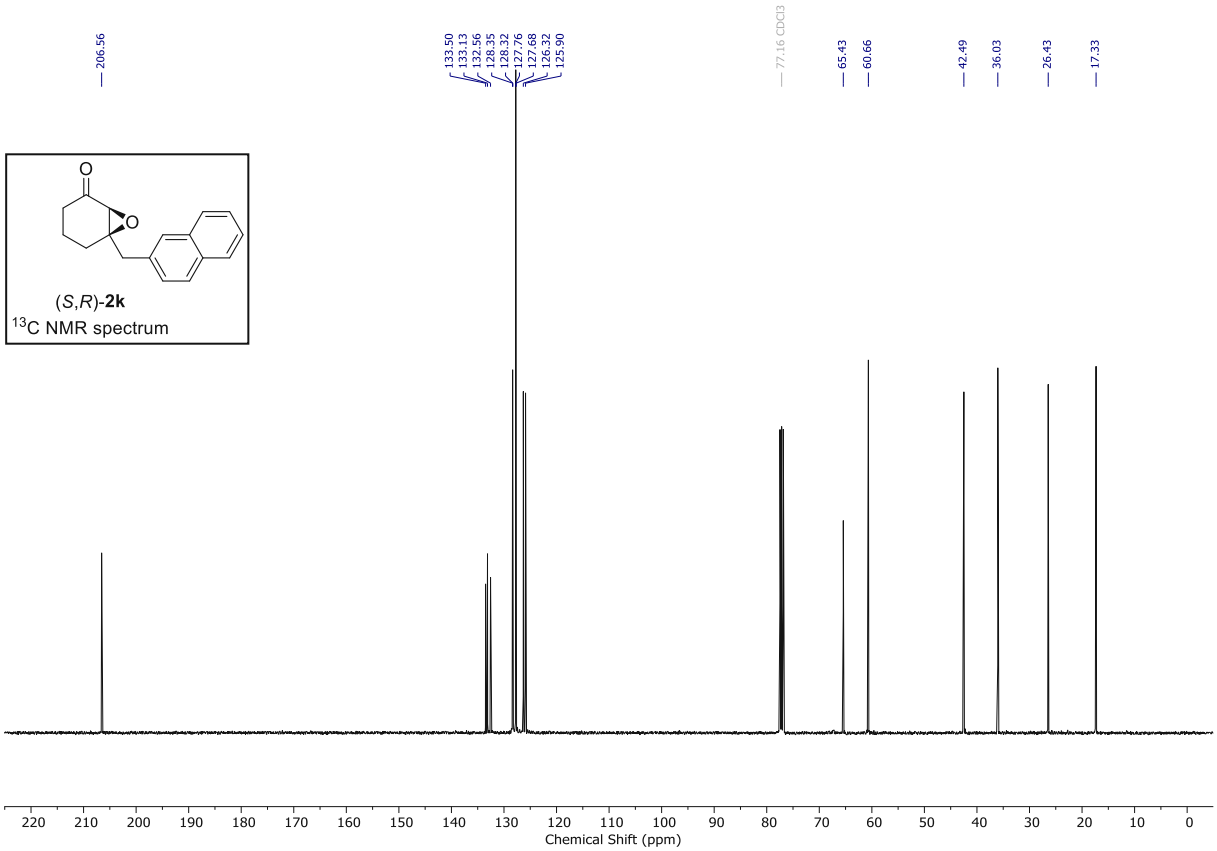




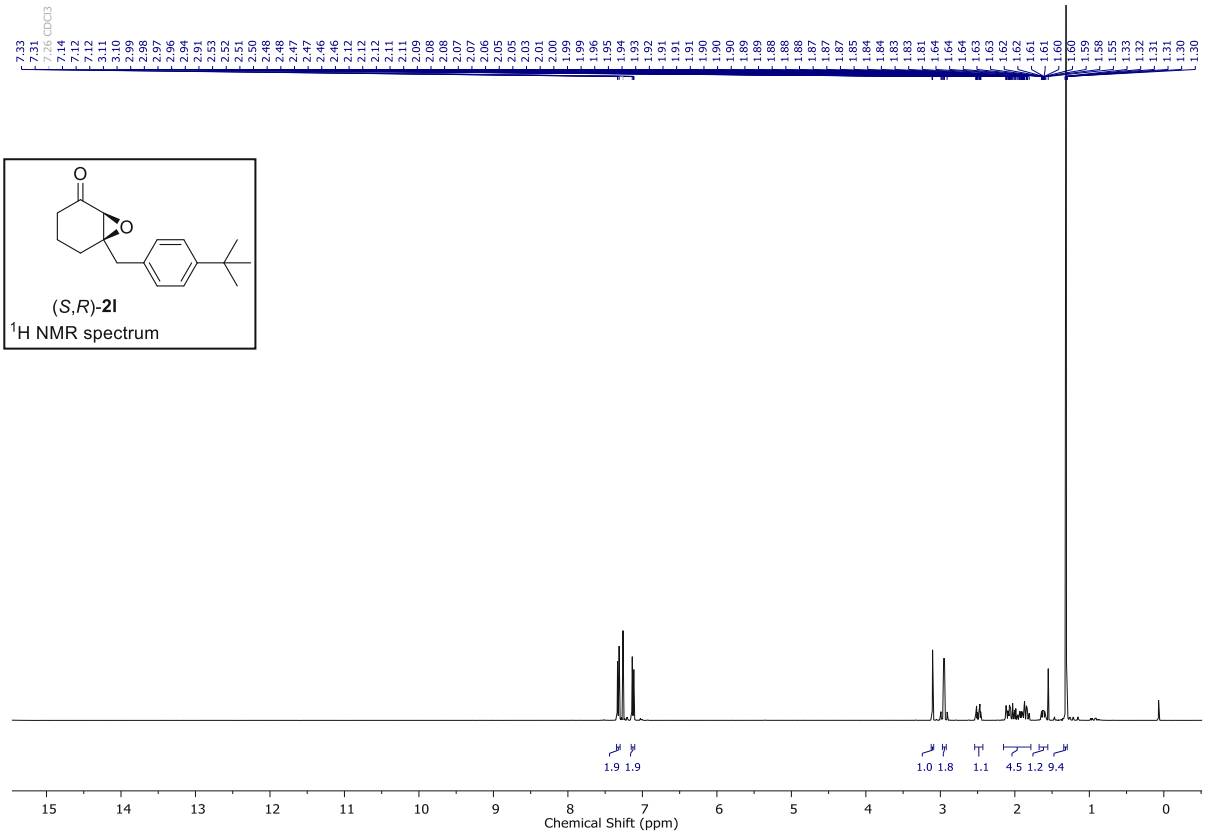
Die approbierte gedruckte Originalversion dieser Dissertation ist an der TU Wien Bibliothek verfügbar.
The approved original version of this doctoral thesis is available in print at TU Wien Bibliothek.

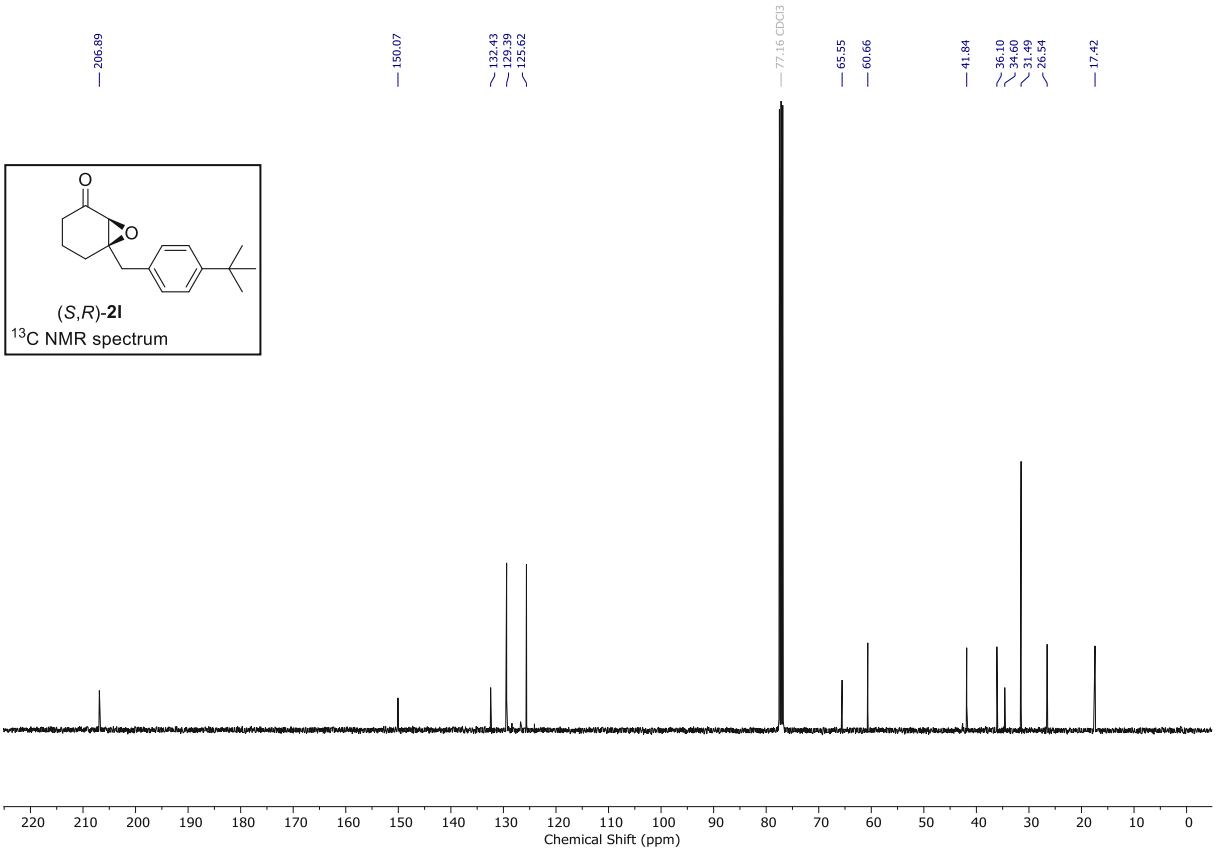




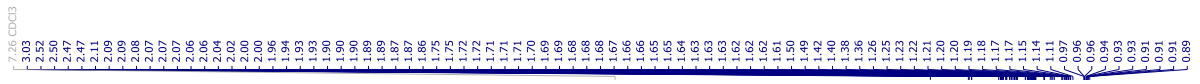


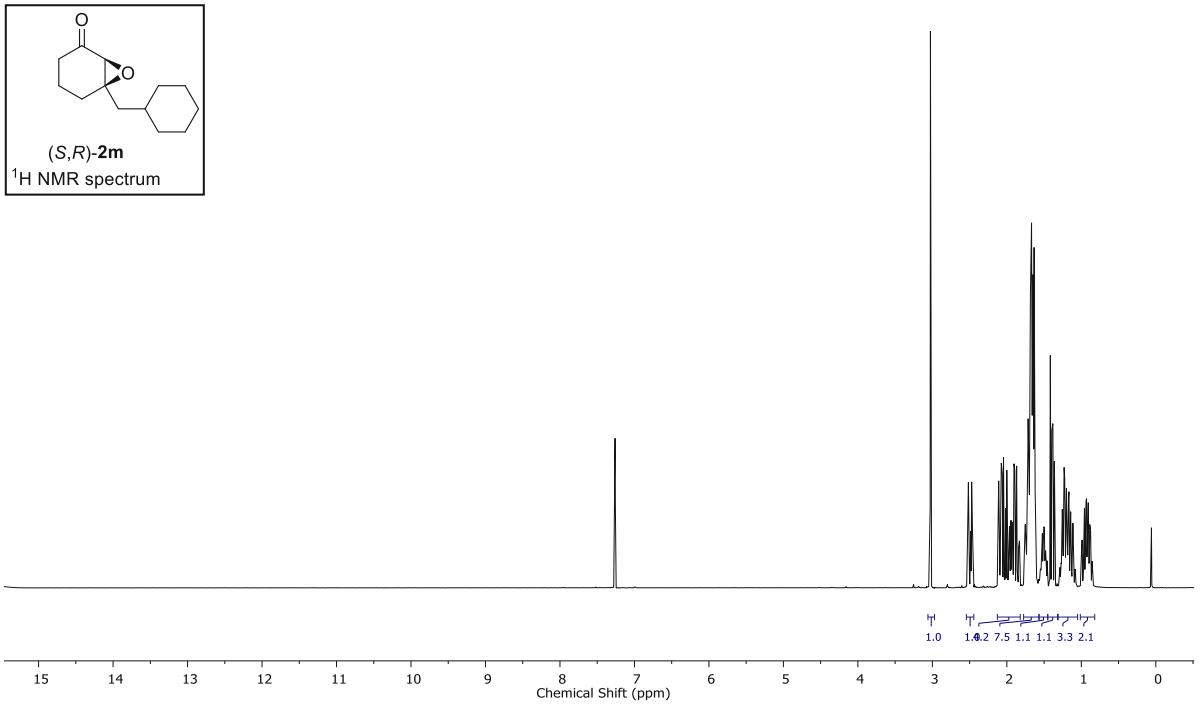
Die approbierte gedruckte Originalversion dieser Dissertation ist an der TU Wien Bibliothek verfügbar.
The approved original version of this doctoral thesis is available in print at TU Wien Bibliothek.

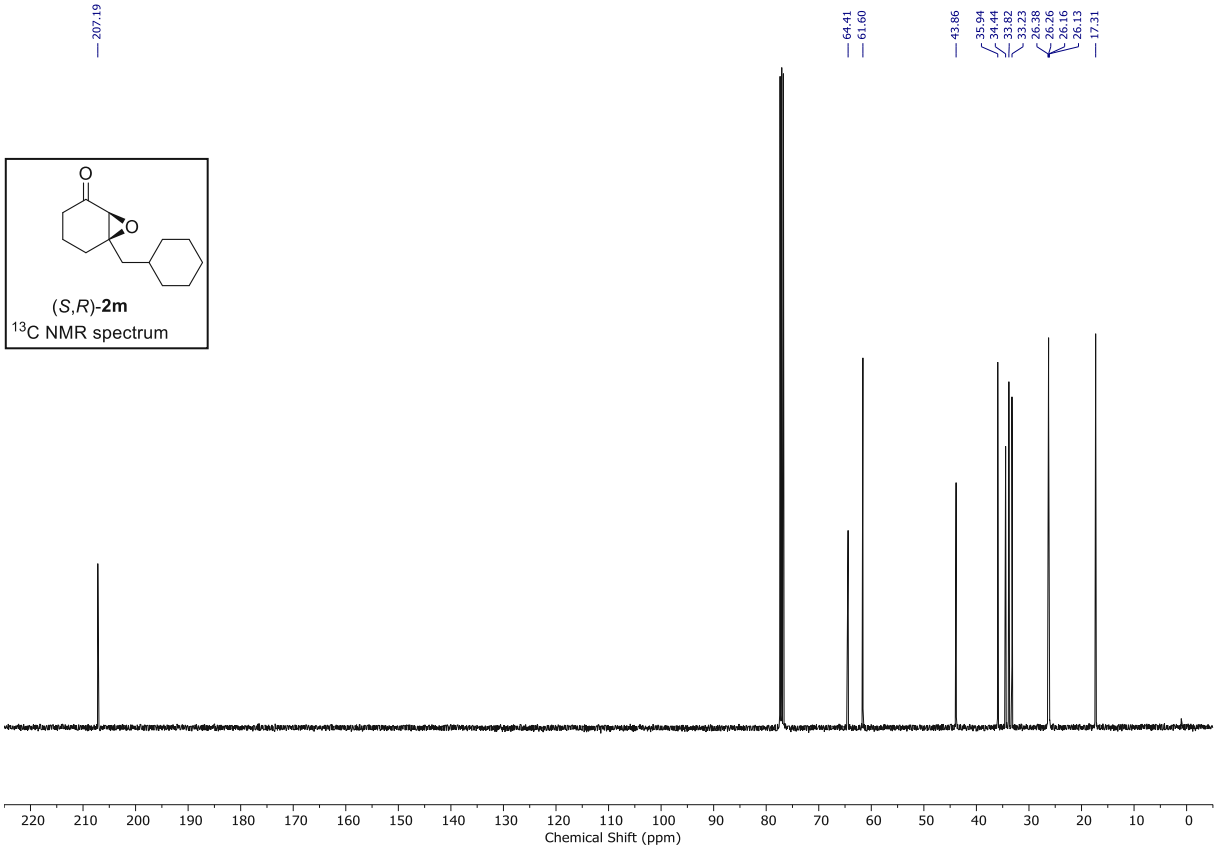




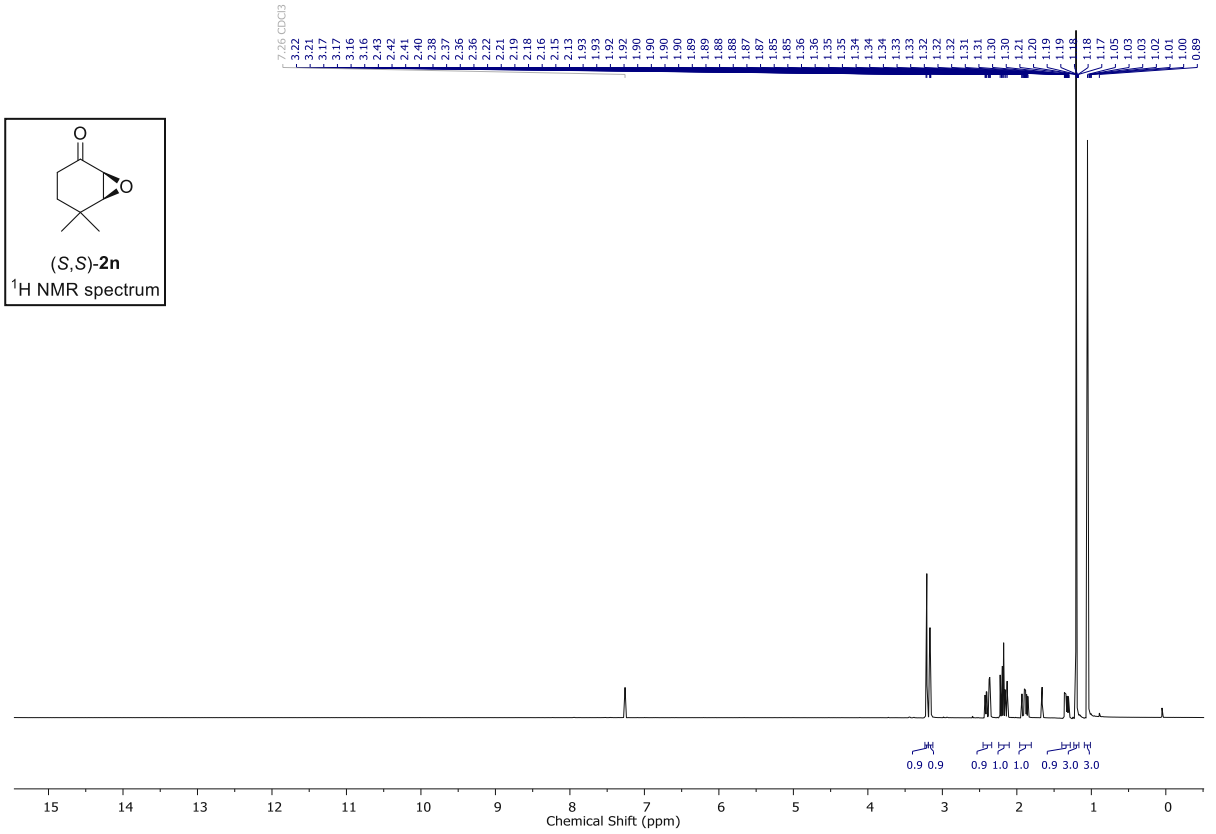
Die approbierte gedruckte Originalversion dieser Dissertation ist an der TU Wien Bibliothek verfügbar.
The approved original version of this doctoral thesis is available in print at TU Wien Bibliothek.

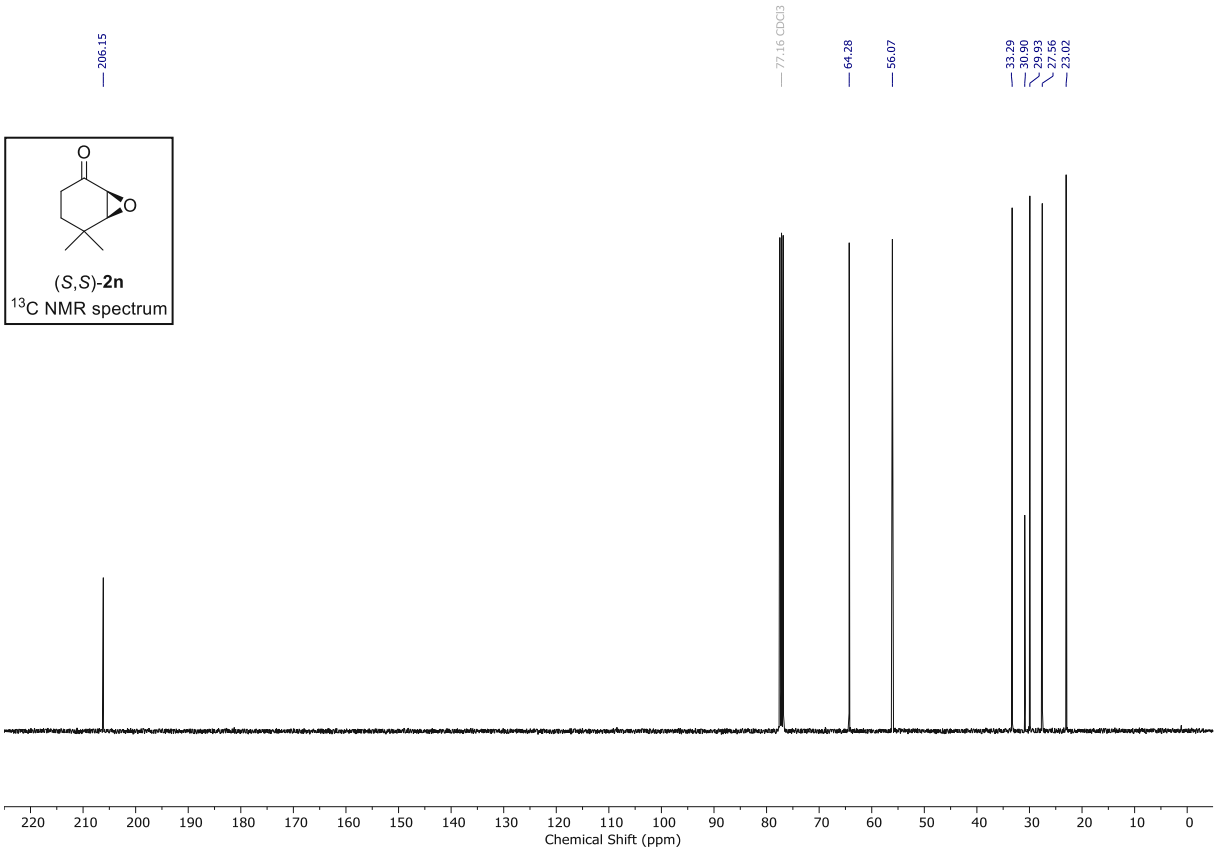




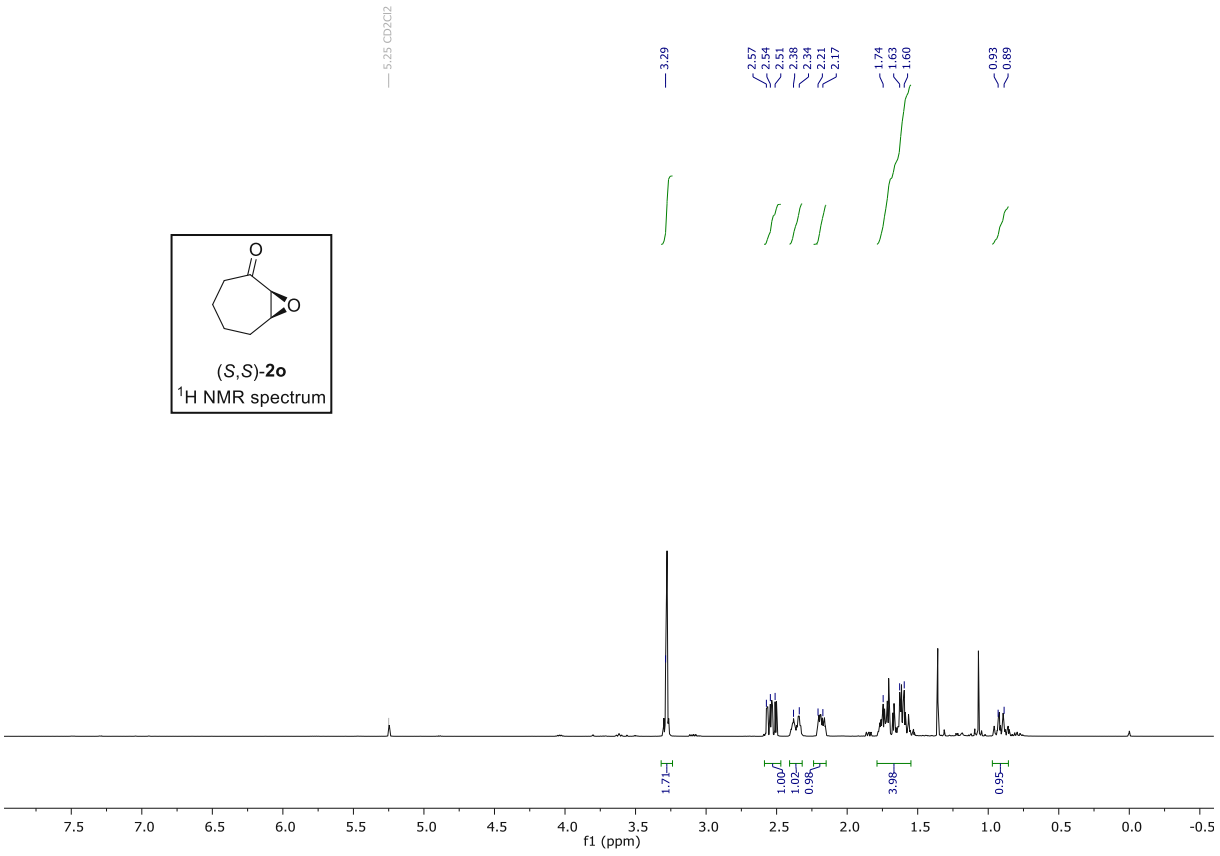


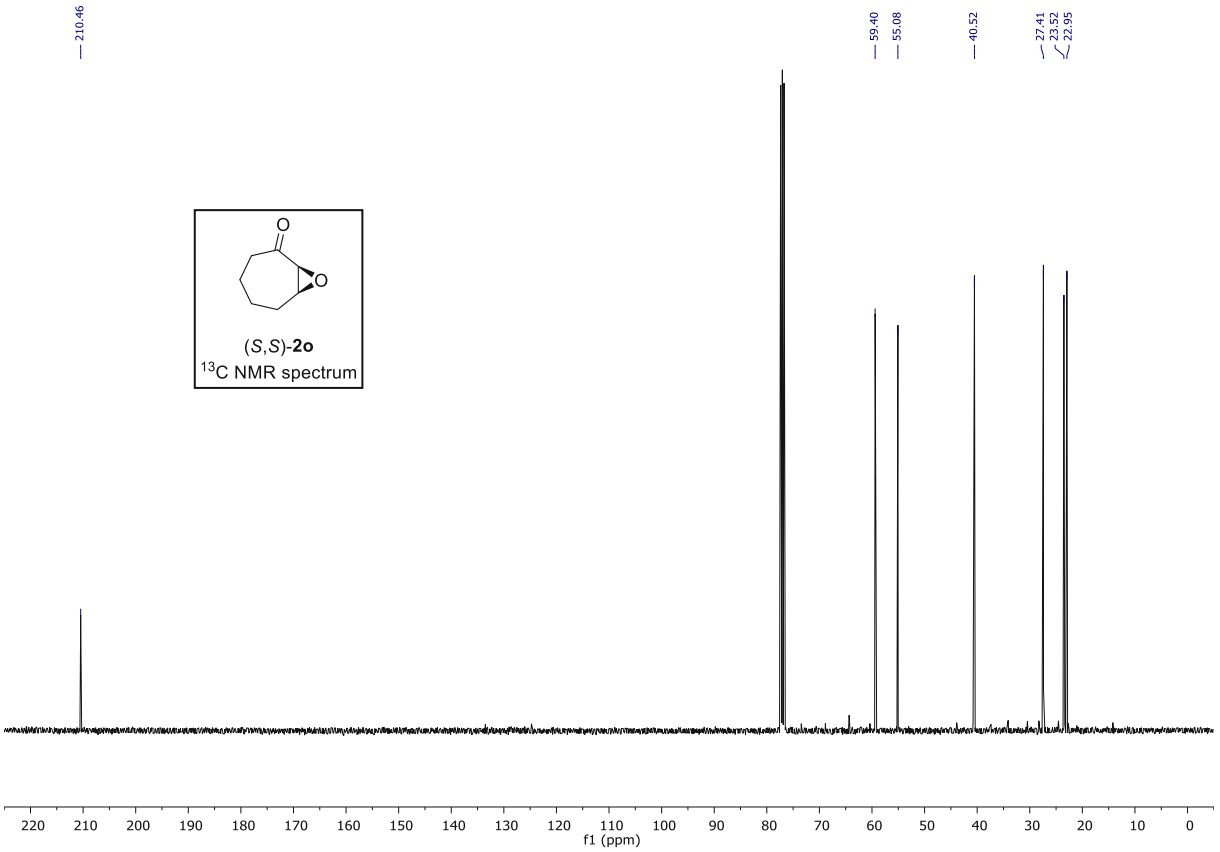
Die approbierte gedruckte Originalversion dieser Dissertation ist an der TU Wien Bibliothek verfügbar.
The approved original version of this doctoral thesis is available in print at TU Wien Bibliothek.



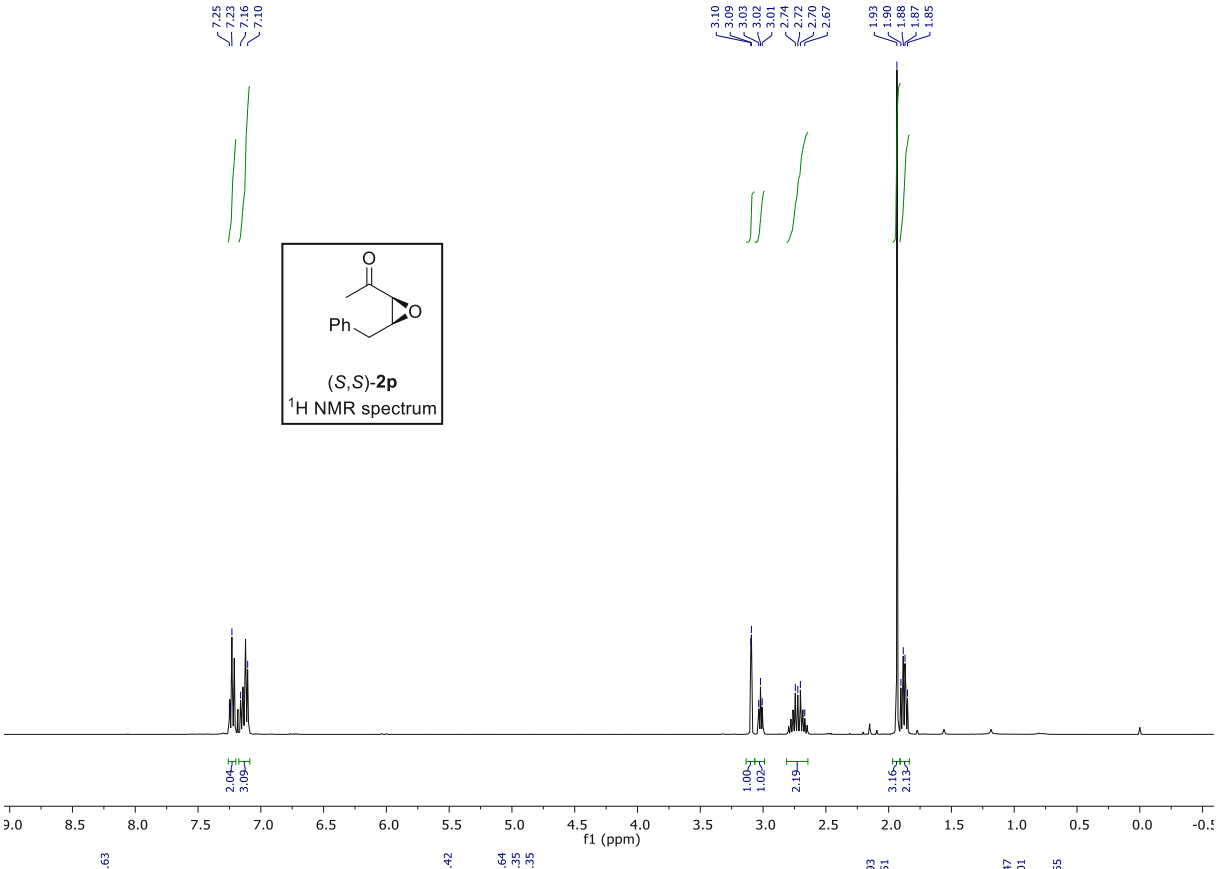


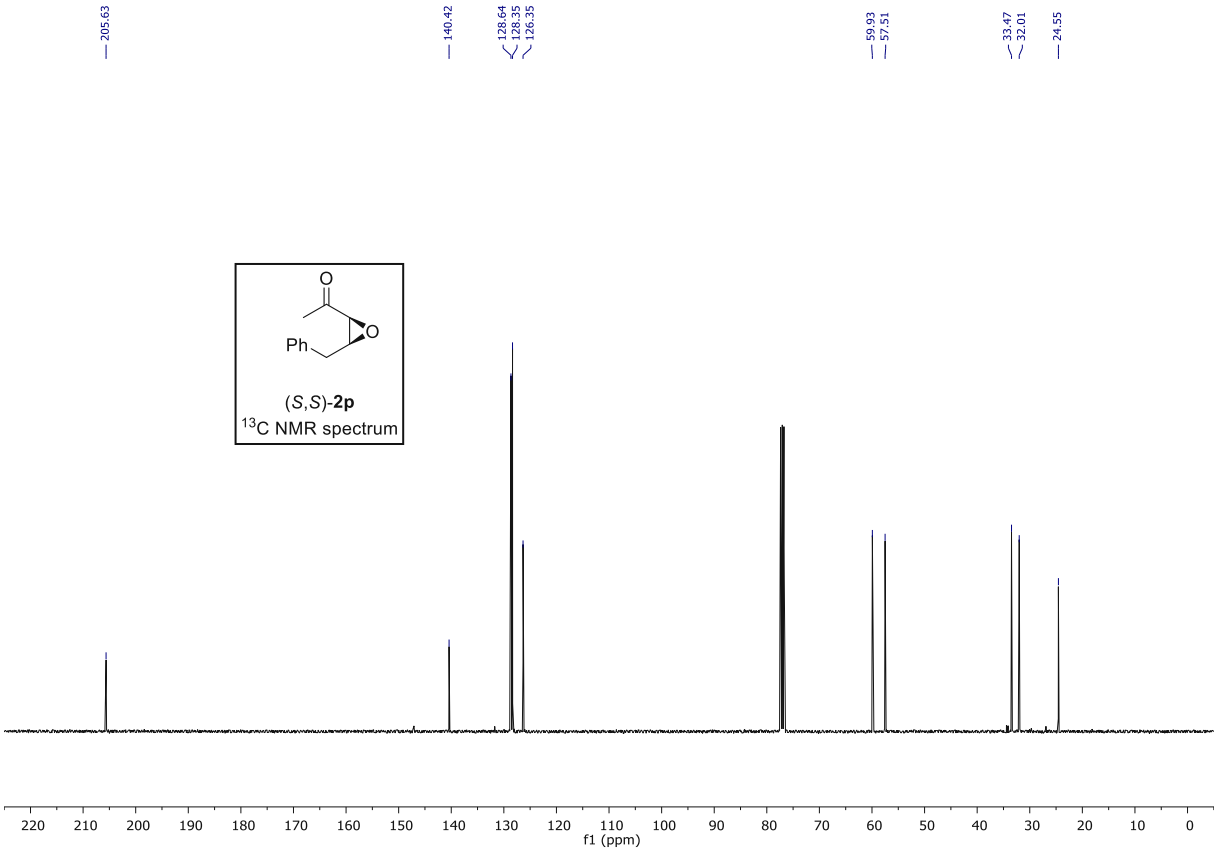
Die approbierte gedruckte Originalversion dieser Dissertation ist an der TU Wien Bibliothek verfügbar.
The approved original version of this doctoral thesis is available in print at TU Wien Bibliothek.



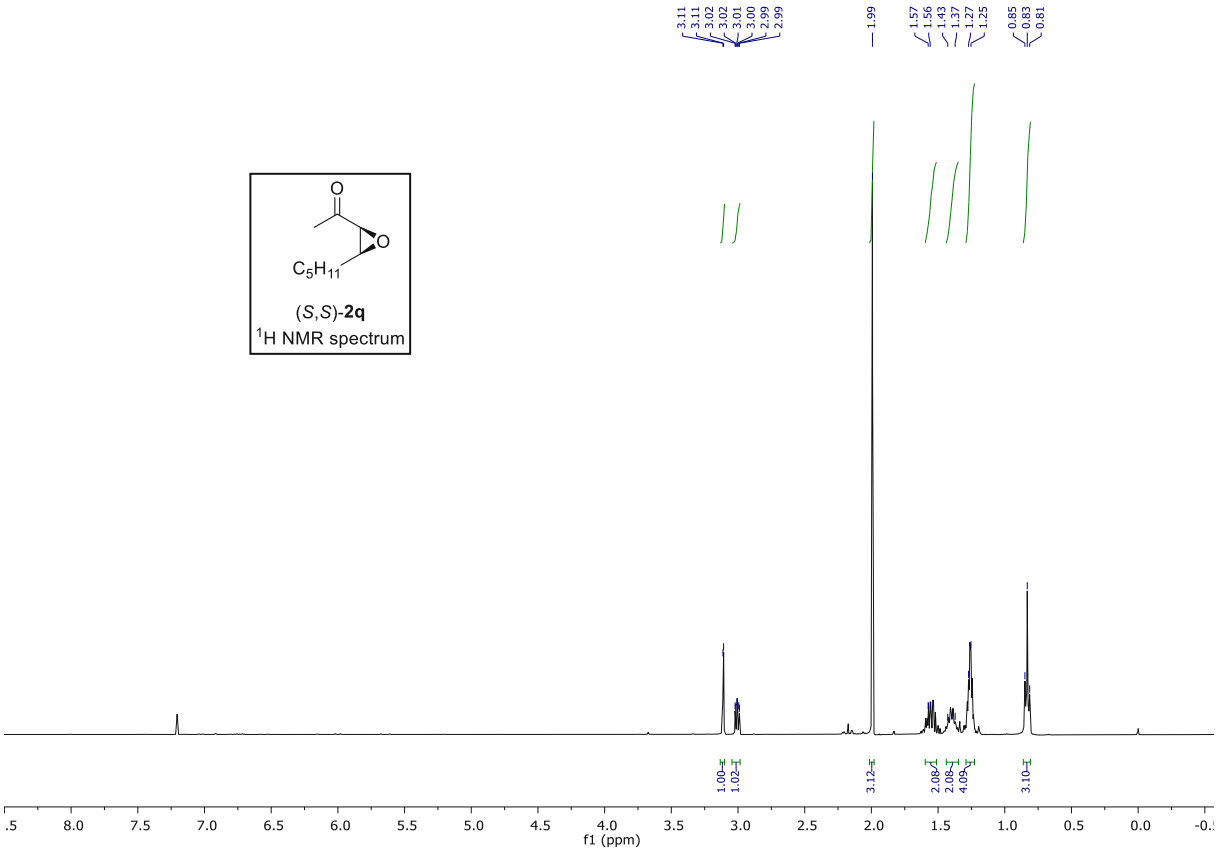


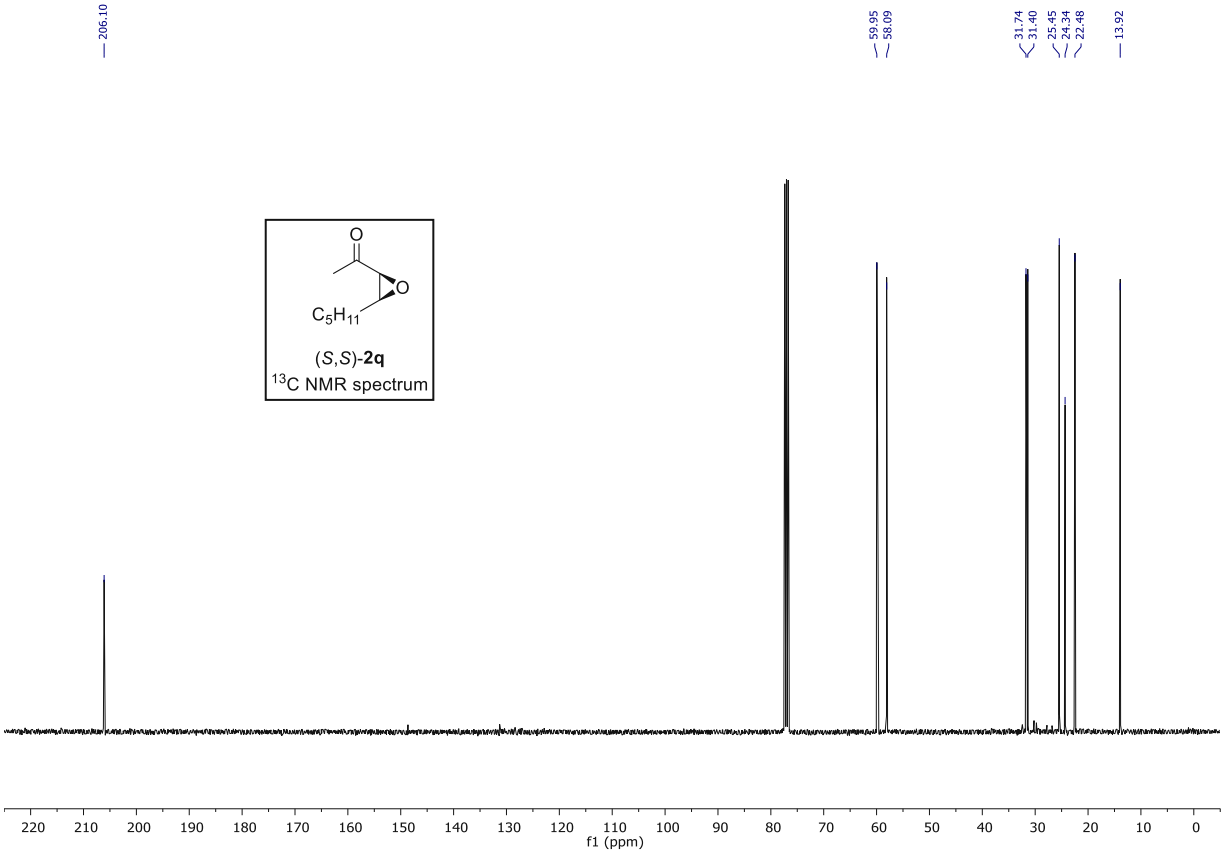
Die approbierte gedruckte Originalversion dieser Dissertation ist an der TU Wien Bibliothek verfügbar.
The approved original version of this doctoral thesis is available in print at TU Wien Bibliothek.





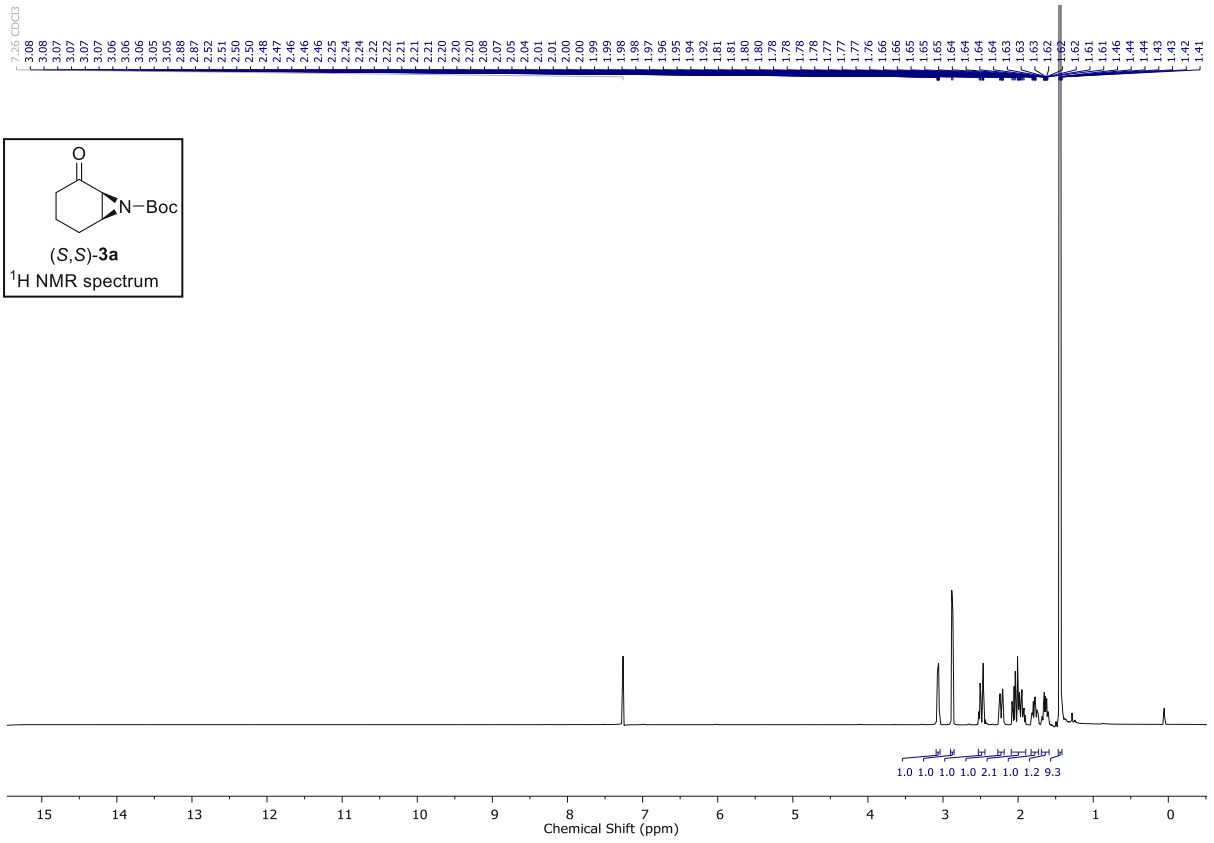
Die approbierte gedruckte Originalversion dieser Dissertation ist an der TU Wien Bibliothek verfügbar.
The approved original version of this doctoral thesis is available in print at TU Wien Bibliothek.

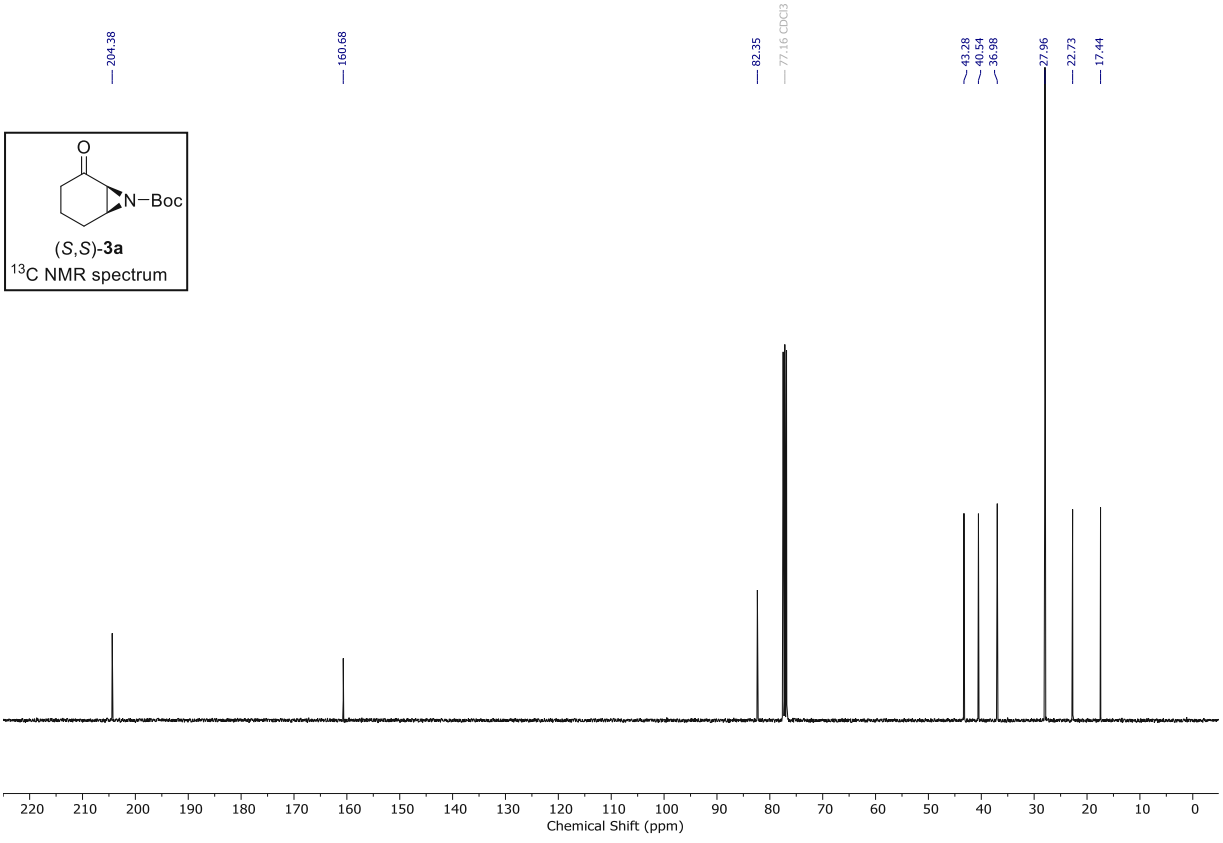




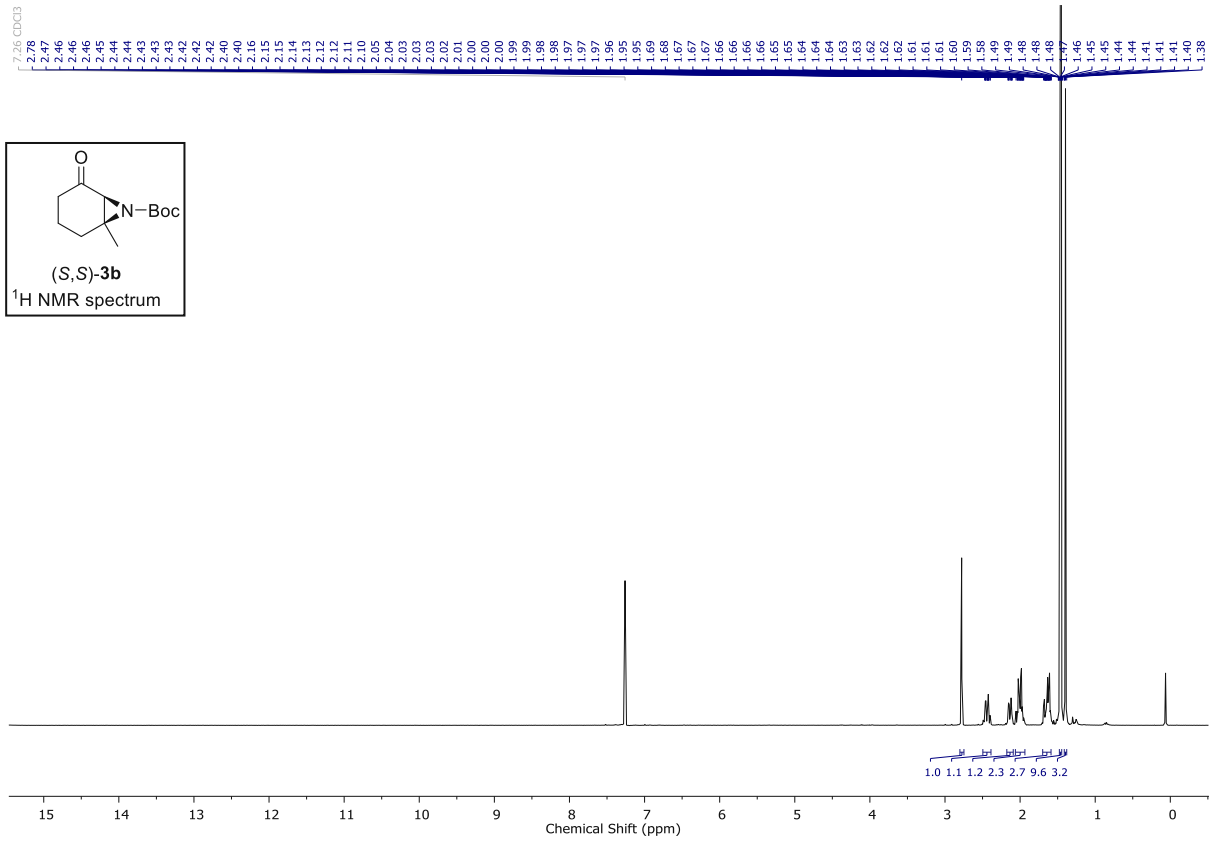
Die approbierte gedruckte Originalversion dieser Dissertation ist an der TU Wien Bibliothek verfügbar.
The approved original version of this doctoral thesis is available in print at TU Wien Bibliothek.

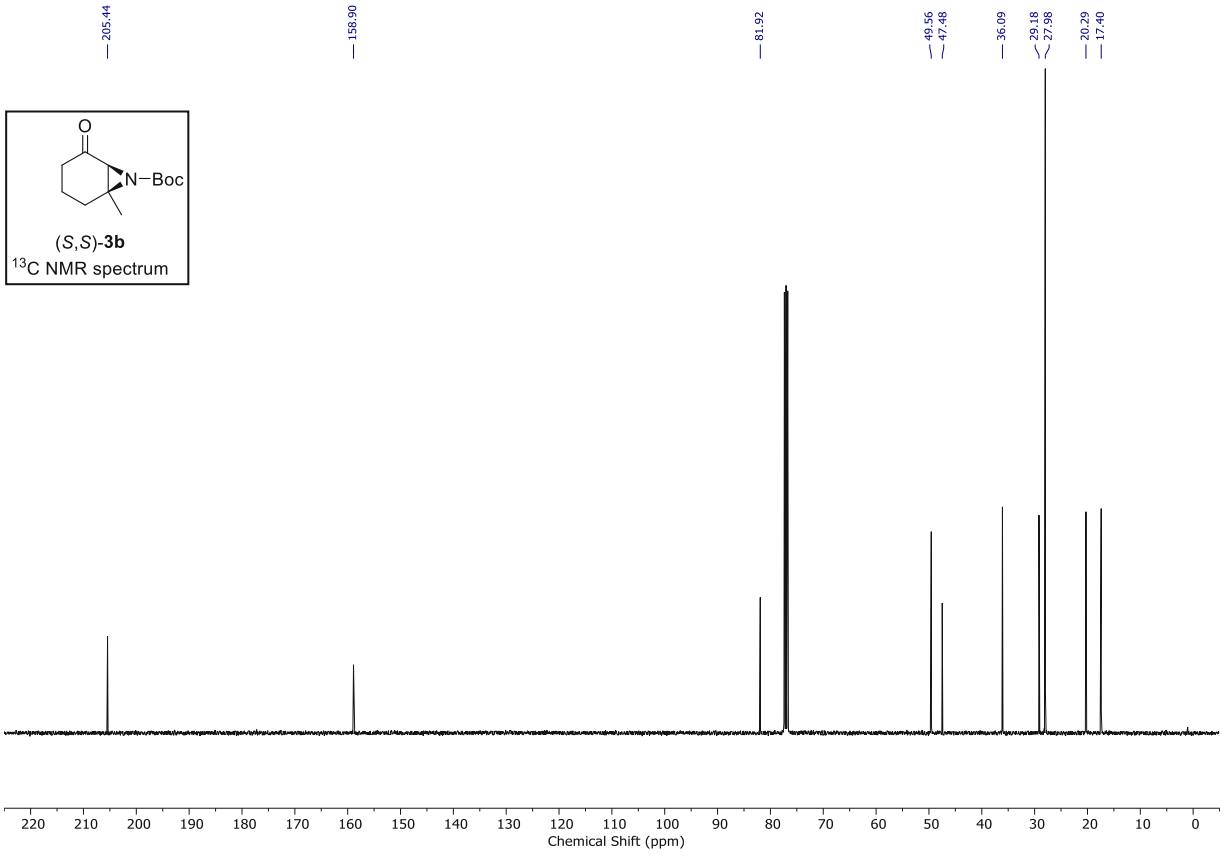
19. NMR spectra for the asymmetric aziridinations



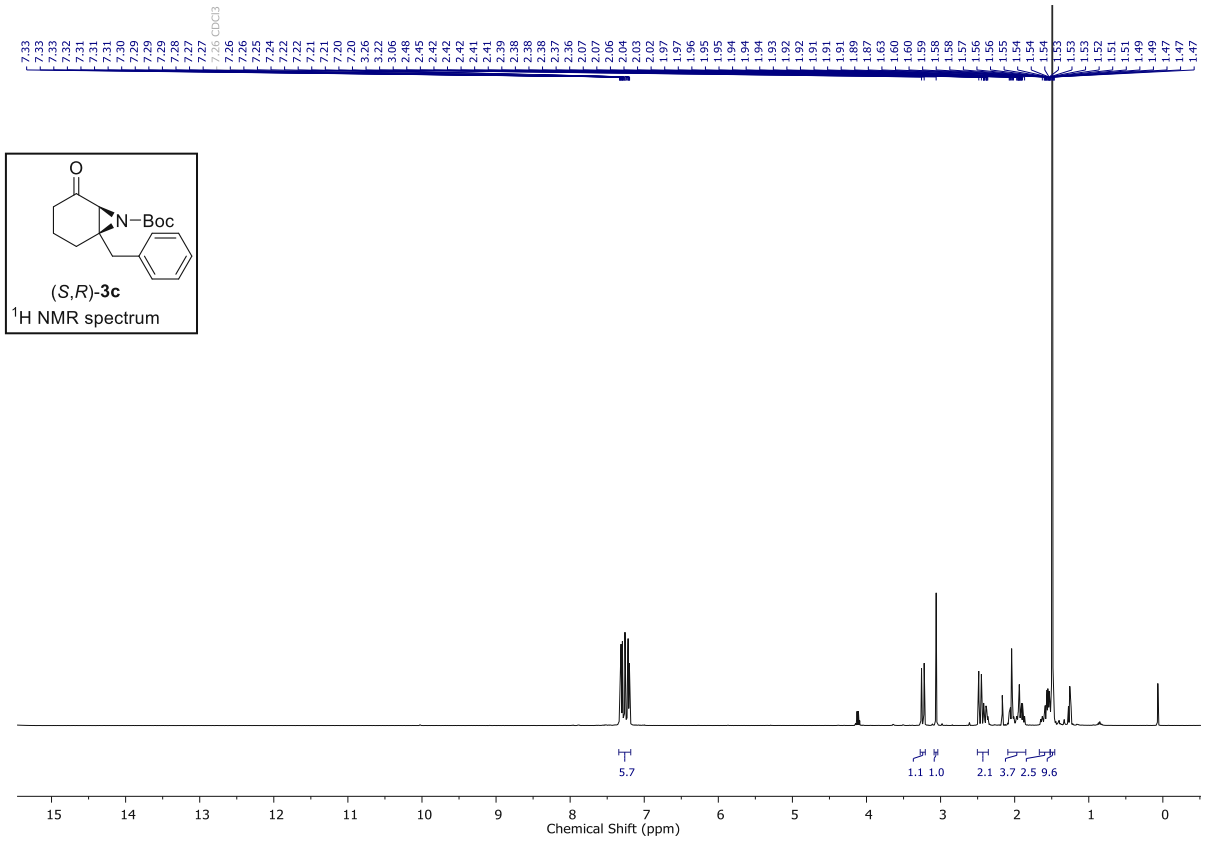


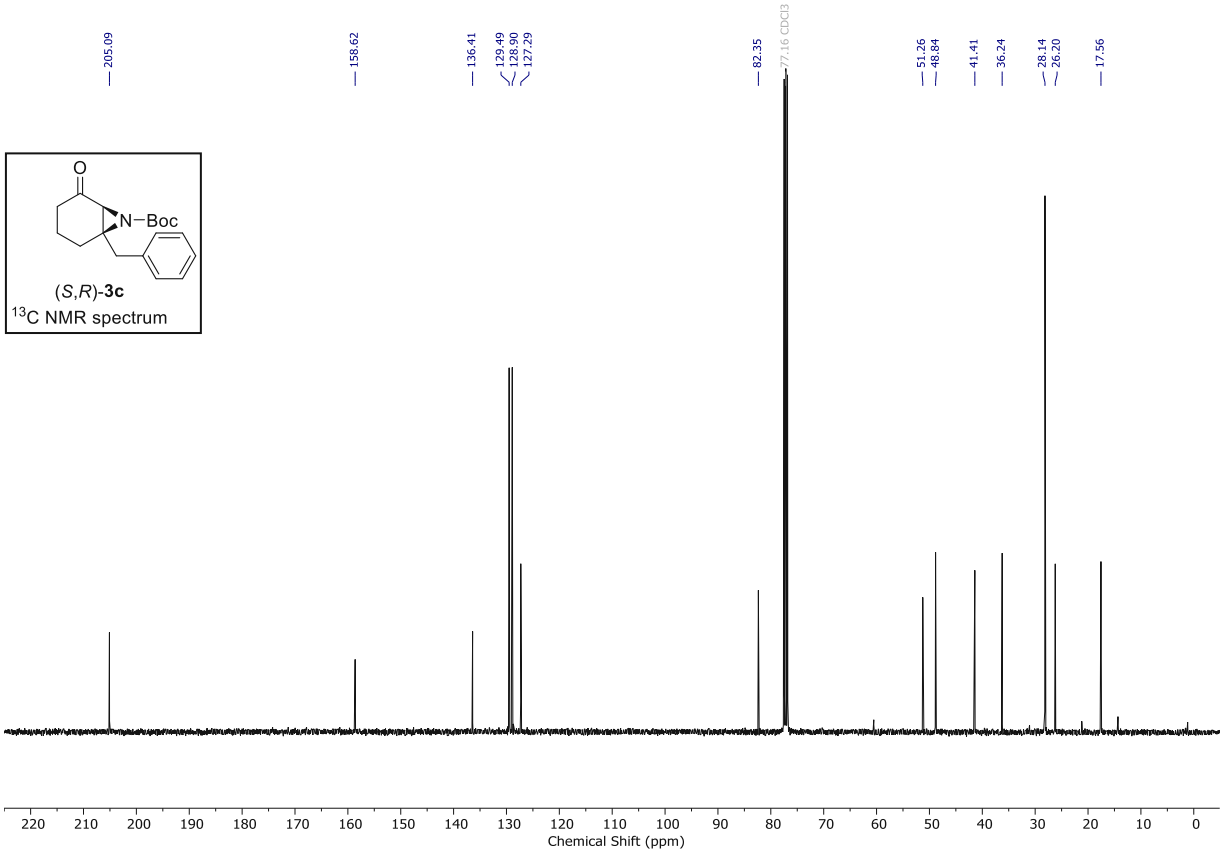
Die approbierte gedruckte Originalversion dieser Dissertation ist an der TU Wien Bibliothek verfügbar.
The approved original version of this doctoral thesis is available in print at TU Wien Bibliothek.



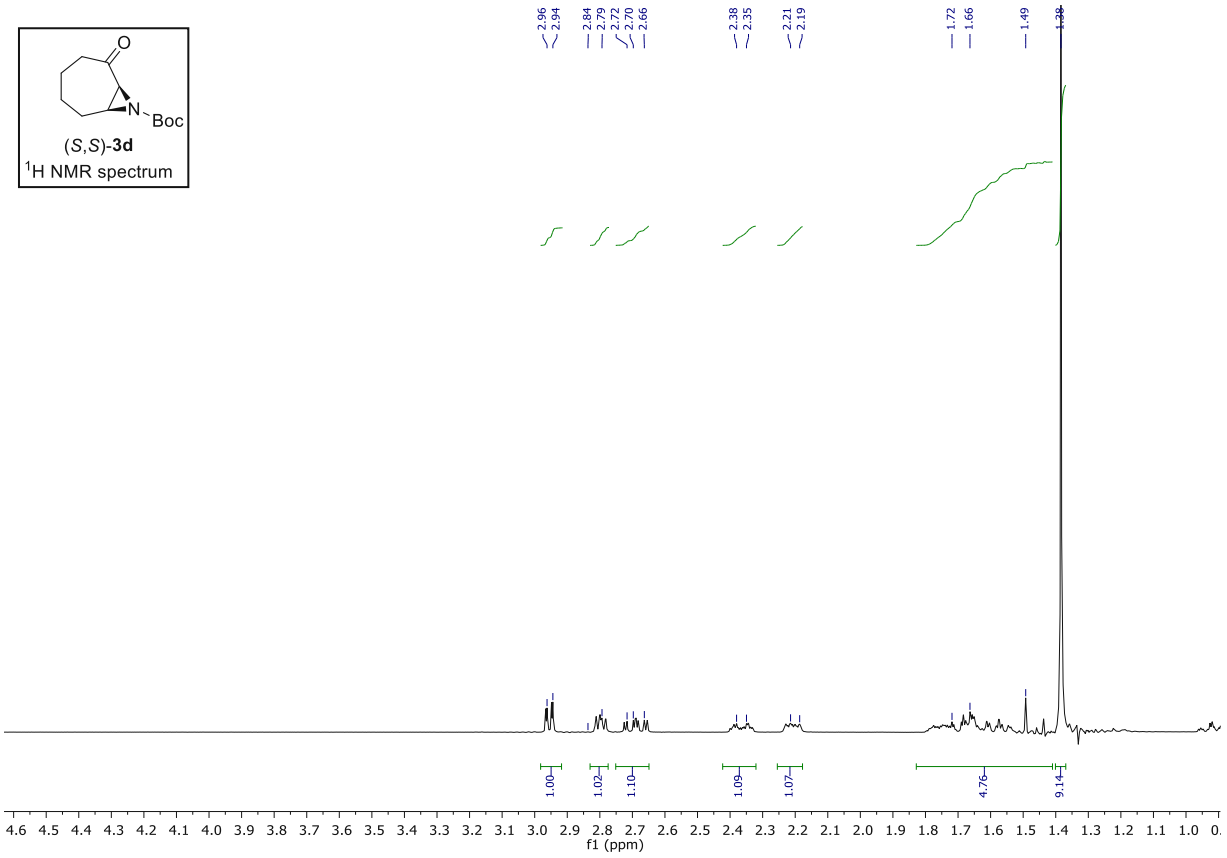


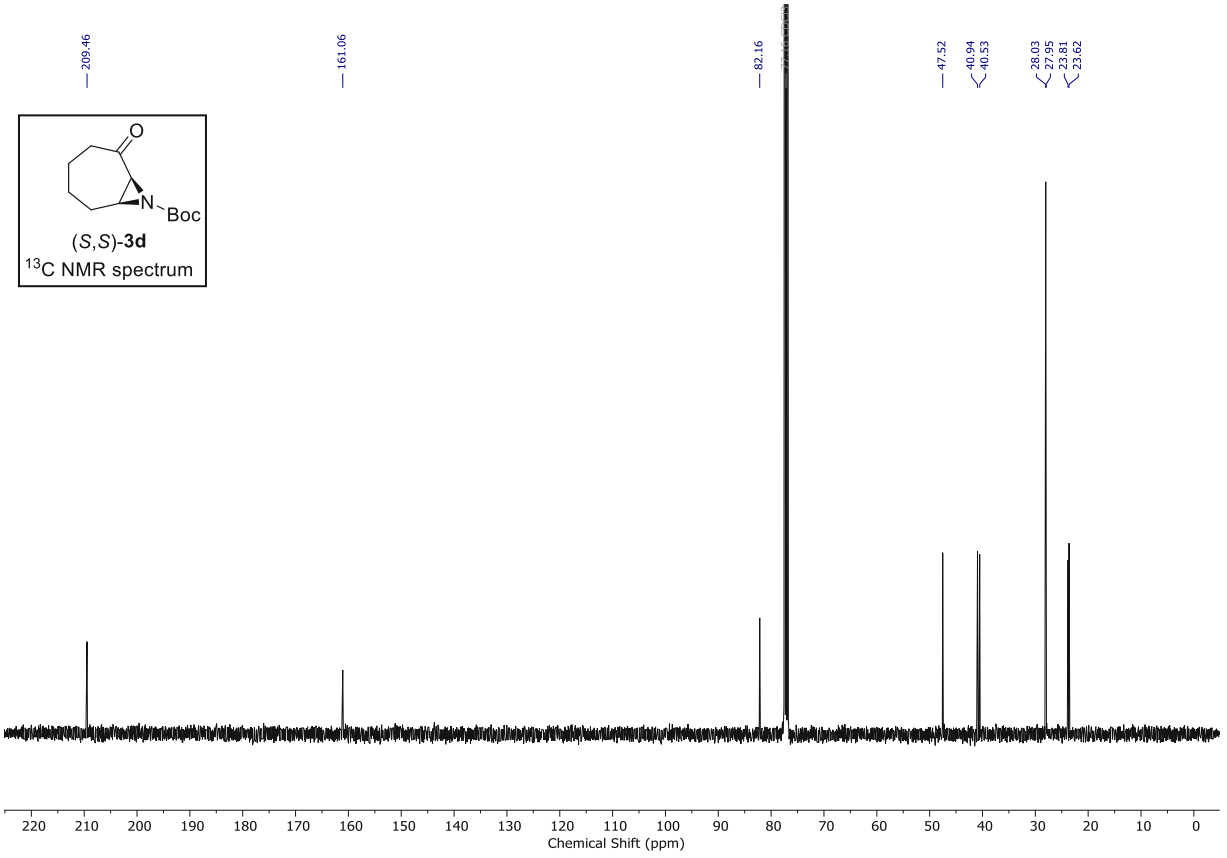
Die approbierte gedruckte Originalversion dieser Dissertation ist an der TU Wien Bibliothek verfügbar.
The approved original version of this doctoral thesis is available in print at TU Wien Bibliothek.



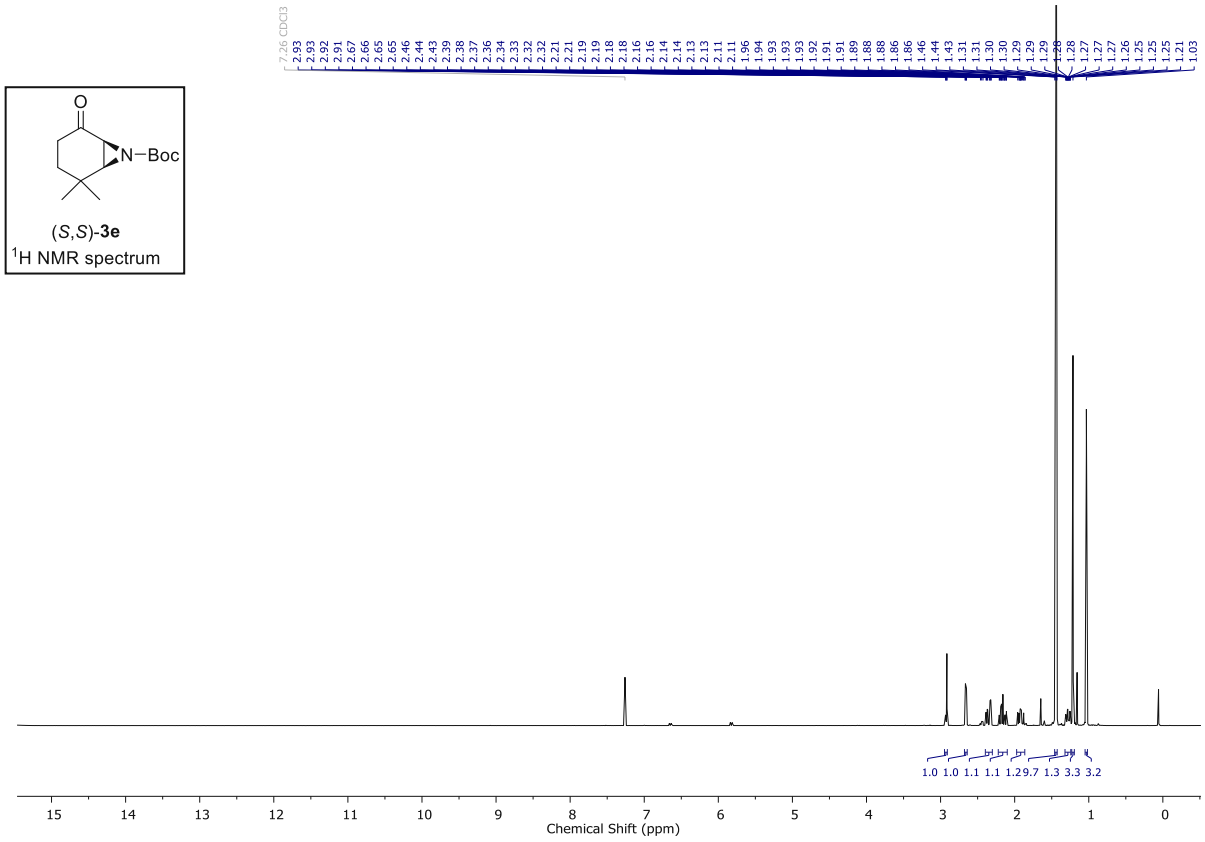


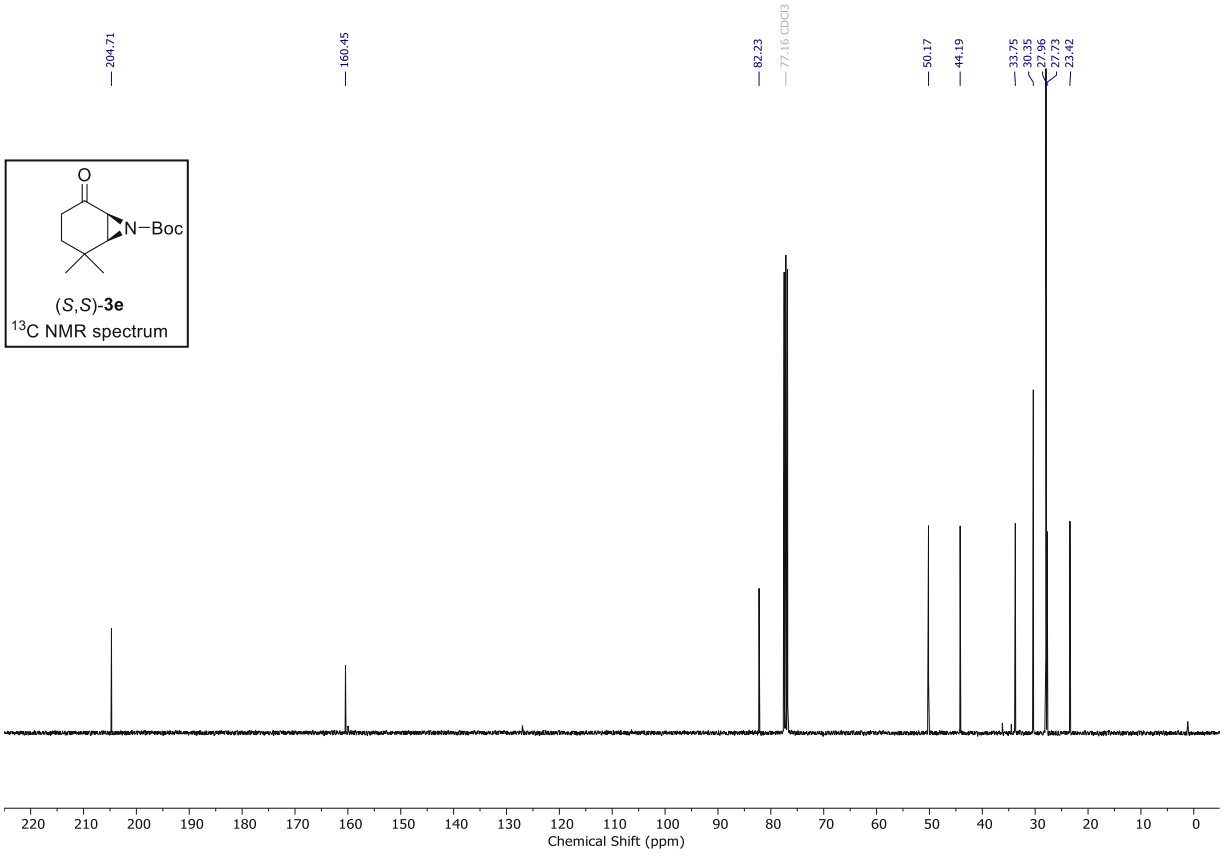
Die approbierte gedruckte Originalversion dieser Dissertation ist an der TU Wien Bibliothek verfügbar.
The approved original version of this doctoral thesis is available in print at TU Wien Bibliothek.



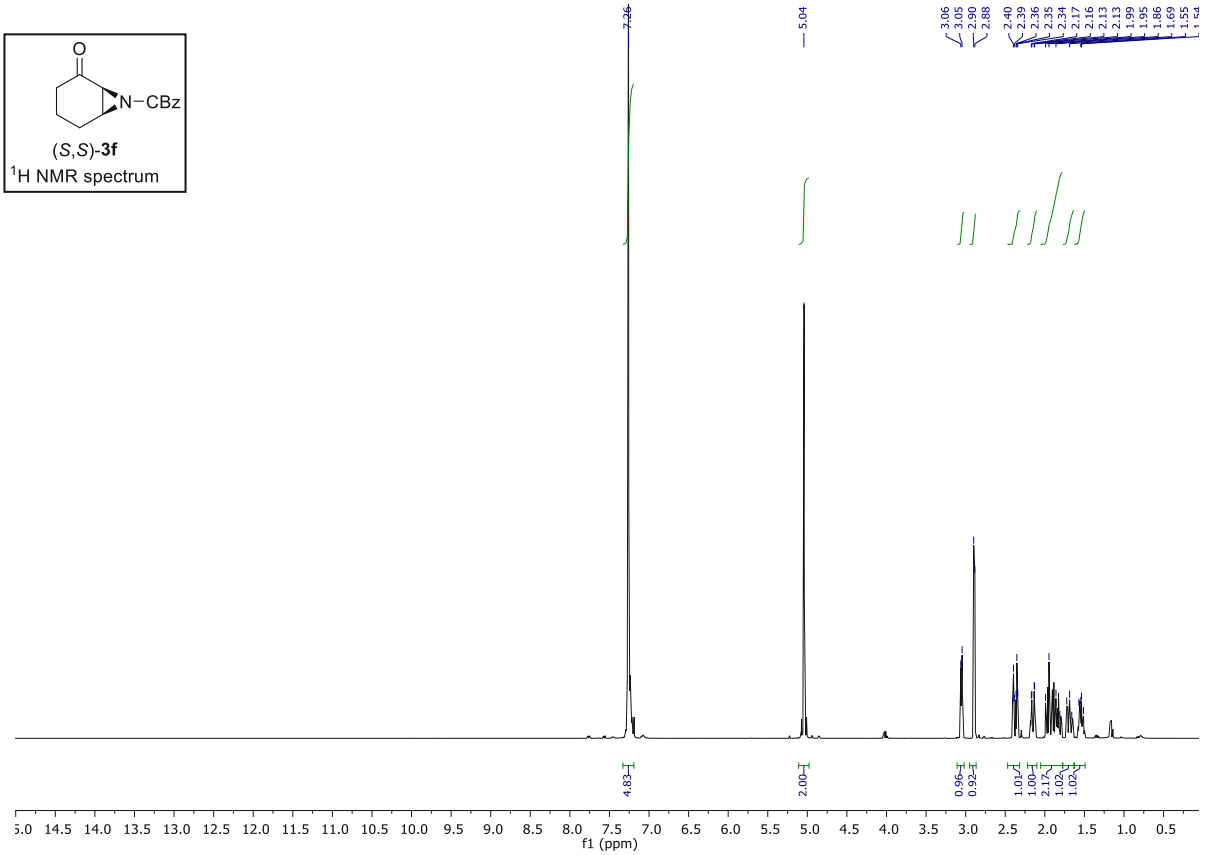


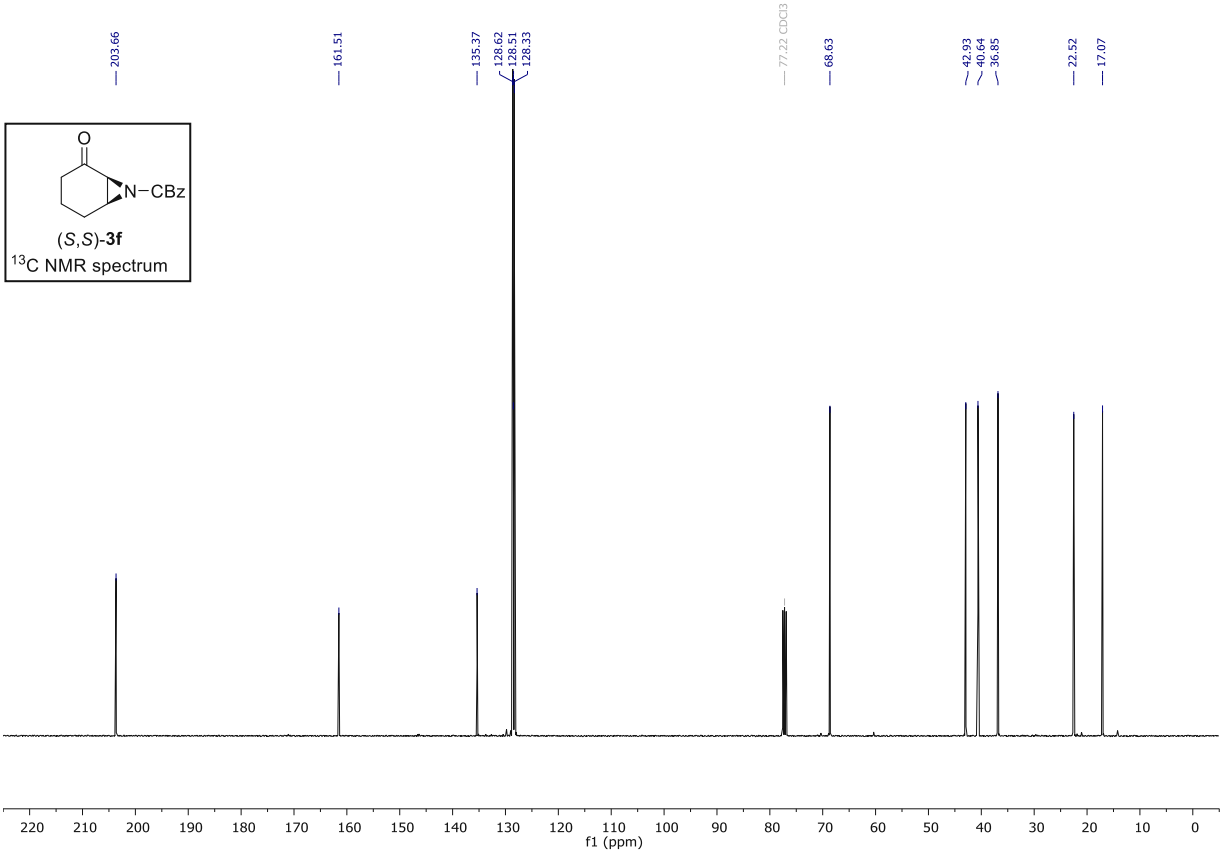
Die approbierte gedruckte Originalversion dieser Dissertation ist an der TU Wien Bibliothek verfügbar.
The approved original version of this doctoral thesis is available in print at TU Wien Bibliothek.



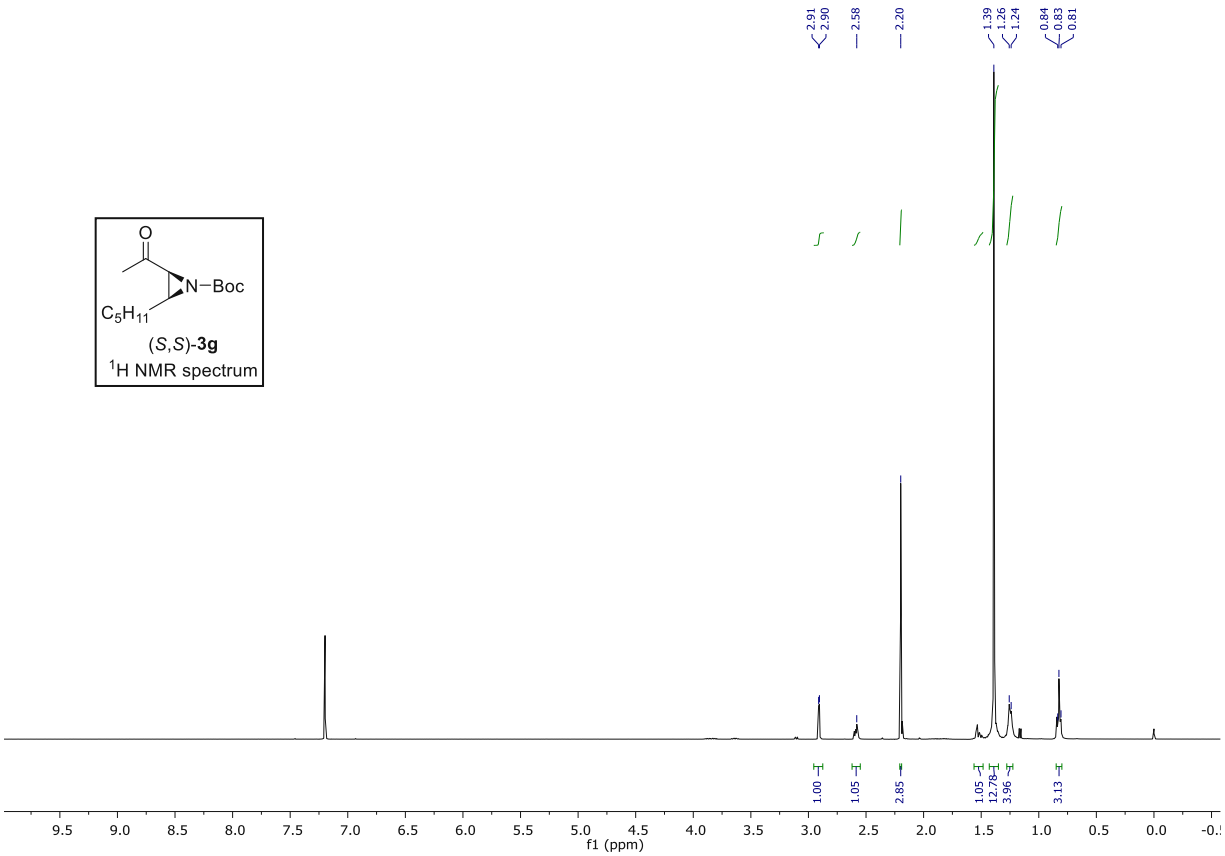


Die approbierte gedruckte Originalversion dieser Dissertation ist an der TU Wien Bibliothek verfügbar.
The approved original version of this doctoral thesis is available in print at TU Wien Bibliothek.

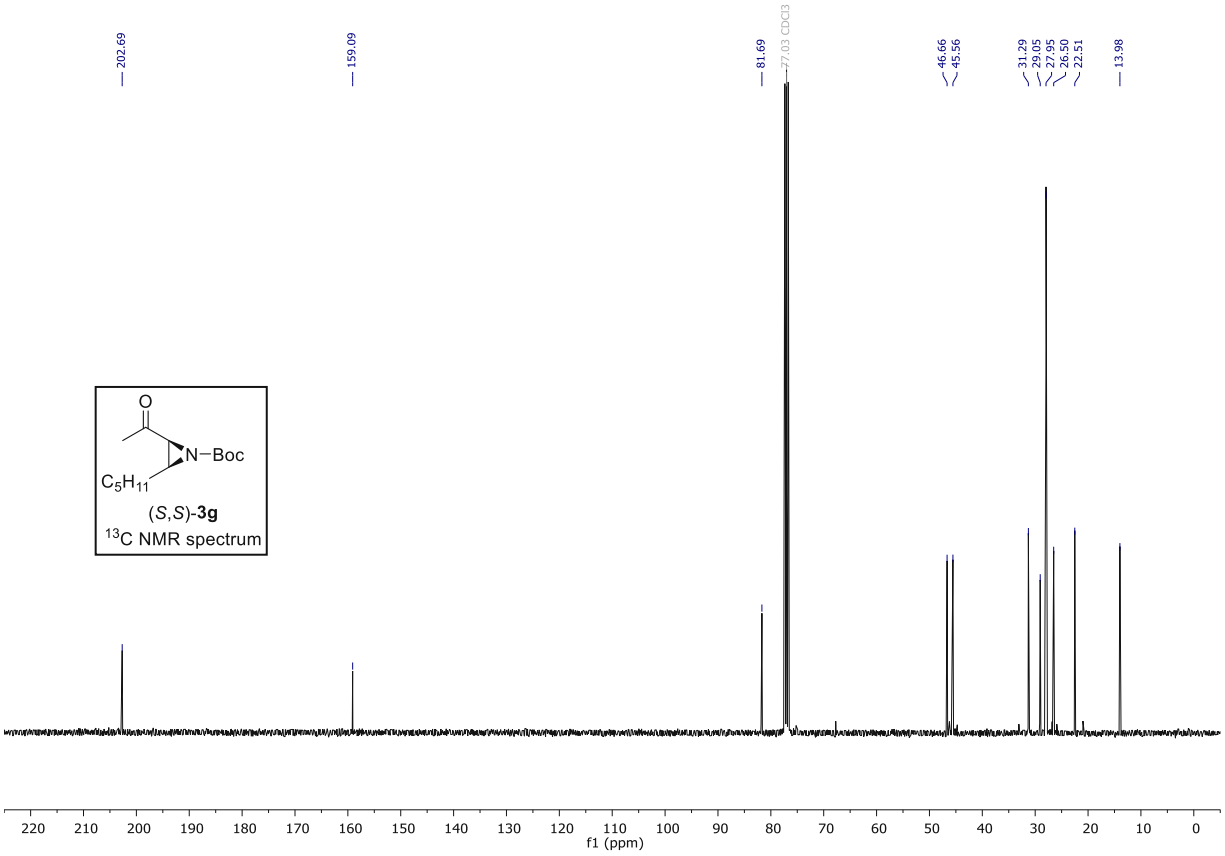




Die approbierte gedruckte Originalversion dieser Dissertation ist an der TU Wien Bibliothek verfügbar.
The approved original version of this doctoral thesis is available in print at TU Wien Bibliothek.

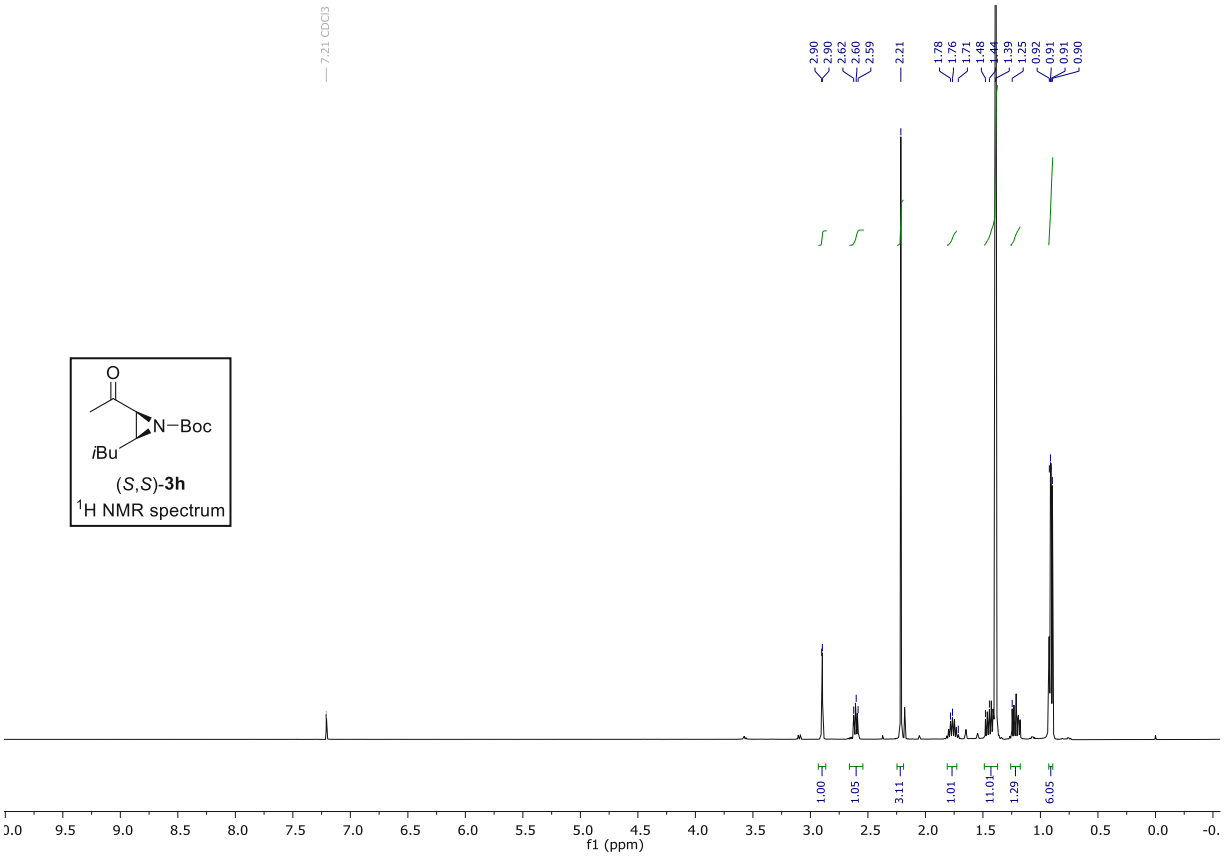


(*S*,*S*)-**3g**
^{1}H NMR spectrum

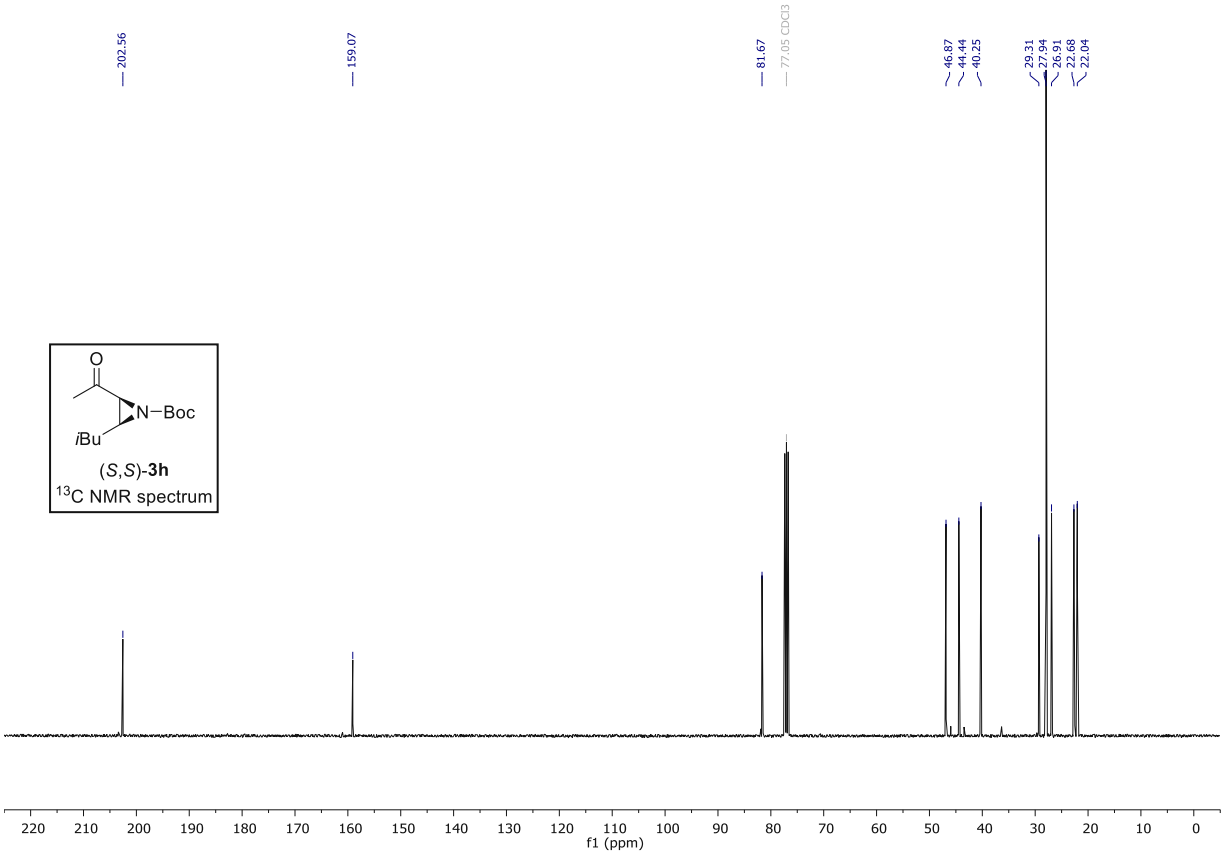


(*S*,*S*)-**3g**
^{13}C NMR spectrum

Die approbierte gedruckte Originalversion dieser Dissertation ist an der TU Wien Bibliothek verfügbar.
The approved original version of this doctoral thesis is available in print at TU Wien Bibliothek.



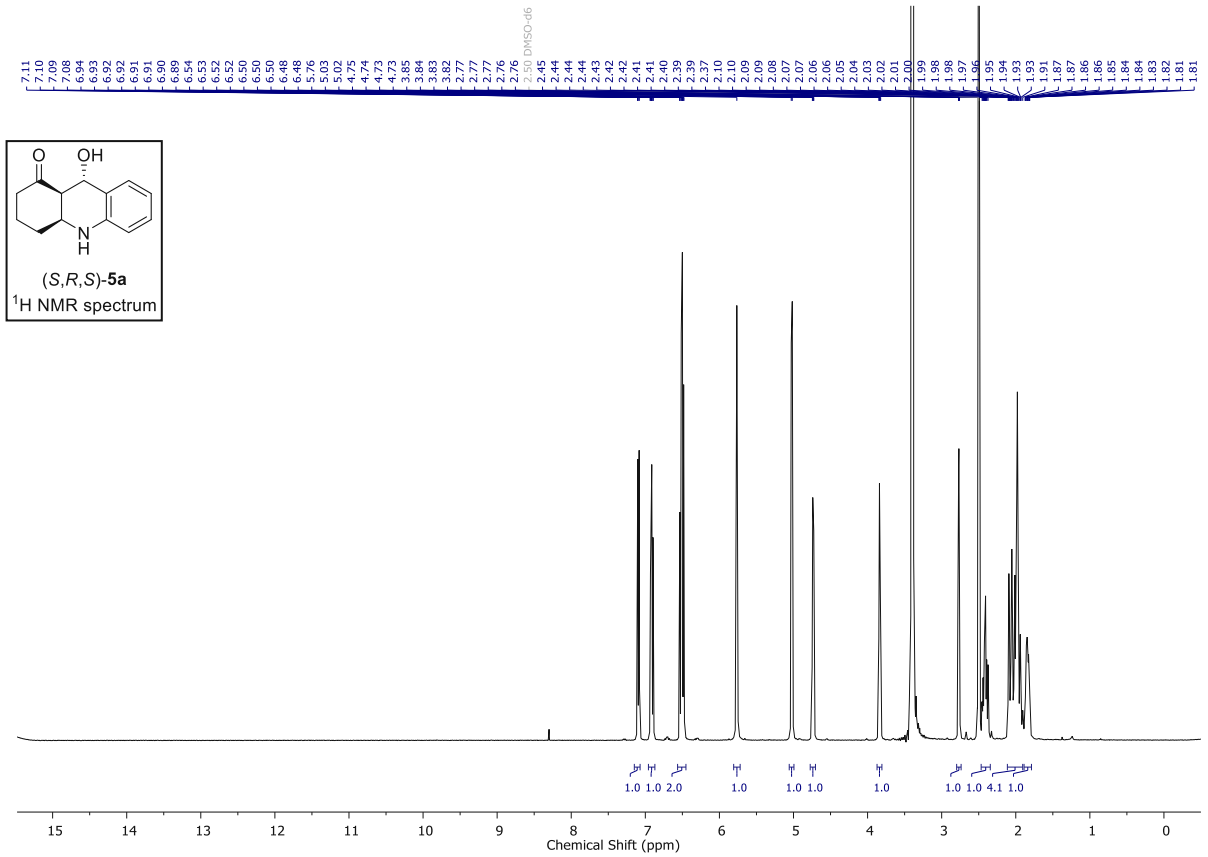
(*S*,*S*)-**3h**
^{1}H NMR spectrum

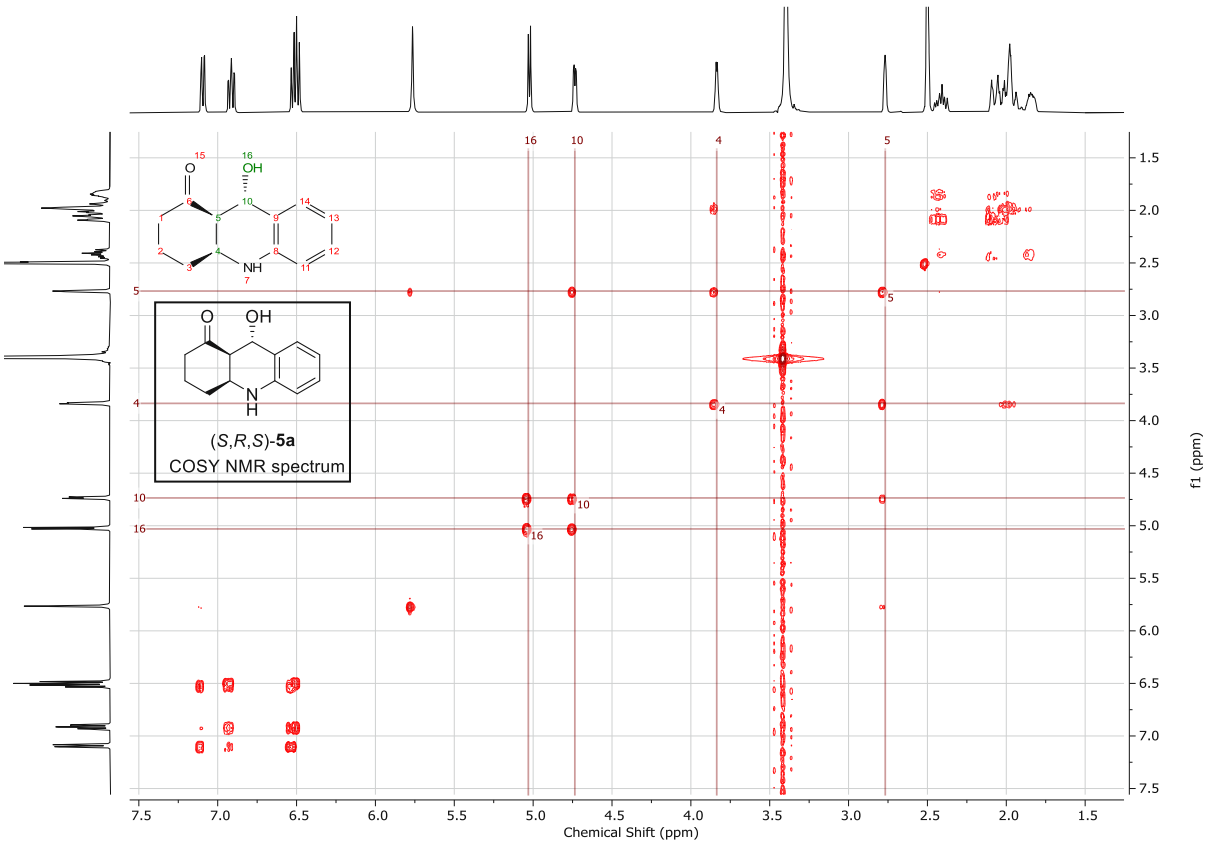


(*S*,*S*)-**3h**
^{13}C NMR spectrum

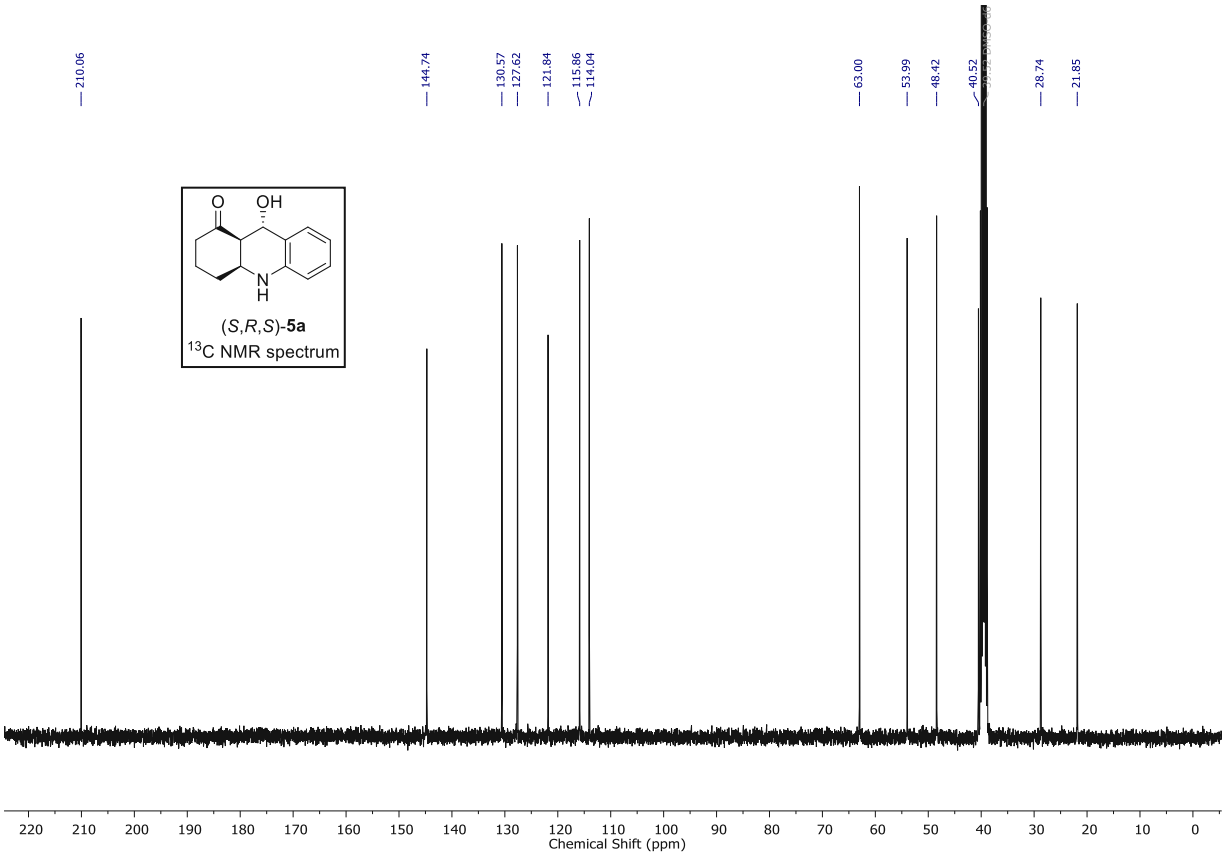
Die approbierte gedruckte Originalversion dieser Dissertation ist an der TU Wien Bibliothek verfügbar.
The approved original version of this doctoral thesis is available in print at TU Wien Bibliothek.

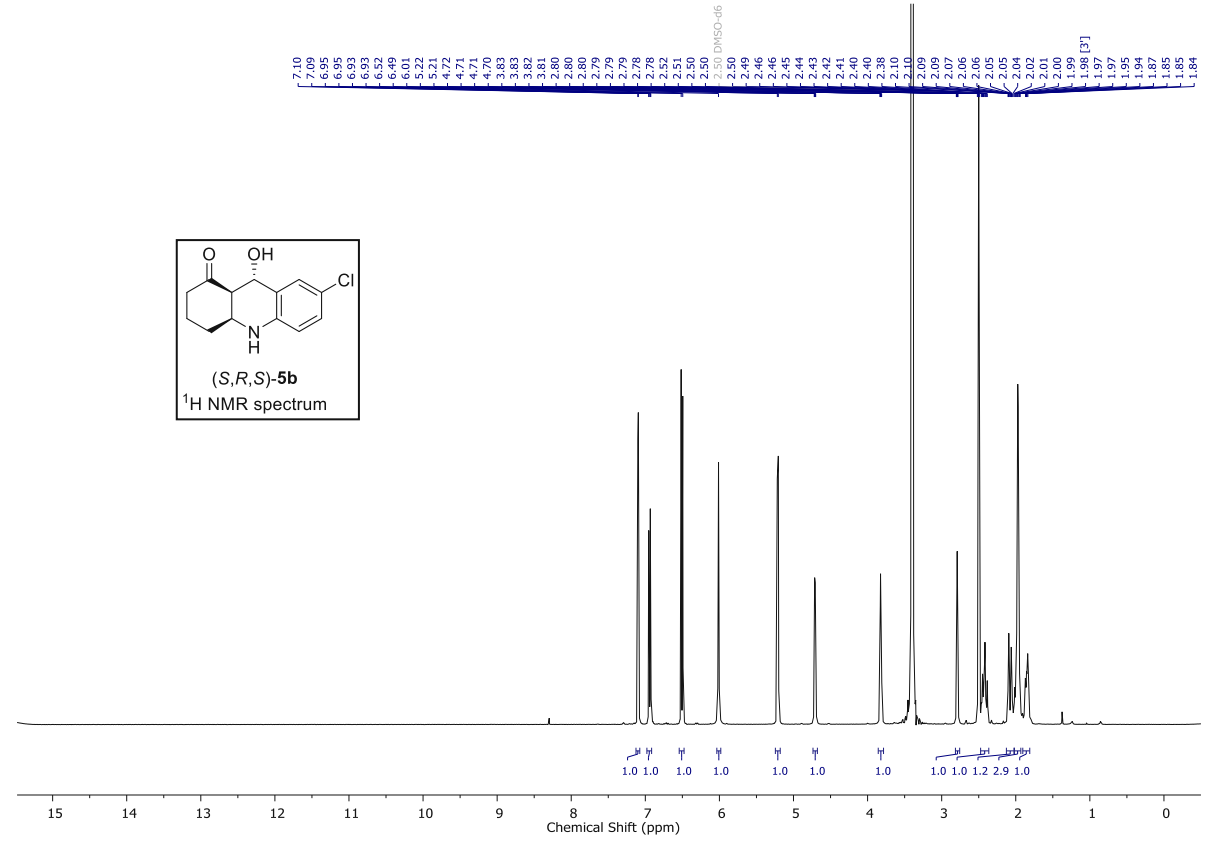
20. NMR spectra of asymmetric Aza-michael/aldol reactions



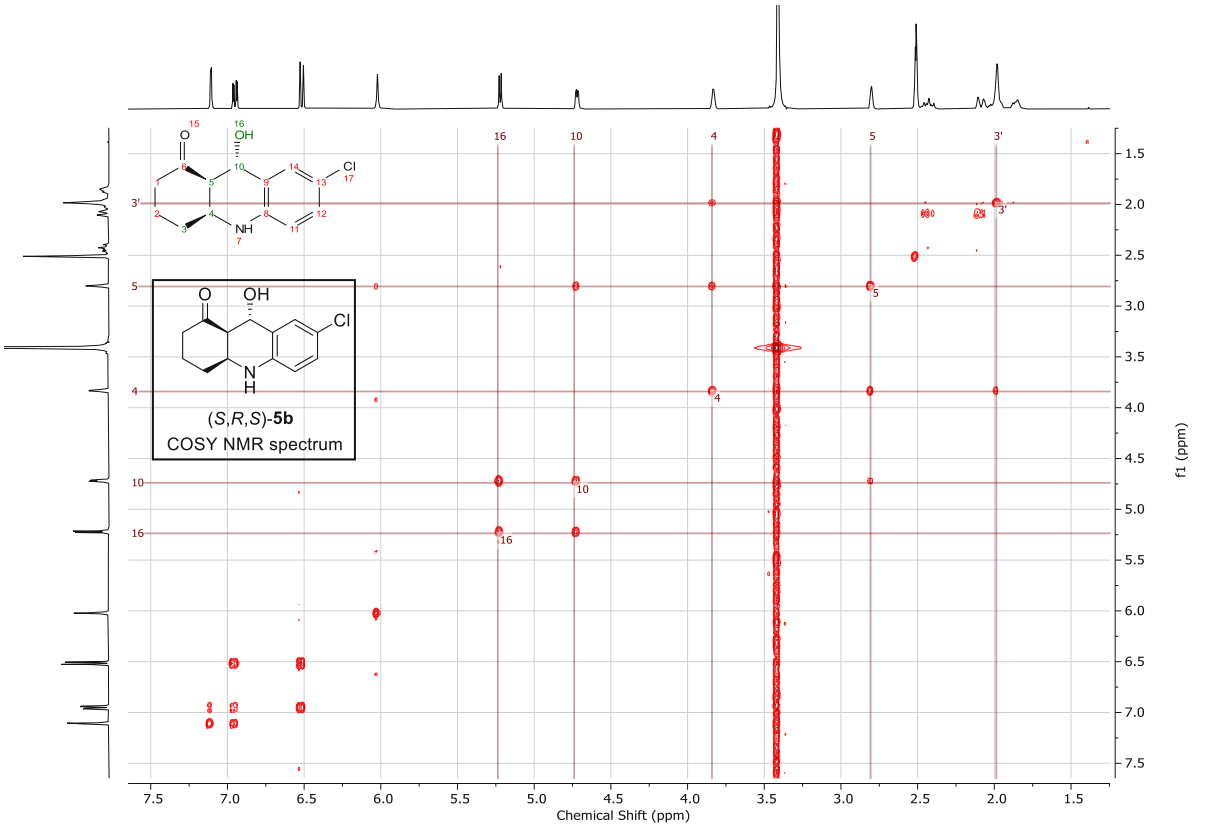


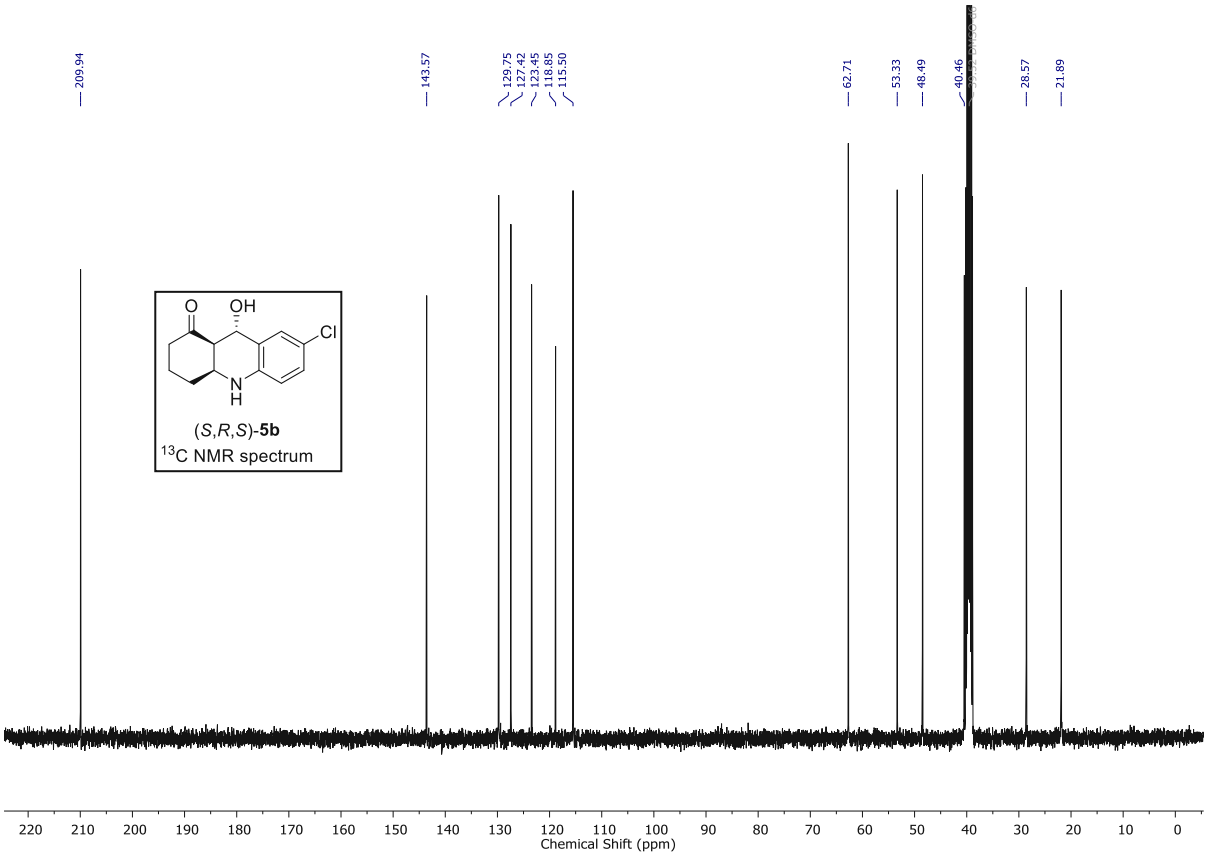
Die approbierte gedruckte Originalversion dieser Dissertation ist an der TU Wien Bibliothek verfügbar.
The approved original version of this doctoral thesis is available in print at TU Wien Bibliothek.
TU Bibliothek Your knowledge hub WIEN





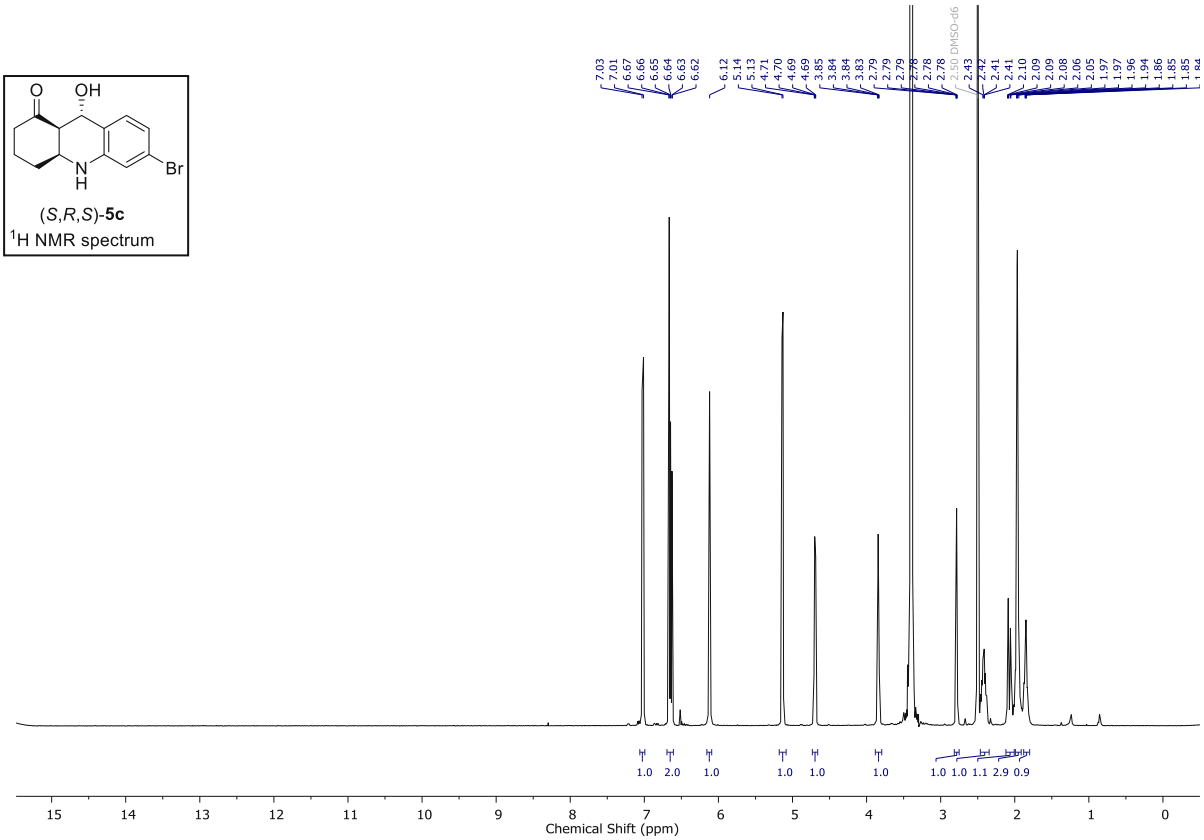
Die approbierte gedruckte Originalversion dieser Dissertation ist an der TU Wien Bibliothek verfügbar.
The approved original version of this doctoral thesis is available in print at TU Wien Bibliothek.

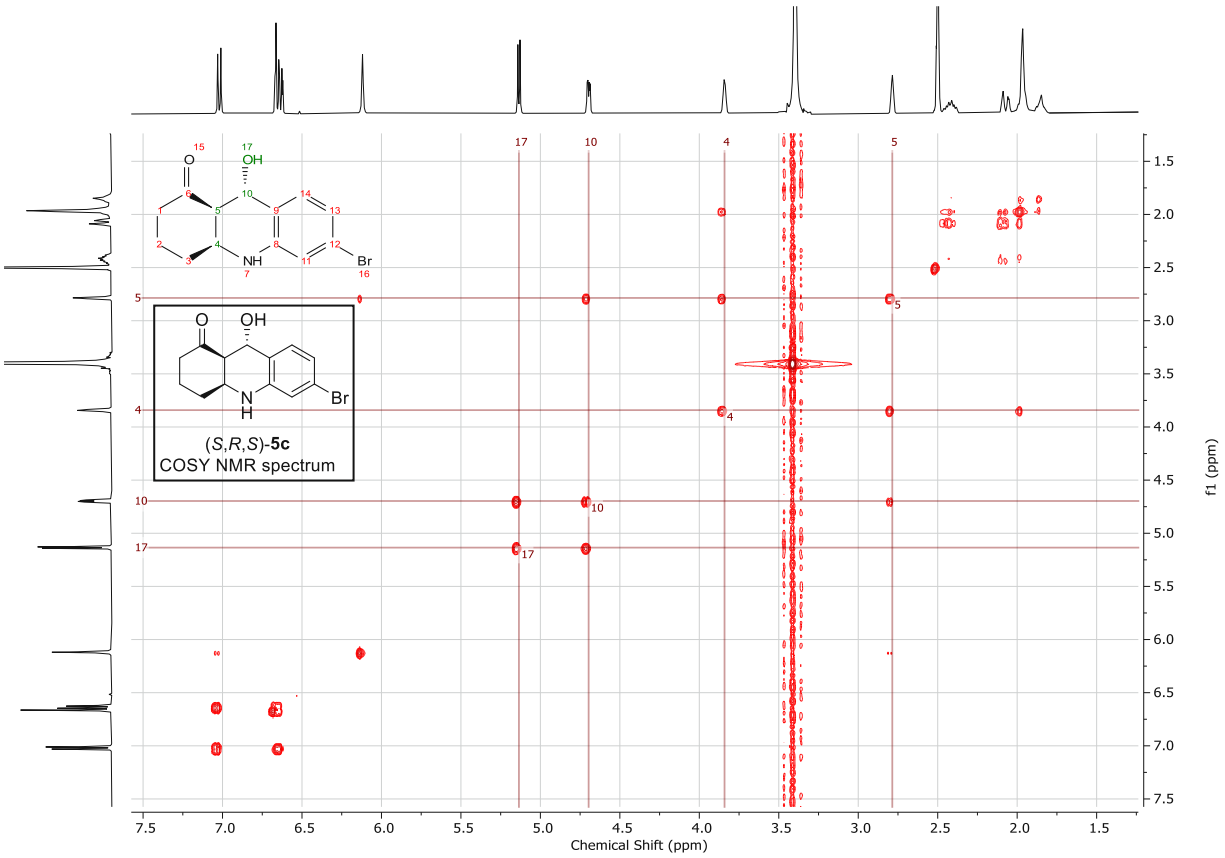




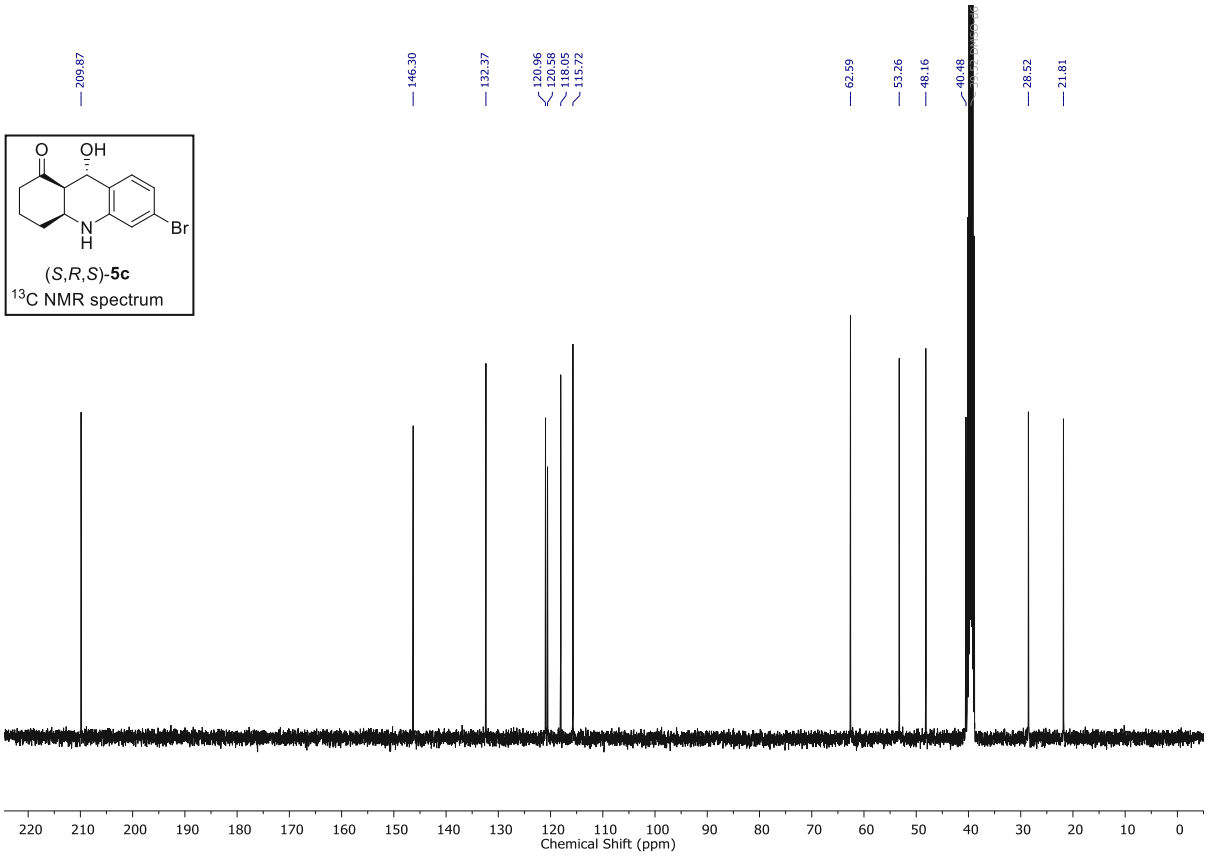
Die approbierte gedruckte Originalversion dieser Dissertation ist an der TU Wien Bibliothek verfügbar.
The approved original version of this doctoral thesis is available in print at TU Wien Bibliothek.

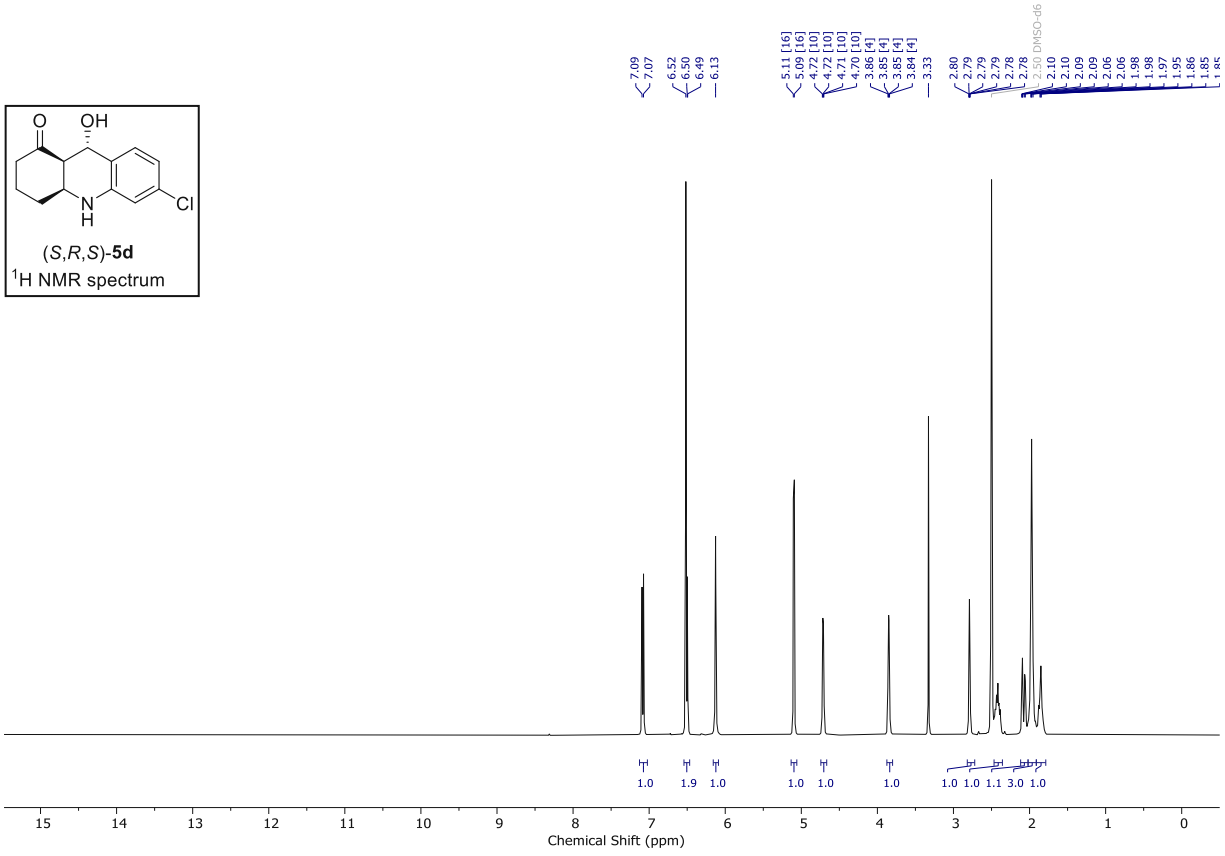
(*S*,*R*,*S*)-**5c**
^{1}H NMR spectrum



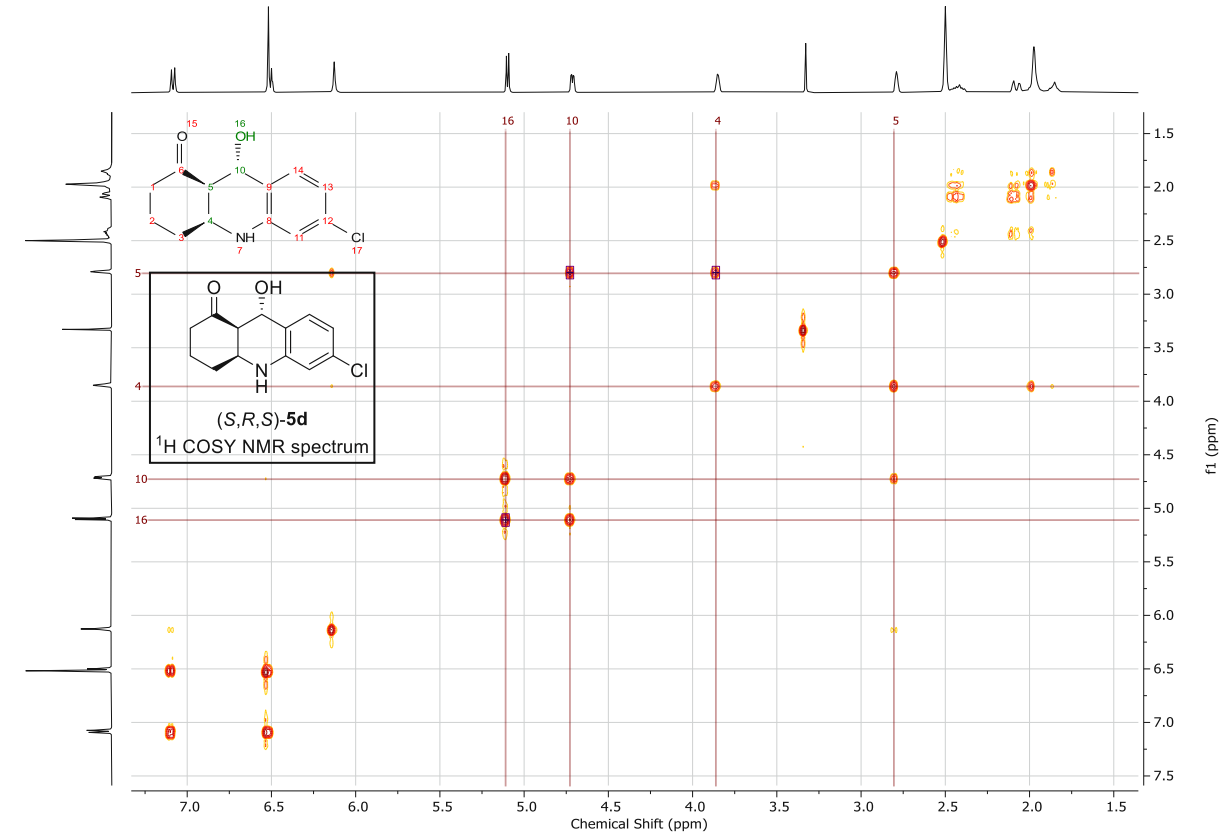


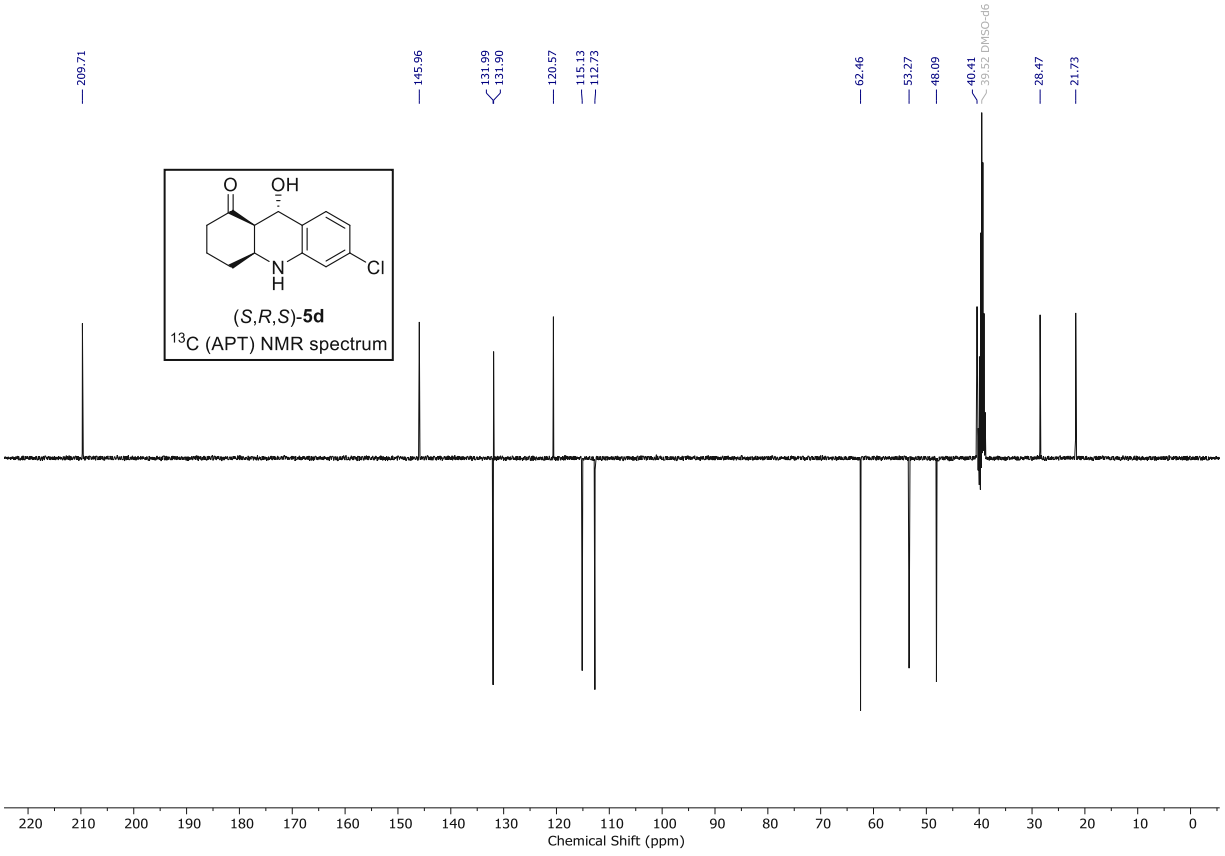
Die approbierte gedruckte Originalversion dieser Dissertation ist an der TU Wien Bibliothek verfügbar.
The approved original version of this doctoral thesis is available in print at TU Wien Bibliothek.



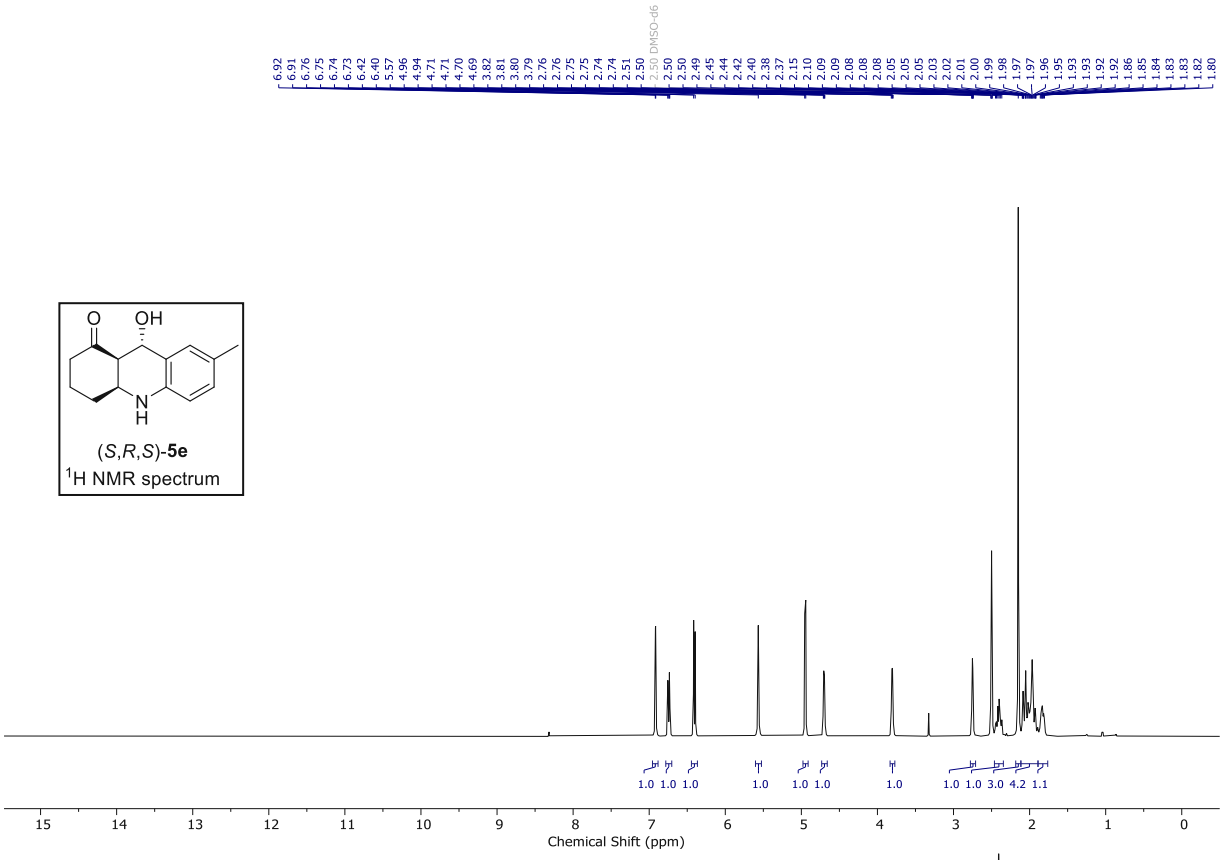


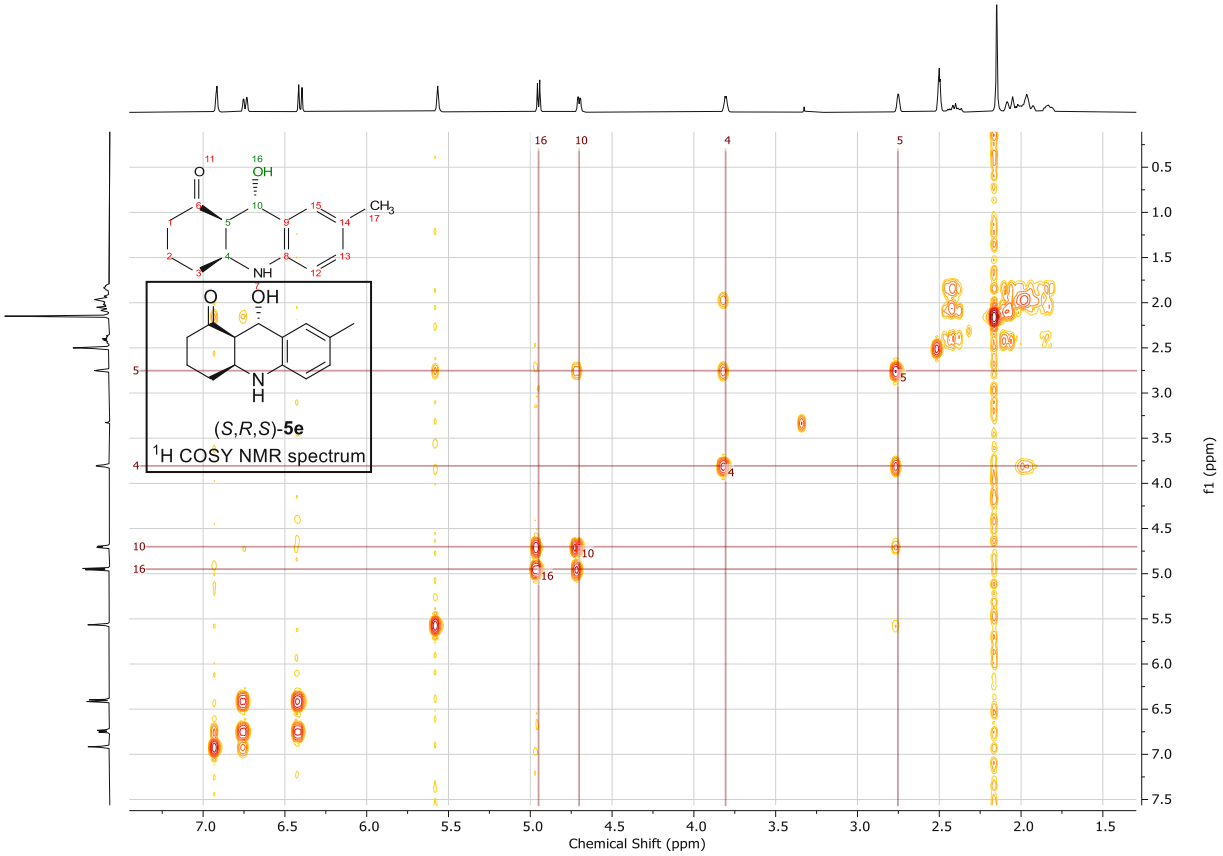
Die approbierte gedruckte Originalversion dieser Dissertation ist an der TU Wien Bibliothek verfügbar.
The approved original version of this doctoral thesis is available in print at TU Wien Bibliothek.



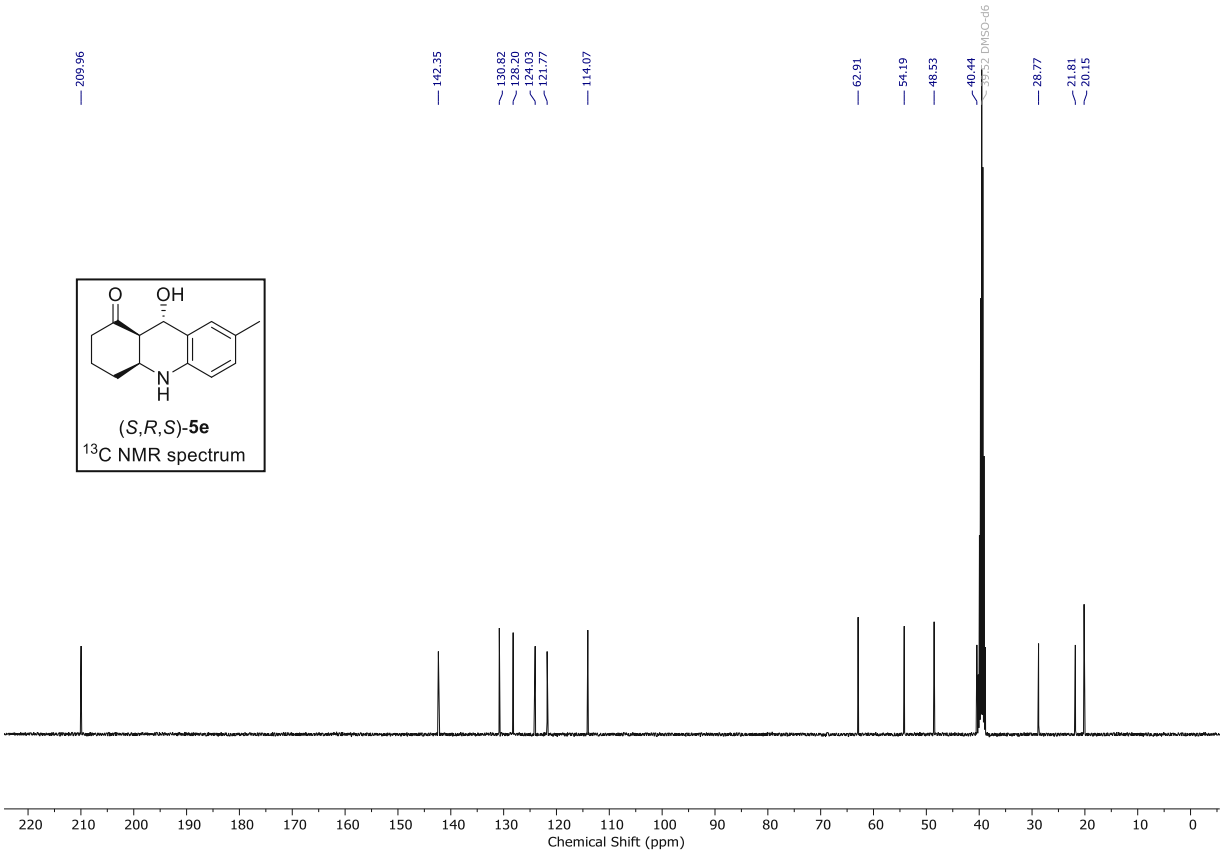


Die approbierte gedruckte Originalversion dieser Dissertation ist an der TU Wien Bibliothek verfügbar.
The approved original version of this doctoral thesis is available in print at TU Wien Bibliothek.



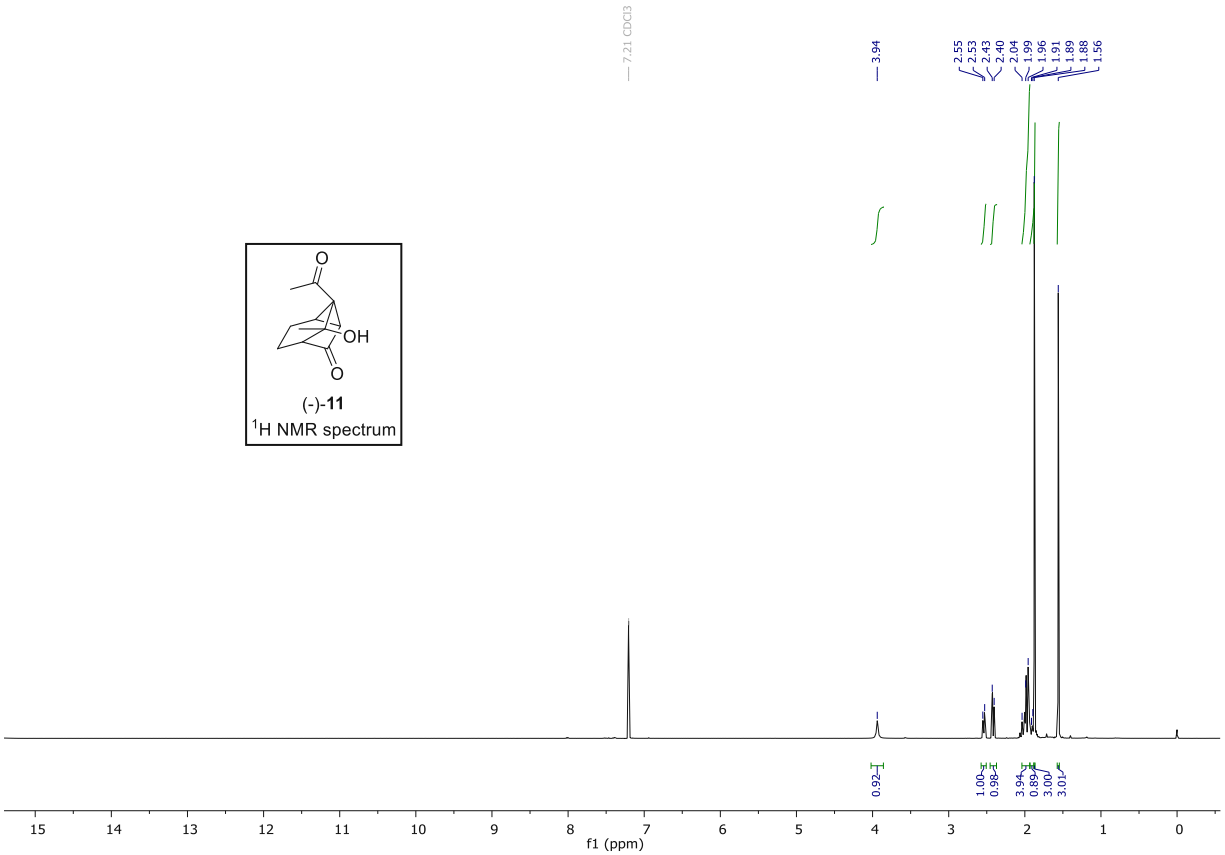


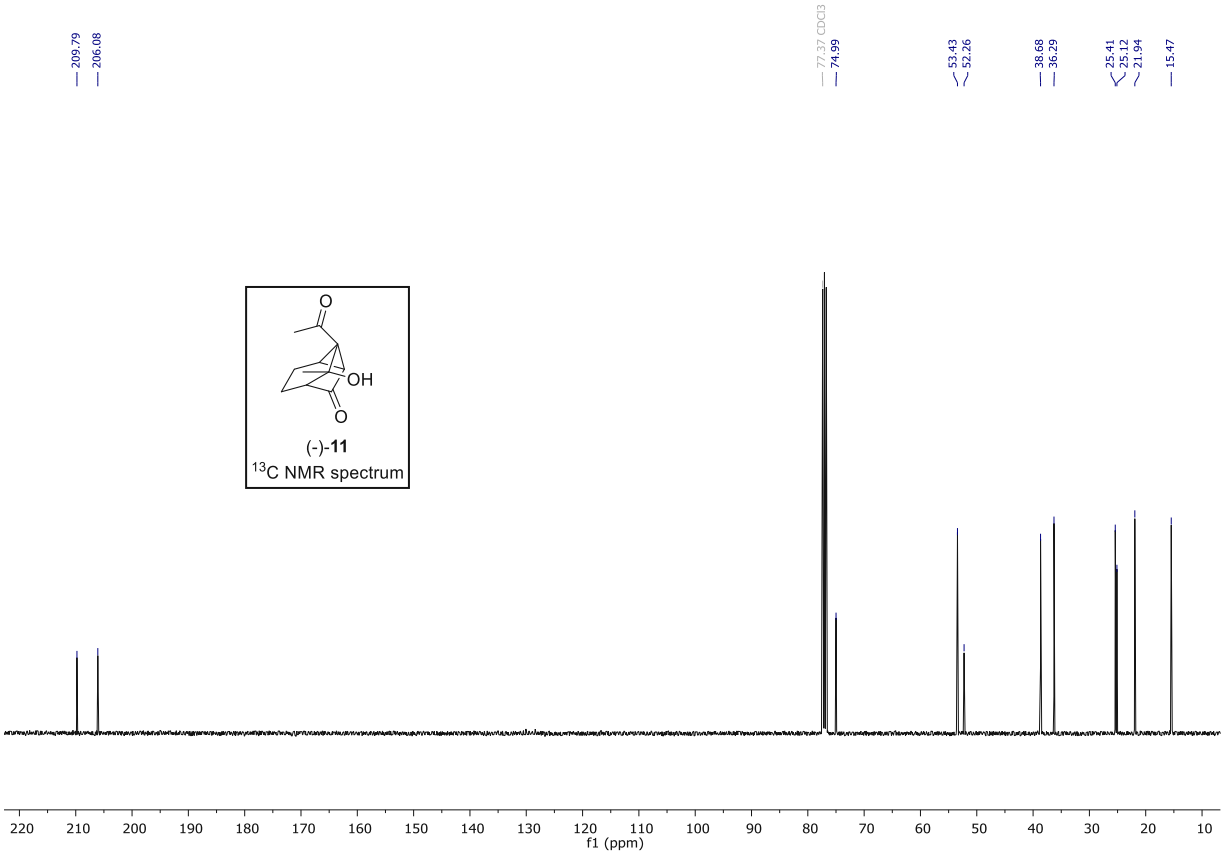
Die approbierte gedruckte Originalversion dieser Dissertation ist an der TU Wien Bibliothek verfügbar.
The approved original version of this doctoral thesis is available in print at TU Wien Bibliothek.



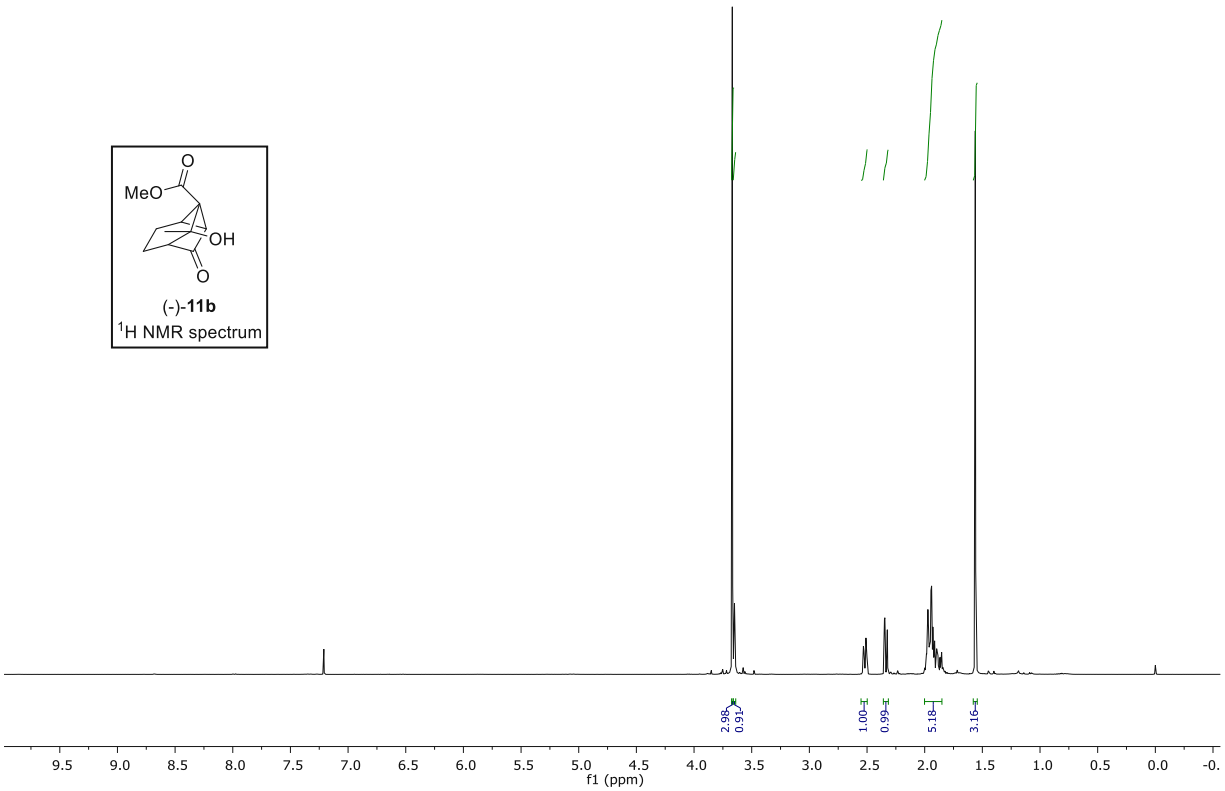
Die approbierte gedruckte Originalversion dieser Dissertation ist an der TU Wien Bibliothek verfügbar.
The approved original version of this doctoral thesis is available in print at TU Wien Bibliothek.

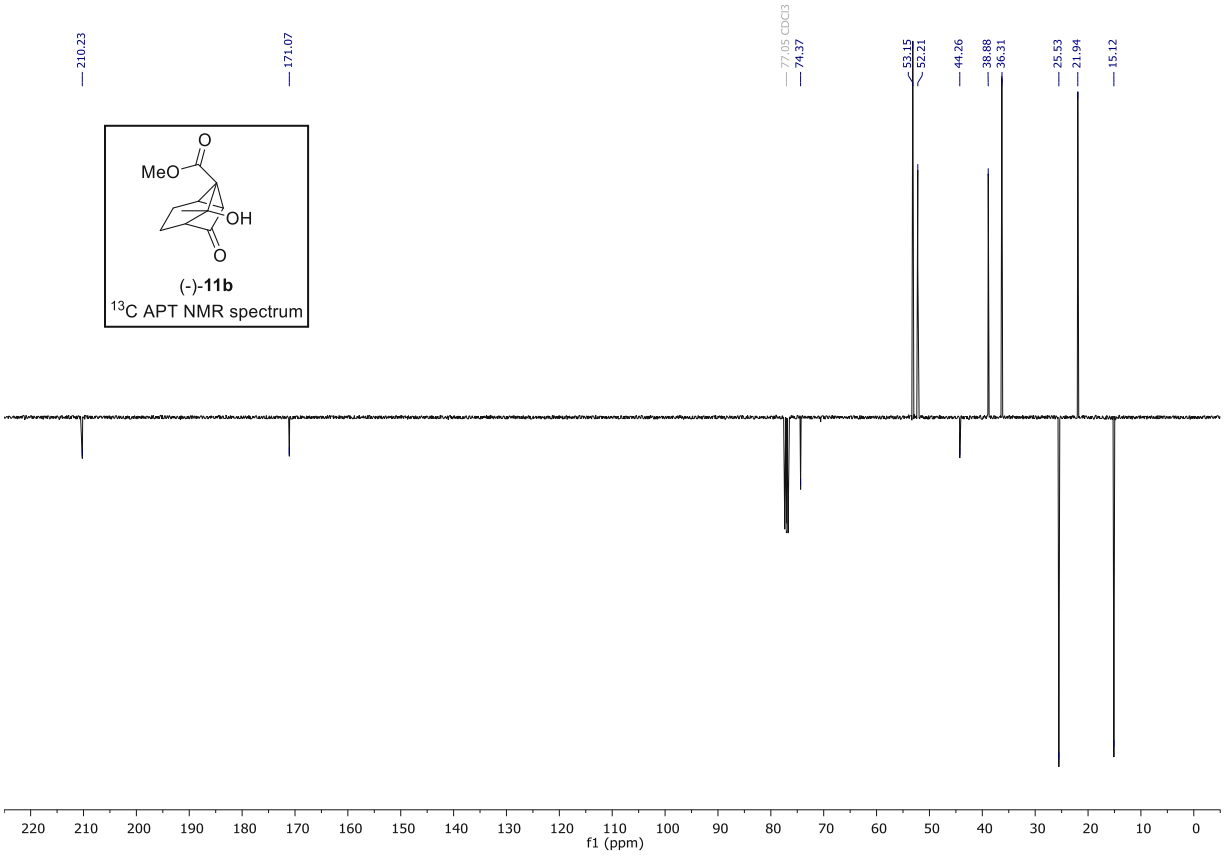
21. NMR spectra of asymmetric Michael-induced Ring-Closure/aldol reaction sequence



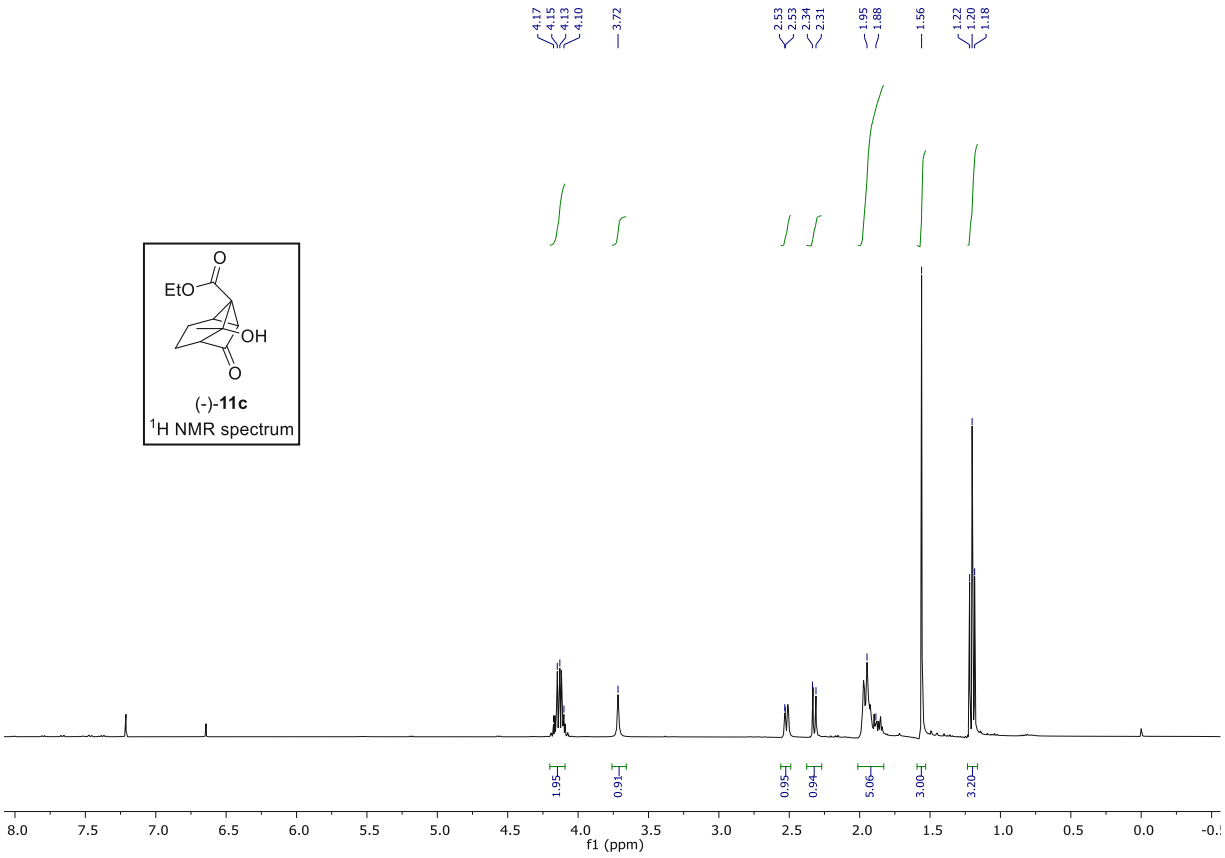


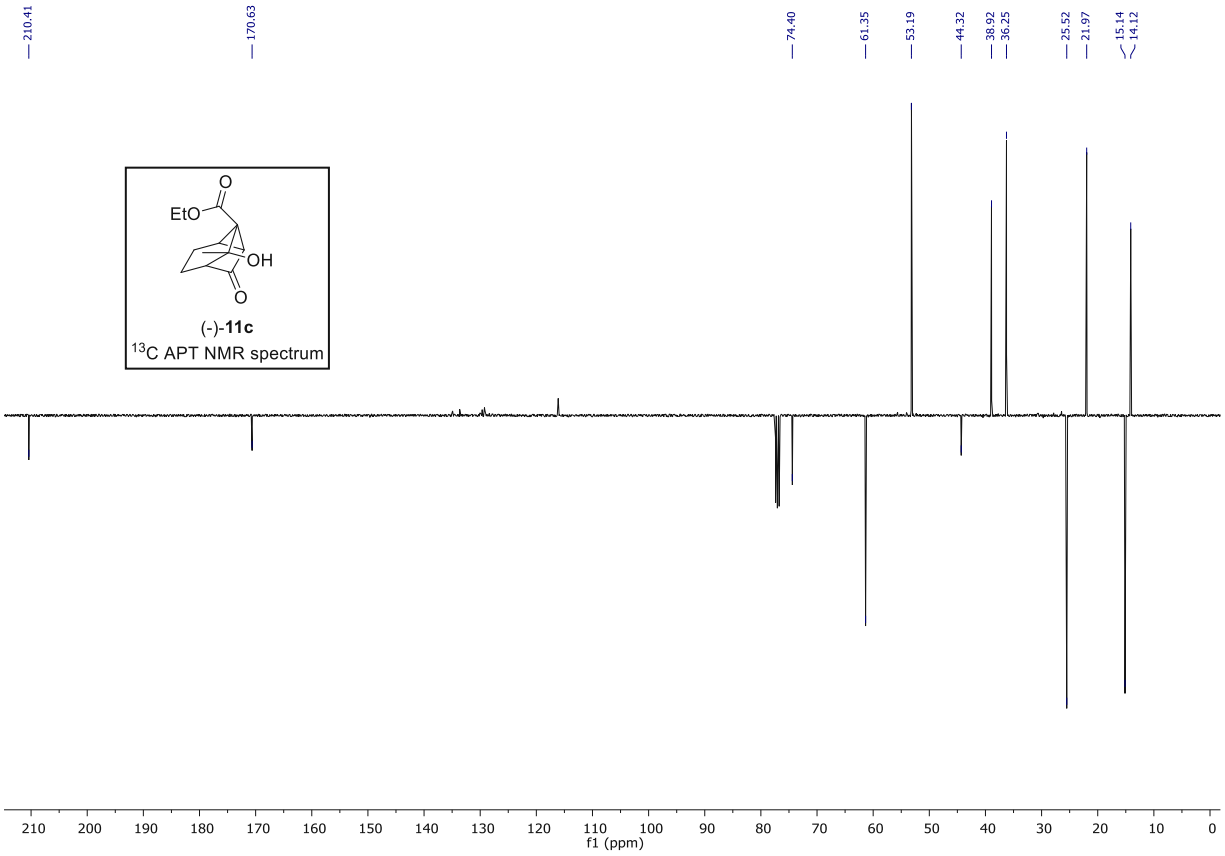
Die approbierte gedruckte Originalversion dieser Dissertation ist an der TU Wien Bibliothek verfügbar.
The approved original version of this doctoral thesis is available in print at TU Wien Bibliothek.



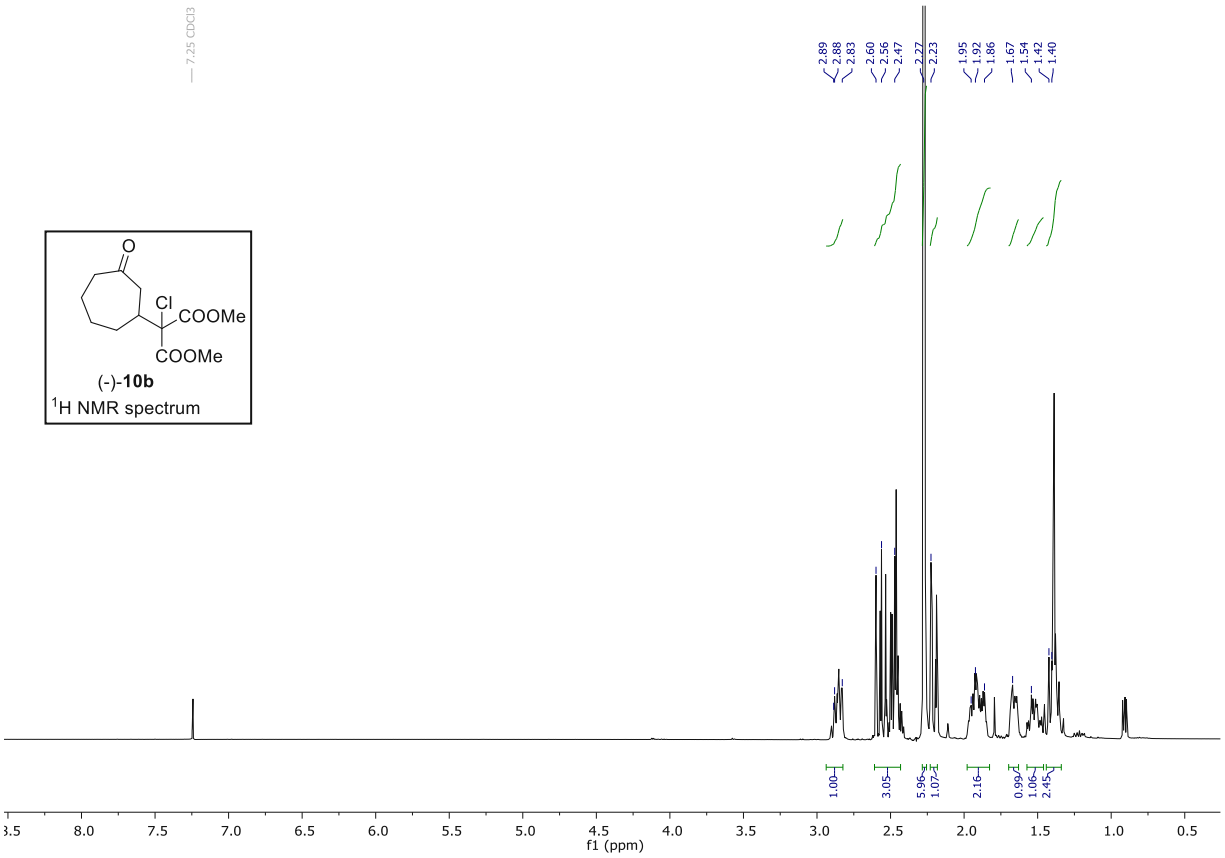


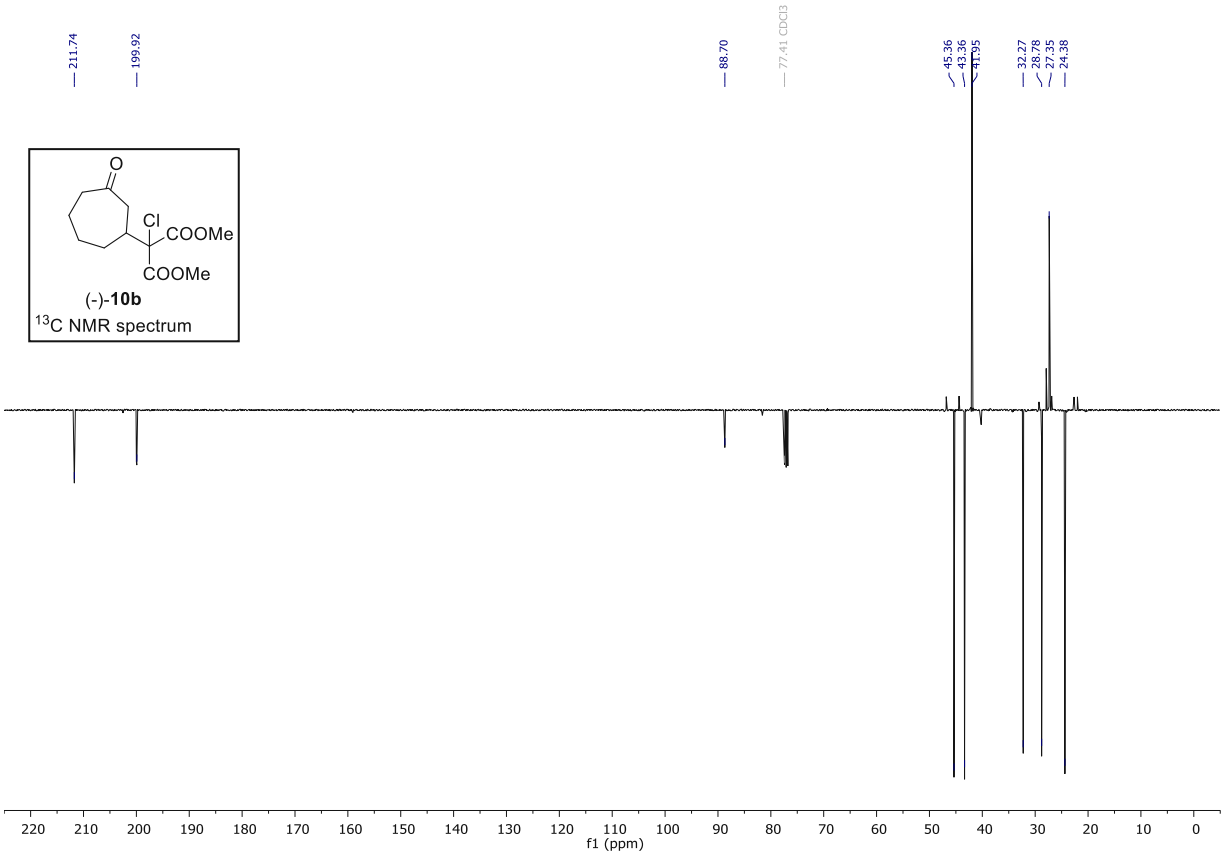
Die approbierte gedruckte Originalversion dieser Dissertation ist an der TU Wien Bibliothek verfügbar.
The approved original version of this doctoral thesis is available in print at TU Wien Bibliothek.





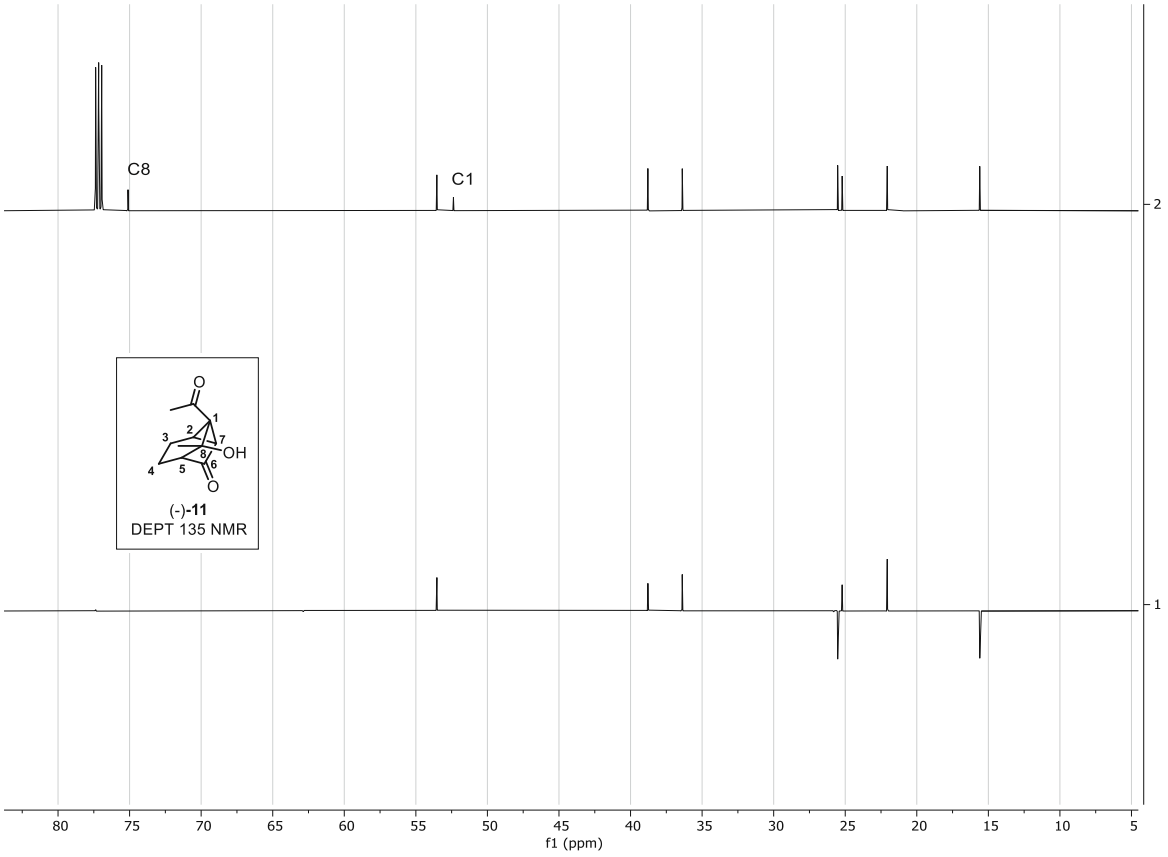
Die approbierte gedruckte Originalversion dieser Dissertation ist an der TU Wien Bibliothek verfügbar.
The approved original version of this doctoral thesis is available in print at TU Wien Bibliothek.

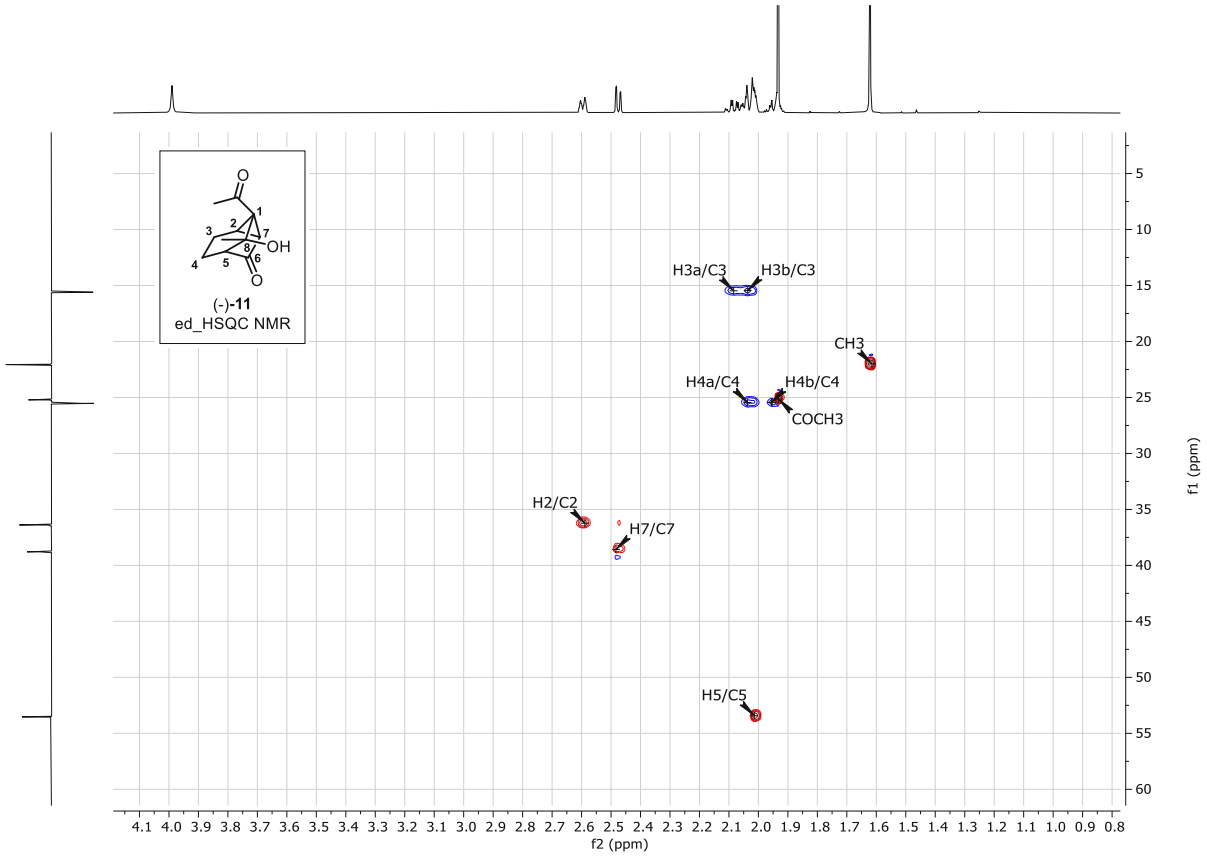




Die approbierte gedruckte Originalversion dieser Dissertation ist an der TU Wien Bibliothek verfügbar.
The approved original version of this doctoral thesis is available in print at TU Wien Bibliothek.

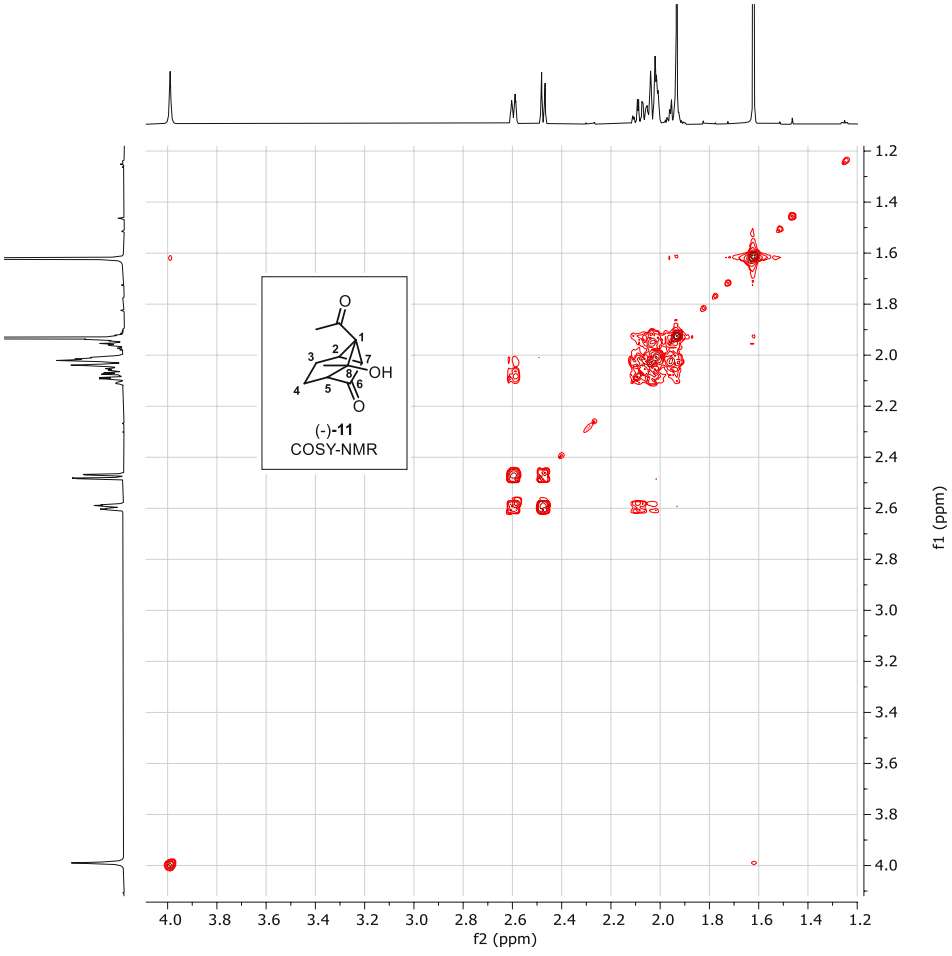
22. Extended 1D/2D-NMR experiments supporting the structure of compound 11





Die approbierte gedruckte Originalversion dieser Dissertation ist an der TU Wien Bibliothek verfügbar.
The approved original version of this doctoral thesis is available in print at TU Wien Bibliothek.

Comparison between the standard C-spectrum and a DEPT-135 experiment identified two CH_2 groups (C2, C4) and besides two carbonyl groups 2 further quaternary signals in the aliphatic region at 75.11 (C8) and 53.37 (C1) ppm. The signal at 75.11 ppm clearly suggesting the vicinity to a strongly withdrawing group/atom like the hydroxyl group. Along with the phase sensitive HSQC spectrum, two CH_3 groups with significantly different chemical environment were identified, one bearing with the typical shifts for an acetyl groups, further assigned as $COCH_3$ and CH_3. Three CH-groups were identified as unambiguous $^{1}H/^{13}C$ shift dupels, corresponding to the 2, 5 and 7-position. This analysis already pointed to an additional bond formation in line with some sort of aldol-type chemistry, additionally to the targeted cyclopropanation transformation. The HSQC also identified the broad singlet at 3.99 ppm as a proton attached to a hetero-atom; considering the starting chemical structure of the starting material most likely an OH group. Measurement of a ^{1}H NMR in DMSO-d_6 confirmed the isolated singlet.



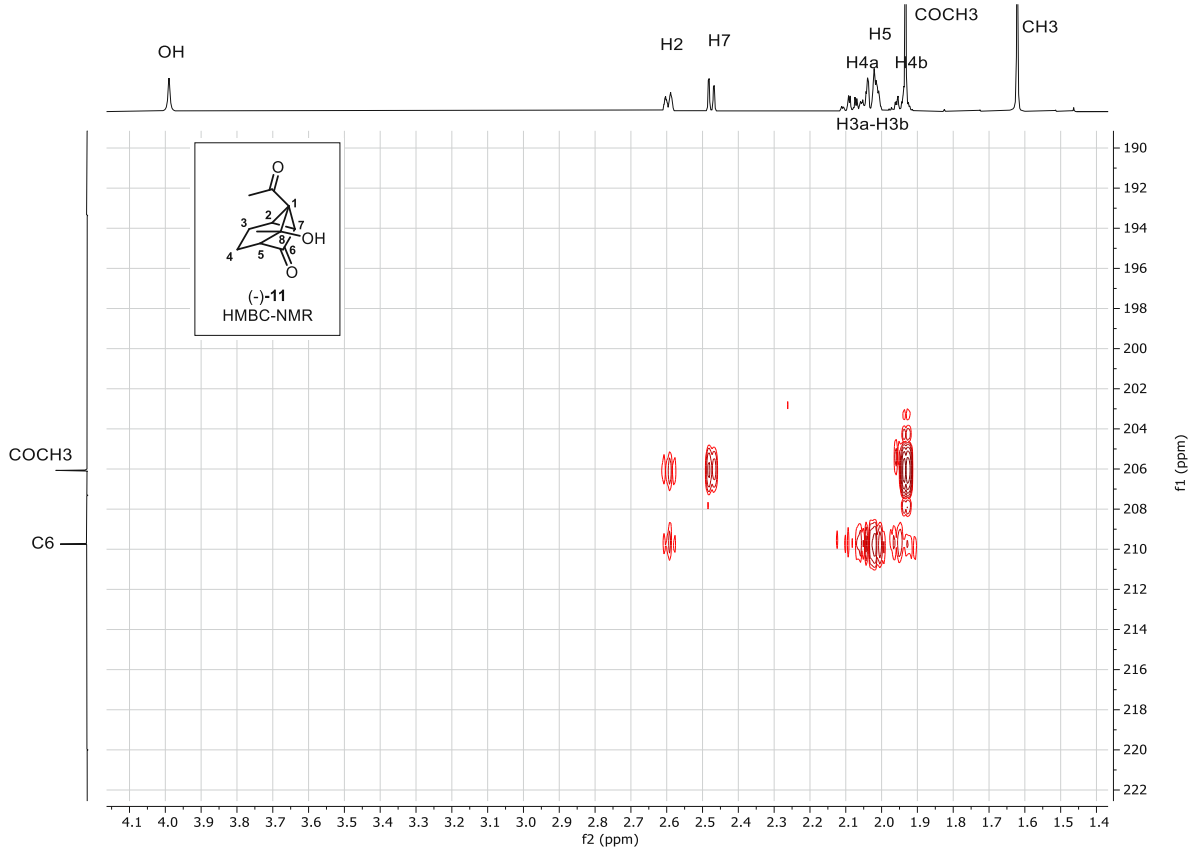
H,H-COSY-correlation

The H,H-COSY spectrum confirmed the two CH_2 groups identified in the HSQC and pointed towards the H7-H2-H3a,b spin system and in line with correlation to the H4a/H4b system, which however is in the crowded region of the spectrum (1.9 - 2.15 ppm). Consequently, also the putative correlation between H5 and H4a/H4b could not be resolved due to complete overlap of the signals as is also visible in the

Die approbierte gedruckte Originalversion dieser Dissertation ist an der TU Wien Bibliothek verfügbar.
The approved original version of this doctoral thesis is available in print at TU Wien Bibliothek.

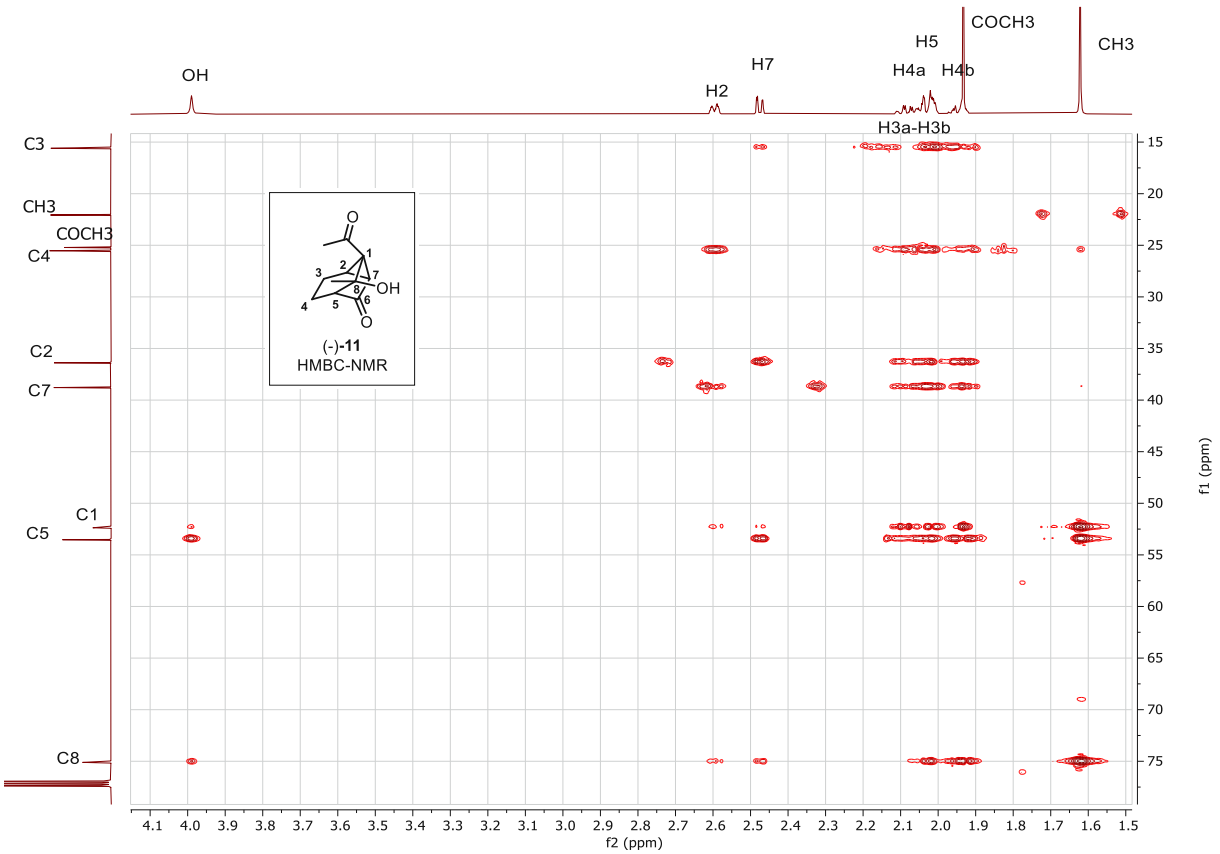
HSQC spectrum. Further, a weak correlation of the OH group with the isolated CH_3 group is also observed, consistent with structure and assignment.

HMBC-Correlation



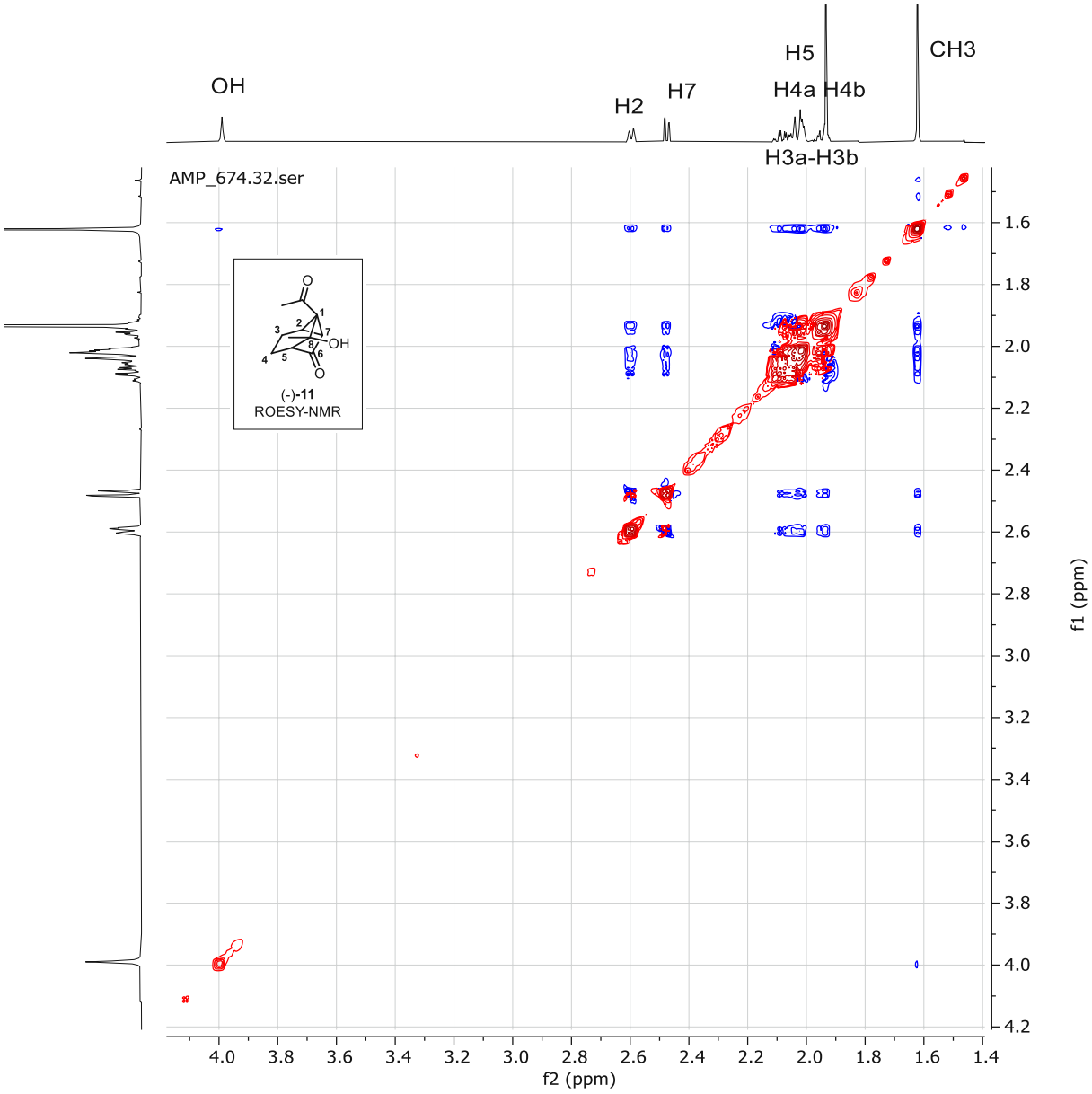
Due to the similar ^{1}H-shifts of many signals the HMBC-correlation is complex but nonetheless allows confirmation of the suggested structure. Only selected correlations are pointed out here. It clearly allowed the assignment of the two carbonyl groups to the remaining acetyl group (206 ppm) based on correlation to the $COCH_3$ signal and the other carbonyl group in the ring-system (210 ppm). All observed correlations over two and particularly three bonds (C6-H2, H4, H5 and **C**OCH_3 to H2, H7) from these carbonyls are consistent with the structure. Further, in the HMBC the vicinity of the hydroxyl-group and the isolated methyl group to both quaternary carbons (C1, C8) is clearly established as well as the additional correlation of the methyl group to the C5-position. Importantly, there are also no correlations conflicting with the suggested structure, which was later also confirmed via the crystal structure.

Die approbierte gedruckte Originalversion dieser Dissertation ist an der TU Wien Bibliothek verfügbar.
The approved original version of this doctoral thesis is available in print at TU Wien Bibliothek.



In respect to the relative stereochemistry at C8, both the NOESY (not shown) and ROESY-correlation exhibit a clear correlation between the methyl group at 1.62 ppm (but not the OH group) and all CH and CH_2 groups of the ring system, indicating that the methyl groups must be in the *endo*-position in respect to the former cyclohexyl ring system which was also later confirmed in the crystal structure.

Die approbierte gedruckte Originalversion dieser Dissertation ist an der TU Wien Bibliothek verfügbar.
The approved original version of this doctoral thesis is available in print at TU Wien Bibliothek.



Die approbierte gedruckte Originalversion dieser Dissertation ist an der TU Wien Bibliothek verfügbar.
The approved original version of this doctoral thesis is available in print at TU Wien Bibliothek.

23. NMR Studies for Phosphoric Acids

In order to probe our hypothesis whether the phosphoric acids **PA5**-**PA9** can eventually form stable enantiomers under the reaction conditions, ^{31}P NMR studies of the salts [(*S*)-**AM6**][**PA3**] and [(*S*)-**AM6**][**PA9**] have been carried out at different temperatures.

The ^{31}P NMR spectra of the salts [(*S*)-**AM6**][**PA3**] resulted in complete peak splitting already when being measured at 27 ˚C, indicating the formation of stable diastereomers in chiral environment, therefore suggesting that the acid **PA3** is chiral and it can form stable, distinguishable enantiomers at room temperature as a result of its steric hindrance (Figures S1-S2).

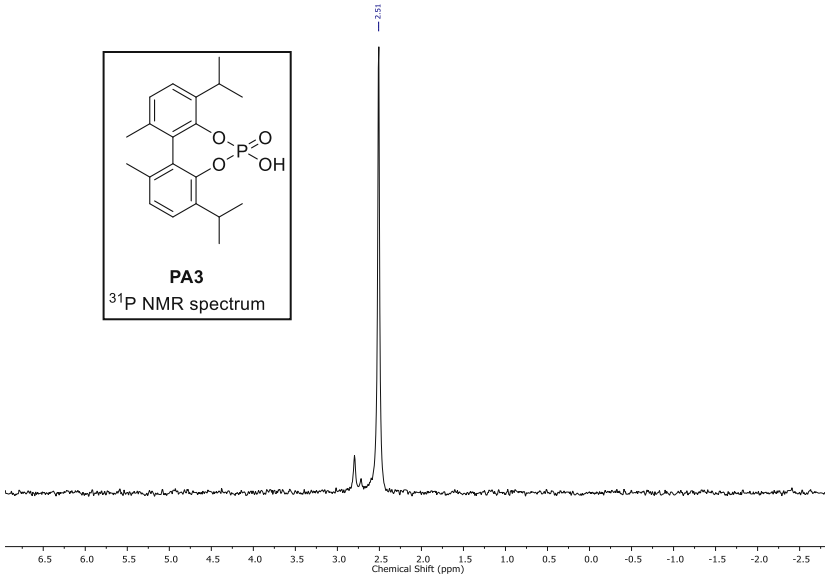


Figure S1. ^{31}P NMR spectrum of the phosphoric acid **PA3** at 27 ˚C.

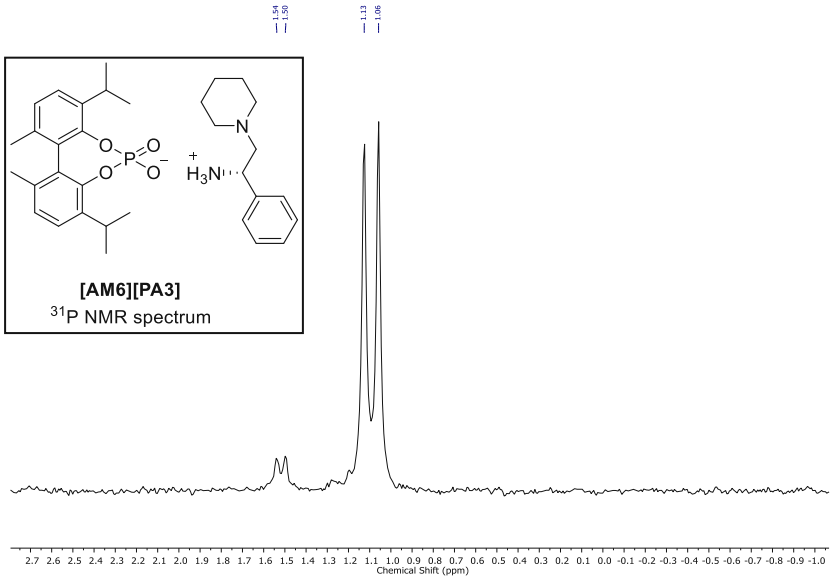


Figure S2. ^{31}P NMR spectrum of the salt [(*S*)-**AM6**][**PA3**] at 27 ˚C.

Die approbierte gedruckte Originalversion dieser Dissertation ist an der TU Wien Bibliothek verfügbar.
The approved original version of this doctoral thesis is available in print at TU Wien Bibliothek.

In contrast, no peak splitting in the NMR spectra of [(*S*)-**AM6**][**PA9**] could be observed at room temperature, suggesting that such ion-paired catalysts based on flexible phosphoric acids might indeed act as a single stereoisomer under the reaction conditions (Figures S3-S4). Measuring the same compounds both at −30 ˚C and − 13 ˚C resulted in no change in this phenomenon (Figures S5-S6).

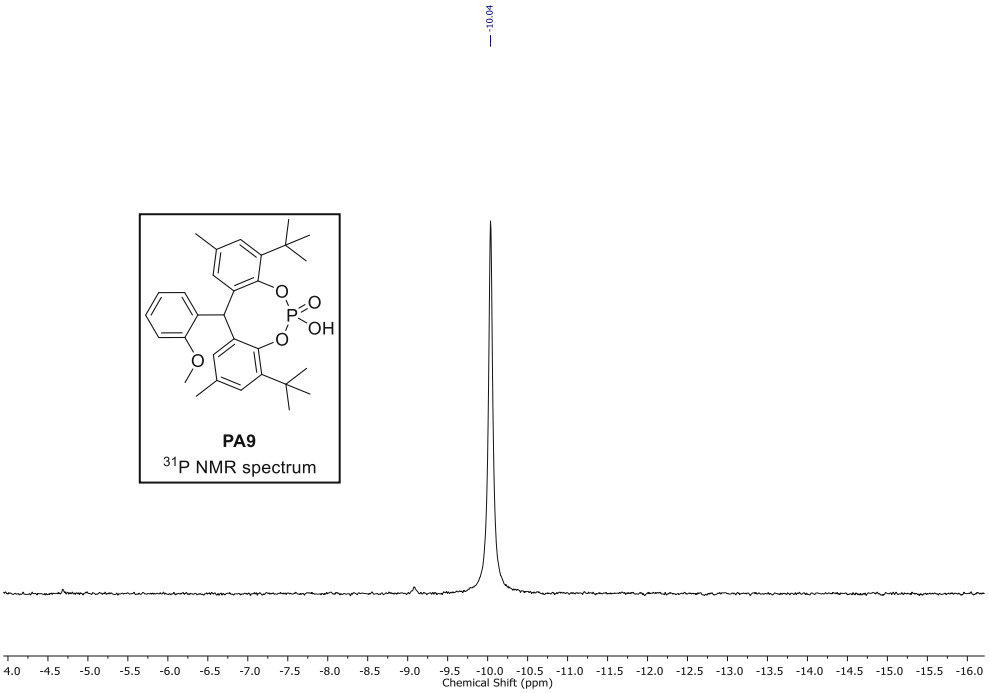


Figure S3. ^{31}P NMR spectrum of the phosphoric acid **PA9** at 27 ˚C.

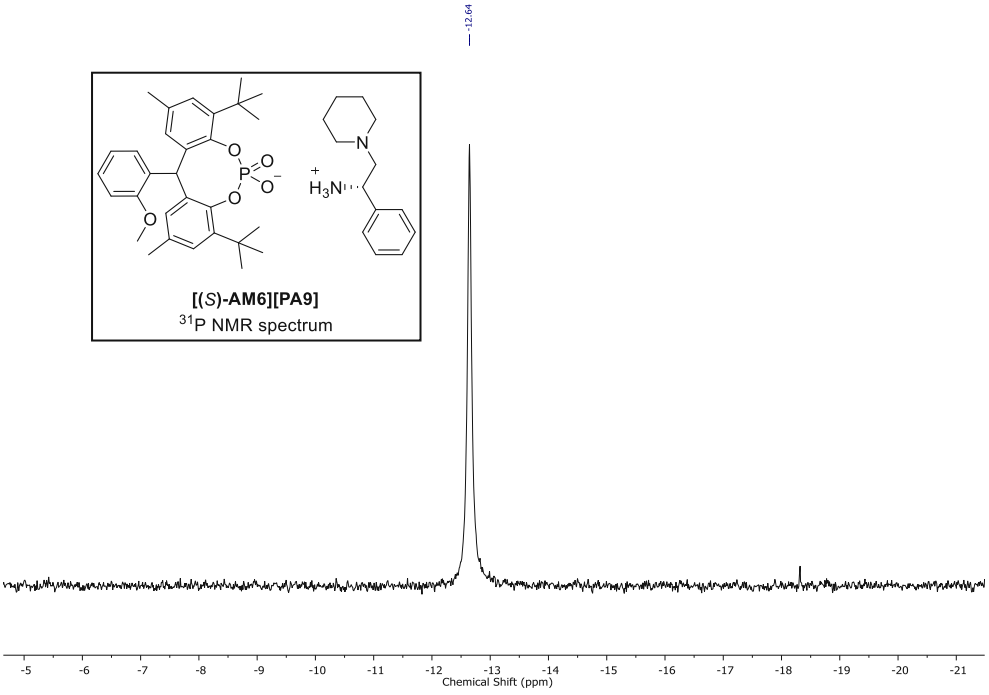


Figure S4. ^{31}P NMR spectrum of the salt [(*S*)-**AM6**][**PA9**] at 27 ˚C.

Die approbierte gedruckte Originalversion dieser Dissertation ist an der TU Wien Bibliothek verfügbar.
The approved original version of this doctoral thesis is available in print at TU Wien Bibliothek.
TU Bibliothek Your knowledge hub WIEN

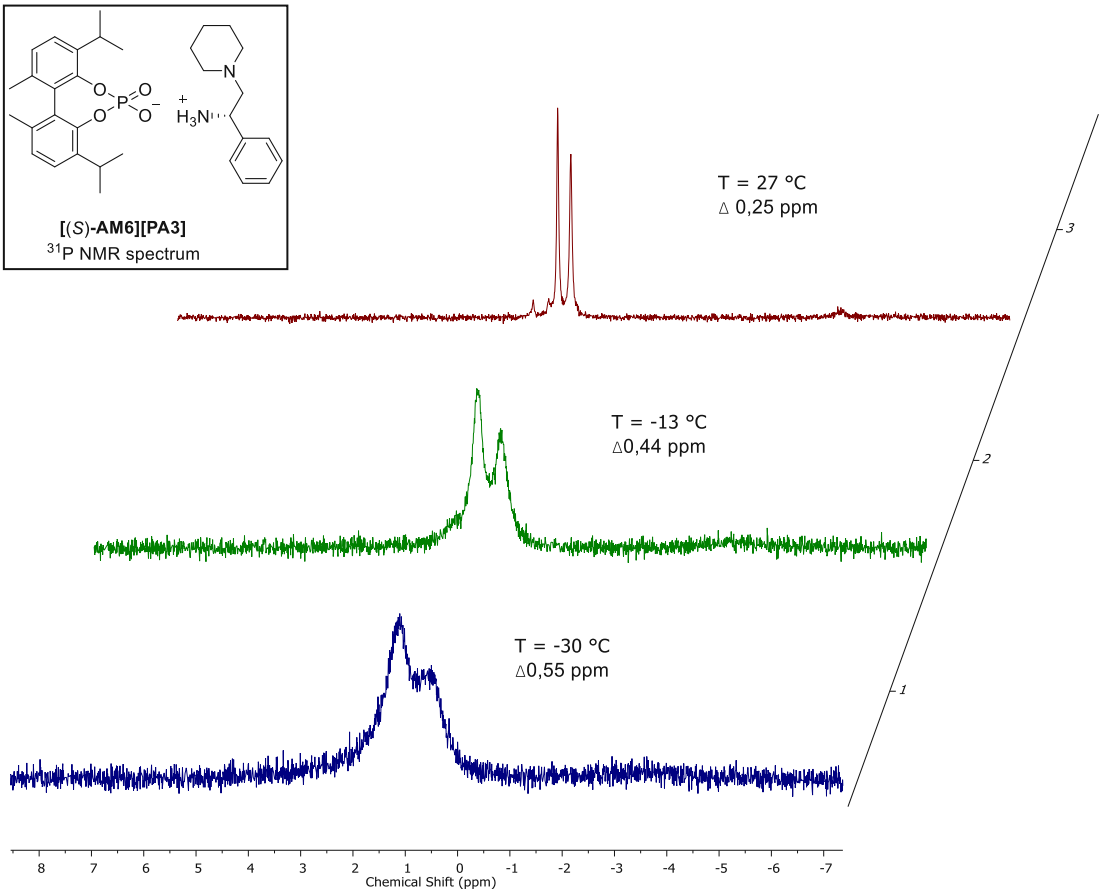


Figure S5. ^{31}P NMR spectrum of the salt [(*S*)-**AM6**][**PA3**] at different temperatures.

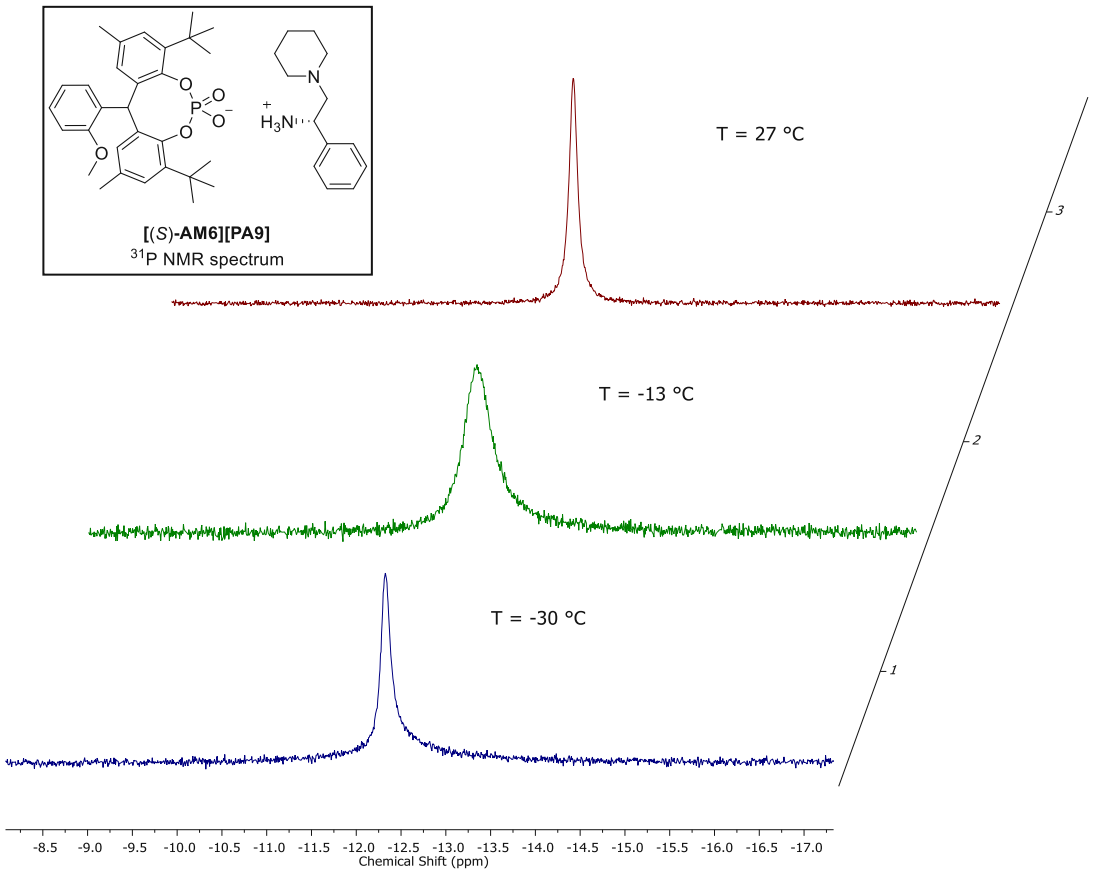


Figure S6. ^{31}P NMR spectrum of the salt [(*S*)-**AM6**][**PA9**] at different temperatures.

Die approbierte gedruckte Originalversion dieser Dissertation ist an der TU Wien Bibliothek verfügbar.
The approved original version of this doctoral thesis is available in print at TU Wien Bibliothek.
TU Bibliothek Your knowledge hub WIEN

In order to further study this phenomenon, the salts of racemic **BINOL-P** and **PA9** with different amines (**AM2**-**AM6**) have been analyzed, respectively. While the former phosphoric acid readily formed stable diastereomers, no peak splitting was observed in any cases when using **PA9** (Figures S7-S8). Even the use of cinchonidine – which was already proven to be efficient for the resolution of chiral phosphoric acids[20] – resulted in no change in this phenomenon (Figures S9-S12).

All these NMR results suggests, that – with the exception of **PA3** – the phosphoric acids of our study can not make stable enantiomers at room temperature, and therefore their salts can act as single stereoisomeric catalyst. This might help avoiding the generation of match-mismatched scenarios and provide an easy access to both product antipodes retaining the enantioselectivity.

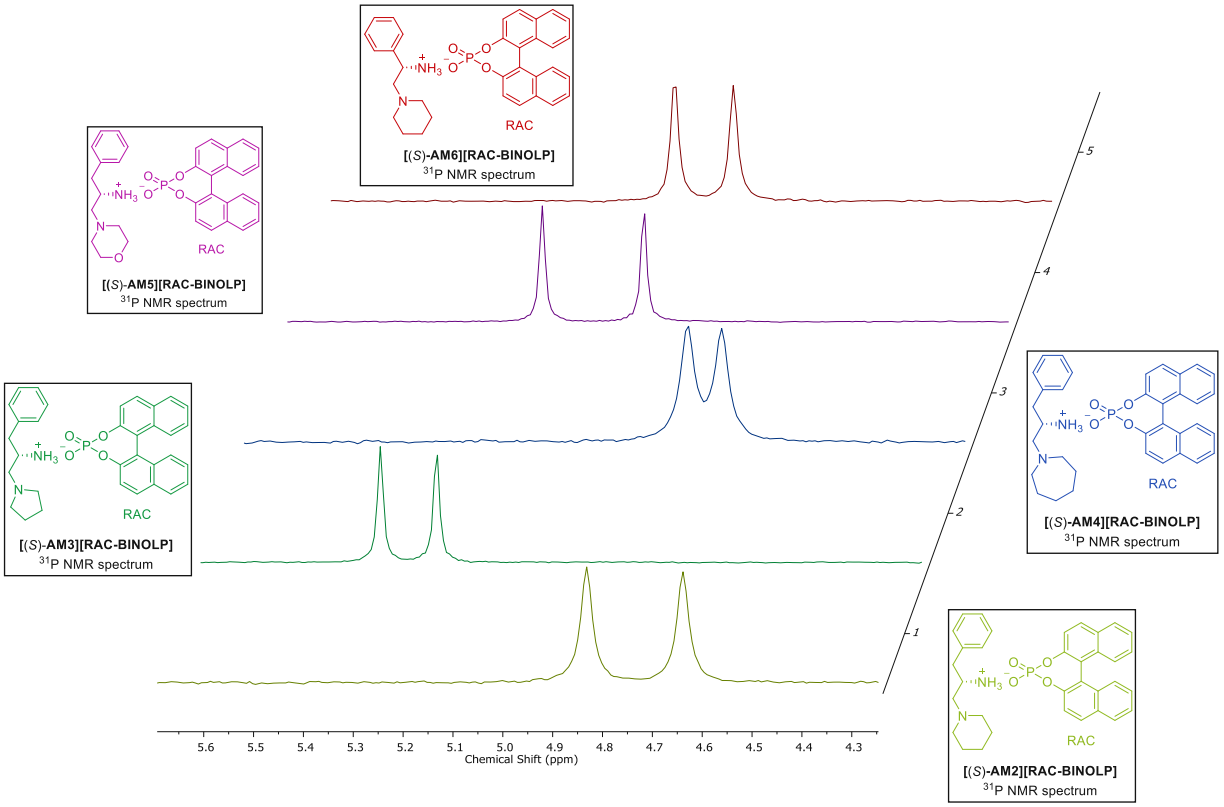


Figure S7. ^{31}P NMR spectra of different diastereomeric salts of chiral amines (*S*)-**AM2**-**AM6** and RAC-**BINOL-P** at room temperature.

Die approbierte gedruckte Originalversion dieser Dissertation ist an der TU Wien Bibliothek verfügbar.
The approved original version of this doctoral thesis is available in print at TU Wien Bibliothek.

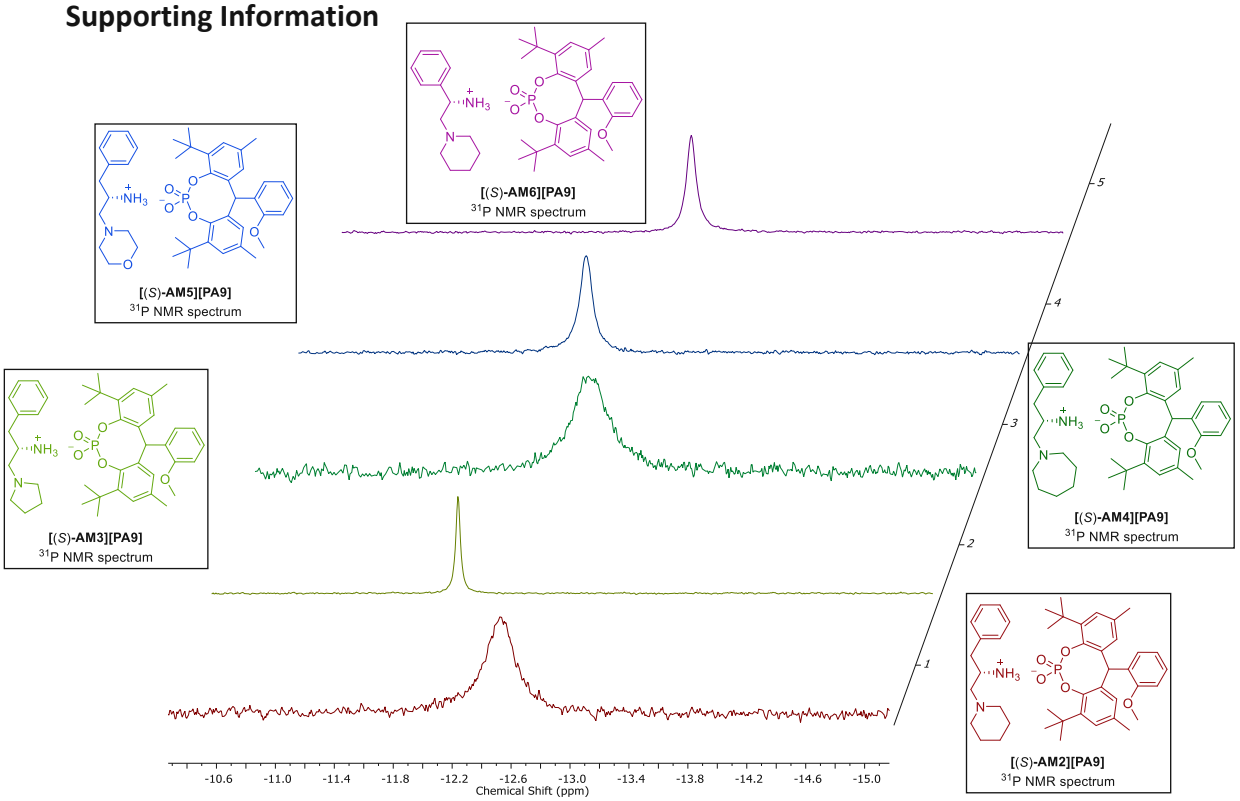


Figure S8. ^{31}P NMR spectra of different salts with chiral amines (*S*)-**AM2**-**AM6** and **PA9** at room temperature, showing no diastereomer formation.

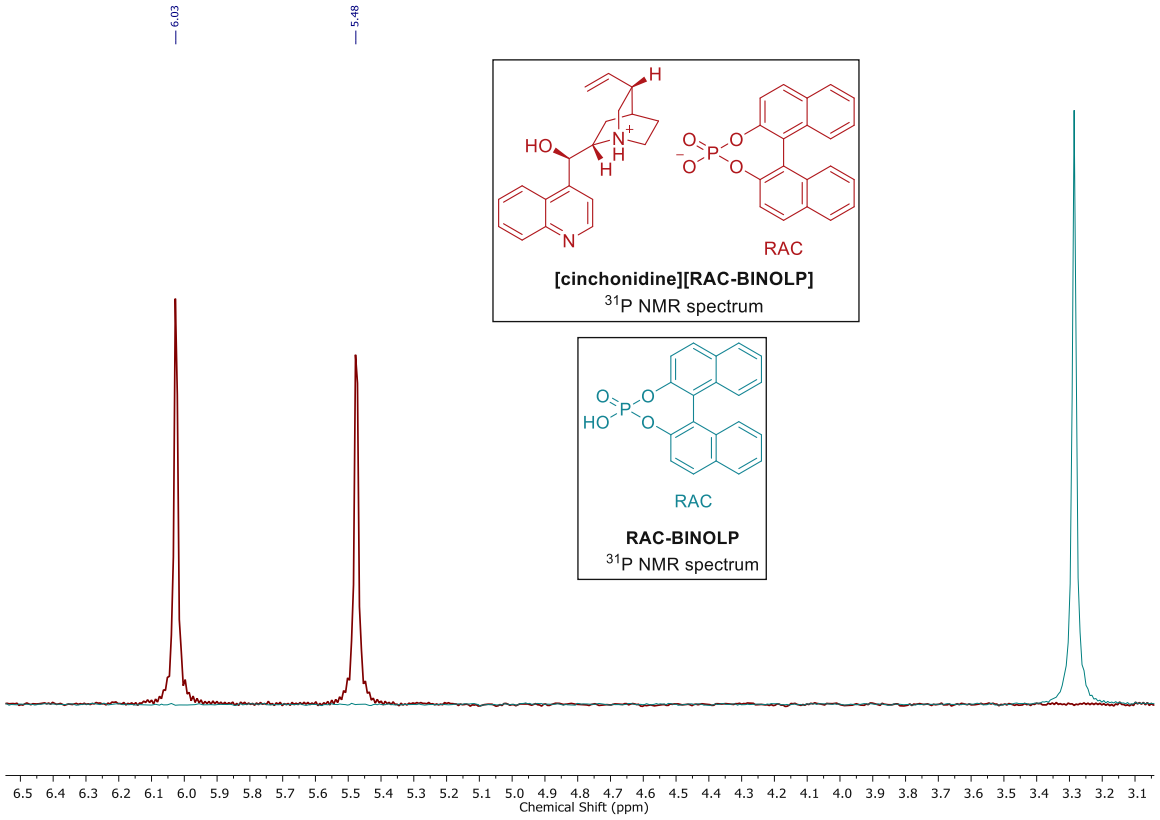


Figure S9. ^{31}P NMR spectra of the salt [cinchonidine][RAC-**BINOLP**] and the phosphoric acid RAC-**BINOLP** at room temperature.

Die approbierte gedruckte Originalversion dieser Dissertation ist an der TU Wien Bibliothek verfügbar.
The approved original version of this doctoral thesis is available in print at TU Wien Bibliothek.

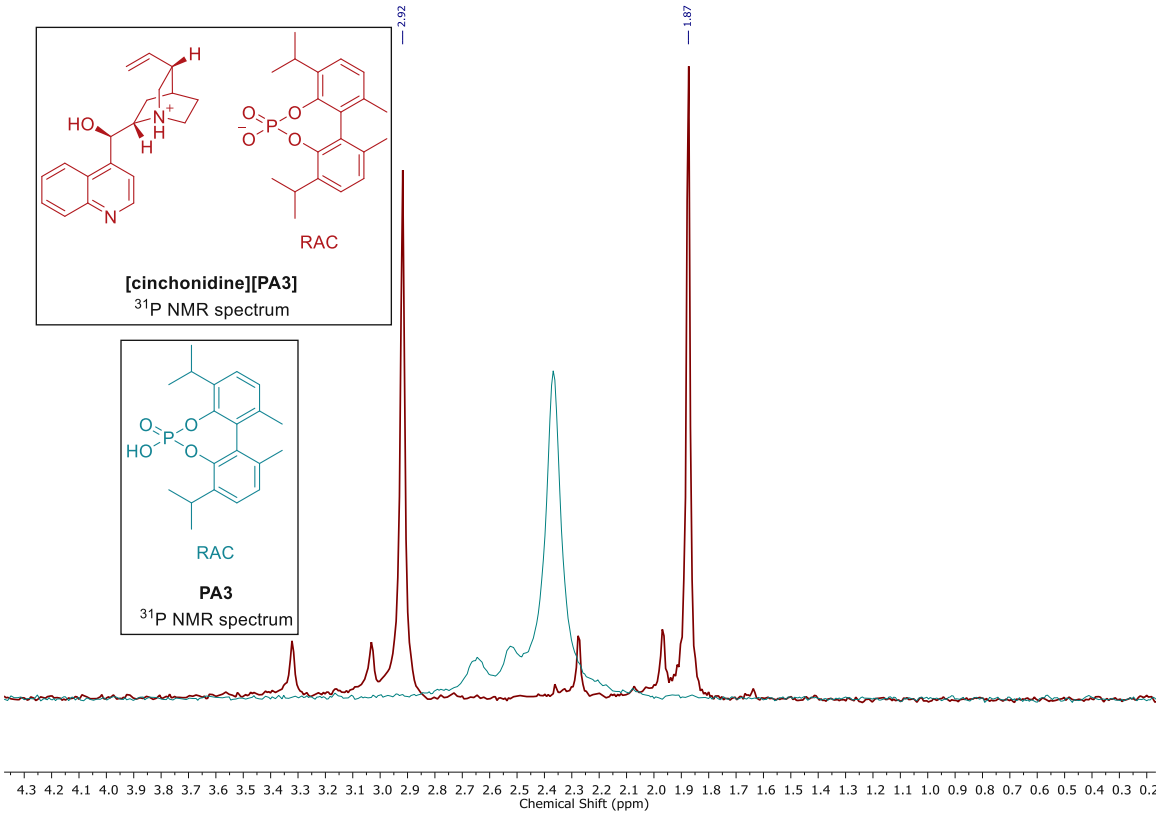


Figure S10. ^{31}P NMR spectra of the salt [cinchonidine]**[PA3]** and the phosphoric acid **PA3** at room temperature.

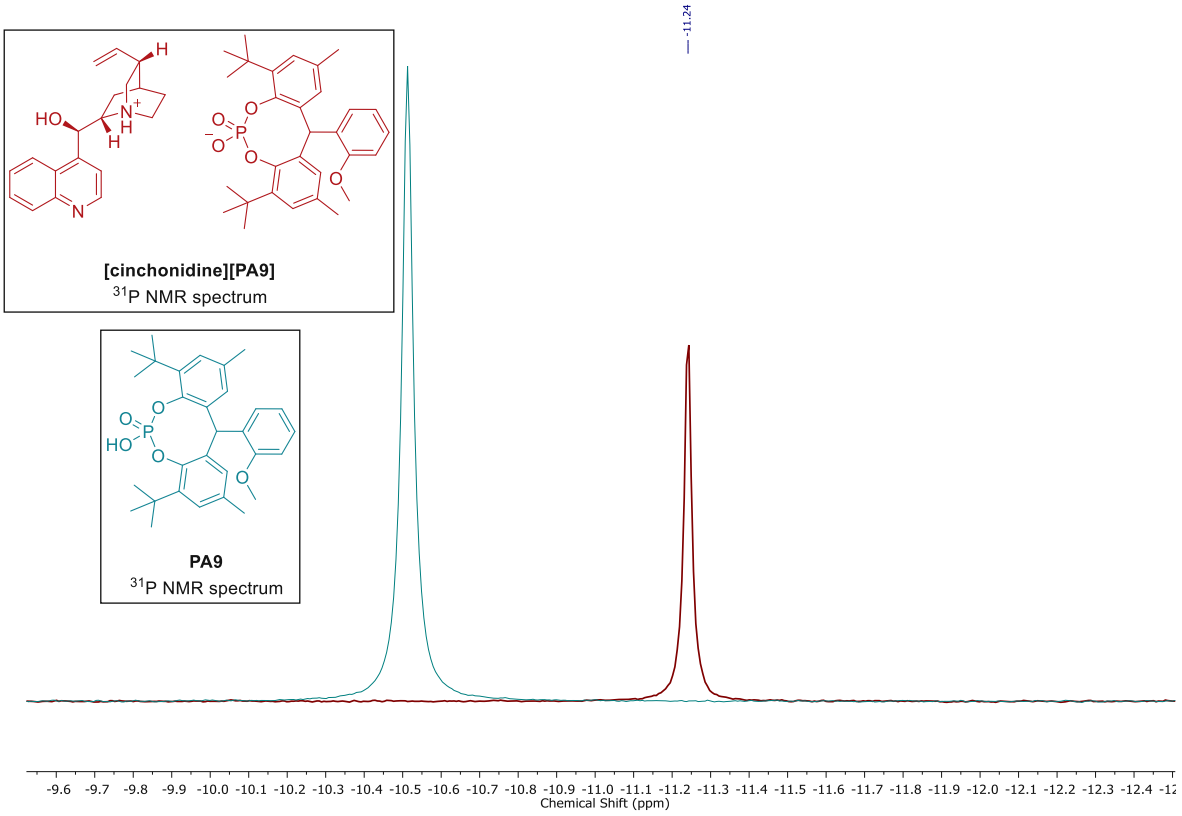


Figure S11. ^{31}P NMR spectra of the salt [cinchonidine]**[PA9]** and the phosphoric acid **PA9** at room temperature showing no diastereomer formation.

Die approbierte gedruckte Originalversion dieser Dissertation ist an der TU Wien Bibliothek verfügbar.
The approved original version of this doctoral thesis is available in print at TU Wien Bibliothek.

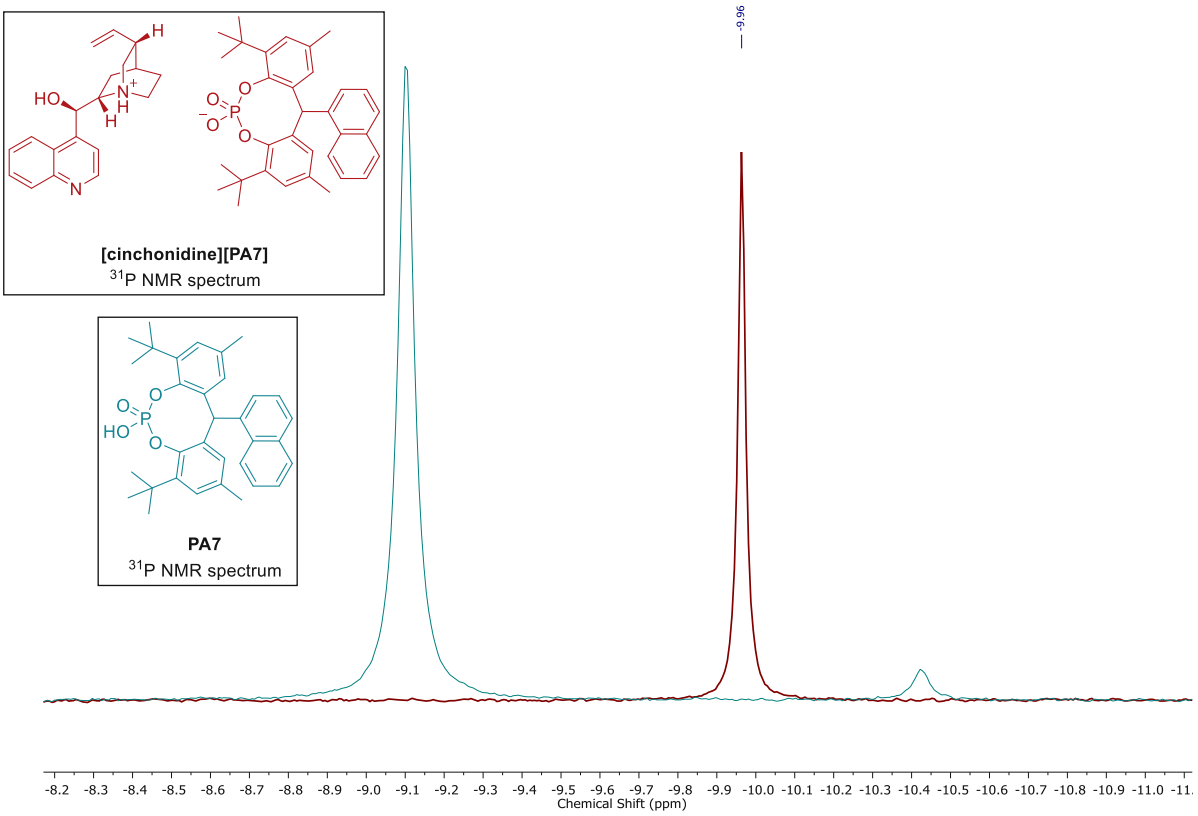


Figure S12. ^{31}P NMR spectrum of the salt [cinchonidine]**[PA7]** and the phosphoric acid **PA7** at room temperature showing no diastereomer formation.

Die approbierte gedruckte Originalversion dieser Dissertation ist an der TU Wien Bibliothek verfügbar.
The approved original version of this doctoral thesis is available in print at TU Wien Bibliothek.

24. XRD data for compounds 5c, 11a and PA9

Methodology

Single crystals of **5c**, **11a** and of the methanol solvate and dioxane disolvate hydrate of **PA9**, *viz*. **PA9-methanol** and **PA9-2dioxane-H_2O**, were pre-selected under a polarising microscope, embedded in perfluorinated polyether and mounted on MiTeGen MicroLoops®. X-ray diffraction data of all crystals were collected at 100 K on a Bruker Kappa APEX-II CCD diffractometer working with graphite-monochromated Mo–Kα radiation (λ = 0.71073 Å) and using narrow ω-scan frames. Corrections for absorption were applied with the multi-scan approach using SADABS.[32] The structures were solved with SHELXT and refined on F^2 with SHELXL.[33] All non-hydrogen atoms were refined with anisotropic displacement parameters. H atoms were placed in calculated positions and thereafter treated as riding, except the H atoms bonded to O atoms that were located from difference Fourier maps and refined freely.

Crystallographic data of (*S*,*R*,*S*)**5c**: $C_{13}H_{14}BrNO_2$; M_r = 296.16, colourless plate, 0.16 × 0.08 × 0.02 mm^3, trigonal, space group $P3_2$ (no. 145), a = 13.3743(8) Å, c = 6.0715(4) Å, V = 940.52(13) Å^3, Z = 3, d_x = 1.569 g/cm^3, T = 100 K. 13390 reflections collected (ϑ_{max} = 30.3°) and merged to 3721 independent data with $I>2\sigma(I)$ (R_{int} = 0.039); final R indices (all data) R_1 = 0.0360, wR_2 = 0.0547, GooF 1.018, 162 parameters, Flack parameter -0.018(5).

Crystallographic data of (-)-**11a**: $C_{11}H_{14}O_3$; M_r = 194.22, colourless fragment, 0.40 × 0.40 × 0.20 mm^3, monoclinic, space group $P2_1$ (no. 4), a = 7.622(2) Å, b = 7.839(2) Å, c = 8.088(2) Å, β = 97.683(6)°, V = 478.9(2) Å^3, Z = 2, d_x = 1.347 g/cm^3, T = 100 K. 5229 reflections collected (ϑ_{max} = 30.3°) and merged to 2778 independent data with $I>2\sigma(I)$ (R_{int} = 0.036); final R indices (all data) R_1 = 0.0571, wR_2 = 0.1540, GooF 1.087, 133 parameters; Flack parameter 0.2(10).

Crystallographic data of **PA9-methanol**: $C_{30}H_{36}O_5P$,CH_5O; M_r = 540.61, colourless block, 0.50 × 0.35 × 0.15 mm^3, triclinic, space group $P\bar{1}$ (no. 2), a = 8.5523(14) Å, b = 13.3715(18) Å, c = 13.6488(18) Å, α = 101.057(9)°, β = 94.356(9)°, γ = 100.883(10)°, V = 1494.1(4) Å^3, Z = 2, d_x = 1.202 g/cm^3, T = 100 K. 44750 reflections collected (ϑ_{max} = 33.1°) and merged to 11293 independent data with $I>2\sigma(I)$ (R_{int} = 0.027); final R indices (all data) R_1 = 0.0471, wR_2 = 0.1126, GooF 1.062, 361 parameters.

Crystallographic data of **PA9-2dioxane-H_2O**: $C_{30}H_{37}O_5P$,2($C_4H_8O_2$),H_2O; M_r = 702.79, colourless fragment, 0.30 × 0.30 × 0.20 mm^3, triclinic, space group $P\bar{1}$ (no. 2), a = 10.3044(9) Å, b = 13.1948(11) Å, c = 15.2341(13) Å, α = 92.285(3)°, β = 103.859(3)°, γ = 112.366(2)°, V = 1839.8(3) Å^3, Z = 2, d_x = 1.269 g/cm^3, T = 100 K. 24690 reflections collected (ϑ_{max} = 25.0°) and merged to 6476 independent

Die approbierte gedruckte Originalversion dieser Dissertation ist an der TU Wien Bibliothek verfügbar.
The approved original version of this doctoral thesis is available in print at TU Wien Bibliothek.
TU Bibliothek Your knowledge hub WIEN

data with $I>2\sigma(I)$ (R_{int} = 0.079); final R indices (all data) R_1 = 0.0913, wR_2 = 0.1590, GooF 1.025, 463 parameters.

Deposition numbers CCDC 2112845 for **5c**, CCDC 2112843 for **11**, CCDC 2112844 for **PA9-methanol** and CCDC 2112846 for **PA9-2dioxane-H_2O** contain the supplementary crystallographic data in CIF format. These data can be obtained free of charge from The Cambridge Crystallographic Data Centre via http://www.ccdc.cam.ac.uk/data_request/cif.

Crystal structures of 5c, 11a, PA9-methanol and PA9-2dioxane-H_2O

In all crystal structures, classical hydrogen bonds are the dominant intermolecular interactions. In **5c**, medium-strong N–H…$O_{carbonyl}$ and strong O–H…$O_{hydroxyl}$ interactions lead to the formation of supramolecular columns running parallel to [001]. Weak Br…Br interactions (3.5 Å) are present between the columns (Figure S13).

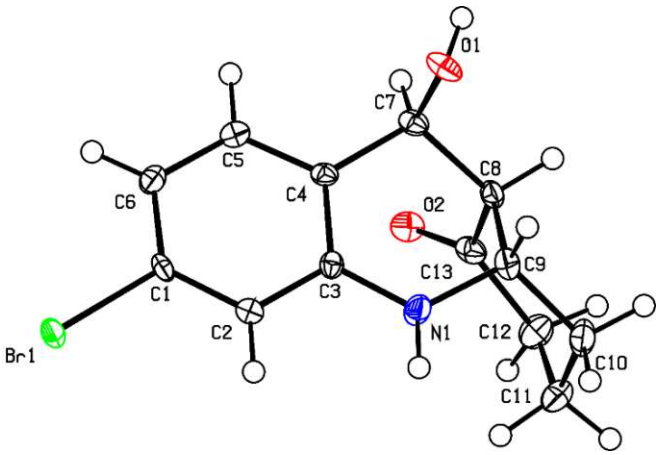


Figure S13. Molecular structure of (*S*,*R*,*S*)-**5c** with atoms shown as displacement ellipsoids at the 50% probability level. H atoms are represented by spheres of arbitrary radius.

Die approbierte gedruckte Originalversion dieser Dissertation ist an der TU Wien Bibliothek verfügbar.
The approved original version of this doctoral thesis is available in print at TU Wien Bibliothek.

In **11a**, adjacent molecules are linked through O–H…$O_{carbonyl}$ hydrogen bonds of medium strength into chains extending parallel to [101] (Figure S14).

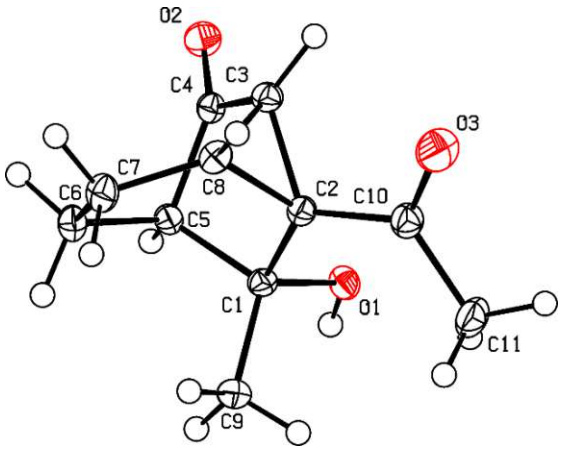


Figure S14. Molecular structure of (-)-**11** with atoms shown as displacement ellipsoids at the 50% probability level. H atoms are represented by spheres of arbitrary radius.

In **PA9-methanol**, a very strong symmetrical hydrogen bond is present between the phosphoric acid OH group and the O atom of the methanol solvate molecule. An additional very strong and likewise symmetrical O–H…O hydrogen bond between the methanol OH group and an O atom of the phosphoric acid moiety leads to a centrosymmetric ring motif with graph-set notation $R^4_4(12)$. In **PA9-2dioxane-H_2O**, again a very strong but asymmetrical hydrogen bond is present between the phosphoric acid moiety and the water molecule, and two more O–H…O hydrogen bonds of medium strengths between the water molecule and an dioxane solvent molecule and a phosphoric acid O atom, respectively, are present. The water molecules function as bridges between a **PA9** entity and a dioxane solvent molecule, leading to a hydrogen-bonded dimer (**PA9**-dioxane-$H_2O)_2$ with ring-set motif $R^4_4(12)$. The second dioxane solvent molecule is only weakly bound through C–H…O interactions (Figures S15 and S16).

Die approbierte gedruckte Originalversion dieser Dissertation ist an der TU Wien Bibliothek verfügbar.
The approved original version of this doctoral thesis is available in print at TU Wien Bibliothek.

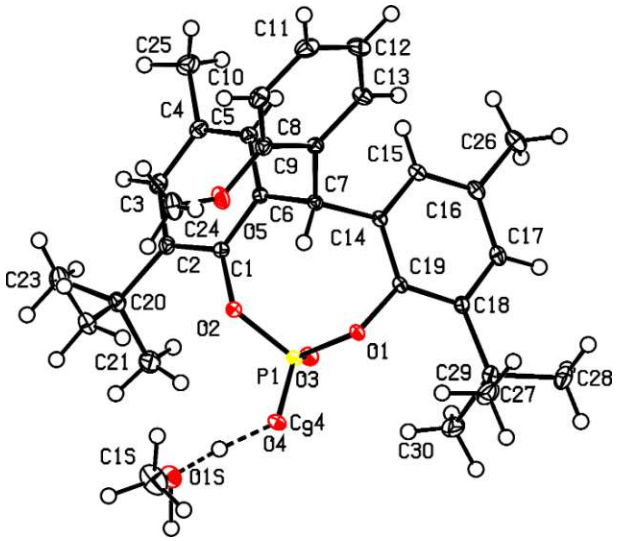


Figure S15. Molecular structure of (**PA9-methanol**) with atoms shown as displacement ellipsoids at the 50% probability level. H atoms are represented by spheres of arbitrary radius. The very strong hydrogen bonds between **PA9** and the methanol molecule is shown as dashed lines.

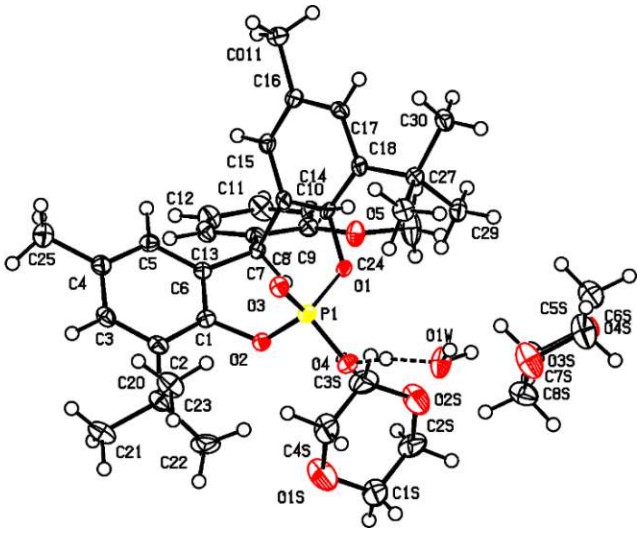


Figure S16. Molecular structure of (**PA9-2dioxane-H_2O**) with atoms shown as displacement ellipsoids at the 50% probability level. H atoms are represented by spheres of arbitrary radius. The very strong hydrogen bond between **PA9** and the water molecule is shown as dashed lines.

Die approbierte gedruckte Originalversion dieser Dissertation ist an der TU Wien Bibliothek verfügbar.
The approved original version of this doctoral thesis is available in print at TU Wien Bibliothek.

24. Bibliography

(1) Yu, G.; Wang, S.; Wang, K.; Hu, Y.; Hu, H. A Novel Approach to 1,2-Dihydro-2-Oxo-3-Pyridinecarboxylic Ester via Aromatization Induced by Deamidation. *Synthesis (Stuttg).* **2004**, No. 7, 1021–1028. https://doi.org/10.1055/s-2004-822325.

(2) Haraguchi, N.; Takenaka, N.; Najwa, A.; Takahara, Y.; Mun, M. K.; Itsuno, S. Synthesis of Main-Chain Ionic Polymers of Chiral Imidazolidinone Organocatalysts and Their Application to Asymmetric Diels-Alder Reactions. *Adv. Synth. Catal.* **2018**, *360* (1), 112–123. https://doi.org/10.1002/adsc.201701016.

(3) Martins, R. de S.; Pereira, M. P.; de Castro, P. P.; Bombonato, F. I. Design and Preparation of a Novel Prolinamide-Based Organocatalyst for the Solvent-Free Asymmetric Aldol Reaction. *Tetrahedron* **2020**, *76* (5), 130855. https://doi.org/10.1016/j.tet.2019.130855.

(4) Katritzky, A. R.; Fali, C. N.; Li, J.; Ager, D. J.; Prakash, I. Synthesis of 1-(T -Butoxycarbonyl)Benzotriazole and 1-(p -Methoxybenzyloxycarbonyl)Benzotriazole and Their Use in the Protection of Amino Acids. *Synth. Commun.* **1997**, *27* (9), 1623–1630. https://doi.org/10.1080/00397919708006101.

(5) Sestito, S.; Daniele, S.; Nesi, G.; Zappelli, E.; Di Maio, D.; Marinelli, L.; Digiacomo, M.; Lapucci, A.; Martini, C.; Novellino, E.; Rapposelli, S. Locking PDK1 in DFG-out Conformation through 2-Oxo-Indole Containing Molecules: Another Tools to Fight Glioblastoma. *Eur. J. Med. Chem.* **2016**, *118*, 47–63. https://doi.org/10.1016/j.ejmech.2016.04.003.

(6) Zhang, E.; Bai, P. Y.; Cui, D. Y.; Chu, W. C.; Hua, Y. G.; Liu, Q.; Yin, H. Y.; Zhang, Y. J.; Qin, S.; Liu, H. M. Synthesis and Bioactivities Study of New Antibacterial Peptide Mimics: The Dialkyl Cationic Amphiphiles. *Eur. J. Med. Chem.* **2018**, *143*, 1489–1509. https://doi.org/10.1016/j.ejmech.2017.10.044.

(7) Karmakar, A.; Basha, M.; Venkatesh Babu, G. T.; Botlagunta, M.; Malik, N. A.; Rampulla, R.; Mathur, A.; Gupta, A. K. Tertiary-Butoxycarbonyl (Boc) – A Strategic Group for N-Protection/Deprotection in the Synthesis of Various Natural/Unnatural N-Unprotected Aminoacid Cyanomethyl Esters. *Tetrahedron Lett.* **2018**, *59* (48), 4267–4271. https://doi.org/10.1016/j.tetlet.2018.10.041.

(8) Hatano, M.; Miyamoto, T.; Ishihara, K. Highly Active Chiral Phosphoramide−Zn(II) Complexes as Conjugate Acid−Base Catalysts for Enantioselective Organozinc Addition to Ketones. *Org. Lett.* **2007**, *9* (22), 4535–4538. https://doi.org/10.1021/ol702074a.

(9) Ando, A.; Shioiri, T. Enantioselective Synthesis of β-Hydroxy-α-Methyl Carbonyl Compounds by Aldol Reaction. *Tetrahedron* **1989**, *45* (16), 4969–4988. https://doi.org/10.1016/S0040-4020(01)81078-4.

(10) Khatik, G. L.; Kumar, V.; Nair, V. A. Reversal of Selectivity in Acetate Aldol Reactions of N -Acetyl-(S)-4-Isopropyl-1-[(R)-1-Phenylethyl]Imidazolidin-2-One. *Org. Lett.* **2012**, *14* (10), 2442–2445. https://doi.org/10.1021/ol300949s.

(11) Li, P.; Chai, Z.; Zhao, S.-L.; Yang, Y.-Q.; Wang, H.-F.; Zheng, C.-W.; Cai, Y.-P.; Zhao, G.; Zhu, S.-Z. Highly Enantio- and Diastereoselective Synthesis of α-Trifluoromethyldihydropyrans Using a Novel Bifunctional Piperazine-Thiourea Catalyst. *Chem. Commun.* **2009**, No. 47, 7369. https://doi.org/10.1039/b915210e.

(12) Li, J.; Luo, S.; Cheng, J. Chiral Primary−Tertiary Diamine Catalysts Derived From Natural Amino Acids for Syn -Aldol Reactions of Hydroxy Ketones. *J. Org. Chem.* **2009**, *74* (4), 1747–1750. https://doi.org/10.1021/jo802557p.

(13) Zhou, Y.; Liu, Q.; Gong, Y. Camphor-Derived C1-Symmetric Chiral Diamine Organocatalysts for Asymmetric Michael Addition of Nitroalkanes to Enones. *Org. Biomol. Chem.* **2012**, *10* (37), 7618. https://doi.org/10.1039/c2ob25922b.

(14) Rossiter, B. E.; Eguchi, M.; Miao, G.; Swingle, N. M.; Hernández, A. E.; Vickers, D.; Fluckiger, E.; Greg Patterson, R.; Vásavi Reddy, K. Enantioselective Conjugate Addition to Cyclic Enones with Scalemic Lithium Organo(Amido)Cuprates, Part IV. Relationship between Ligand Structure and Enantioselectivity. *Tetrahedron* **1993**,

Die approbierte gedruckte Originalversion dieser Dissertation ist an der TU Wien Bibliothek verfügbar.
The approved original version of this doctoral thesis is available in print at TU Wien Bibliothek.
TU Bibliothek Your knowledge hub WIEN

49 (5), 965–986. https://doi.org/10.1016/S0040-4020(01)86278-5.

(15) Kumar, A.; Singh, S.; Kumar, V.; Singh Chimni, S. Asymmetric Syn-Selective Direct Aldol Reaction of Protected Hydroxyacetone Catalyzed by Primary Amino Acid Derived Bifunctional Organocatalyst in the Presence of Water. *Org. Biomol. Chem.* **2011**, *9* (8), 2731. https://doi.org/10.1039/c0ob00898b.

(16) Davis, T. J.; Balsells, J.; Carroll, P. J.; Walsh, P. J. Optimization of Asymmetric Catalysts Using Achiral Ligands: Metal Geometry-Induced Ligand Asymmetry. *Org. Lett.* **2001**, *3* (14), 2161–2164. https://doi.org/10.1021/ol016003d.

(17) Fareghi-Alamdari, R.; Golestanzadeh, M.; Agend, F.; Zekri, N. Regiospecific, One-Pot, and Pseudo-Five-Component Synthesis of 6,6′-(Arylmethylene)Bis(2-(Tert -Butyl)4-Methylphenol) Antioxidants Using Highly Sulfonated Multi-Walled Carbon Nanotubes under Solvent-Free Conditions. *Can. J. Chem.* **2013**, *91* (10), 982–991. https://doi.org/10.1139/cjc-2013-0160.

(18) Hsueh, M.-L.; Huang, B.-H.; Lin, C.-C. Reactions of 2,2′-(2-Methoxybenzylidene)Bis(4-Methyl-6- Tert -Butylphenol) with Trimethylaluminum: Novel Efficient Catalysts for “Living” and “Immortal” Polymerization of ε-Caprolactone. *Macromolecules* **2002**, *35* (15), 5763–5768. https://doi.org/10.1021/ma020574j.

(19) Grant-Overton, S.; Buss, J. A.; Smith, E. H.; Gutierrez, E. G.; Moorhead, E. J.; Lin, V. S.; Wenzel, A. G. Efficient Microwave Method for the Oxidative Coupling of Phenols. *Synth. Commun.* **2015**, *45* (3), 331–337. https://doi.org/10.1080/00397911.2014.956370.

(20) Gutierrez, E. G.; Moorhead, E. J.; Smith, E. H.; Lin, V.; Ackerman, L. K. G.; Knezevic, C. E.; Sun, V.; Grant, S.; Wenzel, A. G. Electron-Withdrawing, Biphenyl-2,2′-diol-Based Compounds for Asymmetric Catalysis. *Eur. J. Org. Chem.* **2010**, *1* (16), 3027–3031. https://doi.org/10.1002/ejoc.201000070.

(21) Kumara Swamy, K. C.; Kumaraswamy, S.; Kommana, P. Very Strong C−H···O, N−H···O, and O−H···O Hydrogen Bonds Involving a Cyclic Phosphate. *J. Am. Chem. Soc.* **2001**, *123* (50), 12642–12649. https://doi.org/10.1021/ja010713x.

(22) Martin, N. J. A.; List, B. Highly Enantioselective Transfer Hydrogenation of α,β- Unsaturated Ketones. *J. Am. Chem. Soc.* **2006**, *128* (41), 13368–13369. https://doi.org/10.1021/ja065708d.

(23) Shintani, R.; Takeda, M.; Nishimura, T.; Hayashi, T. Chiral Tetrafluorobenzobarrelenes as Effective Ligands for Rhodium-Catalyzed Asymmetric 1,4-Addition of Arylboroxines to β,β-Disubstituted α,β-Unsaturated Ketones. *Angew. Chem. Int. Ed.* **2010**, *49* (23), 3969–3971. https://doi.org/10.1002/anie.201000467.

(24) Yasui, N.; Mayne, C. G.; Katzenellenbogen, J. A. Preparation of o -Fluorophenols from Nonaromatic Precursors: Mechanistic Considerations for Adaptation to Fluorine-18 Radiolabeling. *Org. Lett.* **2015**, *17* (22), 5540–5543. https://doi.org/10.1021/acs.orglett.5b02640.

(25) Palais, L.; Alexakis, A. Copper-Catalyzed Asymmetric Conjugate Addition with Chiral SimplePhos Ligands. *Chem. - A Eur. J.* **2009**, *15* (40), 10473–10485. https://doi.org/10.1002/chem.200901577.

(26) LARCHEVÊQUE, M.; VALETTE, G.; CUVIGNY, T. Hyperbasic Media; Synthesis of 1-Alkyl-3-Oxocyclohexenes from 1,5-Diketones. *Synthesis (Stuttg).* **1977**, *1977* (06), 424–427. https://doi.org/10.1055/s-1977-24428.

(27) Wang, X.; Reisinger, C. M.; List, B. Catalytic Asymmetric Epoxidation of Cyclic Enones. *J. Am. Chem. Soc.* **2008**, *130* (19), 6070–6071. https://doi.org/10.1021/ja801181u.

(28) Saini, G.; Mondal, A.; Kapur, M. Palladium-Mediated Remote Functionalization in γ- and ε-Arylations and Alkenylations of Unblocked Cyclic Enones. *Org. Lett.* **2019**, *21* (22), 9071–9075. https://doi.org/10.1021/acs.orglett.9b03462.

(29) Danishefsky, S.; Zimmer, A. The Direction of Base-Catalyzed Aldol Cyclization of 1,5 Diketones. *J. Org. Chem.* **1976**, *41* (26), 4059–4064. https://doi.org/10.1021/jo00888a002.

(30) Cussó, O.; Cianfanelli, M.; Ribas, X.; Klein Gebbink, R. J. M.; Costas, M. Iron Catalyzed Highly Enantioselective Epoxidation of Cyclic Aliphatic Enones with Aqueous H 2 O 2. *J. Am. Chem. Soc.* **2016**, *138* (8), 2732–2738. https://doi.org/10.1021/jacs.5b12681.

Die approbierte gedruckte Originalversion dieser Dissertation ist an der TU Wien Bibliothek verfügbar.
The approved original version of this doctoral thesis is available in print at TU Wien Bibliothek.
TU Bibliothek Your knowledge hub WIEN

(31) De Vincentiis, F.; Bencivenni, G.; Pesciaioli, F.; Mazzanti, A.; Bartoli, G.; Galzerano, P.; Melchiorre, P. Asymmetric Catalytic Aziridination of Cyclic Enones. *Chem. - Asian J.* **2010**, *5* (7), 1652–1656. https://doi.org/10.1002/asia.201000040.

(32) Krause, L.; Herbst-Irmer, R.; Sheldrick, G. M.; Stalke, D. Comparison of Silver and Molybdenum Microfocus X-Ray Sources for Single-Crystal Structure Determination. *J. Appl. Crystallogr.* **2015**, *48* (1), 3–10. https://doi.org/10.1107/S1600576714022985.

(33) Sheldrick, G. M. SHELXT – Integrated Space-Group and Crystal-Structure Determination. *Acta Crystallogr. Sect. A Found. Adv.* **2015**, *71* (1), 3–8. https://doi.org/10.1107/S2053273314026370.

Die approbierte gedruckte Originalversion dieser Dissertation ist an der TU Wien Bibliothek verfügbar.
The approved original version of this doctoral thesis is available in print at TU Wien Bibliothek.

Appendix C

Supporting information:

Synthesis of Chiral Diazabicycloalkanes via Organocatalytic aza-Michael/Aldol Reaction

Die approbierte gedruckte Originalversion dieser Dissertation ist an der TU Wien Bibliothek verfügbar.
The approved original version of this doctoral thesis is available in print at TU Wien Bibliothek.

Supporting Information

Synthesis of Chiral Diaza-Bicycloalkanes via Organocatalytic Aza-Michael/Aldol Reaction

Fabian Scharinger[a], Matthias Weil[b], Michael Schnürch[a] and Katharina Bica-Schröder[a]*

[a] F. Scharinger, Prof. M. Schnürch, Prof. K. Bica-Schröder
Institute of Applied Synthetic Chemistry, TU Wien
Getreidemarkt 9/163, 1060 Wien (Austria)
[b] Prof. M. Weil
Institute of Chemical Technologies and Analytics, TU Wien
Getreidemarkt 9/163, 1060 Wien (Austria)

Die approbierte gedruckte Originalversion dieser Dissertation ist an der TU Wien Bibliothek verfügbar.
The approved original version of this doctoral thesis is available in print at TU Wien Bibliothek.

Table of contents

1 Catalyst synthesis 4

1.1 Synthesis of 9-amino-9-deoxy-epiquinine **AM2** 4

1.2 Synthesis of amino-acid derived diamines **AM3, AM4** 4

1.3 Synthesis of substituted diphenylethylendiamine **AM7**, **AM8** 6

2 Substrate synthesis 7

3 Reagent synthesis 9

4 Screening 12

5 General procedure for the aza-Michael/aldol reaction 14

6 Further transformation 24

7 NMR Spectra 26

7.1 NMR spectra chiral amines 26

7.2 NMR spectra of enals 29

7.3 NMR spectra of reagents 38

7.4 NMR spectra of aza-Michael/aldol products 42

8 HPLC spectra 73

9 XRD data of **6** 131

10 References 132

Die approbierte gedruckte Originalversion dieser Dissertation ist an der TU Wien Bibliothek verfügbar.
The approved original version of this doctoral thesis is available in print at TU Wien Bibliothek.

General remarks

Unless noted otherwise, all purchased chemicals from commercial suppliers were used without further purification. Dry solvents were pre-distilled and desiccated on aluminium oxide columns (PURESOLV, Innovative Technology).

Column chromatography was performed on standard manual glass columns using Merck (40-60 µm) silica gel with pre-distilled solvents (PE: petrolether, EtOAc: ethyl acetate, Et_2O: diethyl ether, DCM: dichloromethane). Precoated aluminium-backed plates were purchased for TLC analysis from Merck (silica gel 60 F_{254}). UV active compounds were detected at 254 nm. Non-UV active compounds have been detected using a vanillin staining solution (5% vanillin in EtOH + H_2SO_4) or $KMnO_4$ staining solution (1.5 g $KmnO_4$ in 10% NaOH + K_2CO_3)

^{1}H, ^{13}C, ^{19}F and ^{31}P NMR spectra were recorded on a Bruker Advance UltraShield 400 MHz spectrometer and chemical shifts are reported in ppm using TMS (tetramethylsilane) as internal standard. Coupling constants (*J*) are given in Hz. For assignation purpose, the following abbreviations are used: s (singlet), d (doublet), t (triplet), q (quartet), m (multiplet), brs (broad singlet), dd (doublet of doublets), ddd (doublets of doublet of doublets), td (triplet of doublets), dt (doublet of triplets).

GC measurements were performed on a Thermo Scientific Focus on a BGB5 column using an FID detector.

GC-MS measurements have been performed on a Thermo Scientific DSQ II on BGB5 column (30m), equipped with a quadrupole MS detector DSQ II.

Chiral HPLC measurements were carried out on a DIONEX UPLC equipped with a photodiode array (PDA) plus detector (190–360 nm), using a Diacel Chiracel AS-H, IB and OJ columns (all 250 × 4.60 mm, 5 µm).

Optical rotation was measured on an Anton Paar MCP500 polarimeter at the specific conditions, and the results have been compared to literature values. Concentrations are given in g / 100 mL.

HR-MS analysis was performed using HTC PAL system autosampler, an Agilent 1100/1200 HPLC and Agilent 6230 AJS ESI-TOF mass spectrometer.

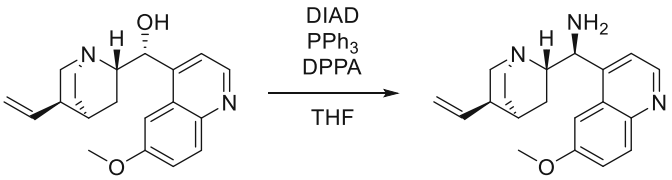
Melting points above room temperature were measured on an automated melting point system OPTI MELT of Stanford Research Systems and are uncorrected.

Infrared spectra were recorded on a Perkin-Elmer Spectrum 65 FT IR spectrometer equipped with a specac MK II Golden Gate Single Reflection ATR unit.

Die approbierte gedruckte Originalversion dieser Dissertation ist an der TU Wien Bibliothek verfügbar.
The approved original version of this doctoral thesis is available in print at TU Wien Bibliothek.
TU Bibliothek Your knowledge hub WIEN

1 Catalyst synthesis

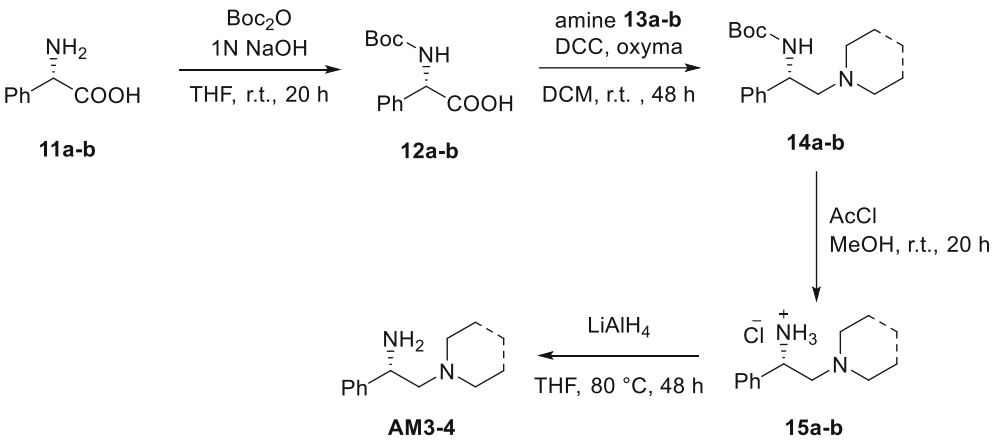
1.1 Synthesis of 9-amino-9-deoxy-epiquinine **AM2**



10 **AM2**

According to the literature procedure:[1] A solution of quinine (2.0 g, 1.0 equiv., 6.2 mmol) and PPh_3 (1.9 g, 1.2 equiv., 7.4 mmol) in anhydrous THF (40 ml) was prepared. Diisopropyl azodicarboxylate (DIAD) (1.5 g, 1.2 equiv., 7.4 mmol) and diphenylphosphoryl azide (DPPA) (2.0 g, 1.2 equiv., 7.4 mmol) were added at 0 °C via syringe, and the mixture was stirred for 20 h at room temperature. The reaction mixture was then heated to reflux for 2 h, followed by cooling to room temperature. Additional PPh_3 (1.9 g, 1.2 equiv., 7.4 mmol) was added, and the mixture was heated to reflux for 5 h. After cooling to room temperature, H_2O (12 ml) was added, and the mixture was stirred for 20 h. The solvent was removed, and the residue was dissolved in DCM. To this solution, 2 N HCl (18 ml) was added, resulting in phase separation. The organic phase was washed with DCM (3x). The aqueous phase was basified using aqueous ammonia (30%) and extracted with DCM (3x). The organic phase was washed with brine (1x), dried with anhydrous Na_2SO_4, filtered, and the solvent was removed in vacuo. The final product, **AM2** (1.4 g, 57%), was obtained as a brown liquid. All analytical data matches with literature.[1] **^{1}H NMR (400 MHz, $CDCl_3$) δ** 8.75 (d, *J* = 4.6 Hz, 1H), 8.03 (d, *J* = 9.2 Hz, 1H), 7.66 (s, 1H), 7.46 (d, *J* = 4.3 Hz, 1H), 7.39 (dd, *J* = 9.2, 2.7 Hz, 1H), 5.80 (ddd, *J* = 17.5, 10.3, 7.5 Hz, 1H), 5.29 (s, 1H), 5.05 – 4.92 (m, 2H), 4.60 (d, *J* = 10.1 Hz, 1H), 3.97 (s, 3H), 3.26 (ddd, *J* = 21.2, 14.2, 8.5 Hz, 2H), 3.09 (d, *J* = 9.0 Hz, 1H), 2.88 – 2.75 (m, 2H), 2.37 – 2.23 (m, 1H), 2.02 (s, 2H), 1.59 (dddd, *J* = 24.6, 12.6, 6.5, 3.2 Hz, 3H), 1.43 (t, *J* = 12.1 Hz, 1H), 0.78 (ddt, *J* = 13.7, 7.5, 2.0 Hz, 1H).

1.2 Synthesis of amino-acid derived diamines **AM3, AM4**



11a-b **12a-b** **14a-b** **15a-b** **AM3-4**

Die approbierte gedruckte Originalversion dieser Dissertation ist an der TU Wien Bibliothek verfügbar.
The approved original version of this doctoral thesis is available in print at TU Wien Bibliothek.
TU Bibliothek Your knowledge hub WIEN

General procedure 2:[2] To the solution of amino acid **11a-b** (1.0 equiv.) in a mixture of THF / 1 N NaOH (1:1, 0.4 M), di-*tert*-butyl-dicarbonate (1.2 equiv.) was added. The solution was stirred for 18 h at room temperature. The THF was removed *in vacuo*, and the resulting aqueous solution was diluted with DCM and acidified to pH 2 with a 1 N HCl solution. The aqueous phase was extracted with DCM (3x), and the combined organic phases were washed with brine, dried over anhydrous Na_2SO_4 and filtered. Removal of the solvent afforded **12a-b** as a colorless, viscous liquid, which was used for the next step without further purification.

To a solution of the Boc-protected amino acid **12a-b** (1.0 equiv.) in dry DCM (0.2 M), DCC (2.0 equiv.), oxyma (1.1 equiv.) and amine **13a-b** (2.5 equiv.) were added at 0 °C. The resulting turbid solution was stirred for another 15 min at 0 °C, allowed to warm up, and stirred at room temperature for 48 h. Then cold EtOAc (50 mL) was added, the mixture was stirred for 10 min, the DCU was filtered off, and the clear solution was concentrated *in vacuo*. The crude mixture was re-dissolved in EtOAc (25 mL) and washed with 1 N HCl (1x). The formed solid was filtered off, and the filtrate was repeatedly washed with 1 N HCl (2x), 1 N NaOH (3x) and brine (1x). The combined organic phases were dried over anhydrous Na_2SO_4, filtered and concentrated. Dry MeOH was added, followed by AcCl (8.0 equiv) dropwise at 0 °C. It was stirred for 20 h at r.t. and concentrated in vacuo to provide the crude **15a-b**.

To a stirred solution of salt **15a-b** (1.0 equiv.) in THF (0.15 M), $LiAlH_4$ (5.0 equiv.) was added in small portions at 0 °C. The resulting dispersion was stirred for 15 min and subsequently stirred at reflux for 48 h. After cooling to room temperature, distilled H_2O (1 mL per g $LiAlH_4$) was added stirred for 10 min and 15% aqueous NaOH (2 mL per g $LiAlH_4$) were added at 0 °C and the mixture was stirred for 10 min. Anhydrous Na_2SO_4 was added to remove the previously added water, and the product was taken up in EtOAc. The solid was filtered off, and was washed with EtOAc (3x). The filtrate was washed with 1 N NaOH (2×) and brine (1×), dried over anhydrous Na_2SO_4 and filtered. Removal of the solvent and subsequent column chromatography (10 % MeOH in DCM, 1% Et_3N, ninhydrin stain) gave the pure product **AM3**-**4**.

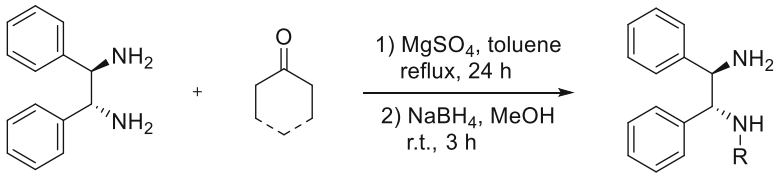
(S)-1-Phenyl-2-(piperidin-1-yl)ethan-1-amine, AM3. Performed on a 6.1 mmol scale from L-phenylglycine with piperidine (2.5 equiv.). Yellow oil (0.99 g, 60% yield). All analytical data matches with literature.[2] **^{1}H NMR (200 MHz, $CDCl_3$) δ** 7.42 – 7.16 (m, 5H), 4.10 (dd, *J* = 9.6, 4.4 Hz, 1H), 2.67 – 2.19 (m, 6H), 1.89 (s, 2H), 1.73 – 1.50 (m, 4H), 1.49 – 1.33 (m, 2H).

(R)-N^1,N^1-diethyl-2-phenylethane-1,2-diamine, AM4. Performed on a 4.1 mmol scale from D-phenylglycine with diethylamine (2.5 equiv.). Yellow oil (0.48 g, 57% yield). All analytical data matches with literature.[3] **^{1}H NMR (600 MHz, $CDCl_3$) δ** 7.30 – 7.22 (m, 4H), 7.22 – 7.15 (m, 1H), 3.91 (dd, *J* = 8.6, 4.7 Hz, 1H), 2.75 (dd, *J* = 11.7, 4.7 Hz, 1H), 2.58 (dd, *J* = 11.7,

Die approbierte gedruckte Originalversion dieser Dissertation ist an der TU Wien Bibliothek verfügbar.
The approved original version of this doctoral thesis is available in print at TU Wien Bibliothek.
TU Bibliothek Your knowledge hub WIEN

8.6 Hz, 1H), 2.29 (p, *J* = 5.9 Hz, 1H), 1.65 (s, 3H), 1.38 – 1.25 (m, 4H), 0.77 (q, *J* = 7.6 Hz, 6H). **^{13}C NMR (151 MHz, $CDCl_3$) δ** 144.94, 128.61, 127.27, 126.53, 60.24, 56.10, 54.96, 26.07, 25.99, 10.03.

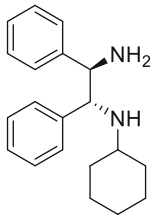
1.3 Synthesis of substituted diphenylethylendiamine **AM7**, **AM8**



7 **8-9** **AM7, AM8**

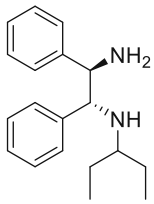
General procedure:[4] In a 250 ml round bottom flask, (R,R)-diphenylethylendiamine (1.0 equiv) was dissolved in dry toluene (0.1 M). $MgSO_4$ (1.2 equiv.) and ketone **8-9** (1.1 equiv.) were added, and the suspension refluxed for 24 h. The mixture was filtered through celite, washed with toluene and concentrated in vacuo. The residue was dissolved in dry MeOH, and $NaBH_4$ (4.0 equiv.) was added at 0 °C portionwise. The ice bath was removed, and the suspension was stirred at r.t. for 3 h. It was then quenched with 1 N NaOH, extracted with ethyl acetate (3x) and brine (1x), dried over anhydrous Na_2SO_4, filtered and concentrated in vacuo. The crude was purified via column chromatography (2.5% MeOH in DCM, 60 g silica, dry loading with silica, ninhydrin stain).

(1R,2R)-N^1-cyclohexyl-1,2-diphenylethane-1,2-diamine, AM7. Performed on a 8.2 mmol scale with



cyclohexanone (2.4 g, 24.7 mmol). Colorless liquid (1.1 g, 79%). All analytical data matches with literature.[4] $[\alpha]_D^{20}$ = +8.93 (c 1.32, $CHCl_3$). **^{1}H NMR (600 MHz, $CDCl_3$)** δ 7.24 – 7.08 (m, 10H), 3.99 (d, *J* = 7.1 Hz, 1H), 3.87 (d, *J* = 7.1 Hz, 1H), 2.22 (tt, *J* = 9.8, 3.8 Hz, 1H), 2.04 – 1.78 (m, 4H), 1.71 – 1.55 (m, 3H), 1.49 (ddd, *J* = 10.3, 6.4, 4.0 Hz, 1H), 1.19 – 1.01 (m, 4H), 0.94 (tdd, *J* = 11.0, 8.5, 2.9 Hz, 1H). **^{13}C NMR (101 MHz, $CDCl_3$)** δ 143.50, 142.12, 128.02, 127.99, 127.79, 127.09, 126.88, 126.81, 66.33, 61.94, 53.52, 34.81, 32.52, 26.14, 25.03, 24.59.

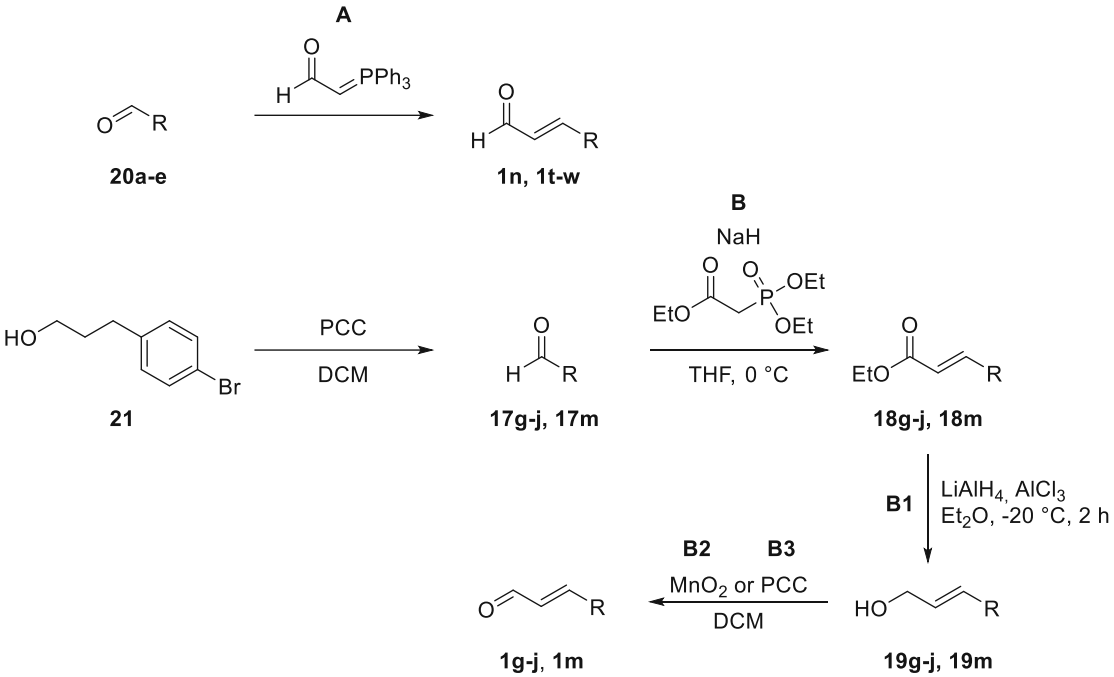
(1R,2R)-N^1-(pentan-3-yl)-1,2-diphenylethane-1,2-diamine, AM8. Performed on a 9.4 mmol scale with



3-pentanone (0.89 g, 10.3 mmol). Colorless liquid (2.0 g, 75%). All analytical data matches with literature.[4] $[\alpha]_D^{20}$ = +2.99 (c 1.34, $CHCl_3$). **^{1}H NMR (400 MHz, $CDCl_3$)** δ 7.25 – 7.06 (m, 10H), 3.98 (d, *J* = 6.9 Hz, 1H), 3.80 (d, *J* = 6.9 Hz, 1H), 2.20 (dq, *J* = 6.7, 5.2 Hz, 1H), 1.73 (s, 3H), 1.41 – 1.18 (m, 4H), 0.78 (t, *J* = 7.4 Hz, 3H), 0.70 (t, *J* = 7.5 Hz, 3H). **^{13}C NMR (101 MHz, $CDCl_3$)** δ 143.78, 142.44, 128.09, 127.99, 127.17, 126.91, 126.84, 66.87, 62.26, 56.42, 26.85, 24.35, 10.48, 8.43.

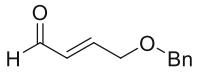
Die approbierte gedruckte Originalversion dieser Dissertation ist an der TU Wien Bibliothek verfügbar.
The approved original version of this doctoral thesis is available in print at TU Wien Bibliothek.
TU Bibliothek Your knowledge hub WIEN

2 Substrate synthesis



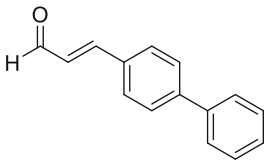
General procedure A:[5] To a solution of (triphenylphosphoanylidene) acetaldehyde (1.0 equiv.) in dry toluene (0.13 M) was added aldehyde **20a-e** (1.0 equiv.) at r.t. and heated to reflux for 20 h under argon atmosphere. After removal of the solvent, column chromatography (25% Et_2O in PE) provided the pure product **1n**, **1t-w**.

(E)-4-(benzyloxy)but-2-enal, 1n. Performed on a 6.7 mmol scale with 2-(benzyloxy)acetaldehyde.



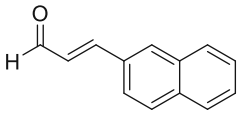
Colorless oil (0.52 g, 44%). All analytical data matches with literature.[6] **^{1}H NMR (400 MHz, $CDCl_3$) δ** 9.59 (d, *J* = 7.9 Hz, 1H), 7.46 – 7.30 (m, 5H), 6.85 (dt, *J* = 15.8, 4.1 Hz, 1H), 6.41 (ddt, *J* = 15.8, 7.9, 1.9 Hz, 1H), 4.60 (s, 2H), 4.29 (dd, *J* = 4.1, 2.0 Hz, 2H).

(E)-3-([1,1'-biphenyl]-4-yl)acrylaldehyde, 1t. Performed on a 6.7 mmol scale with [1,1'-biphenyl]-4-carbaldehyde.



Yellow solid (0.5 g, 32%). All analytical data matches with literature.[7] **^{1}H NMR (400 MHz, $CDCl_3$) δ** 9.73 (d, *J* = 7.7 Hz, 1H), 7.69 – 7.60 (m, 6H), 7.55 – 7.44 (m, 3H), 7.43 – 7.36 (m, 1H), 6.77 (dd, *J* = 15.9, 7.7 Hz, 1H).

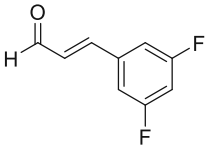
(E)-3-(naphthalen-2-yl)acrylaldehyde, 1u. Performed on a 6.4 mmol scale with 2-naphthaldehyde.



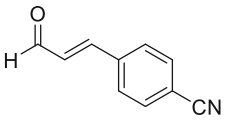
Yellow solid (0.8 g, 69%). All analytical data matches with literature.[8] **^{1}H NMR (400 MHz, $CDCl_3$) δ** 9.77 (d, *J* = 7.7 Hz, 1H), 7.99 (q, *J* = 0.9 Hz, 1H), 7.93 – 7.79 (m, 3H), 7.72 – 7.49 (m, 4H), 6.83 (dd, *J* = 15.9, 7.7 Hz, 1H).

Die approbierte gedruckte Originalversion dieser Dissertation ist an der TU Wien Bibliothek verfügbar.
The approved original version of this doctoral thesis is available in print at TU Wien Bibliothek.

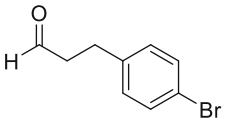
(E)-3-(3,5-difluorophenyl)acrylaldehyde, 1v. Performed on a 4.9 mmol scale with 3,5-difluorobenzaldehyde. Yellow solid (0.5 g, 60%). All analytical data matches with literature.[9] **^{1}H NMR (400 MHz, $CDCl_3$) δ** 9.72 (d, *J* = 7.5 Hz, 1H), 7.38 (d, *J* = 16.0 Hz, 1H), 7.15 – 7.02 (m, 2H), 6.89 (tt, *J* = 8.7, 2.3 Hz, 1H), 6.67 (dd, *J* = 16.0, 7.5 Hz, 1H). **^{19}F NMR (377 MHz, $CDCl_3$) δ** -108.40.



(E)-4-(3-oxoprop-1-en-1-yl)benzonitrile, 1w. Performed on a 4.9 mmol scale with 3,5-difluorobenzaldehyde. Yellow solid (0.5 g, 64%). **^{1}H NMR (400 MHz, $CDCl_3$) δ** 9.73 (dd, *J* = 7.5, 0.9 Hz, 1H), 7.75 – 7.60 (m, 4H), 7.47 (d, *J* = 16.1 Hz, 1H), 6.75 (ddd, *J* = 16.0, 7.5, 0.7 Hz, 1H).



3-(4-bromophenyl)propanal, 17m:[10] To a solution of **21** (3.0 g, 1.0 equiv., 13.9 mmol) in DCM (0.2 M), pyridinium chlorochromate (PCC) (4.5 g, 1.5 equiv., 20.9 mmol) and celite (14g) were added in one batch at r.t. The suspension was stirred vigorously at room temperature for 3 h in argon atmosphere, filtered through a pad of silica, washed with DCM and concentrated to provide the aldehyde **17m** (2.2 g, 74%). All analytical data matches with literature.[11] **^{1}H NMR (400 MHz, $CDCl_3$) δ** 9.80 (s, 1H), 7.40 (d, *J* = 7.9 Hz, 2H), 7.07 (d, *J* = 7.9 Hz, 2H), 2.90 (t, *J* = 7.2 Hz, 2H), 2.76 (t, *J* = 7.2 Hz, 2H).

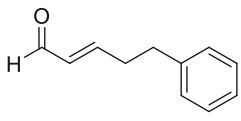


General procedure B:[12] To a suspension of NaH (1.0 equiv) in dry THF (1.6 M), triethyl acetophosphonate (1.1 equiv.) was slowly added at 0 °C and stirred at the same temperature for 30 min. Aldehyde **17g-j**, **17m** was added slowly and stirred at room temperature for 15 min. The resulting mixture was placed into an ultrasonic bath for 5 min, followed by the addition of sat. NH_4Cl, extracted with EtOAc (3x), Brine (1x), dried over anhydrous Na_2SO_4, filtered and concentrated in vacuo. The crude product **18g-j**, **18m** was used for the next step without further purification.

General procedure B1:[13] To a suspension of $LiAlH_4$ (1.1 equiv.) in dry diethylether, $AlCl_3$ (0.38 equiv.) was added slowly at 0 °C. The mixture was stirred for 5 min, followed by the addition of ester **18g-j**, **18m** (1.67M in Et_2O) at 0 °C. It was then stirred at 0° C for 2 h, slowly quenched with 5% HCl, extracted with Et_2O (1x), and sat. $NaHCO_3$ (2x), dried over anhydrous Na_2SO_4, filtered and concentrated. The crude product **19g-j**, **19m** was used for the next step without further purification.

General procedure B2:[14] MnO_2 (4.0 equiv.) was added to a solution of **19g**, **19h**, **19j** in dry DCM (0.16 M). The mixture was stirred for 48 h at r.t. under argon, filtered through celite, washed with DCM and concentrated. Column chromatography (15% Et_2O in PE, vanillin stain) gave the pure product **1g**, **1h**, **1j**.

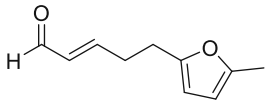
(E)-5-phenylpent-2-enal, 1g. Performed on a 14.9 mmol scale. Colorless liquid (1.16 g, 49%). All analytical data matches with literature.[15] **^{1}H NMR (400 MHz, $CDCl_3$) δ** 9.51 (d, *J*



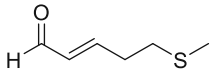
Die approbierte gedruckte Originalversion dieser Dissertation ist an der TU Wien Bibliothek verfügbar.
The approved original version of this doctoral thesis is available in print at TU Wien Bibliothek.
TU Bibliothek Your knowledge hub WIEN

= 7.8 Hz, 1H), 7.46 – 7.13 (m, 5H), 6.87 (dt, *J* = 15.5, 6.5 Hz, 1H), 6.15 (ddt, *J* = 15.7, 7.8, 1.5 Hz, 1H), 2.93 – 2.77 (m, 2H), 2.77 – 2.54 (m, 2H).

(E)-5-(5-methylfuran-2-yl)pent-2-enal, 1h. Performed on a 14.4 mmol scale. Colorless liquid (1.14 g, 48%). All analytical data matches with literature.[16] **^{1}H NMR (400 MHz, $CDCl_3$) δ** 9.50 (d, *J* = 7.9 Hz, 1H), 6.85 (dt, *J* = 15.6, 6.6 Hz, 1H), 6.14 (ddt, *J* = 15.7, 7.9, 1.5 Hz, 1H), 6.01 – 5.79 (m, 2H), 2.80 (t, *J* = 7.3 Hz, 2H), 2.73 – 2.62 (m, 2H), 2.25 (d, *J* = 1.1 Hz, 3H). **^{13}C NMR (101 MHz, $CDCl_3$) δ** 194.05, 157.12, 152.13, 150.98, 133.54, 106.43, 106.06, 31.30, 26.55, 13.61.

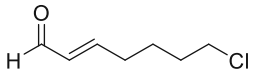


(E)-5-(methylthio)pent-2-enal, 1j. Performed on a 19.2 mmol scale. Yellow liquid (1.1 g, 44%). **^{1}H NMR (400 MHz, $CDCl_3$) δ** 9.54 (d, *J* = 7.8 Hz, 1H), 6.88 (dt, *J* = 15.6, 6.5 Hz, 1H), 6.18 (ddt, *J* = 15.7, 7.8, 1.5 Hz, 1H), 2.76 – 2.57 (m, 4H), 2.15 (s, 3H). **^{13}C NMR (101 MHz, $CDCl_3$) δ** 193.83, 155.80, 133.89, 32.37, 32.17, 15.63. **IR ATR (vmax/cm^{-1})** 1650, 1356, 1178, 1039, 736, 509. **HRMS** (ESI): *m/z* calcd for $C_6H_{10}OS^+$: 130.0452 $[M]^+$; found: 130.008.

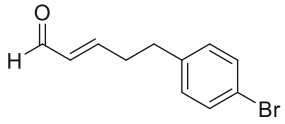


General procedure B3:[10] PCC (1.5 equiv.) and celite (3 g per 1 g PCC) were added to a solution of **19e**, **19i** in DCM (0.21 M) at r.t. and stirred for 3 h. It was filtered through a pad of silica, washed and concentrated in vacuo. Column chromatography (15% Et_2O in PE, vanillin stain) provided the pure product **1i**, **1m**.

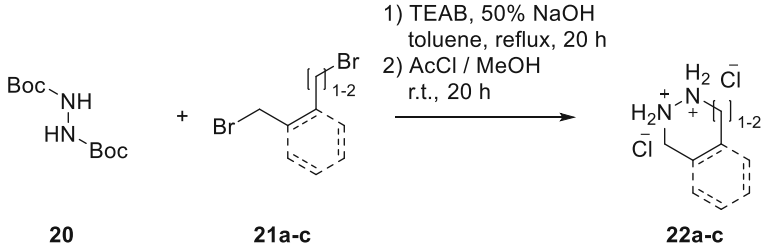
(E)-7-chlorohept-2-enal, 1i. Performed on a 16.6 mmol scale. Yellow oil (1.2 g, 38%). All analytical data matches with literature.[17] **^{1}H NMR (400 MHz, $CDCl_3$) δ** 9.53 (d, *J* = 7.8 Hz, 1H), 6.85 (dt, *J* = 15.6, 6.7 Hz, 1H), 6.15 (ddt, *J* = 15.6, 7.8, 1.5 Hz, 1H), 3.58 (t, *J* = 6.4 Hz, 2H), 2.40 (tdd, *J* = 7.4, 6.7, 1.5 Hz, 2H), 1.92 – 1.78 (m, 2H), 1.78 – 1.64 (m, 2H).



(E)-5-(4-bromophenyl)pent-2-enal, 1m. Performed on a 14.9 mmol scale. Colorless liquid (0.96 g, 42%). All analytical data matches with literature.[18] **^{1}H NMR (400 MHz, $CDCl_3$) δ** 9.49 (d, *J* = 7.8 Hz, 1H), 7.50 – 7.34 (m, 2H), 7.11 – 6.99 (m, 2H), 6.82 (dt, *J* = 15.7, 6.6 Hz, 1H), 6.12 (ddt, *J* = 15.7, 7.8, 1.5 Hz, 1H), 2.79 (t, *J* = 7.8 Hz, 2H), 2.72 – 2.52 (m, 2H).



3 Reagent synthesis

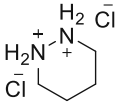


20 **21a-c** **22a-c**

Die approbierte gedruckte Originalversion dieser Dissertation ist an der TU Wien Bibliothek verfügbar.
The approved original version of this doctoral thesis is available in print at TU Wien Bibliothek.

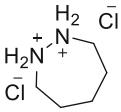
General procedure:[19] To a solution of 50% aqueous NaOH (r.t. 0.5 ml per ml toluene), toluene (0.4 M), tetraethylammonium bromide (TEAB) (15 mol%), dibromoalkane **21a-c** (1.5 equiv.) and **20** (1.0 equiv) were added at r.t. The biphasic system was vigorously stirred at 100 °C for 20 h. After cooling to r.t., the phases were separated, and the aqueous phase was extracted with toluene (3x). The combined organic phase was extracted with H_2O, Brine, dried over anhydrous Na_2SO_4, filtered and concentrated in vacuo. MeOH (0.5 M) was added and cooled to 0 °C. Acetylchloride (AcCl) was slowly added at 0°C via syringe under argon atmosphere. The resulting solution was stirred at r.t. for 20 h. Et_2O was added (1 ml per ml MeOH) and stirred for 30 min at r.t. The solids were filtered, washed with Et_2O (4x) and dried in vacuo to obtain crude **22a-b,** which was used for the next step without further purification.

Hexahydropyridazine dihydrochloride, 22a. Performed on a 64.6 mmol scale. White solid (8.2 g, 80%).



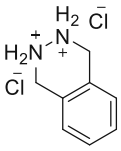
All analytical data matches with literature.[20] **^{1}H NMR (400 MHz, DMSO-d_6) δ** 9.74 (s, 4H), 2.98 (t, *J* = 2.7 Hz, 4H), 1.66 (t, *J* = 3.1 Hz, 4H).

1,2-diazepine dihydrochloride, 22b. Performed on a 34.4 mmol scale. White solid (3.9 g, 65%). All

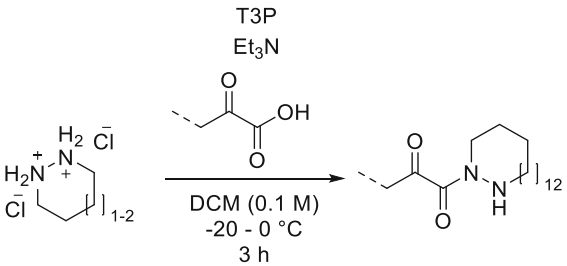


analytical data matches with the literature.[19] **^{1}H NMR (400 MHz, DMSO-d_6) δ** 8.85 (s, 4H), 3.16 – 2.94 (m, 4H), 1.78 – 1.59 (m, 6H).

1,2,3,4-tetrahydrophthalazine-2,3-diium, 22c. Performed on a 34.4 mmol scale. White solid (3.0 g,



42%). All analytical data matches with literature.[21] All analytical data matches with the literature.[19] **^{1}H NMR (400 MHz, DMSO-d_6) δ** 7.66 – 7.10 (m, 4H), 4.33 (s, 4H), 4.19 (s, 4H).



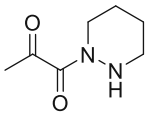
22a-c **2a-d**

General procedure: To a suspension of **22a-b** in dry DCM (0.1 M), Et_3N (1.5 equiv.) was added at 0 °C and stirred for 10 min under argon atmosphere. The solution was cooled to – 20 °C, and keto acid (1.5 equiv.) followed by propanephosphonic acid anhydride (T3P) (2.0 equiv.) were added via syringe and stirred for 5 min. The second batch E_3N (1.5 equiv.) was added slowly at -20 °C, and the resulting solution was stirred at -20 – 0 °C for 3 h. Dist. H_2O was added, the phases separated, and the aqueous phase was washed with DCM (3x). The combined organic phase was extracted with 5% $NaHCO_3$ (3x), dried over anhydrous Na_2SO_4, filtered and concentrated in vacuo. Column chromatography (100% Et_2O,

Die approbierte gedruckte Originalversion dieser Dissertation ist an der TU Wien Bibliothek verfügbar.
The approved original version of this doctoral thesis is available in print at TU Wien Bibliothek.
TU Bibliothek Your knowledge hub WIEN

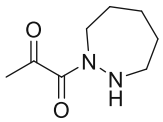
Rf = 0.4, $KMnO_4$ stain) gave the pure product **2a-c**. (comment from the author: 1-[Bis(dimethylamino)methylene]-1H-1,2,3-triazolo[4,5-b]pyridinium 3-oxide hexafluorophosphate (HATU) can be used instead of T3P with comparable yields).

1-(tetrahydropyridazin-1(2H)-yl)propane-1,2-dione, 2a. Performed on a 15.7 mmol scale. White solid



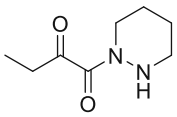
(1.5 g, 63%). **^{1}H NMR (400 MHz, $CDCl_3$) δ** 3.52 (s, 2H), 2.92 – 2.82 (m, 2H), 2.28 (s, 3H), 1.80 – 1.69 (m, 2H), 1.69 – 1.57 (m, 2H). **^{13}C NMR (101 MHz, $CDCl_3$) δ** 200.53, 167.91, 47.95, 42.17, 27.41, 25.14, 23.51. **IR ATR (vmax/cm^{-1})** 3216, 2951, 2931, 1710, 1637, 1439, 1154, 1210, 582, 516. **HRMS** (ESI): *m/z* calcd for $C_7H_{13}N_2O_2^+$: 157.0972 $[M+H]^+$; found: 157.0970.

1-(1,2-diazepan-1-yl)propane-1,2-dione, 2b. Performed on a 11.6 mmol scale. White solid (0.98 g,



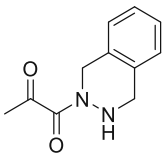
50%). **^{1}H NMR (400 MHz, $CDCl_3$) δ** 3.87 (s, 1H), 3.60 – 3.52 (m, 2H), 2.90 (t, *J* = 5.2 Hz, 2H), 2.25 (s, 3H), 1.82 – 1.70 (m, 2H), 1.70 – 1.53 (m, 4H). **^{13}C NMR (101 MHz, $CDCl_3$) δ** 200.34, 169.47, 51.71, 48.72, 29.88, 27.52, 27.24, 25.42. **IR ATR (vmax/cm^{-1})** 3303, 2924, 2856, 1698, 1643, 1434, 1296, 1183, 831, 751. **HRMS** (ESI): *m/z* calcd for $C_8H_{15}N_2O_2^+$: 185.1285 $[M+H]^+$; found: 185.1293**.**

1-(tetrahydropyridazin-1(2H)-yl)butane-1,2-dione, 2c. Performed on a 6.8 mmol scale from 2-



Oxobutanoic acid. White solid (0.5 g, 43%). **^{1}H NMR (400 MHz, $CDCl_3$) δ** 3.54 (d, *J* = 6.5 Hz, 2H), 2.93 – 2.84 (m, 2H), 2.62 (q, *J* = 7.3 Hz, 2H), 1.82 – 1.71 (m, 2H), 1.71 – 1.59 (m, 2H), 1.12 (t, *J* = 7.3 Hz, 3H). **^{13}C NMR (101 MHz, $CDCl_3$) δ** 203.47, 168.30, 47.92, 42.21, 33.16, 25.20, 23.49, 6.80. **IR ATR (vmax/cm^{-1})** 3241, 2945, 1715, 1634, 1427, 1444, 1161, 1005, 871, 658. **HRMS** (ESI): *m/z* calcd for $C_8H_{15}N_2O_2^+$: 171.1128 $[M+H]^+$; found: 171.1131**.**

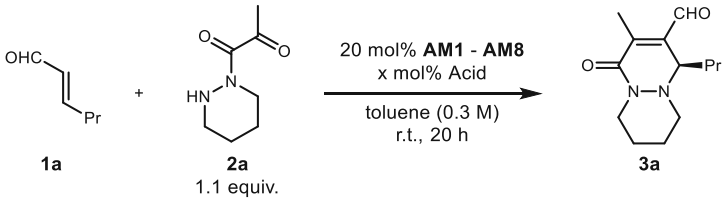
1-(3,4-dihydrophthalazin-2(1H)-yl)propane-1,2-dione, 2d. Performed on a 7.2 mmol scale. Brown

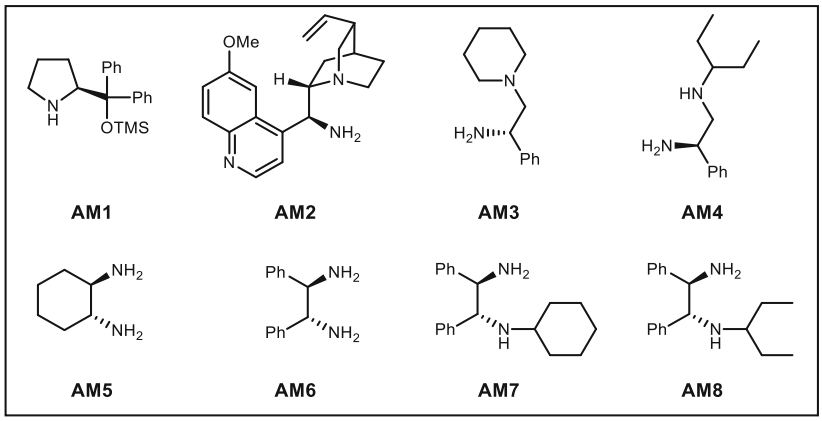


solid (0.32 g, 22%). **^{1}H NMR (400 MHz, $CDCl_3$) δ** 7.29 – 7.18 (m, 2H), 7.18 – 7.12 (m, 1H), 7.11 – 7.05 (m, 1H), 4.70 (s, 2H), 4.04 (d, *J* = 1.4 Hz, 2H), 2.39 (s, 3H). **^{13}C NMR (101 MHz, $CDCl_3$) δ** 199.96, 168.62, 132.45, 129.73, 127.53, 127.24, 127.00, 126.36, 49.04, 42.04, 27.50. **IR ATR (vmax/cm^{-1})** 3265, 2896, 1710, 1646, 1499, 1432, 1178, 934, 735, 574. **HRMS** (ESI): *m/z* calcd for $C_{11}H_{13}N_2O_2^+$: 205.0972 $[M+H]^+$; found: 205.0978**.**

Die approbierte gedruckte Originalversion dieser Dissertation ist an der TU Wien Bibliothek verfügbar.
The approved original version of this doctoral thesis is available in print at TU Wien Bibliothek.

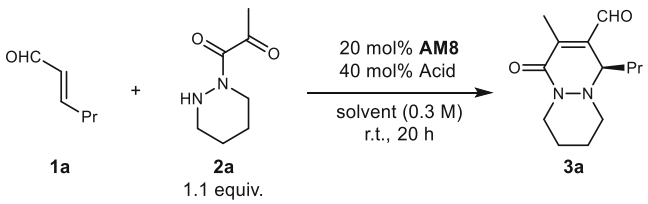
4 Screening





Entry[a]	Amine	Acid	Yield [%][b]	ee [%][c]
1	**AM1**	-	6	rac
2	**AM1**	BA (20 mol%)	17	rac
3	**AM2**	TFA (40 mol%)	87	26 (S)
4	**AM3**	TFA (40 mol%)	70	48 (S)
5	**AM4**	TFA (40 mol%)	89	74 (R)
6	**AM5**	TFA (40 mol%)	96	21 (R)
7	**AM6**	TFA (40 mol%)	62	76 (R)
8	**AM7**	TFA (40 mol%)	60	85 (R)
9	**AM8**	TFA (40 mol%)	79	85 (R)
10[d]	**AM8**	TFA (40 mol%)	61	91 (R)

[a] Reactions were performed with 0.05 mmol **1a**, 1.1 equiv. **2a** and 20 mol% catalyst at 25 °C for 20 h. [b] Determined by GC analysis on a BGB5 column using *n*-dodecane as internal standard. [c] Determined by chiral HPLC on Chiralpak ASH-column. [d] Reaction performed at 0 °C.



Entry[a]	Solvent	Acid	Yield [%][b]	ee [%][c]
1	MeOH	TFA	16	n.d.
2	THF	TFA	51	53

Die approbierte gedruckte Originalversion dieser Dissertation ist an der TU Wien Bibliothek verfügbar.
The approved original version of this doctoral thesis is available in print at TU Wien Bibliothek.
TU Bibliothek Your knowledge hub WIEN

3	dioxane	TFA	25	80
4	$CHCl_3$	TFA	62	78
5	DCM	TFA	56	79
6	Et_2O	TFA	32	68
7	toluene	TFA	79	85
8	toluene	TCA	67	75
9	toluene	PTSA	69	80
10	toluene	AcOH	18	n.d.
11	toluene	BA	19	n.d.
12	toluene	PFBA	60	35

[a] Reactions were performed with 0.05 mmol **1a**, 1.1 equiv. **2a** and 20 mol% diamine, 40 mol% acid, at 25 °C for 20 h. [b] Determined by GC analysis on a BGB5 column using *n*-dodecane as internal standard. [c] Determined by chiral HPLC on Chiralpak ASH-column.

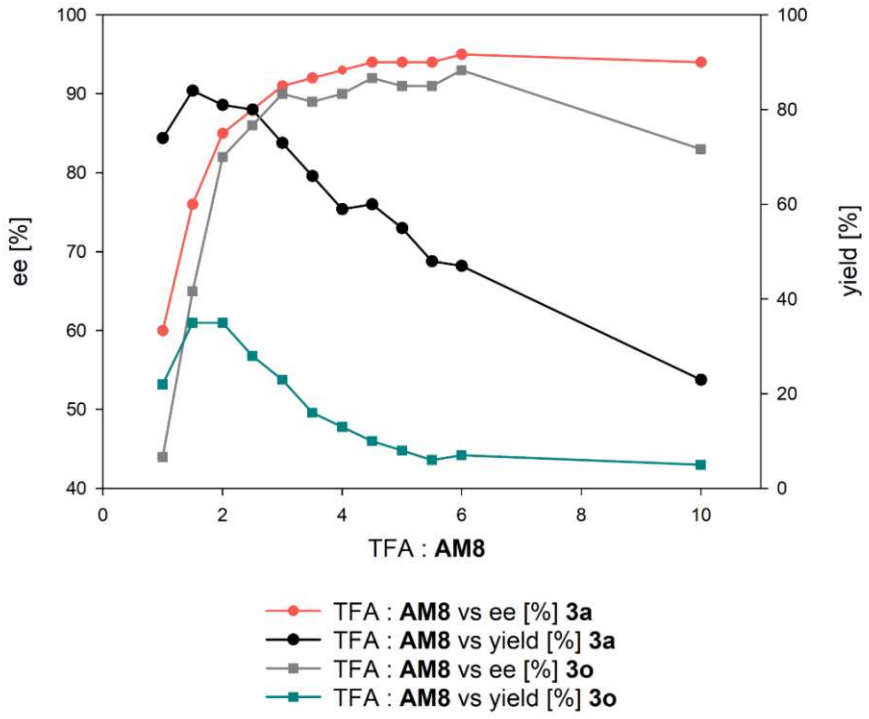
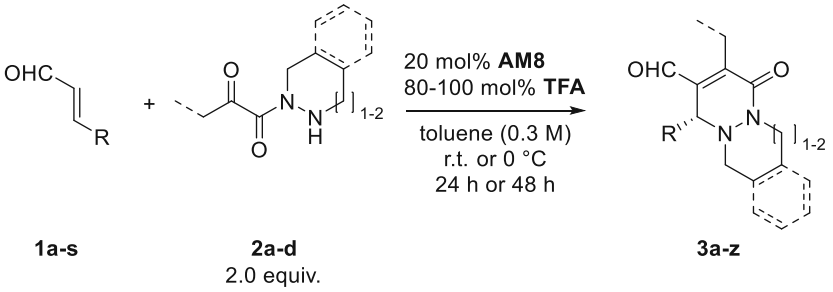


Figure 1. TFA screening TFA quantity screening. Reactions were performed with 0.05 mmol 1a or 1o, 1.1 equiv. 2a and 20 mol% AM8 at 25 °C for 20 h. Yield determined by GC analysis on a BGB5 column using n-dodecane as internal standard. Enantiomeric excess determined by chiral HPLC on Chiralpak ASH-column.

Die approbierte gedruckte Originalversion dieser Dissertation ist an der TU Wien Bibliothek verfügbar.
The approved original version of this doctoral thesis is available in print at TU Wien Bibliothek.

5 General procedure for the aza-Michael/aldol reaction

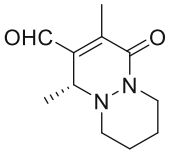


1a-s **2a-d** 2.0 equiv. **3a-z**

Reaction performed in a 7 ml screw cap vial: To a solution of **AM8** (14.4 mg, 20 mol%, 0.05 mmol) in dry toluene (0.85 ml), trifluoracetic acid (TFA) (29.2 mg, 1.0 equiv., 0.25 mmol for **3g-n**, **3t**, **3u**; 23.3 mg, 0.8 equiv. ,0.20 mmol for **3o-s**) was added at r.t. and the solution stirred for 5 min. **2a-c** (2.0 equiv., 0.51 mmol) was added and stirred for another 5 min. **1a-s** (1.0 equiv., 0.25 mmol) was added according to the method below. The crude was directly subjected to column chromatography (50% Et_2O in PE, $KMnO_4$ stain) to provide pure product **3a-u**.

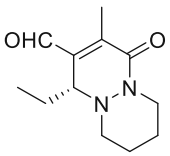
Method A: Substrate added at r.t. and stirred for 20 h at r.t.; Method B: Substrate added at 0 °C and stirred 20 h at 0 °C; Method C: Substrate added at 0 °C and stirred 48 h at 0 °C. Method D: Substrate added at r.t. and stirred for 48 h at r.t.

(R)-1,3-dimethyl-4-oxo-1,4,6,7,8,9-hexahydropyridazino[1,2-a]pyridazine-2-carbaldehyde, 3a.



Method A: Yellow liquid (46 mg, 86%). The **enantiomeric excess** was determined to be 91.4 %ee by chiral HPLC (Chiralpak® AS-H column, *n*-Heptane/EtOH = 98:2, 1 mL/min, λ = 254 nm, 25 °C), minor enantiomer: t_r = 10.6 min, major enantiomer: t_r = 12.8 min. Method B: Yellow liquid (27 mg, 51%). The **enantiomeric excess** was determined to be 94.5 %ee by chiral HPLC (Chiralpak® AS-H column, *n*-Heptane/EtOH = 98:2, 1 mL/min, λ = 254 nm, 25 °C), minor enantiomer: t_r = 10.6 min, major enantiomer: t_r = 12.5 min. $[\alpha]_D^{20}$ = -860.4 (c 0.25, $CHCl_3$). **^{1}H NMR (400 MHz, $CDCl_3$) δ** 10.25 (s, 1H), 4.54 (ddt, *J* = 12.5, 4.6, 1.8 Hz, 1H), 3.80 – 3.67 (m, 1H), 2.88 (td, *J* = 12.5, 3.4 Hz, 1H), 2.75 – 2.56 (m, 2H), 2.29 (d, *J* = 1.0 Hz, 3H), 1.97 – 1.81 (m, 1H), 1.77 – 1.44 (m, 3H), 1.16 (d, *J* = 6.8 Hz, 3H). **^{13}C NMR (101 MHz, $CDCl_3$) δ** 191.85, 163.14, 138.85, 138.59, 54.74, 52.19, 45.90, 24.87, 24.28, 18.98, 10.37. **IR ATR (vmax/cm^{-1})** 1650, 1441, 1367, 1151, 747, 583. **HRMS** (ESI): *m/z* calcd for $C_{11}H_{17}N_2O_2^+$: 209.1285 $[M+H]^+$; found: 209.1285**.**

(R)-1-ethyl-3-methyl-4-oxo-1,4,6,7,8,9-hexahydropyridazino[1,2-a]pyridazine-2-carbaldehyde, 3b.

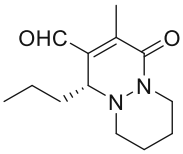


Method A: Yellow liquid (40 mg, 70%). The **enantiomeric excess** was determined to be 92.9 %ee by chiral HPLC (Chiralpak® AS-H column, *n*-Heptane/EtOH = 99:1, 1 mL/min, λ = 235 nm, 25 °C), minor enantiomer: t_r = 12.8 min, major enantiomer: t_r = 31.1 min. Method B: Yellow liquid (28 mg, 49%). The **enantiomeric excess** was determined to be 95.9 %ee by

Die approbierte gedruckte Originalversion dieser Dissertation ist an der TU Wien Bibliothek verfügbar.
The approved original version of this doctoral thesis is available in print at TU Wien Bibliothek.
TU Bibliothek Your knowledge hub WIEN

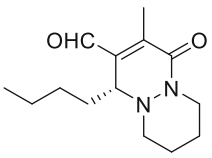
chiral HPLC (Chiralpak® AS-H column, *n*-Heptane/EtOH = 99:1, 1 mL/min, λ = 235 nm, 25 °C), minor enantiomer: t_r = 13.1 min, major enantiomer: t_r = 31 min. $[\alpha]_D^{20}$ = -148.0 (c 0.11, $CHCl_3$). **^{1}H NMR (400 MHz, $CDCl_3$) δ** 10.26 (s, 1H), 4.54 (ddt, *J* = 12.5, 4.8, 1.7 Hz, 1H), 3.51 (dd, *J* = 9.8, 4.3 Hz, 1H), 2.88 (td, *J* = 12.5, 3.4 Hz, 1H), 2.74 (ddd, *J* = 11.8, 10.8, 2.8 Hz, 1H), 2.59 (ddd, *J* = 10.9, 4.8, 2.3 Hz, 1H), 2.29 (d, *J* = 1.0 Hz, 3H), 1.91 (tdt, *J* = 13.1, 11.8, 4.6 Hz, 1H), 1.77 – 1.58 (m, 2H), 1.60 – 1.44 (m, 2H), 1.42 – 1.23 (m, 1H), 0.93 (t, *J* = 7.3 Hz, 3H). **^{13}C NMR (101 MHz, $CDCl_3$) δ** 192.05, 163.12, 139.01, 137.90, 58.07, 54.84, 45.65, 25.58, 24.87, 24.43, 10.72, 10.41. **IR ATR (vmax/cm^{-1})** 1652, 1442, 1200, 721, 577. **HRMS** (ESI): *m/z* calcd for $C_{12}H_{19}N_2O_2^+$: 223.1441 $[M+H]^+$; found: 223.1447.

(R)-3-methyl-4-oxo-1-propyl-1,4,6,7,8,9-hexahydropyridazino[1,2-a]pyridazine-2-carbaldehyde, 3c.



Method A: Yellow liquid (40 mg, 66%). The **enantiomeric excess** was determined to be 92.8 %ee by chiral HPLC (Chiralpak® AS-H column, *n*-Heptane/EtOH = 99:1, 1 mL/min, λ = 254 nm, 25 °C), minor enantiomer: t_r = 10.9 min, major enantiomer: t_r = 19.2 min. Method B: Yellow liquid (36 mg, 60%). The **enantiomeric excess** was determined to be 96.7 %ee by chiral HPLC (Chiralpak® AS-H column, *n*-Heptane/EtOH = 99:1, 1 mL/min, λ = 235 nm, 25 °C), minor enantiomer: t_r = 10.9 min, major enantiomer: t_r = 19.2 min. $[\alpha]_D^{20}$ = -613.5 (c 0.18, $CHCl_3$). **^{1}H NMR (400 MHz, $CDCl_3$) δ** 10.25 (s, 1H), 4.52 (ddt, *J* = 12.5, 4.8, 1.8 Hz, 1H), 3.62 (dd, *J* = 9.5, 4.2 Hz, 1H), 2.86 (td, *J* = 12.5, 3.4 Hz, 1H), 2.80 – 2.69 (m, 1H), 2.58 (ddd, *J* = 11.0, 4.9, 2.3 Hz, 1H), 2.28 (d, *J* = 1.0 Hz, 3H), 1.97 – 1.81 (m, 1H), 1.77 – 1.58 (m, 2H), 1.58 – 1.42 (m, 3H), 1.36 – 1.17 (m, 2H), 0.86 (t, *J* = 7.2 Hz, 3H). **^{13}C NMR (101 MHz, $CDCl_3$) δ** 191.99, 163.17, 138.92, 137.97, 56.24, 54.74, 45.61, 34.42, 24.86, 24.39, 19.20, 13.80, 10.39. **IR ATR (vmax/cm^{-1})** 1671, 1653, 1441, 1372, 1199, 730, 547. **HRMS** (ESI): *m/z* calcd for $C_{13}H_{21}N_2O_2^+$: 237.1598 $[M+H]^+$; found: 237.1597.

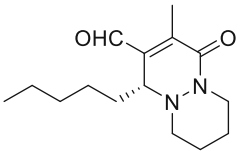
(R)-1-butyl-3-methyl-4-oxo-1,4,6,7,8,9-hexahydropyridazino[1,2-a]pyridazine-2-carbaldehyde, 3d.



Method A: Yellow liquid (41 mg, 64%). The **enantiomeric excess** was determined to be 92.7 %ee by chiral HPLC (Chiralpak® IB column, *n*-Heptane/EtOH = 98:2, 1 mL/min, λ = 254 nm, 25 °C), minor enantiomer: t_r = 8.9 min, major enantiomer: t_r = 8.2 min. Method B: Yellow liquid (33 mg, 51%). The **enantiomeric excess** was determined to be 95.0 %ee by chiral HPLC (Chiralpak® IB column, *n*-Heptane/EtOH = 98:2, 1 mL/min, λ = 254 nm, 25 °C), minor enantiomer: t_r = 8.9 min, major enantiomer: t_r = 8.2 min. $[\alpha]_D^{20}$ = -492.0 (c 0.13, $CHCl_3$). **^{1}H NMR (400 MHz, $CDCl_3$) δ** 10.26 (s, 1H), 4.53 (ddt, *J* = 12.5, 4.8, 1.7 Hz, 1H), 3.60 (dd, *J* = 9.4, 3.5 Hz, 1H), 2.87 (td, *J* = 12.5, 3.3 Hz, 1H), 2.73 (ddd, *J* = 11.9, 10.9, 2.8 Hz, 1H), 2.59 (ddd, *J* = 10.9, 4.8, 2.3 Hz, 1H), 2.28 (d, *J* = 1.0 Hz, 3H), 1.98 – 1.76 (m, 1H), 1.76 – 1.40 (m, 5H), 1.37 – 1.18 (m, 4H), 0.92 – 0.80 (m, 3H). **^{13}C NMR (101 MHz, $CDCl_3$) δ** 192.02, 163.19, 138.90, 138.03, 56.54, 54.78, 45.64, 32.02, 28.17, 24.85, 24.40, 22.41, 14.08, 10.41. **IR ATR (vmax/cm^{-1})** 1671, 1654, 1440, 1372, 1120, 629. **HRMS** (ESI): *m/z* calcd for $C_{14}H_{23}N_2O_2^+$: 251.1754 $[M+H]^+$; found: 251.1763.

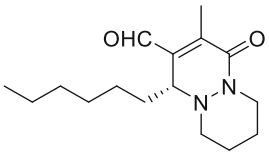
Die approbierte gedruckte Originalversion dieser Dissertation ist an der TU Wien Bibliothek verfügbar.
The approved original version of this doctoral thesis is available in print at TU Wien Bibliothek.
TU Bibliothek Your knowledge hub WIEN

(R)-3-methyl-4-oxo-1-pentyl-1,4,6,7,8,9-hexahydropyridazino[1,2-a]pyridazine-2-carbaldehyde, 3e.



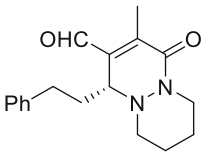
Method A: Yellow liquid (45 mg, 66%). The **enantiomeric excess** was determined to be 92.6 %ee by chiral HPLC (Chiralpak® ASH column, *n*-Heptane/EtOH = 99:1, 1 mL/min, λ = 235 nm, 25 °C), minor enantiomer: t_r = 8.9 min, major enantiomer: t_r = 12.6 min. Method B: Yellow liquid (37 mg, 55%). The **enantiomeric excess** was determined to be 95.9 %ee by chiral HPLC (Chiralpak® ASH column, *n*-Heptane/EtOH = 99:1, 1 mL/min, λ = 235 nm, 25 °C), minor enantiomer: t_r = 8.9 min, major enantiomer: t_r = 12.6 min. $[\alpha]_D^{20}$ = -435.5 (c 0.10, $CHCl_3$). **^{1}H NMR (400 MHz, $CDCl_3$) δ** 10.25 (s, 1H), 4.53 (ddt, *J* = 12.5, 3.9, 1.7 Hz, 1H), 3.60 (dd, *J* = 9.6, 3.9 Hz, 1H), 2.87 (td, *J* = 12.5, 3.3 Hz, 1H), 2.73 (ddd, *J* = 11.9, 10.9, 2.8 Hz, 1H), 2.59 (ddd, *J* = 10.9, 4.8, 2.3 Hz, 1H), 2.28 (d, *J* = 1.0 Hz, 3H), 1.96 – 1.80 (m, 1H), 1.76 – 1.42 (m, 5H), 1.35 – 1.16 (m, 6H), 0.85 (t, *J* = 6.9 Hz, 3H). **^{13}C NMR (101 MHz, $CDCl_3$) δ** 192.02, 163.19, 138.89, 138.04, 56.54, 54.77, 45.64, 32.24, 31.48, 25.62, 24.88, 24.41, 22.59, 14.12, 10.40. **IR ATR (vmax/cm^{-1})** 1671, 1654, 1440, 1372, 1120, 527. **HRMS** (ESI): *m/z* calcd for $C_{15}H_{25}N_2O_2^+$: 265.1911 $[M+H]^+$; found: 265.1926.

(R)-1-hexyl-3-methyl-4-oxo-1,4,6,7,8,9-hexahydropyridazino[1,2-a]pyridazine-2-carbaldehyde, 3f.



Method A: Yellow liquid (48 mg, 67%). The **enantiomeric excess** was determined to be 92.7 %ee by chiral HPLC (Chiralpak® ASH column, *n*-Heptane/EtOH = 99:1, 1 mL/min, λ = 254 nm, 25 °C), minor enantiomer: t_r = 7.9 min, major enantiomer: t_r = 11.2 min. Method B: Yellow liquid (42 mg, 59%). The **enantiomeric excess** was determined to be 95.9 %ee by chiral HPLC (Chiralpak® ASH column, *n*-Heptane/EtOH = 99:1, 1 mL/min, λ = 254 nm, 25 °C), minor enantiomer: t_r = 7.9 min, major enantiomer: t_r = 11.2 min. $[\alpha]_D^{20}$ = -631.4 (c 0.12, $CHCl_3$). **^{1}H NMR (400 MHz, $CDCl_3$) δ** 10.26 (s, 1H), 4.53 (ddd, *J* = 12.5, 4.2, 2.1 Hz, 1H), 3.60 (dd, *J* = 9.4, 3.8 Hz, 1H), 2.87 (td, *J* = 12.5, 3.4 Hz, 1H), 2.73 (ddd, *J* = 11.9, 10.9, 2.8 Hz, 1H), 2.59 (ddd, *J* = 10.9, 4.8, 2.3 Hz, 1H), 2.29 (d, *J* = 1.0 Hz, 3H), 1.90 (tdt, *J* = 13.1, 11.8, 4.6 Hz, 1H), 1.77 – 1.60 (m, 2H), 1.60 – 1.44 (m, 3H), 1.36 – 1.15 (m, 8H), 0.85 (t, *J* = 6.8 Hz, 3H). **^{13}C NMR (101 MHz, $CDCl_3$) δ** 192.34, 163.51, 139.21, 138.37, 56.87, 55.09, 45.96, 32.64, 32.12, 29.28, 26.26, 25.20, 24.74, 23.00, 14.48, 10.73. **IR ATR (vmax/cm^{-1})** 1671, 1654, 1440, 904, 629, 508. **HRMS** (ESI): *m/z* calcd for $C_{16}H_{27}N_2O_2^+$: 279.2067 $[M+H]^+$; found: 279.2087.

(R)-3-methyl-4-oxo-1-phenethyl-1,4,6,7,8,9-hexahydropyridazino[1,2-a]pyridazine-2-carbaldehyde, 3g. Method A: Yellow solid (46 mg, 60%). The **enantiomeric excess** was determined to be 92.8 %ee by

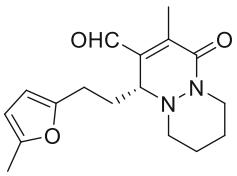


chiral HPLC (Chiralpak® ASH column, *n*-Heptane/EtOH = 99:1, 1 mL/min, λ = 254 nm, 25 °C), minor enantiomer: t_r = 16.5 min, major enantiomer: t_r = 34.4 min. Method C: Yellow solid (42 mg, 55%). The **enantiomeric excess** was determined to be 95.7 %ee by chiral HPLC (Chiralpak® ASH column, *n*-Heptane/EtOH = 99:1, 1 mL/min, λ = 254 nm, 25 °C), minor enantiomer: t_r = 16.5 min, major enantiomer: t_r = 34.4 min. $[\alpha]_D^{20}$ = -559.0 (c 0.14, $CHCl_3$).

Die approbierte gedruckte Originalversion dieser Dissertation ist an der TU Wien Bibliothek verfügbar.
The approved original version of this doctoral thesis is available in print at TU Wien Bibliothek.
TU Bibliothek Your knowledge hub WIEN

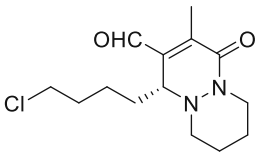
^{1}H NMR (400 MHz, $CDCl_3$) δ 10.24 (s, 1H), 7.32 – 7.22 (m, 2H), 7.17 (ddq, *J* = 7.0, 3.2, 1.8, 1.3 Hz, 3H), 4.57 (ddt, *J* = 12.5, 3.6, 1.7 Hz, 1H), 3.62 (dd, *J* = 10.4, 3.8 Hz, 1H), 2.94 – 2.80 (m, 2H), 2.72 (dddd, *J* = 16.6, 13.9, 10.0, 5.2 Hz, 2H), 2.56 (ddd, *J* = 10.9, 4.7, 2.2 Hz, 1H), 2.29 (d, *J* = 1.0 Hz, 3H), 2.01 – 1.78 (m, 2H), 1.74 (dp, *J* = 13.2, 2.1 Hz, 1H), 1.70 – 1.46 (m, 3H). **^{13}C NMR (101 MHz, $CDCl_3$) δ** 191.82, 163.28, 141.68, 139.19, 137.63, 128.57, 128.41, 125.91, 55.93, 54.63, 45.65, 33.37, 32.17, 24.85, 24.36, 10.42. **IR ATR (vmax/cm^{-1})** 1667, 1651, 1340, 1079, 866, 703, 505. **HRMS** (ESI): *m/z* calcd for $C_{18}H_{23}N_2O_2^+$: 299.1754 $[M+H]^+$; found: 299.1760.

(R)-3-methyl-1-(2-(5-methylfuran-2-yl)ethyl)-4-oxo-1,4,6,7,8,9-hexahydropyridazino[1,2-a] pyridazine-2-carbaldehyde, 3h. Method A: Yellow solid (53 mg, 68%). The **enantiomeric excess** was



determined to be 93.2 %ee by chiral HPLC (Chiralpak® ASH column, *n*-Heptane/EtOH = 99:1, 1 mL/min, λ = 254 nm, 25 °C), minor enantiomer: t_r = 15.6 min, major enantiomer: t_r = 21.7 min. Method C: Yellow solid (39 mg, 50%). The **enantiomeric excess** was determined to be 96.6 %ee by chiral HPLC (Chiralpak® ASH column, *n*-Heptane/EtOH = 99:1, 1 mL/min, λ = 254 nm, 25 °C), minor enantiomer: t_r = 15.6 min, major enantiomer: t_r = 21.7 min. $[\alpha]_D^{20}$ = -504.0 (c 0.13, $CHCl_3$). **^{1}H NMR (400 MHz, $CDCl_3$) δ** 10.25 (s, 1H), 5.85 (d, *J* = 2.9 Hz, 1H), 5.81 (dq, *J* = 3.1, 1.1 Hz, 1H), 4.54 (ddt, *J* = 12.6, 4.9, 1.8 Hz, 1H), 3.70 – 3.59 (m, 1H), 2.97 – 2.50 (m, 5H), 2.29 (d, *J* = 1.0 Hz, 3H), 2.23 (d, *J* = 1.1 Hz, 3H), 1.99 – 1.76 (m, 2H), 1.72 (dp, *J* = 13.1, 2.0 Hz, 1H), 1.69 – 1.45 (m, 3H). **^{13}C NMR (101 MHz, $CDCl_3$) δ** 191.79, 163.15, 153.54, 150.39, 139.22, 137.49, 105.90, 105.67, 55.88, 54.70, 45.66, 30.17, 24.84, 24.48, 24.35, 13.58, 10.43. **IR ATR (vmax/cm^{-1})** 1667, 1654, 1340, 1371, 1115, 705, 534. **HRMS** (ESI): *m/z* calcd for $C_{17}H_{23}N_2O_3^+$: 303.1703 $[M+H]^+$; found: 303.1705.

(R)-1-(4-chlorobutyl)-3-methyl-4-oxo-1,4,6,7,8,9-hexahydropyridazino[1,2-a]pyridazine-2-carbaldehyde, 3i. Method A: Yellow liquid (46 mg, 63%). The **enantiomeric excess** was determined to

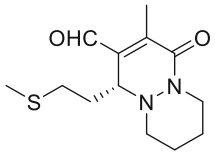


be 91.6 %ee by chiral HPLC (Chiralpak® ASH column, *n*-Heptane/EtOH = 95:5, 1 mL/min, λ = 254 nm, 25 °C), minor enantiomer: t_r = 10.3 min, major enantiomer: t_r = 17.1 min. Method C: Yellow liquid (45 mg, 62%). The **enantiomeric excess** was determined to be 95.7 %ee by chiral HPLC (Chiralpak® ASH column, *n*-Heptane/EtOH = 95:5, 1 mL/min, λ = 254 nm, 25 °C), minor enantiomer: t_r = 10.3 min, major enantiomer: t_r = 17.1 min. $[\alpha]_D^{20}$ = -552.0 (c 0.10, $CHCl_3$). **^{1}H NMR (400 MHz, $CDCl_3$) δ** 10.26 (s, 1H), 4.64 – 4.45 (m, 1H), 3.61 (dd, *J* = 9.8, 3.9 Hz, 1H), 3.51 (td, *J* = 6.5, 2.5 Hz, 2H), 2.88 (td, *J* = 12.5, 3.3 Hz, 1H), 2.75 (td, *J* = 11.4, 2.8 Hz, 1H), 2.60 (ddd, *J* = 11.0, 4.9, 2.3 Hz, 1H), 2.34 – 2.22 (m, 3H), 1.99 – 1.83 (m, 1H), 1.83 – 1.61 (m, 5H), 1.52 (dtt, *J* = 18.0, 12.2, 7.7 Hz, 3H), 1.27 (dddd, *J* = 12.1, 8.6, 5.5, 3.8 Hz, 1H). **^{13}C NMR (101 MHz, $CDCl_3$) δ** 191.94, 163.21, 139.21, 137.65, 56.35, 54.81, 45.70,

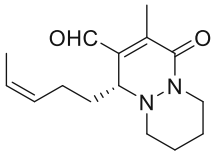
Die approbierte gedruckte Originalversion dieser Dissertation ist an der TU Wien Bibliothek verfügbar.
The approved original version of this doctoral thesis is available in print at TU Wien Bibliothek.
TU Bibliothek Your knowledge hub WIEN

44.97, 32.16, 31.28, 24.86, 24.36, 23.32, 10.43. **IR ATR (vmax/cm^{-1})** 1670, 1654, 1340, 1255, 1115, 903, 718, 543. **HRMS** (ESI): *m/z* calcd for $C_{14}H_{22}ClN_2O_2^+$: 285.1365 [*M+H*]$^+$; found: 285.1370.

(R)-3-methyl-1-(2-(methylthio)ethyl)-4-oxo-1,4,6,7,8,9-hexahydropyridazino[1,2-a]pyridazine-2-carbaldehyde, 3j. Method A: Yellow solid (26 mg, 38%). The **enantiomeric excess** was determined to be 90 %ee by chiral HPLC (Chiralpak® ASH column, *n*-Heptane/EtOH = 95:5, 1 mL/min, λ = 254 nm, 25 °C), minor enantiomer: t_r = 9.8 min, major enantiomer: t_r = 14.0 min. Method C: Yellow solid (21 mg, 30%). The **enantiomeric excess** was determined to be 94.2 %ee by chiral HPLC (Chiralpak® ASH column, *n*-Heptane/EtOH = 95:5, 1 mL/min, λ = 254 nm, 25 °C), minor enantiomer: t_r = 9.8 min, major enantiomer: t_r = 14.0 min. $[\alpha]_D^{20}$ = -571.8 (c 0.12, $CHCl_3$). **^{1}H NMR (400 MHz, $CDCl_3$) δ** 10.27 (s, 1H), 4.54 (ddt, *J* = 12.5, 4.7, 1.8 Hz, 1H), 3.94 – 3.79 (m, 1H), 2.96 – 2.72 (m, 2H), 2.63 (qdd, *J* = 13.2, 8.2, 5.9 Hz, 3H), 2.30 (d, *J* = 1.0 Hz, 3H), 2.07 (s, 3H), 1.94 – 1.44 (m, 6H). **^{13}C NMR (101 MHz, $CDCl_3$) δ** 191.80, 163.29, 139.42, 137.36, 55.04, 54.73, 45.79, 30.69, 30.36, 24.88, 24.32, 15.17, 10.47. **IR ATR (vmax/cm^{-1})** 1664, 1651, 1438, 1350, 1206, 1009, 832, 512. **HRMS** (ESI): *m/z* calcd for $C_{13}H_{21}N_2O_2S^+$: 269.1318 [*M+H*]$^+$; found: 269.1322.



(R,Z)-3-methyl-4-oxo-1-(pent-3-en-1-yl)-1,4,6,7,8,9-hexahydropyridazino[1,2-a]pyridazine-2-carbaldehyde, 3k. Method A: Yellow liquid (43 mg, 61%). The **enantiomeric excess** was determined to be 93.4 %ee by chiral HPLC (Chiralpak® ASH column, *n*-Heptane/EtOH = 99:1, 1 mL/min, λ = 254 nm, 25 °C), minor enantiomer: t_r = 10.5 min, major enantiomer: t_r = 16.9 min. Method C: Yellow liquid (45 mg, 62%). The **enantiomeric excess** was determined to be 96 %ee by chiral HPLC (Chiralpak® ASH column, *n*-Heptane/EtOH = 99:1, 1 mL/min, λ = 254 nm, 25 °C), minor enantiomer: t_r = 10.5 min, major enantiomer: t_r = 16.9 min. $[\alpha]_D^{20}$ = -479.3 (c 0.15, $CHCl_3$). **^{1}H NMR (400 MHz, $CDCl_3$) δ** 10.25 (s, 1H), 5.43 – 5.33 (m, 1H), 5.28 (dddt, *J* = 10.9, 8.0, 6.5, 1.4 Hz, 1H), 4.54 (ddd, *J* = 12.4, 4.2, 2.2 Hz, 1H), 3.62 (dd, *J* = 10.5, 3.7 Hz, 1H), 2.89 (td, *J* = 12.5, 3.4 Hz, 1H), 2.74 (ddd, *J* = 11.9, 10.9, 2.8 Hz, 1H), 2.57 (ddd, *J* = 10.9, 4.8, 2.3 Hz, 1H), 2.29 (d, *J* = 1.0 Hz, 3H), 2.18 (qdd, *J* = 14.9, 8.0, 4.0 Hz, 2H), 2.09 – 1.98 (m, 2H), 1.90 (tdt, *J* = 13.1, 11.9, 4.6 Hz, 1H), 1.82 – 1.45 (m, 4H), 1.27 (dtd, *J* = 13.8, 8.2, 3.7 Hz, 1H), 0.94 (t, *J* = 7.5 Hz, 3H). **^{13}C NMR (101 MHz, $CDCl_3$) δ** 191.89, 163.27, 139.04, 137.87, 132.64, 128.10, 55.78, 54.73, 45.69, 31.82, 24.85, 24.39, 23.42, 20.62, 14.47, 10.41. **IR ATR (vmax/cm^{-1})** 1653, 1614, 1438, 1371, 1200, 1031, 863, 720. **HRMS** (ESI): *m/z* calcd for $C_{16}H_{25}N_2O_2^+$: 277.1911 [*M+H*]$^+$; found: 277.1911.

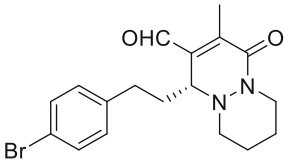


(R,E)-3-methyl-4-oxo-1-(pent-3-en-1-yl)-1,4,6,7,8,9-hexahydropyridazino[1,2-a]pyridazine-2-carbaldehyde, 3l. Method A: Yellow liquid (53 mg, 75%). The **enantiomeric excess** was determined to be 91 %ee by chiral HPLC (Chiralpak® ASH column, *n*-Heptane/EtOH = 99:1, 1 mL/min, λ = 254 nm, 25 °C), minor enantiomer: t_r = 11.1 min, major enantiomer: t_r = 16.1 min. Method C: Yellow liquid (48 mg, 68%). The **enantiomeric excess**

Die approbierte gedruckte Originalversion dieser Dissertation ist an der TU Wien Bibliothek verfügbar.
The approved original version of this doctoral thesis is available in print at TU Wien Bibliothek.
TU Bibliothek Your knowledge hub WIEN

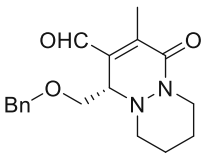
was determined to be 93.1 %ee by chiral HPLC (Chiralpak® ASH column, *n*-Heptane/EtOH = 99:1, 1 mL/min, λ = 254 nm, 25 °C), minor enantiomer: t_r = 11.1 min, major enantiomer: t_r = 16.1 min. $[\alpha]_D^{20}$ = -670.7 (c 0.13, $CHCl_3$). **^{1}H NMR (400 MHz, $CDCl_3$) δ** 10.24 (s, 1H), 5.44 – 5.34 (m, 1H), 5.34 – 5.20 (m, 1H), 4.54 (ddt, *J* = 12.5, 4.9, 1.7 Hz, 1H), 3.65 – 3.56 (m, 1H), 2.88 (td, *J* = 12.5, 3.3 Hz, 1H), 2.74 (ddd, *J* = 11.9, 10.9, 2.9 Hz, 1H), 2.56 (ddd, *J* = 10.9, 4.8, 2.2 Hz, 1H), 2.28 (d, *J* = 1.0 Hz, 3H), 2.25 – 2.08 (m, 2H), 2.08 – 1.97 (m, 2H), 1.89 (tdt, *J* = 13.1, 11.9, 4.7 Hz, 1H), 1.80 – 1.47 (m, 4H), 1.27 (dtd, *J* = 13.7, 8.2, 3.7 Hz, 1H), 0.93 (t, *J* = 7.5 Hz, 3H). **^{13}C NMR (101 MHz, $CDCl_3$) δ** 191.87, 163.25, 139.01, 137.85, 132.61, 128.09, 55.76, 54.70, 45.67, 31.80, 24.83, 24.36, 23.40, 20.60, 14.45, 10.39. **IR ATR (vmax/cm^{-1})** 1671, 1654, 1440, 1252, 1115, 905, 719, 686. **HRMS** (ESI): *m/z* calcd for $C_{16}H_{25}N_2O_2^+$: 277.1911 $[M+H]^+$; found: 277.1911.

(R)-1-(4-bromophenethyl)-3-methyl-4-oxo-1,4,6,7,8,9-hexahydropyridazino[1,2-a]pyridazine-2-carbaldehyde, 3m. Method A: Yellow solid (53 mg, 55%). The **enantiomeric excess** was determined to



be 91.7 %ee by chiral HPLC (Chiralpak® IB column, *n*-Heptane/EtOH = 98:2, 1 mL/min, λ = 210 nm, 25 °C), minor enantiomer: t_r = 16.2 min, major enantiomer: t_r = 14.2 min. Method C: Yellow solid (40 mg, 41%). The **enantiomeric excess** was determined to be 95.5 %ee by chiral HPLC (Chiralpak® IB column, *n*-Heptane/EtOH = 98:2, 1 mL/min, λ = 210 nm, 25 °C), minor enantiomer: t_r = 16.2 min, major enantiomer: t_r = 14.2 min. $[\alpha]_D^{20}$ = -312.1 (c 0.14, $CHCl_3$). **^{1}H NMR (400 MHz, $CDCl_3$) δ** 10.24 (s, 1H), 7.38 (d, *J* = 8.4 Hz, 2H), 7.04 (d, *J* = 8.3 Hz, 2H), 4.63 – 4.47 (m, 1H), 3.58 (dd, *J* = 10.6, 3.8 Hz, 1H), 2.95 – 2.60 (m, 4H), 2.54 (ddd, *J* = 11.0, 4.8, 2.2 Hz, 1H), 2.29 (d, *J* = 1.0 Hz, 3H), 1.98 – 1.71 (m, 3H), 1.70 – 1.47 (m, 3H). **^{13}C NMR (101 MHz, $CDCl_3$) δ** 191.79, 163.32, 140.59, 139.37, 137.49, 131.49, 130.38, 119.68, 55.77, 54.65, 45.73, 33.05, 31.56, 24.86, 24.33, 10.47. **IR ATR (vmax/cm^{-1})** 1671, 1654, 1441, 1159, 905, 729, 631. **HRMS** (ESI): *m/z* calcd for $C_{18}H_{22}BrN_2O_2^+$: 377.0859 $[M+H]^+$; found: 377.0866.

(S)-1-((benzyloxy)methyl)-3-methyl-4-oxo-1,4,6,7,8,9-hexahydropyridazino[1,2-a]pyridazine-2-carbaldehyde, 3n. Method A: Yellow solid (56 mg, 70%). The **enantiomeric excess** was determined to

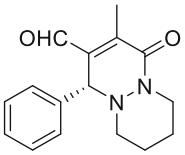


be 85 %ee by chiral HPLC (Chiralpak® ASH column, *n*-Heptane/EtOH = 95:5, 1 mL/min, λ = 254 nm, 25 °C), minor enantiomer: t_r = 11.0 min, major enantiomer: t_r = 13.4 min. Method C: Yellow solid (49 mg, 61%). The **enantiomeric excess** was determined to be 87 %ee by chiral HPLC (Chiralpak® ASH column, *n*-Heptane/EtOH = 95:5, 1 mL/min, λ = 254 nm, 25 °C), minor enantiomer: t_r = 11.0 min, major enantiomer: t_r = 13.4 min. $[\alpha]_D^{20}$ = -516.2. (c 0.12, $CHCl_3$). **^{1}H NMR (400 MHz, $CDCl_3$) δ** 10.22 (s, 1H), 7.39 – 7.17 (m, 5H), 4.62 – 4.46 (m, 3H), 4.07 (ddd, *J* = 8.0, 4.9, 1.2 Hz, 1H), 3.54 (dd, *J* = 10.4, 7.9 Hz, 1H), 3.30 (dd, *J* = 10.4, 4.9 Hz, 1H), 2.92 (td, *J* = 12.5, 3.3 Hz, 1H), 2.82 – 2.63 (m, 2H), 2.29 (d, *J* = 1.0 Hz, 3H), 1.96 (tdt, *J* = 13.2, 11.9, 4.7 Hz, 1H), 1.80 – 1.44 (m, 3H). **^{13}C NMR (101 MHz, $CDCl_3$) δ** 191.54, 162.78, 140.19, 138.19, 134.32, 128.43, 127.68,

Die approbierte gedruckte Originalversion dieser Dissertation ist an der TU Wien Bibliothek verfügbar.
The approved original version of this doctoral thesis is available in print at TU Wien Bibliothek.
TU Bibliothek Your knowledge hub WIEN

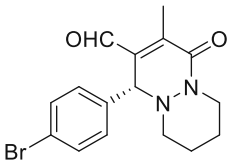
127.58, 73.29, 68.92, 56.77, 54.78, 45.55, 24.70, 24.23, 10.63. **IR ATR (vmax/cm^{-1})** 1617, 1655, 1372, 1443, 1199, 1115, 862, 738, 697, 517. **HRMS** (ESI): *m/z* calcd for $C_{18}H_{23}N_2O_3^+$: 315.1703 $[M+H]^+$; found: 315.1713.

(R)-3-methyl-4-oxo-1-phenyl-1,4,6,7,8,9-hexahydropyridazino[1,2-a]pyridazine-2-carbaldehyde, 3o.



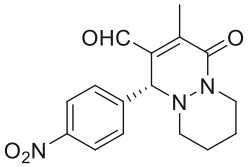
Method D: Yellow solid (35 mg, 51%). The **enantiomeric excess** was determined to be 91.5 %ee by chiral HPLC (Chiralpak® IB column, *n*-Heptane/EtOH = 98:2, 1 mL/min, λ = 254 nm, 25 °C), minor enantiomer: t_r = 22.5 min, major enantiomer: t_r = 17.9 min. $[\alpha]_D^{20}$ = -410.8 (c 0.10, $CHCl_3$). **^{1}H NMR (400 MHz, $CDCl_3$) δ** 10.40 (s, 1H), 7.35 – 7.14 (m, 5H), 4.89 (s, 1H), 4.47 (ddt, *J* = 12.5, 4.8, 1.7 Hz, 1H), 2.94 – 2.79 (m, 3H), 2.42 (d, *J* = 1.0 Hz, 3H), 2.10 – 1.91 (m, 1H), 1.88 – 1.75 (m, 1H), 1.73 – 1.62 (m, 1H), 1.56 (tdt, *J* = 13.2, 8.5, 4.6 Hz, 1H). **^{13}C NMR (101 MHz, $CDCl_3$) δ** 191.78, 162.74, 140.49, 138.63, 135.77, 128.34, 127.84, 127.15, 58.84, 55.16, 45.61, 24.89, 24.04, 10.70. **IR ATR (vmax/cm^{-1})** 1659, 1647, 1493, 1403, 1265, 1033, 904, 592, 502. **HRMS** (ESI): *m/z* calcd for $C_{16}H_{19}N_2O_2^+$: 271.1441 $[M+H]^+$; found: 271.1444.

(R)-1-(4-bromophenyl)-3-methyl-4-oxo-1,4,6,7,8,9-hexahydropyridazino[1,2-a]pyridazine-2-carbaldehyde, 3p. Method D: Yellow solid (52 mg, 58%). The **enantiomeric excess** was determined to



be 98.2 %ee by chiral HPLC (Chiralpak® ASH column, *n*-Heptane/EtOH = 90:10, 1 mL/min, λ = 254 nm, 25 °C), minor enantiomer: t_r = 9.8 min, major enantiomer: t_r = 13.3 min. $[\alpha]_D^{20}$ = -491.1 (c 0.18, $CHCl_3$). **^{1}H NMR (400 MHz, $CDCl_3$) δ** 10.40 (s, 1H), 7.44 – 7.34 (m, 2H), 7.16 – 7.06 (m, 2H), 4.84 (s, 1H), 4.48 (ddt, *J* = 12.6, 4.9, 1.7 Hz, 1H), 2.94 – 2.76 (m, 3H), 2.43 (d, *J* = 1.0 Hz, 3H), 2.08 – 1.93 (m, 1H), 1.81 (ddq, *J* = 13.3, 4.4, 2.2 Hz, 1H), 1.72 – 1.48 (m, 2H). **^{13}C NMR (101 MHz, $CDCl_3$) δ** 191.74, 162.76, 141.00, 137.81, 135.45, 131.53, 129.01, 121.92, 58.42, 55.18, 45.77, 24.95, 24.04, 10.84. **IR ATR (vmax/cm^{-1})** 1655, 1621, 1398, 1374, 1222, 1156, 1072, 824, 722, 578, 537. **HRMS** (ESI): *m/z* calcd for $C_{16}H_{18}BrN_2O_2^+$: 349.0546 $[M+H]^+$; found: 349.0550.

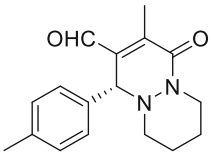
(R)-3-methyl-1-(4-nitrophenyl)-4-oxo-1,4,6,7,8,9-hexahydropyridazino[1,2-a]pyridazine-2-carbaldehyde, 3q. Method D: Yellow solid (55 mg, 68%). The **enantiomeric excess** was determined to



be 88.8 %ee by chiral HPLC (Chiralpak® IB column, *n*-Heptane/EtOH = 70:30, 1 mL/min, λ = 254 nm, 25 °C), minor enantiomer: t_r = 9.6 min, major enantiomer: t_r = 22.3 min. $[\alpha]_D^{20}$ = -413.2 (c 0.13, $CHCl_3$). **^{1}H NMR (400 MHz, $CDCl_3$) δ** 10.44 (s, 1H), 8.18 – 8.04 (m, 2H), 7.50 – 7.36 (m, 2H), 4.97 (s, 1H), 4.49 (ddt, *J* = 12.6, 4.8, 1.7 Hz, 1H), 2.96 – 2.77 (m, 3H), 2.07 – 1.91 (m, 1H), 1.84 (ddq, *J* = 13.4, 4.4, 2.2 Hz, 1H), 1.78 – 1.66 (m, 1H), 1.57 (qt, *J* = 13.2, 4.6 Hz, 1H). **^{13}C NMR (101 MHz, $CDCl_3$) δ** 191.63, 162.54, 147.50, 146.04, 141.67, 134.83, 128.06, 123.51, 58.28, 54.97, 45.76, 24.79, 23.81, 10.87. **IR ATR (vmax/cm^{-1})** 1655, 1618, 1399, 1268, 1010, 906, 726, 566. **HRMS** (ESI): *m/z* calcd for $C_{16}H_{18}N_3O_4^+$: 316.1292 $[M+H]^+$; found: 316.1295.

Die approbierte gedruckte Originalversion dieser Dissertation ist an der TU Wien Bibliothek verfügbar.
The approved original version of this doctoral thesis is available in print at TU Wien Bibliothek.
TU Bibliothek Your knowledge hub WIEN

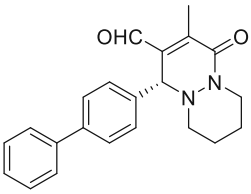
(R)-3-methyl-4-oxo-1-(p-tolyl)-1,4,6,7,8,9-hexahydropyridazino[1,2-a]pyridazine-2-carbaldehyde, 3r.



Method D: Yellow solid (37 mg, 51%). The **enantiomeric excess** was determined to be 91.2 %ee by chiral HPLC (Chiralpak® ASH column, *n*-Heptane/EtOH = 95:5, 1 mL/min, λ = 210 nm, 25 °C), minor enantiomer: t_r = 12.3 min, major enantiomer: t_r = 18.6 min. $[\alpha]_D^{20}$ = -623.5 (c 0.11, $CHCl_3$). **^{1}H NMR (400 MHz, $CDCl_3$) δ** 10.40 (s, 1H), 7.18 – 7.03 (m, 4H), 4.86 (s, 1H), 4.49 (ddt, *J* = 12.6, 4.9, 1.7 Hz, 1H), 2.94 – 2.78 (m, 3H), 2.43 (d, *J* = 1.0 Hz, 3H), 2.30 (s, 3H), 2.09 – 1.94 (m, 1H), 1.85 – 1.76 (m, 1H), 1.71 – 1.63 (m, 1H), 1.58 (ddd, *J* = 17.6, 8.7, 4.6 Hz, 1H). **^{13}C NMR (101 MHz, $CDCl_3$) δ** 191.88, 162.91, 140.37, 137.69, 135.98, 135.75, 129.15, 127.21, 58.83, 55.33, 45.74, 25.02, 24.17, 21.18, 10.77. **IR ATR (vmax/cm^{-1})** 1621, 1655, 1440, 1306, 1238, 941, 707, 516. **HRMS** (ESI): *m/z* calcd for $C_{17}H_{21}N_2O_2^+$: 285.1598 $[M+H]^+$; found: 285.1598.

(R)-1-(4-fluorophenyl)-3-methyl-4-oxo-1,4,6,7,8,9-hexahydropyridazino[1,2-a]pyridazine-2-carbaldehyde, 3s. Method D: Yellow solid (37 mg, 50%). The **enantiomeric excess** was determined to be 92.9 %ee by chiral HPLC (Chiralpak® IB column, *n*-Heptane/EtOH = 98:2, 1 mL/min, λ = 254 nm, 25 °C), minor enantiomer: t_r = 21.9 min, major enantiomer: t_r = 18.8 min. $[\alpha]_D^{20}$ = -494.4 (c 0.12, $CHCl_3$). **^{1}H NMR (400 MHz, $CDCl_3$) δ** 10.40 (s, 1H), 7.24 – 7.15 (m, 2H), 7.01 – 6.88 (m, 2H), 4.86 (s, 1H), 4.49 (ddt, *J* = 12.5, 4.8, 1.7 Hz, 1H), 2.93 – 2.76 (m, 3H), 2.43 (d, *J* = 1.0 Hz, 3H), 2.09 – 1.92 (m, 1H), 1.81 (ddq, *J* = 13.4, 4.4, 2.2 Hz, 1H), 1.73 – 1.63 (m, 1H), 1.56 (qt, *J* = 13.2, 4.6 Hz, 1H). **^{19}F NMR (376 MHz, $CDCl_3$) δ** -114.65. **^{13}C NMR (101 MHz, $CDCl_3$) δ** 191.80, 163.68, 162.83, 161.23, 140.83, 135.76, 134.48, 134.45, 128.99, 128.91, 115.40, 115.19, 58.35, 55.23, 45.78, 24.98, 24.10, 10.82. **IR ATR (vmax/cm^{-1})** 1669, 1654, 1334, 1223, 905, 792, 646. **HRMS** (ESI): *m/z* calcd for $C_{16}H_{18}FN_2O_2^+$: 289.1347 $[M+H]^+$; found: 289.1359.

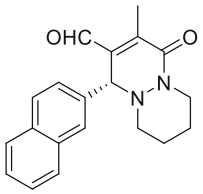
(R)-1-([1,1'-biphenyl]-4-yl)-3-methyl-4-oxo-1,4,6,7,8,9-hexahydropyridazino[1,2-a]pyridazine-2-carbaldehyde, 3t. Method D: Performed on a 0.2 mmol scale. Yellow solid (35 mg, 51%). The



enantiomeric excess was determined to be 88 %ee by chiral HPLC (Chiralpak® ASH column, *n*-Heptane/EtOH = 90:10, 1 mL/min, λ = 235 nm, 25 °C), minor enantiomer: t_r = 10.5 min, major enantiomer: t_r = 13.8 min. $[\alpha]_D^{20}$ = -281.3 (c 0.1, $CHCl_3$). **^{1}H NMR (400 MHz, , $CDCl_3$) δ** 10.44 (s, 1H), 7.56 – 7.47 (m, 4H), 7.45 – 7.38 (m, 2H), 7.37 – 7.29 (m, 3H), 4.96 (s, 1H), 4.53 (ddt, *J* = 12.5, 4.8, 1.7 Hz, 1H), 2.99 – 2.86 (m, 3H), 2.46 (d, *J* = 1.0 Hz, 3H), 2.17 – 1.95 (m, 1H), 1.89 – 1.77 (m, 1H), 1.74 – 1.60 (m, 2H). **^{13}C NMR (101 MHz, $CDCl_3$) δ** 191.81, 162.78, 140.83, 140.74, 140.56, 137.67, 135.75, 128.76, 127.60, 127.33, 127.13, 127.12, 58.69, 55.22, 45.68, 24.92, 24.05, 10.74. **IR ATR (vmax/cm^{-1})** 1669, 1654, 1439, 1262, 1139, 981, 764, 726. **HRMS** (ESI): *m/z* calcd for $C_{22}H_{22}N_2O_2Na^+$: 369.1573 $[M+Na]^+$; found: 369.1577.

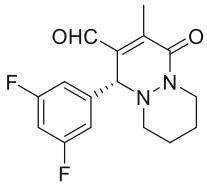
Die approbierte gedruckte Originalversion dieser Dissertation ist an der TU Wien Bibliothek verfügbar.
The approved original version of this doctoral thesis is available in print at TU Wien Bibliothek.

(R)-3-methyl-1-(naphthalen-2-yl)-4-oxo-1,4,6,7,8,9-hexahydropyridazino[1,2-a]pyridazine-2-carbaldehyde, 3u. Method D: Performed on a 0.2 mmol scale. Yellow solid (25 mg, 39%). The



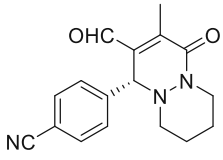
enantiomeric excess was determined to be 97 %ee by chiral HPLC (Chiralpak® ASH column, *n*-Heptane/EtOH = 95:5, 1 mL/min, λ = 254 nm, 25 °C), minor enantiomer: t_r = 10.5 min, major enantiomer: t_r = 17.0 min. $[\alpha]_D^{20}$ = -437.3 (c 0.1, $CHCl_3$). **^{1}H NMR (400 MHz, $CDCl_3$) δ** 10.47 (s, 1H), 7.81 – 7.71 (m, 3H), 7.53 – 7.42 (m, 4H), 5.06 (s, 1H), 4.55 – 4.40 (m, 1H), 3.04 – 2.79 (m, 3H), 2.50 (d, *J* = 1.0 Hz, 3H), 2.06 (tdt, *J* = 13.1, 11.2, 5.1 Hz, 1H), 1.84 (ddq, *J* = 13.4, 4.5, 2.2 Hz, 1H), 1.66 (dddd, *J* = 21.8, 12.8, 6.9, 3.7 Hz, 2H). **^{13}C NMR (101 MHz, $CDCl_3$) δ** 191.86, 162.98, 140.88, 136.07, 135.71, 133.16, 133.09, 128.32, 128.22, 127.63, 126.22, 126.00, 125.83, 59.19, 55.49, 45.79, 25.06, 24.18, 10.91 **IR ATR (vmax/cm^{-1})** 1672, 1654, 1443, 1276, 1110, 907, 727. **HRMS** (ESI): *m/z* calcd for $C_{20}H_{20}N_2O_2Na^+$: 343.1417 [*M+Na*]$^+$; found: 343.1419.

(R)-1-(3,5-difluorophenyl)-3-methyl-4-oxo-1,4,6,7,8,9-hexahydropyridazino[1,2-a]pyridazine-2-carbaldehyde, 3v. Method D: Performed on a 0.2 mmol scale. Yellow solid (42 mg, 69%). The



enantiomeric excess was determined to be 92 %ee by chiral HPLC (Chiralpak® IB column, *n*-Heptane/EtOH = 98:2, 1 mL/min, λ = 254 nm, 25 °C), minor enantiomer: t_r = 19.8 min, major enantiomer: t_r = 16.2 min. $[\alpha]_D^{20}$ = -321.9 (c 0.1, $CHCl_3$). **^{1}H NMR (400 MHz, $CDCl_3$) δ** 10.43 (s, 1H), 6.87 – 6.76 (m, 2H), 6.76 – 6.61 (m, 1H), 4.87 (s, 1H), 4.50 (ddt, *J* = 12.6, 4.8, 1.7 Hz, 1H), 2.95 – 2.80 (m, 3H), 2.43 (d, *J* = 1.0 Hz, 3H), 2.12 – 1.94 (m, 1H), 1.86 – 1.77 (m, 1H), 1.75 – 1.63 (m, 1H), 1.63 – 1.48 (m, 1H). **^{19}F NMR (377 MHz, $CDCl_3$) δ** -109.69. **^{13}C NMR (101 MHz, $CDCl_3$) δ** 191.71, 164.30, 164.18, 162.51, 142.95, 141.57, 134.97, 110.37, 110.30, 110.18, 110.11, 103.62, 103.37, 103.11, 58.10, 58.08, 58.06, 54.92, 45.78, 24.87, 23.94, 10.92. **IR ATR (vmax/cm^{-1})** 1671, 1655, 1618, 1372, 1115, 906, 695, 669, 506. **HRMS** (ESI): *m/z* calcd for $C_{16}H_{17}F_2N_2O_2^+$: 307.1253 [*M+H*]$^+$; found: 307.1255.

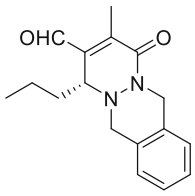
(R)-4-(2-formyl-3-methyl-4-oxo-1,4,6,7,8,9-hexahydropyridazino[1,2-a]pyridazin-1-yl)benzonitrile, 3w. Method D: Performed on a 0.2 mmol scale. Yellow solid (43 mg, 73%). The **enantiomeric excess**



was determined to be 80 %ee by chiral HPLC (Chiralpak® ASH column, *n*-Heptane/EtOH = 80:20, 1 mL/min, λ = 235 nm, 25 °C), minor enantiomer: t_r = 11.5 min, major enantiomer: t_r = 28.7 min. $[\alpha]_D^{20}$ = -411.5 (c 0.1, $CHCl_3$). **^{1}H NMR (400 MHz, $CDCl_3$) δ** 10.43 (s, 1H), 7.62 – 7.49 (m, 2H), 7.44 – 7.32 (m, 2H), 4.93 (d, *J* = 1.4 Hz, 1H), 4.49 (ddt, *J* = 12.5, 4.8, 1.7 Hz, 1H), 2.94 – 2.77 (m, 3H), 2.44 (d, *J* = 0.9 Hz, 3H), 2.02 (tddd, *J* = 13.7, 8.9, 7.3, 4.5 Hz, 1H), 1.91 – 1.78 (m, 1H), 1.76 – 1.57 (m, 2H). **^{13}C NMR (101 MHz, $CDCl_3$) δ** 191.71, 162.63, 144.15, 141.65, 134.95, 132.26, 127.99, 118.73, 111.83, 58.51, 55.08, 45.83, 24.89, 23.92, 10.95. **IR ATR (vmax/cm^{-1})** 1670, 1616, 1405, 1157, 906, 727, 542. **HRMS** (ESI): *m/z* calcd for $C_{17}H_{18}N_2O_2^+$: 296.1394 [*M+H*]$^+$; found: 296.1392.

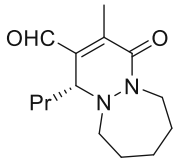
Die approbierte gedruckte Originalversion dieser Dissertation ist an der TU Wien Bibliothek verfügbar.
The approved original version of this doctoral thesis is available in print at TU Wien Bibliothek.
TU Bibliothek Your knowledge hub WIEN

3-methyl-4-oxo-1-propyl-1,4,6,11-tetrahydropyridazino[1,2-b]phthalazine-2-carbaldehyde, 3x.



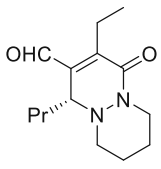
Method D: Performed on a 0.2 mmol scale. Yellow solid (32 mg, 64%). The **enantiomeric excess** was determined to be 85 %ee by chiral HPLC (Chiralpak® ASH column, *n*-Heptane/EtOH = 99:1, 1 mL/min, λ = 235 nm, 25 °C), minor enantiomer: t_r = 30.4 min, major enantiomer: t_r = 23.2 min. $[\alpha]_D^{20}$ = -502.8 (c 0.1, $CHCl_3$). **^{1}H NMR (400 MHz, $CDCl_3$) δ** 10.31 (s, 1H), 7.24 – 7.12 (m, 3H), 7.08 – 6.95 (m, 1H), 5.53 (d, *J* = 15.7 Hz, 1H), 4.32 (dq, *J* = 15.8, 1.1 Hz, 1H), 4.15 (dq, *J* = 13.9, 1.0 Hz, 1H), 3.94 (dd, *J* = 9.9, 3.7 Hz, 1H), 3.65 (d, *J* = 13.9 Hz, 1H), 2.31 (d, *J* = 1.0 Hz, 3H), 1.74 – 1.60 (m, 1H), 1.60 – 1.48 (m, 1H), 1.48 – 1.27 (m, 2H), 0.90 (t, *J* = 7.2 Hz, 3H). **^{13}C NMR (101 MHz, $CDCl_3$) δ** 191.66, 162.67, 139.47, 138.40, 132.73, 131.96, 127.06, 126.79, 126.64, 126.38, 55.43, 54.59, 45.88, 34.28, 19.25, 13.84, 10.55. **IR ATR (νmax/cm^{-1})** 1670, 1655, 1340, 909, 731, 505. **HRMS** (ESI): *m/z* calcd for $C_{17}H_{20}N_2O_2^+$: 284.1519 $[M]^+$; found: 284.1516.

(R)-3-methyl-4-oxo-1-propyl-1,4,7,8,9,10-hexahydro-6H-pyridazino[1,2-a][1,2]diazepine-2-carbaldehyde, 3y. Method C: Yellow liquid (20 mg, 31%). The **enantiomeric excess** was determined to



be 80 %ee by chiral HPLC (Chiralpak® ASH column, *n*-Heptane/EtOH = 99:1, 1 mL/min, λ = 254 nm, 25 °C), minor enantiomer: t_r = 10.9 min, major enantiomer: t_r = 20.8 min. $[\alpha]_D^{20}$ = -268.5 (c 0.11, $CHCl_3$). **^{1}H NMR (400 MHz, $CDCl_3$) δ** 10.25 (s, 1H), 4.34 (ddd, *J* = 13.2, 7.5, 5.9 Hz, 1H), 3.82 – 3.71 (m, 1H), 3.04 – 2.94 (m, 1H), 2.81 – 2.63 (m, 2H), 2.32 (d, *J* = 0.9 Hz, 3H), 1.89 – 1.75 (m, 3H), 1.74 – 1.21 (m, 8H), 0.89 (t, *J* = 7.2 Hz, 3H). **^{13}C NMR (101 MHz, $CDCl_3$) δ** 191.55, 163.77, 140.48, 139.78, 58.09, 57.61, 48.01, 34.51, 28.91, 26.53, 25.30, 19.28, 13.93, 10.54. **IR ATR (νmax/cm^{-1})** 1651, 1671, 1338, 1216, 729, 507. **HRMS** (ESI): *m/z* calcd for $C_{14}H_{23}N_2O_2^+$: 251.1754 $[M+H]^+$; found: 251.1761.

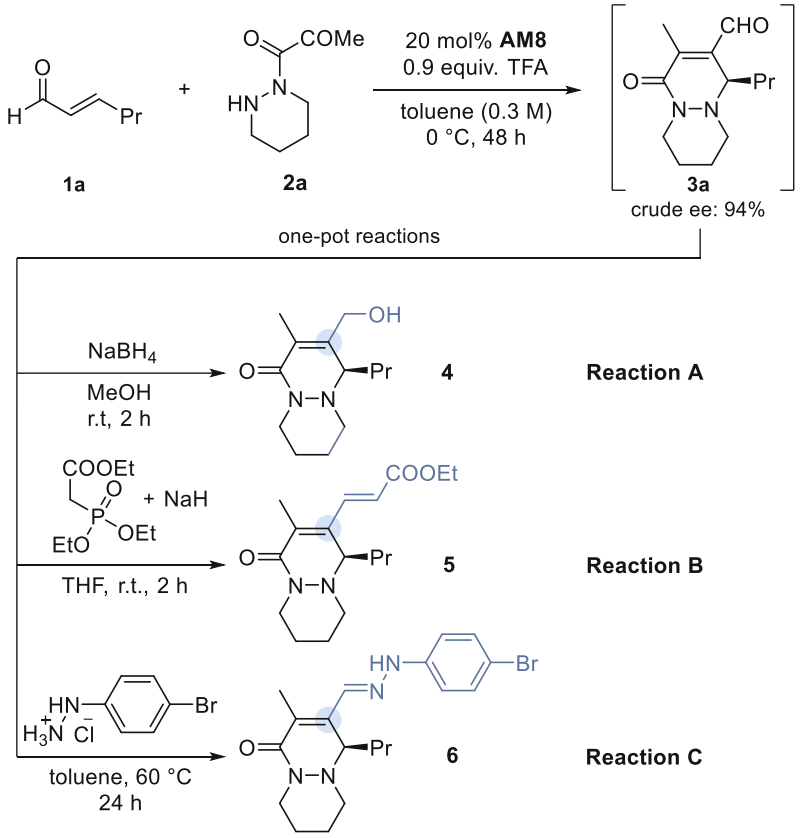
(R)-3-ethyl-4-oxo-1-propyl-1,4,6,7,8,9-hexahydropyridazino[1,2-a]pyridazine-2-carbaldehyde, 3z.



Method C: Yellow liquid (33 mg, 51%). The **enantiomeric excess** was determined to be 98 %ee by chiral HPLC (Chiralpak® ASH column, *n*-Heptane/EtOH = 99:1, 1 mL/min, λ = 254 nm, 25 °C), minor enantiomer: t_r = 7.9 min, major enantiomer: t_r = 11.0 min. $[\alpha]_D^{20}$ = -554.05 (c 0.13, $CHCl_3$). **^{1}H NMR (400 MHz, $CDCl_3$) δ** 10.24 (s, 1H), 4.55 (ddt, *J* = 12.4, 4.8, 1.7 Hz, 1H), 3.64 (dd, *J* = 9.4, 4.3 Hz, 1H), 2.93 – 2.67 (m, 4H), 2.64 – 2.56 (m, 1H), 1.90 (tdt, *J* = 13.1, 11.8, 4.6 Hz, 1H), 1.76 – 1.60 (m, 2H), 1.59 – 1.43 (m, 3H), 1.41 – 1.19 (m, 2H), 1.17 (t, *J* = 7.5 Hz, 3H), 0.88 (t, *J* = 7.2 Hz, 3H). **^{13}C NMR (101 MHz, $CDCl_3$) δ** 191.96, 162.69, 145.27, 137.20, 56.08, 54.72, 45.67, 34.48, 24.89, 24.61, 19.22, 17.80, 16.18, 13.86. **IR ATR (νmax/cm^{-1})** 1671, 1651, 1442, 1259, 1199, 907, 629, 542. **HRMS** (ESI): *m/z* calcd for $C_{14}H_{23}N_2O_2^+$: 251.1754 $[M+H]^+$; found: 251.1720.

Die approbierte gedruckte Originalversion dieser Dissertation ist an der TU Wien Bibliothek verfügbar.
The approved original version of this doctoral thesis is available in print at TU Wien Bibliothek.

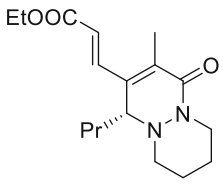
6 Further transformation



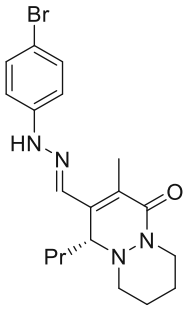
Reaction A, (R)-3-(hydroxymethyl)-2-methyl-4-propyl-6,7,8,9-tetrahydropyridazino[1,2-a]pyridazin-1(4H)-one, 4: After the general Aza-Michael/aldol procedure (chapter 5, 20 mol% **AM8**, 90 mol% TFA, Method C), dry MeOH (0.85 ml) was added followed by batch-wise addition of $NaBH_4$ (29 mg, 3.0 equiv. 0.77 mmol) at r.t. After 2 h (TLC indicated full conversion of **3a**) of stirring, Et_2O and Brine were added, phase separated, aqueous phase washed with Et_2O (3x), the combined organic phase washed with brine, dried over anhydrous Na_2SO_4, filtered and concentrated in vacuo. Column chromatography (100% Et_2O, $KMnO_4$ stain) gave the pure product **4** (37 mg, 61%) as a colorless liquid. The **enantiomeric excess** was determined to be 94.5 %ee by chiral HPLC (Chiralpak® IA3 column, *n*-Hexane/*i*PrOH = 90:10, 1 mL/min, λ = 254 nm, 25 °C), minor enantiomer: t_r = 7.0 min, major enantiomer: t_r = 7.4 min. $[\alpha]_D^{20}$ = -233.4 (c 0.13, $CHCl_3$). **^{1}H NMR (400 MHz, $CDCl_3$) δ** 4.51 – 4.44 (m, 1H), 4.39 (d, *J* = 13.7 Hz, 1H), 4.15 (dd, *J* = 13.7, 1.2 Hz, 1H), 3.35 (dd, *J* = 10.1, 3.1 Hz, 1H), 2.93 – 2.73 (m, 2H), 2.54 (ddd, *J* = 11.0, 4.7, 2.3 Hz, 1H), 1.92 – 1.83 (m, 1H), 1.82 (s, 3H), 1.70 (dp, *J* = 10.8, 2.1 Hz, 1H), 1.65 – 1.44 (m, 4H), 1.40 – 1.30 (m, 2H), 0.89 (t, *J* = 7.1 Hz, 3H). **^{13}C NMR (101 MHz, $CDCl_3$) δ** 164.14, 144.58, 122.37, 60.25, 59.80, 53.87, 45.28, 33.73, 25.06, 24.32, 19.47, 13.99, 10.95. **IR ATR (vmax/cm^{-1})** 3385, 1600, 1292, 1119, 750, 507. **HRMS** (ESI): *m/z* calcd for $C_{13}H_{23}N_2O_2^+$: 239.1754 $[M+H]^+$; found: 239.1755.

Die approbierte gedruckte Originalversion dieser Dissertation ist an der TU Wien Bibliothek verfügbar.
The approved original version of this doctoral thesis is available in print at TU Wien Bibliothek.

Reaction B, ethyl (R,E)-3-(3-methyl-4-oxo-1-propyl-1,4,6,7,8,9-hexahydropyridazino[1,2-a]pyridazin-2-yl)acrylate, 5: To a 0 °C solution of diethoxyphosphoryl-acetic acid ethyl ester (154 mg, 3.0 equiv., 0.77 mmol) in dry THF (0.85 ml) was slowly added NaH (31 mg, 3.0 equiv., 0.77 mmol). After stirring for 30 min at r.t., the solution was added directly to the Aza-Michael/aldol crude solution (chapter 5, 20 mol% **AM8**, 90 mol% TFA, Method C) at 0 °C. After stirring at r.t. for 2 h (TLC indicated full conversion of **3a**), Et_2O and brine were added, and the phase separated. The aqueous phase was extracted with Et_2O (3x), and the combined organic phase was washed with brine, dried over anhydrous Na_2SO_4, filtered and concentrated in vacuo. Column chromatography (50% Et_2O in PE, $KMnO_4$ stain) gave the pure product **5** (55 mg, 70%) as a yellow liquid. The **enantiomeric excess** was determined to be 94 %ee by chiral HPLC (Chiralpak® ASH column, *n*-Heptane/EtOH = 98:2, 1 mL/min, λ = 254 nm, 25 °C), minor enantiomer: t_r = 7.3 min, major enantiomer: t_r = 8.8 min. $[\alpha]_D^{20}$ = -317.8 (c 0.17, $CHCl_3$). **^{1}H NMR (400 MHz, $CDCl_3$) δ** 7.68 (d, *J* = 16.1 Hz, 1H), 5.97 (d, *J* = 16.0 Hz, 1H), 4.51 (ddt, *J* = 12.4, 3.8, 1.7 Hz, 1H), 4.24 (qd, *J* = 7.1, 1.8 Hz, 2H), 3.33 (dd, *J* = 10.2, 3.4 Hz, 1H), 2.91 – 2.72 (m, 2H), 2.53 (ddd, *J* = 10.9, 4.8, 2.3 Hz, 1H), 2.07 (d, *J* = 0.8 Hz, 3H), 1.88 (dddd, *J* = 17.7, 11.9, 9.3, 4.7 Hz, 1H), 1.79 – 1.41 (m, 5H), 1.31 (t, *J* = 7.1 Hz, 5H), 0.90 (t, *J* = 7.2 Hz, 3H). **^{13}C NMR (101 MHz, $CDCl_3$) δ** 166.50, 163.44, 139.69, 137.44, 130.51, 121.58, 60.97, 59.44, 54.34, 45.43, 33.92, 24.97, 24.26, 19.57, 14.37, 13.89, 11.87. **IR ATR (νmax/cm^{-1})** 1712, 1639, 1443, 1378, 1187, 906, 630. **HRMS** (ESI): *m/z* calcd for $C_{17}H_{26}N_2O_3^+$: 306.1943 $[M]^+$; found: 306.1939.



Reaction C, (R,E)-3-((2-(4-bromophenyl)hydrazineylidene)methyl)-2-methyl-4-propyl-6,7,8,9-tetrahydropyridazino[1,2-a]pyridazin-1(4H)-one, 6. After the general aza-Michael/aldol procedure (chapter 5, 20 mol% **AM8**, 90 mol% TFA, Method C), dry MeOH (0.85 ml) was added, followed by 4-bromo-phenylhydrazine-hydrochloride (172 mg, 3.0 equiv. 0.77 mmol) at r.t. The suspension was stirred at 60 °C for 24 h (TLC indicated full conversion of **3a**). The crude was directly subjected to column chromatography (70% Et_2O in PE, $KMnO_4$ stain) to obtain pure **6** (61 mg, 59%) as a yellow solid. m.p. 225-227 °C (Crystalline sample for XRD-measurement was obtained by slow evaporation from MeOH). **enantiomeric excess** was determined to be 94 %ee by chiral HPLC (Chiralpak® ASH column, *n*-Heptane/EtOH = 98:2, 1 mL/min, λ = 254 nm, 25 °C), minor enantiomer: t_r = 15.3 min, major enantiomer: t_r = 18.7 min. $[\alpha]_D^{20}$ = -377.0 (c 0.14, $CHCl_3$). **^{1}H NMR (400 MHz, $CDCl_3$) δ** 8.09 (s, 1H), 7.71 (s, 1H), 7.43 – 7.34 (m, 2H), 6.96 – 6.88 (m, 2H), 4.59 – 4.49 (m, 1H), 3.90 (dd, *J* = 9.9, 3.3 Hz, 1H), 2.93 – 2.80 (m, 2H), 2.65 – 2.57 (m, 1H), 2.01 (d, *J* = 0.8 Hz, 3H), 1.98 – 1.83 (m, 1H), 1.77 – 1.53 (m, 6H), 1.50 – 1.44 (m, 1H), 0.94 (t, *J* = 7.1 Hz, 3H). **^{13}C NMR (101 MHz, $CDCl_3$) δ** 164.24, 142.84, 138.64, 134.31, 132.23, 123.82, 114.44, 112.83, 58.26, 54.13, 45.36, 33.98, 24.88, 24.20, 19.48, 13.87, 10.83. **IR ATR**



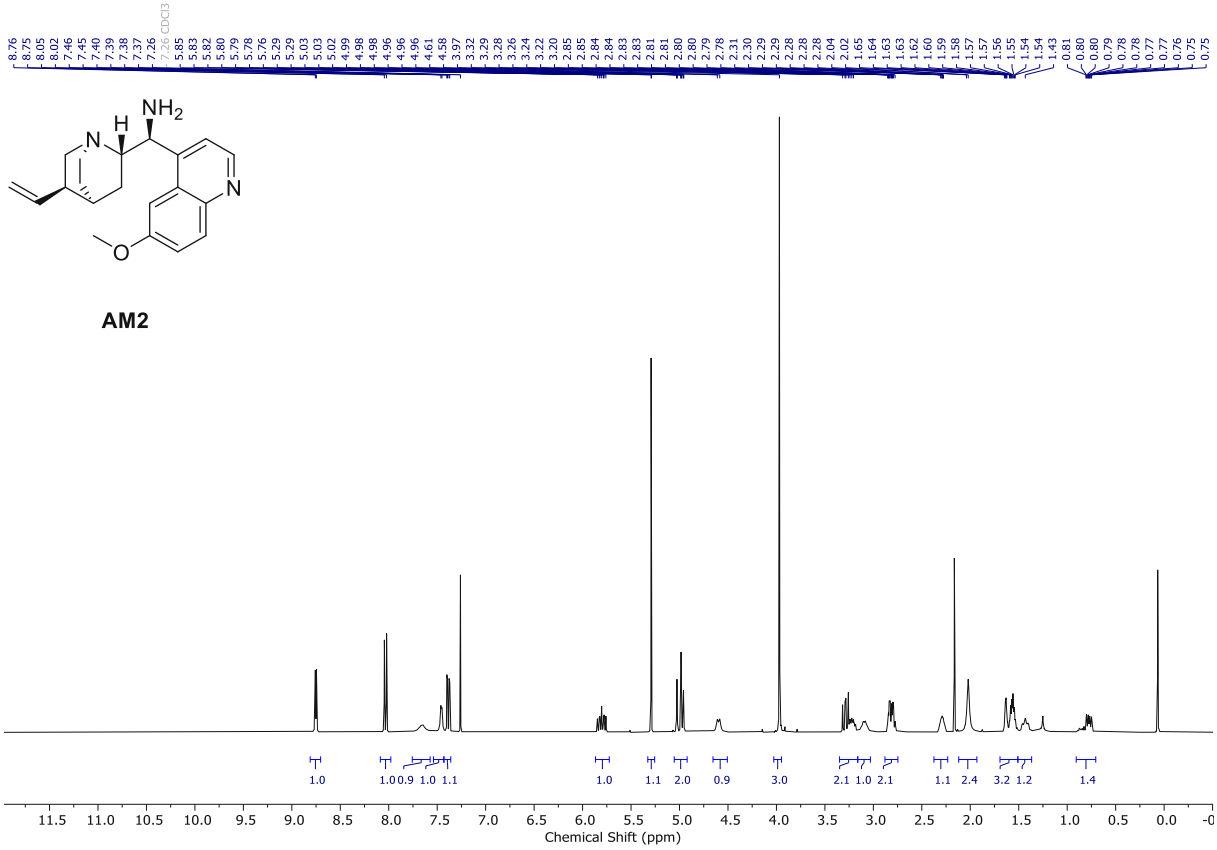
Die approbierte gedruckte Originalversion dieser Dissertation ist an der TU Wien Bibliothek verfügbar.
The approved original version of this doctoral thesis is available in print at TU Wien Bibliothek.
TU Bibliothek Your knowledge hub WIEN

(vmax/cm^{-1}) 3250, 2935, 1592, 1252, 1146, 818. **HRMS** (ESI): *m/z* calcd for $C_{19}H_{25}BrN_2O_3^+$: 405.1212 $[M]^+$; found: 405.1295.

7 NMR Spectra

7.1 NMR spectra chiral amines

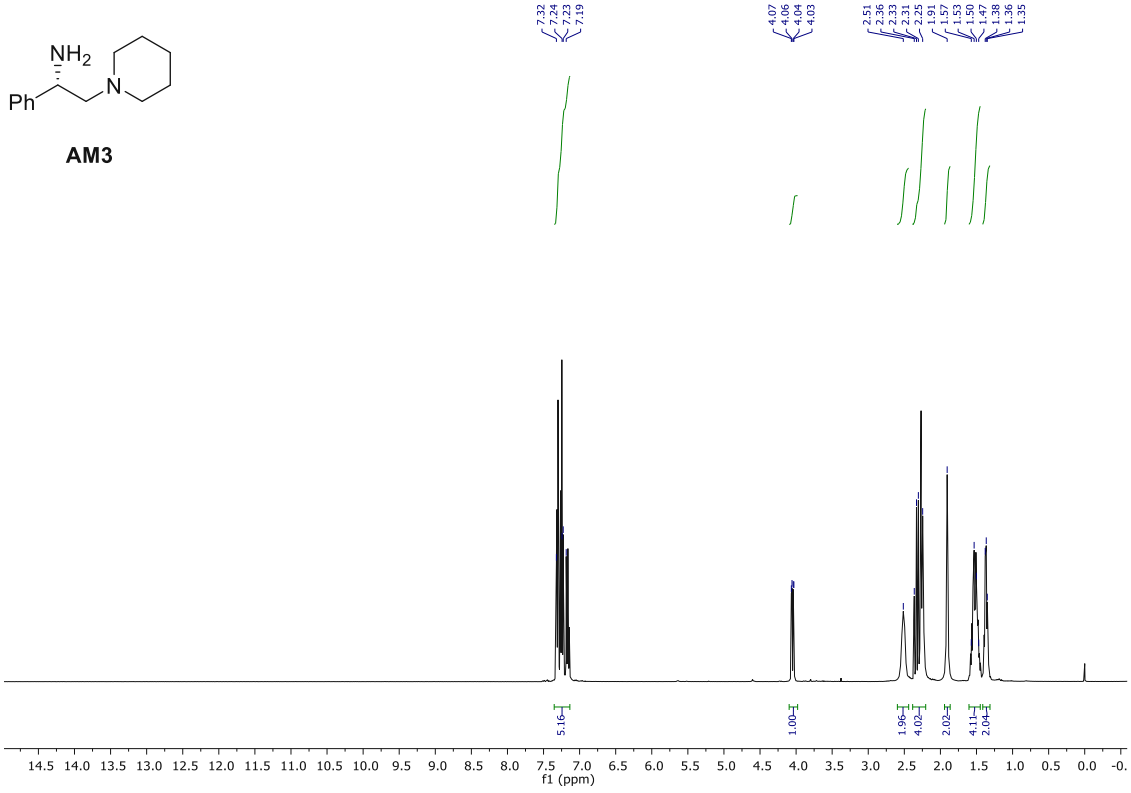
7.1.1 NMR spectra of **AM2**



Die approbierte gedruckte Originalversion dieser Dissertation ist an der TU Wien Bibliothek verfügbar.
The approved original version of this doctoral thesis is available in print at TU Wien Bibliothek.

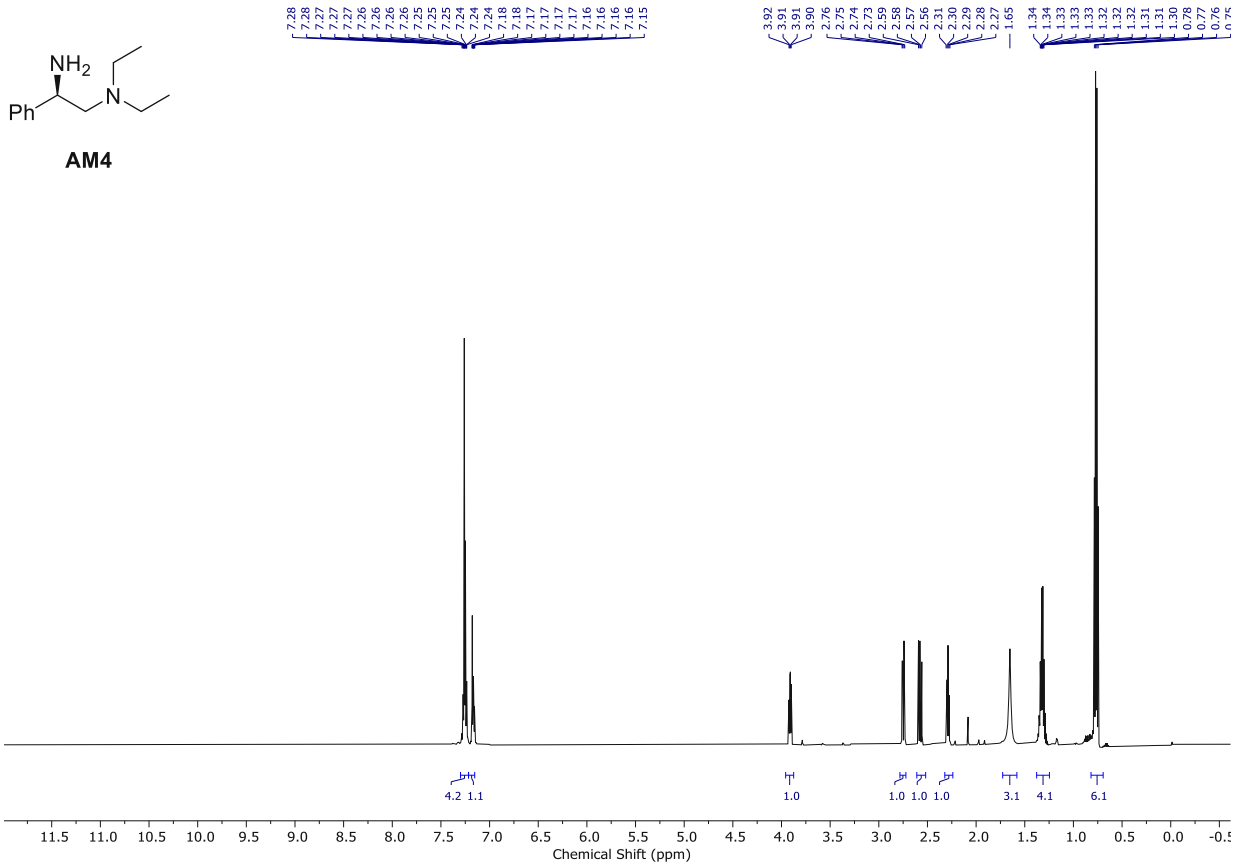
7.1.2 NMR spectra of **AM3**

AM3



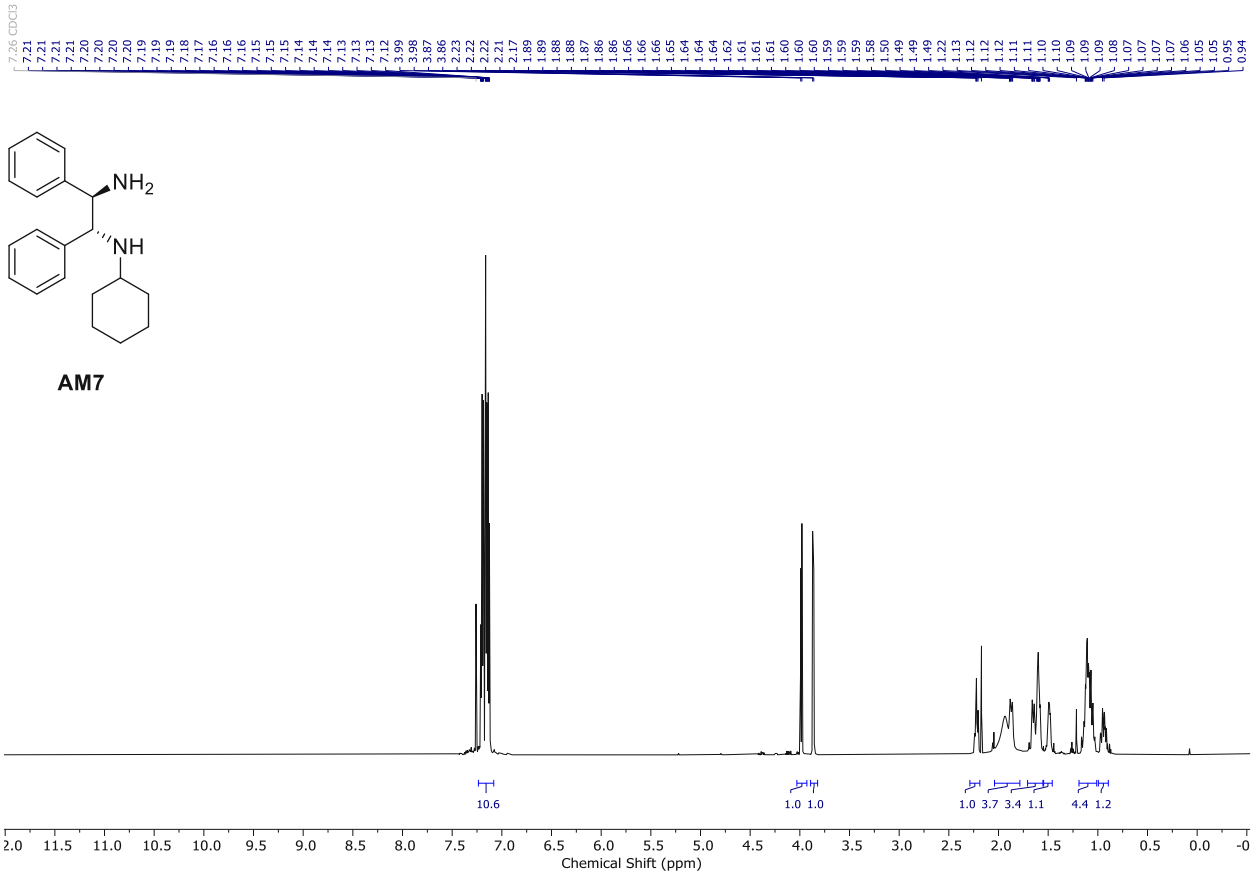
7.1.3 NMR spectra of **AM4**

AM4

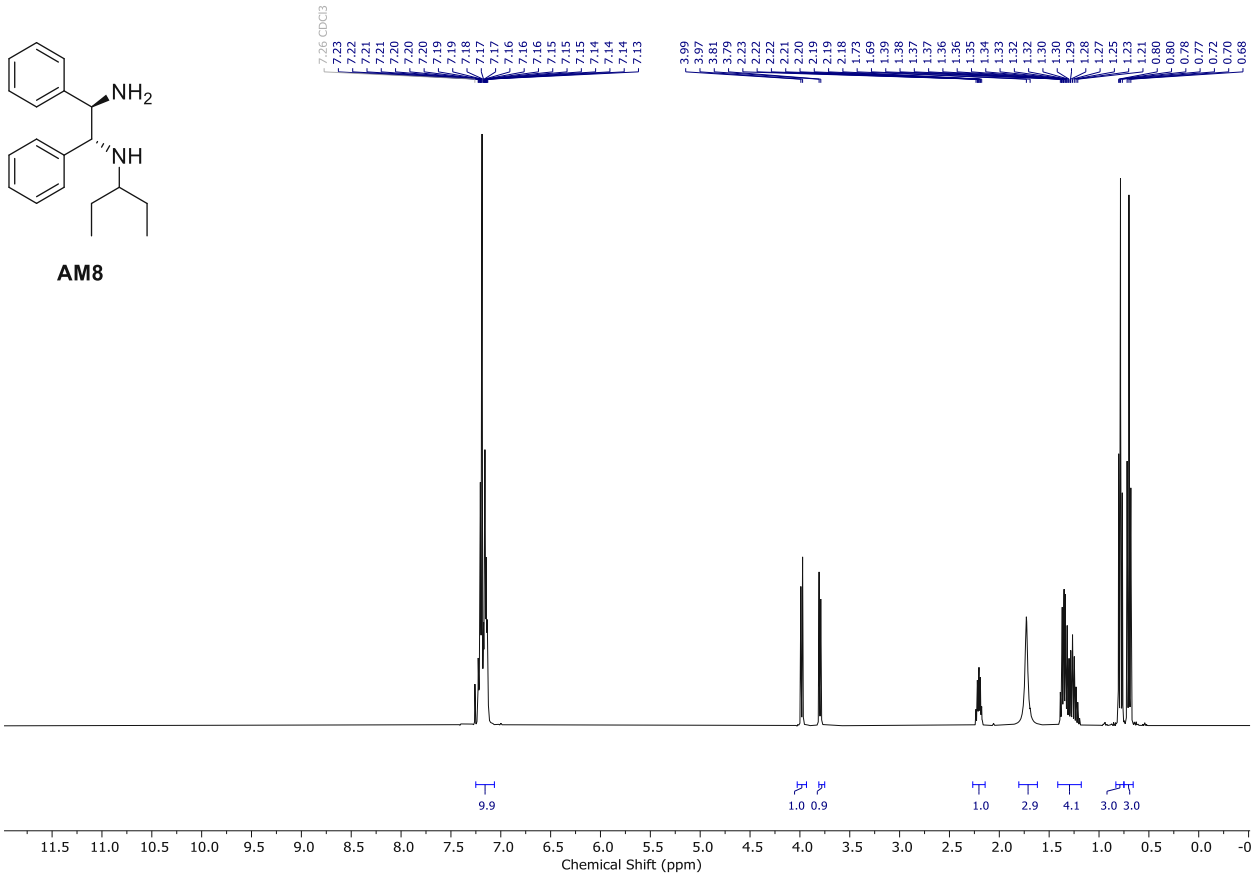


Die approbierte gedruckte Originalversion dieser Dissertation ist an der TU Wien Bibliothek verfügbar.
The approved original version of this doctoral thesis is available in print at TU Wien Bibliothek.
TU Bibliothek Your knowledge hub

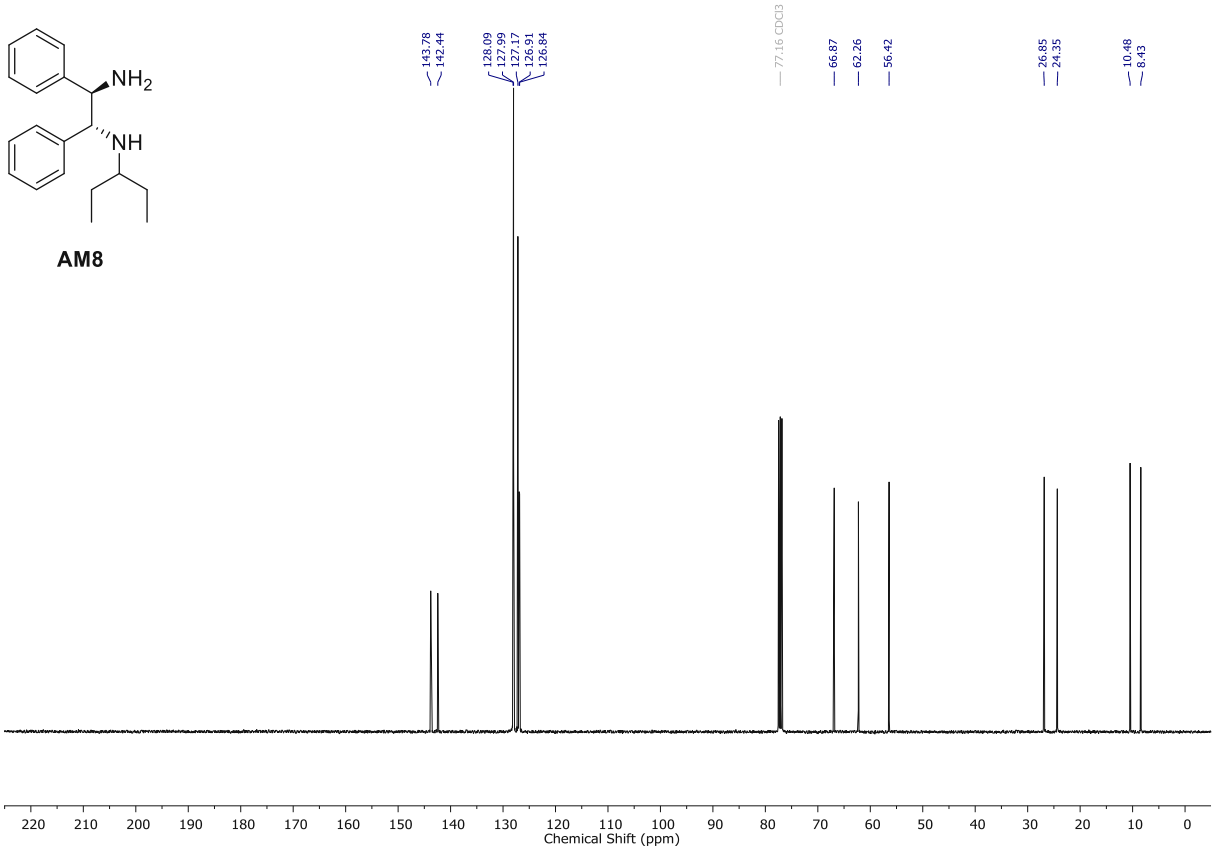
7.1.4 NMR spectra of **AM7**



7.1.5 NMR spectra of **AM8**

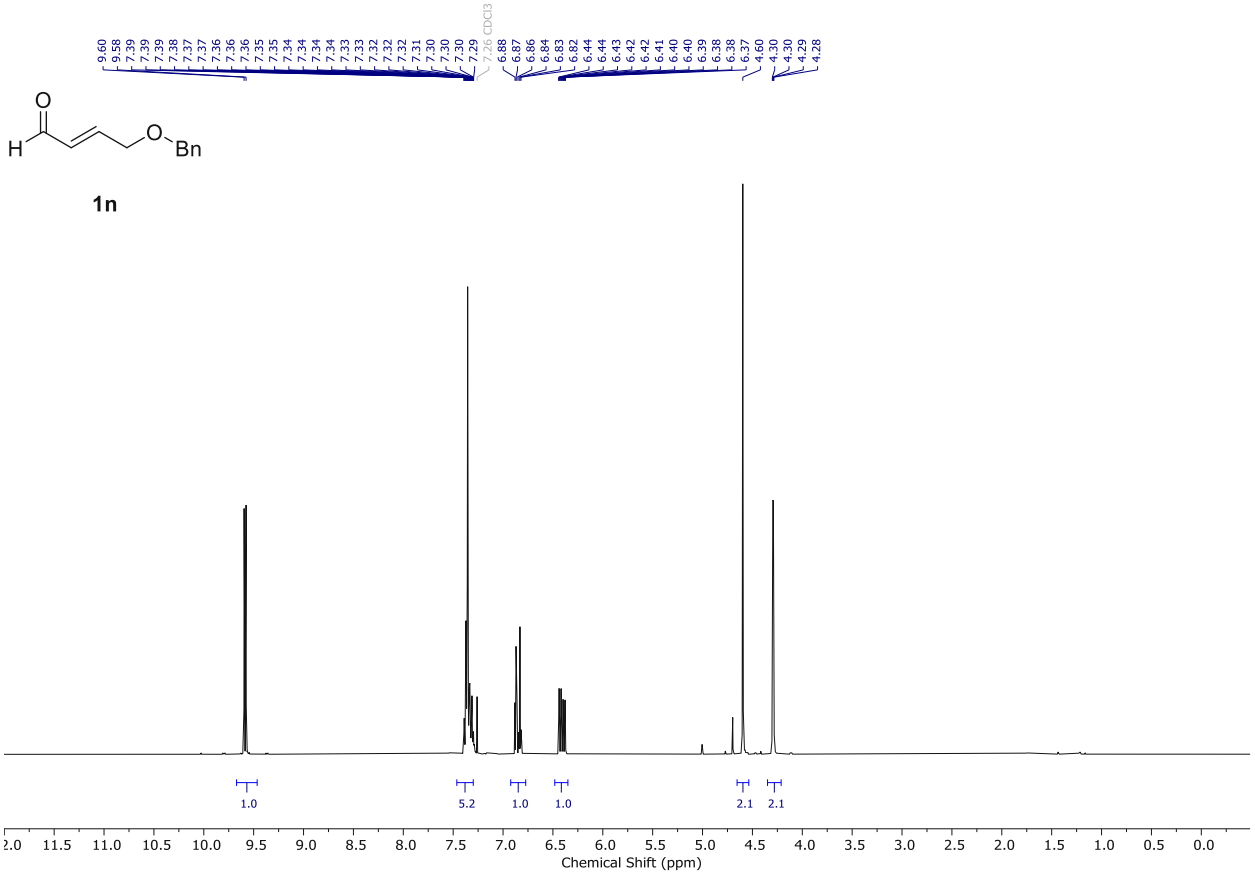


Die approbierte gedruckte Originalversion dieser Dissertation ist an der TU Wien Bibliothek verfügbar.
The approved original version of this doctoral thesis is available in print at TU Wien Bibliothek.
TU Bibliothek Your knowledge hub WIEN



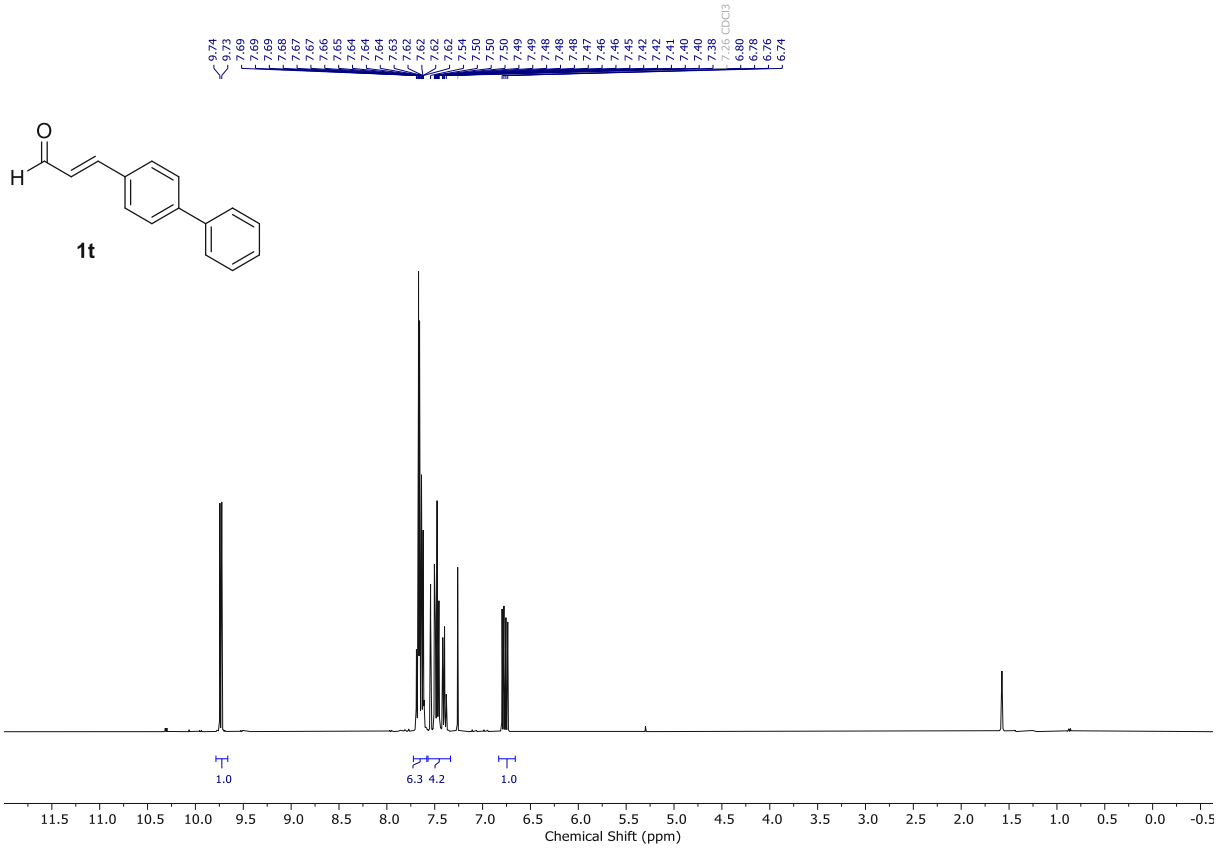
7.2 NMR spectra of enals

7.2.1 NMR spectra of **1n**

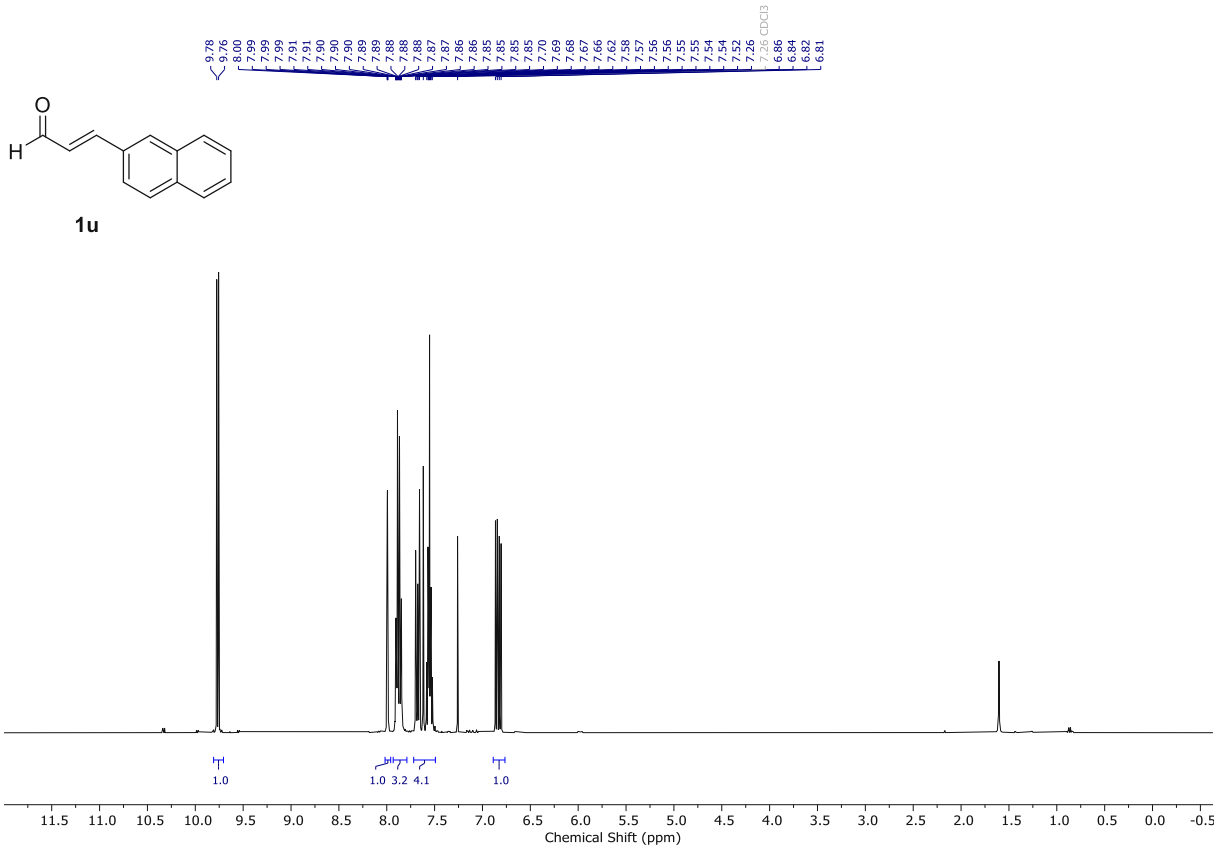


Die approbierte gedruckte Originalversion dieser Dissertation ist an der TU Wien Bibliothek verfügbar.
The approved original version of this doctoral thesis is available in print at TU Wien Bibliothek.

7.2.2 NMR spectra of **1t**

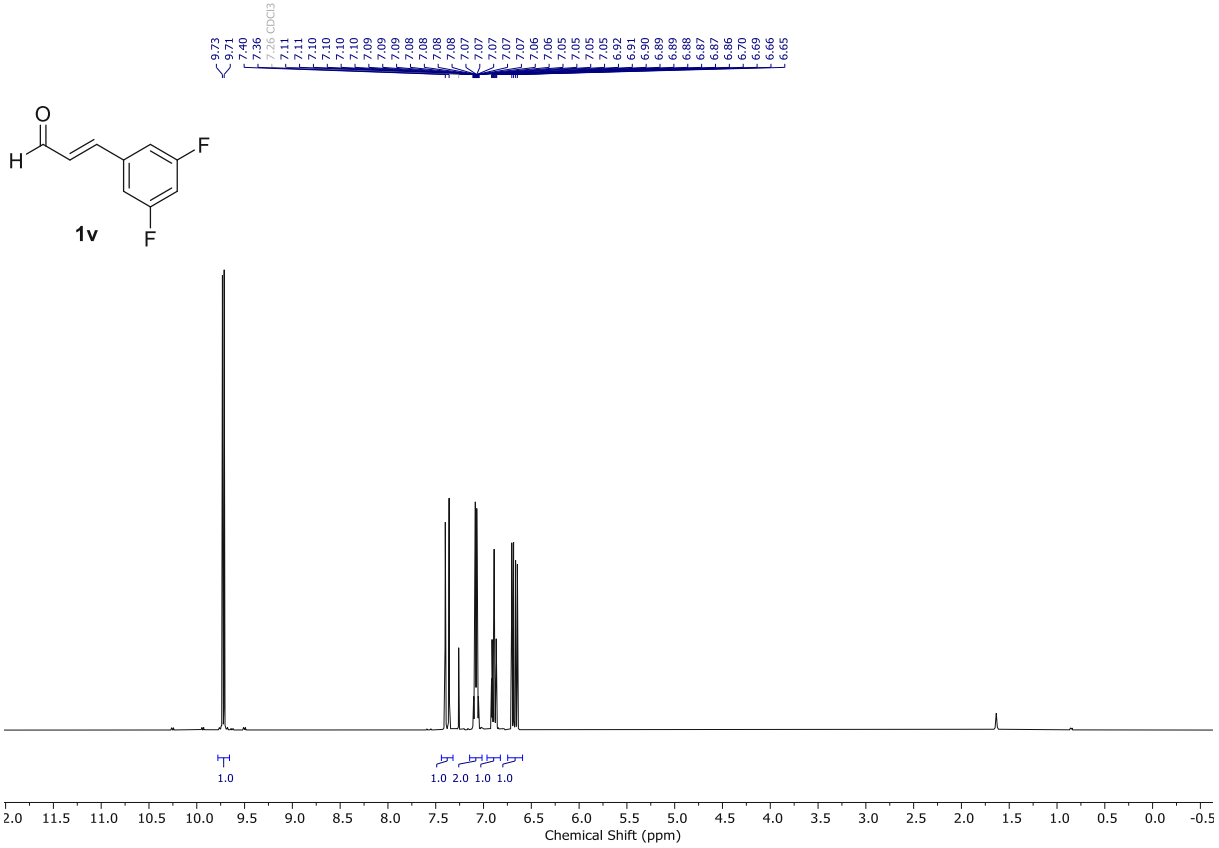


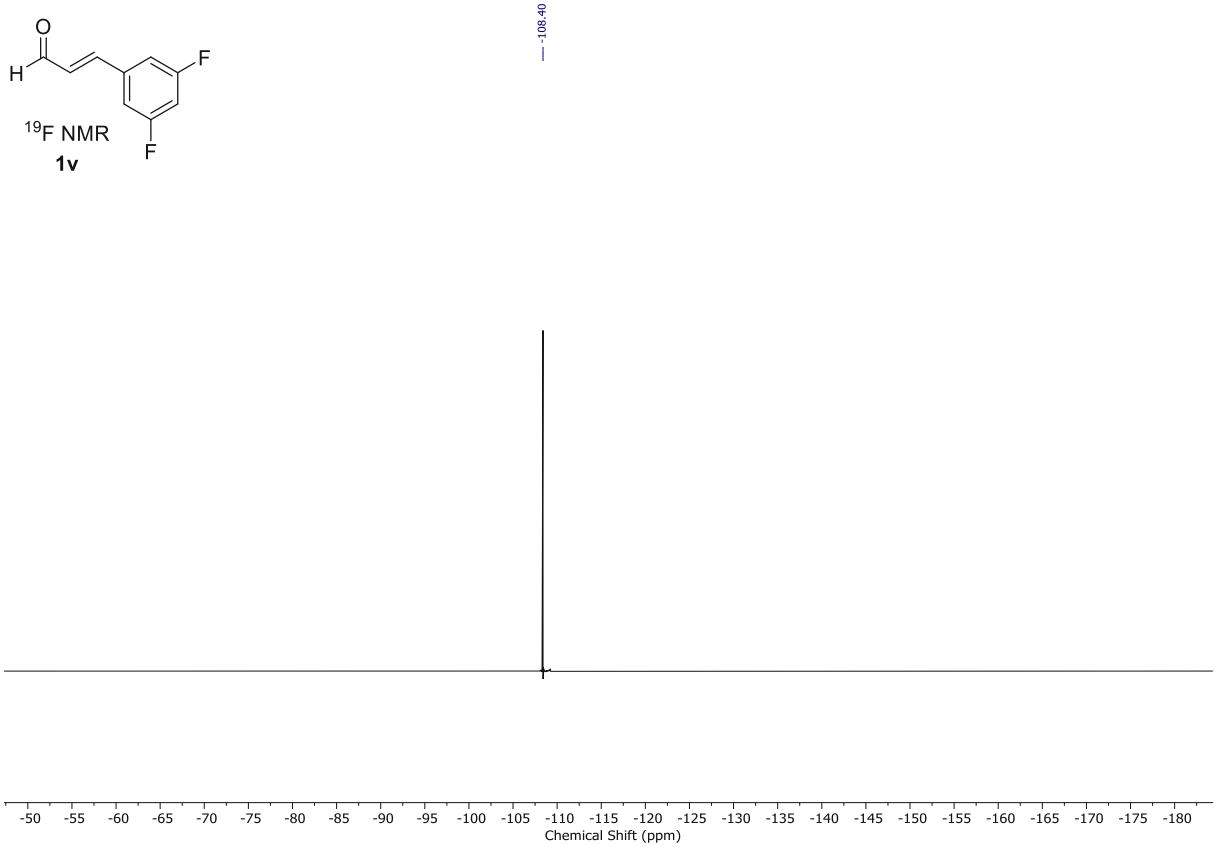
7.2.3 NMR spectra of **1u**



Die approbierte gedruckte Originalversion dieser Dissertation ist an der TU Wien Bibliothek verfügbar.
The approved original version of this doctoral thesis is available in print at TU Wien Bibliothek.
TU Bibliothek Your knowledge hub WIEN

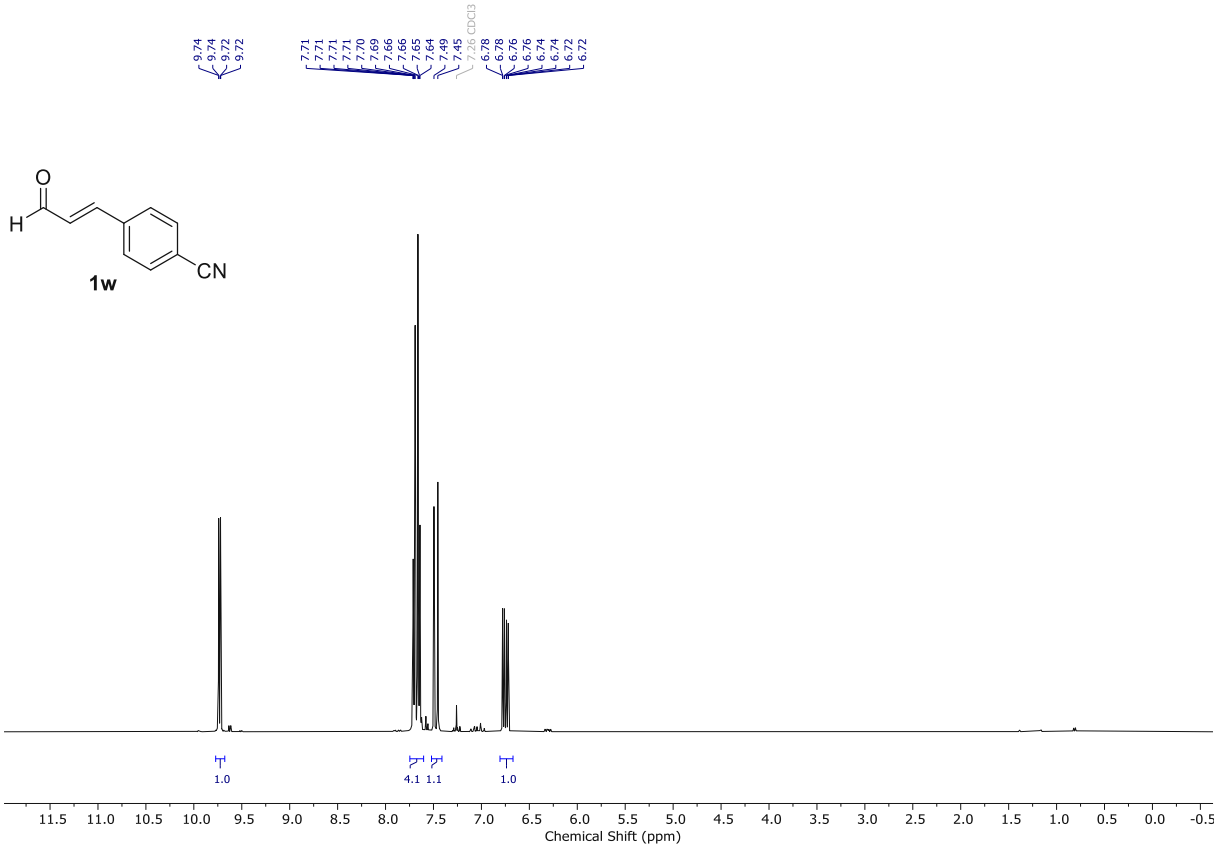
7.2.4 NMR spectra of **1v**



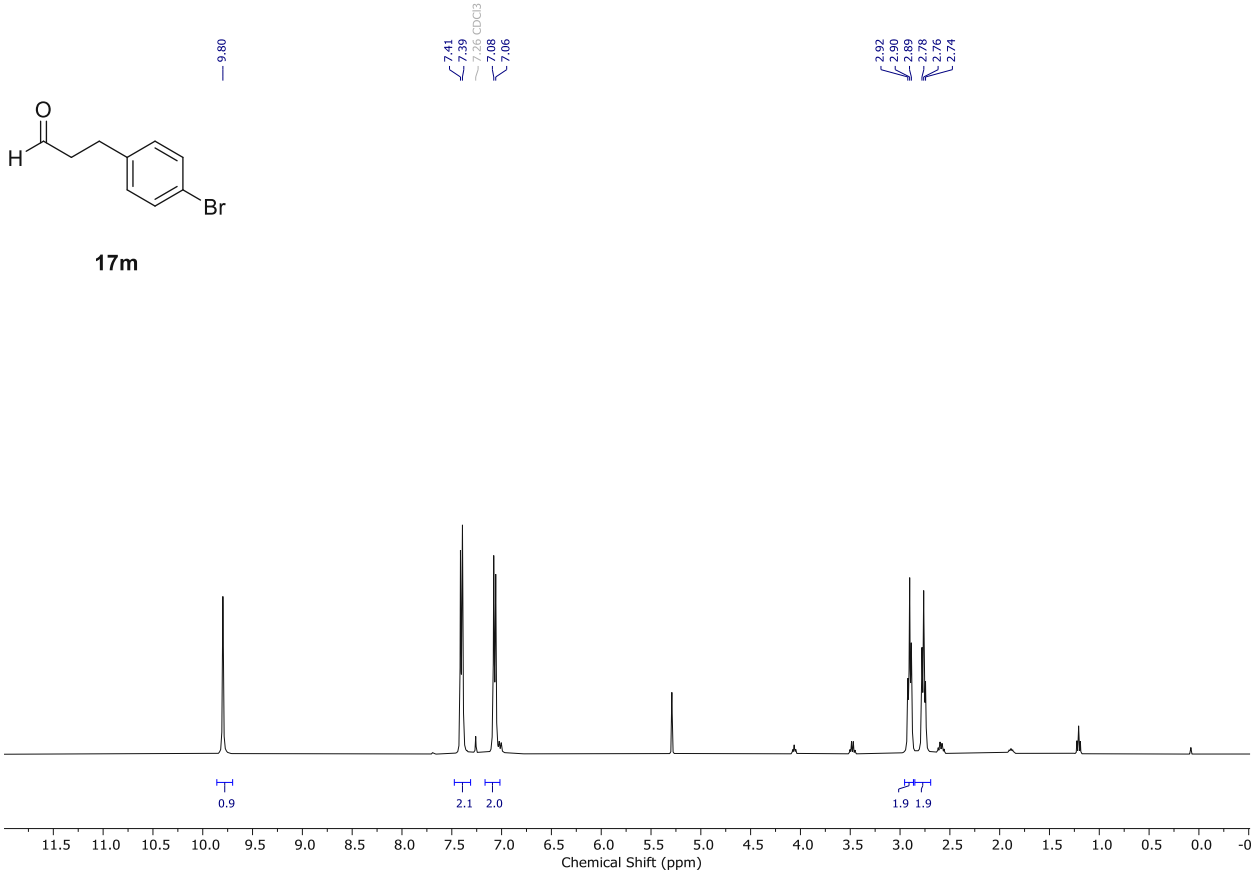


Die approbierte gedruckte Originalversion dieser Dissertation ist an der TU Wien Bibliothek verfügbar.
The approved original version of this doctoral thesis is available in print at TU Wien Bibliothek.

7.2.5 NMR spectra of **1w**

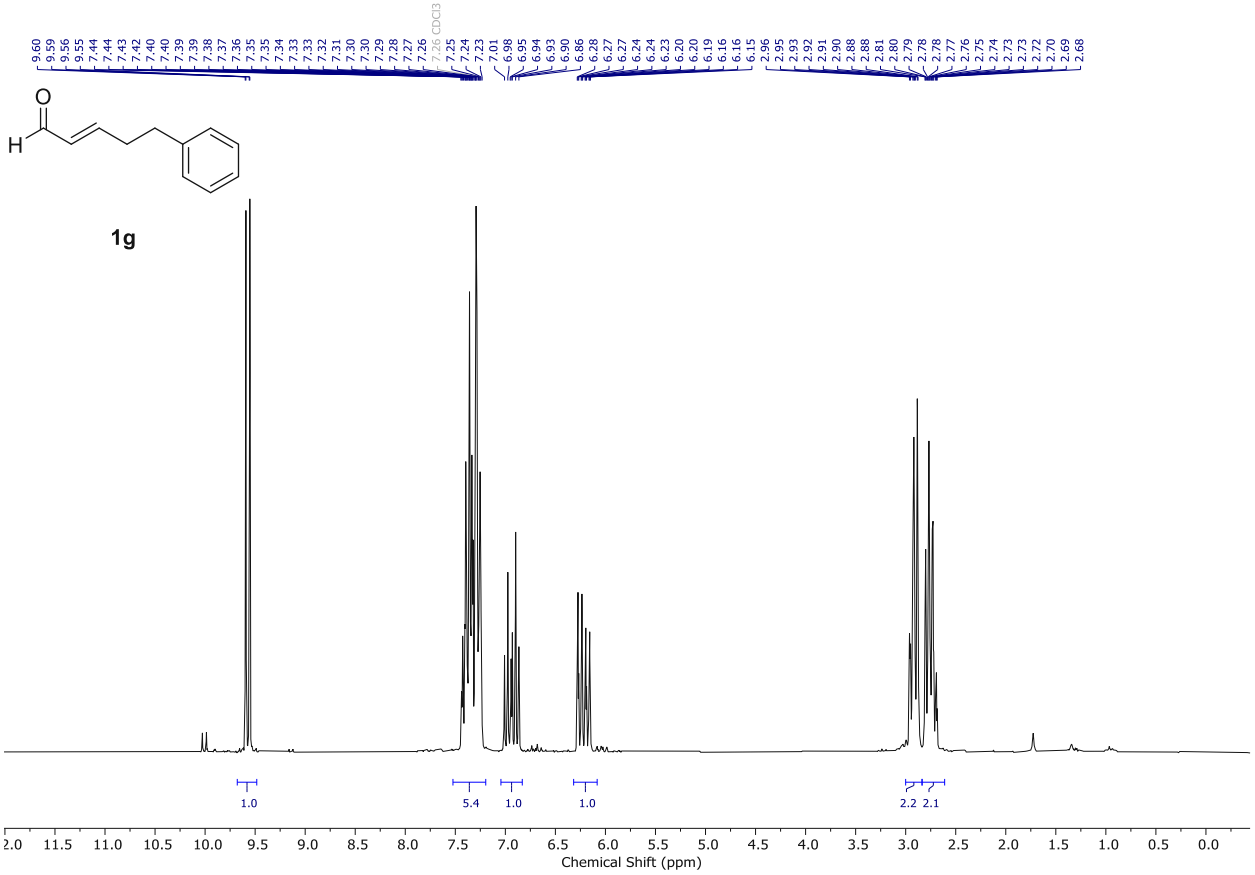


7.2.6 NMR spectra of **17m**

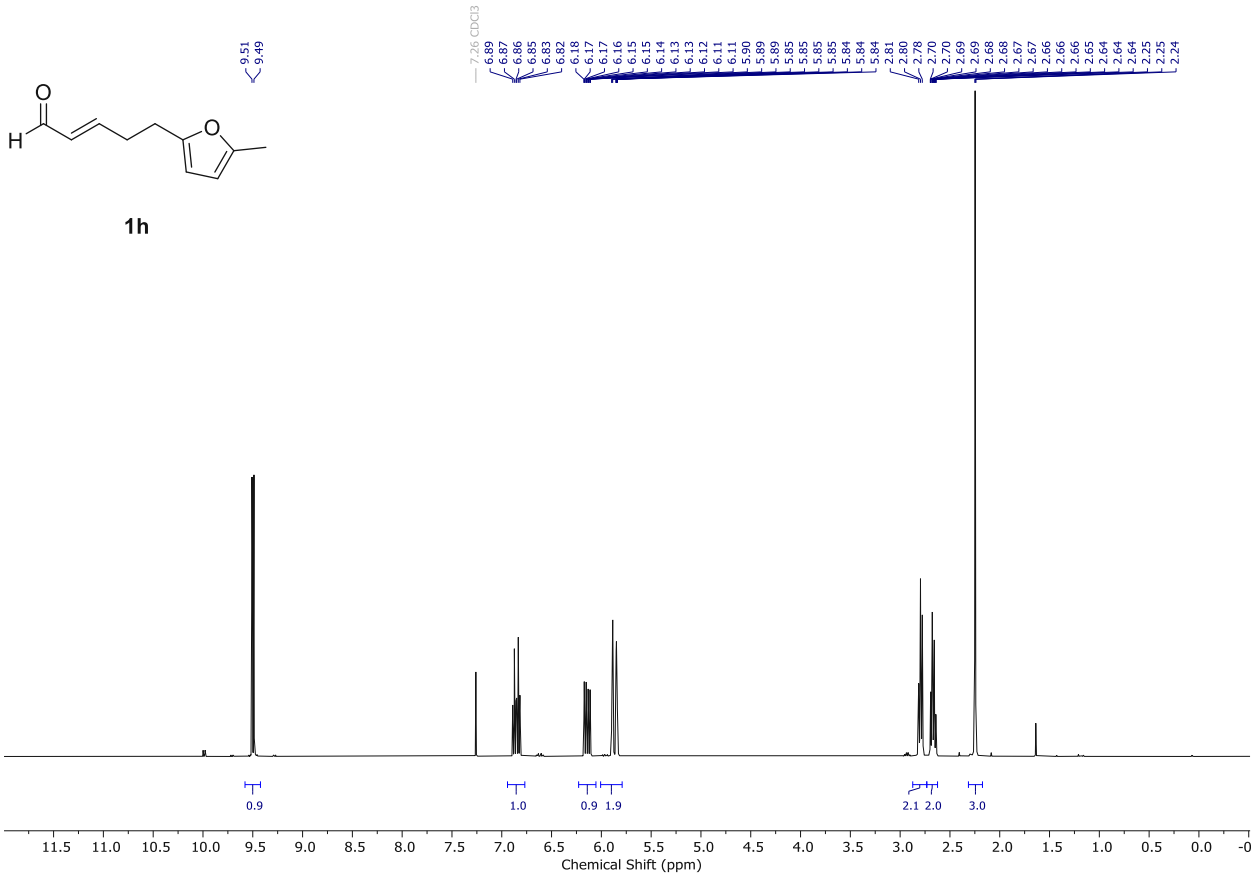


Die approbierte gedruckte Originalversion dieser Dissertation ist an der TU Wien Bibliothek verfügbar.
The approved original version of this doctoral thesis is available in print at TU Wien Bibliothek.

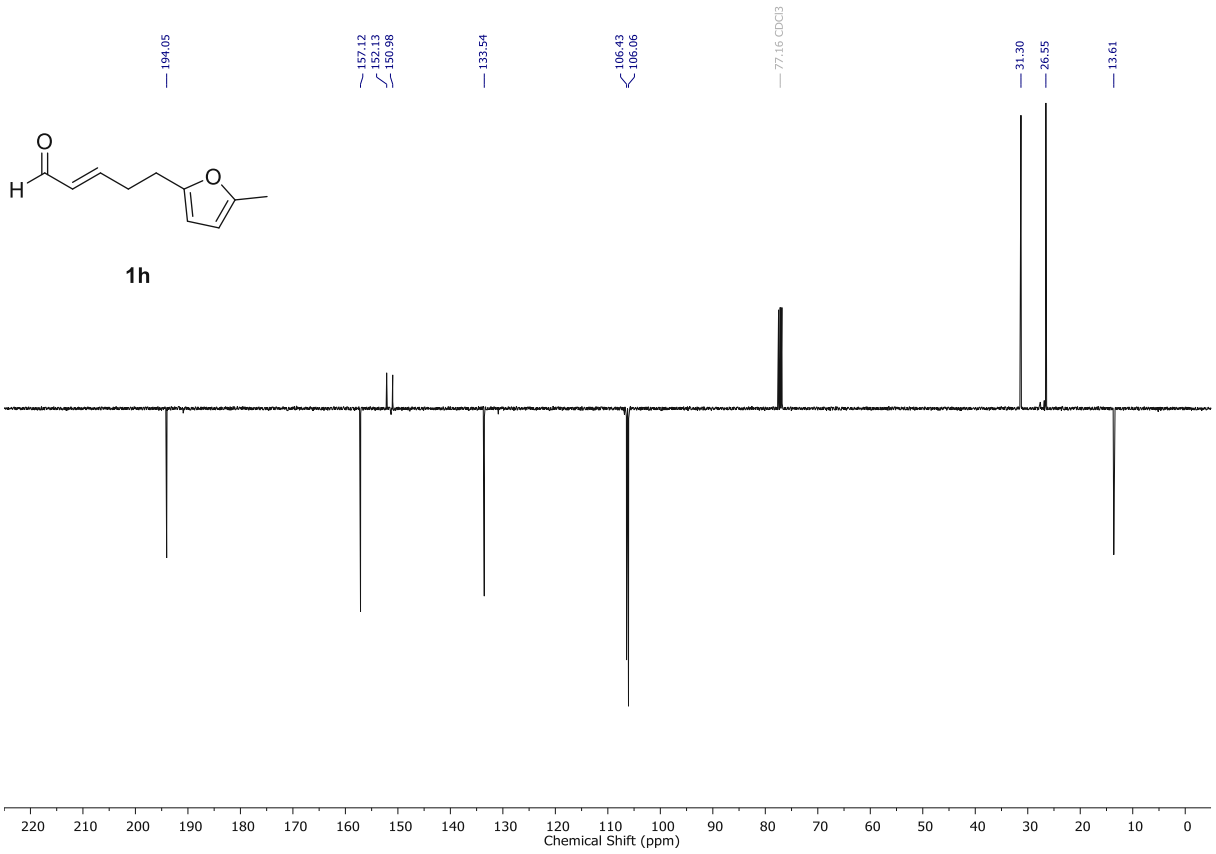
7.2.7 NMR spectra of **1g**



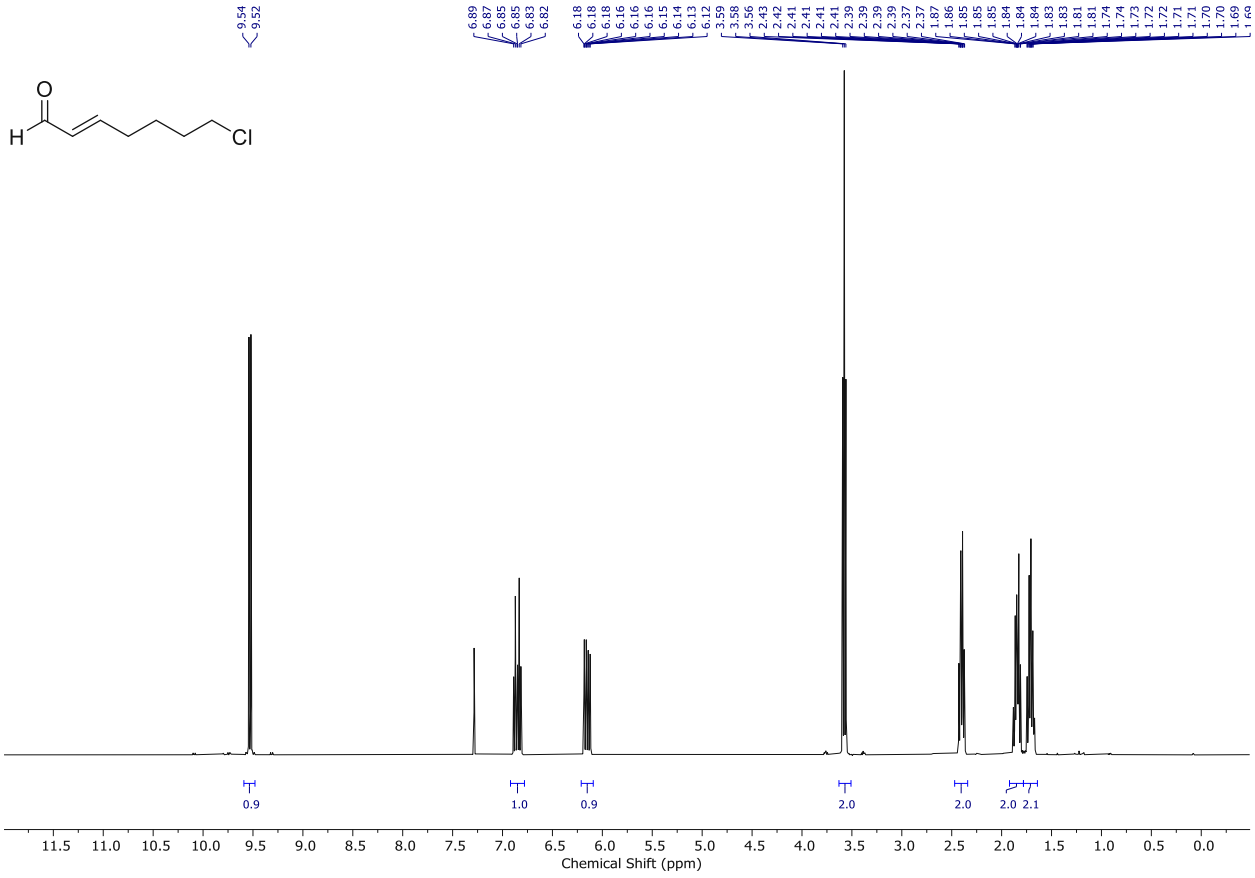
7.2.8 NMR spectra of **1h**



Die approbierte gedruckte Originalversion dieser Dissertation ist an der TU Wien Bibliothek verfügbar.
The approved original version of this doctoral thesis is available in print at TU Wien Bibliothek.

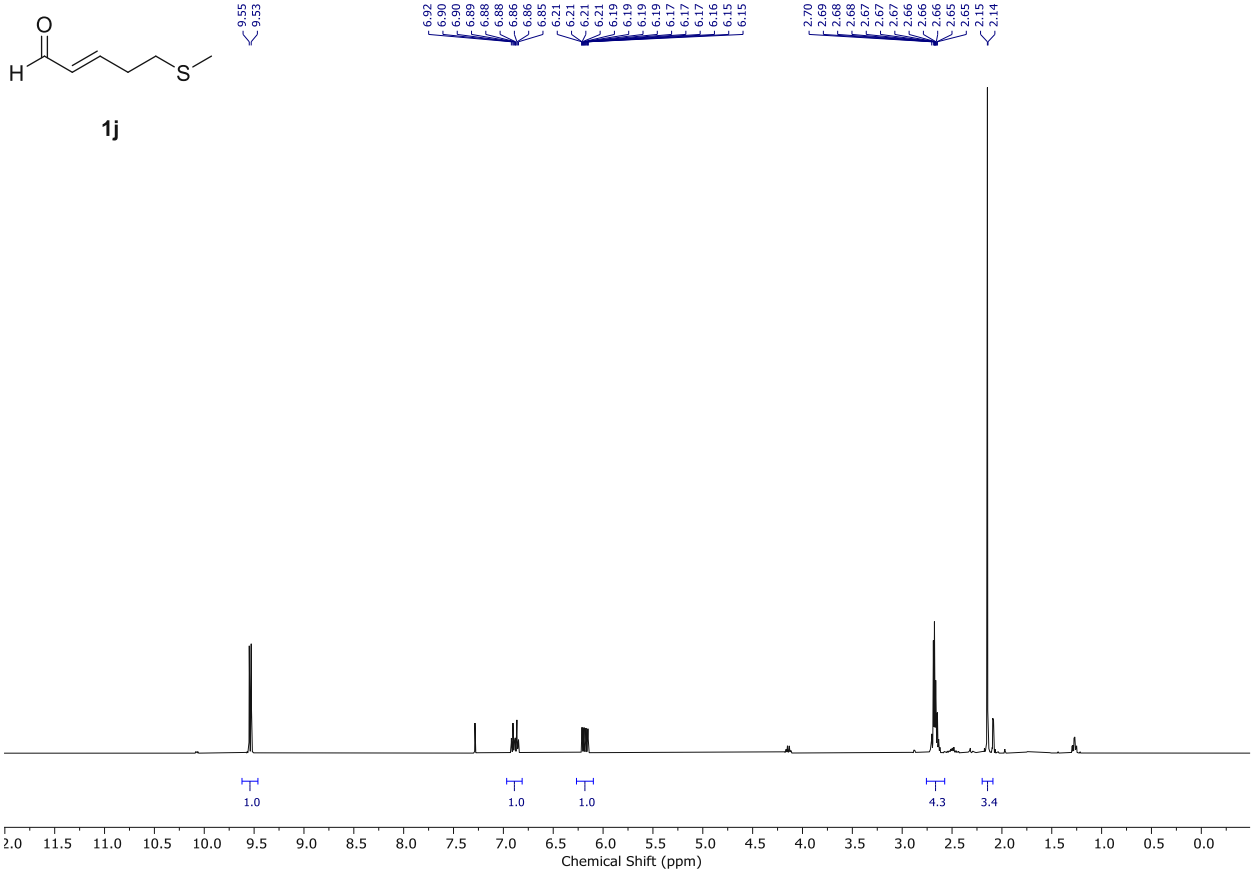


7.2.9 NMR spectra of **1i**

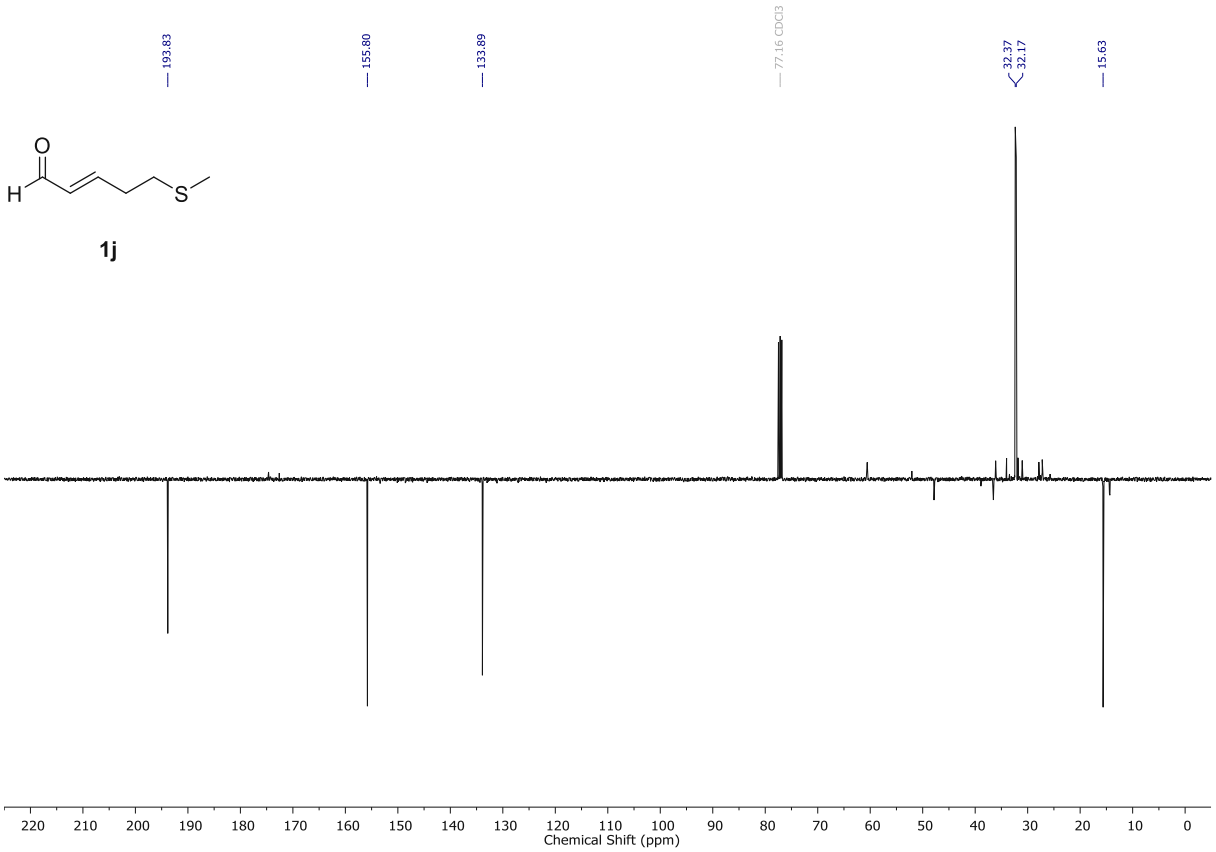


Die approbierte gedruckte Originalversion dieser Dissertation ist an der TU Wien Bibliothek verfügbar.
The approved original version of this doctoral thesis is available in print at TU Wien Bibliothek.
TU Bibliothek Your knowledge hub WIEN

7.2.10 NMR spectra of **1j**



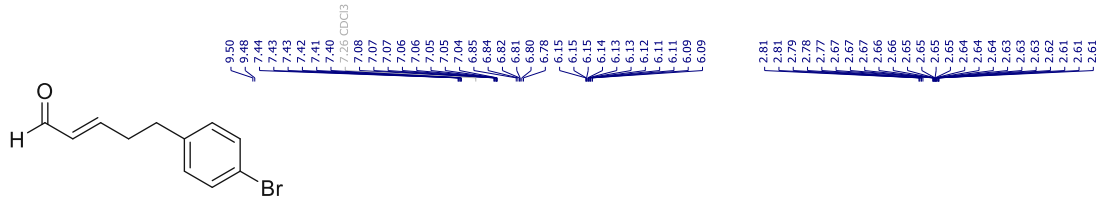
1j



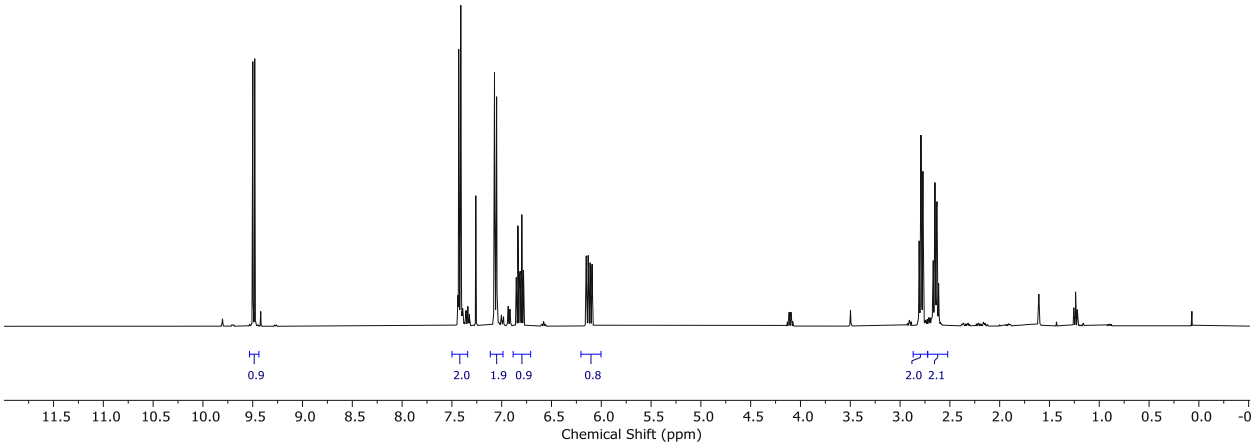
1j

Die approbierte gedruckte Originalversion dieser Dissertation ist an der TU Wien Bibliothek verfügbar.
The approved original version of this doctoral thesis is available in print at TU Wien Bibliothek.

7.2.11 NMR spectra of **1m**

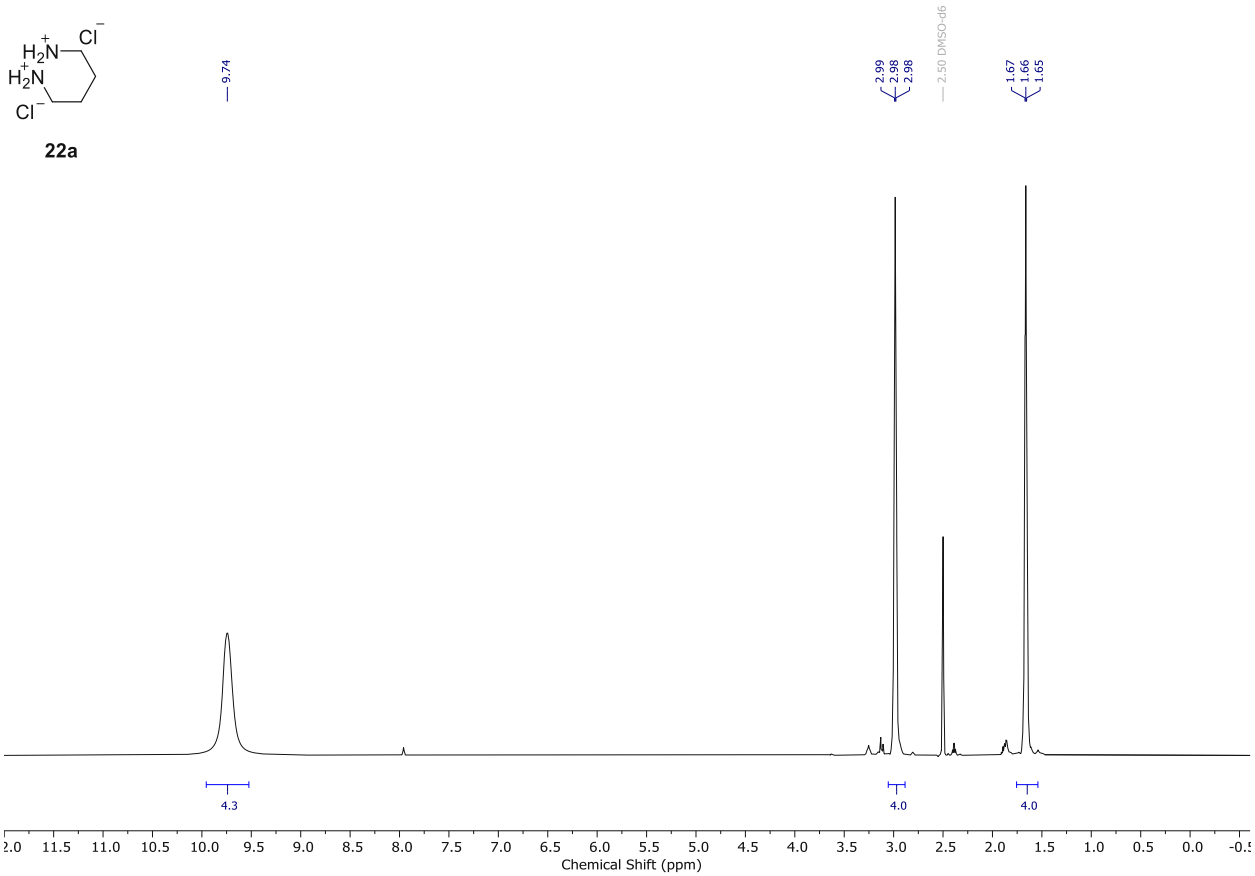


1m



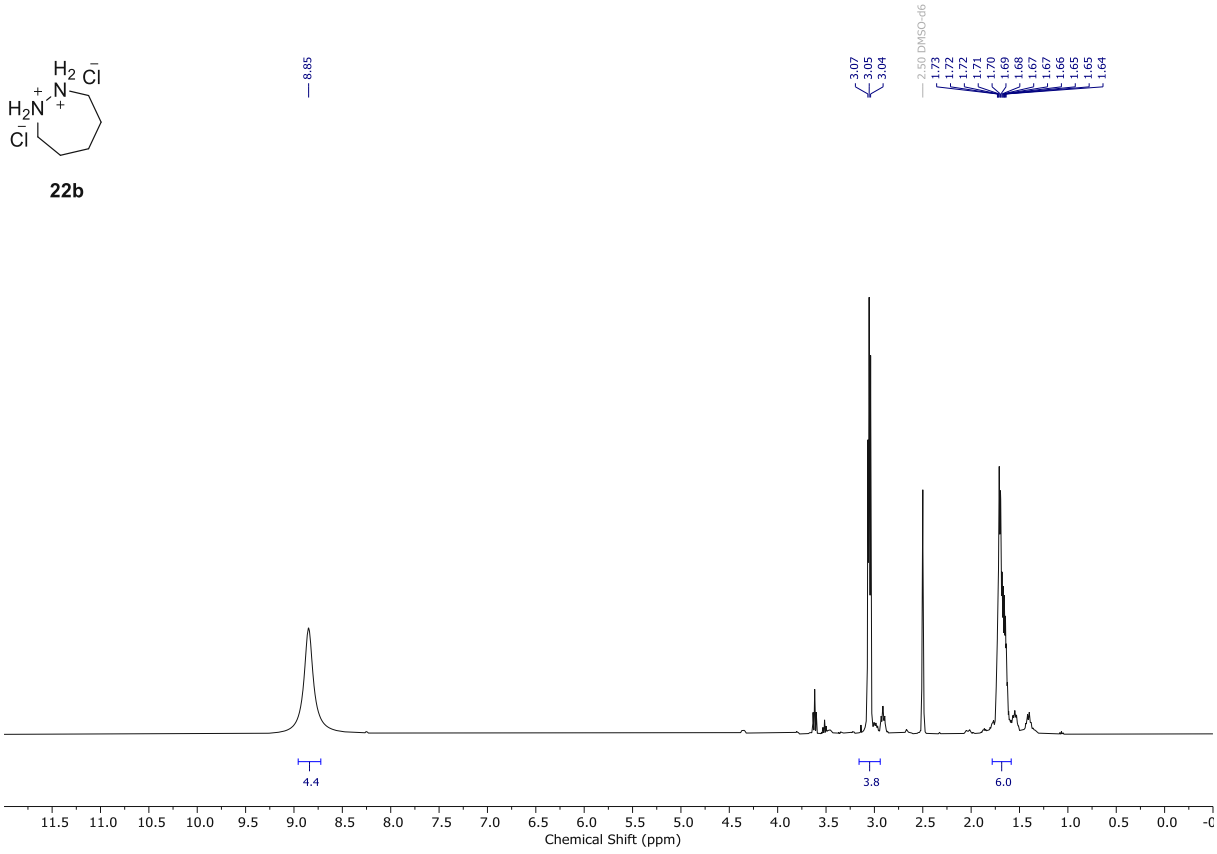
7.2.12 NMR spectra of **22a**

22a



Die approbierte gedruckte Originalversion dieser Dissertation ist an der TU Wien Bibliothek verfügbar.
The approved original version of this doctoral thesis is available in print at TU Wien Bibliothek.

7.2.13 NMR spectra of **22b**



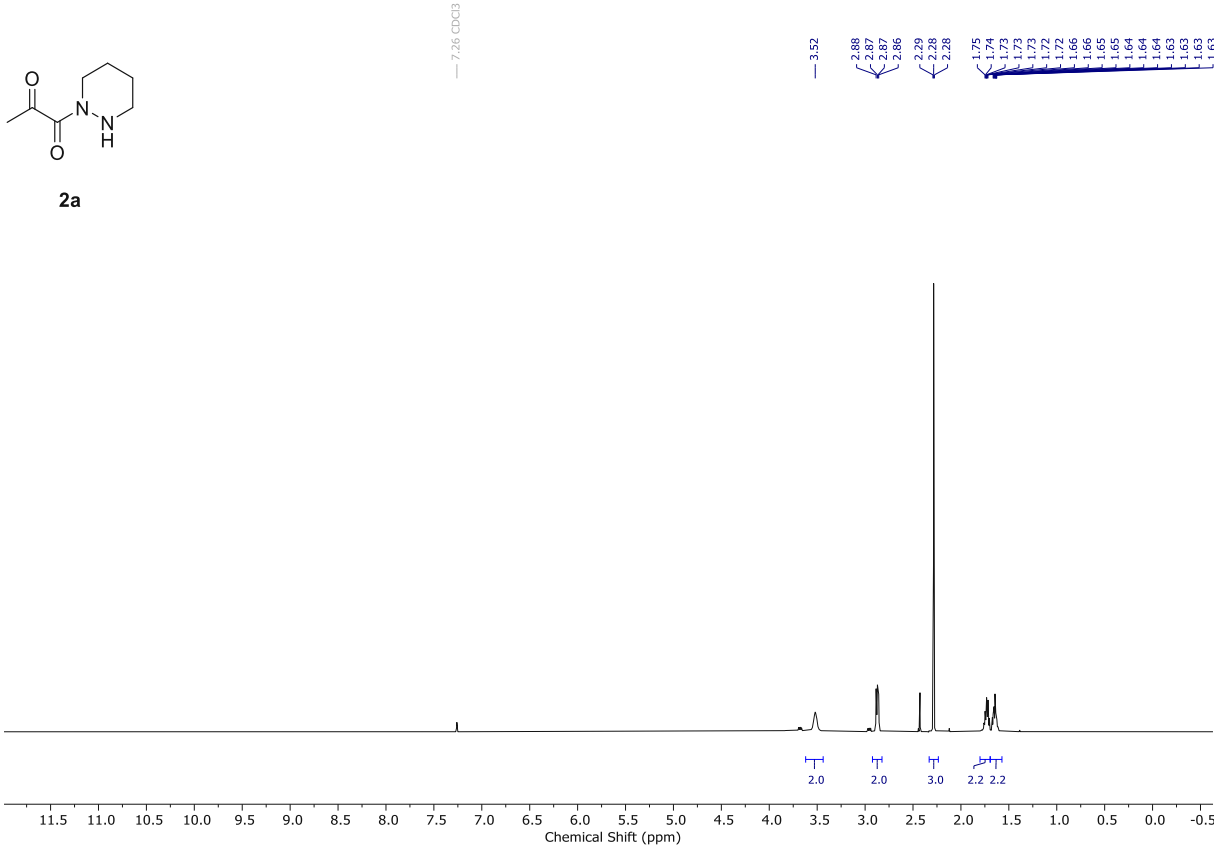
22b

Die approbierte gedruckte Originalversion dieser Dissertation ist an der TU Wien Bibliothek verfügbar.
The approved original version of this doctoral thesis is available in print at TU Wien Bibliothek.

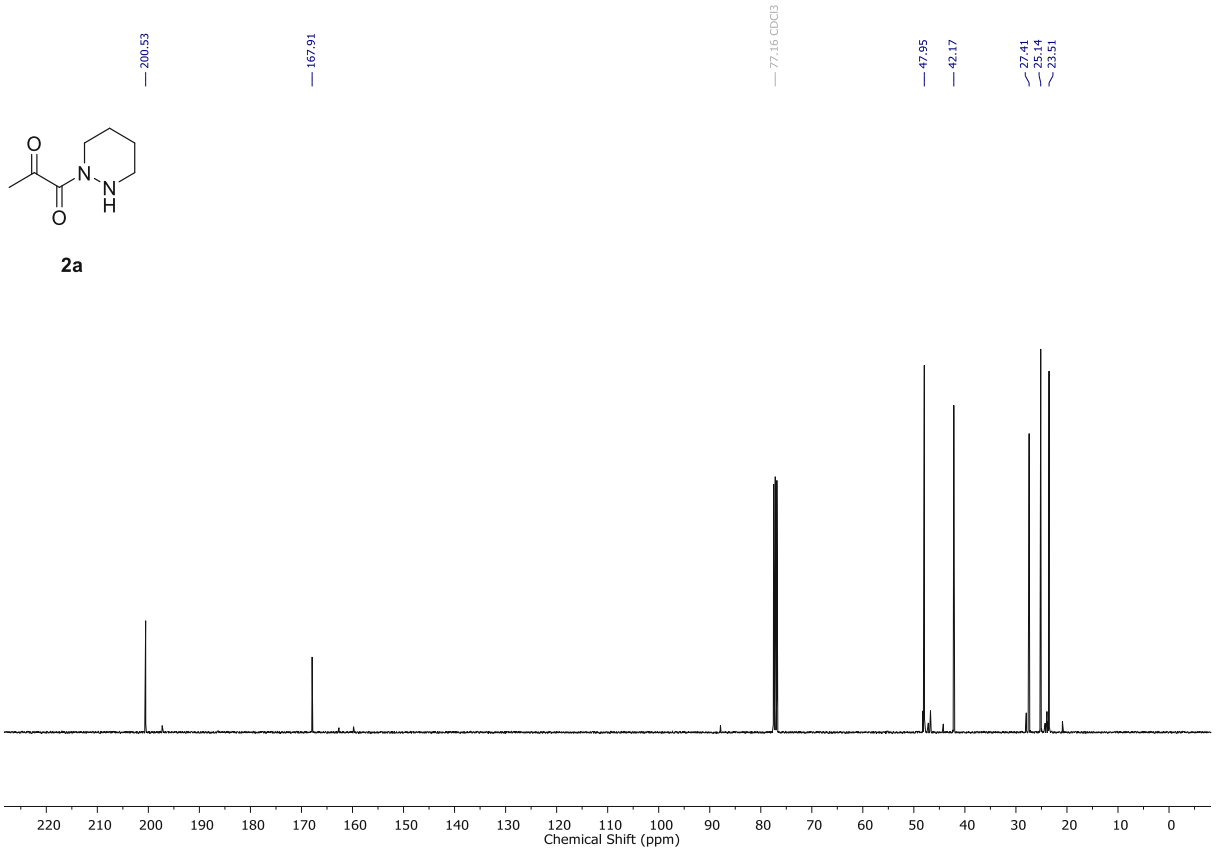
7.3 NMR spectra of reagents

7.3.1 NMR spectra of **2a**

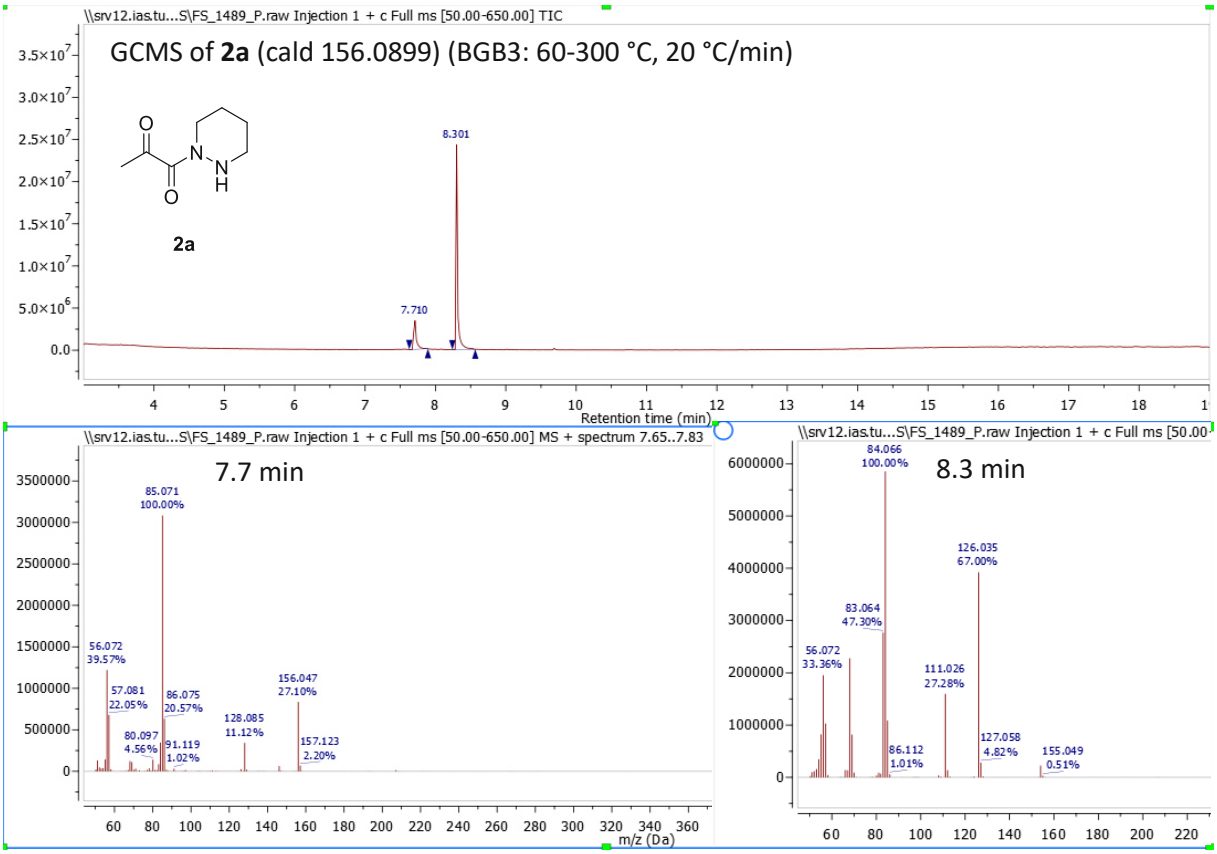
2a



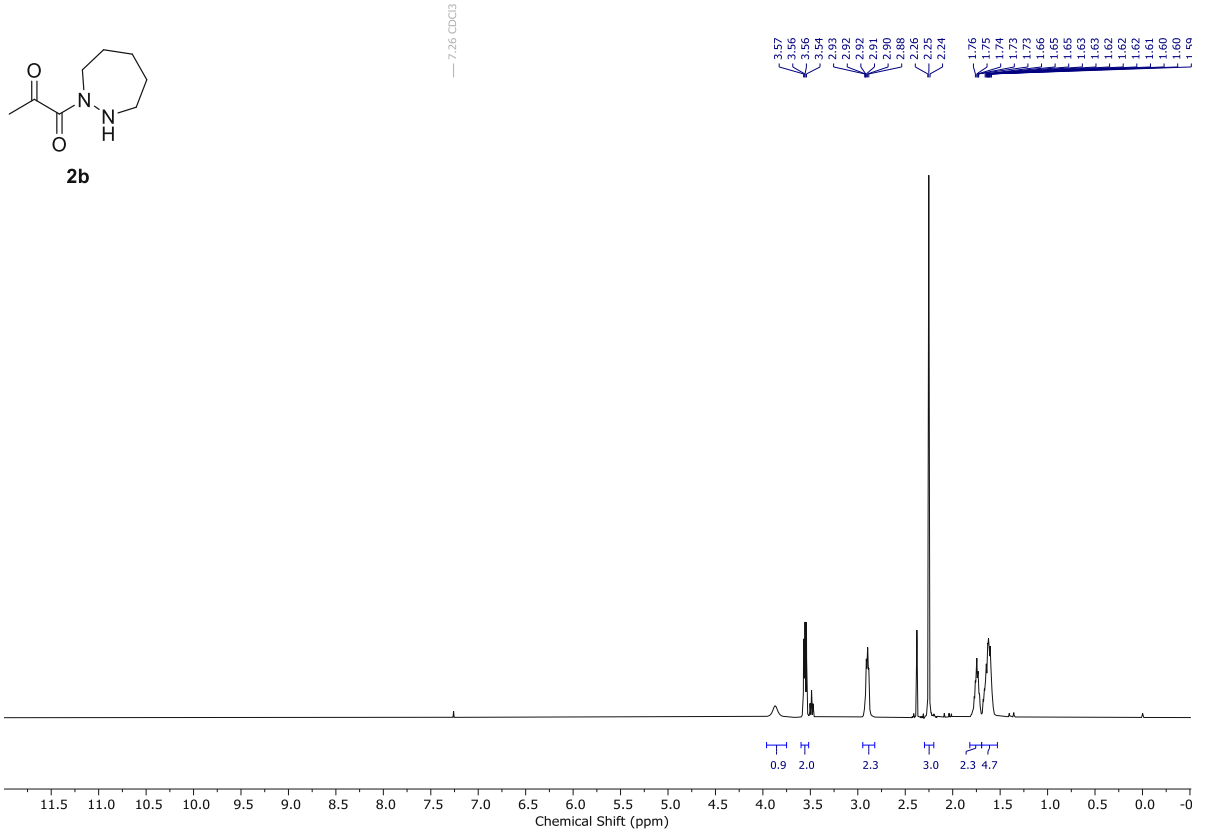
2a



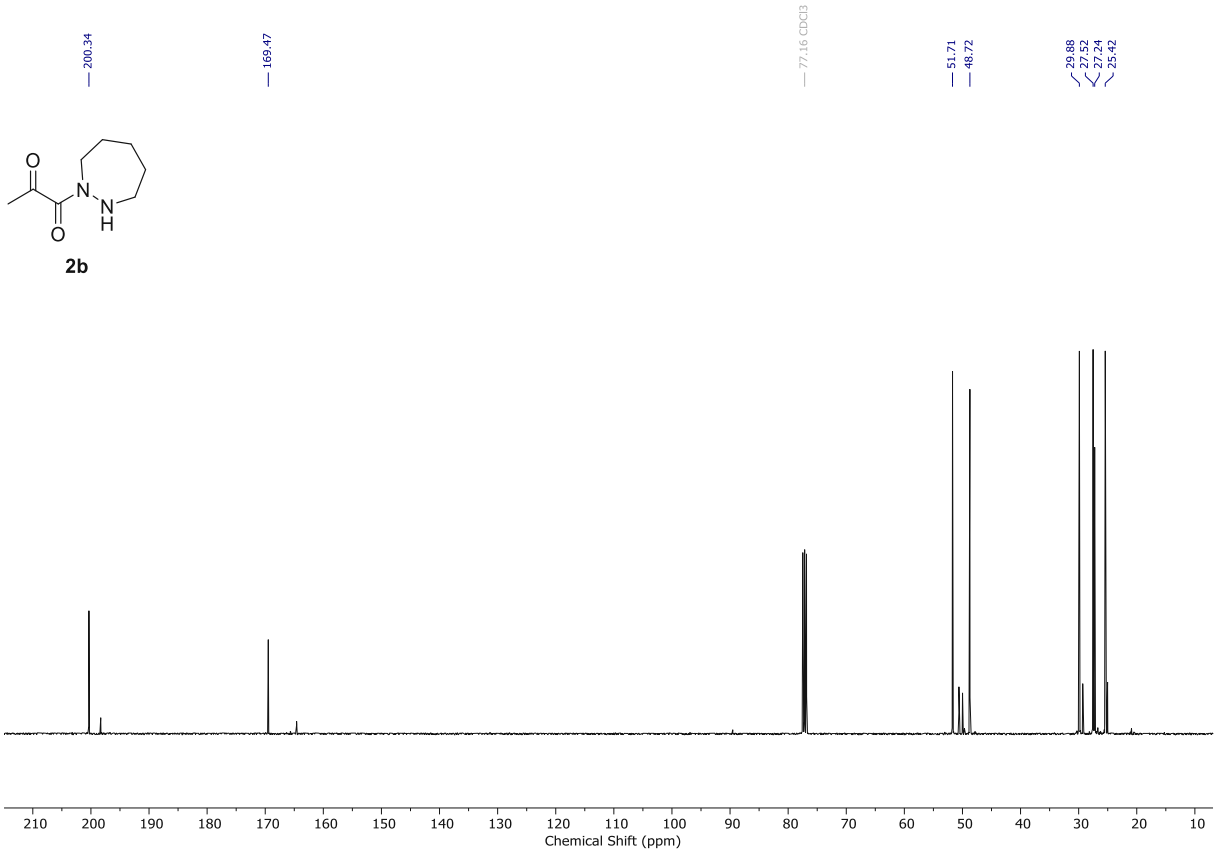
Die approbierte gedruckte Originalversion dieser Dissertation ist an der TU Wien Bibliothek verfügbar.
The approved original version of this doctoral thesis is available in print at TU Wien Bibliothek.



7.3.2 NMR spectra of **2b**

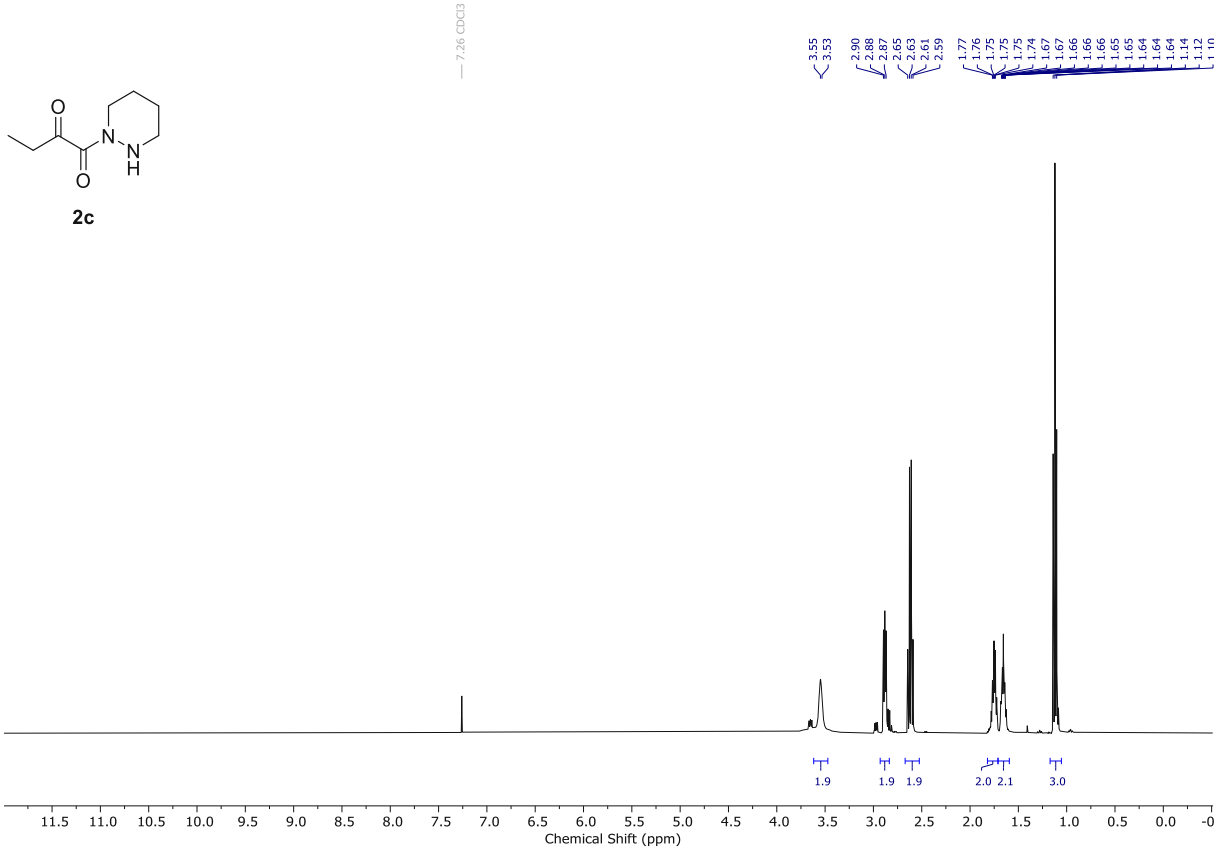


Die approbierte gedruckte Originalversion dieser Dissertation ist an der TU Wien Bibliothek verfügbar.
The approved original version of this doctoral thesis is available in print at TU Wien Bibliothek.



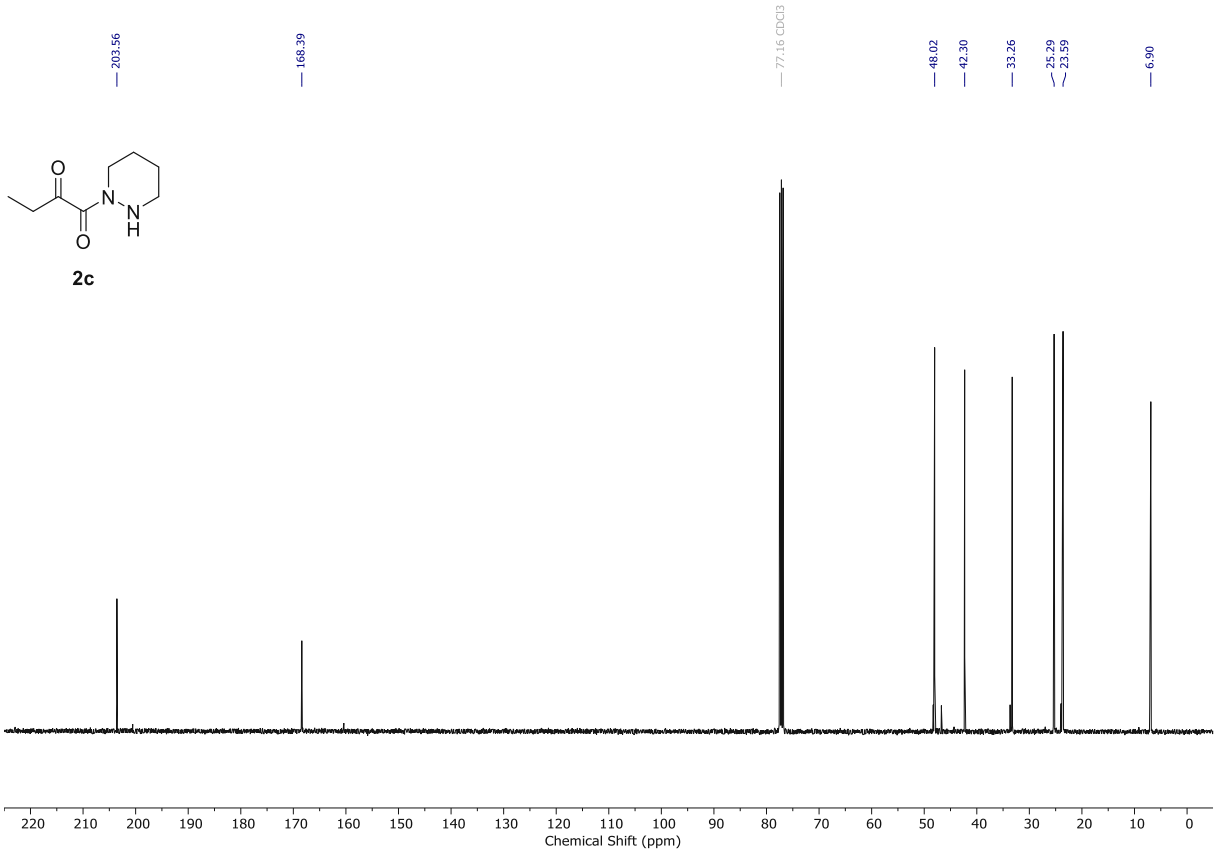
2b

7.3.3 NMR spectra of **2c**

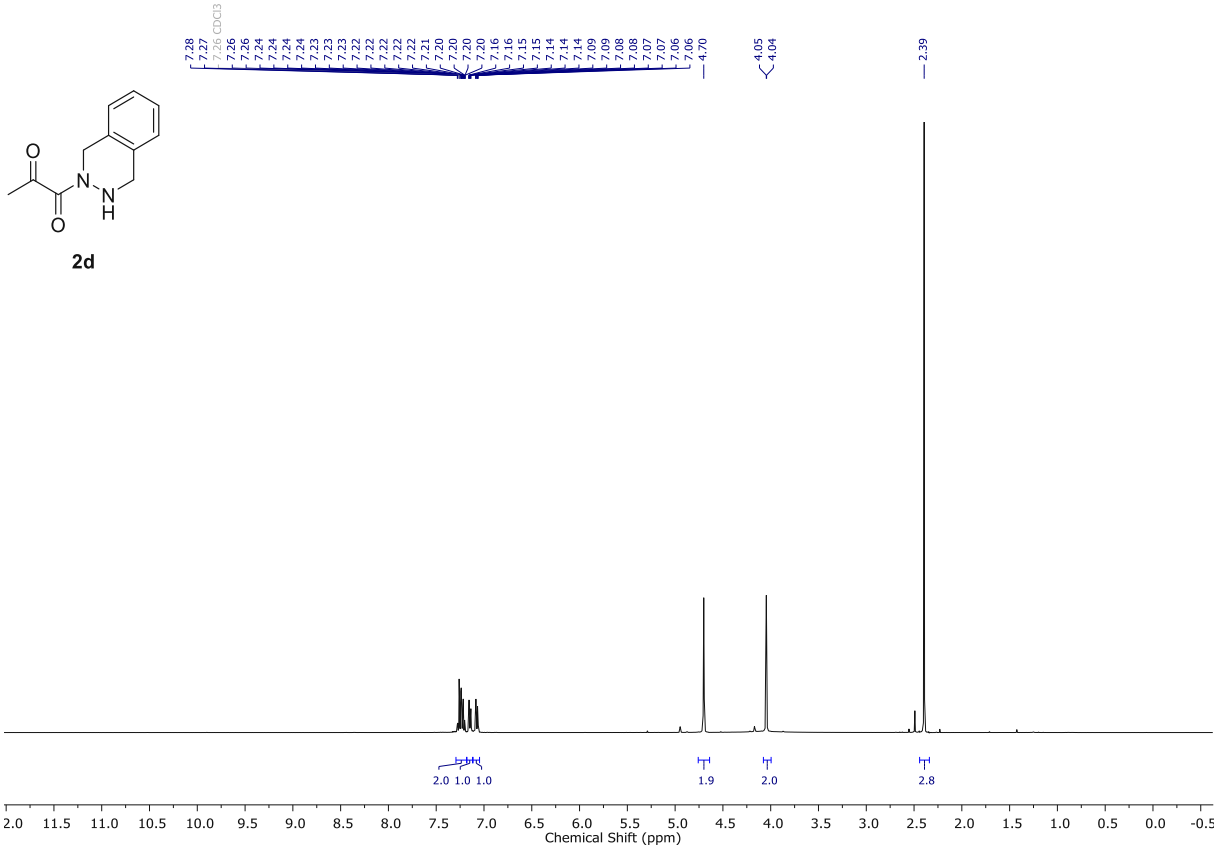


2c

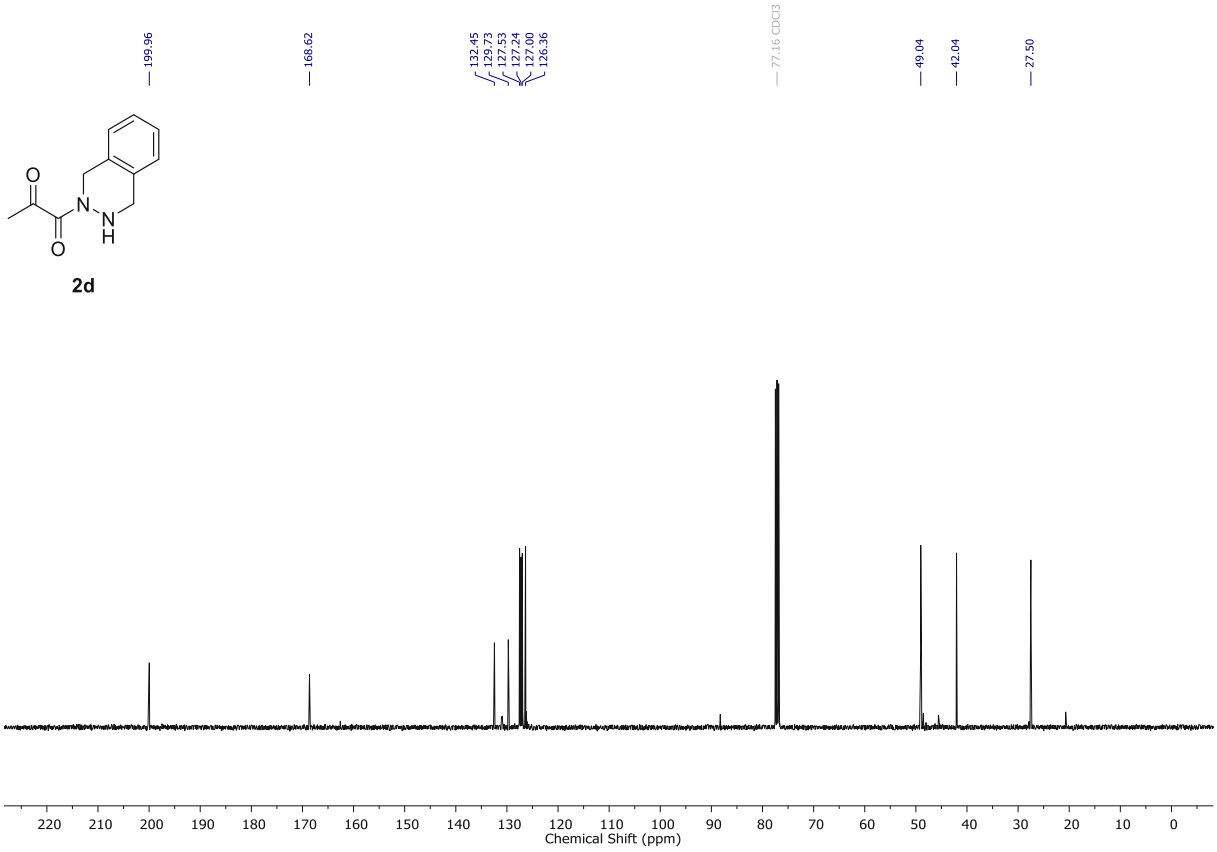
Die approbierte gedruckte Originalversion dieser Dissertation ist an der TU Wien Bibliothek verfügbar.
The approved original version of this doctoral thesis is available in print at TU Wien Bibliothek.



7.3.4 NMR spectra of **2d**

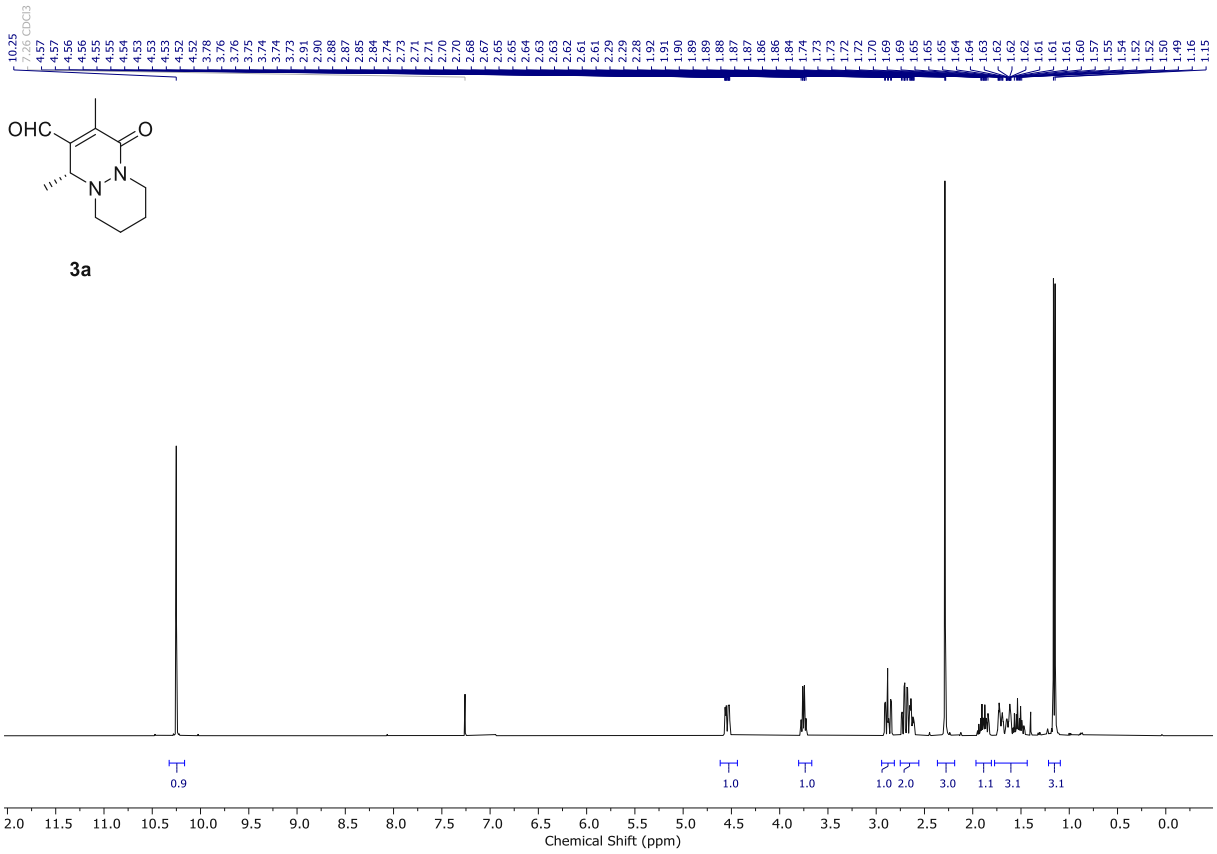


Die approbierte gedruckte Originalversion dieser Dissertation ist an der TU Wien Bibliothek verfügbar.
The approved original version of this doctoral thesis is available in print at TU Wien Bibliothek.
TU Bibliothek Your knowledge hub WIEN

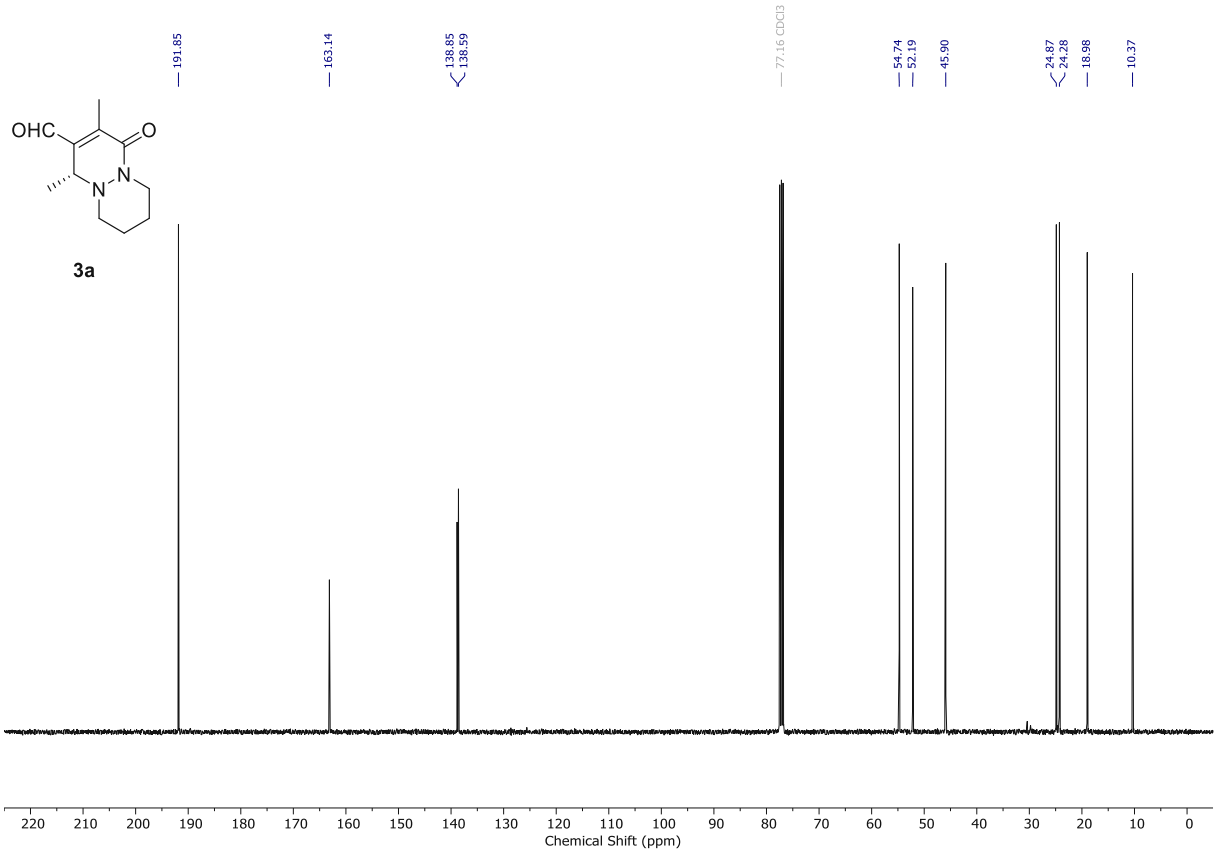


7.4 NMR spectra of aza-Michael/aldol products

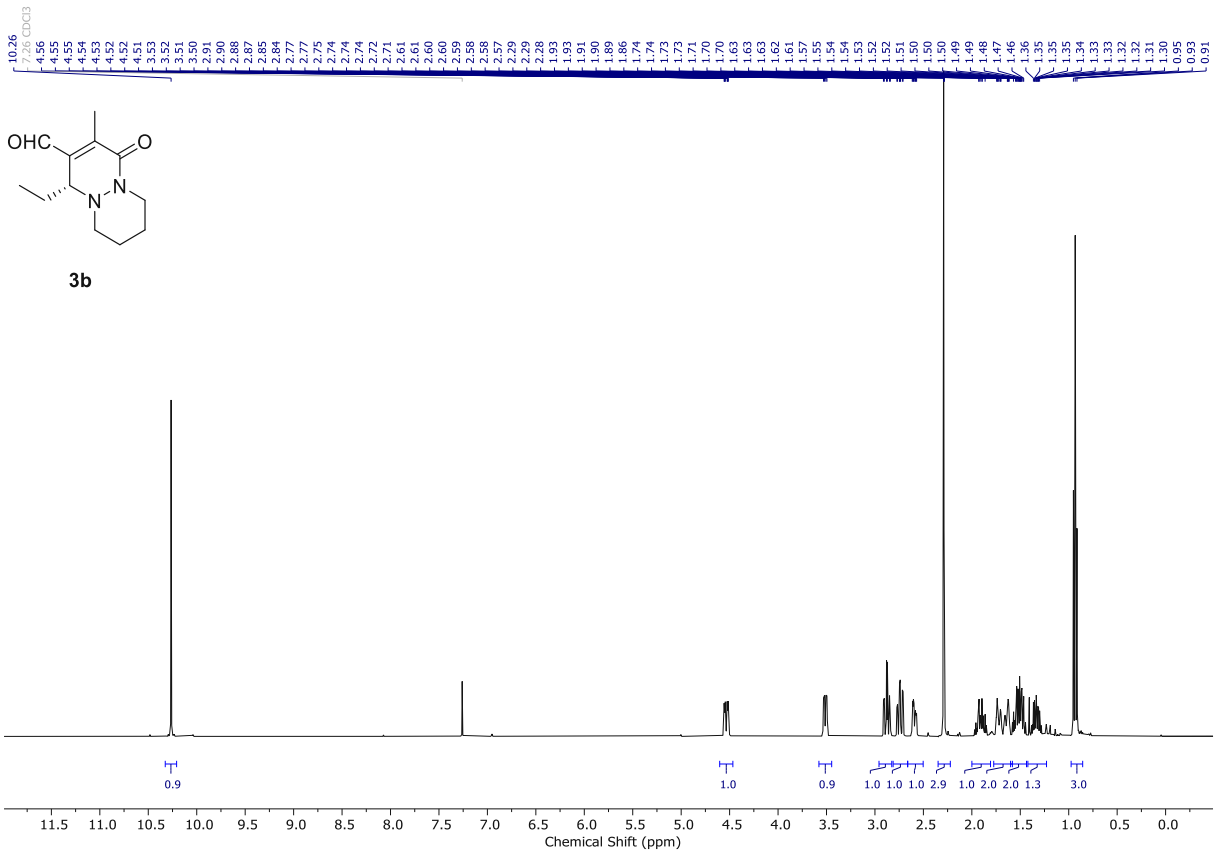
7.4.1 NMR spectra of **3a**



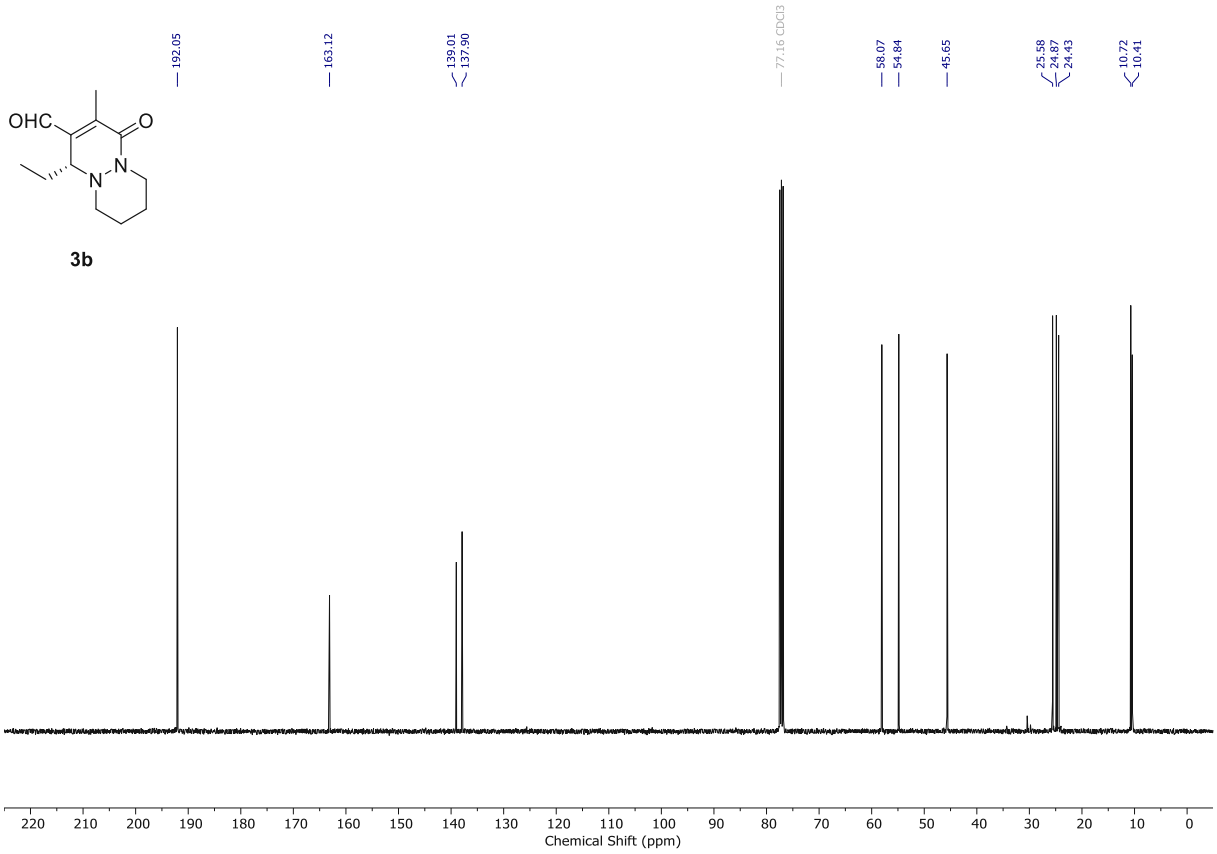
Die approbierte gedruckte Originalversion dieser Dissertation ist an der TU Wien Bibliothek verfügbar.
The approved original version of this doctoral thesis is available in print at TU Wien Bibliothek.
TU Bibliothek Your knowledge hub WIEN



7.4.2 NMR spectra of **3b**

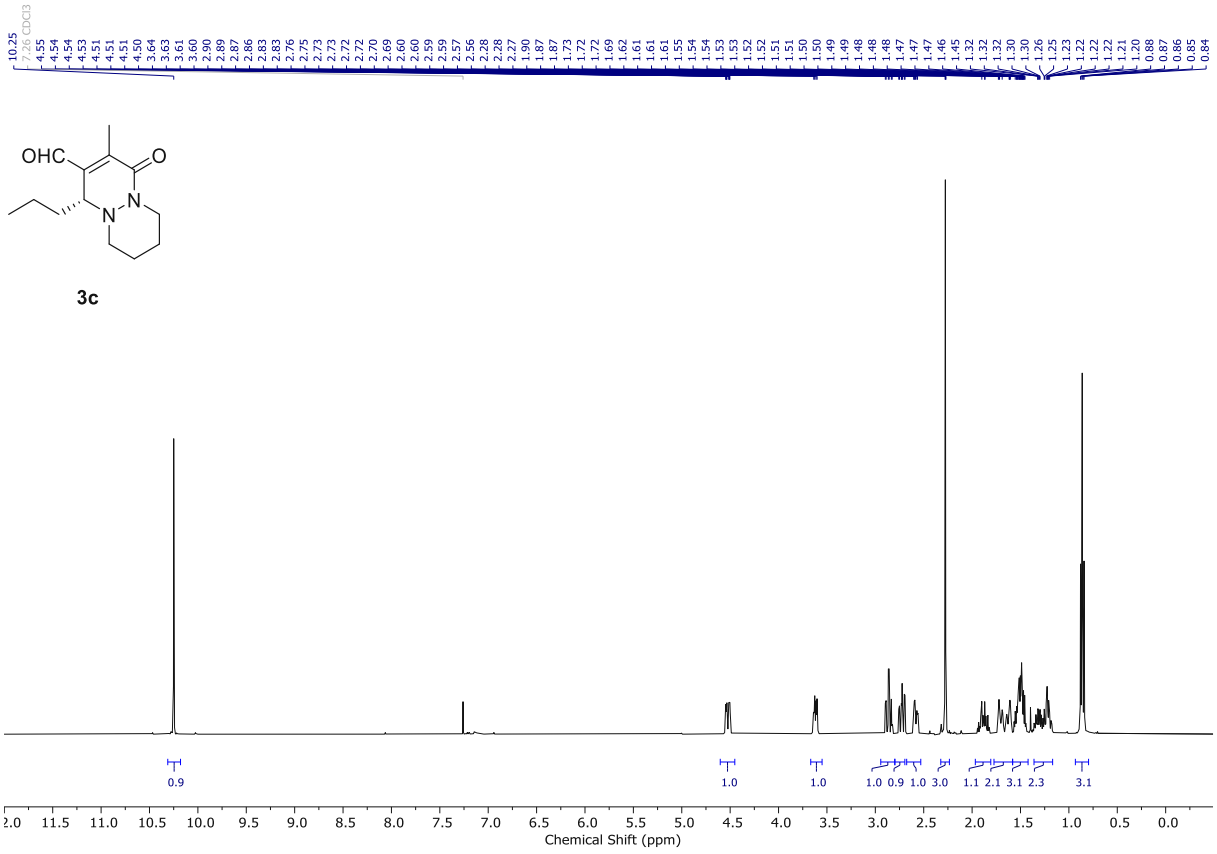


Die approbierte gedruckte Originalversion dieser Dissertation ist an der TU Wien Bibliothek verfügbar.
The approved original version of this doctoral thesis is available in print at TU Wien Bibliothek.



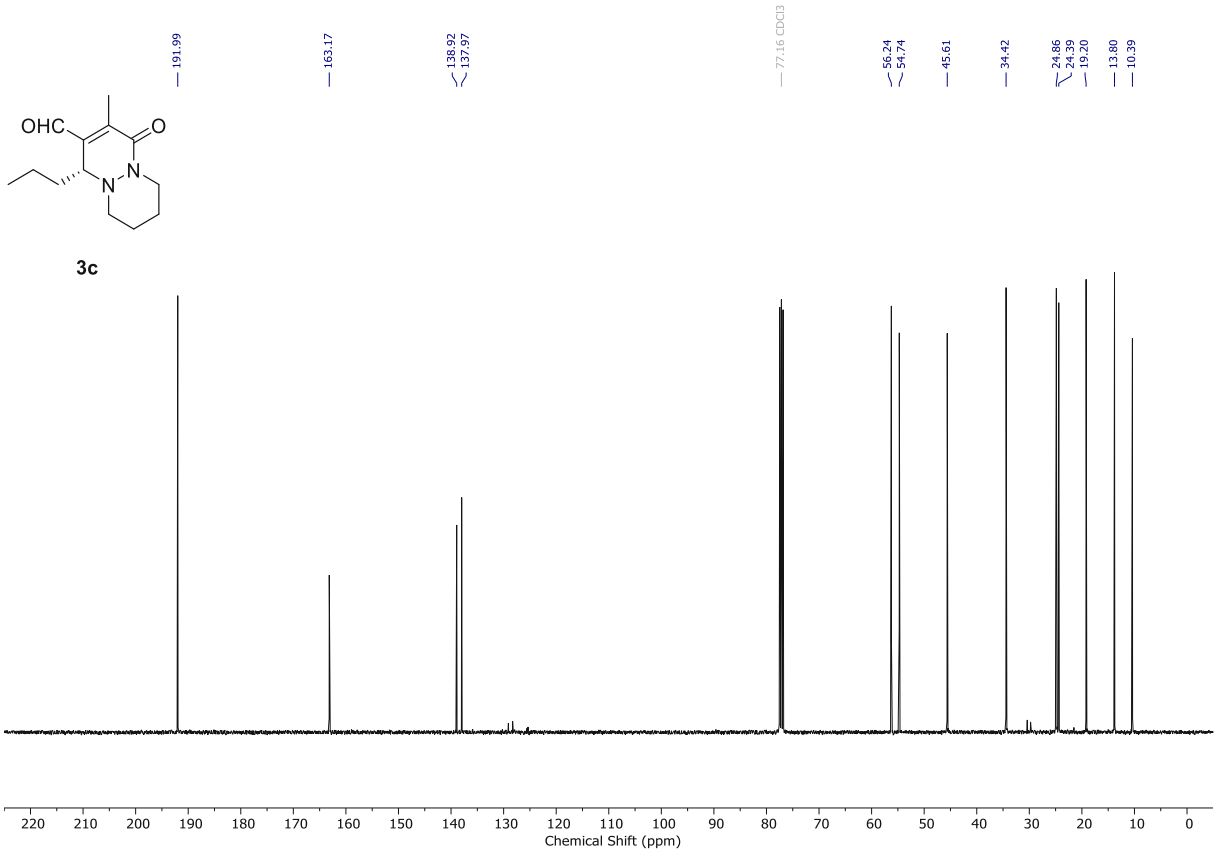
3b

7.4.3 NMR spectra of **3c**

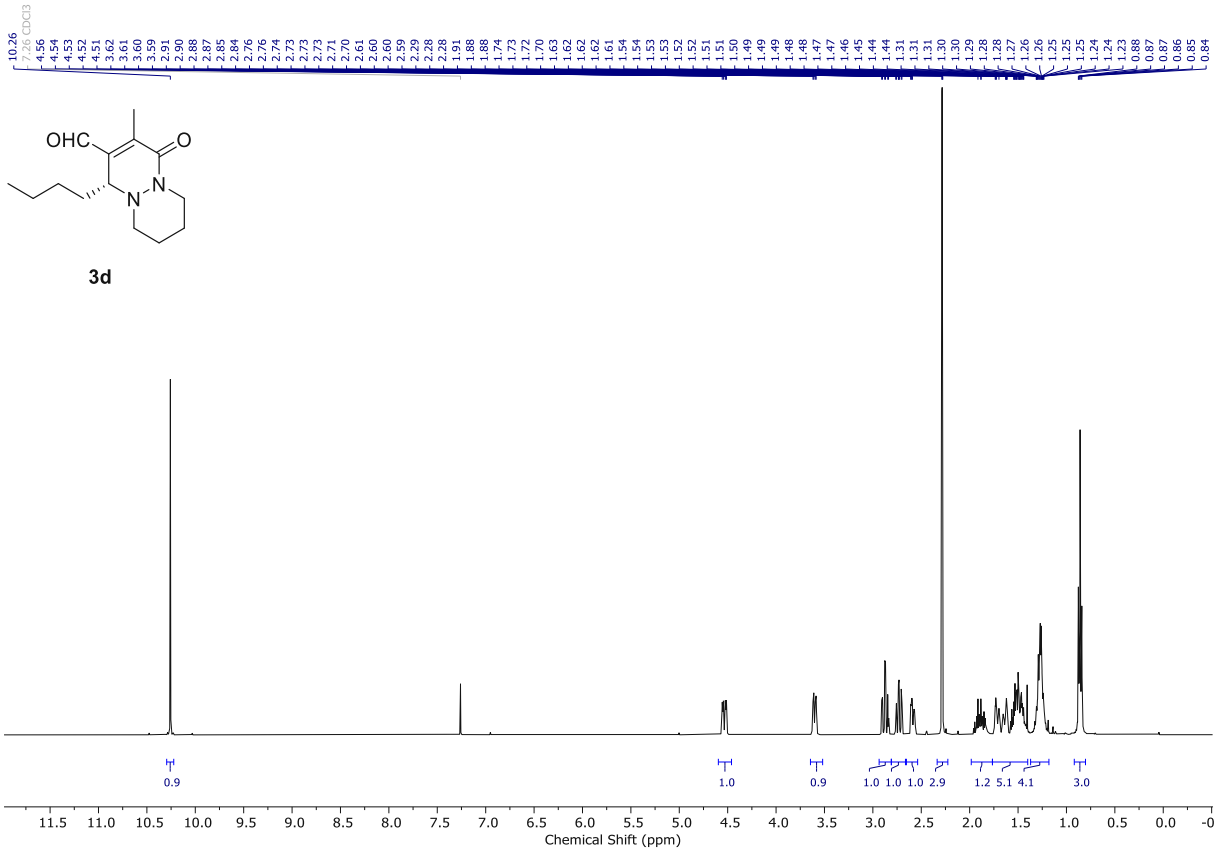


3c

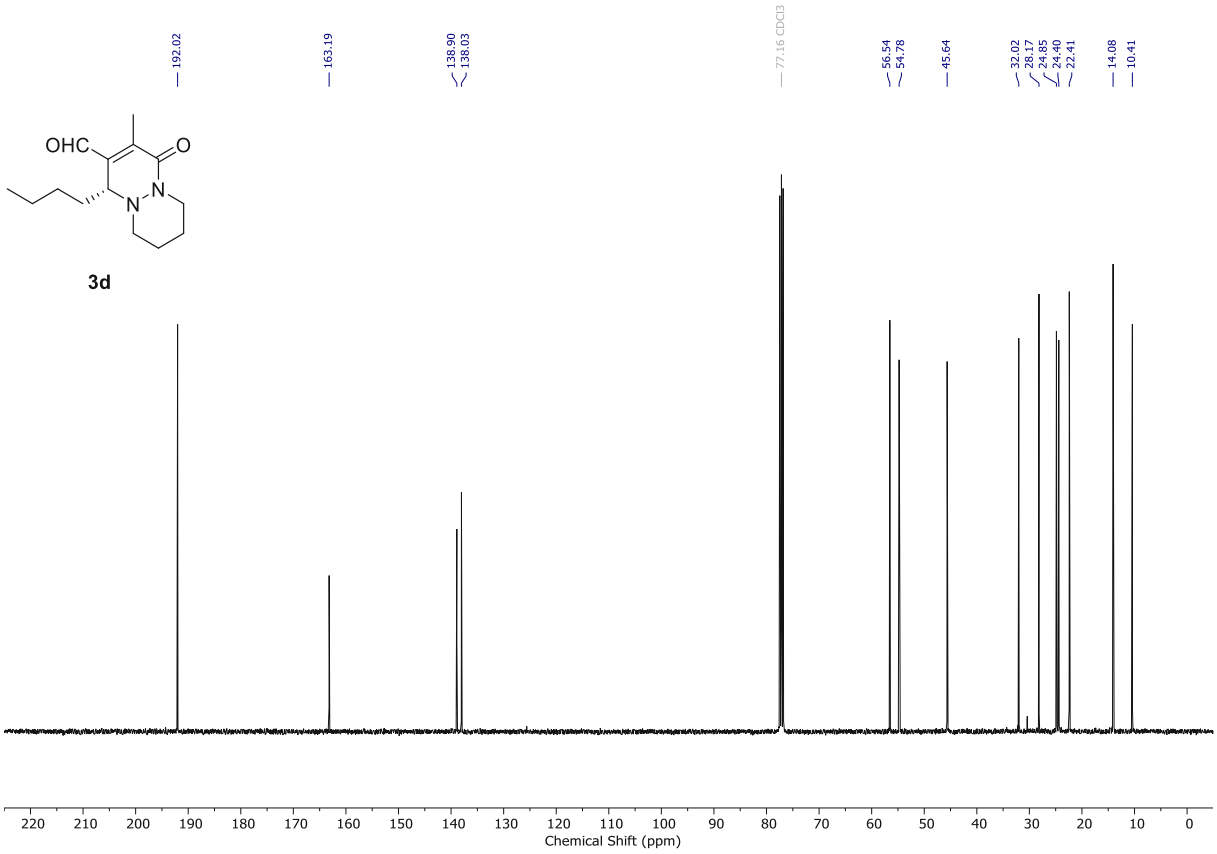
Die approbierte gedruckte Originalversion dieser Dissertation ist an der TU Wien Bibliothek verfügbar.
The approved original version of this doctoral thesis is available in print at TU Wien Bibliothek.



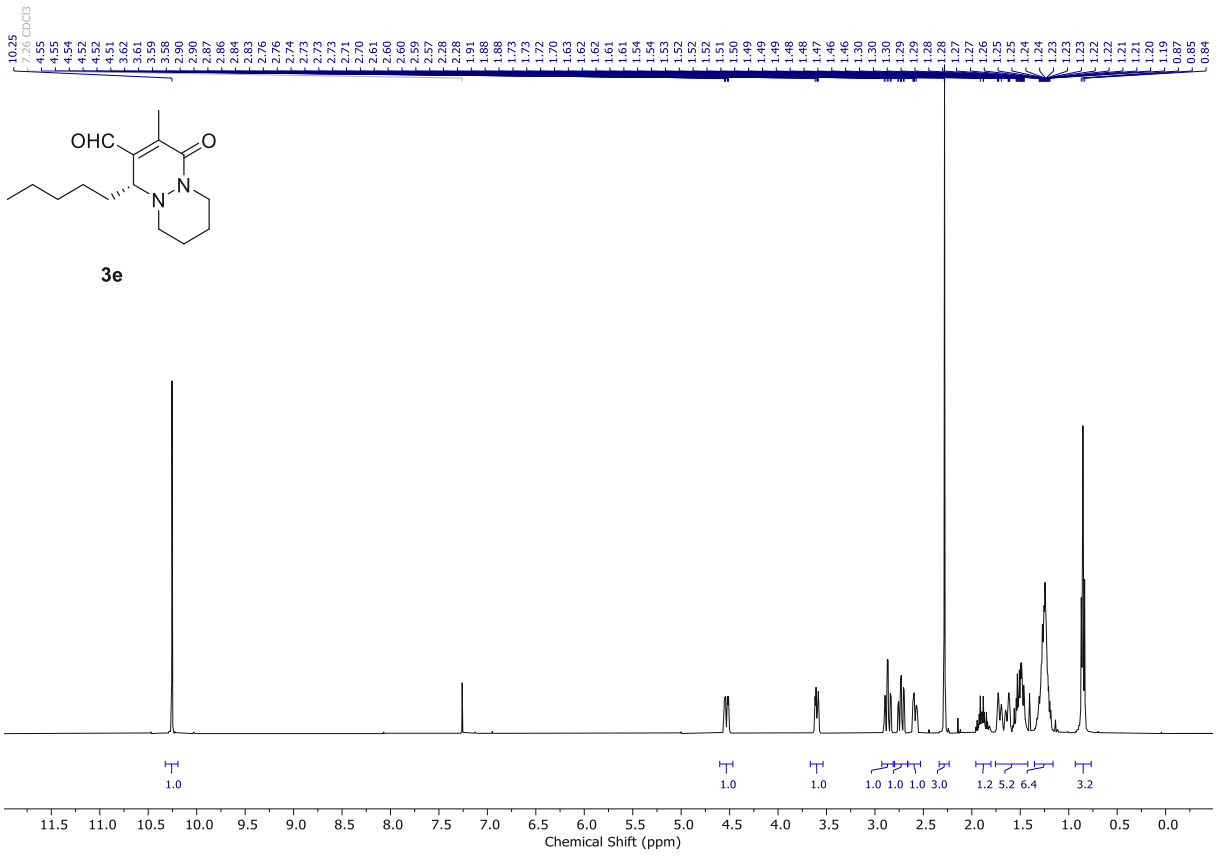
7.4.4 NMR spectra of **3d**



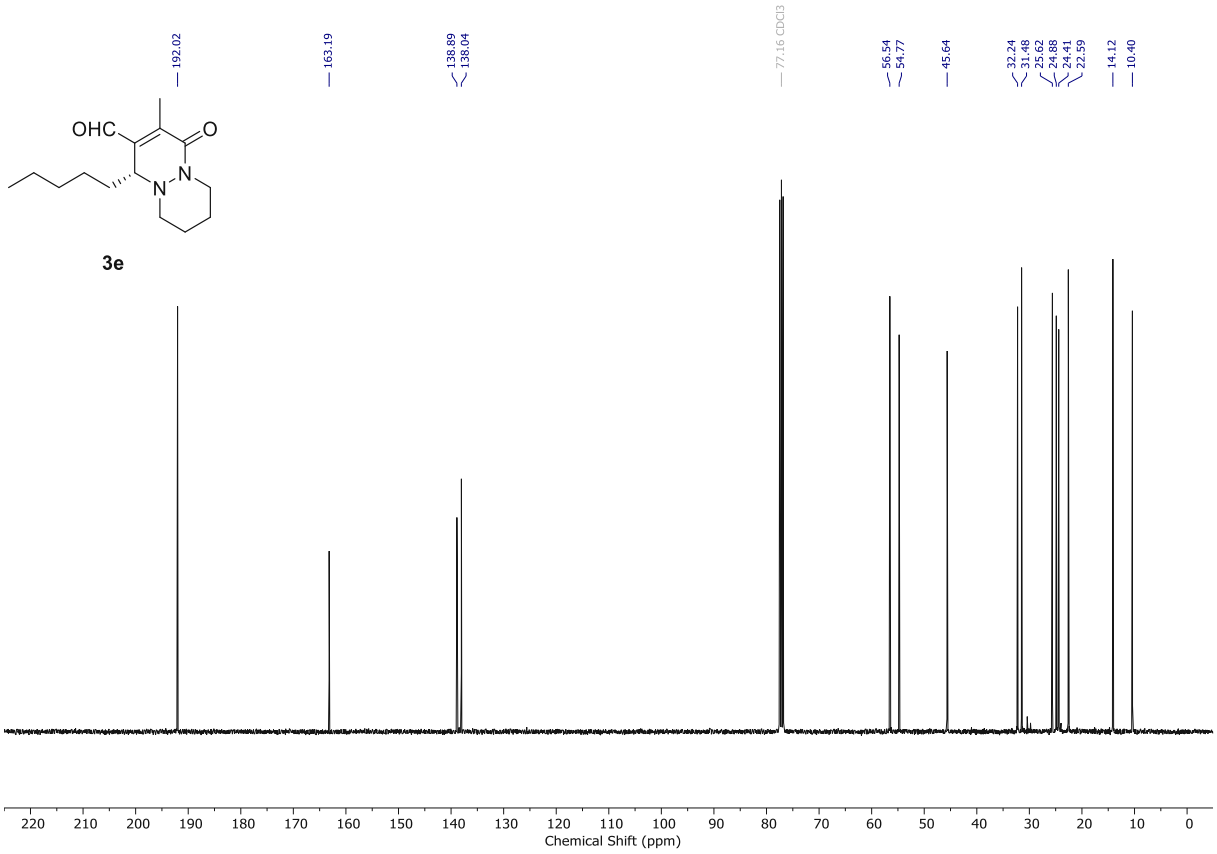
Die approbierte gedruckte Originalversion dieser Dissertation ist an der TU Wien Bibliothek verfügbar.
The approved original version of this doctoral thesis is available in print at TU Wien Bibliothek.



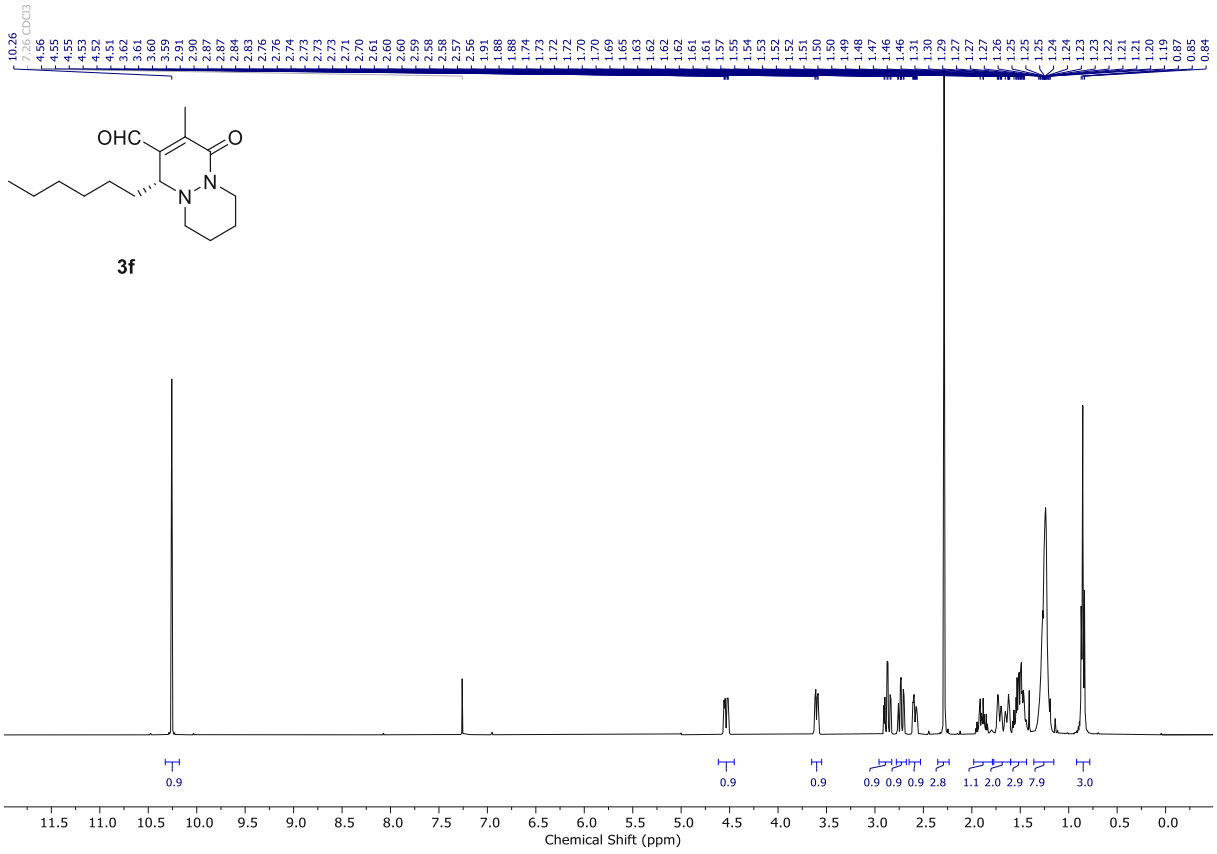
7.4.5 NMR spectra of **3e**



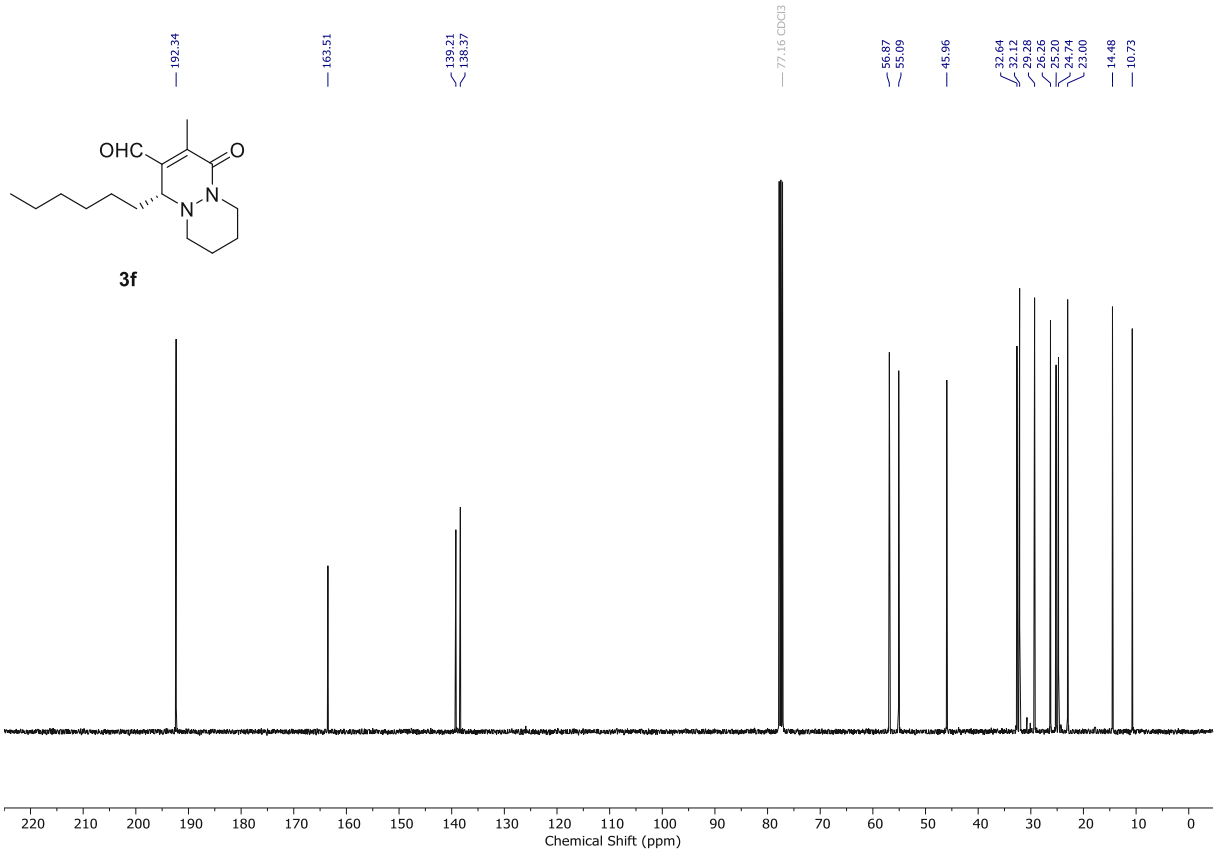
Die approbierte gedruckte Originalversion dieser Dissertation ist an der TU Wien Bibliothek verfügbar.
The approved original version of this doctoral thesis is available in print at TU Wien Bibliothek.



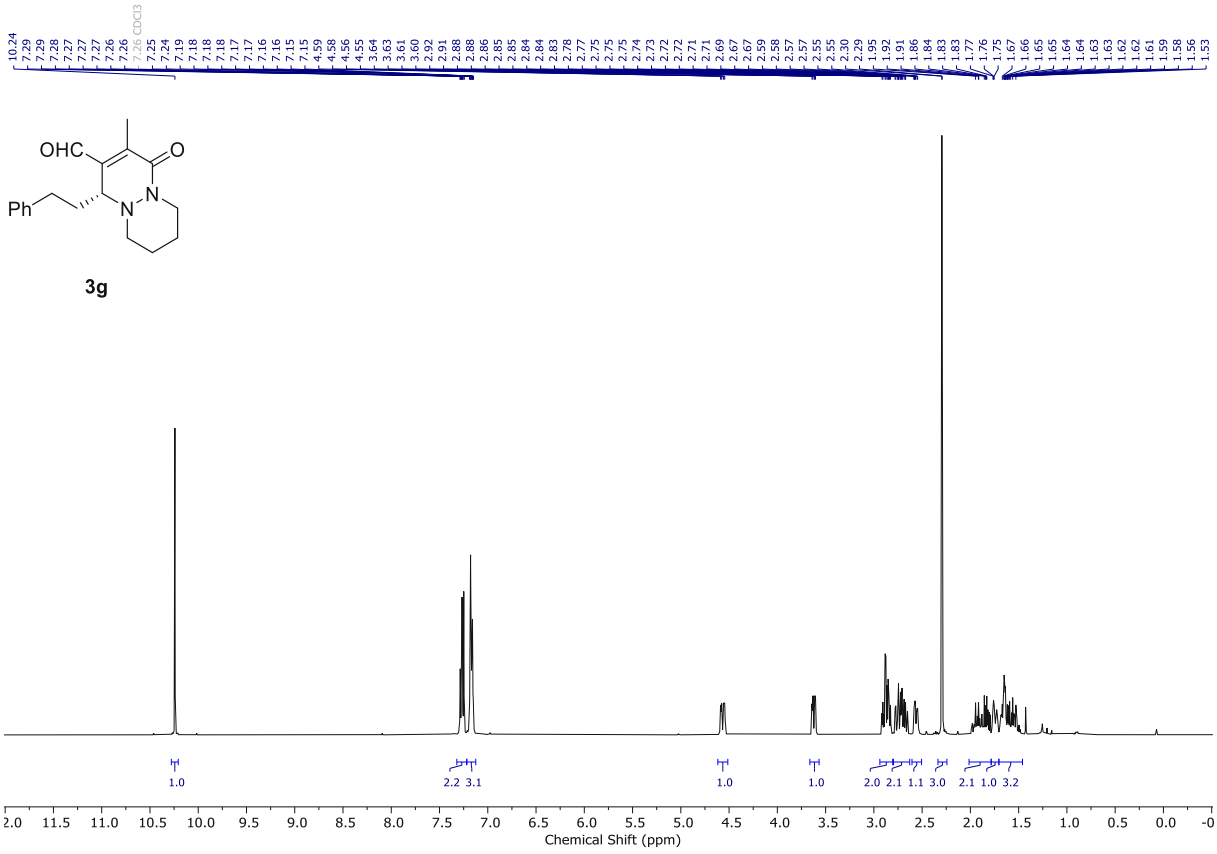
7.4.6 NMR spectra of **3f**



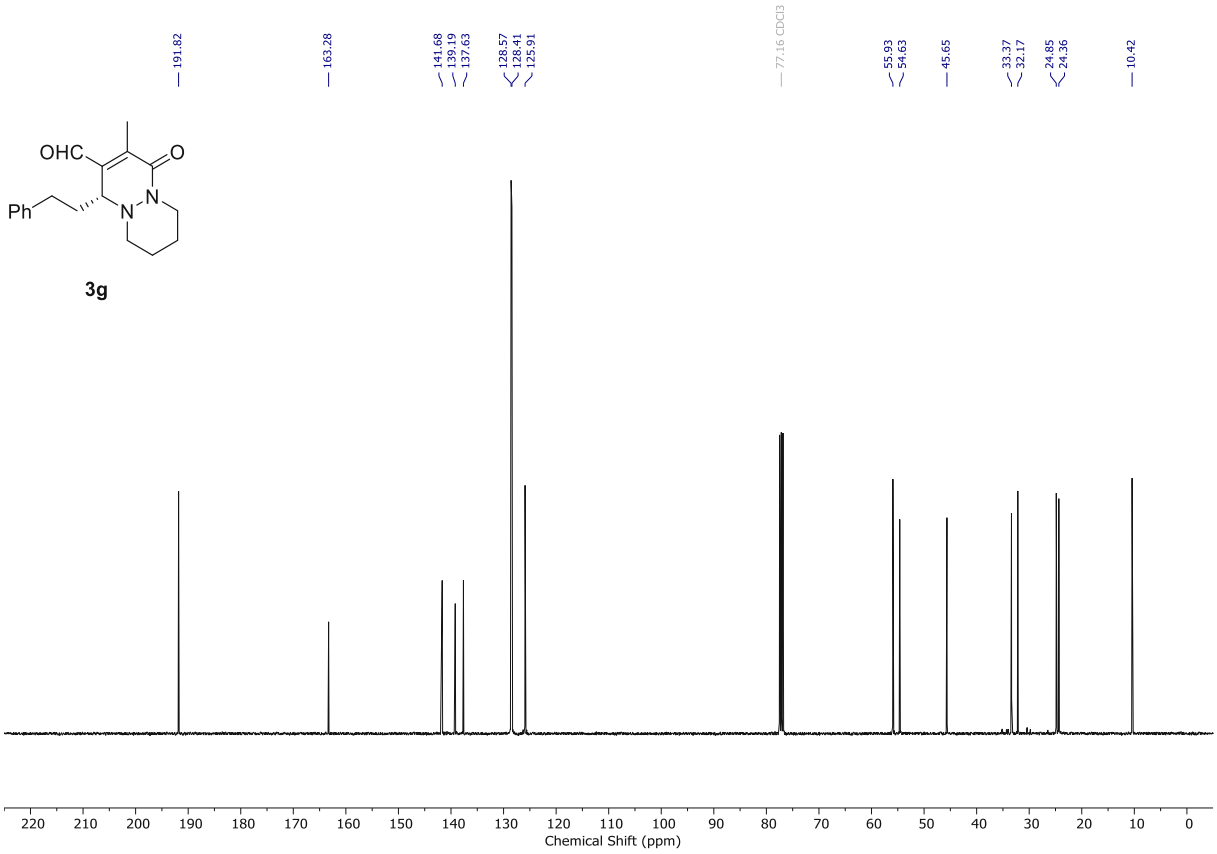
Die approbierte gedruckte Originalversion dieser Dissertation ist an der TU Wien Bibliothek verfügbar.
The approved original version of this doctoral thesis is available in print at TU Wien Bibliothek.



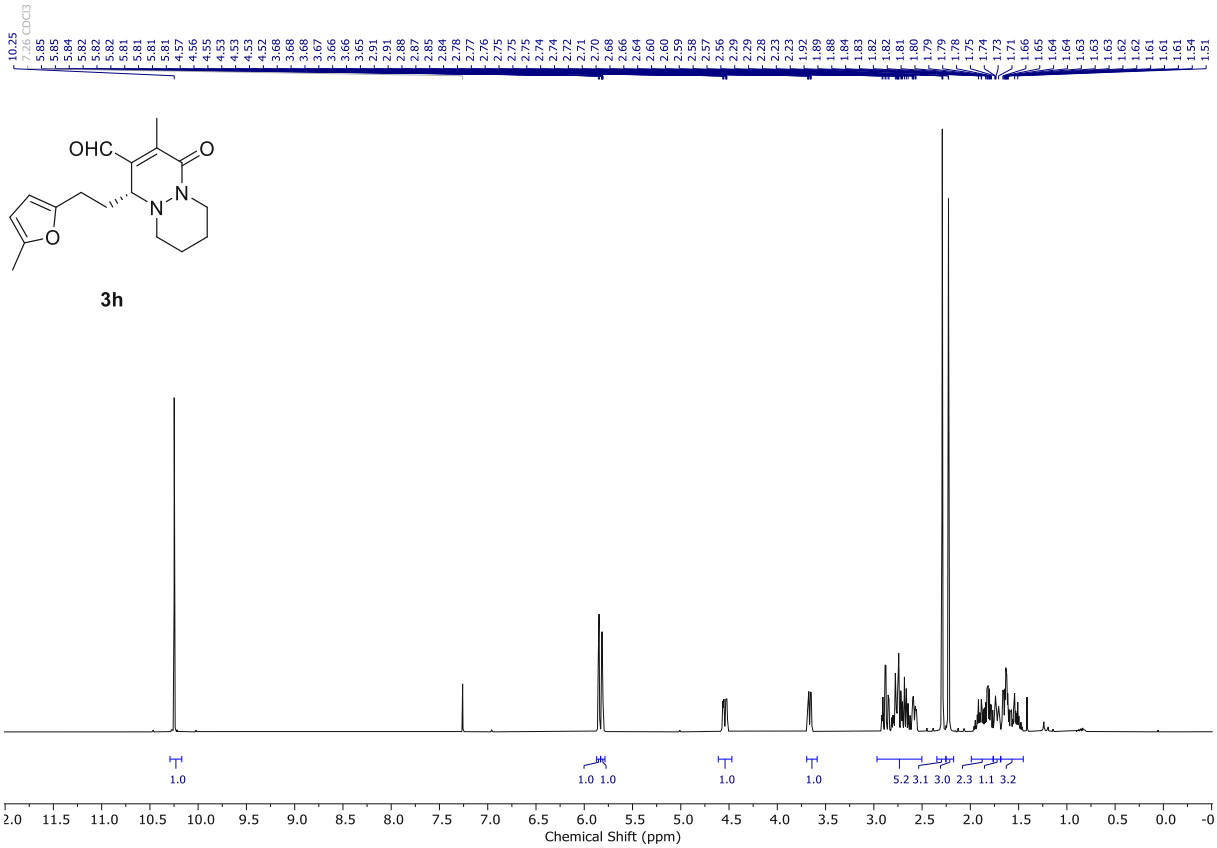
7.4.7 NMR spectra of **3g**



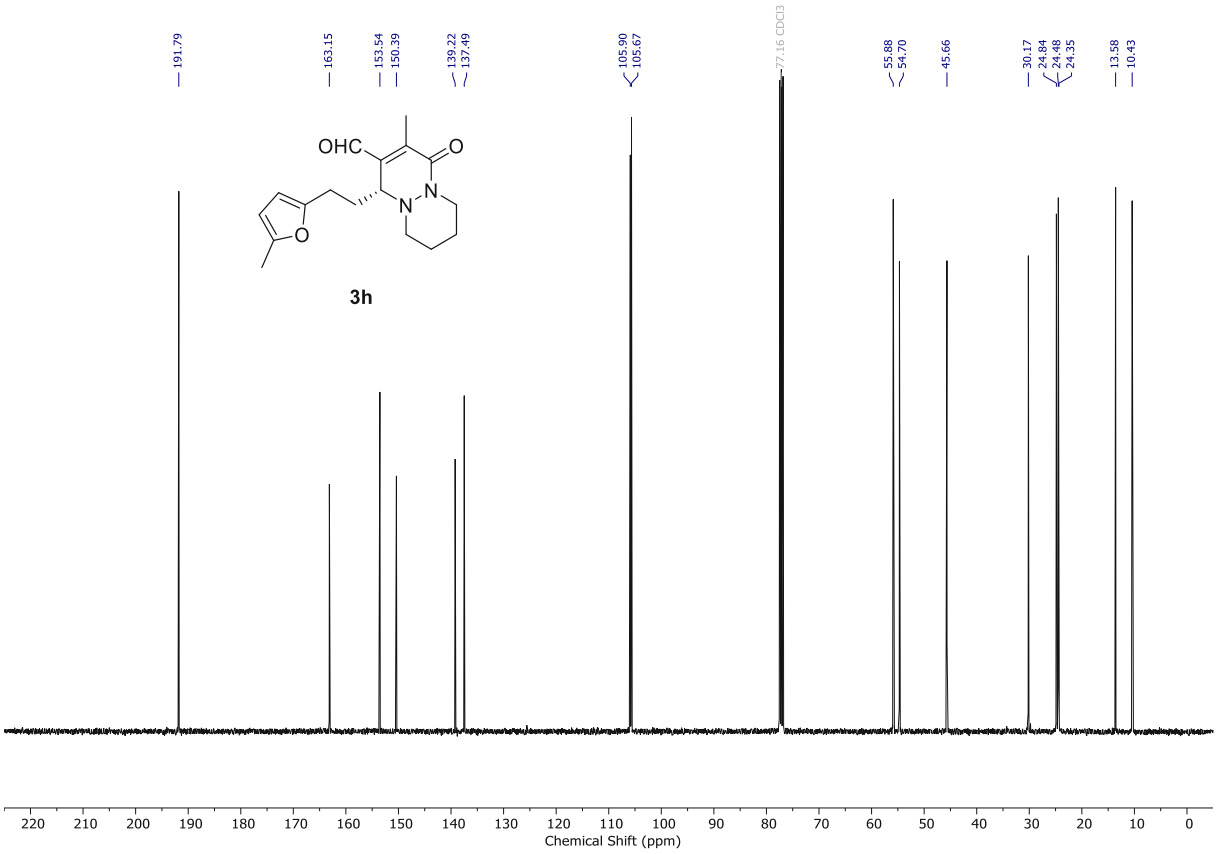
Die approbierte gedruckte Originalversion dieser Dissertation ist an der TU Wien Bibliothek verfügbar.
The approved original version of this doctoral thesis is available in print at TU Wien Bibliothek.



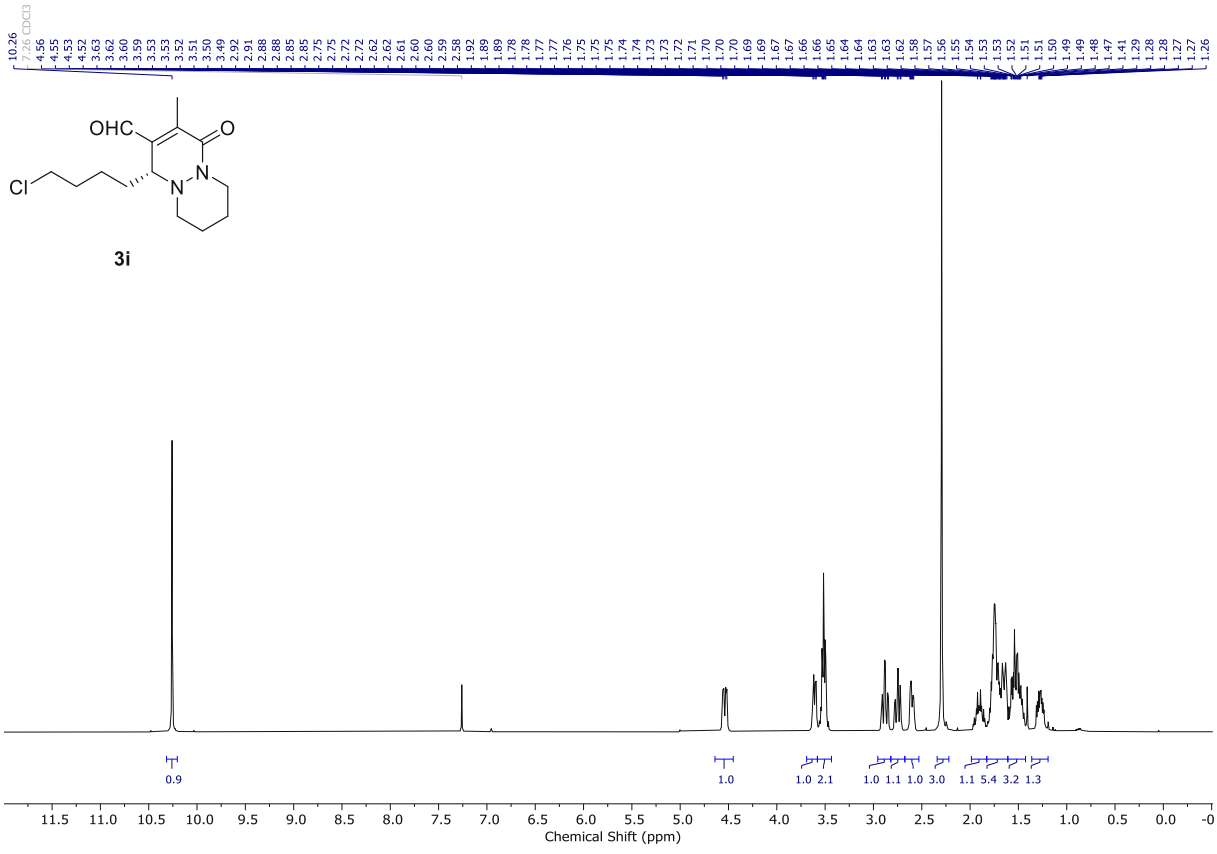
7.4.8 NMR spectra of **3h**



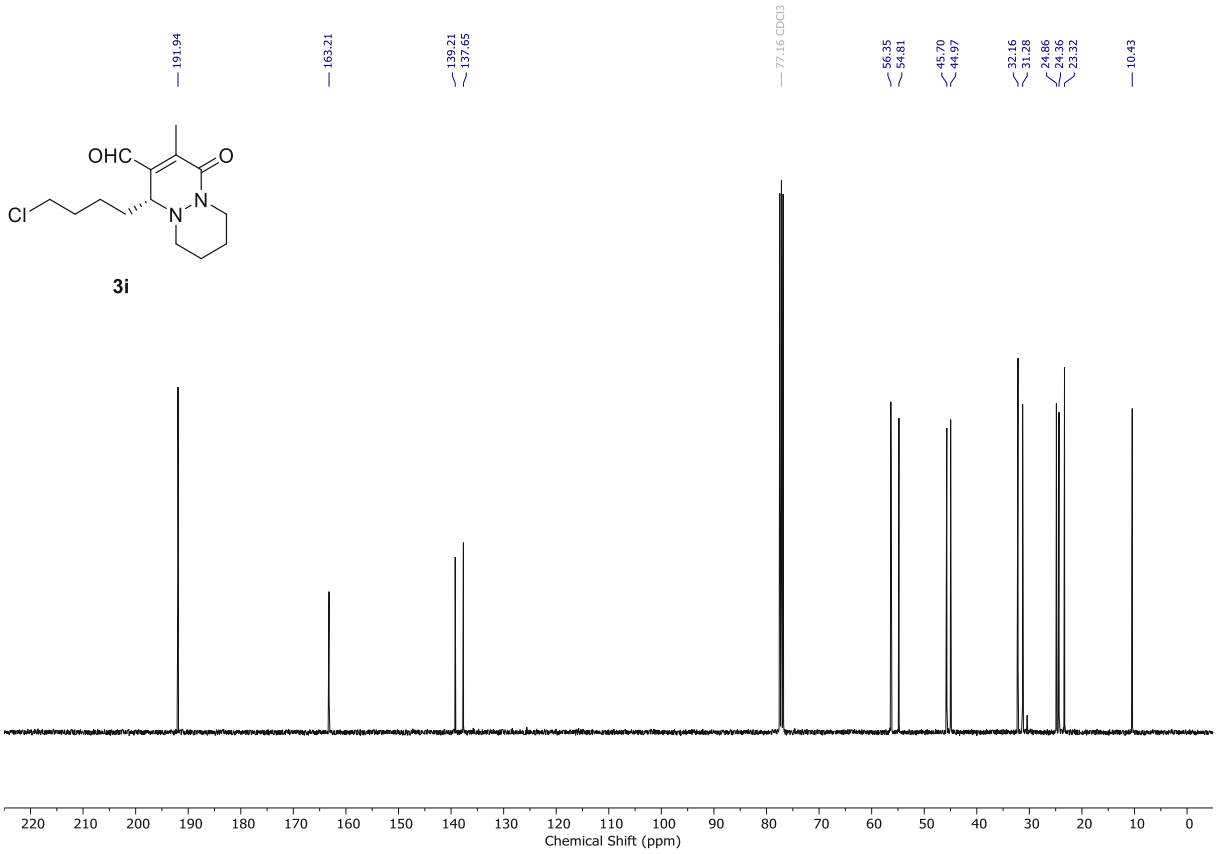
Die approbierte gedruckte Originalversion dieser Dissertation ist an der TU Wien Bibliothek verfügbar.
The approved original version of this doctoral thesis is available in print at TU Wien Bibliothek.



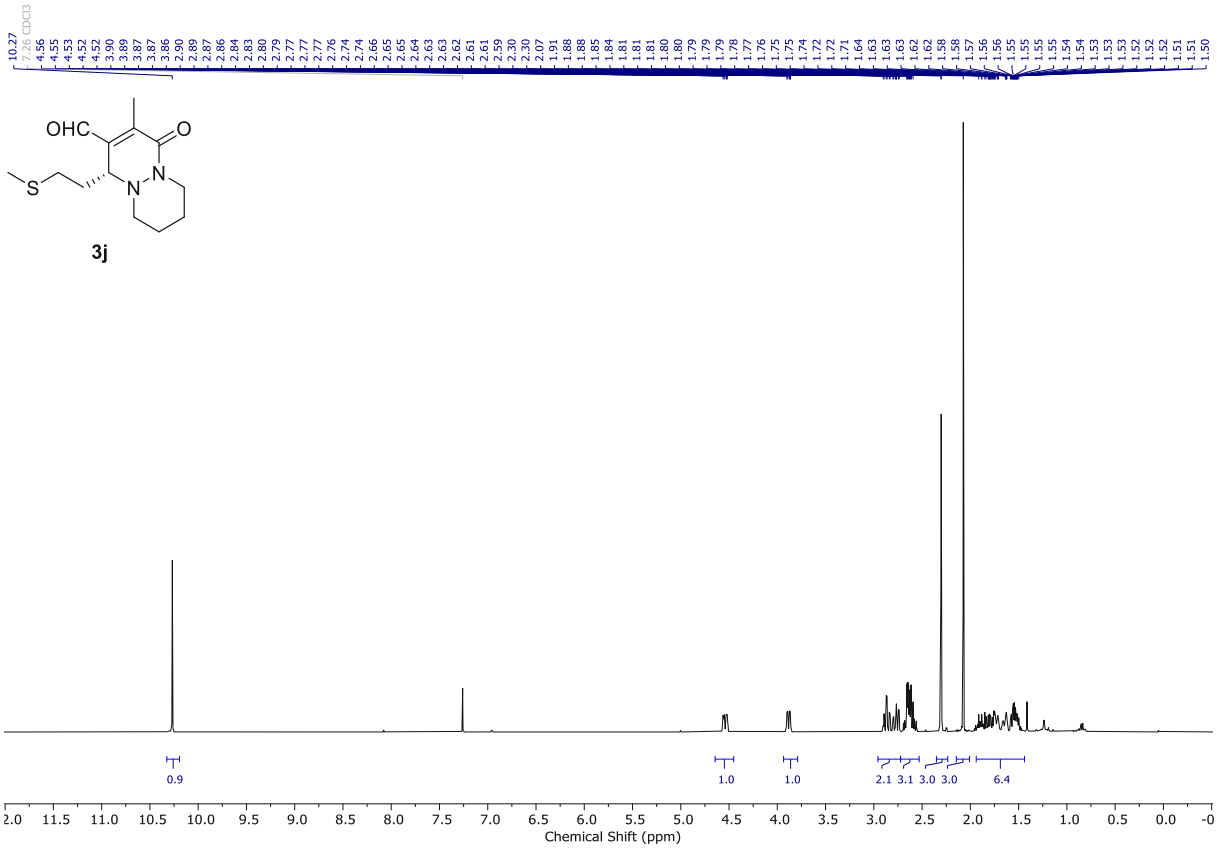
7.4.9 NMR spectra of **3i**



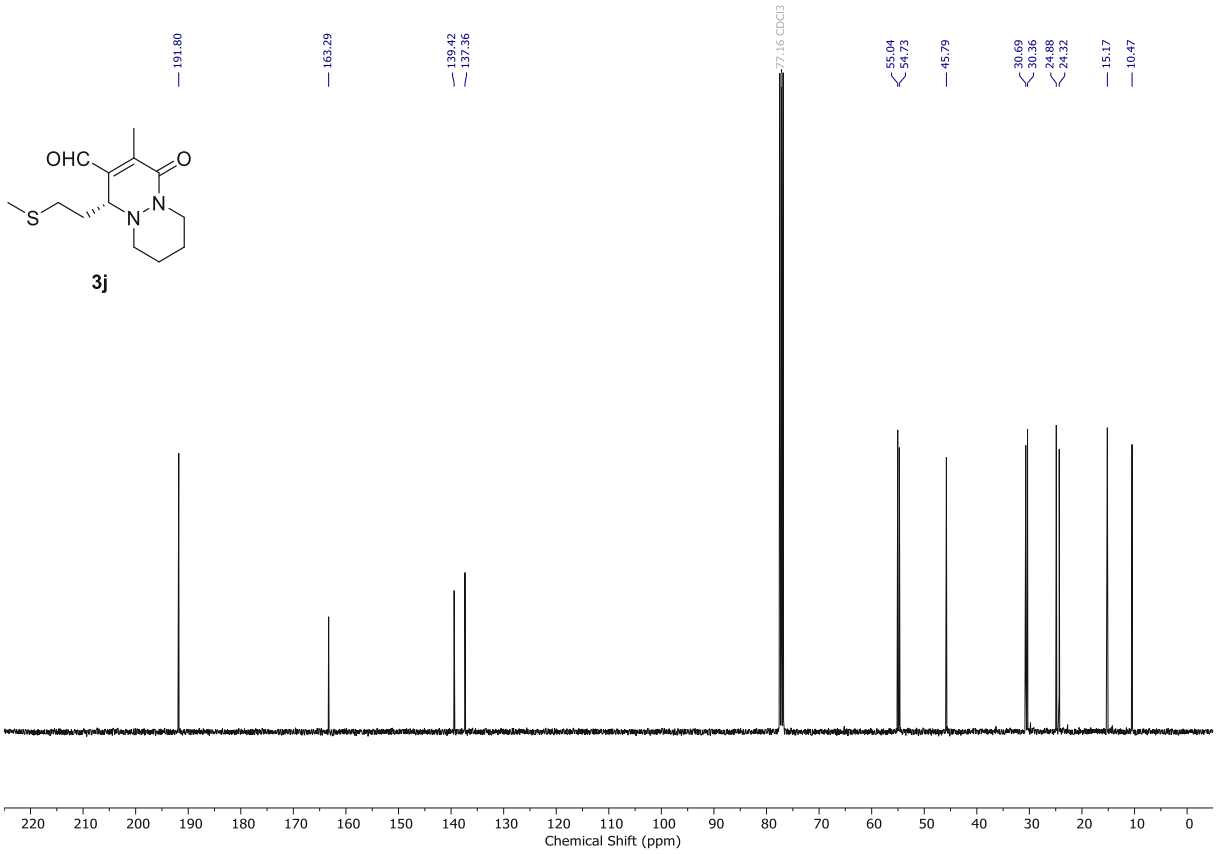
Die approbierte gedruckte Originalversion dieser Dissertation ist an der TU Wien Bibliothek verfügbar.
The approved original version of this doctoral thesis is available in print at TU Wien Bibliothek.



7.4.10 NMR spectra of **3j**

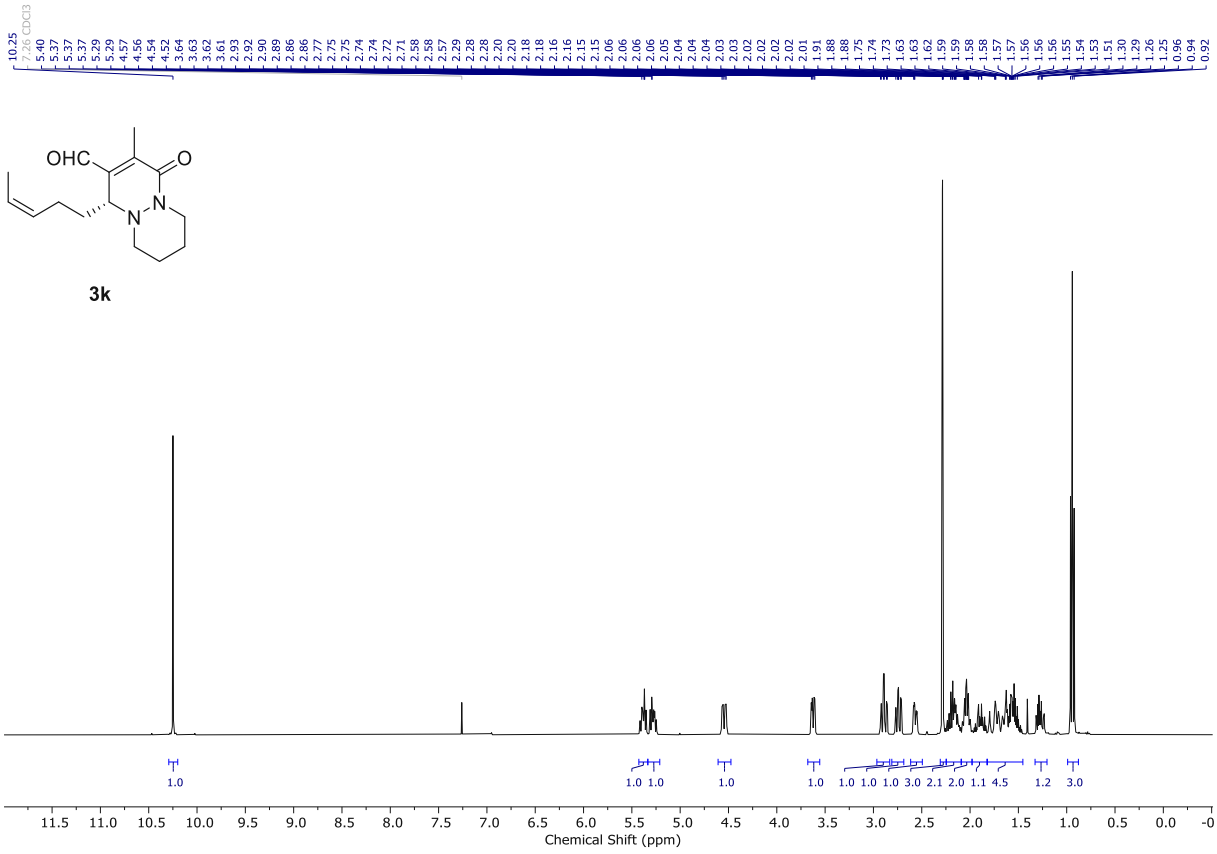


Die approbierte gedruckte Originalversion dieser Dissertation ist an der TU Wien Bibliothek verfügbar.
The approved original version of this doctoral thesis is available in print at TU Wien Bibliothek.



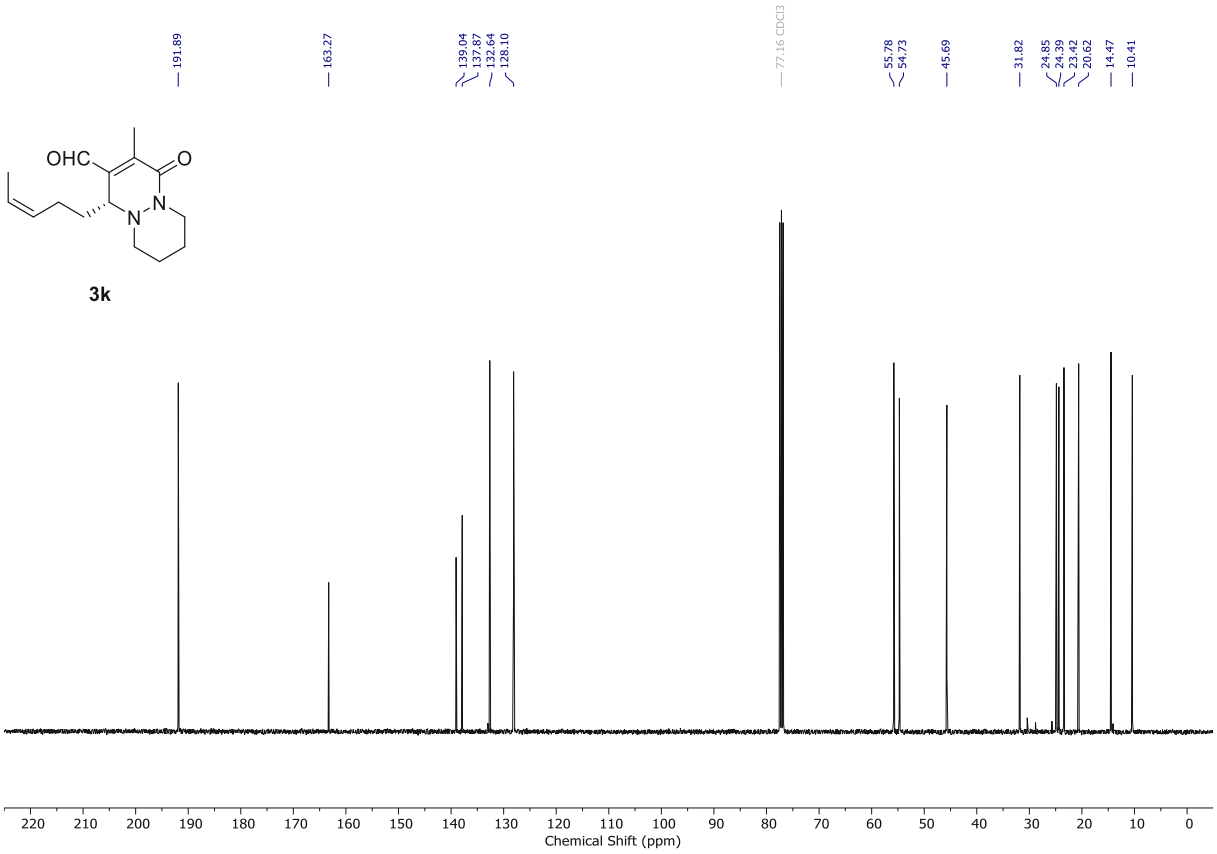
3j

7.4.11 NMR spectra of **3k**

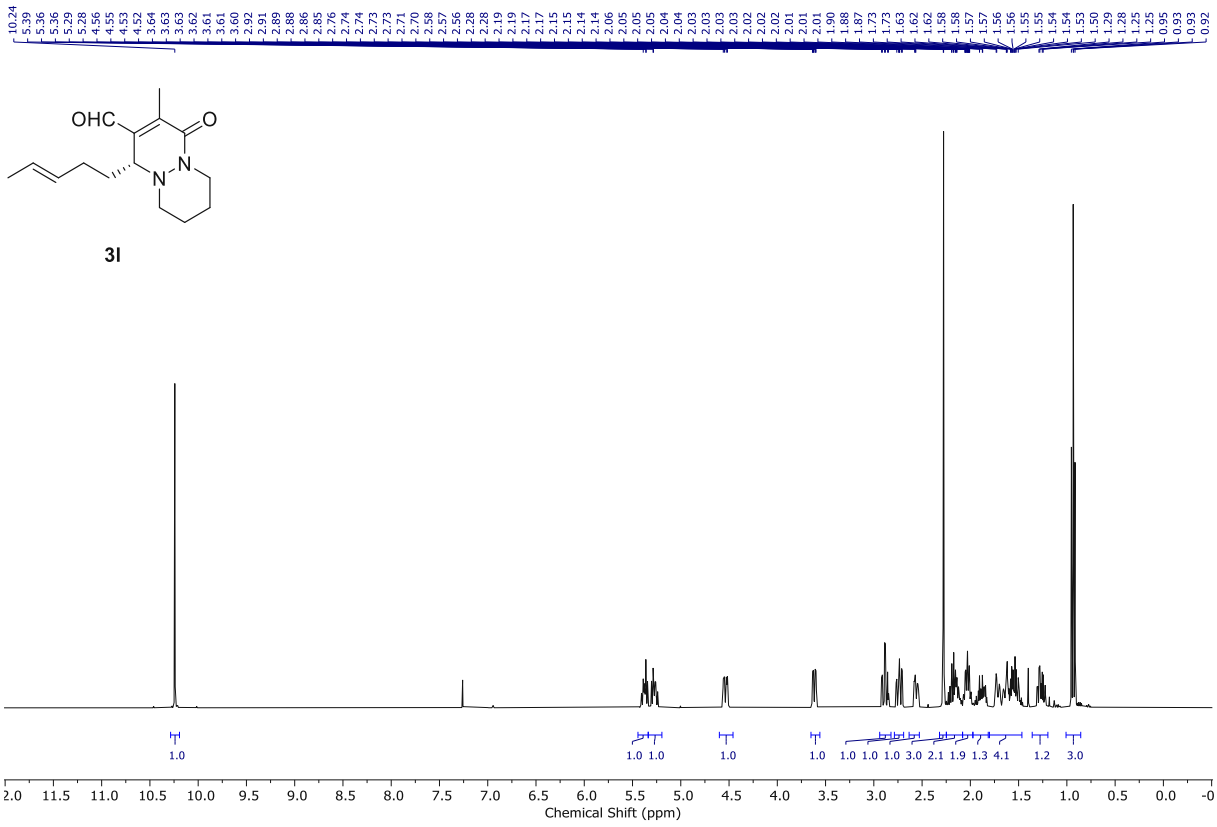


3k

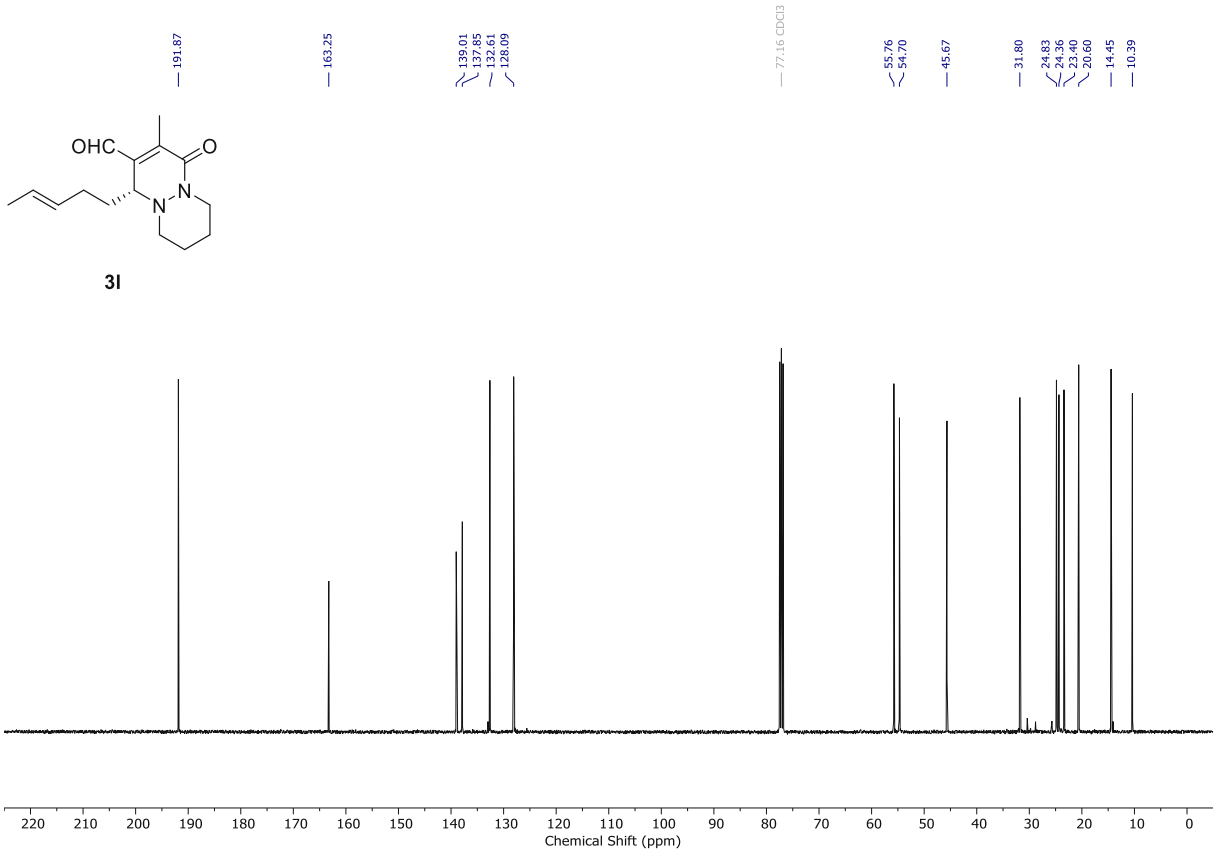
Die approbierte gedruckte Originalversion dieser Dissertation ist an der TU Wien Bibliothek verfügbar.
The approved original version of this doctoral thesis is available in print at TU Wien Bibliothek.



7.4.12 NMR spectra of **3l**

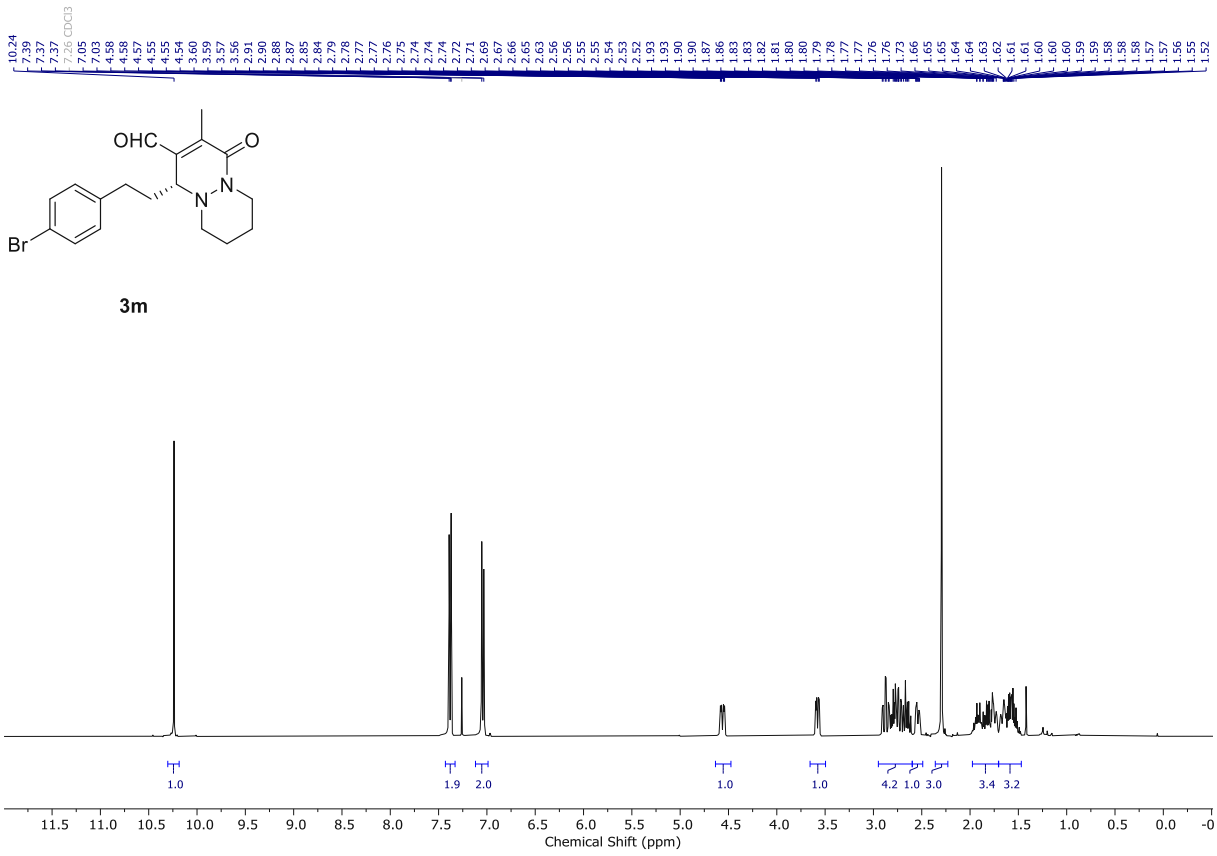


Die approbierte gedruckte Originalversion dieser Dissertation ist an der TU Wien Bibliothek verfügbar.
The approved original version of this doctoral thesis is available in print at TU Wien Bibliothek.
TU Bibliothek Your knowledge hub WIEN



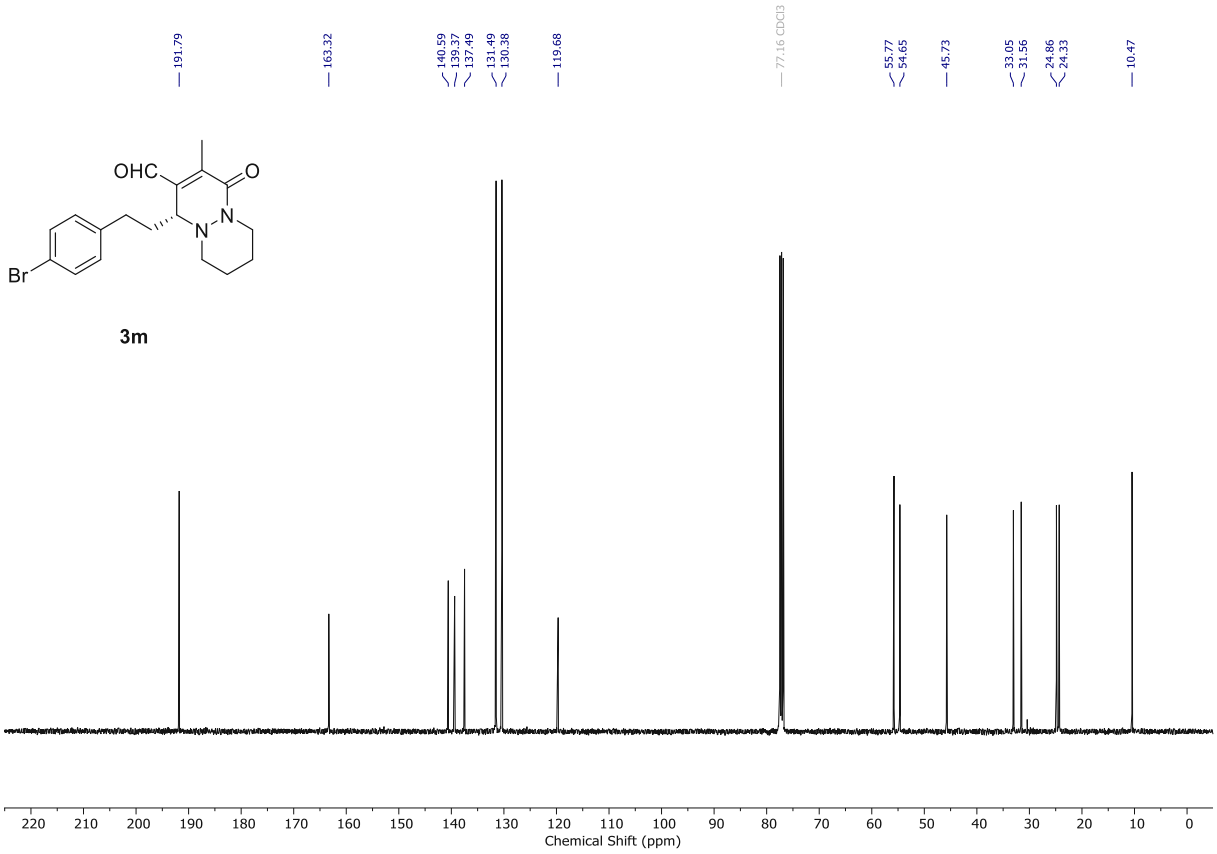
3l

7.4.13 NMR spectra of **3m**

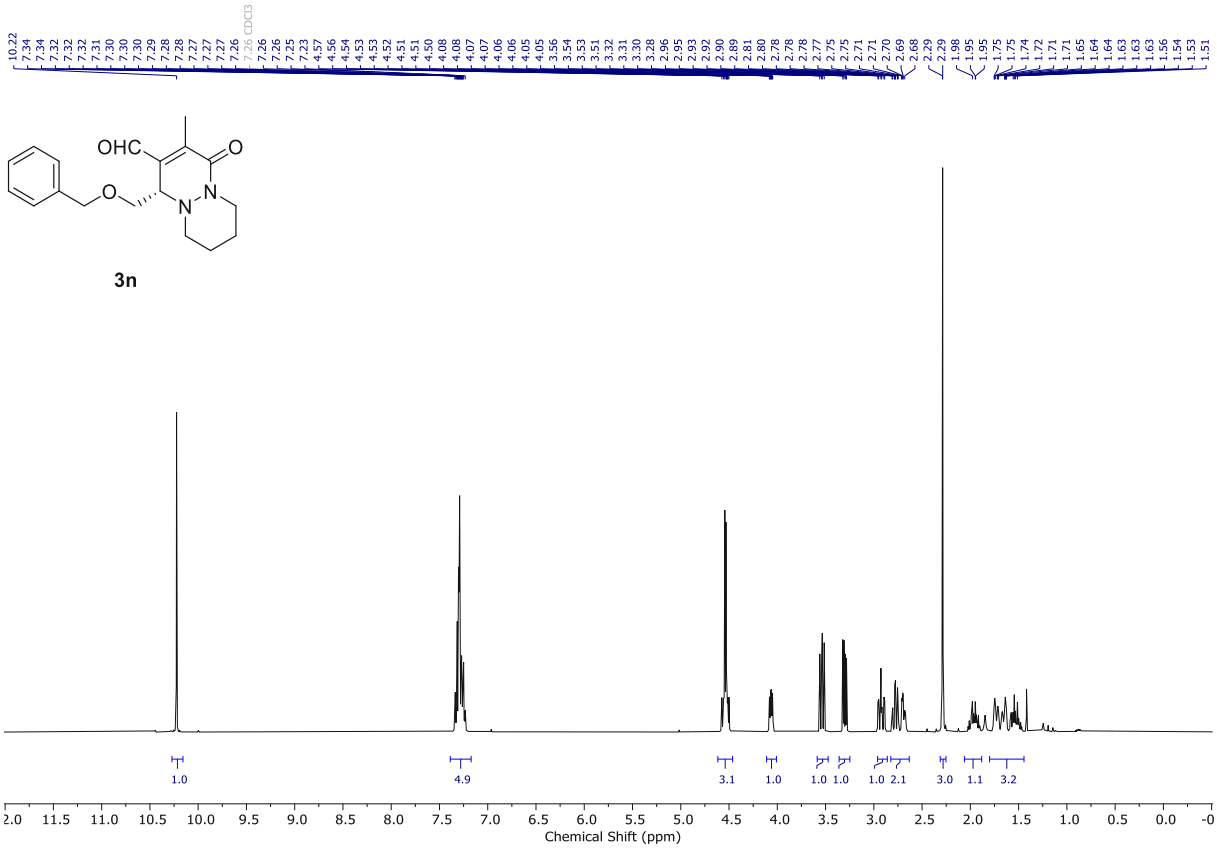


3m

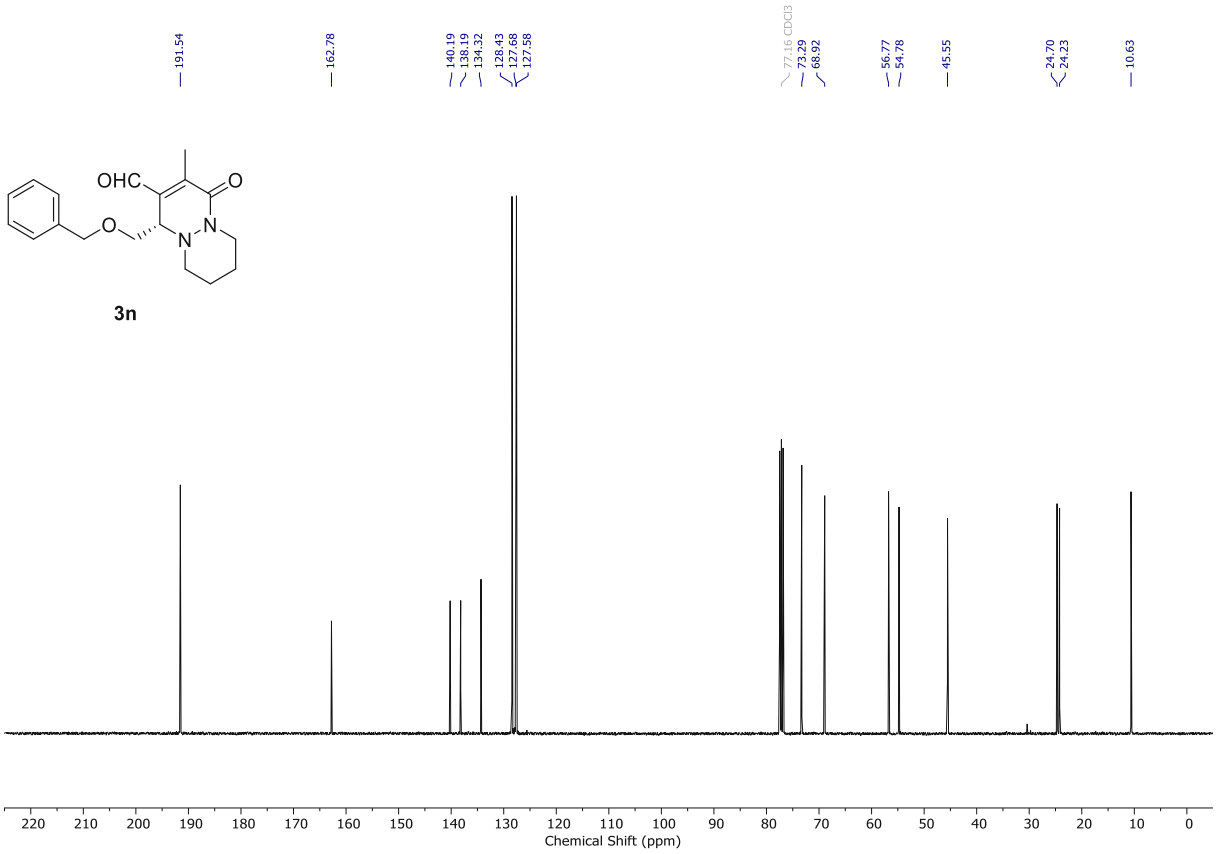
Die approbierte gedruckte Originalversion dieser Dissertation ist an der TU Wien Bibliothek verfügbar.
The approved original version of this doctoral thesis is available in print at TU Wien Bibliothek.



7.4.14 NMR spectra of **3n**

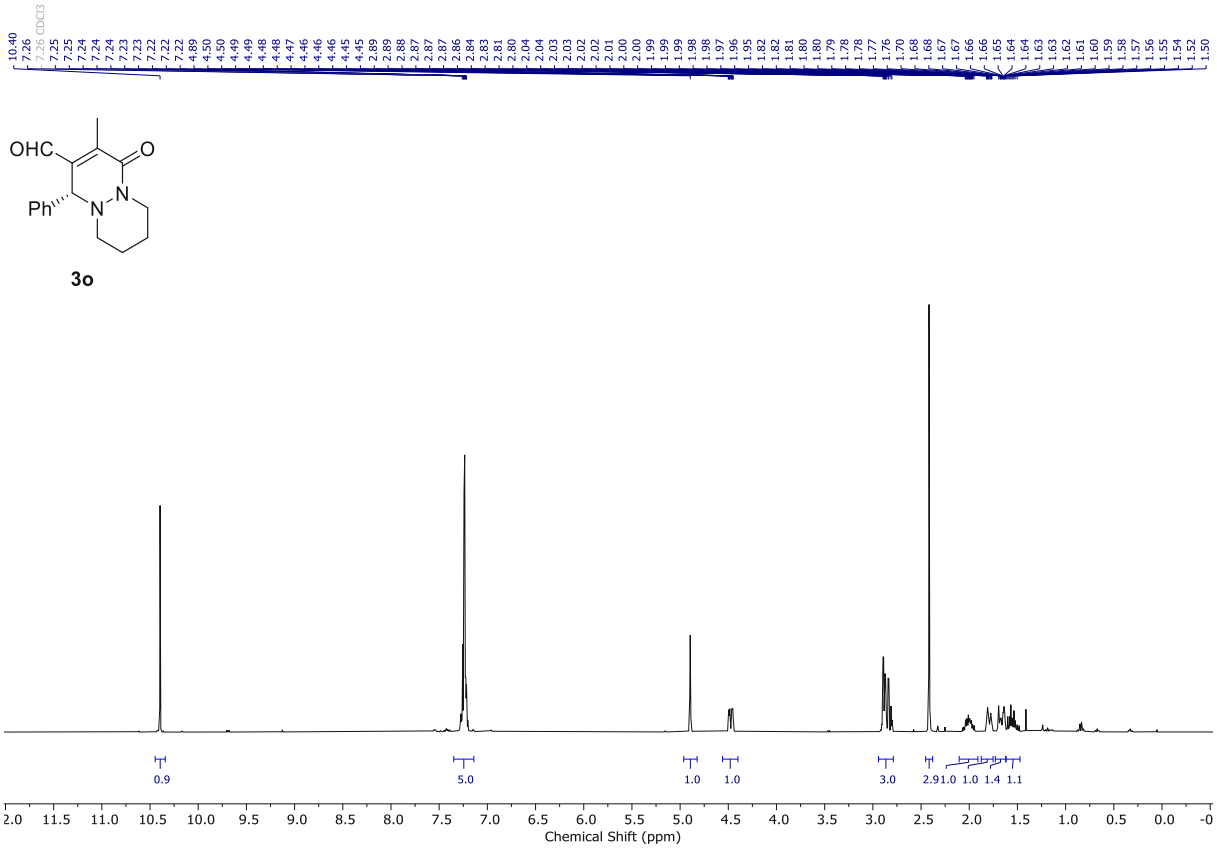


Die approbierte gedruckte Originalversion dieser Dissertation ist an der TU Wien Bibliothek verfügbar.
The approved original version of this doctoral thesis is available in print at TU Wien Bibliothek.



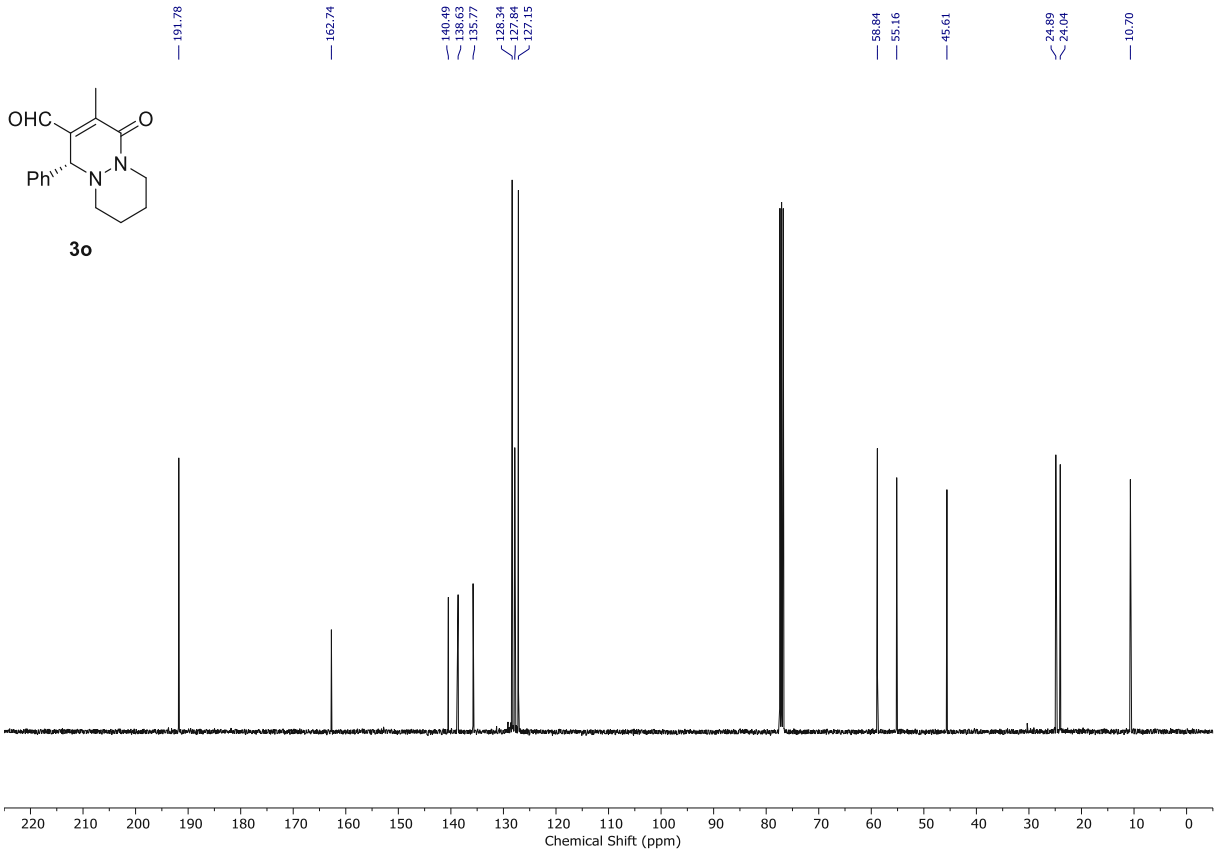
3n

7.4.15 NMR spectra of **3o**



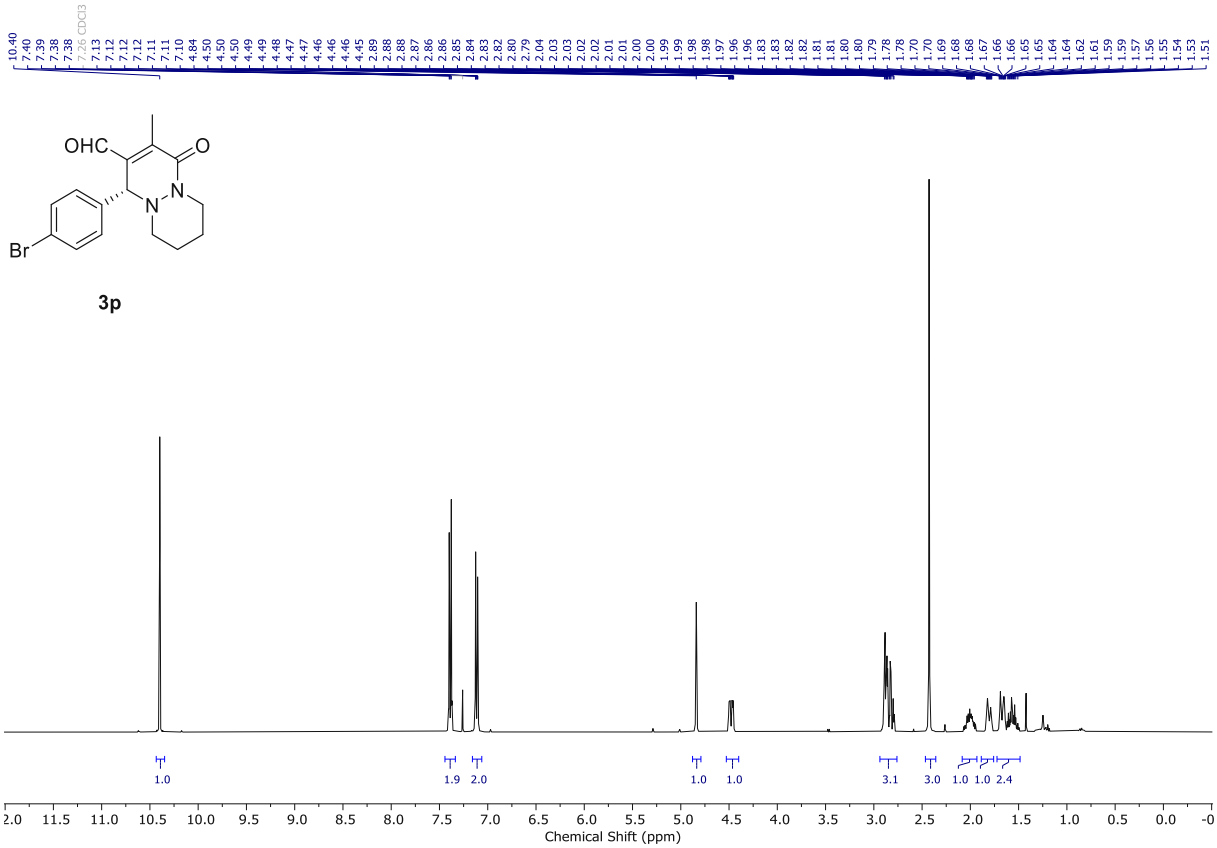
3o

Die approbierte gedruckte Originalversion dieser Dissertation ist an der TU Wien Bibliothek verfügbar.
The approved original version of this doctoral thesis is available in print at TU Wien Bibliothek.



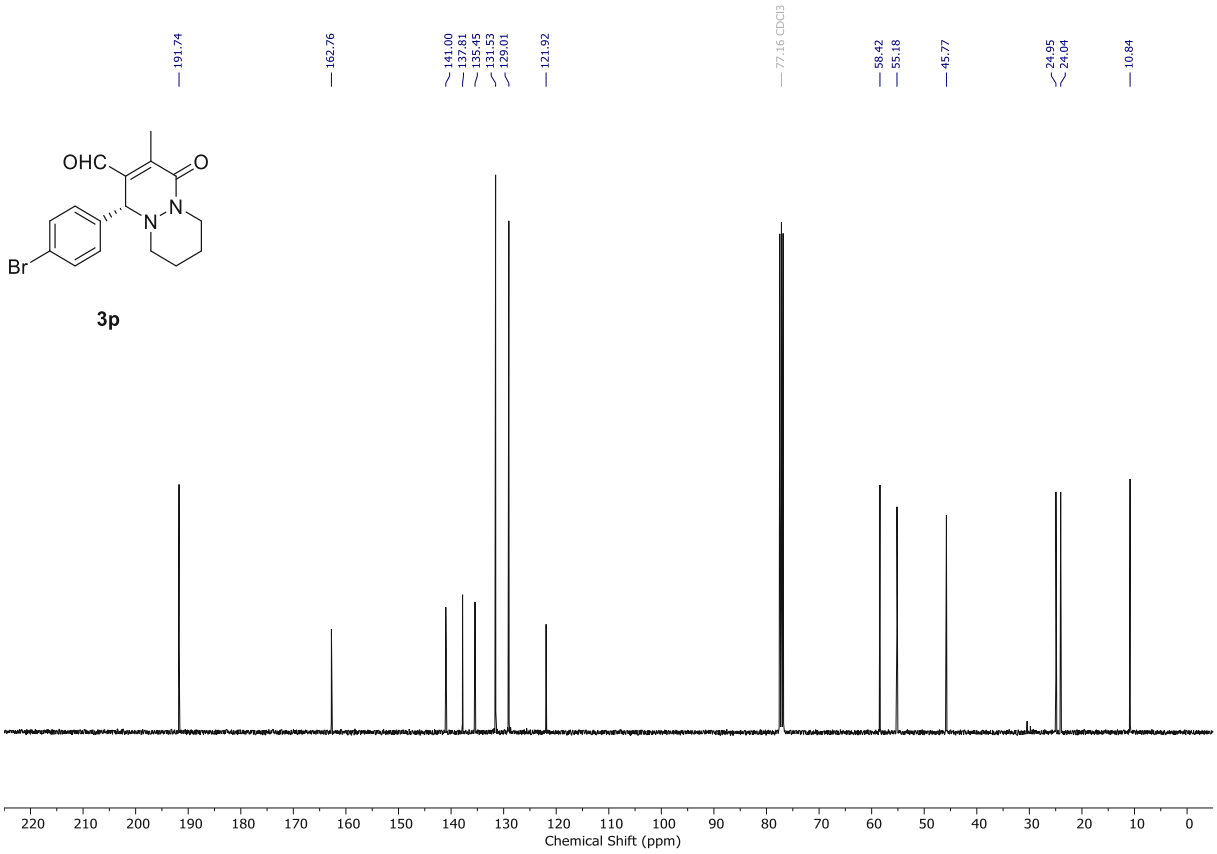
3o

7.4.16 NMR spectra of **3p**



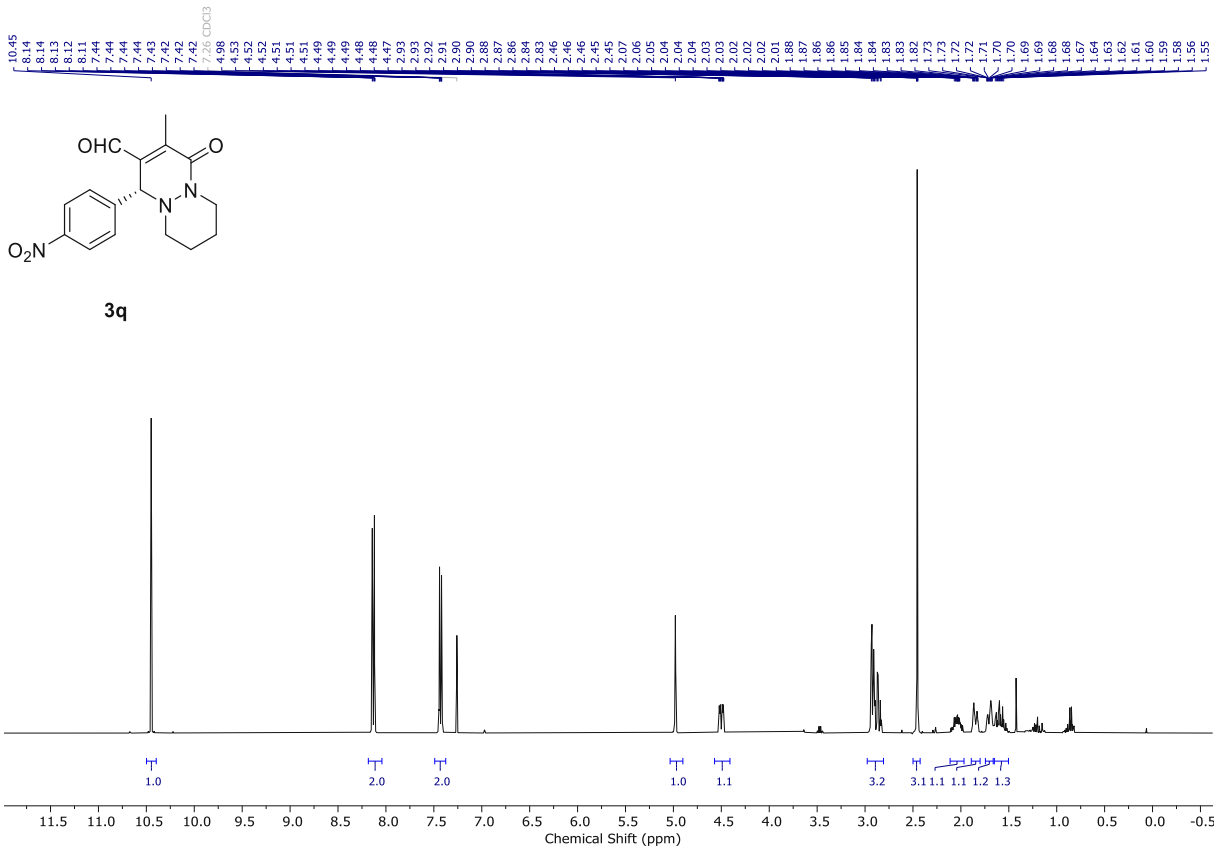
3p

Die approbierte gedruckte Originalversion dieser Dissertation ist an der TU Wien Bibliothek verfügbar.
The approved original version of this doctoral thesis is available in print at TU Wien Bibliothek.



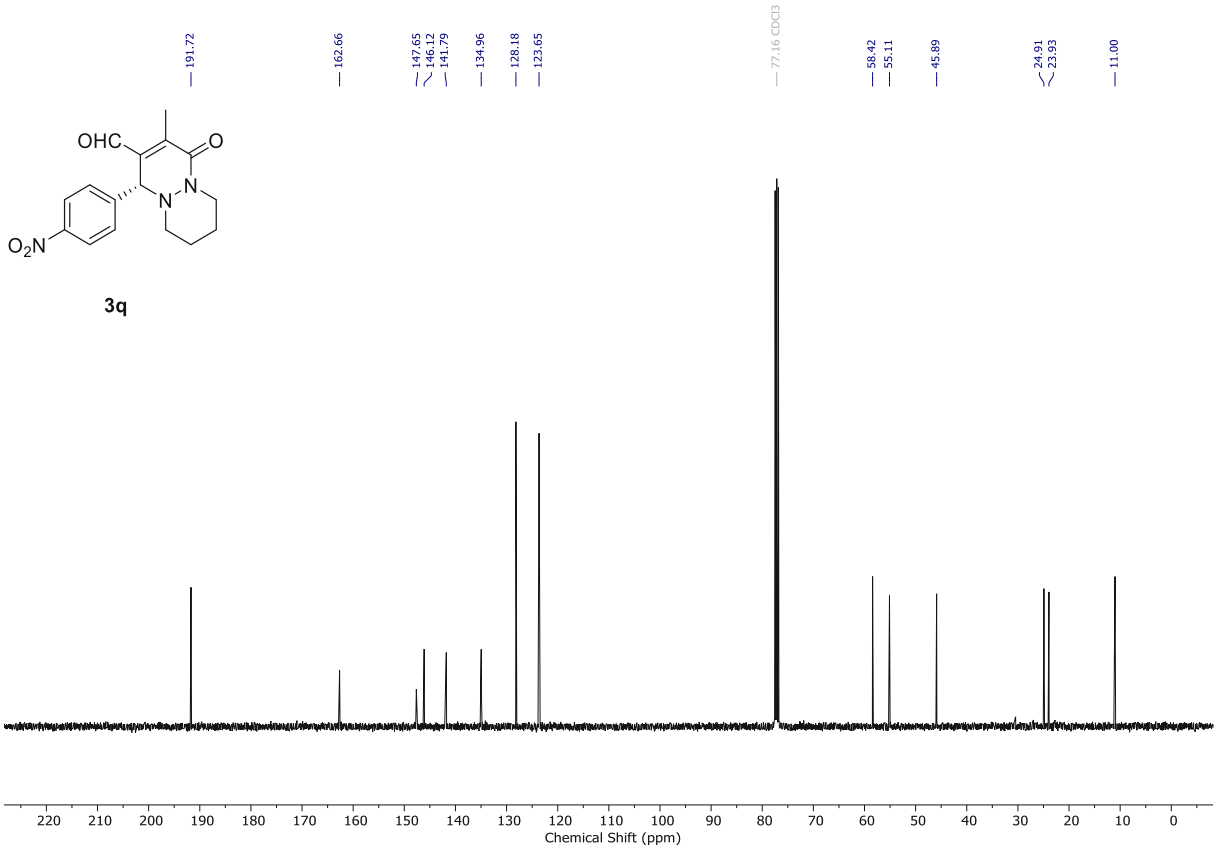
3p

7.4.17 NMR spectra of **3q**

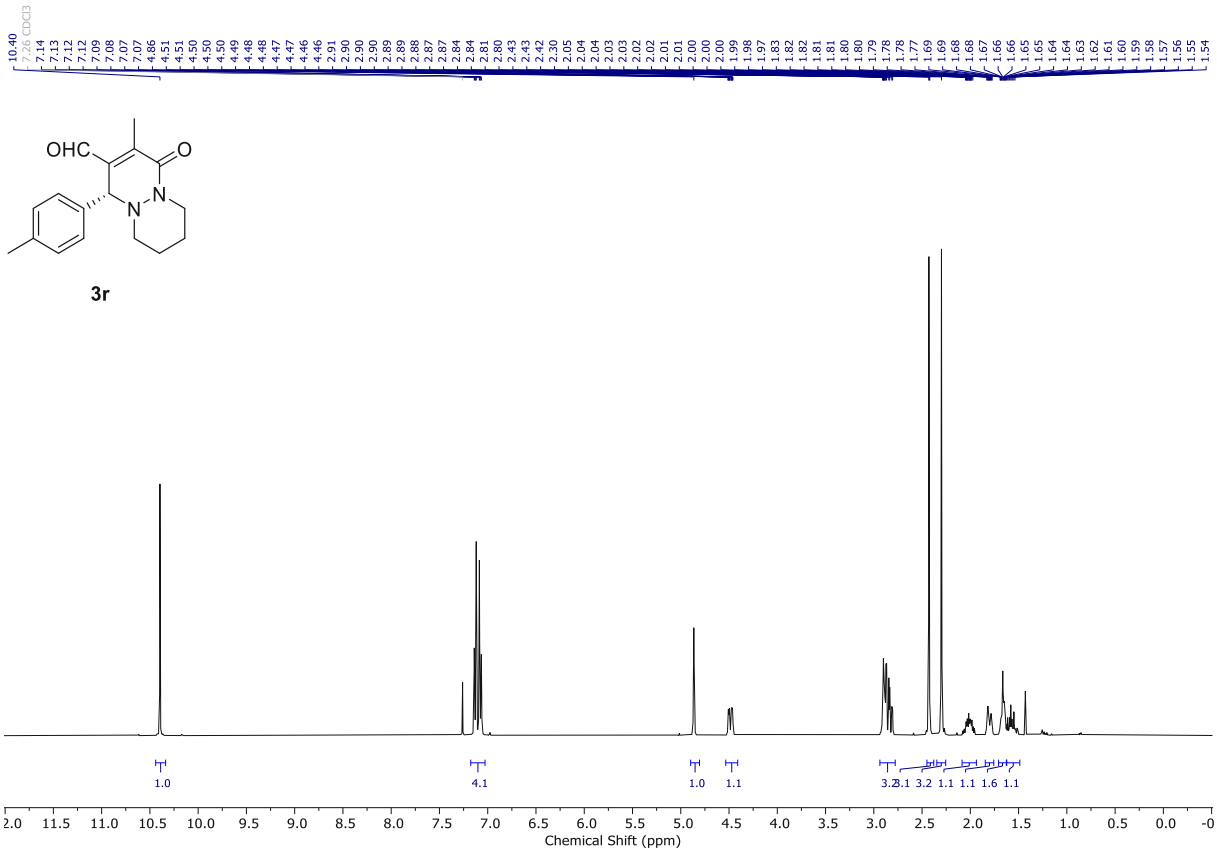


3q

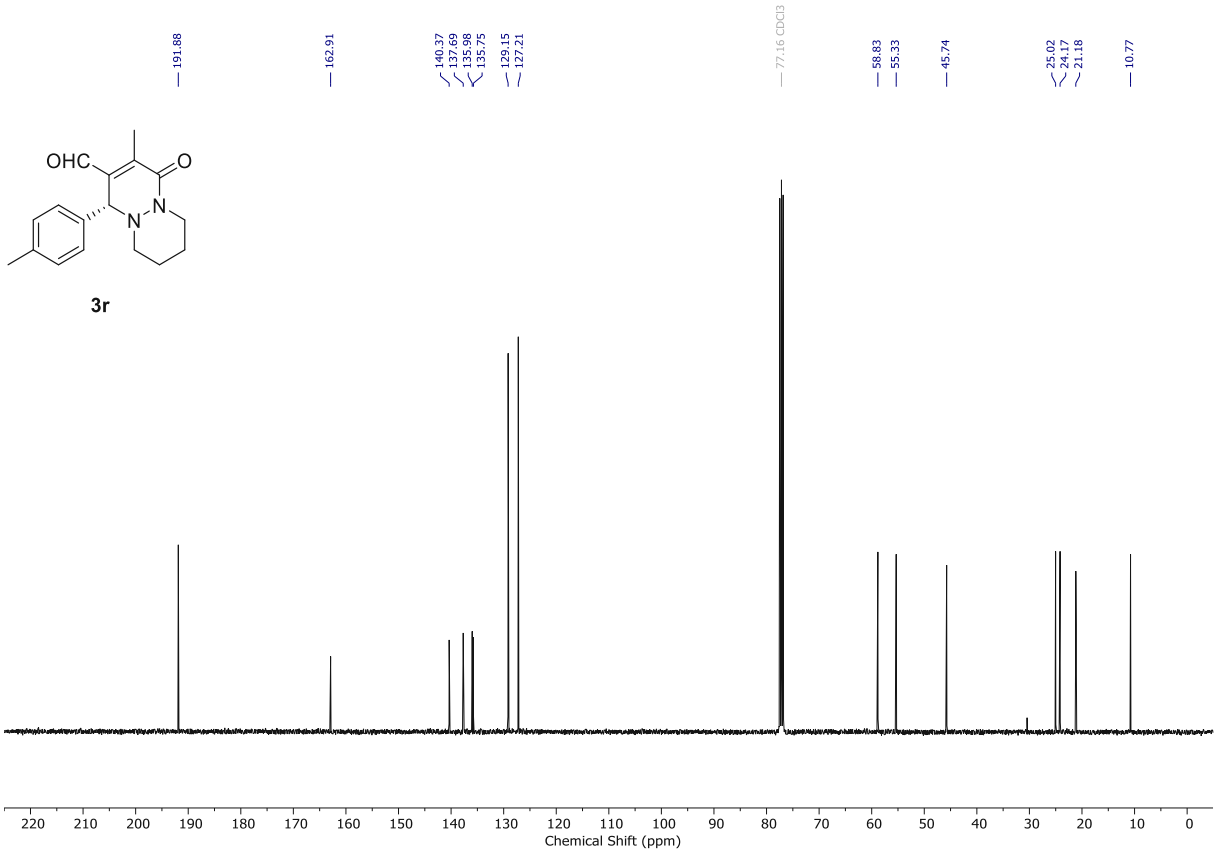
Die approbierte gedruckte Originalversion dieser Dissertation ist an der TU Wien Bibliothek verfügbar.
The approved original version of this doctoral thesis is available in print at TU Wien Bibliothek.
TU Wien Bibliothek Your knowledge hub



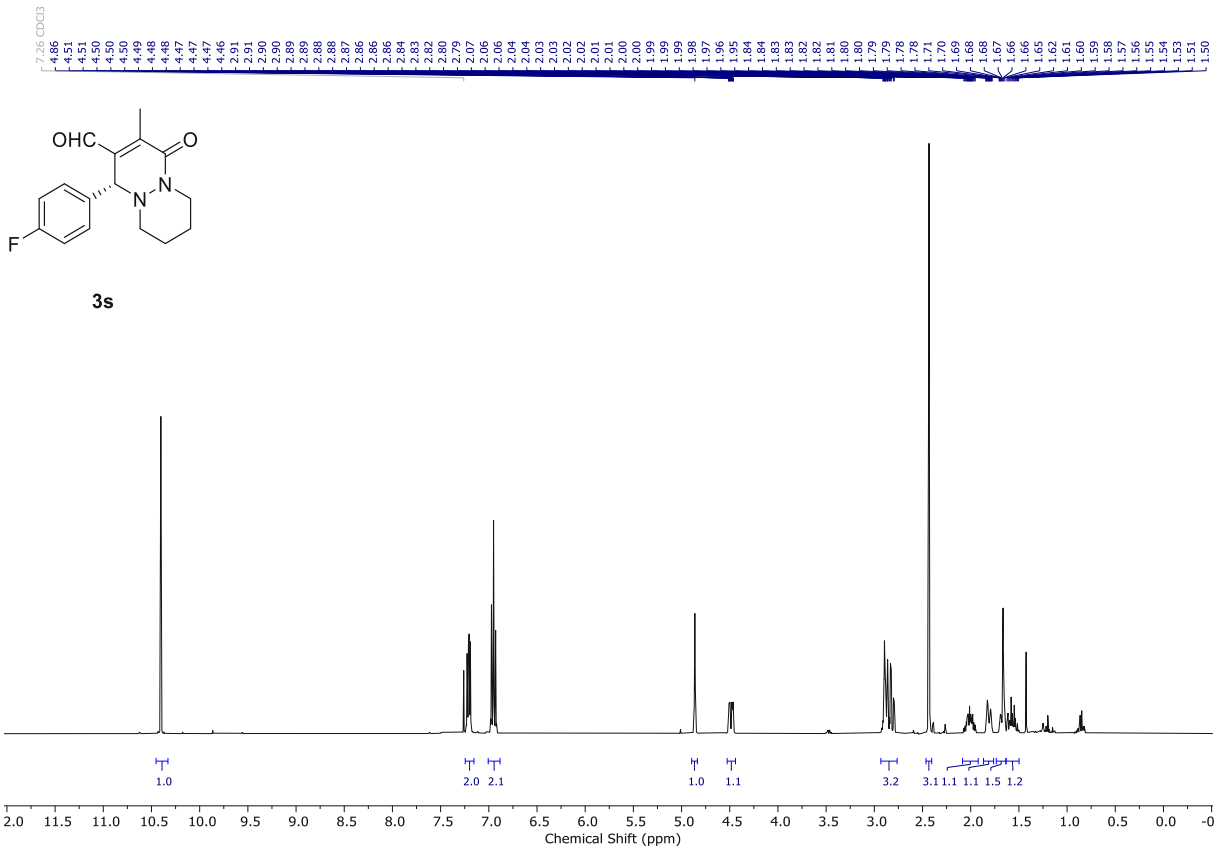
7.4.18 NMR spectra of **3r**



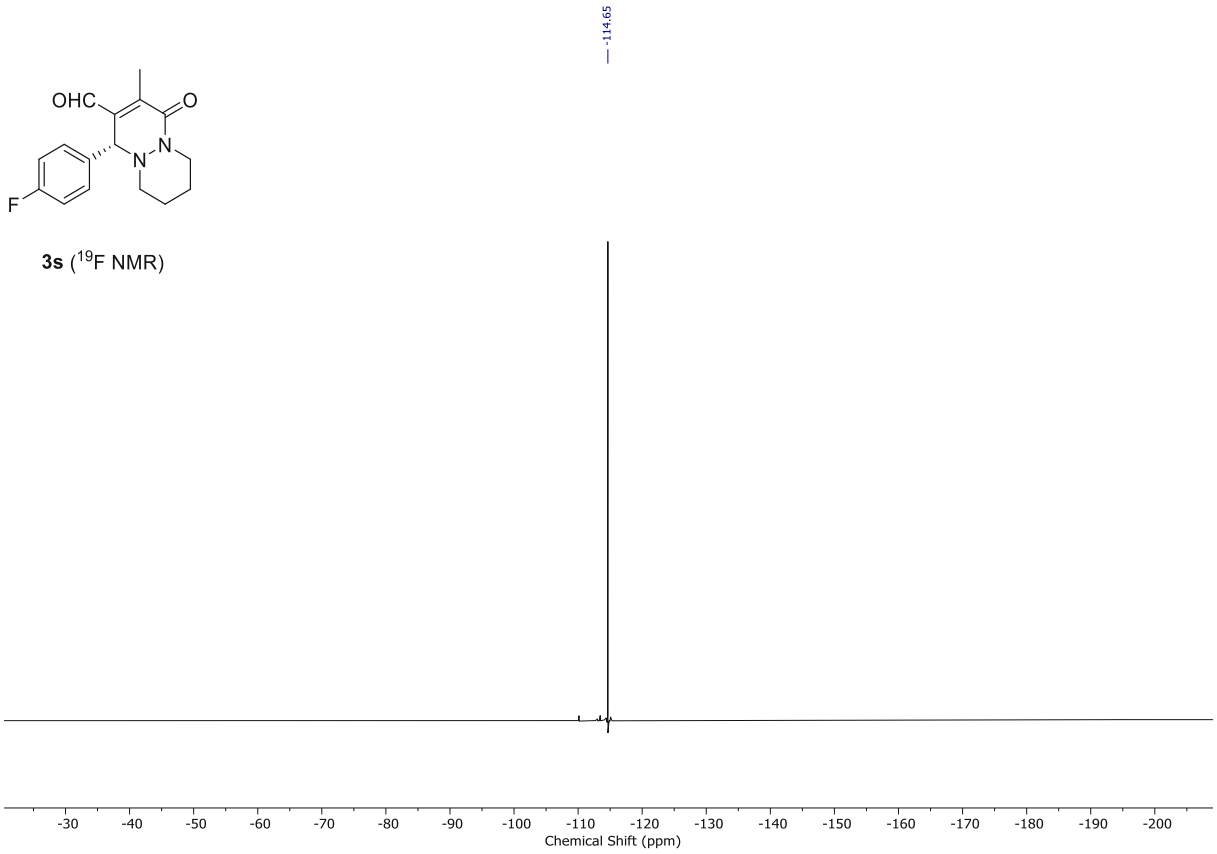
Die approbierte gedruckte Originalversion dieser Dissertation ist an der TU Wien Bibliothek verfügbar.
The approved original version of this doctoral thesis is available in print at TU Wien Bibliothek.



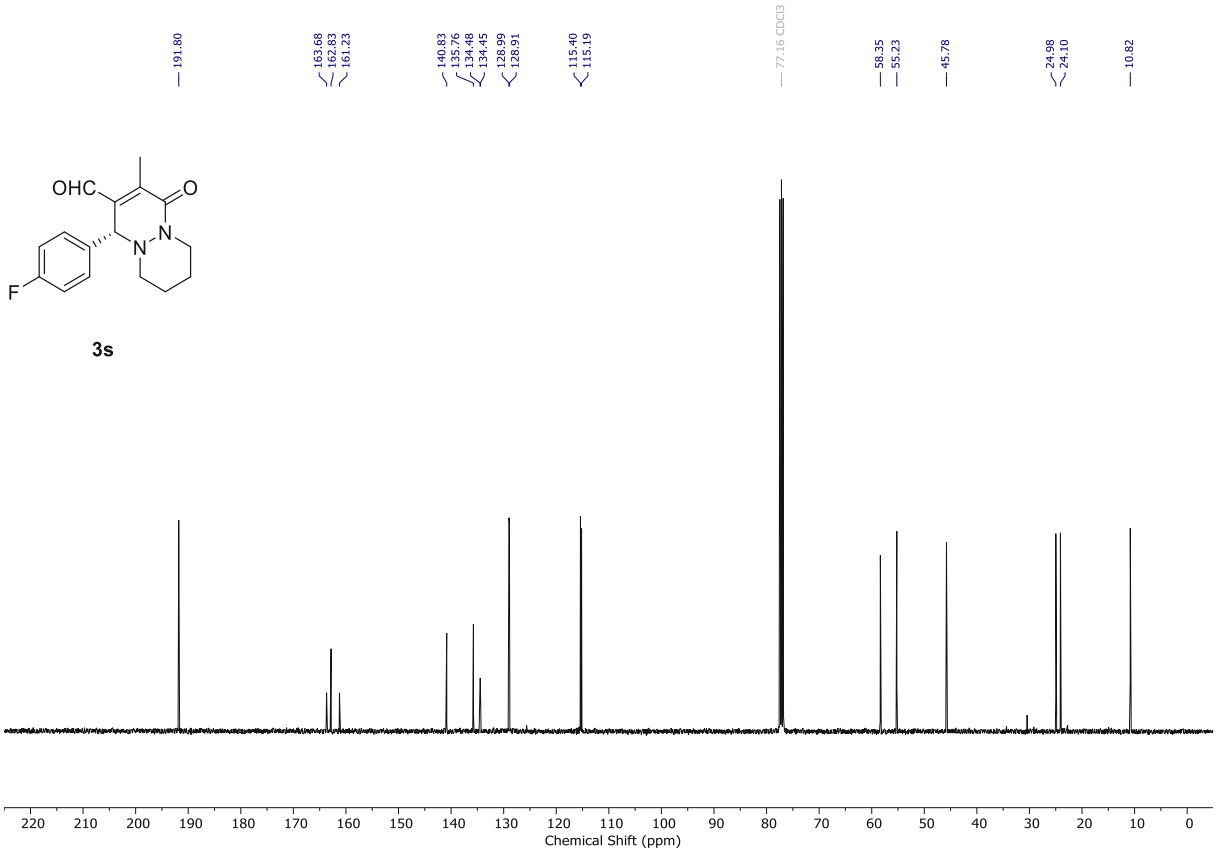
7.4.19 NMR spectra of **3s**



Die approbierte gedruckte Originalversion dieser Dissertation ist an der TU Wien Bibliothek verfügbar.
The approved original version of this doctoral thesis is available in print at TU Wien Bibliothek.
TU Bibliothek Your knowledge hub



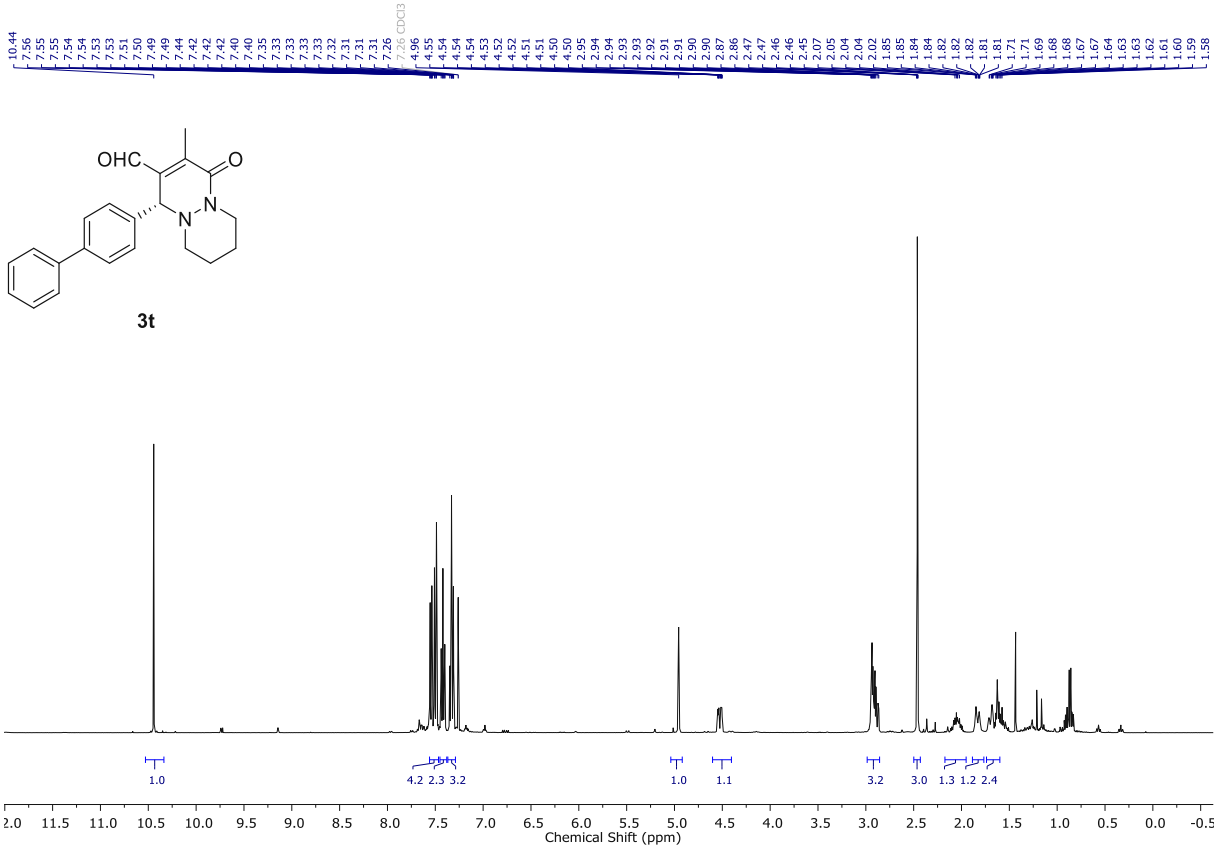
3s (^{19}F NMR)

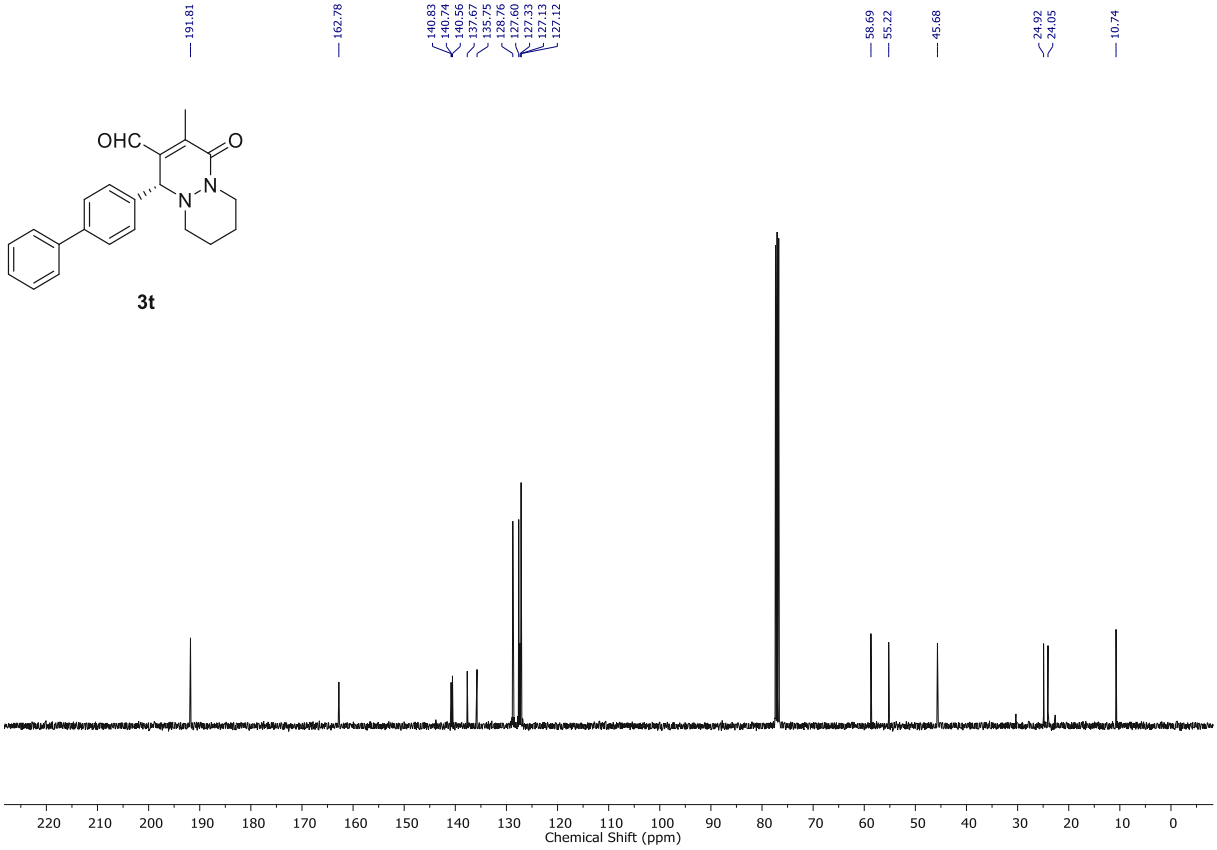


3s

Die approbierte gedruckte Originalversion dieser Dissertation ist an der TU Wien Bibliothek verfügbar.
The approved original version of this doctoral thesis is available in print at TU Wien Bibliothek.

7.4.20 NMR spectra of **3t**

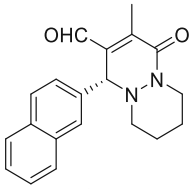




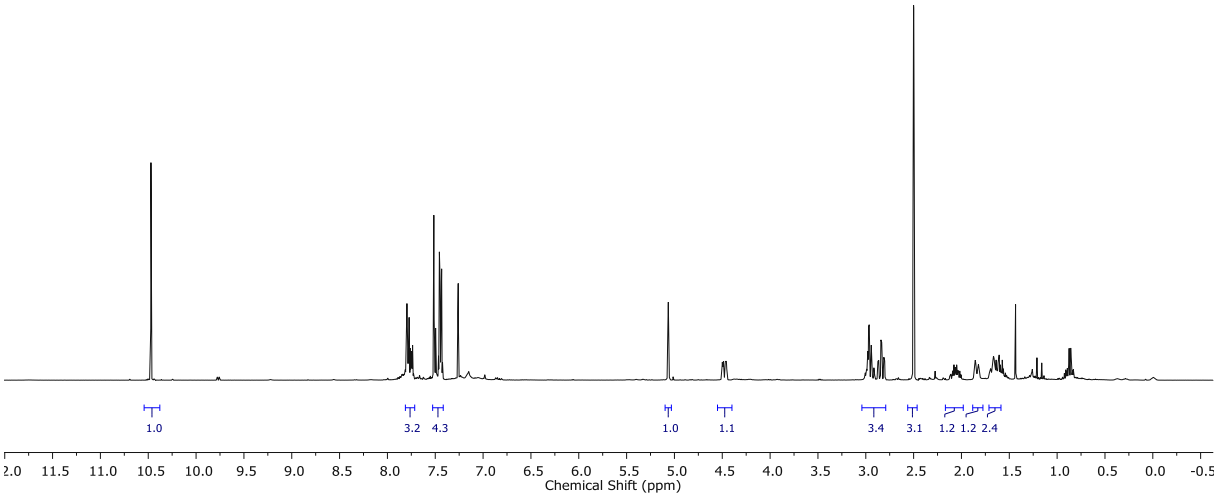
Die approbierte gedruckte Originalversion dieser Dissertation ist an der TU Wien Bibliothek verfügbar.
The approved original version of this doctoral thesis is available in print at TU Wien Bibliothek.

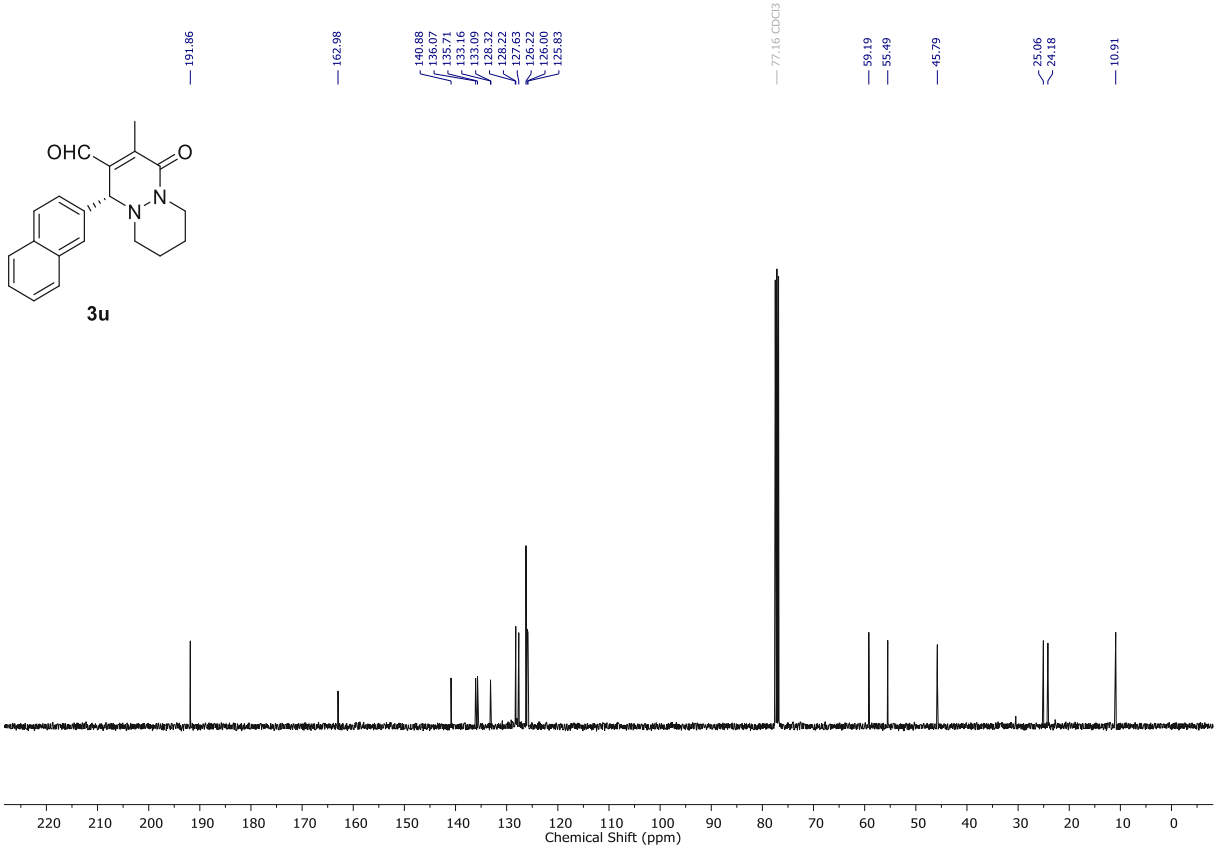
7.4.21 NMR spectra of **3u**





3u

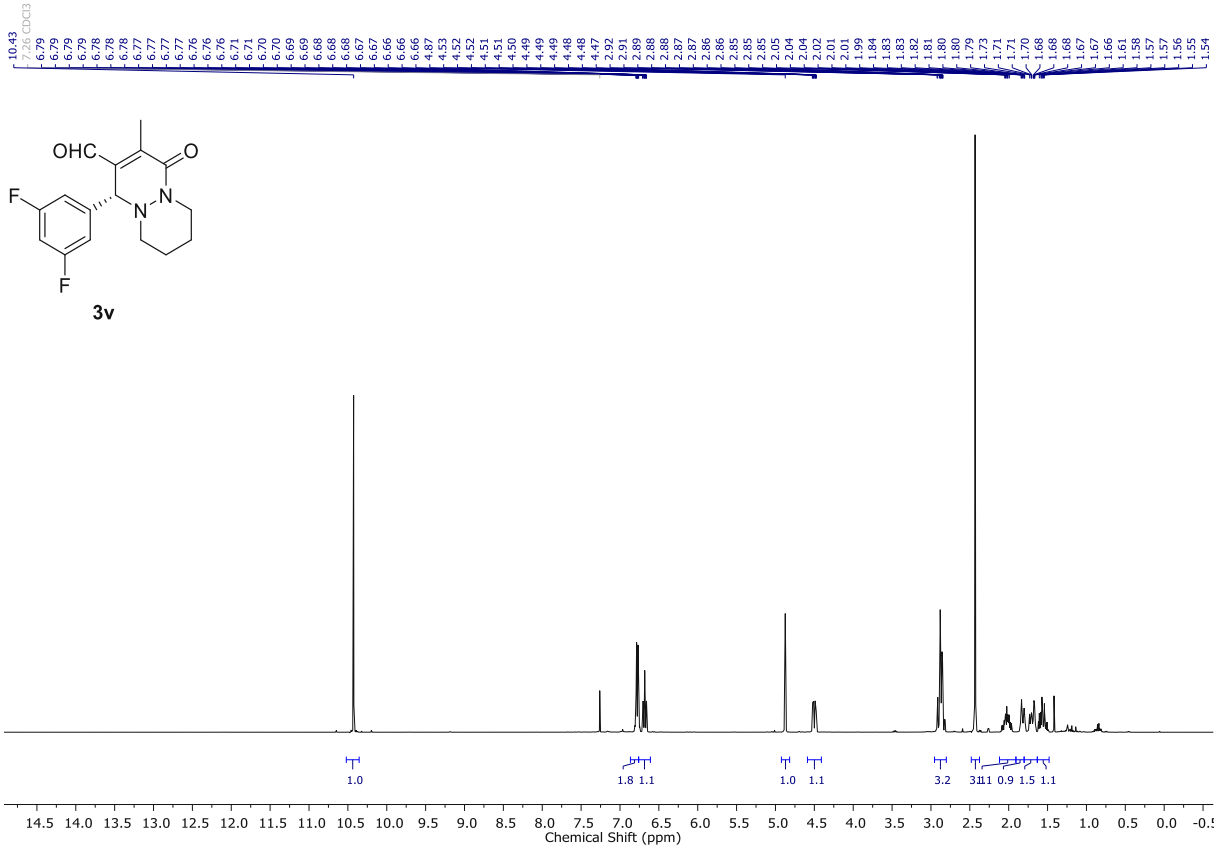


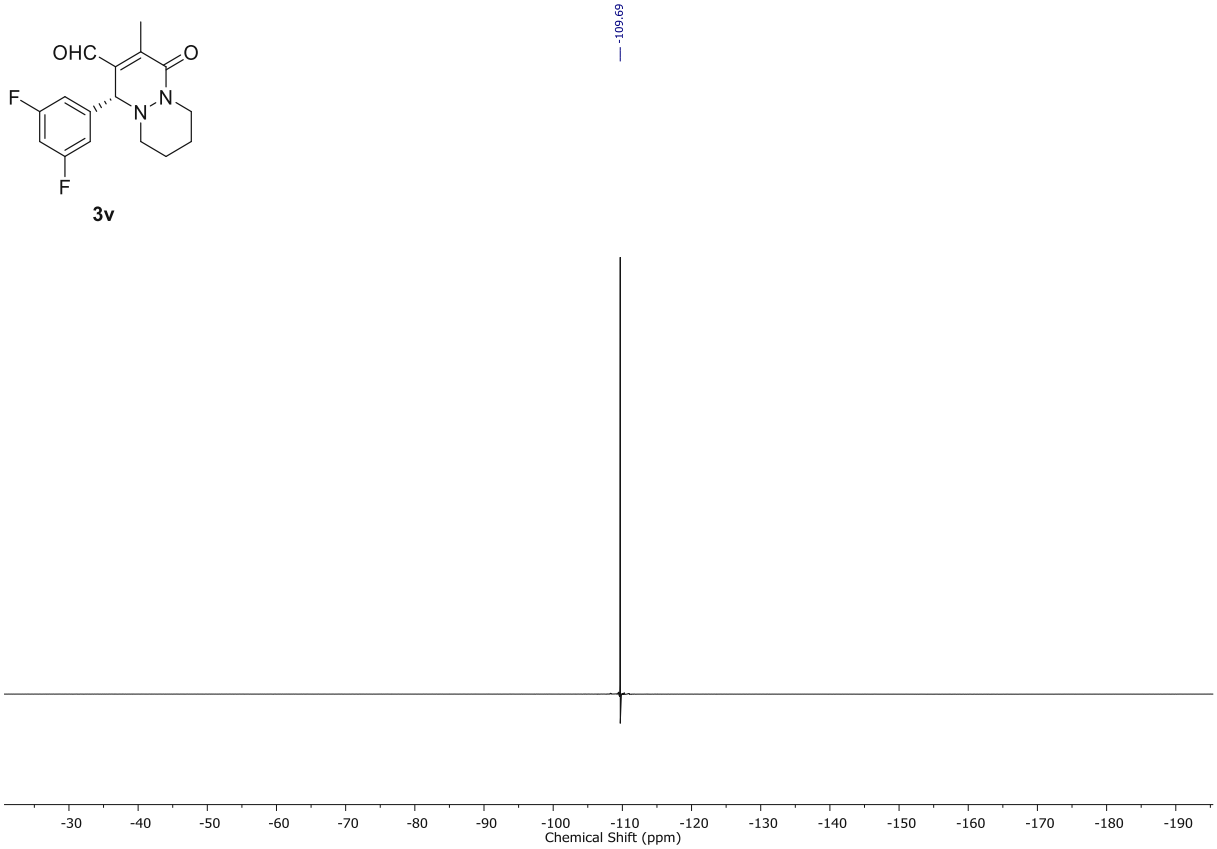


3u

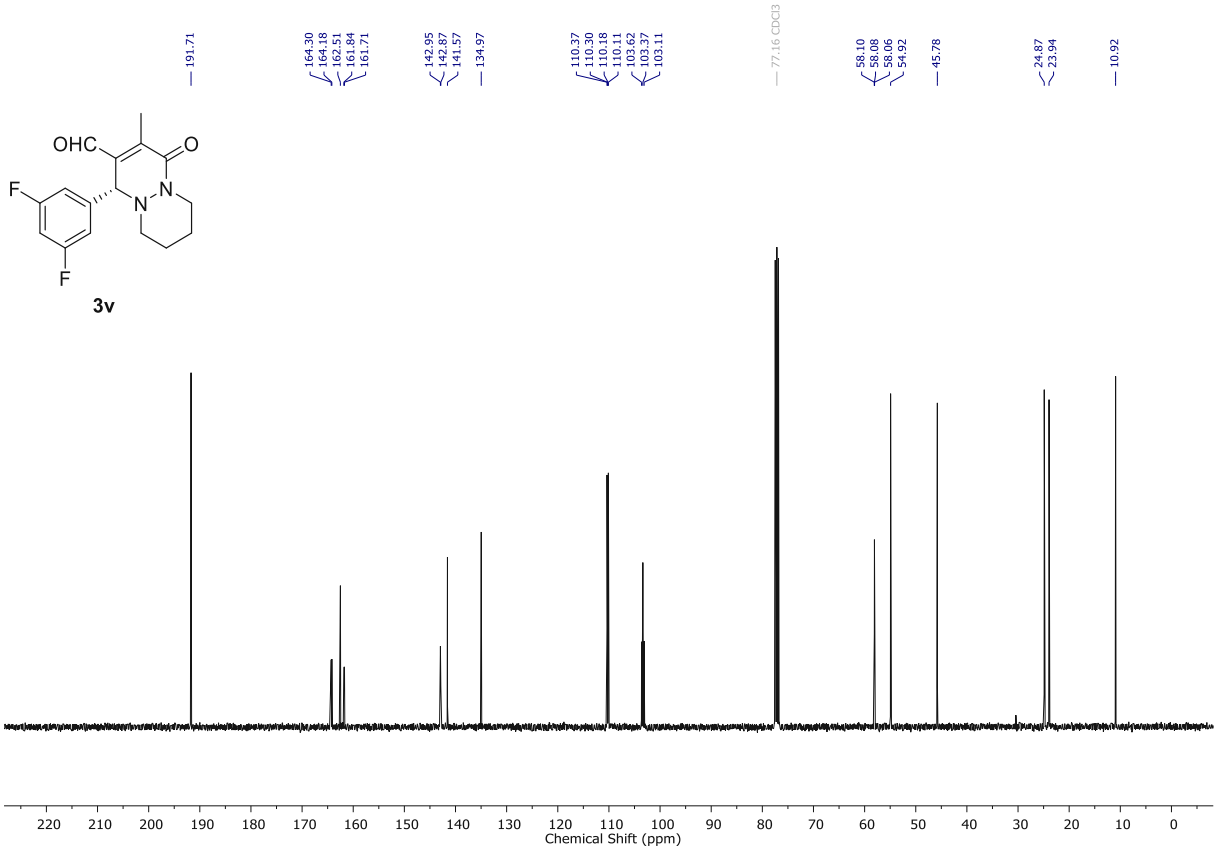
Die approbierte gedruckte Originalversion dieser Dissertation ist an der TU Wien Bibliothek verfügbar.
The approved original version of this doctoral thesis is available in print at TU Wien Bibliothek.

7.4.22 NMR spectra of **3v**

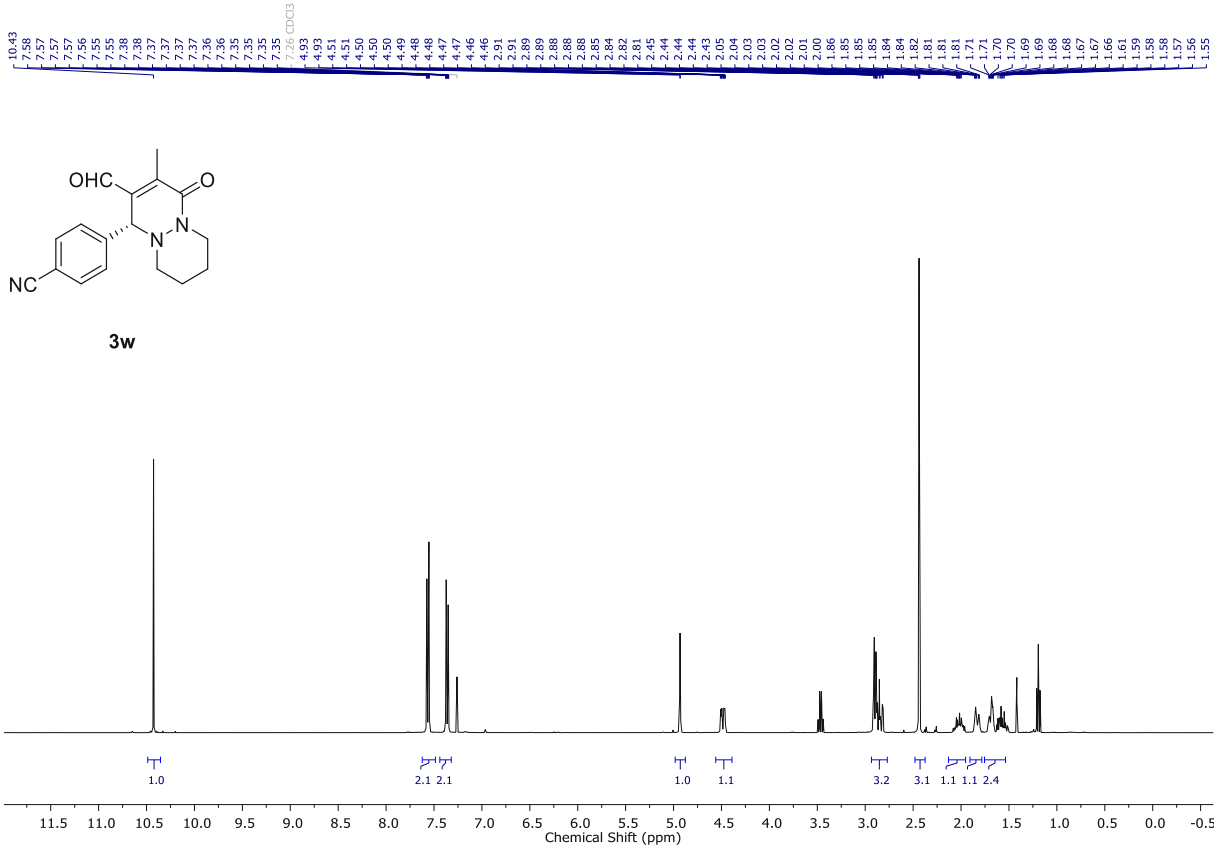




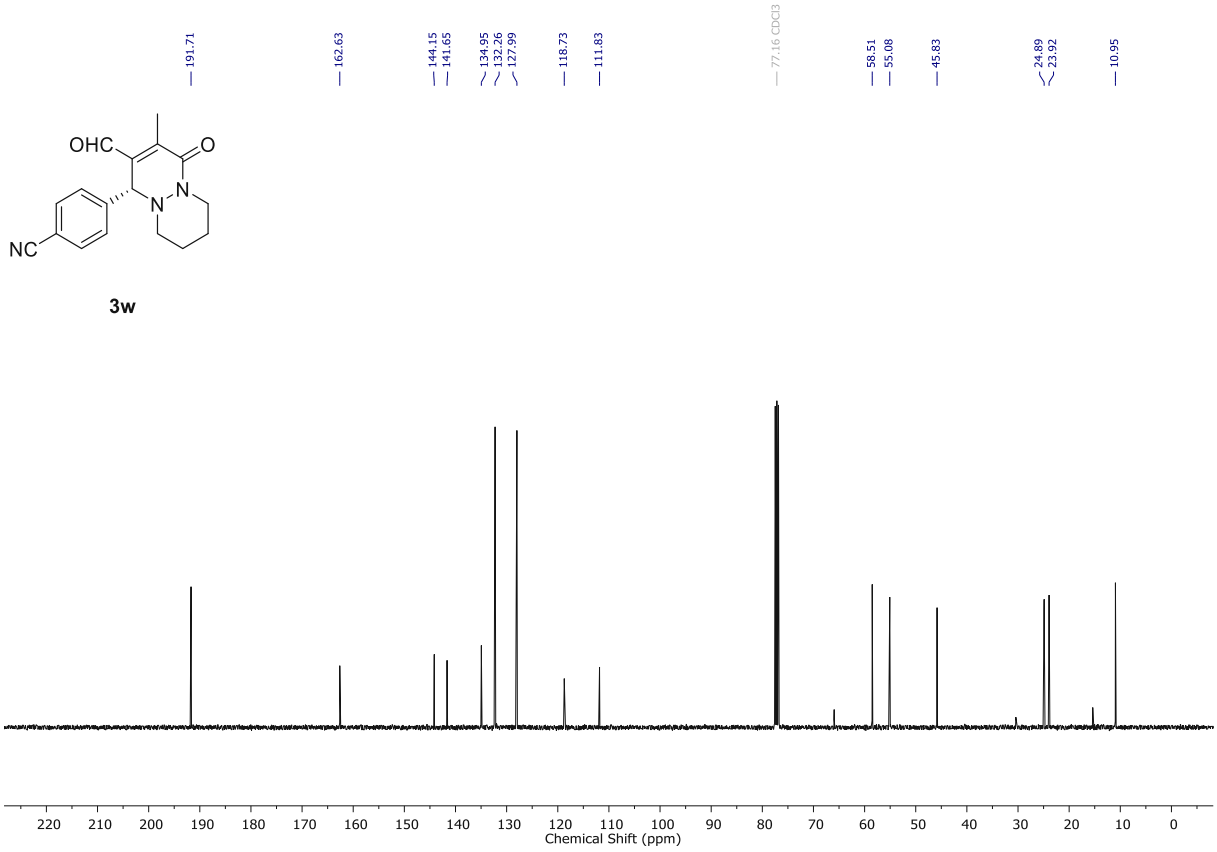
Die approbierte gedruckte Originalversion dieser Dissertation ist an der TU Wien Bibliothek verfügbar.
The approved original version of this doctoral thesis is available in print at TU Wien Bibliothek.



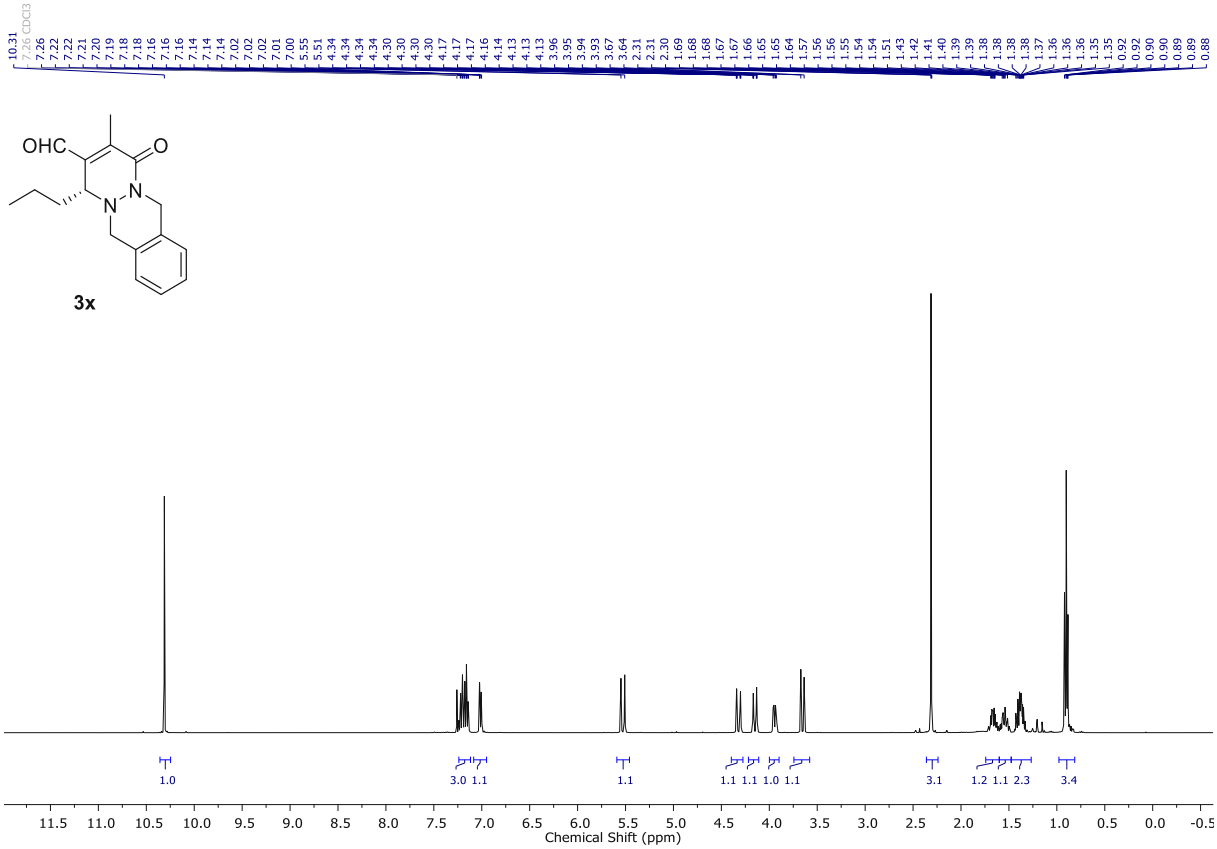
7.4.23 NMR spectra of **3w**



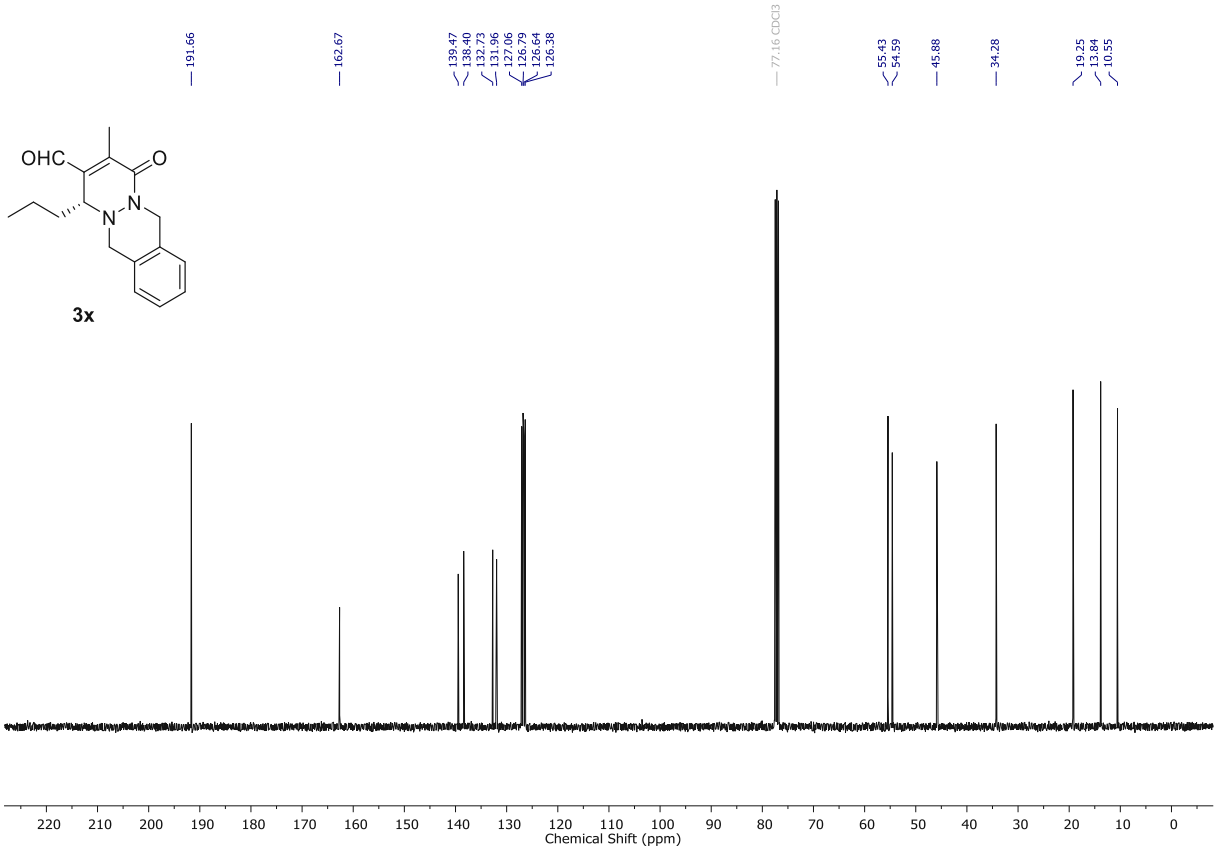
Die approbierte gedruckte Originalversion dieser Dissertation ist an der TU Wien Bibliothek verfügbar.
The approved original version of this doctoral thesis is available in print at TU Wien Bibliothek.



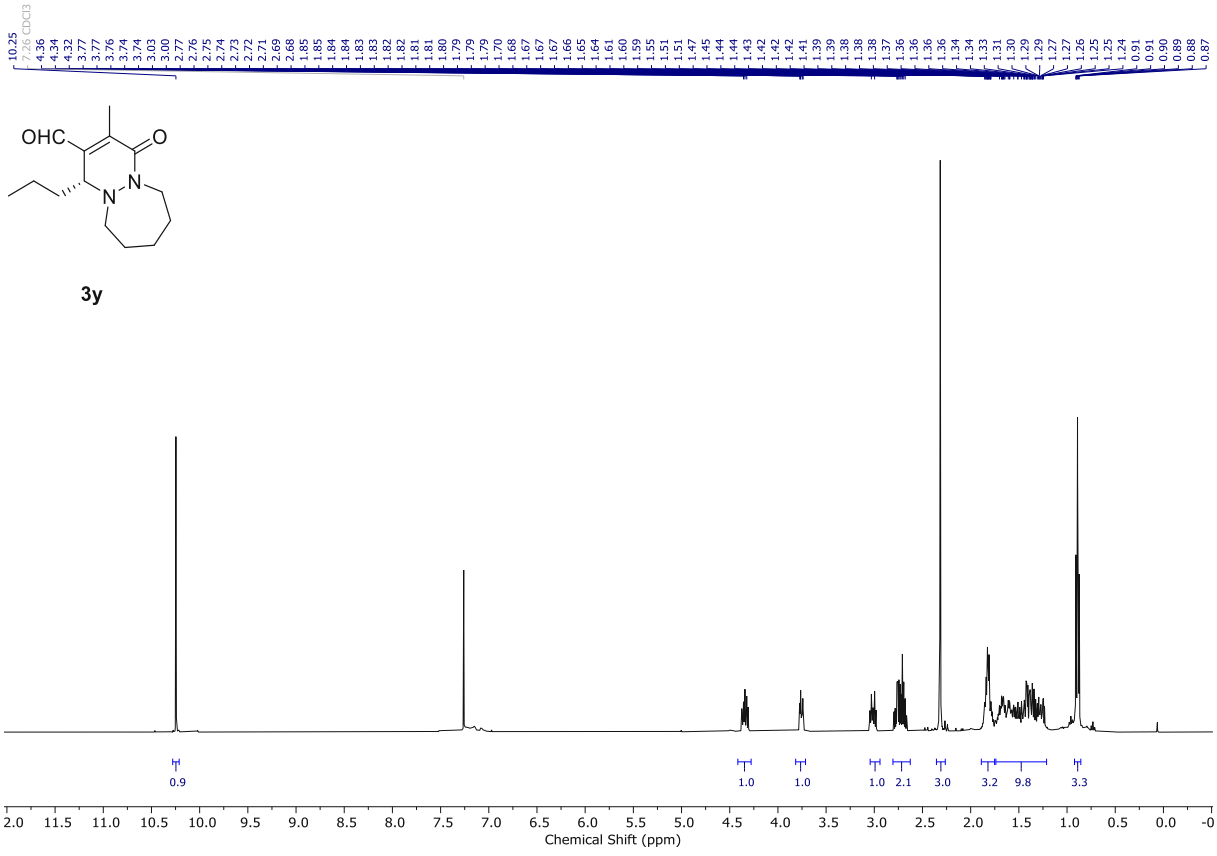
7.4.24 NMR spectra of **3x**



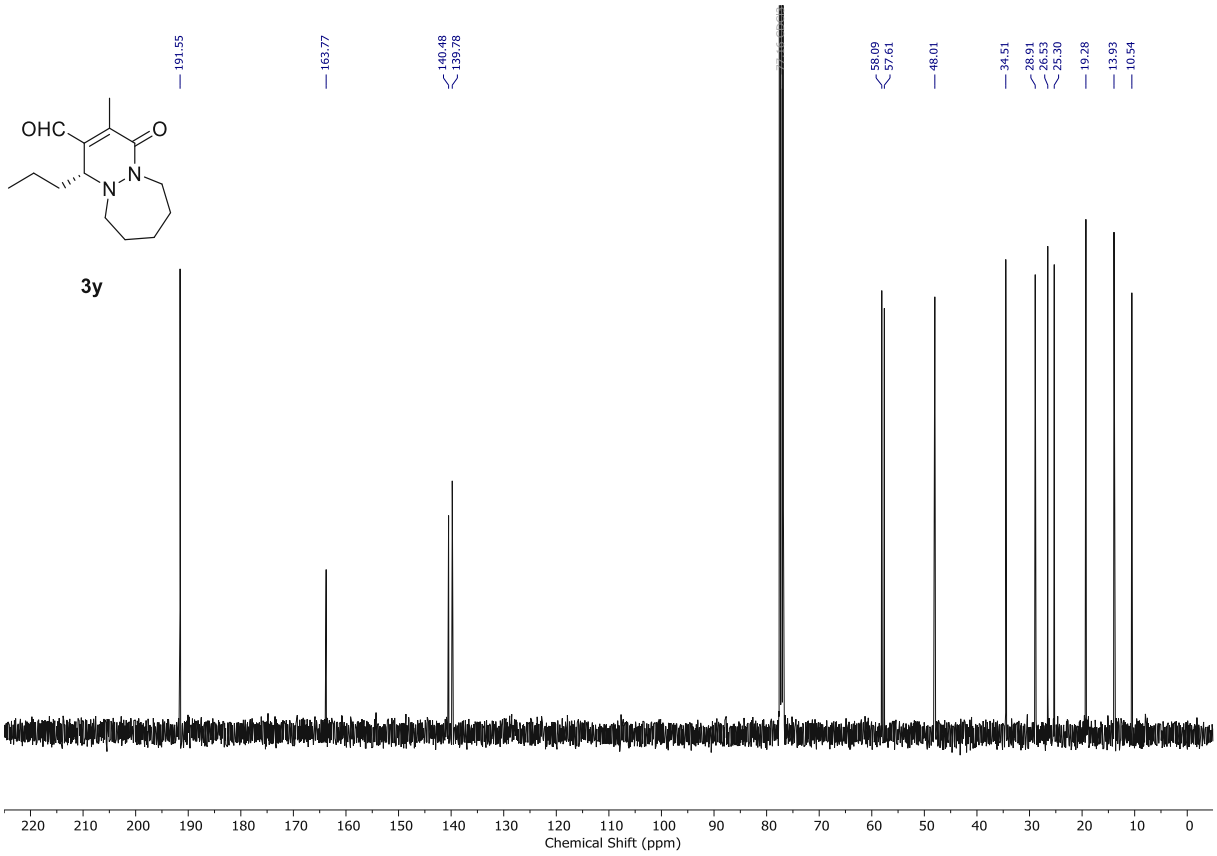
Die approbierte gedruckte Originalversion dieser Dissertation ist an der TU Wien Bibliothek verfügbar.
The approved original version of this doctoral thesis is available in print at TU Wien Bibliothek.



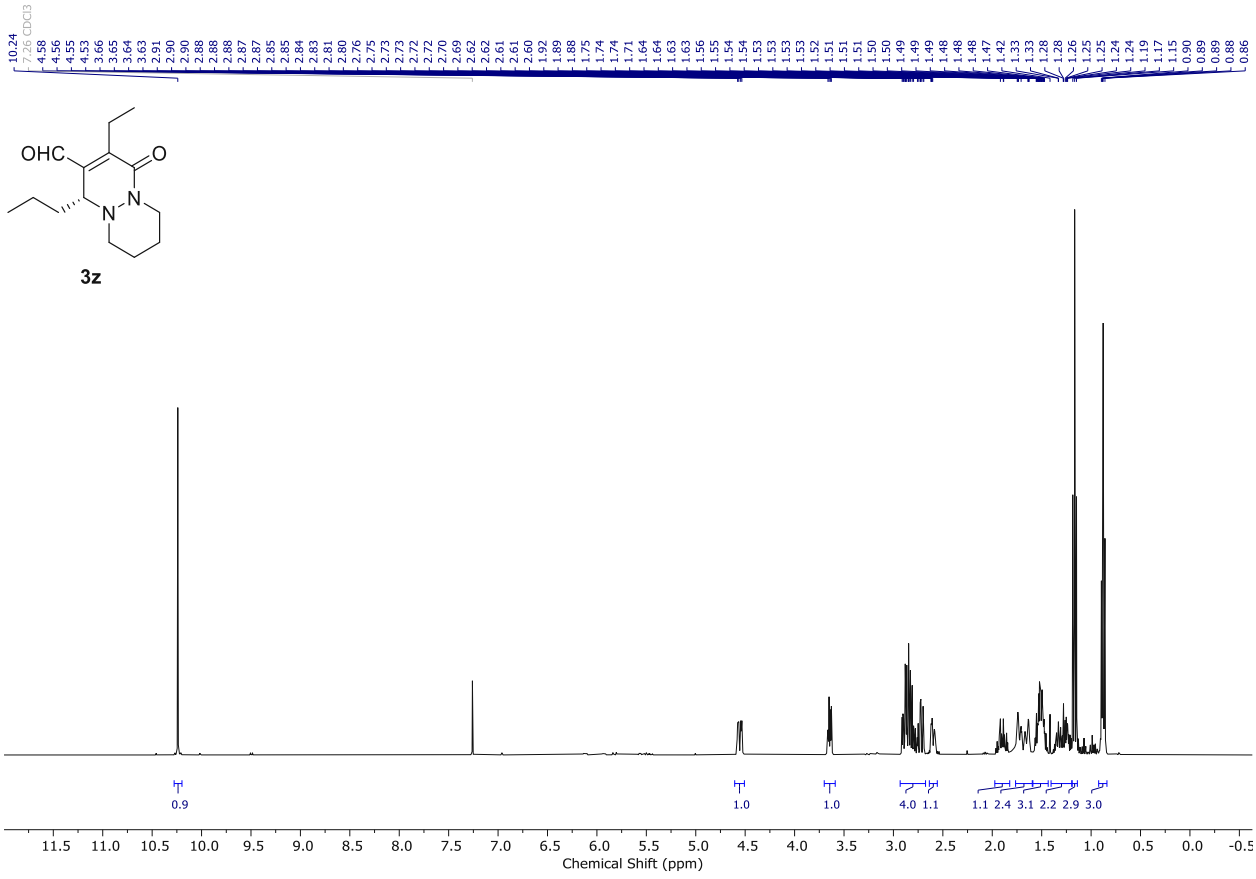
7.4.25 NMR spectra of **3y**



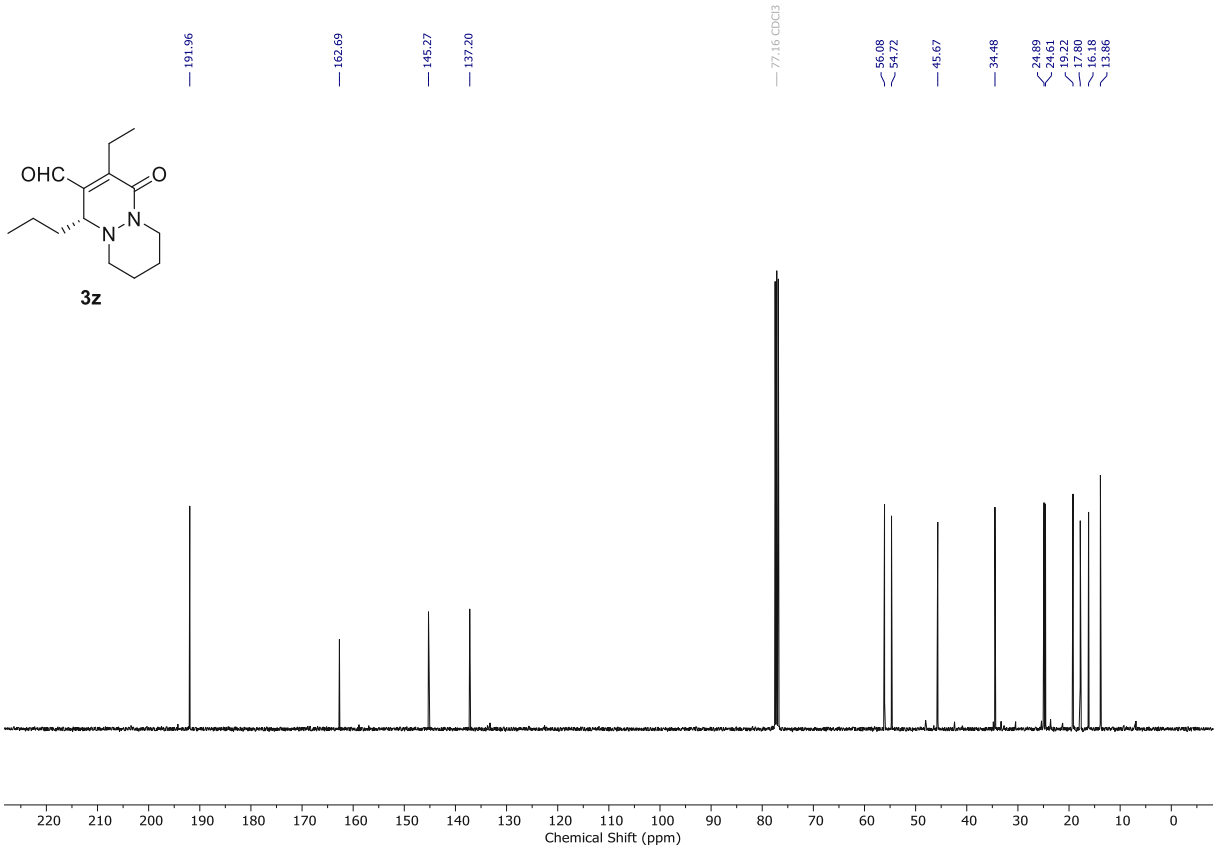
Die approbierte gedruckte Originalversion dieser Dissertation ist an der TU Wien Bibliothek verfügbar.
The approved original version of this doctoral thesis is available in print at TU Wien Bibliothek.



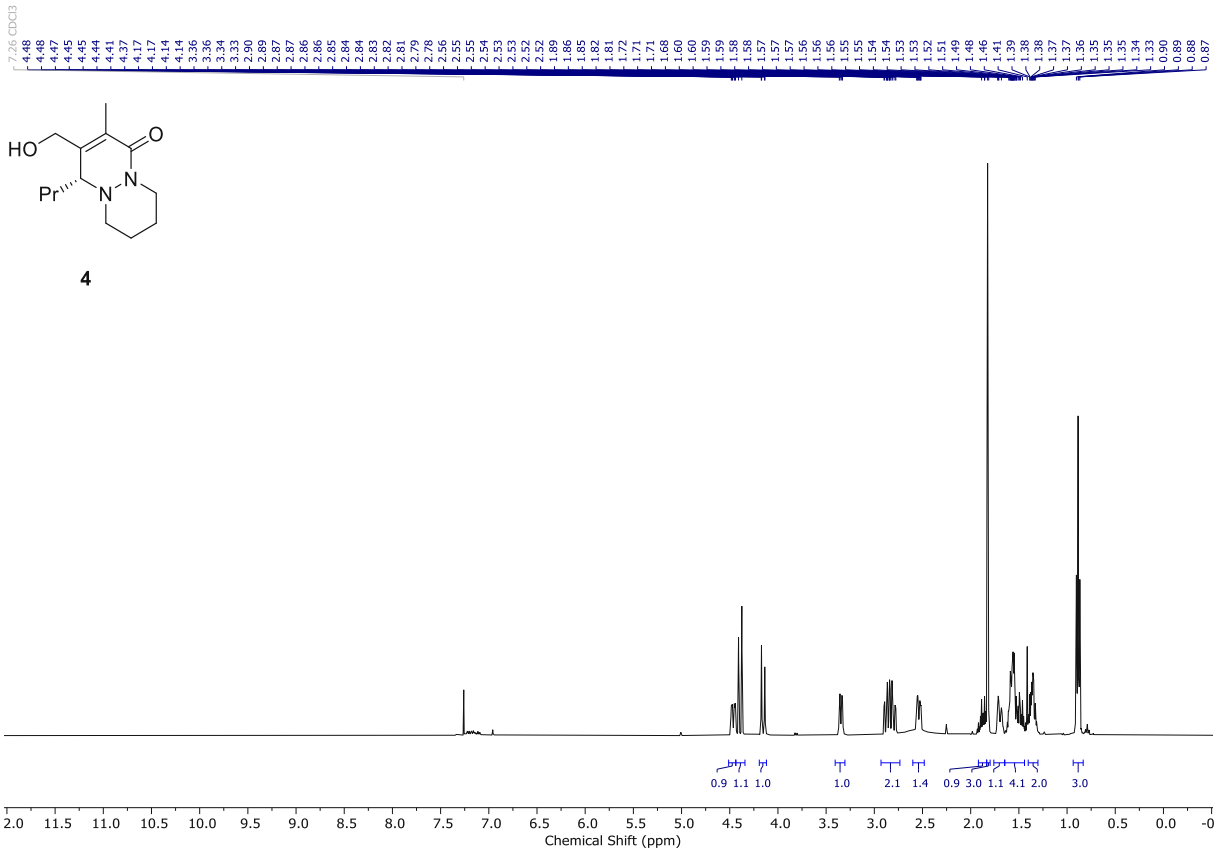
7.4.26 NMR spectra of **3z**



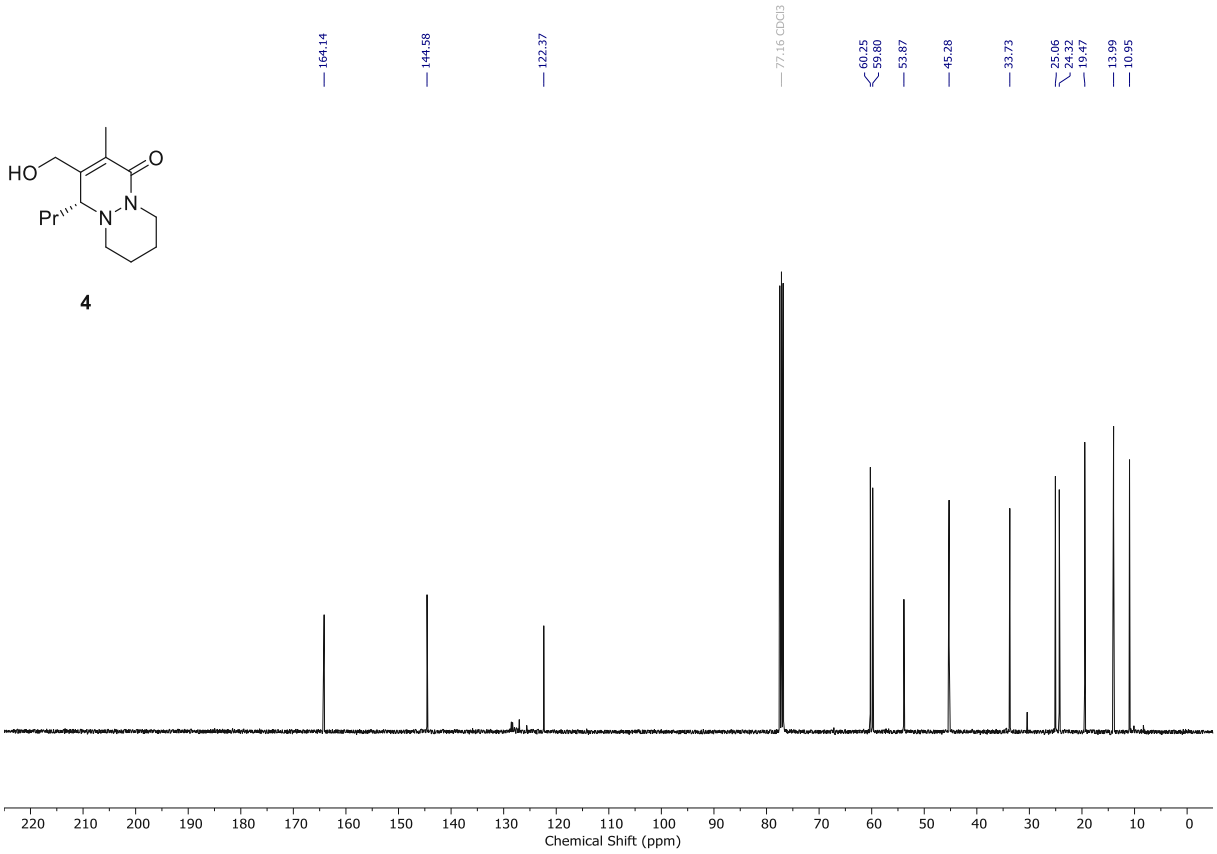
Die approbierte gedruckte Originalversion dieser Dissertation ist an der TU Wien Bibliothek verfügbar.
The approved original version of this doctoral thesis is available in print at TU Wien Bibliothek.



7.4.27 NMR spectra of **4**

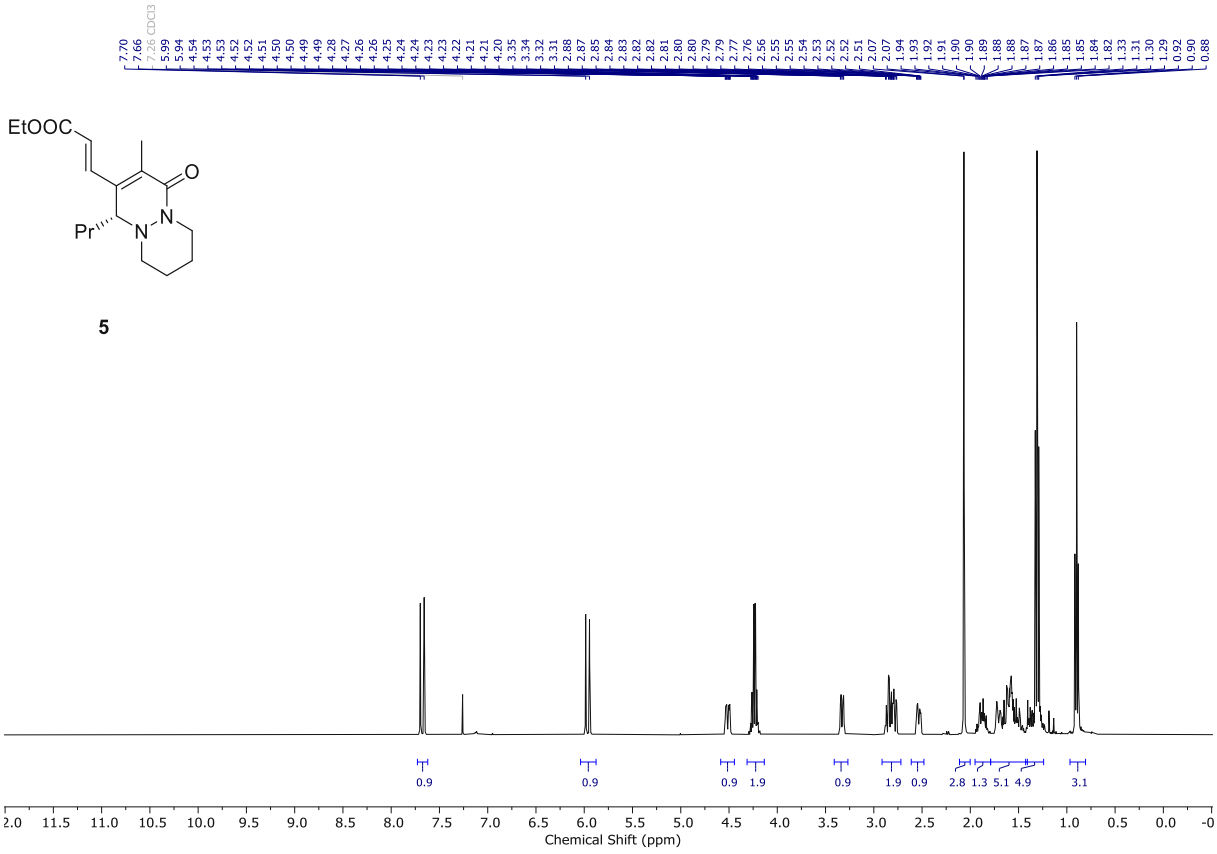


Die approbierte gedruckte Originalversion dieser Dissertation ist an der TU Wien Bibliothek verfügbar.
The approved original version of this doctoral thesis is available in print at TU Wien Bibliothek.

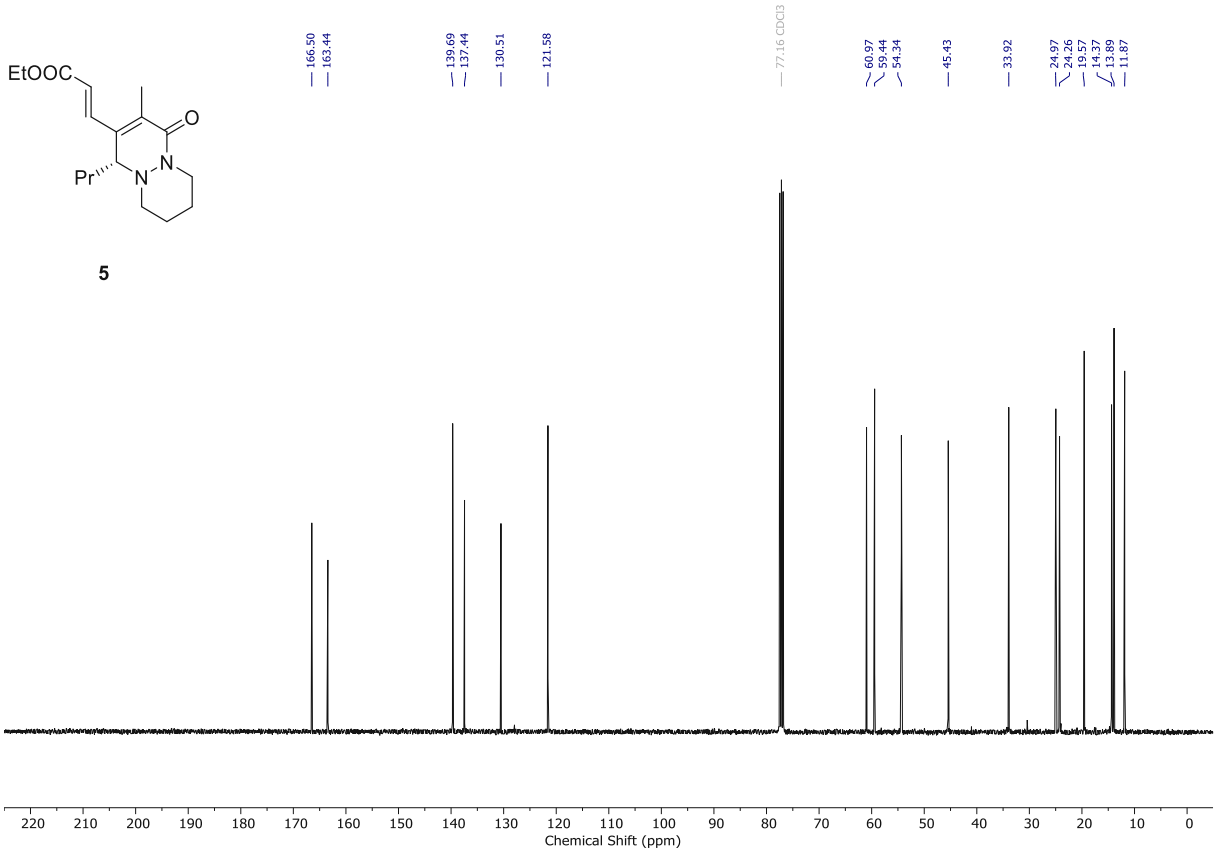


4

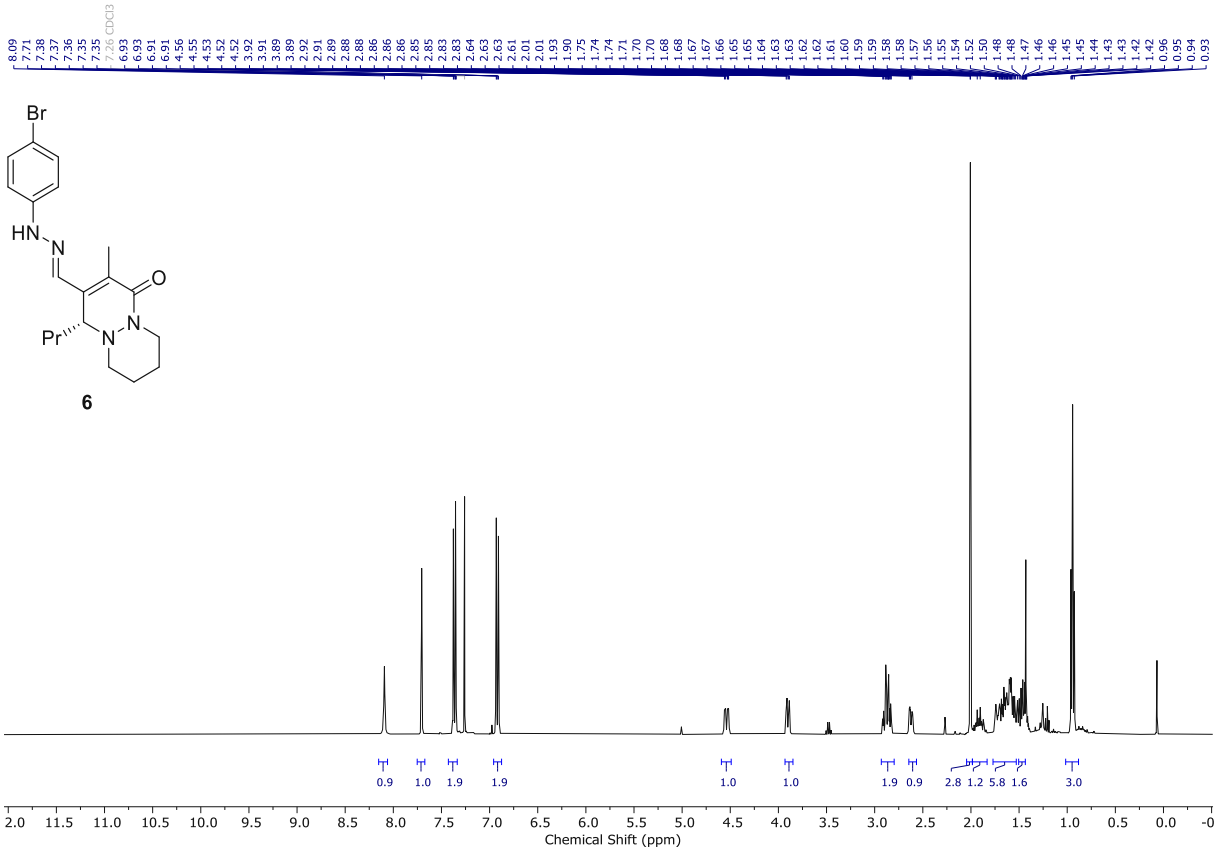
7.4.28 NMR spectra of **5**



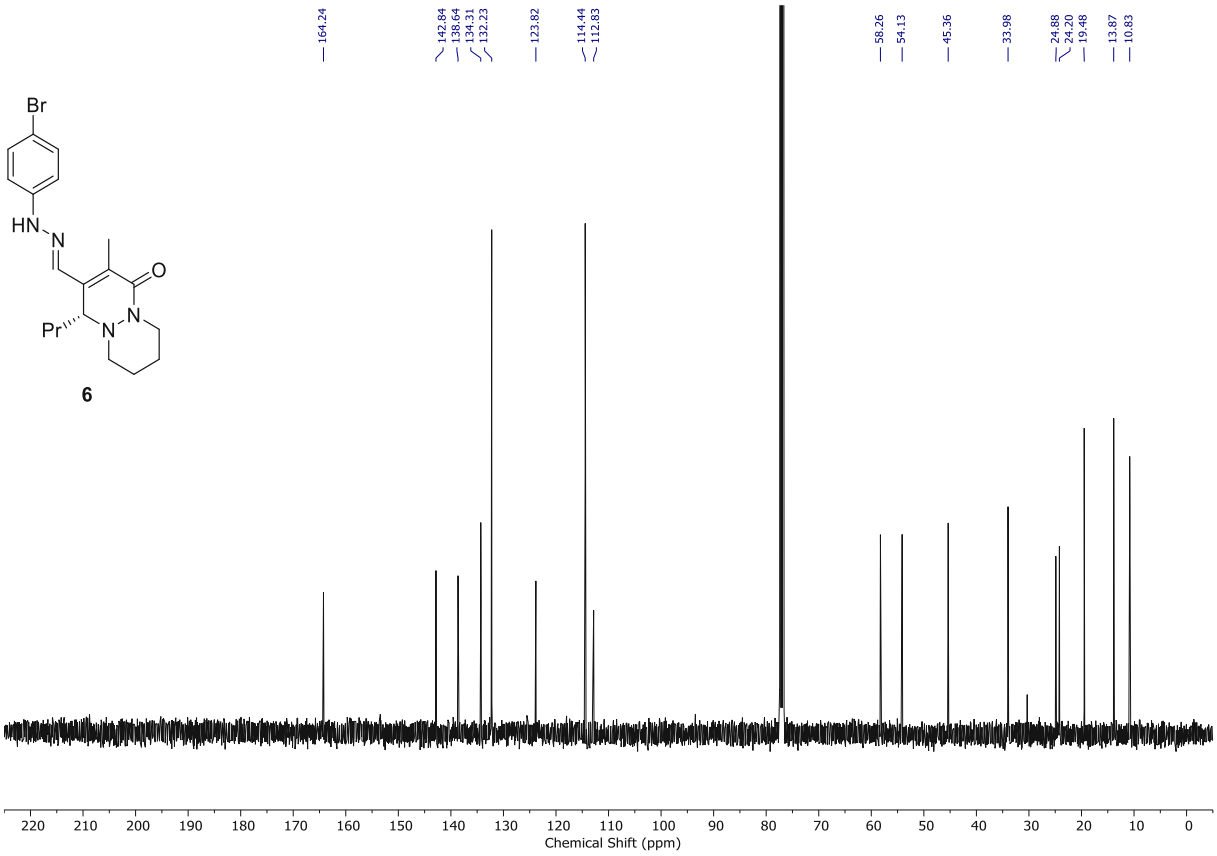
Die approbierte gedruckte Originalversion dieser Dissertation ist an der TU Wien Bibliothek verfügbar.
The approved original version of this doctoral thesis is available in print at TU Wien Bibliothek.



7.4.29 NMR spectra of **6**



Die approbierte gedruckte Originalversion dieser Dissertation ist an der TU Wien Bibliothek verfügbar.
The approved original version of this doctoral thesis is available in print at TU Wien Bibliothek.

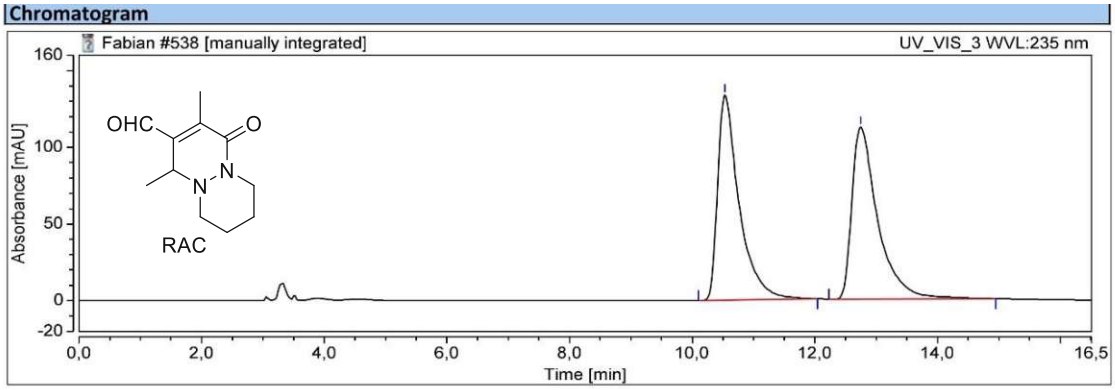


6

Die approbierte gedruckte Originalversion dieser Dissertation ist an der TU Wien Bibliothek verfügbar.
The approved original version of this doctoral thesis is available in print at TU Wien Bibliothek.

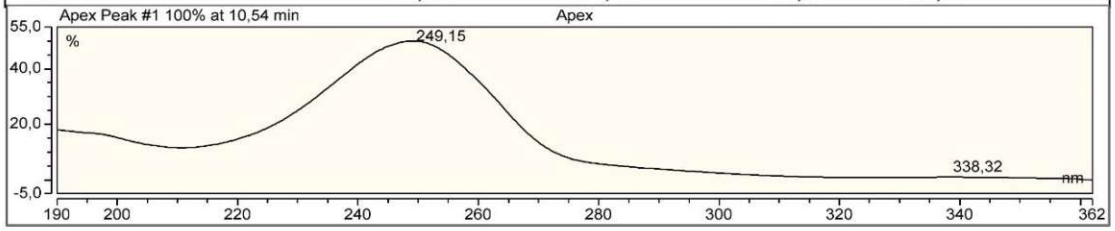
8 HPLC spectra

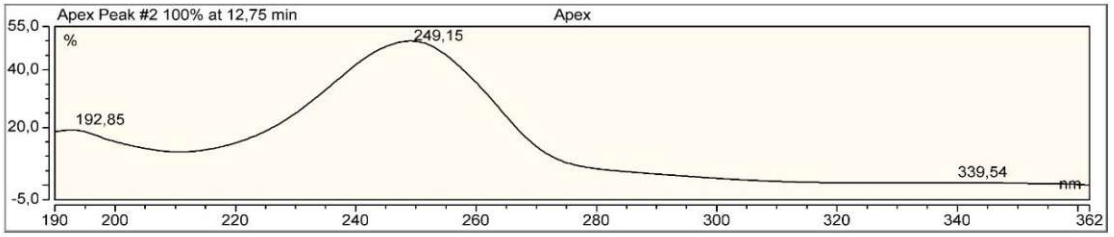
8.1.1 HPLC spectra of **3a**



Integration Results

No.	Peak Name	Retention Time min	Area mAU*min	Height mAU	Relative Area %	Relative Height %	Amount n.a.
1		10,535	54,442	134,173	49,82	54,44	n.a.
2		12,748	54,825	112,277	50,18	45,56	n.a.
Total:			**109,266**	**246,450**	**100,00**	**100,00**	



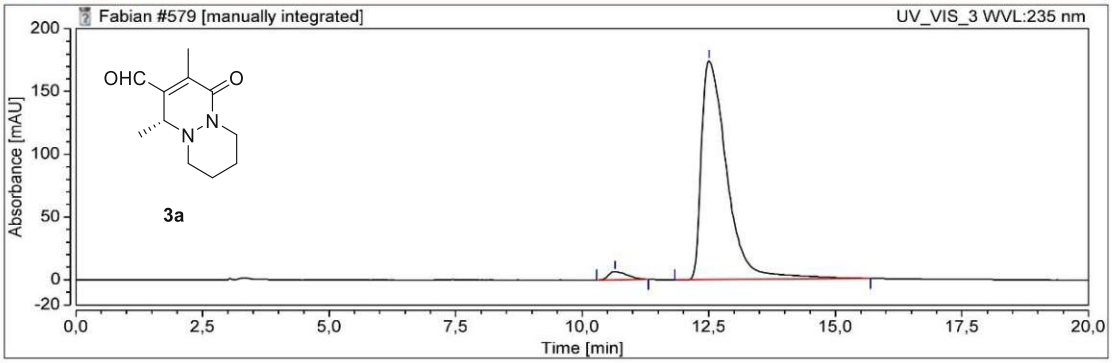


Reports IJD/Integration

Chromeleon (c) Dionex
Version 7.1.1.1127

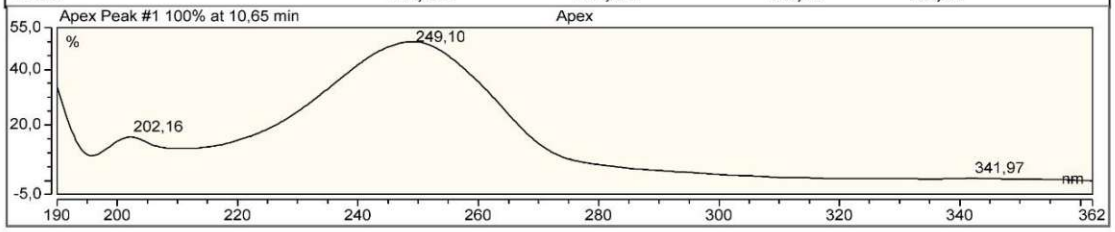
Die approbierte gedruckte Originalversion dieser Dissertation ist an der TU Wien Bibliothek verfügbar.
The approved original version of this doctoral thesis is available in print at TU Wien Bibliothek.

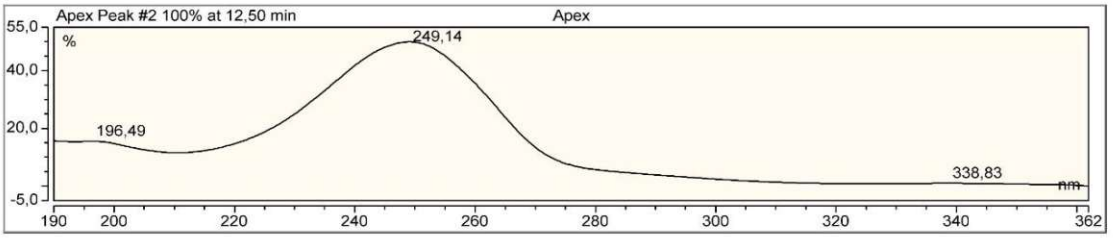
Chromatogram



Integration Results

No.	Peak Name	Retention Time min	Area mAU*min	Height mAU	Relative Area %	Relative Height %	Amount n.a.
1		10,645	2,751	6,652	2,65	3,67	n.a.
2		12,502	101,141	174,375	97,35	96,33	n.a.
Total:			**103,892**	**181,027**	**100,00**	**100,00**	



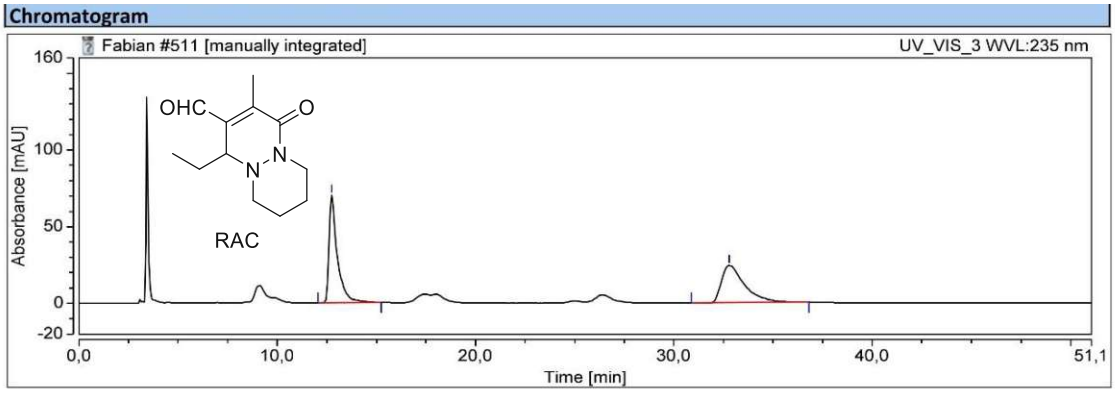


Reports IJD/Integration

Chromeleon (c) Dionex
Version 7.1.1.1127

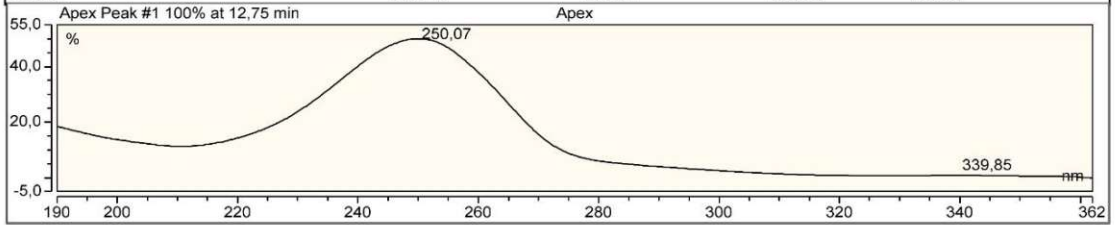
Die approbierte gedruckte Originalversion dieser Dissertation ist an der TU Wien Bibliothek verfügbar.
The approved original version of this doctoral thesis is available in print at TU Wien Bibliothek.

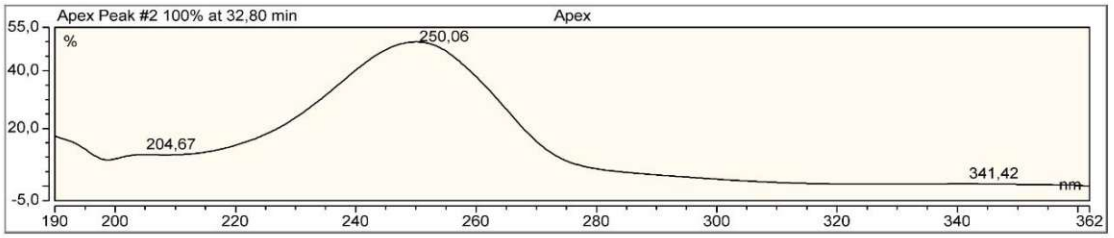
8.1.2 HPLC spectra of **3b**



Integration Results

No.	Peak Name	Retention Time min	Area mAU*min	Height mAU	Relative Area %	Relative Height %	Amount n.a.
1		12,748	34,532	70,235	51,20	74,30	n.a.
2		32,797	32,908	24,289	48,80	25,70	n.a.
Total:			**67,440**	**94,524**	**100,00**	**100,00**	



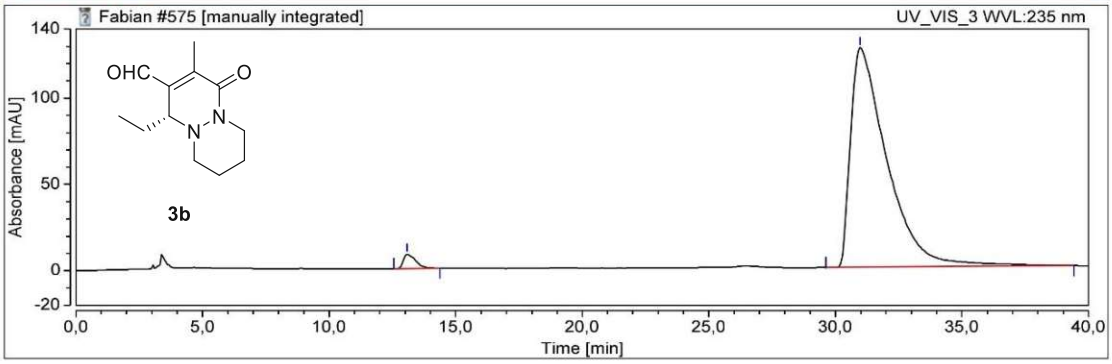


Reports IJD/Integration

Chromeleon (c) Dionex
Version 7.1.1.1127

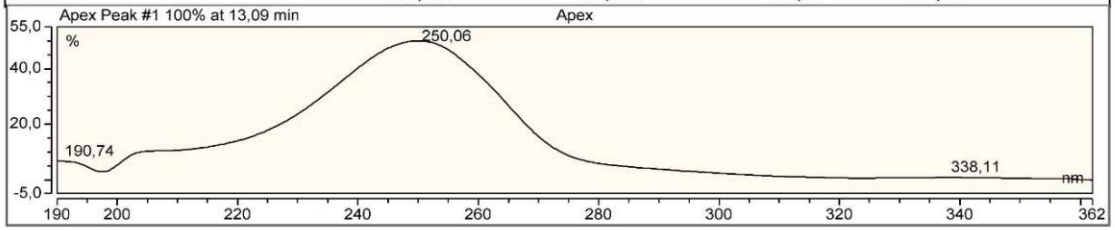
Die approbierte gedruckte Originalversion dieser Dissertation ist an der TU Wien Bibliothek verfügbar.
The approved original version of this doctoral thesis is available in print at TU Wien Bibliothek.

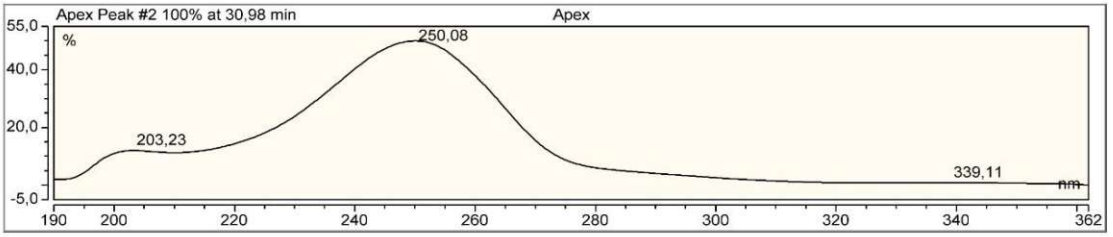
Chromatogram



Integration Results

No.	Peak Name	Retention Time min	Area mAU*min	Height mAU	Relative Area %	Relative Height %	Amount n.a.
1		13,085	4,524	8,258	2,09	6,09	n.a.
2		30,978	212,375	127,377	97,91	93,91	n.a.
Total:			**216,899**	**135,635**	**100,00**	**100,00**	



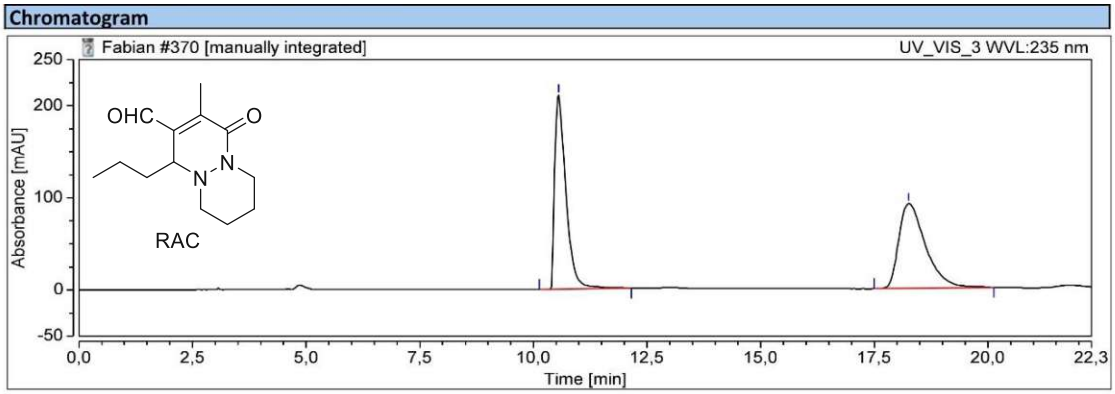


Reports IJD/Integration

Chromeleon (c) Dionex
Version 7.1.1.1127

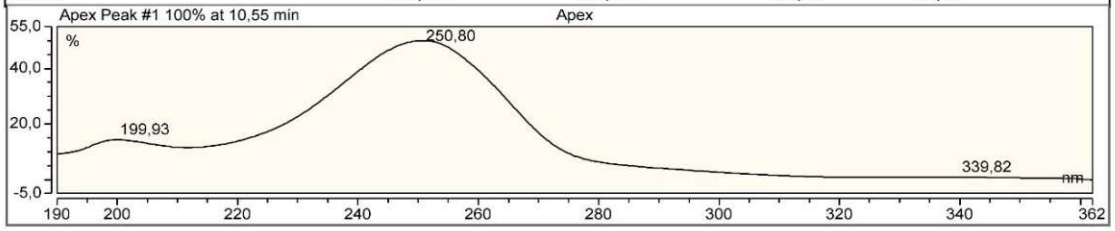
Die approbierte gedruckte Originalversion dieser Dissertation ist an der TU Wien Bibliothek verfügbar.
The approved original version of this doctoral thesis is available in print at TU Wien Bibliothek.

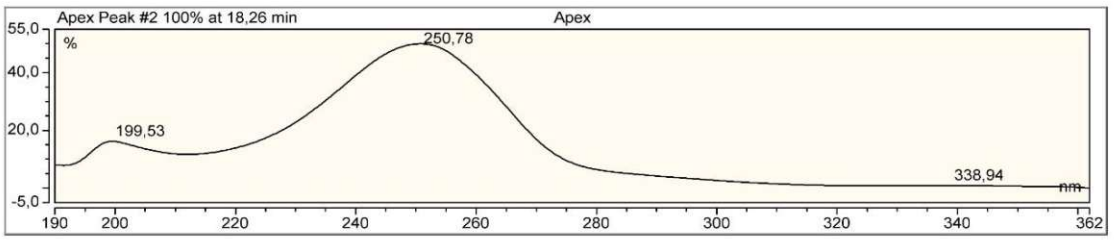
8.1.3 HPLC spectra of **3c**



Integration Results

No.	Peak Name	Retention Time min	Area mAU*min	Height mAU	Relative Area %	Relative Height %	Amount n.a.
1		10,547	60,145	210,897	48,88	69,53	n.a.
2		18,258	62,910	92,427	51,12	30,47	n.a.
Total:			**123,054**	**303,324**	**100,00**	**100,00**	



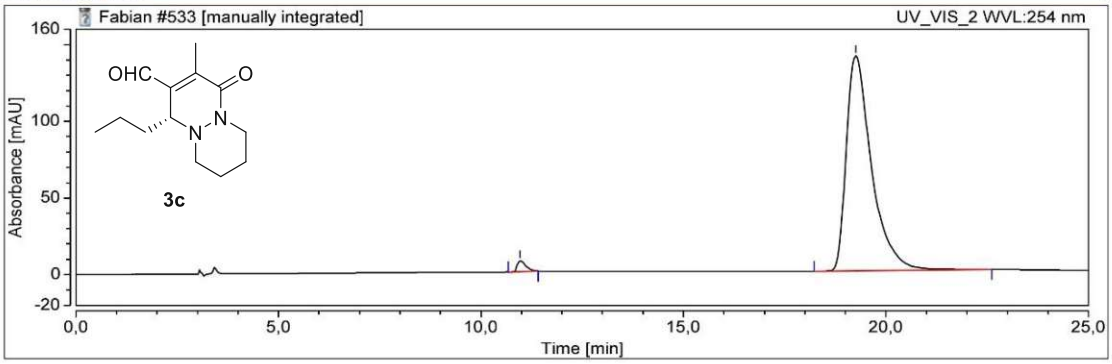


Reports IJD/Integration

Chromeleon (c) Dionex
Version 7.1.1.1127

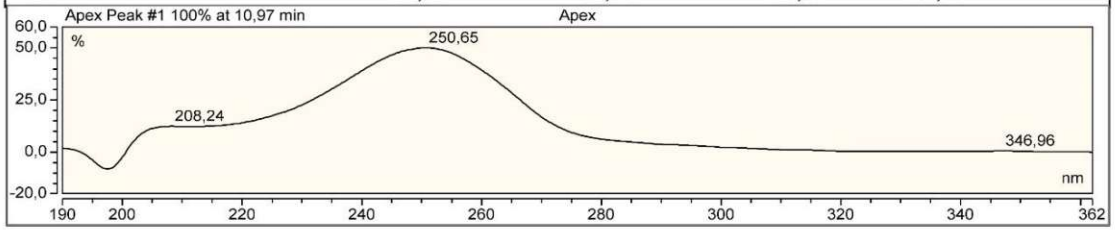
Die approbierte gedruckte Originalversion dieser Dissertation ist an der TU Wien Bibliothek verfügbar.
The approved original version of this doctoral thesis is available in print at TU Wien Bibliothek.

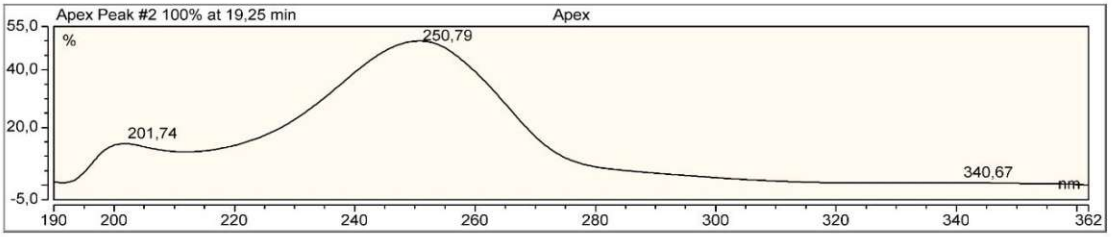
Chromatogram



Integration Results

No.	Peak Name	Retention Time min	Area mAU*min	Height mAU	Relative Area %	Relative Height %	Amount n.a.
1		10,970	1,698	7,028	1,64	4,77	n.a.
2		19,252	101,529	140,222	98,36	95,23	n.a.
Total:			**103,227**	**147,250**	**100,00**	**100,00**	





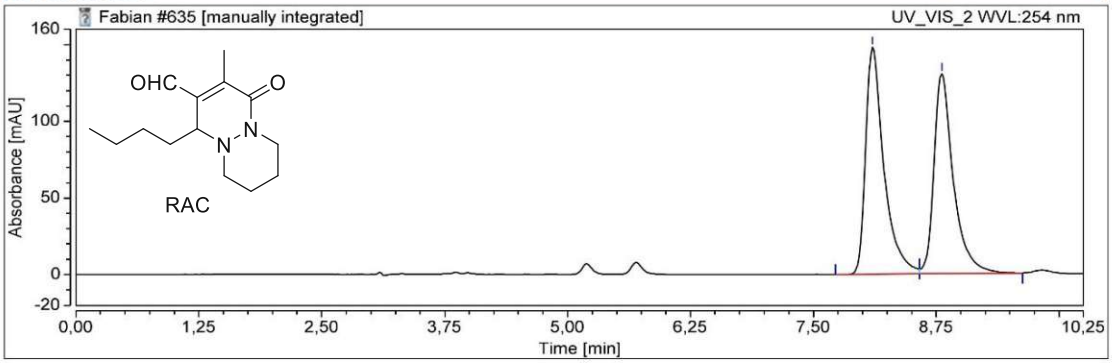
Reports IJD/Integration

Chromeleon (c) Dionex
Version 7.1.1.1127

Die approbierte gedruckte Originalversion dieser Dissertation ist an der TU Wien Bibliothek verfügbar.
The approved original version of this doctoral thesis is available in print at TU Wien Bibliothek.

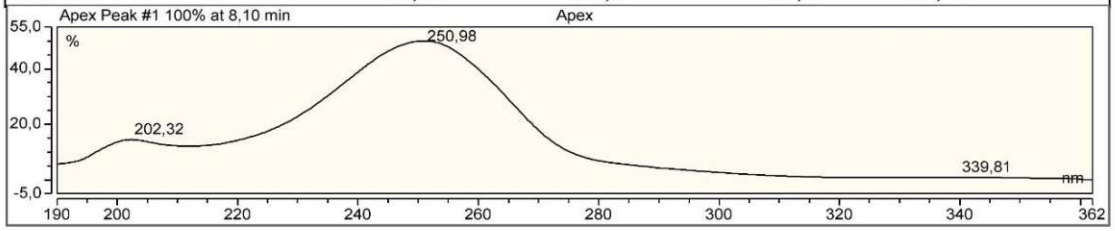
8.1.4 HPLC spectra of **3d**

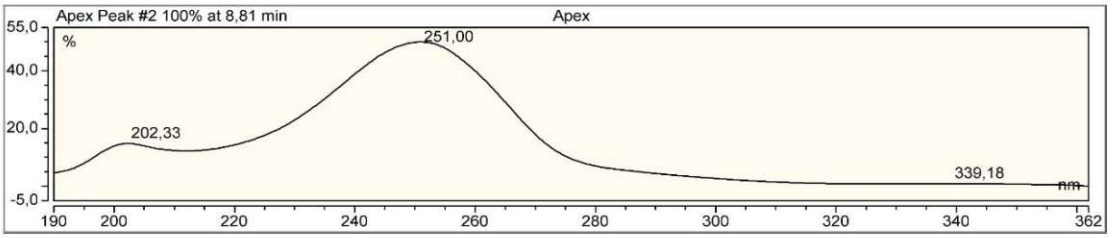
Chromatogram



Integration Results

No.	Peak Name	Retention Time min	Area mAU*min	Height mAU	Relative Area %	Relative Height %	Amount n.a.
1		8,102	31,886	148,113	51,70	53,16	n.a.
2		8,805	29,784	130,529	48,30	46,84	n.a.
Total:			**61,670**	**278,642**	**100,00**	**100,00**	



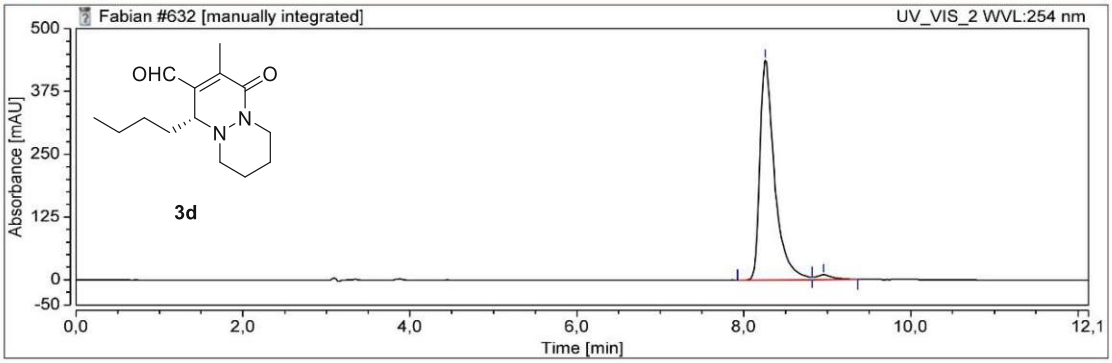


Reports IJD/Integration

Chromeleon (c) Dionex
Version 7.1.1.1127

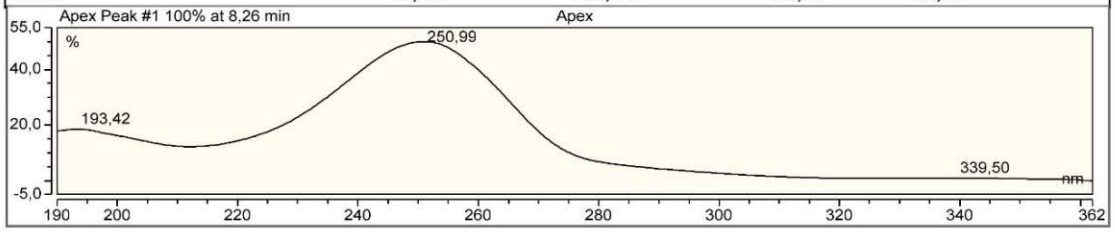
Die approbierte gedruckte Originalversion dieser Dissertation ist an der TU Wien Bibliothek verfügbar.
The approved original version of this doctoral thesis is available in print at TU Wien Bibliothek.

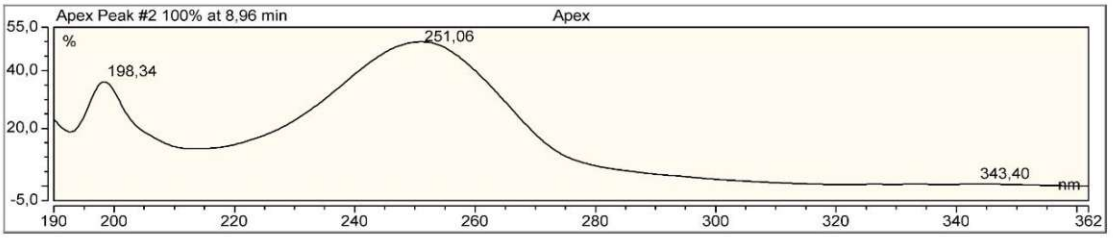
Chromatogram



Integration Results

No.	Peak Name	Retention Time min	Area mAU*min	Height mAU	Relative Area %	Relative Height %	Amount n.a.
1		8,258	88,493	437,799	97,51	97,85	n.a.
2		8,955	2,259	9,640	2,49	2,15	n.a.
Total:			**90,753**	**447,440**	**100,00**	**100,00**	





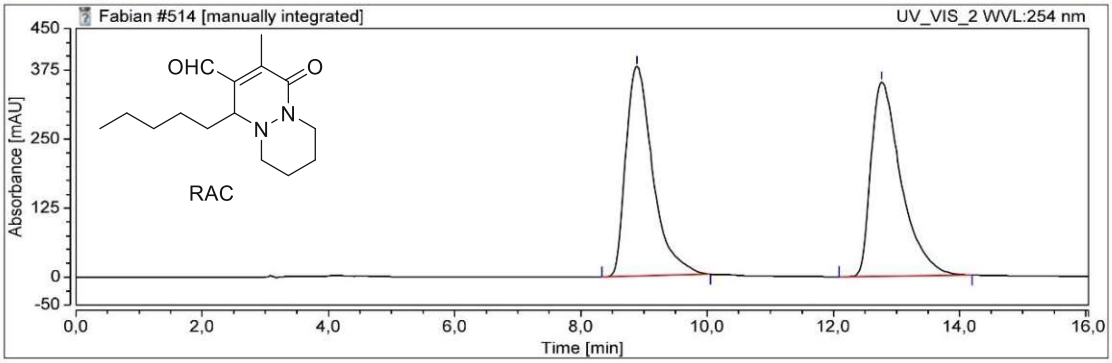
Reports IJD/Integration

Chromeleon (c) Dionex
Version 7.1.1.1127

Die approbierte gedruckte Originalversion dieser Dissertation ist an der TU Wien Bibliothek verfügbar.
The approved original version of this doctoral thesis is available in print at TU Wien Bibliothek.

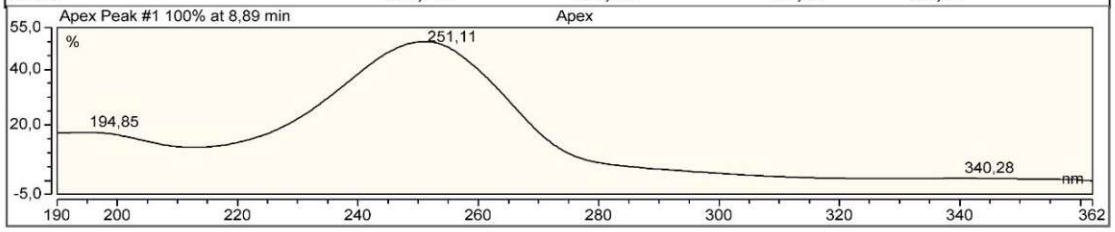
8.1.5 HPLC spectra of **3e**

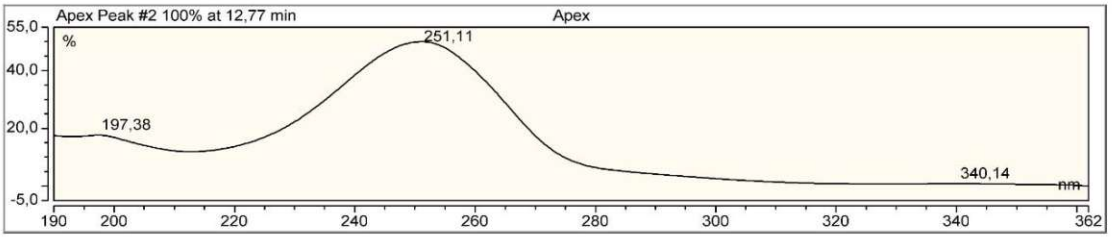
Chromatogram



Integration Results

No.	Peak Name	Retention Time min	Area mAU*min	Height mAU	Relative Area %	Relative Height %	Amount n.a.
1		8,885	188,202	379,667	49,20	51,93	n.a.
2		12,767	194,342	351,390	50,80	48,07	n.a.
Total:			**382,545**	**731,057**	**100,00**	**100,00**	



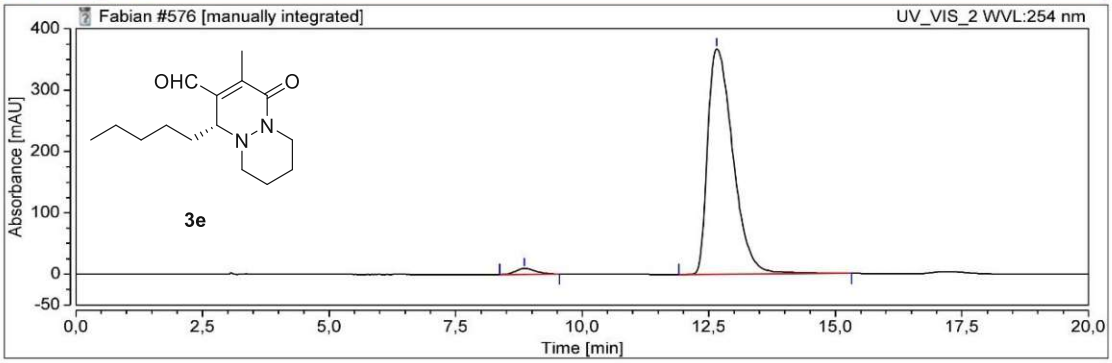


Reports IJD/Integration

Chromeleon (c) Dionex
Version 7.1.1.1127

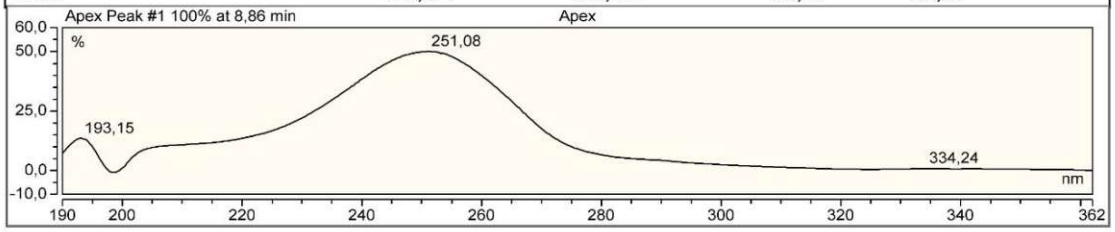
Die approbierte gedruckte Originalversion dieser Dissertation ist an der TU Wien Bibliothek verfügbar.
The approved original version of this doctoral thesis is available in print at TU Wien Bibliothek.

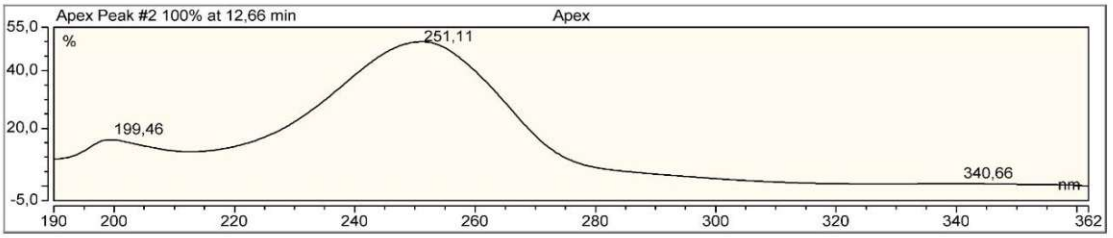
Chromatogram



Integration Results

No.	Peak Name	Retention Time min	Area mAU*min	Height mAU	Relative Area %	Relative Height %	Amount n.a.
1		8,860	4,428	9,675	2,05	2,57	n.a.
2		12,658	212,076	367,479	97,95	97,43	n.a.
Total:			**216,504**	**377,154**	**100,00**	**100,00**	



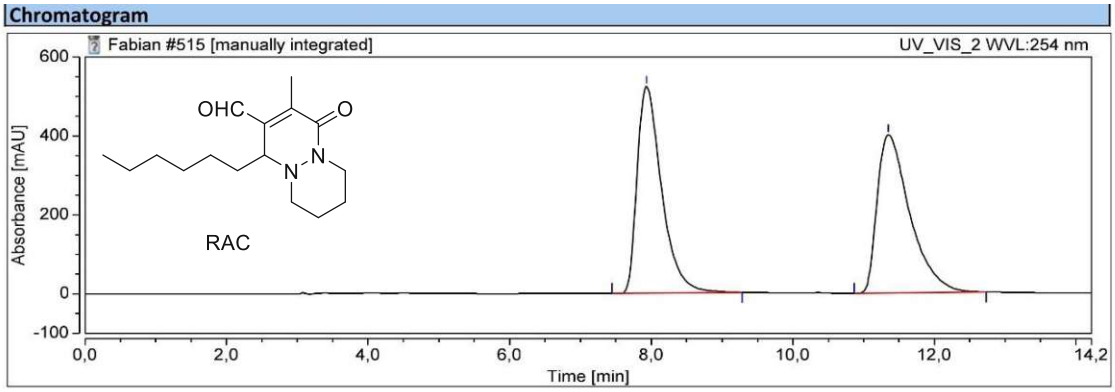


Reports IJD/Integration

Chromeleon (c) Dionex
Version 7.1.1.1127

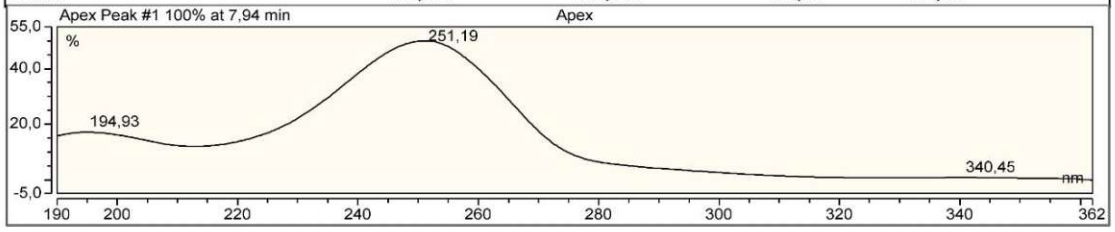
Die approbierte gedruckte Originalversion dieser Dissertation ist an der TU Wien Bibliothek verfügbar.
The approved original version of this doctoral thesis is available in print at TU Wien Bibliothek.

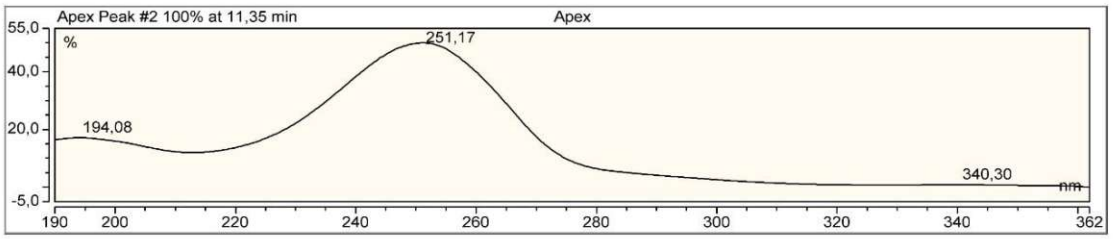
8.1.6 HPLC spectra of **3f**



Integration Results

No.	Peak Name	Retention Time min	Area mAU*min	Height mAU	Relative Area %	Relative Height %	Amount n.a.
1		7,935	210,752	524,653	49,60	56,67	n.a.
2		11,353	214,133	401,192	50,40	43,33	n.a.
Total:			**424,885**	**925,844**	**100,00**	**100,00**	



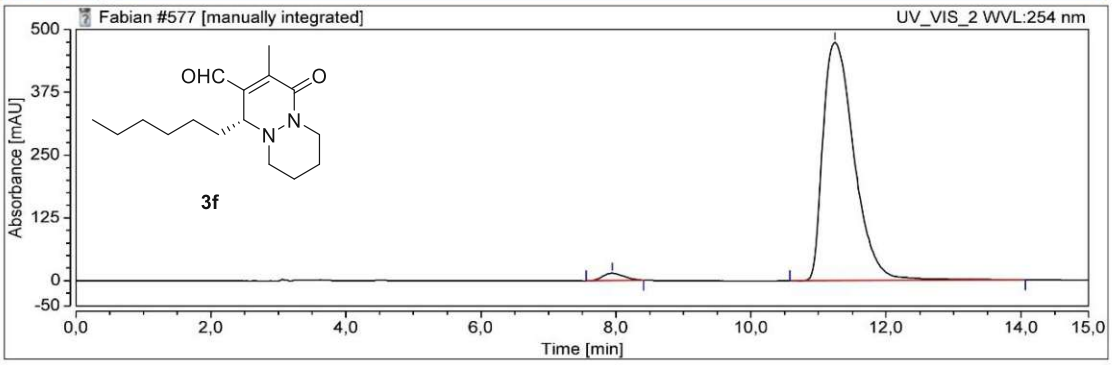


Reports IJD/Integration

Chromeleon (c) Dionex
Version 7.1.1.1127

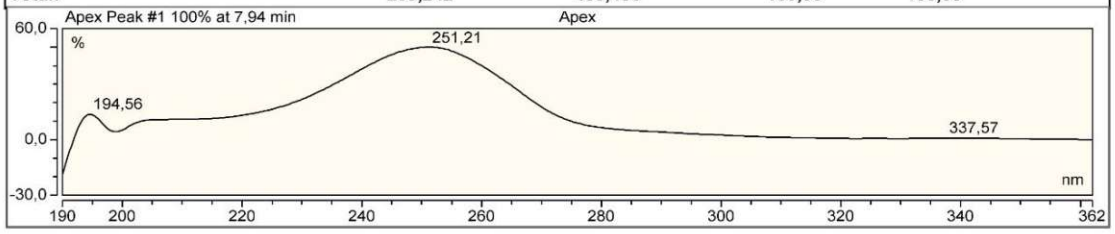
Die approbierte gedruckte Originalversion dieser Dissertation ist an der TU Wien Bibliothek verfügbar.
The approved original version of this doctoral thesis is available in print at TU Wien Bibliothek.

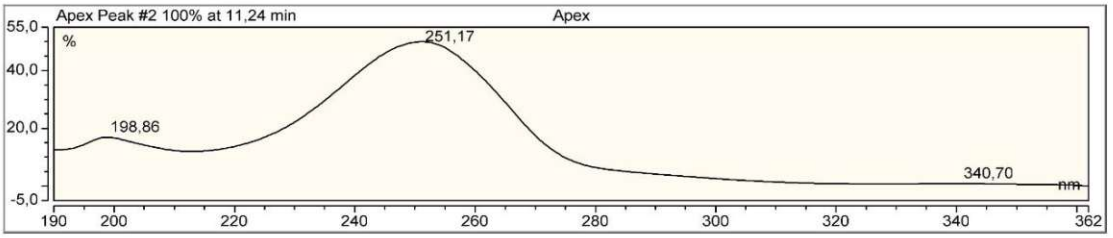
Chromatogram



Integration Results

No.	Peak Name	Retention Time min	Area mAU*min	Height mAU	Relative Area %	Relative Height %	Amount n.a.
1		7,942	5,253	14,431	2,03	2,95	n.a.
2		11,243	253,989	473,974	97,97	97,05	n.a.
Total:			**259,242**	**488,405**	**100,00**	**100,00**	



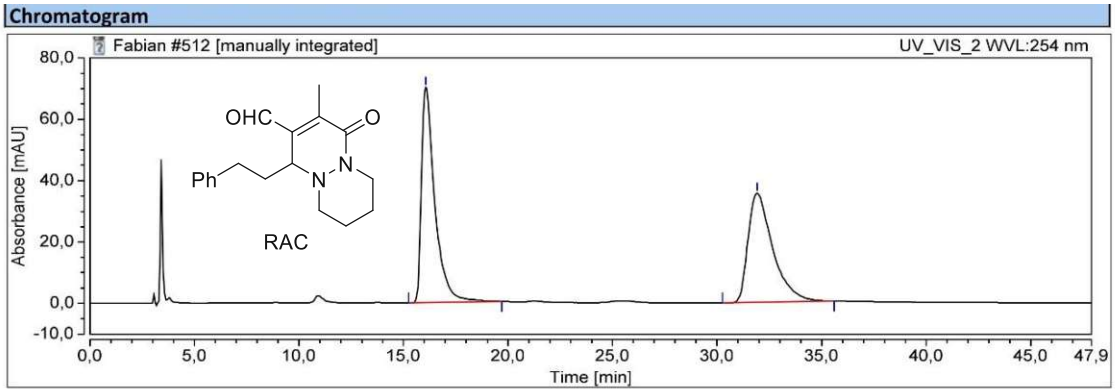


Reports IJD/Integration

Chromeleon (c) Dionex
Version 7.1.1.1127

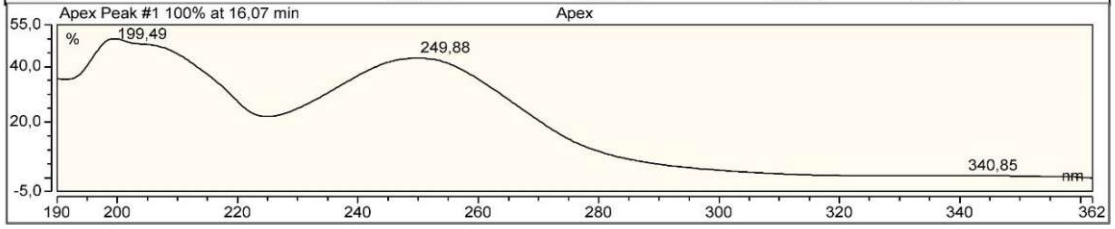
Die approbierte gedruckte Originalversion dieser Dissertation ist an der TU Wien Bibliothek verfügbar.
The approved original version of this doctoral thesis is available in print at TU Wien Bibliothek.

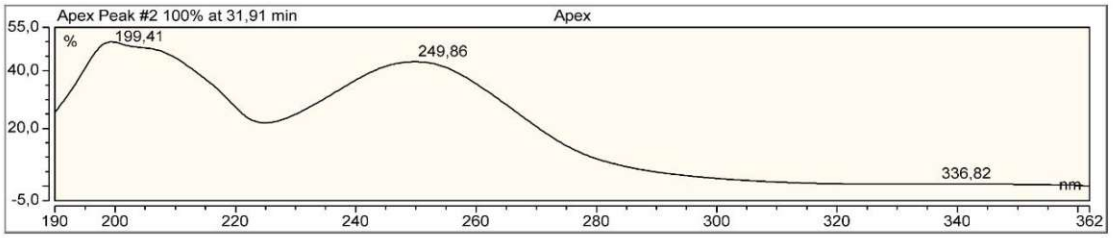
8.1.7 HPLC spectra of **3g**



Integration Results

No.	Peak Name	Retention Time min	Area mAU*min	Height mAU	Relative Area %	Relative Height %	Amount n.a.
1		16,073	51,843	70,183	51,48	66,36	n.a.
2		31,908	48,863	35,582	48,52	33,64	n.a.
Total:			**100,706**	**105,765**	**100,00**	**100,00**	



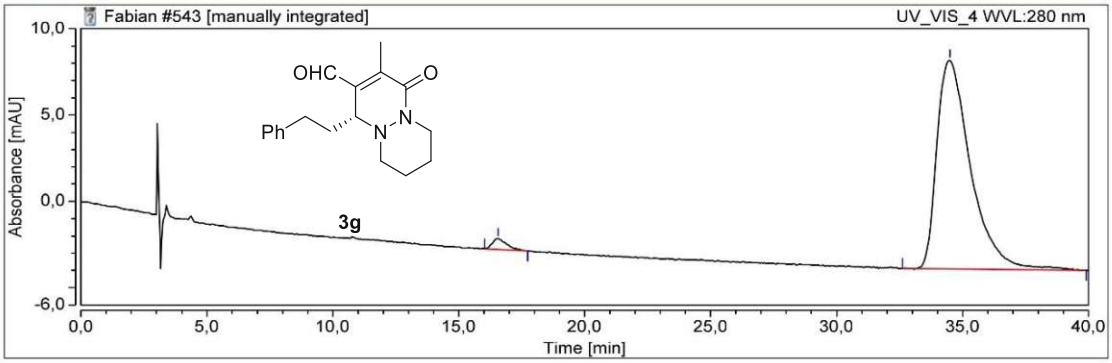


Reports IJD/Integration

Chromeleon (c) Dionex
Version 7.1.1.1127

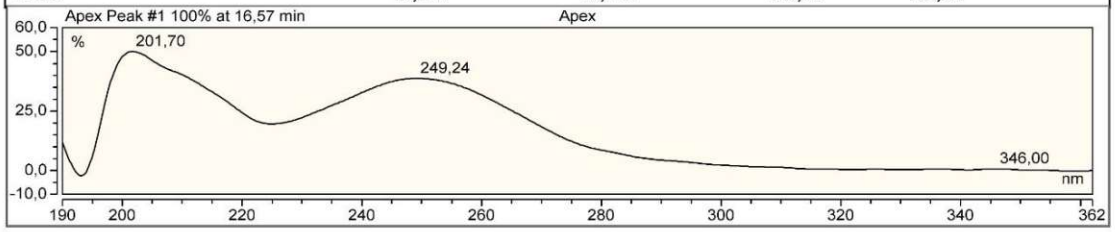
Die approbierte gedruckte Originalversion dieser Dissertation ist an der TU Wien Bibliothek verfügbar.
The approved original version of this doctoral thesis is available in print at TU Wien Bibliothek.

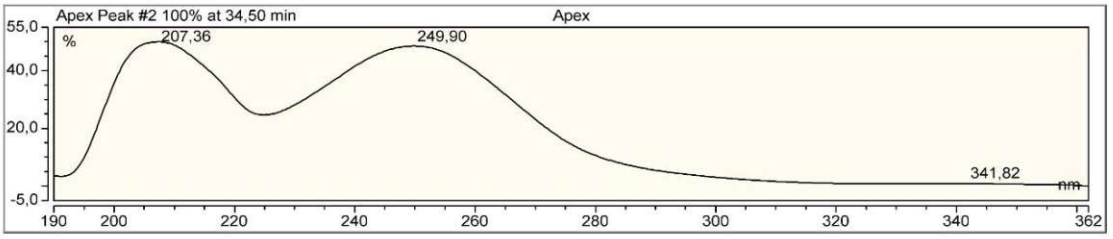
Chromatogram



Integration Results

No.	Peak Name	Retention Time min	Area mAU*min	Height mAU	Relative Area %	Relative Height %	Amount n.a.
1		16,568	0,415	0,645	2,17	5,06	n.a.
2		34,495	18,763	12,103	97,83	94,94	n.a.
Total:			**19,178**	**12,749**	**100,00**	**100,00**	





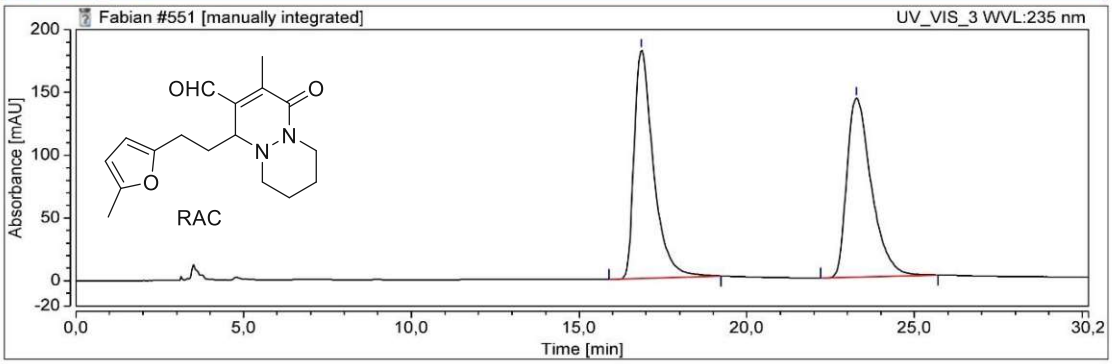
Reports IJD/Integration

Chromeleon (c) Dionex
Version 7.1.1.1127

Die approbierte gedruckte Originalversion dieser Dissertation ist an der TU Wien Bibliothek verfügbar.
The approved original version of this doctoral thesis is available in print at TU Wien Bibliothek.

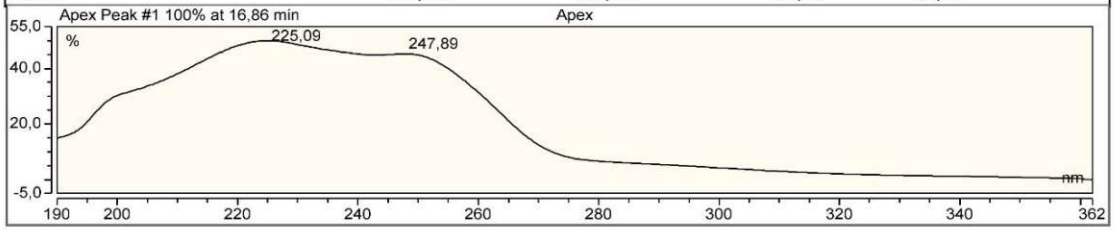
8.1.8 HPLC spectra of **3h**

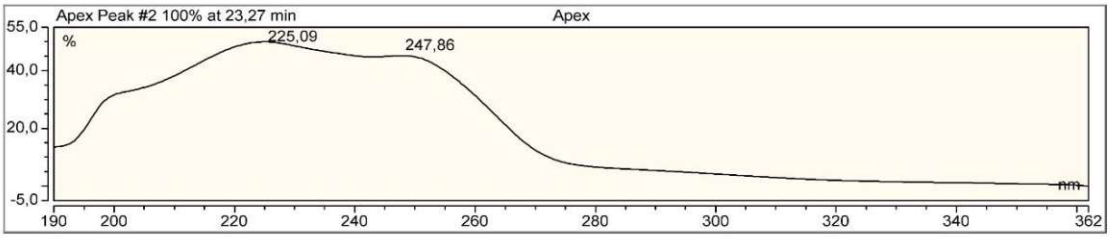
Chromatogram



Integration Results

No.	Peak Name	Retention Time min	Area mAU*min	Height mAU	Relative Area %	Relative Height %	Amount n.a.
1		16,858	121,583	182,238	50,19	56,04	n.a.
2		23,270	120,639	142,943	49,81	43,96	n.a.
Total:			**242,222**	**325,182**	**100,00**	**100,00**	



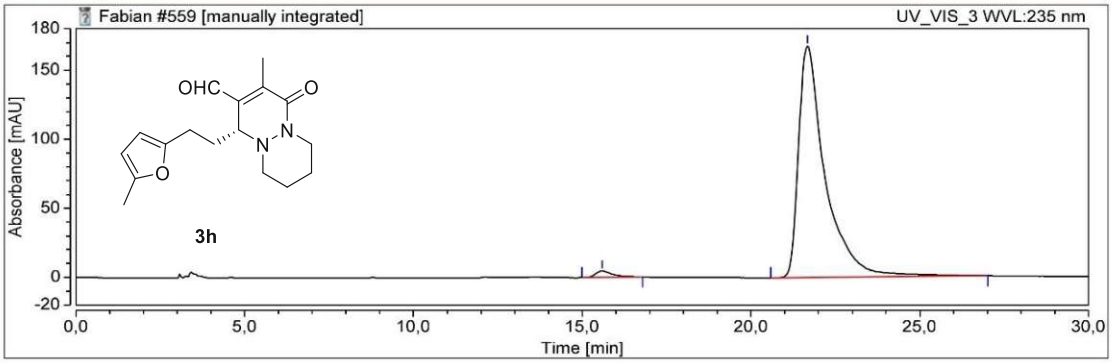


Reports IJD/Integration

Chromeleon (c) Dionex
Version 7.1.1.1127

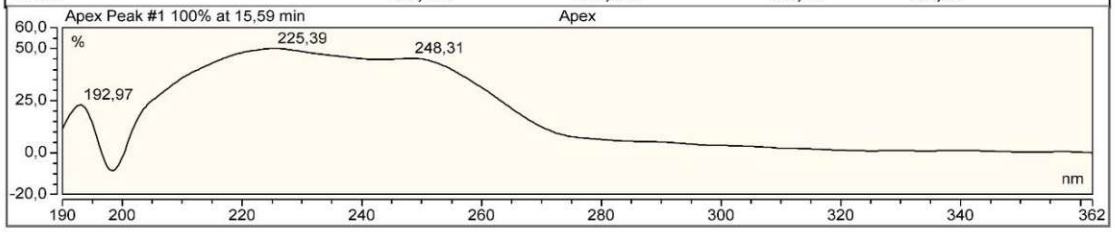
Die approbierte gedruckte Originalversion dieser Dissertation ist an der TU Wien Bibliothek verfügbar.
The approved original version of this doctoral thesis is available in print at TU Wien Bibliothek.

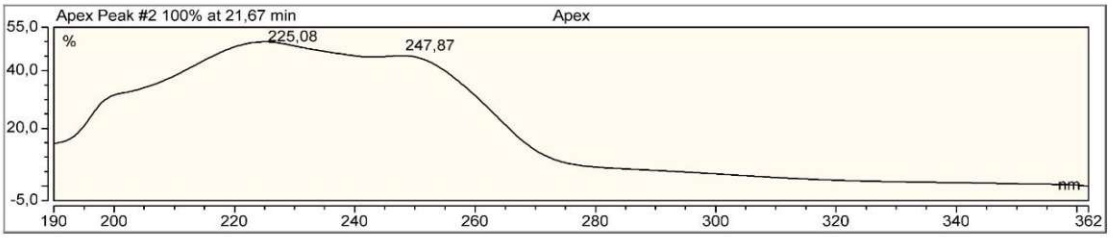
Chromatogram



Integration Results

No.	Peak Name	Retention Time min	Area mAU*min	Height mAU	Relative Area %	Relative Height %	Amount n.a.
1		15,588	2,722	4,642	1,75	2,69	n.a.
2		21,670	153,022	167,703	98,25	97,31	n.a.
Total:			**155,744**	**172,345**	**100,00**	**100,00**	



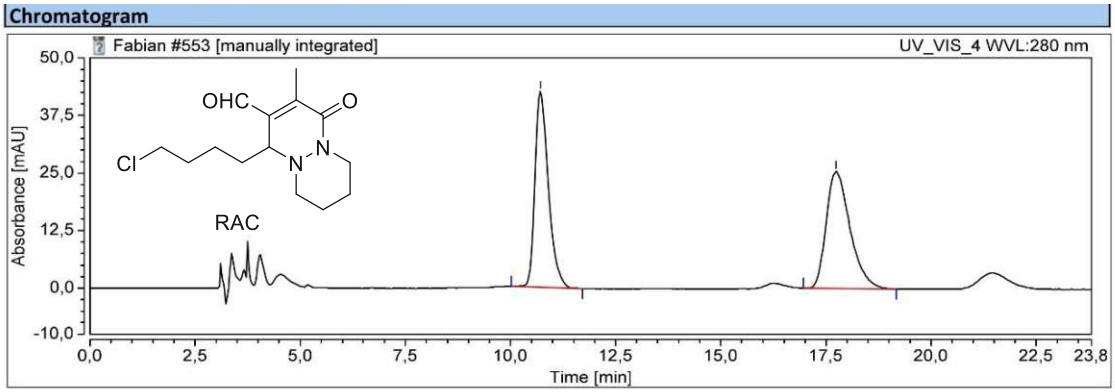


Reports IJD/Integration

Chromeleon (c) Dionex
Version 7.1.1.1127

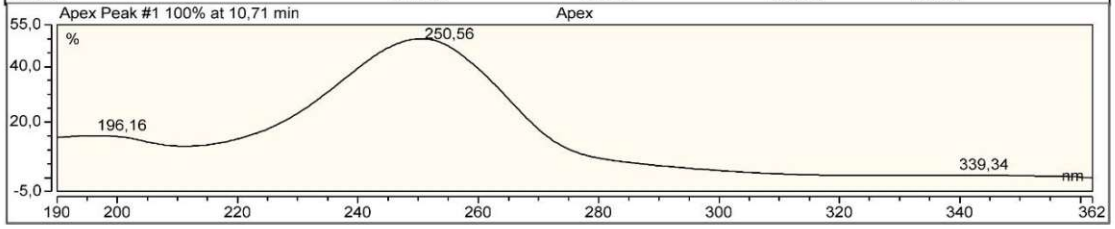
Die approbierte gedruckte Originalversion dieser Dissertation ist an der TU Wien Bibliothek verfügbar.
The approved original version of this doctoral thesis is available in print at TU Wien Bibliothek.

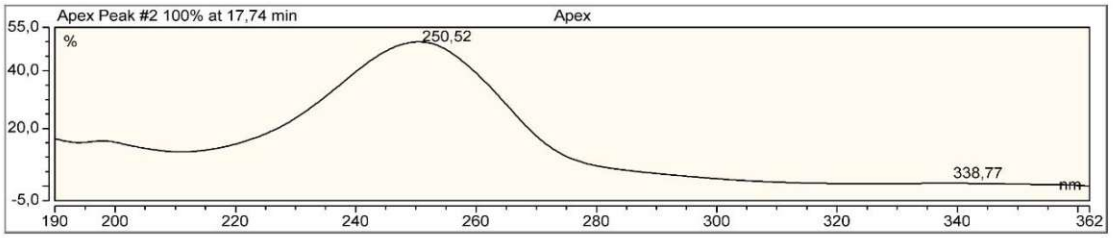
8.1.9 HPLC spectra of **3i**



Integration Results

No.	Peak Name	Retention Time min	Area mAU*min	Height mAU	Relative Area %	Relative Height %	Amount n.a.
1		10,713	15,758	42,564	48,51	62,57	n.a.
2		17,742	16,725	25,463	51,49	37,43	n.a.
Total:			**32,483**	**68,027**	**100,00**	**100,00**	



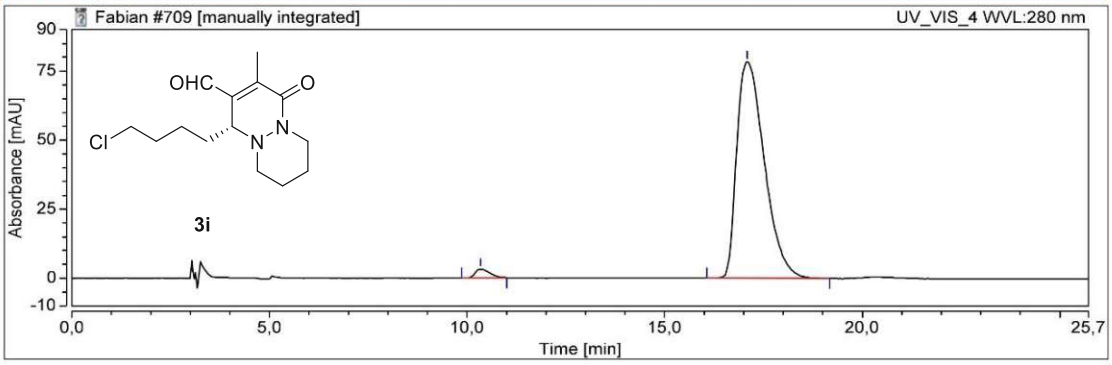


Reports IJD/Integration

Chromeleon (c) Dionex
Version 7.1.1.1127

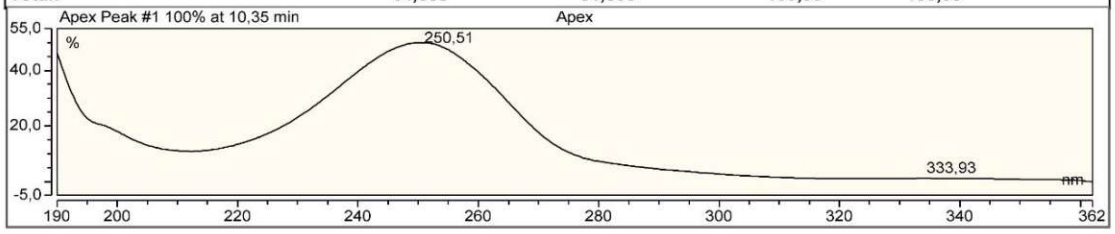
Die approbierte gedruckte Originalversion dieser Dissertation ist an der TU Wien Bibliothek verfügbar.
The approved original version of this doctoral thesis is available in print at TU Wien Bibliothek.

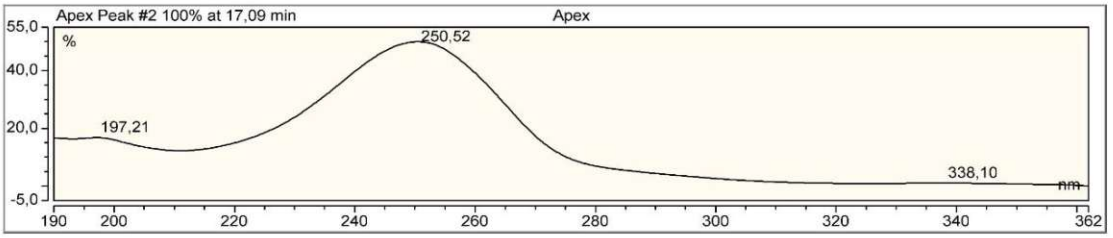
Chromatogram



Integration Results

No.	Peak Name	Retention Time min	Area mAU*min	Height mAU	Relative Area %	Relative Height %	Amount n.a.
1		10,347	1,364	3,258	2,11	3,99	n.a.
2		17,088	63,221	78,410	97,89	96,01	n.a.
Total:			**64,585**	**81,668**	**100,00**	**100,00**	



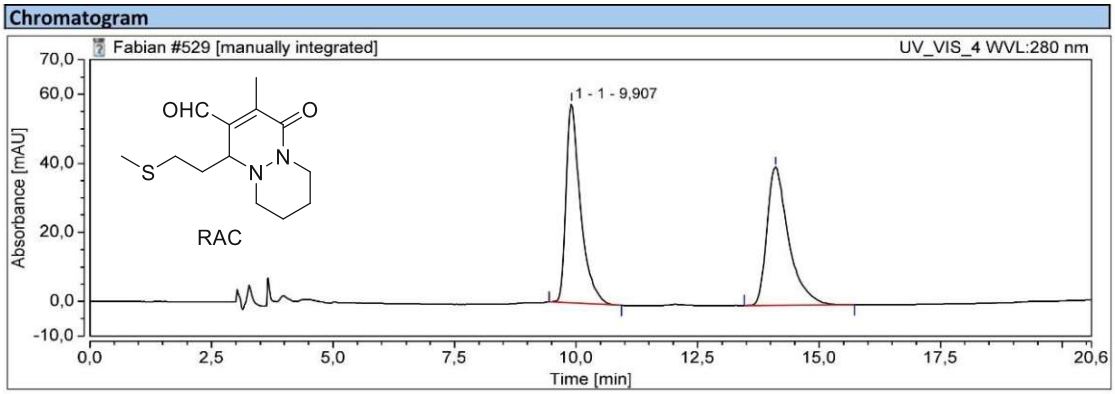


Reports IJD/Integration

Chromeleon (c) Dionex
Version 7.1.1.1127

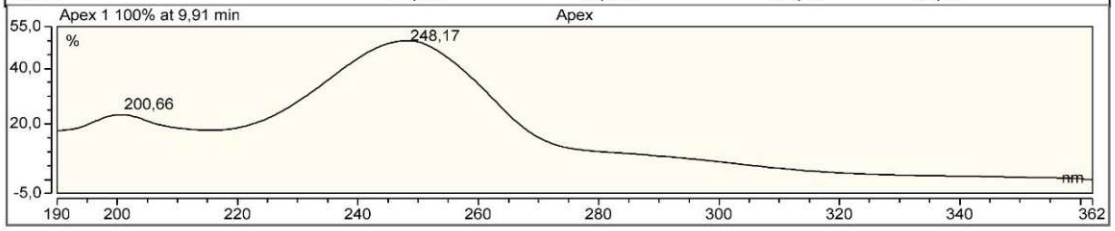
Die approbierte gedruckte Originalversion dieser Dissertation ist an der TU Wien Bibliothek verfügbar.
The approved original version of this doctoral thesis is available in print at TU Wien Bibliothek.

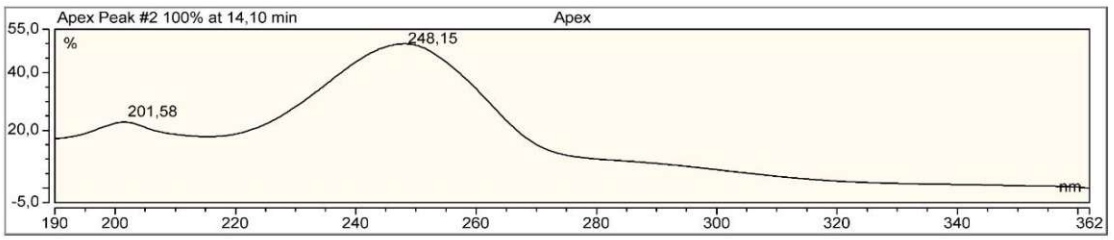
8.1.10 HPLC spectra of **3j**



Integration Results

No.	Peak Name	Retention Time min	Area mAU*min	Height mAU	Relative Area %	Relative Height %	Amount
1	1	9,907	19,938	57,770	49,04	59,06	n.a.
2		14,100	20,716	40,040	50,96	40,94	n.a.
Total:			**40,654**	**97,810**	**100,00**	**100,00**	



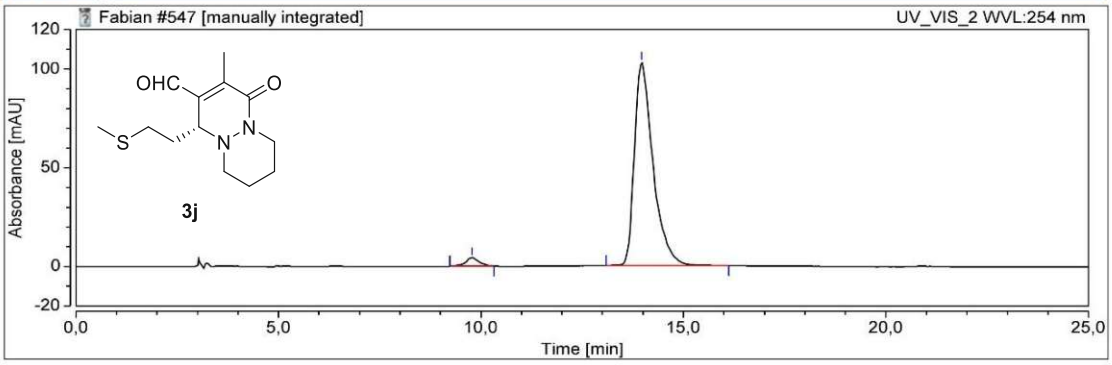


Reports IJD/Integration

Chromeleon (c) Dionex
Version 7.1.1.1127

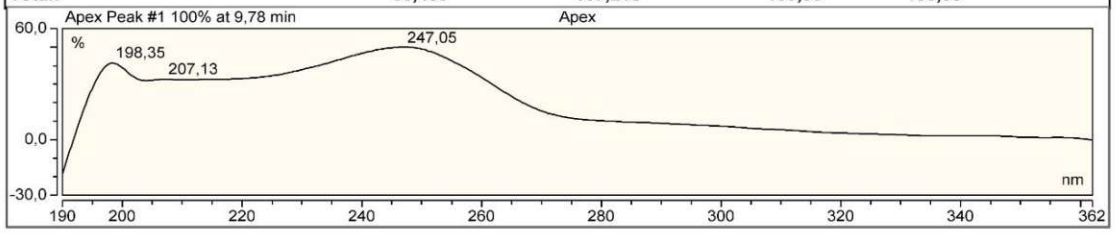
Die approbierte gedruckte Originalversion dieser Dissertation ist an der TU Wien Bibliothek verfügbar.
The approved original version of this doctoral thesis is available in print at TU Wien Bibliothek.

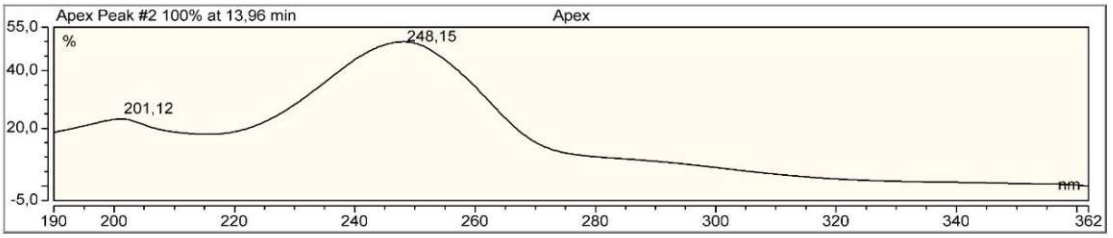
Chromatogram



Integration Results

No.	Peak Name	Retention Time min	Area mAU*min	Height mAU	Relative Area %	Relative Height %	Amount n.a.
1		9,780	1,641	4,303	2,91	4,01	n.a.
2		13,963	54,822	102,915	97,09	95,99	n.a.
Total:			**56,463**	**107,218**	**100,00**	**100,00**	





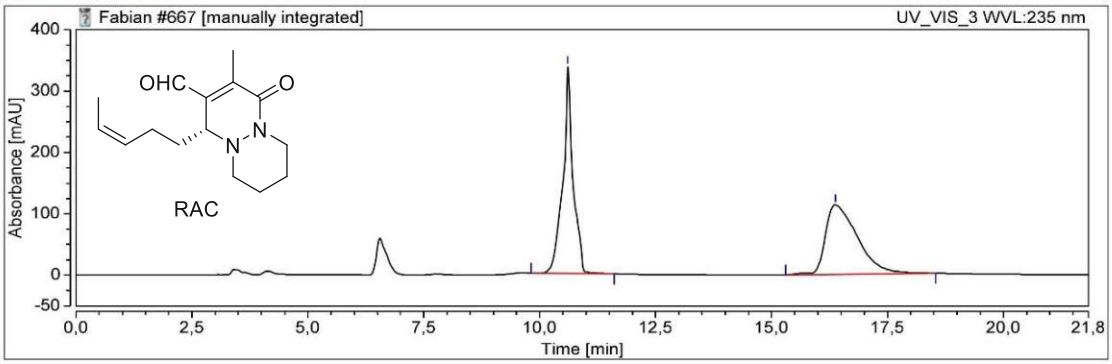
Reports IJD/Integration

Chromeleon (c) Dionex
Version 7.1.1.1127

Die approbierte gedruckte Originalversion dieser Dissertation ist an der TU Wien Bibliothek verfügbar.
The approved original version of this doctoral thesis is available in print at TU Wien Bibliothek.

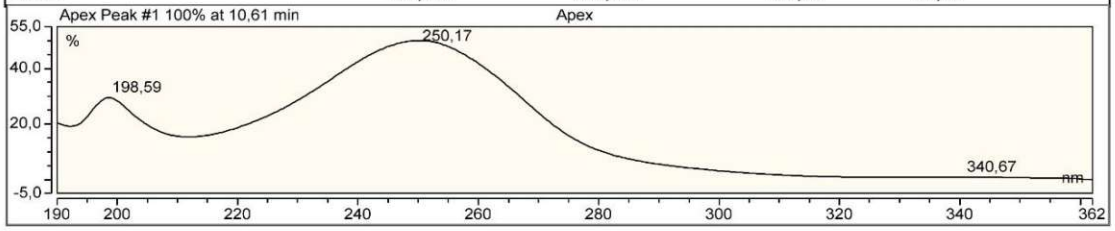
8.1.11 HPLC spectra of **3k**

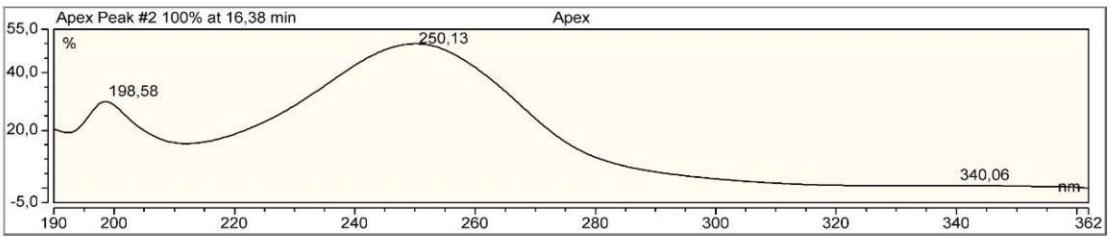
Chromatogram



Integration Results

No.	Peak Name	Retention Time min	Area mAU*min	Height mAU	Relative Area %	Relative Height %	Amount n.a.
1		10,607	85,952	337,044	48,49	74,81	n.a.
2		16,377	91,308	113,470	51,51	25,19	n.a.
Total:			**177,260**	**450,514**	**100,00**	**100,00**	



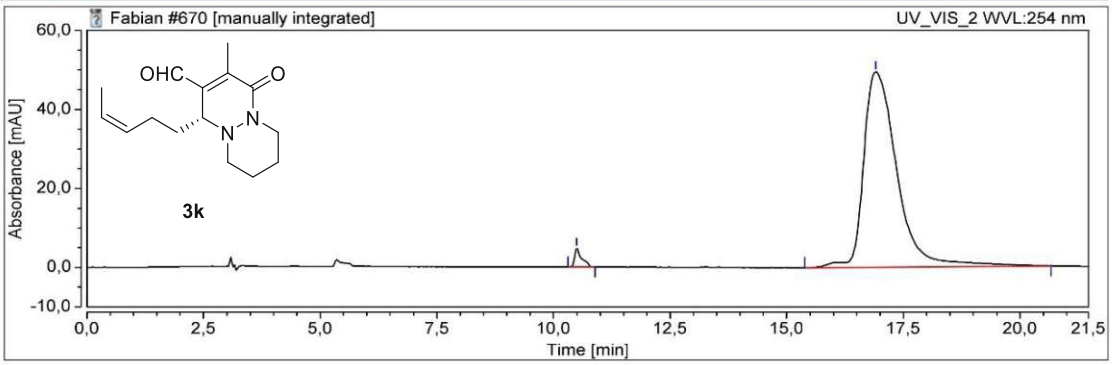


Reports IJD/Integration

Chromeleon (c) Dionex
Version 7.1.1.1127

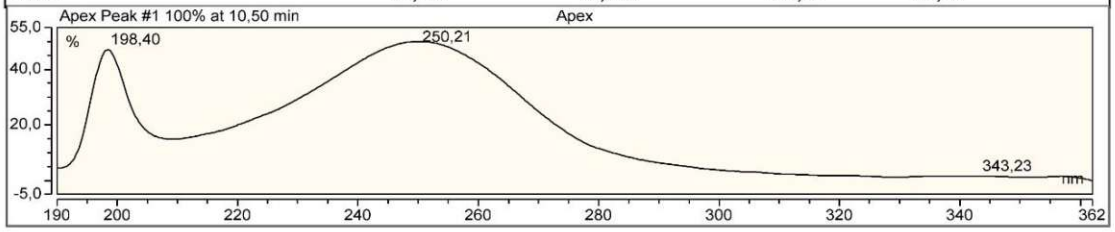
Die approbierte gedruckte Originalversion dieser Dissertation ist an der TU Wien Bibliothek verfügbar.
The approved original version of this doctoral thesis is available in print at TU Wien Bibliothek.

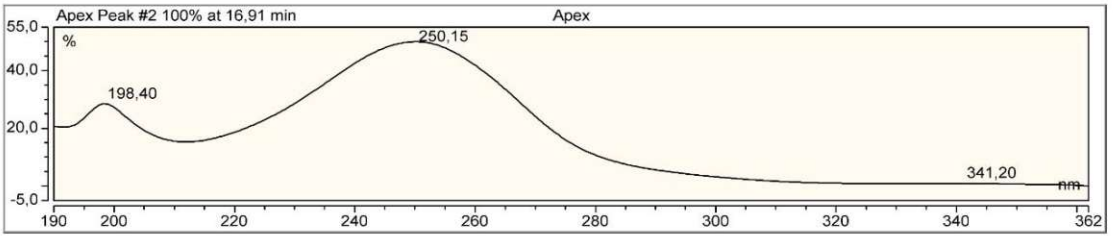
Chromatogram



Integration Results

No.	Peak Name	Retention Time min	Area mAU*min	Height mAU	Relative Area %	Relative Height %	Amount n.a.
1		10,495	0,823	4,738	1,97	8,74	n.a.
2		16,905	40,901	49,467	98,03	91,26	n.a.
Total:			**41,723**	**54,206**	**100,00**	**100,00**	





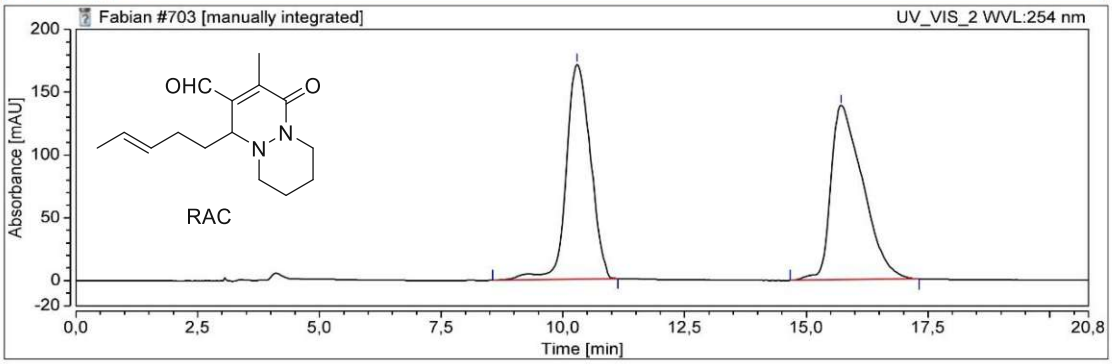
Reports IJD/Integration

Chromeleon (c) Dionex
Version 7.1.1.1127

Die approbierte gedruckte Originalversion dieser Dissertation ist an der TU Wien Bibliothek verfügbar.
The approved original version of this doctoral thesis is available in print at TU Wien Bibliothek.

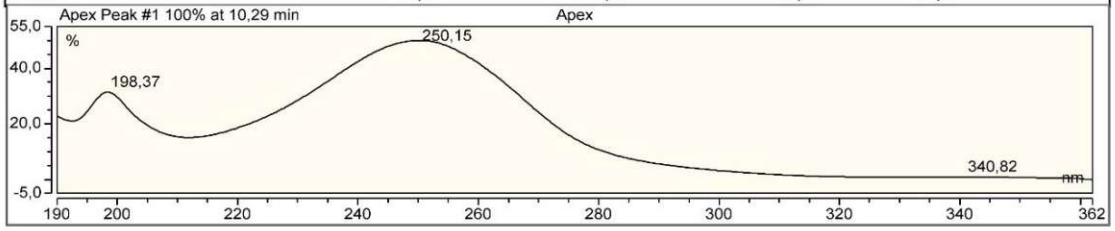
8.1.12 HPLC spectra of **3l**

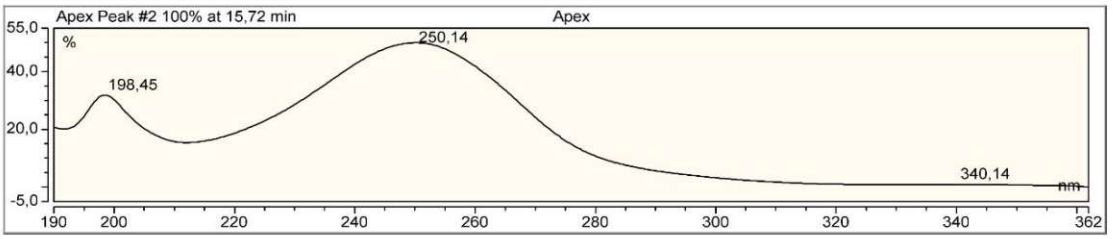
Chromatogram



Integration Results

No.	Peak Name	Retention Time min	Area mAU*min	Height mAU	Relative Area %	Relative Height %	Amount n.a.
1		10,292	98,289	171,210	48,01	55,23	n.a.
2		15,718	106,430	138,805	51,99	44,77	n.a.
Total:			**204,719**	**310,015**	**100,00**	**100,00**	



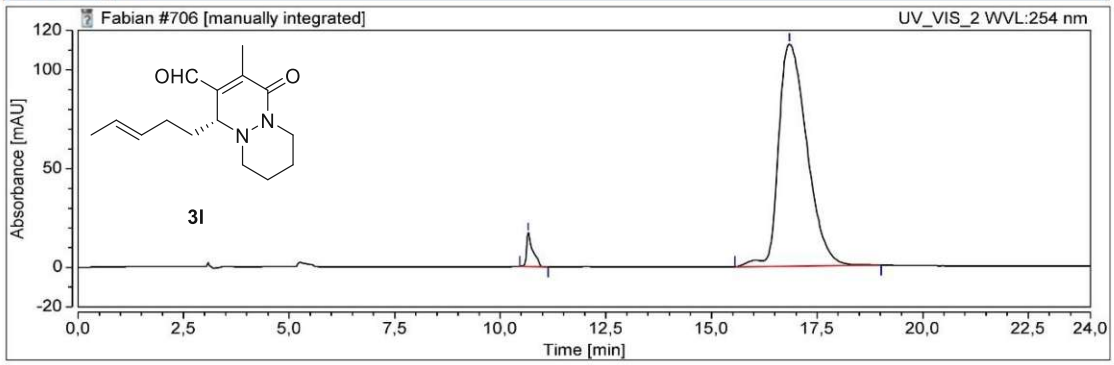


Reports IJD/Integration

Chromeleon (c) Dionex
Version 7.1.1.1127

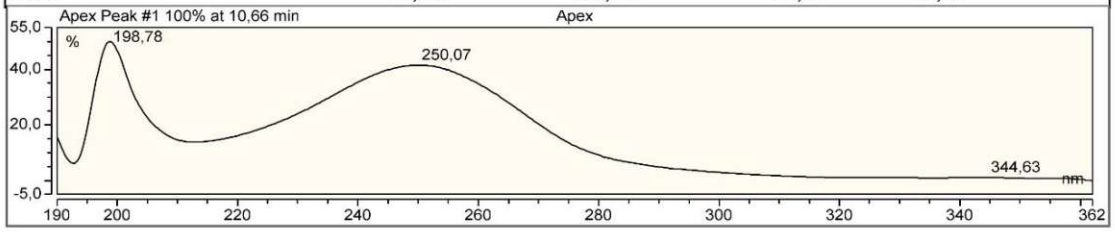
Die approbierte gedruckte Originalversion dieser Dissertation ist an der TU Wien Bibliothek verfügbar.
The approved original version of this doctoral thesis is available in print at TU Wien Bibliothek.

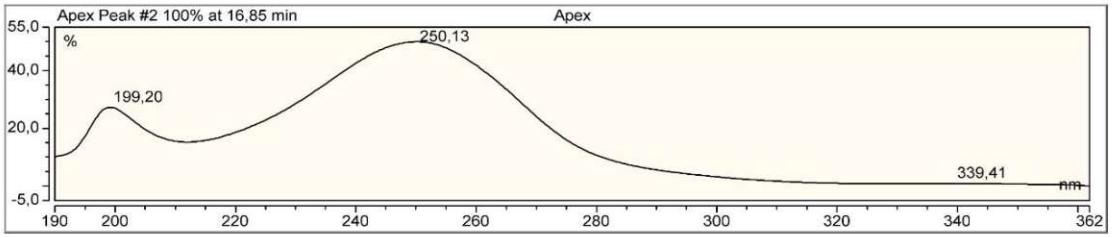
Chromatogram



Integration Results

No.	Peak Name	Retention Time min	Area mAU*min	Height mAU	Relative Area %	Relative Height %	Amount n.a.
1		10,663	2,945	17,079	3,25	13,16	n.a.
2		16,847	87,640	112,654	96,75	86,84	n.a.
Total:			**90,585**	**129,733**	**100,00**	**100,00**	





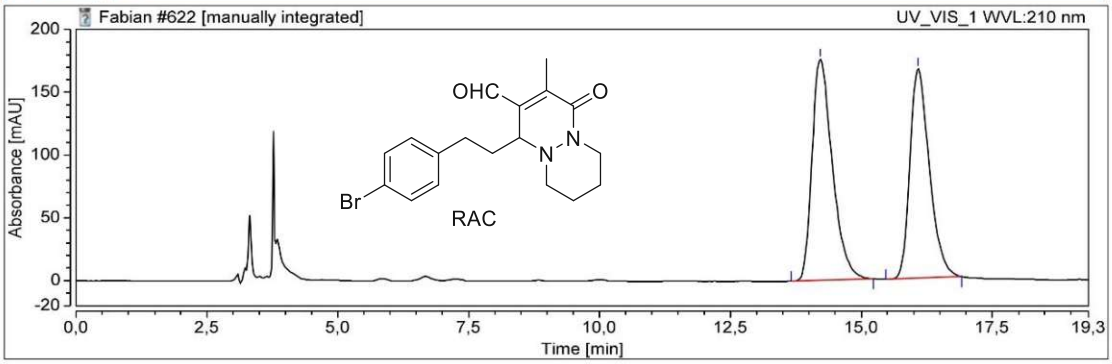
Reports IJD/Integration

Chromeleon (c) Dionex
Version 7.1.1.1127

Die approbierte gedruckte Originalversion dieser Dissertation ist an der TU Wien Bibliothek verfügbar.
The approved original version of this doctoral thesis is available in print at TU Wien Bibliothek.

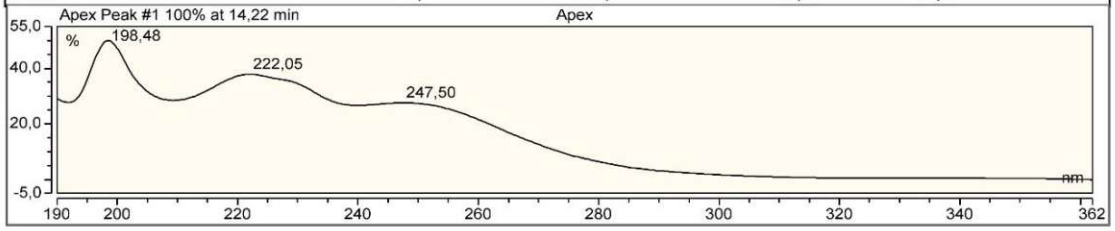
8.1.13 HPLC spectra of **3m**

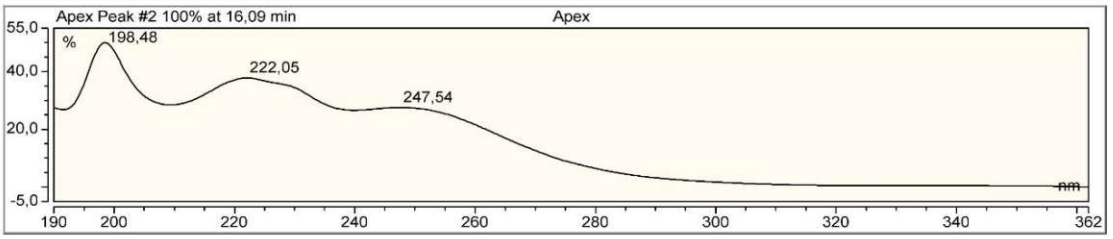
Chromatogram



Integration Results

No.	Peak Name	Retention Time min	Area mAU*min	Height mAU	Relative Area %	Relative Height %	Amount n.a.
1		14,215	79,377	176,234	52,44	51,35	n.a.
2		16,087	71,997	166,951	47,56	48,65	n.a.
Total:			**151,374**	**343,185**	**100,00**	**100,00**	



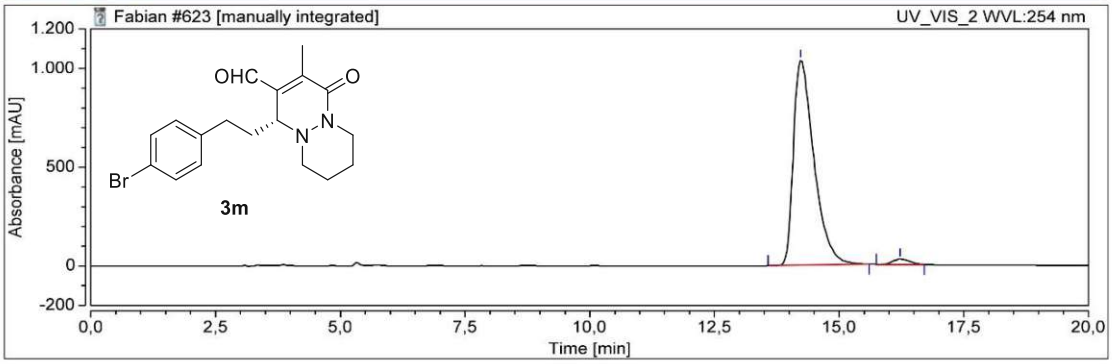


Reports IJD/Integration

Chromeleon (c) Dionex
Version 7.1.1.1127

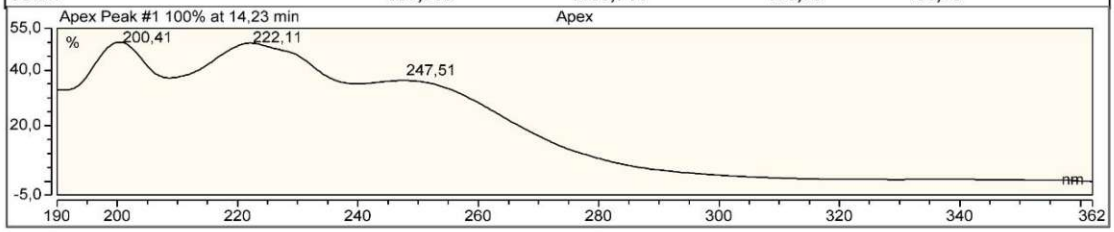
Die approbierte gedruckte Originalversion dieser Dissertation ist an der TU Wien Bibliothek verfügbar.
The approved original version of this doctoral thesis is available in print at TU Wien Bibliothek.

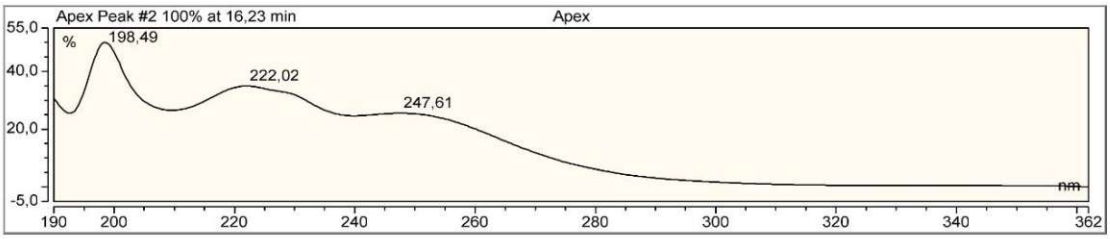
Chromatogram



Integration Results

No.	Peak Name	Retention Time min	Area mAU*min	Height mAU	Relative Area %	Relative Height %	Amount n.a.
1		14,230	496,356	1038,681	97,93	97,46	n.a.
2		16,225	10,513	27,063	2,07	2,54	n.a.
Total:			**506,869**	**1065,744**	**100,00**	**100,00**	



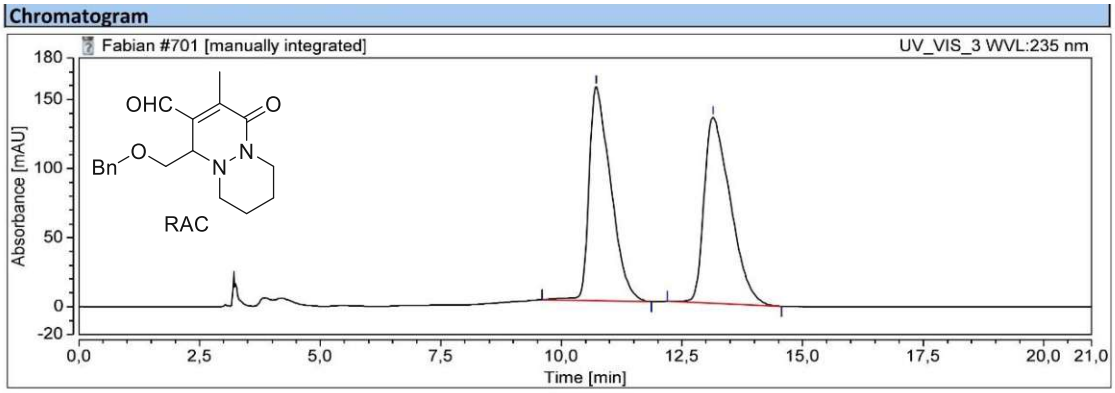


Reports IJD/Integration

Chromeleon (c) Dionex
Version 7.1.1.1127

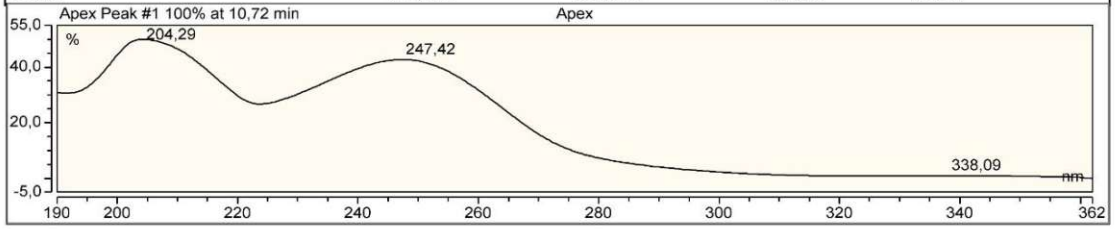
Die approbierte gedruckte Originalversion dieser Dissertation ist an der TU Wien Bibliothek verfügbar.
The approved original version of this doctoral thesis is available in print at TU Wien Bibliothek.

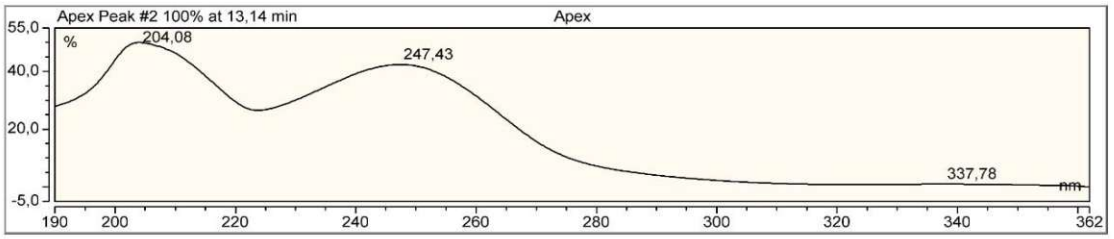
8.1.14 HPLC spectra of **3n**



Integration Results

No.	Peak Name	Retention Time min	Area mAU*min	Height mAU	Relative Area %	Relative Height %	Amount n.a.
1		10,720	80,505	155,380	48,45	53,54	n.a.
2		13,143	85,658	134,814	51,55	46,46	n.a.
Total:			**166,163**	**290,194**	**100,00**	**100,00**	



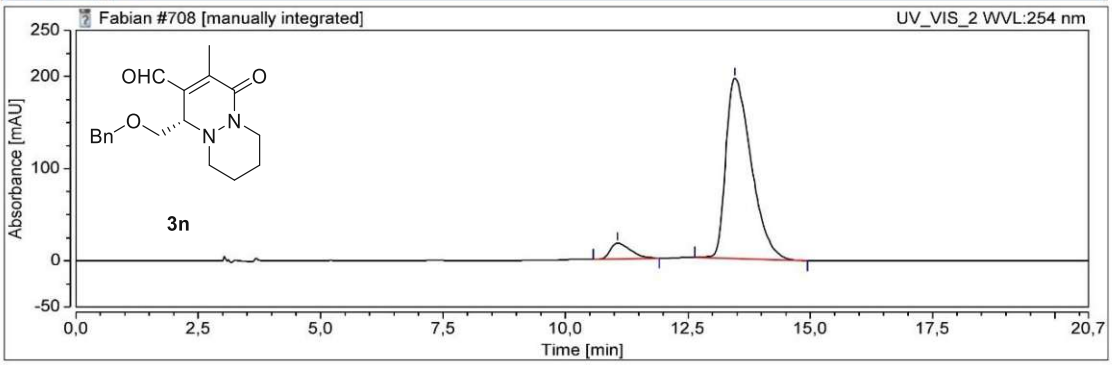


Reports IJD/Integration

Chromeleon (c) Dionex
Version 7.1.1.1127

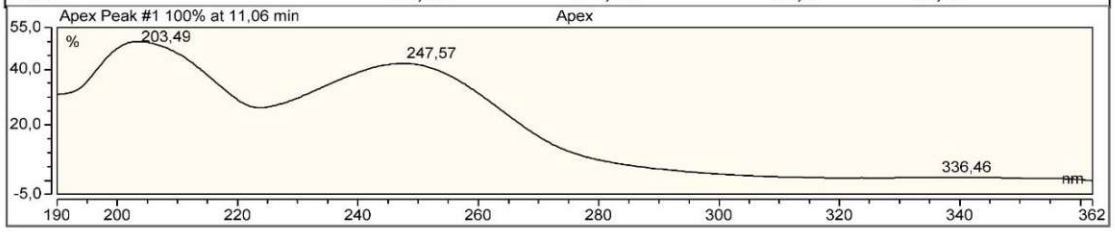
Die approbierte gedruckte Originalversion dieser Dissertation ist an der TU Wien Bibliothek verfügbar.
The approved original version of this doctoral thesis is available in print at TU Wien Bibliothek.

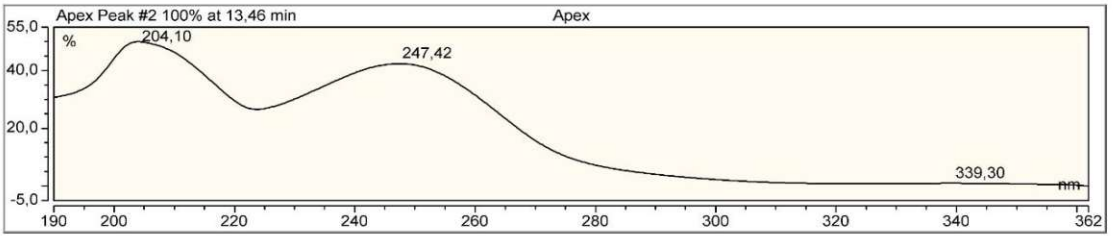
Chromatogram



Integration Results

No.	Peak Name	Retention Time min	Area mAU*min	Height mAU	Relative Area %	Relative Height %	Amount n.a.
1		11,062	8,051	17,177	6,40	8,06	n.a.
2		13,462	117,807	195,969	93,60	91,94	n.a.
Total:			**125,858**	**213,146**	**100,00**	**100,00**	



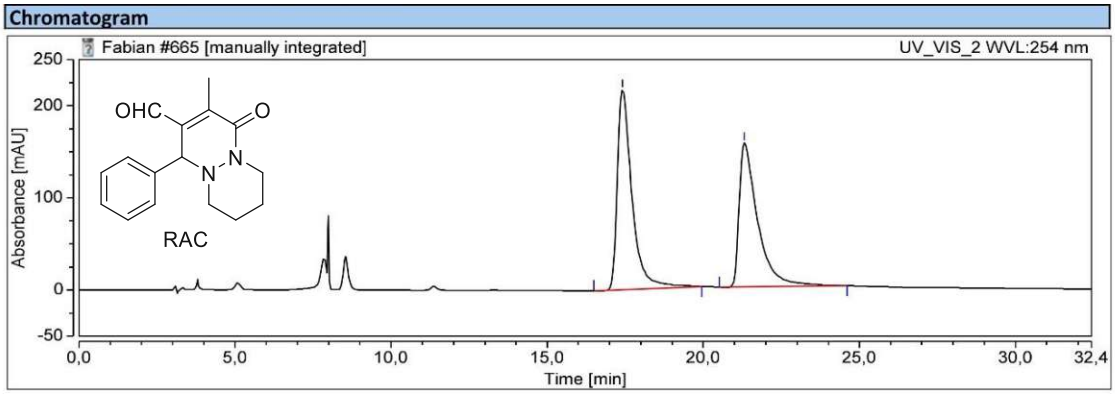


Reports IJD/Integration

Chromeleon (c) Dionex
Version 7.1.1.1127

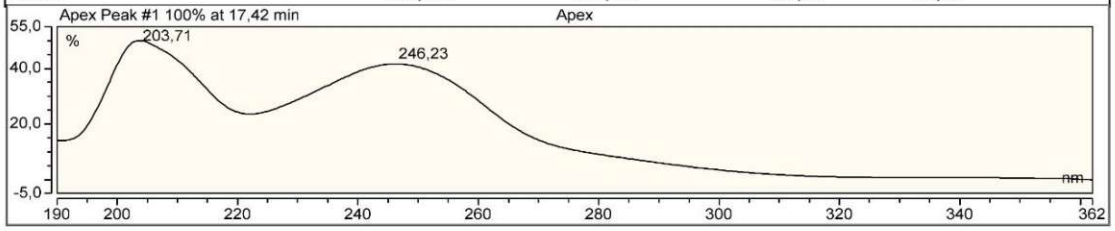
Die approbierte gedruckte Originalversion dieser Dissertation ist an der TU Wien Bibliothek verfügbar.
The approved original version of this doctoral thesis is available in print at TU Wien Bibliothek.

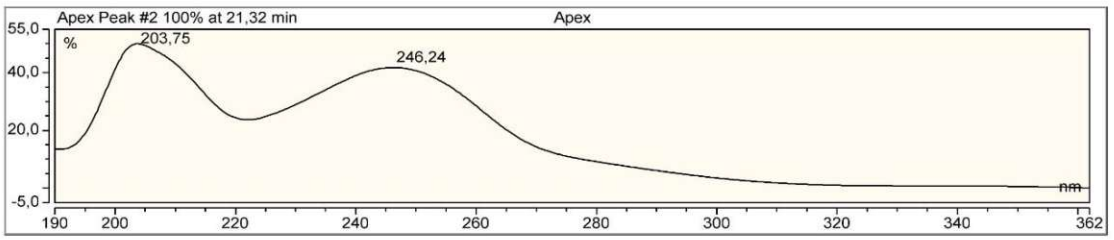
8.1.15 HPLC spectra of **3o**



Integration Results

No.	Peak Name	Retention Time min	Area mAU*min	Height mAU	Relative Area %	Relative Height %	Amount n.a.
1		17,415	117,931	216,696	52,23	58,07	n.a.
2		21,317	107,848	156,455	47,77	41,93	n.a.
Total:			**225,779**	**373,151**	**100,00**	**100,00**	



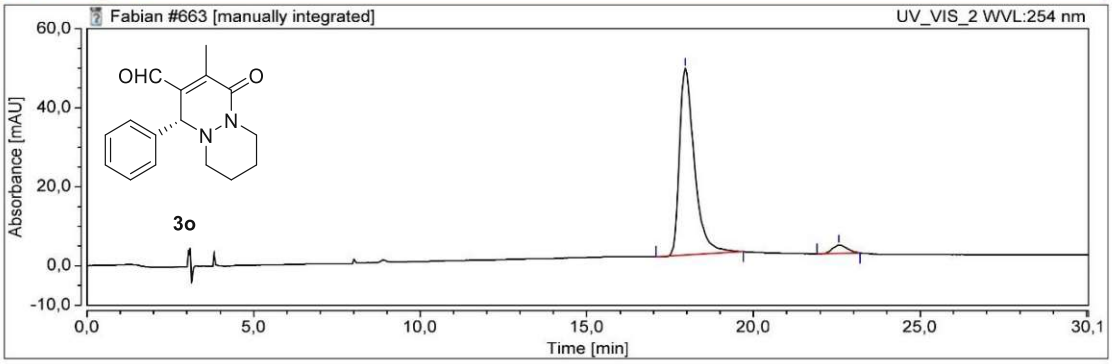


Reports IJD/Integration

Chromeleon (c) Dionex
Version 7.1.1.1127

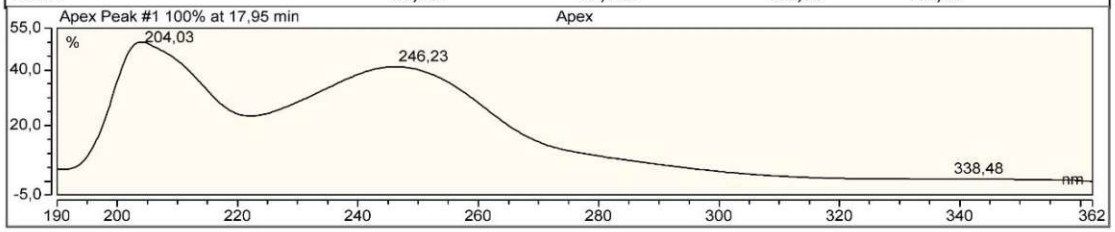
Die approbierte gedruckte Originalversion dieser Dissertation ist an der TU Wien Bibliothek verfügbar.
The approved original version of this doctoral thesis is available in print at TU Wien Bibliothek.

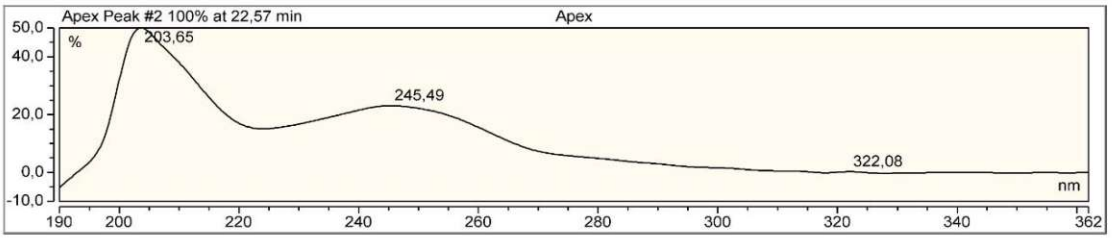
Chromatogram



Integration Results

No.	Peak Name	Retention Time min	Area mAU*min	Height mAU	Relative Area %	Relative Height %	Amount n.a.
1		17,953	24,638	47,299	95,75	95,74	n.a.
2		22,568	1,092	2,103	4,25	4,26	n.a.
Total:			**25,731**	**49,402**	**100,00**	**100,00**	





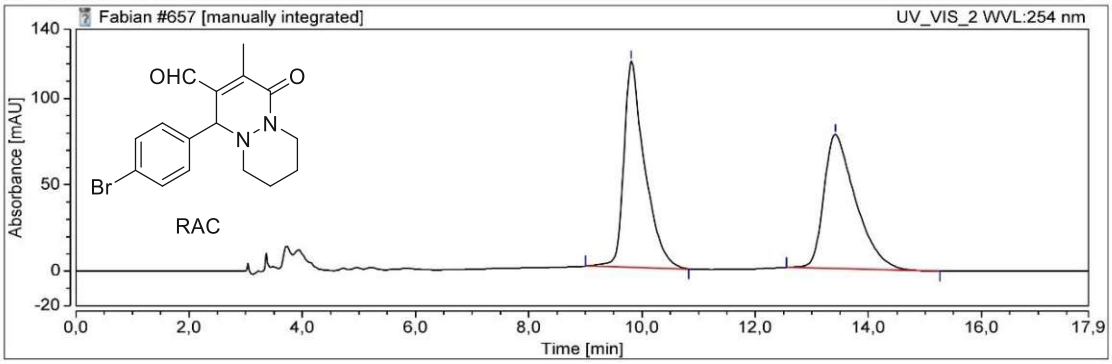
Reports IJD/Integration

Chromeleon (c) Dionex
Version 7.1.1.1127

Die approbierte gedruckte Originalversion dieser Dissertation ist an der TU Wien Bibliothek verfügbar.
The approved original version of this doctoral thesis is available in print at TU Wien Bibliothek.

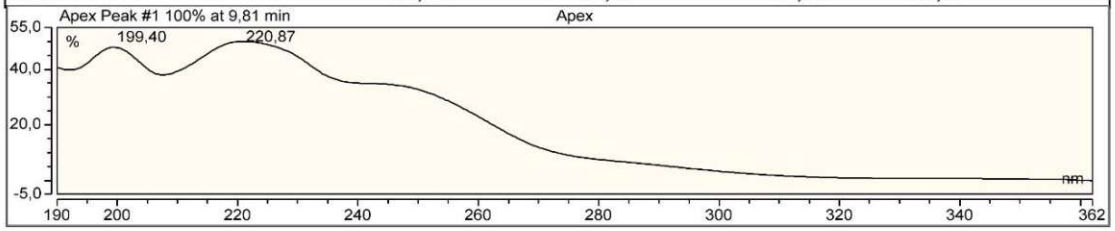
8.1.16 HPLC spectra of **3p**

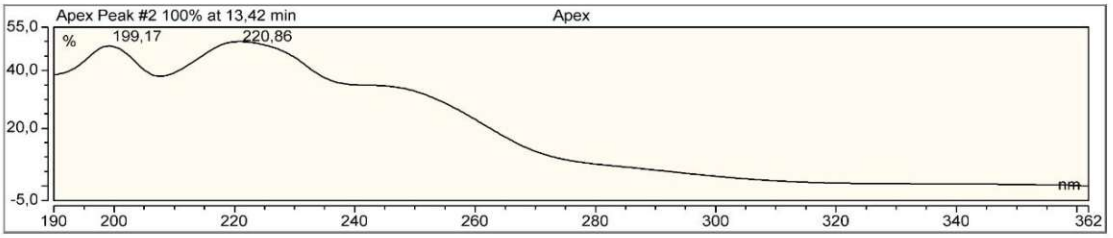
Chromatogram



Integration Results

No.	Peak Name	Retention Time min	Area mAU*min	Height mAU	Relative Area %	Relative Height %	Amount n.a.
1		9,810	51,033	119,488	50,22	60,60	n.a.
2		13,415	50,595	77,699	49,78	39,40	n.a.
Total:			**101,628**	**197,187**	**100,00**	**100,00**	



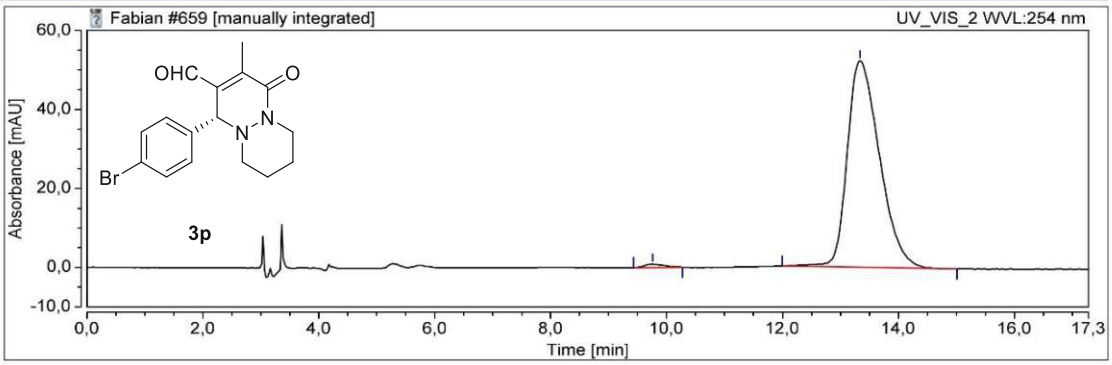


Reports IJD/Integration

Chromeleon (c) Dionex
Version 7.1.1.1127

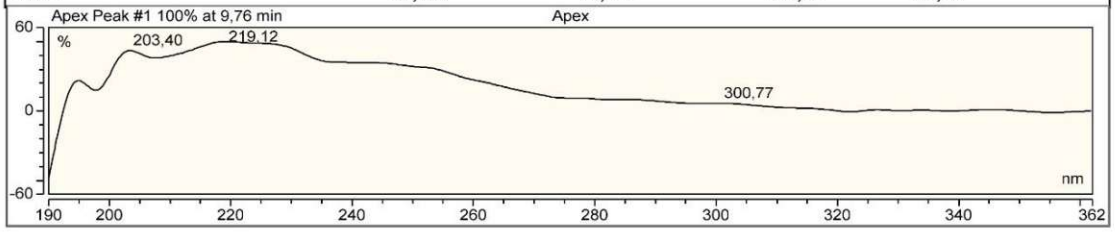
Die approbierte gedruckte Originalversion dieser Dissertation ist an der TU Wien Bibliothek verfügbar.
The approved original version of this doctoral thesis is available in print at TU Wien Bibliothek.

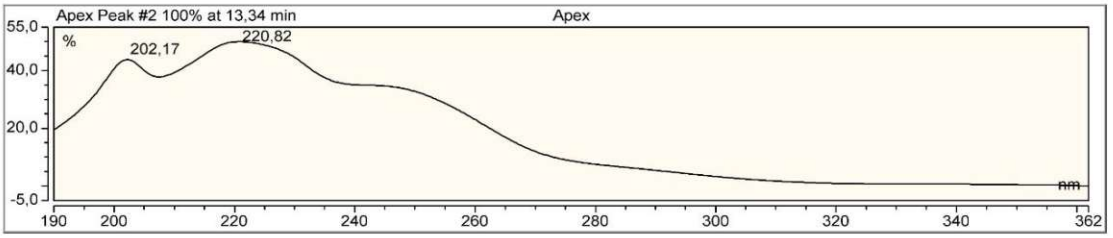
Chromatogram



Integration Results

No.	Peak Name	Retention Time min	Area mAU*min	Height mAU	Relative Area %	Relative Height %	Amount n.a.
1		9,760	0,305	0,806	0,90	1,52	n.a.
2		13,342	33,719	52,335	99,10	98,48	n.a.
Total:			**34,024**	**53,141**	**100,00**	**100,00**	



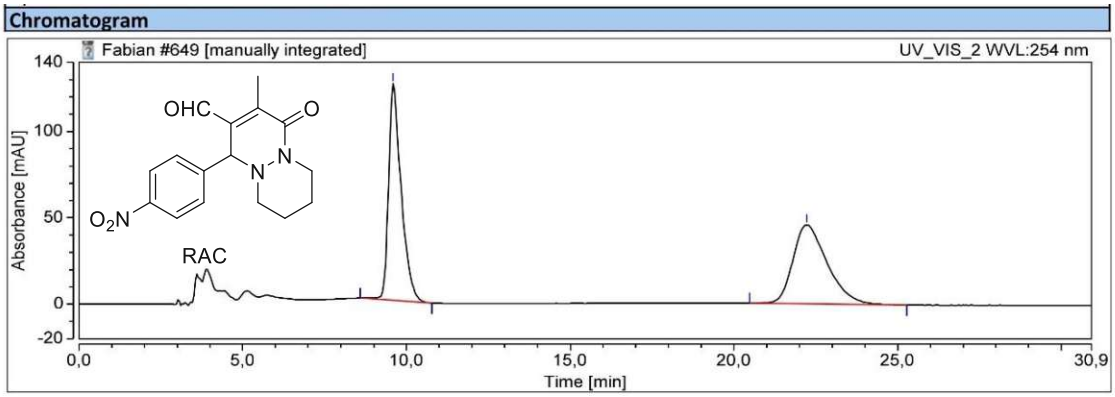


Reports IJD/Integration

Chromeleon (c) Dionex
Version 7.1.1.1127

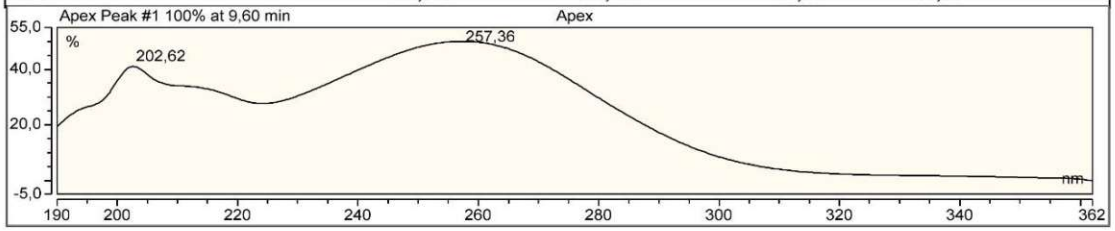
Die approbierte gedruckte Originalversion dieser Dissertation ist an der TU Wien Bibliothek verfügbar.
The approved original version of this doctoral thesis is available in print at TU Wien Bibliothek.

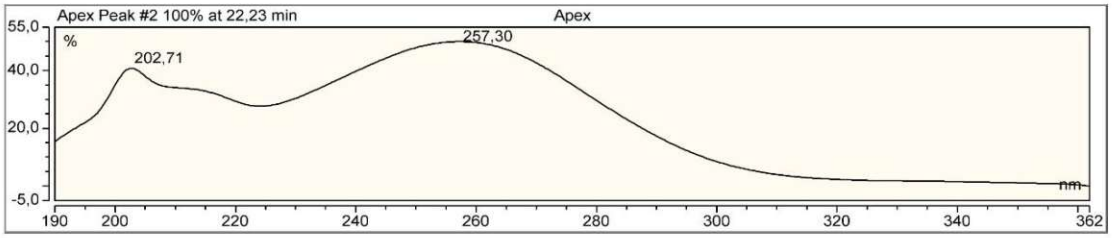
8.1.17 HPLC spectra of **3q**



Integration Results

No.	Peak Name	Retention Time min	Area mAU*min	Height mAU	Relative Area %	Relative Height %	Amount n.a.
1		9,595	56,192	125,473	50,48	73,32	n.a.
2		22,227	55,124	45,650	49,52	26,68	n.a.
Total:			**111,316**	**171,123**	**100,00**	**100,00**	



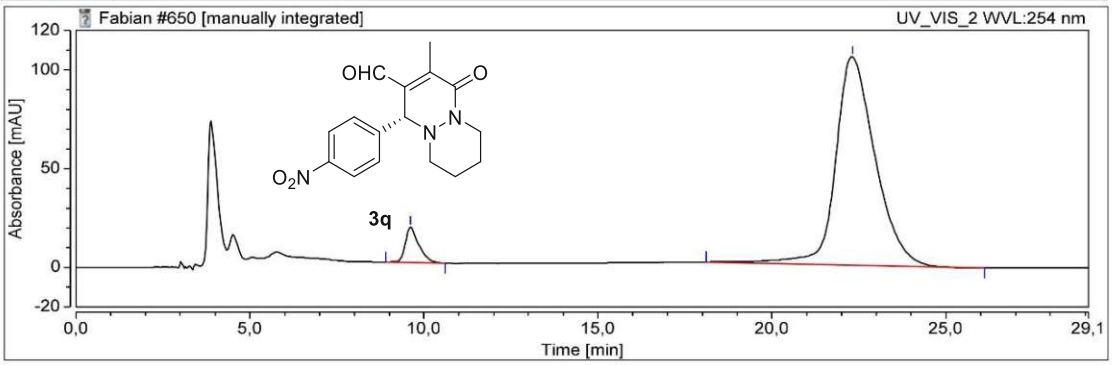


Reports IJD/Integration

Chromeleon (c) Dionex
Version 7.1.1.1127

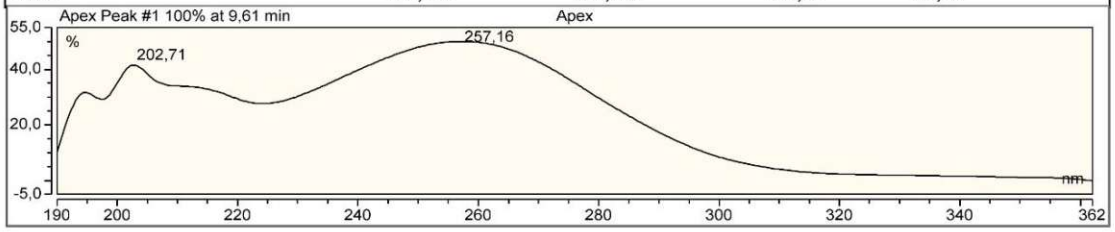
Die approbierte gedruckte Originalversion dieser Dissertation ist an der TU Wien Bibliothek verfügbar.
The approved original version of this doctoral thesis is available in print at TU Wien Bibliothek.

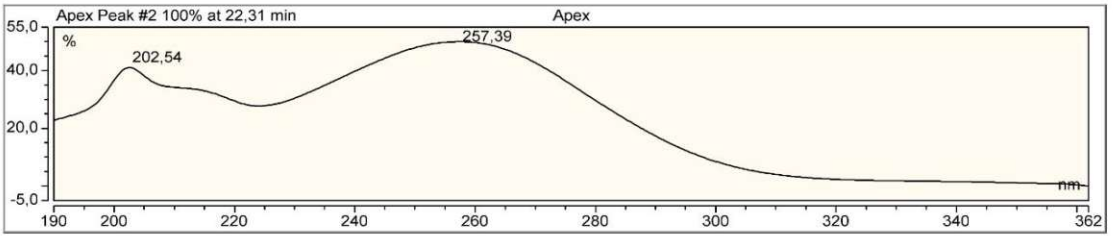
Chromatogram



Integration Results

No.	Peak Name	Retention Time min	Area mAU*min	Height mAU	Relative Area %	Relative Height %	Amount n.a.
1		9,610	8,275	18,148	5,62	14,66	n.a.
2		22,307	138,881	105,604	94,38	85,34	n.a.
Total:			**147,156**	**123,752**	**100,00**	**100,00**	





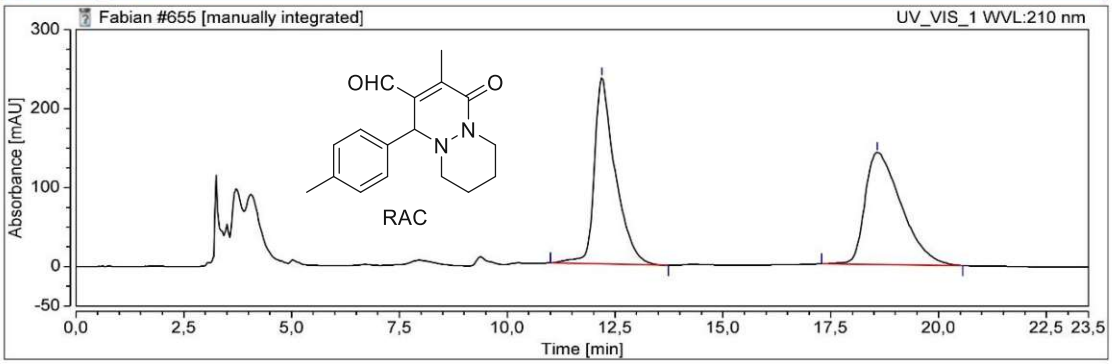
Reports IJD/Integration

Chromeleon (c) Dionex
Version 7.1.1.1127

Die approbierte gedruckte Originalversion dieser Dissertation ist an der TU Wien Bibliothek verfügbar.
The approved original version of this doctoral thesis is available in print at TU Wien Bibliothek.

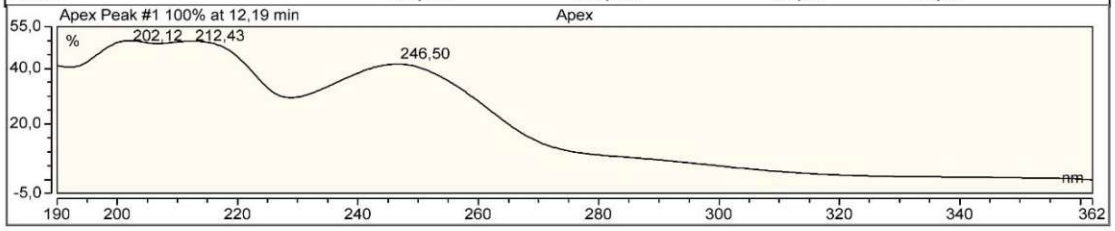
8.1.18 HPLC spectra of **3r**

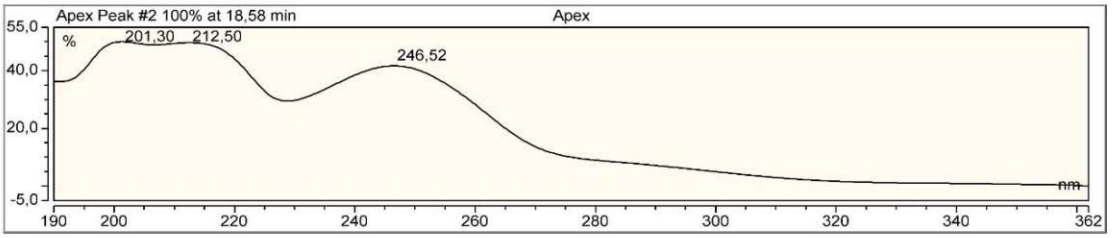
Chromatogram



Integration Results

No.	Peak Name	Retention Time min	Area mAU*min	Height mAU	Relative Area %	Relative Height %	Amount n.a.
1		12,192	132,921	235,935	48,89	62,41	n.a.
2		18,578	138,975	142,113	51,11	37,59	n.a.
Total:			**271,896**	**378,048**	**100,00**	**100,00**	



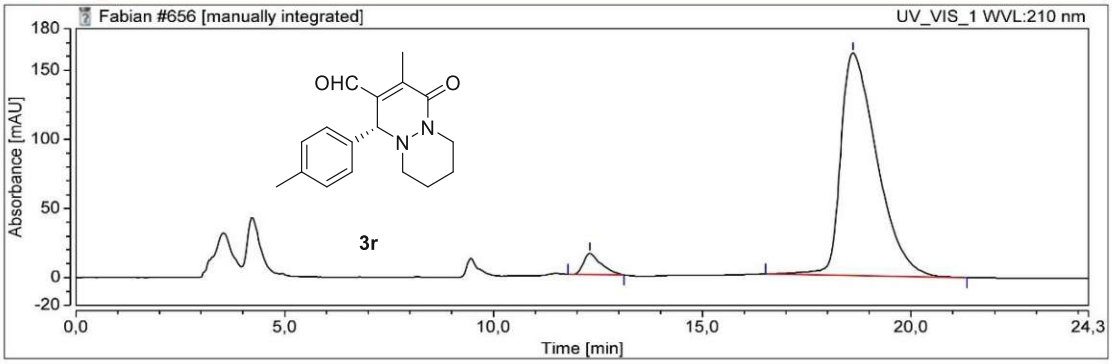


Reports IJD/Integration

Chromeleon (c) Dionex
Version 7.1.1.1127

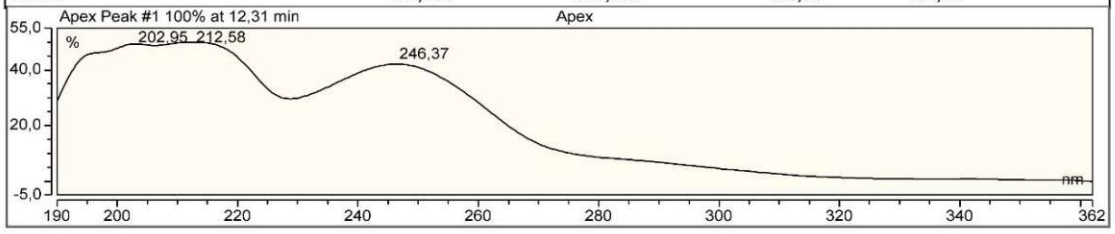
Die approbierte gedruckte Originalversion dieser Dissertation ist an der TU Wien Bibliothek verfügbar.
The approved original version of this doctoral thesis is available in print at TU Wien Bibliothek.

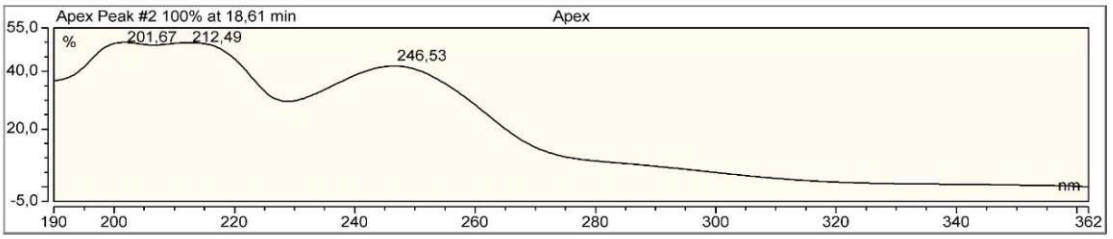
Chromatogram



Integration Results

No.	Peak Name	Retention Time min	Area mAU*min	Height mAU	Relative Area %	Relative Height %	Amount n.a.
1		12,305	7,516	15,448	4,42	8,74	n.a.
2		18,607	162,680	161,218	95,58	91,26	n.a.
Total:			**170,196**	**176,666**	**100,00**	**100,00**	



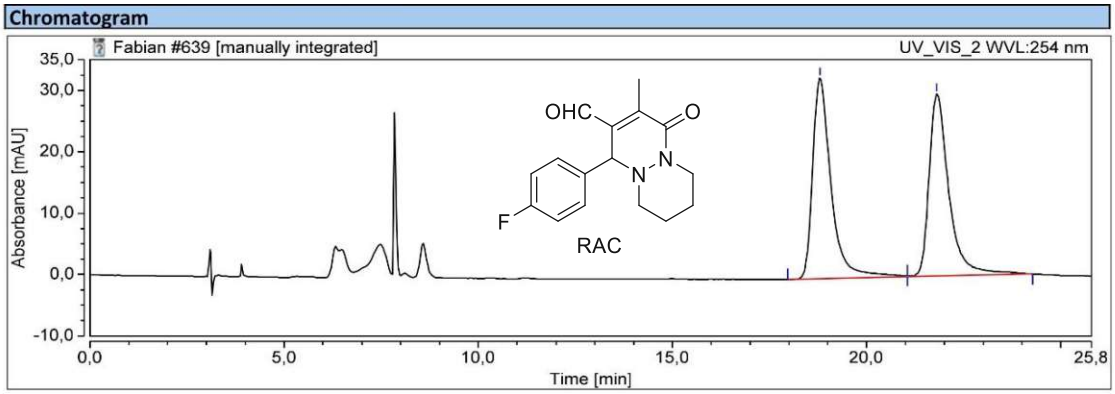


Reports IJD/Integration

Chromeleon (c) Dionex
Version 7.1.1.1127

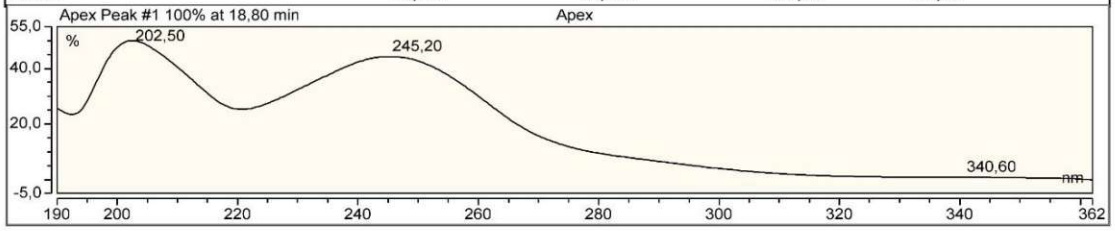
Die approbierte gedruckte Originalversion dieser Dissertation ist an der TU Wien Bibliothek verfügbar.
The approved original version of this doctoral thesis is available in print at TU Wien Bibliothek.

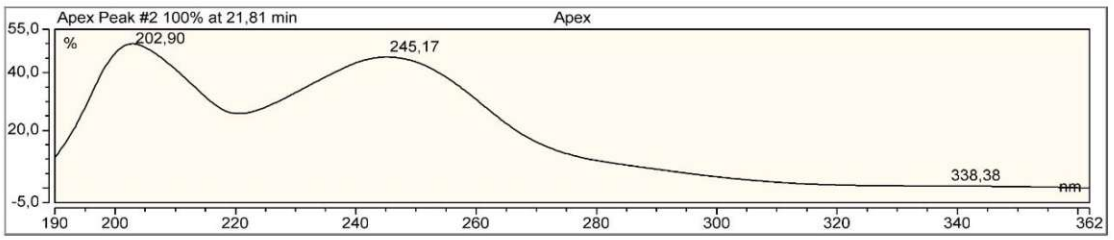
8.1.19 HPLC spectra of **3s**



Integration Results

No.	Peak Name	Retention Time min	Area mAU*min	Height mAU	Relative Area %	Relative Height %	Amount n.a.
1		18,800	18,020	32,719	50,56	52,39	n.a.
2		21,807	17,621	29,731	49,44	47,61	n.a.
Total:			**35,642**	**62,449**	**100,00**	**100,00**	



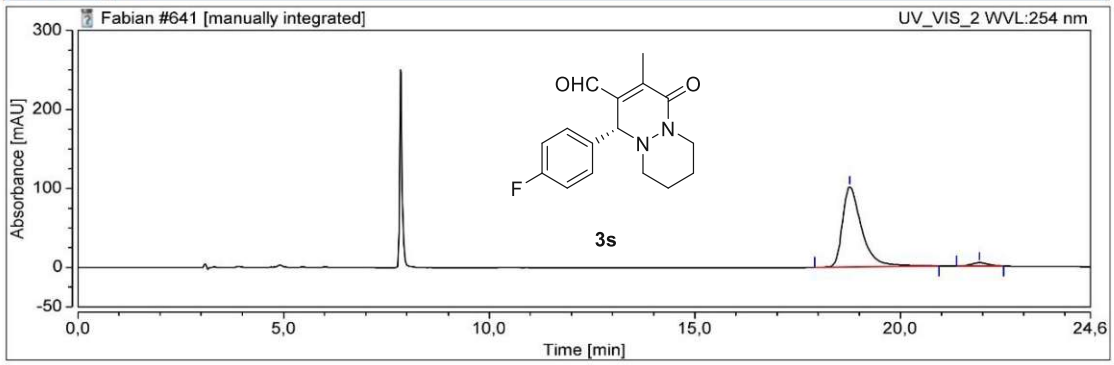


Reports IJD/Integration

Chromeleon (c) Dionex
Version 7.1.1.1127

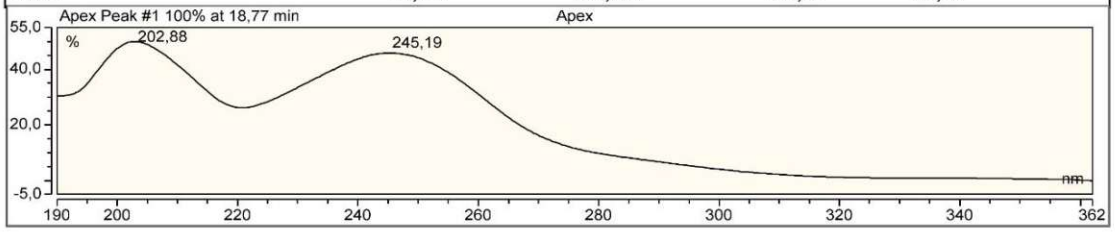
Die approbierte gedruckte Originalversion dieser Dissertation ist an der TU Wien Bibliothek verfügbar.
The approved original version of this doctoral thesis is available in print at TU Wien Bibliothek.

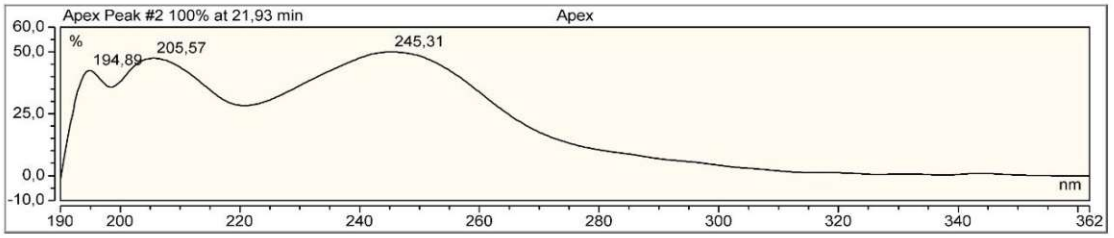
Chromatogram



Integration Results

No.	Peak Name	Retention Time min	Area mAU*min	Height mAU	Relative Area %	Relative Height %	Amount n.a.
1		18,767	55,122	101,522	96,46	96,07	n.a.
2		21,925	2,021	4,152	3,54	3,93	n.a.
Total:			**57,143**	**105,673**	**100,00**	**100,00**	





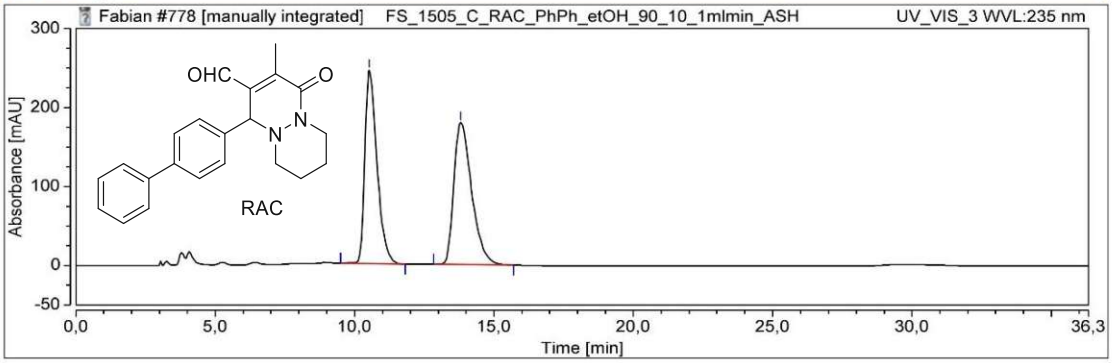
Reports IJD/Integration

Chromeleon (c) Dionex
Version 7.1.1.1127

Die approbierte gedruckte Originalversion dieser Dissertation ist an der TU Wien Bibliothek verfügbar.
The approved original version of this doctoral thesis is available in print at TU Wien Bibliothek.

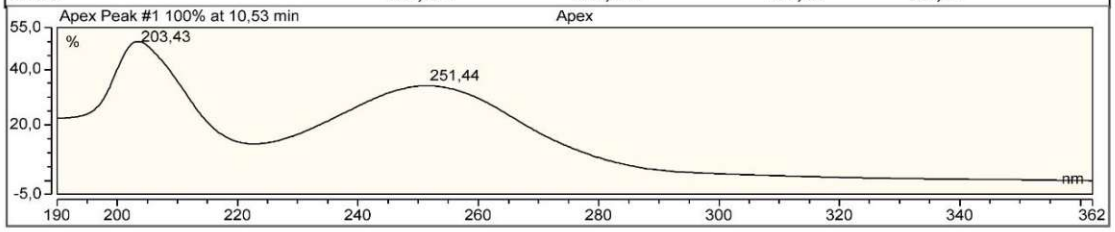
8.1.20 HPLC spectra of **3t**

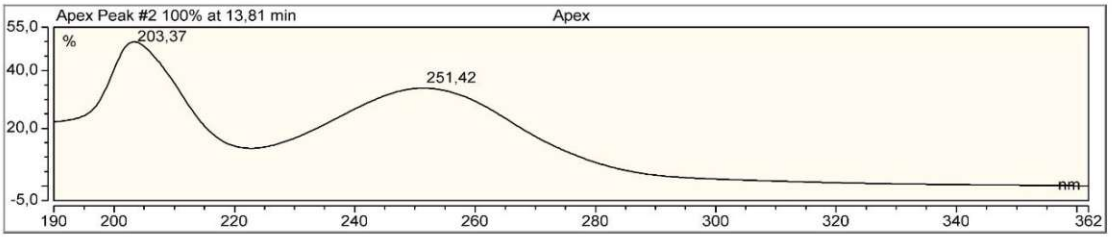
Chromatogram



Integration Results

No.	Peak Name	Retention Time min	Area mAU*min	Height mAU	Relative Area %	Relative Height %	Amount n.a.
1		10,527	123,797	245,122	48,09	57,64	n.a.
2		13,808	133,605	180,150	51,91	42,36	n.a.
Total:			**257,402**	**425,272**	**100,00**	**100,00**	



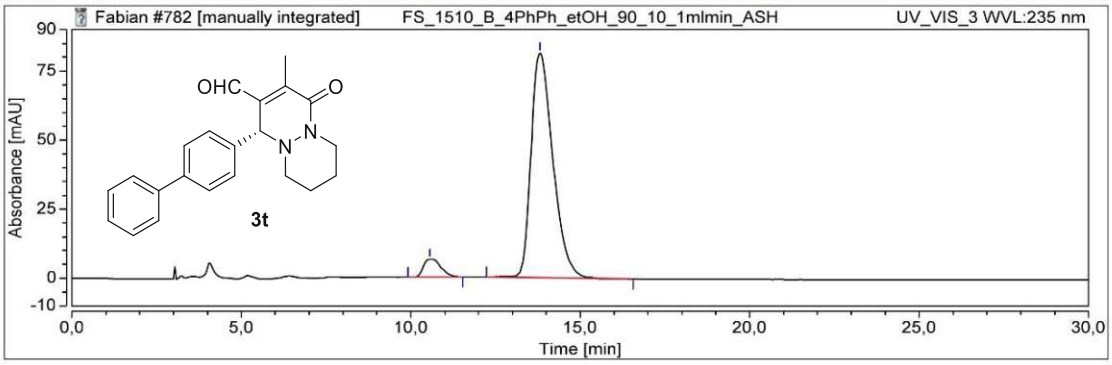


Reports IJD/Integration

Chromeleon (c) Dionex
Version 7.1.1.1127

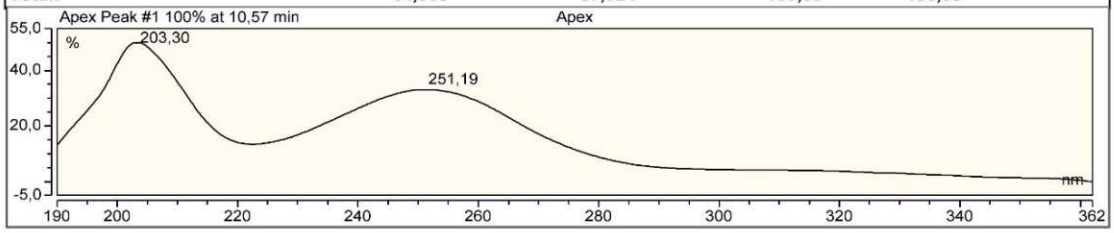
Die approbierte gedruckte Originalversion dieser Dissertation ist an der TU Wien Bibliothek verfügbar.
The approved original version of this doctoral thesis is available in print at TU Wien Bibliothek.

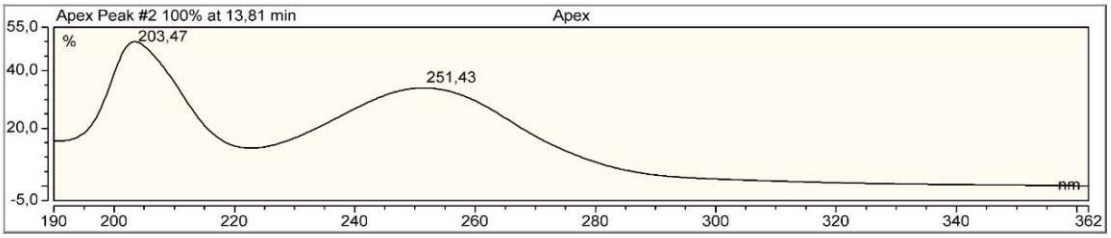
Chromatogram



Integration Results

No.	Peak Name	Retention Time min	Area mAU*min	Height mAU	Relative Area %	Relative Height %	Amount n.a.
1		10,568	3,916	6,541	6,03	7,44	n.a.
2		13,812	61,020	81,383	93,97	92,56	n.a.
Total:			**64,936**	**87,924**	**100,00**	**100,00**	



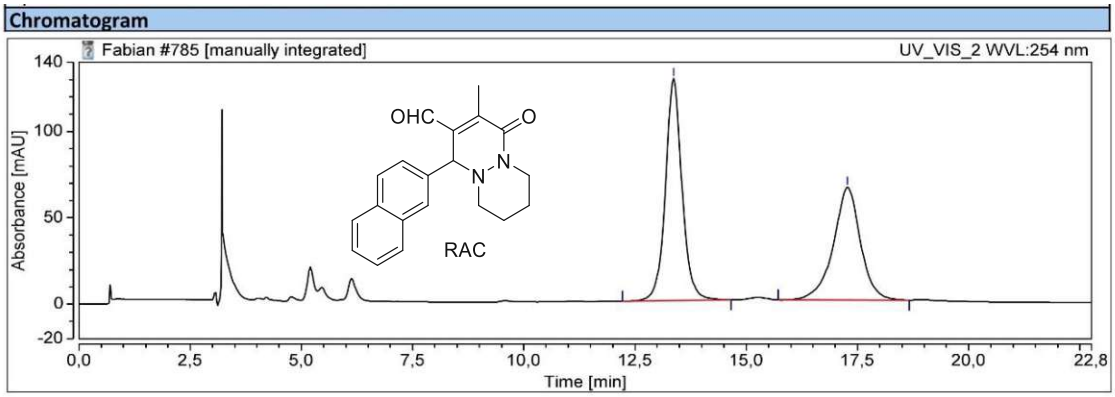


Reports IJD/Integration

Chromeleon (c) Dionex
Version 7.1.1.1127

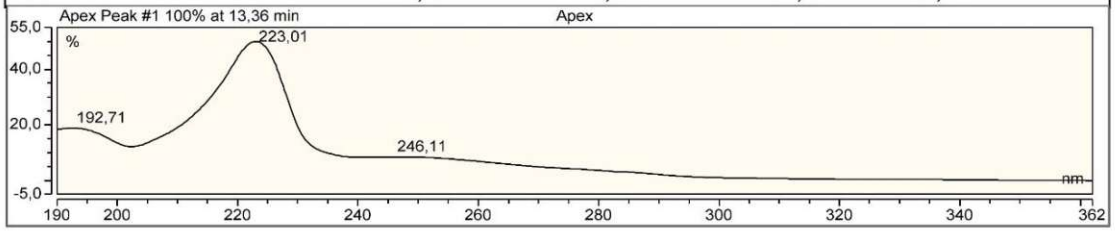
Die approbierte gedruckte Originalversion dieser Dissertation ist an der TU Wien Bibliothek verfügbar.
The approved original version of this doctoral thesis is available in print at TU Wien Bibliothek.

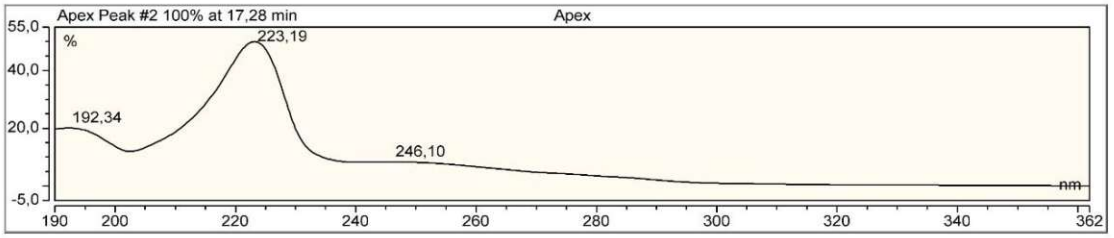
8.1.21 HPLC spectra of **3u**



Integration Results

No.	Peak Name	Retention Time min	Area mAU*min	Height mAU	Relative Area %	Relative Height %	Amount n.a.
1		13,363	55,779	128,735	54,62	66,33	n.a.
2		17,278	46,351	65,339	45,38	33,67	n.a.
Total:			**102,130**	**194,075**	**100,00**	**100,00**	



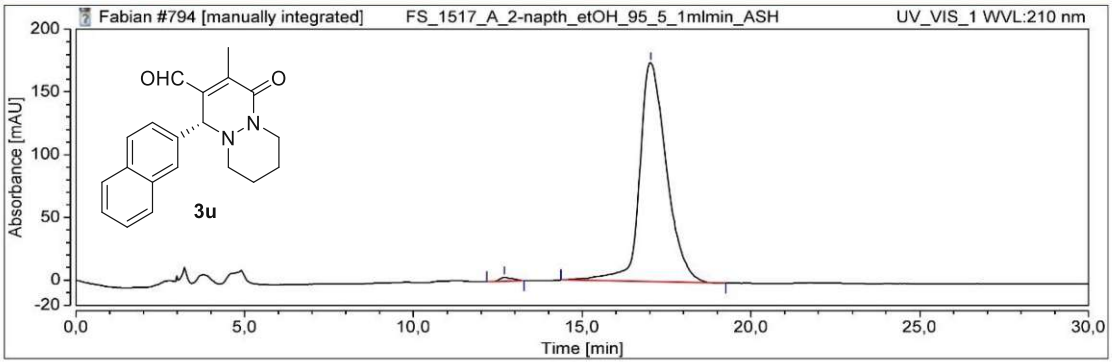


Reports IJD/Integration

Chromeleon (c) Dionex
Version 7.1.1.1127

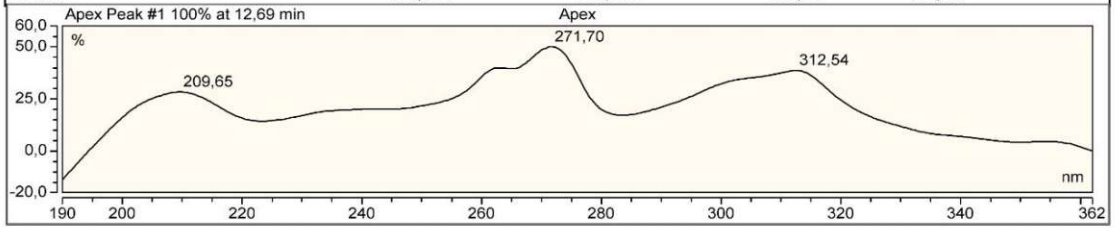
Die approbierte gedruckte Originalversion dieser Dissertation ist an der TU Wien Bibliothek verfügbar.
The approved original version of this doctoral thesis is available in print at TU Wien Bibliothek.

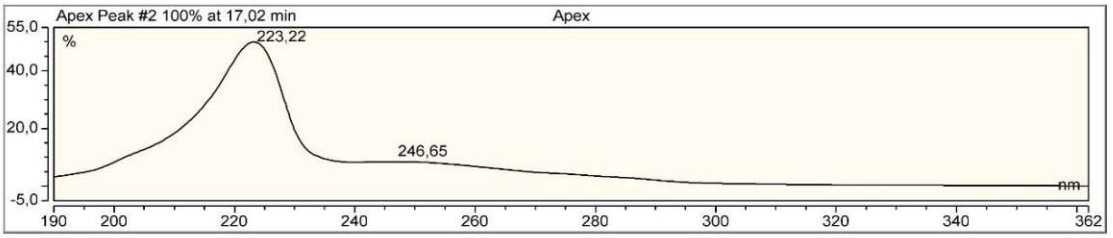
Chromatogram



Integration Results

No.	Peak Name	Retention Time min	Area mAU*min	Height mAU	Relative Area %	Relative Height %	Amount n.a.
1		12,685	1,330	3,159	0,82	1,78	n.a.
2		17,015	161,381	174,733	99,18	98,22	n.a.
Total:			**162,711**	**177,892**	**100,00**	**100,00**	



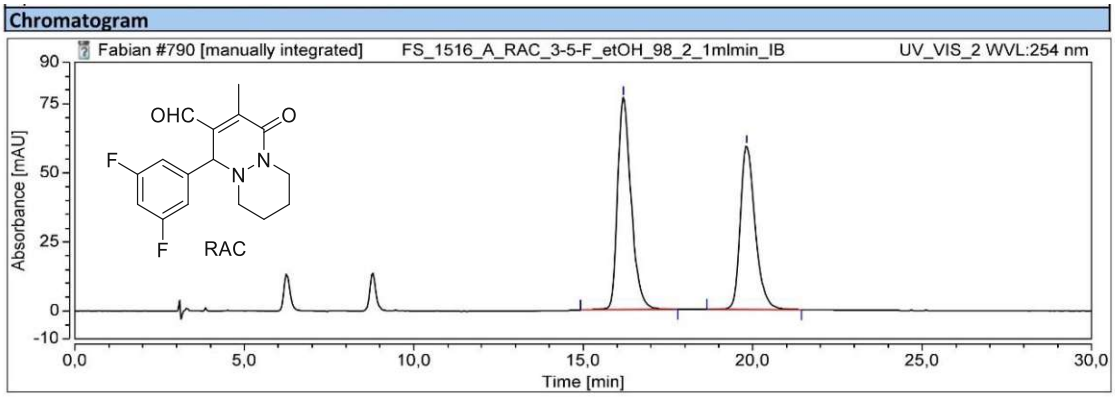


Reports IJD/Integration

Chromeleon (c) Dionex
Version 7.1.1.1127

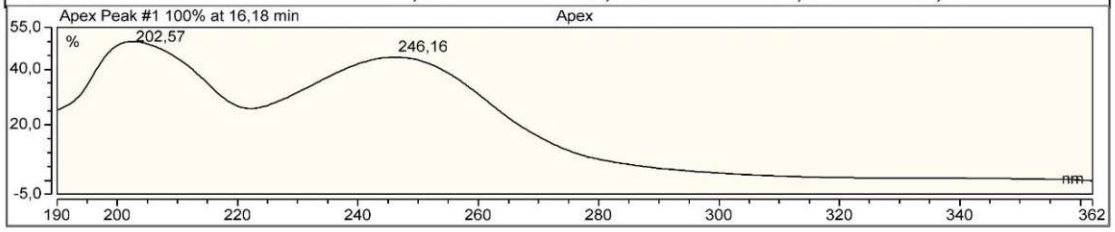
Die approbierte gedruckte Originalversion dieser Dissertation ist an der TU Wien Bibliothek verfügbar.
The approved original version of this doctoral thesis is available in print at TU Wien Bibliothek.

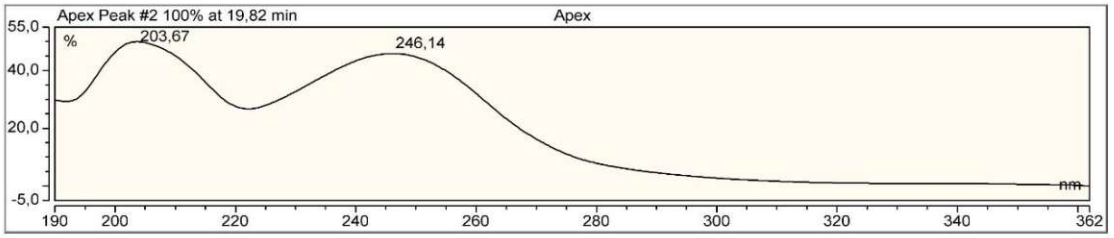
8.1.22 HPLC spectra of **3v**



Integration Results

No.	Peak Name	Retention Time min	Area mAU*min	Height mAU	Relative Area %	Relative Height %	Amount n.a.
1		16,178	35,549	76,922	54,20	56,49	n.a.
2		19,822	30,043	59,243	45,80	43,51	n.a.
Total:			**65,592**	**136,164**	**100,00**	**100,00**	



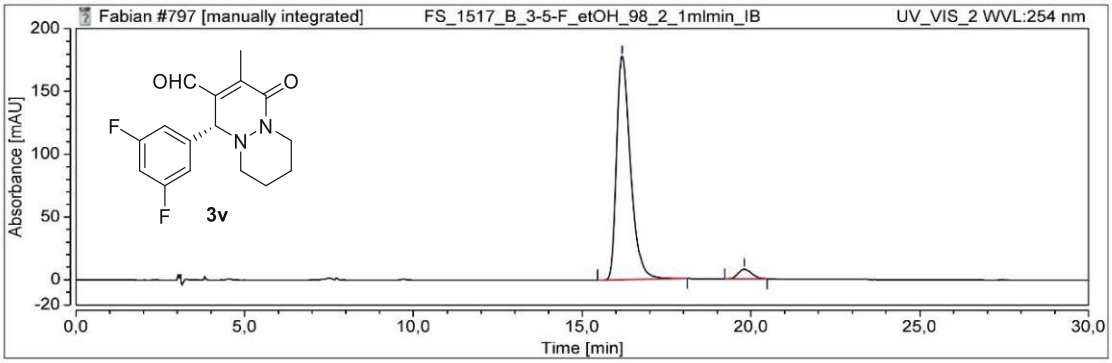


Reports IJD/Integration

Chromeleon (c) Dionex
Version 7.1.1.1127

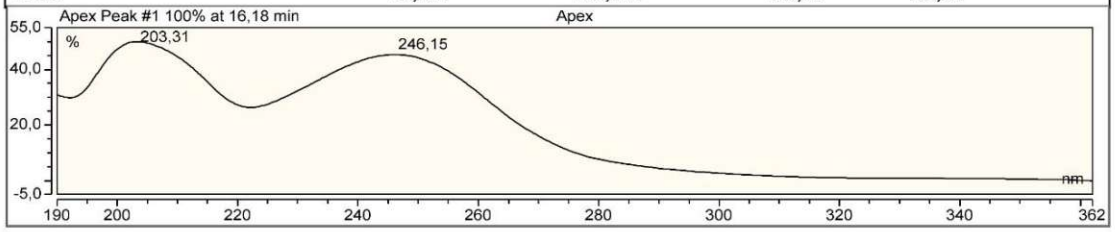
Die approbierte gedruckte Originalversion dieser Dissertation ist an der TU Wien Bibliothek verfügbar.
The approved original version of this doctoral thesis is available in print at TU Wien Bibliothek.

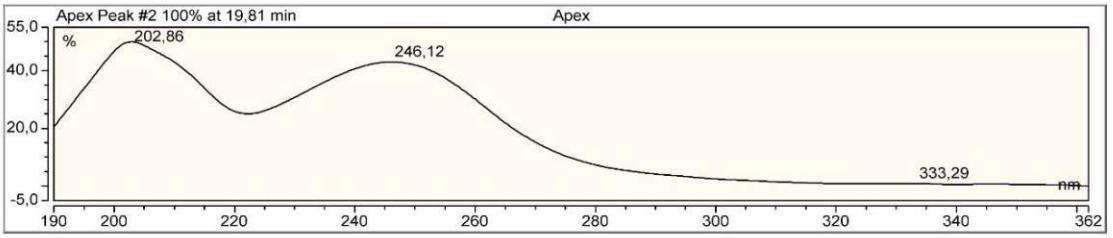
Chromatogram



Integration Results

No.	Peak Name	Retention Time min	Area mAU*min	Height mAU	Relative Area %	Relative Height %	Amount n.a.
1		16,182	84,872	178,021	95,87	95,84	n.a.
2		19,805	3,658	7,728	4,13	4,16	n.a.
Total:			**88,530**	**185,749**	**100,00**	**100,00**	



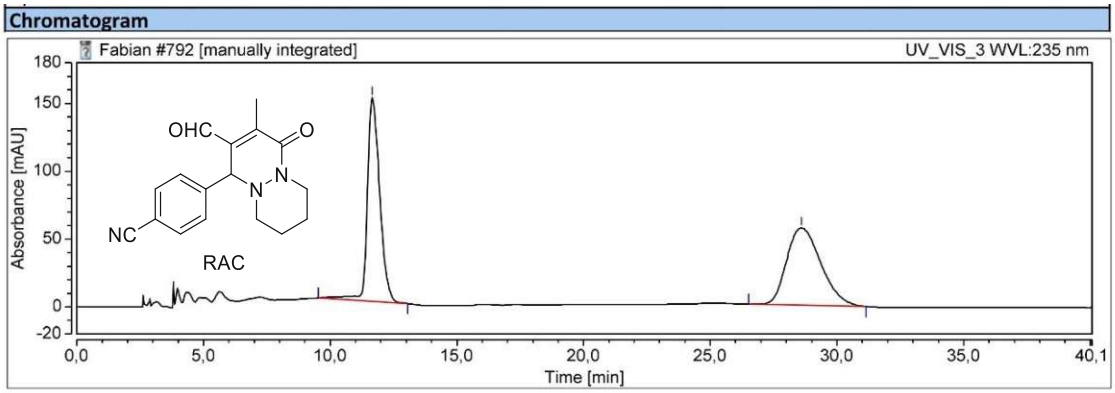


Reports IJD/Integration

Chromeleon (c) Dionex
Version 7.1.1.1127

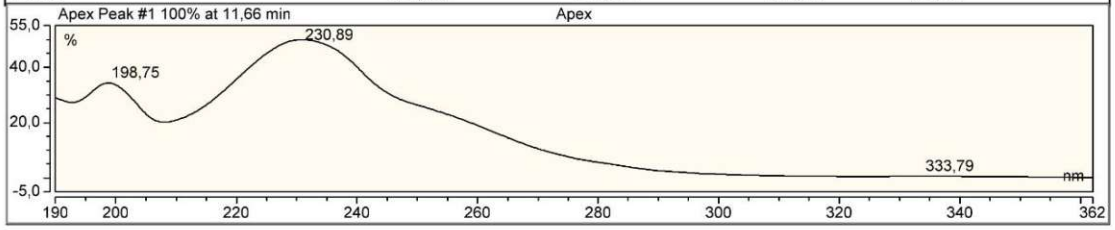
Die approbierte gedruckte Originalversion dieser Dissertation ist an der TU Wien Bibliothek verfügbar.
The approved original version of this doctoral thesis is available in print at TU Wien Bibliothek.

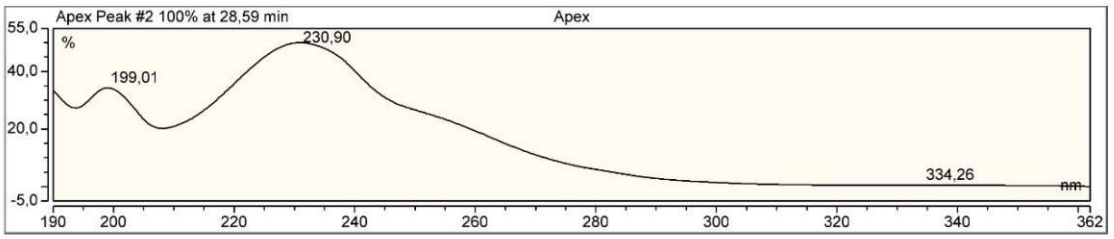
8.1.23 HPLC spectra of **3w**



Integration Results

No.	Peak Name	Retention Time min	Area mAU*min	Height mAU	Relative Area %	Relative Height %	Amount n.a.
1		11,662	84,793	150,488	48,67	72,50	n.a.
2		28,588	89,443	57,089	51,33	27,50	n.a.
Total:			**174,237**	**207,577**	**100,00**	**100,00**	



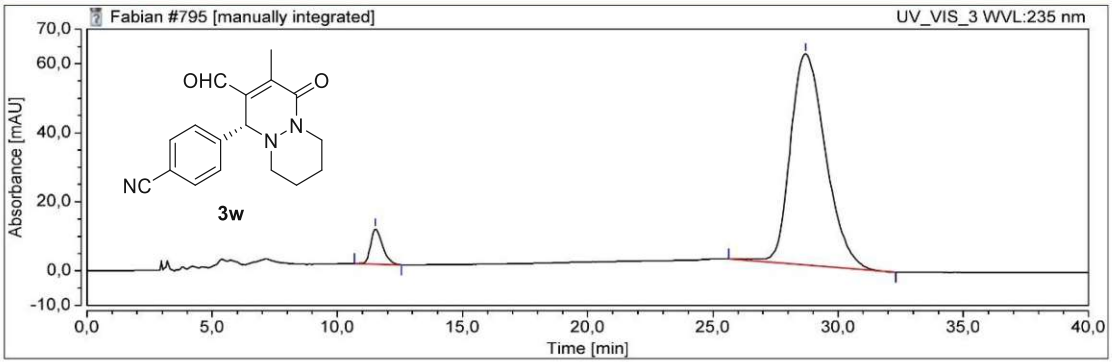


Reports IJD/Integration

Chromeleon (c) Dionex
Version 7.1.1.1127

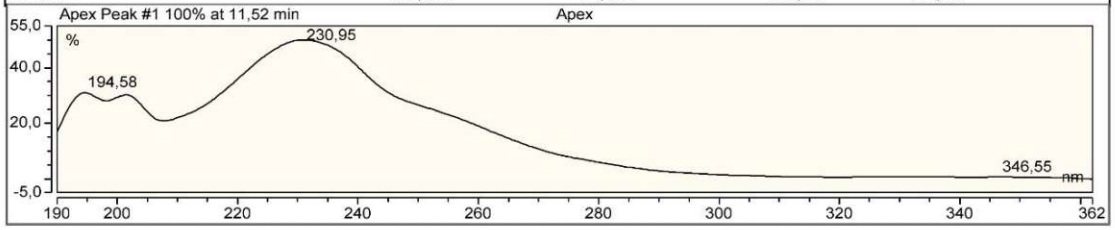
Die approbierte gedruckte Originalversion dieser Dissertation ist an der TU Wien Bibliothek verfügbar.
The approved original version of this doctoral thesis is available in print at TU Wien Bibliothek.

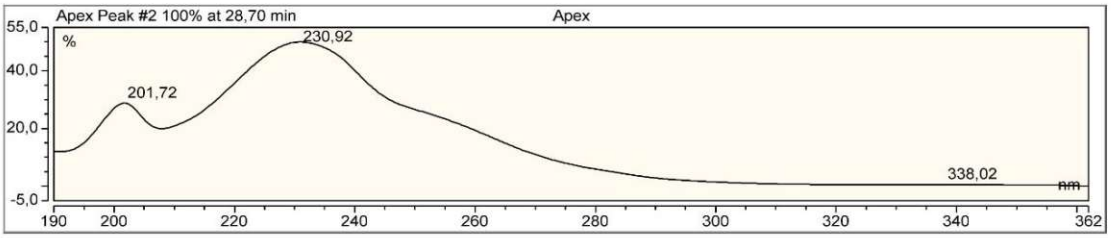
Chromatogram



Integration Results

No.	Peak Name	Retention Time min	Area mAU*min	Height mAU	Relative Area %	Relative Height %	Amount n.a.
1		11,515	5,669	10,207	5,38	14,29	n.a.
2		28,698	99,747	61,207	94,62	85,71	n.a.
Total:			**105,415**	**71,414**	**100,00**	**100,00**	



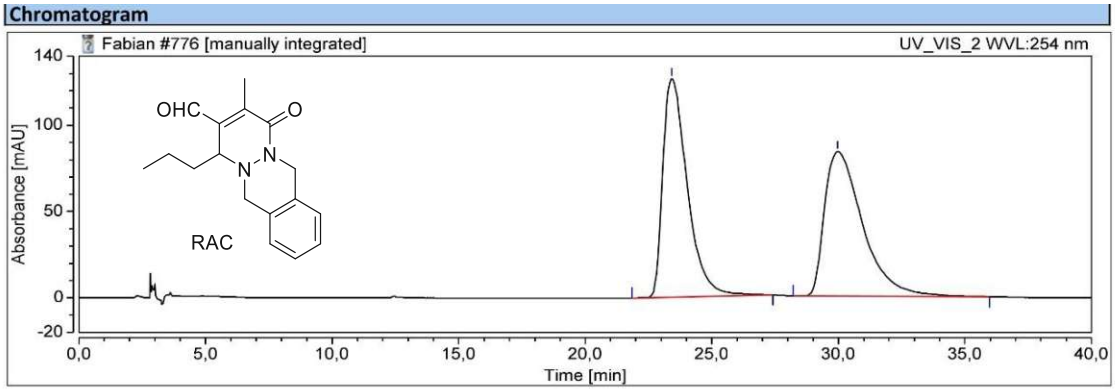


Reports IJD/Integration

Chromeleon (c) Dionex
Version 7.1.1.1127

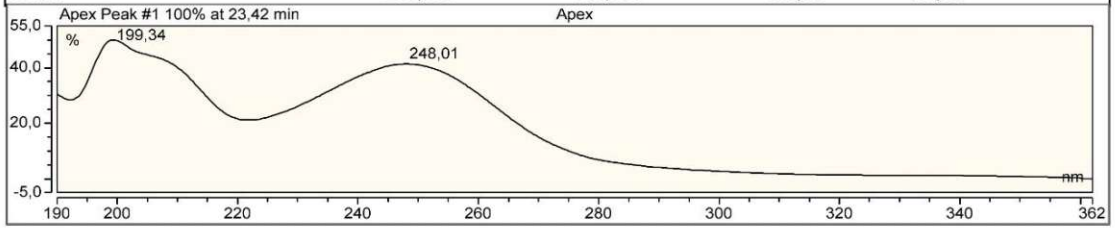
Die approbierte gedruckte Originalversion dieser Dissertation ist an der TU Wien Bibliothek verfügbar.
The approved original version of this doctoral thesis is available in print at TU Wien Bibliothek.

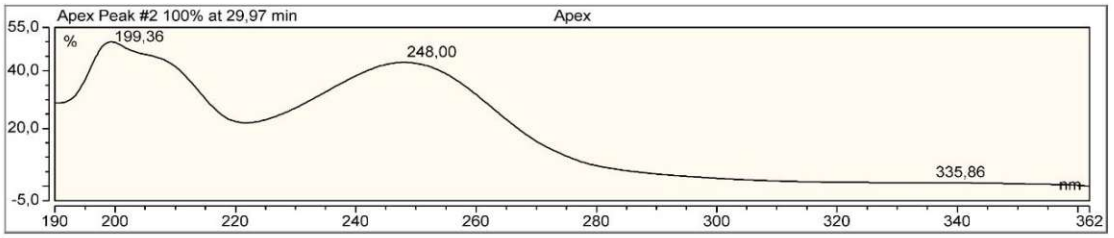
8.1.24 HPLC spectra of **3x**



Integration Results

No.	Peak Name	Retention Time min	Area mAU*min	Height mAU	Relative Area %	Relative Height %	Amount n.a.
1		23,418	142,527	126,826	49,44	60,24	n.a.
2		29,972	145,775	83,708	50,56	39,76	n.a.
Total:			**288,302**	**210,534**	**100,00**	**100,00**	



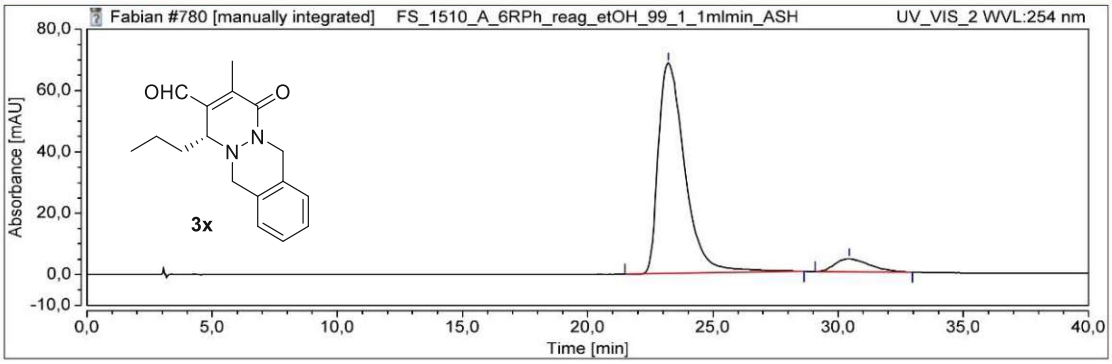


Reports IJD/Integration

Chromeleon (c) Dionex
Version 7.1.1.1127

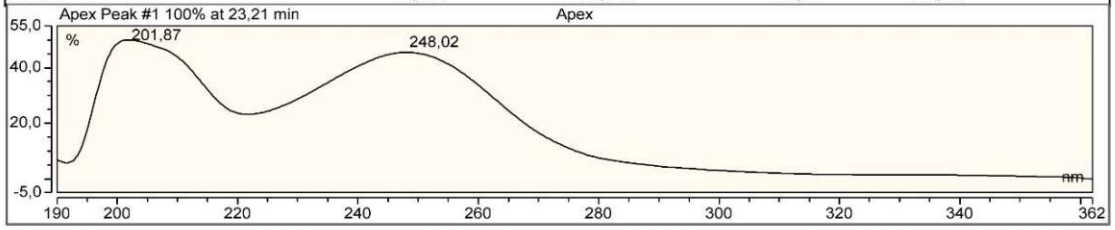
Die approbierte gedruckte Originalversion dieser Dissertation ist an der TU Wien Bibliothek verfügbar.
The approved original version of this doctoral thesis is available in print at TU Wien Bibliothek.

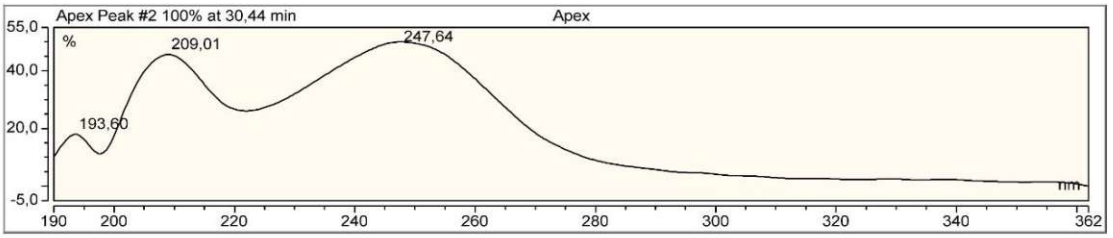
Chromatogram



Integration Results

No.	Peak Name	Retention Time min	Area mAU*min	Height mAU	Relative Area %	Relative Height %	Amount n.a.
1		23,210	84,411	68,648	92,57	94,24	n.a.
2		30,440	6,773	4,196	7,43	5,76	n.a.
Total:			**91,184**	**72,844**	**100,00**	**100,00**	





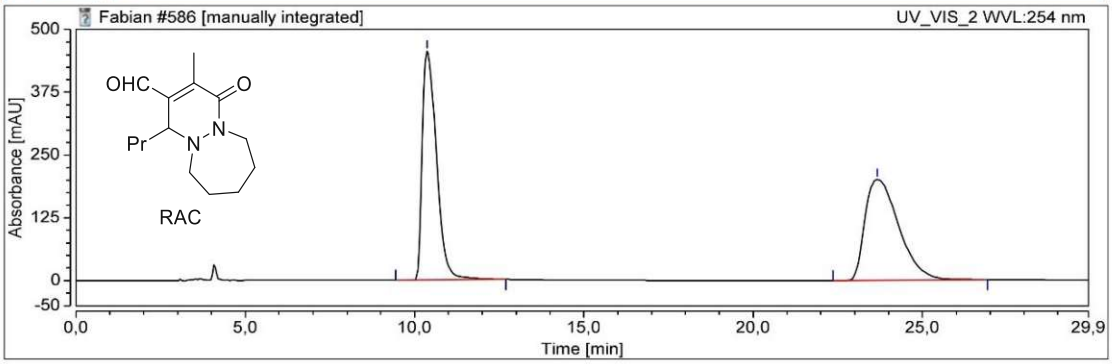
Reports IJD/Integration

Chromeleon (c) Dionex
Version 7.1.1.1127

Die approbierte gedruckte Originalversion dieser Dissertation ist an der TU Wien Bibliothek verfügbar.
The approved original version of this doctoral thesis is available in print at TU Wien Bibliothek.

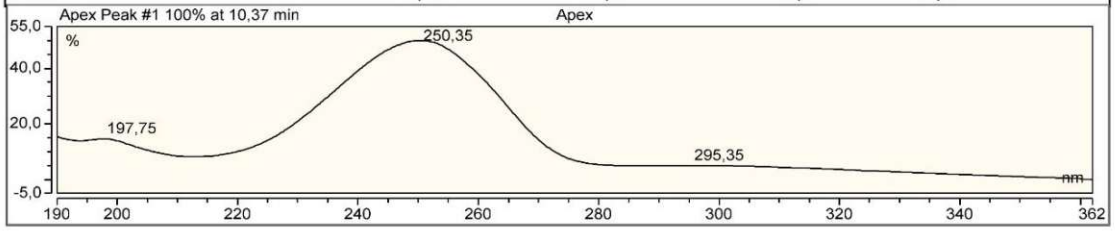
8.1.25 HPLC spectra of **3y**

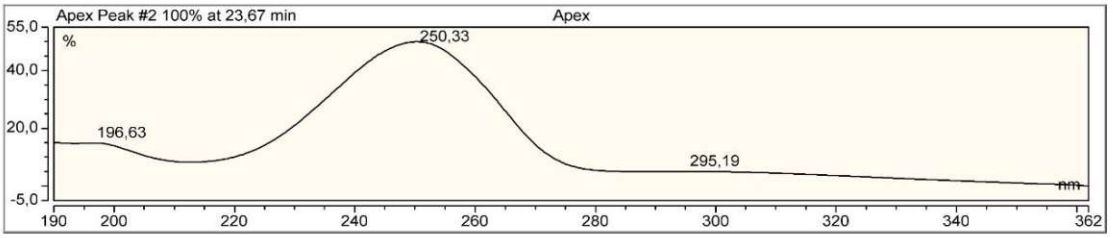
Chromatogram



Integration Results

No.	Peak Name	Retention Time min	Area mAU*min	Height mAU	Relative Area %	Relative Height %	Amount n.a.
1		10,368	224,874	456,670	49,16	69,42	n.a.
2		23,665	232,548	201,187	50,84	30,58	n.a.
Total:			**457,422**	**657,857**	**100,00**	**100,00**	



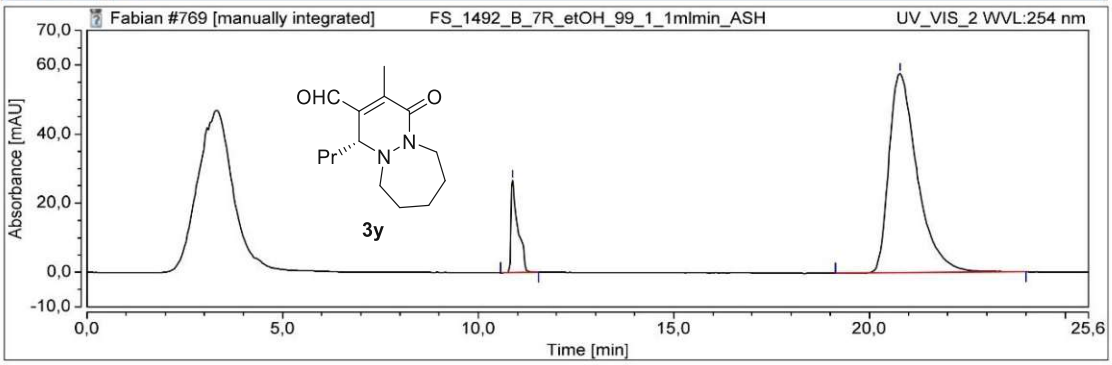


Reports IJD/Integration

Chromeleon (c) Dionex
Version 7.1.1.1127

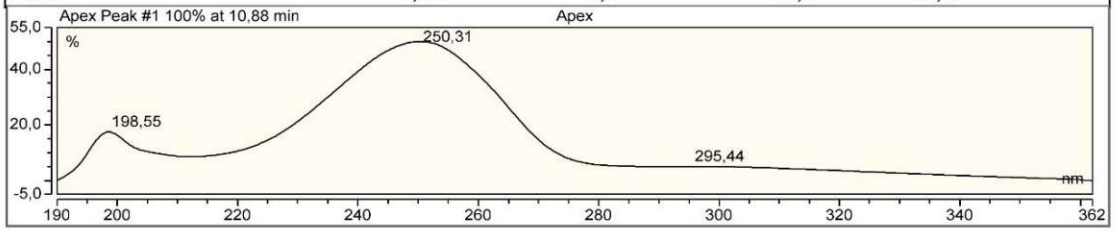
Die approbierte gedruckte Originalversion dieser Dissertation ist an der TU Wien Bibliothek verfügbar.
The approved original version of this doctoral thesis is available in print at TU Wien Bibliothek.

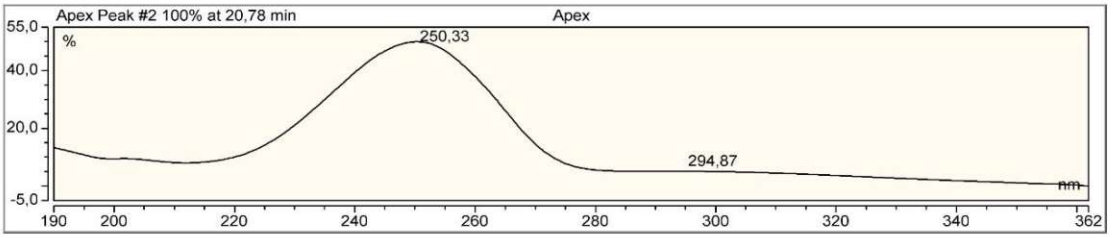
Chromatogram



Integration Results

No.	Peak Name	Retention Time min	Area mAU*min	Height mAU	Relative Area %	Relative Height %	Amount n.a.
1		10,878	5,549	26,687	10,31	31,63	n.a.
2		20,777	48,280	57,683	89,69	68,37	n.a.
Total:			**53,829**	**84,370**	**100,00**	**100,00**	





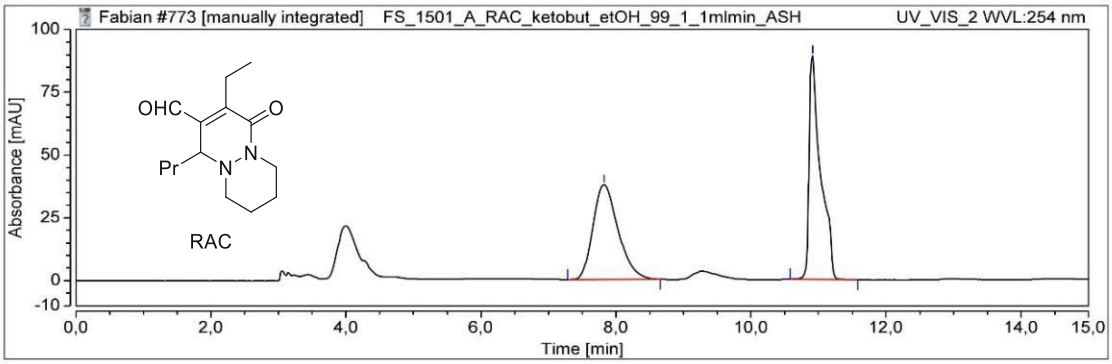
Reports IJD/Integration

Chromeleon (c) Dionex
Version 7.1.1.1127

Die approbierte gedruckte Originalversion dieser Dissertation ist an der TU Wien Bibliothek verfügbar.
The approved original version of this doctoral thesis is available in print at TU Wien Bibliothek.

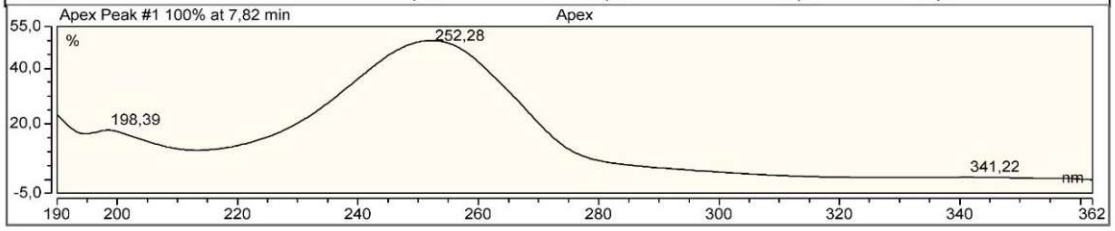
8.1.26 HPLC spectra of **3z**

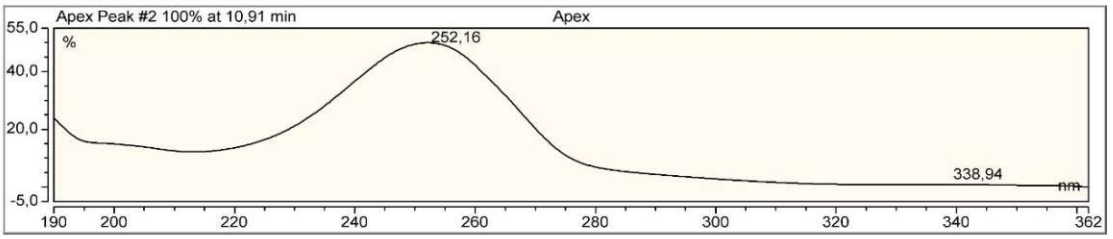
Chromatogram



Integration Results

No.	Peak Name	Retention Time min	Area mAU*min	Height mAU	Relative Area %	Relative Height %	Amount n.a.
1		7,822	16,242	37,681	47,87	29,76	n.a.
2		10,912	17,691	88,937	52,13	70,24	n.a.
Total:			**33,933**	**126,618**	**100,00**	**100,00**	



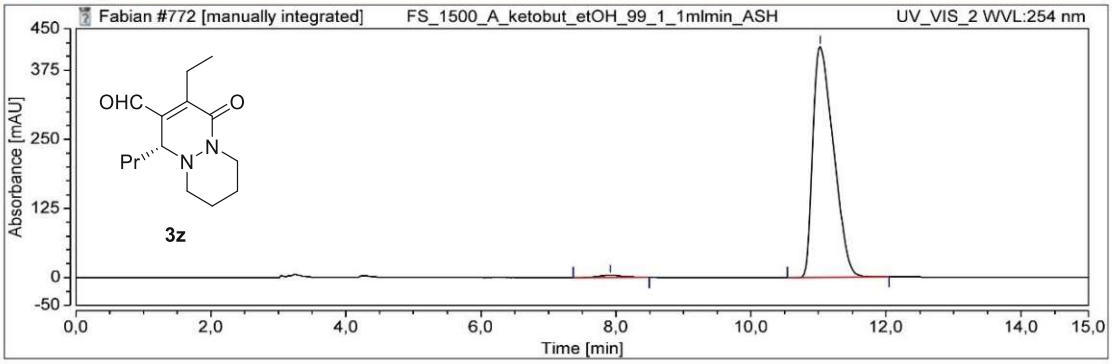


Reports IJD/Integration

Chromeleon (c) Dionex
Version 7.1.1.1127

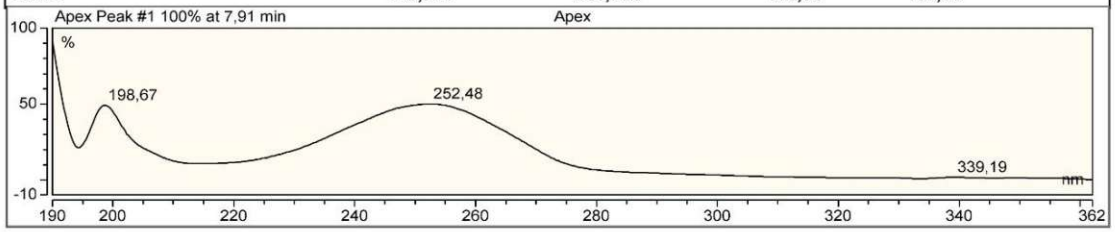
Die approbierte gedruckte Originalversion dieser Dissertation ist an der TU Wien Bibliothek verfügbar.
The approved original version of this doctoral thesis is available in print at TU Wien Bibliothek.

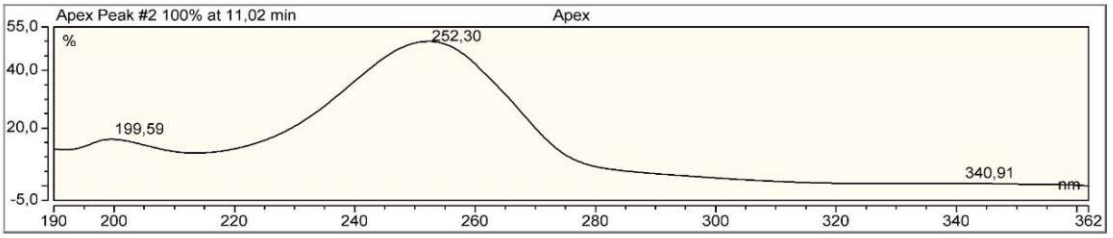
Chromatogram



Integration Results

No.	Peak Name	Retention Time min	Area mAU*min	Height mAU	Relative Area %	Relative Height %	Amount n.a.
1		7,913	1,632	3,884	1,09	0,92	n.a.
2		11,023	148,117	417,678	98,91	99,08	n.a.
Total:			**149,748**	**421,562**	**100,00**	**100,00**	





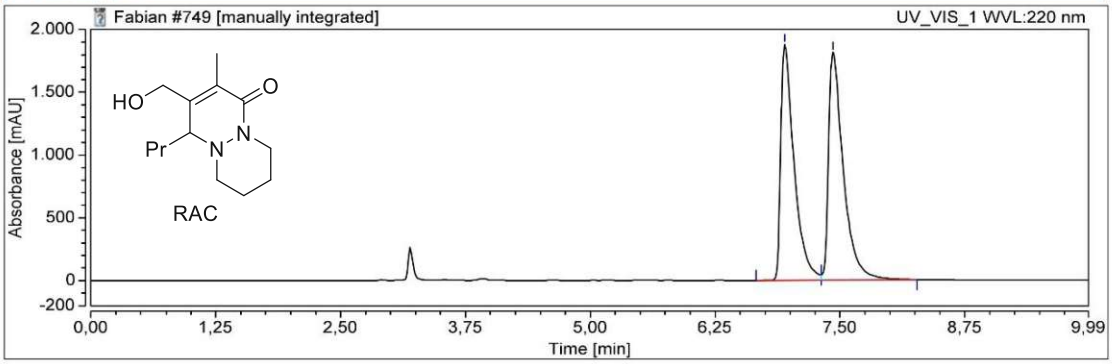
Reports IJD/Integration

Chromeleon (c) Dionex
Version 7.1.1.1127

Die approbierte gedruckte Originalversion dieser Dissertation ist an der TU Wien Bibliothek verfügbar.
The approved original version of this doctoral thesis is available in print at TU Wien Bibliothek.

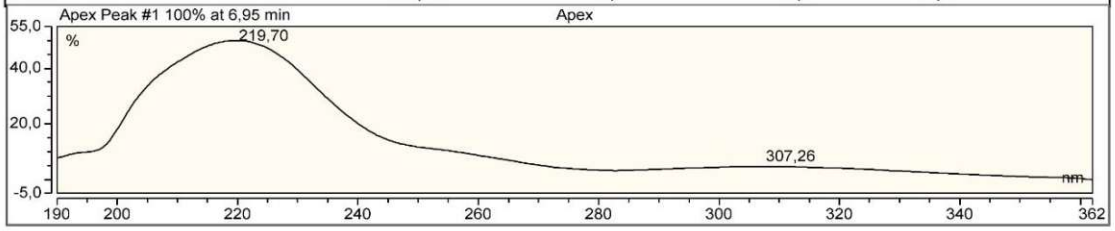
8.1.27 HPLC spectra of **4**

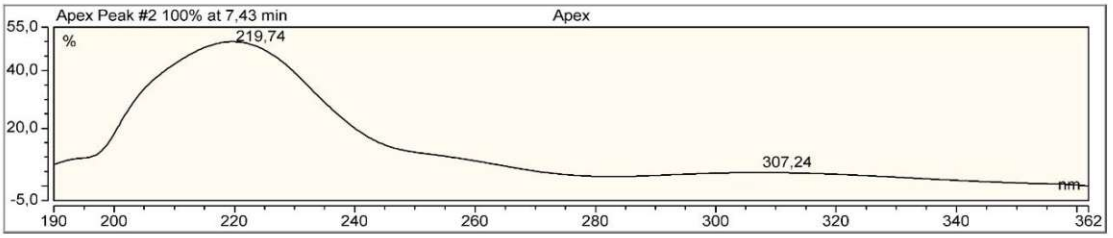
Chromatogram



Integration Results

No.	Peak Name	Retention Time min	Area mAU*min	Height mAU	Relative Area %	Relative Height %	Amount n.a.
1		6,948	290,455	1878,202	48,34	50,84	n.a.
2		7,430	310,350	1815,938	51,66	49,16	n.a.
Total:			**600,805**	**3694,140**	**100,00**	**100,00**	



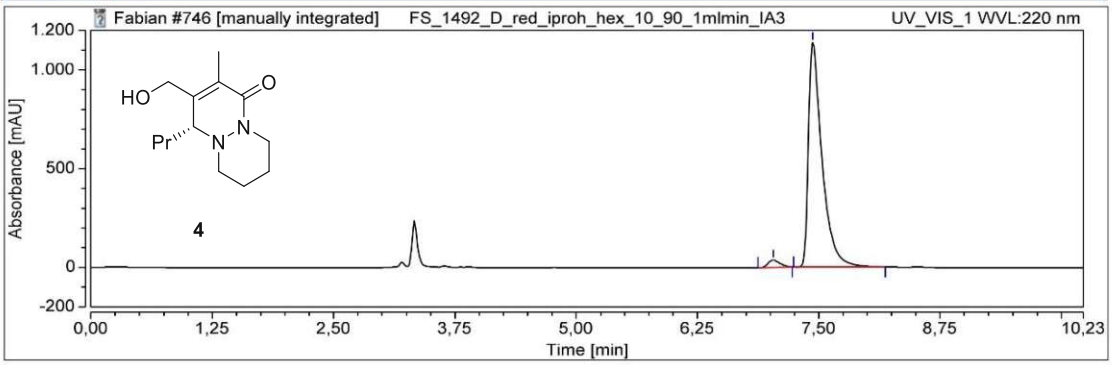


Reports IJD/Integration

Chromeleon (c) Dionex
Version 7.1.1.1127

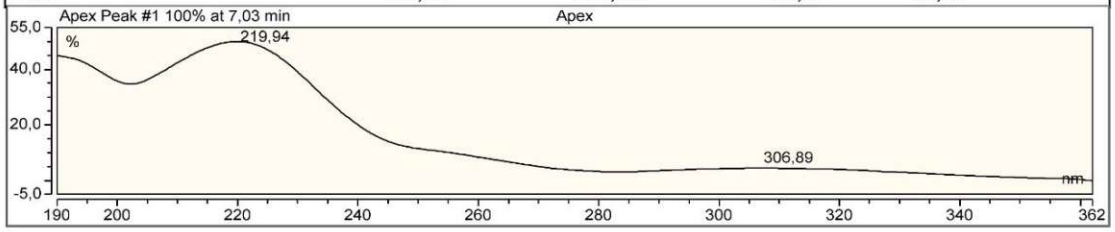
Die approbierte gedruckte Originalversion dieser Dissertation ist an der TU Wien Bibliothek verfügbar.
The approved original version of this doctoral thesis is available in print at TU Wien Bibliothek.

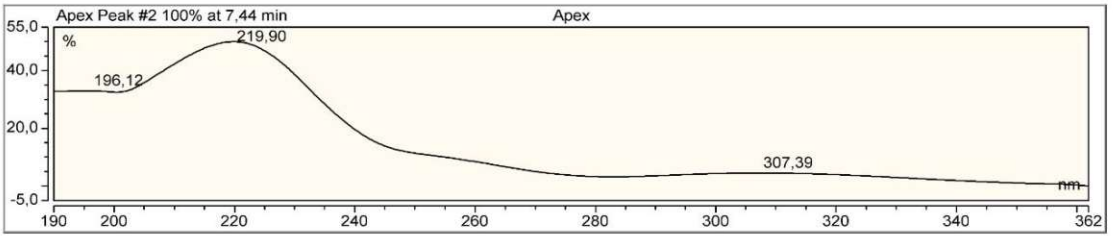
Chromatogram



Integration Results

No.	Peak Name	Retention Time min	Area mAU*min	Height mAU	Relative Area %	Relative Height %	Amount n.a.
1		7,030	5,193	37,296	2,74	3,17	n.a.
2		7,438	184,367	1137,999	97,26	96,83	n.a.
Total:			**189,560**	**1175,294**	**100,00**	**100,00**	



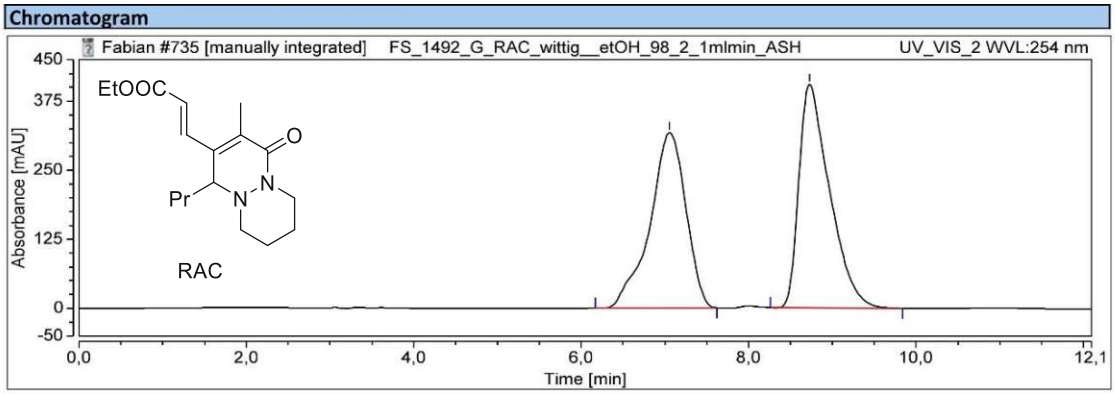


Reports IJD/Integration

Chromeleon (c) Dionex
Version 7.1.1.1127

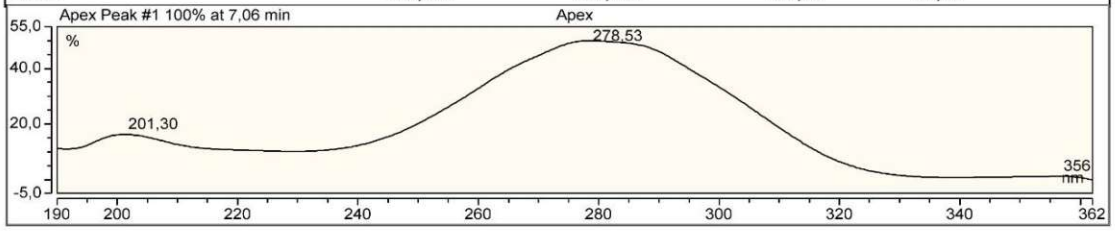
Die approbierte gedruckte Originalversion dieser Dissertation ist an der TU Wien Bibliothek verfügbar.
The approved original version of this doctoral thesis is available in print at TU Wien Bibliothek.

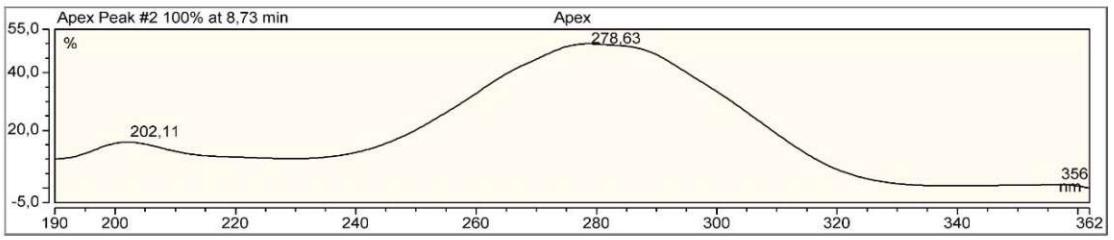
8.1.28 HPLC spectra of **5**



Integration Results

No.	Peak Name	Retention Time min	Area mAU*min	Height mAU	Relative Area %	Relative Height %	Amount n.a.
1		7,055	158,097	317,883	47,94	43,99	n.a.
2		8,727	171,687	404,771	52,06	56,01	n.a.
Total:			**329,784**	**722,655**	**100,00**	**100,00**	



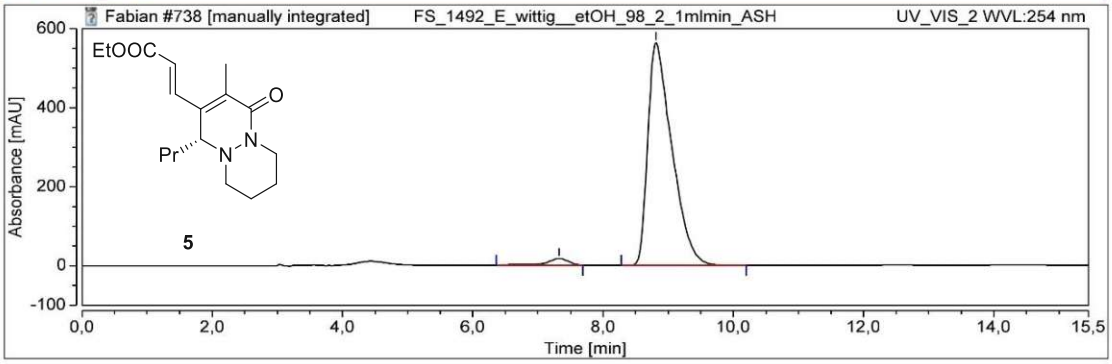


Reports IJD/Integration

Chromeleon (c) Dionex
Version 7.1.1.1127

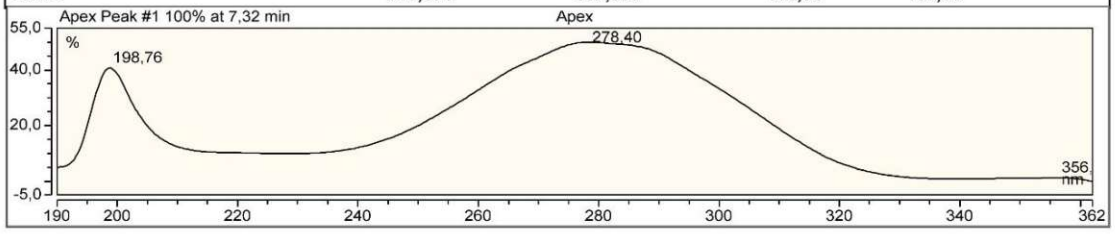
Die approbierte gedruckte Originalversion dieser Dissertation ist an der TU Wien Bibliothek verfügbar.
The approved original version of this doctoral thesis is available in print at TU Wien Bibliothek.

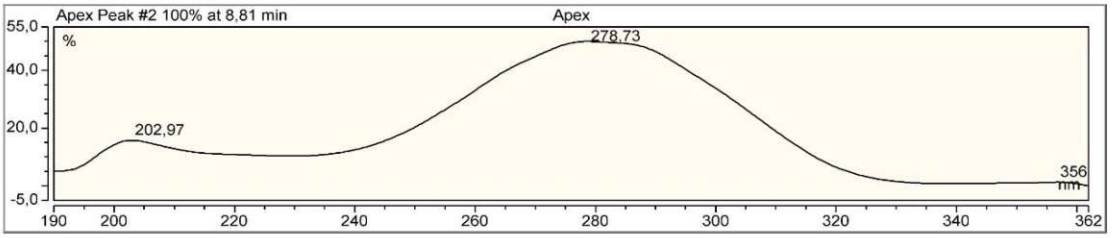
Chromatogram



Integration Results

No.	Peak Name	Retention Time min	Area mAU*min	Height mAU	Relative Area %	Relative Height %	Amount n.a.
1		7,322	7,369	17,618	2,96	3,02	n.a.
2		8,813	241,202	565,381	97,04	96,98	n.a.
Total:			**248,571**	**582,999**	**100,00**	**100,00**	





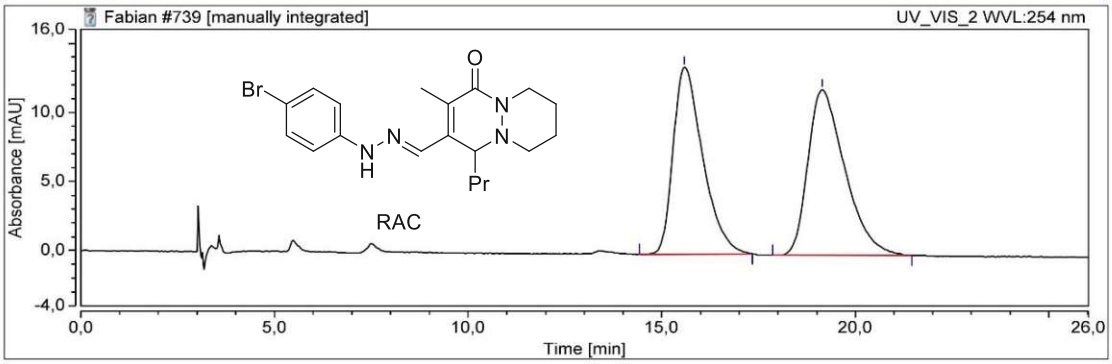
Reports IJD/Integration

Chromeleon (c) Dionex
Version 7.1.1.1127

Die approbierte gedruckte Originalversion dieser Dissertation ist an der TU Wien Bibliothek verfügbar.
The approved original version of this doctoral thesis is available in print at TU Wien Bibliothek.

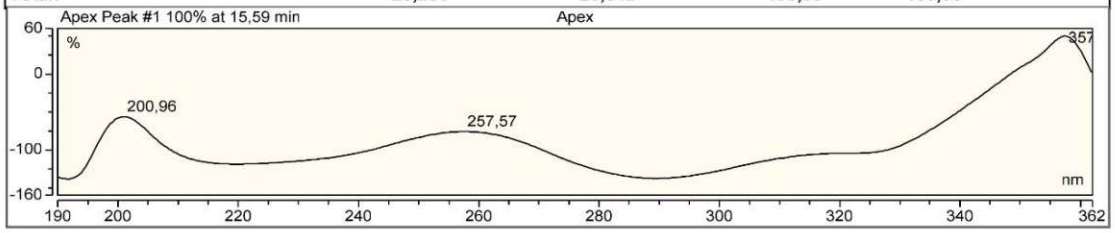
8.1.29 HPLC spectra of **6**

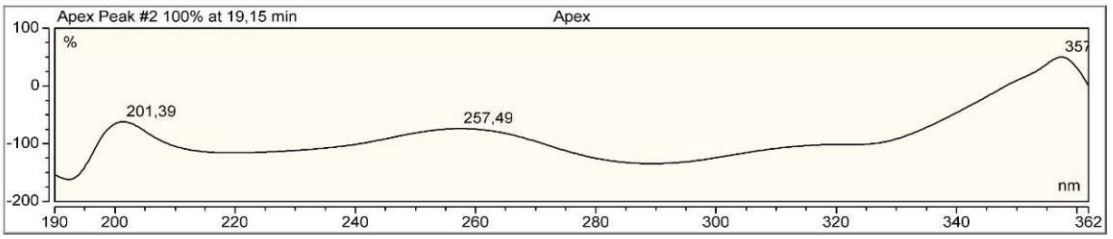
Chromatogram



Integration Results

No.	Peak Name	Retention Time min	Area mAU*min	Height mAU	Relative Area %	Relative Height %	Amount n.a.
1		15,585	11,999	13,548	47,49	53,04	n.a.
2		19,148	13,266	11,994	52,51	46,96	n.a.
Total:			**25,266**	**25,542**	**100,00**	**100,00**	



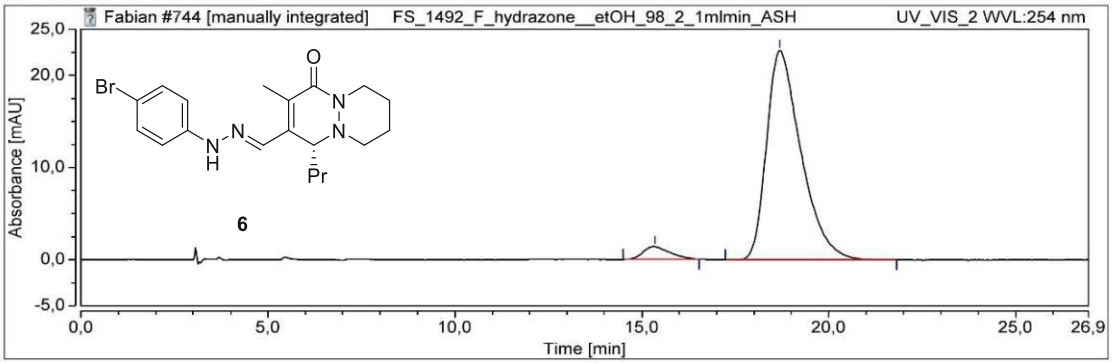


Reports IJD/Integration

Chromeleon (c) Dionex
Version 7.1.1.1127

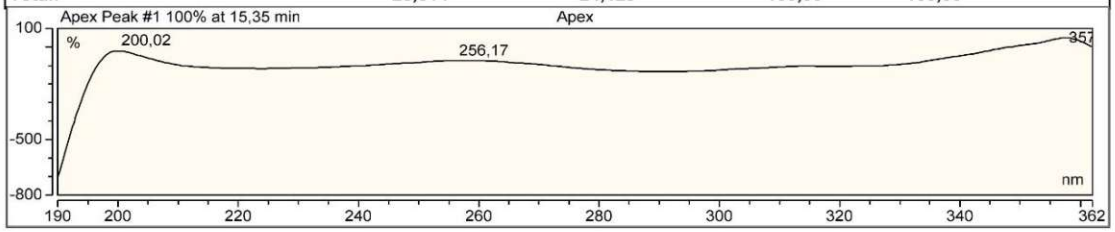
Die approbierte gedruckte Originalversion dieser Dissertation ist an der TU Wien Bibliothek verfügbar.
The approved original version of this doctoral thesis is available in print at TU Wien Bibliothek.

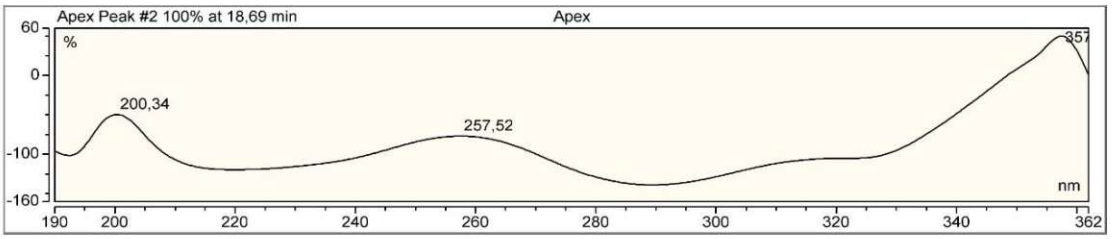
Chromatogram



Integration Results

No.	Peak Name	Retention Time min	Area mAU*min	Height mAU	Relative Area %	Relative Height %	Amount n.a.
1		15,347	1,151	1,396	4,55	5,79	n.a.
2		18,690	24,163	22,733	95,45	94,21	n.a.
Total:			**25,314**	**24,129**	**100,00**	**100,00**	





Reports IJD/Integration

Chromeleon (c) Dionex
Version 7.1.1.1127

Die approbierte gedruckte Originalversion dieser Dissertation ist an der TU Wien Bibliothek verfügbar.
The approved original version of this doctoral thesis is available in print at TU Wien Bibliothek.

9 XRD data of **6**

Solvent for crystal growth: MeOH

Table S1 - Crystal Data and Details of the Structure Determination for compound **6** CCDC 2286183

Crystal Data	
Formula	C19 H25 Br N4 O
Formula Weight	405.34
Crystal System	orthorhombic
Space group	$P2_12_12_1$ (No. 19)
a, b, c [Å]	8.9040(1) 11.8179(3) 18.9284(3)
V [Å^3]	1991.77(6)
Z	4
D(calc) [g/cm^3]	1.352
Mu(CuKa) [/mm]	2.916
F(000)	840
Crystal Size [mm]	0.08 x 0.09 x 0.13
Data Collection	
Temperature (K)	296
Radiation [Å]	CuKa 1.54186
Theta Min-Max [°]	4.4, 67.8
Dataset	-3: 10 ; -13: 13 ; -19: 22
Tot., Uniq. Data, R(int)	20635, 3565, 0.022
Observed Data [I > 2.0 sigma(I)]	3319
Refinement	
Nref, Npar	3565, 233
R, wR2, S	0.0340, 0.0893, 1.07
w = ^2^(FO^2^)+(0.0413P)^2^+0.8190P] WHERE P=(FO^2^+2FC^2^)/3'	
Max. and Av. Shift/Error	0.00, 0.00
Flack x	-0.043(6)
Min. and Max. Resd. Dens. [e/ Å^3]	-0.65, 0.46

CCDC 2286183 contains the supplementary crystallographic data for this paper. These data can be obtained free of charge from The Cambridge Crystallographic Data Centre via www.ccdc.cam.ac.uk/structures

Die approbierte gedruckte Originalversion dieser Dissertation ist an der TU Wien Bibliothek verfügbar.
The approved original version of this doctoral thesis is available in print at TU Wien Bibliothek.

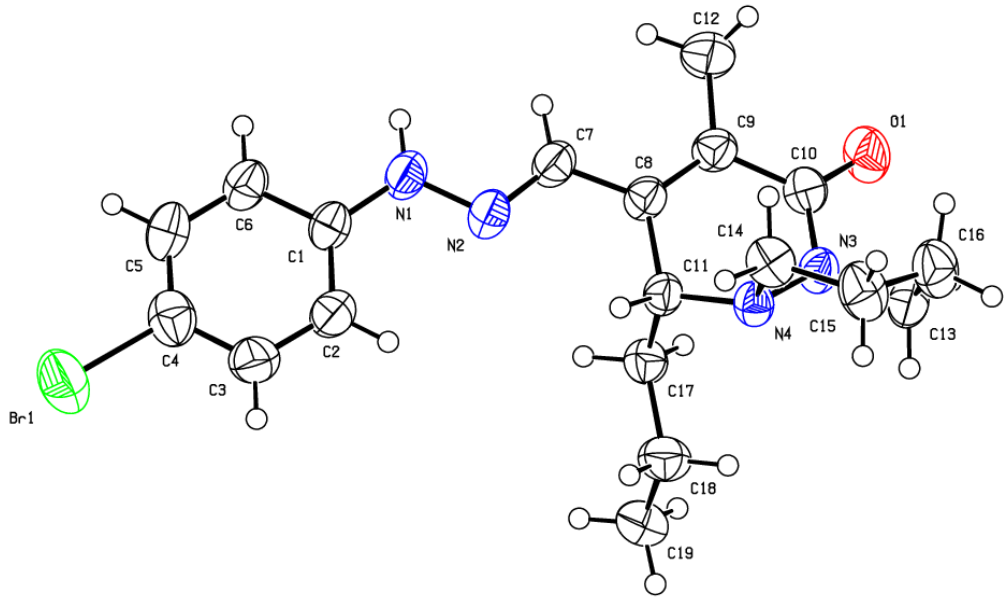


Figure 2.0. Molecular structure of CCDC 2286183 with displacement ellipsoids drawn at the 50% probability level.

10 References

(1) Vakulya, B.; Varga, S.; Csámpai, A.; Soós, T. Highly Enantioselective Conjugate Addition of Nitromethane to Chalcones Using Bifunctional Cinchona Organocatalysts. *Org. Lett.* **2005**, *7* (10), 1967–1969. https://doi.org/10.1021/ol050431s.

(2) Scharinger, F.; Pálvölgyi, Á. M.; Weisz, M.; Weil, M.; Stanetty, C.; Schnürch, M.; Bica-Schröder, K. Sterically Demanding Flexible Phosphoric Acids for Constructing Efficient and Multi-Purpose Asymmetric Organocatalysts. *Angew. Chem. Int. Ed.* **2022**, *61* (26). https://doi.org/10.1002/anie.202202189.

(3) Ooka, H.; Arai, N.; Azuma, K.; Kurono, N.; Ohkuma, T. Asymmetric Hydrogenation of Aromatic Ketones Catalyzed by the TolBINAP/DMAPEN–Ruthenium(II) Complex: A Significant Effect of N -Substituents of Chiral 1,2-Diamine Ligands on Enantioselectivity. *J. Org. Chem.* **2008**, *73* (22), 9084–9093. https://doi.org/10.1021/jo801863q.

(4) Shim, J. H.; Kim, M. J.; Lee, J. Y.; Kim, K. H.; Ha, D. C. Organocatalytic Asymmetric Aldol Reaction Using Protonated Chiral 1,2-Diamines. *Tetrahedron Lett.* **2020**, *61* (36), 152295. https://doi.org/10.1016/j.tetlet.2020.152295.

(5) Ranade, A. R.; Georg, G. I. Enantioselective Synthesis of 3,4-Dihydro-1,2-Oxazepin-5(2 H)-Ones and 2,3-Dihydropyridin-4(1 H)-Ones from β-Substituted β-Hydroxyaminoaldehydes. *J. Org. Chem.* **2014**, *79* (3), 984–992. https://doi.org/10.1021/jo402445r.

(6) Könning, D.; Olbrisch, T.; Sypaseuth, F. D.; Tzschucke, C. C.; Christmann, M. Oxidation of Allylic and Benzylic Alcohols to Aldehydes and Carboxylic Acids. *Chem. Commun.* **2014**, *50* (39), 5014–5016. https://doi.org/10.1039/C4CC01305K.

(7) Zhang, X.-W.; Jiang, G.-Q.; Lei, S.-H.; Shan, X.-H.; Qu, J.-P.; Kang, Y.-B. Iron-Catalyzed α,β-Dehydrogenation of Carbonyl Compounds. *Org. Lett.* **2021**, *23* (5), 1611–1615. https://doi.org/10.1021/acs.orglett.1c00043.

(8) Gan, X.; Fu, Z.; Liu, L.; Yan, Y.; Chen, C.; Zhou, Y.; Dong, J. Phosphorous Acid Promoted Isomerization of Propargyl Alcohols to α,β-Unsaturated Carbonyl Compounds. *Tetrahedron Lett.* **2019**, *60* (32), 150906. https://doi.org/10.1016/j.tetlet.2019.06.065.

(9) McErlain, H.; McLean, E. B.; Morgan, T. E. F.; Burianova, V. K.; Tavares, A. A. S.; Sutherland, A. Organocatalytic Asymmetric Synthesis of SynVesT-1, a Synaptic Density Positron Emission Tomography Imaging Agent. *J. Org. Chem.* **2022**, *87* (21), 14443–14451. https://doi.org/10.1021/acs.joc.2c01895.

(10) Liniger, M.; Neuhaus, C. M.; Altmann, K.-H. Ring-Closing Metathesis Approaches towards the Total Synthesis of Rhizoxins. *Molecules* **2020**, *25* (19), 4527. https://doi.org/10.3390/molecules25194527.

(11) Tu, J.-L.; Gao, H.; Luo, M.; Zhao, L.; Yang, C.; Guo, L.; Xia, W. Iron-Catalyzed Ring-Opening of Cyclic Carboxylic Acids Enabled by Photoinduced Ligand-to-Metal Charge Transfer. *Green Chem.* **2022**, *24* (14), 5553–5558. https://doi.org/10.1039/D2GC01738E.

(12) Wunderlich, J.; Roß, T.; Schröder, M.; Hahn, F. Step-Economic Synthesis of Biomimetic β-Ketopolyene Thioesters and Demonstration of Their Usefulness in Enzymatic Biosynthesis Studies. *Org. Lett.* **2020**, *22* (13), 4955–4959. https://doi.org/10.1021/acs.orglett.0c01348.

Die approbierte gedruckte Originalversion dieser Dissertation ist an der TU Wien Bibliothek verfügbar.
The approved original version of this doctoral thesis is available in print at TU Wien Bibliothek.
TU Bibliothek Your knowledge hub WIEN

(13) Nunez, M. T.; Martin, V. S. Efficient Oxidation of Phenyl Groups to Carboxylic Acids with Ruthenium Tetraoxide. A Simple Synthesis of (R)-.Gamma.-Caprolactone, the Pheromone of Trogoderma Granarium. *J. Org. Chem.* **1990**, *55* (6), 1928–1932. https://doi.org/10.1021/jo00293a044.

(14) Engesser, T.; Brückner, R. Synthesis of Trans -Configured Enol Ethers by a Sequence of Syn -Selective Glycolate Aldol Addition, Hydrolysis, and Grob Fragmentation. *European J. Org. Chem.* **2017**, *2017* (38), 5789–5794. https://doi.org/10.1002/ejoc.201701197.

(15) Ando, K.; Watanabe, H.; Zhu, X. One-Pot Preparation of (E)-α,β-Unsaturated Aldehydes by a Julia–Kocienski Reaction of 2,2-Dimethoxyethyl PT Sulfone Followed by Acid Hydrolysis. *J. Org. Chem.* **2021**, *86* (9), 6969–6973. https://doi.org/10.1021/acs.joc.1c00479.

(16) Williams, P. D.; LeGoff, E. Oxidation of Furans II. Use of Furans as Masked Dienophiles in the Intramolecular Diels-Alder Reaction. *Tetrahedron Lett.* **1985**, *26* (11), 1367–1370. https://doi.org/10.1016/S0040-4039(00)99046-4.

(17) Liao, L.; Guo, R.; Zhao, X. Organoselenium-Catalyzed Regioselective C−H Pyridination of 1,3-Dienes and Alkenes. *Angew. Chem. Int. Ed.* **2017**, *56* (12), 3201–3205. https://doi.org/10.1002/anie.201610657.

(18) Liu, Y.; Izzo, J. A.; McLeod, D.; Ričko, S.; Svenningsen, E. B.; Poulsen, T. B.; Jørgensen, K. A. Organocatalytic Asymmetric Multicomponent Cascade Reaction for the Synthesis of Contiguously Substituted Tetrahydronaphthols. *J. Am. Chem. Soc.* **2021**, *143* (21), 8208–8220. https://doi.org/10.1021/jacs.1c03923.

(19) Ahn, J. H.; Shin, M. S.; Jun, M. A.; Jung, S. H.; Kang, S. K.; Kim, K. R.; Rhee, S. D.; Kang, N. S.; Kim, S. Y.; Sohn, S.-K.; Kim, S. G.; Jin, M. S.; Lee, J. O.; Cheon, H. G.; Kim, S. S. Synthesis, Biological Evaluation and Structural Determination of β-Aminoacyl-Containing Cyclic Hydrazine Derivatives as Dipeptidyl Peptidase IV (DPP-IV) Inhibitors. *Bioorg. Med. Chem. Lett.* **2007**, *17* (9), 2622–2628. https://doi.org/10.1016/j.bmcl.2007.01.111.

(20) Suzuki, I.; Hirata, A.; Takeda, K. Development of Cyclic Hydrazine and Hydrazide Type Organocatalyst – Mechanistic Aspects of Cyclic Hydrazine/Hydrazide-Catalyzed Diels-Alder Reactions. *Heterocycles* **2009**, *79* (1), 851. https://doi.org/10.3987/COM-08-S(D)54.

(21) YONG, L. T. W. X. W. Synthetic and Technological Method of 1,2,3,4-Tetrahydrophthalazine Compound. CN103864696B, 2012.

Die approbierte gedruckte Originalversion dieser Dissertation ist an der TU Wien Bibliothek verfügbar.
The approved original version of this doctoral thesis is available in print at TU Wien Bibliothek.